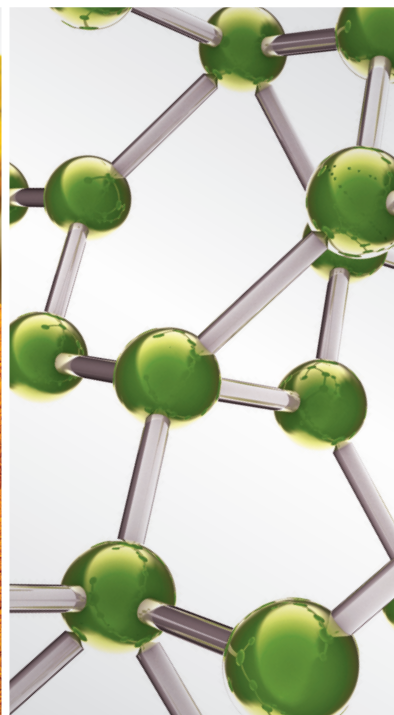
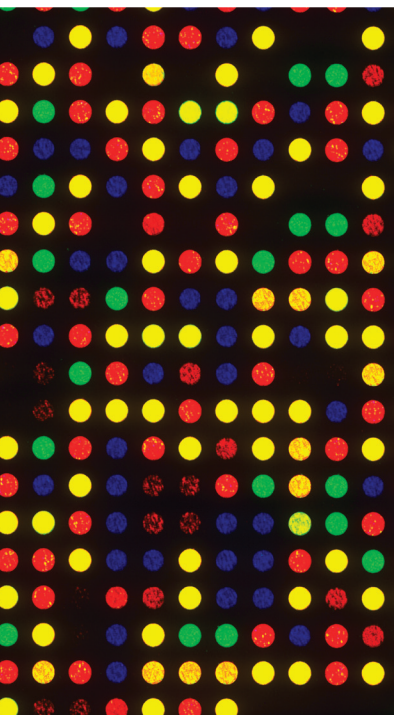


Biophysical Basis for Meridian and Acupoint Functions

GUEST EDITORS: GUANGHONG DING, YING XIA, WOLFGANG SCHWARZ, AND DI ZHANG





Biophysical Basis for Meridian and Acupoint Functions

Biophysical Basis for Meridian and Acupoint Functions

Guest Editors: Guanghong Ding, Ying Xia, Wolfgang Schwarz,
and Di Zhang



Copyright © 2013 Hindawi Publishing Corporation. All rights reserved.

This is a special issue published in "Evidence-Based Complementary and Alternative Medicine." All articles are open access articles distributed under the Creative Commons Attribution License, which permits unrestricted use, distribution, and reproduction in any medium, provided the original work is properly cited.

Editorial Board

- M. A. Abdulla, Malaysia
Jon Adams, Australia
Zuraini Ahmad, Malaysia
U. P. Albuquerque, Brazil
Gianni Allais, Italy
Terje Alraek, Norway
Souliman Amrani, Morocco
Akshay Anand, India
Shrikant Anant, USA
Manuel Arroyo-Morales, Spain
Syed B. Asdaq, Saudi Arabia
Seddigheh Asgary, Iran
Hyunsu Bae, Republic of Korea
Lijun Bai, China
Sandip K. Bandyopadhyay, India
Sarang Bani, India
Vassya Bankova, Bulgaria
Winfried Banzer, Germany
Vernon A. Barnes, USA
Samra Bashir, Pakistan
Jairo Kenupp Bastos, Brazil
Sujit Basu, USA
David Baxter, New Zealand
Andre-Michael Beer, Germany
Alvin J. Beitz, USA
Yong Chool Boo, Republic of Korea
Francesca Borrelli, Italy
Gloria Brusotti, Italy
Ishfaq A. Bukhari, Pakistan
Arndt Büssing, Germany
Rainer W. Bussmann, USA
Raffaele Capasso, Italy
Opher Caspi, Israel
Han Chae, Korea
Shun-Wan Chan, Hong Kong
Il-Moo Chang, Republic of Korea
Rajnish Chaturvedi, India
Chun Tao Che, USA
Tzeng-Ji Chen, Taiwan
Kevin Chen, USA
Jian-Guo Chen, China
Hubiao Chen, Hong Kong
Yunfei Chen, China
Juei-Tang Cheng, Taiwan
Evan Paul Cherniack, USA
Jen-Hwey Chiu, Taiwan
W. Chi-shing Cho, Hong Kong
Jae Youl Cho, Korea
Seung-Hun Cho, Republic of Korea
Chee Yan Choo, Malaysia
Li-Fang Chou, Taiwan
Ryowon Choue, Republic of Korea
Shuang-En Chuang, Taiwan
J.-H. Chung, Republic of Korea
Edwin L. Cooper, USA
Gregory D. Cramer, USA
Meng Cui, China
Roberto N. Cuman, Brazil
Vincenzo De Feo, Italy
R. De la Puerta Vázquez, Spain
Martin Descarreaux, USA
Alexandra Deters, Germany
Siva S. Durairajan, Hong Kong
Mohamed Eddouks, Morocco
Thomas Efferth, Germany
Tobias Esch, USA
Saeed Esmaeili-Mahani, Iran
Nianping Feng, China
Yibin Feng, Hong Kong
Josue Fernandez-Carnero, Spain
Juliano Ferreira, Brazil
Fabio Firenzuoli, Italy
Peter Fisher, UK
W. F. Fong, Hong Kong
Joel J. Gagnier, Canada
Siew Hua Gan, Malaysia
Jian-Li Gao, China
Gabino Garrido, Chile
M. N. Ghayur, Pakistan
Anwarul Hassan Gilani, Pakistan
Michael Goldstein, USA
Mahabir P. Gupta, Panama
Svein Haavik, Norway
Abid Hamid, India
N. Hanazaki, Brazil
K. B. Harikumar, India
Cory S. Harris, Canada
Thierry Hennebelle, France
Seung-Heon Hong, Korea
Markus Horneber, Germany
Ching-Liang Hsieh, Taiwan
Jing Hu, China
Sheng-Teng Huang, Taiwan
Benny Tan Kwong Huat, Singapore
Roman Huber, Germany
Angelo Antonio Izzo, Italy
Suresh Jadhav, India
Kanokwan Jarukamjorn, Thailand
Yong Jiang, China
Zheng L. Jiang, China
Stefanie Joos, Germany
Sirajudeen K. N. S., Malaysia
Z. Kain, USA
Osamu Kanauchi, Japan
Dae Gill Kang, Republic of Korea
Wenyi Kang, China
Shao-Hsuan Kao, Taiwan
Krishna Kaphle, Nepal
Kenji Kawakita, Japan
Jong Yeol Kim, Republic of Korea
Youn Chul Kim, Republic of Korea
Cheorl-Ho Kim, Republic of Korea
Yoshiyuki Kimura, Japan
Joshua K. Ko, China
Toshiaki Kogure, Japan
Jian Kong, USA
Nandakumar Krishnadas, India
Yiu Wa Kwan, Hong Kong
Kuang Chi Lai, Taiwan
Ching Lan, Taiwan
Alfred Längler, Germany
Lixing Lao, Hong Kong
Clara Bik-San Lau, Hong Kong
Jang-Hern Lee, Republic of Korea
Myeong Soo Lee, Republic of Korea
Tat leang Lee, Singapore
Christian Lehmann, Canada
Marco Leonti, Italy
Lawrence Leung, Canada
Kwok Nam Leung, Hong Kong
Ping-Chung Leung, Hong Kong
ChunGuang Li, Australia
Xiu-Min Li, USA
Ping Li, China
Shao Li, China

Man Li, China
Min Li, China
Yong Hong Liao, China
Sabina Lim, Korea
Bi-Fong Lin, Taiwan
Wen Chuan Lin, China
Christopher G. Lis, USA
Gerhard Litscher, Austria
I-Min Liu, Taiwan
Ke Liu, China
Yijun Liu, USA
Cun-Zhi Liu, China
Gaofeng Liu, China
Gail B. Mahady, USA
Juraj Majtan, Slovakia
Subhash C. Mandal, India
Jeanine L. Marnewick, South Africa
Virginia S. Martino, Argentina
James H. McAuley, Australia
Karin Meissner, Germany
Andreas Michalsen, Germany
David Mischoulon, USA
Syam Mohan, Saudi Arabia
J. Molnar, Hungary
Valério Monteiro-Neto, Brazil
Hyung-In Moon, Republic of Korea
Albert Moraska, USA
Mark Moss, UK
Yoshiharu Motoo, Japan
Frauke Musial, Germany
MinKyun Na, Republic of Korea
Richard L. Nahin, USA
Vitaly Napadow, USA
F. R. F. Nascimento, Brazil
S. Nayak, Trinidad And Tobago
Roland Ndip Ndip, South Africa
Isabella Neri, Italy
T. B. Nguenefack, Cameroon
Martin Offenbaecher, Germany
Ki-Wan Oh, Republic of Korea
Yoshiji Ohta, Japan
Olumayokun A. Olajide, UK
Thomas Ostermann, Germany
Stacey A. Page, Canada
Tai-Long Pan, Taiwan
Bhushan Patwardhan, India
Berit Smestad Paulsen, Norway
Andrea Pieroni, Italy
Richard Pietras, USA
Waris Qidwai, Pakistan
Xianqin Qu, Australia
Cassandra L. Quave, USA
Roja Rahimi, Iran
Khalid Rahman, UK
Cheppail Ramachandran, USA
Gamal Ramadan, Egypt
Ke Ren, USA
Man Hee Rhee, Republic of Korea
Mee-Ra Rhyu, Republic of Korea
José Luis Ríos, Spain
Paolo Roberti di Sarsina, Italy
Bashar Saad, Palestinian Authority
Sumaira Sahreen, Pakistan
Omar Said, Israel
Luis A. Salazar-Olivo, Mexico
Mohd. Zaki Salleh, Malaysia
Andreas Sandner-Kiesling, Austria
Adair Santos, Brazil
G. Schmeda-Hirschmann, Chile
Andrew Scholey, Australia
Veronique Seidel, UK
Senthamil R. Selvan, USA
Tuhinadri Sen, India
Hongcai Shang, China
Ronald Sherman, USA
Karen J. Sherman, USA
Kuniyoshi Shimizu, Japan
Kan Shimpo, Japan
Byung-Cheul Shin, Korea
Yukihiro Shoyama, Japan
Chang-Gue Son, Korea
Rachid Soulimani, France
Didier Stien, France
Shan-Yu Su, Taiwan
Mohd Roslan Sulaiman, Malaysia
Venil N. Sumantran, India
John R. S. Tabuti, Uganda
Toku Takahashi, USA
Rabih Talhouk, Lebanon
Wen-Fu Tang, China
Yuping Tang, China
Lay Kek Teh, Malaysia
Mayank Thakur, Germany
Menaka C. Thounaojam, India
Mei Tian, China
Evelin Tiralongo, Australia
Stephanie Tjen-A-Looi, USA
MichaThl Tomczyk, Poland
Yao Tong, Hong Kong
Karl Wah-Keung Tsim, Hong Kong
Volkan Tugcu, Turkey
Yew-Min Tzeng, Taiwan
Dawn M. Upchurch, USA
Maryna Van de Venter, South Africa
Sandy van Vuuren, South Africa
Alfredo Vannacci, Italy
Mani Vasudevan, Malaysia
Carlo Ventura, Italy
Wagner Vilegas, Brazil
Pradeep Visen, Canada
Aristo Vojdani, USA
Shu-Ming Wang, USA
Chong-Zhi Wang, USA
Chenchen Wang, USA
Y. Wang, USA
Kenji Watanabe, Japan
Jintanaporn Wattanathorn, Thailand
Jenny M. Wilkinson, Australia
Darren R. Williams, Republic of Korea
Haruki Yamada, Japan
Nobuo Yamaguchi, Japan
Junqing Yang, China
Yong-Qing Yang, China
Eun Jin Yang, Republic of Korea
Ling Yang, China
Xiufen Yang, China
Ken Yasukawa, Japan
Min Ye, China
M. Yoon, Republic of Korea
Jie Yu, China
Zunjian Zhang, China
Hong Q. Zhang, Hong Kong
Wei-Bo Zhang, China
Jin-Lan Zhang, China
Boli Zhang, China
Ruixin Zhang, USA
Hong Zhang, China
Haibo Zhu, China

Contents

Effect of Electroacupuncture on Rat Ischemic Brain Injury: Importance of Stimulation Duration,

Fei Zhou, Jingchun Guo, Jieshi Cheng, Gencheng Wu, and Ying Xia

Volume 2013, Article ID 878521, 12 pages

Understanding Central Mechanisms of Acupuncture Analgesia Using Dynamic Quantitative Sensory

Testing: A Review, Jiang-Ti Kong, Rosa N. Schnyer, Kevin A. Johnson, and Sean Mackey

Volume 2013, Article ID 187182, 12 pages

Electroacupuncture and Brain Protection against Cerebral Ischemia: Specific Effects of Acupoints,

Fei Zhou, Jingchun Guo, Jieshi Cheng, Gencheng Wu, Jian Sun, and Ying Xia

Volume 2013, Article ID 804397, 14 pages

From Acupuncture to Interaction between δ -Opioid Receptors and Na^+ Channels: A Potential Pathway to Inhibit Epileptic Hyperexcitability,

Dongman Chao, Xueyong Shen, and Ying Xia

Volume 2013, Article ID 216016, 17 pages

Electroacupuncture-Induced Attenuation of Experimental Epilepsy: A Comparative Evaluation of Acupoints and Stimulation Parameters,

Xuezhi Kang, Xueyong Shen, and Ying Xia

Volume 2013, Article ID 149612, 10 pages

Effects of Electroacupuncture at Auricular Concha Region on the Depressive Status of Unpredictable Chronic Mild Stress Rat Models,

Ru-Peng Liu, Ji-Liang Fang, Pei-Jing Rong, Yufeng Zhao, Hong Meng,

Hui Ben, Liang Li, Zhan-Xia Huang, Xia Li, Ying-Ge Ma, and Bing Zhu

Volume 2013, Article ID 789674, 7 pages

An Acupuncture Research Protocol Developed from Historical Writings by Mathematical Reflections: A Rational Individualized Acupoint Selection Method for Immediate Pain Relief,

Sven Schroeder, Gesa Meyer-Hamme, Jianwei Zhang, Susanne Epplée, Thomas Friedemann, and Weiguo Hu

Volume 2013, Article ID 256754, 16 pages

The Neural Pathway of Reflex Regulation of Electroacupuncture at Orofacial Acupoints on Gastric Functions in Rats,

Jianhua Liu, Wenbin Fu, Wei Yi, Zhenhua Xu, and Nenggui Xu

Volume 2012, Article ID 753264, 8 pages

Biophysical Characteristics of Meridians and Acupoints: A Systematic Review,

Juan Li, Qing Wang, Huiling Liang, Haoxu Dong, Yan Li, Ernest Hung Yu Ng, and Xiaoke Wu

Volume 2012, Article ID 793841, 6 pages

Transcutaneous Auricular Vagus Nerve Stimulation Protects Endotoxemic Rat from

Lipopolysaccharide-Induced Inflammation, Yu Xue Zhao, Wei He, Xiang Hong Jing, Jun Ling Liu, Pei Jing Rong, Hui Ben, Kun Liu, and Bing Zhu

Volume 2012, Article ID 627023, 10 pages

Inhibition of Activity of GABA Transporter GAT1 by δ -Opioid Receptor,

Lu Pu, Nanjie Xu, Peng Xia, Quanbao Gu, Shuanglai Ren, Thomas Fucke, Gang Pei, and Wolfgang Schwarz

Volume 2012, Article ID 818451, 12 pages

Electrical Potential of Acupuncture Points: Use of a Noncontact Scanning Kelvin Probe,

Brian J. Gow, Justine L. Cheng, Iain D. Baikie, Ørjan G. Martinsen, Min Zhao, Stephanie Smith, and Andrew C. Ahn

Volume 2012, Article ID 632838, 8 pages

Interstitial Fluid Flow: The Mechanical Environment of Cells and Foundation of Meridians, Wei Yao, Yabei Li, and Guanghong Ding
Volume 2012, Article ID 853516, 9 pages

Research on Nonlinear Feature of Electrical Resistance of Acupuncture Points, Jianzi Wei, Huijuan Mao, Yu Zhou, Lina Wang, Sheng Liu, and Xueyong Shen
Volume 2012, Article ID 179657, 6 pages

Stimulation of TRPV1 by Green Laser Light, Quanbao Gu, Lina Wang, Fang Huang, and Wolfgang Schwarz
Volume 2012, Article ID 857123, 8 pages

Therapeutic Effects of Acupuncture through Enhancement of Functional Angiogenesis and Granulogenesis in Rat Wound Healing, Sang In Park, Yun-Young Sunwoo, Yu Jin Jung, Woo Chul Chang, Moon-Seo Park, Young-An Chung, Lee-So Maeng, Young-Min Han, Hak Soo Shin, Jisoo Lee, and Sang-Hoon Lee
Volume 2012, Article ID 464586, 10 pages

Auricular Acupuncture and Vagal Regulation, Wei He, Xiaoyu Wang, Hong Shi, Hongyan Shang, Liang Li, Xianghong Jing, and Bing Zhu
Volume 2012, Article ID 786839, 6 pages

Hemodynamic Changes in the Brachial Artery Induced by Acupuncture Stimulation on the Lower Limbs: A Single-Blind Randomized Controlled Trial, Masashi Watanabe, Shin Takayama, Atsushi Hirano, Takashi Seki, and Nobuo Yaegashi
Volume 2012, Article ID 958145, 8 pages

Investigation of Acupuncture Sensation Patterns under Sensory Deprivation Using a Geographic Information System, Florian Beissner and Irene Marzolf
Volume 2012, Article ID 591304, 10 pages

Effects of Moxibustion Stimulation on the Intensity of Infrared Radiation of Tianshu (ST25) Acupoints in Rats with Ulcerative Colitis, Xiaomei Wang, Shuang Zhou, Wei Yao, Hua Wan, Huangan Wu, Luyi Wu, Huirong Liu, Xuegui Hua, and Peifeng Shi
Volume 2012, Article ID 704584, 13 pages

Observation of Pain-Sensitive Points along the Meridians in Patients with Gastric Ulcer or Gastritis, Hui Ben, Liang Li, Pei-Jing Rong, Zhi-Gao Jin, Jian-Liang Zhang, Yan-Hua Li, and Xia Li
Volume 2012, Article ID 130802, 7 pages

In Adjuvant-Induced Arthritic Rats, Acupuncture Analgesic Effects Are Histamine Dependent: Potential Reasons for Acupoint Preference in Clinical Practice, Meng Huang, Di Zhang, Zhe-yan Sa, Ying-yuan Xie, Chen-li Gu, and Guang-hong Ding
Volume 2012, Article ID 810512, 6 pages

A Review of Acupoint Specificity Research in China: Status Quo and Prospects, Ling Zhao, Ji Chen, Cun-Zhi Liu, Ying Li, Ding-Jun Cai, Yong Tang, Jie Yang, and Fan-Rong Liang
Volume 2012, Article ID 543943, 16 pages

Effects of Electroacupuncture of Different Frequencies on the Release Profile of Endogenous Opioid Peptides in the Central Nervous System of Goats, Li-Li Cheng, Ming-Xing Ding, Cheng Xiong, Min-Yan Zhou, Zheng-Ying Qiu, and Qiong Wang
Volume 2012, Article ID 476457, 9 pages

Patch Clamp: A Powerful Technique for Studying the Mechanism of Acupuncture, D. Zhang
Volume 2012, Article ID 534219, 7 pages

Systems Biology of Meridians, Acupoints, and Chinese Herbs in Disease, Li-Ling Lin, Ya-Hui Wang, Chi-Yu Lai, Chan-Lao Chau, Guan-Chin Su, Chun-Yi Yang, Shu-Ying Lou, Szu-Kai Chen, Kuan-Hao Hsu, Yen-Ling Lai, Wei-Ming Wu, Jian-Long Huang, Chih-Hsin Liao, and Hsueh-Fen Juan
Volume 2012, Article ID 372670, 13 pages

NMDA Receptor-Dependent Synaptic Activity in Dorsal Motor Nucleus of Vagus Mediates the Enhancement of Gastric Motility by Stimulating ST36, Xinyan Gao, Yongfa Qiao, Baohui Jia, Xianghong Jing, Bin Cheng, Lei Wen, Qiwen Tan, Yi Zhou, Bing Zhu, and Haifa Qiao
Volume 2012, Article ID 438460, 11 pages

Evaluation of the Effect of Laser Acupuncture and Cupping with Ryodoraku and Visual Analog Scale on Low Back Pain, Mu-Lien Lin, Hung-Chien Wu, Ya-Hui Hsieh, Chuan-Tsung Su, Yong-Sheng Shih, Chii-Wann Lin, and Jih-Huah Wu
Volume 2012, Article ID 521612, 7 pages

Acupuncture Alleviates Colorectal Hypersensitivity and Correlates with the Regulatory Mechanism of TrpV1 and p-ERK, Shao-Jun Wang, Hao-Yan Yang, and Guo-Shuang Xu
Volume 2012, Article ID 483123, 10 pages

Are Primo Vessels (PVs) on the Surface of Gastrointestine Involved in Regulation of Gastric Motility Induced by Stimulating Acupoints ST36 or CV12?, Xiaoyu Wang, Hong Shi, Hongyan Shang, Yangshuai Su, Juanjuan Xin, Wei He, Xianghong Jing, and Bing Zhu
Volume 2012, Article ID 787683, 8 pages

Measurements of Location-Dependent Nitric Oxide Levels on Skin Surface in relation to Acupuncture Point, Yejin Ha, Misun Kim, Jiseon Nah, Minah Suh, and Youngmi Lee
Volume 2012, Article ID 781460, 7 pages

Evaluate Laser Needle Effect on Blood Perfusion Signals of Contralateral Hegu Acupoint with Wavelet Analysis, Guangjun Wang, Yuying Tian, Shuyong Jia, Gerhard Litscher, and Weibo Zhang
Volume 2012, Article ID 103729, 9 pages

Research Article

Effect of Electroacupuncture on Rat Ischemic Brain Injury: Importance of Stimulation Duration

Fei Zhou,^{1,2} Jingchun Guo,³ Jieshi Cheng,³ Gengcheng Wu,³ and Ying Xia^{4,5}

¹ Shanghai Research Center for Acupuncture and Meridians, Shanghai 201203, China

² Gongli Hospital, Pudong New District, Shanghai 200135, China

³ Shanghai Medical College of Fudan University, Shanghai 200032, China

⁴ The University of Texas Medical School at Houston, Houston, TX 77030, USA

⁵ Yale University School of Medicine, New Haven, CT 06520, USA

Correspondence should be addressed to Ying Xia; ying.xia@uth.tmc.edu

Received 23 August 2012; Revised 10 November 2012; Accepted 13 December 2012

Academic Editor: Di Zhang

Copyright © 2013 Fei Zhou et al. This is an open access article distributed under the Creative Commons Attribution License, which permits unrestricted use, distribution, and reproduction in any medium, provided the original work is properly cited.

We explored the optimal duration of electroacupuncture (EA) stimulation for protecting the brain against ischemic injury. The experiments were carried out in rats exposed to right middle cerebral artery occlusion (MCAO) for 60 min followed by 24-hr reperfusion. EA was delivered to “Shuigou” (Du 26) and “Baihui” (Du 20) acupoints with sparse-dense wave (5/20 Hz) at 1.0 mA for 5, 15, 30, and 45 min, respectively. The results showed that 30 min EA, starting at 5 minutes after the onset of MCAO (EA during MCAO) or 5 minutes after reperfusion (EA after MCAO), significantly reduced ischemic infarct volume, attenuated neurological deficits, and decreased death rate with a larger reduction of the ischemic infarction in the former group. Also in the group of EA during MCAO, this protective benefit was positively proportional to the increase in the period of stimulation, that is, increased protection in response to EA from 5- to 30-min stimulation. In all groups, EA induced a significant increase in cerebral blood flow and promoted blood flow recovery after reperfusion, and both blood flow volume and blood cell velocity returned to the preischemia level in a short period of time. Surprisingly, EA for 45 min did not show reduction in the neurological deficits or the infarct volume and instead demonstrated an increase in death rate in this group. Although EA for 45 min still increased the blood flow during MCAO, it led to a worsening of perfusion after reperfusion compared to the group subjected only to ischemia. The neuroprotection induced by an “optimal” period (30 min) of EA was completely blocked by Naltrindole, a δ -opioid receptor (DOR) antagonist (10 mg/kg, i.v.). These findings suggest that earlier EA stimulation leads to better outcomes, and that EA-induced neuroprotection against ischemia depends on an optimal EA-duration via multiple pathways including DOR signaling, while “over-length” stimulation exacerbates the ischemic injury.

1. Introduction

Ischemic/hypoxic brain injury, such as stroke, leads to serious and complex pathophysiological changes affecting multiple levels of the brain, and sports a high global mortality rate as the leading cause of neurological disability [1–9]. In spite of extensive research conducted in the past several decades, limited therapeutic options are available against ischemic/hypoxic brain injury till date. The vast physical, emotional, and financial tolls that stroke inflicts upon patients and their families imposes a daunting and continuous challenge to the medical community [5–9]. Previous studies at

our laboratory and at those of others have shown that electroacupuncture (EA), at appropriate acupoints with suitable stimulation parameters, significantly attenuates neurological deficits, infarct volume and mortality in animal models exposed to ischemic insults [10–17], which may potentially shed a new light on developing a better modality for ischemic brain injury. Indeed, there is substantial clinical evidence demonstrating beneficial effects of acupuncture on stroke patients [18–21].

Because of inadequate control, poor methodological quality and small samples seen in previous studies, the efficacy of acupuncture on hypoxic/ischemic injury is still

unproven in clinical settings. In fact, major controversies exist with regards to the effectiveness of acupuncture in stroke patients [22–24]. These may, at least partially, be attributed to the varied approaches adopted in different studies, and since acupuncture induces complex changes at multiple levels in the central nervous system, the outcomes also differ with varying acupunctural methods [25–30]. Therefore, it is extremely important to define what optimal parameters are required for acupuncture treatment in ischemic/hypoxic brain injury.

Towards this goal, our serial studies have established that EA treatment for acute stroke in experimental animals is critically dependent upon specific acupoints along with stimulation currents of specific intensities and frequencies [11–15, 17]. Since the timing and duration of medical treatment has a huge impact on patients with acute stroke [7–9], we conducted this work to address two fundamental issues, that is, (1) when should EA be applied to induce optimal protection, during or after ischemia?, and (2) what duration of EA application is optimal to induce maximal beneficial effect on the ischemic brain?

2. Materials and Methods

2.1. Animals. Adult male Sprague-Dawley rats (240–270 g) were used for the experiments. All animals were purchased with permission from the Experimental Animal Center for the Shanghai Chinese Academy of Science. The animals were housed at an ambient temperature of $24 \pm 1^\circ\text{C}$ and were provided with free access to food and water. All surgical procedures were approved by the Animals Care and Use Committees of Fudan University Shanghai Medical College, Shanghai, China, and were performed under anesthesia (chloral hydrate, 400 mg/kg, i.p.).

2.2. Cerebral Blood Flow Monitoring. The cerebral blood flow was measured using laser-Doppler perfusion monitor (LDPM, PeriFlux5000, Perimed, Sweden). The major steps of the procedure were as follows: first, a small hole was drilled in the right parietal bone at a point 1.5 mm posterior to the bregma and 5 mm lateral to the sagittal suture, as previously described [14, 17, 31]. The superficial micro-vessels of cerebral pia mater were accessed using a laser Doppler probe (0.45 mm diameter) inserted into the hole at a depth of 2 mm and fixed to the skull bone. The probe was used to measure the blood perfusion to the cortex to record the cerebral blood flow. Continuous monitoring of cerebral blood flow was performed beginning 5 minutes prior to the induction of cerebral ischemia until at least 15 minutes after reperfusion. As per the manufacturer's guidelines, the measured change in perfusion values was dependent on the number of blood cells present and their velocity in the area illuminated by the tip of the probe. The changes in the cerebral blood flow of a localized area, recorded as a measure of the dynamic changes in Perfusion Units (PU), concentration of the moving blood cells (CMBC), and the velocity of blood cells (Velocity), were constantly monitored in real-time using LDPM. PU is an index of cerebral blood

flow and is expressed as the product of the number of moving blood cells and their relative velocities.

2.3. Method for Inducing Cerebral Ischemia. We followed the methods described by Longa et al. [32] that are also detailed in our previous publications [14, 17] for creating a focal cerebral ischemia model by middle cerebral artery occlusion (MCAO). Animals were taken under anesthesia to surgically expose their right common carotid, external carotid and internal carotid arteries. After ligation of the distal end of the right external carotid artery, it was incised and a 4–0 monofilament nylon suture (30 mm length, 0.18 mm diameter with a 0.24 mm diameter round tip, MONOSOF, SN-1699G, USA) was introduced to the right external carotid artery and further into the right internal carotid artery for ~20 mm up till the origin of the right middle cerebral artery. The blood flow to the right middle cerebral artery was then occluded at this level.

We constantly monitored the blood flow in all animals to ensure that a uniform cerebral ischemia level was maintained across all groups in a standard fashion. The blood flow was controlled by adjusting the suture in the artery for the induction of ischemia. The ischemic rats that showed a stable drop of ~85% in PU compared to the baseline level (before MCAO), that is, reaching a level of ~15% of the baseline PU, were used for further experimentation. The PU was kept at a low level with minor fluctuations during the entire ischemic period without any significant change except during EA application. After the occlusion, reperfusion of the ischemic area was allowed by withdrawing the suture from the right external carotid artery. Cortical blood flow changes were monitored in all animals beginning 5 minutes prior to the induction of cerebral ischemia until at least 15 minutes after reperfusion. This duration was inclusive of the entire length of MCAO and of EA as well.

Body temperature was maintained at $36.5^\circ\text{C} \pm 0.5^\circ\text{C}$ throughout the surgical procedures till the animal recovered from anesthesia. After the reperfusion, the animals were housed for 24 hours at an ambient temperature of $24 \pm 1^\circ\text{C}$. The same surgical procedures were performed on the animals in the sham-operation group, excluding MCAO.

2.4. Electroacupuncture Methods. WHO standards were followed for the name and localization of acupoints [33, 34]. “Shuigou (Du 26)” and “Baihui (Du 20)” are acupoints located on the head and face. Shuigou (Du 26) is located at a point on the midline of the upper lip 2/3rds from the mouth to the nose. Baihui (Du 20) is located at a point on the midline of the head, approximately midway on the line connecting the apices of both auricles.

To obtain optimal EA effect that induces maximum protection against cerebral ischemia, we applied EA at “Shuigou” (Du 26) and “Baihui” (Du 20) with 5/20 Hz sparse-dense frequency at a constant intensity of ~1.0 mA in all EA groups, beginning at 5 min after the onset of MCAO or 5 min after MCAO. The selection of the acupoints and stimulation parameters was based on the results of our serial studies in the past [14, 17].

In determination of effects of different EA periods on cerebral ischemia, EA was applied using varying lastings-durations, that is, beginning at 5 min after the onset of MCAO and continued up to 5 minutes, 15 minutes, 30 minutes, and 45 minutes, respectively. Five different groups were studied in the present study with the numbers in each group ranging from 16 to 45: MCAO only (Ischemia, $n = 45$), MCAO plus EA for 5 min (EA-5 min, $n = 18$), MCAO plus EA for 15 min (EA-15 min, $n = 16$), MCAO plus EA for 30 min (EA-30 min, $n = 30$), and MCAO plus EA for 45 min (EA-45 min, $n = 30$).

EA was delivered through stainless steel filiform needles (15 mm in length and 0.3 mm in diameter, Suzhou Medical Apparatus Limit Co., China) by an EA apparatus (Model G-6805-II, Shanghai Medical Instruments High-Tech Co., China). The needle on Du 26 is inserted 1 mm deep, vertical to the plane of the skin. At Du 20, the needle is inserted obliquely and to a depth of 2 mm [14, 17, 25, 33, 34]. The intensity and frequency of the output waves with a negative-going pulse on the posterior border (pulse width = 0.5 ms \pm 0.1 ms; component of direct current = Zero) were monitored on a general oscillograph (Model XJ4210A, Shanghai XinJian Instrument and Equipment Co., China).

2.5. δ -Opioid Receptors Blockade. The rats were randomly assigned to one of the four experimental groups: (1) Ischemia alone ($n = 7$); (2) Ischemia + EA at “Shuigou” (DU 26) and “Baihui” (DU 20) ($n = 8$); (3) Ischemia + Naltrindole ($n = 8$), in which rats were administered Naltrindole (10 mg/kg i.v.) 5 min before the onset of MCAO; and (4) Ischemia + EA + Naltrindole ($n = 10$), in which the animals were treated with both EA and Naltrindole. EA was started 5 min after ischemia and continued to 35 min after ischemia in this set of experiments.

2.6. Mortality and Neurological Deficits Monitoring. Some ischemic rats died between 2 and 20 hrs after reperfusion. The death rates were reported for this period based on the number of dead rats and the total number of the rats allocated to the given group. A myriad of factors could be implicated as the cause of death, as for example hemorrhage. However, investigating the precise cause of death was not our aim in this work.

Assessments on neurological deficits were made on animals in all groups. The rats that died within 24 h after MCAO were excluded. Assessments were made 24 h after reperfusion just before the sampling of brain tissue was done. The assessments on neurological deficits were blinded, that is, the person evaluating and scoring the neurological deficits based on pre-set criteria had no prior knowledge on the groups and treatments. The degree of neurological deficits was graded from 0–7 grades [14, 17]. The criteria were set as follows: Grade 0—“normal”, symmetrical movement without any abnormal sign; Grade 1—incomplete stretch of the left anterior limb when the tail was lifted up; Grade 2—dodderly crawl along with the signs of Grade 1; Grade 3—kept the left anterior limb close to the breast when the tail was lifted up; Grade 4—left turn when crawling; Grade 5—left anterior claw

pushed backward along with the signs of Grade 4; Grade 6—repeated rotational motion with an immobile posterior left limb; and Grade 7—left recumbent position because of body supporting incapability.

2.7. Cerebral Infarct Measurement. After the assessment of neurological deficits, animals were sacrificed under anesthesia and samples of brain were taken. The brain slices were prepared as 2.0 mm sections ($n = 12$ –16) and were incubated in a solution of triphenyltetrazolium chloride (TTC, 20 g/L) for 30 minutes at 37°C before being transferred into paraformaldehyde solution (40 g/L) for fixing the infarcted area. The infarct region appeared white or pale while the “normal” tissue appeared red [35, 36]. Pictures were taken of the brain slices with a digital camera and the volume of infarct was analyzed using a computer-assisted image system with ACT-2U software (Nikon). Relative infarct ratio was calculated using the following equation [14, 17, 31]: $(2 * \text{left hemisphere area (non-ischemic side)} - \text{non-infarct area of whole brain slices}) / (2 * \text{left hemisphere areas}) * 100\%$. This equation excludes the factors that could result in an inaccurate calculation of the infarct volume (such as edema).

2.8. Data Analysis. The cerebral blood flow was calculated from PU, CMBC, and velocity measurements. All individual measurements were compared to the baseline values, before MCAO (control level), in each animal. The grouped values were compared between different groups. An average grade of neurological deficits per group was used to make comparisons between groups. Cerebral infarct volume was expressed as a percent fraction of the entire cerebral volume.

All data is presented as mean \pm SD and subjected to statistical analysis. The rate of death was compared using the Chi-square test. All other data was subjected to Analysis of variance (ANOVA), *t*-test, Rank-Sum test, and/or Chi-square test. The changes were considered to be significant if the *P* value was less than 0.05.

3. Results

3.1. Different Effects Induced by EA Starting after the Onset of MCAO versus Post-MCAO. In the group of Ischemia ($n = 45$), with 1 hr MCAO and 24 hr reperfusion, about 18% (8/45) of the rats died within 2–20 hours after the onset of reperfusion. At 24 hours of reperfusion, the living rats displayed serious neurological deficits (Grade 6.0 ± 0.5 , $n = 37$). TTC staining showed that the volume of cerebral infarct was about one third of the whole brain ($32.8\% \pm 3.7\%$, $n = 16$) (Table 1, Figure 1(a)). The infarct areas were mainly localized in the frontoparietal lobes of the cortex and striatum in the right hemisphere (ischemic side, Figure 1(a)).

EA starting at 5 min after the onset of MCAO induced a marked protection against cerebral ischemia, leading to a significant reduction of infarct volume, neurological deficits, and death rate (Table 1, Figures 1(b)–1(d)). EA starting at 5 min after MCAO induced a similar outcome in the ischemic rats (refer to Figure 6). However, it seemed that EA induced a larger reduction of the infarct volume in the former than

TABLE 1: EA period-dependent protection against ischemic injury.

Groups	Neurological deficit	Infarct volume	Death rate
Ischemia	6.0 ± 0.5 (5~7) (<i>n</i> = 37)	32.8% ± 3.7% (<i>n</i> = 16)	18% (8 out of 45)
EA-5 min	5.0 ± 0.5 (4~6) (<i>n</i> = 16) ^{*^}	25.6% ± 5.3% (<i>n</i> = 12) ^{*^}	11% (2 out of 18) ^{***^}
EA-15 min	3.0 ± 0.5 (2~4) (<i>n</i> = 15) ^{***^}	15.4% ± 4.2% (<i>n</i> = 12) ^{***^}	6% (1 out of 16) ^{***^}
EA-30 min	1.0 ± 0.5 (0~2) (<i>n</i> = 28) ^{***^}	4.9% ± 1.2% (<i>n</i> = 12) ^{***^}	7% (2 out of 30) ^{***^}
EA-45 min	7.0 ± 0.0 (~7) (<i>n</i> = 12) [*]	34.3% ± 2.4% (<i>n</i> = 12)	60% (18 out of 30) ^{**}

P* < 0.05 versus Ischemia. *P* < 0.01 versus Ischemia. ^*P* < 0.01 versus EA-45 min. Note that EA significantly reduced the infarct volume, neurological deficit, and death rate and this protective effect became better and better when the length of EA increased from 5 to 30 minutes. However, EA for 45 mins did not improve the neurological deficit and infarct volume and even increased the death rate.

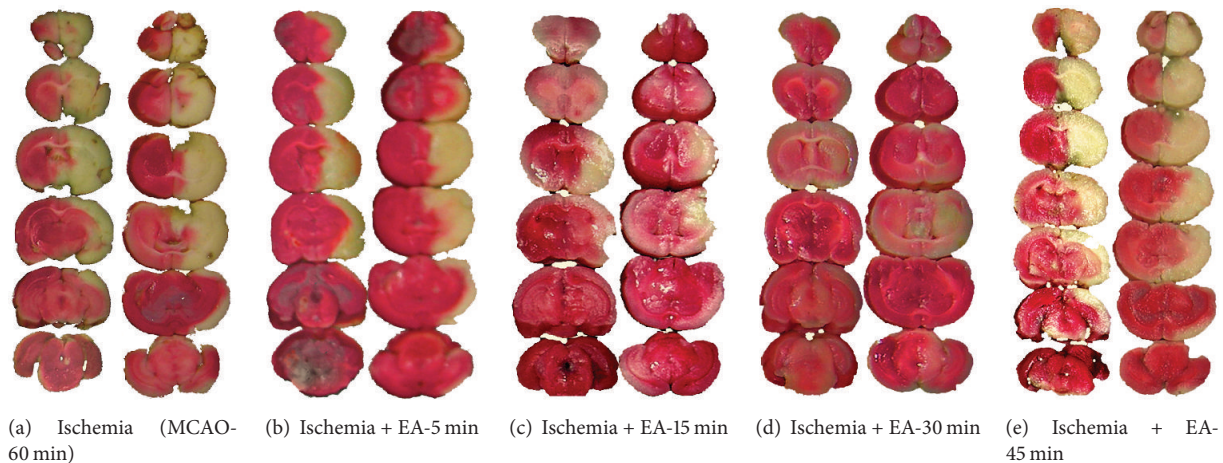


FIGURE 1: EA-induced changes in cerebral infarct size in a time-dependent manner. The brain slices were subjected to TTC staining and the ischemic infarct volume was quantified by a computerized image system. The slices on the *right* of each column show the backside of the *left* slices. Note that the infarct region (pale-white portion) was mainly located in the striatum and the frontoparietal cortex in the right hemisphere. The MCAO-induced infarction (a) was significantly reduced by EA at Du 20 and Du 26 acupoints for 5 min (b), 15 min (c), and 30 min (d). In contrast, EA for 45 min (e) enabled no protection against the cerebral infarction.

the later group. EA after the onset of MCAO reduced the infarct volume by ~85% (Table 1 and Figure 1), while EA after MCAO, by ~45% (refer to Figure 6). These results suggest that early institution of EA stimulation induces better protection against cerebral ischemic injury.

3.2. Increased EA Protection with Increased Periods of the Stimulation from 5 to 30 mins. In the group of MCAO plus EA for 5 min (EA-5 min, *n* = 18), except for 2 rats that died at 5 and 15 hours after the onset of reperfusion (11%, 2/18, *P* < 0.01 versus Ischemia), the degree of average neurological deficits in the living ischemic rats was slightly improved (Grade 5.0 ± 0.5, *n* = 16, *P* < 0.05 versus Ischemia). The infarct volume was slightly reduced (25.6% ± 5.3%, *n* = 12, *P* < 0.05 versus Ischemia) (Table 1 and Figure 1(b)). In the group of MCAO plus EA for 15 min (EA-15 min, *n* = 16), only one rat died at ~3 hours after the onset of reperfusion (6%, 1/16, *P* < 0.01 versus Ischemia), with a greater improvement in average neurological deficits (Grade 3.0 ± 0.5, *n* = 15, *P* < 0.01 versus Ischemia) along with a significant reduction in infarct volume (15.4% ± 4.2%, *n* = 12, *P* < 0.01 versus Ischemia) (Table 1 and Figure 1(c)). In the group of MCAO plus EA for 30 min (EA-30 min, *n* = 30), the neurological

deficits were greatly attenuated (Grade 1.0 ± 0.5, *n* = 28, *P* < 0.01 versus Ischemia) and a significant decrease in death rate (7%, 2/30, *P* < 0.01 versus Ischemia) was noted. The infarct volume was reduced by 85% (4.9% ± 1.2%, *n* = 12, *P* < 0.01 versus Ischemia) (Table 1 and Figure 1(d)). In comparison to the groups of EA for 5 min and EA for 15 min, EA for 30 min induced more beneficial effects in all aspects including neurological deficits, ischemic infarct and death rate (Table 1, Figures 1(b)–1(d)). These results suggest that the EA protection is dependent on an appropriate EA duration.

3.3. Exacerbation of Ischemic Injury by “Over-Length” Stimulation of EA. We investigated to see if the EA protection would be further enhanced by a longer duration of EA stimulation. Therefore, we assigned a few rats to a new group with MCAO plus EA for 45 minutes (EA-45 min, *n* = 30). To our surprise, EA for 45 min significantly increased the mortality in this group of ischemic rats. More than half of the animals in this group (60%, 18/30) died within 0.5 to 10 hours after the onset of reperfusion. All of the dying rats manifested symptoms such as convulsions, tumbling, piloerection, and perspiration (wet feathers) and other abnormalities. When compared the Ischemia group, the death rate increased by 3 folds (60%, 18

out of 30, $P < 0.01$ versus Ischemia) in this group. Although the remaining 12 living rats survived for 24 hours after the reperfusion, they suffered from severe neurological deficits (Grade 7) and were even worse than the group with only Ischemia (Grade 6.0 + 0.5 with range of 5~7, $P < 0.05$). In terms of the infarct volume, EA for 45 min did not reduce the infarct volume at all ($34.3\% \pm 2.4\%$, $n = 12$, $P > 0.05$ versus Ischemia). (Table 1, Figure 1(e)). These results suggest that an increased duration of EA stimulation application further exacerbates the ischemic insult, instead of conferring any protection.

3.4. EA-Induced Increase in Cerebral Blood Flow during MCAO. Using a Laser-Doppler Perfusion Monitor, we continuously monitored the real time changes in cerebral blood flow in all the groups beginning at 5 min prior to MCAO till 15 min after the onset of reperfusion (suture withdrawal), and compared differences in the cerebral blood flow at the pre-MCAO level, during MCAO with/without EA, and early stages of reperfusion between various groups (Figures 2, 3, 4, and 5).

Consistent with our previous studies [14, 17], after the insertion of a nylon suture into the right middle cerebral artery, the blood perfusion (PU) to the monitored cortex immediately decreased by ~85% (i.e., reaching the level at ~15% of the pre-MCAO level). During the entire period of MCAO, the local blood flow was maintained at this low level with a minor fluctuation. CMBC dropped by ~80% of the base-value (i.e., reaching a level at ~20% of the pre-MCAO level) with a slight deceleration of blood cell velocity (reduced by ~25% of the pre-MCAO level). These changes indicated that MCAO induced a greater reduction in the blood volume as compared to the velocity of blood cells (Figures 2(a) and 3–5).

In all the EA groups, EA induced an instant and significant increase in the blood flow of the ischemic brain. The blood flow changed isochronously with the current impulse in response to EA stimulation (Figures 2(b)–2(e) and 3–5). EA induced an increase in PU to ~30% of the control ($P < 0.01$ versus MCAO without EA) (Figure 3) and CMBC to over 65% of the control ($P < 0.01$ versus MCAO without EA) (Figure 4) with a simultaneous decrease in the blood cell velocity to ~55% of the control ($P < 0.05$ versus MCAO without EA) (Figure 5). These results suggest that both “appropriate” and “over” periods of EA stimulation increase the blood flow during MCAO.

3.5. Differential Recovery of the Cerebral Blood Flow after Reperfusion among EA Groups. In the Ischemia group ($n = 30$), following the withdrawal of the nylon suture after 1h MCAO, PU gradually increased to ~25% of the control level (pre-MCAO) ($P < 0.05$ versus during MCAO) and CMBC increased to ~50% of the control ($P < 0.01$ versus during MCAO) with the velocity of blood cells being reduced from ~75% to ~55% ($P < 0.05$, versus during MCAO) in the first 15 minutes after the blood reperfusion (Figures 2(a) and 3–5).

EA changed the pattern of the blood reperfusion. There was, however, a significant difference among different EA

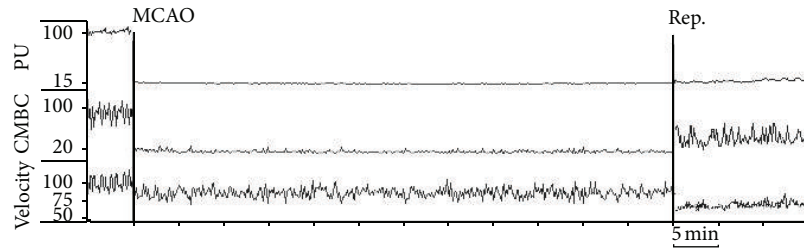
groups, which was evident in the early stage of reperfusion, for instance, during the first 15 minutes after MCAO. In the groups of EA-5 min ($n = 14$), EA-15 min ($n = 12$), and EA-30 min ($n = 30$), blood perfusion (PU) increased to over 90% of the base-value (preischemia) (Figure 3, $P < 0.01$ versus the ischemia group under reperfusion), CMBC recovered to >80% of the preischemia level (Figure 4, $P < 0.01$ versus the ischemia group under reperfusion) and the Velocity increased to >80% of the control level (Figure 5, $P < 0.05$ versus the ischemia group under reperfusion) within 15 minutes after reperfusion.

In sharp contrast, the EA-45 min group ($n = 18$) showed a totally different pattern. For example, PU maintained at a similar level as that during MCAO (~15%), that is, after reperfusion, its level was even lower than those of Ischemia alone (~25%, $P < 0.05$ versus that during reperfusion in the group of Ischemia plus EA for 45 minutes) (Figure 3). Similarly, CMBC still maintained at a low level (~20%) after reperfusion and the level was even lower than that (50%) of the Ischemia group during reperfusion ($P < 0.01$, Figure 4). These findings suggest that EA for 30 minutes or less increases the blood flow during MCAO and promotes the recovery of the blood flow during reperfusion, while an “over-length” (45 min) stimulation, though increasing the blood flow during MCAO, retards the recovery of the blood flow to the brain after MCAO (Figures 2(e) and 3–5).

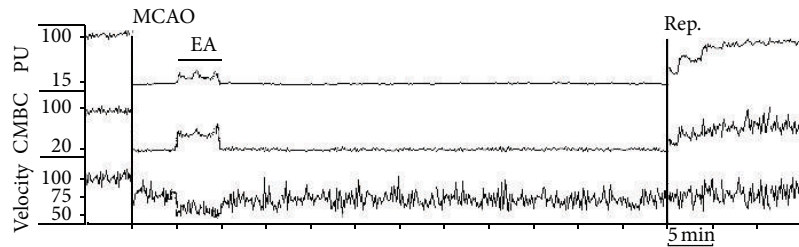
3.6. DOR Antagonist Attenuated EA-Induced Protection against Ischemic Infarction. We previously found that microinjection of DOR antagonist into the lateral cerebral ventricle largely attenuated the EA protection against cerebral ischemic injury [10]. To further reaffirm this observation, we applied Naltrindole to the ischemic rats and determined its effect on the EA-induced neuroprotection. The results showed that in the ischemia group ($n = 7$) the infarct size reduced by ~40% (from $24.8\% \pm 4.1\%$ to $14.7\% \pm 3.4\%$, $P < 0.05$) following treatment with EA beginning immediately after MCAO ($n = 8$). Although Naltrindole (10 mg/kg, i.v.) application did tend to increase the infarct volume, the change was not statistically significant ($30.4\% \pm 4.3\%$, $n = 8$, $P > 0.05$ versus Ischemia alone). However, it completely abolished the EA-induced protection against ischemic infarction ($23.6\% \pm 5.2\%$, $n = 10$, $P > 0.05$ versus Ischemia + EA) (Figure 6). These results indicate that δ -opioid receptor plays a very important role in the EA-induced protection against ischemic injury.

4. Discussion

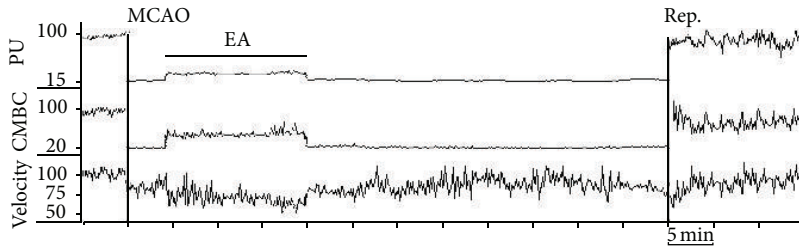
This is the first study to systematically define optimal duration of EA stimulation to induce beneficial effects against ischemic infarction, neurological deficits and mortality. Our results show that EA given for 5–30 minutes significantly reduces ischemic infarct volume and decreases neurological deficits and mortality rate. On the other hand, EA given for 45 min did not show reduction in the neurological deficits or the infarct volume, and rather demonstrated an increase in death rate in this group. However, all groups showed an increase



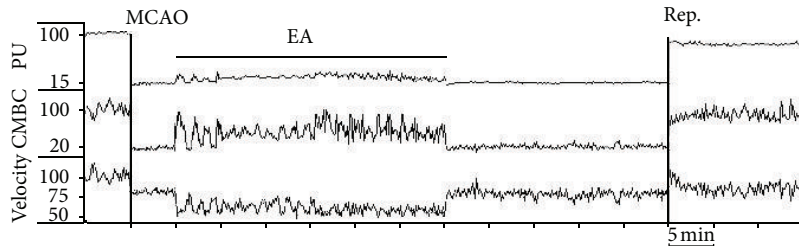
(a) Effect of 60 min MCAO on the blood flow



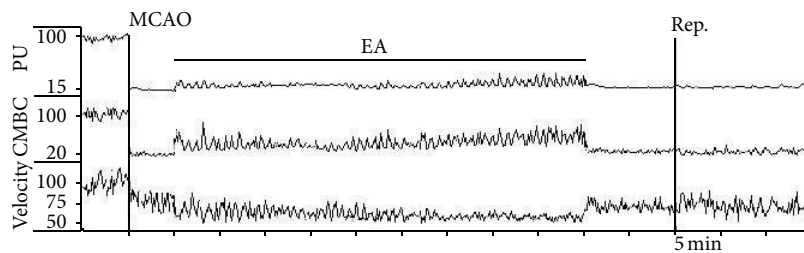
(b) Effect of EA-5 min on the blood flow under ischemia



(c) Effect of EA-15 min on the blood flow under ischemia



(d) Effect of EA-30 min on the blood flow under ischemia



(e) Effect of EA-45 min on the blood flow under ischemia

FIGURE 2: Representative trace recordings of the blood flow in the rats with or without EA. Blood Perfusion (PU), Concentration of Moving Blood Cells (CMBC), and Velocity of Blood Cells (Velocity) were measured in the ischemic rats by a Laser Doppler Perfusion Monitor system. (a) Effect of MCAO-60 min on CBF during ischemia and after reperfusion in Ischemia group. (b) Effect of EA for 5 min at acupoints of Du 20 and Du 26 on CBF. (c) Effect of EA for 15 min on CBF. (d) Effect of EA for 30 min on CBF. (e) Effect of EA for 45 min on CBF. Note that the PU and CMBC decreased immediately after MCAO and the blood flow was maintained at a low level with small fluctuations during the entire period of MCAO with a slight decrease in the velocity. After the onset of reperfusion, PU and CMBC increased with a further decrease in the velocity. EA induced an isochronous increase in PU and CMBC with a decrease in velocity during MCAO. After reperfusion, PU, CMBC, and velocity all increased rapidly and reached the baseline values within 15 min after reperfusion onset in groups of EA for 5–30 min. EA for 45 min, however, induced a greater decrease in PU, CMBC, and velocity than the changes observed in the Ischemia group after reperfusion.

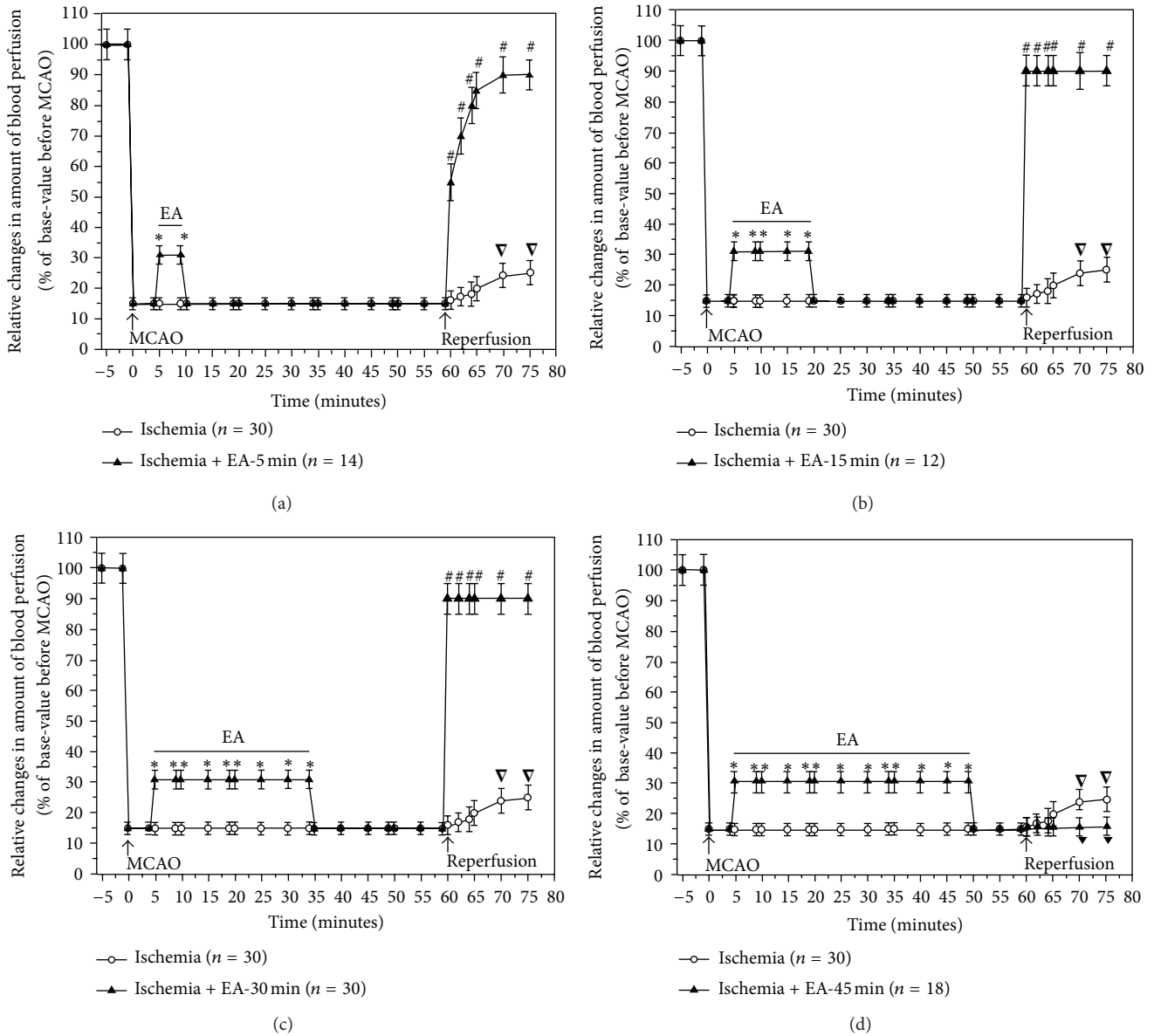


FIGURE 3: Statistical summary of EA effects on PU in the ischemic brain. * $P < 0.01$, Ischemia+EA versus Ischemia group during MCAO; $\nabla P < 0.05$, under reperfusion versus during MCAO in the Ischemia group; # $P < 0.01$, Ischemia + EA versus Ischemia group under reperfusion; $\nabla P < 0.05$, Ischemia + EA versus Ischemia group under reperfusion. Note that MCAO sharply decreased PU to ~15% of the basal value (pre-MCAO), while EA for 5–45 min significantly increased the blood flow to ~30% of the baseline. Within 10–15 minutes after reperfusion, PU gradually increased to ~25% of the baseline (pre-MCAO) in the Ischemia group, whereas it rapidly increased to about 90% of the baseline in the EA for 5–30 minutes groups. In sharp contrast, PU was still at the MCAO level, that is, ~15% of the basal value, during the same period after reperfusion in the group of EA for 45 minutes.

in blood flow after EA stimulation during the period of MCAO. These findings are consistent with our preliminary observations [37] and suggest that the EA protection against ischemic injury is dependent on the length of EA stimulation, and that an “over-length” stimulation can potentially add to the ischemic injury instead of protecting the brain from the injury.

This observation was beyond our expectations. Since the primary cause of ischemic brain injury is insufficient blood supply to the brain, increased blood flow to the brain should

reduce the cerebral ischemic injury. Our previous studies concluded that EA for 30 minutes increases the blood flow during MCAO and reduces ischemic insult to the brain [11, 12, 14, 17]. In extension, we speculated that an extended period of EA stimulation would produce better outcomes. Apparently, this was not the case as we observed opposite results; that is, a prolonged stimulation of EA potentiates, rather than protects against, cerebral damage during ischemic injury to brain. Interestingly, Dr. Wang et al. [38] also observed a similar phenomenon in their studies on EA-induced hypoalgesia in

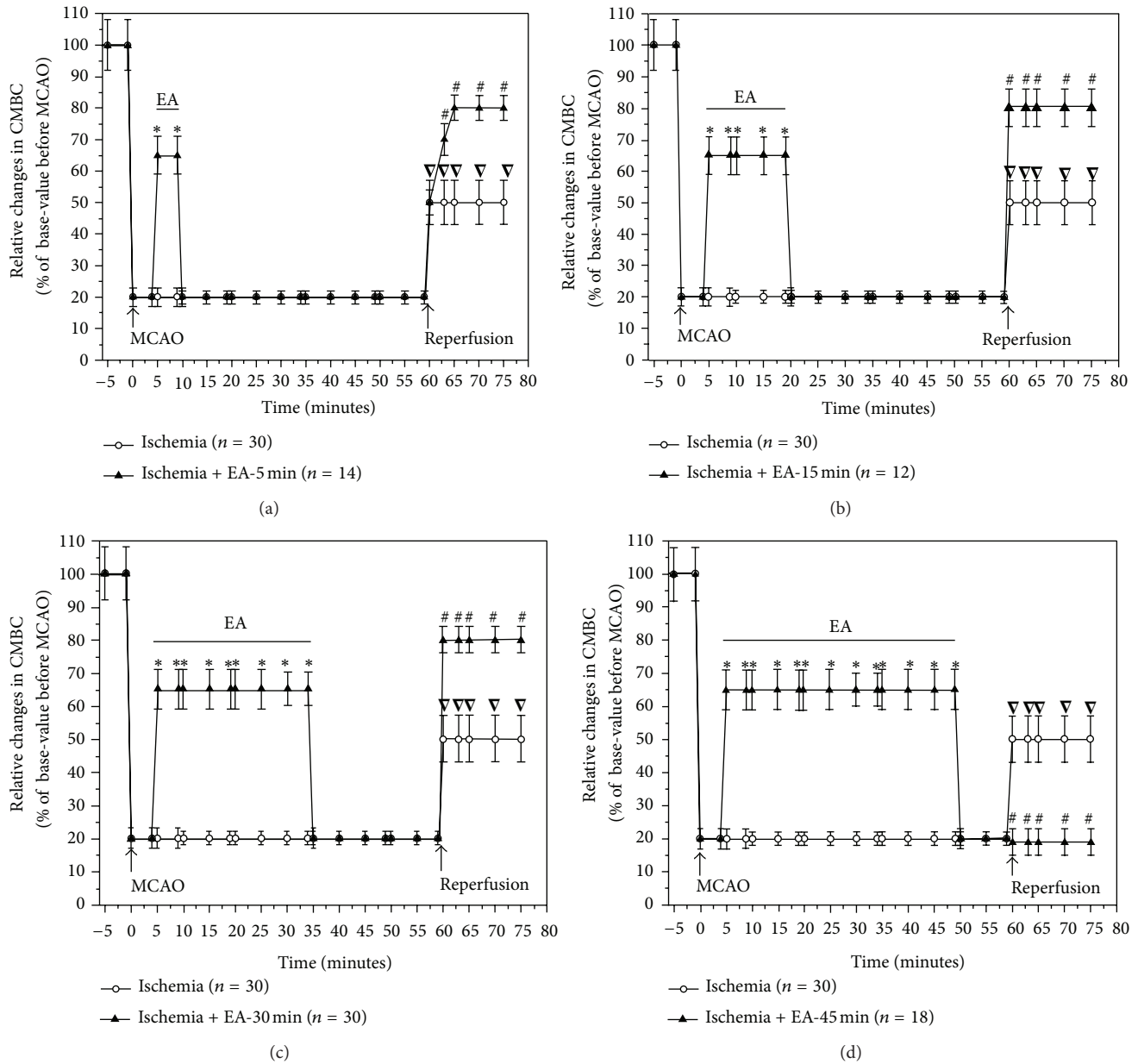


FIGURE 4: Statistical summary of EA effects on concentration of Moving Blood Cells. * $P < 0.01$, Ischemia + EA versus Ischemia group during MCAO; $\nabla P < 0.01$, under reperfusion versus during MCAO in Ischemia group; # $P < 0.01$, Ischemia + EA versus Ischemia group under reperfusion. Note that the MCAO greatly reduced the concentration of Moving Blood Cells (CMBC) to ~20% of the baseline and CMBC quickly increased to ~50% of the baseline after reperfusion. EA for 5–45 minutes significantly increased CMBC during MCAO to ~65% of the baseline. Within 15 minutes after reperfusion, CMBC further increased to ~80% of the baseline in the EA for 5–30 minutes groups, but not in the EA for 45 minutes group with its level being similar to that during MCAO.

healthy volunteers. The subjects were randomized to receive different durations (0 min, 20 min, 30 min, or 40 min) of asynchronous EA stimulations and then subjected to the test of hypoalgesia using a human experimental cold thermal pain threshold model. They found that 30 min of asynchronous EA stimulation resulted in the most significant hypoalgesic effect compared with 0, 20, or 40 min stimulations. Therefore, it seems that a 30 min period is the most optimal duration for EA-induced analgesia and brain protection against ischemic injury.

At present, the mechanism behind this phenomenon is not known. In this work, however, it is noteworthy that EA for 5–30 minutes significantly improves the reperfusion after MCAO and favors quick recovery of blood flow to the pre-ischemic level, in addition to increasing blood flow during MCAO. In sharp contrast, EA for 45 minutes does not promote the recovery of blood flow after MCAO at all, but to the contrary, further worsens it as shown in our present work. This phenomenon partially accounts for the difference in the outcomes between “optimal period” and “over-length” in the

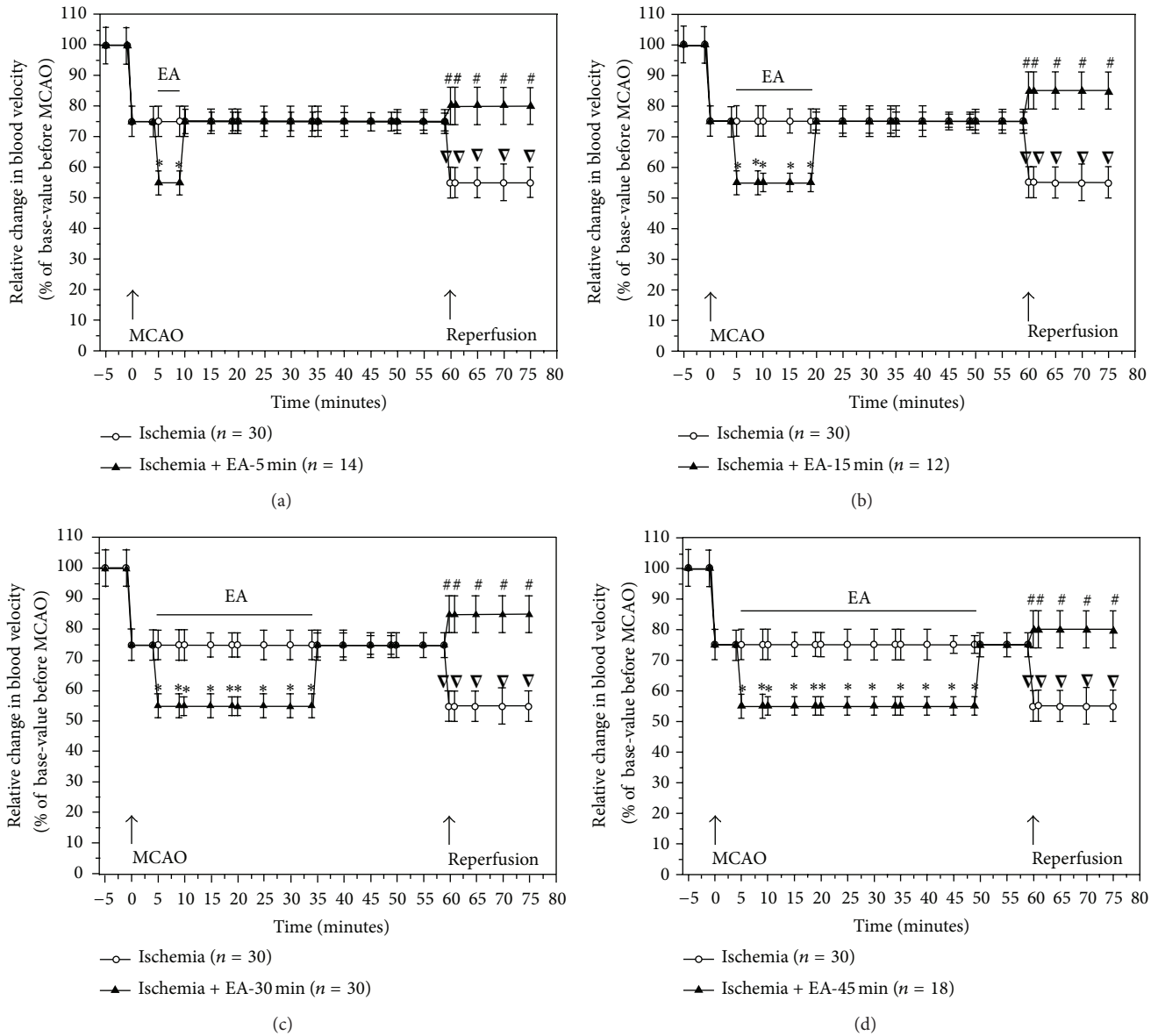


FIGURE 5: Statistical summary of EA effects on the velocity of blood cells. * $P < 0.05$, Ischemia + EA versus Ischemia group during MCAO; $\nabla P < 0.05$, under reperfusion versus during MCAO in Ischemia group; # $P < 0.05$, Ischemia + EA versus Ischemia group under reperfusion. Note that MCAO reduced the velocity of the blood cells to ~75% of the baseline, which was further decreased to ~55% of the baseline after reperfusion. In all EA groups, EA during MCAO immediately decreased the velocity to ~55% of the baseline, and induced a significant increase in it after reperfusion. In contrast to changes in PU and CMBC, the velocity increased to >80% after reperfusion in all EA groups including EA-45 min.

EA treatment although the underlying mechanism remains unknown.

The fact that “over-length” of EA stimulation increases the blood flow under MCAO, but does not lead to any protection against ischemic injury strongly suggests that optimal EA stimulation induces a multi-level regulation in the brain via a complex mechanism. A single factor, such as, an increase in the blood flow under ischemic conditions, may not be enough to induce protection against ischemia. Appropriate stimulation is extremely important for maximal

mobilization of various survival signals and activation of protective pathways in the ischemic brain.

One of these pathways could involve DOR-mediated survival signaling. We have previously demonstrated that DOR is important in inducing neuroprotection [3, 6]. DOR activation attenuates hypoxic, ischemic, or excitatory injury in the neurons and the brain [1, 3, 6]. Evidence shows that both manual acupuncture and EA enhance the activity of the endogenous opioid system, including DOR, in the brain [26–29, 39]. Therefore, the DOR-mediated protection

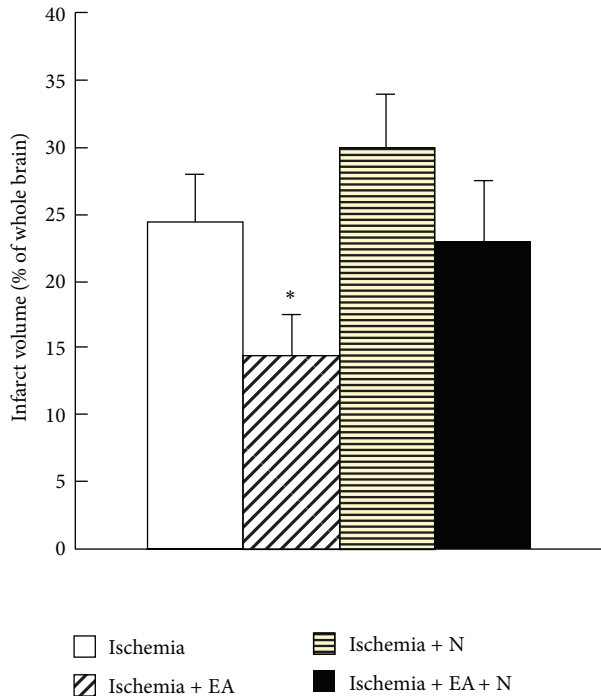


FIGURE 6: Effect of Naltrindole on EA-induced protection against ischemic infarct size. Quantitative volumes of the ischemic infarct were determined based on the percentage of the whole brain volume. Note that the ischemia-induced infarct was reduced by the EA stimulation (* $P < 0.05$ versus ischemia group), which was almost completely reversed after treatment with Naltrindole (N, 10 mg/kg, i.v.) (* $P < 0.05$ versus Ischemia + EA + Naltrindole).

might play a very important role in the EA-induced protection against ischemic injury. Indeed, we first reported that microinjection of a DOR antagonist, Naltrindole, into the cerebral ventricle attenuated the EA-induced cerebral protection against ischemic infarction, suggesting DOR's involvement in the EA-induced protection against brain ischemia [10]. Furthermore, our studies and those of others suggest that EA significantly increases the density of DOR in the ischemic cortex and that DOR signaling could mediate the EA induced neuroprotection against ischemic injury [15, 39, 40]. In the present study, we observed that intravenous injection of Naltrindole almost completely blocked the EA-induced neuroprotection against ischemic injury. All of these observations consistently favor the critical role of DOR in EA-induced neuroprotection against cerebral ischemia. On the other hand, EA can activate additional neurotransmitter systems such as neurotrophic factors in the brain that enable further protection under ischemic conditions [13].

Thus, EA targets multiple mechanisms to achieve a protective effect against ischemic insults, including an increase in the cerebral blood flow under ischemia, an improved recovery of the blood flow after reperfusion, upregulation of the DOR pathway, and other survival signals. An optimal duration of EA stimulation can combine and direct all of these protective pathways against ischemic stress, while an over-stimulation of EA, despite increasing the blood flow

during MCAO, can set this balance of combined protection off.

Moreover, our present results show that EA application during MCAO induces a stronger protection than EA after MCAO, suggesting that an early institution of EA treatment is required to achieve better neuroprotection against ischemic injury. This is similar to the goals of tPA treatment in terms of the importance of the therapeutic window [7, 8]. An early mobilization of protective power may prevent neurons from initiating the process of apoptosis/necrosis in the brain. "Time is brain," which is also true in the case of EA treatment for ischemic brain injury.

In summary, our results suggest early EA treatment with optimal stimulation parameters for an appropriate period is critical to achieve a therapeutic effect for neuroprotection against ischemic insult. The previous controversies in the literature on EA treatment for stroke can be partially attributed to the differences in conditions of the patients and EA parameters. Further in-depth investigations into the "optimal" EA parameters and its underlying mechanisms can help improve clinical outcomes of patients with ischemic/hypoxic injury in the brain.

Acknowledgments

This work was supported by NSFC (30672721, 30873318), NBRP (2009CB522901; 2012CB518502), STCSM (10DZ1975800), NIH (AT-004422 and HD-034852), and Vivian L. Smith Neurologic Foundation.

References

- [1] J. H. Sung, D. M. Chao, and Y. Xia, "Neuronal responses to hypoxia," in *New Frontiers in Neurological Research*, W. Ying and D. Wang, Eds., pp. 73–153, Research Signpost, Kerala, India, 2008.
- [2] Y. Luo, "Cell-based therapy for stroke," *Journal of Neural Transmission*, vol. 118, no. 1, pp. 61–74, 2011.
- [3] D. Chao and Y. Xia, "Tonic storm in hypoxic/ischemic stress: can opioid receptors subside it?" *Progress in Neurobiology*, vol. 90, no. 4, pp. 439–470, 2010.
- [4] K. Arai, J. Lok, S. Guo, K. Hayakawa, C. Xing, and E. H. Lo, "Cellular mechanisms of neurovascular damage and repair after stroke," *Journal of Child Neurology*, vol. 26, pp. 1193–1198, 2011.
- [5] J. H. Zhang, J. Badaut, J. Tang, A. Obenaus, R. Hartman, and W. J. Pearce, "The vascular neural network- a new paradigm in stroke pathophysiology," *Nature Review/Neurology*, vol. 8, no. 12, pp. 711–716, 2012.
- [6] X. Z. He, H. K. Sandhu, Y. L. Yang et al., "Neuroprotection against hypoxia/ischemia: delta-opioid receptor-mediated cellular/molecular events," *Cellular and Molecular Life Sciences*, 2012.
- [7] R. J. Thurman, E. C. Jauch, P. D. Panagos, M. R. Reynolds, and J. Mocco, "Four evolving strategies in the emergent treatment of acute ischemic stroke," *Emergency Medicine Practice*, vol. 14, no. 7, pp. 1–27, 2012.
- [8] K. A. Weant and S. N. Baker, "New windows, same old house: an update on acute stroke management," *Advanced Emergency Nursing Journal*, vol. 34, pp. 112–121, 2012.

- [9] M. Mazighi, E. Meseguer, J. Labreuche, and P. Amarenco, "Bridging therapy in acute ischemic stroke: a systematic review and meta-analysis," *Stroke*, vol. 43, pp. 1302–1308, 2012.
- [10] P. Zhao, J. Guo, S. S. Hong, A. Bazyz-Asaad, J. S. Cheng, and Y. Xia, "Electro-acupuncture and brain protection from cerebral ischemia: the role of delta-opioid receptor," *SfN Abstract*, Program no. 490.13, 2002.
- [11] F. Zhou, J. C. Guo, J. S. Cheng, G. C. Wu, and Y. Xia, "Electro-acupuncture induced protection from cerebral ischemia is dependent on stimulation intensity, and frequency," in *Proceedings of the 3rd Cell Stress Society International Congress on Stress Responses in Biology and Medicine and 2nd World Conference of Stress*, vol. 3, p. 250, Budapest, Hungary, 2007.
- [12] F. Zhou, J. C. Guo, J. S. Cheng, G. C. Wu, and Y. Xia, "Electro-acupuncture and brain protection from cerebral ischemia: differential roles of acupoints," in *Proceedings of the 3rd Cell Stress Society International Congress on Stress Responses in Biology and Medicine and 2nd World Conference of Stress*, vol. 3, p. 249, Budapest, Hungary, 2007.
- [13] J. C. Guo, J. S. Cheng, and Y. Xia, "Acupuncture therapy for stroke," in *Acupuncture Therapy For Neurological Diseases: A Neurobiological View*, Y. Xia, X. Cao, G.-C. Wu, and J. Cheng, Eds., pp. 226–262, Springer-Tsinghua Press, Beijing, China; Heidelberg, Germany; London, UK; and New York, USA, 2010.
- [14] F. Zhou, J. C. Guo, J. S. Cheng, G. C. Wu, and Y. Xia, "Electroacupuncture increased cerebral blood flow and reduced ischemic brain injury: dependence on stimulation intensity and frequency," *Journal of Applied Physiology*, vol. 111, pp. 1877–1887, 2011.
- [15] X. Li, P. Luo, Q. Wang, and L. Z. Xiong, "Electroacupuncture pretreatment as a novel avenue to protect brain against Ischemia and reperfusion injury," *Evidence-Based Complementary and Alternative Medicine*, vol. 2012, Article ID 195397, 12 pages, 2012.
- [16] M. Xu, L. Ge, and D. Zhao, "Electro-acupuncture regulation of central monoamine neurotransmitters in Ischaemia-reperfusion," in *Current Research in Acupuncture*, Y. Xia, G. Ding, and G. C. Wu, Eds., pp. 401–430, Springer, New York, USA; Heidelberg, Germany; Dordrecht, The Netherlands; and London, UK, 2012.
- [17] F. Zhou, J. C. Guo, J. S. Cheng, G. C. Wu, J. Sun, and Y. Xia, "Electroacupuncture and brain protection against cerebral ischemia: specific effects of acupoints," *Evidence-Based Complementary and Alternative Medicine*, vol. 2013, Article ID 804397, 2013.
- [18] V. Hopwood and G. T. Lewith, "Does acupuncture help stroke patients become more independent?" *Journal of Alternative and Complementary Medicine*, vol. 11, no. 1, pp. 175–177, 2005.
- [19] M. H. Rabadi, "Randomized clinical stroke rehabilitation trials in 2005," *Neurochemical Research*, vol. 32, no. 4-5, pp. 807–821, 2007.
- [20] Z. X. Yang and X. M. Shi, "Systematic evaluation of the therapeutic effect and safety of Xingnao Kaiqiao needling method in treatment of stroke," *Zhongguo Zhen Jiu*, vol. 27, no. 8, pp. 601–608, 2007.
- [21] P. Wu, E. Mills, D. Moher, and D. Seely, "Acupuncture in poststroke rehabilitation: a systematic review and meta-analysis of randomized trials," *Stroke*, vol. 41, no. 4, pp. e171–e179, 2010.
- [22] M. Liu, "Acupuncture for stroke in China: needing more high-quality evidence," *International Journal of Stroke*, vol. 1, no. 1, pp. 34–35, 2006.
- [23] Y. Xie, L. Wang, J. He, and T. Wu, "Acupuncture for dysphagia in acute stroke," *Cochrane Database of Systematic Reviews*, vol. 16, no. 3, Article ID CD006076, 2008.
- [24] X. F. Zhao, Y. Du, P. G. Liu, and S. Wang, "Acupuncture for stroke: evidence of effectiveness, safety, and cost from systematic reviews," *Topics in Stroke Rehabilitation*, vol. 19, pp. 226–233, 2012.
- [25] F. Zhou, D. K. Huang, and Y. Xia, "Neuroanatomic basis of acupuncture points," in *Acupuncture Therapy For Neurological Diseases: A Neurobiological View*, Y. Xia, X. Cao, G.-C. Wu, and J. Cheng, Eds., pp. 32–80, Springer-Tsinghua Press, Beijing, China; Heidelberg, Germany; London, UK; and New York, USA, 2010.
- [26] G. Q. Wen, Y. L. Yang, Y. Lu, and Y. Xia, "Acupuncture-induced activation of endogenous opioid system," in *Acupuncture Therapy For Neurological Diseases: A Neurobiological View*, Y. Xia, X. Cao, G.-C. Wu, and J. Cheng, Eds., pp. 104–119, Springer-Tsinghua Press, Beijing, China; Heidelberg, Germany; London, UK; and New York, USA, 2010.
- [27] G. Q. Wen, X. Z. He, Y. Lu, Y. Xia, and Y. Xia, "Effect of acupuncture on neurotransmitters/ modulators," in *Acupuncture Therapy For Neurological Diseases: A Neurobiological View*, Y. Xia, X. Cao, G.-C. Wu, and J. Cheng, Eds., pp. 120–142, Springer-Tsinghua Press, Beijing, China; Heidelberg, Germany; London, UK; and New York, USA, 2010.
- [28] J. F. Liang and Y. Xia, "Acupuncture modulation of central neurotransmitters," in *Current Research in Acupuncture*, Y. Xia, G. Ding, and G. C. Wu, Eds., pp. 1–36, Springer, New York, USA; Heidelberg, Germany; Dordrecht, The Netherlands; and London, UK, 2012.
- [29] Y. Xia, X. D. Cao, G. C. Wu, and J. S. Cheng, "Acupuncture therapy for stroke," in *Acupuncture Therapy For Neurological Diseases: A Neurobiological View*, Y. Xia, X. Cao, G.-C. Wu, and J. Cheng, Eds., pp. 1–480, Springer-Tsinghua Press, Beijing, China; Heidelberg, Germany; London, UK; and New York, USA, 2010.
- [30] Y. Xia, G. H. Ding, and G. C. Wu, *Current Research in Acupuncture*, Springer, New York, USA; Heidelberg, Germany; Dordrecht, The Netherlands; and London, UK, 2012.
- [31] Y. Nishimura, T. Ito, and J. M. Saavedra, "Angiotensin II AT1 blockade normalizes cerebrovascular autoregulation and reduces cerebral ischemia in spontaneously hypertensive rats," *Stroke*, vol. 31, no. 10, pp. 2478–2486, 2000.
- [32] E. Z. Longa, P. R. Weinstein, S. Carlson, and R. Cummins, "Reversible middle cerebral artery occlusion without craniectomy in rats," *Stroke*, vol. 20, no. 1, pp. 84–91, 1989.
- [33] WHO Regional Office for the Western Pacific, *Standardized Nomenclature for Acupuncture*, World Health Organization, Manila, Philippines, 1993.
- [34] WHO Regional Office for the Western Pacific, *WHO Standard Acupuncture Point Locations in the Western Pacific Region*, World Health Organization, Manila, Philippines, 2008.
- [35] J. B. Bederson, L. H. Pitts, and S. M. Germano, "Evaluation of 2,3,5-triphenyltetrazolium chloride as a stain for detection and quantification of experimental cerebral infarction in rats," *Stroke*, vol. 17, no. 6, pp. 1304–1308, 1986.
- [36] R. A. Swanson, M. T. Morton, and G. Tsao-Wu, "Semiautomated method for measuring brain infarct volume," *Journal of Cerebral Blood Flow & Metabolism*, vol. 10, pp. 290–295, 1990.
- [37] F. Zhou, J. C. Guo, R. Yang, J. S. Cheng, G. C. Wu, and Y. Xia, "Electro-acupuncture increases cerebral blood flow and protects the rat brain from ischemic injury," in *Proceedings of the 3rd Cell Stress Society International Congress on Stress Responses in Biology and Medicine and 2nd World Conference of Stress*, vol. 3, pp. 249–250, Budapest, Hungary, 2007.
- [38] S. M. Wang, E. C. Lin, I. Maranets, and Z. N. Kain, "The impact of asynchronous electroacupuncture stimulation duration on cold thermal pain threshold," *Anesthesia and Analgesia*, vol. 109, no. 3, pp. 932–935, 2009.

- [39] X. S. Tian, F. Zhou, R. Yang, Y. Xia, G. C. Wu, and J. C. Guo, "Electroacupuncture protects the brain against acute ischemic injury via up-regulation of delta-opioid receptor in rats," *Journal of Chinese Integrative Medicine*, vol. 6, no. 6, pp. 632–638, 2008.
- [40] L. Z. Xiong, J. Yang, Q. Wang, and Z. H. Lu, "Involvement of δ -and μ -opioid receptors in the delayed cerebral ischemic tolerance induced by repeated electroacupuncture preconditioning in rats," *Chinese Medical Journal*, vol. 120, no. 5, pp. 394–399, 2007.

Review Article

Understanding Central Mechanisms of Acupuncture Analgesia Using Dynamic Quantitative Sensory Testing: A Review

Jiang-Ti Kong,¹ Rosa N. Schnyer,² Kevin A. Johnson,¹ and Sean Mackey¹

¹Stanford Systems Neuroscience & Pain Laboratory, Department of Anesthesiology, Division of Pain Medicine, School of Medicine, Stanford University, 1070 Arastradero Road, Suite 200, Palo Alto, CA 94304, USA

²School of Nursing, The University of Texas at Austin, Austin, TX 78701, USA

Correspondence should be addressed to Jiang-Ti Kong; calypso1@stanford.edu

Received 24 November 2012; Revised 17 March 2013; Accepted 29 March 2013

Academic Editor: Di Zhang

Copyright © 2013 Jiang-Ti Kong et al. This is an open access article distributed under the Creative Commons Attribution License, which permits unrestricted use, distribution, and reproduction in any medium, provided the original work is properly cited.

We discuss the emerging translational tools for the study of acupuncture analgesia with a focus on psychophysical methods. The gap between animal mechanistic studies and human clinical trials of acupuncture analgesia calls for effective translational tools that bridge neurophysiological data with meaningful clinical outcomes. Temporal summation (TS) and conditioned pain modulation (CPM) are two promising tools yet to be widely utilized. These psychophysical measures capture the state of the ascending facilitation and the descending inhibition of nociceptive transmission, respectively. We review the basic concepts and current methodologies underlying these measures in clinical pain research, and illustrate their application to research on acupuncture analgesia. Finally, we highlight the strengths and limitations of these research methods and make recommendations on future directions. The appropriate addition of TS and CPM to our current research armamentarium will facilitate our efforts to elucidate the central analgesic mechanisms of acupuncture in clinical populations.

1. Overview of Research on Acupuncture Analgesia

The treatment of chronic pain is the most well-known clinical application of acupuncture in the west [1, 2]. Acupuncture originated in China more than 2000 years ago and has gained popularity in America since the landmark NIH Consensus Conference in 1997 [3]. Despite broad use, there continues to be ambiguity regarding the efficacy and mechanisms of acupuncture as an analgesic modality. Discrepancies between the results of basic science experiments and clinical trials of acupuncture underscore the controversy surrounding its therapeutic value. The purpose of this review is to outline emerging translational clinical research methods for assessing the central mechanisms of acupuncture analgesia in humans. We begin by summarizing our current understanding of the analgesic mechanisms of acupuncture based on animal and human clinical studies.

1.1. Animal Studies. Animal studies have identified many potential biochemical and neuroanatomical substrates of acupuncture analgesia. Wang et al. [4, 5], Zhao [6], and Han [7, 8] have published excellent comprehensive reviews of these studies. From a biochemical standpoint, it appears that acupuncture may alter the metabolism of substrates involved in both the ascending facilitatory pathways (N-methyl-D-aspartate receptors [9], substance P [10], and interleukin-1 [11]) and the descending inhibitory pain pathways (endogenous opioids [7], serotonin [12], and norepinephrine [13]). From a neuroanatomical standpoint, several central nervous system structures are reported to mediate acupuncture analgesia, including the periaqueductal gray, the nucleus raphe magnus, the locus ceruleus, the arcuate nucleus, the amygdala, and the nucleus accumbens [4, 6]. It is important to note the link between the biochemical and anatomical substrates. For example, low-frequency electroacupuncture triggers the release of enkephalins and endorphins in the periaqueductal

gray, the arcuate nucleus, and the caudate nucleus [14]. These structures then send projections to the spinal dorsal horn via the dorsal lateral funiculi [15]. Increases in serotonin release at the nucleus raphe magnus and norepinephrine release in the locus ceruleus are also crucial to analgesia induced by electroacupuncture [13].

In addition to the classic neurotransmitters and anatomical pathways involved in central pain processing, other mechanisms also contribute to acupuncture analgesia [6], including the hypothalamus-pituitary-adrenal axis (regulating peripheral inflammatory response to pain) [16], the autonomic nervous system (regulating local circulation) [17, 18], and the glial system [19] (contributing to inflammation around spinal and cerebral neural pathways).

1.2. Human Studies. Although animal studies can provide insight into acupuncture's mechanism of action, establishing the efficacy of acupuncture for treating chronic pain in humans is challenging, owing to the variability of study methods and outcomes [20]. However, an increasing body of robust and rigorous evidence indicates that acupuncture may be an effective intervention for the management of chronic pain [21–23]. Researchers from the Acupuncture Trialists' Collaboration, a group, which was established to synthesize data from high-quality randomized trials on acupuncture for chronic pain, recently published a meta-analysis of 29 clinical trials involving 17,922 patients [23]. The analysis showed that acupuncture consistently yielded greater pain reduction as compared with controls in back and neck pain, arthritis, and headaches. When sham acupuncture was used as the control, the differences were modest but remained statistically significant. Larger differences were seen when standard care (which typically included oral medications and regular physician and physical therapy visits) was used as the control [23].

These results indicate that both specific (i.e., site of needling and stimulation techniques) and nonspecific (i.e., context effects, expectations, etc.) components can contribute to acupuncture's therapeutic effect in treating chronic pain. Understanding the possible mechanisms of these effects in chronic pain remains crucial in elucidating the potential therapeutic value of acupuncture in chronic pain.

1.3. Need for Translational Studies Bridging Mechanisms Observed in Animals to Clinical Populations. Animal studies are of limited benefit in fully modeling the human experience of acupuncture and of chronic pain, and the research methods used in clinical trials provide only a limited understanding of acupuncture's mechanism of action in humans. This gap between animal mechanistic studies and human clinical trials remains one of the greatest challenges in acupuncture research today. The white paper published by the Society of Acupuncture Research (SAR) acknowledged this challenge and proposed goals for future studies [24]. One of the key recommendations was the development of biomarkers that can provide meaningful correlations between physiological effects measured in animal studies and patient-reported outcomes in clinical trials.

To this end, we discuss the emerging translational research methods for assessing the central mechanisms of action of acupuncture analgesia in humans. As background, we first review the basic mechanisms of the central nervous system involved in nociception and human pain perception. Next, we focus the review on two research approaches that likely will emerge as valuable tools for understanding pain processing in acupuncture: temporal summation and conditioned pain modulation. We describe the physiologic mechanism, methodology, and applications of these methods in pain research. Then, we examine the current application of temporal summation and conditioned pain modulation to acupuncture research and make recommendations on future directions.

2. Nociceptive Pathways and Neural Processing

2.1. Nociceptive Pathways. Five major components are involved in the perception of pain: (1) the primary peripheral nociceptors; (2) the spinal secondary neurons; (3) the relay neurons (such as those in the thalamus); (4) cortical and subcortical networks responsible for sensory, emotional, and cognitive integration of pain (e.g., the primary sensory cortex, insula, prefrontal cortex, and anterior cingulate cortex); (5) the descending modulatory neurons that originate in subcortical structures (e.g., the periaqueductal grey and locus ceruleus) and project back to the spinal dorsal horn neurons for descending pain processing [25–27].

2.2. Central Nociceptive Processing. Modulation of nociceptive signals occurs beyond the peripheral nociceptors in the central nervous system. This modulation includes processes at the spinal cord and at subcortical and cortical brain structures (components 2, 3, 4, and 5 from above).

First, much of the central nociceptive processing occurs in the spinal dorsal horn [25, 27]. At least two types of spinal secondary neurons are found in the dorsal horn: the nociceptive-specific (NS) neurons and wide dynamic range (WDR) neurons. The WDR neurons are capable of windup, wherein repetitive noxious stimulation with frequencies above 0.3 Hz (the natural frequency of the WDR neurons) leads to amplification in output of the WDR neurons [28]. Such increased wind-up is implicated in a variety of chronic pain conditions [27, 29, 30].

The output of the spinal secondary neurons is dependent on ascending input from the peripheral nociceptors, and it is also modulated by spinal interneurons and descending projections from supraspinal centers. The dynamic balance of these three sources of influence determines the final output from the spinal secondary neurons, which project upward to the relay centers and ultimately to the cerebral cortex for pain perception. This complex interaction of ascending and descending influence on the spinal transmission of pain, commonly referred to as the gate control theory, was originally discovered by Melzack and Wall [31] and has since been validated by many [32, 33].

TABLE 1: Overview of TS and CPM.

	TS	CPM
Experimental construct	Repeats of brief noxious stimuli	A test stimulus measured before and after a conditioning stimulus
Typical magnitudes in healthy subjects	10–20 in a 0–100 visual analog scale (VAS) [42]	~29% reduction in pain rating [43]
Underlying CNS physiology	Windup: increased spinal WDR output due to repetitive C-fiber stimulation at >0.3 Hz	DNIC: global reduction of WDR sensitivity due to a single, heterotopic, noxious stimulation
Pain-processing pathways involved	Ascending facilitation of nociceptive input	Descending inhibition of nociceptive input
Augmenting factors	Advanced age [44], female sex [45, 46], pain catastrophizing [46–49], anxiety, fear of pain, and location (trunk > extremities) [50]	Advanced age [44, 51, 52], female sex (mixed results [43, 45, 53]), pain catastrophizing [54, 55], poor sleep [56, 57], depression [58], and opioid use [59]
Reducing factors		

Second, equally important site of central pain processing occurs in the brain via the complex interaction between the cortex and subcortical nuclei [26, 34–36]. The brain is considered crucial for translating nociceptive signals into the conscious perception of pain. Nociceptive signals are relayed from the thalamus to primary and secondary somatosensory regions, and subsequent brain regions are linked to visceral sensation (i.e., insula), emotion (i.e., limbic system), attention (i.e., anterior cingulate), and cognition (i.e., prefrontal cortex). The brain also exerts descending modulation on nociceptive processing via subcortical structures such as the periaqueductal gray (PAG), the rostroventral medulla (RVM), the hypothalamus, the parabrachial nucleus, and the nucleus tractus solitarius. Complex reciprocal interactions exist between the subcortical and cortical centers of pain processing. Eventually, the descending fibers travel in the dorsal lateral funiculus to reach secondary and inter neurons in the spinal dorsal horn [25].

3. Dynamic Quantitative Sensory Testing

Quantitative sensory testing (QST), also known as psychophysical testing, refers to tests of sensory perception during the administration of stimuli with predetermined physical properties and following specific protocols [37]. These tests are generally safe and noninvasive for use in human studies, and neuroscience research links these tests to biological underpinnings. Backonja, Arendt-Nielsen, and Pfau [37–39] have published in-depth reviews of quantitative sensory testing.

QST can be subdivided into static QST and dynamic QST [38, 39]. Static QST typically refers to the measurement of the threshold that primarily reflects states of the peripheral nervous system. Conversely, dynamic QST involves agitation of the pain-perceiving system in a way that exposes a certain mechanism of pain processing beyond the peripheral nervous system. Two extensively studied dynamic paradigms are temporal summation (TS) and conditioned pain modulation (CPM), which represent the ascending facilitatory and

descending inhibitory aspects of central pain processing, respectively [38]. Table 1 summarizes the basic concept and characteristics of TS and CPM.

3.1. Temporal Summation. Temporal summation (TS) refers to the increased perception of pain in response to repetitive noxious stimuli delivered at frequencies above 0.3 Hz [40, 41]. It is often called “windup pain,” or “temporal summation of second pain.”

3.1.1. Animal Studies and Molecular Mechanisms. Temporal summation is the behavioral correlate of “windup” of spinal wide dynamic range (WDR) neurons at the dorsal horn [28, 75]. In animal studies, researchers made single-fiber recordings from the periphery C fibers and their destined secondary neurons in the spinal dorsal horn. With successive C-fiber activations (by either noxious heat or noxious electrical stimulation) at frequencies over 0.3 pulses per second, WDR neurons displayed increased frequency and amplitude of discharges [75]. These physiologic changes were correlated to behavioral experiments in humans under the same exact stimulation paradigm: they rated the pain with increasing intensity [28]. Thus, TS QST is thought to represent ascending spinal windup of pain processing.

3.1.2. Increase of TS in Chronic Pain and Risk Factors. TS is elevated in a wide variety of pain syndromes, ranging from those that cause idiopathic total body pain (e.g., fibromyalgia [76]) to those considered driven entirely by peripheral factors (e.g., knee arthritis [77]). Increasing evidence suggests that abnormally augmented TS is at least partially responsible for the development of these chronic pain conditions [27]. Furthermore, researchers have identified important risk factors (Table 1) that increase TS, including older age [44], female sex [45, 46], psychological factors (anxiety [50], fear [50], and catastrophizing [46–49]), and location of test (the back exhibits higher TS than the upper or lower extremities [50]).

TABLE 2: Common methods used to generate and compute TS.

Type of stimulus	Experimental paradigms	Variables used to quantify TS
Heat pulses	10–20 heat pulses (0.5–0.75 s each) delivered at 0.3–0.5 Hz either via a continuous contact thermode [44] or intermittent contact probe [60]	TS magnitude: the difference in pain ratings between first and last, or first and most painful pulse, slope of the first few pulses, or the magnitude of 5th pulse [42, 61] Electrical pain threshold (EP-T): intensity at which the subject begins to feel pain at the 4th or 5th pulse [62, 63], or nociceptive withdrawal reflex threshold (NWR-T), the intensity at which limb flexion occurs [64] in response to the electrical stimulation
Electrical stimulation	A single stimulus of a train of five 1-ms pulses at 200 Hz, repeated 5 times at 2 or 3 Hz [62, 63]	
Pin prick	10 stimuli of 56 or 128 mN are delivered, and pain ratings for all ten stimuli averaged versus that of a single stimulus are obtained [65]	Windup ratio: pain of train of 10 pricks delivered at 1 Hz over pain of a single prick [65]
Pressure	Ten 1-s pressure stimuli delivered by an algometer with 1 s between pulses [66, 67]	TS magnitude: difference in pain rating between the first and 10th stimuli [66, 67]

3.1.3. Methodology for Measurement. Although TS is likely a powerful tool for pain research, the lack of a single, standardized, broadly accepted protocol remains a challenge when interpreting previous work and planning future studies. A variety of noxious stimuli can be used to generate TS, including heat, pin pricks, and electrical stimulation [78]. Although there is no consensus on the quantification of TS [79], 5–20 brief repetitions of identical noxious stimuli are typically given, and the research participant is often asked to rate the changing pain sensation after one or several of the stimuli. Table 2 outlines examples of several commonly used experimental protocols to generate and compute TS.

For heat paradigms, the difference in the pain score between the first and most painful pulse, the slope of pain increase, or even the raw pain score from the fifth pulse can be used to calculate the magnitude of TS [42, 61, 79]. When pin pricks are used as the noxious stimuli, the German Research Network on Neuropathic Pain [65] recommends a standard protocol where either 128 or 56 mN pin tips are applied as a single stimulus and as a series of 10 stimuli given at 1 Hz. The participant is asked to give a single pain rating for the single stimulus and then an average rating for the 10 stimuli repeated at 1 Hz. The ratio of average pain rating of the 10 consecutive stimuli to the rating of the single stimulus is defined as TS or, alternatively, as the windup ratio.

3.1.4. Temporal Summation in Acupuncture Studies. The application of TS to acupuncture research in humans is limited despite the fact that the results of several animal studies indicate that acupuncture produces strong, central modulatory effects and that TS reflects the state of central pain facilitation. Currently, only two clinical studies have been performed involving TS in acupuncture.

In the first study, Zheng et al. [63] randomized 36 healthy volunteers to blindly receiving 25 minutes of electroacupuncture, manual acupuncture, and nonpenetrating sham acupuncture in one leg. The TS threshold for trains of electrical stimulation was assessed before, immediately after, and 24 hours after the treatments on the ipsilateral leg,

contralateral leg, and contralateral arm. The results demonstrated that electroacupuncture increased the TS threshold (i.e., reduced TS) in the ipsilateral and contralateral leg up to 24 hours after the treatment. In contrast, manual acupuncture produced no significant change in the TS threshold, although it showed a trend of increase as compared with sham acupuncture. The increase in TS threshold was the greatest in the ipsilateral leg, followed by the contralateral leg; the least change was seen in the contralateral arm, suggesting segmental specificity of the acupuncture interventions. This is one of the very few studies demonstrating that different forms of needle manipulation produced differences in human pain perception linked to a mechanism of central pain processing. Finally, this study demonstrated peripheral influences of acupuncture, as electroacupuncture augmented not only the TS threshold but also the pain detection threshold to single-pulse electrical stimulation.

In the second study, by Tობbackx et al. [80], 39 patients with chronic neck pain due to whiplash injury underwent one session of manual acupuncture (20 minutes) and one session of relaxation therapy (length not specified) in random order with a 1-week between-session washout period. The primary outcomes assessed were pressure pain sensitivity to an analogue algometer and TS scores to 10 consecutive applications of pressure stimuli using the same algometer at a pressure above the pain threshold. The study found that acupuncture caused a greater reduction of the pressure pain threshold as compared with relaxation therapy but produced no change in the TS scores. The authors concluded that in patients with chronic pain, acupuncture does not affect central pain processing.

The inconsistency in the methods used as well as the limited results from these two studies underscore the need for future studies to help further elucidate the role of acupuncture in central pain processing in human subjects. Specifically, both Zheng and Tობbackx demonstrated that after a single session, manual acupuncture did not result in a significant change in TS. However, Zheng was able to demonstrate a significant decrease in TS after electroacupuncture (Tობbackx only studied manual acupuncture). These results suggest that

electroacupuncture may exert a stronger influence on TS than manual acupuncture. Future studies should be conducted to compare electroacupuncture with manual acupuncture in larger cohorts of patients with chronic pain.

It is also important to note that these studies involved only one acupuncture session. In acupuncture practice, a single session is rarely considered sufficient to produce clinically significant effects for the treatment of chronic pain. Therefore, when translating the results of studies of animal models and healthy human subjects to the clinical pain population, multiple acupuncture sessions with treatment frequency of at least once a week should be considered.

We also recommend performing quantitative sensory testing at multiple anatomical sites adjacent to and at a distance from the site treated for pain. Zheng et al. demonstrated a stronger effect of acupuncture in homotopic versus heterotopic sites, while Tobbackx collected data only on the arm, distal to the neck where the pain and the majority of the needling were located.

Last but not least, there is a need to distinguish the peripheral and central components of acupuncture analgesia. Specifically, Zheng demonstrated increase in the threshold to both temporal summation and to single-pulse protocols, suggesting acupuncture's involvement in both central and peripheral nociceptive modulation. The authors further suggest that a mechanism independent of NMDA blockade, such as peripheral opioid receptor activation [81], may play a role. To test this hypothesis, selective blockade of NMDA and μ -opioid receptors should be used. Furthermore, additional biomarkers of central (e.g., secondary hyperalgesia to capsaicin [82]) and peripheral pain processing (pressure and heat pain threshold [38]) may also be used to profile the pain modulatory mechanisms of acupuncture.

3.2. Conditioned Pain Modulation. Conditioned pain modulation (CPM) refers to the phenomenon whereby a noxious stimulus at one body part results in reduced pain perception to another noxious stimulus at a distant, heterotopic body part [83, 84]. The first stimulus is referred to as the conditioning stimulus; the second stimulus, whose pain rating decreases after the application of the conditioning stimulus, is referred to as the test stimulus [84]. CPM has been shown to be a separate phenomenon from cognitive distraction [85, 86]. A variety of other terms have also been used to describe CPM, such as "pain inhibiting pain," "heterotopic noxious conditioning stimulation," and "counterirritation [83, 84]." CPM was also referred to as diffuse noxious inhibitory control (DNIC). However, international experts have agreed to distinguish DNIC, a neurophysiologic process, from CPM, a behavioral correlate of this process (see below) [84].

3.2.1. Animal Studies and Molecular Mechanisms. CPM is the behavioral correlate to diffuse noxious inhibitory control (DNIC) [84], an inhibitory mechanism involving the spinal-bulbo-spinal loop in animal neurophysiological studies [87]. In 1979, Le Bars et al. discovered that when noxious stimuli (A- δ - or C-fiber-mediated) are applied anywhere outside the excitatory receptive field of a spinal or trigeminal

WDR neuron, the response to any noxious input within its receptive field is profoundly inhibited [88, 89]. Le Bars' group subsequently found that DNIC is mediated by the subnucleus reticularis dorsalis (SRD) in the caudal medulla [90], which receives noxious input via pathways in the ventral lateral quadrant of the spinal cord [91], and sends global inhibitory signals to WDR neurons from all spinal levels via the dorsolateral funiculi [92]. Finally, the strong correlation between the signal reduction in the WDR neurons and the pain reduction in a CPM paradigm, in both extent and time course, supports the notion that CPM is the behavioral correlate of DNIC [93–95].

3.2.2. Decrease of CPM in Chronic Pain and Risk Factors. Like TS, CPM is altered in many chronic pain conditions, such as fibromyalgia [96], tension-type headache [97], irritable bowel syndrome [98], and arthritis of the hip [99]. Rather than an increase as with TS, a decrease in CPM is seen. As shown in Table 1, the risk factors for decreased CPM are similar to those for increased TS. These include older age [44, 51, 52], female sex [43, 45, 53], and psychological factors such as catastrophizing [54, 55]. However, the relationship between female sex and decreased CPM is less straight forward as some studies showed clear increase in CPM associated with female sex, while others did not find such association [43, 45, 53]. Large variations in methodology may partially contribute to this discrepancy [43, 53]. Furthermore, chronic opioid use [59], depressed mood [58], and poor sleep also decrease CPM [56, 57].

3.2.3. Measurement Methodology. There is no single, standard protocol for measuring CPM. Table 3 summarizes the key components in generating CPM and demonstrates examples of their variability. Pud et al. [43] published an excellent review of CPM methods. In short, a test stimulus is measured before the application of the conditioning stimulus to obtain a baseline and is measured again during or after the application of the conditioning stimulus to quantify the magnitude of CPM relative to the baseline. The noxious test and conditioning stimuli are typically administered at anatomically distinct locations.

The most common conditioning stimulus is a cold water bath applied to the contralateral hand. However, other conditioning stimuli have been used, including isotonic saline injections and heat pain. It is the general consensus that the conditioning stimulus must be noxious in order to trigger CPM [43, 53]. Once the noxious threshold has been exceeded, the intensity of the conditioning stimulus may not matter, according to reports by Granot et al. [68] and Nir et al. [100]. The duration of the conditioning stimulus is usually between 30 seconds and 2 minutes for the cold water bath [53].

In contrast to the conditioning stimulus, there is a large variation in the choice of test stimulus. Pain recordings of a standard stimulus or pain thresholds from any type of stimulation (electrical, chemical, heat, pressure, etc.) can be used [43]. The magnitude of CPM is measured by the change from baseline in the test stimulus to after the conditioning stimulus is applied. The CPM effect appears to peak during

TABLE 3: Examples of varied parameters in generating CPM.

Parameter	Examples
Conditioning stimulus	Cold water bath (0–10°C) [68], heat (thermode or water bath) [69], hypertonic saline injection [70], and inflated blood pressure cuff [71]
Testing stimulus	Pain detection thresholds [69], rating of a predetermined single pain stimulus [68], and TS protocols [72]
When to measure test stimulus again	Varies widely: from during the conditioning stimulus [73] up to 30 min after the conditioning stimulus [74]
Location of stimulus	Large variation in the relative distance between the testing and conditioning stimuli: for example, upper body to upper body [68] versus upper body to lower body [51]
Computation	Relative or absolute changes in threshold measures or ratings of predetermined pain stimulus [43]

the application of the conditioning stimulus and fades rapidly from 5 to 10 minutes after the conditioning stimulus ceases [43, 53, 101, 102]. One report indicates that the approximate median magnitude of CPM represents about a 29% decrease in pain rating, regardless of the test stimulus used [43]. There is some indication that CPM is stronger when the test and conditioning stimuli are applied at a greater anatomical distance from the CPM stimulus site (e.g., CPM is stronger for the hand-to-contralateral leg than for the hand-to-contralateral hand) [43, 87].

In summary, the best means of capturing robust CPM is to use a strong, noxious conditioning stimulus (such as cold immersion of the contralateral distal extremity) and measure the change in the test stimulus during the latter part of the conditioning stimulus. As with TS, significant variations exist in the methodologies used to generate and compute CPM, making it difficult to make comparisons across studies and subjects. Future efforts should focus on identifying a standardized, broadly accepted protocol for CPM.

3.2.4. CPM in Acupuncture Studies. Similar to TS, the use of CPM to study acupuncture analgesia is limited. There are only two direct studies on acupuncture analgesia and CPM/DNIC, both of which focused on the question of whether acupuncture analgesia is equivalent to CPM/DNIC. To date, no one has studied how acupuncture stimulation may modulate the extent of DNIC.

The first acupuncture-DNIC study was carried out by Bing et al. [103]. Output from WDR neurons in the trigeminal nucleus of rodents was measured using the patch-clamp technique. The conditioning stimuli consisted of manual acupuncture applied to Zusanli (a classic acupuncture point) and to an adjacent nonacupuncture point, both located on the right hind limb, and a standard noxious stimulus—immersion of the left hind limb in a 48°C hot water bath. All three stimuli resulted in a similar degree of inhibition in the firing of the trigeminal WDR neurons (72.5% and 78.5%). Furthermore, the inhibition resulting from all three stimuli demonstrated a similar time course for decay and a similar response to naloxone, which reversed the inhibition by about 30%. The authors concluded that acupuncture maneuvers trigger the neural mechanisms involved in DNIC.

The second acupuncture-DNIC (CPM) study was done in healthy human volunteers using a crossover design [104]. It directly compared the effects of acupuncture, sham acupuncture, and a 1.5°C cold water bath (as a conditioning stimulus in the upper extremity). The test stimulus was the pressure pain threshold at the second toe. The verum acupuncture involved the penetration of Hegu (a classic acupuncture point) with a needle without manipulation, and retaining the needle for 5 minutes. The sham acupuncture involved the tapping and placement of a nonpenetrating Streitberger device [105] at Hegu for 5 minutes. The results showed that the cold bath resulted in much stronger increase in the pressure pain threshold as compared with verum and sham acupuncture. Furthermore, there was no statistically significant difference between the verum and sham. The authors concluded that acupuncture as performed in this trial exerted a small analgesic effect not different from placebo and that the analgesic effect was unlike CPM.

It is difficult to compare these studies because of several reasons. First, the test and conditioning stimuli differed significantly between the two studies. Second, as the authors of the second paper mentioned, their acupuncture needling was only minimally painful (pain score about 2.4 ± 1.5 out of a 10-point scale). Because prior studies have shown that CPM will only work when the conditioning stimulus is beyond the noxious threshold, it is not surprising that acupuncture did not trigger CPM in these studies. Third, Deqi, a unique composite of sensations (such as deep ache and tingling sensation) considered essential for clinical efficacy according to traditional Chinese medicine [106], was not elicited in the second study. In real clinical practice, the acupuncturist aims to achieve Deqi, retains the needles in the body for between 15 and 20 minutes, and often uses more than one needle [107]. Therefore, the treatment performed in the second study does not represent typical clinical practice. Future studies should focus on adapting CPM for the clinical study of acupuncture analgesia using acupuncture methods that are consistent with clinical practice.

Last but not least, the duration of CPM/DNIC is short-lived. Directly comparing acupuncture with CPM will not help understand the clinically relevant long-term analgesia by acupuncture. Because DNIC/CPM is considered to play a role in mediating pain perception in chronic pain conditions [27, 108, 109], it would be more relevant to study how acupuncture

influences CPM rather than simply to treat acupuncture as a form of transient conditioning stimulus.

3.3. Current Trends and Future Directions QST in Acupuncture Research

3.3.1. Clinical Applications of QST. Quantitative sensory testing is increasingly used in clinical research as a helpful marker for central and peripheral nociceptive processing [38, 39, 110]. Specifically, researchers are applying TS and CPM to the following three categories of translational research: (1) to phenotype patient subgroups based on different underlying pain mechanisms [27, 53, 109, 111]; (2) to predict response to treatment based on mechanistic phenotypes thus determined [112–116]; and (3) to characterize the central modulatory effects of new therapies [99, 117–121]. For example, as mentioned separately in the TS and CPM sections, many chronic pain conditions display increased TS and/or reduced CPM as compared with healthy controls. These conditions include fibromyalgia, TMJ disorder, headaches, irritable bowel syndrome, back pain, and arthritis of hip and knee [27]. The next step, then, is to select the appropriate therapies that specifically address an individual patient's mechanistic deficit(s). Recently, Yarnitsky et al. demonstrated this concept of mechanism-based treatment of pain in a landmark study [116]. He found that deficient descending inhibition, as reflected by low CPM, predicted clinical response to duloxetine, an antidepressant that augments descending inhibition by increasing serotonin and norepinephrine levels in the central nervous system [122]. This study represents a future of personalized pain treatment, where QST fingerprinting provides key information on the mechanism of an individual's pain condition. Last but not least, TS and CPM have been used to characterize the central modulatory effects of many drugs and interventions, such as ketamine [123], gabapentin [117], surgery [120], and exercise [121].

3.3.2. Limitations of Current QST Research. Despite the advances described here, there are still significant methodological barriers to the wide utilization of QST in clinical research. First, although the temporal stability of TS and CPM has been established in healthy volunteers [42, 66, 124], it has not been characterized in chronic pain patients [110]. Without stability data in this population, it is difficult to discern if a change in TS or CPM is due to the therapeutic intervention or to the natural fluctuation in these measures. Second, a variety of methods have been used to generate and compute TS [42, 79] and CPM [43], which makes it challenging to make comparisons across studies. Third, individual TS and CPM responses vary widely. For example, a standard thermal TS protocol may not capture TS from 40% to 60% of the individuals tested [61, 125]. This variability imposes restrictions on the external validity of studies involving TS and CPM, particularly in longitudinal studies where some degrees of TS and CPM are expected at baseline. Our group is actively searching for solution to all 3 issues by assessing the stability of TS and CPM in patients with chronic pain,

developing universal protocols to capture TS and CPM in most individuals, and investigating the physiologic bases of the between-individual variations in the response to TS and CPM tests.

In summary, while there is a large body of literature on using TS and CPM to study chronic pain, limitations in methodology still exist. Future studies should address the following three issues: (1) the uncertainty in the temporal stability of TS and CPM in chronic pain conditions; (2) the lack of a universal protocol; (3) the large between-individual variability in both TS and CPM.

3.3.3. QST in Acupuncture Research. The literature contains only sparse data on the use of QST in human acupuncture research. This may be due, in part, to lack of awareness. Advances are being made in applying QST to understand the mechanisms of chronic pain [27, 38, 53, 78, 109] and medications [29, 112, 116–118, 126], and we believe there is a definitive role for QST in the study of acupuncture analgesia.

We make the following practical recommendations for utilizing QST in clinical acupuncture studies. First, because the stability of TS and CPM has not been established in the clinical pain population, we recommend a parallel group design with one group representing the natural course of the disease (waitlist control) and other groups representing active and sham interventions. Second, although there is no single standardized protocol for TS or CPM, there are both more and less established protocols. We recommend choosing the more established protocols. For example, the OPERA trial of several thousands of patients with oral facial pain used reliable heat and pressure pain paradigms to examine TS and CPM [111]. Another example is the comprehensive set of QST measures that encompass both the dynamic and static measures developed by the German Research Network in Neuropathic Pain (DFNS) [65]. With a strong focus on peripheral pathologies, this protocol has been validated on a variety of neuropathic pain syndromes and has been shown to be consistent [127]. Furthermore, both the OPERA and the DFNS protocols include traditional threshold measures to a variety of sensory stimuli. Unlike CPM and TS, these threshold measures offer additional insights on peripheral nociceptive processes. Last but not least, we recommend a two-step approach to determine whether acupuncture leads to analgesia by modifying the central pain-processing pathways. First, research should test whether acupuncture will lead to changes in dynamic QST parameters such as TS and CPM. Second, studies should investigate whether such changes lead to improvement of pain and function.

4. Conclusions

Numerous animal studies suggest that acupuncture leads to analgesia via powerful central pain modulatory mechanisms. However, little is known about whether and how these findings may translate to clinically meaningful outcomes. TS and CPM are emerging behavioral correlates of ascending excitatory and descending inhibitory limbs of central pain

modulation. Both TS and CPM have been widely used in clinical pain research, yet their application to the understanding of acupuncture analgesia is limited. We encourage greater use of TS and CPM in acupuncture research, in conjunction with other psychophysical tools such as pain detection thresholds, and with appropriate attention given to the limitations of these psychophysical methods. The appropriate adaptation of dynamic (TS and CPM) and static QST measures (pain detection threshold) will help advance our understanding of the true mechanisms of acupuncture analgesia in human clinical populations.

Abbreviations

AA:	Acupuncture analgesia
TS:	Temporal summation
CPM:	Conditioned pain modulation
QST:	Quantitative sensory testing
DNIC:	Diffuse noxious inhibitory control
NS:	Nociceptive specific
WDR:	Wide dynamic range
PAG:	Periaqueductal gray
RVM:	Rostroventral medulla
SDR:	Subnucleus dorsalis reticularis
S1:	Somatosensory area 1
S2:	Somatosensory area 2.

Acknowledgments

The authors thank Jarred Younger, PhD, and Katie Martucci, PhD, for constructive feedback on the content and Maureen Donohue, BA, for critical assistance in the preparation of this paper.

References

- [1] A. Burke, D. M. Upchurch, C. Dye, and L. Chyu, "Acupuncture use in the United States: findings from the national health interview survey," *Journal of Alternative and Complementary Medicine*, vol. 12, no. 7, pp. 639–648, 2006.
- [2] A. Vincent, K. M. Kruk, S. S. Cha, B. A. Bauer, and D. P. Martin, "Utilisation of acupuncture at an academic medical centre," *Acupuncture in Medicine*, vol. 28, no. 4, pp. 189–190, 2010.
- [3] Y. Zhang, L. Lao, H. Chen, and R. Ceballos, "Acupuncture use among american adults: what acupuncture practitioners can learn from national health interview survey 2007?" *Evidence-Based Complementary and Alternative Medicine*, vol. 2012, Article ID 710750, 8 pages, 2012.
- [4] S. M. Wang, Z. N. Kain, and P. White, "Acupuncture analgesia: I. The scientific basis," *Anesthesia and Analgesia*, vol. 106, no. 2, pp. 602–610, 2008.
- [5] S. M. Wang, Z. N. Kain, and P. F. White, "Acupuncture analgesia: II. Clinical considerations," *Anesthesia and Analgesia*, vol. 106, no. 2, pp. 611–621, 2008.
- [6] Z. Q. Zhao, "Neural mechanism underlying acupuncture analgesia," *Progress in Neurobiology*, vol. 85, no. 4, pp. 355–375, 2008.
- [7] J. S. Han, "Acupuncture and endorphins," *Neuroscience Letters*, vol. 361, no. 1–3, pp. 258–261, 2004.
- [8] J. S. Han, "Acupuncture analgesia: areas of consensus and controversy," *Pain*, vol. 152, no. 3, pp. S41–S48, 2011.
- [9] R. X. Zhang, L. Wang, X. Wang, K. Ren, B. M. Berman, and L. Lao, "Electroacupuncture combined with MK-801 prolongs anti-hyperalgesia in rats with peripheral inflammation," *Pharmacology Biochemistry and Behavior*, vol. 81, no. 1, pp. 146–151, 2005.
- [10] N. Yonehara, T. Sawada, H. Matsuura, and R. Inoki, "Influence of electro-acupuncture on the release of substance P and the potential evoked by tooth pulp stimulation in the trigeminal nucleus caudalis of the rabbit," *Neuroscience Letters*, vol. 142, no. 1, pp. 53–56, 1992.
- [11] R. X. Zhang, A. Li, B. Liu et al., "Electroacupuncture attenuates bone cancer pain and inhibits spinal interleukin-1 β expression in a rat model," *Anesthesia and Analgesia*, vol. 105, no. 5, pp. 1482–1488, 2007.
- [12] W. B. Hu, Z. J. Wu, and K. M. Wang, "Progress of researches on involvement of serotonin in the central nervous system in acupuncture analgesia and other effects," *Zhen Ci Yan Jiu*, vol. 37, no. 3, pp. 247–251, 2012.
- [13] Y. Zhang, R. X. Zhang, M. Zhang et al., "Electroacupuncture inhibition of hyperalgesia in an inflammatory pain rat model: involvement of distinct spinal serotonin and norepinephrine receptor subtypes," *The British Journal of Anaesthesia*, vol. 109, no. 2, pp. 245–252, 2012.
- [14] L. F. He, "Involvement of endogenous opioid peptides in acupuncture analgesia," *Pain*, vol. 31, no. 1, pp. 99–121, 1987.
- [15] A. Li, Y. Wang, J. Xin et al., "Electroacupuncture suppresses hyperalgesia and spinal Fos expression by activating the descending inhibitory system," *Brain Research*, vol. 1186, no. 1, pp. 171–179, 2007.
- [16] R. X. Zhang, L. Lao, X. Wang et al., "Electroacupuncture attenuates inflammation in a rat model," *Journal of Alternative and Complementary Medicine*, vol. 11, no. 1, pp. 135–142, 2005.
- [17] K. Kubo, H. Yajima, M. Takayama, T. Ikebukuro, H. Mizoguchi, and N. Takakura, "Changes in blood circulation of the contralateral Achilles tendon during and after acupuncture and heating," *International Journal of Sports Medicine*, vol. 32, no. 10, pp. 807–813, 2011.
- [18] C. S. Huang and Y. F. Tsai, "Somatosympathetic reflex and acupuncture-related analgesia," *Chinese Journal of Physiology*, vol. 52, no. 5, pp. 345–357, 2009.
- [19] J. M. Kang, H. J. Park, Y. G. Choi et al., "Acupuncture inhibits microglial activation and inflammatory events in the MPTP-induced mouse model," *Brain Research*, vol. 1131, no. 1, pp. 211–219, 2007.
- [20] E. Ernst, M. S. Lee, and T. Y. Choi, "Acupuncture: does it alleviate pain and are there serious risks? A review of reviews," *Pain*, vol. 152, no. 4, pp. 755–764, 2011.
- [21] B. M. Berman, H. H. Langevin, C. M. Witt, and R. Dubner, "Acupuncture for chronic low back pain," *The New England Journal of Medicine*, vol. 363, no. 5, pp. 454–461, 2010.
- [22] A. Hopton and H. MacPherson, "Acupuncture for chronic pain: is acupuncture more than an effective placebo? A systematic review of pooled data from meta-analyses," *Pain Practice*, vol. 10, no. 2, pp. 94–102, 2010.
- [23] A. J. Vickers, A. M. Cronin, A. C. Maschino et al., "Acupuncture for chronic pain: individual patient data meta-analysis," *Archives of Internal Medicine*, vol. 172, no. 19, pp. 1444–1453, 2012.

- [24] H. M. Langevin et al., "Paradoxes in acupuncture research: strategies for moving forward," *Evidence-Based Complementary and Alternative Medicine*, vol. 2011, Article ID 180805, 11 pages, 2011.
- [25] R. D'Mello and A. H. Dickenson, "Spinal cord mechanisms of pain," *The British Journal of Anaesthesia*, vol. 101, no. 1, pp. 8–16, 2008.
- [26] M. J. Millan, "Descending control of pain," *Progress in Neurobiology*, vol. 66, no. 6, pp. 355–474, 2002.
- [27] K. Phillips and D. J. Clauw, "Central pain mechanisms in chronic pain states—maybe it is all in their head," *Best Practice & Research Clinical Rheumatology*, vol. 25, no. 2, pp. 141–154, 2011.
- [28] D. D. Price, "Characteristics of second pain and flexion reflexes indicative of prolonged central summation," *Experimental Neurology*, vol. 37, no. 2, pp. 371–387, 1972.
- [29] P. K. Eide, "Wind-up and the NMDA receptor complex from a clinical perspective," *The European Journal of Pain*, vol. 4, no. 1, pp. 5–15, 2000.
- [30] R. Kuner, "Central mechanisms of pathological pain," *Nature Medicine*, vol. 16, no. 11, pp. 1258–1266, 2010.
- [31] R. Melzack and P. D. Wall, "Pain mechanisms: a new theory," *Science*, vol. 150, no. 3699, pp. 971–979, 1965.
- [32] A. H. Dickenson, "Gate control theory of pain stands the test of time," *The British Journal of Anaesthesia*, vol. 88, no. 6, pp. 755–757, 2002.
- [33] M. Moayedi and K. D. Davis, "Theories of pain: from specificity to gate control," *Journal of Neurophysiology*, vol. 109, no. 1, pp. 5–12, 2012.
- [34] A. V. Apkarian, M. C. Bushnell, R. D. Treede, and J. K. Zubieta, "Human brain mechanisms of pain perception and regulation in health and disease," *The European Journal of Pain*, vol. 9, no. 4, pp. 463–484, 2005.
- [35] A. D. Craig, "Pain mechanisms: labeled lines versus convergence in central processing," *Annual Review of Neuroscience*, vol. 26, pp. 1–30, 2003.
- [36] S. C. Mackey and F. Maeda, "Functional imaging and the neural systems of chronic pain," *Neurosurgery Clinics of North America*, vol. 15, no. 3, pp. 269–288, 2004.
- [37] M. M. Backonja, D. Walk, R. R. Edwards et al., "Quantitative sensory testing in measurement of neuropathic pain phenomena and other sensory abnormalities," *The Clinical Journal of Pain*, vol. 25, no. 7, pp. 641–647, 2009.
- [38] L. Arendt-Nielsen and D. Yarnitsky, "Experimental and clinical applications of quantitative sensory testing applied to skin, muscles and viscera," *Journal of Pain*, vol. 10, no. 6, pp. 556–572, 2009.
- [39] D. B. Pfau, C. Geber, F. Birklein, and R. D. Treede, "Quantitative sensory testing of neuropathic pain patients: potential mechanistic and therapeutic implications," *Current Pain and Headache Reports*, vol. 16, no. 3, pp. 199–206, 2012.
- [40] I. H. Wagman and D. D. Price, "Responses of dorsal horn cells of M. mulatta to cutaneous and sural nerve A and C fiber stimuli," *Journal of Neurophysiology*, vol. 32, no. 6, pp. 803–817, 1969.
- [41] L. M. Mendell, "Physiological properties of unmyelinated fiber projection to the spinal cord," *Experimental Neurology*, vol. 16, no. 3, pp. 316–332, 1966.
- [42] J. T. Kong, K. A. Johnson, R. R. Balise, and S. Mackey, "Test-retest reliability of thermal temporal summation using an individualized protocol," *Journal of Pain*, vol. 14, no. 1, pp. 79–88, 2013.
- [43] D. Pud, Y. Granovsky, and D. Yarnitsky, "The methodology of experimentally induced diffuse noxious inhibitory control (DNIC)-like effect in humans," *Pain*, vol. 144, no. 1–2, pp. 16–19, 2009.
- [44] R. R. Edwards and R. B. Fillingim, "Effects of age on temporal summation and habituation of thermal pain: clinical relevance in healthy older and younger adults," *Journal of Pain*, vol. 2, no. 6, pp. 307–317, 2001.
- [45] R. B. Fillingim, C. D. King, M. C. Ribeiro-Dasilva, B. Rahim-Williams, and J. L. Riley, "Sex, gender, and pain: a review of recent clinical and experimental findings," *Journal of Pain*, vol. 10, no. 5, pp. 447–485, 2009.
- [46] S. Z. George, V. T. Wittmer, R. B. Fillingim, and M. E. Robinson, "Sex and pain-related psychological variables are associated with thermal pain sensitivity for patients with chronic low back pain," *Journal of Pain*, vol. 8, no. 1, pp. 2–10, 2007.
- [47] R. R. Edwards, M. T. Smith, G. Stonerock, and J. A. Haythornthwaite, "Pain-related catastrophizing in healthy women is associated with greater temporal summation of and reduced habituation to thermal pain," *Clinical Journal of Pain*, vol. 22, no. 8, pp. 730–737, 2006.
- [48] B. R. Goodin, T. L. Glover, A. Sotolongo et al., "The association of greater dispositional optimism with less endogenous pain facilitation is indirectly transmitted through lower levels of pain catastrophizing," *Journal of Pain*, vol. 14, no. 2, pp. 126–135, 2013.
- [49] J. L. Rhudy, S. L. Martin, E. L. Terry et al., "Pain catastrophizing is related to temporal summation of pain but not temporal summation of the nociceptive flexion reflex," *Pain*, vol. 152, no. 4, pp. 794–801, 2011.
- [50] M. E. Robinson, J. E. Bialosky, M. D. Bishop, D. D. Price, and S. Z. George, "Supra-threshold scaling, temporal summation, and after-sensation: relationships to each other and anxiety/fear," *Journal of Pain Research*, vol. 3, pp. 25–32, 2010.
- [51] M. Larivière, P. Goffaux, S. Marchand, and N. Julien, "Changes in pain perception and descending inhibitory controls start at middle age in healthy adults," *Clinical Journal of Pain*, vol. 23, no. 6, pp. 506–510, 2007.
- [52] L. L. Washington, S. J. Gibson, and R. D. Helme, "Age-related differences in the endogenous analgesic response to repeated cold water immersion in human volunteers," *Pain*, vol. 89, no. 1, pp. 89–96, 2000.
- [53] G. van Wijk and D. S. Veldhuijzen, "Perspective on diffuse noxious inhibitory controls as a model of endogenous pain modulation in clinical pain syndromes," *Journal of Pain*, vol. 11, no. 5, pp. 408–419, 2010.
- [54] B. R. Goodin, L. McGuire, M. Allshouse et al., "Associations between catastrophizing and endogenous pain-inhibitory processes: sex differences," *Journal of Pain*, vol. 10, no. 2, pp. 180–190, 2009.
- [55] I. Weissman-Fogel, E. Sprecher, and D. Pud, "Effects of catastrophizing on pain perception and pain modulation," *Experimental Brain Research*, vol. 186, no. 1, pp. 79–85, 2008.
- [56] R. R. Edwards, E. Grace, S. Peterson, B. Klick, J. A. Haythornthwaite, and M. T. Smith, "Sleep continuity and architecture: associations with pain-inhibitory processes in patients with temporomandibular joint disorder," *The European Journal of Pain*, vol. 13, no. 10, pp. 1043–1047, 2009.
- [57] M. T. Smith, R. R. Edwards, U. D. McCann, and J. A. Haythornthwaite, "The effects of sleep deprivation on pain inhibition and spontaneous pain in women," *Sleep*, vol. 30, no. 4, pp. 494–505, 2007.

- [58] J. B. De Souza, S. Potvin, P. Goffaux, J. Charest, and S. Marchand, "The deficit of pain inhibition in fibromyalgia is more pronounced in patients with comorbid depressive symptoms," *Clinical Journal of Pain*, vol. 25, no. 2, pp. 123–127, 2009.
- [59] K. C. Ram, E. Eisenberg, M. Haddad, and D. Pud, "Oral opioid use alters DNIC but not cold pain perception in patients with chronic pain—new perspective of opioid-induced hyperalgesia," *Pain*, vol. 139, no. 2, pp. 431–438, 2008.
- [60] K. G. Raphael, "Temporal summation of heat pain in temporomandibular disorder patients," *Journal of orofacial pain*, vol. 23, no. 1, pp. 54–64, 2009.
- [61] R. J. Anderson, J. G. Craggs, J. E. Bialosky et al., "Temporal summation of second pain: variability in responses to a fixed protocol," *The European Journal of Pain*, vol. 17, no. 1, pp. 67–74, 2013.
- [62] L. Arendt-Nielsen, J. Brennum, S. Sindrup, and P. Bak, "Electrophysiological and psychophysical quantification of temporal summation in the human nociceptive system," *European Journal of Applied Physiology and Occupational Physiology*, vol. 68, no. 3, pp. 266–273, 1994.
- [63] Z. Zheng, S. J. Q. Feng, C. D. Costa, C. G. Li, D. Lu, and C. C. Xue, "Acupuncture analgesia for temporal summation of experimental pain: a randomised controlled study," *The European Journal of Pain*, vol. 14, no. 7, pp. 725–731, 2010.
- [64] J. A. B. Manresa, M. B. Jensen, and O. K. Andersen, "Introducing the reflex probability maps in the quantification of nociceptive withdrawal reflex receptive fields in humans," *Journal of Electromyography and Kinesiology*, vol. 21, no. 1, pp. 67–76, 2011.
- [65] R. Rolke, R. Baron, C. Maier et al., "Quantitative sensory testing in the German Research Network on Neuropathic Pain (DFNS): standardized protocol and reference values," *Pain*, vol. 123, no. 3, pp. 231–243, 2006.
- [66] S. Cathcart, A. H. Winefield, P. Rolan, and K. Lushington, "Reliability of temporal summation and diffuse noxious inhibitory control," *Pain Research and Management*, vol. 14, no. 6, pp. 433–438, 2009.
- [67] H. Nie, L. Arendt-Nielsen, H. Andersen, and T. Graven-Nielsen, "Temporal summation of pain evoked by mechanical stimulation in deep and superficial tissue," *Journal of Pain*, vol. 6, no. 6, pp. 348–355, 2005.
- [68] M. Granot, I. Weissman-Fogel, Y. Crispel et al., "Determinants of endogenous analgesia magnitude in a diffuse noxious inhibitory control (DNIC) paradigm: do conditioning stimulus painfulness, gender and personality variables matter?" *Pain*, vol. 136, no. 1-2, pp. 142–149, 2008.
- [69] S. Lautenbacher, S. Roscher, and F. Strian, "Inhibitory effects do not depend on the subjective experience of pain during heterotopic noxious conditioning stimulation (HNCS): a contribution to the psychophysics of pain inhibition," *The European Journal of Pain*, vol. 6, no. 5, pp. 365–374, 2002.
- [70] M. Valeriani, D. Le Pera, D. Restuccia et al., "Segmental inhibition of cutaneous heat sensation and of laser-evoked potentials by experimental muscle pain," *Neuroscience*, vol. 136, no. 1, pp. 301–309, 2005.
- [71] C. M. Campbell, C. R. France, M. E. Robinson, H. L. Logan, G. R. Geffken, and R. B. Fillingim, "Ethnic differences in diffuse noxious inhibitory controls," *Journal of Pain*, vol. 9, no. 8, pp. 759–766, 2008.
- [72] R. Staud, M. E. Robinson, C. J. Vierck, and D. D. Price, "Diffuse noxious inhibitory controls (DNIC) attenuate temporal summation of second pain in normal males but not in normal females or fibromyalgia patients," *Pain*, vol. 101, no. 1-2, pp. 167–174, 2003.
- [73] P. Svensson, C. H. Hashikawa, and K. L. Casey, "Site- and modality-specific modulation of experimental muscle pain in humans," *Brain Research*, vol. 851, no. 1-2, pp. 32–38, 1999.
- [74] B. Tuveson, A. S. Leffler, and P. Hansson, "Time dependant differences in pain sensitivity during unilateral ischemic pain provocation in healthy volunteers," *The European Journal of Pain*, vol. 10, no. 3, pp. 225–232, 2006.
- [75] D. D. Price and R. Dubner, "Mechanisms of first and second pain in the peripheral and central nervous systems," *Journal of Investigative Dermatology*, vol. 69, no. 1, pp. 167–171, 1977.
- [76] R. Staud, C. E. Bovee, M. E. Robinson, and D. D. Price, "Cutaneous C-fiber pain abnormalities of fibromyalgia patients are specifically related to temporal summation," *Pain*, vol. 139, no. 2, pp. 315–323, 2008.
- [77] P. H. Finan, L. F. Buenaver, S. C. Bounds et al., "Discordance between pain and radiographic severity in knee osteoarthritis findings from quantitative sensory testing of central sensitization," *Arthritis and Rheumatism*, vol. 65, no. 2, pp. 363–372, 2013.
- [78] L. Arendt-Nielsen and S. Petersen-Felix, "Wind-up and neuroplasticity: is there a correlation to clinical pain?" *European Journal of Anaesthesiology, Supplement*, vol. 12, no. 10, pp. 1–7, 1995.
- [79] M. C. Ribeiro-Dasilva, B. R. Goodin, and R. B. Fillingim, "Differences in suprathreshold heat pain responses and self-reported sleep quality between patients with temporomandibular joint disorder and healthy controls," *The European Journal of Pain*, vol. 16, no. 7, pp. 983–993, 2012.
- [80] Y. Tobbackx, M. Meeus, L. Wauters et al., "Does acupuncture activate endogenous analgesia in chronic whiplash-associated disorders? A randomized crossover trial," *The European Journal of Pain*, vol. 17, no. 2, pp. 279–289, 2013.
- [81] G. G. Zhang, C. Yu, W. Lee, L. Lao, K. Ren, and B. M. Berman, "Involvement of peripheral opioid mechanisms in electroacupuncture analgesia," *Explore*, vol. 1, no. 5, pp. 365–371, 2005.
- [82] C. J. Woolf and S. W. N. Thompson, "The induction and maintenance of central sensitization is dependent on N-methyl-D-aspartic acid receptor activation; implications for the treatment of post-injury pain hypersensitivity states," *Pain*, vol. 44, no. 3, pp. 293–299, 1991.
- [83] D. Yarnitsky, "Conditioned pain modulation (the diffuse noxious inhibitory control-like effect): its relevance for acute and chronic pain states," *Current Opinion in Anaesthesiology*, vol. 23, no. 5, pp. 611–615, 2010.
- [84] D. Yarnitsky, L. Arendt-Nielsen, and D. Bouhassira, "Recommendations on terminology and practice of psychophysical DNIC testing," *The European Journal of Pain*, vol. 14, no. 4, article 339, 2010.
- [85] R. Moont, Y. Crispel, R. Lev, D. Pud, and D. Yarnitsky, "Temporal changes in cortical activation during distraction from pain: a comparative LORETA study with conditioned pain modulation," *Brain Research*, vol. 1435, pp. 105–117, 2012.
- [86] R. Moont, D. Pud, E. Sprecher, G. Sharvit, and D. Yarnitsky, "'Pain inhibits pain' mechanisms: is pain modulation simply due to distraction?" *Pain*, vol. 150, no. 1, pp. 113–120, 2010.
- [87] D. le Bars and J.-C. Willer, "Pain modulation triggered by high-intensity stimulation: implication for acupuncture analgesia?" *International Congress Series*, vol. 1238, pp. 11–29, 2002.

- [88] D. Le Bars, A. H. Dickenson, and J. M. Besson, "Diffuse noxious inhibitory controls (DNIC). I. Effects on dorsal horn convergent neurones in the rat," *Pain*, vol. 6, no. 3, pp. 283–304, 1979.
- [89] D. Le Bars, A. H. Dickenson, and J. M. Besson, "Diffuse noxious inhibitory controls (DNIC). II. Lack of effect on non-convergent neurones, supraspinal involvement and theoretical implications," *Pain*, vol. 6, no. 3, pp. 305–327, 1979.
- [90] O. Gall, D. Bouhassira, D. Chitour, and D. Le Bars, "Involvement of the caudal medulla in negative feedback mechanisms triggered by spatial summation of nociceptive inputs," *Journal of Neurophysiology*, vol. 79, no. 1, pp. 304–311, 1998.
- [91] L. Villanueva, M. Peschanski, B. Calvino, and D. Le Bars, "Ascending pathways in the spinal cord involved in triggering diffuse noxious inhibitory controls in the rat," *Journal of Neurophysiology*, vol. 55, no. 1, pp. 34–55, 1986.
- [92] L. Villanueva, D. Chitour, and D. Le Bars, "Involvement of the dorsolateral funiculus in the descending spinal projections responsible for diffuse noxious inhibitory controls in the rat," *Journal of Neurophysiology*, vol. 56, no. 4, pp. 1185–1195, 1986.
- [93] D. Le Bars, L. Villanueva, D. Bouhassira, and J. C. Willer, "Diffuse noxious inhibitory controls (DNIC) in animals and in man," *Patologicheskaya Fiziologiya i Eksperimentalnaya Terapiya*, no. 4, pp. 55–65, 1992.
- [94] A. Roby-Brami, B. Bussel, J. C. Willer, and D. LeBars, "An electrophysiological investigation into the pain-relieving effects of heterotopic nociceptive stimuli. Probable involvement of a supraspinal loop," *Brain*, vol. 110, no. 6, pp. 1497–1508, 1987.
- [95] J. C. Willer, A. Roby, and D. Le Bars, "Psychophysical and electrophysiological approaches to the pain-relieving effects of heterotopic nociceptive stimuli," *Brain*, vol. 107, no. 4, pp. 1095–1112, 1984.
- [96] S. Lautenbacher and G. B. Rollman, "Possible deficiencies of pain modulation in fibromyalgia," *Clinical Journal of Pain*, vol. 13, no. 3, pp. 189–196, 1997.
- [97] A. Pielsticker, G. Haag, M. Zaudig, and S. Lautenbacher, "Impairment of pain inhibition in chronic tension-type headache," *Pain*, vol. 118, no. 1–2, pp. 215–223, 2005.
- [98] C. H. Wilder-Smith, D. Schindler, K. Lovblad, S. M. Redmond, and A. Nirkko, "Brain functional magnetic resonance imaging of rectal pain and activation of endogenous inhibitory mechanisms in irritable bowel syndrome patient subgroups and healthy controls," *Gut*, vol. 53, no. 11, pp. 1595–1601, 2004.
- [99] E. Kosek and G. Ordeberg, "Lack of pressure pain modulation by heterotopic noxious conditioning stimulation in patients with painful osteoarthritis before, but not following, surgical pain relief," *Pain*, vol. 88, no. 1, pp. 69–78, 2000.
- [100] R. R. Nir, Y. Granovsky, D. Yarnitsky, E. Sprecher, and M. Granot, "A psychophysical study of endogenous analgesia: the role of the conditioning pain in the induction and magnitude of conditioned pain modulation," *The European Journal of Pain*, vol. 15, no. 5, pp. 491–497, 2011.
- [101] K. Fujii, K. Motohashi, and M. Umino, "Heterotopic ischemic pain attenuates somatosensory evoked potentials induced by electrical tooth stimulation: diffuse noxious inhibitory controls in the trigeminal nerve territory," *The European Journal of Pain*, vol. 10, no. 6, pp. 495–504, 2006.
- [102] J. C. Willer, T. De Broucker, and D. Le Bars, "Encoding of nociceptive thermal stimuli by diffuse noxious inhibitory controls in humans," *Journal of Neurophysiology*, vol. 62, no. 5, pp. 1028–1038, 1989.
- [103] Z. Bing, L. Villanueva, and D. Le Bars, "Acupuncture and diffuse noxious inhibitory controls: naloxone-reversible depression of activities of trigeminal convergent neurons," *Neuroscience*, vol. 37, no. 3, pp. 809–818, 1990.
- [104] J. Schliessbach, E. van der Klift, A. Siegenthaler, L. Arendt-Nielsen, M. Curatolo, and K. Streitberger, "Does acupuncture needling induce analgesic effects comparable to diffuse noxious inhibitory controls?" *Evidence-Based Complementary and Alternative Medicine*, vol. 2012, Article ID 785613, 2012.
- [105] K. Streitberger and J. Kleinhenz, "Introducing a placebo needle into acupuncture research," *The Lancet*, vol. 352, no. 9125, pp. 364–365, 1998.
- [106] K. K. S. Hui, E. E. Nixon, M. G. Vangel et al., "Characterization of the "deqi" response in acupuncture," *BMC Complementary and Alternative Medicine*, vol. 7, article 33, 2007.
- [107] J. M. Helms, *Acupuncture Energetics*, Medical Acupuncture Publishers, 1995.
- [108] C. D. King, F. Wong, T. Currie, A. P. Mauderli, R. B. Fillingim, and J. L. Riley, "Deficiency in endogenous modulation of prolonged heat pain in patients with irritable bowel syndrome and temporomandibular disorder," *Pain*, vol. 143, no. 3, pp. 172–178, 2009.
- [109] R. Staud, "Abnormal endogenous pain modulation is a shared characteristic of many chronic pain conditions," *Expert Review of Neurotherapeutics*, vol. 12, no. 5, pp. 577–585, 2012.
- [110] M. Curatolo, L. Arendt-Nielsen, and S. Petersen-Felix, "Evidence, mechanisms, and clinical implications of central hypersensitivity in chronic pain after whiplash injury," *Clinical Journal of Pain*, vol. 20, no. 6, pp. 469–476, 2004.
- [111] J. D. Greenspan, G. D. Slade, E. Bair et al., "Pain sensitivity risk factors for chronic TMD: descriptive data and empirically identified domains from the OPPERA case control study," *Journal of Pain*, vol. 12, no. 11 Supplement, pp. T61–T74, 2011.
- [112] E. Eisenberg, A. Midbari, M. Haddad, and D. Pud, "Predicting the analgesic effect to oxycodone by "static" and "dynamic" quantitative sensory testing in healthy subjects," *Pain*, vol. 151, no. 1, pp. 104–109, 2010.
- [113] R. Landau, J. C. Kraft, L. Y. Flint et al., "An experimental paradigm for the prediction of Post-Operative Pain (PPOP)," *Journal of Visualized Experiments*, no. 35, 2010.
- [114] C. Valencia, R. B. Fillingim, and S. Z. George, "Suprathreshold heat pain response is associated with clinical pain intensity for patients with shoulder pain," *Journal of Pain*, vol. 12, no. 1, pp. 133–140, 2011.
- [115] D. Yarnitsky, Y. Crispel, E. Eisenberg et al., "Prediction of chronic post-operative pain: pre-operative DNIC testing identifies patients at risk," *Pain*, vol. 138, no. 1, pp. 22–28, 2008.
- [116] D. Yarnitsky, M. Granot, H. Nahman-Averbuch, M. Khamaisi, and Y. Granovsky, "Conditioned pain modulation predicts duloxetine efficacy in painful diabetic neuropathy," *Pain*, vol. 153, no. 6, pp. 1193–1198, 2012.
- [117] L. Arendt-Nielsen, J. B. Frøkjær, C. Staahl et al., "Effects of gabapentin on experimental somatic pain and temporal summation," *Regional Anesthesia and Pain Medicine*, vol. 32, no. 5, pp. 382–388, 2007.
- [118] D. Kleinböhl, R. Görtelmeyer, H. J. Bender, and R. Hölzl, "Amantadine sulfate reduces experimental sensitization and pain in chronic back pain patients," *Anesthesia and Analgesia*, vol. 102, no. 3, pp. 840–847, 2006.
- [119] D. Pud, E. Eisenberg, A. Spitzer, R. Adler, G. Fried, and D. Yarnitsky, "The NMDA receptor antagonist amantadine reduces surgical neuropathic pain in cancer patients: a double blind, randomized, placebo controlled trial," *Pain*, vol. 75, no. 2–3, pp. 349–354, 1998.

- [120] C. Valencia, L. L. Kindler, R. B. Fillingim, and S. Z. George, "Investigation of central pain processing in shoulder pain: converging results from 2 musculoskeletal pain models," *Journal of Pain*, vol. 13, no. 1, pp. 81–89, 2012.
- [121] C. J. Vierck, R. Staud, D. D. Price, R. L. Cannon, A. P. Mauderli, and A. D. Martin, "The Effect of maximal exercise on temporal summation of second pain (windup) in patients with fibromyalgia syndrome," *Journal of Pain*, vol. 2, no. 6, pp. 334–344, 2001.
- [122] S. Iyengar, A. A. Webster, S. K. Hemrick-Luecke, J. Y. Xu, and R. M. A. Simmons, "Efficacy of duloxetine, a potent and balanced serotonin-norepinephrine reuptake inhibitor in persistent pain models in rats," *Journal of Pharmacology and Experimental Therapeutics*, vol. 311, no. 2, pp. 576–584, 2004.
- [123] L. Arendt-Nielsen, H. Mansikka, C. Staahl et al., "A translational study of the effects of ketamine and pregabalin on temporal summation of experimental pain," *Regional Anesthesia and Pain Medicine*, vol. 36, no. 6, pp. 585–591, 2011.
- [124] M. J. Alappattu, M. D. Bishop, J. E. Bialosky, S. Z. George, and M. E. Robinson, "Stability of behavioral estimates of activity-dependent modulation of pain," *Journal of Pain Research*, vol. 4, pp. 151–157, 2011.
- [125] M. Granot, Y. Granovsky, E. Sprecher, R. R. Nir, and D. Yarnitsky, "Contact heat-evoked temporal summation: tonic versus repetitive-phasic stimulation," *Pain*, vol. 122, no. 3, pp. 295–305, 2006.
- [126] D. D. Price, J. Mao, H. Frenk, and D. J. Mayer, "The N-methyl-D-aspartate receptor antagonist dextromethorphan selectively reduces temporal summation of second pain in man," *Pain*, vol. 59, no. 2, pp. 165–174, 1994.
- [127] C. Maier, R. Baron, T. R. Tölle et al., "Quantitative sensory testing in the German Research Network on Neuropathic Pain (DFNS): somatosensory abnormalities in 1236 patients with different neuropathic pain syndromes," *Pain*, vol. 150, no. 3, pp. 439–450, 2010.

Research Article

Electroacupuncture and Brain Protection against Cerebral Ischemia: Specific Effects of Acupoints

Fei Zhou,^{1,2} Jingchun Guo,³ Jieshi Cheng,³ Gengcheng Wu,³ Jian Sun,² and Ying Xia^{4,5}

¹ Shanghai Research Center for Acupuncture and Meridians, Shanghai 201203, China

² Gongli Hospital, Pudong New District, Shanghai 200135, China

³ Shanghai Medical College of Fudan University, Shanghai 200032, China

⁴ The University of Texas Medical School at Houston, Houston, TX 77030, USA

⁵ Yale University School of Medicine, New Haven, CT 06520, USA

Correspondence should be addressed to Ying Xia; ying.xia@uth.tmc.edu

Received 22 August 2012; Accepted 18 November 2012

Academic Editor: Wolfgang Schwarz

Copyright © 2013 Fei Zhou et al. This is an open access article distributed under the Creative Commons Attribution License, which permits unrestricted use, distribution, and reproduction in any medium, provided the original work is properly cited.

Electroacupuncture (EA) has been shown to increase cerebral blood flow (CBF) and reduce ischemic infarction in the rat model of cerebral ischemia (middle cerebral artery occlusion, MCAO). Since multiple acupoints are recommended to treat cerebral ischemia, we performed this study to investigate if there is any variation in EA protection against cerebral ischemia with the stimulation of certain “acupoints” in rats. One hour of right MCAO with an 85% reduction of blood flow induced an extensive infarction ($32.9\% \pm 3.8\%$ of the brain), serious neurological deficits (scale = 6.0 ± 0.5 , on a scale of 0–7), and a 17% (10 out of 60) mortality. EA, with a sparse-dense wave (5 Hz/20 Hz) at 1.0 mA for 30 minutes, at Du 20 and Du 26 greatly reduced the infarction to $4.5\% \pm 1.5\%$ ($P < 0.01$), significantly improved neurological deficit (scale = 1.0 ± 0.5 , $P < 0.01$), and decreased the death rate to 7% (2 out of 30, $P < 0.01$). Similarly, EA at left LI 11 & PC 6 reduced the infarct volume to $8.6\% \pm 3.8\%$ ($P < 0.01$), improved the neurological deficit (scale = 2.0 ± 1.0 , $P < 0.01$), and decreased the death rate to 8% (2 out of 24, $P < 0.01$). In sharp contrast, EA at right LI 11 & PC 6 did not lead to any significant changes in the infarct volume ($33.4\% \pm 6.3\%$), neurological deficit (scale = 6.5 ± 0.5), and the death rate (20%, 5 out of 24). EA at left GB 34 & SP 6, also had an inconspicuous effect on the ischemic injury. EA at Du 20 & Du 26 or at left LI 11 & PC 6 instantaneously induced a significant increase in cerebral blood flow. Neither EA at right LI 11 & PC 6 nor at GB 34 & SP 6 increased cerebral blood flow. These results revealed that the EA protection against cerebral ischemia is relatively acupoint specific.

1. Introduction

Brain hypoxia/ischemia, as in stroke, causes neuronal injury [1–4] and results in neurological disability and death. Prevention and early treatment are paramount in reducing its devastating effects on affected individuals and their families. However, treatment strategies are presently very limited in spite of extensive research over several decades. Seeking new and effective therapy, including complementary and alternative approaches to prevent/treat ischemic injury, is of utmost importance.

Traditional Chinese Medicine (TCM) has long advocated the use of acupuncture to treat stroke and other neurological disorders. Indeed, several ancient TCM books, for example, Huangdi Nei Jing (*Huangdi's Internal Classic*) and “Handbook

of Prescriptions for Emergencies” (*Zhou Hou Fang*), both contain descriptions of acupuncture therapy for stroke-like disorders. In recent years, a substantial amount of the literature has appeared on the use of manual acupuncture or EA for the brain protection against ischemic injury in both human subjects and animal models [5–15]. However, there are still controversies in terms of the clinical outcome [16–18]. The evidence on the effectiveness of acupuncture in stroke patients was inconclusive under clinical settings, which could be attributed to poor methodological quality and small samples. Further high-quality, randomized controlled trials with long-term followups are needed [18].

Acupuncture induces a complex effect on the central nervous system [19–22] and thus displays therapeutic effects

on the body, which is influenced by multiple factors, especially stimulation manner/parameters and location (acupoints). Differences in various methods and acupoints of acupuncture manipulation may greatly affect immediate efficacy and long-term prognosis of patients. However, there is a lack of knowledge on optimal acupuncture conditions for the treatment of ischemic injury. Traditional Chinese Medicine recommends various acupoints located over different parts of the body along with different methods of acupunctural stimulation. However, most of these recommendations are based on personal experiences and have not been subjected to scientific testing. Therefore, optimizing acupuncture conditions for maximal efficacy is of critical value because different manipulations of acupuncture can result in completely different outcomes. For obvious reasons, it is difficult, if not impossible, to conduct such tests on patients and therefore must be done largely via animal studies.

Recently, we determined the appropriate EA parameters for cerebral protection against ischemia [9, 13]. In fact, our findings suggest that the current frequency and intensity for EA stimulation differentially alters cerebral blood flow and infarct volume in the rat brain exposed to middle cerebral artery occlusion (MCAO). Since there are multiple acupoints all over the body and EA effects are generally acupoint specific, it is equally important to define the specific roles corresponding to each relevant acupoint. Although there are sporadic studies that suggest that Baihui (Du 20) might be better than other acupoints for EA-induced protection against cerebral ischemia [11, 15, 23], a comparative evaluation of various acupoints has yet to be performed.

In order to clarify the fundamental issue concerning the specificity of acupoints in EA-induced cerebral protection against ischemia, we performed a number of experiments on rats to investigate the specific outcomes of stimulation of acupoints located in various regions of the body under ischemic conditions. We specifically chose 4 pairs of “acupoints” in the head, left posterior limb, and left and right anterior limbs, respectively, in addition to the controls. We performed constant monitoring to record the effects on blood flow, neurological deficits, and ischemic infarction in the ischemic brain for a reliable comparison between all groups. Our present data, consistent with our preliminary findings [10], shows that the acupoints in the head and left (contralateral) anterior limb confer maximum protection against ischemic injury in the MCAO rat model, suggesting the importance of these acupoints in the cerebral protection in stroke.

2. Materials and Methods

2.1. Animals. Adult male Sprague-Dawley rats (250 g \pm 10 g) were purchased from the Experimental Animal Center for Shanghai Chinese Academy of Science and housed at an ambient temperature of 24 \pm 1°C with free access to food and water. All surgical procedures were performed under anesthesia (chlorate hydrate, 400 mg/kg, i.p.). All animal procedures were approved by the Animals Care and Use Committees of Fudan University Shanghai Medical College, Shanghai, China.

2.2. Monitoring Cerebral Blood Flow. A laser-Doppler perfusion monitor (LDPM, PeriFlux5000, Perimed, Sweden) was used for the measurement of cerebral blood flow. The main procedure [24] was as follows. A little round hole located at 1.5 mm posterior to the bregma and 5 mm lateral to the sagittal suture was drilled in the right parietal bone and a laser Doppler probe (0.45 mm diameter) was then inserted at a depth of 2 mm to approach the superficial microvessels in the cerebral pia mater to measure blood perfusion of the cortex as an index of cerebral blood flow. The probe was then fixed on the skull bone. Changes in cerebral blood flow were continuously monitored in all animals beginning at least 5 min before the induction of cerebral ischemia to about 15 min after reperfusion (until animal revival). According to the manufacturer, change in perfusion values depends on the number of blood cells present in the area illuminated by the probe tip and the speed at which they move. The changes in blood perfusion recorded as a measure of the dynamic changes in the cerebral blood flow in a localized area were constantly monitored in real time using LDPM. The values measured by LDPM were automatically expressed as perfusion units (PUs), concentration of the moving blood cells (CMBC), and the velocity of blood cells (Velocity). Of these values, PU is the most important index of cerebral blood flow and represents the product of the relative number of moving blood cells and their relative velocities.

2.3. Induction of Cerebral Ischemia. The focal cerebral ischemia model was established by performing the middle cerebral artery occlusion (MCAO) based on the methods described by Longa et al. [25]. Briefly, the rats were surgically operated under anesthesia to expose their right common carotid, the external carotid, and the internal carotid arteries. After ligating the distal end of the right external carotid artery, it was incised and a segment of 4-0 monofilament nylon suture (30 mm length, 0.18 mm diameter with a 0.24 mm diameter round tip, MONOSOF, SN-1699G, USA) was inserted from the right external carotid artery into the right internal carotid artery for a length of ~20 mm (reaching the origin of the right middle cerebral artery) to occlude the blood flow of the right middle cerebral artery.

To standardize our experimental conditions across all experimental groups, we constantly monitored the blood flow in all animals to make sure that a relatively uniform level of cerebral ischemia existed before experimentation. The blood flow was controlled by adjusting the suture in the artery for the induction of ischemia. The ischemic rats that showed a stable drop of ~85% in PU compared to the baseline level (before MCAO), that is, reaching a level of ~15% of the baseline PU, were used for further experimentation. This ischemic condition was kept constant with minor fluctuations during the entire ischemic period. After the occlusion, reperfusion of the ischemic area was allowed by withdrawing the suture from the right external carotid artery. Changes in cortical blood flow were constantly monitored in all animals beginning at least 5 mins before MCAO and continuing up to 15 mins after reperfusion (until animal recovered from the anesthesia). This period included the entire course of MCAO as well as the full length of EA.

Body temperature was monitored by a rectal thermometer and maintained at $36.5^{\circ}\text{C} \pm 0.5^{\circ}\text{C}$ from the start of the surgical procedures till the animal recovered from anesthesia. After the reperfusion, the animals were housed for 24 hours at an ambient temperature of $24 \pm 1^{\circ}\text{C}$. In the sham-operation group, the same surgical procedures other than artery occlusion were performed.

2.4. Application of Electroacupuncture. EA was delivered to 4 pairs of “acupoints” to compare their effects on brain protection and blood flow, those being “Shuigou” (Du 26) and “Baihui” (Du 20), left “Quchi (LI 11)” and “Neiguan” (PC 6), right “Quchi (LI 11)” and “Neiguan” (PC 6), and left “Yanglingquan” (GB 34) and “Sanyinjiao (SP 6). As described previously [13, 19, 26], “Shuigou (Du 26)” and “Baihui (Du 20)” are acupoints on head and face. Shuigou (Du 26) is located in the center of the upper lip situated at a point 2/3rds from the mouth on a line connecting mouth and nose. Baihui (Du 20) is located on the midline of the head, approximately at the midpoint of the line connecting the apices of the two auricles. The depth of the needle used on Du 26 was 1 mm vertically into the skin and 2 mm obliquely into Du 20. “Quchi (LI 11)” and “Neiguan” (PC 6) are acupoints on the anterior limbs. “Quchi (LI 11)” is in the depression on the lateral side of the elbow joint, and “Neiguan” (PC 6) is at the suture between ulnar and radial bones with a distance of 3 mm superior to the wrist joint. Left “Quchi (LI 11)” and “Neiguan” (PC 6) are contralateral to the ischemic cerebral hemisphere. Right “Quchi (LI 11)” and “Neiguan” (PC 6) are ipsilateral to the ischemic cerebral hemisphere. The depth of the needle on LI 11 is 4 mm vertically to the skin and PC 6 is 2 mm vertically. “Yanglingquan” (GB 34) and “Sanyinjiao (SP 6) are acupoints on the posterior limbs. “Yanglingquan” (GB 34) is located in the depression below the capitulum fibulae posterolateral to the knee joint, and “Sanyinjiao (SP 6) is at a point 10 mm superior to the tip of the medial malleolus. Left “Yanglingquan” (GB 34) and “Sanyinjiao (SP 6) are contralateral to the ischemic cerebral hemisphere. The depth of the needle under GB 34 was 5 mm vertically to the skin and that under SP 6 was 6 mm vertically to the skin.

The “optimal” stimulation parameters, that is, sparse-density wave (5 Hz/20 Hz) at 1.0 mA, were chosen based on our previously described reports [9, 13]. In all four EA groups, the same parameters were adopted with only a difference in the acupoint stimulated. EA was started 5 min after the onset of MCAO and was continued for 30 min. It was delivered through stainless steel filiform needles (15 mm length with 0.3 mm in diameter, Suzhou Medical Apparatus Limit Co., China) by an EA apparatus (Model G-6805-II, Shanghai Medical Instruments High-Tech Co., China). This EA apparatus has been widely used in the practice of clinical acupuncture in Traditional Chinese Medicine. The intensity and frequency of the output waves with negative-going pulse on the posterior border (pulse width = 0.5 ± 0.1 ms; component of direct current = 0) were monitored by a general oscillograph (Model XJ4210A, Shanghai XinJian Instrument and Equipment Co., China).

The ischemic rats with MCAO were randomly divided into 5 groups: MACO only (Ischemia, $n = 60$), Ischemia + EA

at Du 20 and Du 26 ($n = 30$), Ischemia + EA at left LI 11 and PC 6 ($n = 24$), Ischemia + EA at right LI 11 and PC 6 ($n = 24$), and Ischemia + EA at left SP 6 and GB 34 ($n = 24$). Finally, to achieve a strict control, we applied comparable acupoint stimulation using the same EA parameters for both ischemic and nonischemic rats and measured the changes in their cerebral blood flow ($n = 8$) to determine if EA has an acupoint-specific effect on the cerebral blood flow under ischemia.

2.5. Evaluation of Death Rate and Neurological Deficits. In our experiments, some ischemic rats died between 2 and 20 hrs after reperfusion. The death rates were calculated based on the number of dead rats within this period and the total number of rats in the given group. Although the deaths could be attributed to a myriad of causes including hemorrhage, we did not investigate the cause of death as part of the study objectives as our aim here was to compare the death rates among various groups.

Neurological behaviors were evaluated in all groups, excluding the rats that died within 24 h after MCAO. Neurological deficits were evaluated at 24 h after the reperfusion (right before sampling brain tissue for detection of ischemic infarction and other tests). The evaluation of neurological deficits was blinded, that is, the one who judged and scored the degree of neurological deficits according to the preset criteria did so without any knowledge about the grouping and treatments. The degree of neurological deficits was graded on a scale of 0 to 7 [13]. The criteria were set as follows: Grade 0—“normal”, symmetrical movement without any abnormal signs; Grade 1—incomplete stretch of the left anterior limb when the tail was lifted up; Grade 2—dodderly crawl along with the signs of Grade 1; Grade 3—kept the left anterior limb close to the breast when the tail was lifted up; Grade 4—left turn when crawling; Grade 5—left anterior claw pushed backward along with the signs of Grade 4; Grade 6—repeated rotational motion with an immotile posterior left limb; Grade 7—left recumbent position because of body supporting incapability.

2.6. Measurement of Cerebral Infarct Volume. Following the evaluation of neurological deficits at 24 h after reperfusion, the rats were sacrificed under anesthesia, and sections of their brains were obtained as 2.0 mm slices ($n = 12 \sim 18$). The brain slices were incubated in a solution of triphenyltetrazolium chloride (TTC, 20 g/L) for 30 minutes at 37°C and then transferred into paraformaldehyde solution (40 g/L) to fix the area of infarct. The infarct region presented as white or pale in color while “normal” tissue showed up as red [13, 27, 28]. The images of the brain slices were taken with a digital camera attached to a computer system. The area/volume of infarct was analyzed by a computer-assisted image system with ACT-2U software (Nikon). Relative infarct ratio was calculated using the following equation [24]: $(2 * \text{left hemisphere area (non-ischemic side)} - \text{noninfarct area of whole brain slices}) / (2 * \text{left hemisphere areas}) * 100\%$. This equation excludes the factors that could result in an inaccurate calculation of the infarct volume (such as edema).

TABLE 1: Effects of EA at different acupoints on cerebral ischemia.

Groups	Scales of neurological deficit	Infarct volume	Death rate
Ischemia	6.0 ± 0.5 (6 ~ 7) (<i>n</i> = 50)	32.9% ± 3.8% (<i>n</i> = 18)	17% (10 out of 60)
Ischemia + EA (Du 20 & Du 26)	1.0 ± 0.5 (0 ~ 2) (<i>n</i> = 28) [△]	4.5% ± 1.5% (<i>n</i> = 12)*	7% (2 out of 30) [▽]
Ischemia + EA (left LI 11 & PC 6)	2.0 ± 1.0 (1 ~ 3) (<i>n</i> = 22) [△]	8.6% ± 3.8% (<i>n</i> = 12)*	8% (2 out of 24) [▽]
Ischemia + EA (right LI 11 & PC 6)	6.5 ± 0.5 (6 ~ 7) (<i>n</i> = 19)	33.4% ± 6.3% (<i>n</i> = 12)	20% (5 out of 24)
Ischemia + EA (left SP 6 & GB 34)	6.0 ± 1.0 (5 ~ 7) (<i>n</i> = 21)	29.8% ± 4.5% (<i>n</i> = 12)	13% (3 out of 24) [#]

Ischemia: the rats were subjected to right MCAO for 1 hour and reperfusion for 24 hours. Ischemia + EA at Du 20 & Du 26: EA (1.0 mA, 5/20 Hz, sparse-density wave) was delivered to the acupoints of “Baihui” (Du 20) and “Shuigou” (Du 26) of the ischemic rats for 30 min. Ischemia + EA at left LI 11 & PC 6: EA was delivered to the acupoints of “Quchi” (LI 11) and “Neiguan” (PC 6) on the left anterior limb of the ischemic rats for 30 min. Ischemia + EA at right LI 11 & PC 6: EA was delivered to the acupoints of “Quchi” (LI 11) and “Neiguan” (PC 6) on the right anterior limb of the ischemic rats for 30 min. Ischemia + EA at left SP 6 & GB 34: EA was delivered to the acupoints of “Sanyinjiao” (SP 6) and “Yanglingquan” (GB 34) on the left posterior limb of the ischemic rats for 30 min. [△]*P* < 0.01 versus Ischemia. **P* < 0.01 versus Ischemia. [▽]*P* < 0.01 versus Ischemia. [#]*P* < 0.05 versus Ischemia. Note that both EA at Du 20 & Du 26 and EA at left LI 11 & PC 6 significantly reduced the neurological deficit, brain infarct volume, and death rate.

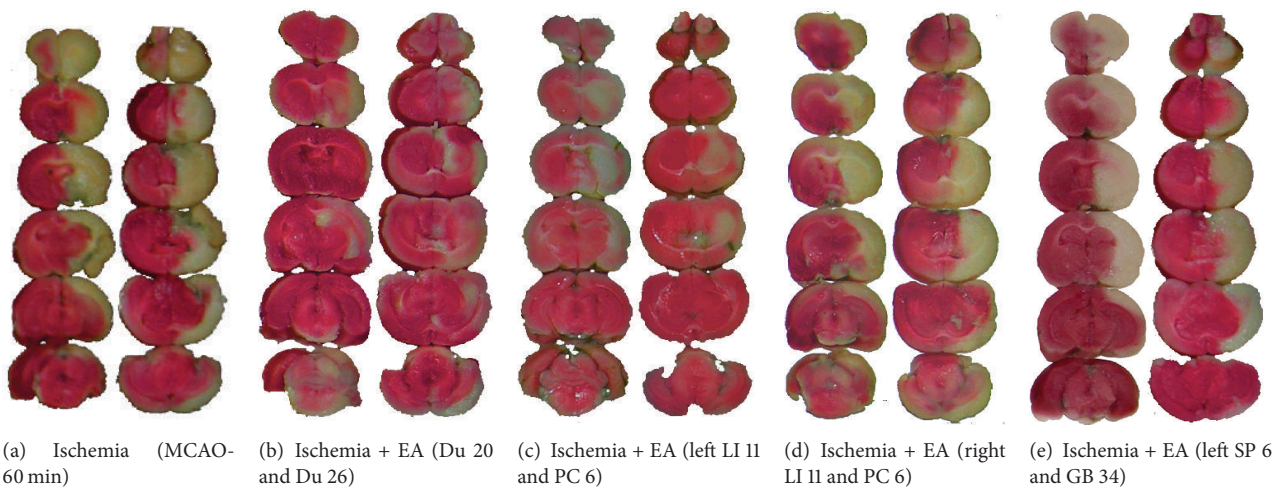


FIGURE 1: EA-induced reduction in the infarct volume varied with stimulation of different acupoints. The brain slices were subjected to TTC staining and the ischemic infarct volume was quantified by a computerized image system. Note that the infarct region (pale-white portion) was mainly located in the striatum and the frontoparietal cortex in the right hemisphere. The slices on the *right* of each column show the backside of the *left* slices. The MCAO-induced infarction (a) was significantly reduced by EA treatment at the acupoints Du 20 and Du 26 (b) and LI 11 and PC 6 on the left anterior limb (c). In contrast, EA treatment with the same parameters at the acupoints LI 11 and PC 6 on the right anterior (d) and SP 6 and GB 34 on the left posterior limbs (e) enabled no appreciable protection against cerebral infarction.

2.7. Data Analysis. Cerebral blood flow was determined as a measure of PU, CMBC, and Velocity. All values in each animal were compared to the baseline values measured before MCAO. The grouped values were compared across various groups. Neurological deficits were evaluated and expressed as an average value of the grade per group. Cerebral infarct volume was expressed as a percentage of the whole cerebrum.

All data are presented as mean ± SD and subjected to statistical analysis. The rate of death was compared using the Chi-square test. All other data were subjected to Analysis of variance (ANOVA), *t*-test, Rank-Sum test, and/or Chi-square test. The changes were considered as significant if the *P* value was less than 0.05.

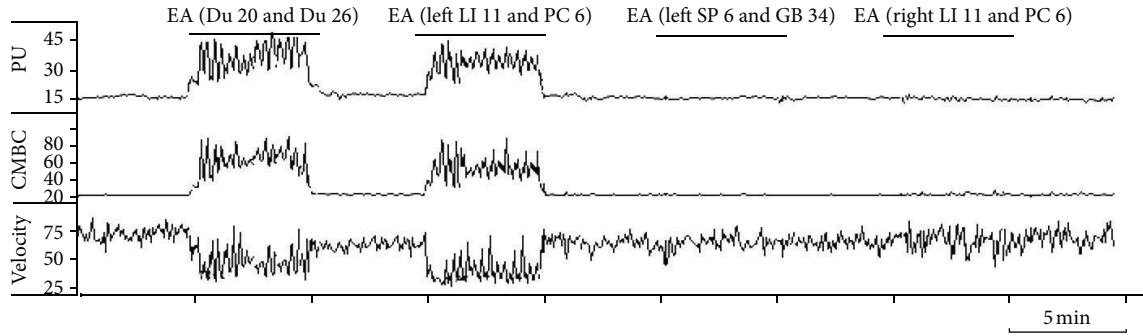
3. Results

3.1. EA Protection against Ischemic Injury Varied with Different Acupoints. In the Ischemia group (MCAO only, *n* = 60), 17% (10/60) of the rats died in less than 24 hrs after 60 min of

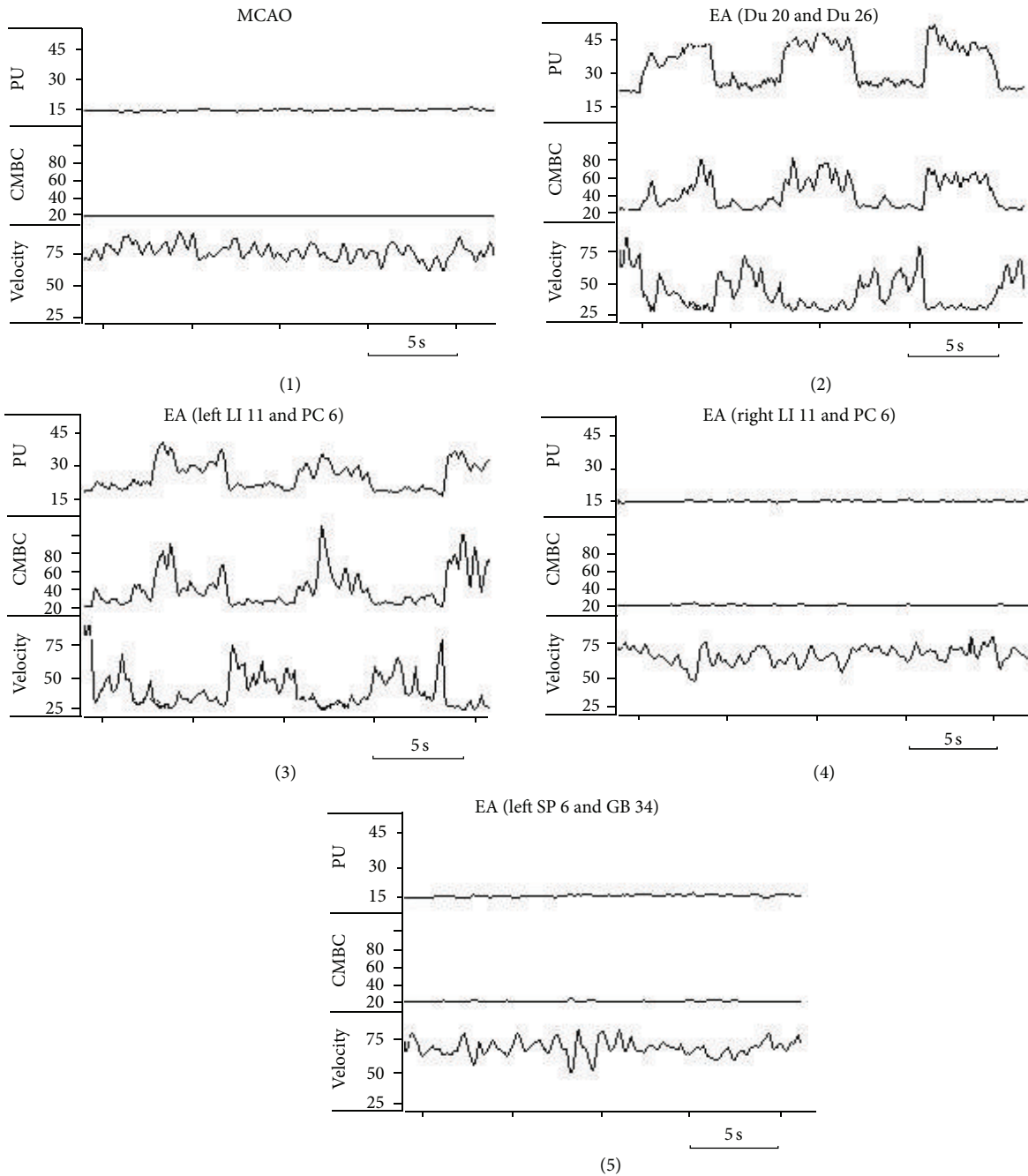
MCAO. At 24 h after reperfusion, the remaining rats showed serious neurological deficits (Grade 6.0 ± 0.5, *n* = 50) with a cerebral infarct volume around one-third of the volume of the whole brain (32.9% ± 3.8%, *n* = 18) (Table 1, and Figure 1(a)). The infarct areas were extensively distributed in the right frontoparietal lobe of the cortex and the striatum. The ischemic side was very swollen.

In the group of Ischemia + EA at Du 20 and Du 26 (*n* = 30), 7% (2/30) of rats died within 2–10 hrs after MCAO (*P* < 0.01 versus Ischemia). At 24 h after reperfusion, the remaining rats showed a significant improvement of neurological deficits as compared to the ischemia alone group (Grade 1.0 ± 0.5, *n* = 28, *P* < 0.01 versus Ischemia) with a greater reduction of infarct volume, chiefly limited to the right striatum (4.5% ± 1.5%, *n* = 12, *P* < 0.01 versus Ischemia) (Table 1 and Figure 1(b)).

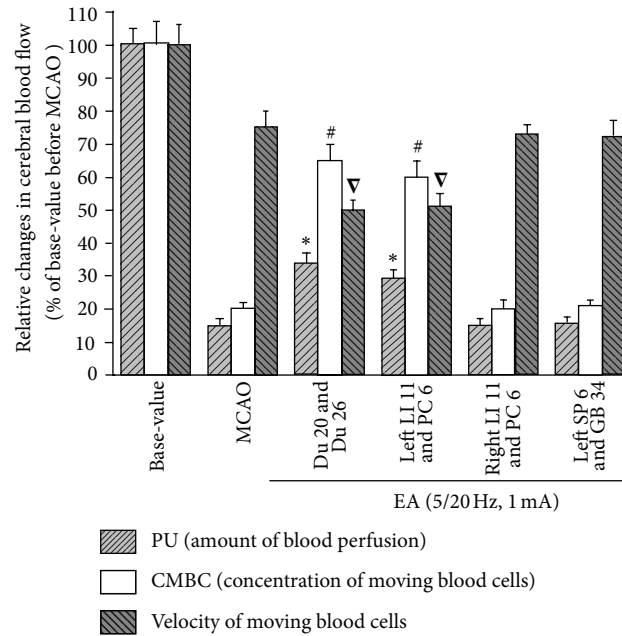
In the group of Ischemia + EA at left LI 11 and PC 6 (*n* = 24), 8% (2/24) of rats died within 2–10 hrs after MCAO (*P* < 0.01 versus Ischemia). At 24 h after reperfusion,



(a) Effects of EA at different acupoints on the blood flow in the ischemic cortex



(b) Major differences in the blood flow in response to EA at different acupoints



(c) Averaged changes in the blood flow in response to EA at different acupoints

FIGURE 2: EA-induced changes in CBF in the ischemic cortex varied with stimulation of different acupoints. The CBF was measured in 6 ischemic rats subjected to EA treatment at different acupoints. Blood perfusion (PU), concentration of moving blood cells (CMBC), and velocity of blood cells (Velocity) were measured by a laser Doppler perfusion monitor system. (a) Changes in CBF in response to EA at different acupoints. (b) CBF in each EA condition. (c) Statistical summary of the changes in CBF in response to EA stimuli. * $P < 0.01$, MCAO versus MCAO plus EA (PU); # $P < 0.01$, MCAO versus MCAO plus EA (CMBC); ∇ $P < 0.05$, MCAO versus MCAO plus EA (Velocity). Note that EA at acupoints Du 20 and Du 26 and left LI 11 and PC 6 induced isochronous increase in PU and CMBC in addition to a decrease in Velocity, but EA at right LI 11 and PC 6 acupoints and left SP 6 and GB 34 acupoints had no significant effects on CBF despite using the same EA parameters.

the remaining rats showed significantly attenuated neurological deficits (Grade 2.0 ± 1.0 , $n = 22$, $P < 0.01$ versus Ischemia) and a greatly reduced infarct volume ($8.6\% \pm 3.8\%$, $n = 12$, $P < 0.01$ versus Ischemia) (Table 1 and Figure 1(c)).

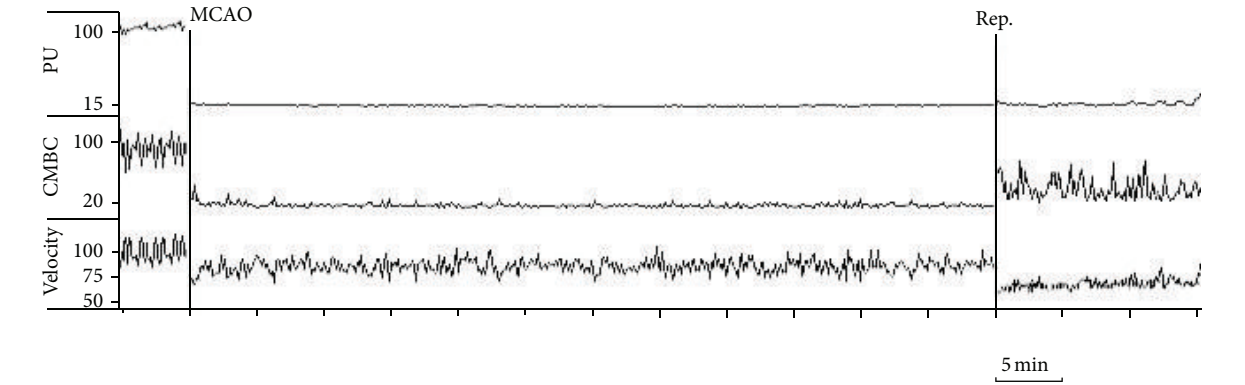
In the group of Ischemia + EA at right LI 11 and PC 6 ($n = 24$), 20% (5/24) of rats died within 2–20 hrs after MCAO ($P > 0.05$ versus Ischemia). At 24 h after reperfusion, the remaining rats showed serious neurological deficits (Grade 6.5 ± 0.5 , $n = 19$, $P > 0.05$ versus Ischemia) with the cerebral infarct volume approximately one-third of the whole brain ($33.4\% \pm 6.3\%$, $n = 12$, $P > 0.05$ versus Ischemia) (Table 1 and Figure 1(d)).

In the group of Ischemia + EA at left SP 6 and GB 34 ($n = 24$), 13% (3/24) rats died within 2–10 hrs after MCAO ($P < 0.05$ versus Ischemia). At 24 h after reperfusion, the remaining rats showed serious neurological deficits (Grade 6.0 ± 1.0 , $n = 21$, $P > 0.05$ versus Ischemia) with the cerebral infarct volume approximately one-third of the whole brain ($29.8\% \pm 4.5\%$, $n = 12$, $P > 0.05$ versus Ischemia) (Table 1 and Figure 1(e)).

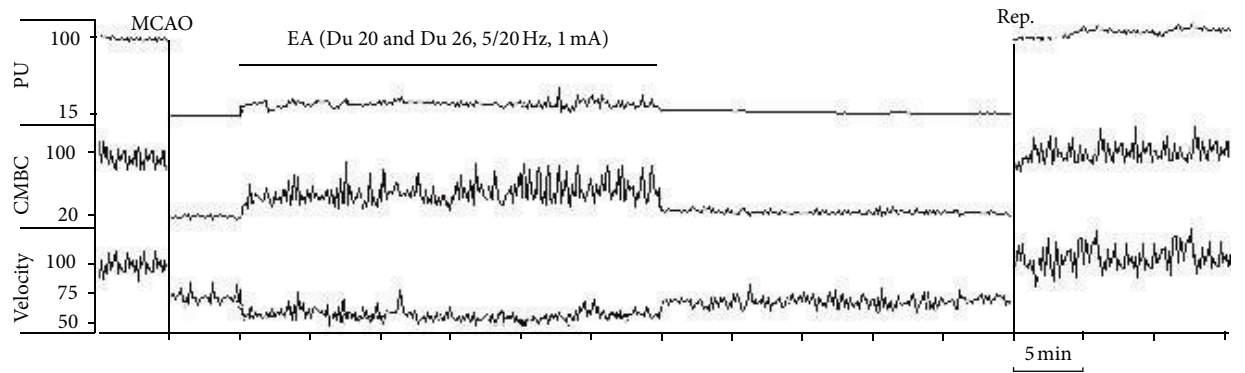
3.2. EA-Induced Changes in Cerebral Blood Flow Varied with Different Acupoints. Considering that an insufficient blood flow causes cerebral ischemic injury, we wondered if EA neuroprotection against cerebral ischemia was rendered

through regulation of the blood supply to the ischemic brain and whether this regulation changed with a difference in the acupoints stimulated. Using a laser-doppler perfusion monitor, we monitored the real-time changes in cerebral blood flow in all experimental groups.

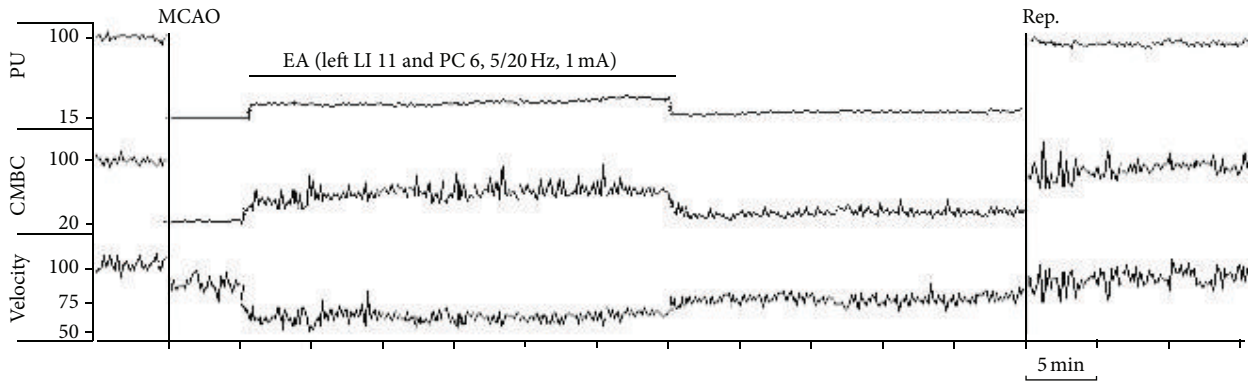
Firstly, we tested if brief stimulation of these acupoints alters the blood flow on the ischemic rats ($n \geq 6$, repeated ≥ 6 times for each pair of acupoints). EA with 5/20 Hz sparse-density current at 1.0 mA was delivered to the acupoints in a manner of 5 min stimulation/5 min cessation. When a nylon suture was successfully inserted into the appropriate place of right middle cerebral artery, the blood perfusion of the monitored cortex decreased immediately from average 100 ± 20 PU to 15 ± 2 PU, that is, a $\sim 85\%$ drop in blood supply with a decrease in CMBC by $\sim 80\%$ and relatively slight deceleration of blood cell velocity by $\sim 25\%$ ($P < 0.05$) (Figures 2(a), 2(b)(1), and 2(c)). EA stimulation at Du 20 and Du 26 immediately induced a significant increase in blood flow. This increase in blood perfusion was synchronous to EA. Among the changes in blood flow, EA induced a 2-fold increase in PU (from $\sim 15\%$ to $\sim 32\%$ of the base level before MCAO, $P < 0.01$) with a 3-fold increase in CMBC (from $\sim 20\%$ to $\sim 65\%$ of the base level, $P < 0.01$) and a slight decrease in the Velocity (from $\sim 75\%$ to $\sim 50\%$ of the base-value, $P < 0.05$) (Figures 2(a), 2(b)(2), and 2(c)). Similarly,



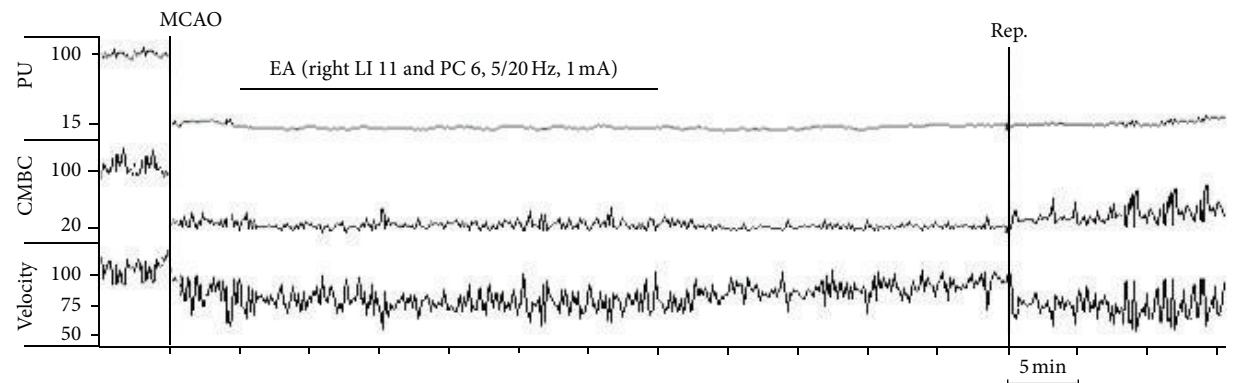
(a) Effect of 60-minute MCAO on cortical blood flow



(b) Effect of EA at "Baihui" (Du 20) and "Shuigou" (Du 26) on cortical blood flow

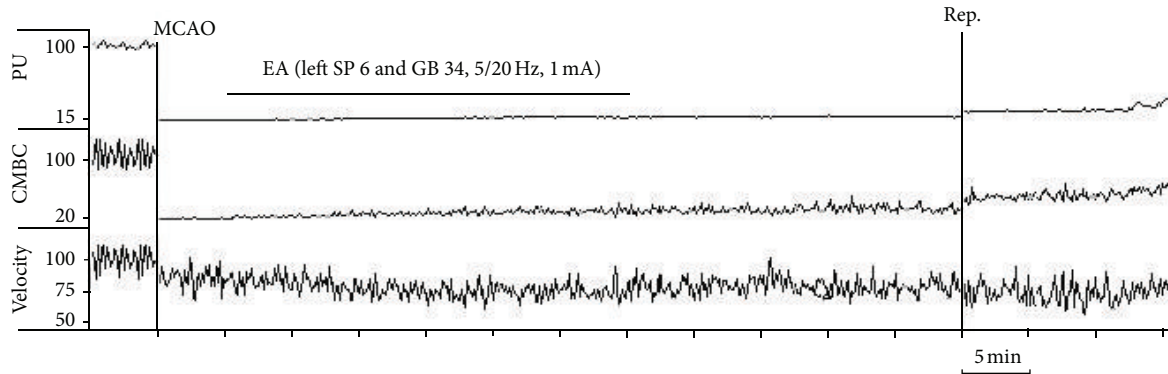


(c) Effect of EA at left "Quchi" (LI 11) and "Neiguan" (PC 6) on cortical blood flow



(d) Effect of EA at right "Quchi" (LI 11) and "Neiguan" (PC 6) on cortical blood flow

FIGURE 3: Continued.



(e) Effect of EA at left “Sanyinjiao” (SP 6) and “Yanglingquan” (GB 34) on cortical blood flow

FIGURE 3: Representative trace recordings of the blood flow. Blood perfusion (PU), concentration of moving blood cells (CMBC), and Velocity of blood cells (Velocity) were measured in the ischemic rats by a laser Doppler perfusion monitor system. (a) Effect of MCAO-60 min on CBF during ischemia and reperfusion in the Ischemia group. (b) Effect of EA at acupoints Du 20 and Du 26 on CBF. (c) Effect of EA at left LI 11 and PC 6 on CBF. (d) Effect of EA at acupoints right LI 11 and PC 6 on CBF. (e) Effect of EA at acupoints left SP 6 and GB 34 on CBF. Note that the PU and CMBC decreased immediately after the right middle cerebral artery was occluded by a nylon suture. The blood flow was kept at a low level with fluctuant waves during the entire MCAO duration. After onset of reperfusion, PU and CMBC increased while the velocity further decreased. EA at right LI 11 and PC 6 acupoints induced no significant change in the CBF during or after MCAO. EA at left SP 6 and GB 34 acupoints induced no significant change in the CBF during the early stages of MCAO, but slightly increased the CMBC after a 10–15 min period of EA. EA stimulation at acupoints Du 20 and Du 26 or left LI 11 and PC 6 induced an isochronous increase in PU and CMBC with a decrease in velocity. After reperfusion, PU, CMBC, and Velocity all increased rapidly and reached the baseline values.

EA at left LI 11 and PC 6 also significantly increased the blood flow immediately after the onset of EA. During the EA stimulation, PU increased almost 2 folds (from ~15% to ~29% of the base-value, $P < 0.01$) with a significant 3-fold increase in CMBC (from ~20% to ~60% of the base level, $P < 0.01$) and a slight decrease in the Velocity (from ~75% to ~50% of the base level, $P < 0.05$) (Figures 2(a), 2(b)(3), and 2(c)). In sharp contrast, EA at right LI 11 and PC 6 (Figures 2(a), 2(b)(4), and 2(c)) and left SP 6 and GB 34 (Figures 2(a), 2(b)(5), and 2(c)) did not induce any significant changes in blood flow despite the use of same EA parameters.

Based on these initial observations, we systematically investigated the changes in blood flow from the time before MCAO to the early stage of the reperfusion. Specifically, the recording started 5 mins prior to MCAO and continued on to 15 mins after the onset of reperfusion (suture withdrawal). EA started at 5 min after the onset of MCAO for a duration of 30 mins with the same stimulation parameters, that is, 5/20 Hz sparse-dense pulse at 1.0 mA in all groups (Figures 3–6). We then compared the differences in cerebral blood flow at the pre-MCAO level, and during MCAO with/without EA in various groups.

In the Ischemia group (MCAO for 60 min, $n = 30$), there was an immediate ~85% decrease in blood perfusion of the monitored cortex. The blood flow was kept constant at this low level for the entire duration of MCAO. The CMBC also decreased to ~20% of the baseline level (the level before MCAO), and the blood cell velocity decreased to 75% of the baseline (Figures 3(a) and 4–6).

In the group of Ischemia + EA at Du 20 and Du 26 ($n = 30$), EA significantly increased the blood flow immediately after the onset of stimulation with the increase in blood

perfusion being synchronous to EA application. The EA-induced changes in blood flow induced a 2-fold increase in PU over the ischemic level ($P < 0.01$), CMBC increased by over 3 folds ($P < 0.01$), and the Velocity slightly decreased by ~33% ($P < 0.05$) (Figures 3(b), 4(a), 5(a), and 6(a)). As the stimulation ceased, the blood flow immediately decreased to the MCAO level.

In the group of Ischemia + EA at left LI 11 and PC 6 ($n = 24$), EA significantly increased regional blood flow immediately after application. Specifically, PU increased by 2 folds over the ischemic (MCAO) level ($P < 0.01$), CMBC significantly increased by 3 folds ($P < 0.01$), and the Velocity slightly decreased by >30% of the MCAO level ($P < 0.05$) (Figures 3(c), 4(b), 5(b), and 6(b)). As the stimulation ceased, the blood flow rapidly returned to the MCAO level.

In sharp contrast to the previous groups, EA at right LI 11 and PC 6 ($n = 12$) did not induce any significant changes in blood flow during MCAO (Figures 3(d), 4(c), 5(c), and 6(c)). The same was true for EA at left SP 6 and GB 34 ($n = 24$). In this group, EA did not significantly alter the blood flow in the first 10–15 minutes. In the later stage of EA, however, CMBC gradually increased with a slight reduction in the Velocity, although, the value of PU showed no significant change (Figures 3(e), 4(d), 5(d), and 6(d)).

3.3. Recovery of the Blood Flow during Reperfusion Varied among Various Groups. In the Ischemia group, following nylon suture removal after a 60-min MCAO, PU slightly increased to 25% of the control (pre-MCAO) level ($P < 0.05$ versus MCAO) and CMBC increased to ~55% of the control level ($P < 0.01$ versus MCAO). However, the velocity of blood cells further decreased during the transition from ischemia

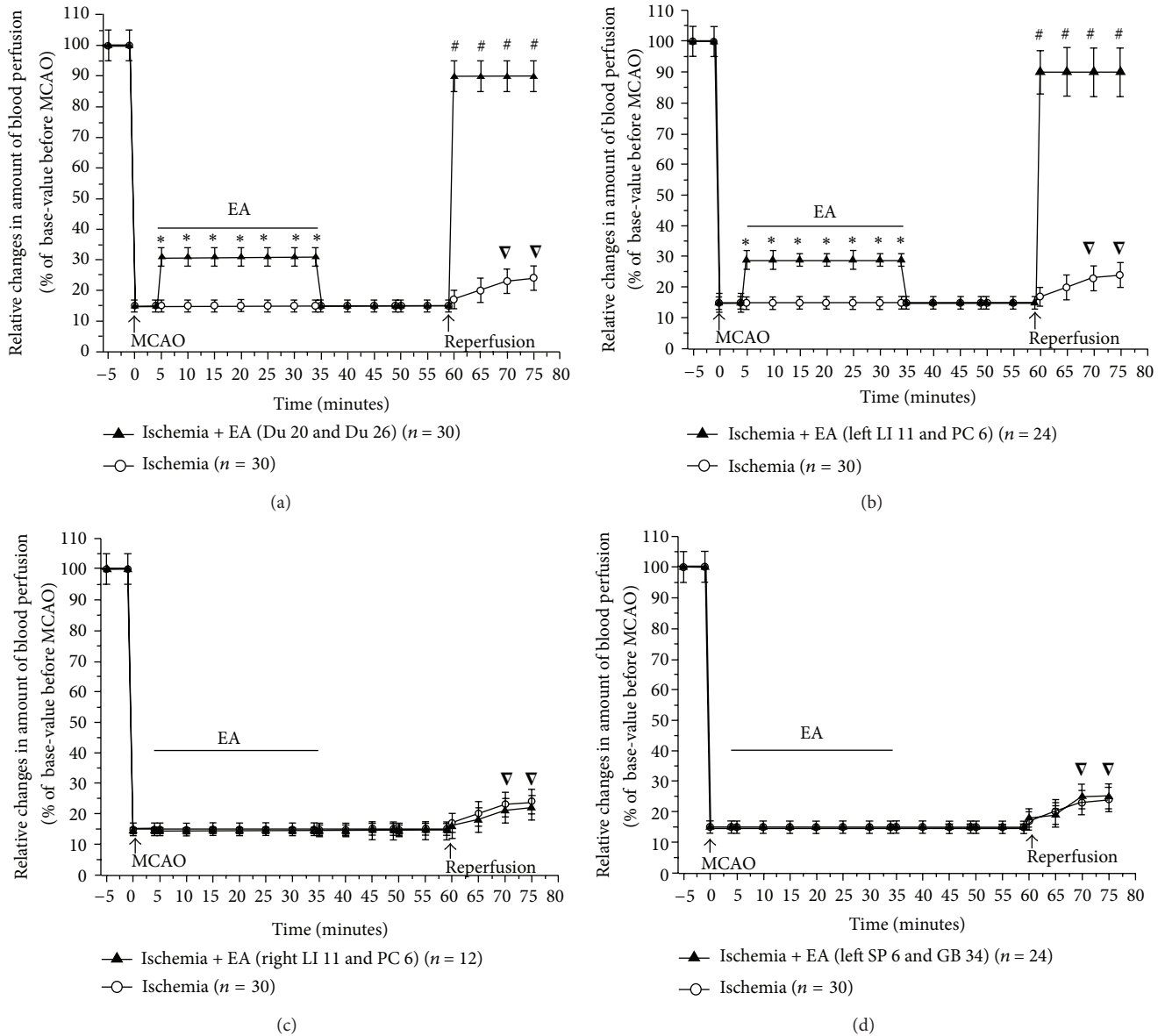


FIGURE 4: Statistical data on cerebral blood flow (PU) in ischemic cortex in MCAO/reperfusion rats with/without EA at different acupoints. PU was measured and compared between the groups. * $P < 0.01$, MCAO + EA versus MCAO; $\nabla P < 0.05$, reperfusion versus MCAO; # $P < 0.01$, reperfusion in MCAO + EA group versus reperfusion in MCAO group. Note that in the Ischemia group, MCAO (0 min) decreased PU to ~15% of the base level before MCAO (-5 min). After the onset of reperfusion, PU increased slightly to ~25%. In the group of EA at Du 20 and Du 26, EA increased PU to ~32% of base level before MCAO. In the group of EA at left LI 11 and PC 6, EA also increased PU to ~29% of base level before MCAO. After the onset of reperfusion, PU in the groups of EA at Du 20 and Du 26 and left LI 11 and PC 6 almost immediately returned to >90% of the pre-MCAO level. However, EA at right LI 11 and PC 6 and left SP 6 and GB 34 did not significantly improve the CBF during MCAO and after reperfusion.

to reperfusion, that is, from 75% to 50% of the control (pre-MCAO) level ($P < 0.05$ versus MCAO) in the first 15 minutes after the blood reperfusion. These results indicate a constant hypoperfusion during MCAO and even after reperfusion, which was mainly due to a decrease in moving blood cells (CMBC) in MCAO or a reduction of blood cell velocity during reperfusion (Figures 3(a) and 4-6).

In the group of Ischemia + EA at Du 20 and Du 26 (Figures 3(b), 4(a), 5(a), and 6(a)) and the the group of

Ischemia + EA at left LI 11 and PC 6 (Figures 3(c), 4(b), 5(b), and 6(b)), the cerebral blood flow (PU, CMBC, and Velocity) gradually increased to the control (pre-MCAO) during reperfusion.

The group of Ischemia + EA at right LI 11 and PC 6 demonstrated a comparable change in the blood flow during reperfusion as seen in the Ischemia alone group (Figures 3(d), 4(c), 5(c), and 6(c)). The group of Ischemia + EA at left SP 6 and GB 34 (Figures 3(e), 4(d), 5(d), and 6(d)) showed changes

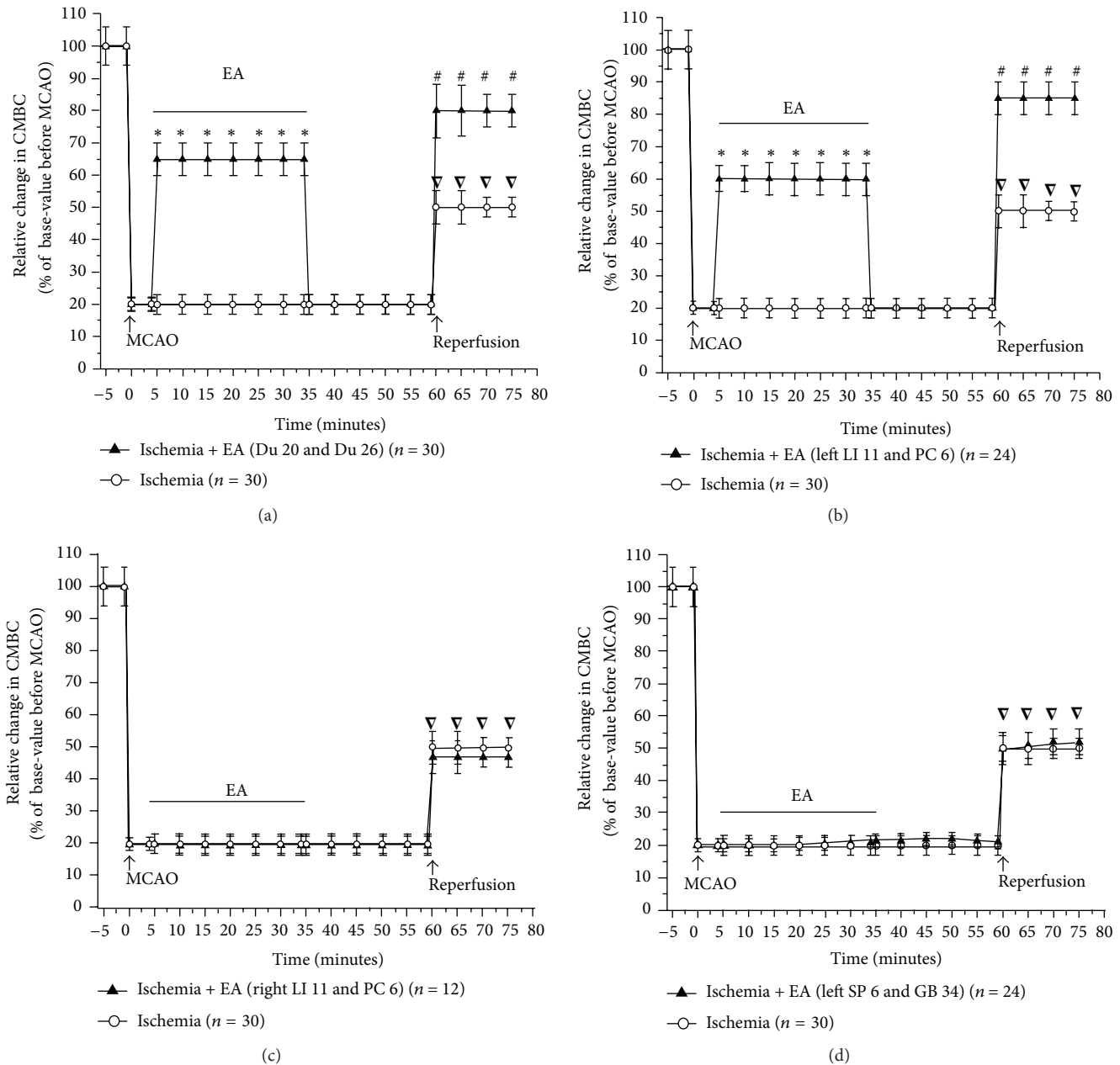


FIGURE 5: Statistical data on the concentration of moving blood cells (CMBC) in the ischemic cortex in MCAO/reperfusion rats with/without EA at different acupoints. CMBCs were measured and compared between the groups. * $P < 0.01$, MCAO + EA versus MCAO; $\nabla P < 0.01$, reperfusion versus MCAO; $\#P < 0.01$, reperfusion in MCAO + EA group versus reperfusion in MCAO group. Note that in the Ischemia group, MCAO (0 min) decreased CMBC to ~20% of the base level before MCAO (-5 min). After the onset of reperfusion, CMBC increased to ~55% of the base level. In the group of EA at Du 20 and Du 26, EA increased CMBC to ~65% of the base level. In the group of EA at left LI 11 and PC 6, EA increased CMBC to ~60% of the base level. After the onset of reperfusion, CMBC in the groups of EA at Du 20 and Du 26 and left LI 11 and PC 6 recovered faster than that in the Ischemia group. However, EA at right LI 11 and PC 6 or at left SP 6 and GB 34 did not significantly improve the CMBC.

in the PU and CMBC comparable to those of the Ischemia alone group during the beginning of reperfusion. However, the velocity recovered faster in this group as opposed to the ischemia alone group. In this EA group, the blood perfusion was largely improved starting from about 10–15 minutes after the onset of perfusion.

3.4. EA Had No Appreciable Effect on Cerebral Blood Flow in the Non-Ischemic Brain. Since EA at some acupoints, like Du 20 and Du 26 and left LI 11 and PC 6, significantly increased the blood flow to the ischemic brain, we further asked whether this response was specific to the ischemic brain or a generic brain response to EA stimulation. To investigate

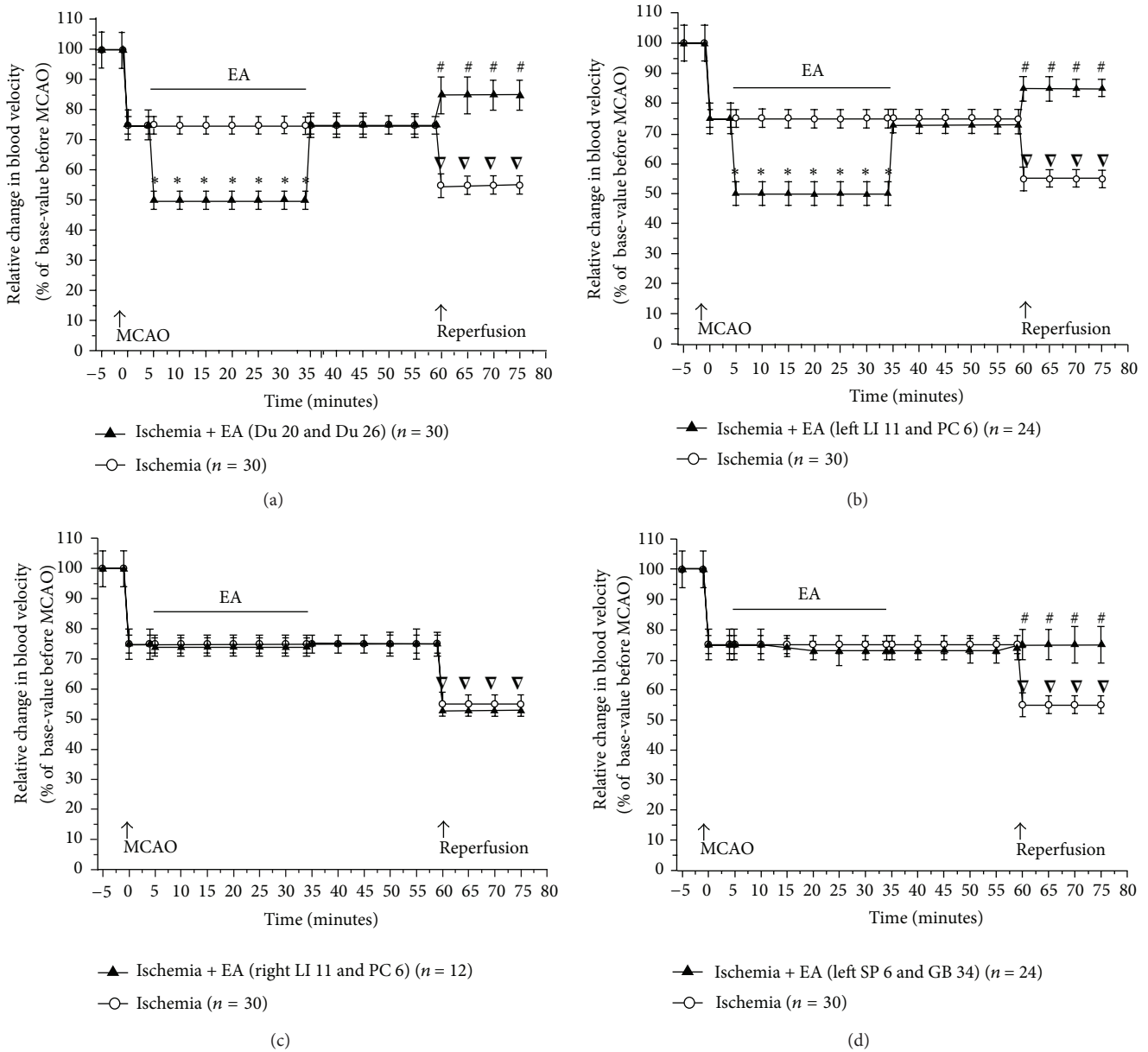


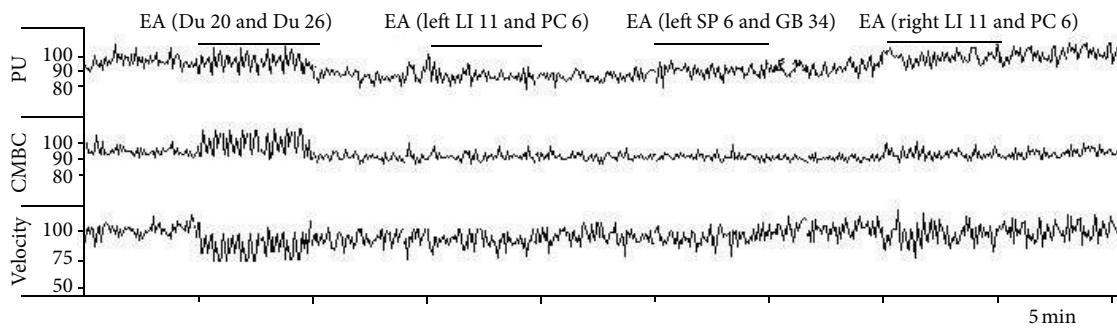
FIGURE 6: Statistical data representing the relative changes in velocity of the moving blood cells (Velocity) in the ischemic cortex in MCAO/reperfusion rats with/without EA at different acupoints. Velocities were measured and compared between the groups. * $P < 0.05$ MCAO + EA versus MCAO; $\nabla P < 0.05$ reperfusion versus MCAO; # $P < 0.05$, reperfusion in MCAO + EA group versus reperfusion in MCAO group. Note that in the Ischemia group, MCAO (0 min) decreased Velocity to ~75% of the base level before MCAO (-5 min). After the onset of reperfusion, Velocity decreased further to 50% of baseline (before MCAO) level. In the EA at Du 20 and Du 26 or left LI 11 and PC 6 groups, EA decreased the Velocity from 75% to 50% of the baseline ($P < 0.05$). After the onset of reperfusion, Velocity in the groups of EA at Du 20 and Du 26 and left LI 11 and PC 6 recovered faster than that in the Ischemia group ($P < 0.05$). However, EA at right LI 11 and PC 6 did not show a significant improvement in the velocity of moving blood cells. EA at left SP 6 and GB 34 acupoints showed a slight improvement in the velocity ($P < 0.05$).

this, we applied EA at 1.0 mA with 5/20 Hz sparse-dense pulse to the same acupoints on the age-matched control rats and measured the changes in cerebral blood flow ($n = 8$). Interestingly, we found no significant effect of EA on cerebral blood flow in the non-ischemic animals despite using the same EA parameters used on the ischemic rats (Figure 7). These observations suggest that the application of EA at

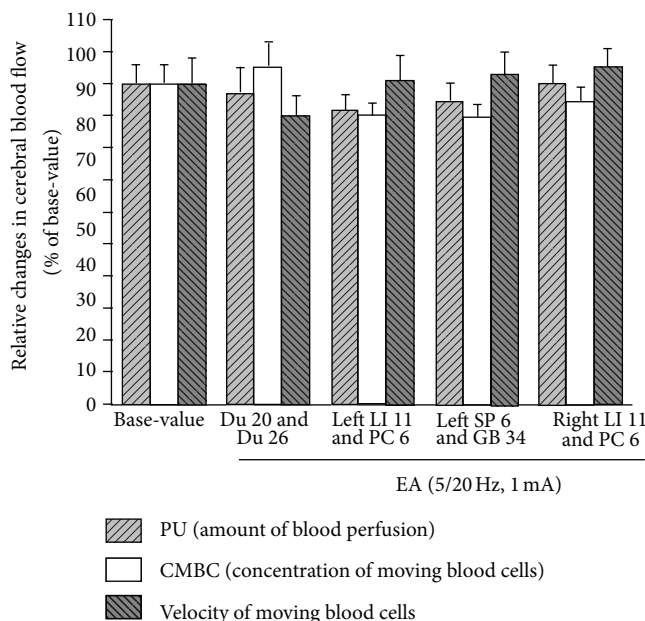
specific acupoints increased blood flow to the ischemic but not to the non-ischemic brain.

4. Discussion

This is the first study to systematically compare the effects of EA at different acupoints on cerebral blood flow and ischemic



(a) Effect of EA at different acupoints on the blood flow in the nonischemic cortex



(b) Averaged changes in the blood flow in the non-ischemic cortex in response to EA at different acupoints

FIGURE 7: EA had no significant effect on the cerebral blood flow in the non-ischemic cortex at different acupoints. Blood perfusion (PU), concentration of moving blood cells (CMBC), and velocity of blood cells (Velocity) were measured in the non-ischemic rats by a laser Doppler perfusion monitor system. (a) Effects of EA at different acupoints on the CBF. (b) Statistical summary. Note that EA had no significant effect on PU, CMBC, and Velocity in response to EA stimulation at different acupoints in the non-ischemic cortex.

injury in the brain. Our comprehensive data specifically shows that EA at Du 20 and Du 26 induced maximum protection against cerebral ischemia as opposed to the limb acupoints. The stimulation of the contralateral (to the ischemic side) acupoints (LI 11 and PC 6) in the left forelimb also induces a significant cerebral protection against ischemic injury, while stimulation of the same acupoints in the ipsilateral forelimb and contralateral acupoints in the hindlimb (SP 6 and GB 34) had no such effect.

In this work, we used optimized parameters, that is, 5/20 Hz parse-dense wave at 1.0 mA, for EA stimulation that confers optimal stimulation based on our previous systematic study [9, 13]. Since we used these parameters for all acupoints under the same experimental conditions, the differences in outcomes observed among all experimental groups can be attributed to specific effects of EA at these acupoints. Therefore, it is important to choose specific acupoints in

the treatment of hypoxic/ischemic encephalopathy, such as stroke. Our observations may provide a useful resource for a standardized application of acupuncture in the treatment of stroke under clinical settings.

Since the major cause of ischemic injury is insufficient blood supply to the brain, any change in blood flow may greatly affect the degree of brain injury. Our results show that in all "EA effective" groups, EA significantly increased the blood flow to the ischemic brain, thereby attenuating the effects of the hypoxic/ischemic environment in the brain. This further suggests the critical dependence of EA-induced protection on the improvement of cerebral blood flow.

The increase in the blood flow started soon after the onset of EA and disappeared almost immediately after the cessation of EA. Therefore, a quick and short-lasting mechanism underlies this action, quite possibly involving the nervous system. During EA stimulation, the muscles around

the acupuncture needles showed slight contractions in response to the EA rhythm. It is possible that the currents directly stretch the tissue and physically affect the blood vessels, thus leading to an increase in the blood flow. However, the facts we noticed in this study do not support this possibility. For example, EA at right LI 11 and PC 6, the acupoints that were physically closer to the ischemic region (right side of the brain), did not increase the blood flow or protect the brain at all. In sharp contrast, EA at left LI 11 and PC 6, contralateral to the ischemic side and relatively farther away from the ischemic region, caused a significant increase in the blood flow and better protected the brain against ischemic injury. This observation provides further evidence in support of the generation of EA signals from peripheral nerves and their transmission to the contralateral brain to regulate the neurotransmitter release and neural function, which in turn regulates various bodily phenomena [19–22]. Altogether, the EA-induced increase in blood flow is most likely based on a neural-controlled regulation. However, the precise mechanisms of how the EA signal upregulates blood flow in the ischemic brain is unknown at this stage and requires further research.

Interestingly, we did not note any appreciable increase in the blood flow of the non-ischemic brain when the animals were stimulated with the same EA parameters. This suggests that the EA-induced regulation of the cerebral blood flow varies with the conditions of the organ/body. Under normal conditions, the EA signal may not change the blood flow to the brain since it is unnecessary. Under a stress like hypoxia/ischemia, however, the same EA signal grants the brain the ability to adapt to the hypoxic/ischemic microenvironment by increasing local blood perfusion. Therefore, this EA-mediated upregulation of cerebral blood flow can be a useful strategy not only for ischemic stroke, but also for cerebral vasospasm and other similar disorders.

In summary, our work evidently demonstrates the specificity of acupoints in EA protection against cerebral ischemia and suggests that acupoints in the head or contralateral forelimb are effective in the treatment of stroke. Stimulation of these acupoints by optimized EA parameters generates a signal to the brain that results in an increase in cerebral blood flow and rescues the brain from ischemic injury. Although the underlying mechanisms need further research, the EA-induced upregulation of cerebral blood flow is an effective strategy with a potential for clinical application in a variety of neurological conditions.

Acknowledgments

This work was supported by NSFC (30672721, 30873318), NBRP (2009CB522901 and 2012CB518502), STCSM (10DZ1975800), NIH (AT-004422 and HD-034852), and Vivian L. Smith Neurologic Foundation.

References

- [1] J. H. Sung, D. M. Chao, and Y. Xia, “Neuronal responses to hypoxia,” in *New Frontiers in Neurological Research*, W. Ying

- and D. Wang, Eds., pp. 73–153, Research Signpost, Kerala, India, 2008.
- [2] D. Chao and Y. Xia, “Tonic storm in hypoxic/ischemic stress: can opioid receptors subside it?” *Progress in Neurobiology*, vol. 90, no. 4, pp. 439–470, 2010.
- [3] K. Arai, J. Lok, S. Guo, K. Hayakawa, C. Xing, and E. H. Lo, “Cellular mechanisms of neurovascular damage and repair after stroke,” *Journal of Child Neurology*, vol. 26, pp. 1193–1198, 2011.
- [4] X. Z. He, H. K. Sandhu, Y. L. Yang et al., “Neuroprotection against hypoxia/ischemia: δ -opioid receptor-mediated cellular/molecular event,” *Cellular and Molecular Life Sciences*. In press.
- [5] P. Zhao, J. Guo, Y. Xia, S. S. Hong, A. Bazy-Asaad, and J. S. Cheng, “Electro-acupuncture and brain protection from cerebral ischemia: the role of delta-opioid receptor,” SfN Abstract. Online Program no. 490. 13, 2002.
- [6] V. Hopwood and G. T. Lewith, “Does acupuncture help stroke patients become more independent?” *Journal of Alternative and Complementary Medicine*, vol. 11, no. 1, pp. 175–177, 2005.
- [7] M. H. Rabadi, “Randomized clinical stroke rehabilitation trials in 2005,” *Neurochemical Research*, vol. 32, no. 4-5, pp. 807–821, 2007.
- [8] Z. X. Yang and X. M. Shi, “Systematic evaluation of the therapeutic effect and safety of Xingnao Kaiqiao needling method in treatment of stroke,” *Zhongguo zhen jiu*, vol. 27, no. 8, pp. 601–608, 2007.
- [9] F. Zhou, J. C. Guo, J. S. Cheng, G. C. Wu, and Y. Xia, “Electroacupuncture induced protection from cerebral ischemia is dependent on stimulation intensity, and frequency,” in *Proceedings of the 3rd Cell Stress Society International Congress on Stress Responses in Biology and Medicine and 2nd World Conference of Stress*, vol. 3, p. 250, Budapest, Hungary, 2007.
- [10] F. Zhou, J. C. Guo, J. S. Cheng, G. C. Wu, and Y. Xia, “Electroacupuncture and brain protection from cerebral ischemia: differential roles of acupoints,” in *Proceedings of the 3rd Cell Stress Society International Congress on Stress Responses in Biology and Medicine and 2nd World Conference of Stress*, vol. 3, p. 249, Budapest, Hungary, 2007.
- [11] J. C. Guo, J. S. Cheng, and Y. Xia, “Acupuncture therapy for stroke,” in *Acupuncture Therapy For Neurological Diseases: A Neurobiological View*, Y. Xia, X. Cao, and G.-C. Wu, Eds., pp. 226–262, Springer, Heidelberg, Germany, 2010.
- [12] P. Wu, E. Mills, D. Moher, and D. Seely, “Acupuncture in poststroke rehabilitation: a systematic review and meta-analysis of randomized trials,” *Stroke*, vol. 41, no. 4, pp. e171–e179, 2010.
- [13] F. Zhou, J. C. Guo, J. S. Cheng, G. C. Wu, and Y. Xia, “Electroacupuncture increased cerebral blood flow and reduced ischemic brain injury: dependence on stimulation intensity and frequency,” *Journal of Applied Physiology*, vol. 111, pp. 1877–1887, 2011.
- [14] M. Xu, L. Ge, and D. Zhao, “Electro-acupuncture regulation of central monoamine neurotransmitters in ischaemia-reperfusion,” in *Current Research in Acupuncture*, Y. Xia, G. Ding, and G.-C. Wu, Eds., pp. 401–430, Springer, New York, NY, USA, 2012.
- [15] X. Li, P. Luo, Q. Wang, and L. Z. Xiong, “Electroacupuncture pretreatment as a novel avenue to protect brain against ischemia and reperfusion injury,” *Evidence-Based Complementary and Alternative Medicine*, vol. 2012, Article ID 195397, 12 pages, 2012.
- [16] M. Liu, “Acupuncture for stroke in China: needing more high-quality evidence,” *International Journal of Stroke*, vol. 1, no. 1, pp. 34–35, 2006.

- [17] Y. Xie, L. Wang, J. He, and T. Wu, "Acupuncture for dysphagia in acute stroke," *Cochrane Database of Systematic Reviews*, vol. 16, no. 3, Article ID CD006076, 2008.
- [18] X. F. Zhao, Y. Du, P. G. Liu, and S. Wang, "Acupuncture for stroke: evidence of effectiveness, safety, and cost from systematic reviews," *Topics in Stroke Rehabilitation*, vol. 19, pp. 226–233, 2012.
- [19] F. Zhou, D. K. Huang, and Y. Xia, "Neuroanatomic basis of acupuncture points," in *Acupuncture Therapy For Neurological Diseases: A Neurobiological View*, Y. Xia, X. Cao, and G.-C. Wu, Eds., pp. 32–80, Springer, Heidelberg, Germany, 2010.
- [20] G. Q. Wen, Y. L. Yang, Y. Lu, and Y. Xia, "Acupuncture-induced activation of endogenous opioid system," in *Acupuncture Therapy for Neurological Diseases: A Neurobiological View*, Y. Xia, X. Cao, and G.-C. Wu, Eds., pp. 104–119, Springer, Heidelberg, Germany, 2010.
- [21] G. Q. Wen, X. Z. He, Y. Lu, and Y. Xia, "Effect of acupuncture on neurotransmitters/modulators," in *Acupuncture Therapy for Neurological Diseases: A Neurobiological View*, Y. Xia, X. Cao, and G.-C. Wu, Eds., pp. 120–142, Springer, Heidelberg, Germany, 2010.
- [22] J. F. Liang and Y. Xia, "Acupuncture Modulation of central neurotransmitters," in *Current Research in Acupuncture*, Y. Xia, G. Ding, and G.-C. Wu, Eds., pp. 1–36, Springer, New York, NY, USA, 2012.
- [23] W. Ouyang, Y. L. Huang, C. D. Da, and J. S. Cheng, "EA reduces rat's neuronal ischemic injury and enhances the expression of basic fibroblast growth factors," *Acupuncture & Electro-Therapeutics Research*, vol. 24, pp. 1–10, 1999.
- [24] Y. Nishimura, T. Ito, and J. M. Saavedra, "Angiotensin II AT1 blockade normalizes cerebrovascular autoregulation and reduces cerebral ischemia in spontaneously hypertensive rats," *Stroke*, vol. 31, no. 10, pp. 2478–2486, 2000.
- [25] E. Z. Longa, P. R. Weinstein, S. Carlson, and R. Cummins, "Reversible middle cerebral artery occlusion without craniectomy in rats," *Stroke*, vol. 20, no. 1, pp. 84–91, 1989.
- [26] X. B. Hua, C. R. Li, D. L. Song, Y. L. Hu, and H. L. Zhou, "Common used acupoints in animals for experimental acupuncture," in *Experimental Acupuncture Science*, Z. R. Li, Ed., pp. 327–329, Chinese Traditional Medicine Press in China, Beijing, China, 2003.
- [27] J. B. Bederson, L. H. Pitts, and S. M. Germano, "Evaluation of 2,3,5-triphenyltetrazolium chloride as a stain for detection and quantification of experimental cerebral infarction in rats," *Stroke*, vol. 17, no. 6, pp. 1304–1308, 1986.
- [28] R. A. Swanson, M. T. Morton, and G. Tsao-Wu, "Semiautomated method for measuring brain infarct volume," *Journal of Cerebral Blood Flow & Metabolism*, vol. 10, pp. 290–295, 1990.

Review Article

From Acupuncture to Interaction between δ -Opioid Receptors and Na^+ Channels: A Potential Pathway to Inhibit Epileptic Hyperexcitability

Dongman Chao,^{1,2,3} Xueyong Shen,^{3,4} and Ying Xia^{1,2}

¹ The University of Texas Medical School at Houston, Houston, TX 77030, USA

² Yale University School of Medicine, New Haven, CT 06520, USA

³ Shanghai Research Center for Acupuncture and Meridians, Shanghai 201203, China

⁴ Shanghai University of Traditional Chinese Medicine, Shanghai 201203, China

Correspondence should be addressed to Ying Xia; ying.xia@uth.tmc.edu

Received 24 August 2012; Revised 10 November 2012; Accepted 13 December 2012

Academic Editor: Di Zhang

Copyright © 2013 Dongman Chao et al. This is an open access article distributed under the Creative Commons Attribution License, which permits unrestricted use, distribution, and reproduction in any medium, provided the original work is properly cited.

Epilepsy is one of the most common neurological disorders affecting about 1% of population. Although the precise mechanism of its pathophysiological changes in the brain is unknown, epilepsy has been recognized as a disorder of brain excitability characterized by recurrent unprovoked seizures that result from the abnormal, excessive, and synchronous activity of clusters of nerve cells in the brain. Currently available therapies, including medical, surgical, and other strategies, such as ketogenic diet and vagus nerve stimulation, are symptomatic with their own limitations and complications. Seeking new strategies to cure this serious disorder still poses a big challenge to the field of medicine. Our recent studies suggest that acupuncture may exert its antiepileptic effects by normalizing the disrupted neuronal and network excitability through several mechanisms, including lowering the overexcited neuronal activity, enhancing the inhibitory system, and attenuating the excitatory system in the brain via regulation of the interaction between δ -opioid receptors (DOR) and Na^+ channels. This paper reviews the progress in this field and summarizes new knowledge based on our work and those of others.

1. Introduction

Epilepsy is one of the most common neurological disorders affecting about 1% of population. Currently available therapies, including medical treatment, surgical treatment, and other treatment strategies such as ketogenic diet and vagus nerve stimulation are symptomatic with their own limitations and complications [1]. Understanding of its cellular and molecular mechanisms and seeking new strategies to cure this disorder still poses a big challenge.

Epilepsy has been recognized as a disorder of brain excitability characterized by recurrent unprovoked seizures that result from the abnormal, excessive, and synchronous activity of clusters of nerve cells in the brain. About 40% of epilepsies are mainly caused by genetic factors, while the other 60% are acquired/etiological epilepsies. Irrespective

of the inherited or acquired type, the changes in neuronal excitability that underlie the pathogenesis of epilepsy are a complex process that induces abnormal activity not only in individual neurons, but also in a population of hyperexcitable neurons in highly synchronous activities that are propagated through normal or pathological pathways.

Epileptic hyperexcitability results from multiple factors such as innate ability of neurons in the cortex and hippocampus, alterations in the membrane properties, imbalance between excitatory and inhibitory transmission, alterations in existing synaptic contacts/circuits and/or establishment of new synaptic contacts/circuits, and the inability of glial cells to maintain glutamate and K^+ homeostasis [1]. Among these factors, the most important determinant is the intrinsic electrogenic property of each neuron that depends on the function of ion channels like Na^+ , K^+ , and Ca^{2+} channels in

the membrane [2]. In particular, Na^+ channels are responsible for the initiation and propagation of action potential, and are critical determinants of intrinsic neuronal excitability.

Acupuncture is one of the oriental medical therapeutic techniques that involves insertion of fine needles into specific body areas (acupoints or meridian points) and swift manual manipulation (e.g., rotating, lifting, thrusting, retaining, etc.) that results in the manifestation of the *Qi* or *De Qi* (acquisition of energy) phenomenon that refers to a mixed sensation of soreness, numbness, swelling, sinking, and heat that appears in the acupoints. *De Qi* is an important component of the therapeutic effect and may be necessary for clinical efficacy of acupuncture [3, 4]. In modern practice, electrical stimulation (versus manual manipulation) of acupoints, that is, electroacupuncture, is increasingly gaining popularity among various acupunctural modalities. Both animal and clinical studies indicate that acupuncture is effective in certain kinds of epilepsy. As compared to the conventional Western medicine and surgical treatments, the significant advantages of acupuncture treatment include its safety, convenience, and minimal side effects [5–7].

Acupuncture exerts its antiepileptic effect through normalization of the disrupted neuronal excitability [1]. Some acupuncture-induced effects involve the activation of the opioid system [8–13]. We have previously demonstrated that electroacupuncture has a neuroprotective role in the brain against ischemic injury via the δ -opioid system [14, 15]. DOR expression/activation inhibits Na^+ channel activity [16, 17] and thus attenuates Na^+ - K^+ homeostasis of the cortex under normoxic/hypoxic conditions [16, 18–22]. Since the electrolyte homeostasis (e.g., Na^+ , Ca^{2+} , K^+ , and Cl^-) gets disrupted between the intra- and extracellular space during epileptic seizures, and since Na^+ channel upregulation participates in the pathological changes of several neurological disorders such as hypoxic/ischemic injury and epilepsy [23–26], acupuncture may attenuate epileptic seizures through the DOR-mediated inhibition of the Na^+ channels [1]. Research in this new field may help us in the pursuit of novel therapeutic solutions for epileptic hyperexcitability and seizures.

2. Pathological Genesis of Epileptic Brain Hyperexcitability

The most prominent feature of epilepsy is the hyperexcitability in the brain. At least two major factors contribute to the hyperexcitability in the epileptic brain. The first and also the most significant contributor is the altered intrinsic electrogenic properties of the neurons (neuronal excitability), which depend on the functioning of membrane ion channels, namely Na^+ , K^+ , and Ca^{2+} channels. The second factor is the synaptic imbalance that involves disruption of chemical transmission from the neighboring cells within the network via ligand-gated ion channels and G-protein-coupled metabotropic receptors and rapid electrical transmission via gap junctions (network excitability) [2]. For both major factors, epilepsy results from the abnormal activity in the neuronal networks. However, hyperexcitability due to altered

ion-channel function contributes to the seizure-prone state [25].

Numerous studies have shown the existence of neuronal networks of epilepsy in the epileptic patients with the aid of EEG-functional magnetic resonance imaging (EEG-fMRI) [1, 27–31]. In epilepsy, synaptic input from neighboring cells within the network is disrupted, which results in a progressive increase in excitability and epileptogenesis. This imbalanced neurotransmission between excitatory and inhibitory activities is the most prominent feature. Exaggerated glutamatergic excitatory transmission, or decreased GABAergic inhibitory transmission between the inhibitory and the excitatory systems, or a combination of these two can lead to an overexcitation of the neurons. A causal association between such imbalances in the neurotransmitter activity has been causatively linked to seizure activity and the development of chronic epilepsy [1]. In addition, aberrant fiber sprouting and robust synaptic reorganization, due to the neuronal injury/loss associated with brain damage under conditions such as status epilepticus, stroke, brain trauma, and developmental malformation or deafferentation often observed in the hippocampus and cortex, also instigate a recurrent excitatory circuit by forming synapses on the dendrites of neighboring neurons (e.g., granule cells in hippocampus). A small cluster of pathologically interconnected neurons in this aberrant recurrent network are capable of generating powerful hyper-synchronous bursts of discharges, initiating epileptogenesis via a kindling effect and development of epileptic discharges that spread throughout the limbic system, and eventually resulting in temporal lobe epilepsy [1, 32–34].

Ion channels in the neuronal membrane have a critical impact on neuronal excitability. Ion channels, especially voltage-gated Na^+ , K^+ , and Ca^{2+} channels, are functional proteins embedded in the plasma membrane. They are critical determinants of neuronal excitability as they influence the generation and propagation of action potential in the neurons. Action potential is the cellular language by which neurons communicate with one another. During the firing of an action potential, the voltage-dependent Na^+ channels dominate the explosive, regenerative activation of inward currents during the rising phase, while a fraction of the voltage-dependent K^+ channels chiefly contribute to the repolarization and hyperpolarizing overshoot phase of the action potential. Voltage-dependent Ca^{2+} channels generally make little contribution to the rising phase of an action potential because their activation kinetics are slower than Na^+ channels. However, Ca^{2+} entry through voltage-gated Ca^{2+} channels activates Ca^{2+} -activated K^+ channels that indirectly contribute to the late repolarization and after hyperpolarization, which follows the rising phase of an action potential [35]. Basically, voltage-gated Na^+ channels along with K^+ and Ca^{2+} channels determine the capacity of action potential generation, the shape of an action potential, and the firing rate and therefore have a great impact on neuronal excitability. Na^+ channel states (opening, closing, and inactivation) make a yes-or-no decision regarding the firing of an action potential, and the channel kinetics (activation and deactivation) and current density play an essential role in the amplitude and

duration of an action potential. Therefore, abnormalities of the function (opening, closing, and inactivation), expression, or structure (e.g., mutation) of ion channels may be responsible for the hyperexcitability of neurons and contribute to the consequent epilepsy.

3. Clinical Practice of Acupuncture Therapy for Epilepsy

Acupuncture treatment for epilepsy has been employed for thousands of years through all of the dynasties in China [50]. The first known description of epilepsy and acupuncture therapy appeared in *Huang Di Nei Jing* (The Yellow Emperor's classic of Internal Medicine), an ancient Chinese medicine book written by a group of Chinese physicians around 770–221 B.C. [50, 51]. Ancient acupuncturists maintained a memorandum of their successful cases based on clinical improvement in their clinical trials. They focused on controlling seizures and compared different acupuncture methods (acupuncture alone with acupuncture plus other therapies) to find how to better control seizures. Therefore, in a way they were using people rather than animals first to perform their experiments [50]. There is no doubt that ancient acupuncturists/physicians made important observations in validating the effects of acupuncture on epilepsy, though mostly through their personal experiences. With the aid of advanced techniques, many modern scientific researchers have demonstrated the antiepileptic effects of acupuncture in animal studies [52–60]. For example, we found that electroacupuncture stimulation of Jinsuo (GV-8) and Fengfu (GV-16) significantly improves epileptic EEG and seizure behaviors through an increase in endogenous melatonin levels in a penicillin-induced rat model [52]. Furthermore, we found in a kainic acid-induced seizure model that electroacupuncture attenuates epileptic seizures, which is relatively specific to stimulation parameters and acupoints [55, 60]. Our findings show that (1) low- or high-frequency electroacupuncture at different acupoints, for example, Renzhong (GV-26) plus Dazhui (GV-14), Jinsuo (GV-8) plus Yaoqi (EXB-9), Neiguan (PC-6) plus Quchi (LI-11), and Fenglong (ST-40) plus Yongquan (KI-1), reduced epileptic seizures with an exception of low-frequency electroacupuncture at Neiguan (PC-6) and Quchi (LI-11); (2) low-frequency electroacupuncture induced a better effect at Fenglong (ST-40) plus Yongquan (KI-1) than other acupoints; (3) there was no significant difference in effects of high-frequency electroacupuncture at these acupoints; and (4) high-frequency electroacupuncture elicited a greater effect than low-frequency electroacupuncture, with an exception of Jinsuo (GV-8) + Yaoqi (EXB-9). The electroacupuncture-induced attenuation appeared 1–1.5 hours after electroacupuncture with no appreciable effect in either EEG or behavioral tests during the first hour after electroacupuncture [55, 60].

Despite substantial evidence from animal research in support of antiepileptic effects of acupuncture, a large number of clinical studies have also shown that patients have benefited from acupuncture for control of their seizures, especially in

cases with refractory epilepsy [36–49], though results from some studies beg to differ [61].

These are extremely heterogenous clinical case series [36–49]. Since many of these reports were written in Chinese and are not understood or easily available to Western peers, we have already summarized the salient information from these reports in Table 1. As shown in this table, the patients treated varied over a range of age from infants to elderly, and the type of epilepsy from absence seizure, febrile convulsion, and generalized clonic-tonic seizure, to even status epilepticus. The case numbers reported also vary from a few to over one hundred, many of which were resistant to antiepileptic drugs. The acupoints and acupuncture methods used in these reports were highly heterogeneous as well. The overall treatment effects of acupuncture are principally manifested by the reduction in symptoms (e.g., a reduction of seizure frequency, shortness of episodes, etc.), functional recovery (e.g., smoothed breath from shortened, quickened, and occasionally stopped breath, recovery from unconsciousness, etc.), improved EEG (e.g., reduction of spike wave, desynchronization, etc.), and/or decreased epilepsy scores. The outcome of acupuncture therapy in these reports is relatively significant, and the total effective rate of treatment is as high as up to 98%.

For the report that was unable to prove a beneficial effect of acupuncture in chronic intractable epilepsy [61], as the authors acknowledged, the negative results could in part be ascribed to the small sample size for this observation [61]. Also, acupoints selected and manipulation/stimulation methods adopted (e.g., frequency, intensity, duration of swift rotation, lifting, thrusting, and retaining) may also be responsible for this observation. In this respect, as has mentioned earlier in this section, electroacupuncture attenuation of epileptic seizures is relatively specific to stimulation parameters and acupoints in our animal studies [60].

4. Potential Mechanisms of Acupuncture Inhibition of Neuronal Hyperexcitability

4.1. Acupuncture and The Opioid System. Classic opioid systems include endogenous peptides and δ -, μ -, and κ -opioid receptors (DOR, MOR, and KOR, resp.). Endogenous opioid peptides enkephalin, β -endorphin, and dynorphin in the brain preferentially bind to DOR, MOR, and KOR, respectively, under physiological concentrations and have multiple functions in the brain. Acupuncture and electroacupuncture have been well recognized to regulate endogenous opioid systems in the central nervous system [8–13, 62].

Along with other biomediators (neurotransmitters, neuromodulators, and/or signaling molecules) [1], the opioid system is also involved in the anticonvulsant effect of acupuncture, though the role of different opioid systems in the acupuncture suppression of epilepsy appears to be very complex.

Some studies show that the blockade of the opioid system in the brain can diminish, while its activation enhances, inhibitory effects of acupuncture on epilepsy. In this regard, Wu and his coworkers reported that in a rat model of

TABLE 1: Clinical reports on acupuncture therapy for epilepsy from some Chinese literature.

Ref. Patients	Age	Types of epilepsy	Acupuncture methods and Acupoints	Therapeutic assessment	Outcome
[36] 114 cases and 8 healthy control	Mean 19 yrs. (6–68) with a history of epilepsy for 1 mo.–35 yr.	Various (Grand mal, petit mal, focal, abdominal pain induced, psychomotor induced, mixed)	Scalp acupuncture (thoracic region, motor region, chorea and parkinsonism control region, foot motor sensory region, optic region) Body acupuncture (HT-7, LR-3, GV-26, GV-20, GB-20, LI-4, ST-36)	EEG; bell sound and verbal suggestion; response to pinching of the neck skin	72.6% with EEG changes mainly as asynchronism (reduction or cessation of epileptic discharges)
[37] 98 cases	Mean 27 yrs. (2–52) with a history of epilepsy for Ave. 17 yr.	Not specified (epileptic attack or EEG confirmed epilepsy)	Scalp acupuncture (Motor area, psychic area, sensory area) Once daily for 15 days as a session, 2–3 sessions in total, 7-day break between sessions, needle retention 30 min	<i>Markedly effective</i> (>75% seizure frequency reduction, or seizure controlled) <i>Effective</i> (50–75% reduction, seizure less severe and interval prolonged) <i>Slightly effective</i> (25–50% reduction) <i>No effect</i> (<25% reduction)	66.3% markedly effective; 23.5% effective; 5.1% effective; 5.1% no effect The overall effective rate is 89.8%
[38] 8 cases	5–16 yrs with a history of epilepsy for 1 mo.–7 yr.	Status epilepticus	Manual acupuncture (LI-4, LR-3, Gv-26, GV-20, KI-1, EX-UE-II, PC-5, HT-7, RN-4, ST-40, EX-HN-3, GB-20, SP-6)	<i>Symptoms</i> (unconscious, white form in mouth, cyanotic face, spastic and convulsive in limbs, short, quick breath with occasional stops, sputum in throat, uncontrolled urine)	Symptoms controlled with 10 min of acupuncture without relapse in 2–8 yr. followup
[39] 78 cases	Mean 24.7 yr. (17–39 yr.)	narcotic abstinence-induced seizures	Manual acupuncture Acupoint: PC-6 Once daily for 10 days, needle retention 30 min with 2 times of stimulation	<i>Markedly effective</i> (the symptoms of drug addiction and abstaining-induced seizures disappear, and no relapse in 6 mo.) <i>Effective</i> (alleviated symptoms, occasional relapse in 1 mo.) <i>No effect</i> (no relief of symptoms, tranquilizer needed for control of symptoms)	70.51% markedly effective; 23.08% effective; 6.41% no effect The overall effective rate is 93.59%
[40] 129 cases (64-catgut implantation group, 65-AED controls)	Mean 21.8 ± 12.0 yrs with a history of epilepsy for Ave. 7.4 yr.	General tonic-clonic epilepsy	Combined catgut implantation and small dose AED (GV-20, BL-18, ST-40, EX-B-9, CV-15, GB-34, BL-15) One time of implantation in every 25–30 days as a session for 4–5 sessions in total	<i>Controlled</i> (>92% of therapeutic efficacy percentile, no relapse), <i>Markedly effective</i> (70–92% of therapeutic efficacy percentile, 75% seizure frequency reduction) <i>Effective</i> (40–70% of therapeutic efficacy percentile, 50% seizure frequency reduction), <i>Slightly effective</i> (20–40% of therapeutic efficacy percentile, <25% seizure frequency reduction) <i>no effect</i> (<20% of therapeutic efficacy percentile, <25% seizure frequency reduction)	28.12% (versus 16.92% for control) controlled; 43.75% (versus 33.85%) markedly effective; 21.88% 9 (versus 35.38%) effective; 4.69% (versus 10.77%) slightly effective; 1.56% (versus 3.08%) not effective The overall effective rate is 93.75% (versus 86.15% for control)

TABLE 1: Continued.

Ref. Patients	Age	Types of epilepsy	Acupuncture methods and Acupoints	Therapeutic assessment	Outcome
[41] 290 cases (160-acupoint catgut embedding group, and 130-acupuncture group)	1-48 Yrs with a history of epilepsy for 10 d-21 yr.	Mixed epilepsy	Acupoint catgut embedding, acupuncture Primary acupoints: For catgut embedding-BL-14 penetrating to BL-15, BL-18 to BL-19, BL-20 to BL-21, EX-B-9 For acupuncture: CV-15, GV-20, EX-B-9, PC-5, ST-40 Secondary acupoints (same for two treatments): BL-12 + GV-20; or ST-36 + ST-34; or ST-40 + ST-36; or BL-17 + SP-10; or BL-23 + GV-4 One time of implantation in every 20 days as a session for 6 sessions in total For acupuncture, 1 time every other day for 6 mo., needle retention 20 min with stimulation 1 time per 5-10 min	<i>Markedly effective</i> (>75% seizure frequency reduction or no relapse in 1 yr.) <i>Effective</i> (50-75% seizure frequency reduction), improved (25-50% seizure frequency reduction), <i>No effect</i> (<25% seizure frequency reduction)	The total effective rate is 89.4% and 77.7% for catgut embedding and acupuncture group, respectively
[42] 120 cases	1.5-55 yrs with a history of epilepsy for 2 mo.-36 yr.	Various (Grand mal, petit mal, focal, abdominal pain induced, psychomotor induced, traumatic, mixed)	Primary acupoints: GV-20, DU-11, EX-B-9 Secondary acupoints: 1: GV-26 + GV-20, PC-6, LI-4, LR-3; 2: ST-36, BL-15, BL-18, BL-20, BL-23; + ST-40 or BL-62 or KI-6. Once daily for 10 days as a session, 3 sessions in total, 3-5-day break between sessions, needle retention 30 min with stimulation 1 time per 10 min	Same as Shi et al., 1987 [37]	71.7% markedly effective; 23.3% effective; 3.3% effective; 1.7% no effect The overall effective rate is 98.3%
[43] 60 cases (30-acupuncture + Xi Feng capsule group, and 30-Xi Feng capsule controls)	<5 yr-16 yrs with a history of epilepsy for < 1 yr-15 yr.	Tonic-clonic epilepsy	Combined acupuncture with Xi Feng capsule Acupoints include GV-26, GV-20, GB-20, PC-6, LR-3, ST-36 Once daily for 8 days as a session, 2 sessions in total, 2-day break between sessions, needle retention 30 min with stimulation 1 time per 10 min	<i>Markedly effective</i> (>75% reduction of seizure duration, >4 reduction of epileptic EEG score) <i>Effective</i> (50-75% reduction of seizure duration, 2-4 reduction of epileptic EEG score) <i>No effect</i> (<50% reduction of seizure duration, <2 reduction of epileptic EEG score)	96.7% (versus 90% for control) overall effective rate in seizure frequency reduction, 80% (versus 60%) in reduction of seizure duration, and 92.3% (versus 88.5%) in EEG improvement
[44] 60 cases (30-acupuncture group, and 30-AED controls)	Mean 65 yrs (40-70 yrs)	Epilepsy secondary to cerebral infarction (focal and general tonic-clonic)	Combined acupuncture and Chinese herb Acupoints include three acupoints on back created by the author (Shaofeng Guo) 1 time daily for 14 days as a session, 2 sessions in total	Controlled (no relapse) <i>Markedly effective</i> (>75% seizure frequency reduction) <i>Effective</i> (50-75% seizure frequency reduction) <i>No effect</i> (<50% seizure frequency reduction, or increased)	The overall effective rate is 93.3% (versus 80% for control) No adverse responses (mild dizziness, hypomnesia, limb numbness, weight loss and lassitude that showed in AED treatment control) appear

TABLE 1: Continued.

Ref. Patients	Age	Types of epilepsy	Acupuncture methods and Acupoints	Therapeutic assessment	Outcome
[45] 90 cases (30-acupuncture group, 30-catgut implantation group, 30-AED controls)	Mean age 35.02, 33.56 and 31.79 yrs, in acupuncture, catgut, and control groups, respectively, with a history of epilepsy for Ave. 7.96, 7.30, and 7.68 yr for acupuncture, catgut implantation, and control, respectively	General tonic-clonic epilepsy	Acupuncture and catgut implantation Primary acupoints include 1: GV-20 + GV-8 + ST-40; 2: BL-15 + BL-18 + GB-34; 3: BL-15 + BL-19 + LI-14 Secondary acupoints include BL-19, GB-20, BL-17, BL-21, BL-23 For catgut embedding, 1 time of embedding in every 15 days for 3 mo For acupuncture, 1 time every other day for 3 mo., needle retention 30 min with stimulation 1 time per 5–10 min	Same as Deng et al., 2001 [40]	The overall effective rate is 93.33%, 86.67%, and 76.67% for catgut implantation, acupuncture group, and control, respectively
[46] 100 cases (50-catgut implantation group, 50-AED controls)	Mean age 30.25 (versus 33.20 in controls) with a history of epilepsy for Ave. 7.71 (versus 7.33 for control) yr.	General paroxysmal epilepsy	Catgut implantation Acupoints and treatment as same as Zhang et al., 2006 [45]	Same as Deng et al., 2001 [40], Zhang et al., 2006 [45]	The overall effective rate is 94.0% and 82.0% for catgut implantation group and control, respectively
[47] 98 cases	12–63 yrs with a history of epilepsy for 5 mo.–20 yr.	Jacksonian epilepsy	Penetrating needling together with scalp acupuncture and strong/electric needling on body points GV-14 penetrating to GV-10, GV-9 to GV-8, GV-6 to GV-4, EX-B9 to GV-1, GV-24 to GV-22, GV-20 to GV-19, CV-15 to CV-12 Bilateral PC-6, ST-40, LR-3, and MS-6 Intermittent dense-loose waves with 2–3 Hz for 30–45 min every other day for 10 times as a session with a total 2 sessions and a break of 3–5 days between 2 sessions	Same as Shi et al., 1987 [37]	The total effective rate is 85.7%
[48] 80 cases (40-catgut implantation group and 40-herbal medicine controls)	6–52 yrs with a history of epilepsy for 1–15 yr.	Grand mal, petit mal, and mixed	Combined catgut implantation and herbal medicine Acupoints include GV-20, EX-B9, PC-6, CV-15 + ST-40 for phlegm, or + CV-12 for abdominal pain, or + BL-23 for uncontrolled urine 1 time of catgut implantation in every 20–30 days for 6 times	Same as Mao and Guo, 2005 [44]	The overall effective rate is 97.5% and 85.0% for catgut implantation group and control, respectively

TABLE 1: Continued.

Ref. Patients	Age	Types of epilepsy	Acupuncture methods and Acupoints	Therapeutic assessment	Outcome
70 cases (36 combined [49] acupuncture and AED group, 34 AED only controls)	6 mo.–6 yr with a history of epilepsy for 1 day	Infantile febrile convulsion	Combined acupuncture and AED Acupoints include GV-26, + KI-1, LI-11, LI-4, and LU-11 for cessation of spasm, or + PC-6 and ST-36 for cessation of vomit	<i>Rapidly effective:</i> spasms cease within 1-2 min of treatment <i>Basically effective:</i> spasms cease in 3-4 min of treatment <i>Ineffective:</i> spasms cease in >5 min of treatment <i>Relapse:</i> >2 times of spasms during 1-3 days of treatment <i>Non relapse:</i> no relapse during 1-3 days of treatment	77.7% (versus 23.5% for control) rapidly effective; 8.3% (versus 55.9%) basically effective; 13.9% (versus 20.6%) ineffective The overall effective rate is 86.1% (versus 79.4% for control) Relapse rate is 8.3% (versus 32.4% for control)

Note: since many of these reports were written in Chinese and are not easily available and/or understood by Western peers, we extracted relevant information from these reports and summarized it in this table.

penicillin-induced seizures, the inhibitory effect of electroacupuncture on cortical epileptiform discharges could be reversed by the injection of a broad spectrum opioid receptor antagonist, naloxone, via various routes including microinjection into the periaqueductal gray matter of the midbrain, accumbens or other nuclei, intraperitoneal, and intracerebroventricular injection, or even direct injection into the cortical site where penicillin was applied. While naloxone injection into the reticular formation of midbrain and the reticular nucleus of the thalamus had little effect on acupuncture attenuation of epilepsy, injection of naloxone into the above-mentioned sites without application of penicillin on the cortex did not induce epileptic burst [63, 64], suggesting a specific activation of the opioid system by electroacupuncture in the epileptic brain. In the hippocampus, activation of KOR with U50488H enhances, while blockade of KOR with antagonist MR2266 or antidynorphin serum abates the antiepileptic effect of electroacupuncture in electroconvulsive rats [65]. Therefore, the authors concluded that endogenously released opioid peptides mediate the suppressive effect of electroacupuncture on seizures [63, 64].

In support of the above viewpoint [63, 64], enhanced biosynthesis of central enkephalin by application of electroacupuncture has been found in the rat brain [66]. In the rat brain of experimental seizures model, hippocampal dynorphin concentration and dynorphin immunoreactivity in hippocampal mossy fiber and hilus are increased by electroacupuncture [67–69]. Also, the seizure-associated increase in leu-enkephalin and β -endorphin levels in the hippocampus and augmented expression of preproenkephalin mRNA in several brain regions (entorhinal cortex, subiculum, hippocampal CA1 area, amygdaloid nucleus, and piriform cortex) in rats are suppressed by electroacupuncture [68, 70–72]. Therefore, acupuncture can suppress epilepsy by regulating the synthesis and release of endogenous opioids.

Acupuncture can also regulate the expression and activity of opioid receptors. Radioreceptor-binding assay combined with autoradiography revealed that repeated electroconvulsive shock resulted in epileptiform EEG, behavioral seizures, and an accompanied increase in the opioid receptor densities in several brain regions (caudate nucleus, hippocampus, habenula nucleus, and amygdale) in rats. Electroacupuncture at Fengfu (GV-16) and Jingsuo (GV-8) was found to suppress the seizure activities and significantly decrease the opioid receptor densities in these brain regions except the caudate nucleus [73].

Electroacupuncture can also upregulate DOR expression in the ischemic brain and thus protect the brain from ischemic injury [15] that can cause epilepsy secondary to cerebral infarction [74]. Most interestingly, direct subacute high-frequency electrical stimulation of the parahippocampal cortex in patients with intractable medial temporal lobe epilepsy also produces an antiepileptic effect, which is associated with reduced opioid peptide binding including ^3H -DAMGO, ^3H -DPDPE, and ^3H -nociceptin (the ligand for MOR, DOR, and a fourth opioid, nociception receptor, resp.) in the same brain regions in patients with epilepsy [75].

Therefore, it is evident in both animals and patients with epilepsy that acupuncture can regulate the activities of endogenous opioids and their receptors in the brain, thereby exerting its antiepileptic effects.

4.2. Opioid Receptors and Na^+ Channels. Opioid receptors are members of the G-protein-coupled receptor superfamily [76], and can functionally couple with ion channels, including Na^+ channels [16, 17, 77]. Our previous data implied an interaction between opioid receptors and Na^+ channels. For example, we observed that DOR downregulation [78] is associated with an upregulation of voltage-gated Na^+ channels in a mutant brain with epileptic seizures [24]. An increased Na^+ channel density [23] along with decreased DOR density [79] occurred in hypoxia-exposed brain. Activation of presynaptic DOR by enkephalin prevents the increase in neuronal Nav1.7 in the dorsal root ganglia, which relieves pain in diabetic neuropathy [17]. More recently, our studies indicated that DOR activation attenuates hypoxic K^+ - Na^+ homeostasis, which largely relies on DOR inhibition of Na^+ influx through Na^+ channels [16, 18–22]. These results suggest that under pathological conditions DOR could mediate an inhibitory regulation of Na^+ channels in the brain.

Furthermore, our direct evidence gained from electrophysiological studies shows that activation of DOR indeed inhibits Na^+ channel activity [16]. Remy et al. observed that SNC80 (1–1000 μM), a putative DOR agonist, reduced the maximal Na^+ current amplitude in a dose-dependent manner and selectively prolonged the course of recovery from slow inactivation without effects on fast inactivation processes [80]. However, the authors concluded that this effect was opioid receptor independent since the effects of SNC80 were not mimicked by another DOR agonist DPDPE (10 μM) and were not inhibited by high concentrations of opioid receptor antagonists, naloxone (50–300 μM), and naltrindole (10 and 100 μM) [80]. This conclusion is arguable due to several important issues (e.g., experimental procedures, specificity and dose of drugs used, etc.) (see review [81]). We recently took the advantages of *Xenopus* oocytes with coexpressed DOR and Na^+ channels to explore a “pure” interaction between DOR and Na^+ channels, and found the following: (1) Nav1.2 expression induced tetrodotoxin- (TTX-) sensitive inward currents; (2) DOR expression reduced the inward currents; (3) activation of DOR reduced the amplitude of the current and rightward shifted the activation curve of the current in the oocytes with both Nav1.2 and DOR, but not in oocytes with Nav1.2 alone; (4) the DOR agonist-induced inhibition of Nav1.2 currents was in a dose-dependent manner and saturable; and (5) the selective DOR agonist had no effect on naive oocytes. These findings present the first demonstration that activation of DOR inhibits Na^+ channel function by decreasing the amplitude of Na^+ currents and increasing its threshold for activation [16]. Similar inhibitory effect of Na^+ channels is also found on MOR and KOR. For example, in acutely isolated cortical neurons, the application of 1 μM of DAMGO, a specific MOR agonist, caused a decrease in the Na^+ current amplitude to approximately 79% of the controls. Moreover, DAMGO decreased the maximum

TABLE 2: Voltage-gated sodium channels.

Subunit	α	β
Subtypes	Nav1.1–Nav1.9	β 1– β 4
Location	Prevalent in the CNS: Nav1.1, Nav1.2, Nav1.3, and Nav1.6 Abundant in muscle: Nav1.4, Nav1.5 Primarily in peripheral nervous system: Nav1.7, Nav1.8, and Nav1.9	Two β subunits associated with an α subunit
Cellular distribution	Primary localized in cell body: Nav1.1 and Nav1.3 High expression in unmyelinated or pre myelinated axons and dendrites: Nav1.2 Nodes of Ranvier and axon initial segments as well as in the somata and dendrites of many projection neurons: Nav1.6	Expressed in a complementary fashion (either β 1 or β 3, and β 2 or β 4) with α subunit
Function	Forms the ion-conducting pore and activation and inactivation gates	Modify the kinetics and voltage dependence of gating Serve as cell adhesion molecules for integrating the channels into the appropriate subcellular domains

current activation rate, prolonged its time-dependent inactivation, shifted the half inactivation voltage from -63.4 mV to -71.5 mV, and prolonged the time constant of recovery from inactivation from 5.4 ms to 7.4 ms [77]. DAMGO also inhibited TTX-resistant voltage-dependent Na^+ current in dorsal root ganglion neurons [82]. U50488, a KOR agonist, decreases voltage-activated Na^+ currents in colon sensory neurons [83]. Therefore, it seems that inhibition of Na^+ channel activities, which depends on signal molecules such as protein kinases [17, 22, 77], is one of the common characteristics of opioid receptors.

4.3. Na^+ Channels and Epileptic Hyperexcitability. As shown by previous reviews [84, 85], brain Na^+ channels consist of a 260 kDa α subunit with two auxiliary β subunits. The α subunit forms the ion-conducting pore and the activation and inactivation gates that regulate voltage-dependent sodium flux across the plasma membrane, while the β subunits modify the kinetics and voltage dependence of the gates. Until now at least nine α subtypes (Nav1.1–Nav1.9) and four β subtypes (β 1– β 4) have been found to express in the excitable cells (Table 2). Nav1.1, Nav1.2, Nav1.3, and Nav1.6 are the primary subtypes in the central nervous system [26, 84–87]. The developmental expression and cellular localization of these subtypes are different in the brain. Nav1.1 expression is first detectable at postnatal day 7, increases during the third postnatal week, and peaks at the end of the first postnatal month, after which levels decrease by about 50%

in the adult. Nav1.2 expression also increases during the third postnatal week and continues to increase thereafter, until the maximal level is reached in adulthood. In rodents, Nav1.3 channels are highly expressed in the brain during the embryonic period, peak at birth, and decline after birth as Nav1.1 and Nav1.2 channels take over, but remain detectable at a lower level during adulthood. Nav1.3 remains at comparatively higher levels in the human adult brain in adulthood. Nav1.1 and Nav1.3 are primary localized in the cell body and are preferentially expressed in the GABAergic neurons. Nav1.2 is particularly highly expressed in the unmyelinated or premyelinated axons and dendrites. Nav1.6 subtype is expressed at the nodes of Ranvier and the initial segments of axons, as well as in the somata and dendrites of many projection neurons [26, 84–87]. Sodium channels are responsible for the initiation and propagation of action potential and influence the subthreshold electrophysiology. Therefore, they are crucial determinants of intrinsic neuronal excitability [25, 35, 86]. Since epilepsy is regarded as an “electrical storm” of brain hyperexcitability [86], altered density or biophysical properties of Na^+ channels may have important consequences on the neuronal excitability and may contribute to the pathophysiology of brain diseases associated with altered excitability, such as epilepsy [26, 86, 88–90]. The importance of Na^+ channels in brain hyperexcitability and the consequent epilepsy is further supported by the fact that a large number of antiepileptic drugs exert their antiepileptic effect by interacting with Na^+ channels [2, 91].

4.3.1. Expressional and Functional Alterations in Na⁺ Channels during Epilepsy. Accumulating evidence indicates that altered expression and functional regulation of Na⁺ channels in the neurons play an important role in the brain hyperexcitability and epileptic phenotype in both acquired and inherited epilepsy. In the cortex of a genetically seizure susceptible EI mouse brain and spontaneously epileptic rat hippocampus, a significant increase in total Na⁺ channel mRNA and protein, as well as in Nav1.1, Nav1.3, and β 1 subunits, was observed to contribute to the generation of epileptiform activity and the observed seizure phenotypes [92, 93]. The expression of Nav1.1 in hippocampal CA1 and that of Nav1.2 in the cortical neurons were found to be significantly increased, which was accompanied with increased neuronal excitability and spontaneous epileptic seizures in the Na⁺/H⁺ exchanger null mutant mouse [24, 94]. In a kindling seizure model, selectively increased expression of Nav1.6 mRNA and protein in hippocampal CA3 neurons and Nav1.6 immunoreactivity in the medial entorhinal neurons resulted in hyperexcitability in these brain regions [95, 96]. In acute status epilepticus models, a transient upregulation of Na⁺ channel mRNAs encoding Nav1.2 and Nav1.3 subunits was observed in the hippocampal neurons [97, 98]. In contrast, the rats with status epilepticus and chronically developed spontaneous epileptic seizures showed a selectively persistent down-regulation of Nav1.2, Nav1.6, and β 1 subunits, as well as short-term down-regulation of β 2 subunit. In addition, an increased excitability, manifested by the augmented window current due to the significant positive shift of inactivation potential and negative shift of activation potential and the resultant increased overlap between the activation and inactivation curve, was observed in the neurons of the hippocampal dentate gyrus [99]. This phenomenon may be caused by the down-regulation of β subunit expression, since β 1/ β 2 subunit, if co-expressed with α subunits, favors inactivation, accelerates recovery of Na⁺ currents [100–102], which increases the number of Na⁺ channels available to be activated, and thus increases the firing rate. In human brain with temporal lobe epilepsy, Nav1.3 mRNA in the pyramidal cells of hippocampal CA4 area is significantly upregulated, and Nav1.2 mRNA in the remaining pyramidal cells of hippocampal CA1, CA2, and CA3 areas is largely downregulated, while Nav1.1 and Nav1.6 do not show any differences in their expression in the hippocampus [103]. *SCN7A* gene that encodes atypical Na⁺ channels (Na_X) was recently reported to be increasingly and persistently expressed in the pyramidal neurons and astrocytes of the hippocampal CA1 and CA3 areas in patients with drug-resistant temporal lobe epilepsy and epileptic rats and is possibly responsible for the enhanced brain excitability and epileptogenesis [104]. In summary, the increased amplitude and density of the voltage-dependent Na⁺ currents, shortened phase of inactivation, and enhanced window currents due to a shift towards depolarization of inactivation currents and more negative activation has been associated with neuronal hyperexcitability and the development of some types of epilepsy [24, 94, 99, 105, 106]. Na⁺ channels, even in the few that fail to inactivate, carry the persistent fraction of Na⁺ currents (that are not sensitive to TTX), though small, and may drive the membrane towards

the firing threshold. Especially under physiological conditions, the persistent sodium currents serve to amplify or spatially integrate synaptic potentials, allow excitable cells to generate subthreshold oscillations, reduce the threshold for repetitive action potential firing, and therefore increase excitability of neurons associated with epilepsy [25, 95, 96, 107, 108]. Despite the differences in epilepsy types/models and Na⁺ channel subtypes in these reports, these findings suggest altered expression and functional regulation of Na⁺ channels (that carry Na⁺ currents including both TTX-sensitive and -resistant ones) are critically involved in brain hyperexcitability and the pathology of epilepsy.

4.3.2. Insights from Genetic Epilepsy Model. Genetic factors are important for the intrinsic excitability of neurons. Studies on Na⁺ channel mutation in the genetic epilepsy model broaden the view on the roles and the underlying mechanisms of Na⁺ channels in brain hyperexcitability and the pathophysiology of epilepsy. Gene mutations that result in channel dysfunction (channelopathies) play an essential role in neuronal excitability, leading to the development of a variety of epilepsy syndromes. The most convincing data on the role of Na⁺ channels in brain hyperexcitability and epileptogenesis comes from the identification of several hundred mutations of Na⁺ channels which lead to inherited epileptic syndromes ranging in severity from relatively mild disorders such as benign familial neonatal-infantile seizures (BFNIS), simple febrile seizures, and generalized epilepsy with febrile seizure plus (GEFS+), to severe epileptic encephalopathy such as severe myoclonic epilepsy of infancy (SMEI, also called Dravet's Syndrome), SMEI borderline, and intractable childhood epilepsy with generalized tonic-clonic seizures (see reviews [25, 86–89]).

So far, several hundred mutations of many Na⁺ channel subtypes, including Nav1.1 (*SCN1A*), Nav1.2 (*SCN2A*), Nav1.3 (*SCN3A*), Nav1.6 (*SCN8A*), even Nav1.7 (*SCN9A*, which is predominantly expressed in peripheral nervous system), and β 1 subunit (*SCN1B*), have been causally linked to a variety of genetic epilepsies [89]. However, the genotype-phenotype correlations for Na⁺ channel epilepsy are very complicated with high heterogeneity. This heterogeneity of genotype-phenotype correlation for Na⁺ channel epilepsy is reflected in the observation that the same gene mutation may result in different phenotypes of epilepsy, and in turn, a single phenotype may be a result of different gene mutations of Na⁺ channels. For example, mutations in *SCN1A* have been reported to cause epilepsy with the symptoms ranging from febrile seizures and GEFS+ to SMEI, and mutations in *SCN2A* are identified to cause BFNIS, GEFS+, SMEI, and intractable epilepsy with mental decline [86–89]. On the other hand, Dravet's Syndrome is reported to have mutations in *SCN1A*, *SCN2A*, and *SCN1B*, and the mutations in both *SCN1A* and *SCN2A* lead to GEFS+ [87, 89]. Among all the mutations, Nav1.1 mutations account for the majority of established epilepsy syndromes in children [86–89, 109]. Approximately 30 *SCN1A* mutations have been identified to account for GEFS+ and all of them are missense mutations.

Many other missense mutations in *SCN1A* also contribute to Dravet's Syndrome, but most of the complications of Dravet's Syndrome result from *SCN1A* mutations caused by frame shift, nonsense, and splice-site mutations, which lead to a truncated protein and haploinsufficiency of *SCN1A* [86–90, 109, 110]. Unlike *SCN1A*-GEFS+ mutations that show a Mendelian inheritance pattern within affected families, most *SCN1A*-SMEI mutations occur *de novo* in the affected child.

Na⁺ channel mutations may result in either gain of function or loss of function that has been proposed to, respectively, increase and decrease the neuronal excitability [87]. The gain of function of Na⁺ channels is manifested by the increased current density, negative shift of activation, positive shift of inactivation, enhanced persistent Na⁺ currents, or mixed effects on channel kinetics but with the net effect of an increase in activity. The loss of function of Na⁺ channels is reflected by the changes that are opposite to those seen with gain of function. However, both gain of function and loss of function in Nav1.1 can predispose the brain to abnormal excitability, that is, brain hyperexcitability and consequent epilepsy syndrome. The increase in neuronal excitability due to gain of function in Na⁺ channels is quite straightforward to be understood and is further supported by the fact that many antiepileptic drugs developed are Na⁺ channel blockers [2, 91]. It is very surprising, however, that “loss of function” in Na⁺ channels also makes the brain very hyperexcitable although it decreases the neuronal excitability. Fortunately, this mystery was unveiled recently with the targeted knockout mice and rats carrying mutated *SCN1A* which developed epileptic seizures (SMEI and GEFS+) and sporadically died within the first postnatal month for the SMEI mice [90, 111–114]. Immunohistochemical analysis revealed that in a developing rodent brain, Nav1.1 was predominantly expressed in the inhibitory GABAergic interneurons of the neocortex and hippocampus, as well as the cerebellar GABAergic Purkinje cells that serve as the output pathway for information on movement, coordination, and balance from the cerebellar cortex [111–114]. Mutations or deletion of Nav1.1 lead to the loss of sustained high-frequency firing of action potential and excitability in the hippocampal and cortical inhibitory interneurons and Purkinje neurons, which allows hyperexcitability of principal neurons (e.g., dentate granule cells and pyramidal neurons) in the neuronal networks, thus leading to brain hyperexcitability and subsequently epilepsy. A unified loss of function hypothesis for Nav1.1 genetic epilepsies has been proposed [86, 88]. According to this hypothesis, the severity of epileptic phenotypes of Nav1.1 mutations is dependent on the extent of Nav1.1 functional damage due to mutations, as, for instance, the spectrum of severity of Nav1.1-associated forms of epilepsy results from an increasing severity of loss of function mutations in Nav1.1 channels and increasing impairment of action potential firing of the GABAergic inhibitory neurons [88]. As mentioned earlier, mild impairment of Nav1.1 channel function causes febrile seizures and moderate to severe impairment of Nav1.1 function due to missense or nonsense mutations causing GEFS+ and SMEI [86, 88].

4.3.3. Na⁺ Channel Based Neuronal and Network Excitability.

The above discussion on altered expression and functions as well as mutations in Na⁺ channels strongly supports the belief that abnormal Na⁺ channel activities are critically involved in neuronal hyperexcitability and the pathology of epilepsy. However, it should be pointed out that emphasizing the important roles of Na⁺ channels in the intrinsic neuronal excitability and the consequent epilepsy does not mean that Na⁺ channels hold any less importance in the network excitability. As we elaborated earlier, both neuronal excitability and network excitability contribute to the hyperexcitability in the epileptic brain. Since epileptic seizures are regarded as an “electrical storm” of brain hyperexcitability [86], they involve not only intrinsic neuronal properties, but also a cluster of anatomically and functionally associated neurons that form epileptic networks and propagate the extremely synchronized “electrical storm” within the networks [1]. Therefore, it is important to realize that Na⁺ channels regulate the brain excitability by altering both intrinsic neuronal and network excitability. The genetic models of SMEI show that the Nav1.1 mutation or deletion affects the inhibitory interneurons in the hippocampus and cortex [90, 111, 113]. Even though the excitatory transmission is not affected, the balance between inhibition and excitation within the networks is severely disrupted [111, 113]. In this model, though the embryonic Nav1.3 channels were found to be upregulated probably as a partial compensatory response to the impaired inhibition and disrupted balance between inhibitory and excitatory transmission [111], the network excitability is greatly enhanced due to Nav1.1 mutation that leads to a loss of sustained high-frequency firing of action potential in the hippocampal and cortical inhibitory interneurons and a limited compensatory capacity of Nav1.3 channels, thereby, making the brain very hyperexcitable. Therefore, Na⁺ channels play a central role in epileptogenesis, which involves interplay of both intrinsic neuronal properties and network activities.

5. Concluding Remarks

Na⁺ channel expressional and functional upregulation has been demonstrated to be critical to epileptic hyperexcitability and seizures, while the inhibitory regulation of Na⁺ channels by DOR [16, 20–22, 81] may contribute to the proper control of neuronal excitability. An impairment of such a balancing mechanism, for example, Na⁺ channel upregulation and/or DOR downregulation in genetic or acquired conditions, may lead to neuronal dysfunction and eventually neurological diseases, especially epileptic seizures. Indeed, Na⁺ channel dysregulation has been casually linked to human epilepsy and well demonstrated in epileptic animals with abundant supporting evidence. For example, in the mutant brain exhibiting spontaneous epilepsy, Na⁺ channel was upregulated [24], while DOR was downregulated in the same brain [78], suggesting a potential role of DOR impairment in the pathophysiology of epilepsy associated with genetic abnormality.

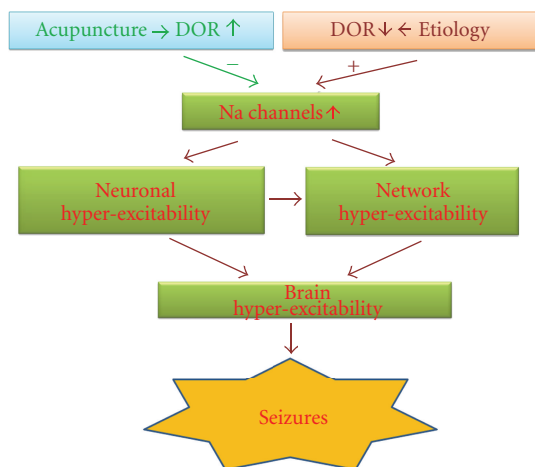


FIGURE 1: Schematic demonstration of the potential relation between acupuncture, opioid, and Na^+ channels in the regulation of brain hyperexcitability and epileptic seizures. Acupuncture can regulate the levels of endogenous opioids and their receptors in the brain. The released opioids activate δ -opioid receptors, and Na^+ channels are inhibited by activated δ -opioid receptors via signaling molecules such as PKC. Thus the neuronal discharges are inhibited and overexcited brain is “cooled” leading to the termination of epilepsy.

Since Na^+ channel upregulation contributes greatly to some kinds of epileptic hyperexcitability that leads to epilepsies, the DOR-mediated inhibition of Na^+ channels could provide a novel clue to open a vast potential of solutions to epileptic seizures. In fact, many antiepileptic drugs are actually inhibitors of Na^+ channels [2, 91]. Moreover, acupuncture can regulate the activities of endogenous opioids and their receptors in both animals and patients with epilepsy, thus exerting its antiepileptic effects. Therefore, stimulating appropriate acupoints with suitable manipulations may be a useful strategy for the treatment of epilepsy. Figure 1 presents a schematic demonstration regarding the interaction between acupuncture, opioids and Na^+ channels in regulation of hyperexcitability and epileptic seizures in the brain.

However, some issues need attention with regard to the association between acupuncture therapy for epilepsy and the role of opioids, and Na^+ channels. As previously discussed, loss of function of Na^+ channels in the inhibitory interneurons can cause brain hyperexcitability and epilepsy. Therefore, it is possible that activation of the opioid system by acupuncture causes inhibition of Na^+ channel activity in inhibitory interneurons, which may further aggravate the symptoms of epilepsy. Despite the demonstration of an antiepileptic effect following DOR activation in some studies [115–118], several other reports showed opposite results. For example, SNC80, a putative DOR agonist, is proconvulsive [119, 120] though it is reported to inhibit Na^+ channel activity [80]. The reasons for the complex and mixed effects of the δ -opioid system on seizures are not well clarified yet, but could be partially related to multiple factors like animal species (e.g., proconvulsive in rats but has little effect in rhesus monkeys) [119–121], seizure types, the methods of drug administration [122], dose used [123], target neurons, and so

forth (also see [1]). Among these factors, the location of DOR on the target neuron seems critical and important. In the hippocampus, both granule cells and inhibitory GABAergic interneurons express DOR [124, 125]. DOR activation in the granule cells inhibits voltage-gated Na^+ channels and thus lowers the excitability of granule neurons [80], which reduces excitatory transmission in the epileptic network and subsequently suppresses seizures. However, DOR activation in inhibitory interneurons leading to the inhibition of Na^+ channels, as observed by Remy et al. [80] in granule neurons, may result in facilitation, rather than suppression, of seizures via postsynaptic disinhibition [126, 127], as has been observed [119, 120]. Therefore, selective activation/inhibition of the opioid system in certain locations of the epileptic networks with acupuncture therapy is critical but also challengeable for the therapeutic outcome. It has been shown that in seizure rat models, acupuncture increases dynorphin synthesis and release, enhances the activity of KOR (which is abundantly distributed in hippocampal granule cell and perforant path) [126, 127] in the hippocampus, and decreases the DOR activity, synthesis, and release of enkephalin (which mainly influences inhibitory interneuron activity) [124, 125]. Therefore, acupuncture balances the inhibition and excitation in the network and thus suppresses the seizures [1]. In this way, acupuncture exerts its antiepileptic effects by normalizing the disrupted neuronal and network excitability (by lowering the overexcited neuronal activity through multiple strategies like enhancing the inhibitory system and attenuating the excitatory system in the brain via regulation of the activities of opioid- Na^+ channels), since the effects of acupuncture on disrupted neuronal function are bidirectional depending on the alterations in the brain functions and activities [128]. We believe that a further clarification on the correlations between acupuncture, opioids, and Na^+ channels can better help us explore the mystery of acupuncture therapy on epilepsy.

Abbreviations

BFNIS:	Benign familial neonatal-infantile seizures
DOR:	δ -opioid receptor
GEFS+:	Generalized epilepsy with febrile seizure plus
KOR:	κ -opioid receptor
MOR:	μ -opioid receptor
SMEI:	Severe myoclonic epilepsy of infancy
TTX:	Tetrodotoxin.

Acknowledgments

This work was supported by NIH (HD-034852, AT-004422), Vivian L. Smith Neurologic Foundation, NBRP (2009CB522901, 2012CB518502), and CSA of TCM.

References

- [1] D. Chao and Y. Xia, “Acupuncture treatment of epilepsy,” in *Current Research in Acupuncture*, Y. Xia, G. Ding, and G. C. Wu, Eds., pp. 129–214, Springer, New York, Heidelberg, Dordrecht, London, USA, 2012.

- [2] A. C. Errington, T. Stöhr, and G. Lees, "Voltage gated ion channels: targets for anticonvulsant drugs," *Current Topics in Medicinal Chemistry*, vol. 5, no. 1, pp. 15–30, 2005.
- [3] J. Kong, R. Gollub, T. Huang et al., "Acupuncture de qi, from qualitative history to quantitative measurement," *Journal of Alternative and Complementary Medicine*, vol. 13, no. 10, pp. 1059–1070, 2007.
- [4] J. J. Mao, J. T. Farrar, K. Armstrong, A. Donahue, J. Ngo, and M. A. Bowman, "De qi: Chinese acupuncture patients' experiences and beliefs regarding acupuncture needling sensation—an exploratory survey," *Acupuncture in Medicine*, vol. 25, no. 4, pp. 158–165, 2007.
- [5] NIH Consensus Development Panel on Acupuncture, "Acupuncture," *The Journal of the American Medical Association*, vol. 280, no. 17, pp. 1518–1524, 1998.
- [6] V. Jindal, A. Ge, and P. J. Mansky, "Safety and efficacy of acupuncture in children: a review of the evidence," *Journal of Pediatric Hematology/Oncology*, vol. 30, no. 6, pp. 431–442, 2008.
- [7] Y. Wu, L. P. Zou, T. L. Han et al., "Randomized controlled trial of traditional Chinese medicine (acupuncture and Tuina) in cerebral palsy—part I: any increase in seizure in integrated acupuncture and rehabilitation group versus rehabilitation group?" *Journal of Alternative and Complementary Medicine*, vol. 14, no. 8, pp. 1005–1009, 2008.
- [8] D. M. Chao, L. L. Shen, S. Tjen-A-Looi, K. F. Pitsillides, P. Li, and J. C. Longhurst, "Naloxone reverses inhibitory effect of electroacupuncture on sympathetic cardiovascular reflex responses," *American Journal of Physiology*, vol. 276, no. 6, pp. H2127–H2134, 1999.
- [9] J. S. Han, "Acupuncture: neuropeptide release produced by electrical stimulation of different frequencies," *Trends in Neurosciences*, vol. 26, no. 1, pp. 17–22, 2003.
- [10] S. M. Wang, Z. N. Kain, and P. White, "Acupuncture analgesia: I. The scientific basis," *Anesthesia and Analgesia*, vol. 106, no. 2, pp. 602–610, 2008.
- [11] G. Wen, Y. Yang, Y. Lu, and Y. Xia, "Acupuncture-induced activation of endogenous opioid system," in *Acupuncture Therapy for Neurological Diseases: A Neurobiological View*, Y. Xia, X. D. Cao, G. C. Wu, and J. S. Cheng, Eds., pp. 104–119, Springer-Tsinghua Press, Beijing, Heidelberg, London, New York, NY, USA, 2010.
- [12] G. Wen, X. He, Y. Lu, and Y. Xia, "Effect of acupuncture on neurotransmitters/modulators," in *Acupuncture Therapy for Neurological Diseases: A Neurobiological View*, Y. Xia, X. D. Cao, G. C. Wu, and J. S. Cheng, Eds., pp. 120–142, Springer-Tsinghua Press, Beijing, Heidelberg, London, New York, NY, USA, 2010.
- [13] J. Liang and Y. Xia, "Acupuncture Modulation of central neurotransmitters," in *Current Research in Acupuncture*, Y. Xia, G. Ding, and G. C. Wu, Eds., pp. 1–36, Springer, New York, NY, USA, 2012.
- [14] P. Zhao, J. C. Guo, S. S. Hong, A. Bazy-Asaad, J. S. Cheng, and Y. Xia, "Electro-acupuncture and brain protection from cerebral ischemia: the role of delta-opioid receptor," *Society for Neuroscience Abstract*, vol. 28, p. 736, 2002.
- [15] X. S. Tian, F. Zhou, R. Yang, Y. Xia, G. C. Wu, and J. C. Guo, "Electroacupuncture protects the brain against acute ischemic injury via up-regulation of delta-opioid receptor in rats," *Zhong Xi Yi Jie He Xue Bao*, vol. 6, no. 6, pp. 632–638, 2008.
- [16] X. Kang, D. Chao, Q. Gu et al., " δ -opioid receptors protect from anoxic disruption of Na^+ homeostasis via Na^+ channel regulation," *Cellular and Molecular Life Sciences*, vol. 66, no. 21, pp. 3505–3516, 2009.
- [17] M. Chattopadhyay, M. Mata, and D. J. Fink, "Continuous δ -opioid receptor activation reduces neuronal voltage-gated sodium channel ($\text{Na}_v1.7$) levels through activation of protein kinase C in painful diabetic neuropathy," *Journal of Neuroscience*, vol. 28, no. 26, pp. 6652–6658, 2008.
- [18] D. Chao, A. Bazy-Asaad, G. Balboni, and Y. Xia, " δ -, but not μ -, opioid receptor stabilizes K^+ homeostasis by reducing Ca^{2+} influx in the cortex during acute hypoxia," *Journal of Cellular Physiology*, vol. 212, no. 1, pp. 60–67, 2007.
- [19] D. Chao, D. F. Donnelly, Y. Feng, A. Bazy-Asaad, and Y. Xia, "Cortical δ -opioid receptors potentiate K^+ homeostasis during anoxia and oxygen-glucose deprivation," *Journal of Cerebral Blood Flow and Metabolism*, vol. 27, no. 2, pp. 356–368, 2007.
- [20] D. Chao, A. Bazy-Asaad, G. Balboni, S. Salvadori, and Y. Xia, "Activation of DOR attenuates anoxic K^+ derangement via inhibition of Na^+ entry in mouse cortex," *Cerebral Cortex*, vol. 18, no. 9, pp. 2217–2227, 2008.
- [21] D. Chao, G. Balboni, L. H. Lazarus, S. Salvadori, and Y. Xia, " Na^+ mechanism of δ -opioid receptor induced protection from anoxic K^+ leakage in the cortex," *Cellular and Molecular Life Sciences*, vol. 66, no. 6, pp. 1105–1115, 2009.
- [22] D. Chao, X. He, Y. Yang et al., "DOR activation inhibits anoxic/ischemic Na^+ influx through Na^+ channels via PKC mechanisms in the cortex," *Experimental Neurology*, vol. 236, no. 2, pp. 228–239, 2012.
- [23] Y. Xia, M. L. Fung, J. P. O'Reilly, and G. G. Haddad, "Increased neuronal excitability after long-term O_2 deprivation is mediated mainly by sodium channels," *Molecular Brain Research*, vol. 76, no. 2, pp. 211–219, 2000.
- [24] Y. Xia, P. Zhao, J. Xue et al., " Na^+ channel expression and neuronal function in the Na^+/H^+ exchanger 1 null mutant mouse," *Journal of Neurophysiology*, vol. 89, no. 1, pp. 229–236, 2003.
- [25] C. E. Stafstrom, "Persistent sodium current and its role in epilepsy," *Epilepsy Currents*, vol. 7, no. 1, pp. 15–22, 2007.
- [26] M. Mantegazza, G. Curia, G. Biagini, D. S. Ragsdale, and M. Avoli, "Voltage-gated sodium channels as therapeutic targets in epilepsy and other neurological disorders," *The Lancet Neurology*, vol. 9, no. 4, pp. 413–424, 2010.
- [27] Y. Aghakhani, A. P. Bagshaw, C. G. Bénar et al., "fMRI activation during spike and wave discharges in idiopathic generalized epilepsy," *Brain*, vol. 127, no. 5, pp. 1127–1144, 2004.
- [28] R. Berman, M. Negishi, M. Vestal et al., "Simultaneous EEG, fMRI, and behavior in typical childhood absence seizures," *Epilepsia*, vol. 51, no. 10, pp. 2011–2022, 2010.
- [29] F. Moeller, H. Muhle, G. Wiegand, S. Wolff, U. Stephani, and M. Siniatchkin, "EEG-fMRI study of generalized spike and wave discharges without transitory cognitive impairment," *Epilepsy and Behavior*, vol. 18, no. 3, pp. 313–316, 2010.
- [30] J. P. Szaflarski, M. DiFrancesco, T. Hirschauer et al., "Cortical and subcortical contributions to absence seizure onset examined with EEG/fMRI," *Epilepsy and Behavior*, vol. 18, no. 4, pp. 404–413, 2010.
- [31] Z. Zhang, G. Lu, Y. Zhong et al., "fMRI study of mesial temporal lobe epilepsy using amplitude of low-frequency fluctuation analysis," *Human Brain Mapping*, vol. 31, no. 12, pp. 1851–1861, 2010.
- [32] A. Bragin, C. L. Wilson, and J. Engel Jr., "Chronic epileptogenesis requires development of a network of pathologically

- interconnected neuron clusters: a hypothesis," *Epilepsia*, vol. 41, supplement 6, pp. S144–S152, 2000.
- [33] P. A. Williams, P. Dou, and F. E. Dudek, "Epilepsy and synaptic reorganization in a perinatal rat model of hypoxia-ischemia," *Epilepsia*, vol. 45, no. 10, pp. 1210–1218, 2004.
- [34] R. J. Morgan and I. Soltesz, "Nonrandom connectivity of the epileptic dentate gyrus predicts a major role for neuronal hubs in seizures," *Proceedings of the National Academy of Sciences of the United States of America*, vol. 105, no. 16, pp. 6179–6184, 2008.
- [35] B. P. Bean, "The action potential in mammalian central neurons," *Nature Reviews Neuroscience*, vol. 8, no. 6, pp. 451–465, 2007.
- [36] K. Y. Chen, G. P. Chen, and X. Feng, "Observation of immediate effect of acupuncture on electroencephalograms in epileptic patients," *Journal of Traditional Chinese Medicine*, vol. 3, no. 2, pp. 121–124, 1983.
- [37] Z. Y. Shi, B. T. Gong, Y. W. Jia, and Z. X. Huo, "The efficacy of electro-acupuncture on 98 cases of epilepsy," *Journal of Traditional Chinese Medicine*, vol. 7, no. 1, pp. 21–22, 1987.
- [38] J. Yang, "Treatment of status epilepticus with acupuncture," *Journal of Traditional Chinese Medicine*, vol. 10, no. 2, pp. 101–102, 1990.
- [39] T. Wen, "Treatment of 78 cases of epilepsy in narcotic abstaining," *Zhongguo Zhen Jiu*, vol. 20, no. 4, p. 226, 2000.
- [40] Y. J. Deng, J. J. Wang, Y. P. Lin, W. Y. Liu, and L. H. Wang, "Clinical observation on treatment of epilepsy general tonic-clonic attack with catgut implantation at acupoint plus antiepileptic Western Medicine of small dose," *Zhongguo Zhen Jiu*, vol. 21, no. 5, pp. 271–273, 2001.
- [41] J. Lin, Q. P. Deng, and J. W. Zhang, "Observation on therapeutic effect of 160 cases of epilepsy treated with acupoint catgut embedding therapy," *Zhongguo Zhen Jiu*, vol. 21, no. 11, pp. 653–654, 2001.
- [42] J. C. Wang, "One hundred and twenty cases of epilepsy treated by three acupoints on back," *Shanghai Zhen Jiu Za Zhi*, vol. 20, no. 2, p. 20, 2001.
- [43] R. Ma, X. Zhang, Y. Liu, X. Li, C. Yang, and J. Xiong, "Clinical observation on treatment of tonic-clonic attack of infantile epilepsy with acupuncture plus Xi Feng capsule," *Journal of Traditional Chinese Medicine*, vol. 42, no. 5, pp. 276–278, 2001.
- [44] K. Y. Mao and Z. Guo, "Observations on the efficacy of combined acupuncture and medicine for treating epilepsy secondary to cerebral infarction," *Shanghai Zhen Jiu Za Zhi*, vol. 24, no. 6, pp. 17–18, 2005.
- [45] J. Zhang, Y. Z. Li, and L. X. Zhuang, "Observation on therapeutic effect of 90 tonic-clonic epilepsy patients treated by catgut implantation therapy," *Zhen Jiu Lin Chuang Za Zhi*, vol. 22, no. 6, pp. 8–10, 2006.
- [46] L. X. Zhuang, J. Zhang, and Y. Z. Li, "Clinical observation on catgut implantation at acupoint for treatment of general paroxysmal epilepsy," *Zhongguo Zhen Jiu*, vol. 26, no. 9, pp. 611–613, 2006.
- [47] Y. Ren, "Acupuncture treatment of Jacksonian epilepsy—a report of 98 cases," *Journal of Traditional Chinese Medicine*, vol. 26, no. 3, pp. 177–178, 2006.
- [48] Z. F. Xu, "Clinical observation on treatment of epileptic seizure by combined catgut embedding and herbal medicine," *Shanghai Zhen Jiu Za Zhi*, vol. 25, no. 12, pp. 13–14, 2006.
- [49] Y. P. Song, W. Yang, H. M. Guo, and Y. Y. Han, "Clinical observation on acupuncture combined with medicine for treatment of infantile febrile convulsion," *Zhongguo Zhen Jiu*, vol. 26, no. 8, pp. 561–562, 2006.
- [50] R. Yang and J. S. Cheng, "Effect of acupuncture on epilepsy," in *Acupuncture Therapy for Neurological Diseases: A Neurobiological View*, Y. Xia, X. D. Cao, G. C. Wu, and J. S. Cheng, Eds., pp. 326–364, Springer-Tsinghua Press, Beijing, Heidelberg, London, New York, 2010.
- [51] C. W. Lai and Y. H. C. Lai, "History of epilepsy in Chinese traditional medicine," *Epilepsia*, vol. 32, no. 3, pp. 299–302, 1991.
- [52] D. M. Chao, G. Chen, and J. S. Cheng, "Melatonin might be one possible medium of electroacupuncture anti-seizures," *Acupuncture and Electro-Therapeutics Research*, vol. 26, no. 1–2, pp. 39–48, 2001.
- [53] J. Guo, J. Liu, W. Fu et al., "The effect of electroacupuncture on spontaneous recurrent seizure and expression of GAD67 mRNA in dentate gyrus in a rat model of epilepsy," *Brain Research*, vol. 1188, no. 1, pp. 165–172, 2008.
- [54] J. Guo, J. Liu, W. Fu et al., "Effect of electroacupuncture stimulation of hindlimb on seizure incidence and supragranular mossy fiber sprouting in a rat model of epilepsy," *The Journal of Physiological Sciences*, vol. 58, no. 5, pp. 309–315, 2008.
- [55] X. Z. Kang and Y. Xia, "Effect of electroacupuncture on experimental epilepsy: roles of different acupoints and stimulation parameters," *Journal of Acupuncture and Tuina Science*, vol. 6, no. 5, pp. 279–280, 2008.
- [56] S. T. Kim, S. Jeon, H. J. Park et al., "Acupuncture inhibits kainic acid-induced hippocampal cell death in mice," *The Journal of Physiological Sciences*, vol. 58, no. 1, pp. 31–38, 2008.
- [57] J. L. Zhang, S. P. Zhang, and H. Q. Zhang, "Antiepileptic effect of electroacupuncture vs. vagus nerve stimulation in the rat thalamus," *Neuroscience Letters*, vol. 441, no. 2, pp. 183–187, 2008.
- [58] J. L. Zhang, S. P. Zhang, and H. Q. Zhang, "Antiepileptic effects of electroacupuncture vs vagus nerve stimulation on cortical epileptiform activities," *Journal of the Neurological Sciences*, vol. 270, no. 1–2, pp. 114–121, 2008.
- [59] G. Goiz-Marquez, S. Caballero, H. Solis, C. Rodriguez, and H. Sumano, "Electroencephalographic evaluation of gold wire implants inserted in acupuncture points in dogs with epileptic seizures," *Research in Veterinary Science*, vol. 86, no. 1, pp. 152–161, 2009.
- [60] X. Kang, X. Shen, and Y. Xia, "Electroacupuncture-induced attenuation of experimental epilepsy: comparative evaluation of acupoints and stimulation parameters," *Evidence-Based Complementary and Alternative Medicine*. In press.
- [61] R. Kloster, P. G. Larsson, R. Lossius et al., "The effect of acupuncture in chronic intractable epilepsy," *Seizure*, vol. 8, no. 3, pp. 170–174, 1999.
- [62] Y. Xia, X. Q. Guo, A. Z. Zhang, X. D. Cao, and P. Li, "Inhibitory effect of analogous electro-acupuncture on experimental arrhythmia," *Acupuncture and Electro-Therapeutics Research*, vol. 10, no. 1–2, pp. 13–34, 1985.
- [63] D. Z. Wu, J. Y. Ma, and W. J. Li, "Inhibitory effect of electroacupuncture on penicillin-induced cortical epileptiform discharges," *Sheng Li Xue Bao*, vol. 38, no. 3, pp. 325–331, 1986.
- [64] D. Wu, "Mechanism of acupuncture in suppressing epileptic seizures," *Journal of Traditional Chinese Medicine*, vol. 12, no. 3, pp. 187–192, 1992.
- [65] H. M. Gao and J. S. Cheng, "Role of intrahippocampal kappa opioid receptors in inhibiting the seizure by electroacupuncture (EA) in rats," *Zhen Ci Yan Jiu*, vol. 23, no. 2, pp. 122–125, 1998.

- [66] H. Yuan and J. S. Han, "Electroacupuncture accelerates the biogenesis of central enkephalins in the rat," *Sheng Li Xue Bao*, vol. 37, no. 3, pp. 265–273, 1985.
- [67] B. E. Wang and J. S. Cheng, "The relationship between dynorphin and acupuncture anticonvulsion in hippocampus," *Chinese Science Bulletin*, vol. 37, no. 13, pp. 1321–1323, 1992.
- [68] B. E. Wang and J. S. Cheng, "Alteration of dynorphin and leu-enkephalin in rat hippocampus during seizure and electroacupuncture," *Zhongguo Yao Li Xue Bao*, vol. 15, no. 2, pp. 155–157, 1994.
- [69] B. E. Wang and J. S. Cheng, "Release of hippocampal dynorphin during electro-stimulated seizure and acupuncture anticonvulsion," *Shanghai Zhen Jiu Za Zhi*, vol. 14, no. 1, pp. 33–34, 1995.
- [70] B. E. Wang, R. Yang, and J. S. Cheng, "Effect of electroacupuncture on the level of preproenkephalin mRNA in rat during penicillin-induced epilepsy," *Acupuncture and Electro-Therapeutics Research*, vol. 19, no. 2-3, pp. 129–140, 1994.
- [71] X. P. He, B. Y. Chen, J. M. Zhu, and X. D. Cao, "Change of Leu-enkephalin- and B-endorphin-like immunoreactivity in the hippocampus after electroconvulsive shock and electroacupuncture," *Acupuncture and Electro-Therapeutics Research*, vol. 14, no. 2, pp. 131–139, 1989.
- [72] X. P. He and X. D. Cao, "Effects of intrahippocampal δ -receptors on inhibition of electroconvulsive shock by electroacupuncture," *Zhongguo Yao Li Xue Bao*, vol. 10, no. 3, pp. 197–201, 1989.
- [73] X. P. He, J. M. Zhu, D. K. Huang, K. Y. Li, and X. D. Cao, "Effect of electroacupuncture on electro-convulsive shock—an autoradiographic study for opioid receptors," *Sheng Li Xue Bao*, vol. 42, no. 2, pp. 149–154, 1990.
- [74] O. Camilo and L. B. Goldstein, "Seizures and epilepsy after ischemic stroke," *Stroke*, vol. 35, no. 7, pp. 1769–1775, 2004.
- [75] L. Rocha, M. Cuellar-Herrera, M. Velasco et al., "Opioid receptor binding in parahippocampus of patients with temporal lobe epilepsy: its association with the antiepileptic effects of subacute electrical stimulation," *Seizure*, vol. 16, no. 7, pp. 645–652, 2007.
- [76] K. Raynor, H. Kong, Y. Chen et al., "Pharmacological characterization of the cloned κ -, δ -, and μ -opioid receptors," *Molecular Pharmacology*, vol. 45, no. 2, pp. 330–334, 1994.
- [77] G. Witkowski and P. Szulczyk, "Opioid μ receptor activation inhibits sodium currents in prefrontal cortical neurons via a protein kinase A- and C-dependent mechanism," *Brain Research*, vol. 1094, no. 1, pp. 92–106, 2006.
- [78] P. Zhao, M. C. Ma, H. Qian, and Y. Xia, "Down-regulation of delta-opioid receptors in Na^+/H^+ exchanger 1 null mutant mouse brain with epilepsy," *Neuroscience Research*, vol. 53, no. 4, pp. 442–446, 2005.
- [79] Y. Xia, H. Cao, J. H. Zhang et al., "Effect of δ -opioid receptor activation on Na^+ channel expression in cortical neurons subjected to prolonged hypoxia in culture," *Society Neuroscience Abstract*, vol. 27, article 381, 2001, Program no. 740.6.
- [80] C. Remy, S. Remy, H. Beck, D. Swandulla, and M. Hans, "Modulation of voltage-dependent sodium channels by the δ -agonist SNC80 in acutely isolated rat hippocampal neurons," *Neuropharmacology*, vol. 47, no. 7, pp. 1102–1112, 2004.
- [81] D. Chao and Y. Xia, "Ionic storm in hypoxic/ischemic stress: can opioid receptors subside it?" *Progress in Neurobiology*, vol. 90, no. 4, pp. 439–470, 2010.
- [82] M. S. Gold and J. D. Levine, "DAMGO inhibits prostaglandin E2-induced potentiation of a TTX-resistant Na^+ current in rat sensory neurons in vitro," *Neuroscience Letters*, vol. 212, no. 2, pp. 83–86, 1996.
- [83] X. Su, S. K. Joshi, S. Kardos, and G. F. Gebhart, "Sodium channel blocking actions of the κ -opioid receptor agonist U50,488 contribute to its visceral antinociceptive effects," *Journal of Neurophysiology*, vol. 87, no. 3, pp. 1271–1279, 2002.
- [84] W. A. Catterall, "From ionic currents to molecular mechanisms: the structure and function of voltage-gated sodium channels," *Neuron*, vol. 26, no. 1, pp. 13–25, 2000.
- [85] A. L. Goldin, "Resurgence of sodium channel research," *Annual Review of Physiology*, vol. 63, pp. 871–894, 2001.
- [86] D. S. Ragsdale, "How do mutant Nav1.1 sodium channels cause epilepsy?" *Brain Research Reviews*, vol. 58, no. 1, pp. 149–159, 2008.
- [87] A. Escayg and A. L. Goldin, "Sodium channel SCN1A and epilepsy: mutations and mechanisms," *Epilepsia*, vol. 51, no. 9, pp. 1650–1658, 2010.
- [88] W. A. Catterall, F. Kalume, and J. C. Oakley, "Nav1.1 channels and epilepsy," *Journal of Physiology*, vol. 588, no. 11, pp. 1849–1859, 2010.
- [89] M. H. Meisler, J. E. O'Brien, and L. M. Sharkey, "Sodium channel gene family: epilepsy mutations, gene interactions and modifier effects," *Journal of Physiology*, vol. 588, no. 11, pp. 1841–1848, 2010.
- [90] C. S. Cheah, F. H. Yu, R. E. Westenbrook et al., "Specific deletion of Nav1.1 sodium channels in inhibitory interneurons causes seizures and premature death in a mouse model of Dravet syndrome," *Proceedings of the National Academy of Sciences of the United States of America*, vol. 109, no. 36, pp. 14646–14651, 2012.
- [91] J. A. Armijo, M. Shushtarjan, E. M. Valdizan, A. Cuadrado, I. de las Cuevas, and J. Adín, "Ion channels and epilepsy," *Current Pharmaceutical Design*, vol. 11, no. 15, pp. 1975–2003, 2005.
- [92] S. Sashihara, N. Yanagihara, H. Kobayashi et al., "Overproduction of voltage-dependent Na^+ channels in the developing brain of genetically seizure-susceptible E1 mice," *Neuroscience*, vol. 48, no. 2, pp. 285–291, 1992.
- [93] F. Guo, N. Yu, J. Q. Cai et al., "Voltage-gated sodium channel Nav1.1, Nav1.3 and β 1 subunit were up-regulated in the hippocampus of spontaneously epileptic rat," *Brain Research Bulletin*, vol. 75, no. 1, pp. 179–187, 2008.
- [94] X. Q. Gu, H. Yao, and G. G. Haddad, "Increased neuronal excitability and seizures in the Na^+/H^+ exchanger null mutant mouse," *American Journal of Physiology*, vol. 281, no. 2, pp. C496–C503, 2001.
- [95] H. Blumenfeld, A. Lampert, J. P. Klein et al., "Role of hippocampal sodium channel Nav1.6 in kindling epileptogenesis," *Epilepsia*, vol. 50, no. 1, pp. 44–55, 2009.
- [96] N. J. Hargus, E. C. Merrick, A. Nigam et al., "Temporal lobe epilepsy induces intrinsic alterations in Na channel gating in layer II medial entorhinal cortex neurons," *Neurobiology of Disease*, vol. 41, no. 2, pp. 361–376, 2011.
- [97] F. Bartolomei, M. Gastaldi, A. Massacrier, R. Planells, S. Nicolas, and P. Cau, "Changes in the mRNAs encoding subtypes I, II and III sodium channel alpha subunits following kainate-induced seizures in rat brain," *Journal of Neurocytology*, vol. 26, no. 10, pp. 667–678, 1997.
- [98] E. Aronica, B. Yankaya, D. Troost, E. A. van Vliet, F. H. Lopes da Silva, and J. A. Gorter, "Induction of neonatal-sodium channel

- II and III (α -isoform mRNAs in neurons and microglia after status epilepticus in the rat hippocampus," *European Journal of Neuroscience*, vol. 13, no. 6, pp. 1261–1266, 2001.
- [99] R. K. Ellerkmann, S. Remy, J. Chen et al., "Molecular and functional changes in voltage-dependent Na^+ channels following pilocarpine-induced status epilepticus in rat dentate granule cells," *Neuroscience*, vol. 119, no. 2, pp. 323–333, 2003.
- [100] A. Toib, V. Lyakhov, and S. Marom, "Interaction between duration of activity and time course of recovery from slow inactivation in mammalian brain Na^+ channels," *Journal of Neuroscience*, vol. 18, no. 5, pp. 1893–1903, 1998.
- [101] C. Chen, V. Bharucha, Y. Chen et al., "Reduced sodium channel density, altered voltage dependence of inactivation, and increased susceptibility to seizures in mice lacking sodium channel β 2-subunits," *Proceedings of the National Academy of Sciences of the United States of America*, vol. 99, no. 26, pp. 17072–17077, 2002.
- [102] T. K. Aman, T. M. Grieco-Calub, C. Chen et al., "Regulation of persistent Na current by interactions between β subunits of voltage-gated Na channels," *Journal of Neuroscience*, vol. 29, no. 7, pp. 2027–2042, 2009.
- [103] W. R. J. Whitaker, R. L. M. Faull, M. Dragunow, E. W. Mee, P. C. Emson, and J. J. Clare, "Changes in the mRNAs encoding voltage-gated sodium channel types II and III in human epileptic hippocampus," *Neuroscience*, vol. 106, no. 2, pp. 275–285, 2001.
- [104] J. A. Gorter, E. Zurolo, A. Iyer et al., "Induction of sodium channel Na_x (SCN7A) expression in rat and human hippocampus in temporal lobe epilepsy," *Epilepsia*, vol. 51, no. 9, pp. 1791–1800, 2010.
- [105] M. Vreugdenhil, G. C. Faas, and W. J. Wadman, "Sodium currents in isolated rat CA1 neurons after kindling epileptogenesis," *Neuroscience*, vol. 86, no. 1, pp. 99–107, 1998.
- [106] S. O. M. Ketelaars, J. A. Gorter, E. A. van Vliet, F. H. Lopes da Silva, and W. J. Wadman, "Sodium currents in isolated rat CA1 pyramidal and dentate granule neurones in the post-status epilepticus model of epilepsy," *Neuroscience*, vol. 105, no. 1, pp. 109–120, 2001.
- [107] T. H. Rhodes, C. Lossin, C. G. Vanoye, D. W. Wang, and A. L. George Jr., "Noninactivating voltage-gated sodium channels in severe myoclonic epilepsy of infancy," *Proceedings of the National Academy of Sciences of the United States of America*, vol. 101, no. 30, pp. 11147–11152, 2004.
- [108] J. Epsztein, E. Sola, A. Represa, Y. Ben-Ari, and V. Crépel, "A selective interplay between aberrant EPSP_{KA} and I_{NaP} reduces spike timing precision in dentate granule cells of epileptic rats," *Cerebral Cortex*, vol. 20, no. 4, pp. 898–911, 2010.
- [109] C. Lossin, "A catalog of SCN1A variants," *Brain and Development*, vol. 31, no. 2, pp. 114–130, 2009.
- [110] G. Bechi, P. Scalmani, E. Schiavon, R. Rusconi, S. Franceschetti, and M. Mantegazza, "Pure haploinsufficiency for Dravet syndrome $\text{Na(V)}1.1$ (SCN1A) sodium channel truncating mutations," *Epilepsia*, vol. 53, no. 1, pp. 87–100, 2012.
- [111] F. H. Yu, M. Mantegazza, R. E. Westenbroek et al., "Reduced sodium current in GABAergic interneurons in a mouse model of severe myoclonic epilepsy in infancy," *Nature Neuroscience*, vol. 9, no. 9, pp. 1142–1149, 2006.
- [112] F. Kalume, F. H. Yu, R. E. Westenbroek, T. Scheuer, and W. A. Catterall, "Reduced sodium current in Purkinje neurons from Nav1.1 mutant mice: implications for ataxia in severe myoclonic epilepsy in infancy," *Journal of Neuroscience*, vol. 27, no. 41, pp. 11065–11074, 2007.
- [113] I. Ogiwara, H. Miyamoto, N. Morita et al., "Nav1.1 localizes to axons of parvalbumin-positive inhibitory interneurons: a circuit basis for epileptic seizures in mice carrying an Scn1a gene mutation," *Journal of Neuroscience*, vol. 27, no. 22, pp. 5903–5914, 2007.
- [114] Y. Ohno, N. Sofue, S. Ishihara, T. Mashimo, M. Sasa, and T. Serikawa, "Scn1a missense mutation impairs GABAA receptor-mediated synaptic transmission in the hippocampus," *Biochemical and Biophysical Research Communications*, vol. 400, no. 1, pp. 117–122, 2010.
- [115] F. C. Tortella and J. B. Long, "Endogenous anticonvulsant substance in rat cerebrospinal fluid after a generalized seizure," *Science*, vol. 228, no. 4703, pp. 1106–1108, 1985.
- [116] F. C. Tortella, E. Echevarria, L. Robles, H. I. Mosberg, and J. W. Holaday, "Anticonvulsant effects of mu (DAGO) and delta (DPDPE) enkephalins in rats," *Peptides*, vol. 9, no. 5, pp. 1177–1181, 1988.
- [117] S. Koide, H. Onishi, S. Yamagami, and Y. Kawakita, "Effects of morphine and D-Ala2-D-Leu5-enkephalin in the seizure-susceptible El mouse," *Neurochemical Research*, vol. 17, no. 8, pp. 779–783, 1992.
- [118] I. Madar, R. P. Lesser, G. Krauss et al., "Imaging of δ - and μ -opioid receptors in temporal lobe epilepsy by positron emission tomography," *Annals of Neurology*, vol. 41, no. 3, pp. 358–367, 1997.
- [119] I. Danielsson, M. Gasior, G. W. Stevenson, J. E. Folk, K. C. Rice, and S. S. Negus, "Electroencephalographic and convulsant effects of the delta opioid agonist SNC80 in rhesus monkeys," *Pharmacology Biochemistry and Behavior*, vol. 85, no. 2, pp. 428–434, 2006.
- [120] E. M. Jutkiewicz, M. G. Baladi, J. E. Folk, K. C. Rice, and J. H. Woods, "The convulsive and electroencephalographic changes produced by nonpeptidic δ -opioid agonists in rats: comparison with pentylenetetrazol," *Journal of Pharmacology and Experimental Therapeutics*, vol. 317, no. 3, pp. 1337–1348, 2006.
- [121] S. S. Negus, M. B. Gatch, N. K. Mello, X. Zhang, and K. Rice, "Behavioral effects of the delta-selective opioid agonist SNC80 and related compounds in rhesus monkeys," *Journal of Pharmacology and Experimental Therapeutics*, vol. 286, no. 1, pp. 362–375, 1998.
- [122] E. M. Jutkiewicz, K. C. Rice, J. R. Traynor, and J. H. Woods, "Separation of the convulsions and antidepressant-like effects produced by the delta-opioid agonist SNC80 in rats," *Psychopharmacology*, vol. 182, no. 4, pp. 588–596, 2005.
- [123] S. B. Bausch, J. P. Garland, and J. Yamada, "The delta opioid receptor agonist, SNC80, has complex, dose-dependent effects on pilocarpine-induced seizures in Sprague-Dawley rats," *Brain Research*, vol. 1045, no. 1-2, pp. 38–44, 2005.
- [124] X. Rezaï, L. Faget, E. Bednarek, Y. Schwab, B. L. Kieffer, and D. Massotte, "Mouse delta opioid receptors are located on presynaptic afferents to hippocampal pyramidal cells," *Cellular and Molecular Neurobiology*, vol. 32, no. 4, pp. 509–516, 2012.
- [125] E. Erbs, L. Faget, G. Scherrer et al., "Distribution of delta opioid receptor-expressing neurons in the mouse hippocampus," *Neuroscience*, vol. 221, pp. 203–213, 2012.
- [126] M. L. Simmons and C. Chavkin, "Endogenous opioid regulation of hippocampal function," *International Review of Neurobiology*, vol. 39, pp. 145–196, 1996.
- [127] C. T. Drake, C. Chavkin, and T. A. Milner, "Opioid systems in the dentate gyrus," *Progress in Brain Research*, vol. 163, pp. 245–263, 2007.

- [128] K. K. S. Hui, O. Marina, J. Liu, B. R. Rosen, and K. K. Kwong, "Acupuncture, the limbic system, and the anticorrelated networks of the brain," *Autonomic Neuroscience: Basic and Clinical*, vol. 157, no. 1-2, pp. 81-90, 2010.

Research Article

Electroacupuncture-Induced Attenuation of Experimental Epilepsy: A Comparative Evaluation of Acupoints and Stimulation Parameters

Xuezhi Kang,^{1,2} Xueyong Shen,^{1,2} and Ying Xia^{3,4}

¹ Shanghai Research Center for Acupuncture and Meridians, Shanghai 201203, China

² Shanghai University of Traditional Chinese Medicine, Shanghai 201203, China

³ The University of Texas Medical School at Houston, Houston, TX 77030, USA

⁴ Yale University School of Medicine, New Haven, CT 06510, USA

Correspondence should be addressed to Ying Xia; ying.xia@uth.tmc.edu

Received 12 August 2012; Revised 10 November 2012; Accepted 15 December 2012

Academic Editor: Guang-Hong Ding

Copyright © 2013 Xuezhi Kang et al. This is an open access article distributed under the Creative Commons Attribution License, which permits unrestricted use, distribution, and reproduction in any medium, provided the original work is properly cited.

The efficacy of electroacupuncture (EA) on epilepsy remains to be verified because of previous controversies that might be due to the complexity of the effects induced by different acupoints and stimulation approaches adopted. Therefore, we investigated the effects of EA on epilepsy to determine the specific acupoints and optimal stimulation parameters in this work. Experimental epilepsy was induced by injecting kainic acid to the lateral cerebral ventricle of adult male SD rats. EA with a low-frequency (10 Hz/1 mA) or high-frequency (100 Hz/1 mA) current was applied to the epileptic model for 30 minutes starting at 0.5 hour after the injection. Four pairs of acupoints were tested, that is, Shuigou (DU26) + Dazhui (DU14), Jinsuo (DU8) + Yaoqi (EXB9), Neiguan (PC6) + Quchi (LI11), and Fenglong (ST40) + Yongquan (KI1). We found that (1) low- or high-frequency EA at different acupoints reduced epileptic seizures ($P < 0.05$ versus the control) with an exception of low-frequency EA at Neiguan (PC6) and Quchi (LI11); (2) low-frequency EA induced a better effect at Fenglong (ST40) plus Yongquan (KI1) than that of the other acupoints ($P < 0.05$); (3) there is no significant difference in the effects of high-frequency EA at these acupoints; and (4) the high-frequency EA elicited a greater effect than that of low-frequency EA in all groups ($P < 0.05$), with an exception at Jinsuo (DU8) + Yaoqi (EXB9). The EA-induced attenuation appeared 1–1.5 hours after EA with no appreciable effect in the first hour after EA in either the EEG or the behavioral tests. We conclude that EA attenuation of epileptic seizures is dependent on the stimulation parameters and acupoints and that the delay in appearance of the EA effect could be a reflection of the time required by the EA signal to regulate neural function in the central nervous system.

1. Introduction

Epilepsy, manifesting as recurrent seizures induced by abnormal electrical discharges in the brain, is a grave neurological disorder and incurs devastating effects on both patients and their families. There are numerous etiological factors implicated in epileptic seizures, including genetic abnormalities, hypoxic/ischemic injury, tumors, and trauma [1–5]. However, the currently available treatment strategies against epileptic seizures are limited and are associated with serious adverse effects [6–8]. In fact, the current treatment of patients with seizure disorders follows a *hit-and-trial* routine involving trial

of various drugs and/or combinations to see works better for the individual. In more than one-third of these patients, no drug has proven to be effective. This includes a huge proportion given the worldwide prevalence of 50 million patients with seizure disorders. Although surgical treatment is successful in certain types of epilepsy, it is expensive, associated with side effects, and may not be easily amenable to all patients. The annual cost of epilepsy is estimated around \$12.5 billion in the United States alone, stemming mostly from loss of productivity by those with intractable or poorly controlled epilepsy [9]. This underscores the need for an alternative and effective epilepsy treatment. Toward this goal,

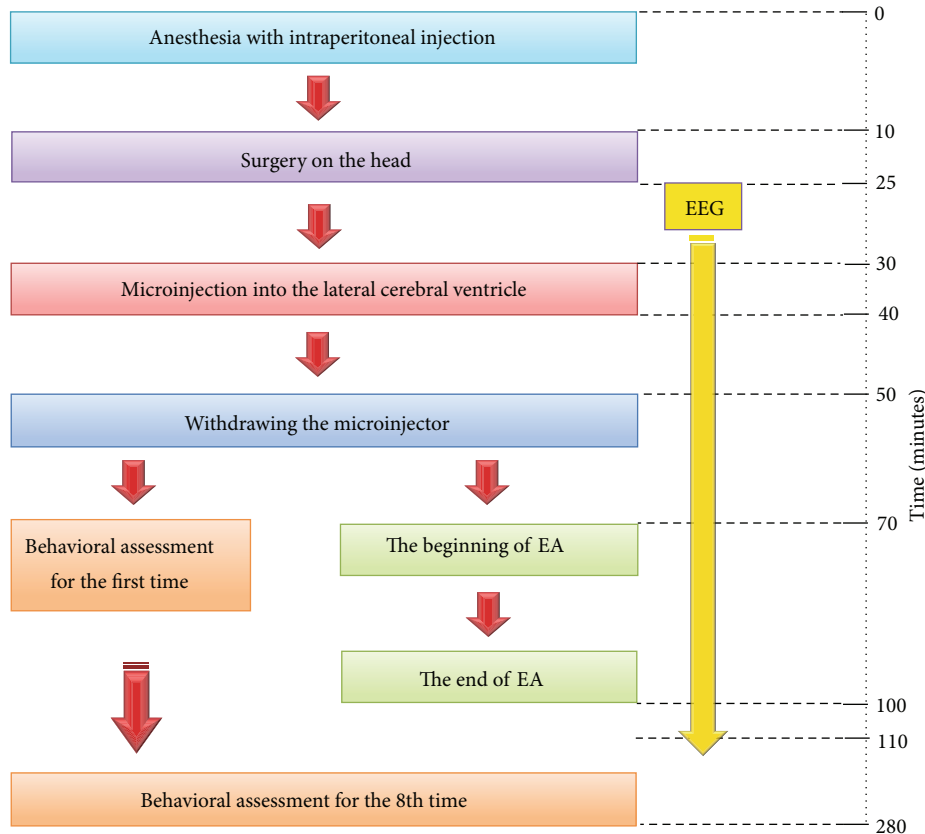


FIGURE 1: Experimental flow chart.

TABLE 1: Racine's 5-point scales*.

Grades	Behavioral changes
1	Mouth and facial movement
2	Head nodding
3	Forelimb clonus
4	Rearing with forelimb clonus
5	Rearing and falling with forelimb clonus (generalized motor convulsions)

* Score 0: without any abnormal activity/sign (i.e., the status before the injection KA).

we have recently made novel observations on utilization of acupuncture in epilepsy treatment.

In traditional Chinese medicine, acupuncture use has a long history in the treatment of epilepsy. Owing to its reproducibility and objectivity, electroacupuncture (EA) is increasingly being accepted and utilized in modern standards of care. In the past, some Chinese and Western investigators demonstrated the attenuation of chemically induced seizures in animals following EA [10–15]. Several scientific investigations published in the Chinese literature have documented a therapeutic effect of acupuncture/EA on epilepsy [16–20]. However, the efficacy of acupuncture/EA in epilepsy is still uncertain due to the limitations of the existing clinical studies and the flaws in their design. First of all, none of these clinical reports adequately describe the selection of

their controls. Moreover, some clinical reports have failed to demonstrate a therapeutic effect of acupuncture/EA in the chronic intractable epilepsy [21–23]. It is very difficult to design a randomized, double-blinded placebo-controlled study in patients with epilepsy. Therefore, a systematic and well-controlled bench study is of utmost importance in order to validate the efficacy of acupuncture/EA before extrapolating its use in a clinical setting.

Multitude of factors can influence the efficacy of EA. Optimal parameters are essential including selection of appropriate regions for stimulation (acupoints), frequency of stimulation, and the method employed for stimulation. Thus, it is possible for these earlier reports to bear inconsistencies in their results owing to the differences in acupuncture parameters and acupoints used. No prior study has been conducted to systematically compare effects of low- and high-frequency EA at different acupoints on epileptic seizures.

In the present work, we have attempted to tackle three fundamental issues: (1) to verify the efficacy of EA in attenuation of epileptic seizures; (2) to examine if low- and high-frequency EA had different effects on epilepsy; and (3) to determine if different acupoints with the same EA parameters lead to different EA effects.

2. Materials and Methods

2.1. Animals. All animal procedures were performed in accordance with the guidelines of the Animal Care and Use

TABLE 2: Frequency & Amplitude of EEG before and after 10 Hz/1 mA EA.

Acupoints	Frequency (Hz)		Amplitude (μ V)	
	Before EA	After EA	Before EA	After EA
DU26 + DU14 ($n = 5$)	24.14 \pm 9.54	14.44 \pm 11.32	44.04 \pm 47.73	56.28 \pm 47.16
DU8 + EXB9 ($n = 7$)	13.89 \pm 11.04	21.27 \pm 12.00	55.47 \pm 41.97	53.16 \pm 51.02
LIII + PC6 ($n = 6$)	23.61 \pm 12.08	19.27 \pm 13.85	39.27 \pm 30.14	26.92 \pm 35.52
ST40 + KII ($n = 7$)	22.41 \pm 12.00	18.37 \pm 14.87	44.17 \pm 39.18	22.16 \pm 21.11

Before EA: Before the initiation of EA (30 minutes after the KA injection).

After EA: 10 minutes after the end of EA (70 minutes after the KA injection).

TABLE 3: Frequency & Amplitude of EEG before and after 100 Hz/1 mA EA.

Acupoints	Frequency (Hz)		Amplitude (μ V)	
	Before EA	After EA	Before EA	After EA
DU26 + DU14 ($n = 6$)	13.57 \pm 12.35	12.85 \pm 12.82	110.48 \pm 72.37	122.10 \pm 160.36
DU8 + EXB9 ($n = 7$)	13.88 \pm 13.03	21.29 \pm 14.20	64.40 \pm 23.86	52.10 \pm 39.08
LIII + PC6 ($n = 6$)	15.28 \pm 9.44	16.57 \pm 17.27	74.33 \pm 35.56	63.42 \pm 37.38
ST40 + KII ($n = 7$)	13.41 \pm 7.56	15.33 \pm 11.01	74.46 \pm 21.65	65.58 \pm 54.1

Before EA: Before the initiation of EA (30 minutes after the KA injection).

After EA: 10 minutes after the end of EA (70 minutes after the KA injection).

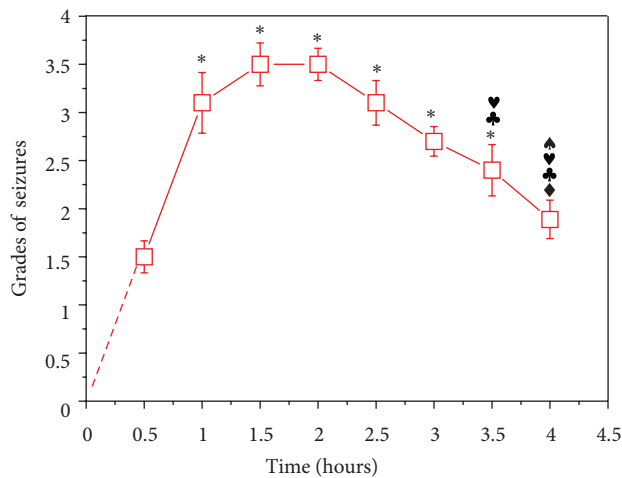


FIGURE 2: Change in grade of seizures against time after the KA injection. KA was injected in the lateral ventricle of the SD rats. * $P < 0.05$ versus that at 0.5 hour; $\spadesuit P < 0.05$ versus that at 1 hour; $\clubsuit P < 0.05$ versus that at 1.5 hours; $\heartsuit P < 0.05$ versus that at 2 hours; $\diamond P < 0.05$ versus that at 2.5 hours. Note that the onset of seizures appeared 0.5 hour after the KA injection, reached the peak 1.5–2 hours later, and then gradually started to decrease.

Committee of Shanghai Research Center for Acupuncture and Meridians. Adult male Sprague Dawley rats with a body weight of 180–220 g were purchased from Shanghai Experimental Animal Center of Chinese Academy of Sciences and were housed at 22–25°C. All the rats were allowed to drink and eat freely and had a controlled circadian rhythm set as 12-hour light/12-hour dark. The animals were randomly grouped into blank control ($n = 4$) and epilepsy ($n = 63$) groups. Furthermore, the epileptic animals were randomly subdivided to a group of epilepsy only ($n = 10$) and epilepsy plus EA groups ($n = 53$).

2.2. Equipment and Materials/Reagents. Kainic Acid (KA) was purchased from Sigma Corporation (USA). All other chemicals and reagents came from China National Pharmaceutical Group Corporation. Equipments used in the study were as follows: stereotaxic apparatus (Model SR-6R, Narishige, Japan), electroacupuncture apparatus (Model G6805-2, Shanghai Medical Instrument High-tech Co., China), oscilloscope (Model XJ4210A; Shanghai Xinjian Instrument & Equipment Co., Ltd., China), bioelectric amplifier (Model ML132, AD Instruments Pty Ltd., Australia), and PowerLab 4/25 data acquisition system (Model ML845, AD Instruments Pty Ltd., Australia).

2.3. Induction of Epileptic Seizures. The rats were anesthetized with intraperitoneal injection of 10% chloral hydrate (0.4 g/kg body weight) and fixed on the stereotaxic instrument. The head epidermis and subgaleal were cut to expose the fonticulus anterior, fonticulus posterior, and the parietal bone. We adjusted and made the fonticulus anterior 1 mm higher than fonticulus posterior and recorded (1) anterior fontanelle sagittal level as R_1 ; (2) anterior fontanelle coronal level as P_1 ; and (3) the height of the anterior fontanelle as H_1 .

For microinjection into the lateral cerebral ventricle, a hole of less than 0.5 mm diameter was drilled at $R_1 + 0.2$ mm (0.2 mm posterior the anterior fontanelle) and $P_1 + 1.5$ mm (1.5 mm from the midline) to penetrate the skull without damaging the meninges. The microinjector filled with KA solution (0.7 μ L, 1 μ g/ μ L) was inserted into the lateral cerebral ventricle at $H_1 - 4.2$ mm (at a depth of 4.2 mm beneath H_1). The KA solution was then injected into the lateral ventricle over 10 minutes at a uniform speed. After the end of injection, the micro-injector was left in place for 10 minutes and then gradually withdrawn.

In the control animals, KA solution was replaced with saline but followed the same injection procedure and into the same ventricle as in the KA animals.

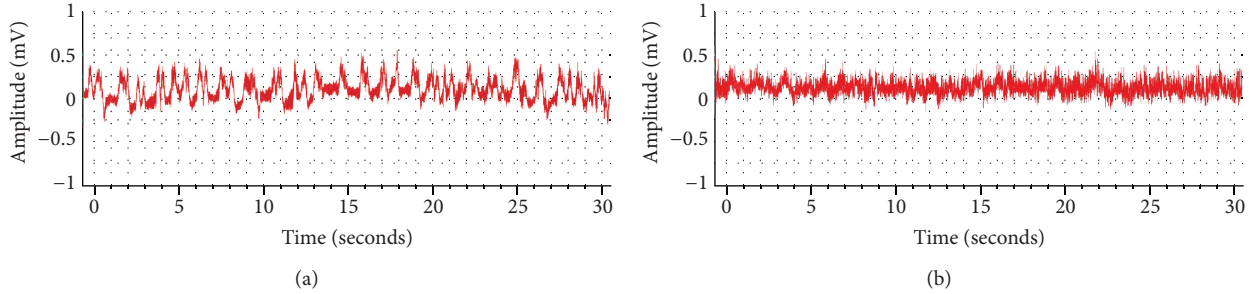


FIGURE 3: Representative EEG recordings from the rat before and after the KA injection. (a) Before KA injection and (b) 30 minutes after the injection. Note that KA induced an epileptic spike wave pattern with a large increase in frequency.

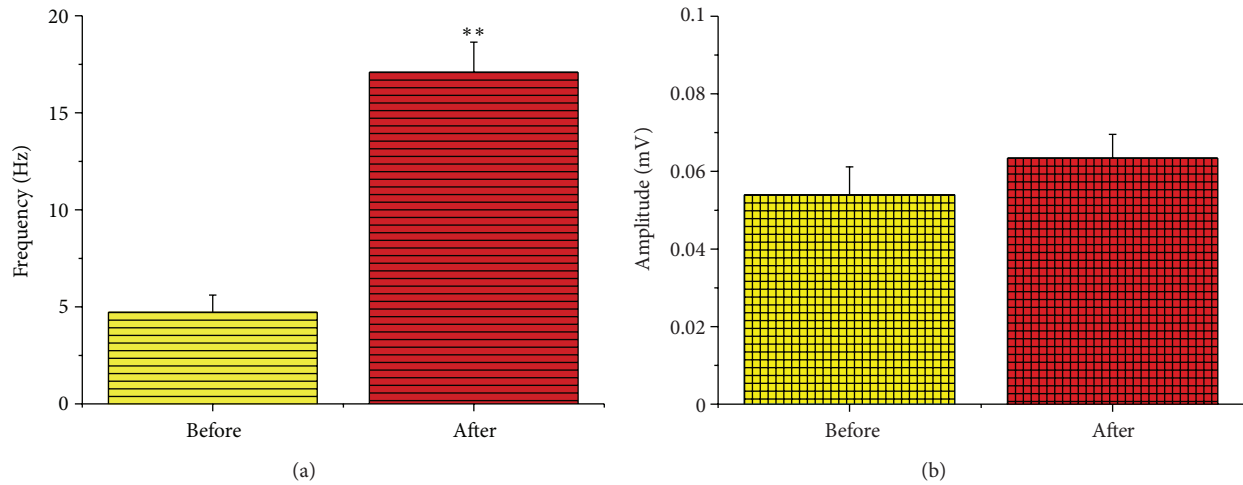


FIGURE 4: Quantitative changes in frequency and amplitude of EEG after the KA injection, (a) frequency and (b) amplitude. $**P < 0.001$. Note that simultaneous to the induction of seizures, the frequency of the EEG waves increased more than 3.5 folds. In contrast, the amplitude had no significant change ($P > 0.05$).

2.4. Evaluation of Epileptic Activity. Every 30 minutes, we conducted a single-blinded behavioral assessment based on the Racine's 5-point scales [24] and recorded the scores at 8-time points in (i.e., 0.5, 1, 1.5, 2, 2.5, 3, 3.5, and 4 hours after the injection of KA). The assessment criteria utilized was shown in Table 1.

2.5. Electroencephalography. Two holes of less than 0.5 mm diameter were drilled in the rat skull at the areas corresponding to the right frontal cortex and right parietal cortex, respectively. Recording and reference electrodes were fixed in the holes using the dental cement and then connected to the PowerLab 4/25 data acquisition system for electroencephalography (EEG) signals. EEG parameters were set at sampling rate 2 k/s; range 50 mV; 100 Hz low-pass and the AC power filter. Since it is impractical to record EEG in the awake state due to unavoidable huge signal noise, we recorded EEG while the animals were under anesthesia, that is, from the beginning of the experiment to 10–15 minutes after EA when the animals were awake from anesthesia.

2.6. Electroacupuncture. After the KA (epileptic model) or saline (control) injection into the lateral ventricle of the rat

brain, the animals were randomly assigned to four major groups: head and neck acupoints (DU26, DU14), forelimb acupoints (PC6, LI11), the back acupoints (DU8, EXB9), and hindlimb acupoints (ST40, KII). In a previous study, we had demonstrated that EA at an intensity of 1 mA is optimal for rats [25], thus in the present work we standardized this parameter and concentrated on the effects of different frequencies, which is another important determinant of the effect of EA [25]. In all the 4 groups, EA was given at both low- (10 Hz/1 mA) and high-frequency (100 Hz/1 mA). It was started 30 mins after the KA injection for a duration of 30 mins (see the experimental flow chart in Figure 1).

2.7. Data Analysis. Data is presented as mean \pm SE. Statistical significance was determined using either student's *t*-test or a one-way ANOVA. Statistical significance was defined by $P < 0.05$. All the data analysis and graphing were carried out using Origin 8.0 software (Origin Lab, USA).

3. Results

3.1. KA-Induced Seizures. We injected 0.7 μ L of KA solution (1 μ g/ μ L) into the lateral ventricle of each rat and applied

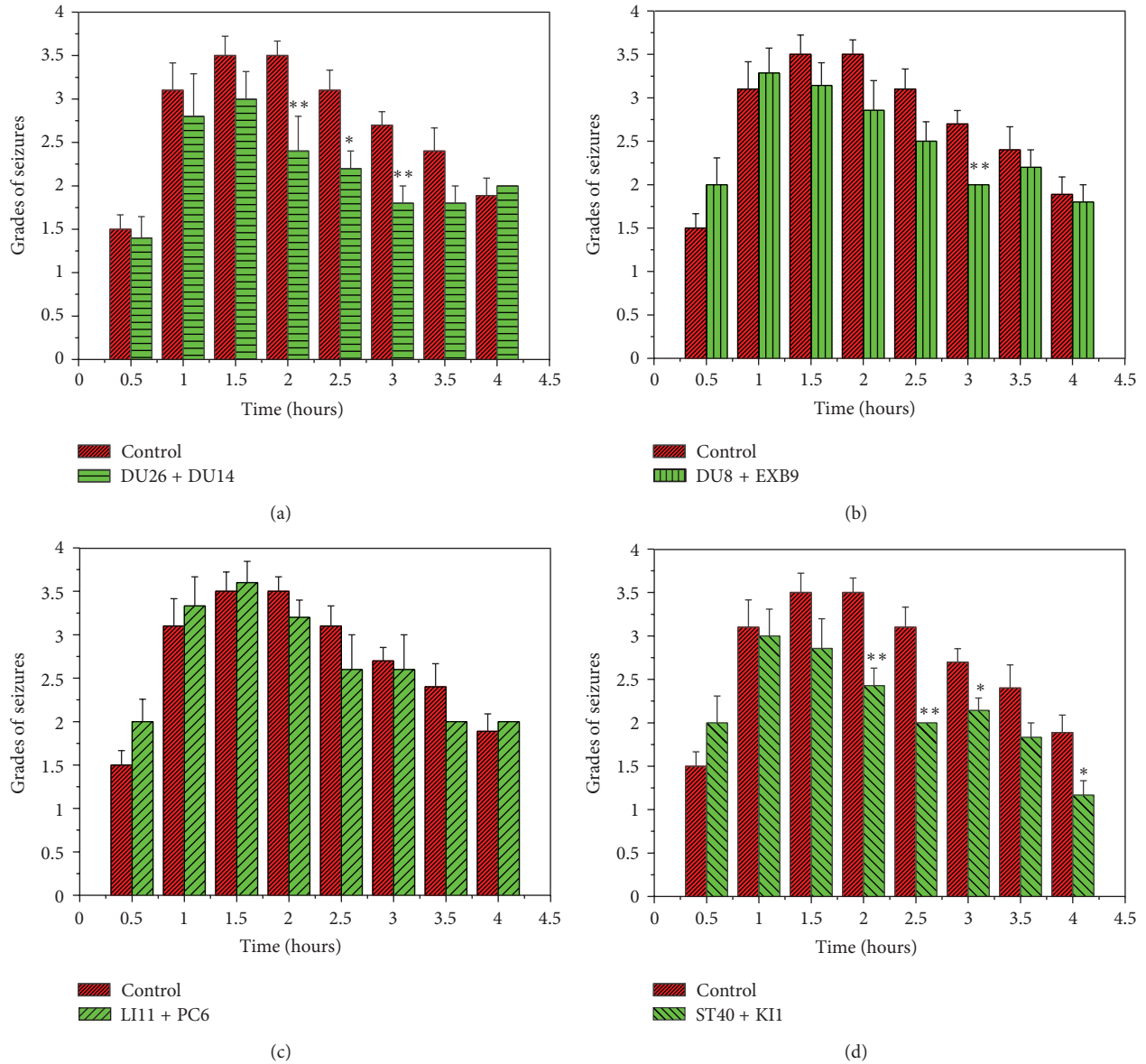


FIGURE 5: Effects of 10 Hz/1 mA EA at different acupoints. (a) DU26 + DU14 ($n = 5$); (b) DU8 + EXB9 ($n = 7$); (c) LI11 + PC6 ($n = 6$); and (d) ST40 + KII ($n = 7$). * $P < 0.05$, ** $P < 0.01$ EA groups versus the control. Note that EA at the acupoints of the head and neck (DU26 + DU14), the back (DU8 + EXB9), and the hindlimb (ST40 + KII), but not the forelimb (LI11 + PC6), significantly attenuated seizures at several points after the KA injection.

Racine’s 5-point scales grading method [24] to obtain the behavioral score. Ten to thirty minutes after the injection, the rats displayed seizure symptoms. The symptoms were most serious at 1.5–2 hours after the injection of KA and then gradually declined. However, epileptic seizure did not completely disappear within 4 hours after the injection (Figure 2). In the control group, same procedures were performed by replacing saline in place of KA, and they did not induce any seizures or any abnormal behaviors.

3.2. KA-Induced EEG Changes. The epilepsy-like spike wave-pattern could be clearly seen on EEG after KA injection (Figure 3). Frequency on EEG wave pattern increased significantly after KA injection (from 4.75954 ± 0.90465 Hz to

17.26694 ± 1.57080 Hz, $n = 51$, $P < 0.001$) (Figures 3(a) and 4(a)). Although there was an increase in the amplitude of the EEG waves in the KA model, it had no statistical difference when compared to the control group, that is, before the KA injection (from 0.05395 ± 0.00722 mV to 0.06342 ± 0.00612 mV, $n = 51$, $P > 0.05$; Figure 4(b)).

3.3. Effects of Low- and High-Frequency EA at Different Acupoints. We utilized two EA frequencies, that is, 10 Hz/1 mA and 100 Hz/1 mA, that have been previously described in the acupuncture literature [25–30], to compare the role of different acupoints in EA effect (Figures 5–7). We tested the following acupoints: DU26 and DU14 in the head and neck, PC6 and LI11 in the forelimb, DU8 and EXB9 in the back,

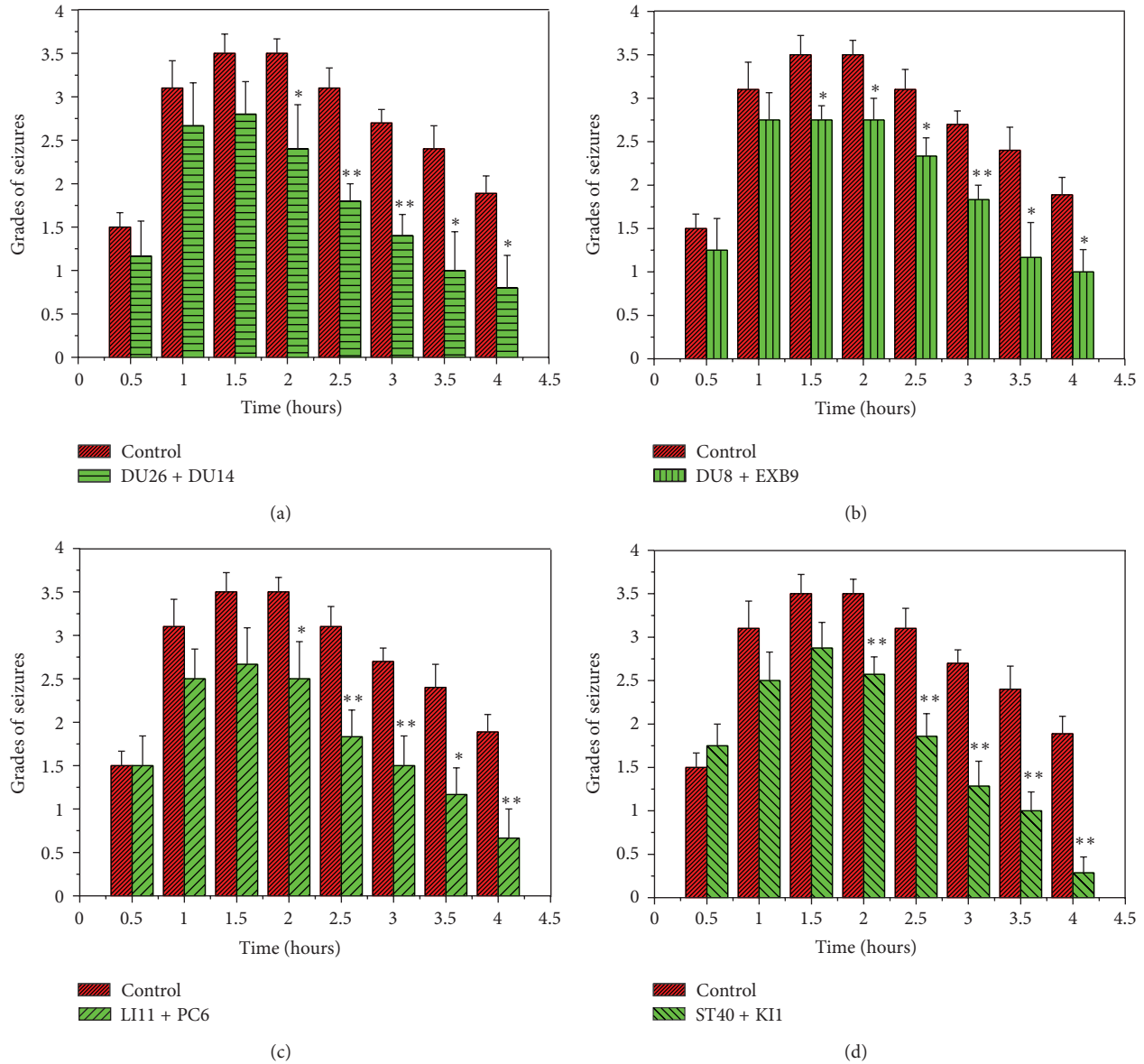


FIGURE 6: Effects of 100 Hz/1 mA EA at different acupoints. (a) DU26 + DU14 ($n = 6$); (b) DU8 + EXB9 ($n = 8$); (c) LI11 + PC6 ($n = 6$); and (d) ST40 + KII ($n = 8$). * $P < 0.05$, ** $P < 0.01$ EA groups versus the control. Note that EA with high frequency stimulation (100 Hz/1 mA) at all these acupoints induced a significant reduction in seizures at most time points, 1–1.5 hours following the KA injection.

and ST40 and KII in the hind limb and found that both EA frequencies were effective in reducing seizures (Figures 5 and 6).

As shown in Figure 5, the low-frequency stimulation (10 Hz/1 mA) at the head and neck, back, and the hind limb acupoints significantly attenuated seizures at several points in time after KA injection. However, EA at PC6 and LI11 did not induce any significant reduction in seizures during the period investigated (Figure 5(c)).

On the other hand, high-frequency stimulation (100 Hz/1 mA) at all the aforementioned acupoints induced a significant reduction in seizures 1–1.5 hours following the KA injection (Figure 6).

With the same stimulating parameters, the comparison among different “effective” acupoints did not show any

significant difference in terms of EA-induced effect on the KA-induced seizures (Figure 7).

3.4. Difference in Low- versus High-Frequency EA on the KA-Induced Seizures. When comparing 100 Hz/1 mA to 10 Hz/1 mA, we found that the high-frequency EA induced a greater attenuation of seizures. As shown in Figure 8, except DU8 + EXB9, all other groups achieved a larger reduction in seizure activity after high-frequency EA when compared to low-frequency EA.

3.5. Effect of EA on EEG. We examined the changes in EEG frequency and amplitude from the initiation of EA (30 minutes after the KA injection) to 10 minutes after stopping EA (70 minutes after the KA injection). No significant

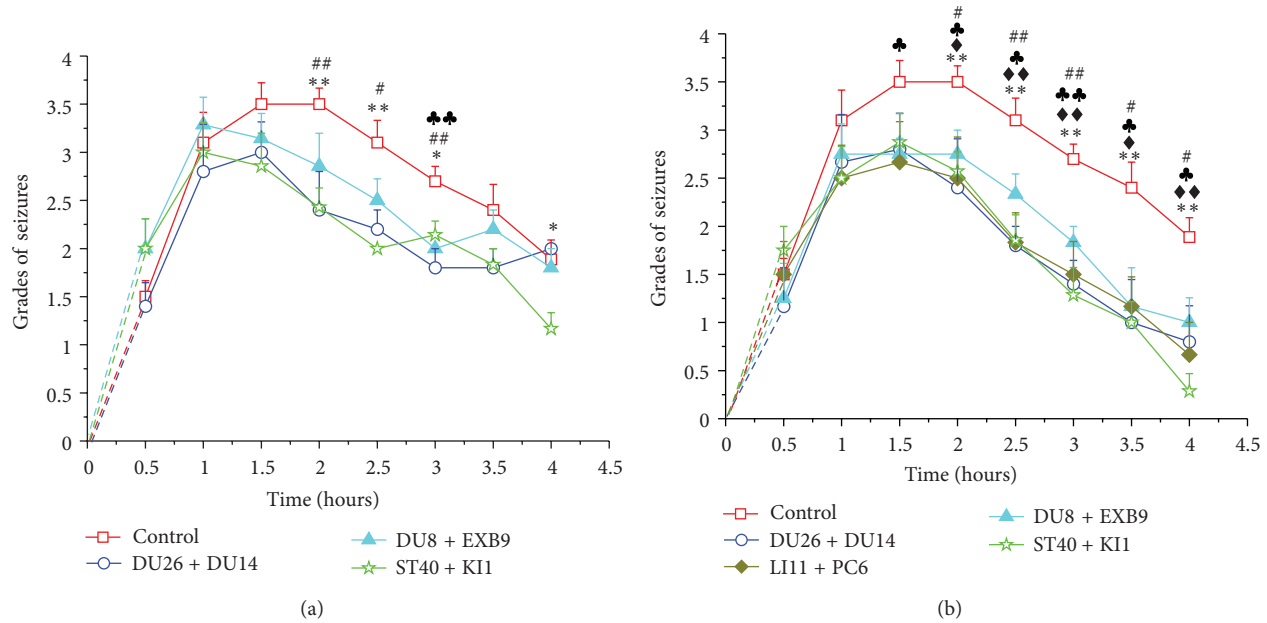


FIGURE 7: Comparisons of EA effects among “effective” acupoints. (a) 10 Hz/1 mA and (b) 100 Hz/1 mA. $^{\#}P < 0.05$, $^{##}P < 0.01$ DU26 + DU14 versus control; $^{\ast}P < 0.05$, $^{**}P < 0.01$ DU8 + EXB9 versus control; $^{\blacklozenge}P < 0.05$, $^{\blacklozenge\blacklozenge}P < 0.01$ LI11 + PC6 versus control; and $^{\ast}P < 0.05$, $^{**}P < 0.01$ ST40 + KI1 versus control. Note that there is no statistical difference among the different “effective” acupoint groups.

changes in the frequency and amplitude were noted either in low- or high-frequency EA groups, or in “effective” versus ineffective acupoint groups. The results are summarized in Tables 2 and 3.

4. Discussion

This is the first study conducting a systematic comparison of different EA stimulation parameters and acupoints in terms of their effects on epileptic seizures. Our results show that (1) EA significantly attenuates KA-induced epilepsy; (2) EA-induced attenuation appears 1–1.5 hours after EA with no appreciable effect from the start of application to 1 hour after EA; and (3) the EA effect was relatively specific to acupoints and EA parameters.

There has been a longstanding controversy in the published literature on the clinical efficacy of EA treatment in epilepsy. Because of the complex etiology and presentation of epilepsy, there are a multitude of factors that can influence the EA effect. Furthermore, it is not feasible to make comparisons as the data were obtained from a varied pool of patients and animal models that utilized different acupuncture/EA parameters and acupoints. Our present study employs a commonly used rat model of epilepsy and provides strong evidence on the attenuation of certain types of epileptic seizures following EA treatment, such as chemical-induced seizures (e.g., KA-induced epilepsy).

It is noteworthy that we failed to observe any significant reduction in epileptic seizures during or immediately after the EA treatment, neither on EEG nor on behavioral assessments. Instead, we found a delay in attenuation of epilepsy

following EA that appeared 1 hour after stimulation. Our unique observations stand in contrast to some of the previous studies [26, 27, 29–31], in which the investigators stated that acupuncture/EA induces an immediate inhibition of epileptic activity [27, 31]. At present, we cannot explain the reasons for such a contrasting effect. However, we believe that this disparity can be attributed to the difference in the methods of EA stimulation in the epilepsy models employed by us and the others. However, we found a few reports documenting a rapid effect of EA using a similar KA-induced epilepsy model of as ours [26].

Among the four major acupoint groups tested, we found that low-frequency (10 Hz/1 mA) EA at head and neck acupoints (DU26 + DU14), back acupoints (DU8 + EXB9), and hindlimb acupoints (ST40 + KI1) induced a significant attenuation of epileptic seizures, while stimulation of forelimb acupoints (PC6 + LI11) had no such effect. These results suggest that the EA effect is relatively specific to acupoints. This could be due to the difference in neural distribution around the acupoints [32, 33] because of differences and complexity in neural transmission from various acupoints to the brain and spinal cord [32–36].

Interestingly, the effectiveness of acupoints varies under different stimulating parameters. For example, the low-frequency EA at the forelimb acupoints (PC6 + LI11) was not effective for epileptic seizures, but the high-frequency EA at the same acupoints induced a significant reduction in epileptic seizures. In general, the high-frequency EA produced a better effect compared to that of low-frequency EA at all acupoints. Based on these observations, we consider high-frequency stimulation as “an optimal parameter” for EA treatment of the KA-induced epilepsy. The underlying

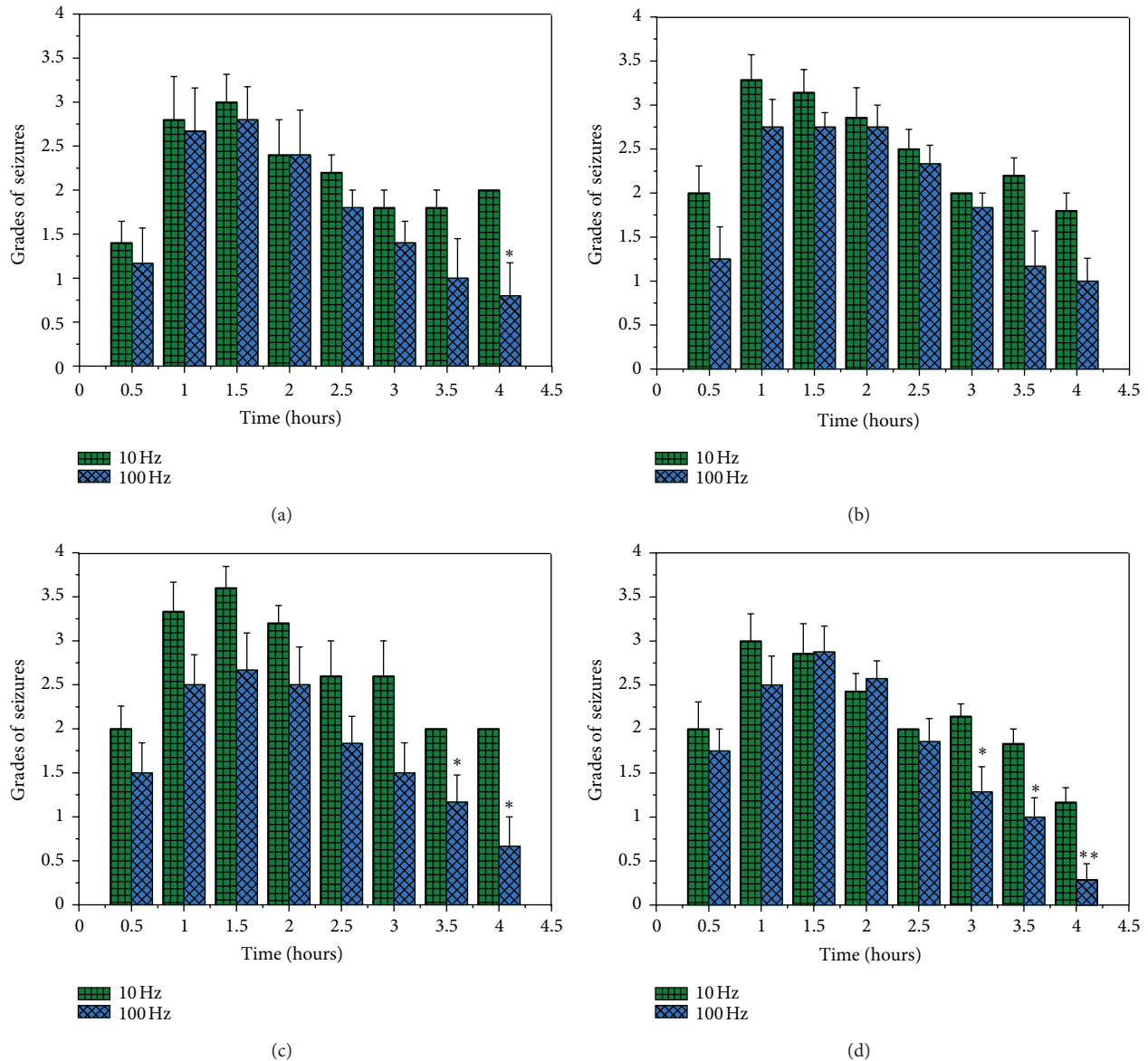


FIGURE 8: Comparisons of low- and high-frequency EA effects on the seizures. Discrepant seizure levels in four acupoint groups after EA with the parameters of 100 Hz/1 mA or 10 Hz/1 mA. (a) DU26 + DU14; (b) DU8 + EXB9; (c) LI11 + PC6; and (d) ST40 + KI1. * $P < 0.05$ or ** $P < 0.01$ versus 10 Hz. Note that except for the group of DU8 + EXB9, all other three groups showed a greater EA effect with 100 Hz/1 mA than 10 Hz/1 mA.

mechanism may be related to specific changes in neural signals generated in the body. High-frequency stimulation may produce neural signals to affect broader brain regions, of which some may respond only to specific acupoints in the case of low-frequency currents.

Several lines of evidence suggest that δ -opioid receptors (DORs) mediated regulation of sodium channels may play a significant role in the molecular mechanism of the EA-induced attenuation of epilepsy [1]. It is well known that neural hyperexcitability during the epileptic seizures may result from dysregulation of sodium channels in the brain [1, 37]. In a mutant model of spontaneous epilepsy [37, 38], for example, sodium channel expression was found to be high

with increased sodium currents and hyperexcitability in the cortical regions [37]. A concomitant low DOR expression was also found in the same model [39]. Furthermore, we found that DOR expression and/or activation decreases sodium currents [40]. Extrapolating from these observations, we hypothesize that DOR expression/activity decreases the sodium channel function thereby reducing sodium currents and hyperexcitability. An impairment of DOR function, on the other hand, will lead to an increase in sodium currents and hyperexcitability that in turn results in an epileptic seizure. Since acupuncture/EA is known to upregulate endogenous opioid expression and function in the brain [34, 36] and increase DOR expression in the cortex

[41], we believe that EA upregulates DOR expression and/or function, thus inhibiting epileptic seizures mediated by neural hyperexcitability due to sodium channel dysfunction. This may also partially explain that EA induced a delayed, not immediate, effect on epilepsy because the upregulation of DOR, particularly expression, requires a certain period of time to make the action in the brain.

In summary, our study reveals that EA induced a significant reduction of epileptic seizures with high frequency as an optimal parameter for EA efficacy in the KA-induced epilepsy model. The EA effect is a delayed response, which is likely to be related to the time involved in the neural regulation of central functions. However, there is a caveat attached that the optimal acupuncture parameters and the underlying mechanisms may vary with different types of epilepsy due to diverse pathophysiological factors causing epileptic seizures. Further investigations on the optimal parameters and mechanisms involved in EA treatment of epilepsy are needed to improve our current knowledge and shed light on better solutions of this neurological disorder.

Acknowledgments

This work was supported by NSFC (81102657, 81001569), NBRP (2009CB522901, 2012CB518502), Chinese SA of TCM, SMSF (11DZ1973300), NIH (HD-034852, AT-004422), and Vivian L. Smith Neurologic Foundation.

References

- [1] D. M. Chao and Y. Xia, "Acupuncture treatment of epilepsy," in *Current Research in Acupuncture*, Y. Xia, G. Ding, and G.-C. Wu, Eds., pp. 129–214, Springer, New York, Heidelberg, Dordrecht, London, 2012.
- [2] A. Merwick, M. O'Brien, and N. Delanty, "Complex single gene disorders and epilepsy," *Epilepsia*, vol. 53, supplement 4, pp. 81–91, 2012.
- [3] M. Wong, "Tumors generate excitement: the role of glutamate in tumor-related epilepsy," *Epilepsy Currents*, vol. 12, pp. 174–175, 2012.
- [4] C. E. Stafstrom and B. L. Tempel, "Epilepsy genes: the link between molecular dysfunction and pathophysiology," *Mental Retardation & Developmental Disabilities Research Reviews*, vol. 6, pp. 281–292, 2000.
- [5] H. Kazemi, S. Hashemi-Fesharaki, S. Razaghi et al., "Intractable epilepsy and craniocerebral trauma: analysis of 163 patients with blunt and penetrating head injuries sustained in war," *Injury*, vol. 43, pp. 2132–2135, 2012.
- [6] M. Simonato, W. Loscher, A. J. Cole et al., "Finding a better drug for epilepsy: preclinical screening strategies and experimental trial design," *Epilepsia*, vol. 53, no. 11, pp. 1860–1867, 2012.
- [7] R. Guerrini, G. Zaccara, G. la Marca, and A. Rosati, "Safety and tolerability of antiepileptic drug treatment in children with epilepsy," *Drug Safety*, vol. 35, pp. 519–533, 2012.
- [8] R. Talati, J. M. Scholle, O. P. Phung et al., "Efficacy and safety of innovator versus generic drugs in patients with epilepsy: a systematic review," *Pharmacotherapy*, vol. 32, pp. 314–322, 2012.
- [9] C. E. Begley, M. Famulari, J. F. Annegers et al., "The cost of epilepsy in the United States: an estimate from population-based clinical and survey data," *Epilepsia*, vol. 41, no. 3, pp. 342–351, 2000.
- [10] V. A. Gusef, N. L. Vol'f, and L. A. Ferdman, "Effect of acupuncture on the activity of experimental epileptogenic foci in the hippocampus of rabbits," *Byulleten Eksperimentalnoi Biologii i Meditsiny*, vol. 99, no. 1, pp. 27–29, 1985.
- [11] G. Goiz-Marquez, S. Caballero, H. Solis, C. Rodriguez, and H. Sumano, "Electroencephalographic evaluation of gold wire implants inserted in acupuncture points in dogs with epileptic seizures," *Research in Veterinary Science*, vol. 86, no. 1, pp. 152–161, 2009.
- [12] A. M. Klide, G. C. Farnbach, and S. M. Gallagher, "Acupuncture therapy for the treatment of intractable, idiopathic epilepsy in five dogs," *Acupuncture and Electro-Therapeutics Research*, vol. 12, no. 1, pp. 71–74, 1987.
- [13] R. B. Panzer and C. L. Chrisman, "An auricular acupuncture treatment for idiopathic canine epilepsy: a preliminary report," *American Journal of Chinese Medicine*, vol. 22, no. 1, pp. 11–17, 1994.
- [14] Z. N. Mao, Z. G. Gao, G. W. Zhang, and S. B. Wang, "Observation on therapeutic effect of acupoint catgut-embedding combined western medicine for epilepsy of generalized seizures type," *Acupuncture Research*, vol. 31, pp. 509–512, 2011.
- [15] Q. Li, J. C. Guo, H. B. Jin, J. S. Cheng, and R. Yang, "Involvement of taurine in penicillin-induced epilepsy and anti-convulsion of acupuncture: a preliminary report," *Acupuncture and Electro-Therapeutics Research*, vol. 30, no. 1-2, pp. 1–14, 2005.
- [16] C. C. Xue, "Comparative study of spinal fractures in electric acupuncture convulsive therapy, electric convulsive therapy and epilepsy," *Chinese Journal of Neurology and Psychiatry*, vol. 20, no. 6, pp. 346–349, 1987.
- [17] J. Yang, "Treatment of status epilepticus with acupuncture," *Journal of Traditional Chinese Medicine*, vol. 10, no. 2, pp. 101–102, 1990.
- [18] N. Shi, "3-directional penetration needling for the treatment of paralysis," *Journal of Traditional Chinese Medicine*, vol. 16, no. 1, pp. 37–40, 1996.
- [19] Z. Y. Shi, B. T. Gong, Y. W. Jia, and Z. X. Huo, "The efficacy of electro-acupuncture on 98 cases of epilepsy," *Journal of Traditional Chinese Medicine*, vol. 7, no. 1, pp. 21–22, 1987.
- [20] X. H. Chen and H. T. Yang, "Effects of acupuncture under guidance of qi streeet theory on endocrine function in the patient of epilepsy," *Chinese Acupuncture & Moxibustion*, vol. 28, no. 7, pp. 481–484, 2008.
- [21] R. Kloster, P. G. Larsson, R. Lossius et al., "The effect of acupuncture in chronic intractable epilepsy," *Seizure*, vol. 8, no. 3, pp. 170–174, 1999.
- [22] K. Stavem, R. Kloster, E. Rössberg et al., "Acupuncture in intractable epilepsy: lack of effect on health-related quality of life," *Seizure*, vol. 9, no. 6, pp. 422–426, 2000.
- [23] D. K. Cheuk and V. Wong, "Acupuncture for epilepsy," *Cochrane Database of Systematic Reviews*, no. 2, Article ID CD005062, 2006.
- [24] R. J. Racine, "Modification of seizure activity by electrical stimulation: II. Motor seizure," *Electroencephalography and Clinical Neurophysiology*, vol. 32, no. 3, pp. 281–294, 1972.
- [25] F. Zhou, J. C. Guo, J. S. Cheng, G. C. Wu, and Y. Xia, "Electroacupuncture increased cerebral blood flow and reduced ischemic brain injury: dependence on stimulation intensity and

- frequency," *Journal of Applied Physiology*, vol. 111, pp. 1877–1887, 2011.
- [26] J. Liu and J. S. Cheng, "Changes of amino acids release in rat's hippocampus during kainic acid induced epilepsy and acupuncture," *Acupuncture Research*, vol. 20, no. 3, pp. 50–54, 1995.
- [27] B. E. Wang and J. S. Cheng, "C-fos expression in rat brain during seizure and electroacupuncture," *Acta Pharmacologica Sinica*, vol. 15, no. 1, pp. 73–75, 1994.
- [28] F. Yang, G. L. Xu, P. Wang et al., "Effect of electroacupuncture on the contents of amino acids in the brain in PTZ kindled epilepsy rats," *Acupuncture Research*, vol. 27, pp. 174–176, 2002.
- [29] Z. N. Huang, R. Yang, G. Chen, and J. S. Cheng, "Effect of electroacupuncture and 7-NI on penicillin-induced epilepsy and their relation with intrahippocampal NO changes," *Acta Physiologica Sinica*, vol. 51, no. 5, pp. 508–514, 1999.
- [30] J. Liu and J. S. Cheng, "Hippocampal non-NMDA and GABA-A receptors in benzylpenicillin-induced epilepsy and electroacupuncture antiepilepsy," *Acta Pharmacologica Sinica*, vol. 18, no. 2, pp. 189–191, 1997.
- [31] Z. Zhang, Z. Yu, and H. Zhang, "Inhibitory effect of electroacupuncture on penicillin-induced amygdala epileptiform discharges," *Acupuncture Research*, vol. 17, no. 2, pp. 96–98, 1992.
- [32] F. Zhou, D. K. Huang, and Y. Xia, "Neuroanatomic basis of acupuncture points," in *Acupuncture Therapy of Neurological Diseases: A Neurobiological View*, pp. 32–80, Springer-Tsinghua Press, Beijing, Heidelberg, London, New York, 2010.
- [33] J. M. Zhu, D. N. Kennedy, and X. D. Cao, "Neural transmission of acupuncture signal," in *Acupuncture Therapy of Neurological Diseases: A Neurobiological View*, pp. 81–103, Springer-Tsinghua Press, Beijing, Heidelberg, London, New York, 2010.
- [34] G. Q. Wen, Y. L. Yang, Y. Lu, and Y. Xia, "Acupuncture-induced activation of endogenous opioid system," in *Acupuncture Therapy of Neurological Diseases: A Neurobiological View*, Y. Xia, X. D. Cao, G. C. Wu, and J. S. Cheng, Eds., pp. 104–119, Springer-Tsinghua Press, Beijing, Heidelberg, London, New York, 2010.
- [35] G. Q. Wen, Y. L. Yang, Y. Lu, and Y. Xia, "Effect of acupuncture on neurotransmitters/modulators," in *Acupuncture Therapy of Neurological Diseases: A Neurobiological View*, Y. Xia, X. D. Cao, G. C. Wu, and J. S. Cheng, Eds., pp. 120–1142, Springer-Tsinghua Press, Beijing, Heidelberg, London, New York, 2010.
- [36] J. F. Liang and Y. Xia, "Acupuncture modulation of neural transmitters/modulators," in *Current Research in Acupuncture*, Y. Xia, G. Ding, and G. C. Wu, Eds., pp. 1–36, Springer, New York, Heidelberg, Dordrecht, London, 2012.
- [37] Y. Xia, P. Zhao, J. Xue et al., "Na⁺ channel expression and neuronal function in the Na⁺/H⁺ exchanger 1 null mutant mouse," *Journal of Neurophysiology*, vol. 89, no. 1, pp. 229–236, 2003.
- [38] G. A. Cox, C. M. Lutz, C. L. Yang et al., "Sodium/hydrogen exchanger gene defect in slow-wave epilepsy mutant mice," *Cell*, vol. 91, no. 1, pp. 139–148, 1997.
- [39] P. Zhao, M. C. Ma, H. Qian, and Y. Xia, "Down-regulation of delta-opioid receptors in Na⁺/H⁺ exchanger 1 null mutant mouse brain with epilepsy," *Neuroscience Research*, vol. 53, no. 4, pp. 442–446, 2005.
- [40] X. Z. Kang, D. Chao, Q. Gu et al., "δ-Opioid receptors protect from anoxic disruption of Na⁺ homeostasis via Na⁺ channel regulation," *Cellular and Molecular Life Sciences*, vol. 66, no. 21, pp. 3505–3516, 2009.
- [41] X. S. Tian, F. Zhou, R. Yang, Y. Xia, G. C. Wu, and J. C. Guo, "Electroacupuncture protects the brain against acute ischemic injury via up-regulation of delta-opioid receptor in rats," *Journal of Chinese Integrative Medicine*, vol. 6, no. 6, pp. 632–638, 2008.

Research Article

Effects of Electroacupuncture at Auricular Concha Region on the Depressive Status of Unpredictable Chronic Mild Stress Rat Models

Ru-Peng Liu,¹ Ji-Liang Fang,^{1,2} Pei-Jing Rong,¹ Yufeng Zhao,³ Hong Meng,¹ Hui Ben,¹ Liang Li,¹ Zhan-Xia Huang,⁴ Xia Li,⁴ Ying-Ge Ma,³ and Bing Zhu¹

¹ Institute of Acupuncture and Moxibustion, China Academy of Chinese Medical Sciences, Beijing 100700, China

² Guanganmen Hospital, China Academy of Chinese Medical Sciences, Beijing 100053, China

³ Clinical Evaluation Center, Institute of Basic Research in Clinical Medicine, China Academy of Chinese Medical Sciences, Beijing 100700, China

⁴ Beijing University of Chinese Medicine, Beijing 100029, China

Correspondence should be addressed to Pei-Jing Rong; rongpj@mail.cintcm.ac.cn

Received 24 August 2012; Revised 21 November 2012; Accepted 14 December 2012

Academic Editor: Wolfgang Schwarz

Copyright © 2013 Ru-Peng Liu et al. This is an open access article distributed under the Creative Commons Attribution License, which permits unrestricted use, distribution, and reproduction in any medium, provided the original work is properly cited.

To explore new noninvasive treatment options for depression, this study investigated the effects of electroacupuncture (EA) at the auricular concha region (ACR) of depression rat models. Depression in rats was induced by unpredictable chronic mild stress (UCMS) combined with isolation for 21 days. Eighty male Wistar rats were randomly assigned into four groups: normal, UCMS alone, UCMS with EA-ACR treatment, and UCMS with EA-ear-tip treatment. Rats under inhaled anesthesia were treated once daily for 14 days. The results showed that blood pressure and heart rate were significantly reduced in the EA-ACR group than in the UCMS alone group or the EA-ear-tip group. The open-field test scores significantly decreased in the UCMS alone and EA-ear-tip groups but not in the EA-ACR group. Both EA treatments downregulated levels of plasma cortisol and ACTH in UCMS rats back to normal levels. The present study suggested that EA-ACR can elicit similar cardioinhibitory effects as vagus nerve stimulation (VNS), and EA-ACR significantly antagonized UCMS-induced depressive status in UCMS rats. The antidepressant effect of EA-ACR is possibly mediated via the normalization of the hypothalamic-pituitary-adrenal (HPA) axis hyperactivity.

1. Introduction

Vagus nerve stimulation (VNS) was approved by the U. S. Food and Drug Administration in 2005 and has been frequently used as a treatment option for treatment-resistant depression (TRD) [1–4]. Its mechanisms of antidepressant action are not fully elucidated; however, its neuromechanisms are based on the direct stimulation of the cervical trunk of the left vagus nerve. The afferent fibers of vagus nerve project to solitary nucleus (SN). Fibers of SN project to the neuroendocrine systems in the limbic system structures and the autonomic nervous system. These areas are strongly interconnected by monoamine-related pathways, including the ventral tegmental area, brainstem, the hypothalamus, thalamus, amygdala, anterior insula, nucleus accumbens, and

the lateral prefrontal cortex [5]. Furthermore, the ventral tegmental area has a dense dopaminergic input to the prefrontal cortex; fibers from the SN project to the locus ceruleus and dorsal raphe nucleus which are major brainstem nuclei related to noradrenergic (NE) and serotonergic (5-HT) innervations of the entire brain cortex, respectively. It is well known that the serotonergic, dopaminergic, and noradrenergic systems are commonly involved in the pathophysiology of depression and in the neuromechanisms of action of antidepressants [6].

Nonetheless, typical implantation of VNS device requires an invasive surgical procedure which may be accompanied by some side effects, such as infection of wound, hoarse voice, dyspnea, difficulty swallowing, neck pain, paresthesia, emesis, laryngospasms, dyspepsia, cardiac asystole, bradycardia,

and even heart failure. Worse still, technical complications of device malfunction may aggravate patient conditions [7, 8].

Enlightened by the mechanism of VNS, researchers in our team found that auricular concha region (ACR) is densely innervated by free nerve endings of the vagus nerve. Our previous animal studies found that electroacupuncture (EA) at ACR (EA-ACR) had significant effects in the management of primary hypertension [9, 10], diabetes mellitus [11, 12], and partial epilepsy [13, 14]. EA-ACR is a noninvasive procedure which requires a portable EA device and no side effects. With a similar mechanism to VNS, EA vagus nerve stimulation may provide beneficial effects in the treatment of depression.

EA-ACR is one of the acupuncture therapeutic methods which can be considered as auriculotherapy. Theories of auriculotherapy dates back to 2000 years ago as first mentioned in the book of *Yellow Emperor's Canon of Medicine* (Huang Di Nei Jing) [15]. Modern auriculotherapy with 42 points was firstly introduced by Dr. P. Nogier (France) in 1956. The international standard map of auricular points was published in China and later was recommended by WHO in 1993. Acupuncture, part of the oriental medicine, has been used in eastern Asian countries for the management of various emotional, psychological, and psychiatric disorders including anxiety, stress, insomnia, and depression. In recent years, acupuncture has become one of the most popular complementary therapies in the West, and the therapeutic effectiveness of acupuncture on depression has been confirmed by modern research studies. Allen et al. [16] found that body acupuncture and auriculotherapy could significantly reduce the severity of depression. Similar results were demonstrated in the studies of Luo et al. [17] and Zhang et al. [18], in which researchers found that electroacupuncture was as efficacious as fluoxetine in the management of major depression. In general, increasing evidences support that acupuncture is an effective treatment for patients with depressive disorders [19–23].

In the current study, we aimed to verify the vagus nerve responses during EA at ACR. Furthermore, antidepressant effects of EA-ACR were investigated by observation of behaviors and measurement of blood biochemicals in the rat models of unpredictable chronic mild stress (UCMS).

The results will provide a fundamental evidence for the anti-depression effects of EA-ACR and will facilitate EA-ACR to become a new noninvasive and low-cost therapy for depression.

2. Methods and Materials

2.1. Animals. Male Wistar rats in 150–170 g were obtained from the Laboratory Animal Resources Center, National Institute for the Control of Pharmaceutical and Biological Products, Beijing (Certificate no. SCXK (jing) 2009-0017). These animals were individually caged on a 12 h light/dark cycle (lights on at 8:00 a.m., lights off at 8:00 p.m.) under controlled temperature ($22 \pm 1^\circ\text{C}$) and humidity ($50\% \pm 5\%$) conditions. Standard rat chow and water were given ad libitum. Animals were allowed to acclimatize for seven

days before the study. All experiment procedures comply with the guidelines of the “Principles of Laboratory Animal Care” (NIH publication number 80-23, revised 1996) and the legislation of the People's Republic of China for the use and care of laboratory animals. The experimental protocols were approved by the Animal Experimentation Ethics Committee of the Institute of Acupuncture and Moxibustion, China Academy of Chinese Medical Sciences. Efforts were made to minimize the number of animal use and the suffering of the experimental animals.

2.2. Open Field Test for Behavioral Scoring. The open field apparatus was constructed of black plywood and measured 80×80 cm with 40 cm walls. White lines were drawn on the floor. The lines divided the floor into twenty-five 16×16 cm squares. A central square ($16 \text{ cm} \times 16 \text{ cm}$) was drawn in the middle of the open field. Rats were put on the central square, at the same time the video camera was turned on for video recording from the top of the open field apparatus. Behaviors of rats were recorded for 3 minutes, with the grid number being counted as the horizontal score and the time of both frontal claws uplifting from the ground as the vertical score. The total locomotor activity of each animal was then scored as the sum of the number of line crosses and rears [24, 25].

2.3. Unpredictable Chronic Mild Stress (UCMS) Model. Eighty Rats were evenly randomized into 4 groups. Forty-two rats were recruited with the total score of 30–120 in the open field test [25]. A successful UCMS model rat was created with the score of the open field test equal or minus 60. Qualified rats were distributed into four groups: the normal control ($n = 10$), UCMS alone ($n = 8$), UCMS with EA-ACR treatment (EA-ACR) ($n = 12$), and UCMS with EA-ear-tip as the treatment control (EA-ear-tip) ($n = 12$). Every five rats in the normal group were housed in one cage. However, rats in the UCMS alone, EA-ACR, and EA-ear-tip groups were caged individually. Depression model was established by 21 days of UCMS combined with isolation. UCMS procedures were based on published studies [25, 26], including seven kinds of stressors: food deprivation, water deprivation, cage tilt 45° (Ugo Basile s.r.l. hot/cold plate, Model 35100–001, Italy), swimming in 4°C ice water, clipping tail 3 min, 50 V electric shock (Electronic stimulator, NIHON KOHDEN, Japan), and overnight illumination. The stressors were given randomly 3 times daily for 21 continuous days. The rats in the normal control group were housed undisturbedly except for necessary procedures such as routine cage cleaning.

2.4. Experimental Procedures (Figure 1). The open field test on all rats was conducted on the day before the study, the 22th day (after UCMS), the 36th day (after treatment), and the 50th day in the study course. After the models of UCMS were established in 21 days, the EA treatment of 14 days was applied to the bilateral auricular concha region (Figure 1) of rats in the EA-ACR group once daily for 20 min. For the EA-ear-tip group, the EA applied to the bilateral ear tips (Figure 1) followed the same procedure and EA parameters as the EA-ACR. All rats in the EA groups

accepted the inhaled anesthesia during the treatment. EA was set at the frequency of 2 Hz, the intensity of 1 mA by using the electroacupuncture stimulator (HANS-100A, Nanjing Gensun Medical Technology Co., Ltd., China). The inhaled anesthesia was conducted on the ISOFLURANE VAPORIZER (Matrx VIP 3000, Midmark corporation, USA) with isoflurane (Hebei Nine Sent Pharmaceutical Co., Ltd., Hebei, China). Blood pressure, including systolic, diastolic and mean pressures, and heart rate of rats were monitored noninvasively by using the apparatus (BP-98A, Beijing Soft Long Biological Technology Co., Ltd., China) during one EA treatment/anesthesia. The data were recorded in numerical values at the starting point of anesthesia (0 min pre-EA), the 1st min of anesthesia (EA begins), the 6th min of anesthesia (EA 5 min), the 11th min of anesthesia (EA 10 min), the 16th min of anesthesia (EA 15 min), and the 21st min of anesthesia (EA 20 min) on the same day for three UCMS groups. At the 51st day of the study, the rats were sacrificed and their neck venous blood was sampled for the tests of plasma cortisol (ELISA, R&D, USA) and ACTH (Acthlisha, R&D, USA) levels.

2.5. Statistical Analysis. The statistical analysis was performed by using one-way analysis of variance (ANOVA) followed by a Turkey test with software SPSS 13.0. $P < 0.05$ which was considered statistically significant, and the data were expressed as means \pm standard deviation.

3. Results

3.1. Effects of EA-ACR Treatment on Heart Rate and Blood Pressure in UCMS Rats (Figures 2 and 3). No statistical difference was found in heart rate and blood pressure among rats of the three UCMS groups at the beginning of the study. Both of the heart rate and blood pressure in three UCMS groups showed a descending trend during the anesthesia period. However, the two EA treatment groups reduced heart rate and blood pressure significantly compared to the UCMS alone group. The mean heart rate from the 6th to 11th min decreased significantly in the EA-ACR group compared to the EA-ear-tip group; furthermore, the mean blood pressure was downregulated significantly in the EA-ACR group compared to the EA-ear-tip group in the treatment period. The EA-ACR treatment resulted in a significant decrease in the heart rate between the starting point of anesthesia and the 11th min of anesthesia ($P < 0.05$) and in the mean pressure between the starting point of anesthesia and the 16th min of anesthesia ($P < 0.05$).

3.2. The Different Influences of EA-Treatments on the Open Field Test Score of UCMS Rats (Figure 4). The total score of rats exposed to the open field test showed a significant decrease on the 22th day compared to the beginning in both the UCMS alone group and the EA-ear-tip group ($P < 0.01$ and $P < 0.01$, resp.). However, the score did not show remarkable differences between the two time spots in the normal group or in the EA-ACR group, respectively. But the EA-ACR group reached the score of 60 in the open field test

and was thus qualified as the UCMS model. In the EA-ear-tip group, the score decreased significantly on the 36th day compared to the 22nd day.

3.3. Effects of EA Treatment on Plasma Cortisol and ACTH Levels in UCMS Rats (Figures 5 and 6). As compared with the normal group, plasma cortisol levels in the three UCMS groups showed significant increases ($P < 0.01$ for all comparisons). On the other hand, the mean plasma cortisol level of the EA-ACR group and the EA-ear-tip group decreased significantly compared to the UCMS alone group ($P < 0.05$ and $P < 0.05$, resp.).

The 21-day UCMS exposure significantly increased the concentration of ACTH in rat blood ($P < 0.01$) when the UCMS group was compared with the normal control on the 51st day of the study. However, EA treatments significantly decreased the concentration of ACTH compared to the UCMS alone group ($P < 0.01$ and $P < 0.01$, resp.), while none of the EA treatment groups showed a significant difference in the concentration of ACTH as the normal control group did.

4. Discussion

In general, EA treatments down-regulated the heart rate and blood pressure as well as the concentration of plasma cortisol and ACTH. However, the heart rate and blood pressure were influenced more intensively by the EA-ACR than the EA-ear-tip, and the open field test score was kept at a higher level by EA-ACR only.

4.1. Cardioinhibitory Effects of EA-ACR Are Similar to the Vagus Nerve Stimulation. In the present study, EA-ACR elicited a significant decrease in heart rate and mean pressure under the anesthesia; however, the EA-ear-tip treatment did not induce similar changes during the treatment. These results suggested that EA stimulation at the auricular concha region induced similar effects as that of the direct vagus nerve electric stimulation had on the heart [7, 27, 28]. VNS, which stimulates the cervical trunk of the vagus nerve directly, is a procedure that was approved by FDA to treat primary hypertension years ago [7, 27]. Our previous research showed that acupuncture at auricular concha area could effectively decrease essential hypertension in rat models [9]. In addition, we found that electric stimulation on nucleus dorsalis nerve vagi could induce immediate decrease in heart rate and corresponding changes of electrocardiogram [29].

Anatomical knowledge of the vagus nerve informs that the auricular fibers of vagus nerve densely distribute in the concha and external auditory meatus of the ear; however, there are a few vagus nerve fibers around the ear tip [30]. The auricular branch of the vagus nerve ascends to the superior vagal ganglion (nucleus dorsalis nerve vagi), where the cholinergic preganglionic parasympathetic neurons give rise to the branchial efferent motor fibers innervating the heart, and stimulating pathway induces cardioinhibitory effects [28]. Afferent signals elicited by EA-ACR may be integrated at the medulla oblongata, which then generates regulatory signals to activate the cardiac vagus nerve. Cardiac vagus



FIGURE 1: Electrical stimulation spot. Black spot 1 on the ear-tip area (nonauricular concha control). Black spot 2 on the auricular concha region (ACR). Positive iron pole (diameter 0.3 mm) on the frontal side of ear, and the negative iron pole (diameter 0.3 mm) on the back side.

nerve activation slows the heart rate and decreases the blood pressure immediately.

4.2. EA-ACR Treatment Improved the Depressive Status of UCMS Rats in the Open Field Test. The unpredictable chronic mild stress (UCMS) has already contributed to the elucidation of the pathophysiological mechanisms of depression such as decreased neurogenesis and HPA axis alterations [26, 31]. In the current study, this model was used to explore the relations between depressive-like behavior in rats and EA-ACR treatment. The open field test provides simultaneous measurement of UCMS. A higher score in the test indicates increased locomotion and exploration and/or a lower level of anxiety [25, 26, 31]. In our study, the scores of open field test were significantly decreased in the UCMS alone and EA-ear-tip groups on day 22 compared to the beginning date, but no significant decrease was found in the EA-ACR group. However, all the rats in the EA-ACR group were qualified for modeling with a standard recruiting score of 60. It was apparent that EA-ACR kept the score on a higher level in the treatment course, while the score of the EA-ear-tip group showed a significant decrease during the treatment. This phenomenon indicated that EA-ACR induced the antidepressive effects. The UCMS model and the open field test were also successfully introduced into previous EA studies on depression. For example, EA at Baihui (GV20) and Yingtang (EX-HN3) on the top and front head scalp for 21 days can significantly improve the symptom of the depressive rats, the crossing and rearing movement times, and the number of p-CREB-positive neuron in the hippocampus as the fluoxetine compared with the UCMS alone group [25].

4.3. EA Treatment Normalized the Hyperactivity of Hypothalamic-Pituitary-Adrenal (HPA) Axis. In the present study, 21 days' UCMS exposure significantly increased the concentrations of plasma cortisol and ACTH in rats. It is

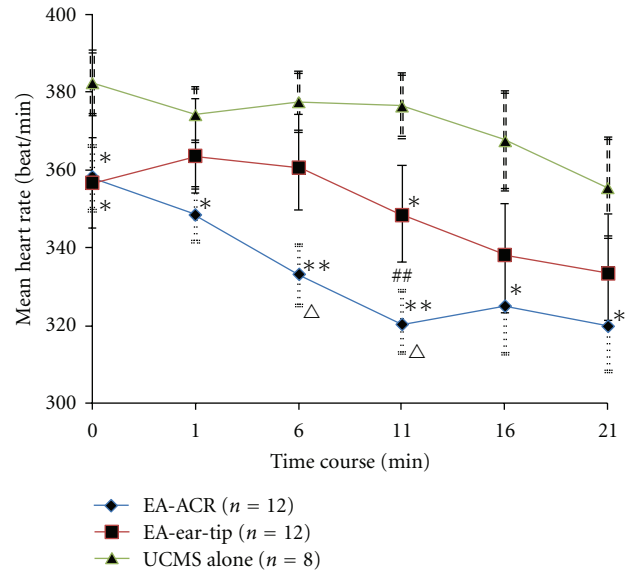


FIGURE 2: The time course of heart rate for three UCMS groups during one EA treatment/anesthesia. Comparison between the EA-treated UCMS group and the UCMS alone group, * $P < 0.05$, ** $P < 0.01$. Comparison between the EA-ACR group and the EA-ear-tip group, $\Delta P < 0.05$, $\Delta\Delta P < 0.01$. Comparison between the starting point of anesthesia and the 11th min in the EA-ACR group, $\#\# P < 0.01$.

consistent with the previous research studies on both human beings and animal models with depressive status [32, 33]. Furthermore, 14 days of EA treatments (both EA-ACR and EA-ear-tip) right after UCMS down-regulated the plasma cortisol and ACTH in UCMS rats to normal levels. Researchers found that EA at acupoints Neiguan(PC6), Sanyinjiao(SP6), and Taichong(LV3) can lower plasma cortisol and ACTH levels and improve symptoms in depression [33].

Several hypotheses have been proposed for the pathological mechanism of depression. Besides disturbed monoaminergic neurotransmission, hyperactivity of hypothalamic-pituitary-adrenal (HPA) axis is closely related to major depression [34–36]. The HPA axis is the primary neuroendocrine system responsible for coordinating the mammalian stress response and has thus been a major focus of neurobiological research of depression. Major components of the HPA axis include corticotropin-releasing factor (CRF), adrenocorticotropin hormone (ACTH), and glucocorticoids. Cortisol is the major glucocorticoid in humans and animals. During stress response, neurons in the paraventricular nucleus (PVN) of the hypothalamus release CRF into the hypothalamo-pituitary portal system. CRF then stimulates the release of adrenocorticotropin (ACTH) from the anterior pituitary into systemic circulation, which in turn stimulates the adrenal cortex to secrete cortisol. Cortisol is responsible for many of the physiological changes associated with the stress response, and it also provides negative feedback to the hypothalamus and pituitary to decrease the synthesis and release of CRF and ACTH.

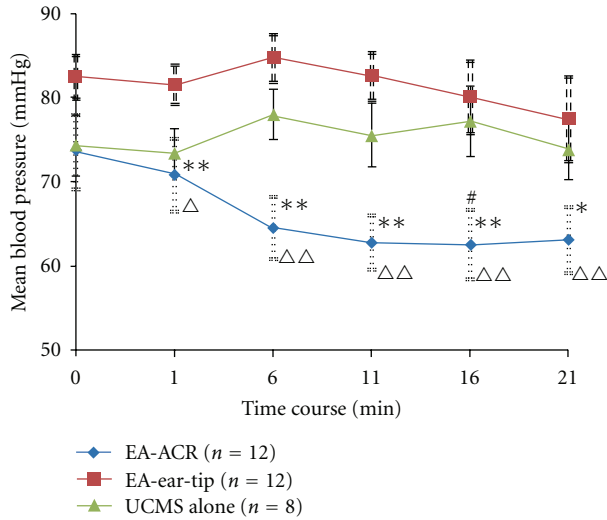


FIGURE 3: The time course of the mean blood pressure for the three UCMS groups during one EA treatment/anesthesia. Comparison between the EA-treated UCMS group and the UCMS alone group, * $P < 0.05$, ** $P < 0.01$. Comparison between the EA-ACR group and the EA-ear-tip group, $\Delta P < 0.05$, $\Delta\Delta P < 0.01$. Comparison between the starting point of anesthesia and the 16th min in the EA-ACR group. # $P < 0.05$.

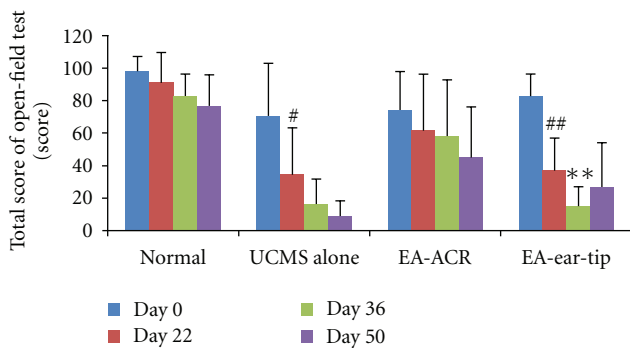


FIGURE 4: The influence of EA-ACR on the open field test score of rats. The 22nd day compared with the day before the test (day 0) in the same group, # $P < 0.05$, ## $P < 0.01$; the 36th day compared with the 22nd day in the EA-ear-tip group, ** $P < 0.01$.

Patients with depression show hyperactivity of the HPA axis that may result from the impaired negative feedback regulation of glucocorticoid release [34]. Moreover, research study also found that normalization of these HPA axis abnormalities is associated with successful antidepressant treatment, and patients whose HPA abnormalities do not normalize are significantly more likely to relapse [37]. In a VNS treatment study, O’Keane et al. [38] found that the CRF/ACTH (adrenocorticotrophic hormone) responses in the depressed group before VNS implantation were significantly higher than in the healthy group and were reduced to normal values after 3 months of VNS treatment; in addition, they also found significant improvement in depression symptoms.

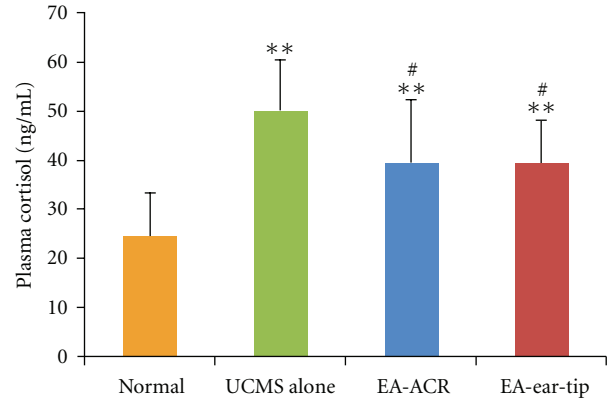


FIGURE 5: The effect of EA-ACR treatment on plasma cortisol in normal and UCMS rats. Comparison of plasma cortisol level between UCMS and normal groups, ** $P < 0.01$. Comparison between the EA-treated UCMS group and the UCMS alone group, # $P < 0.05$.

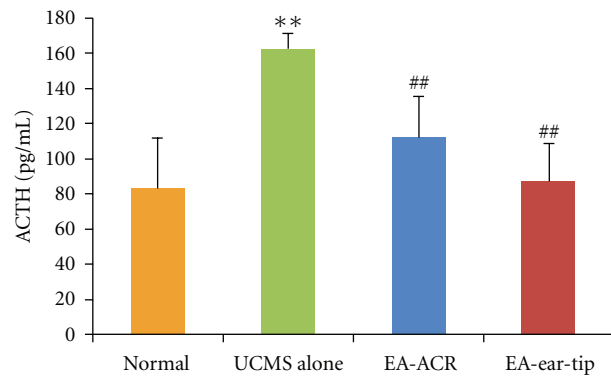


FIGURE 6: The effect of EA-ACR treatment on ACTH in normal and UCMS rats. Comparison of the ACTH level between normal and UCMS groups, ** $P < 0.01$. Comparison between the EA-treated UCMS group and the UCMS alone group, ## $P < 0.01$.

The result of the present study—EA-ACR significantly antagonized UCMS-induced depressive status of rats—is consistent with the findings of the mentioned research studies. As demonstrated through changes in plasma cortisol and ACTH levels, the antidepressant effect of EA-ACR may be mediated via normalization of the HPA axis hyperactivity. Otherwise, EA-ear-tip also was found to be the apparent down-regulation effect on the plasma cortisol and ACTH. It is found that a few vagus nerve fibers are around the ear tip [30], and HPA may be modulated by other nervous pathways beside the vagus nerve, for example, greater auricular nerve and lesser occipital nerve are densely innervated in the area of ear tip, and the EA signals can be transmitted by them to the cervical spinal cord and brain then modulate the HPA. Further investigation has been warranted for this hypothesis.

5. Limitation

This pilot EA-ACR study on depression has a small sample size. Meanwhile, EA-ACR does not only stimulate the

vagus nerve, but also affects other sensory nerves, such as nervous auricularis magnus, lesser occipital nerve, facial nerve, and glossopharyngeal nerve fibers. Although EA-ACR elicited similar effects to VNS, the interaction among the nerves in the area should be explored in the future. Further investigation on EA-ACR for the disturbed monoaminergic neurotransmission of depression has been warranted.

6. Conclusions

EA-ACR can elicit similar cardioinhibitory effects to vagus nerve stimulation (VNS), and EA-ACR significantly antagonized UCMS-induced depressive status of rats. The antidepressant effect of EA-ACR is possibly mediated via normalization of the HPA axis hyperactivity.

Author's Contribution

Ru-Peng Liu and Ji-Liang Fang contributed equally to this paper.

Acknowledgments

This scientific work was supported by the National Natural Science Foundation of China Research Grants (no. 30973798), the Twelfth Five-Year Plan of the National Science and Technology Support Program of China (2012BAF14B10), and the Beijing Natural Science Foundation (no. 711117).

References

- [1] H. A. Sackeim, A. J. Rush, M. S. George et al., "Vagus nerve stimulation (VNS \dot{U}) for treatment-resistant depression: efficacy, side effects, and predictors of outcome," *Neuropsychopharmacology*, vol. 25, no. 5, pp. 713–728, 2001.
- [2] A. J. Rush, L. B. Marangell, H. A. Sackeim et al., "Vagus nerve stimulation for treatment-resistant depression: a randomized, controlled acute phase trial," *Biological Psychiatry*, vol. 58, no. 5, pp. 347–354, 2005.
- [3] A. J. Rush, H. A. Sackeim, L. B. Marangell et al., "Effects of 12 months of vagus nerve stimulation in treatment-resistant depression: a naturalistic study," *Biological Psychiatry*, vol. 58, no. 5, pp. 355–363, 2005.
- [4] A. A. Nierenberg, J. E. Alpert, E. E. Gardner-Schuster, S. Seay, and D. Mischoulon, "Vagus nerve stimulation: 2-year outcomes for bipolar versus unipolar treatment-resistant depression," *Biological Psychiatry*, vol. 64, no. 6, pp. 455–460, 2008.
- [5] M. S. George, H. A. Sackeim, A. J. Rush et al., "Vagus nerve stimulation: a new tool for brain research and therapy," *Biological Psychiatry*, vol. 47, no. 4, pp. 287–295, 2000.
- [6] M. J. Millan, "The role of monoamines in the actions of established and "novel" antidepressant agents: a critical review," *European Journal of Pharmacology*, vol. 500, no. 1–3, pp. 371–384, 2004.
- [7] W. Sperling, U. Reulbach, S. Bleich, F. Padberg, J. Kornhuber, and M. Mueck-Weymann, "Cardiac effects of vagus nerve stimulation in patients with major depression," *Pharmacopsychiatry*, vol. 43, no. 1, pp. 7–11, 2010.
- [8] S. Spuck, V. Tronnier, I. Orosz et al., "Operative and technical complications of vagus nerve stimulator implantation," *Neurosurgery*, vol. 67, no. 2, pp. 489–494, 2010.
- [9] X. Y. Gao, Y. H. Li, P. J. Rong, and B. Zhu, "Effect of acupuncture of auricular concha area on blood pressure in primary hypertension and normal rats and analysis on its mechanism," *Acupuncture Research*, vol. 31, pp. 90–95, 2006.
- [10] X. Y. Gao, Y. H. Li, K. Liu et al., "Acupuncture-like stimulation at auricular point Heart evokes cardiovascular inhibition via activating the cardiac-related neurons in the nucleus tractus solitarius," *Brain Research*, vol. 1397, pp. 19–27, 2011.
- [11] Z. G. Mei, B. Zhu, Y. H. Li, P. J. Rong, H. Ben, and L. Li, "Responses of glucose-sensitive neurons and insulin-sensitive neurons in nucleus tractus solitarius to electroacupuncture at auricular concha in rats," *Chinese Acupuncture & Moxibustion*, vol. 27, no. 12, pp. 917–922, 2007.
- [12] F. Huang, P. J. Rong, H. C. Wang, H. Meng, and B. Zhu, "Clinical observation on the intervention of auricular vagus nerve stimulation treating 35 cases of impaired glucose tolerance patients," *China Journal of Traditional Chinese Medicine and Pharmacy*, vol. 25, no. 12, pp. 2185–2186, 2010.
- [13] W. He, C. L. Zhao, Y. H. Li et al., "Effect of electroacupuncture at auricular concha on behaviors and electroencephalogram in epileptic rats," *Chinese Journal of Pathophysiology*, vol. 27, no. 10, pp. 1913–1916, 2011.
- [14] W. He, Y. H. Li, P. J. Rong, L. Li, H. Ben, and B. Zhu, "Effect of electroacupuncture of different regions of the auricle on epileptic seizures in epilepsy rats," *Acupuncture Research*, vol. 38, no. 6, pp. 417–422, 2011.
- [15] Tang. Wang Bing. Inner Canon of Huang Di. Chinese Ancient Books Publishing House Yin the Qing Dynasty Jingkou Wencheng Tang inscription of Song, Beijing, China, 2003.
- [16] J. J. B. Allen, R. N. Schnyer, and S. K. Hitt, "The efficacy of acupuncture in the treatment of major depression in women," *Psychological Science*, vol. 9, no. 5, pp. 397–401, 1998.
- [17] H. C. Luo, H. Ureil, Y. C. Shen et al., "Comparative study of electroacupuncture and fluoxetine for treatment of depression," *Chinese Journal of Psychiatry*, vol. 36, pp. 215–219, 2003.
- [18] W. J. Zhang, X. B. Yang, and B. L. Zhong, "Combination of acupuncture and fluoxetine for depression: a randomized, double-blind, sham-controlled trial," *Journal of Alternative and Complementary Medicine*, vol. 15, no. 8, pp. 837–844, 2009.
- [19] H. Wang, H. Qi, B. S. Wang et al., "Is acupuncture beneficial in depression: a meta-analysis of 8 randomized controlled trials?" *Journal of Affective Disorders*, vol. 111, no. 2–3, pp. 125–134, 2008.
- [20] Y. L. Sun, S. B. Chen, Y. Gao, and J. Xiong, "Acupuncture versus western medicine for depression in China: a systematic review," *Chinese Journal of Evidence-Based Medicine*, vol. 8, no. 5, pp. 340–345, 2008.
- [21] J. N. Ren, "Auricular acupuncture to treat depression, 50 cases," *Henan Traditional Chinese Medicine*, vol. 25, no. 2, pp. 75–78, 2005.
- [22] Y. M. Liu and H. P. Su, "Observation of clinical efficacy on acupuncture with auricular acupressure to treatment of depression," *Liaoning Journal of Traditional Chinese Medicine*, vol. 35, no. 1, pp. 122–125, 2008.
- [23] J. M. Li, "Observation of clinical curative effect on the treatment of 35 cases of depression with acupuncture and auricular therapy," *Journal of Yunnan University of Traditional Chinese Medicine*, vol. 33, no. 1, pp. 5–6, 2010.

- [24] R. J. Katz, K. A. Roth, and B. J. Carroll, "Acute and chronic stress effects on open field activity in the rat: implications for a model of depression," *Neuroscience & Biobehavioral Reviews*, vol. 5, pp. 247–251, 1981.
- [25] D. M. Duan, Y. Tu, and L. P. Chen, "Effects of electroacupuncture at different acupoint groups on behavior activity and p-CREB expression in hippocampus in the rat of depression," *Chinese Acupuncture & Moxibustion*, vol. 28, no. 5, pp. 369–373, 2008.
- [26] P. Willner, "Validity, reliability and utility of the chronic mild stress model of depression: a 10-year review and evaluation," *Psychopharmacology*, vol. 134, no. 4, pp. 319–329, 1997.
- [27] D. A. Groves and V. J. Brown, "Vagal nerve stimulation: a review of its applications and potential mechanisms that mediate its clinical effects," *Neuroscience and Biobehavioral Reviews*, vol. 29, no. 3, pp. 493–500, 2005.
- [28] T. Kawada, S. Shimizu, M. Li et al., "Contrasting effects of moderate vagal stimulation on heart rate and carotid sinus baroreflex-mediated sympathetic arterial pressure regulation in rats," *Life Sciences*, vol. 89, no. 13, pp. 498–503, 2011.
- [29] H. J. Sun, H. B. Ai, and X. Y. Cui, "Effects of electrical stimulation to the dorsal motor vagal nucleus on HE-ECG signals," *Journal of Shanxi University*, vol. 27, pp. 289–291, 2004.
- [30] S. Standring, *Gray's Anatomy*, Churchill Livingstone, New York, NY, USA, 40th edition, 2008.
- [31] Y. S. Mineur, C. Belzung, and W. E. Crusio, "Effects of unpredictable chronic mild stress on anxiety and depression-like behavior in mice," *Behavioural Brain Research*, vol. 175, no. 1, pp. 43–50, 2006.
- [32] M. P. Boyle, J. A. Brewer, M. Funatsu et al., "Acquired deficit of forebrain glucocorticoid receptor produces depression-like changes in adrenal axis regulation and behavior," *Proceedings of the National Academy of Sciences of the United States of America*, vol. 102, no. 2, pp. 473–478, 2005.
- [33] H. Xu, Z. R. Sun, L. P. Li et al., "Effects of acupuncture on the hypothalamus-pituitary-adrenal axis in the patients of depression," *Chinese Acupuncture and Moxibustion*, vol. 24, no. 2, pp. 78–80, 2004.
- [34] C. B. Nemeroff, H. S. Mayberg, S. E. Krahl et al., "VNS therapy in treatment-resistant depression: clinical evidence and putative neurobiological mechanisms," *Neuropsychopharmacology*, vol. 31, no. 7, pp. 1345–1355, 2006.
- [35] J. P. Herman, H. Figueiredo, N. K. Mueller et al., "Central mechanisms of stress integration: hierarchical circuitry controlling hypothalamo-pituitary-adrenocortical responsiveness," *Frontiers in Neuroendocrinology*, vol. 24, no. 3, pp. 151–180, 2003.
- [36] N. Barden, "Implication of the hypothalamic-pituitary-adrenal axis in the pathophysiology of depression," *Journal of Psychiatry and Neuroscience*, vol. 29, no. 3, pp. 185–193, 2004.
- [37] S. M. O'Toole, L. K. Sekula, and R. T. Rubin, "Pituitary-adrenal cortical axis measures as predictors of sustained remission in major depression," *Biological Psychiatry*, vol. 42, pp. 85–89, 1997.
- [38] V. O'Keane, T. G. Dinan, L. Scott, and C. Corcoran, "Changes in hypothalamic-pituitary-adrenal axis measures after vagus nerve stimulation therapy in chronic depression," *Biological Psychiatry*, vol. 58, no. 12, pp. 963–968, 2005.

Research Article

An Acupuncture Research Protocol Developed from Historical Writings by Mathematical Reflections: A Rational Individualized Acupoint Selection Method for Immediate Pain Relief

Sven Schroeder,¹ Gesa Meyer-Hamme,¹ Jianwei Zhang,² Susanne Epplée,¹
Thomas Friedemann,¹ and Weiguo Hu^{1,3}

¹HanseMercur Center for Traditional Chinese Medicine at the University Medical Center Hamburg-Eppendorf, Martinistrasse 52, House O55, 20246 Hamburg, Germany

²Group TAMS, Department of Informatics, Faculty of Mathematics, Informatics and Natural Science, University of Hamburg, Vogt-Kölln-Strasse 30, 22527 Hamburg, Germany

³World Federation of Acupuncture Societies, B-701, Dongjiu Building, Xizhaosi Street, Dongcheng District, Beijing 100061, China

Correspondence should be addressed to Sven Schroeder; schroeder@tcm-am-uke.de

Received 27 July 2012; Revised 19 September 2012; Accepted 24 September 2012

Academic Editor: Di Zhang

Copyright © 2013 Sven Schroeder et al. This is an open access article distributed under the Creative Commons Attribution License, which permits unrestricted use, distribution, and reproduction in any medium, provided the original work is properly cited.

While balancing yin and yang is one basic principle of Chinese medicine, balancing methods for combination of meridians and acupoints had been described throughout the history of Chinese medicine. We have identified six historical systems for combinations of acupuncture points in historical writings. All of them represent symmetrical combinations which are defined by the steps in the Chinese Clock. Taking the historical systems as a basis, we calculated the possible combinations that fit into these systems they revealed, leading to a total of 19 systems offering new balancing combinations. Merging the data of these 19 systems, there are 7 combinatorial options for every meridian. On the basis of this data, we calculated 4-meridian combinations with an ideal balance pattern, which is given when all meridians balance each other. We identified 5 of these patterns for every meridian, so we end up with 60 patterns for all the 12 meridians but we find multiple overlapping. Finally, 15 distinct patterns remain. By combining this theoretical concept with the *Image and Mirror Concept*, we developed an acupuncture research protocol. This protocol potentially solves some problems of acupuncture trials because it represents a rational reproducible procedure independent of examiner experience, but the resulting treatment is individualized.

1. Introduction

In Chinese Medicine, disease is understood as a loss of balance between the yin and yang energies [1, 2]. Balancing yin and yang is a basic concept of acupuncture treatment [1, 3], so combinations of meridians (or their corresponding organs) and acupoints for the balance of yin and yang had been described throughout the history of Chinese medicine [4]. Meridians are classified as yin or yang meridians. Lung (LU), spleen (SP), heart (HT), kidney (KI), pericardium (PC), and liver (LR) are defined as yin meridians, while large intestines (LI), stomach (ST), small intestines (SI), bladder (BL), triple energizer (TE), and gall-bladder (GB) are defined as yang meridians [5–10]. In our recent article

[11] we have identified the known historical systems for combination of acupuncture points in historical writings and modern textbooks [3, 5–10, 12–27]. All of these represent symmetrical combinations, which were defined by the steps in the Chinese Clock (CC). In TCM theory, a continuous circulation of Qi through 12 meridians in a distinct order (LU, LI, ST, SP, HT, SI, BL, KI, PC, TE, GB, LR) is postulated, described as the Chinese medicine body clock, or Chinese clock (CC).

1.1. Historical Systems. The most common system is the *interior-exterior system*, a single-step system [17, 28–30]. It originates from Ling Shu (Ch. 2, Vol. 1) [23] and was described in detail in *The systematic classic of acupuncture*

TABLE 1: Intrinsic rules of the historical systems.

Every meridian pairs with only other one
Rotation symmetry of 30°, 60°, or 120°
6 pairs of meridian
Maximum of 2 alternating steps
6 yin/yang or 3 yin/yin and 3 yang/yang combinations

and *moxibustion* (Zhen Jiu Jia Yi Jing, Book 9) [17]. Figure 1(a) shows the plotting of the interior-exterior system on the CC. The *neighbouring channels system* is the second option of combining channels in a single-step system. It leads to arm-leg combinations of two yin or two yang channels [30–33]. Figure 1(b) shows the plotting of the neighbouring channels system on the CC. Three systems follow the theory of the 6 stages, originating from the Suwen (Chapter 6, (77 + 79)) and Lingshu (Chapter 5 (948 + 949)) [10, 23] and have been described in detail in the Shanghanlun [10]. Since the description in *The Systematic Classic of Acupuncture and Moxibustion* [17] meridians are named according to the stages and the extremity where the main part of this meridian is running (Hand Tai Yang (SI), Foot Tai Yang (BL), Hand Yang Ming (LI), Foot Yang Ming (ST), Hand Shao Yang (TE), Foot Shao Yang (GB), Hand Tai Yin (LU), Foot Tai Yin (SP), Hand Jue Yin (PC), Foot Jue Yin (LR), Hand Shao Yin (HT), and Foot Shao Yin (KI)). Combining the meridians of one stage is very popular and is called “anatomical system” in some schools [34]. This system represents a 1-step–3-step alternating system. We call it the *6-stage system I*. Figure 1(c) shows the plotting of the 6-stage system I on the CC. The next system we call *6-stage system II*. It combines stages Tai Yang and Shao Yin, stages Yang Ming and Tai Yin as well as stages Shao Yang and Jue Yin. It is widely used in modern schools [18, 29, 31, 32]. Figure 1(d) shows the plotting of the *6-stage system II* on the CC.

6-stage system III originates from the Ming-Dynasty [18]. This system combines Tai Yang with Tai Yin, Jue Yin with Yang Ming and Shao Yang with Shao Yin. Figure 1(e) shows the plotting of the 6-stage system III on the CC.

Cross needling originates from Chapter 63 of the Suwen and is called opposite clock needling in modern school [30] and also used in Japanese acupuncture [18]. Figure 1(f) shows the plotting of the *opposite clock system* on the CC.

1.2. Intrinsic Rules of the Historical Systems. All historically described systems have in common the fact that they build a symmetrical combination in the CC with a rotation symmetry of 30°, 60° or 120°. Every meridian pairs with only one other and no meridian is left over, so there are always 6 pairs of meridians. A maximum of two alternating steps are used, leading to yin-yang/yang-yin or to yin-yin/yang-yang combinations. They can be described as intrinsic rules of the historical systems, summarized in Table 1. A graphical plotting of all historical systems is shown in Figures 1(a)–Figure 1(f).

1.3. Graph Traversal Search for Identification of Further Systems. Our question was to find out whether there are more

TABLE 2: Combinations that follow the intrinsic rules of the historical systems, listed according to steps in the Chinese Clock.

1-step systems	= 2
1-step–3-step alternating systems	= 4
2-step systems	= 4
2-step–6-step alternating systems	= 4
3-step systems	= 2
5-step systems	= 2
6-step systems	= 1
Total number	19

systems than historically described and whether any meridians can be excluded as potentially balancing meridians, so we calculated all symmetrical combinatorial possibilities. We did a graph traversal search for further systems, described in detail in our recent paper, available online [11]. 19 of the symmetrical patterns followed the intrinsic rules of the historical systems (Table 2).

1.4. Additional Combinations from Graph Traversal Search. One 2-step–6-step alternating system we want to emphasize, since it combines stages Tai Yang and Jue Yin, Yang Ming and Shao Yin, as well as Shao Yang and Tai Yin. So we named it *6-stage system IV* (Figure 1(g)).

There are three more 1-step–3-step alternating systems that lead to additional point combinations not covered by those historically described.

Step 5 provides an additional combinatorial possibility, but has no extensive tradition in Chinese medicine except for concepts connected to the extraordinary vessels. All pairs of Yin extraordinary vessels can be opened by using a 5-step combination which includes the very commonly used technique to combine the master points of the paired extraordinary vessels [35]. The master point of the primarily treated extraordinary vessel is needled at first, then the master point of the paired extraordinary vessel, called the coupled point, is needled secondly. Chong Mai (SP-4, Gongsun) and Yin Wei Mai (PC-6, Neiguan), Ren Mai (LU-7, Lique), and Yin Qiao Mai (KI-6, Zhaohai) represent this 5-step combination [24, 35, 36].

With step 5 distant parts of the body are connected. A combination of step 5 with another step in the Chinese Clock is mathematically not possible, if the intrinsic rules of the historical system are to be observed. As described above this is, however, possible for the 1–3-step and for 2–6-step combinations of two steps for an balance in accord with the intrinsic rules (Table 2). This might be an explanation why the points of the extraordinary vessels are usually used alone in a two-point combination [35, 36]. So if you combine a step 5 combination with other meridians, there is a high risk of applying an unbalanced treatment.

The possibilities for finding a balanced treatment strategy can be described by the steps that have to be taken in the Chinese clock to combine acupuncture points. Merging the data of all systems, the steps in the Chinese clock showing a possibility for balancing are the following. Steps 1, 2, and

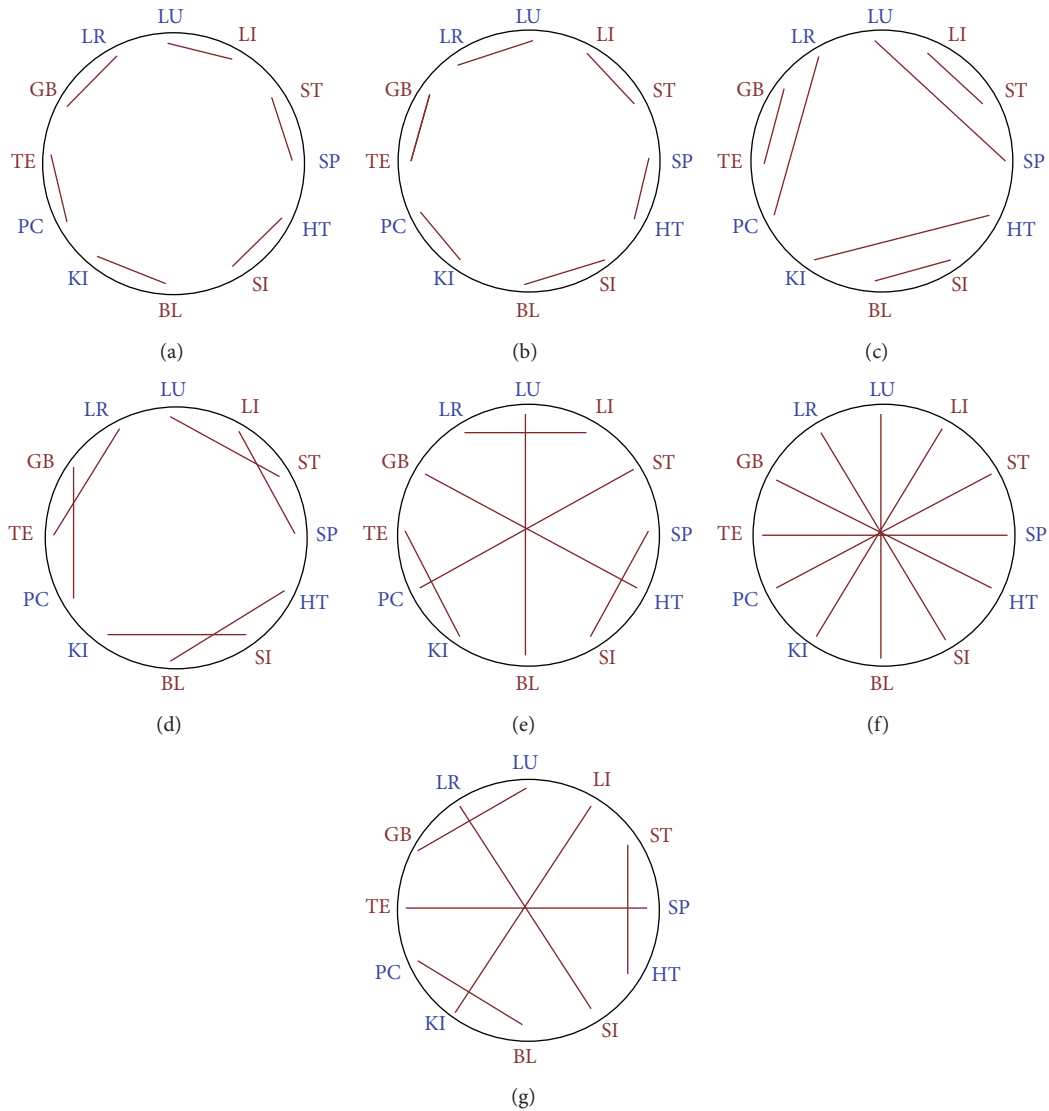


FIGURE 1: Graphical plotting of the historical systems. (a) Interior/exterior; (b) neighbouring channels; (c) 6-stage I; (d) 6-stage II; (e) 6-stage III; (f) opposite clock and one new system; (g) 6-stage IV. Blue: yin meridians, red: yang meridians.

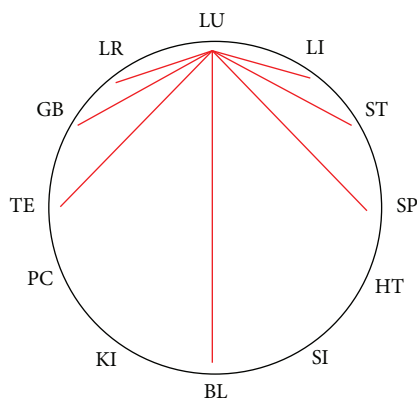


FIGURE 2: Merging of the combinatorial possibilities (this can be done with every meridian in a similar way).

TABLE 3: Possible steps in the Chinese clock for balancing a meridian.

1, 2 and 3 are possible
4 is not possible
5 is possible, but has no tradition in TCM, except in the theory of the extraordinary vessels and might be unbalanced in a multiple point concept
6 is possible

3 are possible so is step 6. Step 4 is not a combinatorial possibility. Step 5 is a combinatorial possibility, but has no tradition in TCM, except in the theory of the extraordinary vessels [35, 36], might lead to an imbalance in multipoint combinations. A summary is given in Table 3.

In Table 4 we list all of the 19 calculated systems, that allow a multimeridian combination. This includes the historical systems, marked in yellow. Systems that allow new combinations are marked in blue, while calculated systems that do not offer new combinations, that are already known by the historical systems, are not marked. The merged data plotted on the CC are shown as an example for the meridians of the lung (see Figure 2). This can be applied for all meridians in a similar way. It shows clearly, that every meridian can be balanced by 7 other meridians. Plotted on the CC these seven options are always step 1, 2, 3 clockwise and counterclockwise as well as step 6. For daily practice this is helpful to quickly identify the treatment options for balancing the affected meridian. It can be used as a tool for quick memorization.

For a TCM practitioner these 7 options might be mainly understood as energetic relationships. We describe this for the example of the LU-Meridian, plotted on the CC in Figure 2. Step 1 clockwise is the internal (LU)-external (LI) relationship, Step 2 clockwise is the Hand-Tai Yin (LU)-Foot-Yang Ming (ST) relationship, described by *6-stage system II*. Step 3 clockwise is the Hand-Tai Yin (LU)-Foot-Tai Yin (SP) from *6-Stage system I*. Step 1 counterclockwise is the *Neighbouring channels* relationship LU-LR, Step 2 counterclockwise is the Hand-Tai Yin (LU)-Foot-Shao Yang (GB) described in the new system *6-stage IV*. Step 3 counterclockwise describes a previously not described combination deriving from mathematical calculations with no obvious theoretical systematic background. Step 6 describes the opposite-clock relationship of LU and BL.

1.5. Combination of More than Two Meridians. Merging of the combinatorial possibilities leads to 7 options for a balanced treatment for every meridian. It might lead to the idea that “everything goes” in acupuncture. This is actually not true. If only two meridians are combined there are these 7 options. Nevertheless, it is very common to combine more than 2 meridians in an acupuncture treatment. For this reason keeping a treatment balanced in accordance with the intrinsic rules of the historical systems becomes complicated. So some acupuncture schools start to describe patterns, usually combining two historical systems treating all four extremities [30–32, 37] to avoid unbalanced combinations.

So a complete balanced treatment of a meridian combines a left-right yin-yang balance and an up-down yin-yang balance (Figure 3). In this context the goal is to identify a pattern which will lead to a balance in which every meridian is balanced by all other meridians employed, in accordance with the above-described intrinsic rules of the historical systems. This is what we call an ideal balance.

1.6. Using Somatotopic Knowledge for the Search of the Right Points on a Balancing Meridian. Somatotopy is the mapping of touch, vibration, and heat signals coming from different parts of the body to distinct and specific locations in the brain’s primary somatosensory cortex (SI). This somatotopic organization is sometimes described as the homunculus of the brain [38]. The somatotopic knowledge is old and is already described in detail in Su Wen (e.g., Chapters 67,

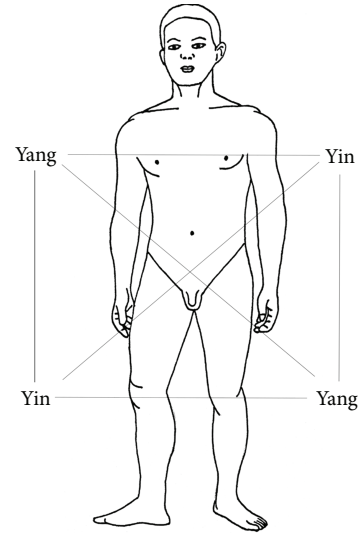


FIGURE 3: Balanced treatment in projection to the body.

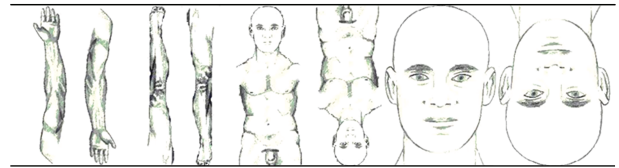


FIGURE 4: . Somatotopic image and mirror of different body areas.

68, and 71) describing the relationship between up and down, left and right, front and back [23]. The most likely form of acupoint specificity lies in the somatotopic response [39]. Some modern schools devote great attention to these somatotopies and use them for point selection, calling this the *Image and Mirror Concept* [30–33]. This *Image and Mirror Concept* describes somatotopic projections of different body areas. It is very useful for the identification of possible areas for treatment, especially when combined with the knowledge of the balancing meridians. Image means in this context, that you can project a part of the body (e.g., the arm) on another part of the body (e.g., the leg) to identify a somatotopic connection. Mirror means in this context, that you also can project an upside-down picture of one body part to another body parts, to find somatotopic connections. So for example, effective points for treatment of the knee region can be found in the region of the elbow, chest, eyes, or nose. In Figure 4 you find a graphical plotting of somatotopically connected body areas.

2. Material and Methods

As a basis for further analysis we took the above described 2-meridian combinations, that follow the intrinsic rules of the historical systems. While the merging of the combinatorial possibilities leads to 7 options for every meridian for a balanced treatment, we were interested in combining more than 2 meridians in a balanced acupuncture procedure. We

TABLE 4: Systems for combinations of meridians for multimeridian combinations.

LU	LI	LR	ST	GB	ST	GB	SP	LR	LI	TE	SP	TE	BL	GB	ST	BL	BL
LI	LU	ST	SP	SP	LR	LR	ST	GB	LU	HT	GB	HT	LR	KI	KI	SP	KI
ST	SP	LI	LU	HT	LU	HT	LI	SI	LR	SP	SI	LV	PC	HT	LU	PC	PC
SP	ST	HT	LI	LI	SI	SI	LU	HT	BL	ST	LU	BL	SI	TE	TE	LI	TE
HT	SI	SP	BL	ST	BL	ST	KI	SP	SI	LI	KI	LI	GB	ST	BL	GB	GB
SI	HT	BL	KI	KI	SP	SP	BL	ST	HT	PC	ST	PC	SP	LR	LR	KI	LR
BL	KI	SI	HT	PC	HT	PC	SI	TE	SP	KI	TE	SP	LU	PC	HT	LU	LU
KI	BL	PC	SI	SI	TE	TE	HT	PC	GB	BL	HT	GB	TE	LI	LI	SI	LI
PC	TE	KI	GB	BL	GB	BL	LR	KI	TE	SI	LV	SI	ST	BL	GB	ST	ST
TE	PC	GB	LR	LR	KI	KI	GB	BL	PC	LU	BL	LU	KI	SP	SP	LR	SP
GB	LR	TE	PC	LU	PC	LU	TE	LI	KI	LR	LI	KI	HT	LU	PC	HT	HT
LR	GB	LU	TE	TE	LI	LI	PC	LU	ST	GB	PC	ST	LI	SI	SI	TE	SI
Step	1	1	2	2	2	2	1-3	1-3	1-3	1-3	3	3	6-2	6-2	6-2	6-2	6-6
Name	Ext./Int.	neighbour	6-stage II				6-stage I						6-stage II	6-stage IV			OPP.CLOCK

Yellow: historical systems, blue: new systems with additional combinations, and white: new systems without new combinations.

decided to calculate the mathematical options for combining 4 meridians to gain an ideal balance, because the human body has four extremities. We defined as an ideal balance a combination of meridians, in which every meridian is balanced by all other meridians employed, in accord with the above-described intrinsic rules of the historical systems.

First we calculated all the possible 4-meridian combinations of the 12 meridians in the CC. Second we reduced the number to the above described 7 options. We listed all possibilities. Third we identified and described the patterns that followed our definition of an ideal balance.

Finally we combined the resulting information with the knowledge of the above described *Image and Mirror Concept* for the development of an research protocol for acupuncture.

3. Results

3.1. Combinatorial Possibilities. The 12 meridians in the circle were labelled 1, 2, 3, ..., 12. There are 6 possible steps in the Chinese clock: 1, 2, 3, 4, 5, and 6. (e.g., step 1 is a connection of two neighbouring meridians, step 2 skips one, combining the first meridian with the third one, etc.). To connect 4 meridian, all solutions can be classified into 3 groups. Every meridian point pairs with other 3 and no meridian is left over. C_n^k is the number of combinations of n things taken k at a time $n!/((n-k)!k!)$. The possible combinatorial number is $C_{12}^4 C_8^4 C_4^4 / (3!) = 5775$.

Then the step of each group was calculated. There are 6 possible steps in the Chinese Clock: 1, 2, 3, 4, 5, 6, as is shown in Figure 1. The number of possible combinations was counted. 4-point combination where every point is a combinatory possibility with every other, following the rule of 2-point combinations, where every point only can be combined with 7 others, as is shown in Figure 2. The combinations with steps 4 and 5 were eliminated, because they did not correspond to the intrinsic rules of the historical system. So the possible steps were only 1, 2, 3, and 6. There

are only 4 kinds of steps, though here are 7 options of combination (as shown in Figure 2) for every meridian.

3.2. Development of 4-Meridian Patterns. An ideal balance pattern for meridian-balancing is given, when all meridians balance each other. So an ideally balanced 4-meridian-pattern is only present, if every meridian is a possible combination (according to one of the 7 options) of every other meridian of this 4-meridian pattern. So we manually evaluated the 4-point combinations according to Table 4.

We listed all possibilities by plotting the combinations on the CC. While there are 12 meridians, there are $12 \times 7 = 84$ options for 2-meridian combinations. These were manually evaluated and the repetitions were deleted, resulting a reduction to 42 options of 2-meridian combinations. This first step of the development of 4-meridian patterns is shown in Figure 5(a).

These 42 pairs of meridians were evaluated for their common potential balancing meridians. We found 24 times 4 shared balancing meridians for the pairs of meridians, 12 times 3 shared balancing meridians and 6 times 2 shared balancing meridians, leading to 144 options for 3-meridian combinations. We deleted the repetitions and found 48 unique options for 3-meridian combinations.

This second step of the development of 4-meridian patterns is shown in Figure 5(b).

The 48 3-meridian combinations were evaluated for their common potential balancing meridians. We found 12 times 2 shared balancing meridians of all 3 meridians and 48 times one shared balancing meridian of all 3 meridians, leading to 60 possible 4-meridian combinations. This third step of the development of 4-meridian patterns is shown in Figure 5(c).

These 60 possible 4-meridian combinations were manually new arranged by the common patterns on the CC and their connection to the 12 meridians. This is shown in Figure 5(d).

For every meridian five ideally balanced 4-meridian-patterns could be identified. They all had a similar pattern on

2-meridian combinations (n = 42)			Possible 3-meridian combinations				
Meridian	Potential balancing meridians	Meridian					
LU	TE GB LR BL LI ST SP	BL KI PC SP GB LR LU	TE	LU GB TE	LU LR TE	LU BL TE	LU SP TE
LU	TE GB LR BL LI ST SP	KI PC TE HT LR LU LI	GB	LU LR GB	LU LI GB	LU TE GB	
LU	TE GB LR BL LI ST SP	PC TE GB SI LU LI ST	LR	LU TE LR	LU GB LR	LU LI LR	LU ST LR
LU	TE GB LR BL LI ST SP	SP HT SI LU KI PC TE	BL	LU TE BL	LU SP BL		
LU	TE GB LR BL LI ST SP	GB LR LU KI ST SP HT	LI	LU GB LI	LU LR LI	LU ST LI	LU SP LI
LU	TE GB LR BL LI ST SP	LR LU LI PC SP HT SI	ST	LU LI ST	LU SP ST	LU LR ST	
LU	TE GB LR BL LI ST SP	LU LI ST TE HT SI BL	SP	LU BL SP	LU ST SP	LU TE SP	LU LI SP
LI	GB LR LU KI ST SP HT	KI PC TE HT LR LU LI	GB	LI LR GB	LI LU GB	LI KI GB	LI HT GB
LI	GB LR LU KI ST SP HT	PC TE GB SI LU LI ST	LR	LI GB LR	LI LU LR	LI ST LR	
LI	GB LR LU KI ST SP HT	HT SI BL LI PC TE GB	KI	LI GB KI	LI HT KI		
LI	GB LR LU KI ST SP HT	LR LU LI PC SP HT SI	ST	LI LR ST	LI LU ST	LI SP ST	LI HT ST
LI	GB LR LU KI ST SP HT	LU LI ST TE HT SI BL	SP	LI LU SP	LI ST SP	LI HT SP	
LI	GB LR LU KI ST SP HT	LI ST SP GB SI BL KI	HT	LI GB HT	LI KI HT	LI ST HT	LI SP HT
ST	LR LU LI PC SP HT SI	PC TE GB SI LU LI ST	LR	ST LU LR	ST LI LR	ST PC LR	ST SI LR
ST	LR LU LI PC SP HT SI	SI BL KI ST TE GB LR	PC	ST LR PC	ST SI PC		
ST	LR LU LI PC SP HT SI	LU LI ST TE HT SI BL	SP	ST LU SP	ST LI SP	ST HT SP	ST SI SP
ST	LR LU LI PC SP HT SI	LI ST SP GB SI BL KI	HT	ST LI HT	ST SP HT	ST SI HT	
ST	LR LU LI PC SP HT SI	ST SP HT LR BL KI PC	SI	ST LR SI	ST PC SI	ST SP SI	ST HT SI
SP	LU LI ST TE HT SI BL	BL KI PC SP GB LR LU	TE	SP LU TE	SP BL TE		
SP	LU LI ST TE HT SI BL	LI ST SP GB SI BL KI	HT	SP LI HT	SP ST HT	SP SI HT	SP BL HT
SP	LU LI ST TE HT SI BL	ST SP HT LR BL KI PC	SI	SP ST SI	SP HT SI	SP BL SI	
SP	LU LI ST TE HT SI BL	SP HT SI LU KI PC TE	BL	SP LU BL	SP TE BL	SP HT BL	SP SI BL
HT	LI ST SP GB SI BL KI	KI PC TE HT LR LU LI	GB	HT LI GB	HT KI GB		
HT	LI ST SP GB SI BL KI	ST SP HT LR BL KI PC	SI	HT ST SI	HT SP SI	HT BL SI	HT KI SI
HT	LI ST SP GB SI BL KI	SP HT SI LU KI PC TE	BL	HT SP BL	HT SI BL	HT KI BL	
HT	LI ST SP GB SI BL KI	HT SI BL LI PC TE GB	KI	HT LI KI	HT GB KI	HT SI KI	HT BL KI
SI	ST SP HT LR BL KI PC	PC TE GB SI LU LI ST	LR	SI ST LR	SI PC LR		
SI	ST SP HT LR BL KI PC	SP HT SI LU KI PC TE	BL	SI SP BL	SI HT BL	SI PC BL	SI KI BL
SI	ST SP HT LR BL KI PC	HT SI BL LI PC TE GB	KI	SI HT KI	SI BL KI	SI PC KI	
SI	ST SP HT LR BL KI PC	SI BL KI ST TE GB LR	PC	SI ST PC	SI LR PC	SI BL PC	SI KI PC
BL	SP HT SI LU KI PC TE	HT SI BL LI PC TE GB	KI	BL HT KI	BL SI KI	BL PC KI	BL TE KI
BL	SP HT SI LU KI PC TE	SI BL KI ST TE GB LR	PC	BL SI PC	BL KI PC	BL TE PC	
BL	SP HT SI LU KI PC TE	BL KI PC SP GB LR LU	TE	BL SP TE	BL LU TE	BL KI TE	BL PC TE
KI	HT SI BL LI PC TE GB	SI BL KI ST TE GB LR	PC	KI SI PC	KI BL PC	KI TE PC	KI GB PC
KI	HT SI BL LI PC TE GB	BL KI PC SP GB LR LU	TE	KI BL TE	KI PC TE	KI GB TE	
KI	HT SI BL LI PC TE GB	KI PC TE HT LR LU LI	GB	KI HT GB	KI LI GB	KI PC GB	KI TE GB
PC	SI BL KI ST TE GB LR	BL KI PC SP GB LR LU	TE	PC BL TE	PC KI TE	PC GB TE	PC LR TE
PC	SI BL KI ST TE GB LR	KI PC TE HT LR LU LI	GB	PC KI GB	PC TE GB	PC LR GB	
PC	SI BL KI ST TE GB LR	PC TE GB SI LU LI ST	LR	PC SI LR	PC ST LR	PC TE LR	PC GB LR
TE	BL KI PC SP GB LR LU	KI PC TE HT LR LU LI	GB	TE KI GB	TE PC GB	TE LR GB	TE LU GB
TE	BL KI PC SP GB LR LU	PC TE GB SI LU LI ST	LR	TE PC LR	TE GB LR	TE LU LR	
GB	KI PC TE HT LR LU LI	PC TE GB SI LU LI ST	LR	GB PC LR	GB TE LR	GB LU LR	GB LI LR

Fat : potential third balancing meridian of both meridians

3-meridian combinations

after deletion of repetitions (n = 48)

(b) Second step of the development of 4-meridian patterns. Potential third balancing meridians of the 2-meridian combinations. Possible 3-meridian combinations and reduction of the 3-meridian combinations by deletion of repetitions

FIGURE 5: Continued.

3-meridian combinations (n = 48)

Possible 4-meridian combinations (n = 60)

	Meridian	Potential balancing meridians	Meridian	Potential balancing meridians	Meridian	Potential balancing meridians		
BL HT KI	BL	SP HT SI LU KI PC TE	HT	LI ST SP GB SI BL KI	KI	HT SI BL LI PC TE GB	⇒	BL HT KI SI
BL KI PC	BL	SP HT SI LU KI PC TE	KI	HT SI BL LI PC TE GB	PC	SI BL KI ST TE GB LR		BL KI PC SI BL KI PC TE
BL KI TE	BL	SP HT SI LU KI PC TE	KI	HT SI BL LI PC TE GB	TE	BL KI PC SP GB LR LU		BL KI TE PC
BL LU TE	BL	SP HT SI LU KI PC TE	LU	TE GB LR BL LI ST SP	TE	BL KI PC SP GB LR LU		BL LU TE SP
BL PC TE	BL	SP HT SI LU KI PC TE	PC	SI BL KI ST TE GB LR	TE	BL KI PC SP GB LR LU		BL PC TE KI
BL SI KI	BL	SP HT SI LU KI PC TE	SI	ST SP HT LR BL KI PC	KI	HT SI BL LI PC TE GB	⇒	BL SI KI HT BL SI KI PC
BL SI PC	BL	SP HT SI LU KI PC TE	SI	ST SP HT LR BL KI PC	PC	SI BL KI ST TE GB LR		BL SI PC KI
BL SP TE	BL	SP HT SI LU KI PC TE	SP	LU LI ST TE HT SI BL	TE	BL KI PC SP GB LR LU		BL SP TE LU
GB LI LR	GB	KI PC TE HT LR LU LI	LI	GB LR LU KI ST SP HT	LR	PC TE GB SI LU LI ST		GB LI LR LU
GB LU LR	GB	KI PC TE HT LR LU LI	LU	TE GB LR BL LI ST SP	LR	PC TE GB SI LU LI ST		GB LU LR TE GB LU LR LI
GB PC LR	GB	KI PC TE HT LR LU LI	PC	SI BL KI ST TE GB LR	LR	PC TE GB SI LU LI ST		GB PC LR TE
GB TE LR	GB	KI PC TE HT LR LU LI	TE	BL KI PC SP GB LR LU	LR	PC TE GB SI LU LI ST		GB TE LR PC GB TE LR LU
HT BL SI	HT	LI ST SP GB SI BL KI	BL	SP HT SI LU KI PC TE	SI	ST SP HT LR BL KI PC		HT BL SI KI HT BL SI SP
HT GB KI	HT	LI ST SP GB SI BL KI	GB	KI PC TE HT LR LU LI	KI	HT SI BL LI PC TE GB		HT GB KI LI
HT KI SI	HT	LI ST SP GB SI BL KI	KI	HT SI BL LI PC TE GB	SI	ST SP HT LR BL KI PC		HT KI SI BL
HT LI GB	HT	LI ST SP GB SI BL KI	LI	GB LR LU KI ST SP HT	GB	KI PC TE HT LR LU LI		HT LI GB KI
HT LI KI	HT	LI ST SP GB SI BL KI	LI	GB LR LU KI ST SP HT	KI	HT SI BL LI PC TE GB		HT LI KI GB
HT SP BL	HT	LI ST SP GB SI BL KI	SP	LU LI ST TE HT SI BL	BL	SP HT SI LU KI PC TE	⇒	HT SP BL SI
HT SP SI	HT	LI ST SP GB SI BL KI	SP	LU LI ST TE HT SI BL	SI	ST SP HT LR BL KI PC		HT SP SI ST HT SP SI BL
HT ST SI	HT	LI ST SP GB SI BL KI	ST	LR LU LI PC SP HT SI	SI	ST SP HT LR BL KI PC		HT ST SI SP
KI GB TE	KI	HT SI BL LI PC TE GB	GB	KI PC TE HT LR LU LI	TE	BL KI PC SP GB LR LU		KI GB TE PC
KI LI GB	KI	HT SI BL LI PC TE GB	LI	GB LR LU KI ST SP HT	GB	KI PC TE HT LR LU LI		KI LI GB HT
KI PC GB	KI	HT SI BL LI PC TE GB	PC	SI BL KI ST TE GB LR	GB	KI PC TE HT LR LU LI		KI PC GB TE
KI PC TE	KI	HT SI BL LI PC TE GB	PC	SI BL KI ST TE GB LR	TE	BL KI PC SP GB LR LU		KI PC TE GB KI PC TE BL
KI SI PC	KI	HT SI BL LI PC TE GB	SI	ST SP HT LR BL KI PC	PC	SI BL KI ST TE GB LR		KI SI PC BL
LI HT SP	LI	GB LR LU KI ST SP HT	HT	LI ST SP GB SI BL KI	SP	LU LI ST TE HT SI BL		LI HT SP ST
LI HT ST	LI	GB LR LU KI ST SP HT	HT	LI ST SP GB SI BL KI	ST	LR LU LI PC SP HT SI		LI HT ST SP
LI LU ST	LI	GB LR LU KI ST SP HT	LU	TE GB LR BL LI ST SP	ST	LR LU LI PC SP HT SI		LI LU ST SP LI LU ST LR
LI SP ST	LI	GB LR LU KI ST SP HT	SP	LU LI ST TE HT SI BL	ST	LR LU LI PC SP HT SI		LI SP ST LU LI SP ST HT
LI ST LR	LI	GB LR LU KI ST SP HT	ST	LR LU LI PC SP HT SI	LR	PC TE GB SI LU LI ST	⇒	LI ST LR LU
LU GB TE	LU	TE GB LR BL LI ST SP	GB	KI PC TE HT LR LU LI	TE	BL KI PC SP GB LR LU		LU GB TE LR
LU LI GB	LU	TE GB LR BL LI ST SP	LI	GB LR LU KI ST SP HT	GB	KI PC TE HT LR LU LI		LU LI GB LR
LU LI LR	LU	TE GB LR BL LI ST SP	LI	GB LR LU KI ST SP HT	LR	PC TE GB SI LU LI ST		LU LI LR GB LU LI LR ST
LU LR TE	LU	TE GB LR BL LI ST SP	LR	PC TE GB SI LU LI ST	TE	BL KI PC SP GB LR LU		LU LR TE GB
LU SP BL	LU	TE GB LR BL LI ST SP	SP	LU LI ST TE HT SI BL	BL	SP HT SI LU KI PC TE		LU SP BL TE
LU SP LI	LU	TE GB LR BL LI ST SP	SP	LU LI ST TE HT SI BL	LI	GB LR LU KI ST SP HT		LU SP LI ST
LU SP ST	LU	TE GB LR BL LI ST SP	SP	LU LI ST TE HT SI BL	ST	LR LU LI PC SP HT SI		LU SP ST LI
LU SP TE	LU	TE GB LR BL LI ST SP	SP	LU LI ST TE HT SI BL	TE	BL KI PC SP GB LR LU		LU SP TE BL
LU ST LR	LU	TE GB LR BL LI ST SP	ST	LR LU LI PC SP HT SI	LR	PC TE GB SI LU LI ST	⇒	LU ST LR LI
PC GB TE	PC	SI BL KI ST TE GB LR	GB	KI PC TE HT LR LU LI	TE	BL KI PC SP GB LR LU		PC GB TE LR PC GB TE KI
PC LR TE	PC	SI BL KI ST TE GB LR	LR	PC TE GB SI LU LI ST	TE	BL KI PC SP GB LR LU		PC LR TE GB
PC SI LR	PC	SI BL KI ST TE GB LR	SI	ST SP HT LR BL KI PC	LR	PC TE GB SI LU LI ST		PC SI LR ST
PC ST LR	PC	SI BL KI ST TE GB LR	ST	LR LU LI PC SP HT SI	LR	PC TE GB SI LU LI ST		PC ST LR SI
SI SP BL	SI	ST SP HT LR BL KI PC	SP	LU LI ST TE HT SI BL	BL	SP HT SI LU KI PC TE	⇒	SI SP BL HT
SI ST LR	SI	ST SP HT LR BL KI PC	ST	LR LU LI PC SP HT SI	LR	PC TE GB SI LU LI ST		SI ST LR PC
SI ST PC	SI	ST SP HT LR BL KI PC	ST	LR LU LI PC SP HT SI	PC	SI BL KI ST TE GB LR		SI ST PC LR
SP ST HT	SP	LU LI ST TE HT SI BL	ST	LR LU LI PC SP HT SI	HT	LI ST SP GB SI BL KI		SP ST HT LI SP ST HT SI
SP ST SI	SP	LU LI ST TE HT SI BL	ST	LR LU LI PC SP HT SI	SI	ST SP HT LR BL KI PC		SP ST SI HT

Fat: potential 4th balancing meridian of all three meridians

(c) The third step of the development of 4-meridian patterns. Potential 4th balancing meridian of all three-meridian and possible 4-meridian combinations

FIGURE 5: Continued.

4-meridian combinations
($n = 60$)

BL HT KI SI
BL KI PC SI
BL KI TE PC
BL LU TE SP
BL PC TE KI
BL SI KI HT
BL SI PC KI
BL SP TE LU
GB LI LR LU
GB LU LR TE
GB PC LR TE
GB TE LR PC
HT BL SI KI
HT GB KI LI
HT KI SI BL
HT LI GB KI
HT LI KI GB
HT SP BL SI
HT SP SI ST
HT ST SI SP
KI GB TE PC
KI LI GB HT
KI PC GB TE
KI PC TE GB
KI SI PC BL
LI HT SP ST
LI HT ST SP
LI LU ST SP
LI SP ST LU
LI ST LR LU
LU GB TE LR
LU LI GB LR
LU LI LR GB
LU LR TE GB
LU SP BL TE
LU SP LI ST
LU SP ST LI
LU SP TE BL
LU ST LR LI
PC GB TE LR
PC LR TE GB
PC SI LR ST
PC ST LR SI
SI SP BL HT
SI ST LR PC
SI ST PC LR
SP ST HT LI
SP ST SI HT
BL KI PC TE
BL SI KI PC
GB LU LR LI
GB TE LR LU
HT BL SI SP
HT SP SI BL
KI PC TE BL
LI LU ST LR
LI SP ST HT
LU LI LR ST
PC GB TE KI
SP ST HT SI

4-meridian combinations
after deletion of repetitions
($n = 15$)

LU LI ST LR
LU LI GB LR
HT SI ST SP
SI HT SP BL
PC TE GB LR
PC TE BL KI
LU LI ST SP
LU TE GB LR
LI HT SP ST
HT SI BL KI
SI PC KI BL
PC TE GB KI
LU TE BL SP
LI HT KI GB
PC SI ST LR

4-meridian combinations, arranged by meridian patterns
($n = 60 = 12 \times 5$)

LU LI ST LR	LU LI GB LR	LU LI ST SP	LU TE GB LR	LU TE BL SP
LI LU SP ST	LI LU LR ST	LI HT SP ST	LI LU LR GB	LI HT KI GB
ST SP HT LI	ST SP LU LI	ST SP HT SI	ST LR LU LI	ST LR PC SI
SP ST SI HT	SP ST LI HT	SP BL SI HT	SP ST LI LU	SP BL TE LU
HT SI BL SP	HT SI ST SP	HT SI BL KI	HT LI ST SP	HT LI GB KI
SI HT KI BL	SI HT SP BL	SI PC KI BL	SI HT SP ST	SI PC LR ST
BL KI PC SI	BL KI HT SI	BL KI PC TE	BL SP HT SI	BL SP LU TE
KI BL TE PC	KI BL SI PC	KI GB TE PC	KI BL SI HT	KI GB HT LI
PC TE GB KI	PC TE BL KI	PC TE GB LR	PC SI BL KI	PC SI ST LR
TE PC LR GB	TE PC KI GB	TE LU LR GB	TE PC KI BL	TE LU SP BL
GB LR LU TE	GB LR PC TE	GB LR LU LI	GB KI PC TE	GB KI HT LI
LR GB LI LU	LR GB TE LU	LR ST LI LU	LR GB TE PC	LR ST SI PC

(d) Fourth step of the development of 4-meridian patterns. Arrangement by meridian patterns and reduction to 15 by deletion of repetitions

FIGURE 5

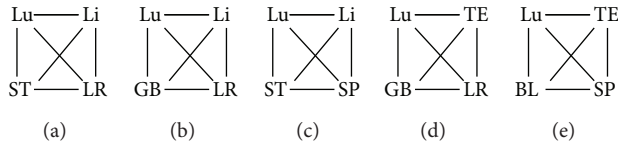


FIGURE 6: Possible patterns for balancing the LU-meridian.

TABLE 5: Possible patterns for an ideal balanced 4-meridian combination.

-1, x, +1, +2
-2, -1, x, +1
x, +1, +2, +3
x, -1, -2, -3
x, +3, 6, -3

x: the balanced meridian, plus: step in the CC clockwise, minus: step in the CC counterclockwise.

the CC. This is shown in Table 5, x is the meridian which is to be balanced; the numbers are the steps in CC, + means clockwise, and - means counterclockwise.

There are always only five ideal balanced options by applying treatment to the three not effected extremities and optionally to the effected meridian itself. So ideal balanced patterns can be plotted similar to Figure 3 with a left-right yin-yang balance and an up-down yin-yang balance. An example for the 5 patterns of the LU-meridian is shown in Figure 6. The pattern can also be plotted on the CC, as shown in Figure 7.

So every meridian can be balanced by 5 different patterns, but we find multiple overlapping. If we delete all repetitions, 15 patterns remain. This is shown as the fourth step of the development of 4-meridian patterns in Figure 5(d). These 15 patterns are plotted a left-right yin-yang-balance and an up-down yin-yang balance in Figure 8. Interestingly all patterns plotted in row 1 and 2 have a balance in two or three of the calculated systems, while all patterns in the third row have only a single balance in one of the above described systems (Table 4).

A graphical plotting, shown in Figure 9, shows that all patterns together build a symmetrical picture on the CC.

3.3. Research Protocol for Pain Relief in Localised Pain. Extremities include not only hand and arm or leg and foot, but as well parts of meridians on trunk, neck, or face of the meridian connected to and named by the extremity (hand or foot). The knowledge of finding the right balancing meridians is even more useful, if it is combined with the somatotopic knowledge of the *Image and Mirror Concept* for finding the right points and the right area on the chosen meridian. In combination, these two methods are extremely useful in the treatment of localized pain and can often produce immediate effects. For best results, first the affected meridian in the region of pain must be identified, then it is detected and treated using a corresponding meridian (according to Table 4) in a corresponding area on an unaffected extremity (according to Figure 4) and then the result is checked.

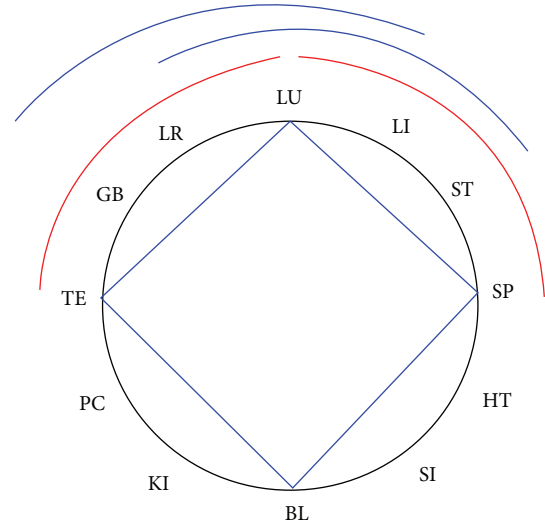


FIGURE 7: Graphical plotting of the 5 pattern for balancing the lung meridian on the Chinese Clock.

In case a change of symptoms but not yet complete pain reduction is found, a corresponding meridian on another extremity should be chosen and treated in the same way until a satisfactory result in the painful area is achieved. Table 6 summarizes the practical approach.

Even though possibilities of choice are listed in the protocol, different approaches lead to similar patterns and success rates. For the example of one pattern see the description in Figure 10.

3.4. Case Example. A 60-year-old carpenter worked overhead for a full day and developed severe shoulder pain. Pain was prominent on the dorsal head of his shoulder. Pain was increased by lateral lifting of the shoulder and by inward rotation of the arm. Pain could be exaggerated by pressure over the lateral scapula; muscles around this area were tight. The active range of movement of the right shoulder was reduced. The shoulder could only be laterally lifted to 50° due to severe pain.

The patient was asked to estimate the pain on a visual analog scale (VAS) from 1 to 10. He described his pain as 9/10 on VAS.

The Right SI-Meridian Was Identified as the Affected Meridian. The area of maximum pain was at point SI-10 (Naoshu) and 2 cun above and below this point. It was decided to start on the legs first and start with a Yang meridian. According to Table 4 the BL- and the ST-meridian are balancing Yang meridians of the SI-meridian. Turning Figure 2 to the IT-meridian, the ST-meridian is the third step from IT if you go clockwise and the BL-meridian is the first step from IT, if you go counterclockwise. These are the only possible yang meridians of the lower extremities. Applying concept on the lower extremities the region around the ankle, the hip region and the region above and below the knee are potentially somatotopic regions of treatment. The BL- and

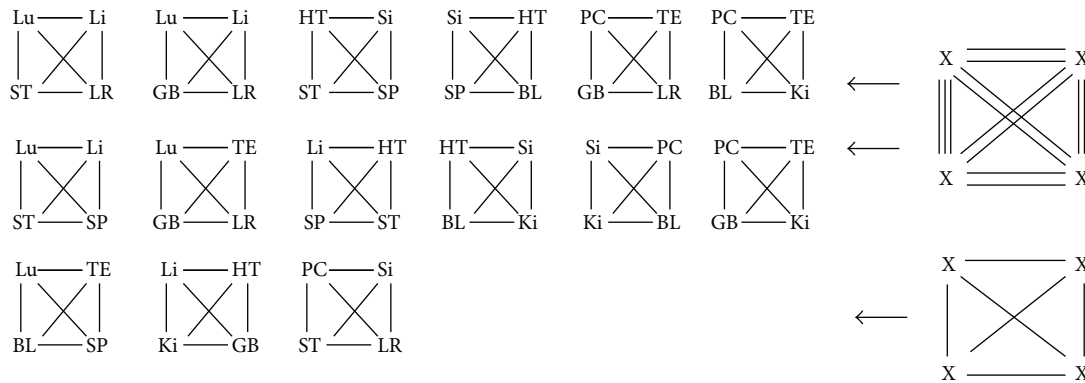


FIGURE 8: 15 ideally balanced patterns.

TABLE 6: Research protocol for immediate pain relief in localised pain.

- (1) Identify the affected meridian in the region of pain and ask the patient to characterize the pain on a visual analog scale (VAS) from 1 to 10.
- (2) Decide which unaffected extremity you want to treat first.
- (3) (a) *In the case that the chosen unaffected extremity is the contralateral arm of the painful arm or the contralateral leg of the painful leg, if the pain is on a yang meridian, the treatment has to applied to a yin meridian (or the other way around).*
 (b) If the pain is on the upper extremities, but the chosen unaffected extremity is a lower extremity (or the other way around), you can decide whether you treat yin or yang meridians first.
- (4) After the decision on which extremity should be treated and whether yin or yang meridians have to be used, look up in Table 4 which meridians are the balancing meridians to the affected meridian.
- (5) (a) Palpate the balancing meridians in a corresponding body region by image or mirror (according to Figure 4) for Ashi points, decide which balancing meridian (according to Table 4) has the most painful Ashi points. Repeat this with other corresponding body regions (according to Figure 4) and decide which is the most painful area.
 (b) If you have followed variant (3b) you have to repeat the examination on the contralateral side of arm or leg. Treatment has to be applied to the more painful side.
- (6) Treat the most painful balancing meridian in the most painful corresponding area. Treat this Ashi area. Insert a needle into the most painful Ashi point. Apply further needles in acupuncture or Ashi points, usually 1-2 proximal the first needle and 1-2 distal the first point on the acupuncture meridian. The number of needles is dependent on the extension of the painful area on the affected meridian.
- (7) Move the affected joint or palpate the original region for pain and ask the patient about a change of symptoms using VAS. In case of 100% pain reduction, don't apply further needles.
- (8) Palpate another non affected extremity on balancing meridians (according to Table 4) in a corresponding body region by image or mirror (according to Figure 4) for Ashi points. But you have to stay in a balance of yin and yang between the legs or the arms. Repeat this with other corresponding body regions and decide on the most painful area.
- (9) See 6.
- (10) See 7.
- (11) Palpate the remaining non affected extremity on balancing meridians (according to Table 4) while staying in the yin-yang-balance of the extremities in a corresponding body region by image or mirroring (according to Figure 4) for Ashi points. Repeat this with other corresponding body regions and decide on the most painful area.
- (12) See 6.
- (13) See 7.
- (14) If the pain relief is still not sufficient, treatment can also applied to the affected meridian itself. But local treatment of the affected area can often produce discomfort to the patient, so the best choices are points by imaging or mirroring of corresponding areas (according to Figure 4) along the affected meridian itself. Repeat this with other corresponding body regions and decide on the most painful area.
- (15) See 6.
- (16) See 7.

ST-meridian was palpated on both legs with a special focus on the somatotopic regions described above for Ashi points.

There was no region of pain on the ST-meridian. There were painful Ashi points on the BL-meridian, very mild above and below the knee but severe in the area of the ankle. The pain was much more prominent on the left side.

So It Was Decided to Treat the Left BL-Meridian. The maximum area of Ashi was at left BL-60 (Kunlun). A sterile 0.2 × 0.22 mm acupuncture needle was perpendicular inserted 0.5 cun at this point and short stimulated by reducing method. 2 other needles approximately 0.25 and 0.5 cun proximal and 2 other needles approximately 0.25 and 0.5 cun distal of BL-60 on the BL-meridian in the maximum area of Ashi were inserted and stimulated in a similar manner. The patient was asked to move his arm. He was able to lift it laterally up to an angle of 90°. Painful areas were palpated again. The patient estimated his pain as 5/10 on VAS.

Then we looked at the right leg for a yin meridian that balances the SI- and the BL-meridian. According to Table 4 the KI- and the SP-meridians were candidates. The KI-meridian is the first step clockwise of the BL-meridian as well as the second step clockwise of the SI-meridian. The SP-meridian is the third step counterclockwise of the BL-meridian as well as the second step of the SI-meridian. Applying *Image and Mirror concept* on the lower extremities we again palpated the KI- and SP-meridian for Ashi point in the region around the ankle, the hip region and the region above and below the knee. There was no region of pain on the KI meridian. There were painful Ashi points on the SP-meridian, very mild above and below the knee but severe in the area of the ankle.

So It Was Decided to Treat the Right SP-Meridian. The maximum area of Ashi was at left SP-5 (Shangqiu). A sterile 0.2 × 0.22 mm acupuncture needle was perpendicular inserted 0.2 cun at this point and suppletively stimulated. 2 other needles approximately 0.25 and 0.5 cun proximal and 2 other needles approximately 0.25 and 0.5 cun distal of SP-5 on the spleen meridian in the maximum area of Ashi were inserted and stimulated in a similar manner. The patient was asked to move his arm. He was able to lift it laterally up to an angle of 110°. Painful areas were palpated again. The patient estimated his pain as 3/10 on VAS.

Then we looked for a yin meridian on the left arm that balances SI, BL and SP. According to Table 4 this is only the HT-meridian. The HT-meridian is the first step counterclockwise of the SI-meridian as well as the second step counterclockwise of the BL-meridian as well as the first step clockwise of the SP-meridian.

So It Was Decided to Treat the Left HT-Meridian. We palpated the HT-meridian of the left arm according to Image and Mirror, searching for Ashi points in the area of the shoulder, the wrist and above and below the elbow. The HT-meridian on the shoulder had some mild Ashi points, but the major region of Ashi was around HT-3 (Shaohai). A sterile 0.2 × 0.22 mm acupuncture needle was obliquely inserted 0.2 cun at this point and suppletively stimulated. 2 other needles

approximately 0.25 and 0.5 cun proximal and 2 other needles approximately 0.25 and 0.5 cun on the HT-meridian were inserted and similarly stimulated.

The patient was asked to move his arm. He was able to lift it laterally up to an angle of 180°. Painful areas were palpated again. The patient estimated his pain as 1/10 on VAS.

Finally, the affected meridian itself was palpated according to image and mirror for Ashi points in the area of the wrist and above and below the elbow.

So It Was Decided to Treat the Affected SI-Meridian Itself. The major region of Ashi was around SI-5 (Yanggu). A sterile 0.2 × 0.22 mm acupuncture needle was perpendicularly inserted 0.3 cun at this point and stimulated by reducing method. 2 other needles were inserted approximately 0.25 and 0.5 cun proximally; one needle was inserted into SI-4 (Wangu) and another needle approximately 0.25 cun distal on the SI-meridian. They were then stimulated as described above.

The patient was asked to move his arm. He was still able to lift it laterally up to an angle of 180°. Painful areas were palpated again. The patient estimated his pain as less than 1/10 on VAS.

So in This Case the Pattern SI-HT-BL-SP Was Used. The patient was given an appointment for the following day. At this time he reported a relapse in the previous night. He estimated his pain as 4/10 on VAS. A similar treatment was applied. After treatment he again estimated his pain as less than 1/10 on VAS. The next day he had his third appointment. His pain had not returned and was reported as less than 1/10 on VAS. He again got a similar treatment on all non-effected extremities. After this no pain was reported any more. His shoulder showed full active and passive movement in all directions. So no extra treatment on the effected meridian was applied.

The patient stayed pain-free and returned to work.

4. Discussion

This paper is based on an analysis of the historically described balancing acupuncture systems found in historical writings and which have been recurrently described in modern textbooks. It uses a mathematical approach to calculate the theoretical options based on the historical systems as a first step. All these historical systems describe combinations of two meridians. They had been determined on the basis of empirical knowledge by generations of experts in Chinese Medicine. But while all the historical systems show a certain symmetry when plotted on the CC and while the order in the CC most likely put a distinct order due to anatomical reasons [11], the CC can be seen as a mathematically organized symmetric description of the three surfaces of the body (back, front, and medial/lateral) [11]. So a search, whether the historical systems offer a complete description of combinatorial possibilities, is only rational. The historically established systems for combining meridians cover many, but not all, of our calculated combinations of meridians. So our mathematical approach offers theoretically calculated

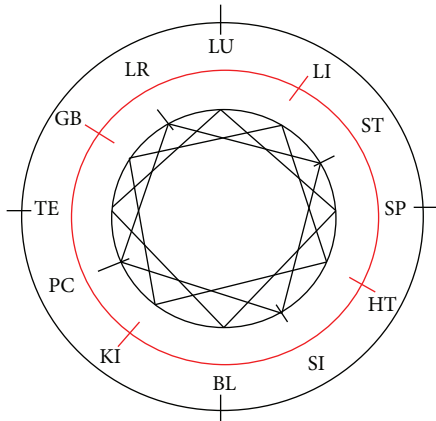


FIGURE 9: Graphical plotting on the Chinese Clock of 15 ideally balanced patterns.

supplementary information to the wisdom of generations of physicians, leading to 7 balancing options for every meridian.

Balancing yin and yang is a basic concept in Chinese medical theory and a basis for acupuncture treatment [1–3]. There is a risk of losing this balance, if the acupuncture plan involves more than two meridians. So as a second step we calculated the option for a balanced acupuncture treatment scheme with more than 2 meridians. Balancing up and down, left and right, and front and back has a long tradition in TCM based on the *Suwen* [23], and the human body has four extremities, we decided to calculate the mathematical options to gain an ideal balance for 4 meridians. An ideal balance means that every chosen meridian balances all other meridians.

All these approaches, determined by way of a mathematical search for combinatorial possibilities is based on theoretical considerations from historical writings and supported by empirical knowledge.

Our observations do not have to be considered as being the only concept in acupuncture. There are more possibilities like balancing yin and yang meridians on one extremity, applying bilateral treatment of the same meridian, there are microsystems like scalp and ear acupuncture, as well as empirically determined point combinations, that do not follow the concept of balancing [29, 40, 41].

But the concept of a balanced treatment has a long tradition in TCM and in the historical writings [23], so we consider it to be a rational basis for logical and reproducible acupuncture strategies.

The authors' experience of achievement of immediate effects in pain management by application of this protocol leads to the question of the mechanisms involved. Acupoints on very distant parts of the body, in some cases even with a completely different segmental innervation in the spinal column, can induce a therapeutic effect on local pain. This contradicts the theory that the main effect of acupuncture treatment is due to peripheral or segmental effects [42–44], so our experience supports the idea of other authors that higher-level central pathways play a central role in pain-releasing

effects of acupuncture [45, 46]. But it has to be considered, that this protocol is only based on theoretical reflections and has to be approved in clinical studies.

Interestingly, there are 5 ideally balanced acupuncture patterns for every meridian. Four of them represent a balance that is found in 2 or 3 of the above calculated systems for every meridian pair (Table 2). These patterns are four neighbours in a row in the Chinese Clock.

In one pattern every balance derives from only one system in Table 2. It combines every third step in the CC. Further research has to be done to determine whether the different patterns represent typical clinical conditions and whether the one pattern with the single balance between 2 meridians represents an exceptional treatment option.

Some schools describe rules whereby it is necessary to combine points by one of the above described systems on the contralateral or ipsilateral side, but no explanations are given [30–32]. Mathematically, at least for the calculated 4-point ideally balanced pattern, it could be either ipsilateral or contralateral retention of the balance. According to our experience in the treatment of localised pain you have to palpate bilaterally for Ashi. The more sensitive area leads to the decision for contralateral or ipsilateral treatment.

Due to multiple overlapping of the 5 patterns for each meridian there only exist a total of 15 distinct patterns for all meridians. Pattern diagnosis has a long tradition in TCM. Syndromes or patterns are described as Zheng diagnosis [47]. TCM Zheng describes major patterns of vegetative disharmonies which are identified by using a comprehensive analysis of clinical information from four main diagnostic TCM methods: observation, listening, questioning, and pulse analysis [48].

Modern research on Zheng diagnosis is devoted to the search for a correlation between Zheng patterns and system biology parameters [48–50].

Further investigation of the correlation of the described ideally balanced acupuncture patterns and the Zheng patterns might lead to an improvement of clinical treatment. The 5 patterns for every meridian described above and the reduction to 15 patterns for all meridians due to overlapping might explain the overlapping of Zheng patterns, resulting in similar patterns to different diseases as well as different patterns for similar diseases [51].

Even though pain has been the focus of most clinical research on acupuncture [52], there are no controlled studies with hard data on the effect of balanced 4-point or meridian combinations in pain research so far. This is a necessity for future trials. By transferring this theoretical consideration into research we have been describing an empirical systematic approach for the achievement of immediate effects in the treatment of localised pain. This can be used as a research protocol for future trials as well as a treatment protocol. While it is a protocol for immediate effects, studies can be cost effective because it can reduce the number of treatments to one.

Acupuncture treatment based on TCM usually requires an individual diagnosis which leads to an individual treatment strategy [29]. This approach is in some aspects con-

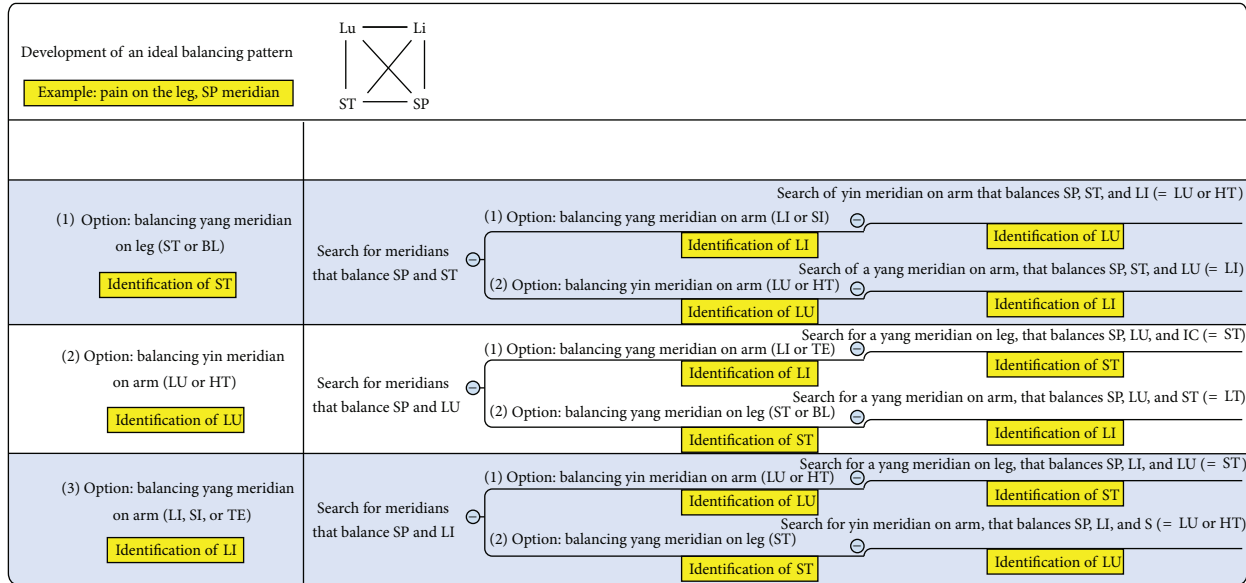


FIGURE 10: Development of an ideal balance pattern.

tradictory to controlled clinical trials in which treatment procedures are usually uniform. Trials with individual treatments are often considered to be less scientific. This is a severe problem for the design of studies on TCM treatments and an obstacle for publication in highly ranked journals. Otherwise TCM experts criticise that controlled trials do not reflect the practice of acupuncture. In controlled trials often no diagnostic framework is applied resulting in a lack of individualisation to address specific TCM imbalances and symptoms [53].

Our protocol potentially solves this problem because it offers a rational, reproducible procedure independent of examiner experience, but the resulting treatment procedure is an individual. This has many advantages. The necessary acupuncture pattern is developed during examination. The pattern of treatment is not fixed before treatment, so probands of the treatment group are not at risk, to get an ineffective treatment for their condition. While the treatment is developed in a rational examination process, the probands will have a good chance to get a corresponding treatment to their body reaction. This will increase the efficacy of the treatment procedures. Anyhow limitation of this protocol are, that it is only based on theoretical consideration and personal experience of the authors. It has to be further approved in clinical trials.

In addition to the test of the efficacy of acupuncture in pain management, information on patterns can be gained in studies following our research protocol.

This might increase the knowledge as to which acupuncture patterns are most sufficient under which clinical conditions and lead to improved treatment strategies as well as to results that help increase the knowledge on the mechanisms of acupuncture.

5. Conclusion

With this systematic description of a mathematical model for the calculation of combinatorial possibilities of meridians as well as the calculation of ideally balanced patterns we describe a theoretical model applicable for acupuncture research and treatment. By sharing our protocol for immediate effects in localized pain treatment we offer researchers a protocol for controlled acupuncture trials with an individualized approach based on historical knowledge. Further research has to approve this theoretical approach and might have influence on understanding mechanism of pain relief in acupuncture. By this approach, theoretical and empirical knowledge is organized into a systematic approach.

Disclosure

This study was not supported by any grant.

References

- [1] G. Soulié de Morant, *Chinese Acupuncture*, Paradigm Publications, Brookline, Mass, USA, 1994.
- [2] Y. Manaka, K. Itaya, and S. Birch, *Chasing the Dragon's Tail: The Theory and Practice of Acupuncture in the Work of Yoshio Manaka*, Paradigm Publications, Brookline, Mass, USA, 1995.
- [3] P. Unschuld, *HuAng Di Nei Jing Su Wen, Nature, Knowledge, Imagery in an Ancient Chinese Medical Text*, Berkeley, Calif, USA, University of California Press edition, 2003.
- [4] J. Zhang, *Clinical Application of Pair Point*, Jiangsu Science and Technology Press, 2008.
- [5] A. Ellis, N. Wiseman, and K. Boss, *Fundamentals of Chinese Acupuncture*, Paradigm Publications, Brookline, Mass, USA, 1991.

- [6] X. Cheng, *Chinese Acupuncture and Moxibustion*, Foreign Language Press, 1999.
- [7] Beijing College of Traditional Chinese Medicine, *Essentials of Chinese Acupuncture*, Foreign Language Press, Beijing, China, 2011.
- [8] S. H. Jiang and X. Lou, *Chinese Acupuncture and Massage*, People's Medical Publishing House, Beijing, China, 2004.
- [9] J. P. Zhao, *Chinese Medicine Study Guide: Acupuncture and Moxibustion*, People's Medical Publishing House, Beijing, China, 2007.
- [10] J. Zhang, B. X. Zhao, and X. L. Lao, *Acupuncture and Moxibustion*, People's Medical Publishing House, Beijing, China, 2011.
- [11] S. Schroeder, S. Epplée, J. Zhang, G. Meyer-Hamme, T. Friedemann, and W. Hu, "Mathematical reflections on acupoint combinations in the traditional meridian systems," *Evidence-Based Complementary and Alternative Medicine*, vol. 2012, Article ID 268237, 10 pages, 2012.
- [12] M. Porkert, *Theoretical Foundations of Chinese Medicine: Systems of Correspondence*, MIT Press, Boston, Mass, USA, 1978.
- [13] P. Unschuld, *The Classic of Difficulties (Nanjing)*. Anonymus, Han, University California Press, Los Angeles, Calif, USA, 1996.
- [14] J. Y. Zhang, *Illustrated Supplementary to the Classified Canon (Lei Jing Tu Yi)*, 1624, People's Health Press, Beijing, China, 1965.
- [15] Z. J. Zhang, Y. Feng, N. Wiseman, C. Mitchell, and Y. Feng, *On Cold Damage (Shang Han Lun)*, Translation & Commentaries, Blue Poppy Press, Boulder, Colo, USA, 2000.
- [16] H. Q. Dou, *Guide to Classical Acupuncture (Zhen Jing Zhi Nan)*, People's Medical Publishing House, Beijing, China, 1983.
- [17] H. F. Mi, *The Systematic Classic of Acupuncture and Moxibustion (Zhen Jiu Jia Yi Jing)*, Blue Poppy Press, Boulder, Colo, USA, 1993.
- [18] M. Shima and C. Chase, *The Channel Divergences*, Blue Poppy Press, Boulder, Colo, USA, 2005.
- [19] Y. Li, "5-Zang extra relationship-theory," in *Introduction To Medicine (Yi Xue Ru Men)*, L. Ting, Ed., vol. 1575, Zang Fu Depth chapter, Tianjin Science and Technology Press, Tianjin, China, 1999.
- [20] G. Wu, *The Glorious Anthology of Acupuncture and Moxibustion (Zhen Jiu Ju Ying)*, *Ode of the Jade Dragon (Yu LongFu)*, vol. 1529, Shanghai Science and Technology Press, Shanghai, China, 1961.
- [21] G. Wu, *The Glorious Anthology of Acupuncture and Moxibustion (Zhen Jiu Ju Ying)* *Song of Points For Miscellaneous Diseases (Za Bing Xue Fa Ge)*, vol. 1529, Shanghai Science and Technology Press, Shanghai, China, 1961.
- [22] G. Wu, *The Glorious Anthology of Acupuncture and Moxibustion (Zhen Jiu Ju Ying)* *Ode of One Hundred Symptoms (Bai Zheng Fu)*, vol. 1529, Shanghai Science and Technology Press, Shanghai, China, 1961.
- [23] A. C. Dun, *The Yellow Emperor's Inner Classic, Spiritual Pivot (Huang Di Nei Jing Su Wen Jiao Zhu Yu Yi)*, Tianjin Science and Technology Press, Tianjin, China, 1989.
- [24] J. Z. Yang, *The Great Compendium of Acupuncture and Moxibustion (Zhen Jiu Da Cheng)*, vol. 1601, Hong Ye Shu Publishing, Taiwan, China, 1967.
- [25] Z. Z. Wang, *The Classic of Supplementing Life with Acupuncture and Moxibustion (Zhen Jiu Zi Sheng Jing)*, vol. 1220, CIREC, 2006.
- [26] S. M. Sun, *Thousand Ducat Formulas (Qian Jin Yao Fang)*, vol. 652, People's Medical Publishing House, Beijing, China, 1955.
- [27] C. T. Liu, Z. C. Liu, and H. Ka, *A Study of Daoist Acupuncture & Moxibustion*, Blue Poppy Enterprises, 1999.
- [28] X. Cheng, *Chinese Acupuncture and Moxibustion*, Foreign Language Press, Beijing, China, 1987.
- [29] J. H. Greten, *Kursbuch Traditionelle Chinesische Medizin*, Thieme, Stuttgart, Germany, 2nd edition, 2007.
- [30] R. . Tan, *Dr. Tan's Strategy of Twelve Magical Points*, Printing, San Diego, California, USA, 2002.
- [31] J. A. Spears, *Meridian Circuit Systems: A Channel Based Approach to Pattern Identification*, vol. 1, CreateSpace, North Charleston, SC, USA, 2010.
- [32] H. G. Ross and F. S. Winarto, *Die Balance-Methode in der Akupunktur: Eine Anleitung zur Schmerztherapie mit Syndromen und Fallbeispiele*, Müller und Steinecke, Munich, Germany, 2010.
- [33] R. Tan, Acupuncture 1, 2, 3 for back pain, elotus update, 2008, <http://www.elotus.org/>.
- [34] S. Y. Li and J. S. Zhao, "Evolution of the connotation of meridians viewed from the changes in the traveling routes: considerations induced from the "eleven meridians" to the "twelve regular meridians," *Zhen Ci Yan Jiu*, vol. 34, no. 2, pp. 132–135, 2009.
- [35] K. Matsumoto and S. Birch, *Extraordinary Vessels*, Paradigm Publications, Brookline, Mass, USA, 1986.
- [36] G. Wu, *The Glorious Anthology of Acupuncture and Moxibustion (Zhen Jiu Ju Ying)*, vol. 1529, Shanghai Science and Technology Press, Shanghai, China, 1961.
- [37] W. C. Young and J. Dong, *Tung's Acupuncture-Elucidation of Tung's Extra Points*, Chih-Yuan Book Store, Taipei, Taiwan, 2005.
- [38] R. P. Dhond, N. Kettner, and V. Napadow, "Neuroimaging acupuncture effects in the human brain," *Journal of Alternative and Complementary Medicine*, vol. 13, no. 6, pp. 603–616, 2007.
- [39] A. Nakagoshi, M. Fukunaga, M. Umeda, Y. Mori, T. Higuchi, and C. Tanaka, "Somatotopic representation of acupoints in human primary somatosensory cortex: an FMRI study," *Magnetic Resonance in Medical Sciences*, vol. 4, no. 4, pp. 187–189, 2005.
- [40] J. Ross, *Acupuncture Point Combinations—The Key to Clinical Success*, Churchill Livingstone, Edinburgh, UK, 1995.
- [41] R. A. Feeley, *Yamamoto New Scalp Acupuncture—Principles and Practice*, Thieme, Stuttgart, Germany, 2011.
- [42] E. D. Al-Chaer, N. B. Lawand, K. N. Westlund, and W. D. Willis, "Pelvic visceral input into the nucleus gracilis is largely mediated by the postsynaptic dorsal column pathway," *Journal of Neurophysiology*, vol. 76, no. 4, pp. 2675–2690, 1996.
- [43] E. D. Al-Chaer, N. B. Lawand, K. N. Westlund, and W. D. Willis, "Visceral nociceptive input into the ventral posterolateral nucleus of the thalamus: a new function for the dorsal column pathway," *Journal of Neurophysiology*, vol. 76, no. 4, pp. 2661–2674, 1996.
- [44] E. D. Al-Chaer, K. N. Westlund, and W. D. Willis, "Nucleus gracilis: an integrator for visceral and somatic information," *Journal of Neurophysiology*, vol. 78, no. 1, pp. 521–527, 1997.
- [45] E. Samsó, N. E. Farber, J. P. Kampine, and W. T. Schmeling, "The effects of halothane on pressor and depressor responses elicited via the somatosympathetic reflex: a potential antinociceptive action," *Anesthesia and Analgesia*, vol. 79, no. 5, pp. 971–979, 1994.
- [46] A. Sato and R. F. Schmidt, "Somatosympathetic reflexes: afferent fibers, central pathways, discharge characteristics," *Physiological Reviews*, vol. 53, no. 4, pp. 916–947, 1973.

- [47] M. Jiang, C. Zhang, G. Zheng et al., "Traditional Chinese medicine Zheng in the era of Evidence-Based Medicine: a literature analysis," *Evidence-Based Complementary and Alternative Medicine*, vol. 2012, Article ID 409568, 9 pages, 2012.
- [48] A. Lu, M. Jiang, C. Zhang, and K. Chan, "An integrative approach of linking traditional Chinese medicine pattern classification and biomedicine diagnosis," *Journal of Ethnopharmacology*, vol. 141, no. 2, pp. 549–556, 2012.
- [49] T. Ma, C. Tan, H. Zhang, M. Wang, W. Ding, and S. Li, "Bridging the gap between traditional Chinese medicine and systems biology: the connection of Cold syndrome and NEI network," *Molecular BioSystems*, vol. 6, no. 4, pp. 613–619, 2010.
- [50] T. Wu, M. Yang, H. F. Wei, S. H. He, S. C. Wang, and G. Ji, "Application of metabolomics in traditional Chinese medicine differentiation of deficiency and excess syndromes in patients with diabetes mellitus," *Evidence-Based Complementary and Alternative Medicine*, vol. 2012, Article ID 968083, 11 pages, 2012.
- [51] Guo, S. Yu, Y. Guan et al., "Molecular mechanisms of same TCM syndrome for different diseases and different TCM syndrome for same disease in chronic hepatitis B and liver cirrhosis," *Evidence-Based Complementary and Alternative Medicine*, vol. 2012, Article ID 120350, 9 pages, 2012.
- [52] A. J. Vickers, A. M. Cronin, A. C. Maschino et al., "Individual patient data meta-analysis of acupuncture for chronic pain: protocol of the acupuncture trialists' collaboration," *Trials*, vol. 11, article 90, 2010.
- [53] B. J. Anderson, F. Haimovici, E. S. Ginsburg, D. J. Schust, and P. M. Wayne, "In vitro fertilization and acupuncture: clinical efficacy and mechanistic basis," *Alternative Therapies in Health and Medicine*, vol. 13, no. 3, pp. 38–48, 2007.

Research Article

The Neural Pathway of Reflex Regulation of Electroacupuncture at Orofacial Acupoints on Gastric Functions in Rats

Jianhua Liu,^{1,2} Wenbin Fu,¹ Wei Yi,² Zhenhua Xu,¹ and Nenggui Xu^{1,2}

¹Laboratory of Electrophysiology, The Secondary Medical College, Guangzhou University of Traditional Chinese Medicine, Guangzhou 510120, China

²Key Laboratory of Acupuncture of Guangdong Province, Guangzhou University of Traditional Chinese Medicine, Guangzhou 510006, China

Correspondence should be addressed to Nenggui Xu, ngxu8018@gzhtcm.edu.cn

Received 21 August 2012; Revised 14 December 2012; Accepted 16 December 2012

Academic Editor: Ying Xia

Copyright © 2012 Jianhua Liu et al. This is an open access article distributed under the Creative Commons Attribution License, which permits unrestricted use, distribution, and reproduction in any medium, provided the original work is properly cited.

Acupuncture has a reflex regulation in gastrointestinal functions, which is characterized with segment. In the present study, the neural pathway of electroacupuncture (EA) at orofacial acupoints (ST2) on gastric myoelectric activity (GMA) in rats was investigated. The results indicated that EA at ST2 facilitated spike bursts of GMA, which is similar to EA at limbs and opposite to EA at abdomen. The excitatory effect was abolished by the transaction of infraorbital nerves, dorsal vagal complex lesion, and vagotomy, respectively. In addition, microinjection of L-glutamate into the nucleus of the solitary tract (NTS) attenuated the excitatory effect. All these data suggest that the dorsal vagal complex is involved in the reflex regulation of EA at orofacial acupoints on gastric functions and NTS-dorsal motor nucleus of the vagus (DMV) inhibitory connections may be essential for it.

1. Introduction

Acupuncture has been applied in the clinic to treat gastrointestinal (GI) diseases for thousands of years in China and Zusanli acupoint (ST36) is viewed as a classic acupoint in treating GI diseases in the textbook of Traditional Chinese Medicine. Recently, numerous clinical and experimental studies have shown that acupuncture is effective in treating GI disorders and regulating GI functions, including gastric motility, gastric acid secretion, and gastric myoelectric activity (GMA) [1–7]. It is noteworthy that, however, acupuncture at different regions induces different effects. For example, acupuncture at limbs enhances GI motility via vagal efferents [2, 3, 7], and acupuncture at the abdomen inhibits GI motility via sympathetic efferents [4], suggesting that the reflex regulation of acupuncture on GI tract is characterized with segment. In these studies, investigators notice that supraspinal structures are involved in this process and dorsal vagal complex (DVC) may be an important candidate [1, 2, 4]. In our previous works, electroacupuncture (EA) at ST36 or orofacial acupoints promote GMA and induce c-fos expression in the nucleus of the solitary tract (NTS)

[2, 8, 9]. Meanwhile, electrophysiological data show that there are convergent neurons of somatoviscera in the NTS simultaneously reactive to acupuncture stimuli and gastric distension [10]. It seems that DVC may be a major target of acupuncture in the regulation of gastric functions.

The DVC consists of the NTS, which receives primary afferent input from the GI tract, and the dorsal motor nucleus of the vagus (DMV), which contains the efferent vagal motor neurons innervating the GI tract. Therefore, the DVC is considered as a parasympathetic preganglionic center in the regulation of GI functions. Anatomical and electrophysiological data demonstrate the existence of excitatory and inhibitory synaptic connections between the NTS and DMV. However, most studies are focused on the inhibitory connections, in which excitation of NST neurons produces inhibition of postsynaptic neurons in the DMV projecting to the GI tract and influences output of the vagus nerves [11–16]. Therefore, the connections, especially inhibitory connections, may play an important role in the regulation of GI functions.

SiBai (ST2) is located on the stomach meridian, which is mainly used to treat eye and GI diseases [17]. YangBai

(GB14), as a control, is located on the urinary bladder meridian, which is mainly applied to treat headache and eye diseases [17]. In the present study, reflex regulation of EA at orofacial acupoints (ST2 and GB14) on GMA in rats and its neural pathway are investigated to clarify the underlying mechanism of EA on GI tract.

2. Experimental Procedure

2.1. Experimental Design. The study was divided into five parts: (1) to observe the effect of EA at ST2, which is located in the infraorbital foramen, on GMA. At the meanwhile, GB14, which is located in the forehead and 2.5 cm directly above the pupil, were chosen as the control. (2) To investigate the afferent pathway of EA at ST2 on GMA by transection of the infraorbital nerves (ION). (3) To study the role of DVC in the EA effect following lesion of the DVC. (4) To explore the effect of microinjection of L-glutamate into the NTS on EA effects. (5) To observe the efferent pathway of EA effects by vagotomy.

2.2. Animals. Adult Sprague-Dawley rats of both sexes, weighing from 220 to 250 g, were used in this study. Each rat was housed in controlled environmental conditions ($25 \pm 1^\circ\text{C}$, relative humidity 40–60%, a 12 h/12 h light-dark cycle from 7:00 am to 19:00 pm), with access to food and water ad libitum. The procedures were performed in accordance with guidelines of Guangzhou University of Traditional Chinese Medicine for Care and Use Committee of Research Animals.

2.3. Implantation of Gastric Electrodes. The surgical procedure was similar to what was previously reported [2]. After an overnight fast, the animal was anesthetized with urethane (1 g/kg, i.p.) and laparotomy was made to expose the stomach. One 2-mm-long ring platinum electrode was sutured to the serosal surface on the anterior wall of the gastric antrum, about 0.5 cm proximal to the pyloric sphincter, and the other about 1.5 cm distal to that. Wires connecting with electrodes were brought out on the scruff of the neck through a subcutaneous tunnel. Finally the abdominal cavity was closed.

2.4. Recording of GMA. Recording of GMA was performed as previously described [2]. The experiment was initiated after the rats were given about 5 days to recover completely from the surgery. All rats were fasted for 24 hours before the experiment and anesthetized with urethane (1 g/kg, i.p.). The low and high cutoff frequency of the amplifier was 10 Hz and 30 Hz, respectively, and both slow waves and spike bursts superimposed in the slow waves were continuously recorded for at least 10 min.

2.5. Transection of ION. ION pretreatment was performed five days before EA at ST2. The animals were anesthetized by an i.p. injection of urethane (1 g/kg.). A vertical incision was made in the skin overlying the infraorbital foramen to expose bilateral ION under a dissecting microscope. For

the transection of ION ($n = 6$), the exposed ION was ligated at two separate points with silk suture, and the nerve bundle between two ligatures was transected. For the sham operation ($n = 6$), the ION were only exposed and did not receive any treatment.

2.6. Lesion of the DVC. Rats ($n = 6$) were anaesthetized with urethane (1 g/kg, i.p.) and were mounted in the stereotaxic apparatus (SR-6N, Narishige, Japan) in the prone position. The atlanto-occipital membrane and cerebellum were removed to expose the dorsal medulla. Obex is defined as the point between the area postrema and calamus scriptorius, where the central canal starts to open into the fourth ventricle [18]. Using this as the reference point, the insulating tungsten electrode was inserted into the DVC and 2 mA cathode current was applied for 10 s. Coordinates of the DVC are 0.5–0.7 mm rostral to the obex, 0.5 mm lateral to the midline bilaterally and 0.4 mm dorsal to the brainstem surface [18]. For the sham lesion ($n = 6$), electrodes were inserted into the same location without current.

2.7. Microinjection of L-Glutamate into the NTS. Rats ($n = 6$) were anaesthetized with urethane and the dorsal medulla was exposed as described above. Before EA at ST2, L-Glutamate (5 nmol/50 nl) (Sigma, USA) was microinjected into the NTS (coordinates: 0.5–0.7 mm rostral to the obex, 0.5 mm lateral to the midline bilaterally and 0.3–0.4 mm dorsal to the brainstem surface). Normal saline was microinjected in the same location as a control ($n = 6$).

2.8. Vagotomy. Prior to EA stimulation, rats ($n = 6$) were anaesthetized with urethane (1 g/kg, i.p.) and pretreated with vagotomy. Bilateral vagus nerves (VN) around the esophagus near the cardia were carefully isolated from the surrounding tissues and ligated at two separate points with silk suture, and the nerve bundle between two ligatures was transected. For the sham operation ($n = 6$), VN were only exposed and did not receive any treatment.

2.9. EA Treatment. Rats were anaesthetized with urethane (1 g/kg, i.p.) and immobilized in a plastic box. Two stainless acupuncture needles (0.28 mm outer diameter) were subcutaneously inserted 5 mm into the ST2 or GB14 acupoints on each side, and were left for 20 min. The electrical stimulation was from a medical EA apparatus (Model G6805-2, Shanghai, China). The stimulation parameters were a frequency of 2 and 20 Hz, alternatively, and intensity strong enough to only elicit slight twitches of the orofacial areas. ST2 and GB14 are located in the infraorbital foramen and 2.5 cm directly above the pupil on the forehead, respectively [19].

2.10. Histology. At the end of microinjection, the microinjection site was marked by injecting 50 nl of 2% pontamine sky blue. The rats were then perfused through the ascending aorta, with 100 ml of normal saline followed by 400 ml of 4% paraformaldehyde. The brainstem was removed and post-fixed in the same fixative solution for 6–8 h and soaked overnight in 20% sucrose solution. 40 μm frozen transverse

sections were obtained at -20°C by a freezing microtome (CM1850, Leica, Germany). Finally, brainstem sections were stained with neutral red to determine placement of micropipette by microscope.

For the lesion of DVC, the rats were perfused and fixed as described above, and frozen transverse sections were treated by hematoxylin-eosin (HE) staining to identify the location of lesion under microscope.

2.11. Statistic Analysis. Data were presented as mean \pm standard error of the mean (SEM) and the significance level was set at $P < 0.05$. The results were analyzed using the paired-samples or independent-samples t test. In case of abnormal distribution or heteroscedasticity, the results were treated by nonparametric tests (Mann-Whitney U).

3. Results

3.1. Effects of EA at Orofacial Acupoints on GMA. EA at ST2 produced a significant increase in the number of cluster of spike bursts per minute (4.50 ± 0.99 versus 7.00 ± 0.82 , $P < 0.05$); however EA at GB14 did not (5.17 ± 0.87 versus 5.00 ± 0.93 , $P > 0.05$). Changes of spike bursts following EA at ST2 was significantly higher than that of EA at GB14 (1.33 ± 0.21 versus 0.17 ± 0.48 , $P < 0.05$) (Figure 1).

3.2. Effects of ION Transaction on GMA Induced by EA. After transaction of ION, EA at ST2 did not produce any change in the GMA (5.00 ± 0.58 versus 5.67 ± 0.55 , $P > 0.05$). In the sham-operated group, EA at ST2 induced remarked increase in the spike bursts (4.83 ± 0.95 versus 7.17 ± 1.31 , $P < 0.05$), which was similar to the change following EA at ST2 alone. Changes of the spike bursts following ION transaction was obviously lower than that in the sham operated group (0.67 ± 0.33 versus 2.33 ± 0.67 , $P < 0.05$) (Figure 2).

3.3. Effects of Lesion of DVC on GMA Induced by EA. Following electrical lesion of the DVC, EA at ST2 had no any effect on the spike bursts (4.50 ± 0.99 versus 3.83 ± 0.48 , $P > 0.05$). In the sham lesion group, EA at ST2 produced significant increase in the number of spike bursts (4.17 ± 0.60 versus 5.83 ± 0.87 , $P < 0.01$). Changes of the spike bursts following lesion of DVC was obviously lower than that in the sham lesion group (0.67 ± 0.42 versus 1.67 ± 0.33 , $P < 0.05$) (Figure 3).

3.4. Effects of Microinjection of Glutamate into the NTS on GMA Induced by EA. Pretreatment of microinjection of L-glutamate into the NTS, EA at ST2 did not induce remarkable changes in the spike bursts (5.67 ± 0.92 versus 5.16 ± 0.91 , $P > 0.05$), which lasted for about 5–10 min. Normal saline microinjection had no effects on changes in the spike bursts elicited by EA at ST2 (5.17 ± 1.40 versus 9.33 ± 1.41 , $P < 0.05$). Histology showed that all microinjections were located within the NTS. Changes of the spike bursts following microinjection of glutamate into the NTS was obviously lower than that in the saline microinjection (0.50 ± 0.56 versus 1.83 ± 0.87 , $P < 0.05$) (Figure 4).

3.5. Effects of Vagotomy on GMA Induced by EA. After bilateral vagotomy, EA at ST2 had no effect on the spike bursts (5.33 ± 1.26 versus 5.83 ± 1.70 , $P > 0.05$). Sham operation did not influence the excitatory effects on GMA induced by EA at ST2 (4.17 ± 0.79 versus 6.67 ± 1.12 , $P < 0.01$). Changes of the spike bursts following vagotomy was obviously lower than that in sham. Changes of the spike bursts following microinjection of glutamate into the NTS was obviously lower than that in the saline microinjection operation (0.50 ± 0.67 versus 2.50 ± 0.5 , $P < 0.05$) (Figure 5).

3.6. Histology. A diagrammatic representation of electrolytic lesion of DVC and microinjection sites into the NTS is shown in Figures 6 and 7, respectively.

4. Discussion

It is well known that somatic inputs from skin and/or muscle induce changes in autonomic functions, which is called somato-autonomic reflex and characterized with segment. In anesthetized rats, pinching abdominal skin inhibits gastric motility and pinching limbs enhances gastric motility [20–22]. As one type of somatic stimuli, acupuncture has similar effects. Acupuncture at abdomen and lower chest inhibits gastric motility via sympathetic efferents, while acupuncture at limb facilitates the gastric motility via vagal efferents [4, 23]. Furthermore, EA at limb accelerates gastric emptying and enhance GMA in human and/or animals, which are also mediated by vagus nerve [6, 24]. In the present study, EA at orofacial acupoints (ST2) produce an increase in the number of cluster of spike bursts of GMA, which is abolished following bilateral vagotomy. GI motility is under the control of GMA, which is composed of slow waves (slow rhythmicity) and spikes (fast rhythmicity). The slow wave determines the frequency and propagation of gastrointestinal contractions and spike activities are superimposed on the slow waves and are electrical counterpart of contractions. GI contractions always occur when spikes are present. Therefore, EA at orofacial acupoints (ST2) produce excitatory effects on gastric motility and the vagus nerve is involved in the process, which is similar to EA at limbs and opposite to EA at abdomen, suggesting that both reflex regulation of acupuncture on gastric functions and the specific relationship between acupoints and viscera is characterized with segment.

In the study, the excitatory effect of EA at ST2 on the GMA is abolished by ION transaction, DVC lesion and vagotomy, respectively, suggesting that the neural pathway comprised by ION-DVC-VN is essential for this response. ST2 is located in the infraorbital foramen and innervated by infraorbital nerves, which have no direct projections to the DVC. Our previous works indicate that EA at ST2 induce c-fos expression in the NTS and inhibit visceral pain in rats, which is mediated by paratrigeminal nucleus and abolished by ION transaction [8, 9]. As a parasympathetic preganglionic center, DVC play an important role in the modulation of EA on GI functions. Anatomical evidence demonstrates that somatic afferents induced by EA at ST-36

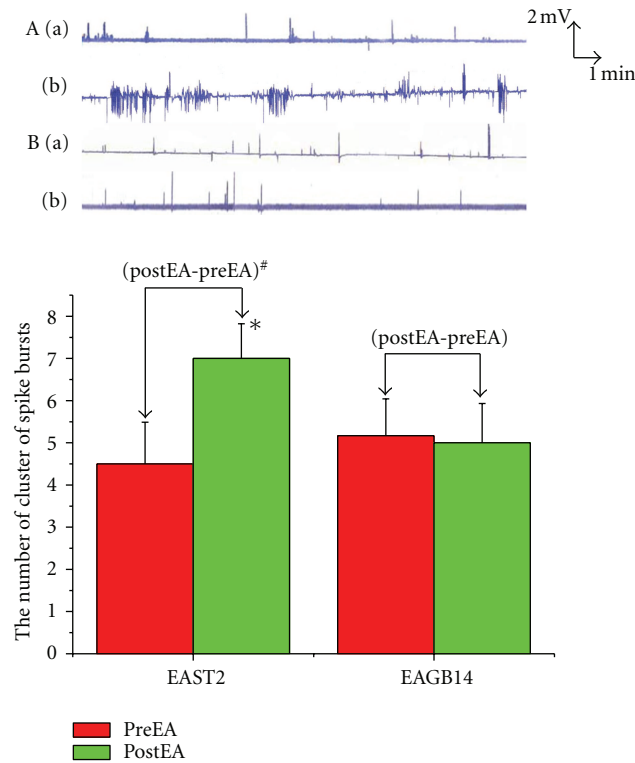


FIGURE 1: : Effects of EA at orofacial acupoints on GMA. * $P < 0.05$ versus preEAST2. # $P < 0.05$ versus (postEA-preEA) EAGB14. (A) EA at ST2 group; (B) EA at GB14 group. (a) PreEA; (b) postEA.

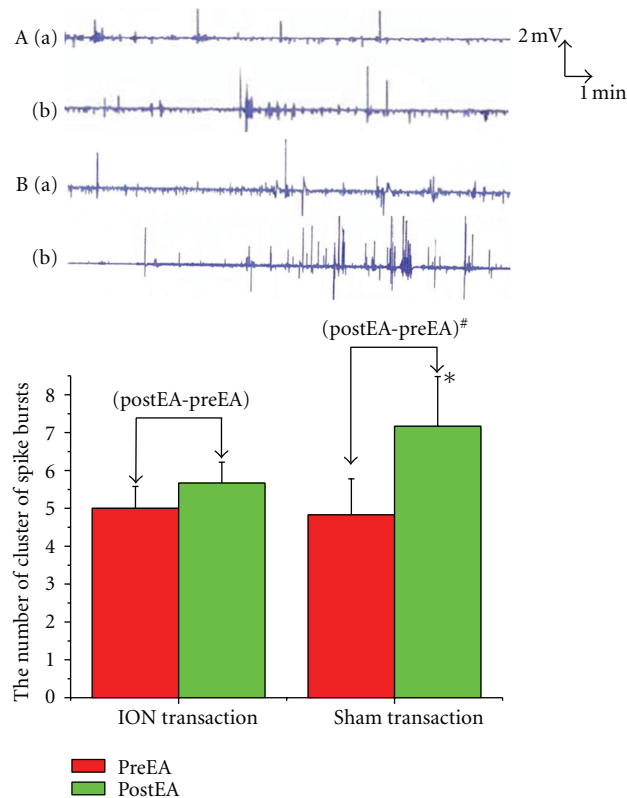


FIGURE 2: Effects of ION transaction on GMA induced by EA. * $P < 0.05$ versus preEA (sham transaction). # $P < 0.05$ versus (postEA-preEA) (ION transaction). (A) EA at ST2 and ION transaction; (B) EA at ST2 and sham transaction. (a) PreEA; (b) postEA.

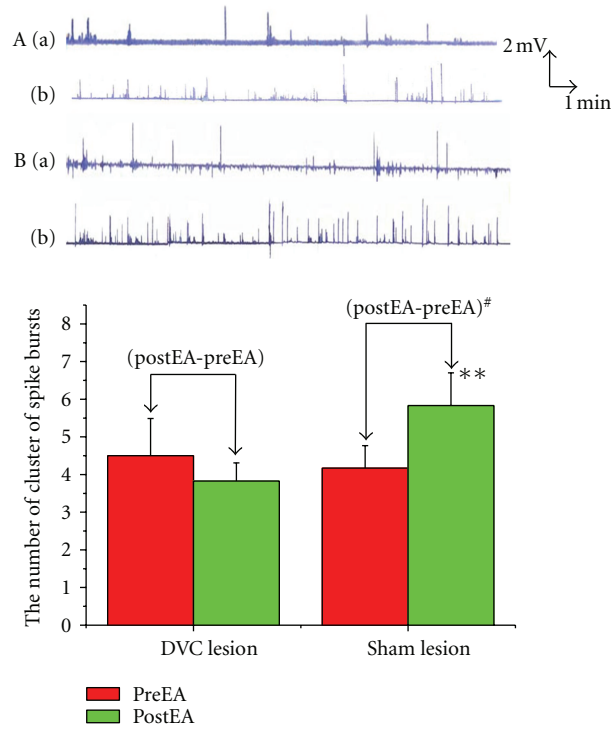


FIGURE 3: Effects of Lesion of DVC on GMA induced by EA. ** $P < 0.01$ versus preEA (sham lesion). # $P < 0.05$ versus (postEA-preEA) (DVC lesion). (A) EA at ST2 and DVC lesion; (B) EA at ST2 and sham lesion. (a) PreEA; (b) postEA.

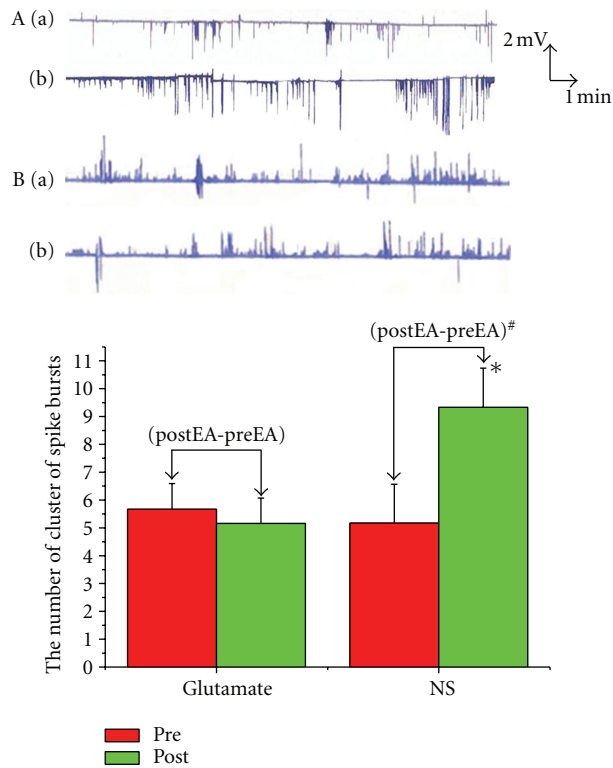


FIGURE 4: Effects of microinjection of glutamate into the NTS on GMA induced by EA. * $P < 0.05$ versus preEA (NS). # $P < 0.05$ versus (postEA-preEA) (Glutamate). (A) EA at ST2 and glutamate microinjection; (B) EA at ST2 and NS microinjection. (a) PreEA; (b) postEA.

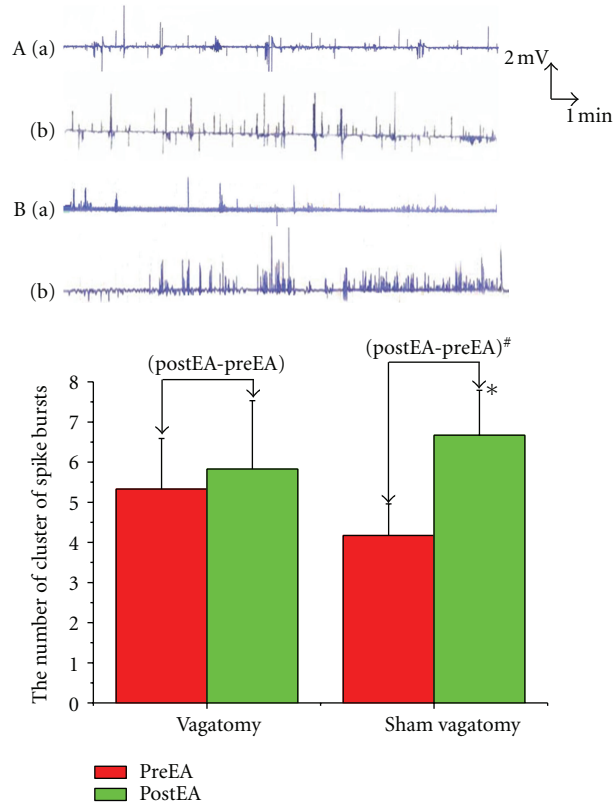


FIGURE 5: Effects of vagotomy on GMA induced by EA. * $P < 0.05$ versus preEA (sham vagotomy). # $P < 0.05$ versus (postEA-preEA) (vagotomy).

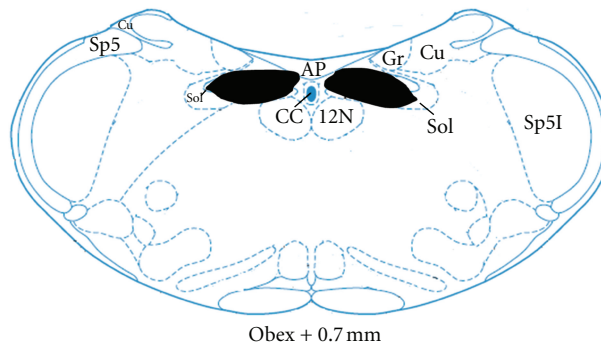


FIGURE 6: A diagrammatic representation of electrolytic lesion of DVC (shaded areas) (adapted from the atlas of Paxinos and Watson [18]). AP: area postrema; CC: central canal; Cu: cuneate fasciculus; Gr: gracile nucleus; Sol: nucleus solitary tract; sol: solitary tract; sp5: spinal trigeminal tract.

is conveyed to the NTS and acts on the DMV, which promote gastric motility [23]. Moreover, NMDA receptors of gastric-projecting neurons in the DMV are involved in the regulation of EA at BL21 on gastric emptying in rats [25]. Our previous works also show that EA at ST36 enhanced the GMI and simultaneously inhibited release of Substance P in the DVC, which is abolished by transaction of vagus nerves [2].

Another interesting issue is that orofacial somatic inputs elicited by EA at ST2 act directly on the DMV neurons or indirectly on the DMV neurons via the NTS. Electrophysiological and anatomical data demonstrate the existence

of substantial synaptic connections between the NTS and DMV and the inhibitory connections is a key for the modulation of GI functions [11–16]. It is well known that numerous neurotransmitters and neuromodulators in the DVC are involved in regulating of GI functions and a primary candidate is glutamate. In the vagovagal reflex, GI sensory inputs terminate in the NTS and release glutamate, which mainly act on non-NMDA receptors and activate the inhibitory neurons in the NTS projecting to the DMV and finally inhibit DMV neurons [26–28]. Several groups of investigators have shown that microinjection of glutamate

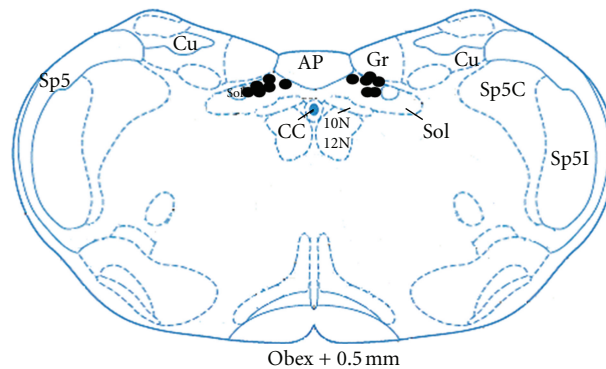


FIGURE 7: A diagrammatic representation of microinjection sites (●) within NTS (adapted from the atlas of Paxinos and Watson [18]). AP: area postrema; CC: central canal; Cu: cuneate fasciculus; Gr: gracile nucleus; Sol: nucleus solitary tract; sol: solitary tract; sp5: spinal trigeminal tract; Sp5C: spinal trigeminal nucleus, caudal part; Sp5I: spinal trigeminal nucleus, interpolar part; 10N: dorsal motor nucleus of vagus; 12N: hypoglossal nucleus.

into the DVC produces inhibitory or excitatory effect on gastric motility. It is seemed that glutamate microinjection into the NTS induces gastric inhibition [29, 30], whereas glutamate microinjection into the DMV results in gastric excitation [31, 32]. Electrophysiological data have shown that the activation of the paraventricular nucleus on gut-sensitive neurons in the DMV may be an indirect result of its effect on NTS neurons [33]. It has been demonstrated that NTS receives visceral and somatic sensory afferents and plays an important role in the somato-visceral processing [2, 8–10]. Somatic inputs from EA at limbs act on DMV via NTS and promote gastric motility, and somatic inputs from EA at abdomen act on the rostral ventrolateral medulla (RVLM) via NTS and inhibit gastric motility [23]. In this study, microinjection of glutamate into the NTS inhibits the excitation of GMA induced by EA at ST2, suggesting that NTS-to-DMV inhibitory connections are involved in the regulation of EA at ST2 on parasympathetic motor output.

In conclusion, taken together, the above findings suggest that the neural pathway of ION-NTS-DMV-VN is involved in the reflex regulation of EA at orofacial acupoints on gastric functions and NTS-DMV inhibitory connections may be essential for it.

Acknowledgments

This work was supported by the National Basic Research Program of China (973 Program; no. 2010CB530500, no. 2010CB530503), Program for New Century Excellent Talents in University (NCET-09-0083), National Natural Science Foundation of China (no. 30873239), and Gudong Natural Science Fund Committee (no. 9351040701000001).

References

- [1] M. Iwa, Y. Nakade, M. Matsushima, T. N. Pappas, M. Fujimiya, and T. Takahashi, "Electroacupuncture at ST-36 accelerates colonic motility and transit in freely moving conscious rats," *American Journal of Physiology*, vol. 290, no. 2, pp. G285–G292, 2006.
- [2] J. H. Liu, J. Yan, S. X. Yi, X. R. Chang, Y. P. Lin, and J. M. Hu, "Effects of electroacupuncture on gastric myoelectric activity and substance P in the dorsal vagal complex of rats," *Neuroscience Letters*, vol. 356, no. 2, pp. 99–102, 2004.
- [3] E. Noguchi, "Mechanism of reflex regulation of the gastroduodenal function by acupuncture," *Evidence-Based Complementary and Alternative Medicine*, vol. 5, no. 3, pp. 251–256, 2008.
- [4] A. Sato, Y. Sato, A. Suzuki, and S. Uchida, "Neural mechanisms of the reflex inhibition and excitation of gastric motility elicited by acupuncture-like stimulation in anesthetized rats," *Neuroscience Research*, vol. 18, no. 1, pp. 53–62, 1993.
- [5] V. Senna-Fernandes, D. L. França, D. de Souza et al., "Acupuncture at "zusanli" (St. 36) and "sanyinjiao" (SP. 6) points on the gastrointestinal tract: a study of the bioavailability of ^{99m}Tc-sodium pertechnetate in rats," *Evid Based Complement Alternat Med*, vol. 2011, Article ID 823941, 6 pages, 2011.
- [6] A. Shiotani, M. Tatewaki, E. Hoshino, and T. Takahashi, "Effects of electroacupuncture on gastric myoelectrical activity in healthy humans," *Neurogastroenterology and Motility*, vol. 16, no. 3, pp. 293–298, 2004.
- [7] M. Tatewaki, M. Harris, K. Uemura et al., "Dual effects of acupuncture on gastric motility in conscious rats," *American Journal of Physiology*, vol. 285, no. 4, pp. R862–R872, 2003.
- [8] J. H. Liu, J. Li, J. Yan et al., "Expression of c-fos in the nucleus of the solitary tract following electroacupuncture at facial acupoints and gastric distension in rats," *Neuroscience Letters*, vol. 366, no. 2, pp. 215–219, 2004.
- [9] J. Liu, W. Fu, W. Yi et al., "Extrasegmental analgesia of heterotopic electroacupuncture stimulation on visceral pain rats," *Brain Research*, vol. 1373, pp. 160–171, 2011.
- [10] J. F. He, J. Yan, X. R. Chang et al., "Neurons in the NTS of rat response to gastric distention stimulation and acupuncture at body surface points," *American Journal of Chinese Medicine*, vol. 34, no. 3, pp. 427–433, 2006.
- [11] S. F. Davis, A. V. Derbenev, K. W. Williams, N. R. Glatzer, and B. N. Smith, "Excitatory and inhibitory local circuit input to the rat dorsal motor nucleus of the vagus originating from the nucleus tractus solitarius," *Brain Research*, vol. 1017, no. 1–2, pp. 208–217, 2004.
- [12] S. F. Davis, K. W. Williams, W. Xu, N. R. Glatzer, and B. N. Smith, "Selective enhancement of synaptic inhibition by hypocretin (orexin) in rat vagal motor neurons: implications

- for autonomic regulation,” *Journal of Neuroscience*, vol. 23, no. 9, pp. 3844–3854, 2003.
- [13] M. J. McCann and R. C. Rogers, “Impact of antral mechanoreceptor activation on the vago-vagal reflex in the rat: functional zonation of responses,” *Journal of Physiology*, vol. 453, pp. 401–411, 1992.
- [14] D. V. Sivarao, Z. K. Krowicki, and P. J. Hornby, “Role of GABA(A) receptors in rat hindbrain nuclei controlling gastric motor function,” *Neurogastroenterology and Motility*, vol. 10, no. 4, pp. 305–313, 1998.
- [15] R. A. Travagli, R. A. Gillis, C. D. Rossiter, and S. Vicini, “Glutamate and GABA-mediated synaptic currents in neurons of the rat dorsal motor nucleus of the vagus,” *The American Journal of Physiology*, vol. 260, no. 3, pp. G531–G536, 1991.
- [16] A. Willis, M. Mihalevich, R. A. Neff, and D. Mendelowitz, “Three types of postsynaptic glutamatergic receptors are activated in DMNX neurons upon stimulation of NTS,” *American Journal of Physiology*, vol. 271, no. 6, pp. R1614–R1619, 1996.
- [17] X. N. Cheng, *Chinese Acupuncture and Moxibustion*, Foreign Language Press, Beijing, China, 1999.
- [18] G. Paxinos and C. Watson, *The Rat Brain in Stereotaxic Coordinates*, Academic Press, Sydney, Australia, 4th edition, 1998.
- [19] Z. R. Li, *Experimental Acupunctureology*, Press of Traditional Chinese Medicine, Beijing, China, 2nd edition, 2007.
- [20] H. Kametani, A. Sato, Y. Sato, and A. Simpson, “Neural mechanisms of reflex facilitation and inhibition of gastric motility to stimulation of various skin areas in rats,” *Journal of Physiology*, vol. 294, pp. 407–418, 1979.
- [21] K. Koizumi, A. Sato, and N. Terui, “Role of somatic afferents in autonomic system control of the intestinal motility,” *Brain Research*, vol. 182, no. 1, pp. 85–97, 1980.
- [22] A. Sato, Y. Sato, F. Shimada, and Y. Torigata, “Changes in gastric motility produced by nociceptive stimulation of the skin in rats,” *Brain Research*, vol. 87, no. 2-3, pp. 151–159, 1975.
- [23] M. Iwa, M. Tateiwa, M. Sakita, M. Fujimiya, and T. Takahashi, “Anatomical evidence of regional specific effects of acupuncture on gastric motor function in rats,” *Autonomic Neuroscience*, vol. 137, no. 1-2, pp. 67–76, 2007.
- [24] X. Lin, “Electrical stimulation of acupuncture points enhances gastric myoelectrical activity in humans,” *American Journal of Gastroenterology*, vol. 92, no. 9, pp. 1527–1530, 1997.
- [25] X. Zhang, B. Cheng, X. Jing et al., “NMDA receptors of gastric-projecting neurons in the dorsal motor nucleus of the vagus mediate the regulation of gastric emptying by EA at weishu (BL21),” *Evidence-Based Complementary and Alternative Medicine*, vol. 2012, Article ID 583479, 7 pages, 2012.
- [26] R. C. Rogers and M. J. McCann, “Intramedullary connections of the gastric region in the solitary nucleus: a biocytin histochemical tracing study in the rat,” *Journal of the Autonomic Nervous System*, vol. 42, no. 2, pp. 119–130, 1993.
- [27] X. G. Zhang and R. Fogel, “Involvement of glutamate in gastrointestinal vago-vagal reflexes initiated by gastrointestinal distention in the rat,” *Autonomic Neuroscience*, vol. 103, no. 1-2, pp. 19–37, 2003.
- [28] X. G. Zhang, W. E. Renehan, and R. Fogel, “Neurons in the vagal complex of the rat respond to mechanical and chemical stimulation of the GI tract,” *American Journal of Physiology*, vol. 274, no. 2, pp. G331–G341, 1998.
- [29] S. E. Spencer and W. T. Talman, “Central modulation of gastric pressure by substance P: a comparison with glutamate and acetylcholine,” *Brain Research*, vol. 385, no. 2, pp. 371–374, 1986.
- [30] S. E. Spencer and W. T. Talman, “Modulation of gastric and arterial pressure by nucleus tractus solitarius in rat,” *American Journal of Physiology*, vol. 250, no. 6, pp. 996–1002, 1986.
- [31] Z. K. Krowicki, A. Arimura, N. A. Nathan, and P. J. Hornby, “Hindbrain effects of PACAP on gastric motor function in the rat,” *American Journal of Physiology*, vol. 272, no. 5, pp. G1221–G1229, 1997.
- [32] D. V. Sivarao, Z. K. Krowicki, T. P. Abrahams, and P. J. Hornby, “Vagally-regulated gastric motor activity: evidence for kainate and NMDA receptor mediation,” *European Journal of Pharmacology*, vol. 368, no. 2-3, pp. 173–182, 1999.
- [33] X. G. Zhang, R. Fogel, and W. E. Renehan, “Stimulation of the paraventricular nucleus modulates the activity of gut-sensitive neurons in the vagal complex,” *American Journal of Physiology*, vol. 277, no. 1, pp. G79–G90, 1999.

Review Article

Biophysical Characteristics of Meridians and Acupoints: A Systematic Review

Juan Li,¹ Qing Wang,¹ Huiling Liang,¹ Haoxu Dong,¹ Yan Li,¹
Ernest Hung Yu Ng,² and Xiaoke Wu¹

¹Department of Obstetrics and Gynecology, National Key Discipline and Clinical Base, Heilongjiang University of Chinese Medicine, 150040 Harbin, China

²Department of Obstetrics & Gynecology, The University of Hong Kong, Hong Kong

Correspondence should be addressed to Xiaoke Wu, xiaokewu2002@vip.sina.com

Received 24 August 2012; Revised 26 November 2012; Accepted 14 December 2012

Academic Editor: Wolfgang Schwarz

Copyright © 2012 Juan Li et al. This is an open access article distributed under the Creative Commons Attribution License, which permits unrestricted use, distribution, and reproduction in any medium, provided the original work is properly cited.

As an integral part of traditional Chinese medicine (TCM), acupuncture is a convenient and effective therapy with fewer adverse effects. Recently, researches on meridian essence have become core issues of modern TCM. Numerous experiments have demonstrated the objective existence of meridians by different technologies since 1950s, such as biophysics, biochemistry, and molecular biology. In this paper, we review biophysical studies on electric, acoustic, thermal, optical, magnetic, isotopic, and myoelectric aspects of meridians and acupoints. These studies suggest that meridians/acupoints have biophysical characteristics which are different from nonacupuncture points. Owing to the limitations of previous studies, future research using high-throughput technologies such as omics and multicenter randomized controlled trials should be performed to explore the acupuncture's mechanisms of action and demonstration of efficacy.

1. Introduction

Acupuncture is an integral part of traditional Chinese medicine (TCM), which dates back about 3,000 years [1]. It is increasingly being accepted as a complementary and alternative medicine (CAM) therapy in the United States [2]. The practice of acupuncture is based on the meridian system [3], and along the meridians lie acupuncture points or acupoints, which may have therapeutic effects for certain medical conditions when stimulated by needling, pressure, or heat [3].

The meridian theory is a fundamental part of TCM and has guided acupuncture for thousands of years [4]. While the clinical effects of acupuncture have drawn extensive attentions from researchers of science and medicine, lots of questions arise: Do meridians exist? What are the mechanisms of their actions? What is the physiological basis of meridians? What are the differences between acupoints and nonacupuncture points? So far, these questions have not been completely answered, but a large number of experiments and clinical trials have been conducted using

advanced biophysical, biochemical, and molecular biological methods [5–8].

In order to have a better understanding of the biophysical basis of meridians/acupoints and their mechanisms of action, we review the biophysical studies of meridians/acupoints after searching the electronic databases MEDLINE, EMBASE, CINAHL, EMBR, CNKI, Wanfang, and Vip from the beginning to June 2012.

2. Biophysical Characteristics of Meridians and Acupoints

2.1. Electrical Characteristics. Low resistance and high capacitance are generally accepted as electrical characteristics of meridians and acupoints [9–11]. Currently, researchers are evaluating the electrophysiological properties of acupoints as a possible means to explore the acting mechanisms of acupuncture [12]. Wang et al. [13] used the infrared thermal images and surface resistance measurement to detect the temperature and resistance at left and right pericardium

(PC) 6, right bladder (BL) 15, and points 1 cm away from all above acupoints as controls in 20 rabbits. The results showed that acupoints had high-temperature and low-resistance characteristics compared with nonacupuncture point controls, and the resistance values were closely related with skin temperature. Other researchers in China [14, 15] have also demonstrated this phenomenon. In addition, Egot-Lemaire and Ziskin [16] found that the dielectric properties of the acupoints were somewhat different from those of the surrounding nonacupuncture points, which ranged from 50 GHz to about 61 GHz.

However, the above findings are not consistent with results of other studies. Ahn et al. [17] used a four-electrode method to measure the electrical impedance along segments of the pericardium and spleen meridians and corresponding parallel control segments in 23 human subjects. The results showed that tissue impedance was on average lower along the pericardium meridian, but not along the spleen meridian, compared with their respective controls. Pearson et al. [18] used two instruments to test the electrical skin impedance at three acupoints and their nearby sites. The results showed that none of the three acupoints tested had lower skin impedance than at either of the nearby control points. Ahn et al. [19] in a systematic review of studies on the electrical characteristics of acupuncture structures found only 5 out of 9 point studies showed positive association between acupoints and lower electrical resistance and impedance, while 7 out of 9 meridian studies showed positive association between acupuncture meridians and lower electrical impedance and higher capacitance. The evidence did not conclusively support the claim that acupoints or meridians were electrically distinguishable. Kramer et al. [20] used an array consisting of 64 (8×8) electrodes to measure the skin resistance. The electrodes were located at corresponding acupoints, and the results of electrical skin resistance measurements (ESRMs) were compared to those of the surrounding electrodes.

Table 1 showed that the electrical skin resistance (ESR) at most acupoints (62.8%) had no significant difference when compared with that of the surrounding areas. This was partly in line with some previous high quality studies, which draw relatively negative conclusions to this topic. Therefore, it could not be concluded that ESRMs could be used for acupoint localization or diagnostic/therapeutic purposes. In this paper, they also found that the reproducibility of the array for measuring ESR was extremely high after 1 minute but was low after 1 hour and 1 week. The phenomenon was characterized by high short-term and low long-term reproducibility. One simple explanation might be a change of environmental conditions, including the factors of artifacts, wide ESR variation inter- and intra-individually, and ESR shift which may be caused by transepidermal water loss or skin hydration [21]. Changes in the thickness of stratum corneum layer (e.g., small abrasions) and the electrode size could also influence ESRMs. And they found that the factor affecting reliability of the results might be that they simply failed to measure the acupoint itself due to the distance of 8 mm between the centers of the electrodes.

TABLE 1: Analysis of electrical skin resistance measurements (ESRMs) at acupoints in healthy humans.

ESR properties	Results of ESRMs
ESR (no significant difference)	397 (62.8%)
ESR↓	163 (25.9%)
ESR↑	71 (11.3%)

Other researchers [22, 23] also found electrode material, size and shape, pressure exerted by the probe, duration of probe application, inclination of the probe tip on the skin, and variations in skin condition (dry/moist, thickness, and integrity of the stratum corneum) might be the potential confounders affecting the reproducibility and reliability of the device for measuring skin electrical current/resistance. To resolve the limitations, Colbert et al. [12] designed a continuous recording system, a fully automatic multichannel device, to record skin impedance at multiple acupoints simultaneously over 24 hours. By using it, they successfully detected that the skin impedance of acupoints was lower than the nearby nonacupuncture points. Moreover, Colbert et al. [24] developed an automated multichannel prototype system and recorded electrical resistance and capacitance at eight skin sites in 33 healthy participants for over 2 hours. The results showed that only the acupoints on the liver and spleen meridians had a lower resistance than their nearby sites (4 mm away), while other comparisons showed no significant differences.

In order to explore the mechanisms of electrical characteristics, Yang [25] analyzed various possible factors that may lead to low resistance. He concluded that a relative higher content of the interstitial fluid (tissue fluid) was the source of low resistance, and the histological essence of meridians was the bands with relative high content of interstitial fluid in loose connective tissues. Others believed that gap junctions might be the structural basis that determined the different skin resistances [26–28]. Tan [29] considered that, besides the inherent organizational factors, the concentration change of charged molecules in the corresponding environment was one of the most important variable factors influencing the resistance in different parts of the body. Furthermore, according to the bioelectric field with rich ion along meridians, he concluded that the resistance of meridians was certain to reduce when propagated sensation along channel (PSC) happened. In other reports [30–35], local tissue-released noradrenalin (NA), nitric oxide (NO), tumor-related factors, and mast cell-released histamine and serotonin (5-HT) were considered to be responsible for the electrical characteristics of meridians and acupoints.

2.2. Acoustic Characteristics. The characteristics of phonation and transmitting sound in meridians were first reported in 1980s and researchers have tried to confirm them in both animal experiments and human trials. Zhang et al. [36] detected 8 acupoints on the conception vessel, 11 acupoints on the governor vessel, and control points on both sides 2 mm apart from the acupoints mentioned above in 30 rabbits. The results showed that the sound wave's amplitude

TABLE 2: The relationship between five different meridians and five musical tones cited in *Huang Di Nei Jin*.

Meridian	The tone name	Western name of the tone	Frequency for tone
Spleen	Gung	Do (C)	261.6 Hz
Lung	Sang	Re (D)	293.7 Hz
Liver	Gak	Mi (E)	329.6 Hz
Heart	Chi	Sol (G)	392.0 Hz
Kidney	Wu	La (A)	440.0 Hz

of acupoints was significantly higher than nonacupuncture points. Wei et al. [37] measured the intensity of sound wave and confirmed that the sound wave could be transmitted in the meridians and acupoints. Its conduction velocity was faster than that of soft tissue but was lower than bone conduction. Furthermore, a significant relationship was found between the tones and the meridians, which were described in the *Yellow Emperor's Internal Medicine (Huang Di Nei Jin)* (Table 2) [38].

The acoustic characteristics of acupoints are concluded as follows: (A) frequency is 2–15 Hz; (B) amplitude is 0.5–10 mV; (C) waveform is similar to sharp wave or sine wave; (D) bidirectional conduction velocity is 6.2–10 cm/s; (E) it could be blocked [39].

The acoustic conduction depends on the media, and orderly the distribution of microscopic particles in the media is a necessary condition to promote the effective conduction. It was reported that the property of transmitting sound in meridians is better than that of the surrounding areas due to the enrichment of isotropic ions along meridians under the action of bioelectric field [26]. Moreover, main and collateral channels are proved to be good medium for mechanical vibration wave and infrasonic wave [39, 40]. Perhaps this is caused by the characteristics of infrasonic wave, that is, long wavelength, weak attenuation extent, difficult to be absorbed while spreading, and strong penetration [40].

In addition, Krevsky et al. [41] found that acoustic characteristics of meridians and acupoints could be used for diagnostic purposes. Transmitted microwave along the meridians was able to detect on the next acupoint of the same meridian. The frequency of microwave in cancer patients was different from that of healthy controls. And the frequency ranges of the microwave transmitted in different meridians were found to be different.

2.3. Thermal Characteristics. Wang [42] reviewed that Borsarello found the trace of facial isotherm detected by the infrared thermal images was similar with human meridians in 1970. Since then, more and more researchers have reported the thermal characteristics of meridians and acupoints from different aspects. For example, Hu et al. [43, 44] observed the infrared radiant by an infrared imaging system and found that the tracks were consistent with the 14 meridians described by the ancient Chinese. Zhang et al. [45] measured the temperature 5 mm and 10 mm subcutaneous,

respectively, along the meridians. They found that the high-temperature line along the meridians was formed after acupuncture, which was mainly emerged in the skin layer.

Furthermore, thermal characteristics may have a role in differentiating the syndromes. It was reported that thermal sensitivity measurement of meridians was used to differentiate the constitutions of yang deficiency, qi deficiency, and peace [46, 47].

2.4. Optical Characteristics. Studies addressing optical properties are relatively less and mainly focus on the high luminous properties and the transmission characteristics of light wave along the meridians. Yan et al. [48] found that there were 14 high luminous lines on the body surface, and the lines were significantly different from those located on both sides 5 mm away. Comparing the high luminous lines where 1934 points lie with the location of the 14 regular meridians on the body surface described by *Huang Di Nei Jin*, the rate of completely overlapped region was 92.97%, and the rate of basically consistent region was 6.72%. The results indicated that meridians and acupoints had high luminous biophysical properties. Liu et al. [49] designed an automatic measurement system to test the transmission characteristics of light wave along the meridians and found that there were significant differences between meridians and nonmeridians. Also, they found that the average attenuation factor of the pericardium meridian was lower than the spleen meridian.

2.5. Magnetic Characteristics. Magnetic characteristics of meridians and acupoints are still not fully defined. Li et al. [50] had examined meridians, acupoints, brain, and relative organs by using superconducting quantum interference device (SQUID) and functional magnetic resonance imaging (fMRI) in the national zero-magnetic laboratory located in China. They found a relatively stable circular current of electromagnetic and chemical oscillation along the low electric resistance pathway. Competition of different frequency oscillation often yielded resonance in some positions of the human body so as to form oscillatory network. Moreover, the electromagnetic and chemical oscillation circulation dominated the position of strange points in the body, which were possibly meridians and acupoints with regulative actions.

The human body is a magnetic field. Recently, the exploration of the relationship between meridians and resting-state brain networks by fMRI has gained popularity. Zhang et al. [51] used fMRI to investigate the specificity of acupuncture. By acupuncturing gallbladder (GB) 40, with kidney (KI) 3 as a control (belonging to the same nerve segment but different meridians), different brain areas were enhanced. It demonstrated that acupuncture at different acupoints could exert different modulatory effects on resting-state networks (RSNs).

Another interesting experiment was performed by Cao [52], who explored effects of acupoints magnetic stimulation on temperature field along meridians. In order to investigate the variation of temperature field before and after magnetic stimulation at acupoints, the infrared imaging temperature

measurement was used to detect the distribution of temperature along the governor vessel on rabbit and human bodies directly. Compared with nonacupuncture points, the temperature of points on the governor vessel varied significantly. This showed that magnetic stimulation of acupoints could cause temperature variation along meridians.

2.6. Migration of Isotope along Meridians. Migration of isotope along channels was first discovered in 1950s. It is a relatively simply physical phenomenon, which follows physical laws. In 1980s, Meng and his group [53] in China had shown that slow movement of $^{99m}\text{TcO}_4^-$ along channels was observed after injecting the isotope into an acupoint, and the channels observed were similar to the meridians recorded in ancient Chinese literature. But they only proved that the channels had nothing to do with lymphatic network. Vessel and neural systems were not concerned.

In 2008, Zhang et al. [54] discovered low hydraulic resistance channels along meridians in minipigs. The low hydraulic resistance causes more fluid to flow along meridian lines compared with nonmeridian areas. The isotope tracing had been used to detect the stomach meridian in six minipigs. It was shown in two cases that, after injecting 0.1 mL $^{99m}\text{TcO}_4^-$ into one low hydraulic resistance point, a migration of isotope could be found along the meridian toward the other low hydraulic resistance point. Based on these findings, they deduced that the migration of isotope in the human body represented the interstitial fluid flow along low hydraulic resistance channels.

2.7. Myoelectric Activities. Myoelectricity is often used to study PSC in China. Zhu et al. [55] proved that PSC was closely related to the nerve-skeletal system. In their study, when large intestine (LI) 4 was stimulated, propagated sensation and myoelectricity along the large intestine meridian appeared. However, brachial plexus block anesthesia could eliminate this phenomenon. Another research in rats conducted by Ma et al. [56] also showed that the myoelectric activity of longissimus muscle was the foundation of PSC. These experiments show that meridians have the character of obvious myoelectric activity, and propagated sensation is closely related to myoelectricity.

3. Summary and Future Directions

Recent studies confirm that meridians and acupoints have many biophysical properties, which are different from those of nonacupuncture points. The characteristics include electric characteristics (i.e., high-electrical potential, conductance, and capacitance, low impedance and resistance), thermal characteristics (i.e., infrared radiant tracking along the meridians), acoustic characteristics (i.e., high guide sound with 2–15 Hz frequency, 0.5–10 mV amplitude, 6.2–10 cm/s bidirectional conduction velocity and being similar with sharp wave or sine wave), optical characteristics (i.e., high luminous properties and light wave spreading along the meridians), magnetic characteristics (i.e., a relative stable circular current of electromagnetic and chemical oscillation

along the low electric resistance pathway), isotopic characteristics (i.e., migration of isotope along meridians), and myoelectric characteristics (i.e., obvious myoelectric activity). Therefore, the existence of meridians is scientifically supported.

These biophysical properties are the bases of PSC and further researches about morphology and acting pathways of meridians. They may also contribute to understanding the changes of body in different function states, diagnosing diseases, exploring new therapy, clarifying the pathogenesis, and differentiating symptomatic types and constitutions in TCM when every property is taken into consideration rather than using single property. Future basic studies should not only use a single method, such as electric, acoustic, optical, and magnetic method, to explore meridian essence, but also employ the methods of systemic biology, such as proteomics, genomics, transcriptomics, and other omics, to reveal the multitarget and multipath mechanisms of action. The basic studies should be further supported by clinical studies especially large randomized controlled trials. And appropriate diseases indicated for acupuncture intervention should be emphasized in this kind of investigations to show the therapeutic benefit.

Authors' Contribution

J. Li, Q. Wang, H. Liang, and H. Dong contributed equally to this work.

Acknowledgments

The authors have no conflict of interests in producing this paper. No funding was obtained for the paper.

References

- [1] E. H. Y. Ng, W. S. So, J. Gao, Y. Y. Wong, and P. C. Ho, "The role of acupuncture in the management of subfertility," *Fertility and Sterility*, vol. 90, no. 1, pp. 1–13, 2008.
- [2] W. Zhou and J. C. Longhurst, "Neuroendocrine mechanisms of acupuncture in the treatment of hypertension," *Evidence-Based Complementary and Alternative Medicine*, vol. 2012, Article ID 878673, 9 pages, 2012.
- [3] J. C. Longhurst, "Defining meridians: a modern basis of understanding," *Journal of Acupuncture and Meridian Studies*, vol. 3, no. 2, pp. 67–74, 2010.
- [4] G. J. Wang, M. H. Ayati, and W. B. Zhang, "Meridian studies in China: a systematic review," *Journal of Acupuncture and Meridian Studies*, vol. 3, no. 1, pp. 1–9, 2010.
- [5] X. H. Yan, X. Y. Zhang, C. L. Liu et al., "Do acupuncture points exist?" *Physics in Medicine and Biology*, vol. 54, no. 9, pp. N143–N150, 2009.
- [6] S. X. Ma, X. Y. Li, B. T. Smith, and N. T. Jou, "Changes in nitric oxide, cGMP, and nitrotyrosine concentrations over skin along the meridians in obese subjects," *Obesity*, vol. 19, no. 8, pp. 1560–1567, 2011.
- [7] N. T. Jou and S. X. Ma, "Responses of nitric oxide—cGMP release in acupuncture point to electroacupuncture in human skin in vivo using dermal microdialysis," *Microcirculation*, vol. 16, no. 5, pp. 434–443, 2009.

- [8] M. Y. Hong, S. S. Park, Y. J. Ha et al., "Heterogeneity of skin surface oxygen level of wrist in relation to acupuncture point," *Evidence-Based Complementary and Alternative Medicine*, vol. 2012, Article ID 106762, 7 pages, 2012.
- [9] C. X. Falk, S. Birch, S. K. Avants, Y. Tsau, and A. Margolin, "Preliminary results of a new method for locating auricular acupuncture points," *Acupuncture and Electro-Therapeutics Research*, vol. 25, no. 3-4, pp. 165-177, 2000.
- [10] H. M. Johng, J. H. Cho, H. S. Shin et al., "Frequency dependence of impedances at the acupuncture point Quze (PC3)," *IEEE Engineering in Medicine and Biology Magazine*, vol. 21, no. 2, pp. 33-36, 2002.
- [11] M. S. Lee, S. Y. Jeong, Y. H. Lee, D. M. Jeong, Y. G. Eo, and S. B. Ko, "Differences in electrical conduction properties between meridians and non-meridians," *American Journal of Chinese Medicine*, vol. 33, no. 5, pp. 723-728, 2005.
- [12] A. P. Colbert, J. Yun, A. Larsen, T. Edinger, W. L. Gregory, and T. Thong, "Skin impedance measurements for acupuncture research: development of a continuous recording system," *Evidence-Based Complementary and Alternative Medicine*, vol. 5, no. 4, pp. 443-450, 2008.
- [13] S. Y. Wang, D. Zhang, Y. G. Zhu et al., "Correlation research of the relations between temperature and resistance of acupoint," *Liaoning Journal of Traditional Chinese Medicine*, vol. 34, no. 1, pp. 5-6, 2007.
- [14] Z. L. Han, "Related researches between the meridian impedance out of balance in the two symmetry sides of human body and diseases," *Journal of Heze Medical College*, vol. 11, no. 1, 9 pages, 1999.
- [15] Y. S. Liu, Y. M. Chen, Y. X. Liu et al., "Research of the resistance change on five shu points in 24 hours," *Chinese Acupuncture & Moxibustion*, vol. 17, no. 7, 401 pages, 1997.
- [16] S. J. Egot-Lemaire and M. C. Ziskin, "Dielectric properties of human skin at an acupuncture point in the 50-75 GHz frequency range, a pilot study," *Bioelectromagnetics*, vol. 32, no. 5, pp. 568-569, 2003.
- [17] A. C. Ahn, J. Wu, G. J. Badger, R. Hammerschlag, and H. M. Langevin, "Electrical impedance along connective tissue planes associated with acupuncture meridians," *BMC Complementary and Alternative Medicine*, vol. 5, article 10, 2005.
- [18] S. Pearson, A. P. Colbert, J. McNames, M. Baumgartner, and R. Hammerschlag, "Electrical skin impedance at acupuncture points," *Journal of Alternative and Complementary Medicine*, vol. 13, no. 4, pp. 409-418, 2007.
- [19] A. C. Ahn, A. P. Colbert, B. J. Anderson et al., "Electrical properties of acupuncture points and meridians: a systematic review," *Bioelectromagnetics*, vol. 29, no. 4, pp. 245-256, 2008.
- [20] S. Kramer, K. Winterhalter, G. Schober et al., "Characteristics of electrical skin resistance at acupuncture points in healthy humans," *Journal of Alternative and Complementary Medicine*, vol. 15, no. 5, pp. 495-500, 2009.
- [21] B. Cravello and A. Ferri, "Relationships between skin properties and environmental parameters," *Skin Research and Technology*, vol. 14, no. 2, pp. 180-186, 2008.
- [22] A. C. Ahn and Ø. G. Martinsen, "Electrical characterization of acupuncture points: technical issues and challenges," *Journal of Alternative and Complementary Medicine*, vol. 13, no. 8, pp. 817-824, 2007.
- [23] O. G. Martinsen, S. Grimnes, L. Mørkrid, and M. Hareide, "Line patterns in the mosaic electrical properties of human skin—a cross-correlation study," *IEEE Transactions on Bio-medical Engineering*, vol. 48, no. 6, pp. 731-734, 2001.
- [24] A. P. Colbert, A. Larsen, S. Chamberlin et al., "A multichannel system for continuous measurements of skin resistance and capacitance at acupuncture points," *Journal of Acupuncture and Meridian Studies*, vol. 2, no. 4, pp. 259-268, 2009.
- [25] W. Yang, "The essence deduce of the meridian organizations based on lower resistance meridian researches," *Acta Scientiarum Naturalium Universitatis Pekinensis*, vol. 44, no. 2, pp. 227-280, 2008.
- [26] J. Y. Fan, S. Y. Xi, Z. Liu et al., "The epidermal structure characteristics of low skin resistance points," *Acta Anatomica Sinica*, vol. 20, no. 4, 429 pages, 1989.
- [27] Z. S. Li, K. Q. Ouyang, X. Q. Zhang et al., "The genesis exploration of low skin resistance points in the big white rats," *Journal of Chongqing University*, vol. 21, no. 3, 101 pages, 1998.
- [28] J. Y. Fan, Q. Huang, Z. M. Wei et al., "The influence of catecholamines to the skin conductivity and epidermal gap bonding in rats," *Basic & Clinical Medicine*, vol. 15, no. 2, 47 pages, 1995.
- [29] C. Y. Tan, "Essence of meridians based on neural electric field," *Chinese Acupuncture & Moxibustion*, vol. 30, no. 10, pp. 835-839, 2010.
- [30] D. Zhang, G. Ding, X. Shen et al., "Role of mast cells in acupuncture effect: a pilot study," *Explore*, vol. 4, no. 3, pp. 170-177, 2008.
- [31] J. X. Chen and S. X. Ma, "Effects of nitric oxide and noradrenergic function on skin electric resistance of acupoints and meridians," *Journal of Alternative and Complementary Medicine*, vol. 11, no. 3, pp. 423-431, 2005.
- [32] J. Y. Fan, Z. M. Wei, Z. Liu et al., "Effect of catecholamines on the skin conductance in mice," *Journal of Beijing Medical University*, vol. 25, pp. 324-326, 1993.
- [33] S. X. Ma, "Enhanced nitric oxide concentrations and expression of nitric oxide synthase in acupuncture points/meridians," *Journal of Alternative and Complementary Medicine*, vol. 9, no. 2, pp. 207-215, 2003.
- [34] V. Ogay, S. K. Min, J. S. Hyo, J. C. Cheon, and K. S. Soh, "Catecholamine-storing cells at acupuncture points of rabbits," *Journal of Acupuncture and Meridian Studies*, vol. 1, no. 2, pp. 83-90, 2008.
- [35] F. Wick, N. Wick, and M. C. Wick, "Morphological analysis of human acupuncture points through immunohistochemistry," *American Journal of Physical Medicine and Rehabilitation*, vol. 86, no. 1, pp. 7-11, 2007.
- [36] K. X. Zhang, X. Wang, R. Cao et al., "Detection of common acupoints in the conception vessel and governor vessel of rabbits and verification of organs effect," *Liaoning Journal of Traditional Chinese Medicine*, vol. 30, no. 7, pp. 568-569, 2003.
- [37] Y. L. Wei, W. Liu, J. Kong et al., "Research of human biological effects and its conduct of gong tune music," in *Chinese Music Therapy Association of the Seventh Symposium*, Fuzhou, China, 2005.
- [38] Y. C. Kim, D. M. Jeong, and M. S. Lee, "An examination of the relationship between five oriental musical tones and corresponding internal organs and meridians," *Acupuncture and Electro-Therapeutics Research*, vol. 29, no. 3-4, pp. 227-233, 2004.
- [39] H. M. Wang, *Research on Meridian and Collateral in China*, Academy Press, Beijing, China, 2006.
- [40] X. M. Wang, "Analysis on the mechanism of acupuncture infrasound energy in treatment of diseases," *Chinese Acupuncture & Moxibustion*, vol. 29, no. 3, pp. 223-226, 2009.
- [41] M. A. Krevsky, E. S. Zinina, Y. Koshurinov et al., "Microwave propagation on acupuncture channels," *Acupuncture & Electro-Therapeutics Research*, vol. 31, no. 1-2, pp. 1-12, 2006.

- [42] B. X. Wang, *Foreign Study of the Meridian*, People's Health Publishing House, Beijing, China, 1984.
- [43] X. L. Hu, P. Q. Wang, J. S. Xu, B. H. Wu, and X. Y. Xu, "Main characteristics of infrared radiant rack along meridian courses over human body surface and the condition of its appearance," *Journal of Infrared and Millimeter Waves*, vol. 20, no. 5, pp. 325–328, 2001.
- [44] P. Q. Wang, X. L. Hu, J. S. Xu et al., "The indication of infrared thermal images on body surface along 14 meridian lines," *Acupuncture Research*, vol. 27, no. 4, 260 pages, 2002.
- [45] D. Zhang, S. Y. Wang, and C. Y. Wang, "Determination of deep temperature under the line of high temperature along meridians," *Chinese Journal of Basic Medicine in Traditional Chinese Medicine*, vol. 7, no. 410, 62 pages, 2001.
- [46] J. X. Zhang, *The Applied Exploration on Using Meridian Thermal Sensitivity Measurement To Identify Yang-Deficiency Constitution and Evaluate Curative Effect*, Guangzhou University of Traditional Chinese Medicine, Guangzhou, China, 2010.
- [47] Y. M. Xian, *The Applied Exploration on the Constitution Properties of Persons With Qi Deficiency Constitution Using Meridian Thermal Sensitivity Measurement*, Guangzhou University of Traditional Chinese Medicine, Guangzhou, China, 2011.
- [48] Z. Q. Yan, Y. Q. Shi, Y. Z. Wang et al., "Research on the biophysical features of strong luminescence phenomena in the 14 regular meridians of human body," *Acupuncture Research*, no. 8, pp. 389–394, 1989.
- [49] X. R. Liu, C. S. Chen, Y. F. Jiang et al., "Light propagation characteristics of meridian and surrounding non-meridian tissue," *Acta Photonica Sinica*, vol. 39, supplement 1, pp. 29–33, 2010.
- [50] D. Z. Li, S. T. Fu, and X. Z. Li, "Study on theory and clinical application of meridians," *Chinese Acupuncture & Moxibustion*, vol. 25, no. 1, pp. 53–59, 2005.
- [51] C. G. Zhang, L. J. Bai, R. W. Dai et al., "Modulatory effects of acupuncture on resting-state networks: a functional MRI study combining independent component analysis and multivariate granger causality analysis," *Journal of Magnetic Resonance Imaging*, vol. 35, no. 3, pp. 572–581, 2012.
- [52] Y. L. Cao, *Research on Effects of Acupoints Magnetic Stimulation on Temperature Field Along Meridian*, Tian Jin University, Tian Jin, China, 2010.
- [53] J. B. Meng, H. H. Gao, P. Wang et al., "A primary study of meridian circulation by isotopic migration," *Acupuncture Research*, vol. 1, pp. 77–80, 1987.
- [54] W. B. Zhang, Y. Y. Tian, H. Li et al., "A discovery of low hydraulic resistance channel along meridians," *Journal of Acupuncture and Meridian Studies*, vol. 1, no. 1, pp. 20–28, 2008.
- [55] B. Zhu, P. J. Rong, Y. Q. Li et al., "Propagated sensation along meridian and myoelectricity activity along meridian," *Science in China*, vol. 31, no. 5, pp. 465–470, 2001.
- [56] C. Ma, Z. Zheng, and Y. K. Xie, "Propagated sensation of rat longissimus muscle's myoelectricity activity," *Chinese Science Bulletin*, vol. 45, no. 18, pp. 1982–1988, 2000.

Research Article

Transcutaneous Auricular Vagus Nerve Stimulation Protects Endotoxemic Rat from Lipopolysaccharide-Induced Inflammation

Yu Xue Zhao, Wei He, Xiang Hong Jing, Jun Ling Liu, Pei Jing Rong, Hui Ben, Kun Liu, and Bing Zhu

Institute of Acupuncture and Moxibustion, China Academy of Chinese Medical Sciences, 16 Nanxiaojie Street, Dongzhimen Nei, Beijing 100700, China

Correspondence should be addressed to Bing Zhu, zhubing@mail.cintcm.ac.cn

Received 21 August 2012; Revised 5 December 2012; Accepted 6 December 2012

Academic Editor: Ying Xia

Copyright © 2012 Yu Xue Zhao et al. This is an open access article distributed under the Creative Commons Attribution License, which permits unrestricted use, distribution, and reproduction in any medium, provided the original work is properly cited.

Background. Transcutaneous auricular vagus nerve stimulation (ta-VNS) could evoke parasympathetic activities via activating the brainstem autonomic nuclei, similar to the effects that are produced after vagus nerve stimulation (VNS). VNS modulates immune function through activating the cholinergic anti-inflammatory pathway. **Methods.** VNS, ta-VNS, or transcutaneous electrical acupoint stimulation (TEAS) on ST36 was performed to modulate the inflammatory response. The concentration of serum proinflammatory cytokines and tissue NF-kappa B p65 (NF- κ B p65) were detected in endotoxaemia affected anesthetized rats. **Results.** Similar to the effect of VNS, ta-VNS suppressed the serum proinflammatory cytokines levels, such as tumour necrosis factor- α (TNF- α), interleukin-1 beta (IL-1 β), and interleukin-6 (IL-6) as well as NF-kappa B p65 expressions of lung tissues. ST36 stimulation also decreases LPS-induced high TNF- α level and NF- κ B signal, but it did not restrain proinflammatory cytokine IL-1 β and IL-6. Neither ta-VNS nor ST36 stimulation could suppress LPS-induced TNF- α and NF- κ B after vagotomy or with α 7nAChR antagonist injection. **Conclusions.** The present paper demonstrated that ta-VNS could be utilized to suppress LPS-induced inflammatory responses via α 7nAChR-mediated cholinergic anti-inflammatory pathway.

1. Introduction

Inflammation is a local, protective response to microbial invasion or injury, which must be fine-tuned and regulated precisely [1]. Several potent cytokines including tumour necrosis factor- α (TNF- α), interleukin-1 beta (IL-1 β), interleukin-6 (IL-6), interleukin-10 (IL-10), and transforming growth factor-beta (TGF- β) are produced by activated macrophages and other immune cells, as necessary and sufficient mediators involved in local and systemic inflammation [2, 3]. Overproduction of cytokines leads to systematic inflammation and tissue injury. If the overproduced cytokines spread into the bloodstream, dangerous inflammatory responses will be induced. In the past ten years, abundant studies have been focused on “the cholinergic anti-inflammatory pathway,” namely, the efferent vagus nerve which inhibits proinflammatory cytokine production and protects

against systemic inflammation via a α 7nAChR-dependent pathway [4]. Vagus nerve stimulation (VNS) prevents the occurrence and development of inflammation effectively via activating the cholinergic anti-inflammatory pathway. VNS and acetylcholine (ACh) attenuated the release of cytokines significantly and improved survival in lethal endotoxemia or sepsis models [5, 6]. For instance, in a rat model of lethal endotoxemia, electrical stimulation of the efferent vagus nerve decreases serum and hepatic TNF levels [6]. Moreover, VNS inhibited all lipopolysaccharide- (LPS-) induced procoagulant responses strongly, attenuated the fibrinolytic response more modestly, and improved hepatic ACh levels significantly in endotoxemia rats [7]. VNS attenuated the LPS-induced increases of the plasma and splenic proinflammatory cytokines, rather than influencing the anti-inflammatory cytokine IL-10 [8]. In addition, activation of this neural immune-modulatory pathway by electrical

stimulation of vagus nerve also protects animals from various circumstances, such as ischemia-reperfusion injury, hypovolemic hemorrhagic shock, heart failure, and myocardial ischemia/reperfusion [9–12].

It was demonstrated that the transcutaneous auricular vagus nerve stimulation (ta-VNS) induced a series of parasympathetic activities [13–17]. Auricular branch of vagus nerve is a special vagal branch that innervates the body surface which could not be found on the other parts of the body [18], mainly innervating the cyma conchae and cavum conchae within the auricle. Our previous studies indicated that there is an intimate connection between auricular concha, the nucleus tractus solitarius (NTS), dorsal motor nucleus of the vagus nerve (DMN), and vagus nerve, which constructs the pathway of the auricular-vagal reflex. Accordingly, there might be some kinds of connection between auricular concha and efferent vagus nerve. In the present study, we reasoned that ta-VNS may have a role in activating the vagus nerve-based cholinergic anti-inflammatory pathway. Here, the effect of ta-VNS on proinflammatory cytokines and NF- κ B p65 was explored to clarify the mechanism of ta-VNS underlying regulating inflammatory diseases.

2. Materials and Methods

2.1. Animals. Male Sprague Dawley rats (12 weeks old) were used in the present study, weighing 275–350 g, supplied by China Academy of Military Science. Rats were housed in groups of 5–6 in standard polycarbonate cages at ambient temperature (22°C) and allowed access to food and water *ad libitum*. Lights were set to an automated 07:00 on and 19:00 off light-dark cycle, and all animal experiments were done between 08:00 and 11:00 a.m. Rats received care consistent with the *National Institutes of Health Guide for the Care and Use of Laboratory Animals*, and the experiments were conducted in accordance with a protocol approved by the Institutional Animal Care and Use Committee of China Academy of Chinese Medical Sciences.

2.2. Experimental Protocols. The present study consisted of 4 main parts. (1) The first detects the effect of ta-VNS, VNS, or transcutaneous electrical acupoint stimulation (TEAS) on ST36 on LPS-induced serum cytokine response. In this part, rats were randomly divided into 5 groups of twelve each: (a) saline-treated animals (NS), (b) endotoxemia model rats (LPS), (c) endotoxemia model rats receiving treatment of ta-VNS (ta-VNS), (d) endotoxemia model rats receiving treatment of VNS (VNS) and (e) endotoxemia model rats received treatment of TEAS on ST36 (ST36). (2) The second detects the effect of ta-VNS, VNS, or TEAS on ST36 on LPS-induced pulmonary NF- κ B p65 expression. In this part, rats were randomly divided into 6 groups, which consisted of the 5 groups aforementioned, and a group of saline-treated animals received treatment of ta-VNS (NS+ta-VNS). (3) The third observes the effect after vagotomy (VGX). In this part, rats were randomly divided into 4 groups: (a) saline-treated animals (NS), (b) endotoxemia model rats (LPS), (c) ta-VNS-treated animals following vagotomy

(VGX+LPS+ta-VNS), and (d) TEAS-treated animals following vagotomy (VGX+LPS+ST36). (4) The fourth observes the effect after α 7nAChR antagonist injection. Rats were randomly divided into 4 groups: (a) saline-treated animals (NS), (b) endotoxemia model rats (LPS), (c) ta-VNS-treated animals following α -bungarotoxin (α -BGT+LPS+ta-VNS), and (d) TEAS-treated animals following α -bungarotoxin (α -BGT+LPS+ST36).

2.3. Endotoxemia Model. LPS is an endotoxin derived from cell wall of gram-negative bacteria, and systemic injection of LPS results in various symptoms of bacterial infection including fever and inflammation [19]. Rats were injected intravenously with lipopolysaccharide (LPS, *Escherichia coli* 0111:B4; Sigma, 5 mg/kg), dissolved in sterile, pyrogen-free saline that was sonicated for 30 minutes immediately before use. Rats ($n = 12$ per group) were killed 2 hours after LPS injection (Figure 1), and the blood was collected from abdominal aorta, allowed to clot for 2 hours at room temperature, and then centrifuged at room temperature for 15 minutes at 2000 rpm. Serum samples were stored at -20°C before cytokine analysis. Lung samples were rapidly excised, rinsed of blood with normal saline, placed into liquid nitrogen immediately and then frozen and stored at -80°C till measurement of NF- κ B p65 expression.

2.4. Electrical Vagus Nerve Stimulation. Rats were anaesthetized with urethane (1 g/kg, intraperitoneally). A midline cervical incision was made to expose the left cervical branch of the vagus nerve. The left carotid sheath was isolated. After blunt preparation, the left vagus nerve trunk was carefully freed from surrounding tissue, separated from the carotid artery trunks, and placed on a custom-made bipolar platinum electrode connected via an isolation unit to a stimulator (SEN-7203, Nihon Kohden). All the exposed nerves were protected from dehydration by covering warm paraffin mineral oil tampons [6]. One and a half hour after LPS administration, constant electrical current stimuli with parameter of 1 mA, 10 Hz, 1 ms were turned on for 20 min (Figure 1(a)).

2.5. Transcutaneous Electrical Acupoint Stimulation (TEAS) on ST36. Transcutaneous surface electrodes were placed bilaterally on the depilatory rat skin at Zusanli (ST36). The ST36 points are located at 5 mm lateral to the anterior tubercle of the tibia and 10 mm below the knee joints. Bilateral surface electrodes at hind limbs were connected via an isolation unit to a stimulator (SEN-7203, Nihon Kohden), and the points were stimulated with the same parameter aforementioned. One and a half hour after LPS administration, the stimulation started and lasted for 20 min (Figure 1). Stimulation intensity was adjusted to a level that elicited a slight muscle twitch at the stimulated site and was limited to a maximum of 1 mA to minimize animal discomfort.

2.6. Transcutaneous Auricular Vagus Nerve Stimulation (ta-VNS). Transcutaneous surface electrodes were placed bilaterally on the auricular concha, which mainly includes cyma conchae and cavum conchae of the auricular. Bilateral surface electrodes at auricular concha were connected via an

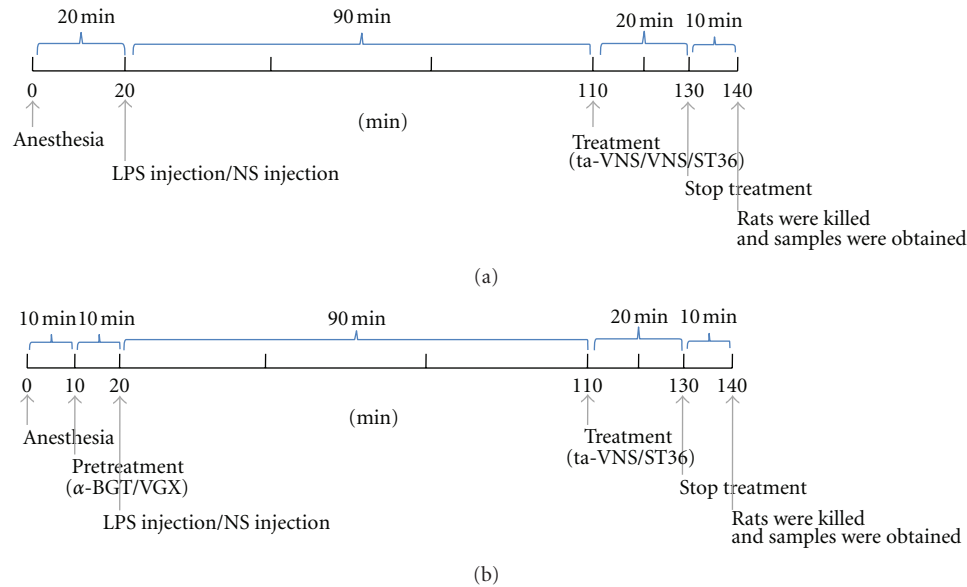


FIGURE 1: The time flow chart indicates the precise time for various operations in the present study, from the time point of anesthetic injection to the time point for sampling. (a) Twenty minutes after anesthesia, rats were injected intravenously with LPS or NS. One and a half hour after modeling, treatment (ta-VNS, VNS, or TEAS on ST36) was performed for twenty minutes. Two hours after LPS injection, rats were killed, and samples were collected. (b) Ten minutes after anesthesia, administration of α -BGT or vagotomy was performed. The rest of the operations were the same with the time flow in (a).

isolation unit to a stimulator (SEN-7203, Nihon Kohden), and the auricular conchae on both sides were stimulated with the same parameter. One and a half hour after LPS administration, the stimulation started and lasted for 20 min (Figure 1). Stimulation intensity was adjusted to a level that elicited a slight twitch of the auricle and was limited to maximum of 1 mA to minimize animal discomfort.

2.7. Vagotomy. Vagotomy was performed before LPS administration (Figure 1(b)). In vagotomized animals, following a ventral cervical midline incision, bilateral vagus trunks were exposed and separated from the common carotid artery, ligated with a 4-0 silk suture.

2.8. Administration of α 7nAChR Antagonist. The specific α 7nAChR antagonist α -bungarotoxin (α -BGT) was obtained from Alexis Biochemicals Corporation (San Diego, CA, USA). The drug was administered intravenously at a dose of 1 μ g/kg before LPS administration [20] (Figure 1(b)).

2.9. Cytokine Analysis. Abdominal aortic blood was collected two hours after LPS administration, allowed to clot for 2 h at room temperature, and centrifuged for 20 min at 2500 rpm. Serum TNF- α , IL-1 β , and IL-6 concentrations were analyzed, respectively, by TNF- α , IL-1 β , and IL-6 ELISA kits (R&D Systems) following the manufacturer's instructions.

2.10. Western Blot. Procedures of western blot analysis were followed as described previously [21]. Protein samples denatured in SDS sample buffer (125 mmol/L Tris-HCl, pH 6.8, 50% glycerol, 2% SDS, 5% mercaptoethanol, and 0.01% bromophenol blue) were subjected to SDS-PAGE and

blotted onto Immobilon-FL transfer membrane (Millipore). Blotted membranes were blocked with 5% skim milk in Tris-buffered saline containing 0.05% Tween-20 for 2 hours and were subsequently incubated with rabbit anti-human-NF- κ B (p65) (diluted 1/200; Santa Cruz Biotechnology Inc., CA, USA) overnight at 4°C. After three washes in Tris-buffered saline containing 0.05% Tween 20, the membranes were incubated with an anti-rabbit IgG antibody-HRP (diluted 1/4000; Santa Cruz Biotechnology Inc., CA, USA) for 1 hour. Quantification of western blots was performed by the Odyssey infrared imaging system (Li-Cor Biosciences) to detect protein expression.

2.11. NF- κ B Immune-Histochemistry. NF- κ B p65 immunohistochemistry staining was performed as described previously [22] to evaluate the lung tissues inflammatory response. Briefly, tissue sections were deparaffinized with xylene and rehydrated through graded series of alcohols. Tissue sections were rinsed in PBS, pretreated with citrate buffer at 93°C, blocked with PBS containing 2% BSA, and then incubated with a primary antibody reactive against rabbit-activated p65 subunit of NF- κ B (Santa Cruz Biotechnology Inc, Santa Cruz, CA, USA). Washed sections were incubated for 10 min with secondary goat anti-rabbit IgG biotin. The reaction product was visualized with DAB chromogenic agent. The sections were counterstained with hematoxylin stain. Slides were analysed on a light microscope (Olympus BX60) using an ImagePro Plus Imaging System (Universal Imaging).

2.12. Statistical Analysis. All the data in the present study were expressed as means \pm SEM and analyzed by one-way

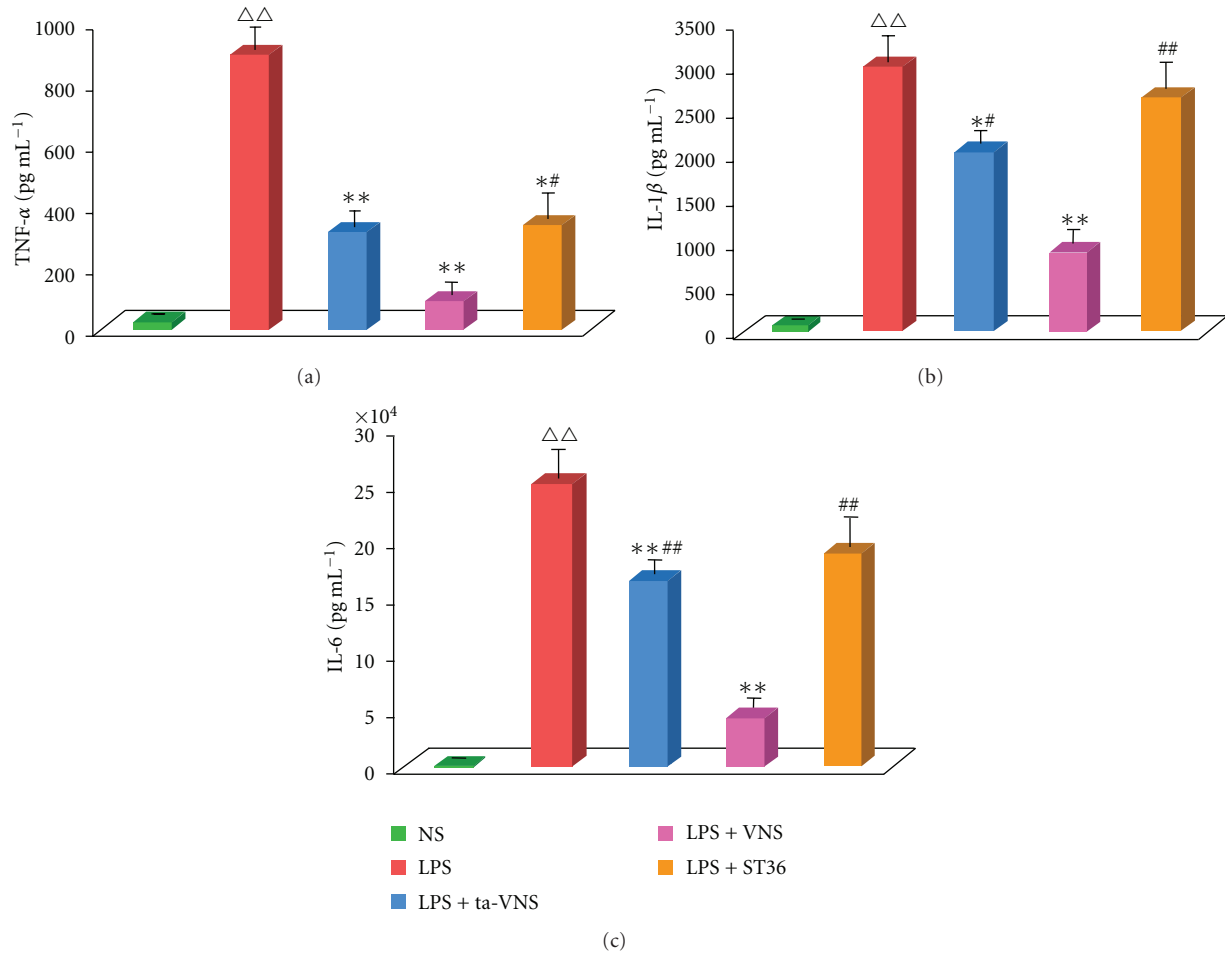


FIGURE 2: Vagus nerve stimulation (VNS) or transcutaneous auricular vagus nerve stimulation (ta-VNS) attenuates the LPS-induced serum cytokine (TNF- α , IL-1 β , and IL-6) response. TEAS on ST36 inhibited TNF- α level significantly. Serum TNF- α (a), IL-1 β (b), and IL-6 (c) contents were measured by ELISA. The columns represent mean \pm SEM for 12 animals in each group. $\Delta\Delta P < 0.01$ versus the normal saline (NS) group; $*P < 0.05$ versus LPS group (LPS); $**P < 0.01$ versus LPS group (LPS); $#P < 0.05$ versus LPS+VNS group; $##P < 0.01$ versus LPS+VNS group.

ANOVA with SPSS software. The two-tailed Student's t -test was used to compare mean values between two groups. P values < 0.05 were considered significant.

3. Results

3.1. Cytokine Levels in the Serum. LPS evoked an inflammatory response characterized by the upregulation of cytokine expressions. After systemic administration of LPS (5 mg/kg, i.v.), TNF- α (Figure 2(a)), IL-1 β (Figure 2(b)), and IL-6 (Figure 2(c)) increased significantly in sera. Both electrical VNS and ta-VNS strongly inhibited LPS-induced proinflammatory cytokine concentrations including TNF- α , IL-1 β , and IL-6 ($n = 12$, $P < 0.01$, $P < 0.05$, resp.). TEAS of ST36 lowered serum TNF- α level ($n = 12$, $P < 0.05$) in endotoxemic rats but failed to significantly alter serum IL-1 β and serum IL-6 levels.

3.2. The Effect of ta-VNS or TEAS on ST36 on Serum TNF- α Level Was Blocked by α -BGT Administration. The above

results showed that ta-VNS has similar effects to VNS on cytokine levels. Previous studies show that VNS-activated "cholinergic anti-inflammatory pathway" regulates systemic inflammatory responses via $\alpha 7$ nAChR, hereby ta-VNS may have the same effect. To test this hypothesis, we pretreated animals with the $\alpha 7$ nAChR antagonist α -BGT. LPS injection induced profound rise in the concentration of serum TNF- α . Either ta-VNS or TEAS on ST36 failed to inhibit TNF- α level after α -BGT administration (Figure 3).

3.3. Effect of ta-VNS or TEAS on ST36 on Serum TNF- α Was Blunted by Vagotomy. To examine the mechanism of ta-VNS in "cholinergic anti-inflammatory pathway," we pretreated animals with vagotomy. The result indicated that intravenous injection of LPS elicited a rapid raise of TNF- α level. Neither ta-VNS nor TEAS on ST36 was effective on inhibiting TNF- α level after vagotomy (Figure 4).

3.4. NF-Kappa B p65 Expressions in Lung Tissues. The systemic administration of LPS was followed with a significantly

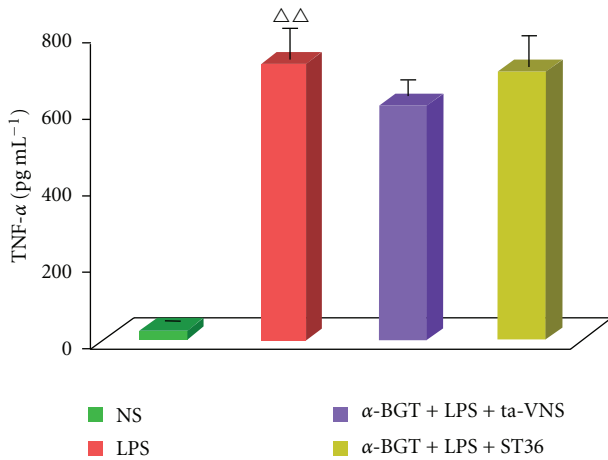


FIGURE 3: ta-VNS or TEAS on ST36 with α -bungarotoxin (α -BGT) administration fails to inhibit the LPS-induced serum TNF- α response. Serum TNF- α concentrations were measured by ELISA. Data are expressed as mean \pm SEM ($n = 12$ per group). $\Delta\Delta P < 0.01$ versus the normal saline (NS) group.

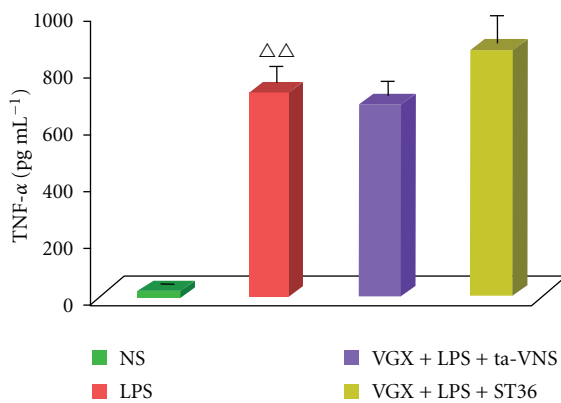


FIGURE 4: ta-VNS or ST36 stimulation with bilateral cervical vagotomy (VGX) fails to inhibit the LPS-induced serum TNF- α response. TNF- α amounts were measured by ELISA. Data are expressed as mean \pm SEM ($n = 12$ per group). $\Delta\Delta P < 0.01$ versus the normal saline (NS) group.

increased expression of NF- κ B p65 in lung tissues (Figures 4 and 5). Both electrical VNS and ta-VNS strongly inhibited LPS-induced NF- κ B p65 ($n = 10$, $P < 0.01$, Figures 4 and 5). TEAS on ST36 did not have the same effect (Figures 5 and 6).

3.5. Effect of ta-VNS or TEAS on ST36 on NF- κ B p65 Was Blunted by Vagotomy. We pretreated animals with vagotomy. The result indicated that ta-VNS or ST36 failed to inhibit the expressions of NF- κ B p65 after vagotomy (Figure 7).

4. Discussion

Here, we reported our original study that auricular concha stimulation is also a potent anti-inflammatory stimulus that can modulate immune factors in endotoxemia rat model. The present study demonstrates that ta-VNS may have an

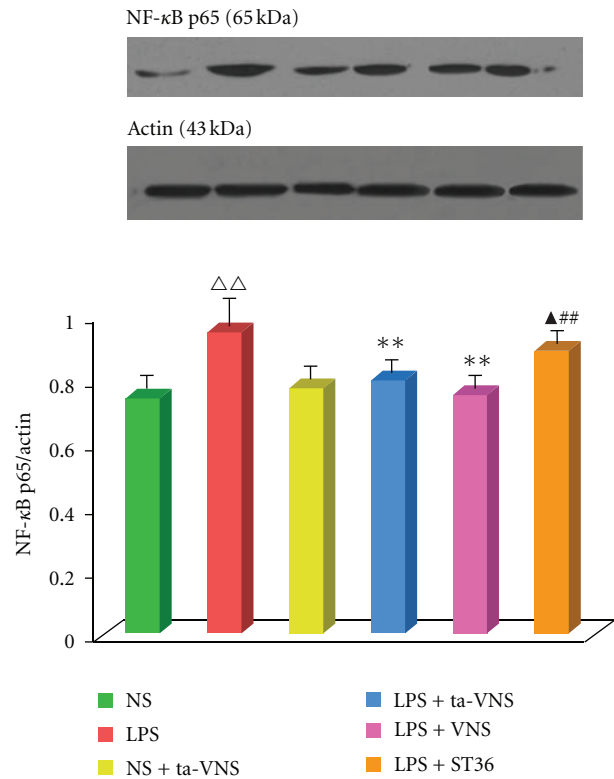


FIGURE 5: VNS or ta-VNS suppresses LPS-induced NF- κ B expression; ST36 stimulation did not affect NF- κ B in endotoxemia animals significantly. ta-VNS did not significantly affect pulmonary NF- κ B expression with normal saline administration. NF- κ B expressions were measured by western blot technique. Data are shown by mean \pm SEM ($n = 12$ per group). $\Delta\Delta P < 0.01$ versus normal saline (NS) group; $**P < 0.01$ versus LPS group (LPS); $##P < 0.01$ versus LPS+VNS group; $\Delta P < 0.05$ versus LPS+ta-VNS.

important role in suppressing inflammatory responses, and this contributes to the involvement of the cholinergic anti-inflammatory pathway in the mechanism.

Previous study demonstrated that the cholinergic anti-inflammatory pathway is a $\alpha 7$ nAChR-dependent, vagus nerve-mediated pathway [1]. It can inhibit macrophage activation through parasympathetic outflow, which functions as an anti-inflammatory pathway in systemic and local inflammation. Inflammatory signals stimulate sensory fibers that ascend in the vagus nerve to synapse in the NTS and then activate efferent fibers in the vagus nerve to suppress peripheral cytokine release through $\alpha 7$ nAChR.

The most important cytokine involved is TNF- α , which activates other proinflammatory cytokines such as IL-1 β , IL-6, and high mobility group B1 (HMGB1) and amplifies other inflammatory mediators. VNS has been demonstrated to inhibit proinflammatory cytokine production [23–25], especially the release and synthesis of TNF- α . The present study indicates that VNS decreases LPS-induced TNF- α , IL-1, and IL-6 in circulation. And ta-VNS reduced the levels of proinflammatory cytokines TNF- α , IL-1 β , and IL-6, which is similar to the effect of VNS. After administration of $\alpha 7$ nAChR antagonist α -BGT, ta-VNS failed to attenuate

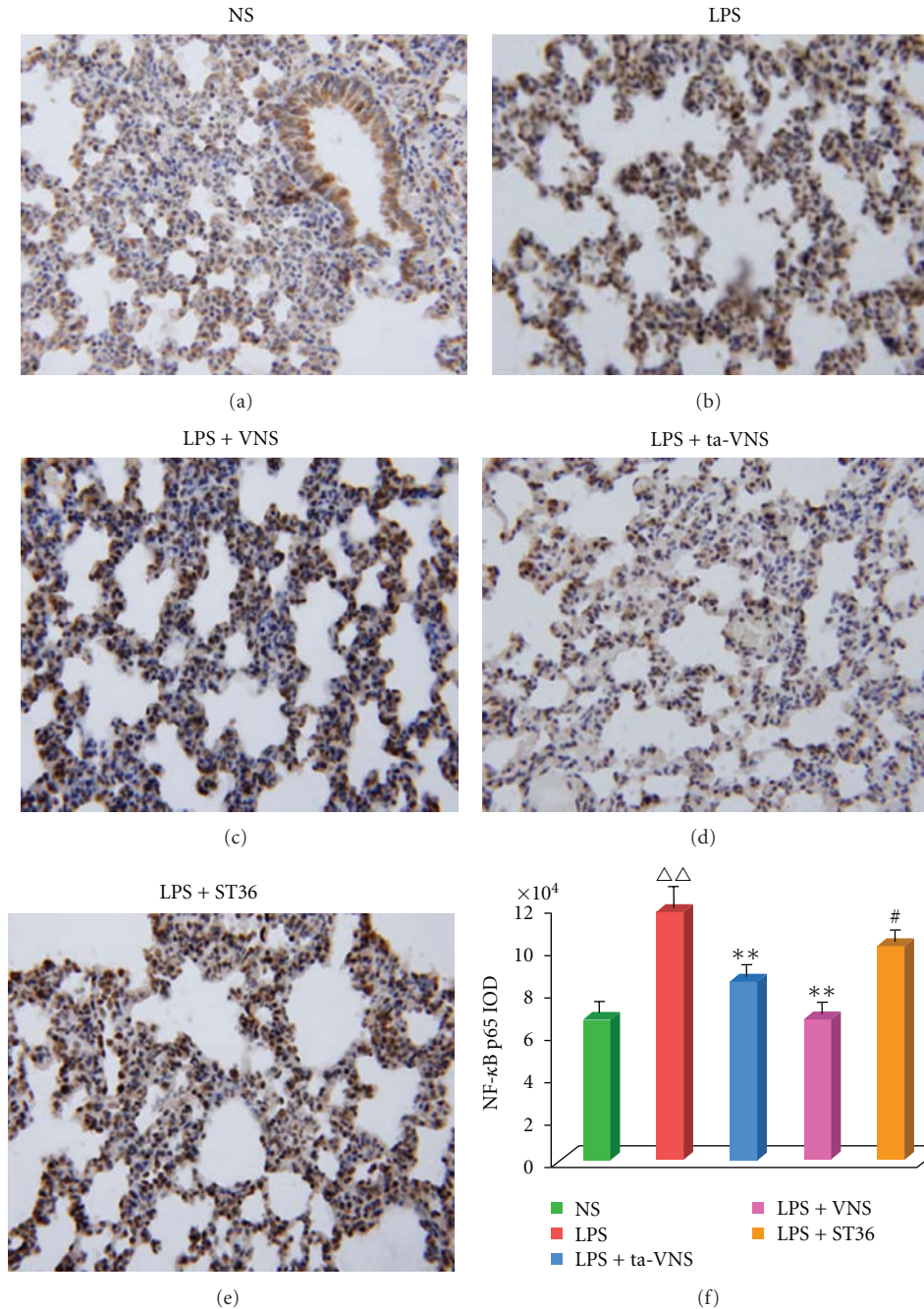


FIGURE 6: Immunohistochemical staining with anti-NF- κ B antibodies reveals significant decrease in LPS-induced NF- κ B immunoreactivity evoked by interventions as of VNS, ta-VNS, and TEAS on ST36. Data are expressed as mean \pm SEM ($n = 12$ per group). $\Delta\Delta P < 0.01$ versus the normal saline (NS) group; $**P < 0.01$ versus LPS group (LPS); $\#P < 0.05$ versus LPS+VNS group. Original magnification: $\times 400$.

serum TNF- α level, which is consistent with previous reports [6–10, 20, 23]. This result indicated that $\alpha 7$ nAChR played a critical role in anti-inflammatory effect of ta-VNS. The present study also demonstrated that vagotomy exacerbated serum TNF responses to inflammatory stimulation, sensitized animals to the lethal effects of endotoxin, and abolished the anti-inflammatory effect of ta-VNS. The results indicated that ta-VNS fails to suppress excessive cytokine response

characterized by exaggerated TNF- α level if there is deficiency in either the $\alpha 7$ nAChR subunit or vagus nerve.

NF- κ B is a master transcription factor controlling the expression of a wide range of proinflammatory genes [26–28]. Previous studies reported that NF- κ B is involved in TNF- α genetic activation and TNF- α production [29, 30]. In the present study, both western blot data and immunohistochemical results indicated that ta-VNS suppresses the

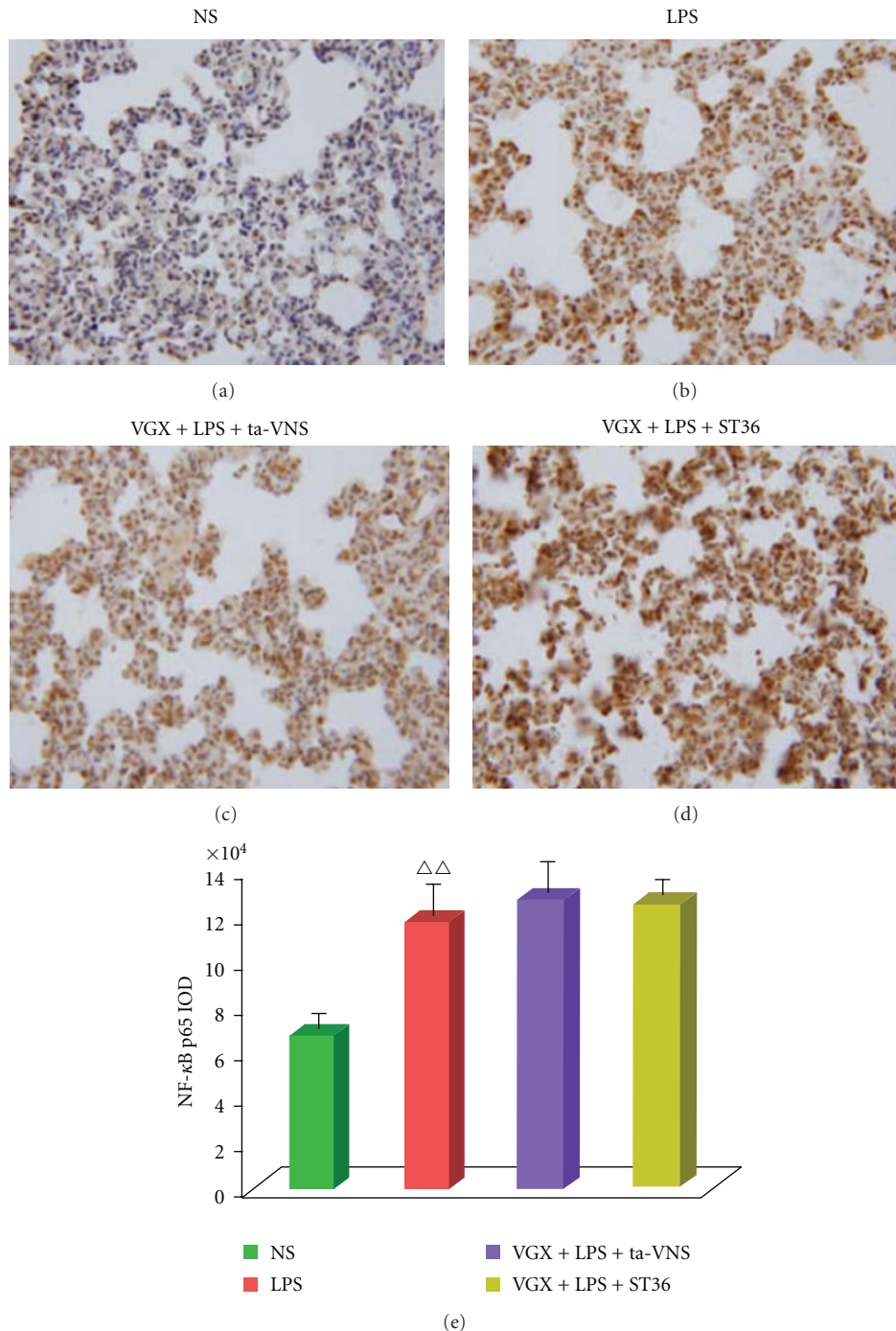


FIGURE 7: ta-VNS or ST36 stimulation with bilateral cervical vagotomy (VGX) fails to inhibit the LPS-induced overexpression of NF- κ B. NF- κ B distribution was measured by immunohistochemical staining. Data are shown as mean \pm SEM ($n = 12$ per group). $\Delta\Delta P < 0.01$ versus the normal saline (NS) group. Original magnification: $\times 400$.

LPS-induced NF- κ B expression in rat lung tissue (Figures 4 and 5), which mimicking the effects of VNS [25, 31]. In vagotomy animals, ta-VNS failed to inhibit increased NF- κ B expression, suggesting ta-VNS functions in situations that require intact vagus nerve.

Some investigators demonstrated that electroacupuncture (EA, on ST36, PC6, and GV20) could increase the vagal activity of experimental animals and human subjects

[13–17, 32–34]. The present study demonstrated that TEAS on ST36 decreased serum TNF- α level in endotoxemia rats. After pretreatment with vagotomy or $\alpha 7$ nAChR antagonist α -BGT, TEAS failed to inhibit serum proinflammatory level in LPS-induced endotoxemia animals.

Auricular acupuncture, as a special form of acupuncture, has been used for the treatment of different disorders for centuries in China. Our research group previously demonstrated

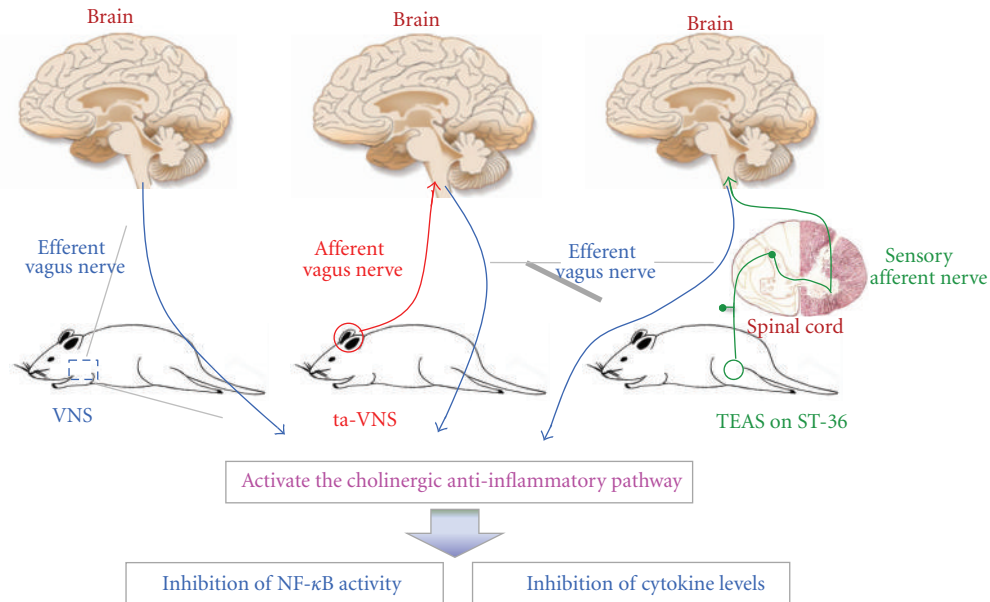


FIGURE 8: The anti-inflammatory mechanisms of the three interventions used in the present study might be as follows: (1) VNS directly activates the cholinergic anti-inflammatory pathway via stimulating efferent vagus nerve. (2) ta-VNS evoked the activity of the auricular branch of vagus nerve (ABVN). The activated signals ascending within afferent vagus nerve are transmitted to the nucleus tractus solitarius. The integrated output is carried by the efferent vagus nerve to inhibit inflammatory responses. (3) TEAS on ST36 activates the somatic fiber endings of the skin around ST36 point, sending signals to the spinal cord via somatic sensory nerve fibers. The nerve impulses were relayed and integrated by NTS by the secondary order neurons in the spinal cord, and the cholinergic anti-inflammatory pathways are activated by the increased efferent vagal output.

that auricular acupuncture stimulation could activate neurons of NTS and upregulate vagal tone, to decrease MAP and HR [35], to trigger gastric motility [36]. Our previous studies also demonstrated that TEAS of auricular concha could activate the parasympathetic nervous system and mimic the effect of VNS to suppress epileptic seizures [18]. In the present study, the results showed that ta-VNS inhibited proinflammatory cytokine levels and suppressed NF- κ B expressions in endotoxaemia rats (Figures 1, 4, and 5), which is similar to the effect of VNS. However, vagotomy or α 7nAChR antagonist α -BGT could diminish the effect of ta-VNS on the anti-inflammatory responses, suggesting that auricular acupuncture may perform an anti-inflammatory effect via cholinergic anti-inflammatory pathway.

In general (Figure 8), VNS directly activates the cholinergic anti-inflammatory pathway via stimulating efferent vagus nerve. As the peripheral branch [18], auricular branch of vagus nerve (ABVN) innervates the auricular concha and the external auditory meatus. Stimulation of the ABVN region could evoke parasympathetic excitation [37–39]. Acupuncture in the area of auricular concha may increase discharge of NTS [18], as the central terminal nuclear for afferent vagal fibers, which primarily transmit signals from local inflammation lesion [4, 40]. Thus, we hypothesize that ABVN could be evoked by ta-VNS, and the activated signals ascend with vagal input to the NTS. The signals are processed within the NTS, and the integrated output signal is carried by efferent vagus nerve to inhibit inflammatory responses. TEAS on the acupoint of ST36 activates the somatic fiber endings around ST36 point, which send the acupuncture

signals to the spinal cord via somatic sensory nerve fibers. In the spinal cord, the nerve impulses are delivered to the NTS by the secondary order neurons, where the signals were processed. Ultimately, the increased efferent vagal output activates the cholinergic anti-inflammatory pathway.

5. Conclusions

The results presented here demonstrate that ta-VNS plays an important role in immunoregulation, through the activation of the cholinergic anti-inflammatory pathway and the down-regulation of proinflammatory cytokine expressions and NF- κ B activities. VNS and TEAS on ST36 might suppress the inflammatory responses via different mechanisms.

Abbreviations

ta-VNS:	Transcutaneous auricular vagus nerve stimulation
LPS:	lipopolysaccharide
NTS:	Nucleus tractus solitarius
DMN:	Dorsal motor nucleus of the vagus
VNS:	Vagus nerve stimulation
TEAS:	Transcutaneous electric acupoint stimulation
Ach:	Acetylcholine
α 7nAChR:	Nicotinic acetylcholine receptors
NF- κ B p65:	NF-kappa B p65
TNF- α :	Tumour necrosis factor-alpha
IL-1 β :	Interleukin-1 beta

IL-6: Interleukin-6
 α -BGT: α -Bungarotoxin
 NS: Normal saline
 VGX: Vagotomy
 ABVN: Auricular branch of vagus nerve.

Acknowledgments

The authors thank Dr. Gao Xinyan for her excellent editorial assistance. They thank Dr. Qiao Haifa for his critical reading of the paper. This work was supported by the National Basic Research Program (973 Program, no. 2011CB505201), the National Natural Science Foundation of China Research Grants (nos. 30973798 and 30901931), and the Beijing Natural Science Foundation (no. 7111007).

References

- [1] K. J. Tracey, "The inflammatory reflex," *Nature*, vol. 420, no. 6917, pp. 853–859, 2002.
- [2] K. J. Tracey, Y. Fong, D. G. Hesse et al., "Anti-cachectin/TNF monoclonal antibodies prevent septic shock during lethal bacteraemia," *Nature*, vol. 330, no. 6149, pp. 662–664, 1987.
- [3] K. J. Tracey, B. Beutler, and S. F. Lowry, "Shock and tissue injury induced by recombinant human cachectin," *Science*, vol. 234, no. 4775, pp. 470–474, 1986.
- [4] V. A. Pavlov and K. J. Tracey, "The cholinergic anti-inflammatory pathway," *Brain, Behavior, and Immunity*, vol. 19, no. 6, pp. 493–499, 2005.
- [5] J. M. Huston, M. Gallowitsch-Puerta, M. Ochani et al., "Transcutaneous vagus nerve stimulation reduces serum high mobility group box 1 levels and improves survival in murine sepsis," *Critical Care Medicine*, vol. 35, no. 12, pp. 2762–2768, 2007.
- [6] L. V. Borovikova, S. Ivanova, M. Zhang et al., "Vagus nerve stimulation attenuates the systemic inflammatory response to endotoxin," *Nature*, vol. 405, no. 6785, pp. 458–462, 2000.
- [7] J. Huang, Y. Wang, D. Jiang, J. Zhou, and X. Huang, "The sympathetic-vagal balance against endotoxemia," *Journal of Neural Transmission*, vol. 117, no. 6, pp. 729–735, 2010.
- [8] D. J. van Westerloo, I. A. J. Giebelen, J. C. M. Meijers et al., "Vagus nerve stimulation inhibits activation of coagulation and fibrinolysis during endotoxemia in rats," *Journal of Thrombosis and Haemostasis*, vol. 4, no. 9, pp. 1997–2002, 2006.
- [9] T. R. Bernik, S. G. Friedman, M. Ochani et al., "Pharmacological stimulation of the cholinergic antiinflammatory pathway," *Journal of Experimental Medicine*, vol. 195, no. 6, pp. 781–788, 2002.
- [10] S. Guarini, D. Altavilla, M. M. Cainazzo et al., "Efferent vagal fibre stimulation blunts nuclear factor- κ B activation and protects against hypovolemic hemorrhagic shock," *Circulation*, vol. 107, no. 8, pp. 1189–1194, 2003.
- [11] M. Li, C. Zheng, T. Sato, T. Kawada, M. Sugimachi, and K. Sunagawa, "Vagal nerve stimulation markedly improves long-term survival after chronic heart failure in rats," *Circulation*, vol. 109, no. 1, pp. 120–124, 2004.
- [12] C. Mioni, C. Bazzani, D. Giuliani et al., "Activation of an efferent cholinergic pathway produces strong protection against myocardial ischemia/reperfusion injury in rats," *Critical Care Medicine*, vol. 33, no. 11, pp. 2621–2628, 2005.
- [13] S. T. Huang, G. Y. Chen, H. M. Lo, J. G. Lin, Y. S. Lee, and C. D. Kuo, "Increase in the vagal modulation by acupuncture at Neiguan point in the healthy subjects," *American Journal of Chinese Medicine*, vol. 33, no. 1, pp. 157–164, 2005.
- [14] Z. Li, K. Jiao, M. Chen, and C. Wang, "Effect of magnitopuncture on sympathetic and parasympathetic nerve activities in healthy driver—assessment by power spectrum analysis of heart rate variability," *European Journal of Applied Physiology*, vol. 88, no. 4-5, pp. 404–410, 2003.
- [15] J. H. Wu, H. Y. Chen, Y. J. Chang et al., "Study of autonomic nervous activity of night shift workers treated with laser acupuncture," *Photomedicine and Laser Surgery*, vol. 27, no. 2, pp. 273–279, 2009.
- [16] C. C. Hsu, C. S. Weng, T. S. Liu, Y. S. Tsai, and Y. H. Chang, "Effects of electrical acupuncture on acupoint BL15 evaluated in terms of heart rate variability, pulse rate variability and skin conductance response," *American Journal of Chinese Medicine*, vol. 34, no. 1, pp. 23–36, 2006.
- [17] K. Imai and H. Kitakoji, "Comparison of transient heart rate reduction associated with acupuncture stimulation in supine and sitting subjects," *Acupuncture in Medicine*, vol. 21, no. 4, pp. 133–137, 2003.
- [18] W. He, P. J. Rong, L. Li, H. Ben, B. Zhu, and G. Litscher, "Auricular acupuncture may suppress epileptic seizures via activating the parasympathetic nervous system: a hypothesis based on innovative methods," *Evidence-Based Complementary and Alternative Medicine*, vol. 2012, Article ID 615476, 5 pages, 2012.
- [19] L. Bertók, "Endotoxins and endocrine system," *Domestic Animal Endocrinology*, vol. 15, no. 5, pp. 305–308, 1998.
- [20] H. Wang, M. Yu, M. Ochani et al., "Nicotinic acetylcholine receptor $\alpha 7$ subunit is an essential regulator of inflammation," *Nature*, vol. 421, no. 6921, pp. 384–388, 2003.
- [21] W. Deng, X. Wang, J. Xiao et al., "Loss of regulator of G protein signaling 5 exacerbates obesity, hepatic steatosis, inflammation and insulin resistance," *PLoS ONE*, vol. 7, no. 1, Article ID e30256, 2012.
- [22] O. J. D'Cruz and F. M. Uckun, "Preclinical evaluation of a dual-acting microbicidal prodrug WHI-07 in combination with vanadocene dithiocarbamate in the female reproductive tract of rabbit, pig, and cat," *Toxicologic Pathology*, vol. 35, no. 7, pp. 910–927, 2007.
- [23] J. M. Huston, M. Ochani, M. Rosas-Ballina et al., "Splenectomy inactivates the cholinergic antiinflammatory pathway during lethal endotoxemia and polymicrobial sepsis," *Journal of Experimental Medicine*, vol. 203, no. 7, pp. 1623–1628, 2006.
- [24] T. R. Bernik, S. G. Friedman, M. Ochani et al., "Cholinergic antiinflammatory pathway inhibition of tumor necrosis factor during ischemia reperfusion," *Journal of Vascular Surgery*, vol. 36, no. 6, pp. 1231–1236, 2002.
- [25] D. Altavilla, S. Guarini, A. Bitto et al., "Activation of the cholinergic anti-inflammatory pathway reduces NF- κ B activation, blunts TNF- α production, and protects against splanchnic artery occlusion shock," *Shock*, vol. 25, no. 5, pp. 500–506, 2006.
- [26] P. A. Bauerle and D. Baltimore, "NF- κ B: ten years after," *Cell*, vol. 87, no. 1, pp. 13–20, 1996.
- [27] M. L. Schmitz and P. A. Bauerle, "Multi step activation of NF- κ B/rel transcriptional factors," *Immunobiology*, vol. 193, no. 2–4, pp. 116–127, 1995.
- [28] R. Schreck, P. Rieber, and P. A. Bauerle, "Reactive oxygen intermediates as apparently widely used messengers in the activation of the NF- κ B transcription factor and HIV-1," *EMBO Journal*, vol. 10, no. 8, pp. 2247–2258, 1991.
- [29] F. Squadrito, D. Altavilla, B. Deodato et al., "Early activation of transcription factor NF- κ B in splanchnic artery occlusion shock," in *Proceedings of the 5th World Congress on Trauma*

Shock Inflammation and Sepsis Pathophysiology Immune Consequences and Therapy, E. Faist, Ed., pp. 389–394, Monduzzi, Munich, Germany, March 2000.

- [30] C. O'Mahony, "Loss of vagal anti-inflammatory effect: in vivo visualization and adoptive transfer," *American Journal of Physiology*, vol. 297, no. 4, pp. R1118–R1126, 2009.
- [31] X. M. Song, J. G. Li, Y. L. Wang et al., "The protective effect of the cholinergic anti-inflammatory pathway against septic shock in rats," *Shock*, vol. 30, no. 4, pp. 468–472, 2008.
- [32] K. Imai, H. Ariga, C. Chen, C. Mantyh, T. N. Pappas, and T. Takahashi, "Effects of electroacupuncture on gastric motility and heart rate variability in conscious rats," *Autonomic Neuroscience: Basic and Clinical*, vol. 138, no. 1-2, pp. 91–98, 2008.
- [33] H. Ouyang, J. Yin, Z. Wang, P. J. Pasricha, and J. D. Z. Chen, "Electroacupuncture accelerates gastric emptying in association with changes in vagal activity," *American Journal of Physiology*, vol. 282, no. 2, pp. G390–G396, 2002.
- [34] Q. Wang, F. Wang, X. Li et al., "Electroacupuncture pretreatment attenuates cerebral ischemic injury through $\alpha 7$ nicotinic acetylcholine receptor-mediated inhibition of high-mobility group box 1 release in rats," *Journal of Neuroinflammation*, vol. 9, article 24, 2012.
- [35] X. Y. Gao, Y. H. Li, K. Liu et al., "Acupuncture-like stimulation at auricular point Heart evokes cardiovascular inhibition via activating the cardiac-related neurons in the nucleus tractus solitarius," *Brain Research*, vol. 1397, pp. 19–27, 2011.
- [36] X. Y. Gao, S. P. Zhang, B. Zhu, and H. Q. Zhang, "Investigation of specificity of auricular acupuncture points in regulation of autonomic function in anesthetized rats," *Autonomic Neuroscience*, vol. 138, no. 1-2, pp. 50–56, 2008.
- [37] I. Tekdemir, A. Asian, and A. Elhan, "A clinico-anatomic study of the auricular branch of the vagus nerve and Arnold's ear-cough reflex," *Surgical and Radiologic Anatomy*, vol. 20, no. 4, pp. 253–257, 1998.
- [38] D. Gupta, S. Verma, and S. K. Vishwakarma, "Anatomic basis of Arnold's ear-cough reflex," *Surgical and Radiologic Anatomy*, vol. 8, no. 4, pp. 217–220, 1986.
- [39] D. Engel, "The gastroauricular phenomenon and related vagus reflexes," *Archiv fur Psychiatrie und Nervenkrankheiten*, vol. 227, no. 3, pp. 271–277, 1979.
- [40] V. A. Pavlov, H. Wang, C. J. Czura, S. G. Friedman, and K. J. Tracey, "The cholinergic anti-inflammatory pathway: a missing link in neuroimmunomodulation," *Molecular Medicine*, vol. 9, no. 5–8, pp. 125–134, 2003.

Research Article

Inhibition of Activity of GABA Transporter GAT1 by δ -Opioid Receptor

Lu Pu,^{1,2,3} Nanjie Xu,² Peng Xia,² Quanbao Gu,^{1,2,4} Shuanglai Ren,^{4,5} Thomas Fucke,^{1,6} Gang Pei,² and Wolfgang Schwarz^{1,4,7}

¹Max-Planck-Institute for Biophysics, Max-von-Laue-Straße 3, 60438 Frankfurt, Germany

²Laboratory of Molecular Cell Biology, Institute of Biochemistry and Cell Biology and Max-Planck Guest Laboratory, Shanghai Institutes for Biological Sciences, Chinese Academy of Sciences, 320 Yue Yang Road, Shanghai 200031, China

³Department of Neurobiology and Behavior, Center for the Neurobiology of Learning and Memory, University of California, Irvine, CA 92697, USA

⁴Shanghai Research Center for Acupuncture and Meridians, 199 Guoshoujing Road, Shanghai 201203, China

⁵Ningxia Key Lab of Cerebrocranial Disease, Ningxia Medical University, 1160 Shengli Street, Ningxia Hui Autonomous Region, Yinchuan 750004, China

⁶Central Institute of Mental Health, BCCN Heidelberg-Mannheim, J5, 68159 Mannheim, Germany

⁷Institute for Biophysics, Goethe-University Frankfurt, Max-von-Laue-Straße 1, 60438 Frankfurt, Germany

Correspondence should be addressed to Wolfgang Schwarz, schwarz@biophys.eu

Received 11 September 2012; Revised 4 November 2012; Accepted 4 November 2012

Academic Editor: Ying Xia

Copyright © 2012 Lu Pu et al. This is an open access article distributed under the Creative Commons Attribution License, which permits unrestricted use, distribution, and reproduction in any medium, provided the original work is properly cited.

Analgesia is a well-documented effect of acupuncture. A critical role in pain sensation plays the nervous system, including the GABAergic system and opioid receptor (OR) activation. Here we investigated regulation of GABA transporter GAT1 by δ OR in rats and in *Xenopus* oocytes. Synaptosomes of brain from rats chronically exposed to opiates exhibited reduced GABA uptake, indicating that GABA transport might be regulated by opioid receptors. For further investigation we have expressed GAT1 of mouse brain together with mouse δ OR and μ OR in *Xenopus* oocytes. The function of GAT1 was analyzed in terms of Na⁺-dependent [³H]GABA uptake as well as GAT1-mediated currents. Coexpression of δ OR led to reduced number of fully functional GAT1 transporters, reduced substrate translocation, and GAT1-mediated current. Activation of δ OR further reduced the rate of GABA uptake as well as GAT1-mediated current. Coexpression of μ OR, as well as μ OR activation, affected neither the number of transporters, nor rate of GABA uptake, nor GAT1-mediated current. Inhibition of GAT1-mediated current by activation of δ OR was confirmed in whole-cell patch-clamp experiments on rat brain slices of periaqueductal gray. We conclude that inhibition of GAT1 function will strengthen the inhibitory action of the GABAergic system and hence may contribute to acupuncture-induced analgesia.

1. Introduction

Neurotransmitter transporters play a key role in the regulation of synaptic transmission. Glutamate and GABA are the dominating excitatory and inhibitory neurotransmitters in the mammalian brain, respectively. The predominate transporters controlling glutamate and GABA in the CNS are the excitatory neurotransmitter transporter EAAC1 [1–3] and the GABA transporter GAT1 [4].

It is generally accepted that pain sensation can be suppressed by acupuncture and that regulation of the glutamatergic and the GABAergic systems is involved in

pain sensation [5]. Inhibition of the excitatory glutamatergic system and stimulation of the inhibitory system will contribute to analgesia. It could be demonstrated that inhibition of excitatory amino acid (EA) receptors [6, 7] and stimulation of GABA-A and GABA-B receptor [5, 8] resulted in pain suppression. Indirect reduction of EA-receptor activity may also be achieved by reduced glutamate concentration in the synaptic cleft, and reduction of glutamate concentration can be achieved by stimulating EAAC activity [9, 10]. In analogy to stimulation of EAAC1, we may expect for the GABAergic system that inhibition of the GABA transporter will result in elevation

of GABA concentration in the synaptic cleft and hence in stimulation of GABA receptor activity; this could contribute to increased inhibitory synaptic transmission and also to reduced pain sensation. Indeed, experiments with transgenic mice with knockout or overexpressed GABA transporters GAT1 have demonstrated that the GAT1 is correspondingly involved in pain sensation [11]. In these experiments it could also be shown that application of GAT1-selective inhibitors, ethyl nipecotate and NO-711, led to analgesia. Though GAT1 is the dominating neuronal GABA transporter, involvement of nonneuronal transporters cannot be excluded.

GAT1 belongs to a family of secondary active systems (see [12]) that are driven by electrochemical gradients for Na^+ and Cl^- . The transport of one GABA is coupled to the cotransport of two Na^+ and one Cl^- [13–18]. As a consequence of the stoichiometry, the translocation of GABA across the cell membrane is associated with a current that can be measured under voltage clamp. In the absence of GABA, the transport cycle is not completed, but transient charge movements can be detected; they reflect extracellular Na^+ binding within the electrical field preceding binding of GABA [19–22]. The GAT1-mediated steady-state current, on the other hand, often reflects only in part the translocation of GABA; another component of GAT1-mediated current represents uncoupled flow of ions through a channel-like mode (see, e.g., [15, 18, 23]).

It was shown previously [24] that acupuncture leads to activation of enkephalinergic neurons and release of endogenous morphines, the endorphins. Activation of opioid receptors has also been shown to regulate pain sensation, and the role of δOR in pain modulation is intriguing [25, 26]. Importantly, δOR has been found to be increasingly targeted to the plasma membrane in the spinal cord dorsal horn in inflammation [27]. Loss of synaptic inhibition including GABAergic inhibition in the spinal dorsal horn is considered to contribute significantly to several forms of chronic pain [8, 28], and regulation of GABA transport has been shown to control pain sensation [11, 29]. Since control and termination of synaptic activity play important roles in physiological and pathophysiological brain functions, regulation of the GABA transporter, which controls the dominating inhibitory transmitter in extracellular space, is a crucial mechanism to regulate neural circuits.

In the present study, potential effects of opiates on GABA transporter were examined, and we found that chronic exposure of rats to morphine reduced GABA uptake into synaptosomes. We have previously shown [9] that the glutamate transporter EAAC1 is downregulated by intermolecular interaction with the Gi-protein-coupled δ -opioid receptor of mouse (δOR) [30] and that this inhibitory interaction is counteracted by activation of the δOR [9]. In the work described here, we present evidence that the δOR interferes with functional surface expression of the GABA transporter GAT1 and that δOR activation results in reduced activity of the GAT1.

2. Materials and Methods

2.1. Experiments on Animals and Synaptosomes. For studying effects of opiates in animal experiments, male Sprague-Dawley rats (200–220 g, Laboratory Animal Center, Chinese Academy of Sciences, Shanghai, China) were used. All experiments were carried out strictly in accordance with the National Institutes of Health Guide for the Care and Use of Laboratory Animals.

Rats were exposed to opioids by s.c. injection of morphine (10 mg/kg) twice per day at 12 h intervals for a period of 10 days as described recently [31, 32]. Control rats were treated similarly, except saline was used throughout. After decapitation of rats, the brains were removed and cooled briefly in chilled balanced salt solution (in mM): 126 NaCl, 5 KCl, 1.25 NaH_2PO_4 , 10 glucose, 25 NaHCO_3 , 2 CaCl_2 , and 2 MgSO_4 , (pH 7.4). Thereafter, hippocampi were rapidly dissected. Hippocampi express both GAT1 [33] and δOR in GABAergic cells [34]. Subcellular fractions were prepared according to standard methods as described previously [35]. The purified synaptosomes were from P2 fraction of the brain lysate [36].

GABA uptake of synaptosomes was initiated by adding 4 nM [^3H]-GABA (Amersham Pharmacia Biotech, Buckinghamshire, UK) and 30 μM unlabeled GABA in a final volume of 500 μL KRH (Krebs Ringer's/HEPES) medium [37]. After incubation at 37°C for 5 min, the uptake was terminated by filtration on a GF/C filter (Whatman) under vacuum, and the filter was washed five times with 10 mL of cold KRH medium. Finally, filters containing synaptosomal particles or neuronal lysates were processed for scintillation counting (Beckman Instruments, Torrance, CA). Nonspecific uptake was determined using Na^+ -free media to block GABA transport.

2.2. Experiments on Oocytes. *Xenopus* oocytes were obtained as described previously (see, e.g., [38]). Full-grown prophase-arrested oocytes were injected with cRNA for GAT1 or/and δOR of mouse brain or μOR of rat brain, or for the rat $\alpha\beta\text{Na}^+$, K^+ pump. cDNA for GAT1 was kindly provided by Dr. Jian Fei (Shanghai, Tongji University). The cells together with noninjected control oocytes were stored at 19°C in oocyte Ringer's solution (ORi (in mM): 90 NaCl, 2 KCl, 2 CaCl_2 , 5 MOPS (adjusted to pH 7.4 with Tris)) containing 70 mg/L gentamicin. The agonist of δOR , [$\text{D-Pen}^{2,5}$]-enkephalin (DPDPE), the agonist [$\text{D-Ala}^2, \text{N-Me-Phe}^4, \text{Gly}^5\text{-ol}$]-enkephalin (DAMGO) of μOR , and the general opioid receptor antagonist naloxone (Sigma) were added at the respective concentrations to ORi. Experiments were performed at room temperature (about 22°C) after 3–5 days of incubation.

Membrane currents were recorded under conventional two-electrode voltage clamp (TurboTec, NPI, Tamm, Germany) during rectangular 200 ms voltage-clamp pulses (from -150 to $+30$ mV in 10 mV increments that were applied from a holding potential of -60 mV (see, e.g., [39])). Voltage dependencies of steady-state and transient membrane currents were analyzed [21]. Steady-state current was determined at the end of the voltage pulses (averaged during

the last 20 ms), and transient currents were analyzed from the entire time course during the respective voltage step.

GAT1-mediated currents were calculated as the difference of current in the presence and absence of GABA. Current values determined before and after the application of GABA were averaged to correct for small drifts with time.

To determine maximum transport activity, uptake of ^3H -labeled GABA (Amersham, Braunschweig, Germany) was measured at 90 mM external Na^+ as describe previously [21] using a total concentration of 100 μM GABA. The number of Na^+ , K^+ pump molecules in the oocyte surface membrane was determined by [^3H]-ouabain binding; the oocytes were preloaded with Na^+ by incubating the cells for 40 min in solution that had the following composition (in mM): 110 NaCl, 2.5 sodium citrate, and 5 MOPS (adjusted to pH 7.6). In the loaded oocytes, intracellular activity of Na^+ was about 80 mM after 40 min of incubation as measured by Na^+ -selective microelectrodes [40]. The number of ouabain binding sites on the oocyte surface was determined in K^+ -free ORI solution containing 2.5 μM [^3H]ouabain (0.86 TBq/mmol, New England Nuclear) and 2.5 μM of cold ouabain at room temperature [38].

2.3. Experiments on Brain Slices. Neonatal Sprague-Dawley rats (10–20 days) were anaesthetized with ether, decapitated and horizontal midbrain slices containing the periaqueductal gray (PAG) were cut (350 μm) in ice-cold (4°C) artificial cerebrospinal fluid (ACSF), and the composition of the ACSF was in mM as follows: NaCl 124, KCl 3.0, NaH_2PO_4 1.25, $\text{MgSO}_4 \cdot 7\text{H}_2\text{O}$ 2.5, NaHCO_3 26, glucose- H_2O 10, and CaCl_2 2.0. For recovery the slices were kept at room temperature (25°C) in ACSF equilibrated with 95% O_2 and 5% CO_2 for ~ 1 hour. The slices were then individually transferred to a chamber and superfused continuously with ACSF (31°C) for electrophysiological experiments.

PAG neurons were visualized using infrared Nomarski optics. Whole-cell recordings were made using patch electrodes (4–5 M Ω); the composition of the electrode filling solution was (in mM) as follows: K-gluconate 95, KCl 30, NaCl 15, MgCl_2 2, HEPES 10, EGTA 11, MgATP 2, and NaGTP 0.25 (pH 7.3, 280–285 mOsmol/L). Liquid junction potentials of ~ 30 mV were corrected. Series resistance (~ 35 M Ω) was compensated automatically and continuously monitored. Whole-cell currents were recorded using EPC10 double amplifier (HEKA Instruments), digitized, filtered (at 2 kHz), and then acquired (sampling at 10 kHz) in PatchMaster (HEKA Instruments). Steady-state currents were determined at the end of 200 ms, rectangular voltage-clamp pulses (from -130 to -30 mV in 10 mV increments, averaged during the last 20 ms) that were applied from a holding potential of -60 mV. GAT1-mediated current was determined as the current component that was inhibited by either 20 μM tiagabine (Biotrend Chemicals AG, Zurich, Switzerland) or 10 μM NNC711 (Tocris Cookson Ltd, Bristol, UK). To reduce background contribution of voltage-gated Na^+ , Ca^{2+} , and K^+ channels, all bath solutions contained 300 nM tetrodotoxin, 10 μM CdCl_2 , and 20 mM tetraethyl ammonium chloride, respectively.

2.4. Western Blot. Yolk-free homogenates of oocytes were prepared 3 days after the injection of cRNA as described previously [41] and by passing the oocytes through 200- μL Eppendorf pipette tips in homogenization buffer (in mM: 20 Tris-HCl (pH 7.4), 5 MgCl_2 , 5 NaH_2PO_4 , 1 EDTA, 100 NaCl, 10 KCl, 1 DTT, and 1 PMSE, and 5 $\mu\text{g}/\text{mL}$ of each of leupeptin, pepstatin, and antipain). Twenty-microliter aliquots of the yolk-free homogenates were electrophoresed on SDS-PAGE. Proteins from nonstained gels were electrophoretically transferred on nitrocellulose membrane for western blot. The primary antibody against GAT1 from rabbit (Chemicon Int. AB1570 W) was applied overnight at 4°C . The secondary antibody against GAT1 from rabbit (abcam. ab426) was applied at room temperature for 1 hr. Band intensities were quantified using ImageJ software.

3. Results

3.1. Exposure of Rats to Morphine Results in Reduced Rate of GABA Uptake. Rate of GABA uptake was determined in synaptosomal preparations of hippocampus of rats that were chronically treated with morphine (Figure 1). Rats were injected twice a day with morphine over a period of 10 days, and GABA uptake into the synaptosomes was significantly reduced 12 h after termination of the morphine treatment compared to untreated controls. Acute injection of morphine (1 h before sacrifice) further decreased the uptake activity. This additional effect of morphine could completely be prevented by the simultaneous use of naloxone, an opioid receptor antagonist, indicating that the acute morphine treatment downregulated GABA transporter activity as a result of activation of opioid receptors.

Among the several canonical opioid receptors, μOR has the highest affinity with morphine [42]; studies with μOR knockout mice also show that μOR is necessary for morphine-induced analgesia and other symptoms [43]. However, at a relatively high concentration, morphine could bind to all three opioid receptors, μOR , δOR , and κOR [44]. In addition, a minor morphine metabolite, morphine-6-glucuronide, showed higher affinity to δOR and lower affinity to μOR , compared to that of morphine in rodents and human [42].

While μOR is constitutively expressed at surface membrane, several studies have shown that the surface expression of δOR is regulated by inflammation, drug exposure, or stimulation [27, 45, 46]. Notably, the physical interactions between μOR and δOR may contribute to long-term changes of morphine-induced analgesia [44, 45]. We reasoned that the changes of either μOR or δOR signaling cascades might be responsible for acute and chronic morphine-induced GABA uptake inhibition. Therefore, we next examined the interaction between GAT1 and μOR or δOR using oocyte as a simplified and well-controlled system.

3.2. Effect of Opioid Receptor Coexpression on Rate of GABA Uptake. To investigate regulation of GAT1 by opioid receptor, we used the *Xenopus* oocytes with heterologously expressed GAT1 and opioid receptor as a model system.

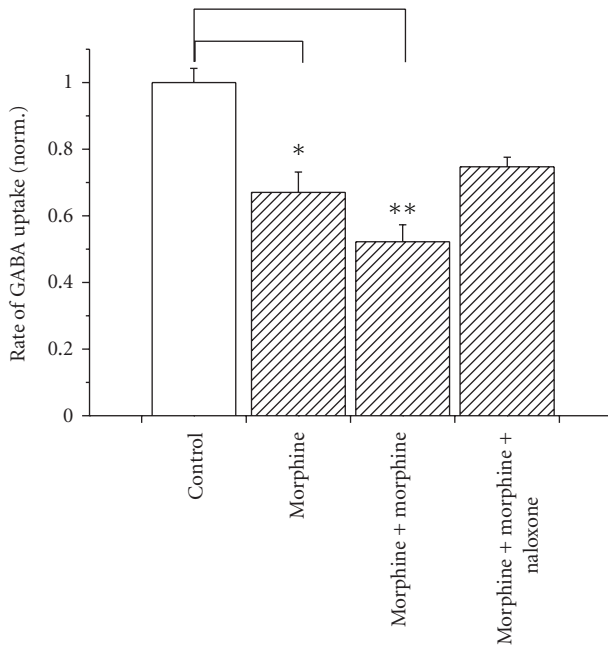


FIGURE 1: Effect of chronic morphine treatment on GABA uptake activity in rats. Uptake activity was measured in synaptosomes of untreated rats (control) and of rats after 10 days of morphine injection twice a day (hatched bars). Data were normalized to the rate of uptake into synaptosomes of controls. For treated rats, rate of GABA uptake was determined 12 hr after the termination of treatment (morphine), with an additional injection of morphine (s.c. 10 mg/kg) 1 hr before sacrificing (morphine + morphine) or with an additional injection of both morphine and naloxone (i.p. 2 mg/kg) 1 hr before sacrificing (morphine + morphine + naloxone). * $P < 0.05$, ** $P < 0.01$ compared to data from control animals; $n = 5$ in each group. Error bars represent SEM.

Functional GABA transporters incorporation into the oocyte membrane was verified by detection of Na^+ -dependent uptake of $[^3\text{H}]\text{GABA}$ at a saturating GABA concentration of $100 \mu\text{M}$ [14, 19]. Only oocytes with heterologously expressed GAT1 showed significant $[^3\text{H}]\text{GABA}$ uptake (see Figure 3(a)). When GAT1 and the δOR of mouse brain were coexpressed in *Xenopus* oocytes by coinjection of cRNA for GAT1 (40 ng) and different amounts for δOR (0, 5, 10, 20, 40 ng), increasing amounts of the coinjected cRNA of δOR led to decreased rate of GAT1-mediated GABA uptake (Figure 2); the dependency was arbitrarily fitted by

$$\text{Rate} = \frac{K_{1/2}^n}{K_{1/2}^n + [\text{cRNA}_{\delta\text{OR}}]^n} \quad (1)$$

with half-maximum inhibition of the rate at $K_{1/2} = 10.7 \text{ ng}$ and $n = 1.7$. Corresponding amounts of cRNA for the rat Na pump, $\alpha 2\beta$, had no significant effect on the GAT1-mediated uptake (Figure 2). To rule out the possibility that expression of δOR in the oocytes may affect translation of other proteins that regulate membrane protein expression, we injected oocytes different amounts of cRNA for δOR together with cRNA for the rat $\alpha 2\beta$ Na^+ pump (40 ng).

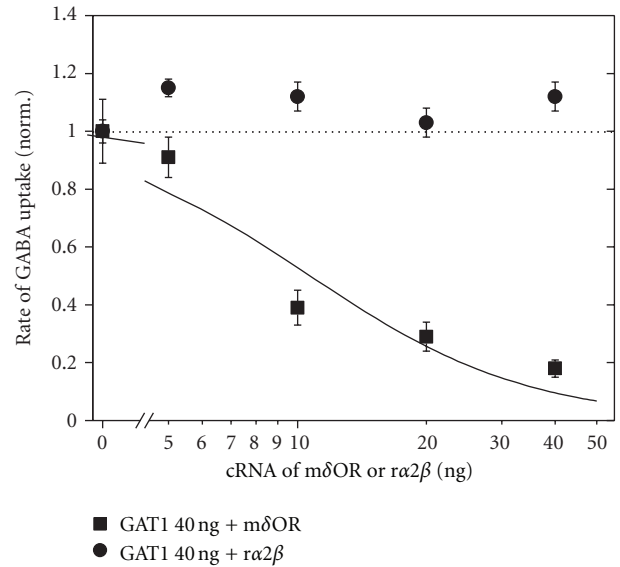


FIGURE 2: Dependence of GAT1-mediated rate of $[^3\text{H}]\text{GABA}$ uptake on different amounts of coinjected cRNA. For cRNA of δOR (filled squares) or $\alpha 2\beta$ pumps (filled circles), the amount of injected cRNA for GAT1 was 40 ng. Data were normalized for each batch of oocytes to the respective value obtained from oocytes not coinjected with cRNA for δOR or $\alpha 2\beta$ and are presented as means \pm SEM from 2 to 3 batches of oocytes (with 8–10 oocytes per batch). The dependence of rate of GABA uptake on δOR -cRNA was fitted by (1).

The coexpression of δOR did not affect surface expression of the pump as judged by $[^3\text{H}]\text{ouabain}$ binding (not illustrated). For the experiments described in the following, we always choose 10 or 20 ng for coinjection of opioid-receptor cRNA.

The reduced uptake in oocytes expressing both the GAT1 and the δOR compared to those expressing GAT1 alone cannot be attributed to background activation of δOR since treatment with the opioid receptor antagonist naloxone ($1 \mu\text{M}$) could only slightly reverse the inhibition (Figure 3(a)). Coinjection of 10 ng cRNA for the μOR instead of cRNA for δOR had no significant effect on the rate of GABA uptake (Figure 3(b)). Functional expression of δOR and μOR was confirmed in the absence of GAT1 activity by application of 100 nM of the δOR or μOR agonists, DPDPE or DAMGO, respectively, and by the resulting activation of the endogenous Ca^{2+} -activated channels (data not shown, see also [30]); it is worth to mention that the voltage dependencies of the currents induced by DPDPE and DAMGO differ from each other indicating that different signaling pathways are activated.

We further tested the effects of the opioid agonists if 10 ng of cRNA for the respective receptor was coinjected. Figure 3(b) shows that activation of δOR by 100 nM DPDPE further reduced the rate of GABA uptake while activation of μOR by 100 nM DAMGO did not significantly change transport activity. Since the heterologous expression of GAT1 with δOR , but not μOR , exhibited significant effect on GABA uptake, we focused the rest of our study on δOR .

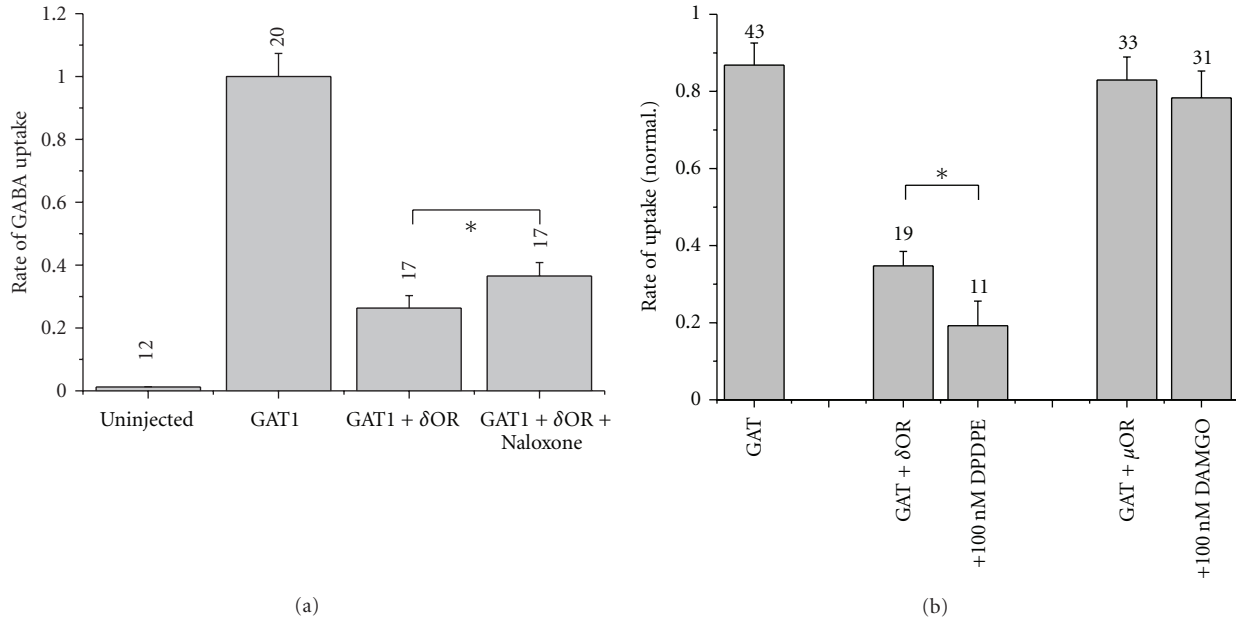


FIGURE 3: Effect of opioid receptor coexpression on GAT1-mediated rate of GABA uptake. (a) 40 ng of GAT1 cRNA alone or 40 ng of GAT1 and 20 ng of cRNA for δ OR were injected into oocytes. Application of 100 nM naloxone gave slight recovery of GAT1 inhibition by the coexpressed δ OR. (b) 40 ng of GAT1 cRNA alone or 40 ng of GAT1 and 10 ng of cRNA for δ OR or μ OR were injected into oocytes. The unspecific rate of uptake was subtracted from the uptake rate of injected oocytes. δ OR was activated by application of 100 nM DPDPE, μ OR by 100 nM DAMGO. Data were normalized for each batch of oocytes to the respective value obtained from oocytes not coinjected with cRNA for δ OR and are presented as means of rates of [3 H]GABA uptake \pm SEM from 2 to 4 batches of oocytes (with 5–10 oocytes per batch), * $P < 0.05$.

3.3. Effect of Opioid Receptor Coexpression on GAT1-Mediated Steady-State Current. Dependence of GAT1-mediated current on membrane potential was determined in voltage-clamp experiments as the difference of membrane current in the presence and the absence of 100 μ M GABA. Figure 4(a) shows original current traces before, during, and after application of GABA. The steady-state GAT1-mediated current was reduced in the oocytes expressing GAT1 when 10 ng cRNA for δ OR were coinjected (Figure 4(b)) to a similar extent as the GABA uptake (compared with Figure 3(b)). As found for the uptake, activation of δ OR by application of DPDPE (100 nM) led to further inhibition of GAT1-mediated current by about 50%. Because DPDPE could induce a Ca^{2+} -dependent current (see above), the effect of DPDPE on GAT1-mediated current was, therefore, determined in the presence of DPDPE as the difference of current in the presence and absence of GABA.

Similar to the findings with the GABA uptake, coexpression of μ OR had no significant effect on the GAT1-mediated steady-state current (Figure 4(b)), and activation of the receptor by 100 nM DAMGO did not significantly influence the current (Figure 4(c)). Also activation of the endogenous acetylcholine (ACh) receptor by 100 μ M ACh did not affect the GAT1-mediated current (data not shown).

3.4. Effect of Opioid Receptor Coexpression on GAT1-Mediated Transient Current. Figure 4(a) illustrates, particularly for depolarizing potential steps, that in the absence of GABA a slow transient current was apparent. The amount of the

corresponding charge movements Q associated with the extracellular Na^+ binding [19] was determined by integration of the transient current signals remaining after subtracting from the responses in the absence of GABA those in the presence of GABA [20, 21]. The voltage-dependent distribution of the charges $Q(E)$ is shown in Figure 5(a) and can be described by a Fermi equation:

$$Q(E) = Q_{-\infty} + \frac{Q_{+\infty} - Q_{-\infty}}{1 + e^{-z_f(E - E_{1/2})F/RT}}, \quad (2)$$

where F , R , and T have their usual meanings, z_f represents the effective valence that is moved during the Na^+ binding step, and $E_{1/2}$ the midpoint potential. Neither z_f nor $E_{1/2}$ was affected by coexpression and activation of δ OR, only the amount of moved charges became reduced (see Table 1). From the ratio of total charge $Q_{\text{max}} = Q_{+\infty} - Q_{-\infty}$ and the effective valence z_f , the number of functionally expressed transporters N can be calculated, and the values are listed in Table 1. The coexpression of δ OR obviously led to a reduction in the number of functioning transporters by about 30% which can only partially account for the reduction of GABA uptake (about 70%, see Figure 3(b)) or of GAT1-mediated current (about 75%, see Figures 4(b) and 4(c)). Also the further inhibition of the current by DPDPE application (about 50%, see Figure 4(c)) can only partially be attributed to a reduction in N which amounts to only 25%.

Analysis of the kinetics of the transient currents yields rate constants k (Figure 5(b)) of the signals that were

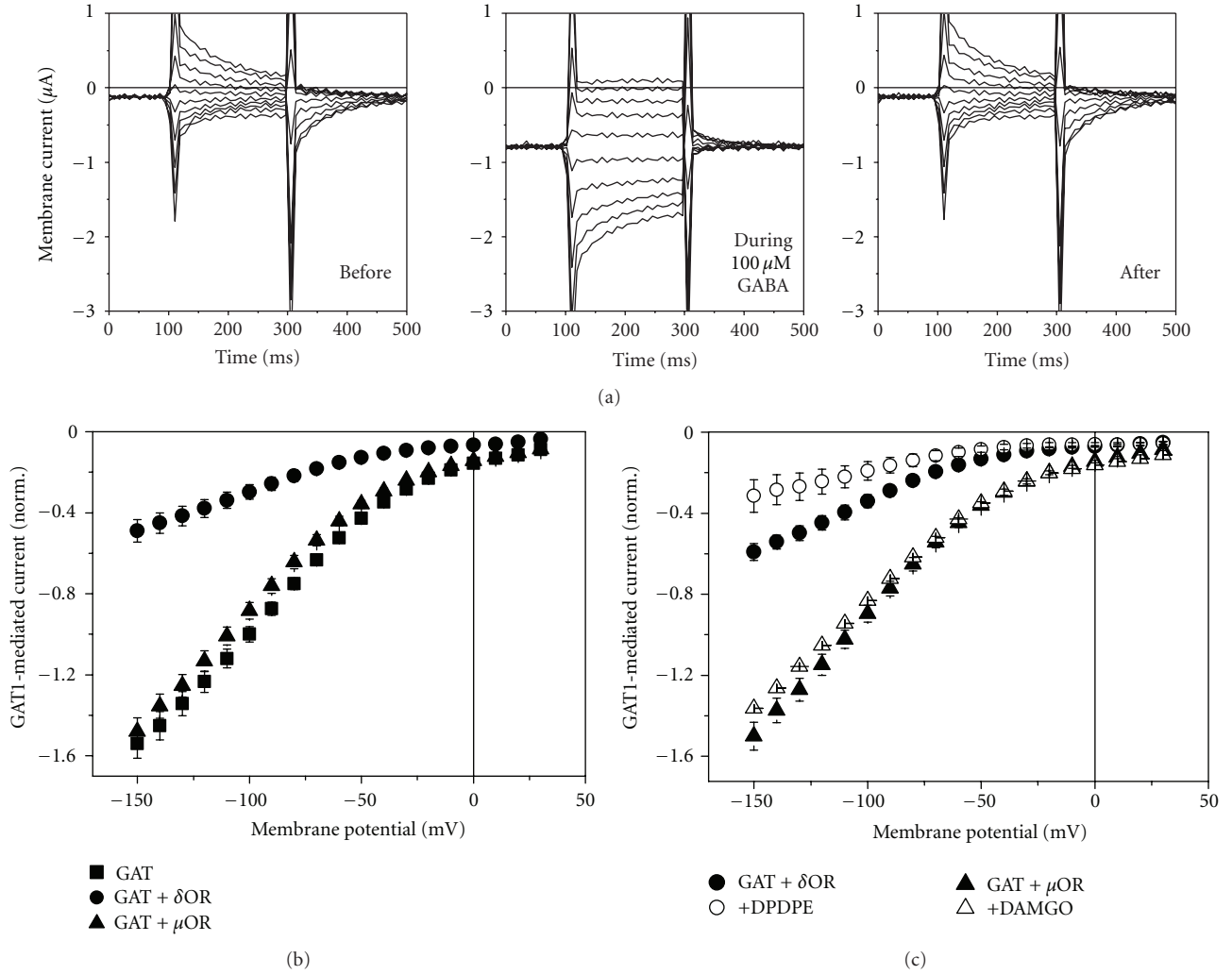


FIGURE 4: Effects of opioid receptor coexpression on GAT1-mediated current. (a) Current traces in response to rectangular voltage pulses before, during, and after application of 100 μM GABA to oocytes with expressed GAT1. Effects on the voltage dependence of steady-state GAT1-mediated currents in oocytes coexpressed with δOR or μOR (10 ng cRNA coinjected) (b) and of their activation by 100 nM DPDPE or DAMGO, respectively (c). Data in (b) and (c) represent averages \pm SEM of at least 6 oocytes.

TABLE 1: Parameters of (1) fitted to the data shown in Figure 5(a).

	Q_{\max} (nC)	$E_{1/2}$ (mV)	z_f	Q_{\max}/z_f (N per oocyte)	k_1^* (s^{-1})	a_1 (mV^{-1})	k_2^* (s^{-1})	a_2 (mV^{-1})
GAT1	73.3			6.1×10^{11}	6.8		7.8	
GAT1 + δOR	49.4	-32.3	1.2	4.1×10^{11}	3.3	85.6	5.4	39.5
GAT1 + δOR (1 μM DPDPE)	39.7			3.3×10^{11}				

obtained by fitting $I = I_{\max}e^{-kt}$ to the transient signal. The voltage dependencies of the k values were fitted by

$$k(V) = k_1(V) + k_2(V) = k_1^*e^{-a_1V} + k_2^*e^{+a_2V}, \quad (3)$$

where k_1 and k_2 represent the forward and backward rate constants, respectively, of a step associated with the extracellular Na^+ binding (fit parameters, see Table 1). All datasets could be fitted by the same voltage dependency; the slowed kinetics on coexpression of δOR was dominated by the reduced forward rate constant that could account

for reduced rate of GABA transport. Activation of δOR by DPDPE did not affect the kinetics. Neither the GAT1-mediated steady-state currents nor the transient charge movements were significantly affected when the $\alpha\alpha2\beta$ Na^+ pump was coexpressed with the GAT1.

Western blot analysis shows that coexpression of δOR does not significantly affect the band intensity for GAT1 (Figure 6(a)). If any there may be a slight increase in band intensity with coexpressed δOR of $7.4 \pm 1.9\%$ (Figure 6(b)). Same loading of the lanes was confirmed by same band intensities for actin.

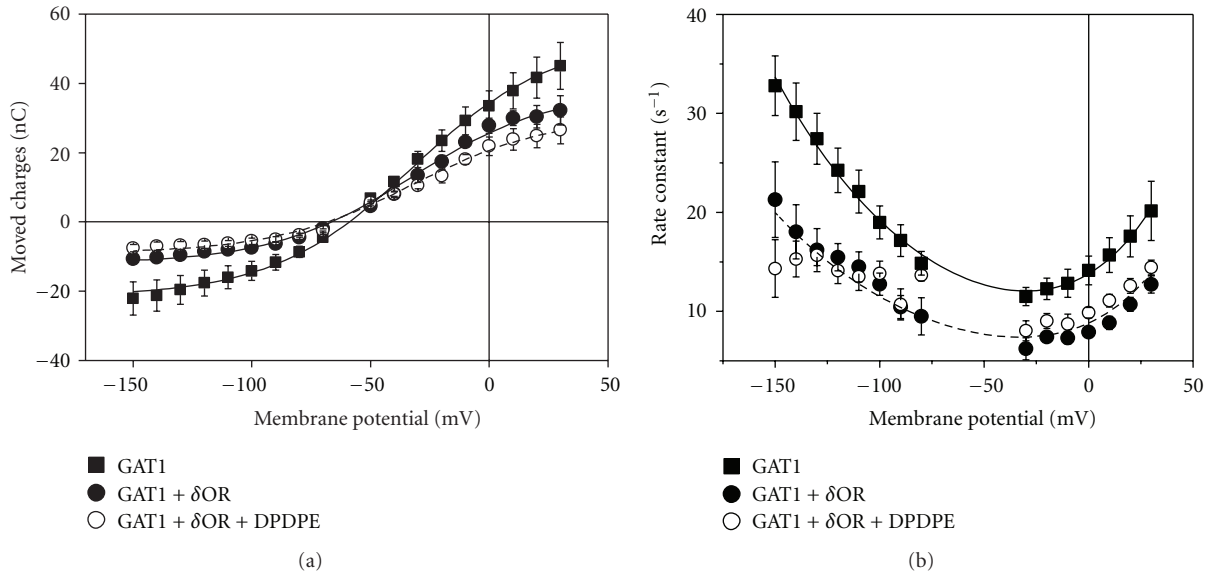


FIGURE 5: Effects of δ OR coexpression and its activation by 100 nM DPDPE on GAT1-mediated transient charge movements. 40 ng of GAT1 cRNA alone or 40 ng of GAT1 and 20 ng of δ OR cRNA were injected into oocytes. (a) Voltage dependencies of moved charge in response to rectangular potential jumps were obtained by integration of the respective transient currents and were fitted by (2) (see lines). (b) The rate constants were obtained by fitting an exponential to the transient current signal, and the voltage dependencies were fitted by (3) (see lines). Data represent means \pm SEM; $n = 6-7$ oocytes for each group.

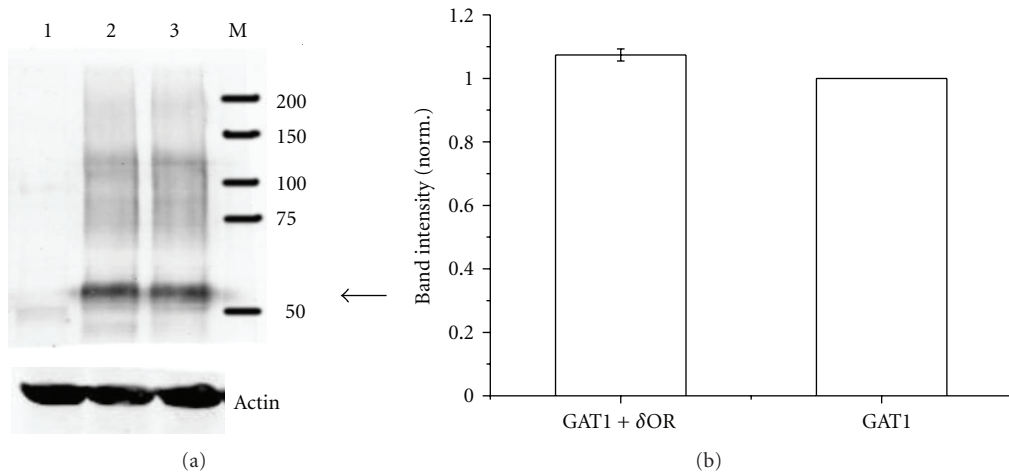


FIGURE 6: GAT1 expression in *Xenopus* oocyte membrane fractions. (a) Lane 1: noninjected oocytes, lane 2: oocytes injected with 40 ng of GAT1 cRNA and 20 ng of δ OR, and lane 3: oocytes injected with 40 ng of GAT1 cRNA alone. The bands at about 60 kDa (see arrow) represent GAT1 monomers. (b) GAT1 monomer band intensities averaged from 5 batches of oocytes and normalized to the respective batch injected with cRNA for GAT1 only.

3.5. Activation of δ -Opioid Receptor Inhibits GAT1-Mediated Current in PAG Neurons. The above data have demonstrated that δ OR interferes with GAT1 activity; in particular, activation of the opioid receptor inhibits GAT1 function. Since these effects might be a result of overexpression in the oocyte model system, we investigated the effect of δ OR activation in brain slices of rat PAG.

Steady-state currents were determined during superfusion of the brain slice with different solutions; in a typical experiment sequence was



with S_{GABA} representing solution with GABA and $S_{GABA+inhibitor}$ solution with additional GAT1-specific inhibitor tiagabine or NNC711. To determine GAT1-mediated current, the currents in S_{GABA} before and after application of the inhibitor were averaged, and the current in the presence of the inhibitor was subtracted to obtain the current component sensitive to the specific inhibitor. Thereafter, solutions in the presence of the δ OR against DPDPE were applied:



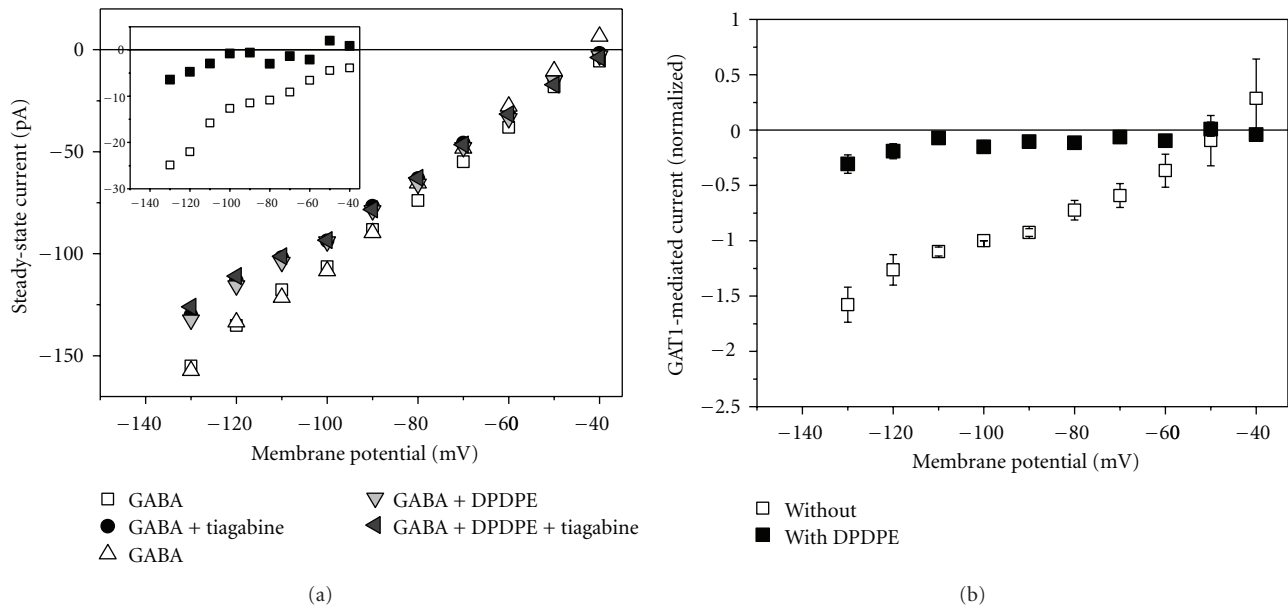


FIGURE 7: Effect of δ OR activation on GAT1-mediated current in rat brain slices from PAG area. Whole-cell patch-clamp recordings were performed on PAG neurons superfusing with different solutions. (a) Steady-state current voltage dependencies of a single experiment with solution sequence as given in the text. The inset shows the GAT1-mediated current determined as tiagabine-sensitive steady-state current. Open squares represent current in the absence and filled squares in the presence of 100 nM DPDPE. (b) GAT1-mediated current from 5 experiments. Data were normalized to the current at -100 mV in the absence of DPDPE and represent averages (\pm SEM). The value of “one” corresponds to 41.4 ± 20.0 pA.

Correspondingly, the GAT1-mediated current was determined as the difference of current in the absence and presence of the GAT1 inhibitor. Figure 7(a) shows an example. For the GAT1-mediated current averaged data are presented in Figure 7(b).

The result revealed strong inhibition of GAT1-mediated current in response to application of the δ OR-specific agonist DPDPE (Figure 7). The nearly complete inhibition of total GAT1-mediated current indicates that in the brain slices all transport modes of GAT1 were blocked. Hence, these data on PAG slices are consistent with the DPDPE-induced reduction of GAT1-mediated GABA uptake and current observed in oocytes.

4. Discussion

The discovery that the opioid receptor antagonist naloxone counteracts acupuncture-induced analgesia [47, 48] led to the suggestion of the involvement of endorphins. Administration of opiates to rats resulted in reduced GABA uptake in brain as determined from measurements in synaptosomes (Figure 1). The GABAergic system also plays a critical role in pain sensation, and in particular inhibition of GAT in mice has antinociceptive effects and transgenic GAT1-overexpressing mice are hyperanalgesic [11]. Since the GABA concentration is controlled to a large extent by the GABA uptake transporter, we investigated effects of opioid receptor expression on GAT1 function. To avoid interference with other GABAergic components, we used the *Xenopus* oocytes as an expression system. This was also useful since the

oocytes do not express endogenous functional Na^+ channels that have been demonstrated to be also regulated by δ OR [49].

4.1. Coexpression of δ OR Reduces Transport Mediated by GAT1. Coexpression of the δ OR with GAT1 from mouse brain led to downregulation of GABA uptake in the oocytes with half maximum inhibition at about 10 ng of cRNA of δ OR (Figure 2); this means at a $\text{cRNA}_{\delta\text{OR}}/\text{cRNA}_{\text{GAT1}}$ ratio of 0.25. The GAT1-mediated current was also reduced (Figure 4(b)). The effects of δ OR coexpression on GABA transport cannot be attributed to competition by the coinjected cRNAs. Neither the translation machinery nor the targeting to the surface membrane was a limiting factor. This became apparent from the observation that GABA uptake was hardly affected by coexpression of another membrane protein (Na^+ pump), and Na^+ -pump expression was not affected by δ OR expression (Figure 2). The reduced transport without activation of δ OR cannot be attributed to a background activity of the receptor since application of the opioid-receptor antagonist naloxone did not have a compensating counteractive effect. Only a slightly stimulated uptake could be detected in the presence of 100 nM naloxone (Figure 3(a)). δ OR seems to directly interfere with the GAT1 leading to the reduced GABA uptake. This effect was specific for δ OR since coexpression of μ OR did affect neither GAT1-mediated GABA uptake (Figure 3(b)) nor current (Figure 4(b)); also transport activities of EAAC1 and the Na, K pump were not affected [9, 50, 51]. Interaction of membrane receptors with transport systems without

activation of the receptor was also reported previously. The glutamate transporter EAAC1 as well as the Na, K pump showed reduced transporter activity with coexpressed δ OR [9, 50, 51], and for the dopamine transporter DAT reduced [52] as well as increased [53] uptake was reported for coexpression with G-protein receptors. This effect was specific for δ OR since coexpression of μ OR did affect neither GAT1-mediated GABA uptake (Figure 3(b)) nor current (Figure 4(b)); also transport activities of EAAC1 and the Na, K pump were not affected [9, 50, 51].

The specificity of the effect of coexpression of δ OR on the GABA transporter becomes also apparent from the observation that targeting of the rat $\alpha 2\beta$ Na⁺, K⁺ pumps to the surface membrane of the oocyte was not affected by coexpression of δ OR (Figure 2). In addition, coexpression of the rat Na⁺, K⁺ pump neither reduced GABA uptake nor GAT1-mediated current, and the number of transporters was not significantly affected either (data not shown).

Western blot analysis also demonstrated that coexpression of δ OR did not affect the amount of GAT1 expressed in the oocytes and targeted to the membrane. Nevertheless, the number of functioning transporters calculated from the Q_{\max} value became reduced by about 30% (see Table 1) on coexpression of δ OR. "Functioning transporter" means that at least Na⁺ can still bind giving rise to the transient current signal, but it does not necessarily mean that GABA can be transported. The inhibition of transport, therefore, might be attributed to a reduced number of GABA-translocating GAT1 molecules in the membrane and to a reduced rate of transport. The reduced apparent affinity for extracellular Na⁺ binding (reduced rate of binding and increased rate of unbinding (Figure 5(b)) supports the view of a contribution of a reduced turnover rate of the transport cycle.

4.2. Activation of δ OR Reduces Transport Mediated by GAT1. As a supraspinal locus for opioid analgesia PAG exhibits high abundance of δ OR (see, e.g., [54, 55]) and also expression of GAT1 has been demonstrated [56]. In *Xenopus* oocytes with coexpressed δ OR and GAT1 activation of δ OR by DPDPE led to further reduction of GAT1-mediated current (Figure 4(c)) compatible with the finding of reduced GABA uptake activity (Figure 3(b)). Compared to nonstimulated δ OR, the inhibition of current amounts to 41% and of uptake to 45%.

Redistribution of transporters between cytoplasmic membranes and the surface membrane resulting in altered transport had been attributed to activity of protein kinase C (PKC) [57]. Opioid receptor activation with activation of PKC had indeed been observed previously [58, 59]. Hence we may speculate that the inhibition of GAT1 activity by δ OR activation might be regulated by PKC; an altered GAT1- δ OR interaction might also be considered as had been suggested for the stimulation of glutamate uptake on activation of δ OR [9]. This of course needs further investigations.

Altered GABA transport as a consequence of activation of G-protein-coupled receptor has been discussed on the basis of indirect effects through altered Na⁺ gradient [60]. Such a mechanism can be excluded for the oocytes since intracellular Na⁺ activity hardly changes during an experiment,

and more direct effects (see, e.g., [61]) have to be considered including the action of protein kinases and phosphatases. Stimulation of PKC alters GABA uptake by redistribution of the transporters between intracellular compartments and the surface membrane [57, 62], but also reduced activity of the GABA transporter has been observed (Eckstein-Ludwig and Schwarz (unpublished)). Mechanisms have been discussed that protein-protein interaction like interaction with syntaxin A or other adaptor proteins modulates the GABA transporter [63] that may be modulated by PKC [64]. Also other transport proteins, channels, G-protein-coupled receptors, and cytoplasmic proteins [65–68] seem to be affected by protein-protein interactions.

The inhibition of GAT1-mediated current cannot be attributed to an overexpression of GAT1 and/or δ OR in the model system "*Xenopus* oocyte." This we demonstrated by patch-clamp experiments on PAG brain slices (Figure 7); application of the δ OR-specific agonist DPDPE resulted in nearly complete inhibition of tiagabine-sensitive current that can be considered to be mediated by GAT1. In *Xenopus* oocyte activation of δ OR did not completely inhibit the GAT1-mediated current as well as uptake. This may be due to the ratio of injected cRNA for GAT1 and δ OR; we found (not shown) that the degree of uptake inhibition by δ OR activation increases with lower amounts of injected cRNA for δ OR.

The signaling pathway in the oocytes definitively differs from that in the brain and might be the reason for the differently pronounced effects on the GAT1 transport modes. Our results suggest that stimulation of δ OR can modulate the GAT1 activity. Interestingly, while δ OR activation leads to inhibition of GAT1-mediated current, the glutamate transporter EAAC1 becomes stimulated [9]. In addition to this modulation of synaptic transmission, modulation of neurotransmitter release by stimulation of opioid receptors has been reported [69, 70].

In the presented work we have demonstrated that GAT1-mediated transport can be regulated by the G-protein-coupled δ -opioid receptor in two ways: (1) by modulation of the number of functional transporters in the membrane and (2) by modulation of transport activity. These modulations are dominated by the presence of δ OR and by receptor activation suggesting that direct transporter-receptor interaction plays the dominating role. Chronic morphine treatment is known to modulate the surface expression of δ OR. For example, it blocks agonist-induced δ OR internalization [71]. The dynamics of δ OR surface expression will thus regulate GABA transporter activity. Since reduced GABA reuptake will lead to elevated GABA concentration in the synaptic cleft, this mechanism may account for the increased GABAergic activity found in chronic opiate-treated rats and its role in pain sensation.

5. Conclusion

It has been shown previously that Na⁺ channel inhibition by δ OR activation may contribute to attenuation of disturbance of ionic homeostasis present under hypoxic/ischemic

conditions [72]. Activation of δ OR can stimulate the neurotransmitter transporters EAAC1 [9] and inhibit the neurotransmitter transporter GAT1 (this work). Stimulation of EAAC1 will lead to reduced concentration of the excitatory neurotransmitter glutamate in the synaptic cleft and inhibition of GAT1 to elevated concentration of the inhibitory transmitter GABA. We like to suggest that the acupuncture-induced elevation of endorphins [24] can contribute to analgesia by regulation of the dominating excitatory and inhibitory neurotransmitter transporters by activation of δ OR.

Abbreviations

ACSF:	Artificial cerebrospinal fluid
DAMGO:	[D-Ala ² ,N-Me-Phe ⁴ ,Gly ⁵ -ol]-enkephalin
δ OR:	δ -Opioid receptor
μ OR:	μ -Opioid receptor
DPDPE:	[D-Pen ^{2,5}]-Enkephalin
EAAC1:	Excitatory amino acid carrier (isoform 1)
GABA:	γ -Amino butyric acid
GAT1:	GABA transporter (isoform 1)
MOPS:	3-(N-morpholino)-propanesulphonic acid
ORi:	Oocyte Ringer's solution
PAG:	Periaqueductal gray
PKC:	Protein kinase C
$\alpha 2\beta$ pump:	Na ⁺ pump of $\alpha 2$ and β subunit of rat.

Acknowledgments

The authors greatly acknowledge the technical assistance of Heike Biehl, Heike Fotis, Eva-Maria Gärtner, Huiming Du, and Yalan WU. This work was financially supported by the Science Foundation of Shanghai Municipal Commission of Science and Technology, the National Basic Research Program of China (973 Program, no. 2012CB518502), and on the basis of an agreement between the Max-Planck Society and the Chinese Academy of Sciences.

References

- [1] J. D. Rothstein, L. Martin, A. I. Levey et al., "Localization of neuronal and glial glutamate transporters," *Neuron*, vol. 13, no. 3, pp. 713–725, 1994.
- [2] Y. He, W. G. Janssen, J. D. Rothstein, and J. H. Morrison, "Differential synaptic localization of the glutamate transporter EAAC1 and glutamate receptor subunit GluR2 in the rat hippocampus," *The Journal of Comparative Neurology*, vol. 418, pp. 255–269, 2000.
- [3] J. Levenson, E. Weeber, J. C. Selcher, L. S. Kategayal, D. J. Sweatt, and A. Eskin, "Long-term potentiation and contextual fear conditioning increase neuronal glutamate uptake," *Nature Neuroscience*, vol. 5, no. 2, pp. 155–161, 2002.
- [4] L. A. Borden and M. J. Caplan, "GABA transporter heterogeneity: pharmacology and cellular localization," *Neurochemistry International*, vol. 29, no. 4, pp. 335–356, 1996.
- [5] T. P. Malan, H. P. Mata, and F. Porreca, "Spinal GABAA and GABAB receptor pharmacology in a rat model of neuropathic pain," *Anesthesiology*, vol. 96, no. 5, pp. 1161–1167, 2002.
- [6] Y. Q. Zhang, G. C. Ji, G. C. Wu, and Z. Q. Zhao, "Excitatory amino acid receptor antagonists and electroacupuncture synergistically inhibit carrageenan-induced behavioral hyperalgesia and spinal fos expression in rats," *Pain*, vol. 99, no. 3, pp. 525–535, 2002.
- [7] J. Zhang, G. T. Gibney, P. Zhao, and Y. Xia, "Neuroprotective role of δ -opioid receptors in cortical neurons," *American Journal of Physiology*, vol. 282, no. 6, pp. C1225–C1234, 2002.
- [8] J. Knabl, R. Witschi, K. Hösl et al., "Reversal of pathological pain through specific spinal GABAA receptor subtypes," *Nature*, vol. 451, no. 7176, pp. 330–334, 2008.
- [9] P. Xia, G. Pei, and W. Schwarz, "Regulation of the glutamate transporter EAAC1 by expression and activation of δ -opioid receptor," *European Journal of Neuroscience*, vol. 24, no. 1, pp. 87–93, 2006.
- [10] W. Schwarz and Q. B. Gu, "Cellular mechanisms in acupuncture points and affected sites," in *Current Research in Acupuncture*, Y. Xia, G. H. Ding, and G.-C. Wu, Eds., pp. 37–51, Springer, 2012.
- [11] J. H. Hu, N. Yang, Y. H. Ma et al., "Hyperalgesic effects of γ -aminobutyric acid transporter I in mice," *Journal of Neuroscience Research*, vol. 73, no. 4, pp. 565–572, 2003.
- [12] P. Schloss, W. Maysner, and H. Betz, "Neurotransmitter transporters. A novel family of integral plasma membrane proteins," *FEBS Letters*, vol. 307, no. 1, pp. 76–80, 1992.
- [13] S. Keynan and B. I. Kanner, " γ -Aminobutyric acid transport in reconstituted preparations from rat brain: coupled sodium and chloride fluxes," *Biochemistry*, vol. 27, no. 1, pp. 12–17, 1988.
- [14] M. P. Kavanaugh, J. L. Arriza, R. A. North, and S. G. Amara, "Electrogenic uptake of γ -aminobutyric acid by a cloned transporter expressed in *Xenopus* oocytes," *Journal of Biological Chemistry*, vol. 267, no. 31, pp. 22007–22009, 1992.
- [15] S. Risso, L. J. DeFelice, and R. D. Blakely, "Sodium-dependent GABA-induced currents in GAT1-transfected HeLa cells," *Journal of Physiology*, vol. 490, no. 3, pp. 691–702, 1996.
- [16] D. W. Hilgemann and C. C. Lu, "GAT1 (GABA:Na⁺:Cl⁻) cotransport function: database reconstruction with an alternating access model," *Journal of General Physiology*, vol. 114, no. 3, pp. 459–475, 1999.
- [17] D. D. F. Loo, S. Eskandari, K. J. Boorer, H. K. Sarkar, and E. M. Wright, "Role of Cl⁻ in electrogenic Na⁺-coupled cotransporters GAT1 and SGLT1," *Journal of Biological Chemistry*, vol. 275, no. 48, pp. 37414–37422, 2000.
- [18] S. Krause and W. Schwarz, "Identification and selective inhibition of the channel mode of the neuronal GABA transporter 1," *Molecular Pharmacology*, vol. 68, no. 6, pp. 1728–1735, 2005.
- [19] S. Mager, J. Naeve, M. Quick, C. Labarca, N. Davidson, and H. A. Lester, "Steady states, charge movements, and rates for a cloned GABA transporter expressed in *Xenopus* oocytes," *Neuron*, vol. 10, no. 2, pp. 177–188, 1993.
- [20] S. Mager, N. Kleinberger-Doron, G. I. Keshet, N. Davidson, B. I. Kanner, and H. A. Lester, "Ion binding and permeation at the GABA transporter GAT1," *Journal of Neuroscience*, vol. 16, no. 17, pp. 5405–5414, 1996.
- [21] Y. Liu, U. Eckstein-Ludwig, J. Fei, and W. Schwarz, "Effect of mutation of glycosylation sites on the Na⁺ dependence of steady-state and transient currents generated by the neuronal GABA transporter," *Biochimica et Biophysica Acta*, vol. 1415, no. 1, pp. 246–254, 1998.
- [22] A. Bicho and C. Grever, "Rapid substrate-induced charge movements of the GABA transporter GAT1," *Biophysical Journal*, vol. 89, pp. 211–231, 2005.

- [23] U. Eckstein-Ludwig, Y. Fueta, J. Fei, and W. Schwarz, "The neuronal GABA transporter GAT1 as a target for action of antiepileptic drugs," in *Control and Diseases of Sodium Transport Proteins and Channels*, Y. Suketa, E. Carafoli, M. Lazdunski, K. Mikoshiba, Y. Okada, and E. M. Wright, Eds., pp. 373–376, Elsevier Press, Amsterdam, The Netherlands, 2000.
- [24] J. S. Han, "Acupuncture and endorphins," *Neuroscience Letters*, vol. 361, no. 1–3, pp. 258–261, 2004.
- [25] M. M. Heinricher and H. Fields, "Molecular and effect of delta opioid compounds," in *The Delta Receptor*, K. J. Chang, F. Porreca, and J. Woods, Eds., pp. 467–480, Marcel Dekker, New York, NY, USA, 2003.
- [26] H. Fields, "State-dependent opioid control of pain," *Nature Reviews Neuroscience*, vol. 5, no. 7, pp. 565–575, 2004.
- [27] C. M. Cahill, A. Morinville, C. Hoffert, D. O'Donnell, and A. Beaudet, "Up-regulation and trafficking of δ opioid receptor in a model of chronic inflammation: implications for pain control," *Pain*, vol. 101, no. 1-2, pp. 199–208, 2003.
- [28] K. A. Moore, T. Kohno, L. A. Karchewski, J. Scholz, H. Baba, and C. J. Woolf, "Partial peripheral nerve injury promotes a selective loss of GABAergic inhibition in the superficial dorsal horn of the spinal cord," *Journal of Neuroscience*, vol. 22, no. 15, pp. 6724–6731, 2002.
- [29] L. Jasmin, M. V. Wu, and P. T. Ohara, "GABA puts a stop to pain," *CNS and Neurological Disorders*, vol. 3, no. 6, pp. 487–505, 2004.
- [30] T. Miyamae, N. Fukushima, Y. Misu, and H. Ueda, " δ Opioid receptor mediates phospholipase C activation via G_i in *Xenopus* oocytes," *FEBS Letters*, vol. 333, no. 3, pp. 311–314, 1993.
- [31] K. A. Trujillo and H. Akil, "Inhibition of morphine tolerance and dependence by the NMDA receptor antagonist MK-801," *Science*, vol. 251, no. 4989, pp. 85–87, 1991.
- [32] L. Pu, G. B. Bao, N. J. Xu, L. Ma, and G. Pei, "Hippocampal long-term potentiation is reduced by chronic opiate treatment and can be restored by re-exposure to opiates," *Journal of Neuroscience*, vol. 22, no. 5, pp. 1914–1921, 2002.
- [33] N. Gong, Y. Li, G. Q. Cai et al., "GABA transporter-1 activity modulates hippocampal theta oscillation and theta burst stimulation-induced long-term potentiation," *Journal of Neuroscience*, vol. 29, no. 50, pp. 15836–15845, 2009.
- [34] E. Erbs, L. Faget, G. Scherrer et al., "Distribution of delta opioid receptor-expressing neurons in the mouse hippocampus," *Neuroscience*, vol. 221, pp. 203–213, 2012.
- [35] J. Ortiz, H. W. Harris, X. Guitart, R. Z. Terwilliger, J. W. Haycock, and E. J. Nestler, "Extracellular signal-regulated protein kinases (ERKs) and ERK kinase (MEK) in brain: regional distribution and regulation by chronic morphine," *Journal of Neuroscience*, vol. 15, no. 2, pp. 1285–1297, 1995.
- [36] N. J. Xu, L. Bao, H. P. Fan et al., "Morphine withdrawal increases glutamate uptake and surface expression of glutamate transporter GLT1 at hippocampal synapses," *Journal of Neuroscience*, vol. 23, no. 11, pp. 4775–4784, 2003.
- [37] K. Ullensvang, K. P. Lehre, J. Storm-Mathisen, and N. C. Danbolt, "Differential developmental expression of the two rat brain glutamate transporter proteins GLAST and GLT," *European Journal of Neuroscience*, vol. 9, no. 8, pp. 1646–1655, 1997.
- [38] G. Schmalzing, S. Gloor, H. Omay, S. Kroner, H. Appelhans, and W. Schwarz, "Up-regulation of sodium pump activity in *Xenopus laevis* oocytes by expression of heterologous β 1 subunits of the sodium pump," *Biochemical Journal*, vol. 279, no. 2, pp. 329–336, 1991.
- [39] A. V. Lafaie and W. Schwarz, "Voltage dependence of the rheogenic Na^+/K^+ ATPase in the membrane of oocytes of *Xenopus laevis*," *Journal of Membrane Biology*, vol. 91, no. 1, pp. 43–51, 1986.
- [40] L. A. Vasilets, T. Ohta, S. Noguchi, M. Kawamura, and W. Schwarz, "Voltage-dependent inhibition of the sodium pump by external sodium: species differences and possible role of the N-terminus of the α -subunit," *European Biophysics Journal*, vol. 21, no. 6, pp. 433–443, 1993.
- [41] Y. Zhu, L. A. Vasilets, J. Fei, L. Guo, and W. Schwarz, "Different functional roles of arginine residues 39 and 61 and tyrosine residue 98 in transport and channel mode of the glutamate transporter EAAC1," *Biochimica et Biophysica Acta*, vol. 1665, no. 1-2, pp. 20–28, 2004.
- [42] K. Oguri, I. Yamada-Mori, and J. Shigezane, "Enhanced binding of morphine and nalorphine to opioid delta receptor by glucuronate and sulfate conjugations at the 6-position," *Life Sciences*, vol. 41, no. 12, pp. 1457–1464, 1987.
- [43] H. W. D. Matthes, R. Maldonado, F. Simonin et al., "Loss of morphine-induced analgesia, reward effect and withdrawal symptoms in mice lacking the μ -opioid-receptor gene," *Nature*, vol. 383, no. 6603, pp. 822–823, 1996.
- [44] C. M. Constantino, I. Gomes, S. D. Stockton, M. P. Lim, and L. A. Devi, "Opioid receptor heteromers in analgesia," *Expert Reviews in Molecular Medicine*, vol. 14, article e9, 2012.
- [45] X. Zhang, L. Bao, and J. S. Guan, "Role of delivery and trafficking of δ -opioid peptide receptors in opioid analgesia and tolerance," *Trends in Pharmacological Sciences*, vol. 27, no. 6, pp. 324–329, 2006.
- [46] K. G. Commons, "Translocation of presynaptic delta opioid receptors in the ventrolateral periaqueductal gray after swim stress," *Journal of Comparative Neurology*, vol. 464, no. 2, pp. 197–207, 2003.
- [47] B. Pomeranz and D. Chiu, "Naloxone blockade of acupuncture analgesia: endorphin implicated," *Life Sciences*, vol. 19, no. 11, pp. 1757–1762, 1976.
- [48] D. J. Mayer, D. D. Price, and A. Rafii, "Antagonism of acupuncture analgesia in man by the narcotic antagonist naloxone," *Brain Research*, vol. 121, no. 2, pp. 368–372, 1977.
- [49] X. Kang, D. Chao, Q. Gu et al., " δ -Opioid receptors protect from anoxic disruption of Na^+ homeostasis via Na^+ channel regulation," *Cellular and Molecular Life Sciences*, vol. 66, no. 21, pp. 3505–3516, 2009.
- [50] H. Deng, Z. Yang, Y. Li et al., "Interactions of Na^+/K^+ -ATPase and co-expressed δ -opioid receptor," *Neuroscience Research*, vol. 65, no. 3, pp. 222–227, 2009.
- [51] Z. J. Yang, G. B. Bao, H. P. Deng et al., "Interaction of δ -opioid receptor with membrane transporters: possible mechanisms in pain suppression by acupuncture," *Journal of Acupuncture and Tuina Science*, vol. 6, no. 5, pp. 298–300, 2008.
- [52] D. Marazziti, S. Mandillo, C. Di Pietro, E. Golini, R. Matteoni, and G. P. Tocchini-Valentini, "GPR37 associates with the dopamine transporter to modulate dopamine uptake and behavioral responses to dopaminergic drugs," *Proceedings of the National Academy of Sciences of the United States of America*, vol. 104, no. 23, pp. 9846–9851, 2007.
- [53] F. J. S. Lee, L. Pei, A. Moszczynska, B. Vukusic, P. J. Fletcher, and F. Liu, "Dopamine transporter cell surface localization facilitated by a direct interaction with the dopamine D2 receptor," *EMBO Journal*, vol. 26, no. 8, pp. 2127–2136, 2007.
- [54] B. Bie and Z. Z. Pan, "Trafficking of central opioid receptors and descending pain inhibition," *Molecular Pain*, vol. 3, article 37, 2007.

- [55] A. Mansour, C. A. Fox, H. Akil, and S. J. Watson, "Opioid-receptor mRNA expression in the rat CNS: anatomical and functional implications," *Trends in Neurosciences*, vol. 18, no. 1, pp. 22–29, 1995.
- [56] P. Barbaresi, G. Gazzanelli, and M. Malatesta, "GABA transporter-1 (GAT-1) immunoreactivity in the cat periaqueductal gray matter," *Neuroscience Letters*, vol. 250, no. 2, pp. 123–126, 1998.
- [57] M. W. Quick, J. L. Corey, N. Davidson, and H. A. Lester, "Second messengers, trafficking-related proteins, and amino acid residues that contribute to the functional regulation of the rat brain GABA transporter GAT1," *Journal of Neuroscience*, vol. 17, no. 9, pp. 2967–2979, 1997.
- [58] L. G. Lou, L. Ma, and G. Pei, "Nociceptin/Orphanin FQ activates protein kinase C, and this effect is mediated through phospholipase C/Ca²⁺ pathway," *Biochemical and Biophysical Research Communications*, vol. 240, no. 2, pp. 304–308, 1997.
- [59] L. G. Lou and G. Pei, "Modulation of protein kinase C and cAMP-dependent protein kinase by δ -opioid," *Biochemical and Biophysical Research Communications*, vol. 236, no. 3, pp. 626–629, 1997.
- [60] A. N. M. Schoffmeier, L. J. M. J. Vanderschuren, T. J. De Vries, F. Hogenboom, G. Wardeh, and A. H. Mulder, "Synergistically interacting dopamine D1 and NMDA receptors mediate nonvesicular transporter-dependent GABA release from rat striatal medium spiny neurons," *Journal of Neuroscience*, vol. 20, no. 9, pp. 3496–3503, 2000.
- [61] M. L. Beckman and M. W. Quick, "Neurotransmitter transporters: regulators of function and functional regulation," *Journal of Membrane Biology*, vol. 164, no. 1, pp. 1–10, 1998.
- [62] J. L. Corey, N. Davidson, H. A. Lester, N. Brecha, and M. W. Quick, "Protein kinase C modulates the activity of a cloned γ -aminobutyric acid transporter expressed in *Xenopus* oocytes via regulated subcellular redistribution of the transporter," *Journal of Biological Chemistry*, vol. 269, no. 20, pp. 14759–14767, 1994.
- [63] S. L. Deken, M. L. Beckman, L. Boos, and M. W. Quick, "Transport rates of GABA transporters: regulation by the N-terminal domain and syntaxin 1A," *Nature Neuroscience*, vol. 3, no. 10, pp. 998–1003, 2000.
- [64] M. L. Beckman, E. M. Bernstein, and M. W. Quick, "Protein kinase C regulates the interaction between a GABA transporter and syntaxin 1A," *Journal of Neuroscience*, vol. 18, no. 16, pp. 6103–6112, 1998.
- [65] G. Ogimoto, G. A. Yudowski, C. J. Barker et al., "G protein-coupled receptors regulate Na⁺,K⁺-ATPase activity and endocytosis by modulating the recruitment of adaptor protein 2 and clathrin," *Proceedings of the National Academy of Sciences of the United States of America*, vol. 97, no. 7, pp. 3242–3247, 2000.
- [66] S. K. Shenoy and R. J. Lefkowitz, "Multifaceted roles of β -arrestins in the regulation of seven-membrane-spanning receptor trafficking and signalling," *Biochemical Journal*, vol. 375, no. 3, pp. 503–515, 2003.
- [67] O. El Far and H. Betz, "G-protein-coupled receptors for neurotransmitter amino acids: C-terminal tails, crowded signalosomes," *Biochemical Journal*, vol. 365, no. 2, pp. 329–336, 2002.
- [68] Y. Zhu, J. Fei, and W. Schwarz, "Expression and transport function of the glutamate transporter EAAC1 in *Xenopus* oocytes is regulated by syntaxin 1A," *Journal of Neuroscience Research*, vol. 79, no. 4, pp. 503–508, 2005.
- [69] P. Illes, "Modulation of transmitter and hormone release by multiple neuronal opioid receptors," *Reviews of Physiology Biochemistry and Pharmacology*, vol. 112, pp. 139–233, 1989.
- [70] M. H. Heijna, F. Hogenboom, A. H. Mulder, and A. N. M. Schoffmeier, "Opioid receptor-mediated inhibition of ³H-dopamine and ¹⁴C-acetylcholine release from rat nucleus accumbens slices. A study on the possible involvement of K⁺ channels and adenylate cyclase," *Naunyn-Schmiedeberg's Archives of Pharmacology*, vol. 345, no. 6, pp. 627–632, 1992.
- [71] D. A. Eisinger, H. Ammer, and R. Schulz, "Chronic morphine treatment inhibits opioid receptor desensitization and internalization," *Journal of Neuroscience*, vol. 22, no. 23, pp. 10192–10200, 2002.
- [72] D. Chao and Y. Xia, "Tonic storm in hypoxic/ischemic stress: can opioid receptors subside it?" *Progress in Neurobiology*, vol. 90, no. 4, pp. 439–470, 2010.

Research Article

Electrical Potential of Acupuncture Points: Use of a Noncontact Scanning Kelvin Probe

**Brian J. Gow,¹ Justine L. Cheng,² Iain D. Baikie,³ Ørjan G. Martinsen,^{4,5} Min Zhao,^{6,7}
Stephanie Smith,⁸ and Andrew C. Ahn^{8,9}**

¹ Osher Center for Integrative Medicine, Brigham and Women's Hospital, 900 Commonwealth Avenue, Boston, MA 02215, USA

² School of Engineering and Applied Sciences and East Asian Programs, Harvard University, Harvard Yard, Cambridge, MA 02138, USA

³ KP Technology Ltd., Wick KW1 5LE, UK

⁴ Department of Physics, University of Oslo, 0316 Oslo, Norway

⁵ Department of Biomedical and Clinical Engineering, Rikshospitalet University Hospital, Oslo University Hospital, 0027 Oslo, Norway

⁶ Departments of Dermatology & Ophthalmology, Research Institute for Regenerative Cures, UC Davis School of Medicine, 2921 Stockton Boulevard, Sacramento, CA 95817, USA

⁷ School of Medical Sciences, University of Aberdeen, Aberdeen AB25 2ZD, UK

⁸ Martinos Center for Biomedical Imaging, Department of Radiology, Massachusetts General Hospital, 149 Thirteenth Street, Charlestown, MA 02129, USA

⁹ Division of General Medicine & Primary Care, Department of Medicine, Beth Israel Deaconess Medical Center, 330 Brookline Avenue, Boston, MA 02215, USA

Correspondence should be addressed to Andrew C. Ahn, aahn1@partners.org

Received 20 September 2012; Revised 1 November 2012; Accepted 4 November 2012

Academic Editor: Wolfgang Schwarz

Copyright © 2012 Brian J. Gow et al. This is an open access article distributed under the Creative Commons Attribution License, which permits unrestricted use, distribution, and reproduction in any medium, provided the original work is properly cited.

Objective. Acupuncture points are reportedly distinguishable by their electrical properties. However, confounders arising from skin-to-electrode contact used in traditional electrodermal methods have contributed to controversies over this claim. The Scanning Kelvin Probe is a state-of-the-art device that measures electrical potential without actually touching the skin and is thus capable of overcoming these confounding effects. In this study, we evaluated the electrical potential profiles of acupoints LI-4 and PC-6 and their adjacent controls. We hypothesize that acupuncture point sites are associated with increased variability in potential compared to adjacent control sites. **Methods.** Twelve healthy individuals were recruited for this study. Acupuncture points LI-4 and PC-6 and their adjacent controls were assessed. A 2 mm probe tip was placed over the predetermined skin site and adjusted to a tip-to-sample distance of 1.0 mm under tip oscillation settings of 62.4 Hz frequency. A 6×6 surface potential scan spanning a $1.0 \text{ cm} \times 1.0 \text{ cm}$ area was obtained. **Results.** At both the PC-6 and LI-4 sites, no significant differences in mean potential were observed compared to their respective controls (Wilcoxon rank-sum test, $P = 0.73$ and 0.79 , resp.). However, the LI-4 site was associated with significant increase in variability compared to its control as denoted by standard deviation and range ($P = 0.002$ and 0.0005 , resp.). At the PC-6 site, no statistical differences in variability were observed. **Conclusion.** Acupuncture points may be associated with increased variability in electrical potential.

1. Introduction

One fundamental question remains largely unaddressed in acupuncture research: what is an acupuncture point? The answer to this question carries substantial implications for research and determines the appropriateness of a sham control, the rationale for employing various techniques

(e.g., electrical stimulation and magnets), and the optimal point localization techniques for animal models. The proper characterization of acupuncture points is arguably as critical to acupuncture research as quality assurances are to botanical research, yet neither researchers nor clinicians have fully arrived at a consensus on how acupuncture points should be defined or localized.

In the acupuncture community, acupuncture points have traditionally been viewed as points of distinct electrical characteristics [1]. This view dates to the 1950s, when Voll (Germany) in 1953 [2], Nakatani (Japan) in 1956 [3, 4], and Niboyet (France) in 1957 [5] independently concluded that skin points with unique electrical characteristics were identifiable and spatially correlated with traditional acupuncture points. Since then, a number of studies have elaborated the electrical properties attached to these “bioactive” points and ascribed these points with increased conductance [6–8], reduced impedance and resistance, increased capacitance [9–14], and elevated electrical potential compared to nonacupuncture points [8, 15–17].

For sixty years, these claims have remained unsettled due, in large part, to confounders inherent to electrodermal devices relying on electrodes contacted with skin. Confounding factors—namely, electrode pressure, choice of contact medium, electrode polarization, and skin moisture—collectively contribute to measurement variability and susceptibilities to bias [18]. To overcome these issues, we have employed a novel Scanning Kelvin Probe to measure surface electrical potential without actually touching the skin, and this study represents the first time, to our knowledge, where this technology has been applied to the study of acupuncture points in an *in vivo* human setting. The Scanning Kelvin Probe relies on capacitive coupling between the probe and the sample and has been used in metal work function determination [19–21], dopant profile characterization in semiconductor devices [22–26], metal corrosion analysis [19, 27], and liquid-air interface characterization [28, 29] with micrometer scale and millivolt resolution. The theoretical basis for applying this technology to biological tissue has been published elsewhere [30].

In this study of 12 healthy subjects, we obtained 1.0 cm × 1.0 cm scans of surface potential over acupuncture points LI-4 and PC-6 and their respective, adjacent controls. We hypothesized that scans of and around the acupuncture point are associated with increased topographic variability in electrical potential compared to the scans of adjacent controls. This hypothesis was derived from the theoretical idea that acupuncture points are electrophysiologically distinct from their adjoining skin and thus engender greater spatial variability in electrical potential for a region encompassing both acupoint and its vicinity.

2. Materials and Methods

2.1. Scanning Kelvin Probe: Setup. The Scanning Kelvin Probe (SKP5050, Kelvin Probe Technology, Ltd., Wick, UK) is a state-of-the-art device that measures surface electrical potential without actually contacting the sample [31]. Its operation can be grossly summarized as follows (Figure 1): a probe tip is positioned close to the skin, creating a capacitor; the probe tip acts as a plate while the skin acts as the contralateral plate and the potential difference between the two (V_s) generates a charge on the probe tip; the probe tip oscillates to vary the distance from the skin (d_0 : tip-to-sample distance, $2d_1$: probe oscillation amplitude); since capacitance

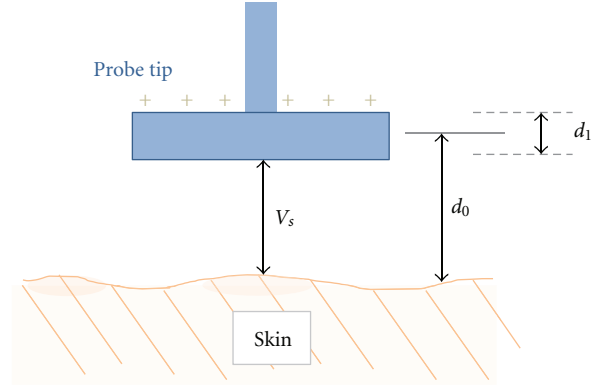


FIGURE 1: Illustration of the Scanning Kelvin Probe arrangement. The Kelvin Probe tip is maintained over the skin at a distance of d_0 to create a capacitor arrangement. Due to the intrinsic potential differences between the tip and the skin (V_s), charges accumulate at the tip once a closed circuit is established. The tip oscillates at an amplitude of d_1 which generates a current through the Scanning Kelvin Probe circuit.

is inversely related to distance, the oscillation changes the capacitance and alters the charge on the probe tip; this generates a measurable current (approximately around 10^{-9} amperes) which is used to calculate the potential difference between the tip and sample; with a constant work function seen with the metallic tip, the skin surface potential can be determined. Our Scanning Kelvin Probe has the added capabilities of (1) calculating the tip-sample distance within an accuracy of $\sim 1\mu\text{m}$ and (2) scanning the surface to produce a two-dimensional potential profile [32, 33].

The probe tip is circular, 2 mm in diameter, and composed of stainless steel. Preliminary studies revealed that biological potential measurements with the steel tip were not sensitive to modest shifts in temperature ($\pm 10^\circ\text{F}$) or humidity ($\pm 5\%$). The tip oscillated at a frequency of 62.4 Hz and an amplitude of $70\mu\text{m}$. The probe tip was set at a constant “gradient” of 210 corresponding to a tip-to-sample distance of approximately 1.0 mm. The “gradient” is a Kelvin Probe measurement that is inversely proportional to the distance squared and is derived from applying a variable backing potential to the tip. A detailed description of this parameter and its derivation is described elsewhere [30, 31]. Data was acquired at a rate of 13,500 Hz, gain of 5, and averaging of 10 to extract the surface electrical potential as previously described [31].

Because the Kelvin Probe is very sensitive to ambient electric fields, a Faraday cage composed of fine copper mesh (16-mesh, TWP Inc., Berkeley, CA) was fabricated and used to enclose the Kelvin Probe head unit and automatic motor scanner unit, along with the subject’s hands and wrists. All conductive materials within the Faraday cage were grounded to an isopotential level using conducting wires connected to a central grounding unit. Insulating materials were either removed or, if required, sprayed with antistatic spray. Furthermore, testing was completed in an electrically shielded room located within the CRC Biomedical Imaging Core at the MGH Charlestown campus. The complete Kelvin

Probe unit was rested on a large 30'' × 36'' Vibration Isolation Workstation (KSI Model number 910R-01-45, Kinetic Systems Inc., Boston, MA) to minimize noise arising from mechanical disturbances.

2.2. Recruitment. Twelve healthy subjects (5 females, 7 males) were recruited to participate in the study. Participants were recruited via postings in Craigslist (<http://www.craigslist.org>). “Healthy” was defined as absence of a chronic medical condition requiring daily medications (e.g., hypertension, diabetes, hypothyroidism, etc.). Individuals with autonomic disorders (sweating irregularities), skin disorders, extensive burns/scars on the hand, tremors, neuromuscular conditions, restless leg syndrome, movement disorders, and implanted cardiac defibrillator/pacemaker were excluded. The subjects’ mean age was 33.7 ± 9.8 (\pm SD) years. Demographic representation was 7 non-Hispanic White, and 5 Asian.

This study was reviewed and approved by the Institutional Review Board at Partners Healthcare. Each study participant read and signed an informed consent form.

2.3. Scanning Measurements. Study volunteers were asked to sit motionless while their wrist and hand were secured with grounding straps to the optical breadboard that served as the base for the Kelvin Probe unit. Because hair may interfere with voltage measurements, each tested site was previously naired to remove all hair within the region. A silver/silver chloride strip electrode (EL-506, Biopac Inc., Goleta, CA) with conductive electrode gel was placed on the ulnar aspect of the forearm approximately 5 cm proximal to the wrist joint. This electrode served as both ground and reference electrode and was intentionally placed close to the test sites to minimize incorporation of physiological electrical activity (e.g., muscle or electrocardiographic) arising from the intervening spaces.

The arm was placed either in a supinated or pronated position depending on the site being evaluated. The hand or wrist was positioned in a way that would keep the surface as flat as possible with respect to the Kelvin Probe tip. In each of the 12 subjects, two acupoints, LI-4 and PC-6, and their corresponding control points were tested. LI-4 was located on the dorsum of the hand, between the first and second metacarpal bones, at the midpoint of the second metacarpal bone and close to its radial border [34]. Its control was exactly 1 cm ulnar to LI-4. PC-6 was located on the flexor aspect of the forearm, 2 cun (a unit of proportional measurements used in acupuncture practice) proximal to the wrist crease and between the tendons of palmaris longus and flexor carpi radialis [34]. Its control was located at either 1 cm radial (7 subjects) or 1 cm ulnar to the point (5 subjects). The radial control was employed for the first seven subjects but switched subsequently to the ulnar control after realizing that the radial control coincided with Japanese-style localization of PC-6. The order of testing by laterality (left versus right), test region (dorsum of the hand versus volar aspect of forearm), and point classification (acupuncture point versus control) was randomized.

Once an acupuncturist identified the points, the corner edges of a 1.0 cm × 1.0 cm square region were marked, centered over the point. The tip was placed over one of the corners and scanning was performed sequentially by rows. The probe was moved with 2 mm intervals to create a 6 × 6 topographic matrix of the surface electrical potential. At each point, a total of 50 electrical potential measurements were acquired continuously to optimize the signal-to-noise ratio, corresponding to a standard error of 6–8 mV per point. After obtaining 50 measurements at a point, the tip was subsequently moved over an adjacent scan point to acquire another set of measurements. These potential measurements were acquired under a “Tracking” algorithm where data were only recorded within a specified range of “gradient,” a marker for probe-to-sample distance. The SKP5050 was equipped with a vertical motor that automatically corrected for any deviations from the desired gradient. Each scan of a test site took approximately 20–25 minutes to perform, corresponding to approximately 35 seconds over each point.

2.4. Calculations and Statistical Analyses. Topographic maps of electrical potentials were obtained by averaging the 50 electrical potential measurements associated with each matrix point. The maps were displayed as a 3-D surface map using Matlab (version 2011b, Mathworks, Natick, MA) to identify any overall electrical potential patterns. In some instances, a consistent elevation or decrease (greater than 50–100 mV) in electrical potential was identified at a matrix point and correlated with subjective sensations of light touch and with the existence of small hairs incompletely removed by Nair. These data points were removed from analyses.

The mean, standard deviation, and range (highest minus smallest potential value) of electrical potential measurements associated with each square scan were calculated, and the Wilcoxon rank sum-tests (Matlab 2011b) were performed to evaluate differences in these variables between acupuncture points and their respective controls.

3. Results

Representative topographic scans of electrical potentials at LI-4 and their corresponding adjacent controls are displayed in Figure 2. Figure 3 shows representative scans of PC-6 and their respective controls. Although a single, coherent peak in potential is seen in several LI-4 topographic scans, no such clear-cut patterns were seen at other sites—including PC-6.

As seen in Table 1, the *mean* potentials at LI4 and PC6 sites were not statistically different from their respective controls (Wilcoxon rank-sum, $P = 0.73$ and 0.79 , resp.). The variability in electrical potential—as evident by both the *standard deviation* and the *range*—was significantly increased at LI-4 site compared to its control ($P = .002$ and 0.0005 , resp.). Except for one subject, every tested individual had greater *standard deviation* in potential at LI-4 site compared to its control, whereas all individuals were found to have greater *range* in electrical potential at LI-4 sites. At PC-6 and PC-6 control sites, on the other hand, no statistical differences in variability were observed ($P = 0.27$ for

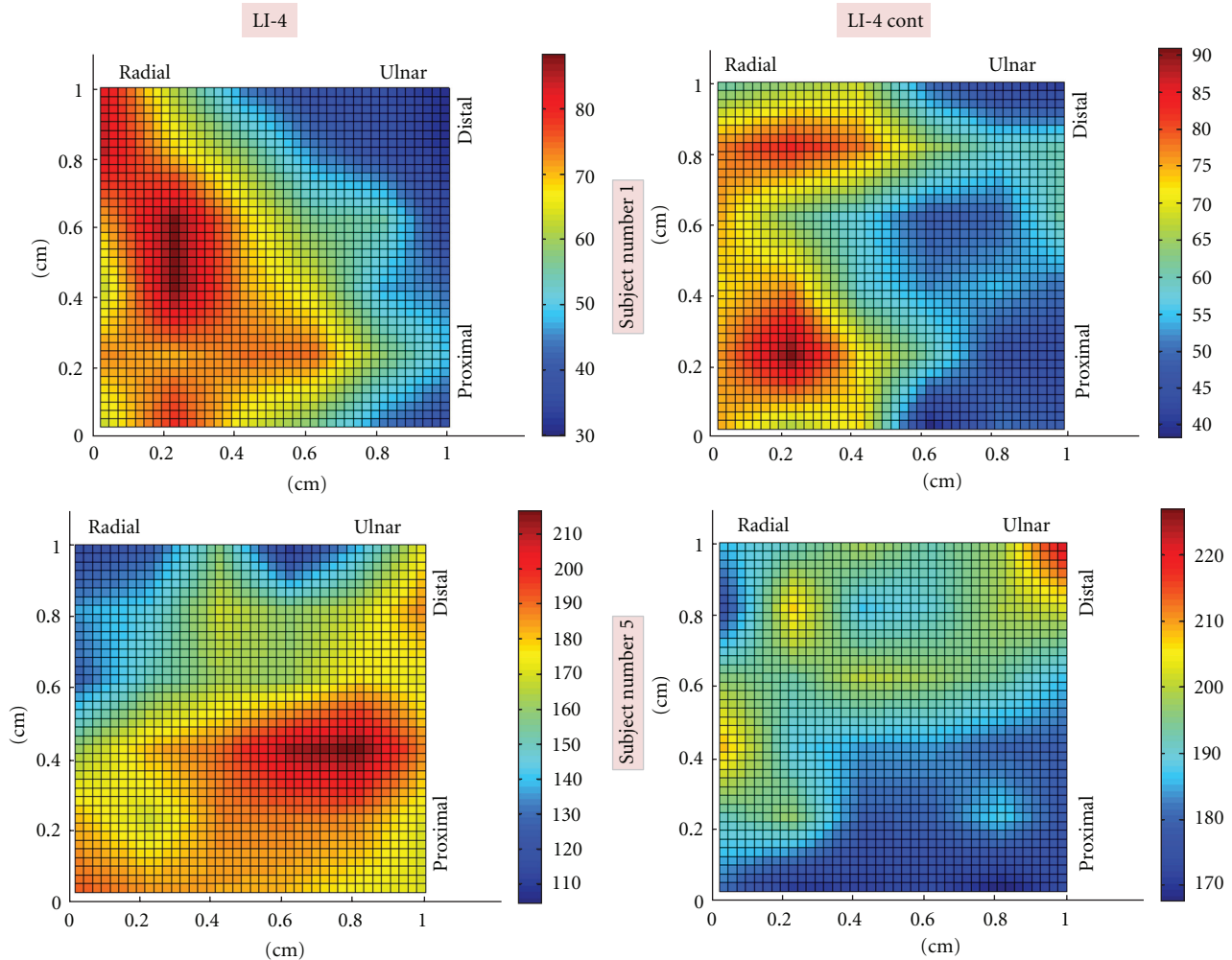


FIGURE 2: Topographic maps of electrical potential at LI-4 and control sites. Representative topographic maps from two subjects are shown here. Images on the left correspond to LI-4 while the images on the right correspond to LI-4 Control. The top images are derived from Subject number 1 and the bottom images are from Subject number 5. For each scan, a color bar is included to display electrical potential magnitudes.

standard deviation and $P = 0.20$ for range). The location of PC-6 controls (radial versus ulnar) had no effect on the study results as no differences in potential variability were seen in either comparisons.

In general, the Scanning Kelvin Probe revealed a not insignificant amount of spatial variability in electrical potential within each 1 cm^2 area. The average difference between the highest and lowest potential within each site was 50 to 80 mV and was found to be as large as 150 mV at some sites.

4. Discussion

This is the first study, to our knowledge, where the electrical properties of acupuncture points were evaluated using a noncontact method. Our approach differs from previous studies in two fundamental ways: first, electrical measurements were obtained without the requirement of an active skin electrode, and second, the Kelvin Probe measures electrical *potential* in contrast to the more common electrical

impedance acquired in other electrodermal studies. These distinctions are associated with several notable advantages and disadvantages.

By obtaining electrical potential without contacting the sample, the Scanning Kelvin Probe bypasses the electrode-skin confounders that plague most, if not all, existing electrodermal devices. The Kelvin Probe is not limited by variable ion accumulation at the electrode, microscopic irregularities of the electrode surface, the effects of contact medium, the variability in mechanical pressure, or the influence of stratum corneum moisture on electrical measures. Moreover, by hovering over the skin surface, the probe tip is capable of scanning the area using a motorized raster unit while maintaining a steady tip-to-sample distance with μm resolution based on a validated Baikie method [31, 33].

However, by virtue of its noncontact approach, the Kelvin Probe is also susceptible to ambient field effects and movement artifacts. Our apparatus involved an electrically shielded room, a local Faraday cage, electrical grounding

TABLE 1: Topographic characteristics of electrical potential scans.

Location	Mean (mean \pm SE, mV)	Scan parameters	
		Standard deviation	Range (mean \pm SE, mV)
Dorsal hand			
LI-4	135.1 \pm 24.2	18.7 \pm 1.8	80.8 \pm 9.2
LI-4 control	139.0 \pm 24.8	12.5 \pm 0.9	52.7 \pm 4.8
<i>P</i> value	0.73	0.002	0.0005
Volar wrist			
PC-6	138.1 \pm 29.3	16.2 \pm 2.8	66.0 \pm 9.2
PC-6 control	138.4 \pm 34.8	17.4 \pm 1.7	76.1 \pm 7.9
<i>P</i> value	0.79	0.27	0.20

of all proximate conductive material, strapping of the hand and wrist to the base board, and a large vibration isolation workstation to attenuate any mechanical perturbations. Even under such controlled conditions, the signal-to-noise ratio was such that numerous potential measurements at each matrix point were required to obtain a sufficiently precise measurement for the purpose of this study. As a consequence, each topographic scan required at least 20 minutes of recording to be completed. In that interim, the wrist and hand could have unwittingly moved and, in few subjects, displaced as much as 6 mm in either longitudinal or lateral directions (although most individuals were able to maintain the position within a 2 mm range).

The volar aspect of the wrist—PC-6 site and its control—in particular, was prone to these movement artifacts since the fully supinated position was more difficult to maintain than the pronated position and the region was frequently traversed by superficial veins that led to slower acquisition of data (interestingly, the respiratory and cardiac mechanical pulsations in the veins could be observed with the Kelvin Probe). These factors may account for why the PC-6 site did not demonstrate a statistical difference compared to its neighboring control. Temporal changes in skin potential over the 20 minute interval may also account for our study results, although ongoing studies with a larger 5 mm tip have demonstrated no substantial change in surface potential over a 40-minute period.

Acquisition of surface electrical potential with the Kelvin Probe has a number of advantages. Without relying on intercalating dyes, strong electrical fields, ionizing beams, or penetrating needles, the Kelvin Probe is well-suited for *in vivo* use. Rather than perturbing the system with substantial electrical currents, as is done in most electrical impedance approaches, surface potential techniques, such as the Scanning Kelvin Probe, introduce little-to-no current and therefore have the theoretical capacity to capture the native and uninhibited endogenous functions of the body. For these reasons, it is not surprising that prior attempts have been made to measure electrical potentials on and around acupuncture points. A total of four studies within the English literature reported that the electrical potential at acupuncture points were, on average, 5 to 100 mV more positive than adjacent skin areas [8, 16, 17, 35]. The non-English literature also agreed with this relative direction in

potential [17, 36]. Our study, in contrast, identified no such consistent relationship and found no statistical differences between mean potentials at acupuncture point and adjacent control sites. Importantly, these prior studies were largely anecdotal in nature and did not have control sites, did not perform statistical analyses, and did not account for skin-electrode factors—such as ionization and redox potentials—that can still confound potential measurements.

The functional significance of the increased variability in electrical potential at LI-4 sites is unclear. Unlike electrical impedance, the physiological factors underlying skin potential measurements have not been fully elaborated and present a significant limitation in our ability to interpret the data. Recent advances in wound healing research, however, have provided some important insights by revealing that a transepithelial potential gradient exists in both amphibian and mammalian skin [37]. Sodium and potassium ions are selectively transported by ion pumps to the inner extracellular layer (i.e., dermal side of the epidermis), while chloride ions are passively transported to the external surface of the skin [38, 39]. This charge separation generates a transepithelial electrical potential that is maintained by apical tight junctions between the outer epidermal cells. In mammalian skin, this transepithelial potential is approximately 70 mV in magnitude—the outer epidermis being more electronegative compared to inner epidermis [40]. Interestingly, this is within the same magnitude of potential changes seen across a 1 cm² span of skin, and it is conceivable that variations in ion pump activities within the epidermis can account for the increased spatial variability in potential seen at LI-4 sites. Certainly, topical applications of pump and channel inhibitors (e.g., amiloride and tetrodotoxin) can be used in future studies to test this hypothesis [41].

This study has a number of limitations. First, as previously stated, the Kelvin Probe is sensitive to ambient field and physical movement artifacts, and potential measurements were affected by superficial structures such as hairs and subcutaneous veins. Second, the prolonged scan time for each site may predispose the topographic map to a number of unintended effects, including lateral displacement of the hand/wrist, changes in local circulation, and subject fatigue. Third, our decision to utilize 2 mm tips and to scan 1.0 cm \times 1.0 cm area may be either too small or too large for the purposes of evaluating an acupuncture point. Future studies

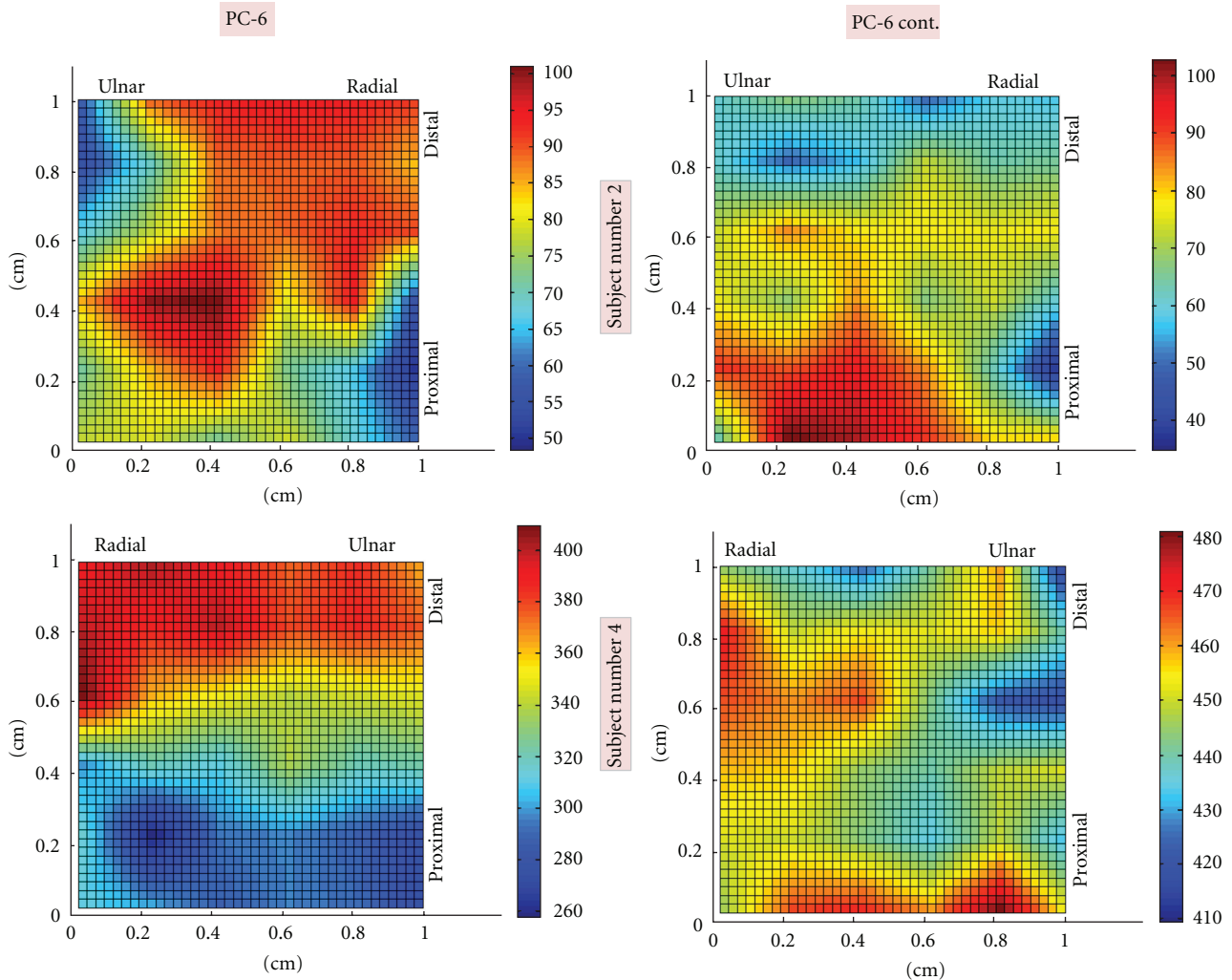


FIGURE 3: Topographic maps of electrical potential at PC-6 and control sites. Representative topographic maps from two subjects are shown here. Images on the left correspond to PC-6 while the images on the right correspond to PC-6 control. The top images are derived from Subject number 2 and the bottom images are from Subject number 4. For each scan, a color bar is included to display electrical potential magnitudes.

should consider evaluating larger scan areas with our present tip or smaller scan areas with smaller tips. Lastly, despite using well-described anatomic landmarks for identifying acupuncture points, we may have incorrectly identified the location of the acupuncture points. Although the scan area provides some level of flexibility, it is worth noting that the exact locations of PC-6 and LI-4 acupuncture points, themselves, are still to some degree disputed. Some of our PC-6 control sites, for instance, can be arguably located on the Japanese-acupuncture-defined PC-6.

Despite these limitations, this study identified a nearly universal increase in variability of potential at LI-4 site compared to its control and provided, for the first time, data on the spatial distribution of *in vivo* electrical potential on intact human skin using a noncontact approach. Future Kelvin Probe studies may consider evaluating the temporal variability of the electrical potential and the electrical field strength over acupuncture points and corresponding controls.

5. Conclusion

The Scanning Kelvin Probe revealed no differences in average electrical potential between acupuncture point and adjacent control sites, but showed a significant increase in variability at the LI-4 area compared to its adjacent control. No such differences were seen at PC-6. The Scanning Kelvin Probe is a promising, novel technology for evaluating *in vivo* skin potentials. Although this application of the Scanning Kelvin Probe is in its early stages, future advances may help yield important insights about the nature of acupuncture points.

Acknowledgments

This research was supported by Grant nos. R21- AT005249 and P30AT005895 of the National Center for Complementary Alternative Medicine (NCCAM). The project described was supported by Clinical Translational Science Award UL1RR025758 to Harvard University and Massachusetts General Hospital from the National Center for Research

Resources. The content is solely the responsibility of the authors and does not necessarily represent the official views of the National Center for Complementary Alternative Medicine or the National Center for Research Resources or the National Institutes of Health. The funders had no role in study design, the data collection and analysis, the decision to publish, or preparation of the paper. Professor I. D. Baikie is the CEO and founder of KP Technology, the manufacturer of the SKP5050 used in this study. The other coauthors have no conflict of interests to report.

References

- [1] A. C. Ahn, A. P. Colbert, B. J. Anderson et al., "Electrical properties of acupuncture points and meridians: a systematic review," *Bioelectromagnetics*, vol. 29, no. 4, pp. 245–256, 2008.
- [2] R. Voll, *Nosodenanwendung in Diagnostik und therapie 13*, ML-Verlage, Uelzen, Germany, 1977.
- [3] Y. Nakatani, "Skin electric resistance and Ryodoraku," *Journal of the Autonomic Nervous System*, vol. 6, p. 5, 1956.
- [4] Y. Nakatani, *A Guide for Application of Ryodoraku Autonomous Nerve Regulatory Therapy*, 1986.
- [5] J. E. H. Niboyet, "Nouvelle constatations sur les propriétés électriques des points Chinois 10," *Bulletin de la Société d'Acupuncture*, vol. 30, pp. 7–13, 1958.
- [6] M. Reichmanis and R. O. Becker, "Physiological effects of stimulation at acupuncture loci: a review," *Comparative Medicine East and West*, vol. 6, no. 1, pp. 67–73, 1978.
- [7] M. Reichmanis, A. A. Marino, and R. O. Becker, "Electrical correlates of acupuncture points," *IEEE Transactions on Biomedical Engineering*, vol. 22, no. 6, pp. 533–535, 1975.
- [8] J. Hyvarinen and M. Karlsson, "Low resistance skin points that may coincide with acupuncture loci," *Medical Biology*, vol. 55, no. 2, pp. 88–94, 1977.
- [9] E. F. Prokhorov, J. González-Hernández, Y. V. Vorobiev, E. Morales-Sánchez, T. E. Prokhorova, and G. Z. Lelo de Larrea, "In vivo electrical characteristics of human skin, including at biological active points," *Medical and Biological Engineering and Computing*, vol. 38, no. 5, pp. 507–511, 2000.
- [10] M. Reichmanis, A. A. Marino, and R. O. Becker, "Laplace plane analysis of transient impedance between acupuncture Li-4 and Li-12," *IEEE Transactions on Biomedical Engineering*, vol. 24, no. 4, pp. 402–405, 1977.
- [11] M. Reichmanis, A. A. Marino, and R. O. Becker, "Laplace plane analysis of impedance on the H meridian," *American Journal of Chinese Medicine*, vol. 7, no. 2, pp. 188–193, 1979.
- [12] H. M. Johng, J. H. Cho, H. S. Shin et al., "Frequency dependence of impedances at the acupuncture point Quze (PC3)," *IEEE Engineering in Medicine and Biology Magazine*, vol. 21, no. 2, pp. 33–36, 2002.
- [13] G. Litscher, R. C. Niemtzw, L. Wang, X. Gao, and C. H. Urak, "Electrodermal mapping of an acupuncture point and a non-acupuncture point," *Journal of Alternative and Complementary Medicine*, vol. 17, no. 9, pp. 781–782, 2011.
- [14] G. Litscher, L. Wang, X. Gao, and I. Gaischek, "Electrodermal mapping: a new technology," *World Journal of Methodology*, vol. 1, no. 1, pp. 22–26, 2011.
- [15] R. O. Becker and A. A. Marino, "Electromagnetism and Life," in *Modern Bioelectricity*, Marcell Dekker, New York, NY, USA, 1988.
- [16] M. L. Brown, G. A. Ulett, and J. A. Stern, "Acupuncture loci: techniques for location," *American Journal of Chinese Medicine*, vol. 2, no. 1, pp. 67–74, 1974.
- [17] C. Ionescu-Tirgoviste and O. Bajenaru, "Electric diagnosis in acupuncture," *American Journal of Acupuncture*, vol. 12, no. 3, pp. 229–238, 1984.
- [18] S. Grimnes and O. G. Martinsen, *Bioimpedance and Bioelectricity Basics*, Academic Press, London, UK, 2000.
- [19] H. N. McMurray, A. J. Coleman, G. Williams, A. Afseth, and G. M. Scamans, "Scanning kelvin probe studies of filiform corrosion on automotive aluminum alloy AA6016," *Journal of the Electrochemical Society*, vol. 154, no. 7, pp. C339–C348, 2007.
- [20] M. Schnippering, M. Carrara, A. Foelske, R. Kötz, and D. J. Fermín, "Electronic properties of Ag nanoparticle arrays. A Kelvin probe and high resolution XPS study," *Physical Chemistry Chemical Physics*, vol. 9, no. 6, pp. 725–730, 2007.
- [21] M. Szymonski, M. Goryl, F. Krok, J. J. Kolodziej, and F. Buatier De Mongeot, "Metal nanostructures assembled at semiconductor surfaces studied with high resolution scanning probes," *Nanotechnology*, vol. 18, no. 4, Article ID 044016, 2007.
- [22] G. Williams, A. Gabriel, A. Cook, and H. N. McMurray, "Dopant effects in polyaniline inhibition of corrosion-driven organic coating cathodic delamination on iron," *Journal of the Electrochemical Society*, vol. 153, no. 10, pp. B425–B433, 2006.
- [23] S. E. Park, N. V. Nguyen, J. J. Kopanski, J. S. Suehle, and E. M. Vogel, "Comparison of scanning capacitance microscopy and scanning Kelvin probe microscopy in determining two-dimensional doping profiles of Si homostructures," *Journal of Vacuum Science and Technology B*, vol. 24, no. 1, pp. 404–407, 2006.
- [24] B. S. Simpkins, E. T. Yu, U. Chowdhury et al., "Local conductivity and surface photovoltage variations due to magnesium segregation in p-type GaN," *Journal of Applied Physics*, vol. 95, no. 11 I, pp. 6225–6231, 2004.
- [25] C. S. Jiang, H. R. Moutinho, D. J. Friedman, J. F. Geisz, and M. M. Al-Jassim, "Measurement of built-in electrical potential in III-V solar cells by scanning Kelvin probe microscopy," *Journal of Applied Physics*, vol. 93, no. 12, pp. 10035–10040, 2003.
- [26] O. A. Semenikhin, L. Jiang, K. Hashimoto, and A. Fujishima, "Kelvin probe force microscopic study of anodically and cathodically doped poly-3-methylthiophene," *Synthetic Metals*, vol. 110, no. 2, pp. 115–122, 2000.
- [27] G. S. Frankel, M. Stratmann, M. Rohwerder et al., "Potential control under thin aqueous layers using a Kelvin Probe," *Corrosion Science*, vol. 49, no. 4, pp. 2021–2036, 2007.
- [28] D. M. Taylor, "Developments in the theoretical modelling and experimental measurement of the surface potential of condensed monolayers," *Advances in Colloid and Interface Science*, vol. 87, no. 2-3, pp. 183–203, 2000.
- [29] D. M. Taylor and G. F. Bayes, "The surface potential of Langmuir monolayers," *Materials Science and Engineering C*, vol. 8-9, pp. 65–71, 1999.
- [30] A. C. Ahn, B. J. Gow, R. G. Martinsen, M. Zhao, and A. J. Grodzinsky, "Applying the Kelvin probe to biological tissues: theoretical and computational analyses," *Physical Review E*, vol. 85, no. 6, Article ID 061901, 2012.
- [31] I. D. Baikie, P. J. S. Smith, D. M. Porterfield, and P. J. Estrup, "Multitip scanning bio-Kelvin probe," *Review of Scientific Instruments*, vol. 70, no. 3, pp. 1842–1850, 1999.
- [32] I. D. Baikie and P. J. Estrup, "Low cost PC based scanning Kelvin probe," *Review of Scientific Instruments*, vol. 69, no. 11, pp. 3902–3907, 1998.

- [33] I. D. Baikie, S. Mackenzie, P. J. Z. Estrup, and J. A. Meyer, "Noise and the Kelvin method," *Review of Scientific Instruments*, vol. 62, no. 5, pp. 1326–1332, 1991.
- [34] P. Deadman, M. Al-Khafaji, and K. Baker, *A Manual of Acupuncture*, Journal of Chinese Medicine Publications, East Sussex, UK, 1998.
- [35] M. Jacob, D. Bruegger, M. Rehm, U. Welsch, P. Conzen, and B. F. Becker, "Contrasting effects of colloid and crystalloid resuscitation fluids on cardiac vascular permeability," *Anesthesiology*, vol. 104, no. 6, pp. 1223–1231, 2006.
- [36] Z.-X. Zhu, "Research advances in the electrical specificity of meridians and acupuncture points," *American Journal of Acupuncture*, vol. 9, no. 3, pp. 203–216, 1981.
- [37] C. D. McCaig, A. M. Rajniecek, B. Song, and M. Zhao, "Controlling cell behavior electrically: current views and future potential," *Physiological Reviews*, vol. 85, no. 3, pp. 943–978, 2005.
- [38] O. A. Candia, "Short-circuit current related to active transport of chloride in frog cornea: effects of furosemide and ethacrynic acid," *Biochimica et Biophysica Acta*, vol. 298, no. 4, pp. 1011–1014, 1973.
- [39] S. D. Klyce, "Transport of Na, Cl, and water by the rabbit corneal epithelium at resting potential," *American Journal of Physiology*, vol. 228, no. 5, pp. 1446–1452, 1975.
- [40] J. J. Vanable, "Integumentary potentials and wound healing," in *Electric Fields in Vertebrate Repair*, R. Borgen, K. R. Robinson, J. W. Vanable, and M. E. McGinnis, Eds., pp. 171–224, Liss, New York, NY, USA, 1989.
- [41] M. Denda, Y. Ashida, K. Inoue, and N. Kumazawa, "Skin surface electric potential induced by ion-flux through epidermal cell layers," *Biochemical and Biophysical Research Communications*, vol. 284, no. 1, pp. 112–117, 2001.

Research Article

Interstitial Fluid Flow: The Mechanical Environment of Cells and Foundation of Meridians

Wei Yao, Yabei Li, and Guanghong Ding

Department of Mechanics and Engineering Science, Shanghai Research Center of Acupuncture, Fudan University, 220 Handan Road, Shanghai 200433, China

Correspondence should be addressed to Guanghong Ding, ghding@fudan.edu.cn

Received 5 July 2012; Revised 3 October 2012; Accepted 20 October 2012

Academic Editor: Wolfgang Schwarz

Copyright © 2012 Wei Yao et al. This is an open access article distributed under the Creative Commons Attribution License, which permits unrestricted use, distribution, and reproduction in any medium, provided the original work is properly cited.

Using information from the deep dissection, microobservation, and measurement of acupoints in the upper and lower limbs of the human body, we developed a three-dimensional porous medium model to simulate the flow field using FLUENT software and to study the shear stress on the surface of interstitial cells (mast cells) caused by interstitial fluid flow. The numerical simulation results show the following: (i) the parallel nature of capillaries will lead to directional interstitial fluid flow, which may explain the long interstitial tissue channels or meridians observed in some experiments; (ii) when the distribution of capillaries is staggered, increases in the velocity alternate, and the velocity tends to be uniform, which is beneficial for substance exchange; (iii) interstitial fluid flow induces a shear stress, with magnitude of several Pa, on interstitial cell membranes, which will activate cells and lead to a biological response; (iv) capillary and interstitial parameters, such as capillary density, blood pressure, capillary permeability, interstitial pressure, and interstitial porosity, affect the shear stress on cell surfaces. The numerical simulation results suggest that *in vivo* interstitial fluid flow constitutes the mechanical environment of cells and plays a key role in guiding cell activities, which may explain the meridian phenomena and the acupuncture effects observed in experiments.

1. Introduction

Interstitial fluid flow is the movement of fluid through the extracellular matrix of tissues, often between blood and lymphatic vessels. This flow provides a necessary mechanism for transporting large proteins through the interstitium and constitutes an important component of microcirculation [1]. Apart from its role in mass transport, interstitial fluid flow also provides a specific mechanical environment that is important for the physiological activities of interstitial cells [2, 3]. Several *in vitro* experiments showed that interstitial fluid flow was very important for cell activities and that a flow of $\mu\text{m/s}$ magnitude induced physiological responses from cells [4–8]. *In vitro* numerical simulations of how the architecture of extracellular fibers affects the shear stress on cell membranes also showed that interstitial fluid flow is important to the fluid force on a cell imbedded in a 3D matrix [9, 10]. Blood flow plays an important role in guiding the physiological activities of endothelial cells (ECs) and smooth muscle cells (SMCs) and during bone remodeling [11–13]. However, studies of the effect of interstitial fluid

flow on interstitial cells (mast cells) are rare. Mast cells are a type of immune cell found in connective tissues. When mast cells are stimulated, they release chemical mediators from their cellular granules into the extracellular matrix and initiate a series of biological responses; many of the responses are correlated with acupuncture effects [14].

Until now, there were no direct *in vivo* measurements of interstitial fluid flow, and information regarding interstitial fluid flow has only been inferred from other possibly correlated measurements. For example, Li et al. visualized regional hypodermic migration channels in the interstitial fluid of humans using magnetic resonance imaging (MRI) [15]. These channels were different from those of lymphatic or blood vessels and partially coincided with the characteristics of meridians. It is believed that interstitial fluid flow can be used to help illustrate the modern physiological mechanism of meridians. In another experiment, nuclide was injected into the “Taiyuan” acupoint of a recently deceased monkey (within a half hour of death). No transmission track was found along the meridian, but a track appeared when saline

solution with heparin was infused simultaneously through an axillary artery and a vein [16]. This phenomenon demonstrates that the movement of an isotope along meridians requires an impetus, which is provided by circulating blood in living beings. We proposed a dynamic model to simulate the interstitial fluid flow near meridians and discovered that the source of direct impetus for this flow was the penetration of plasma between capillaries and interstitial fluid [17]. Furthermore, we developed a two-dimensional (2D) model to study the flow field in connective tissues and observed directional fluid flow [18, 19].

MRI revealed that the tip of an acupuncture needle is normally placed near an interosseous membrane. In this paper, we will investigate the three-dimensional (3D) flow pattern of interstitial fluid in a human interosseous membrane, the effect of physiological parameters on flow velocity and the physiological impact of flow on interstitial cells. The rest of the paper is organized as follows. In Section 2, we present a 3D porous media model to describe the interosseous membrane. The results obtained from the proposed model are presented in Section 3. A discussion and summary of the present study are provided in Section 4.

2. Model and Methods

2.1. The 3D Model. The interosseous membrane is 25 cm long, 2 cm wide, and 0.2 cm thick. Anatomical observations showed that capillaries formed clusters and were distributed in alternating layers. In each cluster, the capillaries were nearly parallel. Figure 1(a) is the sketch map of one membrane unit. The upstream ends of the capillaries connected to a pre-capillary, and the downstream ends connected to a venule. The average length of a capillary group is 2000 μm (see the x -axis in Figure 1(a)), and the average width is 400 μm (see y -axis in Figure 1(a)). The distance between nearby clusters is approximately 1875 μm along the x -axis and approximately 315 μm along the y -axis. Suppose the distance between the capillaries in a cluster is equal, which is approximately 50 μm . According to these characteristics, we develop a 3D model, shown in Figure 1(b). The solid thick lines represent capillaries, and the black and grey colors indicate different layers. The dashed rectangle marks the calculation domain.

To study the effect of flow on interstitial cells, we place a mast cell (a sphere with a diameter of 16 μm) in the center of the domain (the center of the sphere is at $x = 2 \text{ mm}$, $y = z = 0 \text{ mm}$) (Figure 1(b)). The magnified mast cell in Figure 1(b) shows the local Cartesian coordinates $O'x'y'z'$. The origin (O') is at the center of the sphere, and the x' -axis, y' -axis and z' -axis are parallel to the x -axis, y -axis and z -axis, respectively. For mast cells in the interstitium, there is a thin boundary layer near the cell surface, called the Brinkman boundary layer. Therefore, during mesh generation, there is a refined zone near the surface of the mast cell, shown in Figure 1(b) [20].

2.2. Governing Equations. Because the Reynolds number of the interstitial fluid flow is small, inertia can be neglected.

The space in the interstitium composed of parallel collagen fibrils is assumed to be a porous medium. The governing equations are the Brinkman and continuity equations [20]:

$$\nabla p = \mu \Delta \vec{u} - \frac{\mu}{k_p} \vec{u}, \quad (1)$$

$$\nabla \cdot \vec{u} = 0, \quad (2)$$

where ∇ is the gradient operator, Δ is the Laplacian operator, u is the local flow velocity vector, p is the interstitial pressure, μ is the viscosity of interstitial fluid, and k_p is the Darcy permeability of the collagen fibril matrix. The term on the left-hand side of (1) is the pressure gradient. The first term on the right-hand side represents the viscous term, and the last term on the right-hand side represents the Darcy-Forchheimer term, which characterizes flow in a porous medium.

The dimensionless variables are defined as $\vec{u}^* = \vec{u}/U$; $p^* = p/\rho U^2$; $\vec{x}^* = \vec{x}/D$; and $\vec{k} = \vec{k}_p/D^2$, where U is the characteristic velocity, D is the diameter of capillaries, ρ is the fluid density, and \vec{x} is the position vector. Equations (1) and (2) are rewritten in dimensionless forms as:

$$\nabla p^* = \frac{1}{\text{Re}} \Delta \vec{u}^* - \frac{1}{\text{Re} \cdot \vec{k}} \vec{u}^*, \quad (3)$$

$$\nabla \cdot \vec{u}^* = 0, \quad (4)$$

where Re is the Reynolds number, defined as $\text{Re} = \rho U D / \mu$. In our model, \vec{k}_p is small (10^{-16} m^2), and the dimensionless parameter \vec{k} is approximately 10^{-6} . Therefore, the viscous term is small compared with the Darcy-Forchheimer term and can be neglected. Equation (3) reduces to Darcy's law [20]:

$$\nabla p^* = -\frac{1}{\text{Re} \cdot \vec{k}} \vec{u}^*. \quad (5)$$

For the mast cell in the interstitium, the next results will show that the flow field near the cell is almost symmetrical about the x' -axis. Therefore, we use spherical coordinates to analyze the shear stress on the mast cell (τ_{cell}), and the dominant stress is

$$\tau_{r\theta} = -\mu \left\{ r \frac{\partial}{\partial r} \left(\frac{u_\theta}{r} \right) + \frac{1}{r} \frac{\partial u_r}{\partial \theta} \right\}_{\text{cell}}. \quad (6)$$

2.3. Effect of Capillaries on the Interstitial Fluid Flow. Starling's hypothesis that fluid movement across microvascular walls is determined by the transmural difference in hydrostatic and oncotic pressures has become a general principle of physiology [21]:

$$v = k_c [(p_c - p_i) - (\pi_c - \pi_i)], \quad (7)$$

where k_c is the permeability coefficient of the capillary walls, p_c is the hydrostatic pressure in blood, p_i is the interstitial hydrostatic pressure at the capillary wall, π_c is the osmotic pressure in blood, and π_i is the interstitial osmotic pressure at

TABLE 1: Physiological parameter values of the model.

Parameter	Value
Viscosity of interstitial fluid $\mu/(\text{kg}\cdot\text{m}^{-1}\cdot\text{s}^{-1})$	3.5×10^{-3} [22]
Permeability coefficient of capillary wall $k_c/(\text{m}^2\cdot\text{s}\cdot\text{kg}^{-1})$	5×10^{-10} [23]
Plasma colloid osmotic pressure π_c/mmHg	28 [24]
Interstitial colloid osmotic pressure at the capillary wall π_i/mmHg	8 [24]
Density of interstitial fluid $\rho/(\text{kg}\cdot\text{m}^{-3})$	1000
Length of capillary $L/\mu\text{m}$	2000
Diameter of capillary $D/\mu\text{m}$	8 [19]
Distance between adjacent capillaries $d/\mu\text{m}$	48 [19]
Interstitial hydrostatic pressure at the capillary wall p_i/mmHg	-5 [24]
Intravascular capillary pressure at the upstream end p_a/mmHg	25 [24]
Intravascular capillary pressure at the downstream end p_v/mmHg	10 [24]
Width of capillary group W (μm)	392
Length of the calculation domain d_x (μm)	3600
Width of the calculation domain d_y (μm)	784
Height of the calculation domain d_z (μm)	632

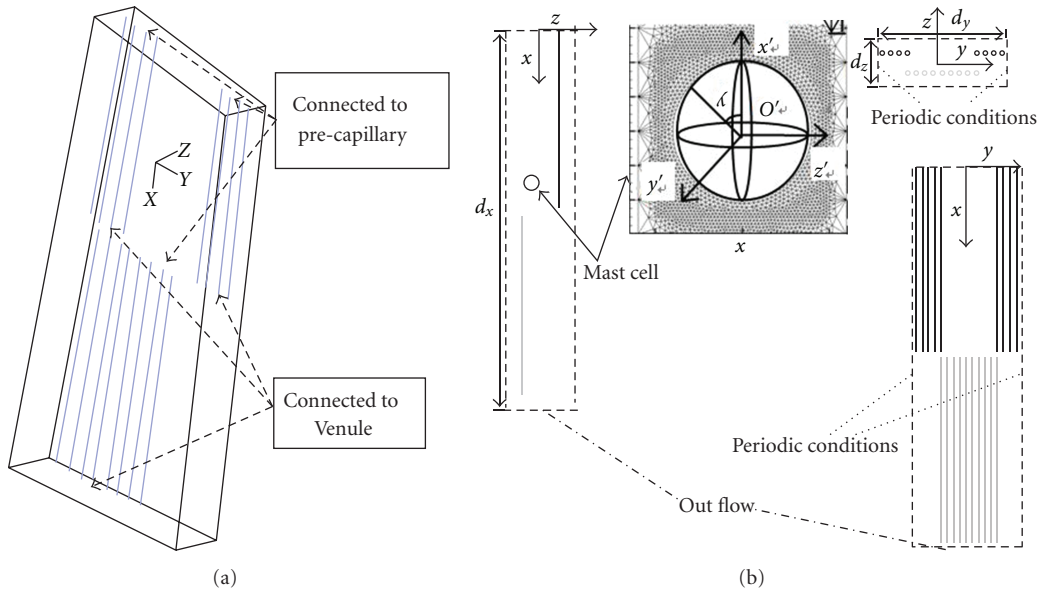


FIGURE 1: Model of the interosseous membrane. (a) The sketch map; (b) 3D porous media model.

the capillary wall. Hu and Weinbaum determined that π_i and p_i (hydrostatic and colloid osmotic pressures, respectively, behind the surface glycocalyx in their model) can differ greatly from the corresponding pressures in the interstitial space [25]. Generally, it is assumed that only p_c varies and that p_c decreases linearly from the pre-capillary side to the venule side along the length of the capillary. Other parameters (p_i , π_c and π_i) are assumed to be constant [21]. Defining the characteristic velocity $U = k_c[(p_a - p_i) - (\pi_c - \pi_i)]$, where p_a is the intravascular capillary pressure at the upstream end, and using the values of the parameters listed in Table 1, the transmural capillary velocity is

$$v = U \left(1 - 1.5 \frac{x}{L} \right), \quad (8)$$

where x is the distance from the upstream end, and L is the length of the capillary.

2.4. Effect of Collagen Fibrils on the Interstitial Fluid Flow.

Parallel collagen fibrils can influence the interstitial fluid flow. Chen et al. developed 2D and 3D finite element models analogous to the parallel collagen fibril arrays in ligaments and tendons to simulate transverse and longitudinal interstitial fluid flows [22]. The flow along collagen fibrils is defined as longitudinal flow with the flow perpendicular to collagen fibrils defined as transverse flow. The computational results provided empirical expressions for Darcy's permeability as a function of the porosity ϕ . Considering the fluid to be

a Newtonian fluid, the empirical expressions are shown as follows:

transverse permeability:

$$k_y = k_z = 1.2 \times 10^{-15} \phi^{0.5} (\phi - \phi_{\min})^{2.5}, \quad (9)$$

longitudinal permeability:

$$k_x = 1.1 \times 10^{-15} \phi^{2.5} (1 - \phi)^{-0.33},$$

where $\phi_{\min} = 1 - \pi/4$ [22]. The physiological range of porosity in ligaments is $0.32 \sim 0.42$ [22]. The structure of an interosseous membrane is similar to that of ligaments. Therefore, the longitudinal permeability is approximately $1.0 \times 10^{-16} \text{ m}^2$, and the ratio of k_x to k_y (ratio = k_x/k_y) is approximately 10.

2.5. Boundary Conditions. The calculation domain is shown in Figure 1(b) and contains one whole and two half capillary clusters. The capillary wall is defined as the velocity-inlet boundary, and the inlet velocity is defined by UDF (8). In addition, because of the periodic geometric character, we define periodic boundary conditions as shown in Figure 1(b). The outward flow (at the bottom boundary) is fully developed, and the x -direction derivative of u_x is zero ($\partial u_x / \partial x = 0$). The upstream flow is neglected, and the inlet velocity (the upper boundary) is defined to be zero. The calculation domain is a porous zone, and the viscous resistance is $1/\overline{k}_p$.

When a mast cell is present in the interstitium, the mast cell region (the sphere in the center) is removed from the original calculation region. The sphere surface is presumed to be a wall; therefore, non-slip boundary conditions ($u_r = 0$, $u_\theta = 0$) are used. The Brinkman boundary layer (δ) has a thickness of magnitude $\sqrt{\overline{k}_p}$.

2.6. Computational Method. The CFD software package FLUENT (version 6.0) is used for the numerical simulation. The grid is generated using the GAMBIT software package. The model is laminar, the solver is segregated and steady, and the solving method is the SIMPLE scheme. The governing equations are solved by iterating. When the iteration is convergent (error of iterated results $e < 0.001$), the velocity field is obtained.

2.7. Physiological Parameters. Table 1 shows the physiological parameters used in the numerical simulation.

3. Results

3.1. Flow Field without Interstitial Cell. Figure 2(a) is the flow field in the x - y plane ($z = 0$, display scale : $y = 1 : 2.5$, $x : z = 1 : 2.5$). The thick black lines represent the capillaries, the arrows point in the direction of the velocity, the arrow length indicates the magnitude of the velocity, and the colored lines are contours of velocity. The interstitial fluid flows from the capillary to the interstitium on the upstream (left) side. Near the x -axis, the flow direction tends to become parallel to the

capillaries. At the venule side, a small amount of the fluid is absorbed by capillaries while most fluid flows outward. In the first cluster, the inlet velocity is zero. However, the penetrating flux through the capillary wall is greater than the absorbing flux. Therefore, fluid flows out at the end of the first cluster. In the second cluster, because there are fluid flows out of the first cluster, the inlet velocity is no longer zero. Comparing the interstitial fluid velocity in the first cluster with that in the second cluster shows that the velocity in the second cluster is obviously greater. This difference occurs because the inlet velocity of the second cluster, which is generated from the first cluster of capillaries, accelerates the interstitial fluid. The outflow of the second cluster is greater than that of the first cluster. Therefore, the velocity in the third cluster will be even greater. Figure 2(b) shows the path lines from the capillaries in the interstitial space (display scale : $y = 1 : 2.5$, $x : z = 1 : 2.5$). The colored lines represent path lines, which are nearly parallel to the capillaries, and the maximum velocity is approximately $1.5 \times 10^{-6} \text{ m/s}$ ($\sim 2.5 \text{ U}$).

3.2. Flow Field around an Interstitial Cell. Using this model, we also investigate the flow field with a cell in the interstitial space. The interstitial cell has little effect on the flow field except near the cell surface. The maximum velocity occurs at the cell surface ($3.25 \times 10^{-6} \text{ m/s}$, 5 U) and is much greater than the velocity at other locations. The flow field near the cell is nearly symmetrical about the x' -axis. Figure 3 displays the stream lines around the cell, with (a) showing the streamlines in the local y' - z' plane ($x' = 0$, represents the cross section), (b) showing the streamlines in the local x' - z' plane ($y' = 0$, represent the r - θ plane), and (c) showing the streamlines in the local x' - y' plane ($z' = 0$). Figures 3(b) and 3(c) are nearly identical. The direction of the velocity is along the x -axis, and the maximum velocity is at $x' = 0 \text{ mm}$.

3.3. Mechanical Environment of Interstitial Cell. Interstitial fluid flow provides mechanical stimuli to the interstitial cell. The shear stress on the surface of the mast cell (τ_{cell}) is calculated using (6). The shear stress is affected by the Darcy permeability k . Figure 4 shows the τ_{cell} distribution on the cell surface for (a) an isotropic condition (ratio = 1) and (b) an anisotropic condition (ratio = 10). The results show that τ_{cell} has bilateral symmetry and that the maximum τ_{cell} ($\tau_{\text{cell,max}}$) is at $x' = 0 \text{ mm}$ for ratio ≥ 1 (ratio = 1 and ratio = 10). τ_{cell} increases as k_x decreases. As ratio increases, the τ_{cell} near $\tau_{\text{cell,max}}$ changes significantly. The τ_{cell} distribution on the cell surface in Figure 4 is also shown for (c) fixed k_y ($k_y = 4 \times 10^{-17} \text{ m}^2$) and (d) fixed k_x ($k_x = 4 \times 10^{-16} \text{ m}^2$). The results show that k_x is the main factor affecting τ_{cell} . When k_y is fixed, τ_{cell} increases as k_x decreases (Figure 4(c)). When k_x is fixed, as k_y decreases, the distribution of τ_{cell} becomes more uneven (Figure 4(d)).

3.4. The Effect of Physiological Parameters on $\tau_{\text{cell,max}}$. The capillary density in the interstitium can affect the interstitial fluid flow and τ_{cell} . With the cross-sectional area defined as $S = d_y * d_z$, Figure 5 shows the relationship between $\tau_{\text{cell,max}}$ and S . Obviously, $\tau_{\text{cell,max}}$ decreases as S increases, and the

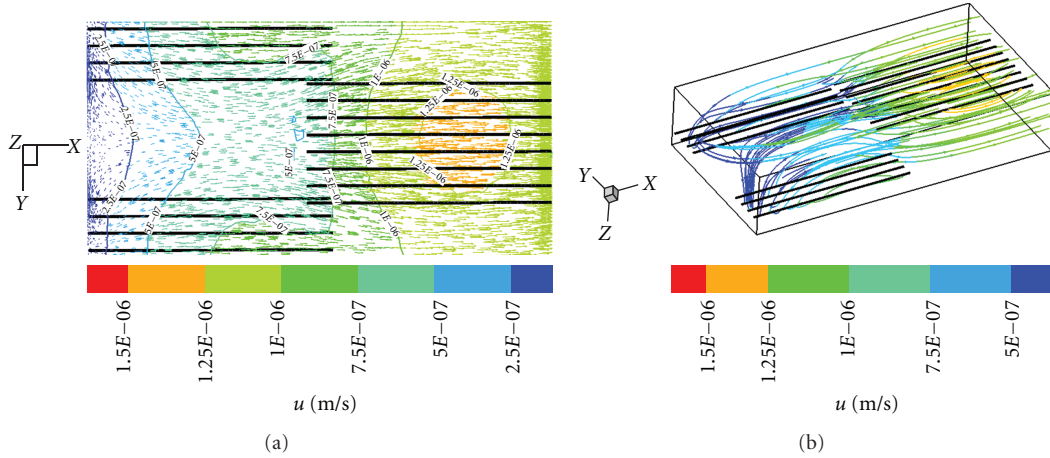


FIGURE 2: (a) Flow field in the x - y plane; (b) path lines from the capillaries.

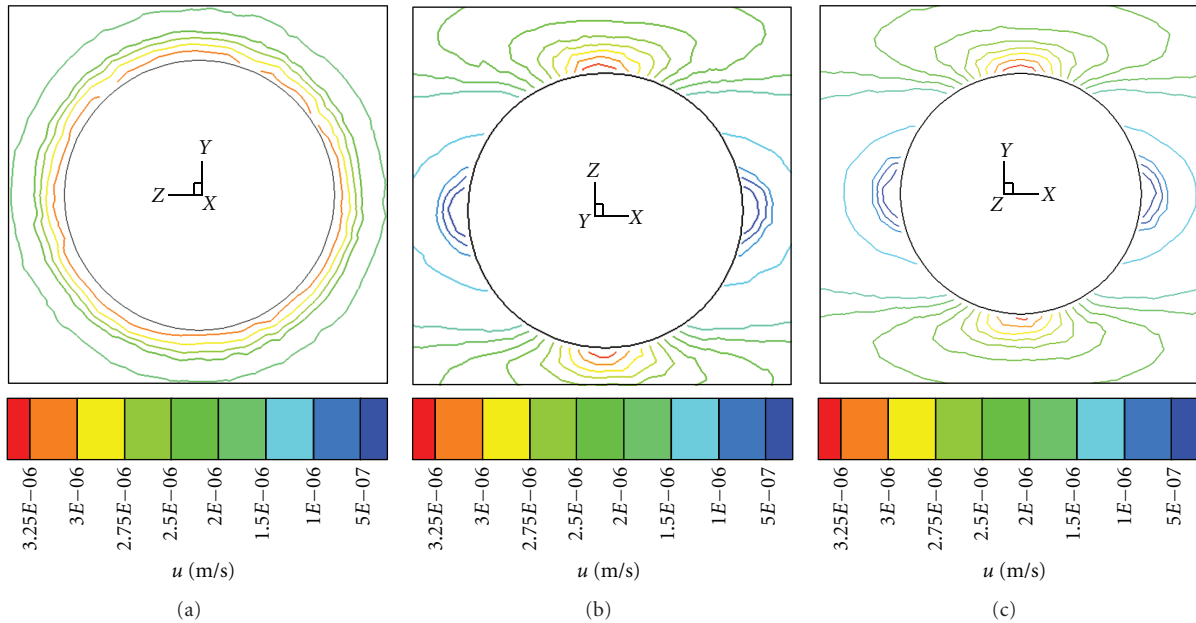


FIGURE 3: Streamlines of velocity around the cell. (a) y' - z' plane; (b) x' - z' plane; (c) y' - z' plane.

relationship is nonlinear. For smaller S , larger changes occur in $\tau_{\text{cell, max}}$.

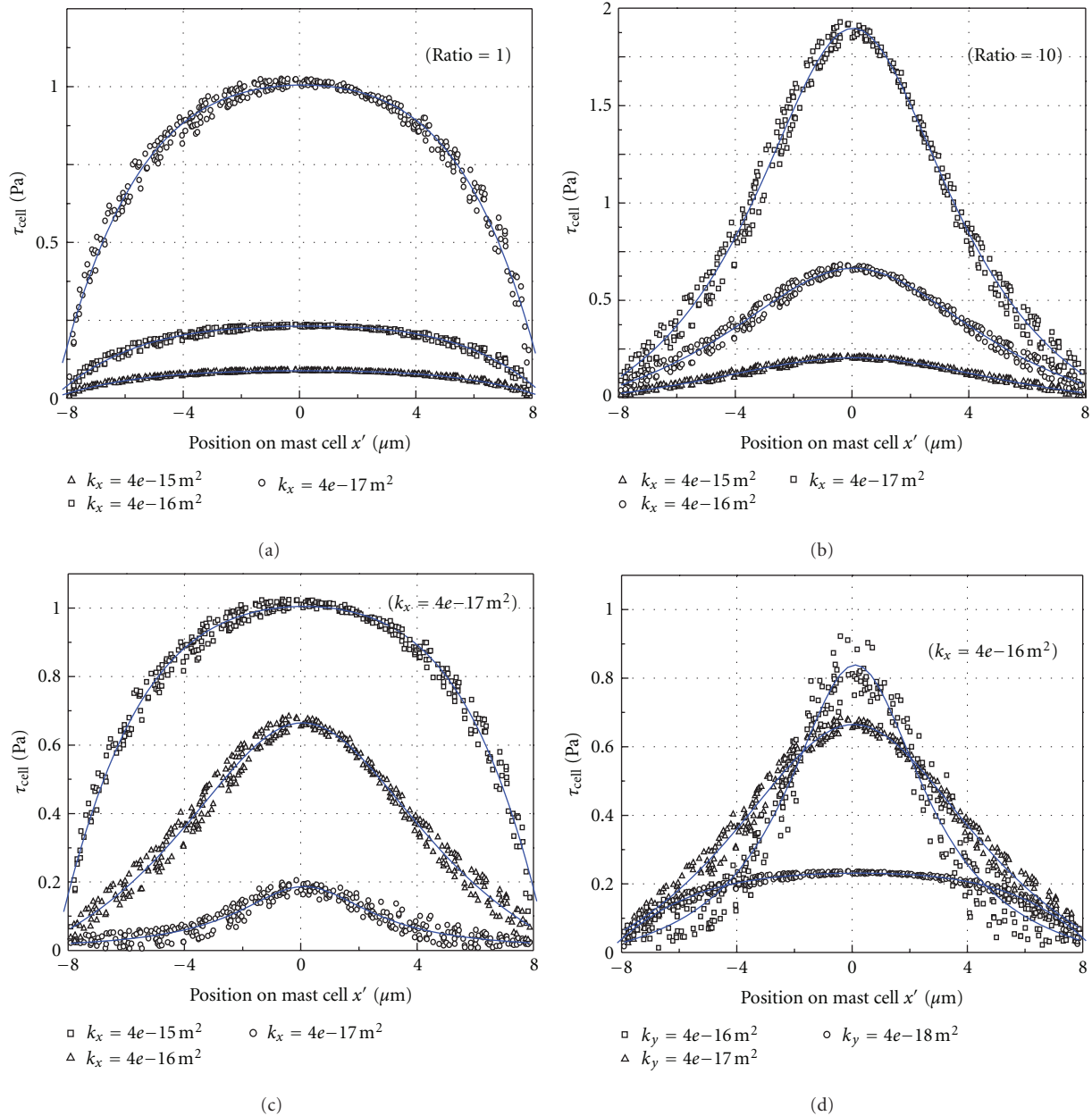
The permeability coefficient of the capillary wall (k_c) can also affect the interstitial fluid flow and τ_{cell} . As shown in Figure 6, $\tau_{\text{cell, max}}$ increases linearly with k_c .

Both the intravascular capillary pressure (p_c) and the interstitial hydrostatic pressure at the capillary wall (p_i) can affect the permeability velocity of the capillary wall (7) and thus the interstitial fluid flow and τ_{cell} . Figure 7 shows how changes in p_i , intravascular capillary pressure at the upstream end (p_a), and intravascular capillary pressure at the downstream end (p_v) affect $\tau_{\text{cell, max}}$. The abscissa is the change in p_a , p_v , and p_i compared to the standard values p_{a0} , p_{v0} , and p_{i0} , respectively; that is, $\Delta p_* = p_* - p_{*0}$. $\tau_{\text{cell, max}}$ increases linearly with increasing p_a and p_v , and decreases linearly with increasing p_i . The effect of p_i is the greatest, whereas the effect of p_v is the least.

Based on the numerical results, we can make the following observations. Capillaries in a parallel array can induce parallel interstitial fluid flow. Interstitial fluid flow can induce shear stress on the cell surface. The ratio determines the distribution of the shear stress, and k_x greatly affects the maximum shear stress. The shear stress can be increased by decreasing the cross-sectional area, which corresponds to increasing the capillary density. The shear stress can also be increased by increasing capillary permeability, increasing intravascular capillary pressure and decreasing interstitial pressure.

4. Discussion

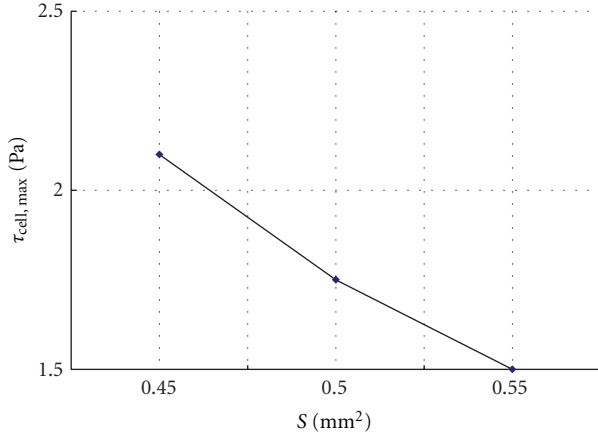
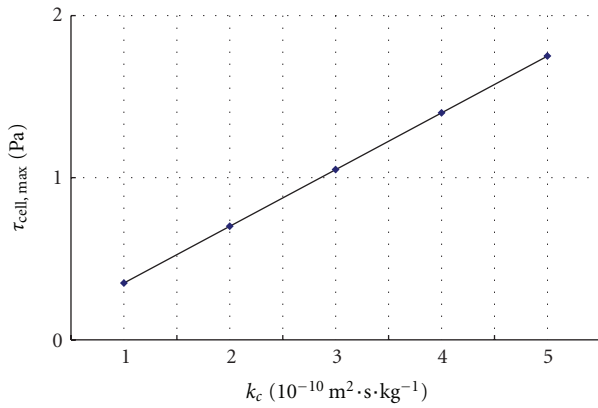
4.1. Directional Interstitial Flow May Explain Some Experimental Observations. The velocity field shows that the direction of the interstitial fluid flow is parallel to the

FIGURE 4: τ_{cell} distribution on the surface of the mast cell.

orientation of the capillaries. The first cluster of capillaries can generate an interstitial fluid flow with a velocity of approximately $0.75 \times 10^{-6} \text{ m/s}$. This flow then enters the space surrounding the second cluster of capillaries and accelerates to $1.25 \times 10^{-6} \text{ m/s}$. The maximum velocity in the space surrounding the second cluster of capillaries is $1.5 \times 10^{-6} \text{ m/s}$. If the fluid is not absorbed by the lymphatic system, it will flow downstream and be accelerated by the downstream capillaries. In the past, it was accepted that most of the seepage from the arteriole side of a capillary is absorbed at the venule side, and the surplus is immediately absorbed by lymphatic vessels. In reality, capillaries are not always near lymphatic vessels, and the amount of fluid that seeps from capillaries is always greater than the amount of

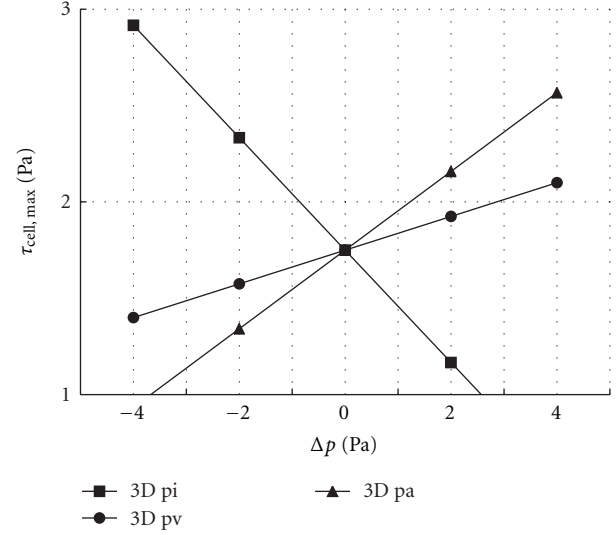
fluid absorbed by capillaries. Therefore, the unabsorbed fluid will travel some distance or even a long distance before being reabsorbed by blood or lymphatic vessels. It is possible that the long interstitial tracks observed in a previous experiment are in fact the interstitial fluid flow [16]. The tracer (Gd-DTPA) injected into the acupoint travels with the interstitial fluid flow. Therefore, the observance of flow along a meridian that differs from blood and lymph flow may be interstitial fluid flow [15].

4.2. A Staggered Distribution of Capillaries Results in a Uniform Interstitial Fluid Velocity. The distribution of the capillaries can influence the velocity distribution of the interstitial fluid flow. Figure 2(a) shows this influence.

FIGURE 5: Variation of $\tau_{cell,max}$ with cross-sectional area S .FIGURE 6: Variation of $\tau_{cell,max}$ with k_c .

In the first cluster, the capillaries are located farther from the x -axis, and thus the interstitial fluid velocity farther from the x -axis increases more quickly than the velocity near the x -axis. In contrast, the capillaries in the second cluster are located near the x -axis, and this interstitial fluid velocity near the x -axis increases faster than the flow farther from the x -axis. With this staggered distribution of capillaries, the increases in velocity alternate, and the velocity tends to be uniform, which is beneficial for substance exchange. Interstitial fluid flow will affect the bioactivities of cells. When tissues are poorly vascularized, such as ligaments and tendons, interstitial fluid flow is more important for metabolism than it is for well-vascularized tissues.

4.3. The Shear Stress Induced by Interstitial Fluid Flow Will Affect Cell Bioactivities. The numerical simulation shows that the flow has a velocity of magnitude 10^{-6} m/s and that the flow induces several Pa shear stresses on the mast cell surface. Many studies showed that subtle fluid mechanical environment played an important role in the ability of cells to proliferate, differentiate, form functional structures, and release chemical mediators [26, 27]. Recent studies showed that interstitial flow influences the immune microenvironment in cancer [28]. The immune microenvironment

FIGURE 7: $\tau_{cell,max}$ as p_a , p_v , and p_i change.

of the tumor consists of multiple cell types, cytokines, and stromal components that can further attract immune cells and guide their fate. Civelek et al. presented the first direct evidence that SMCs with a contractile phenotype will indeed contract when exposed to 2D fluid shear stress [29]. Studies suggest that both laminar shear stress (2D) and interstitial flow (3D) can induce SMC contraction [30]. These studies provide a different perspective regarding the mechanism for myogenic control of blood flow that regulates flow distribution in response to blood pressure changes. Wang found intracellular Ca^{2+} increases in mast cells and mediators release immediately after mechanical stimulation [31]. Further research showed that the mechanosensitive Ca^{2+} channel TRPV_2 may be involved in this process [32].

The mechanism for how interstitial flow affects cell bioactivities is still unknown. It was once generally believed that the shear stress induced by the flow was the main factor. Further studies suggest that cell membrane-related receptors, ion channels, cell surface glycocalyx, integrins, and signaling messengers are all involved in this process. A recent paper shows that the fluid shear stress on cells is rather small and that the solid stress induced by interstitial flow through cell surface glycocalyx is much higher [33]. The solid stress more likely plays a major role in regulating cell function and behavior. However, it is difficult to evaluate solid stress because doing so requires detailed knowledge of the glycocalyx microstructure and extracellular matrix properties. In this paper, we do not focus on the complex mechanism of membrane ion channel activation and solid stress induced by interstitial flow through the cell surface glycocalyx. Instead, we only compare the shear stresses on the mast cell surface in different conditions.

4.4. Physiological Parameters Variation Has Effect on τ_{cell} . The longitudinal permeability and the ratio determined the distribution of τ_{cell} . From (9), we know that k_x and k_y are functions of the porosity ϕ . Therefore, ϕ affects τ_{cell} . Actually,

the smaller ϕ is, the greater effect on $\tau_{\text{cell, max}}$ is. At normal physiological values, ϕ has much smaller effects than when the values are outside of the normal physiological range [19]. Increasing intravascular capillary pressure or capillary permeability can increase τ_{cell} . Therefore, blood microcirculation can affect the living conditions of interstitial cells, and changing the blood supply is an effective method for adjusting the circulation of interstitial fluid. Decreasing the interstitial pressure can also increase τ_{cell} , and doing so has a greater impact than changing the intravascular capillary pressure.

4.5. TCM Treatments and Acupuncture Effect. With traditional Chinese treatments such as massage and cupping, the interstitial pressure can be changed by applying periodic or negative pressure on the body surface [34]. The above results show that interstitial pressure is a main factor affecting interstitial flow and τ_{cell} . Therefore, there may be a correlation between these treatments and interstitial flow.

Acupuncture is a therapeutic treatment in which a needle is inserted into specific parts (acupoints). When the needle is twirled, lifted and thrust, the winding of collagen on the acupuncture needle changes the interstitial microenvironment [35, 36], which produces mechanical stimulation. The stimulation causes degranulation in local mast cells and the release of biological mediators such as histamine, substance P, and leukotriene C_4 , and so forth [14]. These mediators can further activate mast cells and excite nerve endings, which may lead to “De-qi” (a local sensation of heaviness, numbness, soreness, or paresthesia, which is believed to be an important aspect of acupuncture treatment). Moreover, these mediators have a powerful effect in increasing capillary permeability and increasing interstitial flow [24]. The increased flow not only increases the τ_{cell} to activate local mast cells but also transports biological mediators secreted by mast cells to activate other mast cells along the flow path [2, 37]. In summary, the meridian phenomena and the “De-qi” sensations along the meridian during acupuncture may be closely related to the interstitial flow.

Acknowledgments

This work was supported by National Natural Science Foundation of China (11202053), Shanghai Science Foundation (12ZR1401100), and 973 Project (2012CB518502).

References

- [1] M. L. Knothe Tate, “Interstitial fluid flow,” in *Bone Mechanics Handbook*, S. C. Cowin, Ed., vol. 22, pp. 1–29, CRC press, Boca Raton, Fla, USA, 2nd edition, 2002.
- [2] J. M. Tarbell, S. Weinbaum, and R. D. Kamm, “Cellular fluid mechanics and mechanotransduction,” *Annals of Biomedical Engineering*, vol. 33, no. 12, pp. 1719–1723, 2005.
- [3] C. P. Ng and M. A. Swartz, “Fibroblast alignment under interstitial fluid flow using a novel 3-D tissue culture model,” *American Journal of Physiology*, vol. 284, no. 5, pp. H1771–H1777, 2003.
- [4] C. P. Ng and M. A. Swartz, “Mechanisms of interstitial flow-induced remodeling of fibroblast-collagen cultures,” *Annals of Biomedical Engineering*, vol. 34, no. 3, pp. 446–454, 2006.
- [5] K. C. Boardman and M. A. Swartz, “Interstitial flow as a guide for lymphangiogenesis,” *Circulation Research*, vol. 92, no. 7, pp. 801–808, 2003.
- [6] C. P. Ng, B. Hinz, and M. A. Swartz, “Interstitial fluid flow induces myofibroblast differentiation and collagen alignment in vitro,” *Journal of Cell Science*, vol. 118, no. 20, pp. 4731–4739, 2005.
- [7] R. H. Vera, E. Genové, L. Alvarez et al., “Interstitial fluid flow intensity modulates endothelial sprouting in restricted Src-activated cell clusters during capillary morphogenesis,” *Tissue Engineering A*, vol. 15, no. 1, pp. 175–185, 2009.
- [8] L. N. M. Hayward and E. F. Morgan, “Assessment of a mechano-regulation theory of skeletal tissue differentiation in an in vivo model of mechanically induced cartilage formation,” *Biomechanics and Modeling in Mechanobiology*, vol. 8, no. 6, pp. 447–455, 2009.
- [9] J. A. Pedersen, F. Boschetti, and M. A. Swartz, “Effects of extracellular fiber architecture on cell membrane shear stress in a 3D fibrous matrix,” *Journal of Biomechanics*, vol. 40, no. 7, pp. 1484–1492, 2007.
- [10] J. A. Pedersen, S. Lichter, and M. A. Swartz, “Cells in 3D matrices under interstitial flow: effects of extracellular matrix alignment on cell shear stress and drag forces,” *Journal of Biomechanics*, vol. 43, no. 5, pp. 900–905, 2010.
- [11] J. M. Tarbell and M. Y. Pahakis, “Mechanotransduction and the glycocalyx,” *Journal of Internal Medicine*, vol. 259, no. 4, pp. 339–350, 2006.
- [12] R. C. Riddle and H. J. Donahue, “From streaming potentials to shear stress: 25 years of bone cell mechanotransduction,” *Journal of Orthopaedic Research*, vol. 27, no. 2, pp. 143–149, 2009.
- [13] S. P. Fritton and S. Weinbaum, “Fluid and solute transport in bone: flow-induced mechanotransduction,” *Annual Review of Fluid Mechanics*, vol. 41, pp. 347–374, 2009.
- [14] D. Zhang, G. H. Ding, X. Y. Shen et al., “Role of mast cells in acupuncture effect: a pilot study,” *Explore*, vol. 4, no. 3, pp. 170–177, 2008.
- [15] H. Y. Li, J. F. Yang, M. Chen et al., “Visualized regional hypodermic migration channels of interstitial fluid in human beings: are these ancient meridians?” *Journal of Alternative and Complementary Medicine*, vol. 14, no. 6, pp. 621–628, 2008.
- [16] R. W. Li, S. Wen, J. Mong et al., “Analysis of the linear migration of the radionuclide along meridians in perfused extremities of monkey,” *Acupuncture Research*, vol. 17, no. 1, pp. 67–70, 1992 (Chinese).
- [17] G. H. Ding, X. Y. Shen, W. Yao et al., “Dynamic mechanism of directional interstitial fluid flow and meridian,” *Progress in Natural Science*, vol. 5, no. 1, pp. 61–70, 2005 (Chinese).
- [18] W. Yao, N. Chen, and G. H. Ding, “Numerical simulation of interstitial fluid based on a new view of Starling’s hypothesis of capillary wall,” *Chinese Journal of Theoretical and Applied Mechanics*, vol. 41, no. 1, pp. 35–40, 2009 (Chinese).
- [19] W. Yao and G. H. Ding, “Interstitial fluid flow: simulation of mechanical environment of cells in the interosseous membrane,” *Acta Mechanica Sinica*, vol. 27, no. 4, pp. 602–610, 2011.
- [20] R. Y. Tsay and S. Weinbaum, “Viscous flow in a channel with periodic cross-bridging fibres. Exact solutions and Brinkman approximation,” *Journal of Fluid Mechanics*, vol. 226, pp. 125–148, 1991.

- [21] J. Keener and J. Sneyd, *Mathematical Physiology*, Springer, New York, NY, USA, 2nd edition, 2009.
- [22] C. T. Chen, D. S. Malkus, and R. Vanderby, "A fiber matrix model for interstitial fluid flow and permeability in ligaments and tendons," *Biorheology*, vol. 35, no. 2, pp. 103–118, 1998.
- [23] X. Hu, R. H. Adamson, B. Liu, F. E. Curry, and S. Weinbaum, "Starling forces that oppose filtration after tissue oncotic pressure is increased," *American Journal of Physiology*, vol. 279, no. 4, pp. H1724–H1736, 2000.
- [24] C. Guyton and J. E. Hall, *Textbook of Medical Physiology*, Elsevier, Philadelphia, Pa, USA, Eleven edition, 2006.
- [25] X. P. Hu and S. Weinbaum, "A new view of Starling's hypothesis at the microstructural level," *Microvascular Research*, vol. 58, no. 3, pp. 281–304, 1999.
- [26] C. P. Ng, C. L. E. Helm, and M. A. Swartz, "Interstitial flow differentially stimulates blood and lymphatic endothelial cell morphogenesis in vitro," *Microvascular Research*, vol. 68, no. 3, pp. 258–264, 2004.
- [27] S. N. Alshihabi, Y. S. Chang, J. A. Frangos, and J. M. Tarbell, "Shear stress-induced release of PGE2 and PGI2 by vascular smooth muscle cells," *Biochemical and Biophysical Research Communications*, vol. 224, no. 3, pp. 808–814, 1996.
- [28] M. A. Swartz and A. W. Lund, "Lymphatic and interstitial flow in the tumour microenvironment: linking mechanobiology with immunity," *Nature Reviews Cancer*, vol. 12, no. 3, pp. 210–219, 2012.
- [29] M. Civelek, K. Ainslie, J. S. Garanich, and J. M. Tarbell, "Smooth muscle cells contract in response to fluid flow via a Ca^{2+} -independent signaling mechanism," *Journal of Applied Physiology*, vol. 93, no. 6, pp. 1907–1917, 2002.
- [30] Z. D. Shi and J. M. Tarbell, "Fluid flow mechanotransduction in vascular smooth muscle cells and fibroblasts," *Annals of Biomedical Engineering*, vol. 39, no. 6, pp. 1608–1619, 2011.
- [31] L. N. Wang, *Investigation of mechanical sensitive channels on mast cell [Ph.D. thesis]*, Fudan University, Shanghai, China, 2010.
- [32] D. Zhang, A. Spielmann, G. H. Ding et al., "Activation of mast-cell degranulation by different physical stimuli involves activation of the transient-receptor-potential channel TRPV2," *Physiological Research*, vol. 61, no. 1, pp. 113–124, 2012.
- [33] J. M. Tarbell and Z. D. Shi, "Effect of the glycocalyx layer on transmission of interstitial flow shear stress to embedded cells," *Biomechanics and Modeling in Mechanobiology*. In press, <http://link.springer.com/journal/10237/onlineFirst/page/3>.
- [34] E. Cafarelli and F. Flint, "The role of massage in preparation for and recovery from exercise. An overview," *Sports Medicine*, vol. 14, no. 1, pp. 1–9, 1992.
- [35] H. M. Langevin and J. A. Yandow, "Relationship of acupuncture points and meridians to connective tissue planes," *The Anatomical Record*, vol. 269, no. 6, pp. 257–265, 2002.
- [36] X. J. Yu, G. H. Ding, H. Huang, J. Lin, W. Yao, and R. Zhan, "Role of collagen fibers in acupuncture analgesia therapy on rats," *Connective Tissue Research*, vol. 50, no. 2, pp. 110–120, 2009.
- [37] M. A. Swartz and M. E. Fleury, "Interstitial flow and its effects in soft tissues," *Annual Review of Biomedical Engineering*, vol. 9, pp. 229–256, 2007.

Research Article

Research on Nonlinear Feature of Electrical Resistance of Acupuncture Points

Jianzi Wei,¹ Huijuan Mao,¹ Yu Zhou,¹ Lina Wang,¹ Sheng Liu,¹ and Xueyong Shen^{1,2}

¹Laboratory of Acupuncture and Moxibustion, Shanghai University of Traditional Chinese Medicine, 1200 Cailun Road, Shanghai 201203, China

²Systemic Physiology Laboratory for Acupuncture and Meridian, Shanghai Research Center of Acupuncture and Meridians, 199 Guoshoujing Road, Shanghai 201203, China

Correspondence should be addressed to Xueyong Shen, snowysh@hotmail.com

Received 19 September 2012; Accepted 16 November 2012

Academic Editor: Wolfgang Schwarz

Copyright © 2012 Jianzi Wei et al. This is an open access article distributed under the Creative Commons Attribution License, which permits unrestricted use, distribution, and reproduction in any medium, provided the original work is properly cited.

A highly sensitive volt-ampere characteristics detecting system was applied to measure the volt-ampere curves of nine acupuncture points, LU9, HT7, LI4, PC6, ST36, SP6, KI3, LR3, and SP3, and corresponding nonacupuncture points bilaterally from 42 healthy volunteers. Electric currents intensity was increased from $0\ \mu\text{A}$ to $20\ \mu\text{A}$ and then returned to $0\ \mu\text{A}$ again. The results showed that the volt-ampere curves of acupuncture points had nonlinear property and magnetic hysteresis-like feature. On all acupuncture point spots, the volt-ampere areas of the increasing phase were significantly larger than that of the decreasing phase ($P < 0.01$). The volt-ampere areas of ten acupuncture point spots were significantly smaller than those of the corresponding nonacupuncture point spots when intensity was increase ($P < 0.05 \sim P < 0.001$). And when intensity was decrease, eleven acupuncture point spots showed the same property as above ($P < 0.05 \sim P < 0.001$), while two acupuncture point spots showed opposite phenomenon in which the areas of two acupuncture point spots were larger than those of the corresponding nonacupuncture point spots ($P < 0.05 \sim P < 0.01$). These results show that the phenomenon of low skin resistance does not exist to all acupuncture points.

1. Introduction

Skin resistance, one of the important biophysical indexes supporting the objective reality of acupuncture points, had been detected since the 1950s, when Voll [1] found that skin points electrical characteristics in traditional acupuncture points areas were different from other areas. Since then, a number of studies have concluded that acupuncture points exhibit low skin resistance [2–4] and increased conductivity [5–7], but different opinions on the electrical characteristics of acupuncture points have remained. Pei and Liu put forward their dissent years ago [8], while Korr et al. found that the distribution of low-resistance areas varied from individual to individual, and not all were located at acupuncture points [9]. Recently, Pearson et al. reported that right GB 14, right PC 8, and left TE1 showed no low skin resistance at all [10]. Kramer et al. tested six commonly used acupuncture points on 53 subjects and found that the

occurrence rate of low resistance was only 25.9 percent [11]. Besides the complexity of detecting skin resistance at acupuncture points, which may be influenced by numerous factors [12, 13], the root of these contradictory results is that skin resistance of acupuncture points is nonlinear. Because of the complexity of its composition, acupuncture points electrical impedance has some typical characteristics different from linear impedance component (e.g., the space distribution of acupuncture point tissues is anisotropic, and the acupuncture point tissues are actively responsive to external input). Thus, acupuncture point electrical impedance is nonlinear and flexible; its values change when the detected voltages or currents vary [14]. Since the resistance value of an acupuncture point varies according to current and voltage, the electrical characteristics of acupuncture points must be expressed by a volt-ampere curve.

Classification of the electrical properties of acupuncture points will provide an objective index for studying

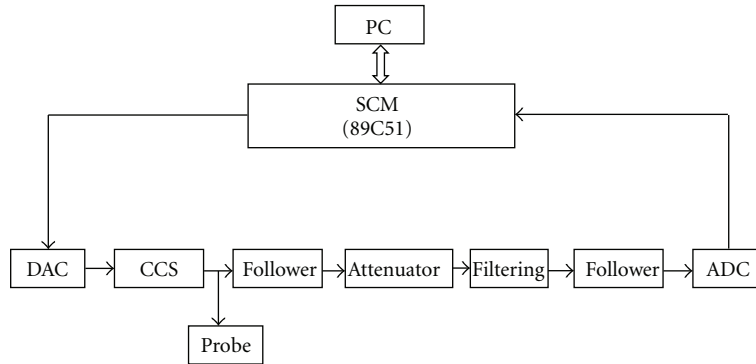


FIGURE 1: Hardware schematic diagram of volt-ampere characteristic detection system. A highly sensitive volt-ampere characteristic detecting system was constructed using a single chip microcontroller (SCM), a digital-analog component (DAC), a constant current source component (CCS), a voltage follower, an attenuator, an analog-digital component (ADC), and two electrodes. The detecting electrode was a plane electrode installed with a silver head 4 mm in diameter. The negative electrode was silver-gilt like that of the limb lead of an electrocardiograph. The SCM was connected to the USB of a personal computer (PC) through a data line.

the functions of the points. Active response to external stimulation and the reflection of symptoms are the main characteristics of acupuncture points, of which the former is more important as it is the means by which acupuncture can be applied therapeutically. When external stimuli such as needling, moxibustion, electrostimulation, lasers, and infrared irradiation act on acupuncture points, they may produce obvious reactions that subsequently regulate and balance bodily functions. However, due to the lack of objective indexes, research on the active response of acupuncture points to external stimulation is still quite limited.

The purpose of this study is threefold: to use a nonlinear detecting method to ascertain the volt-ampere curves of acupuncture points and observe their basic features, to compare volt-ampere areas of acupuncture points and non-acupuncture points to determine their skin resistance, and to probe the relationship between an acupuncture point's volt-ampere characteristics and its response to external stimulation.

2. Methods

2.1. Subjects. 42 healthy volunteers, 23 males and 19 females, aged 23–36, with a mean age of 26.73 ± 3.02 , were recruited. “Healthy” was defined as normal body temperature and no known autonomic nervous system dysfunction, coronary heart disease, systemic disease, or skin disease [15]. All subjects were informed of the nature of the experiment and willingly signed the consent form before participation. The research protocol was approved by the Human Study Ethics Committee of the Shanghai Research Center of Acupuncture and Meridians.

The acupuncture points tested were bilateral LU9 (Taiyuan), HT7 (Shenmen), LI4 (Hegu), PC6 (Neiguan), ST36 (Zusanli), SP6 (Sanyinjiao), KI3 (Taixi), LR3 (Taichong), SP3 (Taibai) and; thus, 18 acupuncture point spots and their relevant non-acupuncture points controls. The control for LU9 was the midpoint between LU9 and PC7 (Daling). The control for HT7 was the midpoint between HT7 and PC7.

The control for LR3 and SP3 was the midpoint between these two acupuncture points. Each control for the remaining acupuncture points was on the same level as the respective point and 1 cm lateral to it.

2.2. Experimental Device. A highly sensitive volt-ampere characteristic detecting system and its working mechanism are used as referenced in [16, 17] (see Figure 1).

2.3. Experimental Procedures. The experiment was performed under quiet, controlled environmental conditions: temperature $22^{\circ}\text{C} \pm 3^{\circ}\text{C}$, minimal air flow, relative humidity $55 \pm 10\%$, and shielding from electromagnetic radiation [17].

The subjects were asked to arrive at the laboratory more than 15 minutes prior to the experiment and sit quietly to relax their muscles to become acclimated to the testing conditions. The detecting electrode was placed on the points with $160 \text{ g} \pm 5\%$ pressure ten minutes after 75% alcohol was applied to the detected spots.

The negative electrode was applied with cardio cream made by Nihon Kohden Corporation. When LU9, HT7, PC6, and their relevant control points were detected, the inert electrode was placed three cun from the cubital crease on the palm aspect of the forearm. When ST36, KI3, SP3, LR3, and their relevant control points were detected, it was placed three cun above the tip of the medial malleolus. When SP6 and its control point were detected, it was placed three cun below ST35 (Dubi).

The parameters of the detecting system were adjusted to 30V, the maximum voltage detection range, and $0 \mu\text{A}$ – $20 \mu\text{A}$, the scanning range of constant current, in order to avoid stimulating or polarizing effects [18]. The total scanning time was 20 seconds. The electrical current scanning was increasing steadily and linearly from $0 \mu\text{A}$ to $20 \mu\text{A}$ in the first 10 seconds and decreasing steadily from $20 \mu\text{A}$ to $0 \mu\text{A}$ in the second 10 seconds. The data was recorded every $0.1 \mu\text{A}$; each spot was designed to measure 3 times in advance, and the value showed was already the average of them (see Figure 2).

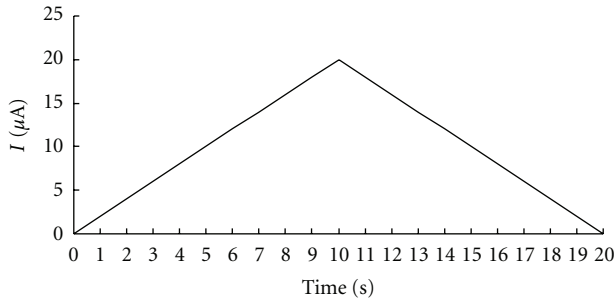


FIGURE 2: Electrical current-time I - T curve of detecting system. The electrical current first increase from $0 \mu\text{A}$ to $20 \mu\text{A}$ (0–10 s), then decrease from $20 \mu\text{A}$ to $0 \mu\text{A}$ (10–20 s).

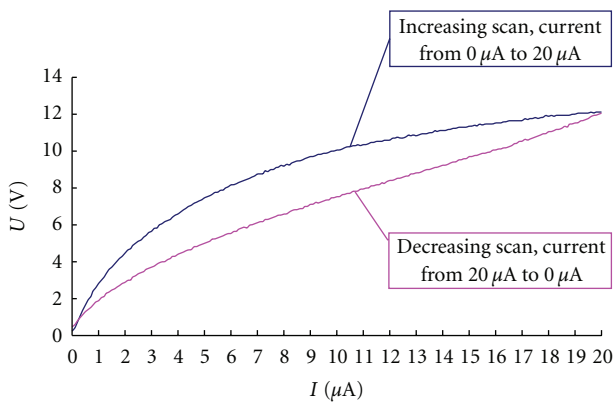


FIGURE 3: Schematic diagram of volt-ampere curve of the acupuncture points.

The system recorded the value of the corresponding voltage automatically, and during the biphasc scanning, it traced the volt-ampere curve as well. Each detected spot had two volt-ampere curves, recorded respectively with $0 \mu\text{A} \sim 20 \mu\text{A}$ and $20 \mu\text{A} \sim 0 \mu\text{A}$ (see Figure 3).

2.4. Statistics. The original data was filtered before statistical analysis. If the voltage at the acupuncture points or control points of a subject exceeded 30V, that whole data wasn't fit into statistics.

The volt-ampere area refers to the area comprised by the volt-ampere curve and abscissa, which was calculated by integral calculus ($\int U dI$). As the data were collected discontinuously, the volt-ampere area was calculated as $S = \sum U \Delta I$.

The SPSS10.0 software package was used, and the paired-sample t -test was applied to compare the difference of volt-ampere areas between acupuncture points and control points as well as the difference between the volt-ampere areas of the increasing and decreasing scans of each point. In all cases, $\alpha = 0.05$ or less was considered significant.

3. Result

Bilaterally, thirty-four spots were scanned on 42 healthy volunteers: nine bilateral acupuncture points and eight relevant

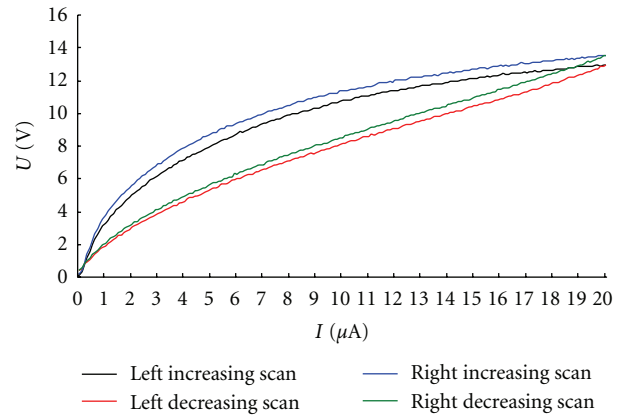


FIGURE 4: Volt-ampere curve of PC 6. The volt-ampere curves of acupuncture points were parabola-like rather than straight. The curves produced by increasing current intensity did not totally overlap those produced by decreasing current intensity.

bilateral control points, since LR3 and SP3 shared the same control.

Qualitative analysis showed that all detected spots had nonlinear and magnetic hysteresis-like characteristics. With regard to nonlinearity, the volt-ampere curves of acupuncture points were parabola-like rather than straight. This was most obvious at the very weak current, $0 \mu\text{A}$ to $5 \mu\text{A}$, in the course of scanning from $0 \mu\text{A}$ to $20 \mu\text{A}$. During decreasing scanning, that is from $20 \mu\text{A}$ to $0 \mu\text{A}$, they became almost straight (see Figure 4). With regard to magnetic hysteresis, the curves produced by the increasing intensity did not totally overlap those produced by decreasing intensity. This was quite similar to the B-H curves that occur in ferromagnetic materials (see Figure 4).

Further quantitative analysis showed that in both acupuncture points and the control the volt-ampere areas produced by the increasing intensity were all larger than those of the decreasing intensity ($P < 0.01$) (see Table 1).

When the acupuncture points and control points were compared, four acupuncture point spots, bilateral LI4 and bilateral SP3, had larger volt-ampere areas than those of their relevant control spots when intensity was increasing, but the differences were not statistically significant. The other fourteen acupuncture point spots had smaller volt-ampere areas than their relevant control spots did. The differences in ten of these, five bilateral points, reached statistical significance ($P < 0.05 \sim P < 0.001$). These were LU9, PC6, ST36, SP6, and KI3 (see Table 1).

During decreasing intensity, five acupuncture point spots, right HT7, bilateral ILI4, and bilateral SP3, had larger volt-ampere areas than their relevant control spots did; the differences for right LI4 and right SP3 reached statistical significance. Each of the other thirteen acupuncture point spots had smaller volt-ampere areas than those of their relevant control spots; of these, eleven acupuncture point spots reached statistical significance ($P < 0.05 \sim P < 0.001$). They were bilateral LU9, bilateral PC6, bilateral ST36, bilateral KI3, bilateral LR3, and left SP6 (see Table 1).

TABLE 1: Volt-ampere areas of acupuncture points at human bodies.

		Right increasing scan	Left increasing scan	Right decreasing scan	Left decreasing scan
LU9	(n = 39)	169.83 ± 104.30**** [^]	172.82 ± 89.55**** [^]	151.95 ± 77.63****	154.36 ± 66.58****
Control point of LU9		249.27 ± 97.82 [^]	227.31 ± 103.34 [^]	218.89 ± 76.96	198.43 ± 74.39
HT7	(n = 37)	272.30 ± 113.63 [^]	245.28 ± 109.48 [^]	239.73 ± 88.99	217.69 ± 87.27
Control point of HT7		277.38 ± 103.41 [^]	255.53 ± 94.83 [^]	238.10 ± 79.92	226.31 ± 70.41
LI4	(n = 36)	244.83 ± 106.56 [^]	244.40 ± 115.35 [^]	197.87 ± 71.71*	191.88 ± 77.26
Control point of LI4		226.53 ± 102.00 [^]	227.89 ± 111.78 [^]	178.56 ± 70.65	182.05 ± 76.23
PC6	(n = 38)	208.72 ± 112.58** [^]	190.58 ± 92.47** [^] *	164.05 ± 79.60***	151.38 ± 60.60****
Control point of PC6		231.81 ± 124.30 [^]	213.01 ± 97.60 [^]	183.09 ± 87.69	166.43 ± 64.45
ST36	(n = 34)	178.14 ± 89.23**** [^]	186.57 ± 109.47**** [^]	141.57 ± 61.71****	147.46 ± 72.01****
Control point of ST36		221.76 ± 98.97 [^]	240.41 ± 124.20 [^]	172.61 ± 65.90	179.18 ± 82.20
SP6	(n = 35)	225.24 ± 104.14**** [^]	231.55 ± 106.51** [^]	178.29 ± 75.88	179.91 ± 71.66**
Control point of SP6		258.02 ± 122.97 [^]	252.07 ± 114.07 [^]	188.38 ± 81.09	193.26 ± 73.30
KI3	(n = 28)	187.65 ± 116.88**** [^]	209.78 ± 114.49** [^]	157.43 ± 81.57****	169.14 ± 79.60**
Control point of KI3		257.00 ± 146.53 [^]	262.43 ± 134.84 [^]	213.14 ± 112.28	212.54 ± 90.84
LR3		212.60 ± 100.70 [^]	220.67 ± 103.65 [^]	177.58 ± 69.11**	180.98 ± 68.45***
Control point of LR3 and SP3	(n = 34)	227.19 ± 104.57 [^]	245.27 ± 95.29 [^]	197.35 ± 73.69	211.21 ± 65.99
SP3		247.47 ± 100.95 [^]	252.68 ± 90.14 [^]	229.31 ± 82.53***	228.73 ± 70.15

Compare to decreasing-scan [^] $P < 0.01$.

Compare to control point * $P < 0.05$; ** $P < 0.01$; *** $P < 0.005$; **** $P < 0.0001$.

4. Discussion

Our data showed that the volt-ampere curves of acupuncture points are clearly nonlinear (Figure 3), further substantiating previous reports [19–21] and indicating that only with nonlinear detecting methods can the panorama of electrical characteristics of acupuncture points be obtained. Conversely, linear detecting methods will not yield precise results even when experimental conditions are strictly controlled.

Besides their methodological significance, the nonlinear characteristics of the volt-ampere curve also have biological significance. The human being is both a complex living organism and a complicated open system. The behaviors and physiological activities of the human body possess the features of nonlinearity and unpredictability that correspond to complex systems. During the course of evolution, the human body has adapted to its environment. Homeostasis regulates and maintains the cells to play their physiological roles smoothly, permitting the body to eliminate various kinds of internal and external factors that disturb the normal physiochemical state of its internal environment. As a result, a dynamic balance of the internal environment can be maintained. The nonlinearity of skin resistance, one of the biophysical characteristics of acupuncture points, may be regarded as a response to the complexity of the functions of the body.

The volt-ampere area is the integral of voltage response resulting from the scanning current on the acupuncture points. It is the average strength of the current during the time of scanning, and its value reflects the resistance/impedance of the acupuncture points to that scanning current. A higher value at the volt-ampere area means greater resistance/impedance.

In this study, left and right LI4 and left and right SP3 had larger volt-ampere areas than the relevant control during the increase, as did the right HT7, left and right LI4, and left and right SP3 during the decrease, among which right LI4 and right SP3 reached statistical significance. Thus, not all acupuncture point spots volt-ampere areas were smaller than those of control. This indicates that the phenomenon of low acupuncture points skin resistance does not always exist, which is consistent with the results of our previous research [17, 18, 20]. The data showed that acupuncture points skin resistance may either be lower or higher, depending on different points. The prevalent methods of detecting acupuncture points according to the lower skin resistance are not reliable.

Acupuncture points actively respond to external electric stimulation. In this study, two manifestations were observed when acupuncture points were stimulated by increasing and decreasing electric current intensity. First, the degree of nonlinearity declined as the scanning time went on, and second, volt-ampere curves from $0 \mu\text{A}$ to $20 \mu\text{A}$ were totally different from those of $20 \mu\text{A}$ to $0 \mu\text{A}$ (see Figure 2). When analyzed quantitatively, the volt-ampere areas during the decreasing intensity were smaller than those of the increasing intensity (Table 1). The active response to external electric stimulation further confirms that an acupuncture point is sensitive to stimulation, as do the myoelectric signal sent out when an acupuncture point is needled [22] and the degranulation of a mastocyte when an acupuncture point is stimulated by needles [23] or lasers [24].

As in our previous research [21, 25–27], the data suggests that the volt-ampere areas under increasing intensity and those under decreasing intensity vary with physiological and

pathological changes of the body. Does this suggest that acupuncture points respond differently to external stimulation under different physiological and pathological states? Can the difference values be regarded as an index for studying acupuncture points response to external stimulation? This warrants further study.

The volt-ampere curve of the increasing intensity was totally different from that of the decreasing. The fact that it was larger when intensity was increasing suggests a similarity to the magnetic hysteresis characteristics of ferromagnetic materials. The magnetic hysteresis-like characteristic of the volt-ampere curve of an acupuncture point may be quantitatively expressed by the difference value, that is, the value of the volt-ampere area increasing scanning minus that of decreasing scanning. With Potter's method, Chen studied the resistance characteristics of the heart meridian on the forearm. It was found that an acupuncture point has the general properties of a resistance-capacitor circuit. Topologically it was the parallel connection of a resistance and a capacitor, which has a series connection with a resistance [28]. The same results were obtained when Reichmanis applied Laplace analysis to the segment of the heart meridian from HT4 to HT3 [3]. Since acupuncture points possess resistance-capacitor circuit-like properties which can store and release electric current, this may explain the magnetic hysteresis-like phenomenon of the volt-ampere curves of acupuncture points in this study. The time curves of the electric current under increasing and decreasing intensity were symmetrical (see Figure 2), but the volt-ampere area during the increase was larger. This demonstrates that some part of the current going into the acupuncture point during the increase must have remained in the acupuncture point, suggesting that acupuncture points have the ability to store energy and also warrants further study.

5. Conclusion

The phenomenon of low skin resistance does not exist at all acupuncture points. The volt-ampere curves of human acupuncture points are clearly nonlinear; consequently, nonlinear-detecting methods should be applied. The volt-ampere curve-detecting device used in this study is noninvasive and convenient and provides a valuable new method for studying acupuncture points response to external stimulation. Although only the volt-ampere characteristics were detected, the complete picture of electrical characteristics can be obtained with the device. The magnetic hysteresis-like characteristics of the volt-ampere curve of acupuncture points indicate that the points store part of the electric energy they get during external electrical stimulation. Our main focus during followup will concern the relationship between the energy of acupuncture points and their functions.

Conflict of Interests

The authors do not have any conflict of interests or any circumstances that could be perceived as a potential conflict of interests.

Acknowledgments

The authors would like to thank Lixing Lao for advice and Lyn Lowry for English editorial support. This project was supported by the National Basic Research Program of China (2009CB522901), National Natural Science Foundation of China (81102635, 81202648), the Key Program of State Administration of Traditional Chinese Medicine of China, and Innovation Program of Shanghai Municipal Education Commission (11YZ68).

References

- [1] R. Voll, "Twenty years of electroacupuncture diagnosis in Germany. A progress report," *American Journal of Acupuncture*, vol. 3, no. 1, pp. 7–17, 1975.
- [2] E. F. Prokhorov, J. González-Hernández, Y. V. Vorobiev, E. Morales-Sánchez, T. E. Prokhorova, and G. Z. Lelo de Larrea, "In vivo electrical characteristics of human skin, including at biological active points," *Medical and Biological Engineering and Computing*, vol. 38, no. 5, pp. 507–511, 2000.
- [3] M. Reichmanis, A. A. Marino, and R. O. Becker, "Laplace plane analysis of impedance on the H meridian.," *American Journal of Chinese Medicine*, vol. 7, no. 2, pp. 188–193, 1979.
- [4] H. M. Johng, J. H. Cho, H. S. Shin et al., "Frequency dependence of impedances at the acupuncture point Quze (PC3)," *IEEE Engineering in Medicine and Biology Magazine*, vol. 21, no. 2, pp. 33–36, 2002.
- [5] M. Reichmanis and R. O. Becker, "Physiological effects of stimulation at acupuncture loci: a review," *Comparative Medicine East and West*, vol. 6, no. 1, pp. 67–73, 1978.
- [6] M. Reichmanis, A. A. Marino, and R. O. Becker, "Electrical correlates of acupuncture points," *IEEE Transactions on Biomedical Engineering*, vol. 22, no. 6, pp. 533–535, 1975.
- [7] J. Hyvarinen and M. Karlsson, "Low resistance skin points that may coincide with acupuncture loci," *Medical Biology*, vol. 55, no. 2, pp. 88–94, 1977.
- [8] T. F. Pei and H. L. Liu, "Test and preliminary analysis on electrical skin impedance in 6 patients with ulcers," *Haerbin Journal of Traditional Chinese Medicine*, vol. 3, no. 4, pp. 40–41, 1960.
- [9] I. M. Korr, P. E. Thomas, and H. M. Wright, "Patterns of electrical skin resistance in man," *Acta Neurovegetativa*, vol. 17, no. 1-2, pp. 77–96, 1958.
- [10] S. Pearson, A. P. Colbert, J. McNamers, M. Baumgartner, and R. Hammerschlag, "Electrical skin impedance at acupuncture points," *Journal of Alternative and Complementary Medicine*, vol. 13, no. 4, pp. 409–418, 2007.
- [11] S. Kramer, K. Winterhalter, G. Schober et al., "Characteristics of electrical skin resistance at acupuncture points in healthy humans," *Journal of Alternative and Complementary Medicine*, vol. 15, no. 5, pp. 495–500, 2009.
- [12] A. C. Ahn and Ø. G. Martinsen, "Electrical characterization of acupuncture points: technical issues and challenges," *Journal of Alternative and Complementary Medicine*, vol. 13, no. 8, pp. 817–824, 2007.
- [13] J. Wei, X. Shen, and T. Wang, "The resistance of acupoint and its measurement," *Sheng wu yi xue gong cheng xue za zhi = Journal of biomedical engineering = Shengwu yixue gongchengxue zazhi*, vol. 23, no. 3, pp. 509–511, 2006.
- [14] B. Wu, X. Hu, and J. Xu, "Effect of increase and decrease of measurement voltage on skin impedance," *Acupuncture Research*, vol. 18, no. 2, pp. 104–107, 1993.

- [15] H. M. Langevin, D. L. Churchill, J. R. Fox, G. J. Badger, B. S. Garra, and M. H. Krag, "Biomechanical response to acupuncture needling in humans," *Journal of Applied Physiology*, vol. 91, no. 6, pp. 2471–2478, 2001.
- [16] T. Wang, X. Y. Shen, J. Z. Wei, and G. H. Ding, "Develop on computer-based detection system of volt-ampere characteristic of acupoints.," *Chinese Archives of Traditional Chinese Medicine*, vol. 26, no. 7, pp. 1427–1429, 2008.
- [17] J. Z. Wei, A. M. Zhang, X. Y. Shen, Y. Zhou, and L. Zhao, "Volt-ampere characteristics of Yuan points of three yin channels of hand in women before, during and after menstruation," *Journal of Chinese Integrative Medicine*, vol. 4, no. 3, pp. 260–264, 2006.
- [18] C. P. Richter and B. G. Woodruff, "Changes produced by sympathectomy in the electrical resistance of the skin," *Surgery*, vol. 10, no. 6, pp. 957–970, 1941.
- [19] J. Fraden and S. Gelman, "Investigation of nonlinear effects in surface electroacupuncture," *American Journal of Acupuncture*, vol. 7, no. 1, pp. 21–30, 1979.
- [20] T. Yamamoto and Y. Yamamoto, "Non-linear electrical properties of skin in the low frequency range," *Medical and Biological Engineering and Computing*, vol. 19, no. 3, pp. 302–310, 1981.
- [21] X. Y. Shen, J. Z. Wei, Y. H. Zhang et al., "Study on Volt-ampere (V-A) characteristics of human acupoints," *Zhongguo zhen jiu = Chinese acupuncture & moxibustion.*, vol. 26, no. 4, pp. 267–271, 2006.
- [22] Z. P. Liu, T. Yin, X. G. Guan et al., "Primary study on objective evaluation parameter and method of acupuncture deqi and maneuver," *Chinese Journal of Clinical Rehabilitation*, vol. 9, no. 29, pp. 119–121, 2005.
- [23] D. Zhang, G. Ding, X. Shen et al., "Role of mast cells in acupuncture effect: a pilot study," *Explore*, vol. 4, no. 3, pp. 170–177, 2008.
- [24] K. Cheng, X. Y. Shen, G. H. Ding, and F. Wu, "Relationship between laser acupuncture analgesia and the function of mast cells," *Chinese Acupuncture and Moxibustion*, vol. 29, no. 6, pp. 478–483, 2009.
- [25] Y. Zhou, J. Z. Wei, and X. Y. Shen, "Research on circadian rhythm of volt-ampere characteristic at Taiyuan(LU9)," *China Journal of Basic Medicine in Traditional Chinese Medicine*, vol. 9, no. 2, pp. 54–56, 2003.
- [26] J. Z. Wei, Y. Zhou, L. M. Hua, X. Y. Shen, C. H. Wan, and Y. B. Zhou, "Research on circadian rhythm of volt-ampere characteristic at six-yin-meridian yuan- primary points," *Chinese Archives of Traditional Chinese Medicine*, vol. 22, no. 2, pp. 233–234, 2004.
- [27] J. Z. Wei, X. Y. Shen, T. Wang, H. J. Mao, Y. Zhou, and L. X. Lao, "Circadian difference of volt-ampere characteristics of acupoints daling (PC7)," *Journal of Alternative and Complementary Medicine*, vol. 13, no. 8, article 903, 2007.
- [28] C. Rixin, "Porter analyze on the electrical resistance of forearm area of heart meridian," *Chinese Acupuncture and Moxibustion*, vol. 7, no. 6, pp. 26–28, 1987.

Research Article

Stimulation of TRPV1 by Green Laser Light

Quanbao Gu,¹ Lina Wang,^{1,2} Fang Huang,³ and Wolfgang Schwarz^{1,4}

¹ Shanghai Research Center for Acupuncture and Meridians, 199 Guoshoujing Road, Shanghai 201203, China

² Acupuncture and Moxibustion College, Shanghai University of Traditional Chinese Medicine, 1200 Cailun Road, Shanghai 201203, China

³ State Key Laboratory of Medical Neurobiology, Shanghai Medical College, Fudan University, Shanghai 200031, China

⁴ Institute for Biophysics, J. W. Goethe University, Max-von-Laue Straße 1, 60438 Frankfurt am Main, Germany

Correspondence should be addressed to Wolfgang Schwarz, schwarz@biophys.eu

Received 20 September 2012; Revised 6 November 2012; Accepted 14 November 2012

Academic Editor: Di Zhang

Copyright © 2012 Quanbao Gu et al. This is an open access article distributed under the Creative Commons Attribution License, which permits unrestricted use, distribution, and reproduction in any medium, provided the original work is properly cited.

Low-level laser irradiation of visible light had been introduced as a medical treatment already more than 40 years ago, but its medical application still remains controversial. Laser stimulation of acupuncture points has also been introduced, and mast-cells degranulation has been suggested. Activation of TRPV ion channels may be involved in the degranulation. Here, we investigated whether TRPV1 could serve as candidate for laser-induced mast cell activation. Activation of TRPV1 by capsaicin resulted in degranulation. To investigate the effect of laser irradiation on TRPV1, we used the *Xenopus* oocyte as expression and model system. We show that TRPV1 can functionally be expressed in the oocyte by (a) activation by capsaicin ($K_{1/2} = 1.1 \mu\text{M}$), (b) activation by temperatures exceeding 42°C , (c) activation by reduced pH (from 7.4 to 6.2), and (d) inhibition by ruthenium red. Red (637 nm) as well as blue (406 nm) light neither affected membrane currents in oocytes nor did it modulate capsaicin-induced current. In contrast, green laser light (532 nm) produced power-dependent activation of TRPV1. In conclusion, we could show that green light is effective at the cellular level to activate TRPV1. To which extend green light is of medical relevance needs further investigation.

1. Introduction

Low-level laser irradiation in the mW/cm^2 range of visible and near-infrared (NIR) light had been introduced as a medical treatment already in the late 60s (see [1]), but its medical application still remains controversial. One major reason is that the cellular and molecular photo/biological responses are highly complex.

Since light below 600 nm is strongly absorbed in tissue by haemoglobin and melanin, and above 1200 nm by the water, medical application focused on the red and NIR range (see e.g., [2]). As possible photoreceptor cytochrome oxidase C has been suggested [3, 4]. Also in a modern variant of Chinese medicine, laser light is used to stimulate acupuncture points (see e.g., [5]). In traditional Chinese medicine, acupuncture points are stimulated by the needling procedure; it could be demonstrated that this leads to the degranulation of mast cells, which forms an essential early step in acupuncture-induced analgesia [6]. The degranulation in acupuncture points cannot only be induced by the

mechanical stress during needle manipulation or osmotic stress, but also by high temperatures like those that are applied during moxibustion. Even irradiation of mast cells with red laser light, that is used in the laser acupuncture [5, 7], results in degranulation [8]. More recently, irradiation of acupoints with blue laser light has been introduced in medical treatment [9].

In the work by Zhang et al. [8], it was shown that the degranulation induced by mechanical stress, high temperature, and red light involves activation of TRPV2, a member of the family of transient-receptor-potential (TRP) ion channels. Application of blue laser light was also demonstrated to elicit mast-cell degranulation, and the involvement of another TRP channel, TRPV4, was suggested [10]. In addition to these two TRPV channels, mast cells also express TRPV1 [8]. In our work presented here we investigated to which extent TRPV1 can be activated by blue, green, and red laser light.

To investigate effects of laser light on TRPV1 and to avoid interference with the other members of TRPV family in the

mast cells, we used *Xenopus* oocytes as a model system with heterologously expressed TRPV1. Activity of TRPV1 was monitored under voltage clamp as TRPV1-mediated current.

2. Materials and Methods

2.1. Transcription of TRPV1 cDNA. Full length human TRPV1 cDNA was cut from the vector pCAGGSM2-IRES-GFP-R1R2/TrpV1 (kindly provided by Dr. B. Nilius, University of Leuven, Belgium) with restriction enzyme Cla I and EcoR I and subcloned into the in vitro transcription vector pTLN digested with the same enzymes. The recombinant plasmid named pTLN-hTRPV1 was confirmed by DNA sequencing. 5 μ g pTLN-hTRPV1 were linearized by Hpa I and purified. The in vitro transcription was carried out using 2 μ g linearized pTLN-hTRPV1 under the guideline of SP6 transcription kit (Ambion). TRPV1 cRNA was stored at -20°C for the following experiments.

2.2. Cell Culture. Human mast cells HMC-1 (kindly provided by Dr. J. H. Butterfield, Mayo Clinic, USA) were cultured in IMDM (Gibco, Invitrogen, USA), supplemented with 2 mM L-glutamine, 25 mM HEPES, 10% (v/v) fetal bovine serum (Gibco, Invitrogen), and 1% penicillin and streptomycin (Gibco, Invitrogen, USA) in a 95% humidity-controlled incubator with 5% CO_2 at 37°C .

2.3. Expression of TRPV1 Protein in *Xenopus* Oocytes. To investigate effects of laser irradiation on the TRPV1 protein, we used the *Xenopus* oocyte for heterologous expression and applied voltage-clamp techniques. Females of the clawed toad *Xenopus laevis* (Maosheng Bio-Technology Co., Shanghai, China) were anaesthetized with tricaine (1 g/L H_2O , MS222, Sandoz, Basel, Switzerland) or in ice water. Parts of the ovary were removed and treated with 0.3 units per mL liberase (Roche) for 3 h to remove enveloping tissue and to obtain isolated oocytes. For expression of TRPV1 protein, oocytes of stage V or VI [11] were selected and injected with 20 ng cRNA (at 1 ng/1 nL) two to three days before the experiments; uninjected oocytes served as controls. The cells were stored at 19°C in oocyte Ringer's-like solution (G-ORi, see Section 2.6). Experiments were performed at room temperature (24 – 26°C).

2.4. Voltage-Clamp Experiments. We applied conventional two-electrode voltage clamp using Turbo TEC-03 with Cell-Works software (NPI electronic, Tamm, Germany) to measure membrane currents. To determine steady-state current-voltage dependencies (IV curves), membrane currents were averaged during the last 20 ms of 200 ms, rectangular voltage pulses from -150 to $+30$ mV in 10 mV increments; the pulses were applied from a holding potential of -60 mV. To avoid changes at the reference bath electrode due to changes in Cl^- activity, the electrode was uncoupled from the bath via an ORi-filled channel.

2.5. Laser Stimulation. For laser stimulation of the oocytes continuous-wave (CW) lasers were used, for 406 nm the CW

Laser 1051390/AF (COHERENT), for 532 nm the CW Laser SUWTECH LDC 1500 (Shanghai Uniwave Technology Co., Ltd), and for 657 nm the CW Laser SB2007047 (Shanghai University of Traditional Chinese Medicine). Fibre optics were used to guide the laser light close to the oocyte (5 mm) with output powers of 5 mW, 36 mW, and 5–40 mW—for the blue, red, and green laser light, respectively. The spot size at the position to the oocyte was 2 mm in diameter, oocytes had a diameter of 1–1.2 mm. In several experiments using a one-millimetre thermoprobe, we confirmed that the applied laser light could not produce any significant change in temperature; at most an increase of 0.5 degrees was detectable after 30 min of irradiation. Taking into account that the oocyte was in addition continuously superfused with fresh solution of room temperature, effects of changing temperature can be excluded.

2.6. Solutions. Standard ORi (Oocyte Ringer's) solution contained (in mM) 90 NaCl, 2 KCl, 2 CaCl_2 , and 5 MOPS (pH 7.4, adjusted with Tris). For incubation of the oocytes, the ORi was supplemented with 70 mg/L Gentamycin (G-ORi). Stock solutions of capsaicin (1 mM) were prepared in ethanol and of ruthenium red (RuR, 6 mM) in distilled water. The bath solution for HMC-1 cells contained (in mM) 150 NaCl, 5 KCl, 2 CaCl_2 , 5 MgCl_2 , 4 D-sorbitol, and 10 HEPES (pH 7.4 adjusted with NaOH).

2.7. Data Analysis. For judging statistical significant effects of laser irradiation on current-voltage dependencies, *t*-tests were performed for at least 2 different potentials (-100 and -50 mV). Mean values were considered as statistically different on the basis of *t*, $P < 0.03$.

3. Results

3.1. Functional Expression of TRPV1 in the Oocytes. To demonstrate that TRPV1 was functionally expressed in the oocytes, several specific characteristics of TRPV1-mediated current were investigated.

TRPV1 is known to be activated by capsaicin [12, 13]. Oocytes injected with cRNA for TRPV1 responded to application of 500 nM capsaicin with an increase in membrane current that completely disappeared after washout (Figure 1(a)). To correct for possible drift with time, capsaicin-induced current I_{cap} was calculated according to

$$I_{\text{cap}} = \frac{I1_{\text{before}} - I1_{\text{after}}}{2} - I2, \quad (1)$$

where $I1$ is the current in the absence of capsaicin (before or after the application of the agonist) and $I2$ the current in the presence. The difference current will be considered as current mediated by TRPV1 (Figure 1(b)); oocytes not injected with cRNA, never exhibited any capsaicin-sensitive current (Figure 1(b)). The current-voltage dependence is characterised by outward rectification. Oocytes not injected with cRNA exhibited no response to capsaicin.

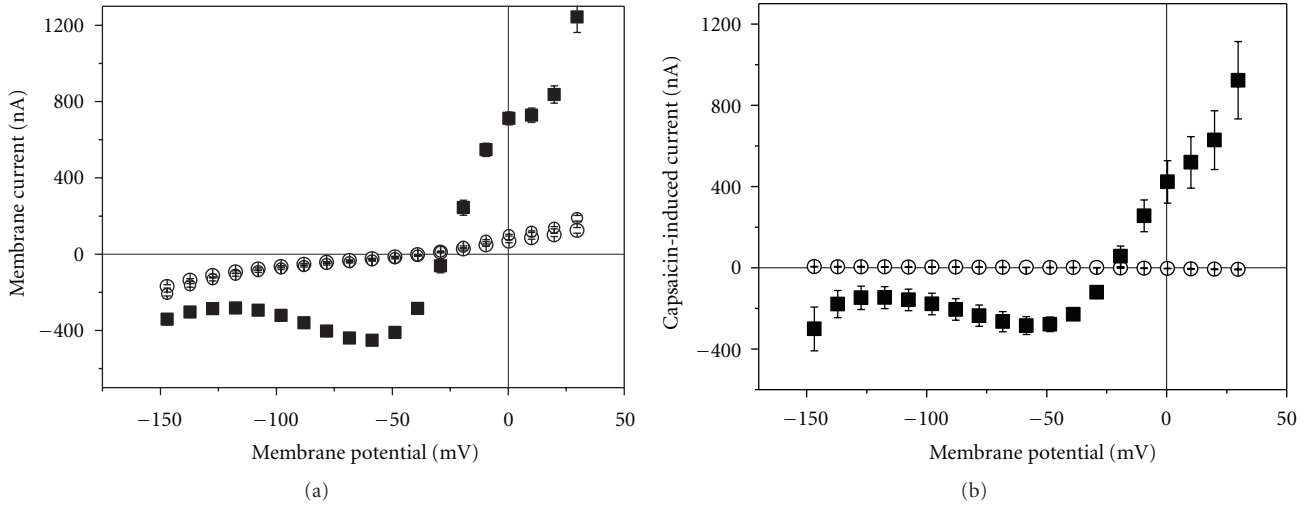


FIGURE 1: Effect of capsaicin application on current-voltage curves. (a) Membrane current in oocytes injected with TRPV1-cRNA. Large open circles before, filled squares during, and small open circles after application of 500 nM capsaicin. (b) Capsaicin-induced current in uninjected oocytes (open circles) and cRNA-injected oocytes (filled squares). All data are averages from 8 experiments (\pm SEM).

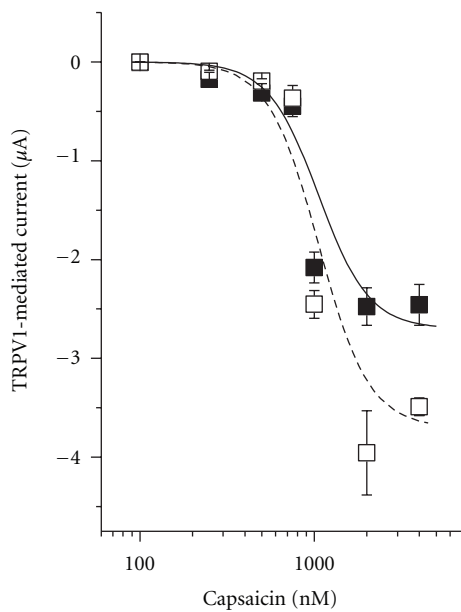


FIGURE 2: Dependence of TRPV1-mediated current on capsaicin concentration. Filled squares current at -60 mV and open squares at -100 mV. Data are averages from 7 experiments (\pm SEM). Lines represent approximations of the concentration dependencies with the same $K_{1/2}$ value of $1.06 \mu\text{M}$.

The dependence of the TRPV1-mediated current showed strong dependence on capsaicin concentration (Figure 2) and can be approximated by

$$I = I_{\text{max}} \frac{[\text{capsaicin}]^3}{[\text{capsaicin}]^3 + K_{1/2}^3}, \quad (2)$$

with an $K_{1/2}$ value of $1.06 \mu\text{M}$ for -60 as well as -100 mV.

Another characteristic of TRPV1 is its inhibition by ruthenium red (RuR) [14]. Figure 3 shows that $12 \mu\text{M}$ RuR

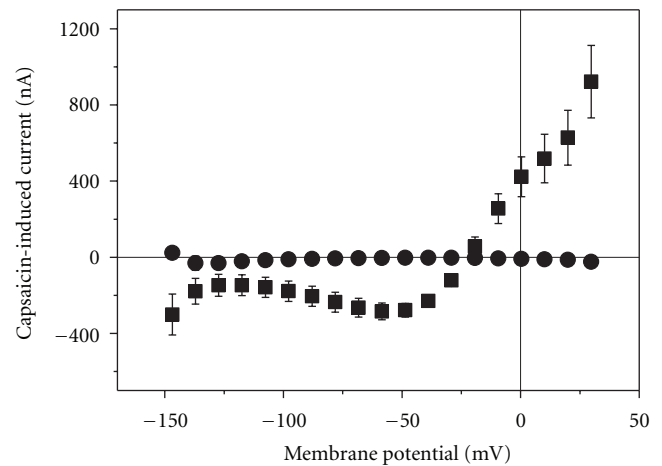


FIGURE 3: Inhibition of capsaicin-induced current by RuR. Filled square current-voltage dependence of current induced by $500 \mu\text{M}$ capsaicin, filled circles in the simultaneous presence of $12 \mu\text{M}$ RuR. Data are averages (\pm SEM) of 14 measurements in the absence and of 4 measurements in the presence of RuR.

completely blocked the capsaicin-induced current in the oocytes over the entire potential range. In control oocytes not injected with cRNA, no RuR-sensitive current component could be detected.

TRPV1 can also be activated by reduced pH [12]. Over the potential range of -40 to -120 mV, reducing the extracellular pH hardly affected the membrane current in noninjected oocytes (Figure 4). In cRNA-injected oocytes, the change in pH from 7.4 to 6.2 activated a current (Figure 4) with similar voltage dependence as the capsaicin-induced current (compare Figure 1(b)).

Physiologically TRPV1 functions as thermosensor responding to noxious temperatures exceeding 42°C . If the temperature of the solution superfusing the oocyte was increased

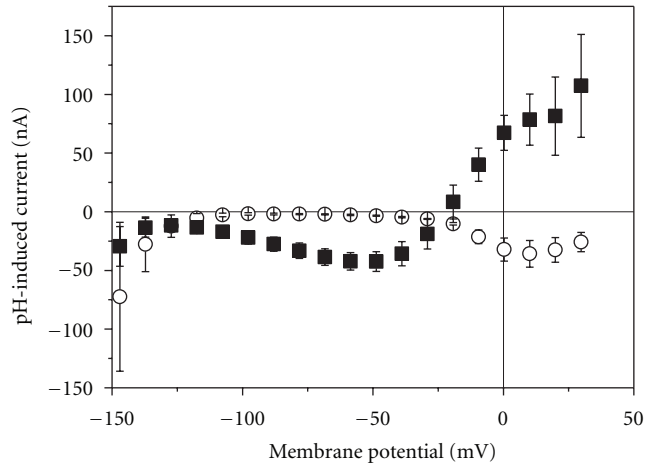


FIGURE 4: Effect of pH reduction on membrane current. Change current in response to a reduction of external pH from 7.4 to 6.2 in noninjected oocytes (open circles) and in cRNA-injected cells (filled squares). Data for injected cells are averages (\pm SEM) of 7 measurement; for the control cells 2 measurements were performed.

from room temperature of 25°C to 42°C, outward-rectifier current, typical for the capsaicin-induced current, was stimulated (Figure 5(a)). This increase in current was completely reversible when the temperature was returned to 25°C. In the presence of RuR, no such current could be activated at 42°C (not illustrated). Also at 35°C only a tiny current component became apparent with voltage-dependence different from TRPV1-mediated current (Figure 5(b)).

In the following we investigated to which extent TRPV1 function can be modulated by laser light of three different wave lengths: red light of 637 nm, blue light of 406 nm, and green light of 532 nm. In oocytes not expressing TRPV1 with none of the wavelengths, any current modulation was detectable, even at the highest output powers of 40 mW.

3.2. Effect of Red Laser Light on TRPV1-Mediated Current. In medical low-level laser application, including laser acupuncture, red laser light is often applied. In the absence of capsaicin, no change in membrane current was detectable when red laser light (637 nm, 5 mW) was applied (not shown); even at 36 mW no sign of light-induced current was visible (for holding current at -60 mV see Figure 9). Also when TRPV1 was activated by 500 nM capsaicin, a 2 min time period of irradiation could not be significantly modulated TRPV1-mediated current (Figure 6).

3.3. Effect of Blue Laser Light on TRPV1-Mediated Current. Recently, low-level blue laser light was introduced in laser acupuncture [9]. Therefore, we also tested for the effect of 406 nm on TRPV1-mediated current. Similarly to the red laser light, an output power of 5 mW could not affect membrane current (for holding current at -60 mV see Figure 9). Also when TRPV1 was activated by 500 nM capsaicin, a 2 min time period of irradiation could not significantly modulate TRPV1-mediated current (Figure 7).

3.4. Effect of Green Laser Light on TRPV1-Mediated Current. In contrast to the red and blue laser light, green laser light (532 nm) activated in cRNA-injected oocytes even in the absence of capsaicin a current that increased with increasing output power (Figure 8(a)). Already at 5 mW a significant TRPV1-mediated current could be activated. The effect gradually increased with time reaching a maximum steady-state current within 2 min of irradiation (for 40 mW compare Figure 9). When the laser light was turned off, the current instantaneously dropped to the same level as before irradiation. At laser output power of 40 mW, the typical outward rectification of TRPV1 channel was clearly apparent (Figure 8(b)).

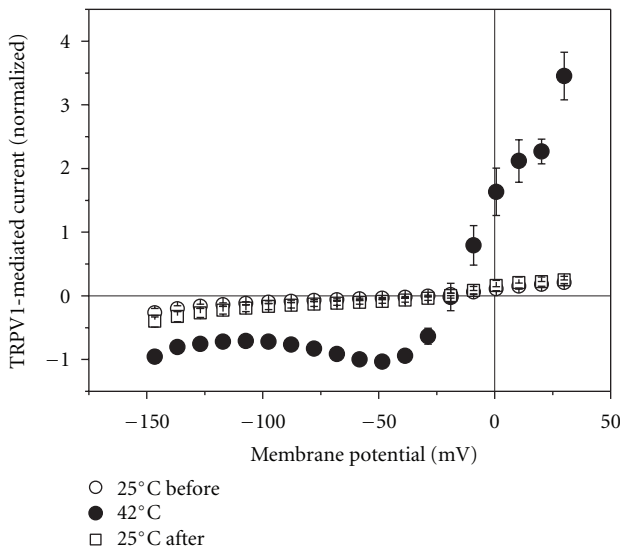
3.5. Capsaicin Induces Degranulation in HMC-1. The experiments described above were done on the model system *Xenopus* oocyte. To support the idea that mast cell degranulation and activation of TRPV1 might be involved in acupuncture effects, we tested whether TRPV1 activation can induce mast cell degranulation. Figures 10(a) and 10(b) illustrate that application of 1 μ M capsaicin (about $K_{1/2}$ value for TRPV1 activation, see Figure 2) indeed led to degranulation. Already at 500 nM clear activation of TRPV1 was possible (Figure 1); after application of 500 nM capsaicin for 5 min $62 \pm 8\%$ of the cells had degranulated (Figure 10(c)).

4. Discussion

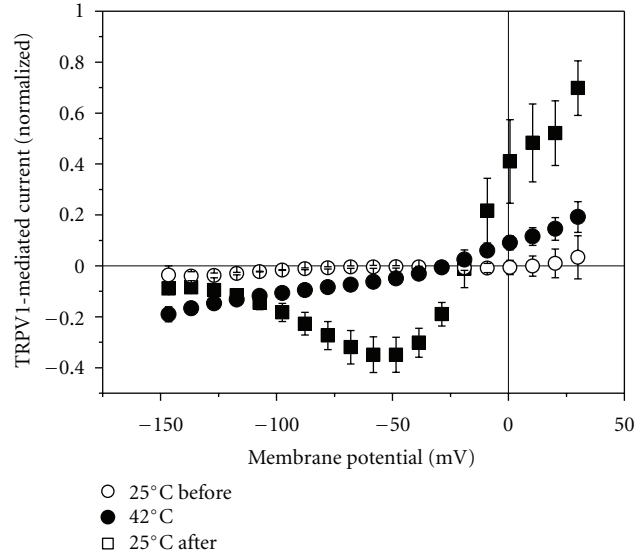
4.1. TRPV1 Is Functionally Expressed in the Oocytes. We have demonstrated that TRPV1 was functionally expressed in the oocytes by showing TRPV1-specific characteristics. Oocytes injected with the cRNA for TRPV1 exhibited capsaicin-inducible current (Figure 1) with a $K_{1/2}$ value of about 1 μ M (Figure 2) which is similar to the value reported by others [12, 13]. Also the current-voltage dependence with outward-rectifier characteristic was reported for TRPV1-mediated current [14, 15]. The inhibition by RuR (Figure 3) and activation by reduced pH (Figure 4) of such outward-rectifying current are additional indications [12, 14] that TRPV1 was functionally expressed in the oocytes.

Within the TRPV family, TRPV1 is characterized also by temperature sensitivity with activation by temperature above 42°C [16, 17]. Increasing the temperature even to 35°C only slightly increased the membrane conductance (Figure 5(a)), but as soon as the temperature reached about 42°C, current was induced with the outward-rectifying current-voltage dependence typical for TRPV1 (Figure 5(b)).

4.2. TRPV1 as a Candidate for Laser-Induced Degranulation. It was demonstrated previously that degranulation of mast cell is an essential initial step in acupuncture-induced pain relief [6]. In addition, it was demonstrated that various physical stimuli used in Chinese Medical Treatment can produce mast-cell degranulation [8]. These stimuli include mechanical stress, which is applied during the acupuncture needle manipulation [18–20] via the connective tissue to the mast cells, and high temperatures, which are applied during moxibustion to the acupuncture points [21]. Also



(a)



(b)

FIGURE 5: Effect of elevated temperature on membrane current of TRPV1-expressing oocytes. (a) Effect of 42°C (filled circles) in comparison to 25°C before and after the raise in temperature. (b) Effect of 35°C (filled circles) in comparison to 25°C before the raise in temperature and to the current induced by 500 nM capsaicin (filled squares).

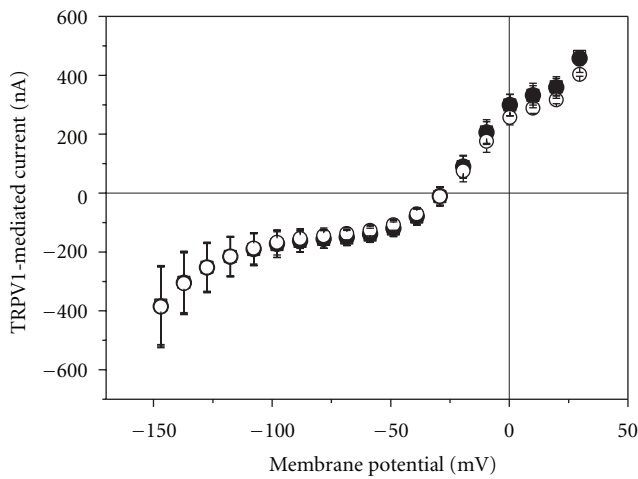


FIGURE 6: Effect of red laser light on current-voltage curve of TRPV1-mediated current. TRPV1 was activated by 500 nM capsaicin. Open square were obtained before irradiation, filled circles at the end of a 2 min lasting irradiation period (637 nm, 36 mW), and open circles 2 min after the laser light was turned off. Data represent averages from 3 oocytes (\pm SEM).

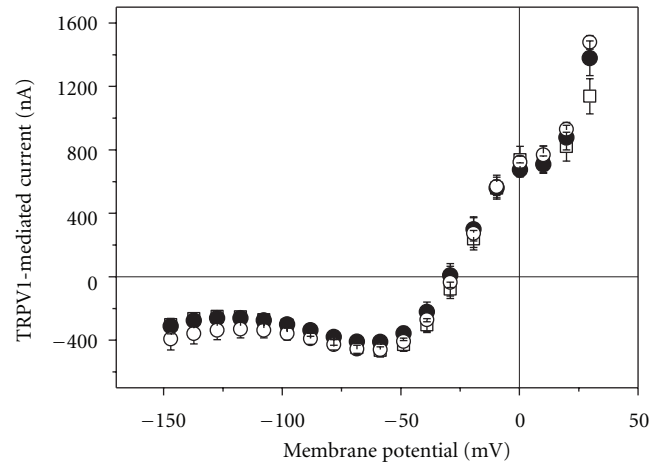


FIGURE 7: Effect of blue laser light on current-voltage curve of TRPV1-mediated current. TRPV1 was activated by 500 nM capsaicin. Open square were obtained before irradiation, filled circles at the end of a 2-min lasting irradiation period (406 nm, 5 mW), and open circles 2 min after the laser light was turned off. Data represent averages from 3 oocytes (\pm SEM).

red laser light in the 630 to 640 nm range is often applied to acupuncture points [7, 9, 22]. All three physical stimuli can elicit mast-cell degranulation that involves activation of TRPV2 ion channels [8].

Because of the optical window of tissue in the range of 600 to 1200 nm, red and NIR light have a penetration depth of up to several mm [23] and have mainly been used to investigate photo biomodulation and stimulation including its application in laser acupuncture. Despite the

fact that blue light has a penetration depth in only the sub-mm range, nevertheless, irradiation of acupuncture points by blue laser light was introduced into laser acupuncture recently [24]. Irradiation of mast cells with a 405 nm laser indeed leads to mast-cell degranulation that was attributed to an intracellular increase of Ca^{2+} by activation of TRPV4 [10]; TRPV4 is also expressed in mast cells [8, 10].

While red and blue laser light seem to stimulate activation of TRPV2 and TRPV4, respectively, these wave lengths were ineffective for TRPV1 (Figures 6 and 7). On the other

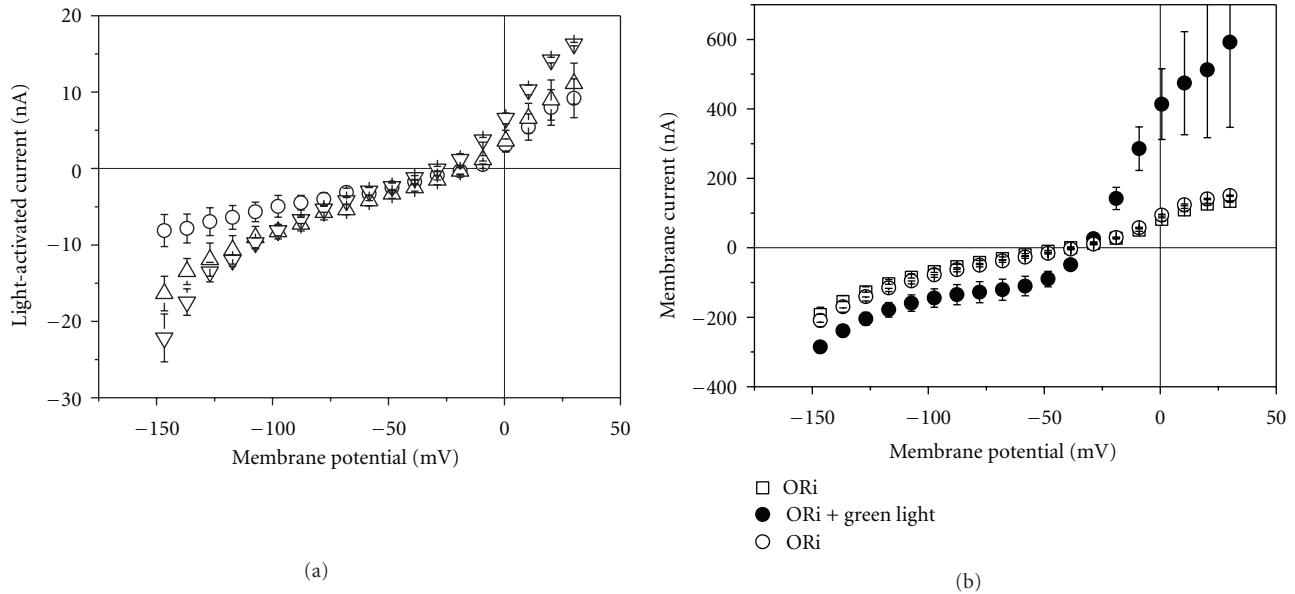


FIGURE 8: Effect of green laser light on current-voltage curve of TRPV1-mediated current. (a) Light-activated current in oocytes injected with cRNA for TRPV1; output power 5 mW (circles), 10 mW (triangle up), and 20 mW (triangles down). Data represent averages from 3 oocytes (\pm SEM). (b) Membrane current before (open squares), during (2 min after light was turned on, filled circles), and after irradiation at 40 mW. Data represent averages from 5 oocytes (\pm SEM).

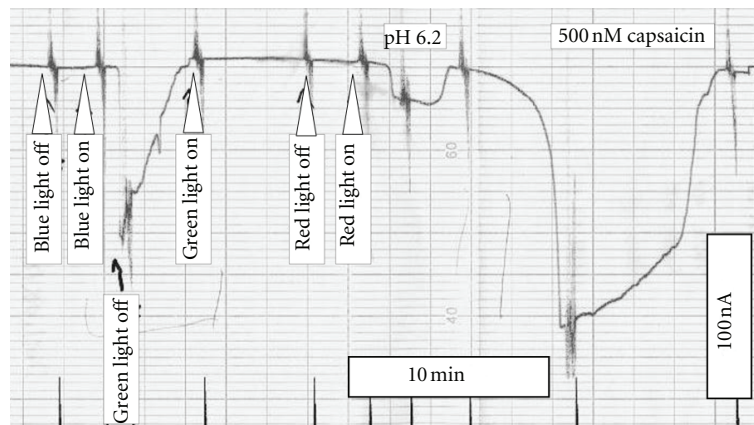


FIGURE 9: Pen recording of holding current at -60 mV. Downward deflexions represent activation of inward current. Red light of 637 nm was applied at 36 mW, green light of 532 nm at 40 mW, and blue light of 406 nm at 5 mW.

hand, for TRPV1 green laser light was a very effective stimulus (Figure 8). At 40 mW, the light induced current amounted to about 80 nA (at -60 mV, see Figure 9), which is comparable to the 85 nA of current that can be activated by 250 nM capsaicin (Figure 2).

Photo biostimulation particularly in the red and NIR range have been attributed to absorption by cytochrome oxidase C. Interestingly, the stimulation of TRPV1 by the green light is dose-dependent, but after about 2 min a steady state is reached, and when turning off the light the TRPV1-mediated current instantaneously vanishes. The physical basis for this is currently under investigation.

In our work, we focused on laser-light-induced mast-cell degranulation that might form an initial step in acupuncture

induced analgesia. Detailed investigations have elucidated that irradiation of peripheral nerve with red or NIR laser light may also be of relevance for analgesic effects (for a detailed review see [25]). In particular, decreased conduction velocities have been reported in experiments on humans and animals with involvement of A δ and C fibres. In our experiments, we could demonstrate the effectiveness of green laser light on TRPV1. Interestingly, TRPV1 is highly expressed in peripheral A δ and C fibres [12], and hence, may also form in the nerve cells a target for green laser-light stimulation. It was reported that within acupuncture points, TRPV1 shows higher expression on A δ and C fibres than in nonacupuncture points and this becomes even increased after electroacupuncture [26]. The authors conclude that the

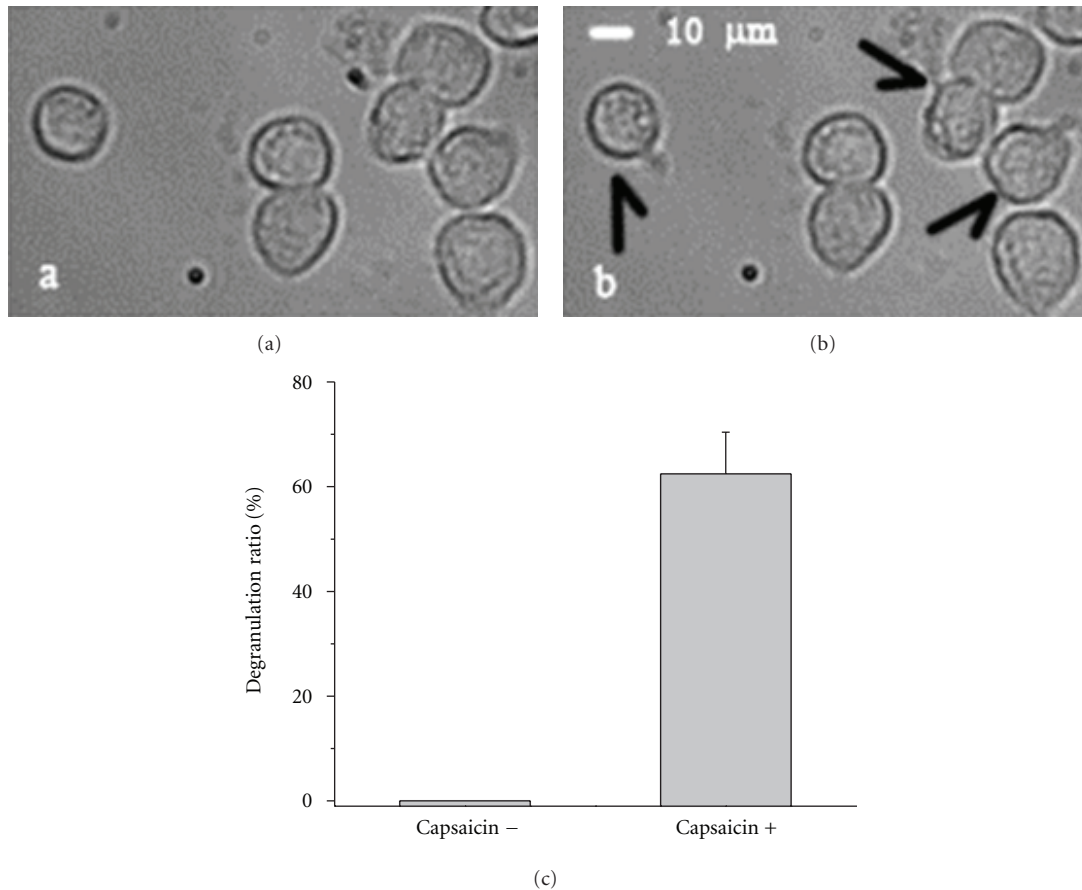


FIGURE 10: Degranulation of human mast cells induced by capsaicin. (a) Human mast cells HMC-1 incubated in bath solution in the absence of the TRPV1-specific agonist capsaicin. (b) HMC-1 cells having been superfused for 5 min with bath solution containing 1 μ M capsaicin. The arrows point to the degranulating cell. (c) Percentage of degranulated HMC-1 cells in the absence and presence of 500 nM capsaicin (exposition time 10 min, values present averages of 3 independent experiments \pm SEM).

higher expression of TRPV1 and its upregulation in response to acupuncture may be involved in the transmission of the acupuncture signal.

In addition to the results in our model system *Xenopus* oocyte, we could show that activation of TRPV1 by the specific agonist capsaicin can indeed induce degranulation (Figure 10). We, therefore, like to suggest that in addition to red and blue laser light also green light with its intermediate penetration depth might be a useful tool in medical treatment.

Abbreviations

CW laser:	Continuous-wave laser
ORi:	Oocyte Ringer's
RuR:	Ruthenium red
TRP:	Transient receptor potential
TRPV1:	Transient receptor potential valinoid-sensitive, isoform 1.

Acknowledgments

The authors are very grateful to Dr. Bernd NILIUS for providing them the cDNA for TRPV1 and to Huiming

DU for his excellent technical assistance. The work was financially supported by the Science Foundation of Shanghai Municipal Commission of Science and Technology, the National Basic Research Program of China (973 Program, no. 2012CB518502), and the National Natural Science Foundation of China (no. 81102635).

References

- [1] E. Mester, A. F. Mester, and A. Mester, "The biomedical effects of laser application," *Lasers in Surgery and Medicine*, vol. 5, no. 1, pp. 31–39, 1985.
- [2] P. Whittaker, "Laser acupuncture: past, present, and future," *Lasers in Medical Science*, vol. 19, no. 2, pp. 69–80, 2004.
- [3] T. Karu, "Primary and secondary mechanisms of action of visible to near-IR radiation on cells," *Journal of Photochemistry and Photobiology B*, vol. 49, no. 1, pp. 1–17, 1999.
- [4] T. I. Karu, L. V. Pyatibrat, and N. I. Afanasyeva, "A novel mitochondrial signaling pathway activated by visible-to-near infrared radiation," *Photochemistry and Photobiology*, vol. 80, no. 2, pp. 366–372, 2004.
- [5] G. Litscher, *High-Tech Acupuncture & Integrative Laser Medicine*, Pabst Science Publishers, Lengerich, Germany, 2012, edited by G. Litscher, X. Y. Gao, L. Wang and B. Zhu.

- [6] D. Zhang, G. Ding, X. Shen et al., "Role of mast cells in acupuncture effect: a pilot study," *Explore*, vol. 4, no. 3, pp. 170–177, 2008.
- [7] X. Y. Shen, L. Zhao, G. H. Ding et al., "Effect of combined laser acupuncture on knee osteoarthritis: a pilot study," *Lasers in Medical Science*, vol. 24, no. 2, pp. 129–136, 2009.
- [8] D. Zhang, A. Spielmann, L. Wang, G. Ding, F. Huang, and Q. Gu, "Mast-cell degranulation induced by physical stimuli involves the activation of transient-receptor-potential channel TRPV2," *Physiological Research*, vol. 61, no. 1, pp. 113–124, 2012.
- [9] G. Litscher, "Integrative laser medicine and high-tech acupuncture at the Medical University of Graz," *Evidence-Based Complementary and Alternative Medicine*, vol. 2012, Article ID 103109, 21 pages, 2012.
- [10] W. Z. Yang, J. Y. Chen, J. T. Yu, and L. W. Zhou, "Effects of low power laser irradiation on intracellular calcium and histamine release in RBL-2H3 mast cells," *Photochemistry and Photobiology*, vol. 83, no. 4, pp. 979–984, 2007.
- [11] J. N. Dumont, "Oogenesis in *Xenopus laevis* (Daudin). I. Stages of oocyte development in laboratory maintained animals," *Journal of Morphology*, vol. 136, no. 2, pp. 153–179, 1972.
- [12] M. J. Caterina, M. A. Schumacher, M. Tominaga, T. A. Rosen, J. D. Levine, and D. Julius, "The capsaicin receptor: a heat-activated ion channel in the pain pathway," *Nature*, vol. 389, no. 6653, pp. 816–824, 1997.
- [13] J. Vriens, G. Appendino, and B. Nilius, "Pharmacology of vanilloid transient receptor potential cation channels," *Molecular Pharmacology*, vol. 75, no. 6, pp. 1262–1279, 2009.
- [14] C. Garcia-Martinez, C. Morenilla-Palao, R. Planells-Cases, J. M. Merino, and A. Ferrer-Montiel, "Identification of an aspartic residue in the P-loop of the vanilloid receptor that modulates pore properties," *The Journal of Biological Chemistry*, vol. 275, no. 42, pp. 32552–32558, 2000.
- [15] M. Raisinghani, R. M. Pabbidi, and L. S. Premkumar, "Activation of transient receptor potential vanilloid 1 (TRPV1) by resiniferatoxin," *Journal of Physiology*, vol. 567, no. 3, pp. 771–786, 2005.
- [16] M. J. Caterina, A. Leffler, A. B. Malmberg et al., "Impaired nociception and pain sensation in mice lacking the capsaicin receptor," *Science*, vol. 288, no. 5464, pp. 306–313, 2000.
- [17] R. Vennekens, G. Owsianik, and B. Nilius, "Vanilloid transient receptor potential cation channels: an overview," *Current Pharmaceutical Design*, vol. 14, no. 1, pp. 18–31, 2008.
- [18] H. M. Langevin, D. L. Churchill, J. R. Fox, G. J. Badger, B. S. Garra, and M. H. Krag, "Biomechanical response to acupuncture needling in humans," *Journal of Applied Physiology*, vol. 91, no. 6, pp. 2471–2478, 2001.
- [19] H. M. Langevin, "Connective tissue: a body-wide signaling network?" *Medical Hypotheses*, vol. 66, no. 6, pp. 1074–1077, 2006.
- [20] H. M. Langevin, D. L. Churchill, J. Wu et al., "Evidence of connective tissue involvement in acupuncture," *The FASEB Journal*, vol. 16, no. 8, pp. 872–874, 2002.
- [21] J. F. Zhang and Y. C. Wu, "Modern progress of mechanism of moxibustion therapy," *Journal of Acupuncture and Tuina Science*, vol. 4, no. 5, pp. 257–260, 2006.
- [22] G. Litscher and D. Schikora, *Laserneedle—Acupuncture: Science and Practice*, Pabst Science Publishers, Lengerich, Germany, 2007, edited by G. Litscher and D. Schikora.
- [23] R. R. Anderson and J. A. Parrish, "The optics of human skin," *Journal of Investigative Dermatology*, vol. 77, no. 1, pp. 13–19, 1981.
- [24] X. Y. Gao, G. Litscher, K. Liu, and B. Zhu, "Sino-European transcontinental basic and clinical high-tech acupuncture studies-part 3: violet laser stimulation in anesthetized rats," *Evidence-Based Complementary and Alternative Medicine*, vol. 2012, Article ID 402590, 8 pages, 2012.
- [25] R. Chow, P. Armati, E. L. Laakso, J. M. Bjordal, and G. D. Baxter, "Inhibitory effects of laser irradiation on peripheral mammalian nerves and relevance to analgesic effects: a systematic review," *Photomedicine and Laser Surgery*, vol. 29, no. 6, pp. 365–381, 2011.
- [26] T. S. Abraham, M. L. Chen, and S. X. Ma, "TRPV1 expression in acupuncture points: response to electroacupuncture stimulation," *Journal of Chemical Neuroanatomy*, vol. 41, no. 3, pp. 129–136, 2011.

Research Article

Therapeutic Effects of Acupuncture through Enhancement of Functional Angiogenesis and Granulogenesis in Rat Wound Healing

Sang In Park,¹ Yun-Young Sunwoo,¹ Yu Jin Jung,¹ Woo Chul Chang,¹ Moon-Seo Park,¹ Young-An Chung,^{1,2} Lee-So Maeng,¹ Young-Min Han,¹ Hak Soo Shin,¹ Jisoo Lee,³ and Sang-Hoon Lee⁴

¹Institute of Catholic Integrative Medicine (ICIM), Incheon St. Mary's Hospital, The Catholic University of Korea, Incheon 403-720, Republic of Korea

²Department of Radiology, Incheon St. Mary's Hospital, The Catholic University of Korea, Incheon, Republic of Korea

³Chicago Medical School, Rosalind Franklin University of Medicine and Science, North Chicago, USA

⁴Department of Radiology, St. Mary's Hospital, The Catholic University of Korea, Seoul, Republic of Korea

Correspondence should be addressed to Sang-Hoon Lee, nm@catholic.ac.kr

Received 27 July 2012; Revised 8 November 2012; Accepted 14 November 2012

Academic Editor: Wolfgang Schwarz

Copyright © 2012 Sang In Park et al. This is an open access article distributed under the Creative Commons Attribution License, which permits unrestricted use, distribution, and reproduction in any medium, provided the original work is properly cited.

Acupuncture regulates inflammation process and growth factors by increasing blood circulation in affected areas. In this study, we examined whether acupuncture has an effect on wound healing in injured rat. Rats were assigned randomly into two groups: control group and acupuncture group. Acupuncture treatment was carried out at 8 sites around the wounded area. We analyzed the wound area, inflammatory cytokines, proliferation of resident cells, and angiogenesis and induction of extracellular matrix remodeling. At 7 days after-wounding the wound size in acupuncture-treat group was decreased more significantly compared to control group. In addition, the protein levels of proinflammatory cytokines such as tumor necrosis factor- α (TNF- α) and interleukin-1 β (IL-1 β) were significantly decreased compared to the control at 2 and 7 days post-wounding. Also, we analyzed newly generated cells by performing immunostaining for PCNA and using several phenotype markers such as CD-31, α -SMA, and collagen type I. In acupuncture-treated group, PCNA-positive cell was increased and PCNA labeled CD-31-positive vessels, α -SMA- and collagen type I-positive fibroblastic cells, were increased compared to the control group at 7 days post-wounding. These results suggest that acupuncture may improve wound healing through decreasing pro-inflammatory response, increasing cell proliferation and angiogenesis, and inducing extracellular matrix remodeling.

1. Introduction

In normal wound repair, well-controlled and coordinated balance between immune defense and epithelial cell proliferation and differentiation is essential. Wound healing involves a complex process that includes inflammation, proliferation, epithelialization, angiogenesis, and collagen matrix formation [1, 2]. During the inflammatory phase of skin repair, neutrophils and macrophages infiltrate the wounded area to clear damaged tissue and produce cytokines such as macrophage inflammatory protein (MIP)-1 α , interleukin (IL) family, and tumor necrosis factor- α (TNF- α) to expedite

the repair process [3]. Epithelialization occurs by migration and proliferation of keratinocytes from the wound edges and by differentiation of stem cells from the remaining hair follicle bulbs [4, 5]. Also, collagen deposition occurs by the influx of growth factors such as transforming growth factor- β , fibroblast growth factor (FGF), and vascular endothelial growth factor (VEGF) that are secreted by macrophages, platelets, and fibroblasts. Moreover, angiogenesis is a multistep process that involves endothelial cell sprouting from the parent vessel, by migration, proliferation, alignment, and tube formation to other vessels [6, 7]. Angiogenesis plays important roles in the healing process of wound [7–9].

This process is associated with the expression of angiogenic factors such VEGF and platelet derived growth factor (PDGF).

Acupuncture is an Asian medical procedure with a long history that involves peripheral sensory stimulation for treatment of various ailments. Recently, a number of studies tried to elucidate the physiology of acupuncture. Our previous study demonstrated that acupuncture on specific acupoints induces changes of glucose metabolism in the brain [10]. Furthermore, acupuncture attenuates inflammation increasing blood circulation at the affected area [11]. Some studies reported therapeutic effect of acupuncture on Ashi point. As we know, Ashi-point is pain site that is found on the body by the practitioner. Since Ashi points can be anywhere, there is an unlimited number of them. Sun group demonstrated that there is similar therapeutic effect of acupuncture site between acupoint and Ashi-point in orthopedic postoperative pain [12]. Lee et al. and Nakajima et al. reported that acupuncture treatment in wound and around bone fracture accelerates healing process by reducing proinflammation and stimulating epidermal regeneration [13, 14]. Therefore, we believe acupuncture may provide a non-toxic and natural alternative to wound healing. However, the exact mechanisms behind the effects of acupuncture are still not clear.

In this study, we investigated whether acupuncture treatment around the edges of wound improved wound healing and promoted the proliferation of resident cells in wounded area of rats. Also, we studied the effects of acupuncture on angiogenesis and induction of extracellular matrix remodeling and change of pro-inflammatory cytokines in wound area.

2. Methods

2.1. Animals. The experimental protocol used in this study was designed in compliance with the guidelines established by the Institutional Animal Care and Use Committee of Catholic University Medical School. Male Sprague-Dawley rats (270–300 g) were initially anesthetized with 5% isoflurane in 70% nitrous oxide and 30% oxygen using an induction chamber, and were maintained by a mixture of 2% isoflurane under temperature controlled conditions ($37 \pm 0.1^\circ\text{C}$) using a rectal thermometer and heating pad (Harvard Apparatus Inc., Holliston, Massachusetts, USA). After shaving and cleaning with 70% ethanol, the dorsal skin was picked up at the midline and punched through two layer of skin (10 mm in diameter). The animals were divided into two groups: (1) inhalation anesthesia group after wound ($n = 7$, Control group) and (2) acupuncture-treated experimental group ($n = 7$, acupuncture group). Each group was subdivided into three time point group (2 and 7 days after wound; $n = 6$ for each time point).

2.2. Acupuncture Treatment Procedure. The acupuncture treatment was given daily for 20 min at 9 sites in wound area, by using a stainless press-needle of 0.25 mm in diameter



FIGURE 1: Acupuncture treatment after wound. Image obtained at 1 day after wound showing wounded skin being treated with acupuncture.

and 30 mm in length (Suzhou Hua Tuo Medical Instruments Co. Ltd Suzhou, China). The rats were maintained under inhalation anesthesia in thermally regulated conditions ($37 \pm 0.1^\circ\text{C}$) using a rectal thermometer and heating pad (Harvard Apparatus Inc., Holliston, Massachusetts, USA). The acupuncture needles were placed and fixed on the skin around the wound (Figure 1). Needles were accurately inserted to the targeted depth of 1.5 mm and were sustained with 20 min per day for 5 days after wound.

2.3. Wound Closure Measurements. Immediately after creating the wounds, the initial wound sizes were measured using a caliper at 0, 1, 3, 5, and 7 days following wound. Changes in wound areas over time were expressed as the percentage of the initial wound areas. Also, wound area was digitally photographed using a digital camera in red box (3×3 cm) (Canon ES350, Ohta-ku, Tokyo, Japan).

2.4. Immunohistofluorescence Staining. At 7 days post-wound, the rats were sacrificed and the skin was removed for histological examination. Skin tissue samples were fixed in 10% formalin for 24 h before embedding in paraffin. The blocks were cut into $5 \mu\text{m}$ section in order to perform hematoxylin and eosin (H&E) and immunohistostaining. The sections were dewaxed in histoclear (Sigma, St. Louis, MO, USA) and rehydrated through a graded alcohol series. After retrieval (Abcam, Cambridge, MA, USA), the sections were blocked with normal goat serum for 1 h at room temperature. The sections were incubated at 4°C overnight with the following antibodies: mouse antiproliferation cell nuclei antigen (PCNA; Millipore, Billerica, MA, USA), rabbit polyclonal antibody to CD-31 (CD-31; Abcam), Collagen type I (Abcam), α -smooth muscle (α -SMA, Abcam). After washing, sections were incubated in Alexa 546-conjugated goat anti-mouse IgM (Molecular probe, Eugene, Oregon,

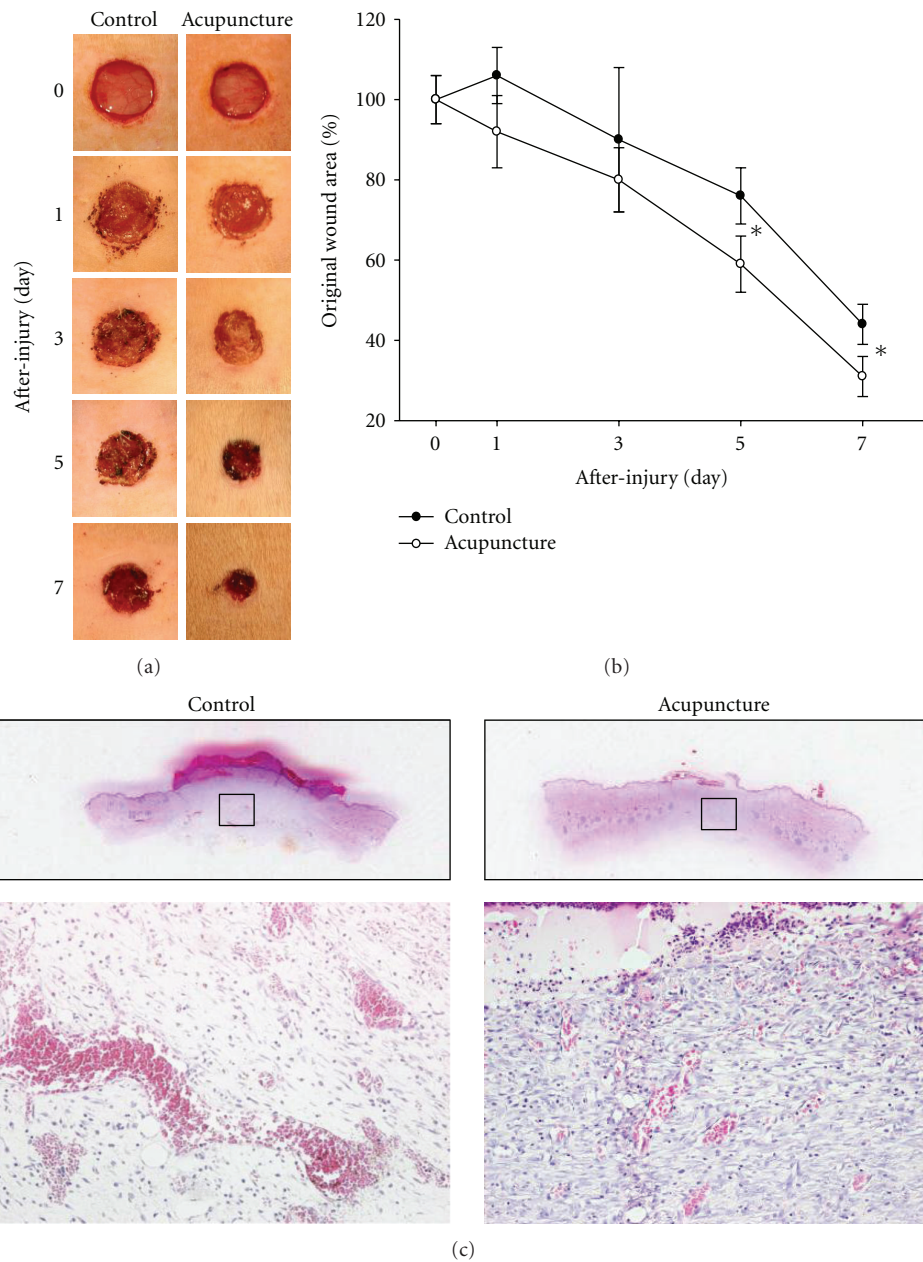


FIGURE 2: Wound closure in wound rat. Image shown in the wound image of acupuncture and control group at 0, 1, 3, 5, and 7 days after-wounding (a). Wound area was measured at the indicated time points of after-wounding (b). Area of the wounds was determined by quantitative analysis using caliper. Cutaneous wounds at 7 days were stained with (H&E) and photographed with a digital camera mounted on a light microscope (c). The wound sizes of acupuncture-treated group significantly decreased compared to the control group. Also red blood cells within the number of blood vessels decreased compared to the control group. Data are expressed as mean \pm SD, * $P < 0.05$, Scale bars denote, 100 μ m.

USA) and Cy2-conjugated goat anti-rabbit IgG (Jackson ImmunoResearch) for 1 h at room temperature. After washing, the sections were counterstained with 4',6-diamidino-2-phenylindole (DAPI; Sigma-Aldrich). Fluorescent images were acquired using a fluorescence microscope equipped with a spot digital camera (Nikon, Chiyoda-ku, Tokyo, Japan) and a Zeiss LSM 510 confocal scanning laser microscope ($\times 200$ oil objective) (Carl Zeiss, Jena, Germany).

To determine PCNA and PCNA labeled-CD-31, α -SMA, and collagen type I-positive cells, every fifth coronal section per animal was prepared and counting was performed on three randomly selected non-overlapping per section. The measurement was made in a predefined field (300 μ m \times 300 μ m) and the number of positive cells of wound area were obtained by multiplying by three. Using Meta-Morph imaging program (Molecular Devices Inc, Downingtown, PA, USA),

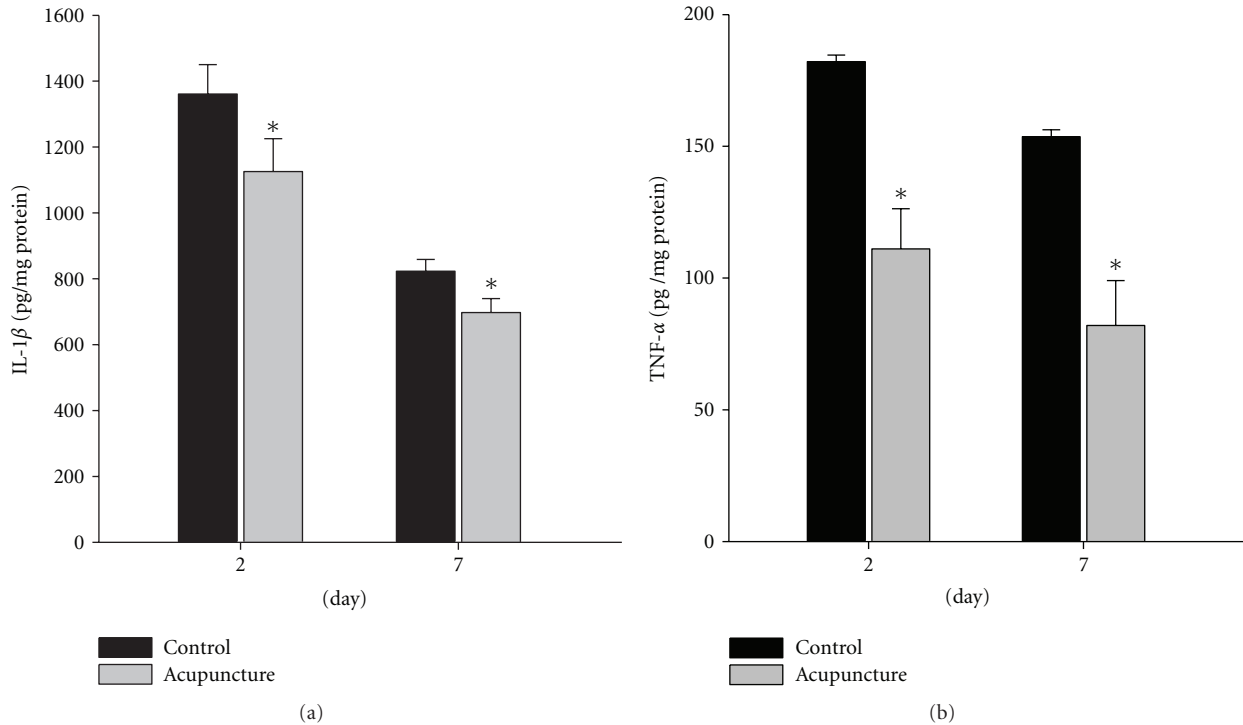


FIGURE 3: Expression of inflammatory cytokines in wound area. TNF- α and IL-1 β were detected by ELISA at days after-wound. Protein levels of these factors show the quantitative analysis data (a-b). TNF- α and IL-1 β were significantly decreased compared with the control group (a-b). Data are expressed as mean \pm SD, * $P < 0.05$.

wound area was determined by counting PCNA, CD-31, α -SMA, and collagen type I-positive cells.

2.5. Enzyme-Linked Immunosorbent Analysis. At 2 and 7 days following wound, wound samples were homogenized in t-per tissue protein extraction buffer (Pierce, Rockford, IL, USA) with protease inhibitor. The lysates were cleared by centrifugation (10,000 g) for 30 min at 4°C and the supernatant was kept at -70°C. The supernatant was examined using the enzyme-linked immunosorbent assay (ELISA) to detect the protein levels of angiogenic factor and inflammatory cytokines. The supernatant was further analyzed to quantify the concentration of VEGF (R&D system, Minneapolis, USA), TNF- α (R&D system), and IL-1 β (R&D system) in strict accordance with the manufacturer's protocols.

2.6. Statistical Analysis. The behavior tests, cerebral ischemic volume, and cell count of apoptotic cells for both rat groups were subjected to one-way ANOVA with post hoc analysis, independent *T*-test, or Mann-Whitney *U* test. Data are presented as the mean value \pm standard deviation of the mean. Probability values less than 0.05 were considered statistically significant.

3. Results

3.1. Wound Area. Wound sizes were measured at 0, 1, 3, 5, and 7 days post-wounding. Wound closure was noted

to progress more rapidly in acupuncture-treated group compared to the control group (Figure 2). At 7 days post-wounding, the wound sizes of acupuncture-treated group significantly decreased compared to the control group (31 ± 5 versus $44 \pm 5\%$, $P < 0.05$). These results suggest that acupuncture can accelerate the restoration of wound healing.

3.2. Expression of Inflammatory Cytokine. We hypothesized that acupuncture may protect an injured area following a wound by reducing the production of inflammatory cytokines. We used the ELISA to detect protein levels of inflammatory cytokines at 2 and 7 days in the wound area. At 2 and 7 days post-wounding, pro-inflammatory cytokines such as IL-1 β and TNF- α were significantly reduced compared to the control group (Figure 3). These results suggest that acupuncture could promote wound healing to regulate inflammatory cytokines.

3.3. Endogenous Cell Proliferation. To investigate whether acupuncture treatment improved newly generated cell during wound healing, the number of proliferating cells were determined by anti-PCNA antibody. At 7 days after wound, proliferation of the newly generated cells increased greatly in acupuncture treated group compared to the control group within the wound area (Figure 4). These results suggest that acupuncture could have potentially improved cell proliferation during wound healing.

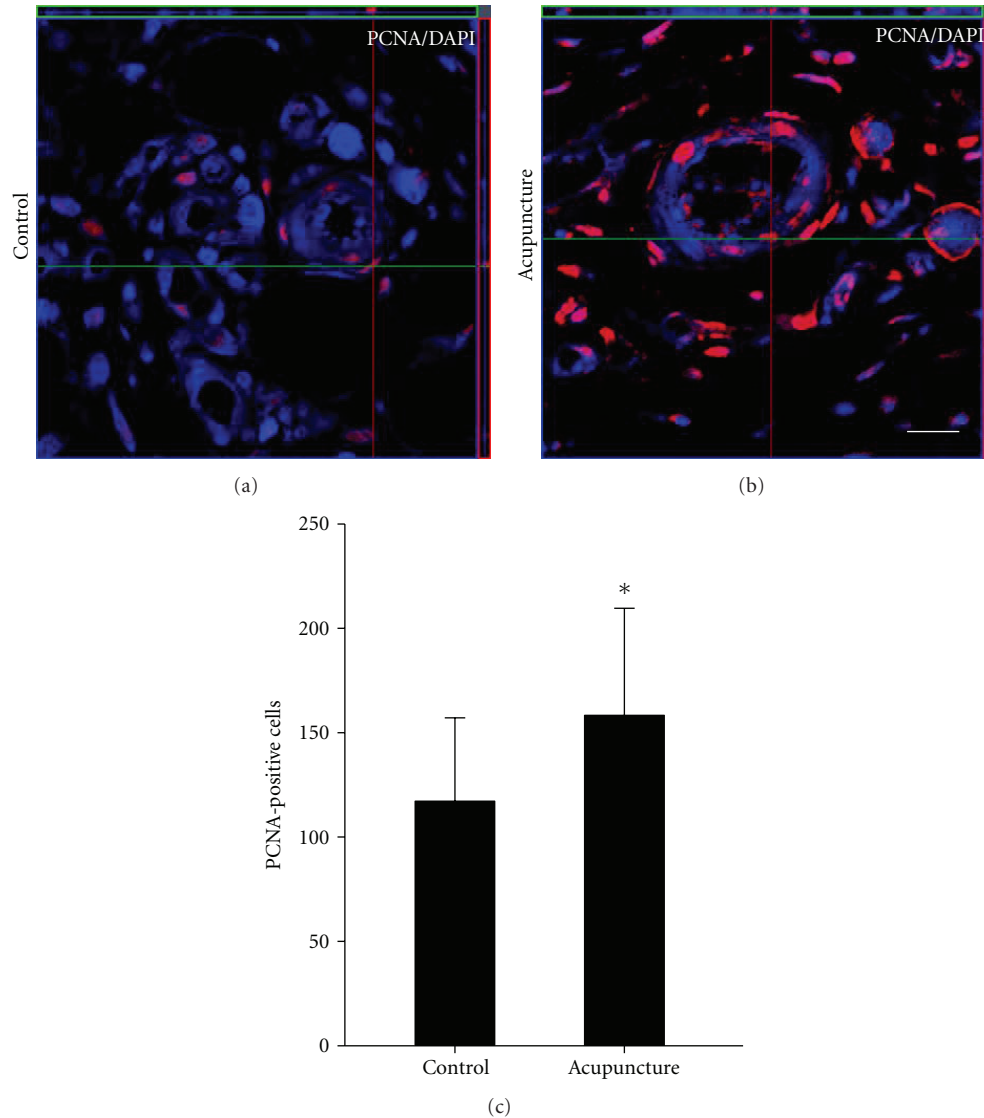


FIGURE 4: Quantitative analysis of PCNA-labeled cells in the wound area. Cell proliferation was measured by immunostaining using anti-PCNA antibody. At 7 days after-wounding, PCNA-labeled cells were present in wound area (a-b). PCNA positive cells were counted. In acupuncture-treated group, proliferation of endogenous cell was significantly increased compared to the control group (c). Data are expressed as mean \pm SD, * $P < 0.05$, Scale bars denote, 50 μm .

3.4. Angiogenesis. To investigate whether acupuncture treatment promotes angiogenesis, angiogenesis factor, and endothelial cell of newly generated cells such as VEGF and CD-31 were analyzed using the ELISA and immunostaining. The VEGF is produced by a variety of cell types during wound healing, and is a potent stimulator of proliferation and migration in endothelial cells [15–17]. The expression of VEGF was significantly increased compared to the control group at 7 days after wound (16.6 ± 0.7 versus 12.9 ± 2.9 pg/mg, $P < 0.05$) (Figure 5(h)). This suggests that acupuncture may enhance angiogenesis of newly generated cells. In acupuncture-treated group, PCNA labeled CD-31-positive cells were increased compare to the control group in the wound area (172 ± 9.6 versus 118 ± 18.2 , $P < 0.05$) (Figure 5(g)). These results suggest that the acupuncture

could effectively promote angiogenesis by increasing VEGF expression in wound model.

3.5. Epidermal Regeneration. We examine whether acupuncture could promote the induction of extracellular matrix remodeling by immunostaining for PCNA and several phenotype markers including α -SMA and collagen type I in the wound area. At the wound edge, vascular smooth muscle cells were analyzed using α -SMA antibody. The expression of α -SMA was observed at vascular smooth muscle cells of subcutaneous tissue (Figures 6(a) and 6(d)). In acupuncture-treated group at 7 days post-wounding, the PCNA labeled α -SMA-positive cells were significantly increased compared to the control (169 ± 33 versus 129 ± 26 , $P < 0.05$)

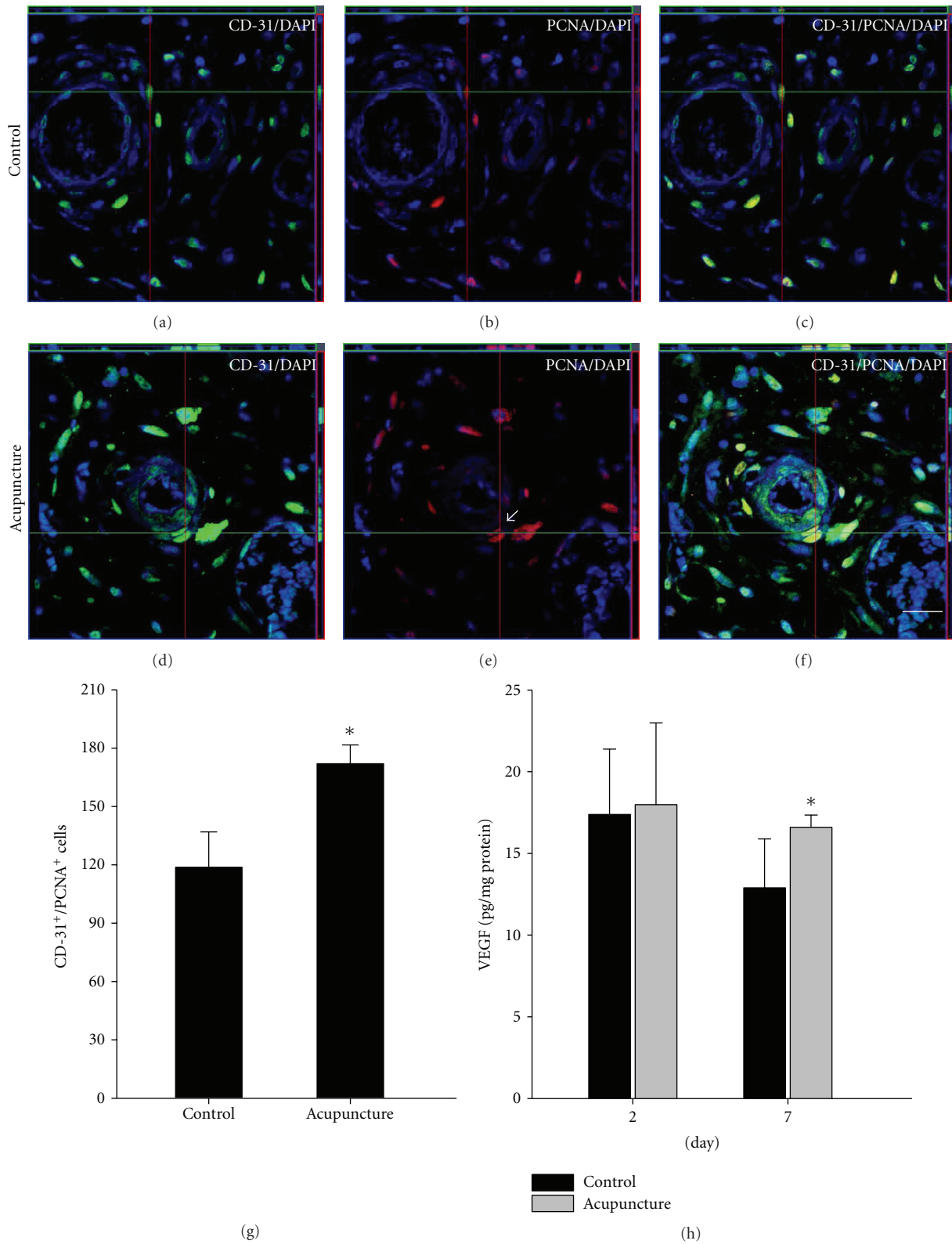


FIGURE 5: Quantitative analysis of angiogenesis by acupuncture in wound area. Histological analysis was shown into PCNA and CD-31 staining at 7 days after wound (a–f). The numbers of PCNA/CD-31-labeled cells were quantified present in wound area (g). At 7 days after-wounding, the expression of VEGF was significantly increased compared to the control group (h). Data are expressed as mean ± SD, * $P < 0.05$, Scale bars denote, 50 μm.

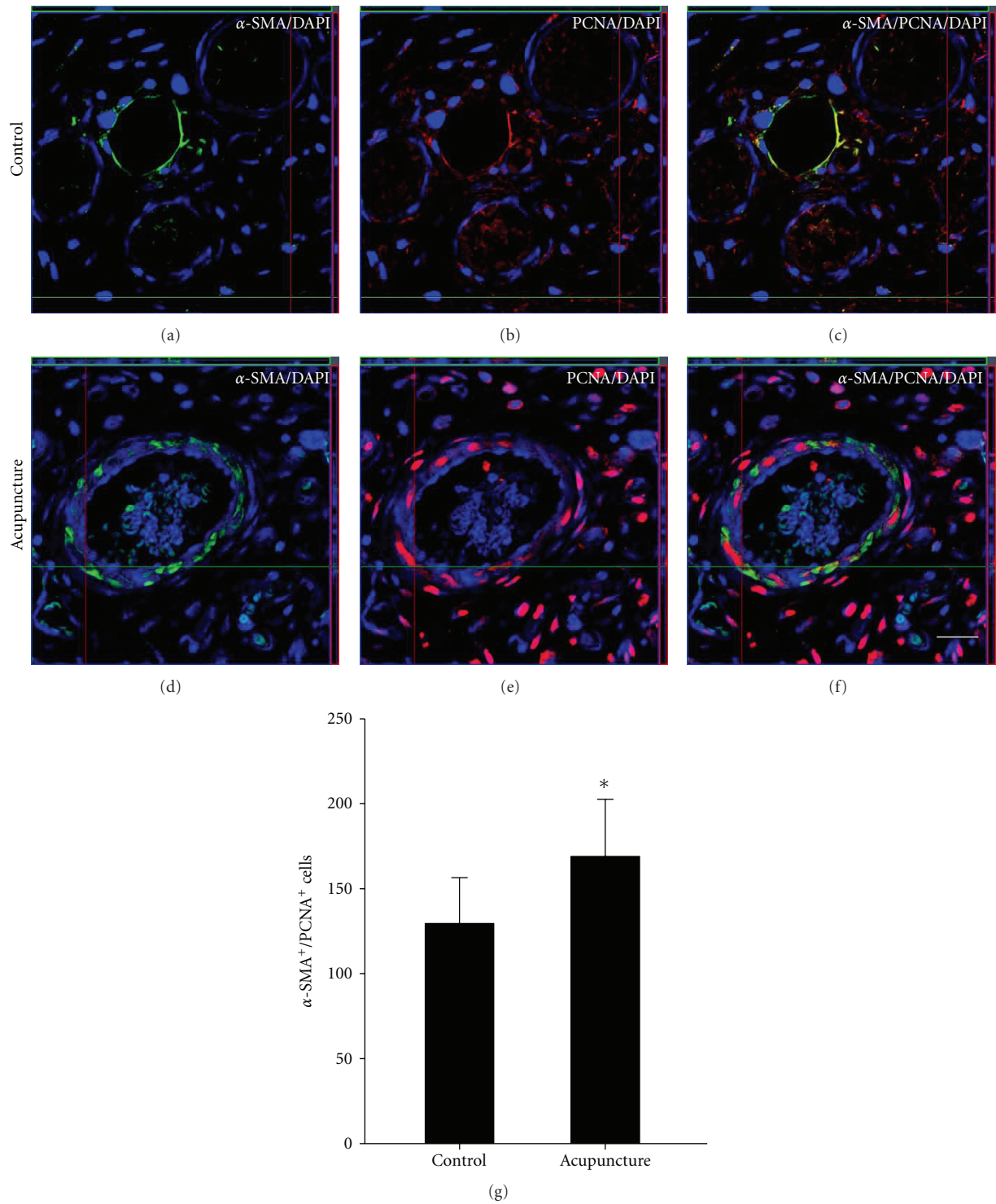


FIGURE 6: Quantitative analysis of epidermal regeneration by acupuncture in wound area. Histological analysis was shown into PCNA and α -SMA staining at 7 days after wounding (a–f). The numbers of PCNA/ α -SMA-labeled cells present were quantified in wound area (g). At 7 days after-wounding, the PCNA/ α -SMA-labeled cells were decreased compared to the control group. Data are expressed as mean \pm SD, * $P < 0.05$, Scale bars denote, 50 μ m.

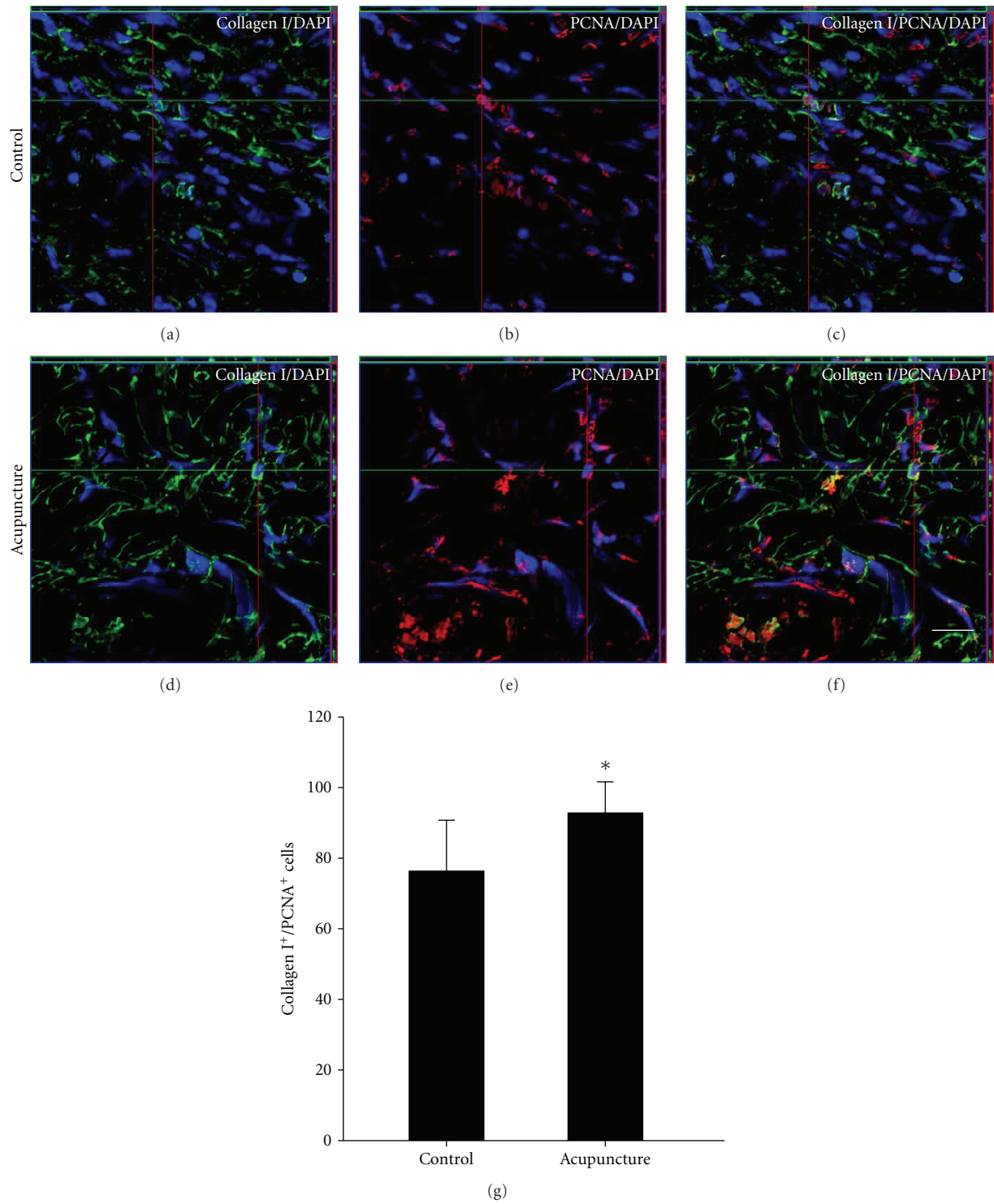


FIGURE 7: Quantitative analysis of epidermal regeneration by acupuncture in wound area. Histological analysis was shown in PCNA and collagen type I staining at 7 days after wounding (a–f). The numbers of PCNA/collagen type I-labeled cells present were quantified in wound area (g). At 7 days after-wounding, the PCNA/collagen type I-labeled cells were increased compared to the control group. Data are expressed as mean \pm SD, * $P < 0.05$, Scale bars denote, 50 μ m.

(Figure 6(g)). Also, PCNA labeled collagen type I-positive cells were significantly increased compared to the control (93 ± 8 versus 76 ± 14 , $P < 0.05$) (Figure 7). These results suggest that the acupuncture may be associated with mechanisms involved in stimulating wound healing through increasing extracellular matrix protein such as α -SMA and collagen type I.

4. Discussion

The aim of wound healing is to promote rapid wound closure and recover functional properties. In this study, we examined the effect of the acupuncture treatment on wound model such as healing of the wound area, expression of inflammatory cytokines, cell proliferation, angiogenesis, and granulation tissue formation.

Acupuncture has a long history as an Asian medical procedure that was used to treat various diseases such as inflammatory diseases, complex regional pain syndromes, and neurological diseases [18]. Previously studies reported therapeutic effect of acupuncture on Ashi-point in pain, bruise, and bone fracture disease [12–14]. Also they suggested that acupuncture could have effects on wound healing process through inhibition of inflammatory cytokines, improvement of proliferative cells, and stimulation of epidermal regeneration. Therefore, we suggest that acupuncture treatment around the edges of wound might improve healing process. In this study, we observed wound healing at 1, 3, 5, and 7 days. The acupuncture-treated group showed a more reduced compared to the control group.

Also, we analyzed in the pro-inflammatory cytokines such as TNF- α and IL-1 β in the early phases of wound healing using the ELISA. We demonstrated that the expression of TNF- α decreased in acupuncture-treated group compared to the control at 2 and 7 days. Also, the expression of IL-1 β was decreased compared to control group. These results suggest that acupuncture stimulation may have protective effects in wound model through the suppression of pro-inflammatory cytokines, which are secreted by macrophages [19, 20].

We investigated whether the acupuncture treatment could promote proliferation of newly generated cells and enhance the angiogenesis and granulation formation of newly generated cells by performing immunostaining for PCNA and several phenotype markers including CD-31, α -SMA, and collagen type I. PCNA-positive cells were counted at the edge of the wound at 7 days after wound model. In the acupuncture treated group, PCNA-positive cells were significantly increased compared to the control group. Also, we evaluated angiogenesis of newly generated cells by counting PCNA and CD-31-positive cells. PCNA-labeled CD-31 cells were increased in acupuncture group compared to the control at 7 days. Further, we observed the expression levels of VEGF at 2, and 7 days after wound model. The expression of VEGF was also increased compared to the control group at 7 days. The increase of expression of angiogenesis factors over time might be related to the acceleration of wound healing.

Granulation-tissue formation and contraction are fundamental steps during the wound healing process, which can be analyzed by observing newly generated α -SMA and collagen type I. The expression of α -SMA was observed not only at vascular smooth muscle cells of subcutaneous tissue but also at myofibroblasts around granulated area in connective tissue. Also, increase in the deposition of collagen type I, the major collagen type in skin, is consistent with a more organized and stronger repaired skin [21]. Furthermore, collagen type I play an important role guiding keratinocytes and dermal fibroblasts migration in the wounded area. In acupuncture treated group, the PCNA labeled α -SMA and collagen type I-positive cells were significantly increased compared to the control. These results suggest that acupuncture may be associated with the wound healing effect by increasing extracellular matrix proteins.

In conclusion, the result of our study suggests that acupuncture treatment around the edges of wound promotes wound healing through decreasing inflammatory cytokine release, increasing newly generated cells, and stimulating angiogenesis and granulation-tissue formation. Further studies are needed to identify the precise mechanism of action behind acupuncture.

Conflict of Interests

The authors report no conflict of interests.

Authors' Contribution

S.I. Park and Y.-Y. Sunwoo equally contributed to this work as joint first authors.

Acknowledgment

The research was supported by Grant 2012K001409 from the Converging Research Center Program through the Ministry of Education, Science, and Technology.

References

- [1] A. J. Singer and R. A. F. Clark, "Cutaneous wound healing," *New England Journal of Medicine*, vol. 341, no. 10, pp. 738–746, 1999.
- [2] G. Chodorowska and D. Roguś-Skorupska, "Cutaneous wound healing," *Annales Universitatis Mariae Curie-Skłodowska. Sectio D*, vol. 59, no. 2, pp. 403–407, 2004.
- [3] S. C. Heo, E. S. Jeon, I. H. Lee, H. S. Kim, M. B. Kim, and J. H. Kim, "Tumor necrosis factor- α -activated human adipose tissue-derived mesenchymal stem cells accelerate cutaneous wound healing through paracrine mechanisms," *Journal of Investigative Dermatology*, vol. 131, no. 7, pp. 1559–1567, 2011.
- [4] R. L. Eckert, T. Efimova, S. R. Dashti et al., "Keratinocyte survival, differentiation, and death: many roads lead to mitogen-activated protein kinase," *Journal of Investigative Dermatology Symposium Proceedings*, vol. 7, no. 1, pp. 36–40, 2002.
- [5] J. Schaubert, R. A. Dorschner, A. B. Coda et al., "Injury enhances TLR2 function and antimicrobial peptide expression through a vitamin D-dependent mechanism," *Journal of Clinical Investigation*, vol. 117, no. 3, pp. 803–811, 2007.

- [6] E. M. Conway, D. Collen, and P. Carmeliet, "Molecular mechanisms of blood vessel growth," *Cardiovascular Research*, vol. 49, no. 3, pp. 507–521, 2001.
- [7] A. Bitto, L. Minutoli, M. R. Galeano et al., "Angiopoietin-1 gene transfer improves impaired wound healing in genetically diabetic mice without increasing VEGF expression," *Clinical Science*, vol. 114, no. 11-12, pp. 707–718, 2008.
- [8] P. Bao, A. Kodra, M. Tomic-Canic, M. S. Golinko, H. P. Ehrlich, and H. Brem, "The role of vascular endothelial growth factor in wound healing," *Journal of Surgical Research*, vol. 153, no. 2, pp. 347–358, 2009.
- [9] M. Kimura, N. Shibahara, H. Hikiami et al., "Traditional Japanese formula kigikenchuto accelerates healing of pressure-loading skin ulcer in rats," *Evidence-Based Complementary and Alternative Medicine*, vol. 2011, Article ID 592791, 13 pages, 2011.
- [10] M. S. Park, Y. Y. Sunwoo, K. S. Jang et al., "Changes in brain FDG metabolism induced by acupuncture in healthy volunteers," *Acta Radiologica*, vol. 51, no. 8, pp. 947–952, 2010.
- [11] M. Braddock, C. J. Campbell, and D. Zuder, "Current therapies for wound healing: electrical stimulation, biological therapeutics, and the potential for gene therapy," *International Journal of Dermatology*, vol. 38, no. 11, pp. 808–817, 1999.
- [12] Z. H. Sun and C. X. Feng, "The clinical observation on acupuncture at Xuanzhong (GB 39) and Ashi points for treatment of orthopedic postoperative pain," *Zhongguo Zhen Jiu*, vol. 27, no. 12, pp. 895–897, 2007.
- [13] J. A. Lee, H. J. Jeong, H. J. Park, S. Jeon, and S. U. Hong, "Acupuncture accelerates wound healing in burn-injured mice," *Burns*, vol. 37, no. 1, pp. 117–125, 2011.
- [14] M. Nakajima, M. Inoue, T. Hojo et al., "Effect of electroacupuncture on the healing process of tibia fracture in a rat model: a randomised controlled trial," *Acupuncture in Medicine*, vol. 28, no. 3, pp. 140–143, 2010.
- [15] E. Kiwanuka, J. Junker, and E. Eriksson, "Harnessing growth factors to influence wound healing," *Clinics in Plastic Surgery*, vol. 39, no. 3, pp. 239–248, 2012.
- [16] N. N. Nissen, P. J. Polverini, A. E. Koch, M. V. Volin, R. L. Gamelli, and L. A. DiPietro, "Vascular endothelial growth factor mediates angiogenic activity during the proliferative phase of wound healing," *American Journal of Pathology*, vol. 152, no. 6, pp. 1445–1452, 1998.
- [17] M. Gaudry, O. Br gerie, V. Andrieu, J. El Benna, M. A. Poci-dalo, and J. Hakim, "Intracellular pool of vascular endothelial growth factor in human neutrophils," *Blood*, vol. 90, no. 10, pp. 4153–4161, 1997.
- [18] F. J. Zijlstra, I. van den Berg-de Lange, F. J. P. M. Huygen, and J. Klein, "Anti-inflammatory actions of acupuncture," *Mediators of Inflammation*, vol. 12, no. 2, pp. 59–69, 2003.
- [19] E. Aoki, T. Kasahara, H. Hagiwara, M. Sunaga, N. Hisamitsu, and T. Hisamitsu, "Electroacupuncture and moxibustion influence the lipopolysaccharide-induced TNF- α production by macrophages," *In Vivo*, vol. 19, no. 3, pp. 495–500, 2005.
- [20] C. C. Finnerty, D. N. Herndon, R. Przkora et al., "Cytokine expression profile over time in severely burned pediatric patients," *Shock*, vol. 26, no. 1, pp. 13–19, 2006.
- [21] E. M. C. Sant'Ana, C. M. C. P. Gouv a, J. L. Q. Durigan, M. R. Cominetti, E. R. Pimentel, and H. S. Selistre-de-Ara jo, "Rat skin wound healing induced by alternagin-C, a disintegrin-like, Cys-rich protein from *Bothrops alternatus* venom," *International Wound Journal*, vol. 8, no. 3, pp. 245–252, 2011.

Review Article

Auricular Acupuncture and Vagal Regulation

Wei He, Xiaoyu Wang, Hong Shi, Hongyan Shang, Liang Li, Xianghong Jing, and Bing Zhu

Institute of Acupuncture and Moxibustion, China Academy of Chinese Medical Sciences, Beijing 100700, China

Correspondence should be addressed to Xianghong Jing, xianghongjing@hotmail.com and Bing Zhu, zhubing@mail.cintcm.ac.cn

Received 30 September 2012; Accepted 2 November 2012

Academic Editor: Di Zhang

Copyright © 2012 Wei He et al. This is an open access article distributed under the Creative Commons Attribution License, which permits unrestricted use, distribution, and reproduction in any medium, provided the original work is properly cited.

Auricular acupuncture has been utilized in the treatment of diseases for thousands of years. Dr. Paul Nogier firstly originated the concept of an inverted fetus map on the external ear. In the present study, the relationship between the auricular acupuncture and the vagal regulation has been reviewed. It has been shown that auricular acupuncture plays a role in vagal activity of autonomic functions of cardiovascular, respiratory, and gastrointestinal systems. Mechanism studies suggested that afferent projections from especially the auricular branch of the vagus nerve (ABVN) to the nucleus of the solitary tract (NTS) form the anatomical basis for the vagal regulation of auricular acupuncture. Therefore, we proposed the “auriculovagal afferent pathway” (AVAP): both the autonomic and the central nervous system could be modified by auricular vagal stimulation via projections from the ABVN to the NTS. Auricular acupuncture is also proposed to prevent neurodegenerative diseases via vagal regulation. There is a controversy on the specificity and the efficacy of auricular acupoints for treating diseases. More clinical RCT trials on auricular acupuncture and experimental studies on the mechanism of auricular acupuncture should be further investigated.

1. The History of Auricular Acupuncture

Acupuncture is a part of traditional Chinese medicine (TCM). It has been accepted in China and has been used as one of the alternative and complementary treatments in western countries. Auricular acupuncture has been also used in the treatment of diseases for thousands of years. In the classic TCM text of Huang Di Nei Jing, which was compiled in around 500 B.C, the correlation between the auricle and the body had been described; all six Yang meridians were directly connected to the auricle, whereas the six Yin meridians were indirectly connected to the ear by their corresponding yang meridian, respectively [1]. In Hippocrates' time, around 450 BC, bleeding points on the posterior (mastoid) surface of the ear were used to facilitate ejaculation, reduce impotency problem, and treat leg pain [2]. It was also reported that the auricle was associated with emotion [2]. During Renaissance sporadic trading between China and Europe made it possible to introduce needles, moxa, and cauterization of the external ear or cutting the veins behind the ears for relieving diseases in Europe [3]. In 1957, Dr. Paul Nogier, a physician in France, firstly originated the concept of an inverted fetus map on the external ear [2]. He proposed the concept after visiting a folk doctor, who

cauterized the very small auricular area “sciatic point” of the patients for the treatment of sciatica. The folk doctor learned this technique from a Chinese who resided in Marseilles [3].

Nogier presented his discovery in several congresses and published it in an international circulation journal, which eventually led to the widespread acceptance of his approach. With some exceptions, the Chinese charts were very similar to Nogier's originals [4].

2. Auricular Acupuncture for Vagal Regulation

The autonomic nervous system (ANS), which plays a crucial role in the maintenance of homeostasis, is mainly composed of two anatomically and functionally distinct divisions: the sympathetic system and the parasympathetic system. In terms of the influence of the parasympathetic system, the physiological significance of the vagus nerve is clearly illustrated by its widespread distribution [5]. It controls the activity of the cardiovascular, respiratory, and gastrointestinal systems and has effects on smooth muscles, blood vessels, sweat glands, and the endocrine system. Numerous investigations showed that vagal tone was elicited by auricular acupuncture or auricular acupressure [6–8]. It is

described as a reflexive treatment of physical, emotional, and neurological dysfunctions via specific zones on the ear where these dysfunctions are reflected [9].

2.1. Cardiovascular Regulation. Cardiac vagal postganglionic fiber endings release acetylcholine, which are bound with cholinergic M receptors on the myocardial cell membrane or vascular smooth muscle. Activation of the vagus nerve typically leads to a reduction in heart rate and blood pressure. Cardiovascular vagal regulations by auricular acupuncture have been investigated in clinical trials and animal experiments [6, 10–18]. In elite basketball athletes, the value of heart rate decreased at 30th and 60th minutes postexercise in auricular acupuncture group compared with that in normal control group [6]. In fourteen healthy men, auricular electrical acupuncture stimulation was found to have a positive effect on respiratory sinus arrhythmia adjusted for tidal volume, which indicated an increase in vagal activity [10]. The systolic pressure and diastolic pressure in 20 cases of hypertension rabbits were decreased by ear electroacupuncture inserting at the “Er Jian” (HX_{6,7i}) point [11]. Acupuncture at “shenmen” (TF4) slowed down the heart rate and activated the parasympathetic nerves [12].

Several investigations had focused on the relationship between auricular acupoint “Heart” (CO₁₅) and cardiovascular regulation. In healthy volunteers, a significant decrease in heart rate and a significant increase in heart rate variability after manual ear acupressure at auricular acupoint CO₁₅ have been shown [13]. In anesthetized Sprague Dawley rats, acupuncture at auricular point “Heart” showed a more significant inhibitory effect on arterial pressure and heart rate than acupuncture at acupoints Zusanli (ST36) and Neiguan (PC6) [14]. Decrease in blood pressure and a small bradycardia had been induced by auricular acupuncture at different points in rats [8]. A significant increase in total heart rate variability was found after auricular acupuncture at the ear point CO₁₅ [15]. In addition, mean blood flow velocity of the ophthalmic artery was significantly increased during needling vision-related acupoints of auricular acupuncture, which may be induced by parasympathetic tone [16]. In 30 cases of vascular hypertensive patients, it was found that acupuncture at acupoint CO₁₅ produced marked short-term and long-term depressor effect as well as evident immediate effects on cardiac functional activities in grade II and grade III hypertension and marked effects on angiotensin II in grade III hypertension [17].

After receiving 4-week-treatment of auricular acupuncture therapy, a greater percentage change in Pittsburgh sleep quality index was moderately correlated with both a lower percentage change in high frequency power of heart rate variability (HRV) and a greater percentage change in normalized low frequency power of HRV, thus, it suggested that auricular acupuncture intervention led to more cardiac parasympathetic and less cardiac sympathetic activities, which contributed to the improvement of postmenopausal insomnia [18].

2.2. Respiratory Regulation. In a controlled single-blind study, a significant decrease in the olfactory recognition

threshold by auricular acupuncture at the auricular “Lung” point was found in 23 healthy volunteers [7]. Bilateral stimulation of auricular acupoint TF₄ combined with other acupoints of Daimai (GB26), ST36, and Sanyinjiao (SP6) resulted in a net increase in vital capacity during the period of acupuncture analgesia which lasted for 3 to 4 hours after stimulation [19]. In fourteen healthy men, auricular electrical acupuncture stimulation was found to have a positive effect on respiratory sinus arrhythmia adjusted for tidal volume, which indicated an increase in vagal activity [10].

2.3. Gastrointestinal Regulation. Increase in intragastric pressure has been induced by auricular acupuncture in rats [8]. By comparison of the width of corpus and antrum of the stomach, as well as duodenum before and after the application of auricular acupuncture in 60 patients, the results showed that the effects of auricular acupuncture and usual drugs on the motility and tone of gastrointestinal tract were equal [20]. In order to relieve the abdominal distension and other discomforts due to gastrointestinal dysfunction after abdominal operations, the patients were treated by auricular-plaster therapy plus acupuncture at ST36. The results indicated that auricular-plaster therapy plus acupuncture at ST36 may promote postoperative recovery of the intestinal function [21].

3. Mechanisms of Auricular Acupuncture for Vagal Regulation

3.1. The Nerve Supply of the Auricle. The auricle is innervated by cranial nerves and spinal nerves. Innervations of at least four nerves supply the anterior auricle: the auriculotemporal nerve, the auricular branch of the vagus nerve (ABVN), the lesser occipital nerve, and the greater auricular nerve. The auriculotemporal nerve is a mandibular branch of the trigeminal nerve, which mainly supplies the anterosuperior and anteromedial areas of the external ear. The auricular branch of the vagus nerve, which is the only peripheral branch of the vagus nerve, mainly supplies the auricular concha and most of the area around the auditory meatus. The lesser occipital nerve mainly innervates the skin of the upper and back parts of the auricular. The greater auricular nerve (GAN) from the cervical plexus supplies both surfaces of the lower parts of the auricle. The innervation of the auricle is characterized by a great deal of overlap between multiple nerves [22] (see Figure 1).

3.2. Auriculovagal Relation. Both Chinese and Western researchers have recognized the relationship between the auricle and vagal regulation. Arnold’s reflex was first described in 1832 by Friedrich Arnold, professor of anatomy at Heidelberg University in Germany. It is one of the somato-parasympathetic reflexes. Physical stimulation of the external acoustic meatus innervated by the ABVN elicits a cough much like the other cough reflexes induced by vagal tone. There were also clinic reports on vagal tone responses such as cardiac deceleration and even asystole



FIGURE 1: The innervations of the external auricle. The innervations of the auricular branch of the vagus nerve are marked by green color. The innervations of the auriculotemporal nerve are marked by red color. The innervations of the lesser occipital nerve are marked by blue color. The innervations of the greater auricular nerve are marked by yellow color.

and depressor response, induced by stimulations including cerumen crumming in auditory canal or auricular concha [23, 24]. Engel [25] groups together eight reflexes including gastroauricular phenomenon in man, auricular phenomenon in man, pulmoauricular phenomenon in man, auriculogenital reflex in cat, auriculouterine reflex in women, oculocardiac reflex in man, Kalchschmidt's reflex in cattle, and coughing attack with heartburn in man. According to the national standards of the location of auricular acupoints [26], auricular acupoints treating visceral diseases are mainly located at auricular concha (see Figure 2). Perhaps the ABVN forms a connection between the auricle and the autonomic regulations.

3.3. Relationship between the ABVN and the Nucleus of the Solitary Tract. The anatomical relationship between the ABVN and the nucleus of the solitary tract (NTS) has been investigated. After applying horseradish peroxidase (HRP) to the central cut end of the ABVN in the cat, some labeled neuronal terminals were seen in the interstitial, dorsal, dorsolateral, and commissural subnuclei of the NTS; some of these terminals may be connected monosynaptically with solitary nucleus neurons which send their axons to visceromotor centers in the brainstem [27].

The auricular concha is mainly innervated by the ABVN. The relationship between the acupuncture stimulation at auricular concha and the NTS has also been investigated. In an animal study, acupuncture stimulation at auricular concha induced the hypoglycemic effect by activating the firing activities of the neurons in NTS [28]. It is also found that acupuncture-like stimulation at auricular acupoint CO₁₅ activates the cardiac-related neurons in the NTS to

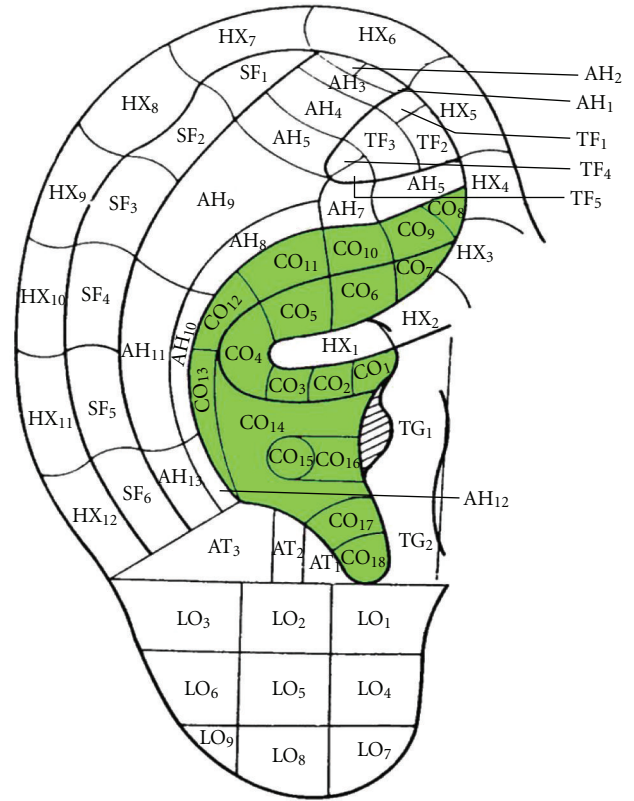


FIGURE 2: Auricular acupoints treating visceral diseases are mainly located at auricular concha.

evoke cardiovascular inhibition, whereas the inactivation of the NTS with local anesthetics decreased the cardiovascular inhibitory responses evoked by auricular acupuncture [14].

Recently, it is suggested to assess the function of the vagus nerve through transcutaneous electric stimulation of the ABVN innervating parts of the ear. The 8 mA stimulation was performed at five different electrode positions at the subject's right ear. A clear, reproducible vagus sensory evoked potential (VSEP) was recorded after stimulation at the inner side of the tragus of the right ear, instead of the other stimulation positions at the lobulus auriculæ, the scapha, thecus antihelices superior, and the top of the helix. It is considered that cutaneous stimuli of this region are transported via the auricular nerve to the jugular ganglion and from there with the vagus nerve into the medulla oblongata and to the NTS [29]. Although other regions of the auricle might be innervated by a small amount of innervation of the ABVN, the inner side of the tragus is a large amount of innervation the ABVN to mediate the VSEP.

3.4. Extensive Connections between the NTS with Visceral Organs and Other Brain Structures. The NTS in the brainstem carries and receives visceral primary afferent signals from a variety of visceral regions and organs. Neurons that synapse in the NTS participate into the autonomic reflexes, with a result to regulate the autonomic function. Outputs that go from the NTS are transferred to a large number

of other regions of the brain including the paraventricular nucleus of the hypothalamus and the central nucleus of the amygdala as well as to other nuclei in the brainstem (such as the parabrachial area and other visceral motor or respiratory networks). Perhaps, extensive connections between the NTS with visceral organs and other brain structures [30] may elucidate the mechanism of auricular acupuncture.

Therefore, we proposed the “auriculovagal afferent pathway” (AVAP); both the autonomic and the central nervous system could be modified by auricular vagal stimulation via projections from the ABVN to the NTS (see Figure 3).

4. Prevention and Treatment of Diseases via Vagal Regulation of Auricular Acupuncture

The nuclei of the vagus nerve in the brainstem have been implicated as one of the earliest regions in the pathophysiological process of both Alzheimer’s and Parkinson’s diseases. Far-field potentials from brainstem after transcutaneous vagus nerve stimulation at the auricle have been utilized as a noninvasive method in the early diagnosis of neurodegenerative disorders [31–33]. We suggest that further study is needed on whether auricular acupuncture plays a role in the prevention and treatment of these neurodegenerative disorders via activating the vagal nuclei in the brainstem.

Vagus nerve stimulation has been approved by FDA as an alternative treatment for neuropsychiatric diseases such as epilepsy and depression. In order to avoid the disadvantages of cervical vagus nerve stimulation, less invasive methods including transcutaneous vagus nerve stimulation [34–36] and electrical auricula-vagus stimulation [37] to stimulate vagal afferences have been proposed. In a pilot study, an overall reduction of seizure frequency was observed in five of seven patients after 9 months of electrical stimulation of the ABVN. It is also found that the electrical stimulation of the ABVN is safe and well tolerated [38]. As a complementary method, it is also proposed that auricular acupuncture may suppress epileptic seizures via activating the parasympathetic nervous system [39–41].

5. Complications on Auricular Acupuncture

5.1. Controversy on Specificity of Auricular Acupoint. Several studies investigated the specificity of auricular acupoints. Parts of the studies agree on the concept that specific areas of the ear are related to specific areas of the body. Acupuncture at CO₁₅, but not Stomach (CO₄), produced depressor effect on vascular hypertension [17, 42]. Specificity of auricular acupoint is also identified by two quantified examinations of the electrical properties [43, 44].

There is still disagreement on the specificity of auricular acupoint. Similar patterns of cardiovascular and gastric responses could be evoked by stimulation at different areas of the auricle, which do not support the theory of a highly specific functional map in the ear [8]. Auricular acupuncture appears to be effective for smoking cessation, but the effect may not depend on point location [45].

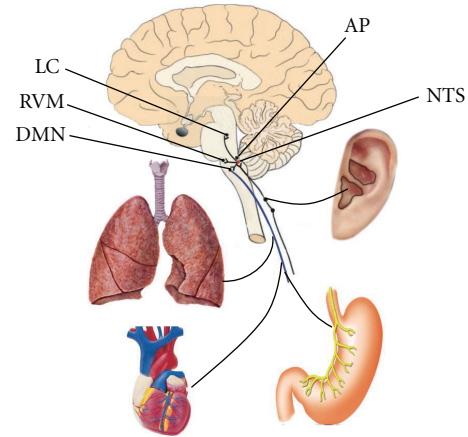


FIGURE 3: “Auriculovagal afferent pathway” (AVAP): both the autonomic and the central nervous system could be modified by auricular vagal stimulation via projections from the ABVN at the auricular concha to the NTS (see Figure 3). NTS: nucleus of the solitary tract; DMN: dorsal motor nucleus of the vagus; AP: area postrema; RVM: rostral ventrolateral medulla; LC: locus coeruleus.

5.2. Inconsistent Results on the Study of Auricular Acupuncture.

There are inconsistent study results related to the treatment effects of auricular acupuncture, which may be related to trial designing, clinical observation measures, the set of sham acupuncture, and statistical analyses [46–48]. In clinical studies, most studies on the clinical observation of auricular acupuncture were not sufficiently convincing. More RCT evaluations of effect of auricular acupuncture should be performed to obtain objective and consistent results. Besides, there are almost 200 auricular acupoints in each ear that represent all parts of the body and many functional areas. It is not easy to locate the acupoint accurately. Therefore, in a clinical trial, the acupuncture operator should be trained well. In experimental studies, anatomical and morphological studies on auricular acupoints and neuroimaging study such as fMRI on the effect of auricular acupuncture should be encouraged to investigate the mechanism of auricular acupuncture.

Conflict of Interests

It should be understood that none of the authors has any financial or scientific conflict of interests with regard to the research described in this paper.

Acknowledgments

This work was supported by National Basic Research Program (973 Program, no. 2011CB505201), Beijing Natural Science Foundation (no. 7102120), and National Natural Science Foundation of China Research Grants (no. 30901931). The authors are grateful to Dr. Jianghui Li for her reading of the paper.

References

- [1] H. Yang, "A brief analysis on the treatise of ears in Huangdi Neijing," *Zhejiang Journal of Traditional Chinese Medicine*, vol. 44, no. 1, pp. 14–15, 2009.
- [2] P. Nogier, *From Auriculotherapy to Auriculomedicine*, Maisonneuve, Sainte-Ruffine, France, 1981.
- [3] L. Gori and F. Firenzuoli, "Ear acupuncture in European traditional medicine," *Evidence-Based Complementary and Alternative Medicine*, vol. 4, supplement 1, pp. 13–16, 2007.
- [4] J. Chalmers, "Modern auricular therapy: a brief history and the discovery of the vascular autonomic signal," *Journal of Chinese Medicine*, no. 84, pp. 5–8, 2007.
- [5] L. K. McCorry, "Physiology of the autonomic nervous system," *American Journal of Pharmaceutical Education*, vol. 71, no. 4, article 78, 2007.
- [6] Z. P. Lin, Y. H. Chen, C. Fan, H. J. Wu, L. W. Lan, and J. G. Lin, "Effects of auricular acupuncture on heart rate, oxygen consumption and blood lactic acid for elite basketball athletes," *The American Journal of Chinese Medicine*, vol. 39, no. 6, pp. 1131–1138, 2011.
- [7] O. Tanaka and Y. Mukaino, "The effect of auricular acupuncture on olfactory acuity," *American Journal of Chinese Medicine*, vol. 27, no. 1, pp. 19–24, 1999.
- [8] X. Y. Gao, S. P. Zhang, B. Zhu, and H. Q. Zhang, "Investigation of specificity of auricular acupuncture points in regulation of autonomic function in anesthetized rats," *Autonomic Neuroscience*, vol. 138, no. 1–2, pp. 50–56, 2008.
- [9] T. Oleson, "Auriculotherapy stimulation for neuro-rehabilitation," *NeuroRehabilitation*, vol. 17, no. 1, pp. 49–62, 2002.
- [10] R. La Marca, M. Nedeljkovic, L. Yuan, A. Maercker, and U. Ehlert, "Effects of auricular electrical stimulation on vagal activity in healthy men: evidence from a three-armed randomized trial," *Clinical Science*, vol. 118, no. 8, pp. 537–546, 2010.
- [11] F. Xu, X. Liu, Z. Liu, J. Chen, and B. Dong, "The role of ear electroacupuncture on arterial pressure and respiration during asphyxia in rabbits," *Zhen Ci Yan Jiu*, vol. 17, no. 1, pp. 36–32, 1992.
- [12] C. C. Hsu, C. S. Weng, M. F. Sun, L. Y. Shyu, W. C. Hu, and Y. H. Chang, "Evaluation of scalp and auricular acupuncture on EEG, HRV, and PRV," *American Journal of Chinese Medicine*, vol. 35, no. 2, pp. 219–230, 2007.
- [13] X. Y. Gao, L. Wang, I. Gaischek, Y. Michenthaler, B. Zhu, and G. Litscher, "Brain-modulated effects of auricular acupressure on the regulation of autonomic function in healthy volunteers," *Evidence-Based Complementary and Alternative Medicine*, vol. 2012, Article ID 714391, 8 pages, 2012.
- [14] X. Y. Gao, Y. H. Li, K. Liu et al., "Acupuncture-like stimulation at auricular point heart evokes cardiovascular inhibition via activating the cardiac-related neurons in the nucleus tractus solitarius," *Brain Research*, vol. 1397, pp. 19–27, 2011.
- [15] X. Y. Gao, K. Liu, B. Zhu, and G. Litscher, "Sino-European transcontinental basic and clinical high-tech acupuncture studies-part I: auricular acupuncture increases heart rate variability in anesthetized rats," *Evidence-Based Complementary and Alternative Medicine*, vol. 2012, Article ID 817378, 5 pages, 2012.
- [16] G. Litscher, "Computer-based quantification of traditional Chinese-, ear- and Korean hand acupuncture: needle-induced changes of regional cerebral blood flow velocity," *Neurological Research*, vol. 24, no. 4, pp. 377–380, 2002.
- [17] H. Huang and S. Liang, "Acupuncture at otoacupoint heart for treatment of vascular hypertension," *Journal of Traditional Chinese Medicine*, vol. 12, no. 2, pp. 133–136, 1992.
- [18] Y. Y. Kung, C. C. H. Yang, J. H. Chiu, and T. B. J. Kuo, "The relationship of subjective sleep quality and cardiac autonomic nervous system in postmenopausal women with insomnia under auricular acupressure," *Menopause*, vol. 18, no. 6, pp. 638–645, 2011.
- [19] E. Facco, G. Manani, A. Angel et al., "Comparison study between acupuncture and pentazocine analgesic and respiratory post-operative effects," *American Journal of Chinese Medicine*, vol. 9, no. 3, pp. 225–235, 1981.
- [20] S. Borozan and G. Petković, "Ear acupuncture has a hypotonic effect on the gastrointestinal tract," *Vojnosanitetski Pregled*, vol. 53, no. 1, pp. 31–33, 1996.
- [21] Q. Wan, "Auricular-plaster therapy plus acupuncture at zusanli for postoperative recovery of intestinal function," *Journal of Traditional Chinese Medicine*, vol. 20, no. 2, pp. 134–135, 2000.
- [22] N. Ueno, H. Sudo, Y. Hattori, K. Yuge, T. Miyaki, and H. Ito, "Innervation of the external ear in humans and the musk shrew," *Nihon Jibiinkoka Gakkai Kaiho*, vol. 96, no. 2, pp. 212–218, 1993.
- [23] D. Gupta, S. Verma, and S. K. Vishwakarma, "Anatomic basis of Arnold's ear-cough reflex," *Surgical and Radiologic Anatomy*, vol. 8, no. 4, pp. 217–220, 1986.
- [24] A. Thakar, K. K. Deepak, and S. S. Kumar, "Auricular syncope," *Journal of Laryngology and Otolaryngology*, vol. 122, no. 10, pp. 1115–1117, 2008.
- [25] D. Engel, "The gastroauricular phenomenon and related vagus reflexes," *Archiv fur Psychiatrie und Nervenkrankheiten*, vol. 227, no. 3, pp. 271–277, 1979.
- [26] L. Q. Zhou and B. X. Zhao, *Nomenclature and Location of Auricular Points*, Standard Publishing House, Beijing, China, 1st edition, 2008.
- [27] S. Nomura and N. Mizuno, "Central distribution of primary afferent fibers in the Arnold's nerve (the auricular branch of the vagus nerve): a transganglionic HRP study in the cat," *Brain Research*, vol. 292, no. 2, pp. 199–205, 1984.
- [28] Z. G. Mei, B. Zhu, Y. H. Li, P. J. Rong, H. Ben, and L. Li, "Responses of glucose-sensitive neurons and insulin-sensitive neurons in nucleus tractus solitarius to electroacupuncture at auricular concha in rats," *Zhongguo Zhen Jiu*, vol. 27, no. 12, pp. 917–922, 2007.
- [29] A. J. Fallgatter, B. Neuhauser, M. J. Herrmann et al., "Far field potentials from the brain stem after transcutaneous vagus nerve stimulation," *Journal of Neural Transmission*, vol. 110, no. 12, pp. 1437–1443, 2003.
- [30] T. R. Henry, "Therapeutic mechanisms of vagus nerve stimulation," *Neurology*, vol. 59, no. 6, supplement 4, pp. S3–S14, 2002.
- [31] T. Polak, F. Markulin, A. C. Ehlis, J. B. M. Langer, T. M. Ringel, and A. J. Fallgatter, "Far field potentials from brain stem after transcutaneous Vagus nerve stimulation: optimization of stimulation and recording parameters," *Journal of Neural Transmission*, vol. 116, no. 10, pp. 1237–1242, 2009.
- [32] A. J. Fallgatter, A. C. Ehlis, T. M. Ringel, and M. J. Herrmann, "Age effect on far field potentials from the brain stem after transcutaneous vagus nerve stimulation," *International Journal of Psychophysiology*, vol. 56, no. 1, pp. 37–43, 2005.
- [33] F. G. Metzger, T. Polak, Y. Aghazadeh, A. C. Ehlis, K. Hagen, and A. J. Fallgatter, "Vagus somatosensory evoked potentials—a possibility for diagnostic improvement in patients with

- mild cognitive impairment?" *Dementia and Geriatric Cognitive Disorders*, vol. 33, no. 5, pp. 289–296, 2005.
- [34] T. Kraus, K. Hösl, O. Kiess, A. Schanze, J. Kornhuber, and C. Forster, "BOLD fMRI deactivation of limbic and temporal brain structures and mood enhancing effect by transcutaneous vagus nerve stimulation," *Journal of Neural Transmission*, vol. 114, no. 11, pp. 1485–1493, 2007.
- [35] S. Dietrich, J. Smith, C. Scherzinger et al., "A novel transcutaneous vagus nerve stimulation leads to brainstem and cerebral activations measured by functional MRI," *Biomedizinische Technik*, vol. 53, no. 3, pp. 104–111, 2008.
- [36] E. C. G. Ventureyra, "Transcutaneous vagus nerve stimulation for partial onset seizure therapy. A new concept," *Child's Nervous System*, vol. 16, no. 2, pp. 101–102, 2000.
- [37] A. C. Yang, J. G. Zhang, P. J. Rong, H. G. Liu, N. Chen, and B. Zhu, "A new choice for the treatment of epilepsy: electrical auricula-vagus-stimulation," *Medical Hypotheses*, vol. 77, no. 2, pp. 244–245, 2011.
- [38] H. Stefan, G. Kreiselmeyer, F. Kerling et al., "Transcutaneous vagus nerve stimulation (t-VNS) in pharmacoresistant epilepsies: a proof of concept trial," *Epilepsia*, vol. 53, no. 7, pp. 115–118, 2012.
- [39] W. He, P. J. Rong, L. Li, H. Ben, B. Zhu, and G. Litscher, "Auricular acupuncture may suppress epileptic seizures via activating the parasympathetic nervous system: a hypothesis based on innovative methods," *Evidence-Based Complementary and Alternative Medicine*, vol. 2012, Article ID 615476, 5 pages, 2012.
- [40] W. He, Y. H. Li, P. J. Rong, L. Li, H. Ben, and B. Zhu, "Effect of electroacupuncture of different regions of the auricle on epileptic seizures in epilepsy rats," *Zhen Ci Yan Jiu*, vol. 36, no. 6, pp. 414–418, 2011.
- [41] W. He, C. L. Zhao, Y. H. Li et al., "Effect of electroacupuncture at auricular concha on behaviors and electroencephalogram in epileptic rats," *Chinese Journal of Pathophysiology*, vol. 12, no. 10, pp. 1913–1916, 2011.
- [42] H. Q. Huang and S. Z. Liang, "Improvement of blood pressure and left cardiac function in patients with hypertension by auricular acupuncture," *Zhong Xi Yi Jie He Za Zhi*, vol. 11, no. 11, pp. 654–656, 1991.
- [43] T. D. Oleson, R. J. Kroening, and D. E. Bresler, "An experimental evaluation of auricular diagnosis: the somatotopic mapping of musculoskeletal pain at ear acupuncture points," *Pain*, vol. 8, no. 2, pp. 217–229, 1980.
- [44] K. Saku, Y. Mukaino, H. Ying, and K. Arakawa, "Characteristics of reactive electropermeable points on the auricles of coronary heart disease patients," *Clinical Cardiology*, vol. 16, no. 5, pp. 415–419, 1993.
- [45] A. White and R. Moody, "The effects of auricular acupuncture on smoking cessation may not depend on the point chosen—an exploratory meta-analysis," *Acupuncture in Medicine*, vol. 24, no. 4, pp. 149–156, 2006.
- [46] M. S. Lee, B. C. Shin, L. K. P. Suen, T. Y. Park, and E. Ernst, "Auricular acupuncture for insomnia: a systematic review," *International Journal of Clinical Practice*, vol. 62, no. 11, pp. 1744–1752, 2008.
- [47] K. Pilkington, G. Kirkwood, H. Rampes, M. Cummings, and J. Richardson, "Acupuncture for anxiety and anxiety disorders—a systematic literature review," *Acupuncture in Medicine*, vol. 25, no. 1-2, pp. 1–10, 2007.
- [48] A. R. White, R. C. Moody, and J. L. Campbell, "Acupressure for smoking cessation—a pilot study," *BMC Complementary and Alternative Medicine*, vol. 7, article 8, 2007.

Research Article

Hemodynamic Changes in the Brachial Artery Induced by Acupuncture Stimulation on the Lower Limbs: A Single-Blind Randomized Controlled Trial

Masashi Watanabe, Shin Takayama, Atsushi Hirano, Takashi Seki, and Nobuo Yaegashi

Department of Traditional Asian Medicine, Graduate School of Medicine, Tohoku University, Sendai 980-8575, Japan

Correspondence should be addressed to Takashi Seki, tseki.tohoku@gmail.com

Received 9 August 2012; Revised 16 October 2012; Accepted 30 October 2012

Academic Editor: Wolfgang Schwarz

Copyright © 2012 Masashi Watanabe et al. This is an open access article distributed under the Creative Commons Attribution License, which permits unrestricted use, distribution, and reproduction in any medium, provided the original work is properly cited.

Acupuncture is commonly performed at acupoints. No comparisons of quantitative physiological alterations in the brachial artery (BA) induced by the stimulation of different acupoints in the lower limbs have been performed in humans. Therefore, we investigated changes in blood flow volume (BFV) in the BA as an indicator of the physiological effects induced by stimulation at 3 points. Seventy-five healthy participants aged 33 ± 9 years (mean \pm SD) were enrolled and randomly assigned to 3 groups; they received stimulation at 3 different points located on the lower limbs: ST36, LR3, and a non-acupoint. Stimulation was performed bilaterally with manual rotation of the needles. Using ultrasonography, BFV was measured continuously from rest to 180 seconds after stimulation. LR3 stimulation significantly increased BFV compared to that before needle insertion. Meanwhile, stimulation at ST36 and the non-acupoint significantly decreased BFV compared to that before needle insertion. Stimulation at LR3 elicited a significant increase in BFV compared to that at ST36 and the non-acupoint. The results suggest that the stimulation of different points on the lower limbs causes distinct physiological effects on BFV in the BA.

1. Introduction

Acupuncture is an important facet of traditional Chinese medicine [1]. Acupuncture points, called acupoints, are gateways located on meridians that can restore the flow of *qi* [2]. The treatment of specific acupuncture points depends on the particular diagnosis [3]. The acupuncture theory is based on the meridian system, which connects acupoints to the organs. However, it has been difficult to verify the meridian and acupoint structures as well as and the connections between organs and meridians. The Zusanli (ST36) acupoint is located on the stomach meridian. This acupoint is known to be effective for the treatment of digestive system disorders; it improves digestive function and decreases abdominal pain [1, 4]. The Taichong (LR3) acupoint is located on the liver meridian; stimulation at this point is known to regulate liver function [1, 4]. One of the functions of the liver is to regulate the free movement of *qi*. Stagnation of liver *qi* may impede blood circulation [4] and cause frequent limb chills.

However, there is currently no evidence supporting the findings mentioned above.

Blood flow volume (BFV) is an important index for representing the condition of organs and tissues. Therefore, we employed BFV as a quantitative indicator of the effects of traditional interventions on the human body. There are some reports in the literature about the hemodynamic responses to acupuncture stimulation at several acupoints [5–9]. Acupuncture is reported to be effective for treating Raynaud syndrome [10] and chills in the hand [11] as well as improving blood circulation in the forearm. However, these reports only show changes in temperature or blood flow at the skin surface. We previously reported the effects of acupuncture at a single acupoint on the BFV of the upper limb in humans, measured by ultrasonography [12, 13]. In addition, we reported the effects of acupuncture on BFV in the superior mesenteric artery by acupuncture at different acupoints in the lower limbs [14]. To our knowledge, no study has reported changes in the BFV of the brachial

artery (BA) induced by acupuncture stimulation at different acupoints on the lower limbs. Therefore, this study aimed to clarify the effects of acupuncture stimulation at 2 different acupoints, ST36 and LR3, and a non-acupoint on the hemodynamics in the BA of healthy participants.

2. Methods

2.1. Participants. Seventy-five healthy adult volunteers (45 men and 30 women) aged 33 ± 9 years (mean \pm SD; range 20–53 years) were enrolled in this study. No participants had cardiovascular disease. None of the participants took any medicine 1 month before the experiment. All participants were examined after fasting and abstaining from alcohol and caffeine for at least 3 hours. The study protocol was approved by the Ethics Committee of Tohoku University, Graduate School of Medicine. All participants provided written informed consent prior to the beginning of the experiment.

2.2. Setting. The participants rested in the supine position in a quiet, air-conditioned room (temperature 25–26°C). Three monitoring electrocardiographic electrodes were attached to the anterior part of the chest of each participant. Four electrodes for impedance cardiography (ICG) (Bioz ICG Module, Dash 3000®, GE Healthcare, USA) were placed at the base of the neck and the level of the xiphoid process in the midaxillary line. ICG utilizes 4 dual sensors on the neck and chest to apply low-amplitude high-frequency alternating electrical current to the participant's thorax. Pulsatile changes in BFV and velocity are measured as changes in impedance. These changes are subsequently synchronized with the electrocardiogram to automatically calculate hemodynamic parameters such as stroke volume and the cardiac index (CI) [15]. ICG is a noninvasive monitoring method that allows the measurement of the CI according to the changes in thoracic resistance that result from variations in intrathoracic BFV [16, 17]. The CI was calculated on the basis of the stroke volume, heart rate, and body surface area measured by ICG [18]. The systemic vascular resistance index (SVRI) was calculated using the CI and blood pressure. Blood pressure was measured with an oscillometer (BP-608 Evolution II®, Colin Healthcare Co. Ltd., Kyoto, Japan) on the left upper arm. BA hemodynamics was measured by an ultrasonograph (Prosound α 10®, Hitachi-Aloka Medical Ltd., Tokyo, Japan) on the right arm; this system contains a high-resolution linear array transducer (13 MHz) and a computer-assisted analysis software (e-tracking system® Hitachi-Aloka Medical Ltd., Tokyo, Japan). The software automatically detected the vessel edge and measured the vessel diameter and BFV continuously [19]. The combination of ultrasonography and pulsed Doppler enables the noninvasive investigation of the blood flow in small vessels such as the coronary, splenic, and adrenal arteries as well as the superior mesenteric artery and BA [20]. The right arm was fixed, and the right BA was scanned longitudinally where the vessel diameter and Doppler wave readings were stable. The transducer was fixed in a special probe holder

(MP-PH0001®, Hitachi-Aloka Medical Ltd., Tokyo, Japan) at the site where the clearest B-mode image of the anterior and posterior vessel wall was obtained (Figure 1). Care was taken to avoid compressing the artery. The BA diameter was monitored automatically when the tracking gate was placed on the intima of the vessel. The waveform of the changes of vessel diameter over the cardiac cycle was displayed in real time using the e-tracking system® (Figure 1). To obtain accurate measurements, the Doppler angle was maintained at 60° or less [21, 22]. BFV was calculated automatically as the Doppler flow velocity (corrected for the angle) multiplied by heart rate and vessel cross-sectional area [21–23]. To ensure consistent images were obtained, the probe was maintained in the same position throughout the test using a special holder. The e-tracking system® automatically measured changes of vessel diameter with a precision of 0.01 mm. The use of this system avoids operator bias, increases reproducibility, and improves accuracy. The system and software were developed to measure flow-mediated dilatation (FMD), which is usually measured at the BA [24, 25]. Ultrasonography is a noninvasive method for evaluating blood flow velocity. Blood flow changes rapidly in the arteries of the extremities, especially in the peripheral arteries [26]. Changes in venous return due to respiration cause oscillations in stroke volume and blood pressure [27]. Thus, the arterial pulse should be modified by breathing [28]. Therefore, the participants were asked to breathe every 6 seconds during the test, and hemodynamic parameters were calculated as the average values of each 6-second period to minimize the influence of respiration. The following hemodynamic parameters were determined: (1) blood pressure (mmHg), (2) heart rate (beats/min), (3) cardiac index ($L \cdot \text{min}^{-1} \cdot \text{m}^{-2}$), and (4) blood flow volume ($\text{mL} \cdot \text{min}^{-1} \cdot \text{m}^{-2}$).

2.3. Study Protocol. A single-blind randomized controlled trial was performed. The experimental outline of the study is shown in Figure 2. All participants ($n = 75$) were randomly assigned to 1 of 3 groups receiving the following treatments: (1) needle stimulation at ST36 ($n = 25$, Zusanli; located on the lower leg, 3 units below the lateral “eye” of the knee, approximately 1 finger width lateral to the tibia [29]) (Figure 3); (2) needle stimulation at LR3 ($n = 25$, Taichong; located on the foot, 1.5–2 units above the web between the first and second toes [29]) (Figure 3); (3) needle stimulation at a non-acupoint ($n = 25$; located on the lower leg, 3 units lateral to and below ST36, midpoint of the stomach and gallbladder meridian) (Figure 3). The participants had no knowledge about acupuncture or acupoints.

After the ultrasonograph was positioned, the participants rested in the supine position for 10 minutes. We then measured the BA hemodynamics, blood pressure, heart rate, and the CI at rest (i.e., before needle insertion), during needle stimulation, and 30, 60, and 180 seconds after needle stimulation. Needle stimulation was performed by a licensed acupuncturist. Disposable fine stainless-steel needles (0.16 mm diameter, 40 mm length, Seirin Co. Ltd., Shizuoka, Japan) were inserted bilaterally on the target point

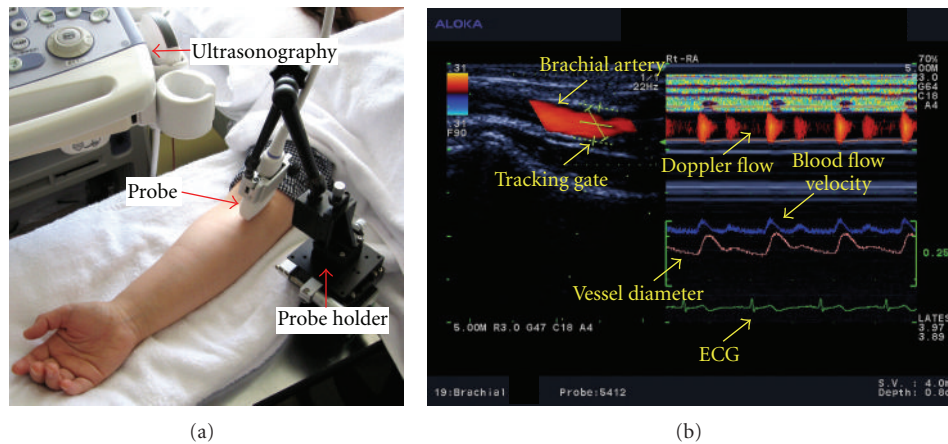


FIGURE 1: (a) An ultrasonographic measurement of the brachial artery with a special probe holder (MP-PH001®), Hitachi-Aloka Medical Ltd., Tokyo, Japan). (b) Hemodynamic data obtained by ultrasonography. The left image shows the vessel image and position of the tracking gate of the brachial artery. The right image shows the changes in vessel diameter, Doppler flow, and blood flow velocity determined by an automated edge detection device and computer analysis software (e-tracking system®, Hitachi-Aloka Medical Ltd., Tokyo, Japan).

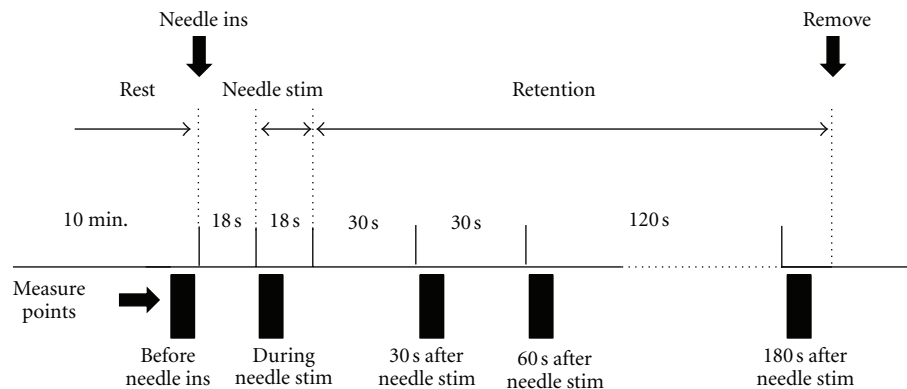


FIGURE 2: Experimental diagram. Before needle insertion (ins) and stimulation (stim) bilaterally at ST36, LR3, and the non-acupoint. After the needles were inserted, needle stimulation was applied for 18 s with manual rotation. The needles were retained for 180 s after needle stimulation and then removed. Hemodynamic parameters were measured before needle insertion, during, and 30, 60, and 180 s after needle stimulation. min.: minutes, s: seconds.

and maintained at a depth of 10 mm during the test to ensure they reached the muscle. After the needles were inserted, the stimulation was performed for 18 seconds by rotating the needles $<90^\circ$ manually. The needles were retained for the duration of the test following stimulation and were then removed.

2.4. Statistical Analysis. Statistical analysis was performed with PASW software (version 17.0, SPSS Japan Inc., Tokyo, Japan). Comparisons between the ST36, LR3, and non-acupoint groups were performed by two-way analysis of variance (ANOVA) with a post hoc Tukey test. Repeated-measures one-way ANOVA with a post hoc Dunnett's test were used for statistical comparison between pre- and post-needle insertion values. Mean values between groups were compared using the Kruskal-Wallis H test. The level of statistical significance was set at $P < 0.05$. Individual variations were analyzed as percent changes.

3. Results

3.1. Participants. One participant assigned to the LR3 group was excluded from the analysis because of arrhythmia. There were no significant differences among the clinical profiles of the 3 groups (Table 1).

3.2. Data Summary. Table 2 summarizes the hemodynamic measurements performed before and after needle insertion in the ST36, LR3, and non-acupoint groups. Stimulation at ST36 elicited a decrease in BFV in the BA during needle stimulation compared with that before needle insertion. The basal values of BFV in the BA were not significantly different among the 3 groups. Similarly, no significant differences were observed in any parameters measured at rest before needle insertion.

3.3. Blood Pressure. No significant differences were observed among the 3 groups or with respect to the percent change

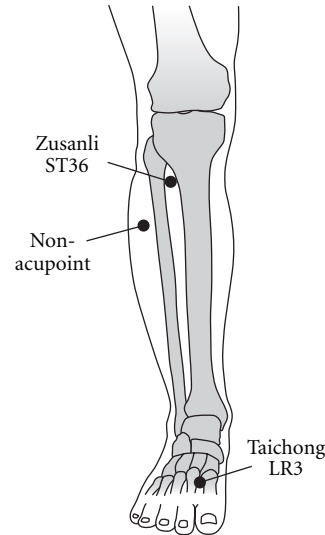


FIGURE 3: Needle positions of ST36, LR3, and the non-acupoint.

TABLE 1: Clinical profiles by group.

Profile	Stimulation points		
	ST36	LR3	Non-acupoint
Person	25	24	25
Sex (men : women)	15 : 10	14 : 10	15 : 10
Age (year)	31.0 ± 9.7	34.6 ± 8.4	33.1 ± 8.3
Height (cm)	166.9 ± 9.2	167.7 ± 8.9	165.5 ± 8.1
Weight (kg)	64.0 ± 12.1	61.7 ± 10.9	60.3 ± 9.5
Body surface area (m ²)	1.71 ± 0.19	1.70 ± 0.19	1.66 ± 0.15

in systolic or diastolic blood pressure in each test before and after needle insertion.

3.4. Heart Rate. No significant differences were observed among the 3 groups with respect to the percent change in heart rate in each test. Regarding the percent change in heart rate, stimulation at LR3 elicited a significant decrease in heart rate measured during needle stimulation compared to that before needle insertion. The heart rate tended to decrease during needle stimulation.

3.5. Cardiac Index. No significant differences were observed among the 3 groups with respect to the percent change in the CI in each test. Regarding the percent change in the CI, the stimulation at the non-acupoint elicited a significant increase in the CI in the BA 180 seconds after needle stimulation compared to that before needle insertion.

3.6. Systemic Vascular Resistance Index. No significant differences were observed among the 3 groups with respect to the percent change in SVRI in each test (Figure 4). Regarding the percent change in SVRI, the stimulation at LR3 and the non-acupoint elicited a significant decrease in SVRI in the BA

180 seconds after needle stimulation compared to that before needle insertion.

3.7. Blood Flow Volume of the Brachial Artery. Figure 5 shows the percent change in BFV in the BA in each test. The percent change in BFV in the BA was significantly different between the LR3 group and the other 2 groups. The stimulation at LR3 elicited a significant increase in BFV in the BA 60 and 180 seconds after needle stimulation compared to that before needle insertion. Meanwhile, the stimulation at ST36 elicited a significant decrease in BFV in the BA during and 60 and 180 seconds after needle stimulation compared to that before needle insertion. Furthermore, stimulation at the non-acupoint elicited a significant decrease in BFV in the BA during and 60 seconds after needle stimulation compared to that before needle insertion.

4. Discussion

To our knowledge, this is the first study comparing the differences in BFV in the BA induced by needle stimulation at 3 acupoints as assessed by ultrasonography. The results show that BFV in the BA increased significantly after needle stimulation at LR3, whereas it decreased significantly after needle stimulation at ST36 and the non-acupoint. Furthermore, after needle stimulation at the non-acupoint, the CI increased significantly while SVRI decreased significantly. These results indicate that the physiological effects on the BFV in the BA triggered by needle stimulation vary depending on the acupoint stimulated. Needle stimulation at the lower limbs is known to elicit systemic visceral responses via supraspinal reflexes [30–32]. However, visceral responses vary, as observed in the present study.

Stimulation at ST36 and the non-acupoint elicited significant decreases in BFV in the BA during needle stimulation compared to that before needle insertion. The physiological mechanism involved in the decrease in BFV in the BA

TABLE 2: Summary of measured hemodynamic parameters.

Parameter/test condition	Before needle ins	During needle stim	30 s after needle stim	60 s after needle stim	180 s after needle stim
Systolic blood pressure (mm Hg)					
ST36	116.1 ± 11.0				116.2 ± 10.2
LR3	114.7 ± 12.7				112.1 ± 12.3
Non-acupoint	117.5 ± 15.5				116.0 ± 14.0
Diastolic blood pressure (mm Hg)					
ST36	69.1 ± 8.0				69.0 ± 8.6
LR3	68.2 ± 9.1				66.1 ± 9.0
Non-acupoint	70.4 ± 12.2				70.0 ± 11.0
Heart rate (beats/min)					
ST36	66.2 ± 10.2	64.1 ± 10.7	67.0 ± 10.7	66.4 ± 10.5	68.0 ± 11.7
LR3	63.4 ± 9.0	60.4 ± 7.8	63.0 ± 9.1	63.4 ± 9.1	63.6 ± 9.1
Non-acupoint	65.0 ± 9.5	62.6 ± 10.5	64.5 ± 9.4	64.8 ± 9.6	64.8 ± 10.4
Cardiac index ($L \cdot \text{min}^{-1} \cdot \text{m}^{-2}$)					
ST36	3.0 ± 0.7	3.0 ± 0.6	3.0 ± 0.6	3.0 ± 0.7	3.0 ± 0.7
LR3	2.7 ± 0.4	2.7 ± 0.4	2.7 ± 0.5	2.7 ± 0.5	2.7 ± 0.5
Non-acupoint	2.7 ± 0.4	2.7 ± 0.4	2.7 ± 0.4	2.8 ± 0.4	2.8 ± 0.4
Systemic vascular resistance index ($\text{dyne sec/cm}^5 \cdot \text{m}^2$)					
ST36	2390 ± 513				2347 ± 556
LR3	2507 ± 429				2414 ± 431
Non-acupoint	2602 ± 654				2522 ± 586
Blood flow volume in brachial artery ($\text{mL} \cdot \text{min}^{-1} \cdot \text{m}^{-2}$)					
ST36	55.4 ± 29.3**	33.4 ± 13.1**	48.0 ± 21.5	44.0 ± 20.8	45.5 ± 25.4
LR3	38.9 ± 25.9	29.8 ± 20.6	41.8 ± 25.1	47.7 ± 30.7	54.8 ± 32.6
Non-acupoint	59.0 ± 52.4	37.7 ± 31.0	57.8 ± 50.6	48.0 ± 40.5	53.3 ± 40.7

The values represent the mean ± SD. **Significant difference ($P < 0.01$) in the blood flow volume in the brachial artery between before needle insertion (ins) and during needle stimulation (stim) at ST36.

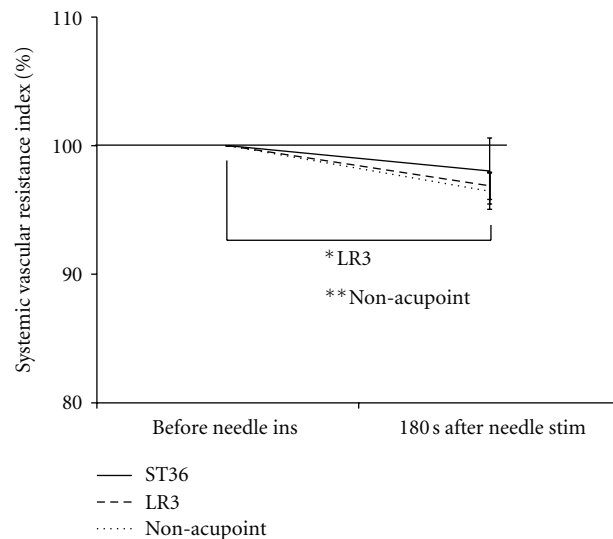


FIGURE 4: Percent change in the systemic vascular resistance index before needle insertion (ins) and at stimulation (stim) at ST36, LR3, and the non-acupoint. Values represent means and standard errors (SEM). ***Significantly different ($P < 0.05$, $P < 0.01$, resp.) relative to the resting condition in each test setup.

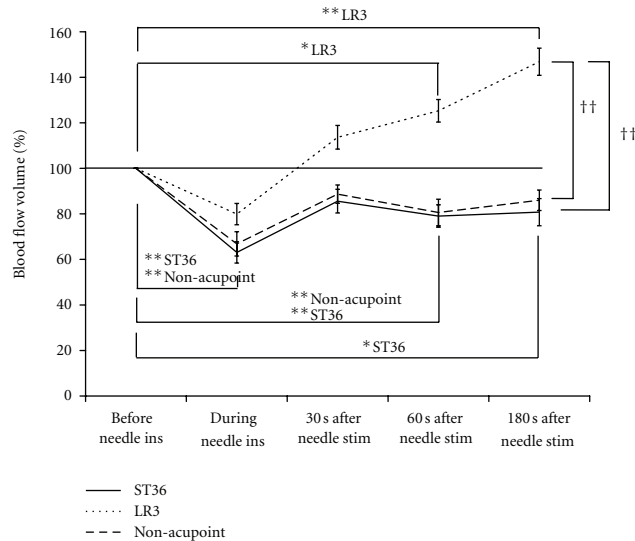


FIGURE 5: Percent change in blood flow volume in the brachial artery before needle insertion (ins) and during and after needle stimulation (stim) at ST36, LR3, and the non-acupoint. The values represent means and corresponding standard errors (SEM). ***,** Significant difference ($P < 0.05$ and $P < 0.01$, resp.) relative to the blood flow volume before needle insertion at LR3, ST36, or the non-acupoint. †† Significant difference ($P < 0.01$) between the LR3 and ST36/non-acupoint groups.

induced by the stimulations applied to the skin is a peripheral vascular resistance caused by an instantaneous increase in sympathetic tone [33]. During needle stimulation, heart rate tended to decrease without a change in the CI. Previous studies report that the mechanism of the acupuncture induced decrease in heart rate is based on somatoautonomic reflexes, which occur via the cardiac sympathetic nerves [34–36]. These mechanisms are involved in the supraspinal reflex.

Stimulation at LR3 elicited a significant increase in BFV in the BA 60 and 180 seconds after needle stimulation compared to that before needle insertion. In addition, for LR3 stimulation, a systemic reaction was elicited such that the SVRI decreased significantly 180 seconds after needle stimulation without any changes in blood pressure, heart rate, or the CI compared to those before needle insertion. This reaction suggests that the increase of BFV in the BA after stimulation at LR3 depends on the decrease of SVRI. A previous report suggests that the changes in BFV in the BA caused by needle stimulation at LR3 depend on the decrease of the resistive index of the peripheral artery after needle stimulation [13]. This report supports the relationship between the increase of BFV in the BA and the decrease of SVRI observed in the present study. A previous study found that adrenal sympathetic nerve activity and catecholamine secretion rate increase as a result of stimulating the hind limb of rats [30, 37–39]. In addition, vasodilation is reported to be elicited via adrenalin beta-2 receptor activation [40]. However, in the present study, the BFV of the BA decreased after needle stimulation at the non-acupoint with the decrease of SVRI. This result may suggest that BFV increased in other organs but not in the BA and that the shift of BFV to other organs is induced by needle stimulation. Similar speculation can be applied to the reaction with ST36 stimulation. However, further investigations are required to clarify these reactions.

The physiological reactions mentioned earlier may support the idea that stimulations at ST36, LR3, and the non-acupoint have different impacts on the autonomic nervous system, which regulates BFV in the BA. A recent report also suggested that opposite cardiovascular effects were shown in the response to stimulation of LR3 and ST36 in rats [41]. We can deduce that the various reactions mediated by the autonomic nervous system depend on the characteristics of a specific stimulation, such as the site, intensity, and duration. The 3 points used in this study (ST36, LR3, and the non-acupoint) are located along the boundary of the same dermatomes, and their innervations are complex [42]. Therefore, each point likely has different sensitivities to stimulation. Among other factors, differences in signal transmission via afferent and efferent fibers depend on anatomical structures such as the dermatomes and myotomes as well as the innervation and thickness of the muscle and skin at the stimulation points.

The present study was a human observational study. Measuring sympathetic and parasympathetic activities in human subjects is invasive and difficult. Therefore, we observed the effects of stimulation at 2 acupoints and 1 non-acupoint on BFV and speculated on the mechanism using previous experimental studies as a basis. In a previous study with 25 participants per group, we reported the changes in BFV in the BA measured by ultrasonography when acupuncture was performed at a single acupoint [12, 13]. According to these results, we enrolled 25 participants in each of the 3 groups in the present study. The use of ultrasound methods to assess FMD has a good reproducibility [43–45]. However, a previous study evaluating the reproducibility of FMD indicates that 62 subjects per group are required to detect a treatment difference of 2 FMD% with a probability of 0.05 and a power of 0.80 in a parallel design comparing intergroup changes [46]. Therefore, the small sample size

of each group may be a limitation of the present study. The findings of this study suggest that acupuncture induces endothelium-dependent FMD, providing an interesting pathophysiological basis for the explanation of observed blood flow changes.

5. Conclusions

The present study revealed that BFV in the BA increased after needle stimulation at LR3 without changes in the CI. Needle stimulation at ST36 and the non-acupoint affected the hemodynamics of the BA. These physiological effects may be dependent on acupoint location.

Conflict of Interests

No conflict of interests exists.

Acknowledgments

The authors would like to thank all of the participants. M. Watanabe planned the study, recruited participants, performed the experiments, performed data analysis, and wrote the paper. S. Takayama planned the study, provided advice on the experiments, and provided advice on the paper. A. Hirano performed the experiments. T. Seki planned the study and provided advice on the paper. N. Yaegashi was the authority for the study planning as well as execution, and assisted paper writing. This work was supported by Health and Labour Science Research Grants for Clinical Research from the Japanese Ministry of Health, Labour, and Welfare.

References

- [1] M. Giovanni, *The Foundations of Chinese Medicine: A Comprehensive Text for Acupuncturists and Herbalists*, Churchill Livingstone, Edinburgh, UK, 1989.
- [2] S. P. C. Ngai, A. Y. M. Jones, and E. K. W. Cheng, "Lung meridian acupuncture point skin impedance in asthma and description of a mathematical relationship with FEV₁," *Respiratory Physiology and Neurobiology*, vol. 179, no. 2-3, pp. 187–191, 2011.
- [3] J. A. Sutherland, "Meridian therapy: current research and implications for critical care," *AACN Clinical Issues*, vol. 11, no. 1, pp. 97–104, 2000.
- [4] G. Liu, A. Hyodo, Q. Cao et al., *Fundamentals of Acupuncture & Moxibustion*, Huaxia Publishing House, Beijing, China, 2006.
- [5] E. Haker, H. Egekvist, and P. Bjerring, "Effect of sensory stimulation (acupuncture) on sympathetic and parasympathetic activities in healthy subjects," *Journal of the Autonomic Nervous System*, vol. 79, no. 1, pp. 52–59, 2000.
- [6] Y. Syuu, H. Matsubara, T. Kiyooka et al., "Cardiovascular beneficial effects of electroacupuncture at Neiguan (PC-6) acupoint in anesthetized open-chest dog," *Japanese Journal of Physiology*, vol. 51, no. 2, pp. 231–238, 2001.
- [7] W. K. Wang, T. Lin Hsu, H. C. Chang, and Y. Y. Lin Wang, "Effect of acupuncture at Hsien-Ku (St-43) on the pulse spectrum and a discussion of the evidence for the frequency structure of Chinese medicine," *American Journal of Chinese Medicine*, vol. 28, no. 1, pp. 41–55, 2000.
- [8] Y. Kurono, M. Minagawa, T. Ishigami, A. Yamada, T. Kakamu, and J. Hayano, "Acupuncture to Danzhong but not to Zhongting increases the cardiac vagal component of heart rate variability," *Autonomic Neuroscience*, vol. 161, no. 1-2, pp. 116–120, 2011.
- [9] L. Tough, "Lack of effect of acupuncture on electromyographic (EMG) activity—a randomised controlled trial in healthy volunteers," *Acupuncture in Medicine*, vol. 24, no. 2, pp. 55–60, 2006.
- [10] R. Appiah, S. Hiller, L. Caspary, K. Alexander, and A. Creutzig, "Treatment of primary Raynaud's syndrome with traditional Chinese acupuncture," *Journal of Internal Medicine*, vol. 241, no. 2, pp. 119–124, 1997.
- [11] T. C. Kuo, C. W. Lin, and F. M. Ho, "The soreness and numbness effect of acupuncture on skin blood flow," *American Journal of Chinese Medicine*, vol. 32, no. 1, pp. 117–129, 2004.
- [12] S. Takayama, T. Seki, N. Sugita et al., "Radial artery hemodynamic changes related to acupuncture," *Explore*, vol. 6, no. 2, pp. 100–105, 2010.
- [13] S. Takayama, T. Seki, M. Watanabe et al., "Brief effect of acupuncture on the peripheral arterial system of the upper limb and systemic hemodynamics in humans," *Journal of Alternative and Complementary Medicine*, vol. 16, no. 7, pp. 707–713, 2010.
- [14] M. Watanabe, S. Takayama, and T. Seki, "Haemodynamic changes in the superior mesenteric artery induced by acupuncture stimulation on the lower limbs," *Evidence-Based Complementary and Alternative Medicine*, vol. 2012, Article ID 908546, 9 pages, 2012.
- [15] C. L. Springfield, F. Sebat, D. Johnson, S. Lenge, and C. Sebat, "Utility of impedance cardiography to determine cardiac vs. noncardiac cause of dyspnea in the emergency department," *Congestive Heart Failure*, vol. 10, no. 2, pp. 14–16, 2004.
- [16] A. C. Perrino, A. Lippman, C. Ariyan, T. Z. O'Connor, and M. Luther, "Intraoperative cardiac output monitoring: comparison of impedance cardiography and thermodilution," *Journal of Cardiothoracic and Vascular Anesthesia*, vol. 8, no. 1, pp. 24–29, 1994.
- [17] N. M. Albert, M. D. Hail, J. Li, and J. B. Young, "Equivalence of the bioimpedance and thermodilution methods in measuring cardiac output in hospitalized patients with advanced, decompensated chronic heart failure," *American Journal of Critical Care*, vol. 13, no. 6, pp. 469–479, 2004.
- [18] J. L. Fellahi, V. Caille, C. Charron, P. H. Deschamps-Berger, and A. Vieillard-Baron, "Noninvasive assessment of cardiac index in healthy volunteers: a comparison between thoracic impedance cardiography and doppler echocardiography," *Anesthesia and Analgesia*, vol. 108, no. 5, pp. 1553–1559, 2009.
- [19] J. Soga, K. Nishioka, S. Nakamura et al., "Measurement of flow-mediated vasodilation of the brachial artery—a comparison of measurements in the seated and supine positions," *Circulation Journal*, vol. 71, no. 5, pp. 736–740, 2007.
- [20] U. Gembruch, "Assessment of the fetal circulatory state in uteroplacental insufficiency by Doppler ultrasound: which vessels are the most practicable?" *Ultrasound in Obstetrics & Gynecology*, vol. 8, no. 2, pp. 77–81, 1996.
- [21] P. N. Burns and C. C. Jaffe, "Quantitative flow measurements with Doppler ultrasound: techniques, accuracy, and limitations," *Radiologic Clinics of North America*, vol. 23, no. 4, pp. 641–657, 1985.

- [22] K. J. W. Taylor and S. Holland, "Doppler US—part I. Basic principles, instrumentation, and pitfalls," *Radiology*, vol. 174, no. 2, pp. 297–307, 1990.
- [23] R. W. Gill, "Measurement of blood flow by ultrasound: accuracy and sources of error," *Ultrasound in Medicine and Biology*, vol. 11, no. 4, pp. 625–641, 1985.
- [24] J. Deanfield, A. Donald, C. Ferri et al., "Endothelial function and dysfunction—part I: methodological issues for assessment in the different vascular beds: a statement by the working group on endothelin and endothelial factors of the European society of hypertension," *Journal of Hypertension*, vol. 23, no. 1, pp. 7–17, 2005.
- [25] M. C. Corretti, T. J. Anderson, E. J. Benjamin et al., "Guidelines for the ultrasound assessment of endothelial-dependent flow-mediated vasodilation of the brachial artery: a report of the international brachial artery reactivity task force," *Journal of the American College of Cardiology*, vol. 39, no. 2, pp. 257–265, 2002.
- [26] Y. Nimura, H. Matsuo, and T. Hayashi, "Studies on arterial flow patterns—instantaneous velocity spectrums and their phasic changes—with directional ultrasonic Doppler technique," *British Heart Journal*, vol. 36, no. 9, pp. 899–907, 1974.
- [27] C. W. Hsieh, C. W. Mao, M. S. Young, T. L. Yeh, and S. J. Yeh, "Respiratory effect on the pulse spectrum," *Journal of Medical Engineering and Technology*, vol. 27, no. 2, pp. 77–84, 2003.
- [28] D. Korpas and J. Halek, "Pulse wave variability within two short-term measurements," *Biomedical Papers of the Medical Faculty of the University Palacký, Olomouc, Czechoslovakia*, vol. 150, no. 2, pp. 339–344, 2006.
- [29] C. H. Chen, *Acupuncture: A Comprehensive Text*, Eastland Press, Seattle, Wash, USA, 1981.
- [30] A. Sato, Y. Sato, A. Suzuki, and S. Uchida, "Reflex modulation of catecholamine secretion and adrenal sympathetic nerve activity by acupuncture-like stimulation in anesthetized rat," *Japanese Journal of Physiology*, vol. 46, no. 5, pp. 411–421, 1996.
- [31] S. Uchida and H. Hotta, "Acupuncture affects regional blood flow in various organs," *Evidence-Based Complementary and Alternative Medicine*, vol. 5, no. 2, pp. 145–151, 2008.
- [32] E. Noguchi, "Mechanism of reflex regulation of the gastroduodenal function by acupuncture," *Evidence-Based Complementary and Alternative Medicine*, vol. 5, no. 3, pp. 251–256, 2008.
- [33] B. Johansson, "Circulatory responses to stimulation of somatic afferents with special reference to depressor effects from muscle nerves," *Acta Physiologica Scandinavica*, vol. 198, pp. 1–91, 1962.
- [34] S. Uchida, M. Shimura, H. Ohsawa, and A. Suzuki, "Neural mechanism of bradycardiac responses elicited by acupuncture-like stimulation to a hind limb in anesthetized rats," *Journal of Physiological Sciences*, vol. 57, no. 6, pp. 377–382, 2007.
- [35] H. Ohsawa, K. Okada, K. Nishijo, and Y. Sato, "Neural mechanism of depressor responses of arterial pressure elicited by acupuncture-like stimulation to a hindlimb in anesthetized rats," *Journal of the Autonomic Nervous System*, vol. 51, no. 1, pp. 27–35, 1995.
- [36] K. Nishijo, H. Mori, K. Yosikawa, and K. Yazawa, "Decreased heart rate by acupuncture stimulation in humans via facilitation of cardiac vagal activity and suppression of cardiac sympathetic nerve," *Neuroscience Letters*, vol. 227, no. 3, pp. 165–168, 1997.
- [37] J. Li, J. Li, Z. Chen et al., "The influence of PC6 on cardiovascular disorders: a review of central neural mechanisms," *Acupuncture in Medicine*, vol. 30, no. 1, pp. 47–50, 2012.
- [38] E. Stener-Victorin, S. Fujisawa, and M. Kurosawa, "Ovarian blood flow responses to electroacupuncture stimulation depend on estrous cycle and on site and frequency of stimulation in anesthetized rats," *Journal of Applied Physiology*, vol. 101, no. 1, pp. 84–91, 2006.
- [39] S. Stock and K. Uvnas-Moberg, "Increased plasma levels of oxytocin in response to afferent electrical stimulation of the sciatic and vagal nerves and in response to touch and pinch in anaesthetized rats," *Acta Physiologica Scandinavica*, vol. 132, no. 1, pp. 29–34, 1988.
- [40] D. Robertson, *Primer on the Autonomic Nervous System*, Elsevier, 3rd edition, 2012.
- [41] T. Friedemann, X. Shen, J. Bereiter-Hahn, and W. Schwarz, "Regulation of the cardiovascular function by CO₂ laser stimulation in anesthetized rats," *Lasers in Medical Science*, vol. 27, pp. 469–477, 2012.
- [42] S. Standring, *Gray's Anatomy: The Anatomical Basis of Clinical Practice*, Churchill Livingstone Elsevier, UK, 40th edition, 2008.
- [43] S. L. Magda, A. O. Ciobanu, and M. Florescu, "Comparative reproducibility of the noninvasive ultrasound methods for the assessment of vascular function," *Heart Vessels*. In press.
- [44] A. E. Donald, J. P. Halcox, M. Charakida et al., "Methodological approaches to optimize reproducibility and power in clinical studies of flow-mediated dilation," *Journal of the American College of Cardiology*, vol. 51, no. 20, pp. 1959–1964, 2008.
- [45] L. Ghiadoni, F. Fajta, M. Salvetti et al., "Assessment of flow-mediated dilation reproducibility: a nationwide multicenter study," *Journal of Hypertension*, vol. 30, no. 7, pp. 1399–1405, 2012.
- [46] N. M. De Roos, M. L. Bots, E. G. Schouten, and M. B. Katan, "Within-subject variability of flow-mediated vasodilation of the brachial artery in healthy men and women: implications for experimental studies," *Ultrasound in Medicine and Biology*, vol. 29, no. 3, pp. 401–406, 2003.

Research Article

Investigation of Acupuncture Sensation Patterns under Sensory Deprivation Using a Geographic Information System

Florian Beissner¹ and Irene Marzolff²

¹ Pain & Autonomics-Integrative Research (PAIR), Department of Psychiatry and Psychotherapy, Jena University Hospital, 07743 Jena, Germany

² Institute for Physical Geography, Goethe University, 60438 Frankfurt am Main, Germany

Correspondence should be addressed to Florian Beissner, coffeeefellow@gmail.com

Received 20 July 2012; Revised 30 August 2012; Accepted 3 September 2012

Academic Editor: Wolfgang Schwarz

Copyright © 2012 F. Beissner and I. Marzolff. This is an open access article distributed under the Creative Commons Attribution License, which permits unrestricted use, distribution, and reproduction in any medium, provided the original work is properly cited.

The study of acupuncture-related sensations, like *deqi* and propagated sensations along channels (PSCs), has a long tradition in acupuncture basic research. The phenomenon itself, however, remains poorly understood. To study the connection between PSC and classical meridians, we applied a geographic information system (GIS) to analyze sketches of acupuncture sensations from healthy volunteers after laser acupuncture. As PSC can be subtle, we aimed at reducing the confounding impact of external stimuli by carrying out the experiment in a floatation tank under restricted environmental stimulation. 82.4% of the subjects experienced PSC, that is, they had line-like or 2-dimensional sensations, although there were some doubts that these were related to the laser stimulation. Line-like sensations on the same limb were averaged to calculate sensation mean courses, which were then compared to classical meridians by measuring the mean distance between the two. Distances ranged from 0.83 cm in the case of the heart (HT) and spleen (SP) meridian to 6.27 cm in the case of the kidney (KI) meridian. Furthermore, PSC was observed to “jump” between adjacent meridians. In summary, GIS has proven to be a valuable tool to study PSC, and our results suggest a close connection between PSC and classical meridians.

1. Introduction

Acupuncture is a medical intervention originating from ancient Asia, where needles are used to stimulate certain points on the body. Despite more than five decades of intensive research in Asia and the West, the underlying mechanisms of acupuncture are still largely unknown. A phenomenon that may be of great importance for the understanding of these mechanisms is a specific sensation upon stimulation of acupuncture points that is called *deqi* (“the arrival of *qi*”, 得氣) in Chinese medicine. Previous works have shown that the perception of this sensation usually described by words like “aching,” “soreness,” “pressure,” or “tingling” [1] is similar between subjects, irrespective of their expectation, sex, or cultural background [2–4]. Judging from the adjectives that are most frequently used to describe *deqi*, it is a mixed sensation with a strong component of C-fiber-mediated pain [5]. Another important feature of *deqi*

is that it often spreads or radiates from the point of its elicitation. This has led to the term “propagated sensation along meridians” (PSM) or, more commonly, “propagated sensation along channels” (PSC) [2].

So far, the investigation of PSC has been limited by a lack of appropriate methods for its assessment. Questionnaires like the MASS (MGH acupuncture sensation scale) [6] have been developed to measure sensory qualities and intensity of *deqi*. But they give only a rough estimate of the spreading/radiation experienced by the subject. To gain a deeper understanding of PSC, however, it is crucial to measure its exact course and compare it between subjects.

To close this gap, we developed a new method by combining standardized subjects’ drawings, a method often used for pain assessment [7], with an analysis based on a geographic information system (GIS) [8]. Geographical information systems allow to map, visualize, and analyze the patterns, dimensions, relationships, and changes of spatial

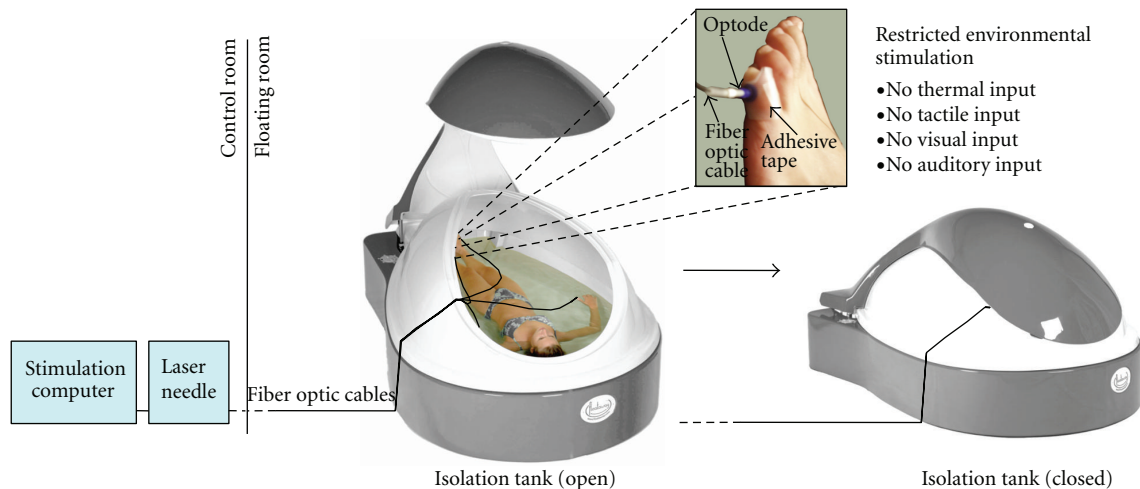


FIGURE 1: Experimental design. The subject inside the tank was stimulated with an acupuncture laser, while floating on the water surface to reduce tactile input. Laser light was transmitted by fiber optic cables from the control room. Laser optodes were attached to the skin using silicone adapters and adhesive tape. After the tank was closed, there was also reduced visual, auditory, and thermal input, so that subjects could concentrate on sensations occurring during laser acupuncture. Tank images courtesy of Floataway, Norfolk, UK.

data. The spatial reference is usually a coordinate system of the Earth such as latitudes and longitudes, metric units in a map projection or postal codes, but any other local system may be used as well. In health care and medical science, spatial data analyses on local to global scales have a long tradition, beginning with the classic study of London's 1854 cholera epidemic by British epidemiologist John Snow [9]. GIS today plays an important role in public and private health care, medical research and insurance for management, planning and analysis [10, 11], but few studies have so far been conducted on the basis of body maps. Our approach allows for the first time to map the detailed course of PSC in a sample of subjects, compare the results between subjects, and calculate mean courses. The results can then be compared to the so-called *meridians* (chin.: “*jingluo*”, 经络), vessel-like structures that according to Chinese medical theory traverse the human body circulating an immaterial substance (chin.: “*qi*”, 氣). Based on acupuncture classics as well as previous reports, we hypothesized a strong resemblance between the courses of certain meridians and those of PSC. Since no anatomical correlate has been found for the concept of meridians despite decades of research [12, 13], it is very likely that these structures were originally inspired by the line-like appearance of PSC patterns.

As PSC can sometimes be subtle, we aimed at reducing the confounding impact of tactile stimuli that can hardly be controlled under normal circumstances. Therefore, all measurements were carried out in a floatation tank [14] under restricted environmental stimulation [15]. A floatation tank is filled with saline that is constantly kept at skin temperature as is the surrounding air. It is soundproof and either dark or illuminated by very dim light. The subject inside the tank floats supine on the saline without effort, which greatly reduces the amount of tactile, visual, and auditory input and allows full concentration on sensations inside the body.

2. Methods

2.1. Study Design. All measurements were carried out at floatbase GmbH (Frankfurt am Main, Germany). The experimental design is shown in Figure 1. When subjects arrived at the floatbase, they were first familiarized with the isolation tank and its emergency facilities to reduce anxiety. Next, subjects were shown the questionnaire with the body schemes, which were used after the experiment to sketch their sensations. Silicone adapters for the laser optodes were attached to the following points of the body using adhesive tape: (1) Little toe of the left foot, acupuncture point Bladder 67 (BL-67), (2) Big toe of the right foot, acupuncture point Spleen 1 (SP-1), (3) Index finger of the left hand, acupuncture point Large Intestine 1 (LI-1), (4) Little finger of the right hand, acupuncture point Small Intestine 1 (SI-1). For the exact localization of the points, see Supplementary Figure 1 in Supplementary Material available online at doi:10.1155/2012/591304. Subjects were instructed how to enter the tank, take a comfortable position, insert the laser optodes into the silicone adapters, and close the tank from the inside. They were also informed about the timing of the experiment, which is described in detail below. The investigator then left the room so that subjects could undress and enter the tank.

The closing of the tank was indicated to the investigator by a signal light and marked the official beginning of the experiment. In a first period, lasting 10 minutes, subjects did not receive any stimulation, so they could adapt to the new environment. In the second period, lasting 16 minutes, a randomly chosen set of three of the four points were stimulated one after another with the laser in a randomized order. Each stimulation lasted three minutes followed by one minute without stimulation. For the point that was not stimulated, the laser was simply left switched off during the entire four (3 + 1) minutes. The end of the stimulation

paradigm was indicated to the subjects by a special sound (sea rushing). From this point, subjects had four minutes to prepare themselves to leave the tank. After this time, the tank opened automatically.

After taking a shower to remove excess saline from the body, subjects were handed out the questionnaire, which they were asked to fill out immediately.

2.2. Subjects. 20 healthy subjects (10 male/10 female) took part in the study. The mean age was 28.8 ± 4.1 (S.D.) years. Prior to the measurement, subjects were screened for any acute diseases or contraindications for using the floatation tank (skin diseases, epilepsy, claustrophobia, and pregnancy). All subjects were healthy on the day of the measurement. None of them had any history of neurological disease or took any kind of medication on a regular basis. The intake of analgesics as rescue medication was prohibited during the five days before the measurement. None of the subjects had any prior knowledge of acupuncture theory as a student or practitioner.

After the measurement, three subjects (1 male, 2 female) were excluded. Two mentioned the intake of antihistaminic drugs not until after the measurement, and one developed severe vertigo and nausea inside the tank.

2.3. Laser Stimulation Device. Low-level laser stimulation was administered using a Laserneedle (Laserneedle EG GmbH, Wehrden, Germany) emitting a combination of 655 nm (red) and 785 nm (infrared) laser light with an irradiation power of about 15 W/cm^2 at the distal output. Laser optodes were applied in contact mode using silicone adapters, which were attached to the skin using adhesive tape. The laser power at the distal output of each optode was about 40 mW. Reflection losses could be neglected due to the direct contact of the optode with the skin. Acupuncture Lasers like this have been used before in a number of studies [16, 17].

2.4. Isolation Tank. All measurements were performed using the same isolation tank (floataway, Norfolk, UK) at floatbase. The size of the tank was $2.20 \text{ m} \times 1.50 \text{ m}$ with a water depth of 25 cm. The water inside the tank was loaded with 300 kg magnesium sulfate to achieve the floatation effect, that is, make subjects float on its surface. The water temperature was kept at a constant 34°C to minimize temperature sensations. The tank and the surrounding room were soundproof and subjects were asked to keep their eyes shut throughout the whole experiment, thus minimizing auditory and visual sensations. A dim red light illuminated the tank during the whole experiment to prevent subjects from noticing changes in ambient light due to switching of the laser.

2.5. Body Schemes and Questionnaires. To assess and compare bodily sensations experienced by the subjects, body schemes were developed based on the illustrations in [18] (see Supplementary Figure 1). When these body schemes were first shown to the subjects before the measurements, the following instructions were given: "Please pay attention

to any sensation that you believe is an effect of the laser stimulation. You will later be asked to sketch your sensations on these body schemes. You will also be asked about the quality and intensity of the sensations." Directly after the end of the measurements, subjects were given the body schemes as well as the German version of the McGill pain questionnaire [19, 20] with its 77 descriptors (sensory, affective, and evaluative) and an additional visual analogue scale. The order of the descriptors was randomized for each subject. The following instructions were read aloud to the subjects: "Please describe any sensation that you believe was an effect of the laser stimulation. Sketch the localization of these sensations on the body schemes using the following three signs: A dot for every point-like sensation, a line for every line-like sensation and hachures for every two-dimensional sensation. Please choose any number of descriptors from the questionnaire that describe the sensations you have experienced. Please rate the overall intensity of these sensations on the vertical line between 0 (no sensation) and 100 (maximally tolerable sensation). Finally, please indicate, which of the points you believe have been stimulated and, what your perceived order of stimulation was."

2.6. Analysis of Psychophysical Data. Descriptors chosen by the subjects to describe their sensations were ranked by their absolute frequency (see Table 1). Only those descriptors that were chosen five times or more were taken into account.

Based on subjects' estimation concerning the point selection, that is, the three stimulated points out of four points with attached optodes, results were sorted into four standard categories for every point: hits, misses, correct rejects, and false positives (see Table 2). The sum over all subjects was calculated for each category. A one-tailed Fisher's exact test was used to analyze a possible connection between stimulation and perception. A P value of <0.05 was considered significant.

Finally, the perceived order of stimulation was compared to the actual order.

2.7. Analysis of the Sketched Sensations. In order to compare the localization and extent of the sensations between subjects, a GIS body-map template (front and back) was created in ESRI ArcGIS 10.0 by digitizing the body scheme used in the questionnaire and scaling it to the mean body height of all subjects (175 cm). All body sketches were scanned, transferred into the GIS database, and georeferenced to the body-map template. The database was then populated with the subjects' mapped sensations in point, polyline, and polygon format by digitizing them on-screen from the scanned sketches, and attributing each feature with a key ID and the subject code. For point-like sensations, the radius as drawn in the sketch was added to the attribute table and for line-like and two-dimensional sensations, the line lengths or polygon area, respectively, were calculated in the GIS (see Supplementary Table 1). In the case of multiple objects of the same kind for one subject (e.g., two line-like sensations), these objects were given different roman numbers as indices. Note that GIS calculations in this case were based on a 2D

TABLE 1: The most frequently used descriptors chosen by the subjects to describe their sensations during laser acupuncture. Only descriptors that were chosen by at least five subjects are shown.

Subjects	Descriptors										
	Tingling	Radiating	Spreading	Hot	Dull	Pulsing	Throbbing	Pricking	Stinging	Tender	Pinching
1	X	X									
2	X		X		X					X	
3		X		X			X				
4	X	X	X	X		X	X	X			X
5	X	X	X	X	X	X		X	X		
6	X	X	X		X			X			
7	X	X	X		X	X	X	X	X		
8	X										X
9					X					X	
10				X							
11				X						X	
12	X					X	X			X	
13						X	X	X	X		X
14	X	X	X	X	X	X	X				
15		X	X	X	X					X	
16	X	X	X	X			X	X	X		X
17	X	X	X			X		X	X		X
Sum	11	10	9	8	7	7	7	7	5	5	5

representation of the body, not taking account of the actual 3D surface of the body.

To be able to overlay all sensations in one plot (see Figure 2), lines representing the line-like sensations were converted to polygons by a buffering algorithm in the GIS, resulting in 1.5 cm wide swaths. Point-like sensations were converted to circles using the radius drawn in the sketches by the subjects. All sensations were then overlaid and intersected, resulting in a dataset of overlapping sensation polygons. The choice of 1.5 cm width for the line-like sensations was based on previous literature reports on PSC [21].

2.8. Calculation of Sensation Mean Courses and Comparison to Classical Meridians. Depending on the subject's sensation and way of sketching, the line-like sensations were represented by single or multiple line features, sometimes arranged in parallel or radially. In order to analyze their general direction and compare them to classical meridians, mean courses of all lines related to a certain body part (e.g., lower right leg) were calculated as follows: each line was subdivided into 10 parts of equal length that were numbered 1 to 10 and attributed with their length. For all lines belonging to the same body part, the length-weighted mean center point of each group of sublines with the same part number was then calculated. Finally, the resulting 10 center points were converted back to a polyline, thus representing a mean course and length of the mapped sensations within a given body part. Only sensation mean courses longer than 5 cm were further considered.

To be able to compare sensation mean courses to classical meridians, an approach was needed to incorporate the variability of different literature sources concerning the exact

course of meridians. We decided to include two well-known reference works [22, 23] as well as drawings from two specialists, each with more than 10 years of experience in application and teaching of traditional chinese medicine. While the latter two drew their sketches directly on the body scheme, meridian courses from the reference works were transferred to the schemes by one of the authors (FB). After scanning and georeferencing the sketches, the four versions of all meridians were digitized and added to the GIS database. For each of the four versions, distance maps in the form of raster datasets with 1 cm resolution were computed by calculating the Euclidean distance for each raster cell to the meridian. The four versions were then averaged using Map Algebra, yielding a map of mean distance to each meridian (see Supplementary Figure 2). Using a GIS tool originally developed to extract 3D properties such as mean elevations for features located on a terrain surface, the minimum, maximum, and mean distance for each sensation mean course recorded by the subjects could then be calculated (Table 3, Figures 3 and 4).

3. Results

3.1. Psychophysical Data. The mean intensity of subjects' sensations had a VAS score of 26.47 ± 20.09 (SD) (see Supplementary Table 2).

Subjects chose 7.76 ± 5.23 (mean \pm SD) descriptors for their sensations. Eleven descriptors were chosen by five or more subjects (see Table 1). These were *tingling*, *radiating*, *spreading*, *hot*, *dull*, *pulsing*, *throbbing*, *pricking*, *stinging*, *tender*, and *pinching*. It should be mentioned that some subjects, while filling out the questionnaire, mentioned the

TABLE 2: Comparison of subjects' perceived and actually exerted stimulation. Fisher's exact test was calculated independently for each of the four stimulated points as well as for the overall effect.

Subjects	Left little toe (BL-67)			Right big toe (SP-1)			Left index finger (LI-1)			Right little finger (SI-1)			All points						
	Hits	Misses	Correct rejects	Hits	Misses	False positives	Hits	Misses	Correct rejects	Hits	Misses	False positives	Hits	Misses	Correct rejects	Hits	Misses	False positives	
1			X		X						X					1	2	1	0
2	X			X		X		X						X		3	0	0	1
3	X			X		X		X						X		3	0	1	0
4		X		X				X			X					2	1	0	1
5	X			X				X			X					3	0	1	0
6	X			X				X			X					3	0	1	0
7	X			X				X								3	0	0	1
8		X		X				X								2	1	0	1
9	X			X				X								2	1	1	0
10	X			X				X								2	1	1	0
11		X		X		X		X			X					1	2	0	1
12	X			X				X								1	1	1	0
13	X			X				X								2	1	1	0
14	X			X				X								3	0	0	1
15		X		X		X		X			X					1	2	0	1
16	X			X				X			X					3	0	1	0
17	X			X				X								3	0	1	0
Sum	12	2	1	2	8	4	2	3	10	2	4	1	8	4	3	38	12	10	7
Fisher's exact test	P = 0.46			P = 1.00			P = 0.03			P = 0.26			P = 0.02						

TABLE 3: Distances of sensation mean courses to meridians at the same limb.

	Stimulated point	Front/back	Length of sensation mean course/cm	Meridian	Distance to meridian/cm		
					Min	Mean	Max
Front	Right big toe (SP-1)	f	25.00	SP	0.46	0.83	1.28
	Right big toe (SP-1)	f	25.00	LR	0.61	1.07	2.03
	Right little finger (SI-1)	f	27.07	HT	0.06	1.39	2.53
	Left little toe (BL-67)	f	11.71	KI	4.05	6.27	10.08
Back	Left little toe (BL-67)	b	20.28 (lower line)	BL	1.06	3.38	4.53
	Left little toe (BL-67)	b	16.18 (upper line)	BL	1.22	1.30	1.37
	Left index finger (LI-1)	b	30.35	LI	0.02	0.83	2.53
	Right little finger (SI-1)	b	27.88	SI	0.38	1.30	1.82

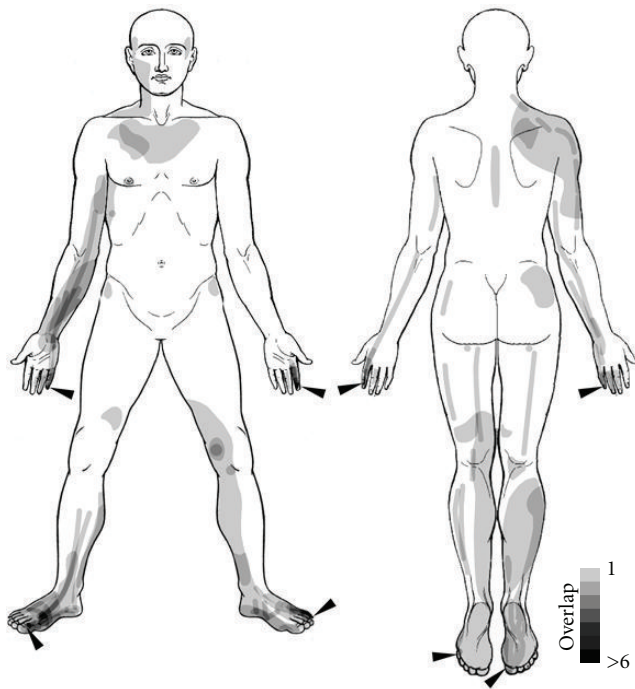


FIGURE 2: Exploratory GIS analysis of subjects' sensations experienced during laser acupuncture. The grey level of the superimposed polygons indicates the number of subjects who experienced a point-like, line-like or 2-dimensional sensation in this area.

lack of the descriptor *warm* that seemed to describe their sensations. As no further explanations by the experimenter were allowed, most of them decided to use the descriptor *hot* instead.

Five subjects correctly identified the three out of four points that had been stimulated (see Table 2). Nine subjects missed one or more points, and seven subjects had false positives, that is, one of the points they chose had not been stimulated. Fisher's exact test over all points (pooled data) was significant ($P < 0.02$) showing a connection between stimulation and perception. For the single points, however, only LI-1 at the left index finger showed a significant result ($P < 0.03$).

Interestingly, the order of stimulation of the points was not estimated correctly by a single subject.

3.2. Sketched Sensations. 13 subjects experienced point-like, 12 line-like, and 13 2-dimensional sensations during laser acupuncture. 10 subjects experienced all three kinds of sensations. The detailed results of the GIS analysis can be found in Supplementary Table 1. While the majority of subjects (10) reported all three kinds of sensations, two subjects drew only points, and one returned an empty body scheme. Excluding the latter three subjects, we can, thus, say that 14 out of 17 subjects (82.4%) experienced PSC. The mean radius of the point-like sensations was 1.67 ± 1.35 cm. Line-like sensations had a mean length of 13.81 ± 11.81 cm, while the average length per subject of all summed up single lines was 38.19 ± 40.50 cm. 2-dimensional sensations had a mean area of 67.31 ± 94.72 cm² or 201.94 ± 222.87 cm², if summed up per subject. Figure 2 shows an overlay of all sensations with dots represented by circles and lines represented by swaths. The majority of sensations were reported from the limbs, while relatively few subjects sketched sensations on the trunk. Point-like sensations were mostly restricted to the stimulation loci. One eye-catching exception was a point experienced by one subject bilaterally at the location of acupuncture point BL-36, directly below the buttock. Furthermore, for the SI Meridian, there was a single subject showing line-like sensations almost along the whole course (see lines in the back shoulder region in the upper right of Figure 3).

3.3. Comparison of Sensation Mean Courses to Classical Meridians. There were eight subregions on the limbs where sensation mean courses could be calculated. These are shown in Figure 3 (for the upper half of the body) and Figure 4 (for the lower half of the body). Three of the mean courses were on the front (inner side of the right arm, inner and outer side of the left arm), and five lines on the back side of the body scheme (inner side of the right leg, sole of the right foot, dorsum of the left foot, and posterior thigh area). The mean length of the sensation mean courses was 12.33 ± 7.32 cm.

The assessment of distances between sensation mean courses and classical meridians (see Table 3) showed an overall good agreement between the two. The smallest mean deviation of the sensation mean from the meridian course was 0.83 cm, seen on the right leg (inner side), where SP-1 had been stimulated, and on the left arm (back side), where LI-1 had been stimulated. For the sole of the foot, no distance

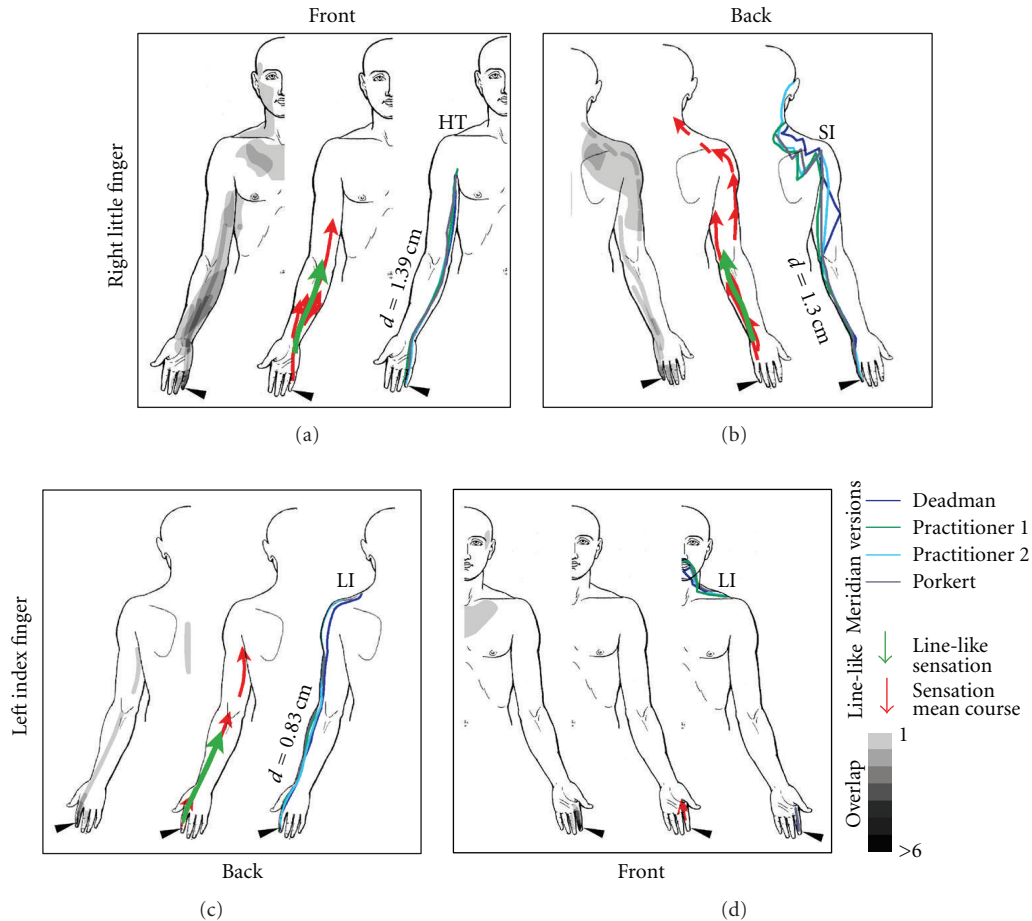


FIGURE 3: Comparison of subjects' sensations and the courses of meridians on the upper body. In each frame, the left image depicts all sensations in the respective quadrant of the body (see also Figure 2). The middle image shows all line-like sensations as well as sensation mean courses. The right image depicts the course of the meridian taking into account differences from the literature. The mean distance of the sensation mean course from the respective meridian as calculated with the GIS is given and denoted with a small d (for explanation see Supplementary Figure 2). For the minimum and maximum distance, the reader is referred to Table 3.

calculation was possible, as neither SP nor LR Meridians traverse this part of the body. On the inner side of the right leg (SP-1), agreement with the sensation mean course was better for the SP Meridian ($d = 0.83$ cm) than for the LR Meridian ($d = 1.07$ cm). However, this clear connection between stimulated point and associated meridian was not always found. For example, sensations on the right arm that should be related to stimulation of the point SI-1, showed good agreement with, both, the SI Meridian ($d = 1.30$ cm) and the HT Meridian ($d = 1.39$ cm). A general observation was the low variance of the distance: Maximum distances of sensation mean courses and meridians were as low as 1.28 cm (for SP-1 and the SP meridian) and 1.37 cm (for BL-67 and the BL meridian), meaning that the sensation never deviated more than this value from the meridian. Minimum distances showed points, where sensation mean courses virtually intersected with meridians (0.02 cm for LI-1 and the LI meridian, 0.06 cm for SI-1 and the HT meridian, and 0.38 cm for SI-1 and the SI meridian). Interestingly, due to our calculation method, such small values also imply a negligible variability in meridian courses. These points,

where all lines come very close to each other, were all located on the distal part of the extremities (see Figure 3).

4. Discussion

In this paper, we have demonstrated the general feasibility of two experimental concepts: firstly, we have shown that propagated sensations along channels (PSC) can be studied under sensory deprivation in a single-blinded design, when using laser acupuncture. Secondly, we applied for the first time a geographic information system (GIS) to the study of PSC phenomena.

We used sensory deprivation in an isolation tank to reduce environmental stimuli (visual, auditory, tactile, and temperature), to allow subjects to fully concentrate on sensations occurring during laser acupuncture stimulation. Judging from the ratio of occurrence of PSC (82.4%) in our experiment, we can say that this strategy seems to be a successful one, as other studies have reported much lower ratios: the largest cohort that has so far been investigated,

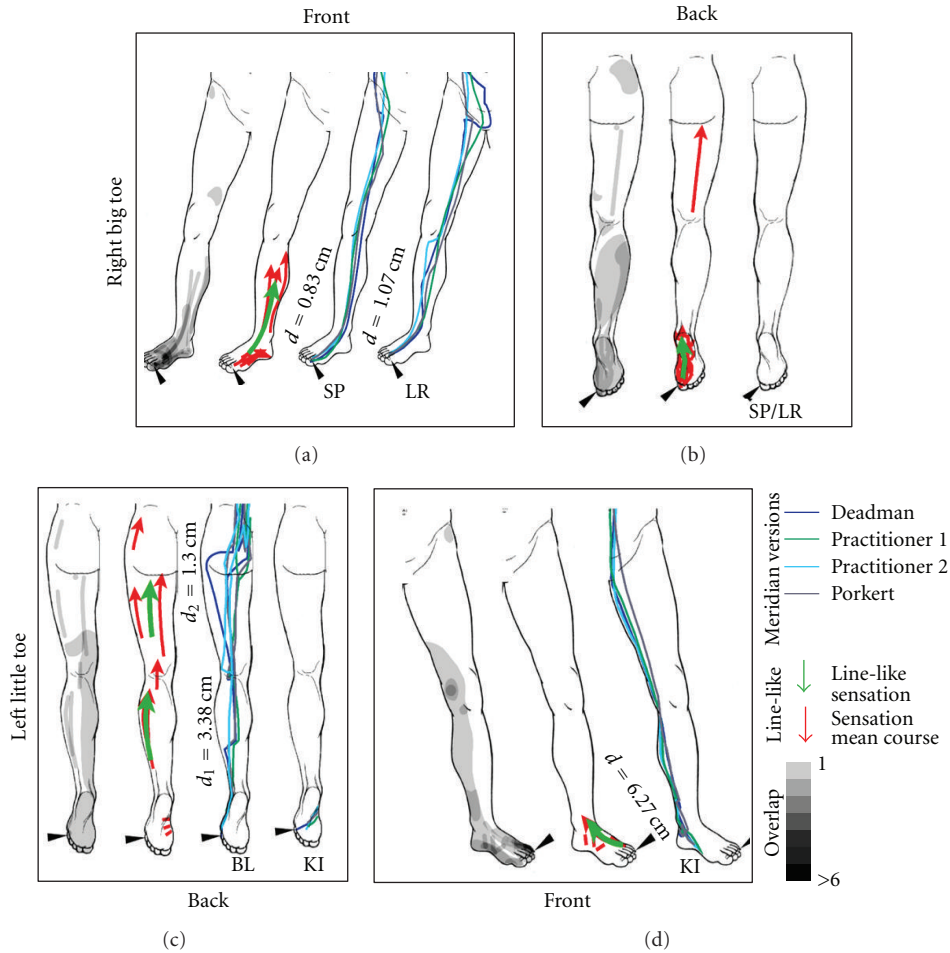


FIGURE 4: Comparison of subjects' sensations and the courses of meridians on the lower body. In each frame, the left image depicts all sensations in the respective quadrant of the body (see also Figure 2). The middle image shows all line-like sensations as well as sensation mean courses. The right image depicts the course of the meridian taking into account differences from the literature. The mean distance of the sensation mean course from the respective meridian as calculated with the GIS is given and denoted with a small d (for explanation see Supplementary Figure 2). For the minimum and maximum distance, the reader is referred to Table 3. Note, that for the right big toe, none of the relevant meridians (SP/LR) runs on the backside of the leg.

comprised incredible 63,228 individuals in more than 20 districts in China in the late 1970s [24]. The authors reached the conclusion that PSC occurs in 20.7% of subjects, although these studies used needles instead of an acupuncture laser. Thus, the use of an isolation tank to study PSC in detail can be recommended despite the increased effort of such an endeavor.

Using laser instead of conventional needle acupuncture produced very similar sensations to those usually reported in studies on the acupuncture sensation *deqi*. *Tingling, radiating, spreading, hot (warm), dull, and throbbing* are descriptors that have often been reported in this context [1, 3, 25]. However, also sham laser acupuncture has previously been reported to induce such sensations [26, 27]. This reminds us of our own observations of false-positive results, when subjects were asked, which points they believed had been stimulated. Only one of the single points (LI-1) showed a significant correlation of stimulation and sensation. Even more strangely, none of the subjects

estimated the stimulation order correctly. Contemplating these results in conjunction with our rather small sample size, we must not neglect the possibility that the actual laser stimulation (i.e., laser on or off) may not be of central importance for the elicitation of *deqi* and PSC. In other words, the phenomenon of PSC may be unrelated to actual laser stimulation taking place. This should be tested in further experiments.

Within the GIS framework, we have introduced a new approach to calculate mean courses of line-like sensations, which now allows group analysis of spatial PSC patterns. This method can be used to compare PSC lines (i.e., sensation mean courses) to any other data, whose spatial pattern can be mapped on a body scheme similar to that used in our study (Supplementary Figure 1), which constitutes an important step forward in the study of the still unknown physiological basis of PSC and its relation to other acupuncture effects. In our study, PSC lines were compared to classical meridians, as this connection has been reported

numerous times before [28]. Despite the purely descriptive character of our analysis, we believe that an average distance between sensation mean courses and meridians of around 1 cm, as observed in our study, clearly points towards a close connection of the two entities. We also sought to include possible variability of meridian courses between different literature sources [29] and, thus, developed an approach to incorporate this variability in the distance measurement by means of Euclidean distance fields. An interesting side observation was that variability seemed to be larger for some meridians than for others. Meridians with a rather smooth course, like HT, LI, KI, and SP showed less variability than those with sharp edges, like SI and BL. Although not the focus of this study, GIS may in general provide a means for further investigation of meridian variability. This should be of importance for the study of the underlying mechanism of PSC as well as acupuncture in general. We speculate that the paradigmatic concept of meridians as small-diameter, line-like vessels with clear anatomical courses cannot withstand closer investigation.

Although this study was more like a proof-of-concept, some limitations need to be addressed:

Firstly, the small sample size precludes a detailed interpretation especially of the results concerning the connection of stimulated and sensed points. Furthermore, a design where only two of the four points had been stimulated, would have probably made the results clearer in the sense that it would have been easier to achieve significant results in Fisher's exact test. One could also argue, that we have not tested, how well the participants of the study were able to remember the sensations after each single laser stimulation. So they may give unreliable answers after receiving three stimulations in a row.

From the GIS-methodological point of view, the use of body schemes as a base map within the GIS is not quite correct, as the complex 3-dimensional shape of the human body is transferred into 2D by a simple orthogonal projection. In cartography, the shape of the Earth is described by 3D bodies such as spheres (for small scales), ellipsoids (usually locally optimized), or the geophysical Geoid model (for highest precision) and transferred to the plane by a map projection. The wide choice of possible projections allows preserving selected metric properties such as areas or local angles. Both 3D models for representing the shape of the Earth and map projection methods are integrated into GIS software, but there is, so far, no "standard human body" model implemented in these systems. In our case, the body maps do not precisely preserve areas or distances, resulting in distortions mainly around the edges of the body maps. Therefore, small differences in calculated distances, for example between meridians running along the middle of the body trunk and along the sides of the body must be interpreted with caution.

Furthermore, our choice of meridians for distance calculation might be criticized, as we did not restrict ourselves to the meridian connected to the stimulated point (e.g., the SP meridian for the point SP-1), but also included other meridians with a known connection to the stimulated finger or toe. This was done, after first results showed that many

subjects experienced PSC following the course of the HT meridian, despite SI-1 being the stimulation locus. Such "jumping" of PSC from one meridian to an adjacent one has been reported from the very beginning of PSC research in China [24] and we believe that despite the obvious connection between PSC and meridians, the latter may be the result of some oversystematization of early PSC observations during the last two millennia.

For the future, it would be desirable to make the transition from descriptive to predictive PSC analyses using GIS. This could be accomplished by including null data for comparison. Such null data may either be generated by some model or by changing the position and shape of existing objects with Monte-Carlo-like methods. Once this is accomplished, *P* values could be calculated expressing the likelihood of findings, like those presented here, thus paving the way to finally understand the physiological underpinnings of *deqi*, PSC, and acupuncture in general.

Acknowledgments

The authors thank floatbase GmbH, Frankfurt (Gunnar Ehrke, Stefan Eckhardt, Mark Neuberger) for their generous and friendly support in carrying out the experiments. F. Beissner thanks Mark Neuberger, Anna Kristina Beissner, and Professor Hans-Georg Schaible for helpful discussions. F. Beissner was supported by Horst Görtz Foundation.

References

- [1] K. K. S. Hui, E. E. Nixon, M. G. Vangel et al., "Characterization of the "deqi" response in acupuncture," *BMC Complementary and Alternative Medicine*, vol. 7, article 33, 2007.
- [2] Z. P. Ji, "Studies on propagated sensation along channels. Present status and future prospects," *Journal of Traditional Chinese Medicine*, vol. 1, no. 1, pp. 3–6, 1981.
- [3] K. K. S. Hui, T. N. Sporko, M. G. Vangel, M. Li, J. Fang, and L. Lao, "Perception of *Deqi* by Chinese and American acupuncturists: a pilot survey," *Chinese Medicine*, vol. 6, article 2, 2011.
- [4] H. Park, J. Park, H. Lee, and H. Lee, "Does *Deqi* (needle sensation) exist?" *American Journal of Chinese Medicine*, vol. 30, no. 1, pp. 45–50, 2002.
- [5] F. Beissner, A. Brandau, C. Henke et al., "Quick discrimination of Adelta and C fiber mediated pain based on three verbal descriptors," *PLoS ONE*, vol. 5, no. 9, Article ID e12944, 2010.
- [6] J. Kong, R. Gollub, T. Huang et al., "Acupuncture *De Qi*, from qualitative history to quantitative measurement," *Journal of Alternative and Complementary Medicine*, vol. 13, no. 10, pp. 1059–1070, 2007.
- [7] M. Margolis, "The pain chart: spatial properties of pain," in *Pain Measurement and Assessment*, R. Melzack, Ed., pp. 309–321, Raven Press, New York, NY, USA, 1983.
- [8] P. A. Longley, M. F. Goodchild, D. J. Maguire, and D. W. Rhind, *Geographic Information Systems and Science*, Wiley, Chichester, UK, 2005.
- [9] J. Snow, *Snow on Cholera: Being a Reprint of Two Papers*, The Commonwealth Fund, New York, NY, USA, 1936.
- [10] A. C. Gatrell and M. Löytönen, *GIS and Health*, Taylor & Francis, London, UK, 1998.

- [11] E. K. Cromley and S. L. McLafferty, *GIS and Public Health*, Guilford Press, New York, NY, USA, 2002.
- [12] G. J. Wang, M. H. Ayati, and W. B. Zhang, "Meridian studies in China: a systematic review," *Journal of Acupuncture and Meridian Studies*, vol. 3, no. 1, pp. 1–9, 2010.
- [13] J. C. Longhurst, "Defining meridians: a modern basis of understanding," *Journal of Acupuncture and Meridian Studies*, vol. 3, no. 2, pp. 67–74, 2010.
- [14] J. Lilly, *The Deep Self, Profound Relaxation and Isolation Tank Technique*, Warner Books, New York, NY, USA, 1977.
- [15] P. Suedfeld and R. A. Borrie, "Health and therapeutic applications of chamber and flotation restricted environmental stimulation therapy (rest)," *Psychology and Health*, vol. 14, no. 3, pp. 545–566, 1999.
- [16] P. Whittaker, "Laser acupuncture: past, present, and future," *Lasers in Medical Science*, vol. 19, no. 2, pp. 69–80, 2004.
- [17] G. Litscher, L. Wang, D. Schikora et al., "Biological effects of painless laser needle acupuncture," *2004 Medical Acupuncture*, vol. 16, pp. 24–29.
- [18] H. Head, "On disturbances of sensation with especial reference to the pain of visceral disease," *Brain*, vol. 16, pp. 1–133, 1893.
- [19] C. Stein and G. Mendl, "The German counterpart to McGill pain questionnaire," *Pain*, vol. 32, no. 2, pp. 251–255, 1988.
- [20] R. Melzack, "The McGill pain questionnaire: major properties and scoring methods," *Pain*, vol. 1, no. 3, pp. 277–299, 1975.
- [21] B. Li, *A Survey of Propagated Sensation Along Channels Phenomenon of 203 Mozambicans. Advances in Acupuncture and Acupuncture Anaesthesia*, The People's Medical Publishing House, Beijing, China, 1980.
- [22] P. Deadman, K. Baker, and M. Al-Khafaji, *A Manual of Acupuncture*, Journal of Chinese Medicine Publications, 1998.
- [23] M. Porkert, C. Hempen, J. Bao et al., *Classical Acupuncture—The Standard Textbook*, Phainon, Dinkelscherben, Germany, 1995.
- [24] Cooperative Group of Investigation of PSC, *A Survey of Occurrence of the Propagated Sensation Along Channels (PSC) in the Mass and Its Basic Properties*, Advances in Acupuncture and Acupuncture Anaesthesia, 1980.
- [25] P. White, F. Bishop, H. Hardy et al., "Southampton needle sensation questionnaire: development and validation of a measure to gauge acupuncture needle sensation," *Journal of Alternative and Complementary Medicine*, vol. 14, no. 4, pp. 373–379, 2008.
- [26] N. Salih, P. I. Bäuml, M. Simang, and D. Irnich, "Deqi sensations without cutaneous sensory input: results of an RCT," *BMC Complementary and Alternative Medicine*, vol. 10, article 81, 2010.
- [27] D. Irnich, N. Salih, M. Offenbächer, and J. Fleckenstein, "Is sham laser a valid control for acupuncture trials?" *Evidence-Based Complementary and Alternative Medicine*, vol. 2011, Article ID 485945, 8 pages, 2011.
- [28] Z. Zongxiang, Y. Zhiqiang, and Y. Shuzhang, "Studies on the phenomenon of latent propagated sensation along the channels. I. The discovery of a latent PSC and a preliminary study of its skin electrical conductance," *American Journal of Chinese Medicine*, vol. 9, no. 3, pp. 216–224, 1981.
- [29] I. F. Tao, "A critical evaluation of acupuncture research: physiologization of Chinese medicine in Germany," *East Asian Science, Technology and Society*, vol. 2, no. 4, pp. 507–524, 2009.

Research Article

Effects of Moxibustion Stimulation on the Intensity of Infrared Radiation of Tianshu (ST25) Acupoints in Rats with Ulcerative Colitis

Xiaomei Wang,¹ Shuang Zhou,^{1,2} Wei Yao,³ Hua Wan,⁴ Huangan Wu,¹ Luyi Wu,¹ Huirong Liu,¹ Xuegui Hua,¹ and Peifeng Shi¹

¹Key Laboratory of Acupuncture-Moxibustion and Immunological Effects, Shanghai University of Traditional Chinese Medicine, Shanghai 200030, China

²Department of Traditional Chinese Medicine, The Second Military Medical University, Shanghai 200433, China

³Department of Mechanics and Engineering Science, Fudan University, Shanghai 200433, China

⁴Division of Surgery of Chinese Medicine, Shuguang Hospital, Shanghai University of Traditional Chinese Medicine, Shanghai 201203, China

Correspondence should be addressed to Huangan Wu, wuhuangan@126.com

Received 14 August 2012; Revised 7 October 2012; Accepted 14 October 2012

Academic Editor: Wolfgang Schwarz

Copyright © 2012 Xiaomei Wang et al. This is an open access article distributed under the Creative Commons Attribution License, which permits unrestricted use, distribution, and reproduction in any medium, provided the original work is properly cited.

ST25 is a key acupoint used in the treatment of ulcerative colitis by moxibustion stimulation, but the biophysical mechanism underlying its effects is still unknown. The aim of the present study was to explore the biophysical properties of ST25 acupoint stimulated by moxibustion in a rat model of ulcerative colitis. The infrared radiation intensity of fourteen wavelengths of ST25 showed significant differences between the normal and model control groups. The intensity of infrared radiation of forty wavelengths showed significant differences compared with the corresponding control points in normal rats. The intensity of infrared radiation of twenty-eight wavelengths showed significant differences compared with the corresponding control points in model rats. The intensity of infrared radiation of nine wavelengths in the herb-partition moxibustion group, eighteen wavelengths in the ginger-partition moxibustion group, seventeen wavelengths in the garlic-partition moxibustion group, and fourteen wavelengths in the warming moxibustion group of the left ST25 showed significant differences compared with that of the model control group. For the right-hand-side ST25, these values were 33, 33, 2, and 8 wavelengths, respectively. This indicated that one possible biophysical mechanism of moxibustion on ST25 in ulcerative colitis model rats might involve changes in the intensity of infrared radiation of ST25 at different wavelengths.

1. Introduction

The human body is a biological heater that emits infrared rays. Infrared rays can be easily absorbed by objects and penetrate deep into the tissues, where they are transformed into internal energy. The human body is both a source and absorber of infrared radiation [1, 2]. The reported research indicates a significant difference between the infrared radiation patterns of healthy persons and ill ones [3–5]. Infrared radiation can be absorbed if acupuncture points are stimulated by moxibustion [6, 7].

Moxibustion is a reputable alternative and complementary therapy with a history of use in eastern countries

spanning many thousands of years. Its therapeutic effects depend on meridians and acupoints of the human body [8–11]. Over the past few years, research teams have used thermal infrared imaging to study the patterns of infrared radiation on the surface of the human body along the meridian channel [12, 13]. Studies have found that the infrared radiation spectra of the acupuncture points specifically related to disease changes under disease conditions. In certain morbid conditions of the human body, the infrared radiation of acupoints can differ significantly on the heart meridian and pericardium meridian in patients with coronary artery diseases [14–16]. Patients with chronic stomachaches are distinguished by the patterns of infrared

radiation at the stomach Shu (BL21) and Zusanli (ST36) acupoints [17, 18]. Studies have shown a correlation between the meridians and viscera, and the meridian function is closely related to infrared transmission inside and outside of human body [19, 20]. Research has shown that the radiation spectra of moxibustion with ginger, garlic, and monkshood cake were identical to those of healthy human bodies but different from those of bodies subjected to moxa-moxibustion [21]. The acupoints and their infrared resonance radiation patterns have been shown to play an important role in indirect moxibustion stimulation [22, 23]. This indicates that there may be an internal link between moxibustion, acupoints, and meridians that involves infrared transmission.

Tianshu (ST25) points are key acupoints in stomach channel of foot yangming, and moxibustion is an intrinsic part of traditional Chinese medicine (TCM). In clinical practice, acupuncturists apply moxibustion at the specific acupuncture points to treat the corresponding diseases of the viscera; this treatment has been shown to be effective. Research has indicated that moxibustion can modulate gastrointestinal functions [24]. Acupuncture and moxibustion at ST25 can alleviate symptoms and improve quality of life in patients with ulcerative colitis (UC) [25–27]. They have also been shown to improve immune function in UC model rats [28–30]. Our previous study indicated that both Hegu (LI4) and Shangjuxu (ST37) involve changes in infrared radiation spectra in UC patients with intestinal lesions [31]. However, the biophysical mechanism of ST25 stimulated by moxibustion in UC remains unknown.

The present study was performed to establish an UC model in rats, to investigate the intensity of infrared radiation of ST25 stimulated by moxibustion, and to explore the biophysical properties of ST25 acupoint in UC model rats.

2. Materials and Methods

2.1. Experimental Animals and Model Establishment. Sixty male Sprague-Dawley (SD) rats (weighing 140 ± 20 g) were obtained from the Experimental Animal Center of Shanghai University of Traditional Chinese Medicine. Five male rats were housed in a cage at room temperature ($22 \pm 2^\circ\text{C}$) and $60 \pm 5\%$ humidity. All rats were performed in strict accordance with the National Institutions of Health Guide for the Care and Use of Laboratory Animals. This study was approved by the Ethics Committee of Yueyang Hospital, which is affiliated with Shanghai University of Traditional Chinese Medicine, China. After three days, the 60 rats were randomly divided into the following experimental groups: normal ($n = 10$), model ($n = 10$), herb-partition moxibustion (HPM) ($n = 10$), ginger-partition moxibustion (GPM) ($n = 10$), garlic-partition moxibustion (GLM) ($n = 10$), and warming moxibustion (WM) ($n = 10$).

The UC rat model was established using an immunological method and local stimulation [32]. In brief, fresh human colonic mucosa was obtained from surgical colonic specimens, homogenized in normal saline, and centrifuged

for 30 min at 3000 rpm. The supernatant, containing antigens released from colon of UC patients, was diluted to an appropriate protein concentration and mixed with Freund's adjuvant (Shanghai Chemical Reagent Company, Shanghai, China). One milliliter of the antigen-adjuvant mixture containing a total of 6 mg protein was injected into the front footpad of each rat on day 0. After this initial dose, the same mixture was then injected into the rear footpad, dorsa, inguina, and abdominal cavities on days 10, 17, 24, and 31, respectively. On day 38, in order to stimulate the colonic immune response, rats were anesthetized intraperitoneally with 2% pentobarbital sodium (30 mg/kg) and a 3 mL enema of 3% formalin was administered for 1 hour, then washed with saline, and a 2 mL enema of antigen fluid (without Freund's adjuvant) lasting 2 hours was performed. One rat in model group died of intestinal perforation.

The establishment of the UC rat model was confirmed using hematoxylin-eosin (HE) for pathological observation.

2.2. Moxibustion Stimulation. After the UC model was established in the rats, four moxibustion stimulations were performed during days 39–46 in the moxibustion groups, and anesthesia was not applied. Rat holders (Beijing Jintotai Technology Development Co., Ltd. China) were used to hold the animals in position.

HPM ($n = 10$): as indicated in Figure 1, moxa cones (Figure 1A) (0.5 cm in diameter and 0.6 cm high) (Nanyang Hanyi Moxa Co., Ltd. China) were placed vertically on a medicinal formula (diameter 0.5 cm, height 0.3 cm) composed of radix aconite, cortex, radix, carthami, and salviae miltiorrhizae (Figure 1B). The medicinal formula was then placed on ST25 acupoints [33, 34]. The moxa cones were then ignited, and each acupoint was treated twice lasting 15 min.

GPM ($n = 10$): as indicated in Figure 1, moxa cones were placed vertically on a fresh ginger (diameter 0.5 cm, high 0.3 cm) instead of medicinal formula (Figure 1B). The fresh ginger was then placed on ST25 acupoints. The moxa cones were then ignited, and each acupoint was treated twice lasting 15 min.

GLM ($n = 10$): as indicated in Figure 1, moxa cones were placed vertically on a fresh garlic (diameter 0.5 cm, height 0.3 cm) instead of medicinal formula (Figure 1B). The fresh garlic was then placed on ST25 acupoints. The moxa cones were then ignited, and each acupoint was treated twice lasting 15 min.

WM ($n = 10$): as indicated in Figure 2, the moxa stick (Figure 2A) (diameter 0.5 cm, length 20 cm) was ignited and hung 2 cm above the ST25 acupoints (Figure 2B). Each acupoint was treated once for 10 min.

NC ($n = 10$): no treatment. The same fixation as the moxibustion groups was administered.

MC ($n = 10$): no treatment. The same fixation as the moxibustion groups was administered.

All treatments were repeated once daily for a total of 14 d [35].

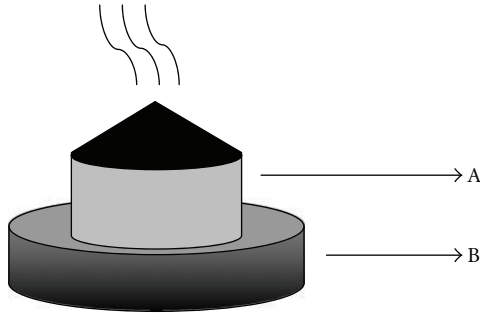


FIGURE 1: Sketch of herb-partition moxibustion. A: Moxa segment. B: Herb-tablet.

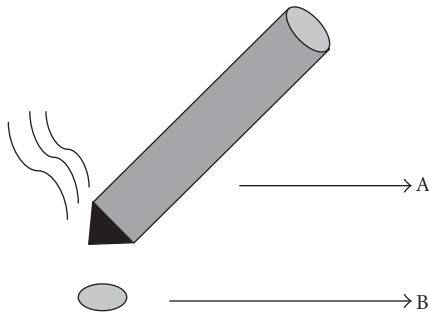


FIGURE 2: Sketch of warm moxibustion. A: Moxa stick. B: Acupoint.

2.3. Morphological Observation of Colon Samples. After the infrared measurements finished, all rats were killed by cervical dislocation. The samples were collected from the descending colon (5 cm above the anus) and cleaned with normal saline. General morphology was then assessed and scored. The samples were fixed in 10% formalin, dehydrated, embedded in paraffin, and sectioned into 4 μm thick slices. These sections were then stained with hematoxylin-eosin for pathological observation [36].

2.4. Detection of the Intensity of Infrared Radiation. A hypersensitivity PHE201 infrared spectrum analyzer was used to detect the intensity of infrared radiation on bilateral ST25 and negative control points (0.5 cm from ST25) of experimental rats. The 59 measurement wavelengths range from 1.5–16 μm [1, 22].

In the morning of the next day after moxibustion treatments finished, all rats were brought into a darkroom. None were anesthetized. The room was maintained at $22 \pm 3^\circ\text{C}$ room temperature and $55 \pm 10\%$ humidity and it had no obvious airflow, strong noises, or electromagnetic fields. Thirty minutes later, the acupoints were defatted using 75% alcohol. An analyzer probe (diameter 3 mm) (Figure 3) was gently placed on the acupoints. The analyzer was initialized to scan the wavelengths from 1.5 to 6 μm . The analyzer automatically recorded the intensity of infrared radiation at a total of 59 detection points every 0.25 μm .

2.5. Statistical Analysis. All data were analyzed using SPSS 11.0 statistical software (SPSS Inc., USA). All data are

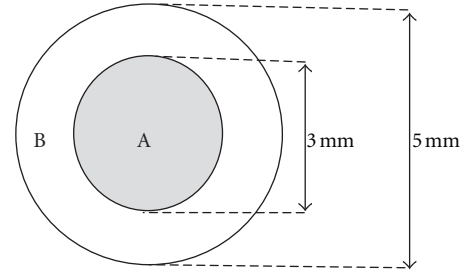


FIGURE 3: Sketch of points of detection and moxibustion stimulation. A: Point of detection. B: Point of moxibustion stimulation.

expressed as mean \pm SD for normally distributed continuous variables. Rank-sum testing was used to compare the four moxibustion groups with normal and model control groups. The pairing rank-sum test was used to compare the right- and left-hand-side acupoints. $P < 0.05$ was considered statistically significant.

3. Results

3.1. Morphological Observation of UC Rat Model [37]. As shown in Figure 4, the NC group showed complete colonic mucosa epithelium and regular colonic gland with inconspicuous inflammatory cell infiltration. The colonic mucosa and mucosa villi were damaged or missing in the UC model group, and large numbers of mononuclear cells and macrophages appeared in the mucosa or submucosa. There was also more congestion, edema, and ulceration than in the normal group. However, moxibustion stimulation with herbs, ginger, garlic, and moxa sticks decreased the inflammatory cell infiltration and improved the condition of the colonic mucosa and mucosa villi. Only slight submucosal edema and inflammatory cell infiltration were observed in the treated groups, and the colonic mucosa epithelium and the colonic gland were more regularly arranged in all treated groups except the mild moxibustion group than in the model group. New epithelial cells were observed, covering the ulcers. This indicates that moxibustion treatment can inhibit inflammatory cell infiltration under UC conditions and induce recovery of these ulcers in the colon tissue.

3.2. Infrared Spectrum Characteristic of ST25 and Control Points. Each curve showed the average infrared radiation of ST25 in rats from each group. The intensity of infrared radiation of ST25 showed significant individual and intergroup differences, but each group showed the same spectral peak. The first peak value appeared at about 10 μm , and the second, which was weaker than the first, appeared at about 13.75 μm .

3.3. Intensity of Infrared Radiation at ST25 and Control Points in Normal Rats (Table 1). NC group rats showed significant differences in the intensity of infrared radiation of the left ST25 and control point at 4.00, 4.75, 5.00, 5.50, 6.25, 6.50, 6.75, 15.50, and 16.00 μm ($P < 0.05$) and extremely significant differences at 5.25 μm ($P < 0.01$). On the right side, the intensity of infrared radiation of ST25 differed

TABLE 1: Intensity of infrared radiation of ST25 and the control points in normal rats (mean \pm SD).

WL (μm)	N	L-ST25	L-ST25-N	R-ST25	R-ST25-N
1.50	10	0.032 \pm 0.027	0.041 \pm 0.018	0.035 \pm 0.024	0.031 \pm 0.013
1.75	10	-0.002 \pm 0.022	0.004 \pm 0.027	0.001 \pm 0.022	-0.005 \pm 0.030
2.00	10	0.002 \pm 0.025	-0.001 \pm 0.023	-0.002 \pm 0.024	-0.004 \pm 0.027
2.25	10	-0.003 \pm 0.021	0.008 \pm 0.019	0.005 \pm 0.020	0.007 \pm 0.023
2.50	10	-0.003 \pm 0.020	0.005 \pm 0.025	0.005 \pm 0.029	-0.003 \pm 0.024
2.75	10	-0.004 \pm 0.022	0.005 \pm 0.023	0.001 \pm 0.022	-0.002 \pm 0.031
3.00	10	-0.006 \pm 0.019	0.007 \pm 0.034	0.002 \pm 0.025	-0.002 \pm 0.030
3.25	10	0.001 \pm 0.019	0.007 \pm 0.019	0.005 \pm 0.023	0.004 \pm 0.026
3.50	10	0.023 \pm 0.020	0.035 \pm 0.031	0.021 \pm 0.028	0.028 \pm 0.030
3.75	10	0.019 \pm 0.029	0.025 \pm 0.020	0.032 \pm 0.031	0.036 \pm 0.028
4.00	10	0.006 \pm 0.023	0.031 \pm 0.023 ^Δ	0.016 \pm 0.015	0.024 \pm 0.028
4.25	10	0.037 \pm 0.023	0.058 \pm 0.020	0.048 \pm 0.021	0.060 \pm 0.033
4.50	10	0.067 \pm 0.018	0.075 \pm 0.028	0.068 \pm 0.021	0.082 \pm 0.032
4.75	10	0.063 \pm 0.030	0.094 \pm 0.024 ^Δ	0.076 \pm 0.029	0.092 \pm 0.037
5.00	10	0.074 \pm 0.020	0.099 \pm 0.030 ^Δ	0.094 \pm 0.025	0.100 \pm 0.031
5.25	10	0.079 \pm 0.024	0.118 \pm 0.026 ^{ΔΔ}	0.106 \pm 0.024*	0.123 \pm 0.025
5.50	10	0.059 \pm 0.023	0.086 \pm 0.026 ^Δ	0.082 \pm 0.022*	0.095 \pm 0.026
5.75	10	0.048 \pm 0.020	0.064 \pm 0.026	0.057 \pm 0.017	0.070 \pm 0.040
6.00	10	0.066 \pm 0.024	0.086 \pm 0.028	0.082 \pm 0.017	0.103 \pm 0.031
6.25	10	0.044 \pm 0.023	0.070 \pm 0.027 ^Δ	0.068 \pm 0.026*	0.075 \pm 0.026
6.50	10	0.046 \pm 0.022	0.078 \pm 0.026 ^Δ	0.059 \pm 0.028	0.077 \pm 0.030
6.75	10	0.143 \pm 0.026	0.182 \pm 0.032 ^Δ	0.147 \pm 0.038	0.174 \pm 0.050
7.00	10	0.224 \pm 0.040	0.275 \pm 0.032	0.230 \pm 0.065	0.274 \pm 0.078
7.25	10	0.322 \pm 0.055	0.365 \pm 0.066	0.341 \pm 0.076	0.395 \pm 0.087
7.50	10	0.374 \pm 0.058	0.422 \pm 0.070	0.393 \pm 0.064	0.455 \pm 0.081
7.75	10	0.404 \pm 0.066	0.458 \pm 0.073	0.428 \pm 0.077	0.493 \pm 0.090
8.00	10	0.473 \pm 0.075	0.522 \pm 0.094	0.477 \pm 0.087	0.563 \pm 0.104 ^Δ
8.25	10	0.480 \pm 0.080	0.541 \pm 0.079	0.509 \pm 0.086	0.606 \pm 0.118 ^Δ
8.50	10	0.494 \pm 0.077	0.555 \pm 0.094	0.519 \pm 0.095	0.609 \pm 0.103 ^Δ
8.75	10	0.571 \pm 0.078	0.642 \pm 0.114	0.590 \pm 0.105	0.684 \pm 0.130
9.00	10	0.660 \pm 0.100	0.744 \pm 0.122	0.686 \pm 0.122	0.808 \pm 0.152 ^Δ
9.25	10	0.690 \pm 0.099	0.794 \pm 0.140	0.721 \pm 0.134	0.865 \pm 0.157 ^Δ
9.50	10	0.750 \pm 0.096	0.856 \pm 0.149	0.791 \pm 0.133	0.923 \pm 0.161 ^Δ
9.75	10	0.809 \pm 0.118	0.911 \pm 0.161	0.850 \pm 0.138	0.997 \pm 0.163 ^Δ
10.00	10	0.846 \pm 0.123	0.953 \pm 0.162	0.892 \pm 0.150	1.043 \pm 0.176 ^Δ
10.25	10	0.835 \pm 0.135	0.936 \pm 0.141	0.874 \pm 0.138	1.047 \pm 0.173 ^Δ
10.50	10	0.739 \pm 0.140	0.825 \pm 0.138	0.768 \pm 0.117	0.933 \pm 0.157 ^Δ
10.75	10	0.655 \pm 0.121	0.732 \pm 0.120	0.679 \pm 0.118	0.834 \pm 0.144 ^{ΔΔ}
11.00	10	0.580 \pm 0.115	0.658 \pm 0.108	0.620 \pm 0.110	0.753 \pm 0.123 ^Δ
11.25	10	0.548 \pm 0.094	0.613 \pm 0.100	0.556 \pm 0.094	0.683 \pm 0.121 ^{ΔΔ}
11.50	10	0.496 \pm 0.090	0.549 \pm 0.091	0.501 \pm 0.093	0.627 \pm 0.123 ^{ΔΔ}
11.75	10	0.433 \pm 0.086	0.488 \pm 0.090	0.448 \pm 0.085	0.559 \pm 0.098 ^{ΔΔ}
12.00	10	0.407 \pm 0.067	0.466 \pm 0.073	0.427 \pm 0.072	0.510 \pm 0.080 ^Δ
12.25	10	0.410 \pm 0.057	0.466 \pm 0.065	0.430 \pm 0.061	0.518 \pm 0.086 ^{ΔΔ}
12.50	10	0.387 \pm 0.064	0.445 \pm 0.070	0.420 \pm 0.074	0.511 \pm 0.088 ^{ΔΔ}
12.75	10	0.359 \pm 0.077	0.409 \pm 0.082	0.385 \pm 0.070	0.460 \pm 0.085 ^Δ
13.00	10	0.362 \pm 0.065	0.415 \pm 0.058	0.372 \pm 0.067	0.449 \pm 0.075 ^Δ
13.25	10	0.462 \pm 0.054	0.529 \pm 0.088	0.465 \pm 0.092	0.534 \pm 0.109
13.50	10	0.587 \pm 0.073	0.661 \pm 0.110	0.605 \pm 0.101	0.699 \pm 0.124 ^Δ
13.75	10	0.590 \pm 0.092	0.660 \pm 0.119	0.616 \pm 0.106	0.735 \pm 0.133 ^Δ
14.00	10	0.509 \pm 0.113	0.560 \pm 0.107	0.531 \pm 0.100	0.651 \pm 0.123 ^Δ

TABLE 1: Continued.

WL (μm)	N	L-ST25	L-ST25-N	R-ST25	R-ST25-N
14.25	10	0.426 \pm 0.095	0.485 \pm 0.085	0.467 \pm 0.098	0.561 \pm 0.108 ^Δ
14.50	10	0.363 \pm 0.076	0.416 \pm 0.072	0.399 \pm 0.083	0.487 \pm 0.092 ^Δ
14.75	10	0.258 \pm 0.072	0.299 \pm 0.058	0.286 \pm 0.066	0.356 \pm 0.060 ^Δ
15.00	10	0.205 \pm 0.058	0.240 \pm 0.040	0.227 \pm 0.059	0.278 \pm 0.054 ^Δ
15.25	10	0.177 \pm 0.050	0.200 \pm 0.031	0.190 \pm 0.043	0.226 \pm 0.038 ^Δ
15.50	10	0.178 \pm 0.033	0.212 \pm 0.026 ^Δ	0.201 \pm 0.041	0.241 \pm 0.033 ^Δ
15.75	10	0.172 \pm 0.037	0.198 \pm 0.026	0.192 \pm 0.029	0.234 \pm 0.042 ^{ΔΔ}
16.00	10	0.137 \pm 0.038	0.168 \pm 0.034 ^Δ	0.170 \pm 0.026*	0.195 \pm 0.036

WL: wavelength, L-ST25: left ST25, L-ST25-N: left ST25 control point, R-ST25: right ST25, R-ST25-N: right control point. The intensity of the left-hand-side infrared radiation of ST25 in normal rats is significantly different from that of right-hand-side ST25 (* $P < 0.05$, ** $P < 0.01$). The intensity of infrared radiation of ST25 in normal rats is significantly different from that of the ipsilateral control point (^Δ $P < 0.05$, ^{ΔΔ} $P < 0.01$).

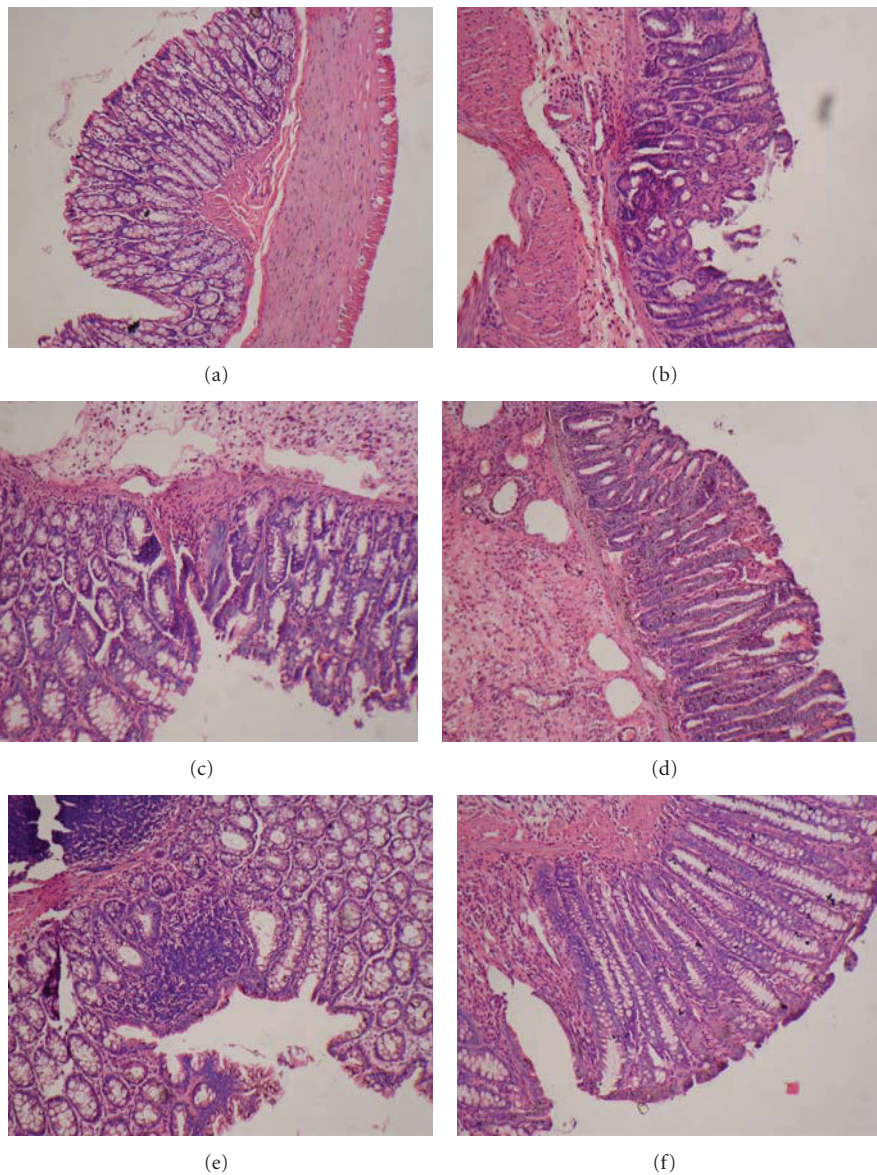


FIGURE 4: Morphological observation of UC rat model. (a) Normal group. (b) Model group. (c) Herb-partition moxibustion group. (d) Ginger-partition moxibustion group. (e) Garlic-partition moxibustion group. (f) Warming moxibustion group.

TABLE 2: Intensity of infrared radiation of ST25 and the control points in UC model rats (mean \pm SD).

WL (μm)	N	L-ST25	L-ST25-N	R-ST25	R-ST25-N
1.50	9	-0.003 \pm 0.035	0.023 \pm 0.025 ^A	0.009 \pm 0.014	0.010 \pm 0.022
1.75	9	0.005 \pm 0.025	0.013 \pm 0.024	0.021 \pm 0.028	0.016 \pm 0.021
2.00	9	0.017 \pm 0.030	0.026 \pm 0.021	0.007 \pm 0.025	0.020 \pm 0.030
2.25	9	0.008 \pm 0.033	0.016 \pm 0.024	0.018 \pm 0.026	0.025 \pm 0.023
2.50	9	0.022 \pm 0.018	0.018 \pm 0.023	0.013 \pm 0.027	0.022 \pm 0.025
2.75	9	0.024 \pm 0.019	0.025 \pm 0.020	0.022 \pm 0.017	0.028 \pm 0.019
3.00	9	0.021 \pm 0.023	0.023 \pm 0.022	0.029 \pm 0.021	0.025 \pm 0.020
3.25	9	0.015 \pm 0.030	0.027 \pm 0.023	0.016 \pm 0.024	0.028 \pm 0.028
3.50	9	0.030 \pm 0.021	0.045 \pm 0.027	0.036 \pm 0.026	0.052 \pm 0.029
3.75	9	0.043 \pm 0.017	0.053 \pm 0.020	0.039 \pm 0.022	0.051 \pm 0.030
4.00	9	0.031 \pm 0.033	0.040 \pm 0.033	0.038 \pm 0.036	0.034 \pm 0.031
4.25	9	0.059 \pm 0.035	0.075 \pm 0.036	0.077 \pm 0.041	0.071 \pm 0.042
4.50	9	0.073 \pm 0.018	0.091 \pm 0.014	0.074 \pm 0.025	0.093 \pm 0.028
4.75	9	0.084 \pm 0.023	0.107 \pm 0.021 ^A	0.096 \pm 0.026	0.103 \pm 0.020
5.00	9	0.085 \pm 0.016	0.105 \pm 0.022 ^A	0.087 \pm 0.019	0.112 \pm 0.022 ^A
5.25	9	0.109 \pm 0.041	0.124 \pm 0.035	0.121 \pm 0.039	0.128 \pm 0.030
5.50	9	0.079 \pm 0.022	0.101 \pm 0.028	0.088 \pm 0.030	0.111 \pm 0.028
5.75	9	0.070 \pm 0.019	0.086 \pm 0.028	0.075 \pm 0.029	0.084 \pm 0.025
6.00	9	0.095 \pm 0.028	0.111 \pm 0.027	0.102 \pm 0.024	0.116 \pm 0.024
6.25	9	0.065 \pm 0.019	0.078 \pm 0.023	0.073 \pm 0.034	0.085 \pm 0.029
6.50	9	0.062 \pm 0.033	0.082 \pm 0.035	0.067 \pm 0.035	0.084 \pm 0.032
6.75	9	0.164 \pm 0.028	0.170 \pm 0.021	0.165 \pm 0.039	0.191 \pm 0.037
7.00	9	0.232 \pm 0.030	0.246 \pm 0.032	0.234 \pm 0.042	0.282 \pm 0.049 ^A
7.25	9	0.328 \pm 0.049	0.348 \pm 0.023	0.334 \pm 0.053	0.394 \pm 0.049 ^{AA}
7.50	9	0.359 \pm 0.054	0.378 \pm 0.046	0.378 \pm 0.074	0.452 \pm 0.067 ^A
7.75	9	0.408 \pm 0.066	0.414 \pm 0.041	0.408 \pm 0.078	0.492 \pm 0.065 ^{AA}
8.00	9	0.457 \pm 0.075	0.482 \pm 0.035	0.472 \pm 0.078	0.559 \pm 0.076 ^A
8.25	9	0.474 \pm 0.075	0.504 \pm 0.055	0.484 \pm 0.088	0.586 \pm 0.087 ^{AA}
8.50	9	0.482 \pm 0.072	0.506 \pm 0.060	0.491 \pm 0.081	0.590 \pm 0.084 ^{AA}
8.75	9	0.546 \pm 0.088	0.575 \pm 0.056	0.569 \pm 0.088	0.671 \pm 0.095 ^A
9.00	9	0.635 \pm 0.095	0.666 \pm 0.072	0.657 \pm 0.105	0.792 \pm 0.117 ^{AA}
9.25	9	0.671 \pm 0.104	0.705 \pm 0.070	0.698 \pm 0.102	0.835 \pm 0.102 ^{AA}
9.50	9	0.738 \pm 0.114	0.788 \pm 0.072	0.772 \pm 0.115	0.912 \pm 0.113 ^{AA}
9.75	9	0.778 \pm 0.117	0.824 \pm 0.090	0.805 \pm 0.124	0.946 \pm 0.126 ^A
10.00	9	0.791 \pm 0.113	0.834 \pm 0.095	0.817 \pm 0.131	0.971 \pm 0.116 ^{AA}
10.25	9	0.791 \pm 0.117	0.827 \pm 0.093	0.814 \pm 0.134	0.964 \pm 0.118 ^A
10.50	9	0.676 \pm 0.118	0.715 \pm 0.100	0.711 \pm 0.126	0.852 \pm 0.119 ^A
10.75	9	0.600 \pm 0.099	0.642 \pm 0.086	0.633 \pm 0.115	0.742 \pm 0.111 ^A
11.00	9	0.551 \pm 0.097	0.588 \pm 0.083	0.573 \pm 0.111	0.660 \pm 0.097
11.25	9	0.505 \pm 0.081	0.549 \pm 0.090	0.541 \pm 0.107	0.616 \pm 0.104
11.50	9	0.456 \pm 0.091	0.485 \pm 0.078	0.488 \pm 0.095	0.567 \pm 0.085
11.75	9	0.415 \pm 0.086	0.447 \pm 0.061	0.433 \pm 0.092	0.513 \pm 0.069 ^A
12.00	9	0.377 \pm 0.067	0.414 \pm 0.045	0.407 \pm 0.069	0.474 \pm 0.062 ^A
12.25	9	0.383 \pm 0.065	0.430 \pm 0.061	0.413 \pm 0.070	0.473 \pm 0.070
12.50	9	0.385 \pm 0.057	0.414 \pm 0.047	0.402 \pm 0.065	0.473 \pm 0.070 ^A
12.75	9	0.377 \pm 0.060	0.396 \pm 0.050	0.380 \pm 0.069	0.453 \pm 0.059 ^A
13.00	9	0.351 \pm 0.074	0.385 \pm 0.047	0.365 \pm 0.070	0.440 \pm 0.061 ^A
13.25	9	0.447 \pm 0.072	0.477 \pm 0.050	0.465 \pm 0.068	0.548 \pm 0.077 ^A
13.50	9	0.554 \pm 0.071	0.590 \pm 0.046	0.578 \pm 0.091	0.674 \pm 0.092 ^A
13.75	9	0.555 \pm 0.092	0.597 \pm 0.070	0.580 \pm 0.091	0.677 \pm 0.097 ^A
14.00	9	0.454 \pm 0.091	0.488 \pm 0.073	0.473 \pm 0.095	0.564 \pm 0.089 ^A

TABLE 2: Continued.

WL (μm)	N	L-ST25	L-ST25-N	R-ST25	R-ST25-N
14.25	9	0.396 \pm 0.078	0.444 \pm 0.066	0.423 \pm 0.086	0.500 \pm 0.091
14.50	9	0.351 \pm 0.076	0.383 \pm 0.070	0.375 \pm 0.074	0.444 \pm 0.073
14.75	9	0.255 \pm 0.048	0.288 \pm 0.051	0.267 \pm 0.064	0.312 \pm 0.053
15.00	9	0.217 \pm 0.041	0.238 \pm 0.043	0.221 \pm 0.050	0.254 \pm 0.041
15.25	9	0.185 \pm 0.032	0.202 \pm 0.030	0.196 \pm 0.040	0.215 \pm 0.049
15.50	9	0.196 \pm 0.035	0.205 \pm 0.035	0.201 \pm 0.044	0.221 \pm 0.041
15.75	9	0.193 \pm 0.026	0.211 \pm 0.035	0.208 \pm 0.037	0.219 \pm 0.040
16.00	9	0.158 \pm 0.030	0.171 \pm 0.033	0.164 \pm 0.035	0.180 \pm 0.040

WL: wavelength, L-ST25: left ST25, L-ST25-N: left ST25 control point, R-ST25: right ST25, R-ST25-N: right control point. The intensity of infrared radiation of ST25 in model rats was found to be significantly different from that of the ipsilateral control point ($^{\Delta}P < 0.05$, $^{\Delta\Delta}P < 0.01$).

significantly from control point at 8.00, 8.25, 8.50, 9.00, 9.25, 9.5, 9.75, 10.00, 10.25, 10.50, 11.00, 12.00, 12.75, 13.00, 13.50, 13.75, 14.00, 14.25, 14.5, 14.75, 15.00, 15.25, and 15.5 μm ($P < 0.05$) and differed extremely significantly at 10.75, 11.25, 11.50, 11.75, 12.25, 12.50, and 15.75 μm ($P < 0.01$). The intensities of infrared radiation of the left-hand-side ST25 differed significantly from the right-hand-side ST25 at 5.25, 5.50, 6.25, and 16.00 μm ($P < 0.05$).

3.4. Intensity of Infrared Radiation at ST25 and Control Points in UC Model Rats (Table 2). In MC group rats, the intensity of infrared radiation showed significant differences across the left ST25 and control point at 1.50, 4.75, and 5.00 μm ($P < 0.05$). On the right-hand side, the intensities of infrared radiation of ST25 differed from control point at 5.00, 7.00, 8.00, 8.75, 9.75, 10.25, 10.50, 10.75, 11.75, 12.00, 12.50, 12.75, 13.00, 13.25, 13.50, 13.75, and 14.00 μm ($P < 0.05$) and differed very significantly at 7.25, 7.75, 8.25, 8.50, 9.00, 9.25, 9.50, and 10.00 μm ($P < 0.01$). However, there was no difference between the intensity of infrared radiation at the left and right ST25.

3.5. Intensities of Infrared Radiation of the Left ST25 after Different Moxibustion Stimulations (Table 3). There were significant differences in the intensity of infrared radiation of the left ST25 between the NC and the MC groups at 3.00, 3.75, 4.75, 5.75, 6.00 μm ($P < 0.05$) and at 2.50, 2.75, 5.25 μm ($P < 0.01$).

After different types of moxibustion stimulation, the intensity of infrared radiation of the left ST25 of the HPM group was significantly different from that of the MC group at 2.50, 3.00, 10.25, 10.50, 11.00, 11.25, and 11.50 μm ($P < 0.05$) and very significantly different at 2.75 and 10.75 μm ($P < 0.01$). The differences between GPM group and MC group were significant at 2.50, 7.50, 8.00, 8.25, 8.50, 9.00, 9.25, 9.75, 10.00, 10.25, 10.75, 11.00, 11.25, 11.50, 11.75, and 14.00 μm ($P < 0.05$) and very significant at 2.75, 9.25, and 10.50 μm ($P < 0.01$). The differences between GLM group and MC group were significant at 2.75, 3.00, 7.50, 8.00, 8.50, 8.75, 9.00, 9.25, 9.50, 9.75, 10.00, 10.25, 10.50, 10.75, 11.50, and 12.00 μm ($P < 0.05$) and very significant at 8.25 μm ($P < 0.01$). The intensity of infrared radiation of the left ST25 in the WM group was significantly different

from those of the MC group at 2.50, 10.00, 10.25, 11.00, 11.25, 11.75, 12.00, 13.75, and 14.25 μm ($P < 0.05$) and very significantly different at 2.75, 10.50, 10.75, 11.50, and 14.00 μm ($P < 0.01$).

For the intensity of infrared radiation of left ST25, eight wavelengths showed a statistically significant difference between the NC and MC groups. After moxibustion stimulation, there were 9 wavelengths in the HPM group, 18 wavelengths in the GPM group, 17 wavelengths in the GLM group, and 14 wavelengths in the WM group that showed statistically significant differences from the MC group.

3.6. Intensity of Infrared Radiation of the Right ST25 after Different Moxibustion Stimulations (Table 4). The intensity of infrared radiation of the right ST25 showed significant differences between the NC and MC groups at 1.75, 4.00, 4.25, and 4.75 μm ($P < 0.05$) and at 2.75 and 3.00 μm ($P < 0.01$).

After different types of moxibustion stimulation, the intensity of infrared radiation of the right ST25 of the HPM group was significantly different from that of the MC group at 2.25, 7.25, 7.50, 7.75, 8.00, 8.50, 8.75, 9.50, 12.50, 13.25, and 14.25 μm ($P < 0.05$) and very significantly different at 1.75, 2.75, 3.00, 8.25, 9.00, 9.25, 9.75, 10.00, 10.25, 10.50, 10.75, 11.00, 11.25, 11.50, 11.75, 12.00, 12.25, 12.75, 13.00, 13.50, 13.75, and 14.00 μm ($P < 0.01$). The differences between GPM group and MC group were significant at 13.50, 14.75, and 15.00 μm ($P < 0.05$) and very significant at 3.00, 7.00, 7.25, 7.50, 7.75, 8.00, 8.25, 8.50, 8.75, 9.00, 9.25, 9.50, 9.75, 10.00, 10.25, 10.50, 10.75, 11.00, 11.25, 11.50, 11.75, 12.00, 12.25, 12.50, 12.75, 13.00, 13.75, 14.00, 14.25, and 14.50 μm ($P < 0.01$). The differences between the GLM group and MC group were significant at 3.00 and 8.25 μm ($P < 0.05$). The intensity of infrared radiation of the right ST25 in the WM group and MC group was significantly different at 1.75, 3.00, 10.25, 10.50, 10.75, 11.00, and 14.00 μm ($P < 0.05$) and very significantly different at 2.75 μm ($P < 0.01$).

For the intensity of infrared radiation of the right ST25, 6 wavelengths showed a statistically significant difference between the NC and MC groups. After moxibustion stimulation, 33 wavelengths in the HPM group, 33 wavelengths in the GPM group, 2 wavelengths in the GLM group,

TABLE 3: Intensity of infrared radiation of left-hand-side ST25 after different moxibustion treatments.

WL (μm)	NC	MC	HPM	GPM	GLM	WM
1.50	-0.008 ± 0.030	-0.003 ± 0.035	0.007 ± 0.015	0.008 ± 0.014	0.009 ± 0.013	0.002 ± 0.011
1.75	-0.002 ± 0.022	0.005 ± 0.025	0.003 ± 0.013	0.009 ± 0.015	0.012 ± 0.023	-0.002 ± 0.009
2.00	0.002 ± 0.025	0.017 ± 0.030	0.012 ± 0.011	0.015 ± 0.012	0.003 ± 0.025	0.006 ± 0.012
2.25	-0.003 ± 0.021	0.008 ± 0.033	0.004 ± 0.018	0.020 ± 0.021	0.006 ± 0.020	0.004 ± 0.016
2.50	-0.003 ± 0.020	$0.022 \pm 0.018^{**}$	$0.002 \pm 0.016^{\Delta}$	$0.004 \pm 0.015^{\Delta}$	0.006 ± 0.013	$0.006 \pm 0.015^{\Delta}$
2.75	-0.004 ± 0.022	$0.024 \pm 0.019^{**}$	$-0.001 \pm 0.016^{\Delta\Delta}$	0.010 ± 0.015	$0.007 \pm 0.011^{\Delta}$	$0.004 \pm 0.015^{\Delta\Delta}$
3.00	-0.006 ± 0.019	$0.021 \pm 0.023^*$	$0.003 \pm 0.020^{\Delta}$	0.005 ± 0.019	$0.001 \pm 0.017^{\Delta}$	0.009 ± 0.013
3.25	0.001 ± 0.019	0.015 ± 0.030	0.011 ± 0.017	0.012 ± 0.019	0.017 ± 0.012	0.004 ± 0.023
3.50	0.022 ± 0.020	0.030 ± 0.021	0.025 ± 0.035	0.032 ± 0.020	0.029 ± 0.018	0.017 ± 0.015
3.75	0.019 ± 0.029	$0.043 \pm 0.017^*$	0.031 ± 0.020	0.040 ± 0.017	0.036 ± 0.024	0.034 ± 0.012
4.00	0.006 ± 0.023	0.031 ± 0.033	0.023 ± 0.030	0.024 ± 0.017	0.035 ± 0.034	0.034 ± 0.029
4.25	0.037 ± 0.023	0.059 ± 0.035	0.056 ± 0.025	0.058 ± 0.021	0.055 ± 0.031	0.059 ± 0.030
4.50	0.067 ± 0.018	0.073 ± 0.018	0.057 ± 0.032	0.078 ± 0.015	0.072 ± 0.027	0.058 ± 0.024
4.75	0.063 ± 0.030	$0.084 \pm 0.023^*$	0.071 ± 0.018	0.093 ± 0.015	0.083 ± 0.021	0.074 ± 0.015
5.00	0.074 ± 0.020	0.085 ± 0.016	0.071 ± 0.017	0.094 ± 0.019	0.087 ± 0.016	0.095 ± 0.020
5.25	0.079 ± 0.024	$0.109 \pm 0.041^{**}$	0.099 ± 0.018	0.114 ± 0.016	0.100 ± 0.032	0.102 ± 0.013
5.50	0.059 ± 0.023	0.079 ± 0.022	0.088 ± 0.033	0.090 ± 0.018	0.079 ± 0.028	0.079 ± 0.031
5.75	0.048 ± 0.020	$0.070 \pm 0.019^*$	0.059 ± 0.025	0.067 ± 0.026	0.057 ± 0.021	0.061 ± 0.009
6.00	0.066 ± 0.024	$0.095 \pm 0.028^*$	0.071 ± 0.025	0.083 ± 0.020	0.082 ± 0.032	0.083 ± 0.026
6.25	0.044 ± 0.023	0.065 ± 0.019	0.058 ± 0.032	0.072 ± 0.020	0.059 ± 0.030	0.071 ± 0.027
6.50	0.046 ± 0.022	0.062 ± 0.033	0.056 ± 0.025	0.063 ± 0.023	0.052 ± 0.022	0.064 ± 0.018
6.75	0.143 ± 0.026	0.164 ± 0.028	0.146 ± 0.042	0.153 ± 0.026	0.170 ± 0.049	0.142 ± 0.029
7.00	0.224 ± 0.040	0.232 ± 0.030	0.231 ± 0.041	0.236 ± 0.046	0.250 ± 0.050	0.237 ± 0.036
7.25	0.322 ± 0.055	0.328 ± 0.049	0.345 ± 0.066	0.366 ± 0.038	0.367 ± 0.083	0.355 ± 0.029
7.50	0.374 ± 0.058	0.359 ± 0.054	0.377 ± 0.078	$0.434 \pm 0.042^{\Delta}$	$0.434 \pm 0.097^{\Delta}$	0.393 ± 0.032
7.75	0.404 ± 0.066	0.408 ± 0.066	0.415 ± 0.074	0.470 ± 0.047	0.462 ± 0.104	0.441 ± 0.047
8.00	0.473 ± 0.075	0.457 ± 0.075	0.470 ± 0.084	$0.540 \pm 0.041^{\Delta}$	$0.536 \pm 0.100^{\Delta}$	0.496 ± 0.058
8.25	0.480 ± 0.080	0.474 ± 0.075	0.503 ± 0.087	$0.565 \pm 0.056^{\Delta}$	$0.572 \pm 0.104^{\Delta\Delta}$	0.525 ± 0.049
8.50	0.494 ± 0.077	0.482 ± 0.072	0.489 ± 0.079	$0.555 \pm 0.048^{\Delta}$	$0.559 \pm 0.106^{\Delta}$	0.521 ± 0.046
8.75	0.571 ± 0.078	0.546 ± 0.088	0.582 ± 0.105	0.624 ± 0.076	$0.633 \pm 0.121^{\Delta}$	0.581 ± 0.077
9.00	0.660 ± 0.100	0.635 ± 0.095	0.682 ± 0.105	$0.741 \pm 0.066^{\Delta}$	$0.741 \pm 0.162^{\Delta}$	0.686 ± 0.060
9.25	0.690 ± 0.099	0.671 ± 0.104	0.729 ± 0.114	$0.800 \pm 0.068^{\Delta\Delta}$	$0.787 \pm 0.152^{\Delta}$	0.740 ± 0.070
9.50	0.750 ± 0.096	0.738 ± 0.114	0.783 ± 0.120	$0.841 \pm 0.051^{\Delta}$	$0.846 \pm 0.147^{\Delta}$	0.808 ± 0.070
9.75	0.809 ± 0.118	0.778 ± 0.117	0.856 ± 0.137	$0.891 \pm 0.080^{\Delta}$	$0.890 \pm 0.163^{\Delta}$	0.874 ± 0.069
10.00	0.846 ± 0.123	0.791 ± 0.113	0.891 ± 0.140	$0.930 \pm 0.102^{\Delta}$	$0.906 \pm 0.168^{\Delta}$	$0.926 \pm 0.074^{\Delta}$
10.25	0.835 ± 0.135	0.791 ± 0.117	$0.899 \pm 0.136^{\Delta}$	$0.911 \pm 0.086^{\Delta}$	$0.898 \pm 0.146^{\Delta}$	$0.920 \pm 0.086^{\Delta}$
10.50	0.739 ± 0.140	0.676 ± 0.118	$0.801 \pm 0.121^{\Delta}$	$0.822 \pm 0.081^{\Delta\Delta}$	$0.785 \pm 0.119^{\Delta}$	$0.824 \pm 0.070^{\Delta\Delta}$
10.75	0.655 ± 0.121	0.600 ± 0.099	$0.722 \pm 0.104^{\Delta\Delta}$	$0.698 \pm 0.077^{\Delta}$	$0.693 \pm 0.110^{\Delta}$	$0.739 \pm 0.072^{\Delta\Delta}$
11.00	0.580 ± 0.115	0.551 ± 0.097	$0.640 \pm 0.100^{\Delta}$	$0.633 \pm 0.045^{\Delta}$	0.616 ± 0.100	$0.645 \pm 0.059^{\Delta}$
11.25	0.548 ± 0.094	0.505 ± 0.081	$0.590 \pm 0.089^{\Delta}$	$0.585 \pm 0.047^{\Delta}$	0.564 ± 0.079	$0.595 \pm 0.067^{\Delta}$
11.50	0.496 ± 0.090	0.456 ± 0.091	$0.540 \pm 0.082^{\Delta}$	$0.544 \pm 0.041^{\Delta}$	$0.526 \pm 0.083^{\Delta}$	$0.551 \pm 0.048^{\Delta\Delta}$
11.75	0.433 ± 0.086	0.415 ± 0.086	0.469 ± 0.061	$0.483 \pm 0.071^{\Delta}$	0.475 ± 0.081	$0.491 \pm 0.040^{\Delta}$
12.00	0.407 ± 0.067	0.377 ± 0.067	0.428 ± 0.062	0.429 ± 0.048	$0.432 \pm 0.071^{\Delta}$	$0.439 \pm 0.040^{\Delta}$
12.25	0.410 ± 0.057	0.383 ± 0.065	0.422 ± 0.065	0.430 ± 0.039	0.432 ± 0.079	0.434 ± 0.039
12.50	0.387 ± 0.064	0.385 ± 0.057	0.405 ± 0.064	0.427 ± 0.044	0.419 ± 0.068	0.428 ± 0.036
12.75	0.360 ± 0.077	0.377 ± 0.060	0.399 ± 0.051	0.408 ± 0.042	0.407 ± 0.057	0.403 ± 0.037
13.00	0.362 ± 0.065	0.351 ± 0.075	0.387 ± 0.056	0.394 ± 0.031	0.379 ± 0.051	0.393 ± 0.033
13.25	0.462 ± 0.051	0.447 ± 0.072	0.473 ± 0.072	0.441 ± 0.058	0.452 ± 0.093	0.474 ± 0.059
13.50	0.587 ± 0.073	0.554 ± 0.071	0.595 ± 0.099	0.584 ± 0.064	0.586 ± 0.095	0.621 ± 0.076
13.75	0.590 ± 0.092	0.555 ± 0.092	0.629 ± 0.091	0.592 ± 0.091	0.582 ± 0.087	$0.640 \pm 0.060^{\Delta}$
14.00	0.509 ± 0.113	0.454 ± 0.091	0.519 ± 0.072	$0.534 \pm 0.076^{\Delta}$	0.513 ± 0.077	$0.555 \pm 0.047^{\Delta\Delta}$

TABLE 3: Continued.

WL (μm)	NC	MC	HPM	GPM	GLM	WM
14.25	0.426 \pm 0.095	0.396 \pm 0.078	0.427 \pm 0.063	0.450 \pm 0.079	0.440 \pm 0.063	0.465 \pm 0.035 ^{Δ}
14.50	0.363 \pm 0.076	0.351 \pm 0.076	0.366 \pm 0.053	0.380 \pm 0.058	0.375 \pm 0.050	0.390 \pm 0.044
14.75	0.258 \pm 0.072	0.255 \pm 0.048	0.266 \pm 0.050	0.267 \pm 0.047	0.275 \pm 0.052	0.268 \pm 0.032
15.00	0.205 \pm 0.058	0.217 \pm 0.041	0.214 \pm 0.043	0.219 \pm 0.035	0.226 \pm 0.030	0.222 \pm 0.023
15.25	0.177 \pm 0.050	0.185 \pm 0.032	0.169 \pm 0.032	0.172 \pm 0.032	0.173 \pm 0.035	0.180 \pm 0.015
15.50	0.178 \pm 0.033	0.196 \pm 0.035	0.185 \pm 0.032	0.179 \pm 0.019	0.202 \pm 0.043	0.190 \pm 0.028
15.75	0.172 \pm 0.037	0.193 \pm 0.026	0.184 \pm 0.044	0.180 \pm 0.022	0.189 \pm 0.033	0.180 \pm 0.011
16.00	0.137 \pm 0.038	0.158 \pm 0.030	0.152 \pm 0.027	0.139 \pm 0.030	0.166 \pm 0.031	0.146 \pm 0.016

WL: wavelength, NC: normal control group, MC: model control group, HPM: herb-partition moxibustion, GPM: ginger-partition moxibustion, GLM: garlic-partition moxibustion, WM: warming moxibustion. The intensity of infrared radiation of the left-hand-side ST25 showed significant differences between normal rats and model rats ($*P < 0.05$, $**P < 0.01$). After moxibustion stimulations, the intensity of infrared radiation of ST25 in moxibustion groups were significantly different from those of the model groups ($\Delta P < 0.05$, $\Delta\Delta P < 0.01$).

and 8 wavelengths in the WM group showed statistically significant differences from the MC group.

4. Discussion

In traditional Chinese medicine, acupoints are the points of infusion and transmission of qi and blood of viscus and meridians onto the surface of the human body and the windows of connection between the human body and its surroundings. In this way, infrared radiation and the transmission characteristics of acupoints can indicate the state of infusion of qi and blood and of the body's physiological response to pathological changes in the visceral organs.

Traditional Chinese medicine, which includes moxibustion, has been developing for more than 2500 years, and it has a long history of being used to prevent and treat diseases in Eastern cultures. Moxibustion therapy is a stimulation of acupoints by the burning of moxa. Moxibustion therapy includes both direct moxibustion and indirect moxibustion. Indirect moxibustion is a relatively common clinical therapy, and it includes herb-partition moxibustion, ginger-partition moxibustion, garlic-partition moxibustion, and other types of moxibustion. Moxibustion, through its warming effect and medicinal properties, improves the flow of both qi and blood through the acupoints and meridians, regulating the functions of viscus and organs to prevent and treat illnesses. Studies have indicated that moxibustion therapy can improve human immunity and regulate digestive function [24, 26, 38]. However, the biophysical mechanism underlying moxibustion and the role of acupoints in this process are unknown.

Several studies have indicated that infrared radiation is natural on the surface of the human body [39–41]. Ever since French scientist J. Borsarello photographed the infrared thermogram to show meridians and acupoints in human body in 1970, researchers at home and abroad have carried out many studies regarding the infrared thermography characteristics of the human body. Progress has been made on the meridian phenomenon, the characteristics of acupoints, acupuncture technique, and the therapeutic effects of acupuncture. Research has shown that the body emits infrared radiation along specific tracks and that acupuncture

may cause changes in skin temperature [42–48]. Reinforcing acupuncture techniques can increase skin temperature and reducing methods can decrease skin temperature [49–55]. The duration of retaining needle and the warming effects of acupuncture has certain relation [56]. The body may experience acupoint temperature imbalances during pathologic states [57]. However, the human body shows individual differences with respect to infrared radiation, and the infrared radiation is readily influenced by physiological factors such as sweating and nervousness and by environment factors such as atmospheric convection. In this way, data concerning skin temperature and changes in it are questionable and cannot alone be used to determine the mechanism underlying acupoint infrared radiation.

In the theory of traditional Chinese medicine, the Tianshu (ST25) acupoint is located at the stomach channel of foot yangming. It is the frontmost Mu point of the large intestine channel of hand yangming and the hub of ascending lucidity and descending turbidity in the human body. It can recruit qi and blood along the stomach channel and transmit both to the large intestinal channel. Therefore, ST25 is closely related to the gastrointestinal tract for the regulation of gastrointestinal function [33, 58]. Because it has antidiarrheal and cathartic effects, it is used to treat gastrointestinal diseases in clinic practice. Previous studies have indicated that ST25 plays an important role in the treatment of gastrointestinal diseases [59–64]. Acupuncture and moxibustion stimulation at ST25 can activate mast cell degranulation and downregulate colonic epithelial cell apoptosis in colitis model rats [59, 60]. They have also been shown to have analgesic effects in rats subjected to chronic visceral hypersensitivity [61, 62]. They regulate gastrointestinal function in human patients [63, 64]. In the present study, the intensity of infrared radiation of bilateral ST25 and the control points in UC rats were measured using a hypersensitivity PHE201 infrared spectrum analyzer [1, 22]. Results indicated that the intensities of infrared radiation of ST25 in the NC and MC groups differed from control points and that the difference on the right side was more marked than on the left side. However, there was little difference between the right and left ST25. This indicated the specificity of ST25 acupoint relative to control points. The intensities of infrared radiation of ST25 showed differences

TABLE 4: Intensity of infrared radiation of right-hand-side ST25 after different moxibustion treatments.

WL (μm)	NC	MC	HPM	GPM	GLM	WM
1.50	-0.004 ± 0.031	0.009 ± 0.014	0.004 ± 0.022	0.006 ± 0.015	0.012 ± 0.020	0.005 ± 0.018
1.75	0.001 ± 0.022	$0.021 \pm 0.028^*$	$-0.005 \pm 0.015^{\Delta\Delta}$	0.015 ± 0.011	0.020 ± 0.022	$0.003 \pm 0.011^{\Delta}$
2.00	-0.002 ± 0.024	0.007 ± 0.025	-0.003 ± 0.021	0.013 ± 0.021	0.009 ± 0.021	0.006 ± 0.020
2.25	0.005 ± 0.020	0.018 ± 0.026	$-0.001 \pm 0.019^{\Delta}$	0.014 ± 0.017	0.011 ± 0.024	0.007 ± 0.019
2.50	0.005 ± 0.029	0.013 ± 0.027	-0.005 ± 0.011	0.009 ± 0.014	0.006 ± 0.020	0.004 ± 0.014
2.75	0.001 ± 0.022	$0.022 \pm 0.017^{**}$	$0.002 \pm 0.011^{\Delta\Delta}$	0.010 ± 0.011	0.010 ± 0.016	$0.000 \pm 0.008^{\Delta\Delta}$
3.00	0.002 ± 0.025	$0.029 \pm 0.021^{**}$	$0.001 \pm 0.023^{\Delta\Delta}$	$0.003 \pm 0.012^{\Delta\Delta}$	$0.008 \pm 0.017^{\Delta}$	$0.008 \pm 0.014^{\Delta}$
3.25	0.005 ± 0.023	0.016 ± 0.024	0.024 ± 0.024	0.011 ± 0.021	0.022 ± 0.017	0.014 ± 0.028
3.50	0.021 ± 0.028	0.036 ± 0.026	0.032 ± 0.030	0.016 ± 0.021	0.033 ± 0.021	0.025 ± 0.022
3.75	0.032 ± 0.031	0.039 ± 0.022	0.036 ± 0.022	0.039 ± 0.018	0.047 ± 0.022	0.041 ± 0.016
4.00	0.016 ± 0.015	$0.038 \pm 0.036^*$	0.039 ± 0.023	0.026 ± 0.018	0.040 ± 0.025	0.047 ± 0.010
4.25	0.048 ± 0.021	$0.077 \pm 0.041^*$	0.062 ± 0.030	0.053 ± 0.016	0.063 ± 0.029	0.062 ± 0.025
4.50	0.068 ± 0.021	0.074 ± 0.025	0.079 ± 0.025	0.083 ± 0.023	0.084 ± 0.031	0.074 ± 0.018
4.75	0.076 ± 0.029	$0.096 \pm 0.026^*$	0.085 ± 0.023	0.089 ± 0.014	0.091 ± 0.020	0.084 ± 0.012
5.00	0.094 ± 0.025	0.087 ± 0.019	0.090 ± 0.025	0.098 ± 0.018	0.097 ± 0.029	0.092 ± 0.015
5.25	0.106 ± 0.024	0.121 ± 0.039	0.109 ± 0.026	0.119 ± 0.010	0.113 ± 0.022	0.116 ± 0.019
5.50	0.082 ± 0.022	0.088 ± 0.030	0.093 ± 0.024	0.092 ± 0.015	0.089 ± 0.023	0.087 ± 0.019
5.75	0.057 ± 0.017	0.075 ± 0.029	0.074 ± 0.024	0.068 ± 0.030	0.063 ± 0.029	0.060 ± 0.013
6.00	0.082 ± 0.017	0.102 ± 0.024	0.088 ± 0.028	0.094 ± 0.016	0.093 ± 0.030	0.090 ± 0.020
6.25	0.068 ± 0.026	0.073 ± 0.034	0.072 ± 0.016	0.072 ± 0.016	0.071 ± 0.024	0.069 ± 0.024
6.50	0.059 ± 0.028	0.067 ± 0.035	0.068 ± 0.021	0.063 ± 0.022	0.057 ± 0.036	0.067 ± 0.017
6.75	0.147 ± 0.038	0.165 ± 0.039	0.177 ± 0.031	0.184 ± 0.025	0.169 ± 0.047	0.156 ± 0.020
7.00	0.230 ± 0.065	0.234 ± 0.042	0.270 ± 0.033	$0.294 \pm 0.036^{\Delta\Delta}$	0.256 ± 0.062	0.242 ± 0.026
7.25	0.341 ± 0.076	0.334 ± 0.053	$0.401 \pm 0.047^{\Delta}$	$0.420 \pm 0.042^{\Delta\Delta}$	0.367 ± 0.082	0.352 ± 0.028
7.50	0.393 ± 0.064	0.378 ± 0.074	$0.445 \pm 0.048^{\Delta}$	$0.491 \pm 0.060^{\Delta\Delta}$	0.421 ± 0.097	0.403 ± 0.037
7.75	0.428 ± 0.077	0.408 ± 0.078	$0.482 \pm 0.052^{\Delta}$	$0.524 \pm 0.053^{\Delta\Delta}$	0.466 ± 0.094	0.442 ± 0.031
8.00	0.477 ± 0.087	0.472 ± 0.078	$0.555 \pm 0.062^{\Delta}$	$0.620 \pm 0.062^{\Delta\Delta}$	0.541 ± 0.101	0.511 ± 0.058
8.25	0.509 ± 0.086	0.484 ± 0.088	$0.591 \pm 0.066^{\Delta\Delta}$	$0.648 \pm 0.070^{\Delta\Delta}$	$0.565 \pm 0.110^{\Delta}$	0.536 ± 0.044
8.50	0.519 ± 0.095	0.491 ± 0.081	$0.583 \pm 0.063^{\Delta}$	$0.639 \pm 0.077^{\Delta\Delta}$	0.559 ± 0.109	0.537 ± 0.041
8.75	0.590 ± 0.105	0.569 ± 0.088	$0.678 \pm 0.079^{\Delta}$	$0.720 \pm 0.087^{\Delta\Delta}$	0.630 ± 0.133	0.609 ± 0.074
9.00	0.686 ± 0.122	0.657 ± 0.105	$0.789 \pm 0.074^{\Delta\Delta}$	$0.850 \pm 0.092^{\Delta\Delta}$	0.739 ± 0.132	0.711 ± 0.072
9.25	0.721 ± 0.134	0.698 ± 0.102	$0.846 \pm 0.088^{\Delta\Delta}$	$0.914 \pm 0.085^{\Delta\Delta}$	0.790 ± 0.153	0.761 ± 0.084
9.50	0.791 ± 0.133	0.772 ± 0.115	$0.915 \pm 0.087^{\Delta}$	$0.961 \pm 0.087^{\Delta\Delta}$	0.828 ± 0.158	0.821 ± 0.083
9.75	0.850 ± 0.138	0.805 ± 0.124	$0.984 \pm 0.085^{\Delta\Delta}$	$1.018 \pm 0.071^{\Delta\Delta}$	0.893 ± 0.171	0.884 ± 0.094
10.00	0.892 ± 0.150	0.817 ± 0.131	$1.027 \pm 0.096^{\Delta\Delta}$	$1.062 \pm 0.072^{\Delta\Delta}$	0.905 ± 0.175	0.924 ± 0.088
10.25	0.874 ± 0.138	0.814 ± 0.134	$1.030 \pm 0.096^{\Delta\Delta}$	$1.031 \pm 0.073^{\Delta\Delta}$	0.866 ± 0.154	$0.923 \pm 0.087^{\Delta}$
10.50	0.768 ± 0.117	0.711 ± 0.126	$0.930 \pm 0.089^{\Delta\Delta}$	$0.908 \pm 0.069^{\Delta\Delta}$	0.766 ± 0.130	$0.822 \pm 0.069^{\Delta}$
10.75	0.679 ± 0.118	0.633 ± 0.115	$0.834 \pm 0.080^{\Delta\Delta}$	$0.798 \pm 0.055^{\Delta\Delta}$	0.677 ± 0.123	$0.732 \pm 0.075^{\Delta}$
11.00	0.620 ± 0.110	0.573 ± 0.111	$0.734 \pm 0.061^{\Delta\Delta}$	$0.712 \pm 0.023^{\Delta\Delta}$	0.608 ± 0.112	$0.655 \pm 0.050^{\Delta}$
11.25	0.556 ± 0.094	0.541 ± 0.107	$0.674 \pm 0.073^{\Delta\Delta}$	$0.659 \pm 0.031^{\Delta\Delta}$	0.551 ± 0.104	0.604 ± 0.055
11.50	0.501 ± 0.093	0.488 ± 0.095	$0.619 \pm 0.069^{\Delta\Delta}$	$0.611 \pm 0.031^{\Delta\Delta}$	0.515 ± 0.100	0.554 ± 0.045
11.75	0.448 ± 0.085	0.433 ± 0.092	$0.548 \pm 0.064^{\Delta\Delta}$	$0.550 \pm 0.032^{\Delta\Delta}$	0.457 ± 0.087	0.492 ± 0.033
12.00	0.427 ± 0.072	0.407 ± 0.069	$0.496 \pm 0.055^{\Delta\Delta}$	$0.499 \pm 0.023^{\Delta\Delta}$	0.431 ± 0.092	0.437 ± 0.029
12.25	0.430 ± 0.061	0.413 ± 0.070	$0.490 \pm 0.057^{\Delta\Delta}$	$0.492 \pm 0.028^{\Delta\Delta}$	0.419 ± 0.086	0.440 ± 0.030
12.50	0.420 ± 0.074	0.402 ± 0.065	$0.475 \pm 0.047^{\Delta}$	$0.483 \pm 0.033^{\Delta\Delta}$	0.411 ± 0.087	0.431 ± 0.033
12.75	0.385 ± 0.070	0.380 ± 0.069	$0.455 \pm 0.052^{\Delta\Delta}$	$0.470 \pm 0.030^{\Delta\Delta}$	0.403 ± 0.072	0.410 ± 0.030
13.00	0.372 ± 0.067	0.365 ± 0.070	$0.451 \pm 0.049^{\Delta\Delta}$	$0.449 \pm 0.026^{\Delta\Delta}$	0.372 ± 0.076	0.398 ± 0.032
13.25	0.465 ± 0.092	0.465 ± 0.068	$0.534 \pm 0.051^{\Delta}$	0.528 ± 0.051	0.448 ± 0.100	0.478 ± 0.050
13.50	0.605 ± 0.101	0.578 ± 0.091	$0.692 \pm 0.066^{\Delta\Delta}$	$0.679 \pm 0.044^{\Delta}$	0.575 ± 0.112	0.617 ± 0.074
13.75	0.616 ± 0.106	0.580 ± 0.091	$0.717 \pm 0.074^{\Delta\Delta}$	$0.704 \pm 0.034^{\Delta\Delta}$	0.578 ± 0.115	0.640 ± 0.049
14.00	0.531 ± 0.100	0.473 ± 0.095	$0.601 \pm 0.069^{\Delta\Delta}$	$0.617 \pm 0.026^{\Delta\Delta}$	0.513 ± 0.105	$0.555 \pm 0.051^{\Delta}$

TABLE 4: Continued.

WL (μm)	NC	MC	HPM	GPM	GLM	WM
14.25	0.467 \pm 0.098	0.423 \pm 0.086	0.503 \pm 0.046 ^Δ	0.528 \pm 0.043 ^{ΔΔ}	0.435 \pm 0.084	0.467 \pm 0.045
14.50	0.399 \pm 0.083	0.375 \pm 0.074	0.430 \pm 0.040	0.451 \pm 0.034 ^{ΔΔ}	0.376 \pm 0.076	0.395 \pm 0.038
14.75	0.286 \pm 0.066	0.267 \pm 0.064	0.293 \pm 0.035	0.314 \pm 0.021 ^Δ	0.274 \pm 0.067	0.279 \pm 0.025
15.00	0.227 \pm 0.059	0.221 \pm 0.050	0.238 \pm 0.033	0.261 \pm 0.032 ^Δ	0.231 \pm 0.035	0.223 \pm 0.027
15.25	0.190 \pm 0.043	0.196 \pm 0.040	0.196 \pm 0.025	0.203 \pm 0.028	0.171 \pm 0.045	0.189 \pm 0.013
15.50	0.201 \pm 0.041	0.201 \pm 0.044	0.213 \pm 0.028	0.218 \pm 0.020	0.201 \pm 0.050	0.191 \pm 0.025
15.75	0.192 \pm 0.029	0.208 \pm 0.037	0.210 \pm 0.020	0.209 \pm 0.019	0.197 \pm 0.045	0.189 \pm 0.019
16.00	0.170 \pm 0.026	0.164 \pm 0.035	0.168 \pm 0.029	0.174 \pm 0.024	0.169 \pm 0.035	0.157 \pm 0.015

WL: wavelength, NC: normal control group, MC: model control group, HPM: herb-partition moxibustion, GPM: ginger-partition moxibustion, GLM: garlic-partition moxibustion, WM: warming moxibustion. The intensity of infrared radiation of right-hand-side ST25 showed significant differences between normal rats and model rats (* $P < 0.05$, ** $P < 0.01$). After moxibustion stimulations, the intensity of infrared radiation of ST25 in moxibustion groups was significantly different from that of model groups ($\Delta P < 0.05$, $\Delta\Delta P < 0.01$).

between the NC and MC groups and between the HPM and MC groups. However, further research must be performed using larger samples. Some studies have indicated that the near-infrared radiation from the moxa moxibustion burning process can energize hydrogen bonds inside the acupoints and allow them to absorb the stimulated resonance. They would then transmit energy to the cells through the nerve-fluid system [38]. This also showed that moxibustion stimulation could improve the condition of colon tissue in UC model rats, indicating that the infrared radiation of acupoints and moxibustion treatment has a biophysical foundation. Other studies have reported that the infrared radiation spectra of radix aconite-partition moxibustion and acupoints are amazingly consistent. The therapeutic effects of indirect moxibustion include the physical effects of moxibustion thermal radiation, the therapeutic effect of moxa and partition, and the resonance of the infrared radiation of indirect moxibustion and acupoints [65, 66].

5. Conclusion

Acupoints are specific, and moxibustion, especially thing-partition moxibustion, can regulate the running state of both qi and blood in acupoints. In this way, they can be used to treat illness by influencing the infrared physical effect of the corresponding acupoints. An in-depth study of these effects would reveal the biophysical properties of these acupoints, the pathologic characteristics of UC, and the biophysical mechanisms underlying the therapeutic effects of moxibustion. It may also provide new research methods that can be used to diagnose illness and explore the effects of acupuncture and moxibustion stimulation.

Abbreviations

ST25: Tianshu acupoint
 NC: Normal control group
 MC: Model control group
 HPM: Herb-partition moxibustion
 GPM: Ginger-partition moxibustion

GLM: Garlic-partition moxibustion

WM: Warming moxibustion

UC: Ulcerative colitis.

Conflict of Interests

The authors have no conflict of interests to declare.

Acknowledgments

The authors thank the National Basic Research Program of China (973 program, no. 2009CB522900), National Natural Science Foundation of China (no. 81001549 and 81173331), Shanghai Health System of Outstanding Young Talent Cultivation Program (no. XYQ2011068), and Shanghai Rising-Star Program (no. 10QA1406100) for their support.

References

- [1] G. Ding, W. Yao, J. Chu et al., "Spectral characteristic of infrared radiations of some acupoint and non-acupoint areas in human arm surface," *Chinese Science Bulletin*, vol. 46, no. 8, pp. 678–682, 2001.
- [2] Y. H. Han, G. H. Ding, X. Y. Shen, H. P. Deng, and W. Yao, "Infrared radicalization spectrum of human surface and the relationship with ATP energy metabolize," *Shanghai Journal of Biomedical Engineering*, vol. 26, no. 4, pp. 198–200, 2005.
- [3] X. Shen, G. Ding, H. Deng et al., "Infrared radiation spectrum of acupuncture point on patients with coronary heart disease," *American Journal of Chinese Medicine*, vol. 36, no. 2, pp. 211–218, 2008.
- [4] X. Y. Shen, G. H. Ding, H. P. Deng et al., "Analysis on pathological information of infrared radiation spectrums at acupuncture point neiguan (PC6) for patients with coronary heart disease," *Journal of Infrared and Millimeter Waves*, vol. 25, no. 6, pp. 443–446, 2006.
- [5] Y. Ding, G. Ding, X. Shen et al., "Observation on the characters of infrared radiation spectrum of acupoints in normal humans and CHD patients," *Journal of Biomedical Engineering*, vol. 23, no. 2, pp. 309–312, 2006.
- [6] H. P. Deng, X. Y. Shen, and G. H. Ding, "Characteristics of infrared radiation of moxibustion and meridian-acupoints," *Zhongguo Zhen Jiu*, vol. 24, no. 2, pp. 105–108, 2004.

- [7] X. Shen, G. Ding, J. Wei et al., "An infrared radiation study of the biophysical characteristics of traditional moxibustion," *Complementary Therapies in Medicine*, vol. 14, no. 3, pp. 213–219, 2006.
- [8] T. Philp, P. J. R. Shah, and P. H. L. Worth, "Acupuncture in the treatment of bladder instability," *British Journal of Urology*, vol. 61, no. 6, pp. 490–493, 1988.
- [9] S. P. Yun, W. S. Jung, S. U. Park et al., "Effects of moxibustion on the recovery of post-stroke urinary symptoms," *American Journal of Chinese Medicine*, vol. 35, no. 6, pp. 947–954, 2007.
- [10] J. W. Joo and Y. T. Choi, "The clinical study of the effect of electroacupuncture and moxibustion on urinary disturbance as a complication of cerebrovascular accidents," *Journal of Korean Acupuncture Moxibustion Society*, vol. 14, pp. 1–14, 1997.
- [11] S. Uchida, A. Suzuki, F. Kagitani, K. Nakajima, and Y. Aikawa, "Effect of moxibustion stimulation of various skin areas on cortical cerebral blood flow in anesthetized rats," *American Journal of Chinese Medicine*, vol. 31, no. 4, pp. 611–621, 2003.
- [12] X. L. Hu, P. Q. Wang, B. H. Wu, and J. S. Xu, "Displaying of the meridian courses over human body surface with thermal imaging system," *Revista Paulista de Acupuntura*, vol. 2, no. 1, pp. 7–12, 1996.
- [13] Y. W. Ding and G. H. Ding, "Application of infrared radiation spectrum to acu-moxibustion research," *Zhen Ci Yan Jiu*, vol. 32, no. 4, pp. 252–255, 2006.
- [14] Y. Q. Zhang, G. H. Ding, X. Y. Shen, H. P. Liu, W. Yao, and H. P. Deng, "Difference of the infrared spectra radiated from the acupoints between healthy volunteers and patients of coronary heart disease," *Zhongguo Zhen Jiu*, vol. 24, no. 12, pp. 846–849, 2004.
- [15] H. P. Deng, X. Y. Shen, G. H. Ding et al., "Infrared radiation spectrum from point shenmen in patients with coronary heart disease," *Shanghai Journal of Acupuncture and Moxibustion*, vol. 23, no. 11, pp. 31–34, 2004.
- [16] H. P. Liu, X. Y. Shen, H. P. Deng et al., "Infrared spectrum research in patients with coronary heart disease," *Shanghai Journal of Traditional Chinese Medicine*, vol. 38, no. 4, pp. 52–53, 2004.
- [17] S. Chen, J. Yan, and J. B. Zhu, "Research on infrared radiation of Wei Shu and Zusanli acupoints applying in differentiation of symptoms and signs of chronic stomachache," *Hunan College Journal of Traditional Chinese Medicine*, vol. 3, no. 1, pp. 52–53, 2002.
- [18] X. R. Chang, J. Yan, S. X. Yi, Z. H. Yue, and Y. P. Lin, "Relation of the infrared radiation on Zusanli, Liangmen and Weishu area with chronic gastric pain and its application," *World Chinese Journal of Digestology*, vol. 17, no. 5, pp. 516–520, 2009.
- [19] L. Fei, H. S. Cheng, D. H. Cai et al., "The experimental explore and research outlook of essential fundamental of meridian and functional characters," *Chinese Science Bulletin*, vol. 43, no. 6, pp. 658–672, 1998.
- [20] H. P. Deng, X. Y. Shen, and G. H. Ding, "Relationship between spontaneous infrared radiation of Taiyuan(LU9) and pulmonary function," *Journal of Traditional Chinese Medicine*, vol. 48, no. 1, pp. 47–49, 2007.
- [21] G. H. Ding, X. Y. Shen, J. H. Chu et al., "Research on infrared radiation spectrum of moxibustion and acupoints in human body in traditional Chinese medicine," *Chinese Journal of Biomedical Engineering*, vol. 21, no. 4, pp. 356–360, 2002.
- [22] X. Y. Shen, G. H. Ding, J. H. Zhu et al., "Human acupoints and moxibustion infrared radiation spectrum with infrared transmission in acupoints," *Acta University Tradition Medicinal Science Pharmacologiaeque Shanghai*, vol. 15, no. 4, pp. 33–35, 2001.
- [23] Y. Zheng, "Research and application progress of the infrared effects of moxibustion," *Zhong Xi Yi Jie He Xue Bao*, vol. 10, no. 2, pp. 135–140, 2012.
- [24] J. H. Chiu, "How is the motility of gastrointestinal sphincters modulated by acupmoxa?" *International Congress Series*, vol. 12, no. 38, pp. 141–147, 2002.
- [25] Y. B. Jia, X. X. Feng, and X. F. Liu, "Clinical study on electroacupuncture combined with acupoint sticking therapy for treatment of chronic ulcerative colitis," *Chinese Acupuncture & Moxibustion*, vol. 30, no. 9, pp. 717–719, 2010.
- [26] J. P. Mu, H. G. Wu, Z. Q. Zhang et al., "Meta-analysis on acupuncture and moxibustion for treatment of ulcerative colitis," *Chinese Acupuncture & Moxibustion*, vol. 27, no. 9, pp. 687–690, 2007.
- [27] E. H. Zhou, H. R. Liu, H. G. Wu et al., "Down-regulation of protein and mRNA expression of IL-8 and ICAM-1 in colon tissue of ulcerative colitis patients by partition-herb moxibustion," *Digestive Diseases and Sciences*, vol. 54, no. 10, pp. 2198–2206, 2009.
- [28] H. G. Wu, Z. Huang, H. R. Liu et al., "Experimental study on influence of acupuncture and moxibustion therapy on apoptosis of colonic epithelial cells in rats of ulcerative colitis," *Zhongguo Zhen Jiu*, vol. 25, no. 2, pp. 119–122, 2005.
- [29] H. G. Wu, L. B. Zhou, Y. Y. Pan et al., "Study of the mechanisms of acupuncture and moxibustion treatment for ulcerative colitis rats in view of the gene expression of cytokines," *World Journal of Gastroenterology*, vol. 5, no. 6, pp. 515–517, 1999.
- [30] H. G. Wu, Y. Yao, X. Y. Shen et al., "Comparative study on infrared radiation spectrum of yuan point and Xiahe point of the large intestine channel in the patient of ulcerative colitis," *Chinese Acupuncture & Moxibustion*, vol. 28, no. 1, pp. 49–55, 2008.
- [31] H. G. Wu, H. R. Liu, L. Y. Tan et al., "Electroacupuncture and moxibustion promote neutrophil apoptosis and improve ulcerative colitis in rats," *Digestive Diseases and Sciences*, vol. 52, no. 2, pp. 379–384, 2007.
- [32] H. Ogawa, *Organ Inflammation and Disease Model*, Medical Academy Press, Tokyo, Japan, 1971.
- [33] G. C. Sugai, A. O. Freire, A. Tabosa, Y. Yamamura, S. Tufik, and L. E. Mello, "Serotonin involvement in the electroacupuncture- and moxibustion-induced gastric emptying in rats," *Physiology and Behavior*, vol. 82, no. 5, pp. 855–861, 2004.
- [34] Z. R. Li, *Experimental Acupuncture Science*, China press of Traditional Chinese Medicine, Beijing, China, 2007.
- [35] H. G. Wu, L. B. Zhou, D. R. Shi et al., "Morphological study on colonic pathology ulcerative colitis treated by moxibustion," *World Journal of Gastroenterology*, vol. 6, no. 6, pp. 861–865, 2000.
- [36] Y. Z. Chen, *Practical Internal Medicine*, People's Medical Publishing House, Beijing, China, 2001.
- [37] H. R. Liu, S. Zhou, X. M. Wang, and H. G. Wu, "Regulating effects of different moxibustion therapies on bax and Bcl-2 in rats with ulcerative colitis," *Journal of Acupuncture and Tuina Science*, vol. 8, no. 3, pp. 174–180, 2010.
- [38] H. Y. Yang and T. Y. Liu, "Preliminary study on biophysics mechanisms of moxibustion therapy," *Zhongguo Zhen Jiu*, vol. 16, no. 10, pp. 17–18, 1996.
- [39] D. Zhang, W. Fu, S. Wang, Z. Wei, and F. Wang, "Displaying of infrared thermogram of temperature character on meridians," *Acupuncture Research*, vol. 21, no. 3, pp. 63–67, 1996.

- [40] J. Ying, X. Y. Shen, H. P. Liu et al., "Comparison of infrared radiation spectrum detected from Tai Chong point between patients with coronary heart disease and health adults," *Zhejiang Journal of Traditional Chinese Medicine*, vol. 11, no. 3, pp. 100–101, 2005.
- [41] X. Hu, B. Wu, and P. Wang, "Displaying of meridian courses travelling over human body surface under natural conditions," *Acupuncture Research*, vol. 18, no. 2, pp. 83–89, 1993.
- [42] D. Zhang and S. Y. Wang, "Study on effects of α -Receptor blocker on high temperature lines along channels in the cholecystitis model rabbit by infrared thermogram," *Zhongguo Zhen Jiu*, vol. 22, no. 11, pp. 745–748, 2002.
- [43] J. S. Xu, P. Q. Wang, X. L. Hu, B. H. Wu, and F. Q. Zhang, "The usage of isothermal display and full temperature display of infrared radiation imaging in the study of meridian," *Journal of Fujian College of Traditional Chinese Medicine*, vol. 14, no. 2, pp. 20–22, 2004.
- [44] P. Wang, X. Hu, J. Hu, and B. Wu, "Investigation on the displaying of the infrared radiant track along the governor vessel meridian and conception vessel of human body surface," *Chinese Journal of Clinical Rehabilitation*, vol. 7, no. 9, pp. 1379–1380, 2003.
- [45] D. Zhang, S. Y. Wang, H. M. Ma, Y. Y. Ye, and Y. G. Zhu, "Display on the infrared thermal image of body surface temperature reaction of viceral diseases (pericarditis)," *Chinese Journal of Basic Medicine in Traditional Chinese Medicine*, vol. 10, no. 7, pp. 52–54, 2004.
- [46] Z. B. Lü, M. Blank, A. Angielczyk, and H. Büttng, "Changes in the thermogram of the body surface induced by acupuncture in human beings," *Acupuncture Research*, vol. 12, no. 3, pp. 239–243, 1987.
- [47] R. Liu, D. Zhuang, X. Yang et al., "Objective display on phenomena of propagated sensation along channels (PSC)—changes on the infrared thermal image channels pathway of upper extremity," *Acupuncture Research*, vol. 15, no. 3, pp. 239–244, 1990.
- [48] D. Zhang, J. B. Meng, and H. H. Gao, "Objective display on characteristics of meridian temperature—changes on the infrared thermal image channels pathway of meridians after acupuncture," *Nature Magazine*, vol. 12, no. 11, pp. 845–847, 1989.
- [49] J. S. Xu, X. L. Hu, P. Q. Wang, and B. H. Wu, "Effect of acupuncture on infrared radiant track along meridians over the human body surface," *Zhen Ci Yan Jiu*, vol. 27, no. 4, pp. 255–258, 2002.
- [50] C. H. Zhang, "Changes on acupoints temperature pre and post acupuncture," *Zhongguo Zhen Jiu*, vol. 8, no. 5, pp. 37–38, 1988.
- [51] D. Zhang and Z. X. Wei, "Heating effect of acupuncture at Guangming," *Shanghai Journal of Acupuncture and Moxibustion*, vol. 16, no. 4, pp. 3–5, 1997.
- [52] D. Zhang and D. Peng, "Infrared thermal image of therapeutic effect on Hegu by acupuncture," *Journal of Traditional Chinese Medicine*, vol. 30, no. 5, pp. 32–34, 1989.
- [53] Y. Cheng and P. Li, "Effect on temperature field by acupuncture on eight confluent points," *Journal of Tianjin College of Traditional Chinese Medicine*, vol. 18, no. 3, pp. 43–45, 1999.
- [54] D. Zhang, J. Meng, H. Gao, B. Wen, L. Xue, and N. Chen, "Effects of the heat-tonification method on the surface temperature of the body observed by infra-red thermography," *Journal of Traditional Chinese Medicine*, vol. 10, no. 1, pp. 36–41, 1990.
- [55] D. Zhang, "Computerized thermovision for study of principles of acupuncture and meridian phenomena," *Hongwai Jishu*, vol. 14, no. 4, pp. 28–32, 1992.
- [56] D. Zhang, H. Gao, Z. Wei, and B. Wen, "The thermographic observation of the relationship between the retention of acupuncture needles and the effect of nose temperatures," *Acupuncture Research*, vol. 16, no. 1, pp. 73–75, 1991.
- [57] J. T. Xie and J. B. Li, "Photothermal detection of acupuncture in patients with cold and fever syndrome of lung-stomach," *Chinese Journal of Traditional Medical Science and Technology*, vol. 4, no. 3, pp. 139–140, 1997.
- [58] E. H. Zhou, H. R. Liu, H. G. Wu et al., "Suspended moxibustion relieves chronic visceral hyperalgesia via serotonin pathway in the colon," *Neuroscience Letters*, vol. 451, no. 2, pp. 144–147, 2009.
- [59] Y. Shi, L. Qi, J. Wang et al., "Moxibustion activates mast cell degranulation at the ST25 in rats with colitis," *World Journal of Gastroenterology*, vol. 17, no. 32, pp. 3733–3738, 2011.
- [60] C. H. Bao, L. Y. Wu, Y. Shi et al., "Moxibustion down-regulates colonic epithelial cell apoptosis and repairs tight junctions in rats with Crohn's disease," *World Journal of Gastroenterology*, vol. 17, no. 45, pp. 4960–4970, 2011.
- [61] H. R. Liu, X. M. Wang, E. H. Zhou et al., "Acupuncture at both ST25 and ST37 improves the pain threshold of chronic visceral hypersensitivity rats," *Neurochemical Research*, vol. 34, no. 11, pp. 1914–1918, 2009.
- [62] E. H. Zhou, X. M. Wang, G. H. Ding et al., "Suspended moxibustion relieves chronic visceral hyperalgesia and decreases hypothalamic corticotropin-releasing hormone levels," *World Journal of Gastroenterology*, vol. 17, no. 5, pp. 662–665, 2011.
- [63] L. K. Guo, C. X. Zhang, and X. F. Guo, "Acupuncture combined with Chinese herbal medicine Plantain and Senna Granule in treatment of functional constipation: a randomized, controlled trial," *Journal of Chinese Integrative Medicine*, vol. 9, no. 11, pp. 1206–1214, 2011.
- [64] H. G. Wu, Z. Shi, Y. Zhu et al., "Clinical research of ulcerative colitis treated with herbal cake-partitioned moxibustion," *Journal of Acupuncture and Tuina Science*, vol. 7, no. 2, pp. 80–83, 2009.
- [65] G. H. Ding, X. Y. Shen, J. H. Chu, Z. M. Huang, and W. Yao, "Observation on the characters of the infrared radiation spectrum of acupoints and four types of moxibustion in the human body," *Zhen Ci Yan Jiu*, vol. 27, no. 4, pp. 269–273, 2002.
- [66] X. Y. Shen, G. H. Ding, J. H. Chu et al., "Comparison of infrared radiation spectrum of traditional moxibustion, substitute moxibustion and acupoints of human body," *Journal of Infrared and Millimeter Waves*, vol. 22, no. 2, pp. 123–126, 2003.

Research Article

Observation of Pain-Sensitive Points along the Meridians in Patients with Gastric Ulcer or Gastritis

Hui Ben,¹ Liang Li,¹ Pei-Jing Rong,¹ Zhi-Gao Jin,² Jian-Liang Zhang,¹
Yan-Hua Li,¹ and Xia Li³

¹Institute of Acupuncture and Moxibustion, China Academy of Chinese Medical Sciences, Beijing 100700, China

²Beijing Coal General Hospital, Beijing 100028, China

³Beijing University of Traditional Chinese Medicine, Beijing 100029, China

Correspondence should be addressed to Pei-Jing Rong, rongpj@mail.cintcm.ac.cn

Received 20 August 2012; Accepted 14 October 2012

Academic Editor: Wolfgang Schwarz

Copyright © 2012 Hui Ben et al. This is an open access article distributed under the Creative Commons Attribution License, which permits unrestricted use, distribution, and reproduction in any medium, provided the original work is properly cited.

This study aims to investigate the sensitization of human skin points along certain meridians related to visceral disease by using the pressure-pain threshold (PPT) as an indicator. We detected and compared the PPTs of people with and without gastric ulcer or gastritis on the related acupoints, abdomen area, and back area with von Frey detector and observed the similarities and differences under their respective physiological and pathological states. The results showed that (1) the PPTs of patients with gastric ulcer on related acupoints decreased significantly compared with the control group; (2) there was no significant difference in PPT between the chosen points of the measured meridian and the adjacent nonacupoints; (3) there was an apparent distribution of tender points on the relevant abdomen and back regions of patients with gastric ulcer or gastritis, but none was found on the control group; (4) the pain-sensitive points of gastric ulcer and gastritis patients were BURONG (ST19), LIANGMEN (ST21), and HUAROU MEN (ST24) of the stomach meridian on the abdominal region and PISHU (BL20), WEISHU (BL21), and WEICANG (BL50) on the back, among others. The results suggest that the practical significance of acupoints may lie in its role as a relatively sensitive functional area. In a pathological state, the reflex points on the skin which are related to certain visceral organs become sensitive and functionally intensify.

1. Introduction

The pressure-pain threshold (PPT) of skin is the minimum force applied on the skin by external pressure which induces pain. It is one of the traditional measures to quantitatively evaluate pain that has been widely used in basic as well as clinic studies. In most cases, reporting of perceived pain by the subjects is usually influenced by factors like the expectancy, and pressure algometry however provides objective information of the local pain conditions.

According to the theory of meridians in traditional Chinese medicine, there are connections between the internal organs and their respective somatic meridians. Therefore, visceral lesions can lead to changes of pain sensation, which exhibited as tenderness point(s), or pigmentations and so forth in certain areas of the body surface. And similarly, the stimulation of acupoints can result in the regulation of function of the responding internal organs.

Previous studies have shown that the sensitive points on the body surface accompanied with some visceral disorders including the digestive diseases which are characterized with abdominal pain and tenderness as the common sign and symptom. In this study, by the help of von Frey detector, we measured the PPT of acupoints along meridians of subjects with gastric ulcer or gastritis to assess their sensitization under the pathological conditions.

2. Materials and Methods

2.1. Detection of Pressure-Pain Threshold

2.1.1. Detection Equipment. The 2390-type von Frey detector produced by the IITC Company of the United States was used to detect the PPTs of acupoints along the related meridians so as to compare the similarities and differences

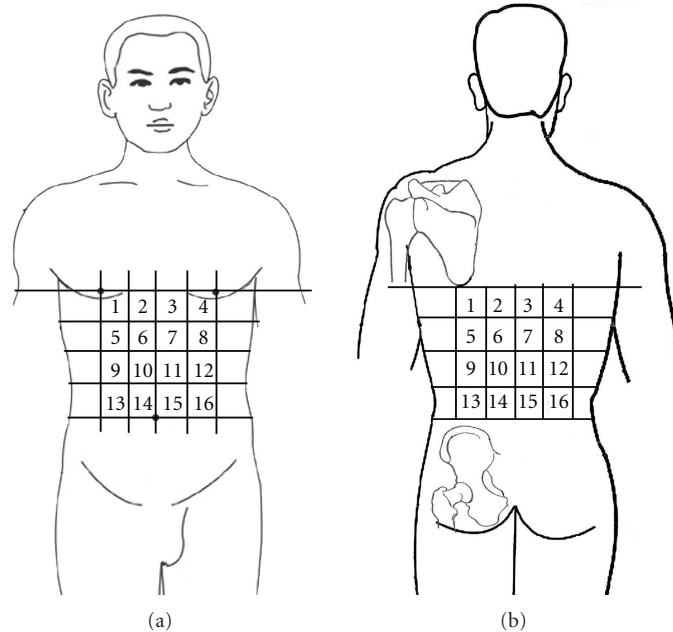


FIGURE 1: Abdominal and back testing zones. The abdominal and back regions of the subject were divided into 16 testing zones, respectively.

between the results acquired in normal and pathological states.

2.1.2. Detection of Acupoints. *Tested acupoints* (1) Stomach Meridian: ZUSANLI (ST36), SHANGJUXU (ST37), XIAJUXU (ST39); (2) Large Intestine Meridian: SHOUWULI (LI13), QUCHI (LI11), SHOUSANLI (LI10), HEGU (LI4); (3) back acupoints: WEISHU (BL21), DACHANGSHU (BL25); (4) points which are 1.0–1.5 cm adjacent to the above acupoints were selected as the control acupoints; (5) the abdominal and back acupoints.

2.1.3. Methods. The probe tip was kept moving vertically downward toward the skin at an even speed. When the subject felt the pain, the probe was removed immediately and the data on the detector were recorded simultaneously. Each point was tested three times at an interval of three minutes. The average of the data was taken as the threshold.

2.2. Partition of the Testing Zones on the Abdomen and Back. The abdominal and back regions of the subject were divided into 16 testing areas, respectively (Figure 1). In each testing area three points were tested, and each point had a certain distance to the other two points.

2.3. Identification of Tender Points on the Abdomen and Back. Tender points in the testing zones of the subject's abdomen and back were identified by finger-pressure method. Tender points were determined when the subject expressed obvious pain or a quasinstringy pain while the thumb pressed vertically downward at an even speed.

2.4. Selection of Pain-Sensitive Points on the Abdomen and Back. Data are expressed as means of the values acquired from the three test points in each of the 16 testing zones mentioned above. The three points with the lowest pain threshold (i.e., pain-sensitive point) were selected and marked in Figure 5. The points marked for each group were cumulatively displayed in Figure 5 to demonstrate the different responses to pain of the relevant areas on the surface of body between healthy people and patients with gastric ulcer or gastritis.

2.5. Grouping

2.5.1. Control Group 1. Twenty healthy volunteers were selected (10 male and 10 female, aged 25–50). The PPTs were measured, respectively, on the stomach meridian, large intestine meridian, back meridian, and those adjacent to open acupoints.

2.5.2. Gastric Ulcer Group 1. Sixteen volunteers with gastric ulcer were selected (8 male and 8 female, aged 30–55). The PPTs were measured, respectively, on the stomach meridian, large intestine meridian, back meridian, and those adjacent to open acupoints.

2.5.3. Control Group 2. Twenty one healthy volunteers were selected (11 male and 10 female, aged 30–55). The PPTs were measured, respectively, in each testing zone on the abdomen and back.

2.5.4. Gastric Ulcer Group 2. Sixteen volunteers with gastric ulcer were selected (8 male and 8 female, aged 30–55).

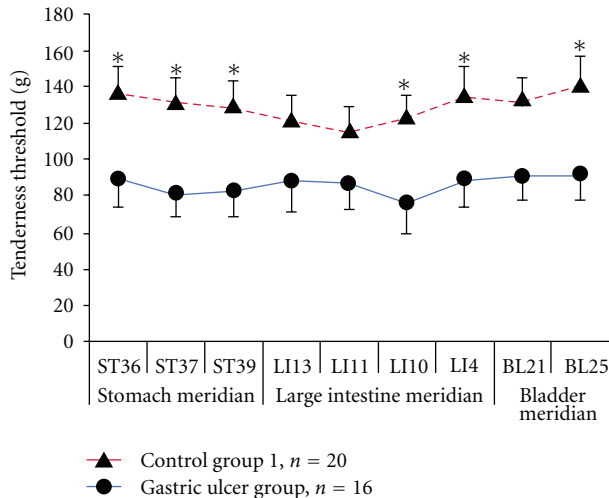


FIGURE 2: The PPTs of the gastric ulcer group decreased significantly compared with that of the control group.

The PPTs were measured, respectively, in each testing zone on the abdomen and back.

2.5.5. Gastritis Group. Twenty one volunteers with gastritis were selected (9 male and 12 female, aged 30–60). The PPTs were measured, respectively, in each testing zone on the abdomen and back.

3. Results

3.1. The Comparison between Gastric Ulcer Group 1 and Control Group 1

3.1.1. The Comparison of PPTs between the Gastric Ulcer Group and the Control Group. The results showed a significant decrease of PPTs of the test points on related meridians of patients with gastric ulcer in disease state compared with the control group ($P < 0.05$) (Figure 2).

3.1.2. The Comparison of PPTs between the Selected Acupoints and Adjacent Points. There was no significant difference in PPTs between the points along the tested meridians and the adjacent open points (Figure 3).

3.2. The Comparison of PPTs among Gastric Ulcer Group 2, Gastritis Group, and Control Group 2

3.2.1. The Distribution of Tender Points on the Abdomen and Back. The distribution of tender points in the abdominal and back testing zones was detected by using the finger-pressure method. The results showed that there was no apparent tender point in the normal control group, but, in the gastric ulcer group, tender points appeared more often on the left side of the abdomen and the lower right side of the back (Figure 4).

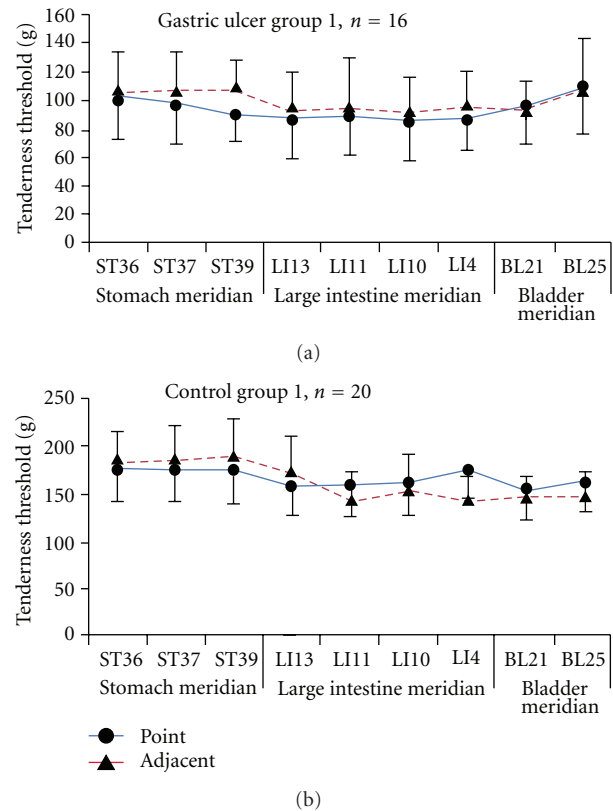


FIGURE 3: There was no significant difference in PPTs between points on meridians and nonmeridians.

3.2.2. The Distribution of the Pain-Sensitive Points on the Abdomen and Back. The PPTs of pain-sensitive points displayed in Figures 5(a) and 5(b) were measured by von Frey detector. Figure 5 shows a dispersed distribution of pain-sensitive points on the abdomen and back in the control group, and there was no relative specificity. The pain-sensitive points of the gastric ulcer group were relatively concentrated. They were mainly distributed at BURONG (ST19); LIANGMEN (ST21), and HUAROUMEN (ST24), among others of the stomach meridian on the abdomen and PISHU (BL20), WEISHU (BL21), YANGGANG (BL48), WEICANG (BL50), among others of the bladder meridian on the back (Figure 6). The distribution of the pain-sensitive points was basically consistent with the distribution of tender points obtained by using the finger-pressure method. In the gastritis group, the distribution of the pain-sensitive points was less concentrated than that of the gastric ulcer group. It may be attributed to the fact that the clinical symptoms of patients with gastritis were less severe than that of patients with gastric ulcer.

4. Discussion

Mechanical tenderness is not only a symptom of local skin or muscle tissue, but also a typical performance of some pain syndromes. It has diagnostic significance in clinical settings. The PPT can be used as an indicator for the evaluation of

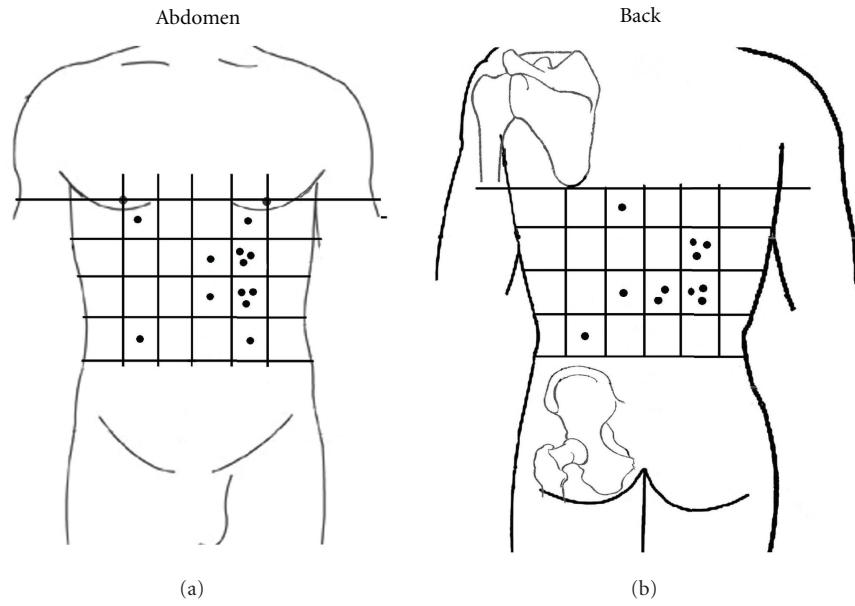


FIGURE 4: There were more tender points distributed on the left side of the abdomen and the lower right side of the back in the gastric ulcer group.

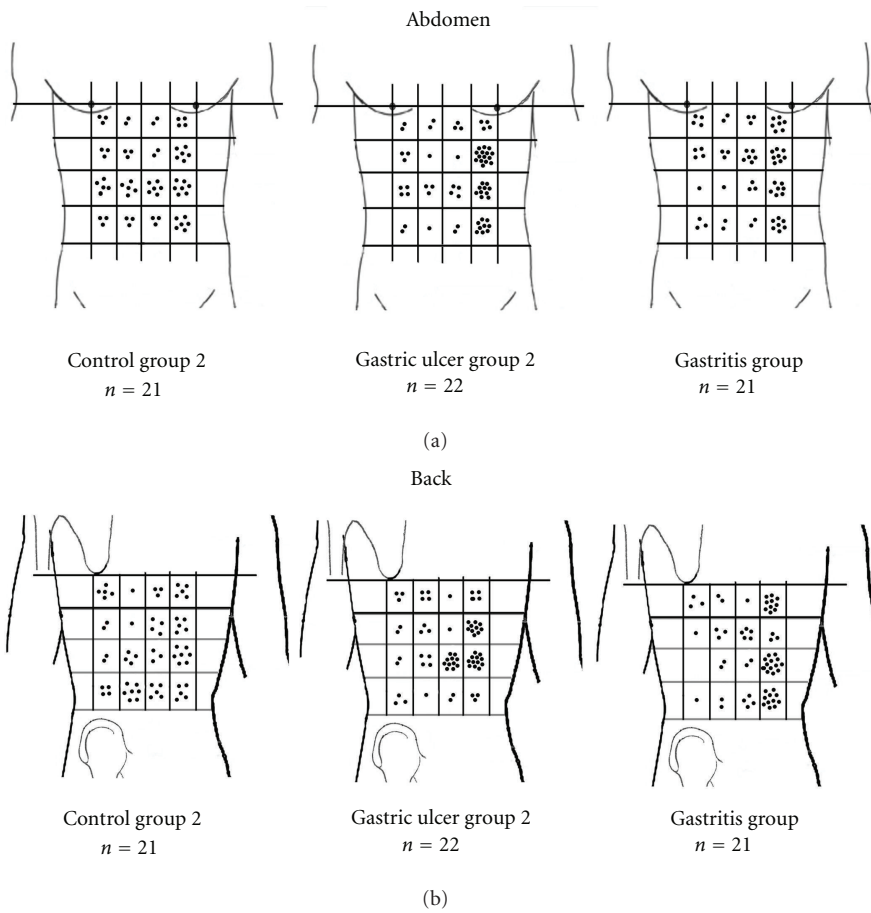


FIGURE 5: (a) The distribution of the pain-sensitive points on the abdomen. (b) The distribution of the pain-sensitive points on the back.

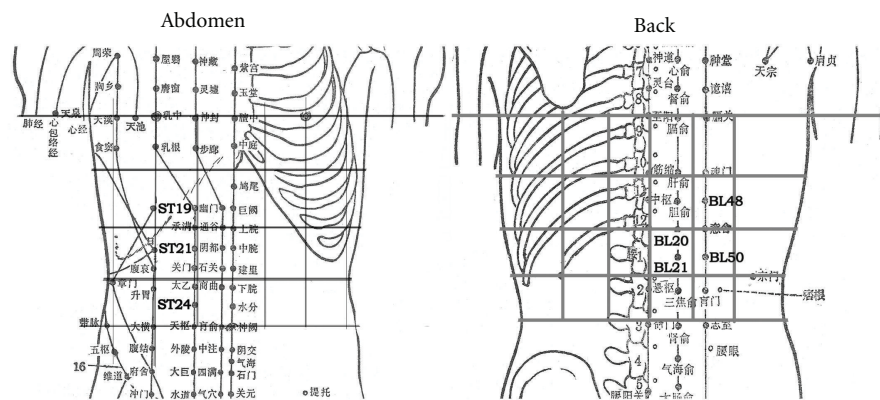


FIGURE 6: The pain-sensitive points were mainly distributed at ST19, ST21, ST24, among others of the stomach meridian on the abdomen and at BL20, BL21, BL48, BL50, among others of the bladder meridian on the back.

the body's inflammatory activity, subcutaneous tissue sensitivity, and pain tolerance. It has been applied in the assessment of the efficacy of various clinical treatment therapies [1, 2].

Research has shown that the primary afferent transmission of pain may be affected by the neuroendocrine interaction [3]. As visceral diseases increase the chemical substances that cause pain (5-HT, histamine, peptides, and others) in the body, the pain sensitivity of the patients increases as well [4]. In 1999, British scholar Kosek [5] reported that the PPTs at the muscle-nerve points were significantly lower than the PPTs of "pure" muscle and/or bone. These "muscle-nerve" points are similar to what we call the meridian points.

Meridian points are the reaction points and the treatment points of visceral diseases in traditional Chinese Medicine. The correlation between meridians and internal organs means that the meridians not only have close correlation with their corresponding organs in terms of physiological function, but also demonstrate specific reactions of visceral disorders on the surface of body in pathological states. The therapeutic stimulation on meridians has a regulatory effect on the function of internal organs [6]. In recent years, Yu et al. have proposed the idea that acupoints are "dynamic" and the functioning of acupoints is a dynamic process [7]. He believes that area size of acupoints on the body surface and the function of acupoints are not fixed. On the contrary, the function and area size of acupoints change with the state of the body and the function of their corresponding internal organs. He suggests that acupoints have two states, namely, on/off. The switch between the two states is a dynamic process and reflects the transition of the body from a "dormant" healthy state to an "activated" pathological state. At the same time, the process is accompanied with changes of the microphysical and chemical environments; that is, at the time of visceral disorder, the acupoints turn from the dormant state to the sensitized state. Thus it is possible to regulate the functioning of internal organs by stimulating acupoints.

In recent years, many studies on acupoint specificity have shown that the function and characteristics of acupoints are closely related to the distribution of specific nerves [8, 9] and blood vessels [10, 11]. Acupoints also exhibit unique physical properties, such as optical specificity [12], thermal specificity [13], and electromagnetic specificity [14]. In addition, gene expression in the brain caused by stimulating acupoints has significantly increased comparing with the gene expression caused by stimulating nonacupoints. The result suggests that the effect of acupuncture on acupoints is different from the effect of acupuncture on nonacupoints [15]. Another study has shown that acupuncture can regulate the nitric oxide (NO) content and the activity of nitric oxide synthase (NOS) in body tissues [16–18]. The increase of NO content in the pathological state reflects the activity of the acupoints from one side.

Results showed that the PPTs of skin in the gastric ulcer group were significantly lower than that of the normal control group, regardless of whether it was tested on related meridians or on the adjacent open points. There was no significant difference in PPTs between points on the meridians and adjacent open points. It showed that in pathological states the meridian points were more sensitive and had lower PPTs than in the normal state. Meridian points had no significant difference compared with the adjacent open points. It suggests that acupoint was not just an isolated point but represents a relatively sensitive point area with certain special function. Previous studies have shown that meridian has an optimized and inclusive systematic structure instead of a single channel structure [19].

The distribution of pain-sensitive points on the abdomen and back also suggests that, in the gastric ulcer group, there were obvious tender points in the reflex zones on the body surface associated with the disease. The PPTs were lower, and the pain-sensitive points were more concentrated. Tender points and pain-sensitive points were mainly concentrated at ST19, ST21, and ST24 on the Stomach Meridian of Foot-Yangming of the abdomen and at BL20, BL21, BL48, and BL50 on the Bladder Meridian of Foot-Taiyang of the back.

A previous research showed that the LIANGMEN point area on the abdomen and the WEISHU point area on the back had a clear overlap with the segmental distribution of nerves of the stomach [20]. The Foot-Yangming Meridian points and the back points were closely related to the stomach [21, 22]. According to the responses of subjects, they felt apparent pain or tingling when these areas were pressed or tested, and sometimes the string pain goes up and down along the meridian. It is evident that there is a relatively specific link between the meridians (acupoints) on the body surface and the stomach diseases. But based on the feeling of subjects and the tested results, the correlation was not apparent in all states. We observed that there was no tender point on the body of subjects in the normal control group, and the distribution of pain-sensitive points was relatively dispersed. But in pathological states the subjects felt clear pain at meridian points (acupoints). This showed that, in pathological states, acupoints and meridian areas on the body surface were more sensitive and active compared with the normal state. This performance was positively correlated to the alleviation of clinical symptoms and pain [1, 2].

The above results suggest that the practical significance of acupoint may lie in its role as a relatively sensitive functional area. The reflex area of internal organs on the surface of body is more sensitive and functionally more active than other areas of the body surface, particularly in pathological states. Therefore, acupoints (point areas) cannot only “mirror the disease” in diagnosis, but also help to “cure the disease” in treatment.

5. Conclusions

In conclusion, tender points appeared on the abdomen and back regions of patients with gastric ulcer or gastritis, suggesting that the essence of acupoints goes beyond a mere site for stimulation. Thus, our study provides scientific evidence for the theory of “correlation between meridians and viscera” and, further, helps elucidate the mechanism of acupuncture in the management of gastrointestinal diseases.

Appendix

The positions of mentioned acupoints in this paper

ST19: on the upper abdomen, 6 *cun* above the centre of the umbilicus and 2 *cun* lateral to the anterior midline.

ST21: on the upper abdomen, 4 *cun* above the centre of the umbilicus and 2 *cun* lateral to the anterior midline.

ST24: on the upper abdomen, 1 *cun* above the centre of the umbilicus and 2 *cun* lateral to the anterior midline.

ST36: on the anteriolateral side of the leg, 3 *cun* below Dubi (ST35), one finger breadth (middle finger) from the anterior crest of the tibia.

ST37: on the anteriolateral side of the leg, 6 *cun* below Dubi (ST35), one finger breadth (middle finger) from the anterior crest of the tibia.

ST39: on the anteriolateral side of the leg, 9 *cun* below Dubi (ST35), one finger breadth (middle finger) from the anterior crest of the tibia.

LI10: 2 *cun* above Quchi (LI11) when a fist is made.

LI11: between the humerus and radius when the elbow is flexed and the hand is put on the chest.

LI13: 3 *cun* above the elbow, mid the Zhouliao (LI12), and on the big vessel (probably the cephalic vein), when the elbow is flexed.

LI14: 7 *cun* above the elbow, at the lower end of the deltoid muscle.

BL20: on the back below the spinous process of the 11th thoracic vertebra, 1.5 *cun* lateral to the posterior midline.

BL21: on the back below the spinous process of the 12th thoracic vertebra, 1.5 *cun* lateral to the posterior midline.

BL25: on the low back, below the spinous process of the 4th lumbar vertebra, 1.5 *cun* lateral to the posterior midline.

BL48: on the back, below the spinous process of the 10th thoracic vertebra, 3 *cun* lateral to the posterior midline.

BL50: on the back, below the spinous process of the 12th thoracic vertebra, 3 *cun* lateral to the posterior midline.

Acknowledgments

This scientific work was supported by a National Basic Research Program of China (973 program, no. 2012CB518503) and a National Natural Science Foundation of China (no. 30772830) Grant to P.-J. Rong. The first two authors (H. Ben and L. Li) contributed equally to this study. P.-J. Rong designed the study and was responsible for obtaining approval by the Institutional Animal Care and Use Committee of the China Academy of Chinese Medical Sciences. Z.-G. Jin, J.-L. Zhang, Y.-H. Li, and X. Li performed the measurements in Beijing. H. Ben and L. Li analyzed the data and wrote the paper. W.-C. Li helped us to modify the manuscript. All authors approved the paper and there is no competing financial interests for this paper.

References

- [1] Y. Huang, G. L. Liu, and S. M. Zhao, “Changes in the stomach and duodenal ulcers in patients with ear tenderness threshold,” *Chinese Acupuncture & Moxibustion*, vol. 8, pp. 39–40, 1996.
- [2] N. H. Wang, “One of the experimental pain evaluation methods: the tenderness threshold. *Foreign Medical Sciences, Physical Medicine and Rehabilitation*, vol. 24, no. 3, pp. 97–99, 2004.

- [3] Z. F. Zhao, J. H. Lu, Q. Y. Liu et al., "Influence of interaction between endocrine and nervous factors on the pain threshold, calcitonin gene-related peptide immunoreactivity of dorsal root ganglia and spinal dorsal horn in rat," *Acta Universitatis Medicinae Tangji*, vol. 29, no. 6, pp. 493–496, 2000.
- [4] L. Huang, "Effect of cognitive operation on pain threshold and pain tolerance," *Chinese Mental Health Journal*, vol. 17, no. 4, pp. 261–262, 2003.
- [5] E. Kosek, J. Ekholm, and P. Hansson, "Pressure pain thresholds in different tissues in one body region. The influence of skin sensitivity in pressure algometry," *Scandinavian Journal of Rehabilitation Medicine*, vol. 31, no. 2, pp. 89–93, 1999.
- [6] Y. Wang, K. Ji, and X. H. Zang, "Meridian—organs doctrine of progress and discussion of problems," *Journal of Clinical Acupuncture and Moxibustion*, vol. 21, no. 6, pp. 54–56, 2005.
- [7] X. C. Yu, B. Zhu, J. H. Gao et al., "The scientific basis of the points dynamic process," *Journal of Traditional Chinese Medicine*, vol. 48, no. 11, pp. 17–23, 2007.
- [8] k. Liu, W. Wang, A. H. Li et al., "Morphological research of Liver Meridian and effects of capsaicin on genitofemoral nerve discharge frequency in rats," *Anatomía Clínica*, vol. 11, no. 4, pp. 232–235, 2006.
- [9] Y. L. Zhao, X. R. Chang, J. Yan et al., "Study on the specificity of effects of electroacupuncture at acupoints of Stomach Meridian on gastric myoelectric activity and its efferent pathway in the rat," *Chinese Archives of Traditional Chinese Medicine*, vol. 23, no. 10, pp. 1788–1790, 2005.
- [10] F. Liu and E. Y. Chen, "Distribution of vessels in the frontal part of the interosseous membrane of leg and its relationship with points," *Shanghai Journal of Traditional Chinese Medicine*, vol. 34, no. 12, pp. 40–41, 2000.
- [11] X. Mu, H. Q. Duan, W. Chen et al., "Physiological study on the relationship between the essence of acupuncture point and the microvasalium," *Chinese Journal of Basic Medicine in Traditional Chinese Medicine*, vol. 7, no. 12, pp. 47–52, 2001.
- [12] Y. W. Ding, G. H. Ding, X. Y. Shen et al., "Observation on the characters of infrared radiation spectrum of acupoints in normal humans and CHD patients," *Journal of Biomedical Engineering*, vol. 23, no. 2, pp. 309–312, 2006.
- [13] H. P. Deng, X. Y. Shen, and G. H. Ding, "Characteristics of infrared radiation of moxi and meridian-acupoints," *Chinese Acupuncture & Moxibustion*, vol. 24, no. 2, pp. 105–107, 2004.
- [14] D. Z. Li, S. T. Fu, and X. Z. Li, "Study on the theory and clinical application of meridians (III)," *Chinese Acupuncture & Moxibustion*, vol. 25, no. 1, pp. 53–59, 2005.
- [15] J. C. Yu, T. Yu, and J. X. Han, "Analysis on difference of acupuncture effects between acupoint and non-acupoint from difference of gene expression," *Chinese Acupuncture & Moxibustion*, vol. 22, no. 11, pp. 749–751, 2002.
- [16] Z. H. Zhu, Z. Ding, X. M. Tang, and K. X. Ding, "Experimental study on effects of acupuncture at Zusanli (ST36) on NO and NOS in brain tissue of mice of spleen deficiency," *Chinese Acupuncture & Moxibustion*, vol. 5, no. 6, pp. 309–312, 2000.
- [17] Z. C. Liu, F. M. Sun, M. H. Zhu, Z. Sun et al., "Effects of acupuncture on contents of nitric oxide and nitric oxide synthase in the hippocampus in the obese rat," *Chinese Acupuncture & Moxibustion*, vol. 23, no. 1, pp. 52–54, 2007.
- [18] W. Y. Liu and B. Bai, "The effect of nitric oxide in brain on pain threshold of rats," *Chinese Journal of Behavioral Medical Science*, vol. 8, no. 4, pp. 255–257, 2007.
- [19] H. Shi, Y. Wan, and J. S. Han, "Sex differences of analgesia induced by 100 Hz electroacupuncture and intrathecal injection of dynorphin a in rats," *Chinese Journal of Pain Medicine*, vol. 5, no. 2, pp. 97–101, 1999.
- [20] J. Yan and B. Zhu, *Basic and Clinic of Acupuncture*, Hunan Science and Technology Press, Hunan, China, 2010.
- [21] J. S. Li, J. Yan, and X. R. Chang, "Influence of electric acupuncture at acupoints of the foot-yangming meridian on gastric motion and motilin in rabbits," *China Journal of Basic Medicine in Traditional Chinese Medicine*, vol. 10, no. 3, pp. 36–39, 2004.
- [22] J. Yan, X. R. Chang, J. H. Liu et al., "Study on protective action of electroacupuncture at acupoints of the foot-yangming channel on lesion of gastric mucosa in rabbits," *Chinese Acupuncture & Moxibustion*, vol. 21, no. 6, pp. 30–32, 2001.

Research Article

In Adjuvant-Induced Arthritic Rats, Acupuncture Analgesic Effects Are Histamine Dependent: Potential Reasons for Acupoint Preference in Clinical Practice

Meng Huang,¹ Di Zhang,^{1,2} Zhe-yan Sa,¹ Ying-yuan Xie,³
Chen-li Gu,⁴ and Guang-hong Ding^{1,2}

¹ Department of Mechanics and Engineering Science, Fudan University, Shanghai 200433, China

² Shanghai Research Center for Acupuncture and Meridians, Shanghai 201203, China

³ College of Acupuncture and Moxibustion, Shanghai University of Traditional Chinese Medicine, Shanghai 201203, China

⁴ Medical School, Fudan University, Shanghai 200433, China

Correspondence should be addressed to Guang-hong Ding, ghding@fudan.edu.cn

Received 18 August 2012; Accepted 27 September 2012

Academic Editor: Ying Xia

Copyright © 2012 Meng Huang et al. This is an open access article distributed under the Creative Commons Attribution License, which permits unrestricted use, distribution, and reproduction in any medium, provided the original work is properly cited.

This study investigated whether immediate acupuncture effects in the acupoint are histamine dependent. Both histamine injection and manual acupuncture stimulation increased the pain threshold (PT) after treatment compared with the model group ($P < 0.01$), producing an analgesic effect. After pretreatment with clemastine, an H1 receptor antagonist and an antipruritic, the increase in the animals' pain threshold after acupuncture was suppressed compared with the Acu group ($P < 0.01$); however, there was no interference with the acupuncture-induced degranulation of mast cells. Pretreatment with disodium cromolyn did not suppress the increase in PT induced by the histamine injection at Zusanli (ST-36). We conclude that in adjuvant-induced arthritic rats, acupuncture analgesic effects are histamine dependent, and this histamine dependence determines the acupoint preference of acupoints away from the target site in acupuncture practice.

1. Introduction

During the last two decades, research on acupuncture has determined that acupuncture is based on relationships between structures and functions that have been studied under physiological conditions. Regarding the initiation of local acupoint effects after acupuncture, the degranulation of mast cells was found to be related to acupuncture analgesia in adjuvant-induced arthritic rats [1]. Moreover, these analgesic effects depend on the transduction of neural signals above the acupunctured acupoint [2]. However, the characteristics of this neural activation induced by mast cell degranulation after acupuncture remain unclear. In this study, we tested the histamine dependence of acupuncture analgesia and presented a hypothesis for the mechanism of acupoint preference in acupuncture analgesia clinical practice.

2. Methods

2.1. Animals. The present study was performed in accordance with the guidelines of the Animal Care and Use Committee of Shanghai Research Center for Acupuncture and Meridians. Male Sprague-Dawley (SD) rats (150 ± 20 g), from the Shanghai Experimental Animal Center of the Chinese Academy of Science, were housed in cages with a temperature-controlled environment (22–25°C) and a 12/12-hour light/dark cycle. Food and water were made available ad lib. All animals were handled with care to prevent infection and to minimize stress. All behavioral experiments were performed between 9 am and 4 pm. For each experimental group, animals were chosen randomly.

2.2. Adjuvant Arthritis Model. To achieve the adjuvant arthritis model, rats under anesthesia (10% chloral hydrate

0.4 mL/100 g i.p.) were injected with 0.05 mL of Complete Freund's Adjuvant (Sigma-Aldrich) in the left ankle joint. On the second day after modeling, the injected ankle joint was dropsical; some rats also lifted the left hind paw while moving.

2.3. Disposal for Each Group. 50 μ L of histamine (100 μ g/mL in normal saline vehicle, histamine from Sigma-Aldrich) was injected at Zusanli (ST-36) (half under the skin, half in the muscle) in the His group. The Acu group was treated with acupuncture (described below). Prior to histamine injection (5 min), 20 μ L of a mast cell stabilizer, disodium cromolyn (0.02 g/mL in normal saline vehicle, disodium cromolyn from Sigma-Aldrich), was injected at the acupoint (half under the skin, half in the muscle) in the Cro + His group as a control for the other mast cell-degranulating substance. 50 μ L of the histamine H1 receptor antagonist clemastine (0.01 μ g/mL in normal saline vehicle, clemastine from Intech) was injected 5 min before acupuncture in the Cle + Acu group to study histamine function during animal acupuncture. To determine the efficiency of clemastine, a Cle group with a clemastine injection and a Cle + His group with an additional histamine injection were studied. To determine the efficiency of disodium cromolyn, a Cro + Acu group, which received a disodium cromolyn injection 5 min before acupuncture, was studied. The other groups included the Control group without modeling, the model group without treatment, and the NS group, which received an injection of 50 μ L of normal saline solution.

2.4. Nociceptive Testing Model. The thermal-induced paw withdraw test was used to assess analgesic responses. An analgesia meter (IITC, Life Sciences, Woodland Hills, C.A., U.S.) was used to apply heat stimulation. Each time, rats were acclimated to the test chamber for 30–40 min prior to testing. The triangle area of the underside of the left ankle joint was stimulated with 30% of maximum light strength. The room temperature was controlled at $24 \pm 2^\circ\text{C}$. A 20 sec cutoff maximum was programmed into the timer to prevent tissue damage. We tested three times successively to obtain an average PT (10 min intervals were allowed between each test).

Three PTs were tested in this study. Before modeling (BM), the PT was obtained before anesthesia for modeling; after modeling (AM), the PT was obtained on the second day after modeling. The treatment for each group was performed 1 hour after the AM test, and after treatment (AT), the PT was obtained 20 min after treatment. For the control and model groups, the AM and AT values were obtained according to the duration of the other groups.

2.5. Acupuncture Stimulation. Since Zusanli (ST-36) is a popular acupoint for analgesia studies in animal experiments as well as for clinical treatment, it was selected as the acupoint for our experiments. Sterilized, stainless steel acupuncture needles (0.25 mm in diameter, 1 inch in length, Suzhou Kangnian Medical Devices Co., Ltd., Suzhou,

China) were inserted into ST-36 at the left hind leg, located 5 mm lateral and distal to the anterior tubercle of the tibia. The perpendicular needling depth was approximately 5 mm, and we alternately applied the lift-thrusting and twisting manipulation for 30 sec with 30 sec intervals. The acupuncture was performed for 30 min.

2.6. Specimen Preparations and Microscopic Examination. Tissue samples from acupoints and nearby sham points were collected after decapitation of the animals under narcosis (10% chloral hydrate 0.4 mL/100 g i.p.). We took the upper part of tissue from ST-36. After cutting, the final size of the tissue sample with skin and muscle was $5 \times 5 \times 5 \text{ mm}^3$. Sequential paraffin slices with 4- μ m thickness were made after 48 h of fixation at 4°C in fixing solution (10% formalin). The sections were longitudinal to the skin and the muscle tissue. The sample was stained with 0.5% toluidine blue. Mast cells could with more than three granules outside of the cell membrane or with empty cavities in the cytoplasm were considered degranulated (Figure 1). The numbers of mast cells per sample were counted and then averaged. Degranulation ratios (DR) which stands for the ratios of degranulated to total mast cells were calculated. Representative photomicrographs were taken at 400x magnification for morphological evaluation.

2.7. Data Analysis. Data were analyzed using SPSS 10.0. PT data were compared using a multivariable analysis. The mast cell degranulation rate was determined using a one-way ANOVA.

3. Results

3.1. Validity for Methods. The BM values for all the groups were not significantly different from each other, which indicated the stability of the animals' sensitivity to the thermal stimulation. After modeling, all of the other groups exhibited significant different sensitivity (versus control, Table 1), indicating hyperalgesia due to adjuvant-induced arthritis.

The clemastine injection had no influence on the PT or DR (Cle versus NS, Table 1; Figure 1(j)). Disodium cromolyn successfully suppressed acupuncture-induced analgesia and reduced DR (Cro + Acu versus Acu, Table 1; Figures 1(d) and 1(g)). Both of these chemicals presented no effects other than their desired functions.

3.2. Acupuncture Analgesia Is Histaminergic. After the acupuncture treatment, both the PT and DR increased compared with the model group, which indicates that the analgesic effect was related to mast cell activation. In the Cle + Acu group, pretreatment with clemastine suppressed acupuncture-induced analgesia (versus Acu, Table 1). However, the mast cells were still activated by acupuncture-induced mechanical stimulations (versus Cle, Table 1; Figures 1(h) and 1(j)), which indicates that the acupuncture-induced analgesia is histaminergic in this case.

TABLE 1: Comparison of PT and degranulation ratios of MCs near ST-36 among different groups.

Groups	N	Pain thresholds ($\bar{x} \pm$ s.e., s)			Degranulation ratios ($\bar{x} \pm$ s.e., %)
		Before model	After model	After treatment	
Control	12	9.04 \pm 0.20	9.38 \pm 0.19	9.27 \pm 0.17	33.59 \pm 0.72
Model	12	8.90 \pm 0.40	6.48 \pm 0.28 [#]	6.58 \pm 0.35 [△]	39.71 \pm 2.09
NS	11	9.23 \pm 0.31	6.10 \pm 0.33 [#]	6.68 \pm 0.33 [△]	37.72 \pm 2.33
Acu	12	9.52 \pm 0.18	6.58 \pm 0.17 [#]	8.77 \pm 0.26 [*]	57.61 \pm 1.42 [*]
His	12	9.21 \pm 0.20	6.27 \pm 0.22 [#]	8.50 \pm 0.28 [*]	57.03 \pm 2.95 ^{*▲}
Cro + His	13	9.21 \pm 0.12	6.41 \pm 0.19 [#]	7.86 \pm 0.30	25.40 \pm 1.80 [†]
Cro + Acu	12	8.91 \pm 0.18	6.51 \pm 0.19 [#]	6.40 \pm 0.36 [‡]	36.03 \pm 2.28 [‡]
Cle + Acu	12	9.56 \pm 0.32	6.90 \pm 0.21 [#]	6.54 \pm 0.26 [‡]	51.54 \pm 2.32
Cle + His	12	9.36 \pm 0.17	6.66 \pm 0.18 [#]	5.85 \pm 0.28 [†]	37.13 \pm 1.90
Cle	22	9.56 \pm 0.16	6.70 \pm 0.21 [#]	7.41 \pm 0.2	32.24 \pm 1.40

[#] $P < 0.01$ versus control; ^{*} $P < 0.01$ versus model; [△] $P < 0.01$ versus control; [†] $P < 0.01$ versus His; [‡] $P < 0.01$ versus Acu; [▲] $P < 0.01$ versus NS.

Data of control, model, NS, Acu, His groups were from earlier publication [4].

3.3. Histamine Injection in the Acupoint Induces Analgesic Effects. Histamine injection had an analgesic effect (versus model, Table 1), while clemastine pretreatment suppressed this effect (versus His, Table 1). However, disodium cromolyn pretreatment had no significant effects (versus His, Table 1), and mast cells were stabilized without a significant increase in DR (versus His, Table 1; Figures 1(f) and 1(i)). Combined with the fact that there is no histamine H1 receptors on mast cells, the activation of mast cells in His group might be caused by substance P released from those afferents expressing histamine H1 receptors [3].

4. Discussion

In the acupoint, there are neural targets, including A δ and C-type fiber, which respond to manual acupuncture by inducing the central release of morphine peptide and thus the analgesic effect [5]. However, in clinical practice, the so-called “De-Qi” sensation determines the acupuncture’s analgesic effects, which indicates the difference between acupuncture and nociceptive stimuli [6]. This kind of difference among acupuncture techniques might be caused by the mechanical activation of mast cells in the acupoint.

The activation of mast cells is often related to the itch sensation, and this activation can be either histaminergic or nonhistaminergic (see Figure 2). A histamine-dependent itch (or pruritus) is a common itch sensation [7]. It is characterized by the triad effects of histamine in the skin, including flare, wheal, and itch. In the skin, histamine is synthesized in the Golgi apparatus of basophils and mast cells and is stored in granules inside of these cells. Mast cells in the skin can be activated by IgE, neurotransmitters, endocrines, or mechanical forces [8] and expel the granules, releasing histamine into the local environment [9]. Histamine-independent itch was first reported in 1953; papain and cowhage spicules were shown to induce the itch sensation [10]. The papain and cowhage spicules both activate polymodal C-fibers, which are in charge of pain sensation under mechanical and thermal stimuli as well [11].

The receptor target in this case is likely to be proteinase-activated receptor 2 (PAR2) [12], which can be activated by mast cell tryptase released from mast cells in both rat and human skin [13, 14].

In our study, we used the histamine H1 receptor antagonist clemastine to test the histamine dependence of acupuncture analgesia. We found that pretreatment with clemastine at the acupoint can suppress the analgesic effect of acupuncture, but it has no effect on the degranulation induced by acupuncture. The activation of neural regulation in the acupoint is histaminergic.

Since the 1990s, some important discoveries regarding histamine-dependent itch had been made: Schemmlz found a distinct subgroup of C-fibers that are preferentially excited by histamine [15]; Andrew and Craig found histamine-sensitive central projection neurons [16]. Both these authors suggested a histaminergic itch sensation pathway separate from that of pain. This hypothesis is also supported by the modulation of itch by pain in both direction [17] and displacement of pain and itch in pathological conditions [18, 19]. On human subject pain could markedly suppress itch in a range about 10 cm [20]. Histamine injection has direct effects on pain that cause dysesthesias around the site [21].

Considering these facts, in the present study, we tested histamine administration at the acupoint. We found that histamine injection in the acupoint provoked analgesia in a different segment. This effect was accompanied by mast cell degranulation, which might be the result of histamine-induced axon reflex. However, with disodium cromolyn pretreatment, this analgesic effect was not suppressed, which indicates that histamine plays a key role in the activation of the analgesic effect.

One unique characteristic of acupuncture remains: although there are about 360 acupoints in the human body, in practice, there is a preference for sites away from the target site. In traditional Chinese medicine, this preference is explained by the concept of balance. However, to date, not many efforts have been made in scientific acupuncture research on this topic. According to our findings, we believe,

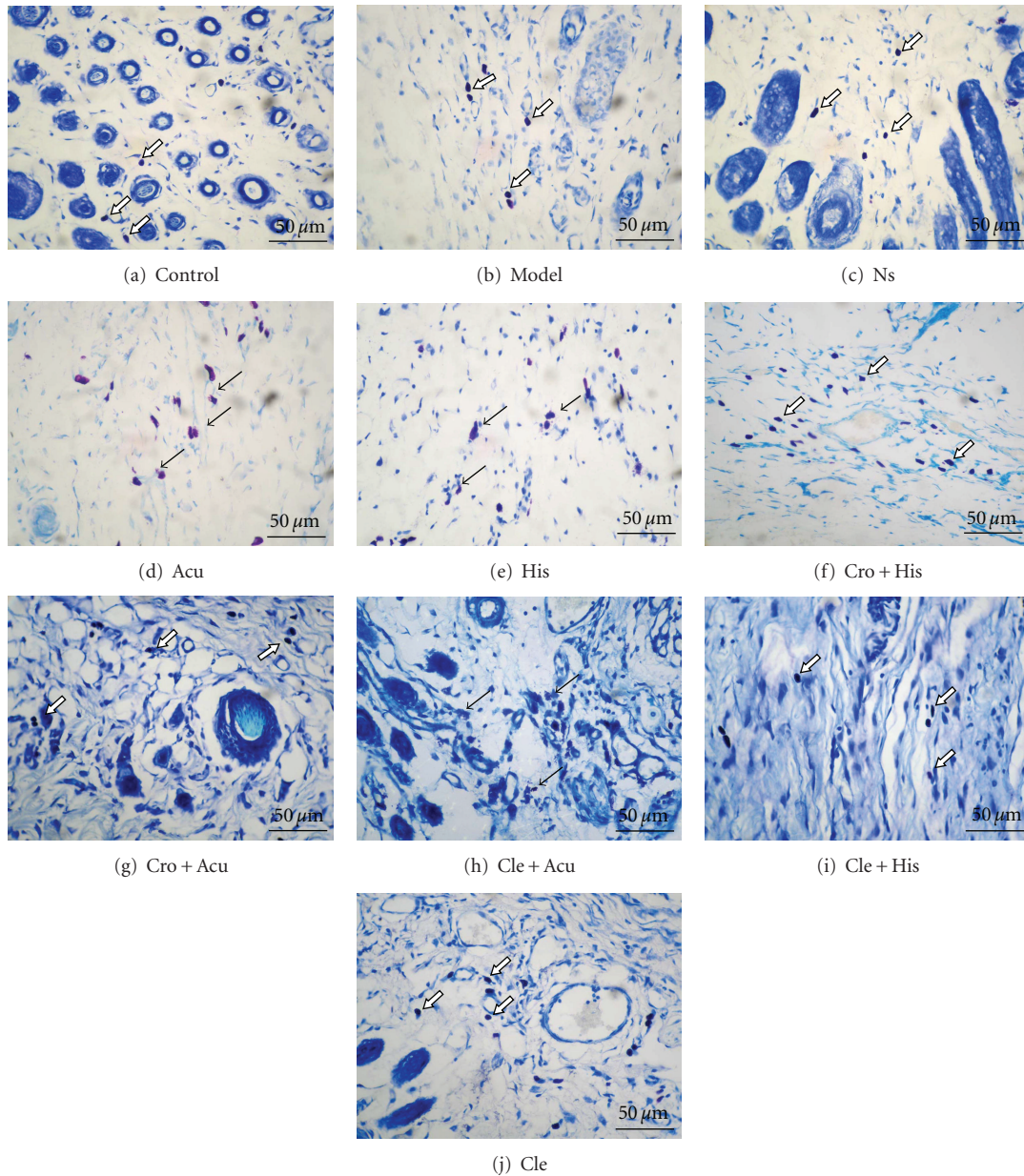


FIGURE 1: Mast cells in the skin and connective tissue near the acupoint area. (a) Control group; (b) Model group; (c) NS group; (d) Acu group; (e) His group; (f) Cro + His group; (g) Cro + Acu group; (h) Cle + Acu group; (i) Cle + His group; (j) Cle group. All pictures were taken at the dermis of ST-36, for groups receiving acupuncture (d), (g), (h) the textures are disoriented, for other group fibers are orderly placed. Blank arrows indicate mast cells in a stable state, and black arrows indicate degranulated mast cells (TB staining 400x).

at least in the case of acupuncture analgesia, that this kind of preference might be caused by histamine-dependent initiation in the acupoint. As shown in Figure 2, in a pathological condition, at the painful site, both kinds of itch sensation will be suppressed by the activation of pain (blue line) on the spinal level. In this case, the histamine released from mast cells cannot generate activation in the central nervous system. Figure 2(b) shows that in the case of acupuncture, mast cells are activated by mechanical force through the manipulation of needles. The histamine release activates the histamine-dependent fiber through H1 receptor, and since the acupoint is away from the pain site, it is not

interrupted by pain sensation and activates the histamine-related center in brain, which might be responsible for acupuncture analgesia.

Clinical research of the past 40 years has demonstrated the effectiveness of acupuncture for relieving pain [22]. Studies on the central mechanism of acupuncture analgesia have been gaining attention for a long time [23]. However, because of the lack of knowledge about brain function and the mechanism of interactions between different sensations, the central mechanism of acupuncture's immediate effect had not previously been related to any physiological mechanism.

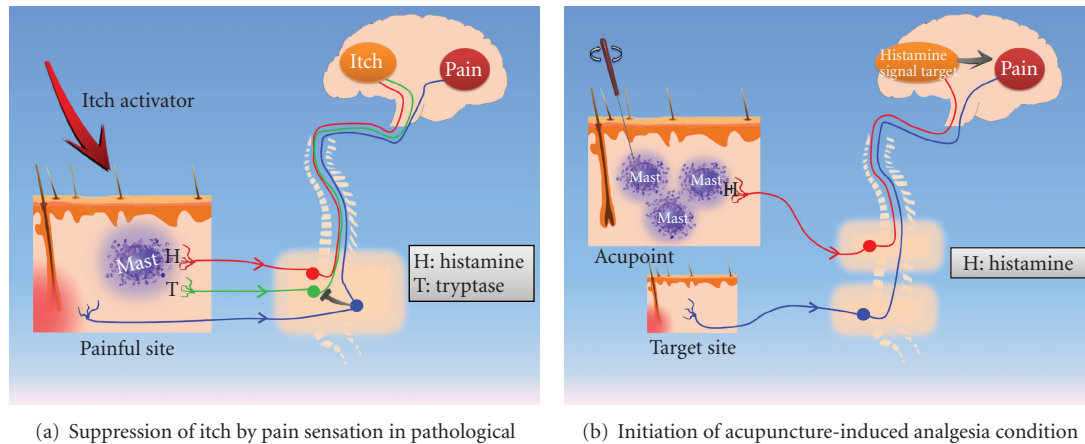


FIGURE 2: Interaction of histamine signal and pain sensation in case of itch suppression by pain and acupuncture analgesia. (a) In a pathological condition, pain suppresses the itch sensation. Mast cells are involved in the itch sensation in two possible ways: the activation of histamine receptors in a histamine-dependent fiber (red line) and the activation of PAR-2 by tryptase (green line). Both of these forms of activation are suppressed by the activation of pain (blue line) at the spinal level. (b) In the case of acupuncture, mast cells are activated by the mechanical force through the manipulation of the needle. The histamine release activated the histamine-dependent fiber through H1 receptors. Since the acupoint is away from the pain site, it is not interrupted by the activation of the pain sensation but activates the histamine target in the brain and initiates acupuncture analgesia.

5. Conclusion

In our research, we found that during acupuncture, mast cells in the acupoint are activated and degranulated by the mechanical stimuli, and they can release histamine into the acupoint through the H1 receptor. The histamine modulates the microenvironment in the acupoint, generating an upstream signal and modulating pain sensation in the central nervous system. Moreover, the histamine dependence of the acupuncture analgesia indicates that acupuncture in the acupoint close to the target site is less effective because of the interruption of pathological pain in the target site. This finding reveals strategic differences between acupuncture analgesia and conventional pain regulation.

Acknowledgments

This work was supported by the National Basic Research Program of China (973 Program, no. 2012CB518502), the National Natural Science Foundation of China (no. 81102630), and the Science Foundation of Shanghai Municipal Commission of Science and Technology (no. 10DZ1975800).

References

- [1] D. Zhang, G. H. Ding, X. Y. Shen et al., "Role of mast cells in acupuncture effect: a pilot study," *Explore*, vol. 4, no. 3, pp. 170–177, 2008.
- [2] H. Huang, R. Zhan, X. J. Yu, D. Zhang, W. M. Li, and G. H. Ding, "Effects of acupoint-nerve block on mast cell activity, manual acupuncture- and electroacupuncture-induced analgesia in adjuvant arthritis rats," *Zhen Ci Yan Jiu*, vol. 34, no. 1, pp. 31–56, 2009.
- [3] M. Ninkovic and S. P. Hunt, "Opiate and histamine H1 receptors are present on some substance P-containing dorsal root ganglion cells," *Neuroscience Letters*, vol. 53, no. 1, pp. 133–137, 1985.
- [4] M. Huang, Y. Y. Xie, and G. H. Ding, "Acupoint-injection of histamine induced analgesic effect in acute adjuvant-induced-arthritis rats," *Zhen ci Yan Jiu*, vol. 35, no. 2, pp. 99–103, 2010.
- [5] K. Okada, M. Oshima, and K. Kawakita, "Examination of the afferent fiber responsible for the suppression of jaw-opening reflex in heat, cold, and manual acupuncture stimulation in rats," *Brain Research*, vol. 740, no. 1–2, pp. 201–207, 1996.
- [6] J. Xiong, F. Liu, M. M. Zhang, W. Wang, and G. Y. Huang, "De-qi, not psychological factors, determines the therapeutic efficacy of acupuncture treatment for primary dysmenorrhea," *Chinese Journal of Integrated Medicine*, vol. 18, no. 1, pp. 7–15, 2012.
- [7] S. Ständer, M. Steinhoff, M. Schmelz, E. Weisshaar, D. Metzke, and T. Luger, "Neurophysiology of Pruritus: cutaneous Elicitation of Itch," *Archives of Dermatology*, vol. 139, no. 11, pp. 1463–1470, 2003.
- [8] A. M. Gilfillan and C. Tkaczyk, "Integrated signalling pathways for mast-cell activation," *Nature Reviews Immunology*, vol. 6, no. 3, pp. 218–230, 2006.
- [9] M. Maurer, T. Theoharides, R. D. Granstein et al., "What is the physiological function of mast cells? Introduction," *Experimental Dermatology*, vol. 12, no. 6, pp. 886–910, 2003.
- [10] W. B. Shelley and R. P. Arthur, "Studies on cowhage (*Mucuna pruriens*) and its pruritogenic proteinase, mucunain," *A.M.A. Archives of Dermatology*, vol. 72, no. 5, pp. 399–406, 1955.
- [11] L. M. Johaneck, R. A. Meyer, R. M. Friedman et al., "A role for polymodal C-fiber afferents in nonhistaminergic itch," *Journal of Neuroscience*, vol. 28, no. 30, pp. 7659–7669, 2008.
- [12] M. Steinhoff, C. U. Corvera, M. S. Thoma et al., "Proteinase-activated receptor-2 in human skin: tissue distribution and activation of keratinocytes by mast cell tryptase," *Experimental Dermatology*, vol. 8, no. 4, pp. 282–294, 1999.

- [13] T. Akiyama, M. I. Carstens, and E. Carstens, "Excitation of mouse superficial dorsal horn neurons by histamine and/or PAR-2 agonist: potential role in itch," *Journal of Neurophysiology*, vol. 102, no. 4, pp. 2176–2183, 2009.
- [14] K. P. Valchanov, G. B. Proctor, R. H. Hartley, K. L. Paterson, and D. K. Shori, "Enzyme histochemistry of rat mast cell tryptase," *Histochemical Journal*, vol. 30, no. 2, pp. 97–103, 1998.
- [15] M. Schmelz, R. Schmidt, A. Bickel, H. O. Handwerker, and H. E. Torebjörk, "Specific C-receptors for itch in human skin," *Journal of Neuroscience*, vol. 17, no. 20, pp. 8003–8008, 1997.
- [16] D. Andrew and A. D. Craig, "Spinothalamic lamina I neurons selectively sensitive to histamine: a central neural pathway for itch," *Nature Neuroscience*, vol. 4, no. 1, pp. 72–77, 2001.
- [17] M. Steinhoff, J. Bienenstock, M. Schmelz, M. Maurer, E. Wei, and T. Biro, "Neurophysiological, neuroimmunological, and neuroendocrine basis of pruritus," *Journal of Investigative Dermatology*, vol. 126, no. 8, pp. 1705–1718, 2006.
- [18] A. Ikoma, M. Fartasch, G. Heyer, Y. Miyachi, H. Handwerker, and M. Schmelz, "Painful stimuli evoke itch in patients with chronic pruritus: central sensitization for itch," *Neurology*, vol. 62, no. 2, pp. 212–217, 2004.
- [19] S. Davidson, X. Zhang, S. G. Khasabov, D. A. Simone, and G. J. Giesler, "Relief of itch by scratching: state-dependent inhibition of primate spinothalamic tract neurons," *Nature Neuroscience*, vol. 12, no. 5, pp. 544–546, 2009.
- [20] H. J. Nilsson, A. Levinsson, and J. Schouenborg, "Cutaneous field stimulation (CFS): a new powerful method to combat itch," *Pain*, vol. 71, no. 1, pp. 49–55, 1997.
- [21] P. Sikand, S. G. Shimada, B. G. Green, and R. H. LaMotte, "Similar itch and nociceptive sensations evoked by punctate cutaneous application of capsaicin, histamine and cowhage," *Pain*, vol. 144, no. 1-2, pp. 66–75, 2009.
- [22] J. G. Lin and W. L. Chen, "Review: acupuncture analgesia in clinical trials," *American Journal of Chinese Medicine*, vol. 37, no. 1, pp. 1–18, 2009.
- [23] B. Pomeranz and D. Chiu, "Naloxone blockade of acupuncture analgesia: endorphin implicated," *Life Sciences*, vol. 19, no. 11, pp. 1757–1762, 1976.

Review Article

A Review of Acupoint Specificity Research in China: Status Quo and Prospects

Ling Zhao,¹ Ji Chen,² Cun-Zhi Liu,³ Ying Li,¹ Ding-Jun Cai,¹ Yong Tang,¹ Jie Yang,¹ and Fan-Rong Liang¹

¹ Chengdu University of Traditional Chinese Medicine, Sichuan, Chengdu 610075, China

² Foreign Languages School, Chengdu University of Traditional Chinese Medicine, Sichuan, Chengdu 610075, China

³ Beijing Hospital of Traditional Chinese Medicine Affiliated to Capital Medical University, Beijing 100010, China

Correspondence should be addressed to Fan-Rong Liang, acuresearch@126.com

Received 15 April 2012; Revised 17 September 2012; Accepted 19 September 2012

Academic Editor: Wolfgang Schwarz

Copyright © 2012 Ling Zhao et al. This is an open access article distributed under the Creative Commons Attribution License, which permits unrestricted use, distribution, and reproduction in any medium, provided the original work is properly cited.

The theory of acupoint specificity is the basis for elucidating the actions of acupoints as employed in clinical practice. Acupoint specificity has become a focus of attention in international research efforts by scholars in the areas of acupuncture and moxibustion. In 2006, the Chinese Ministry of Science approved and initiated the National Basic Research Program (973 Program), one area of which was entitled Basic Research on Acupoint Specificity Based on Clinical Efficacy. Using such approaches as data mining, evidence-based medicine, clinical epidemiology, neuroimaging, molecular biology, neurophysiology, and metabolomics, fruitful research has been conducted in the form of literature research, clinical assessments, and biological studies. Acupoint specificity has been proved to exist, and it features meridian-propagated, relative, persistent, and conditional effects. Preliminary investigations have been made into the biological basis for acupoint specificity.

1. Introduction

For over 2500 years in China, acupuncture has been practiced to treat diseases and maintain well-being. Some traditional theories relating to acupuncture adopt non-Western concepts, and so they would appear to be incompatible with modern medical practice. Nevertheless, acupuncture has gradually won acceptance in Western countries as an alternative or complementary treatment for various conditions. Many reliable studies, including systematic reviews and randomized controlled trials, have indicated that acupuncture is safe and effective in treating a wide range of diseases [1–6]. A number of neuroimaging studies have examined the neural correlates of acupuncture as well as its other biological mechanisms [7–11]. Recently, the doubtful effects of acupuncture with respect to acupoints and nonacupoints have been investigated in clinical research [12–14], and neuroimaging results have also raised questions regarding the existence of acupoint specificity [15, 16]. At the Society for Acupuncture Research (SAR) international symposium held in November 2007, there was intense debate among scholars from different countries about acupoint specificity, and it was regarded

as a core scientific problem with respect to the practice of acupuncture. In 2010, the American Association of Acupuncture reported in a white paper that acupoint specificity was one of the paradoxes of acupuncture research [17].

In 2006, the Chinese government launched the National Basic Research Program (973 Program), one area of which was entitled Basic Research on Acupoint Specificity Based on Clinical Efficacy, which aimed to obtain more accurate data on acupoint specificity. By means of multisubject collaboration, traditional research methods were combined with modern approaches to examine clinical improvement and the biological basis for acupuncture. As a result, major progress was made with regard to acupoint specificity after five years of this research project in China.

2. Advance in the Literature Research of Acupoint Specificity

Using data mining and computer-processing technology, over 2,600,000 pieces of ancient and modern texts relating to migraine, functional dyspepsia (FD), uterus-related

disorders, and dysmenorrhea were collected and compiled by scholars in China. Following the ideas and approaches of evidence-based medicine, this database was filtered and assessed. Acupuncture prescriptions were examined as a key element, and the data relating to the acupoint effect were extracted; in this way, a database with regard to acupoint specificity based on the historical literature was established [18]. On the basis of this, using Microsoft.NET as the system development tool, C# language as the development language, and SQL Server 2005 developed by Microsoft as the database-management system, we established the Data Excavation Platform of Acupoint Specificity. With this platform, we were able to carry out multidimensional and multilayer association analysis using the following four major functions: standardization of acupuncture prescription; standardization of moxibustion prescription; analysis of acupoints; analysis of meridians [19].

Data mining of the literature revealed that acupoints on the *Shaoyang* meridian were the ones chiefly selected for migraine; second, the most commonly selected were acupoints on the *Yangming* meridian. *Fengchi* (GB20) and *Waiguan* (TE5) on the *Shaoyang* meridian were most frequently used for migraine, though *Touwei* (ST8) and *Zusanli* (ST36) on the *Yangming* meridian were also by doctors to treat migraine [20, 21]. The acupoints on the meridian of the foot *Yangming* were the prime choice for treating FD; among them, *Zusanli* (ST36) and *Liangqiu* (ST34) were especially employed. In addition, *Zhongwan* (CV12) and *Weishu* (BL21) as the alarm and transport (*Fu* and *Mu*) points of the stomach were frequent points of application [22, 23]. The acupoints employed for uterus-related disorders and dysmenorrhea were mainly on the spleen meridian, the *Ren* meridian, and the kidney meridian; among these, *Sanyinjiao* (SP6), *Guanyuan* (CV4), and *Taixi* (KI3) were, respectively, the ones most frequently employed for each meridian [24, 25]. These findings indicate that acupoint specificity is closely related to the paths of the meridians; this is because the meridian is the prerequisite for achieving acupoint specificity. Furthermore, acupoint specificity was correlated with the degree of convergence of the meridian's *qi*.

3. Advances in Clinical Studies of Acupoint Specificity

In accordance with the concepts and methods of evidence-based medicine, the principles of clinical epidemiology, and good clinical practice, 2429 participants with migraine, FD, primary dysmenorrhea (PD), and ischemic stroke were recruited for a study. Seven multicentered randomized controlled trials (RCTs) were carried out to verify acupoint specificity (Table 1).

In an RCT on the immediate effect of treating acute migraine with acupuncture, 180 participants were centrally randomized into the verum acupuncture group (acupoints on the *Shaoyang* meridian), sham acupuncture group 1 (some fixed points on a distant nonmeridian reported in the literature), and sham acupuncture group 2 (points located halfway between the two meridians). It was clear from the

trial that among the three groups, significant differences were observed in pain relief, relapse, or aggravation as well as in general evaluations ($P < 0.05$) within 24 hours after treatment. Significant decreases in visual analogue scale (VAS) scores from baseline were observed in the 4th hour after treatment among patients in all three groups ($P < 0.05$). The VAS scores in the 4th hour after treatment decreased by a median of 1.0 cm, 0.5 cm, and 0.1 cm, respectively, in the verum acupuncture group, sham acupuncture group 1, and sham acupuncture group 2. Similarly, there was a significant difference in the change in VAS scores from baseline in the 2nd hour after treatment among the three groups ($P < 0.05$). However, in the 2nd hour after treatment, only patients treated with verum acupuncture showed significant decreases in VAS scores from baseline by a median of 0.7 cm ($P < 0.01$). These findings support the contention that specific physiological effects are produced from genuine acupoints rather than from nonacupoints [26].

In the next RCT on the long-term analgesic effect of acupuncture on migraine, 480 participants from three clinical centers were centrally randomized into treatment group 1 (*Shaoyang*-specific acupuncture), treatment group 2 (*Shaoyang*-nonspecific acupuncture), treatment group 3 (*Yangming*-specific acupuncture), and the control group (nonacupoint group). The left and right acupoints were employed alternatively using needles connected to Han's acupoint nerve stimulator (HANS, Model LH 200A TENS, Nanjing, China) for 30 minutes. Treatments were administered once a day for 5 continuous days followed by a 2-day rest interval. Patients in the acupuncture treatment groups and the nonacupoint control group received a total of 20 treatments over a 4-week period. The primary outcome was the number of days when the subjects experienced a migraine during weeks 5–8 after randomization. Secondary outcomes included the frequency of migraine attacks, migraine intensity, and Migraine-Specific Quality-of-Life Questionnaire. Results showed that compared with patients in the control group, patients in the acupuncture groups reported fewer days with a migraine during weeks 5–8; however, the difference between the treatments was not significant ($P > 0.05$). There was a significant reduction in the number of days with a migraine during weeks 13–16 in all acupuncture groups compared with control (*Shaoyang*-specific acupuncture versus control, $P < 0.01$; *Shaoyang*-nonspecific acupuncture versus control, $P < 0.01$; *Yangming*-specific acupuncture versus control, $P < 0.05$). There was a significant, but not clinically relevant, benefit for almost all secondary outcomes in the three acupuncture groups compared with the control group. There were no relevant differences among the three acupuncture groups [27].

In all, 712 patients with FD included in the multicenter RCT of acupuncture were centrally randomized into six groups: group 1, specific acupoints of the stomach meridian; group 2, nonspecific acupoints of the stomach meridian; group 3, specific acupoints of the alarm and transport (*Fu* and *Mu*) points; group 4, specific acupoints of the gallbladder meridian; group 5, sham acupuncture of nonacupoints; group 6, itopride. Han's acupoint nerve stimulator was used for the electroacupuncture stimulation of each acupoint

TABLE 1: RCT studies of acupoint specificity in China.

Trial	Research object	Sample size	Groups	Primary outcome	Result
Li et al. [26]	Patients with acute migraine attacks	180	Verum acupuncture group: Waiguan (TE5), Yanglingquan (GB 34), Qiuxu (GB 40), Jiaosun (TE 20), Fengchi (GB 20) Sham acupuncture group one: (1) At the medial arm on the anterior border of the insertion of the deltoid muscle at the junction of the deltoid and biceps muscles; (2) Halfway between the tip of the elbow and the axillae; (3) Ulnar side, halfway between the epicodylus medialis of the humerus and the ulnar side of the wrist; (4) The edge of the tibia 1-2 cm lateral to the Zusanli (ST36) horizontally; (5) The inside of the mid-thigh region 2 cm lateral to half the distance from the anterior superior iliac spine to the lateral superior corner of the patella on the rectus femoris; Sham acupuncture group two: (1) located halfway between the triple energizer and small intestine meridians lateral to Waiguan (TE 5) horizontally; (2) halfway between the line from Qiuxu (GB 40) to Jiexi (ST 41); (3) halfway between the gallbladder and bladder meridians lateral to Yanglingquan (GB 34) horizontally; (4) halfway between the line from Jiaosun (TE 20) to Shuaigu (GB 8); (5) halfway between the line from Fengchi (GB 20) to Anmian (extra point) bilaterally	Pain (VAS scores)	+
Li et al. [27]	Migraine patients	480	Group one: Waiguan (TE5), Yanglingquan (GB34), Qiuxu (GB40), Fengchi (GB20) Group two: Luxi (TE19), Sanyangluo (TE8), Xiyangguan (GB33), Diwuhui (GB42) Group three: Touwei (ST8), Pianli (LI6), Zusanli (ST36), Chongyang (ST42) Group four: (1) At the medial arm on the anterior border of the insertion of the deltoid muscle at the junction of the deltoid and biceps muscles; (2) Halfway between the tip of the elbow and the axillae; (3) Ulnar side, halfway between the epicodylus medialis of the humerus and the ulnar side of the wrist; (4) The edge of the tibia 1-2 cm lateral to the Zusanli (ST36) horizontally	Number of days with a migraine	-
Ma et al. [29]	FD patients	712	Group one: Chongyang (ST42), Fenglong (ST40), Zusanli (ST36), Liangqiu (ST34) Group two: Tiaokou (ST38), Dubi (ST35), Yinshi (ST33), Futu (ST32) Group three: Weishu (BL21), Zhongwan (CV12) Group four: Qiuxu (GB40), Guangming (GB37), Yanglingquan (GB34), Waiqiu (GB36) Group five: the same with group four in migraine study (sample size: 480) Group six: itopride (take orally)	SID scores	+
Yu et al. [30]	PD patients	66	Treatment group: <i>Sanyinjiao</i> (SP6) Control group: <i>Xuanzhong</i> (GB39)	PI, RI, A/B	+
Liu et al. [31]	PD patients	200	Acupoint group: <i>Sanyinjiao</i> (SP6) Unrelated acupoint group: <i>Xuanzhong</i> (GB39) Non-acupoint group: lateral side of lower leg, 3 inches above the tip of external malleolus, 1.5 inches behind anterior crest of the tibia No acupuncture group	Pain (VAS scores)	-
Liu, Ma	PD patients	501	Acupoint group: <i>Sanyinjiao</i> (SP6) Unrelated acupoint group: <i>Xuanzhong</i> (GB39) Non-acupoint group: lateral side of lower leg, 3 inches above the tip of external malleolus, 1.5 inches behind anterior crest of the tibia	Pain (VAS scores)	+
Shen et al. [34]	Patients with ischemic stroke	290	Acupoint group: basic acupoints-Neiguan (PC6), Shuigou (DU26), <i>Sanyinjiao</i> (SP6); additional acupoints-Jiquan (HT1), Weizhong (BL40), Chize (LU5) Non-acupoint group: located 3 mm apart from acupoints mentioned above	Global symptoms (BI, relapse rate,	+

Notes: "+" refers to the trial detected different outcomes between acupoint and non-acupoint/inactive acupoint; "-" denotes that the trial did not detect different outcomes between acupoint and non-acupoint/inactive acupoint.

PI: pulsatility index; RI: resistance index; BI: barthel index.

or nonacupoint after needle insertion for 30 minutes. All patients received a total of 20 treatments over a 4-week period. The treatments were administered once a day for 5 continuous days followed by a 2-day rest interval. This trial included both a 4-week and a 12-week followup period. The outcomes were the patient's response, improvement in symptoms measured using the Symptom Index of Dyspepsia (SID), and quality-of-life (QOL) improvement based on the Nepean Dyspepsia Index (NDI) [28]. The results indicated that acupuncture was effective in the treatment of FD and superior to nonacupoint treatment. All the groups showed an improvement in SID and QOL at the end of the treatment, and the improvement was sustained for 4 and 12 weeks. The overall response rate was significantly higher in acupuncture group 1 and lower in the sham acupuncture group than in the itopride and other acupuncture groups ($P < 0.05$). Similarly, the difference in symptoms and QOL improvement was significant between group 1 and the other acupuncture groups ($P < 0.05$) [29].

Three clinical trials were conducted to examine the effect of acupuncture on PD. The first trial included 66 patients with PD, who were randomized into two groups by means of a random-number table. The treatment group received manual acupuncture bilaterally at *Sanyinjiao* (SP6) for 5 minutes after needling sensation (*deqi*) was elicited during the period of menstrual pain; in the control group, the needle was bilaterally at *Xuanzhong* (GB39) for 5 minutes during the period of menstrual pain. Compared with the control group, patients in the treatment group showed significant reductions 5 minutes after treatment in terms of changes in menstrual pain scores ($P < 0.001$), values of pulsatility index ($P < 0.001$), resistance index ($P < 0.01$), and ratio of the systolic and diastolic peaks (A/B) in the uterine arteries ($P < 0.01$). These trials suggest that needling at SP6 can immediately improve uterine arterial blood flow in patients with PD, whereas GB39 did not achieve these effects [30]. In the second RCT, 200 eligible participants with PD were recruited. Patients were randomly assigned to the acupoint group, unrelated acupoint group, nonacupoint group, or no-acupuncture group. Acupuncture and sham acupuncture were administered once a day for 3 days with electroacupuncture at *Sanyinjiao* (SP6), which was specifically intended to treat PD, at an unrelated acupoint (*Xuanzhong*, GB39), or at a nonacupoint location. The primary outcome was pain intensity as measured by VAS at baseline and at 5, 10, 30, and 60 minutes after the start of the first intervention. The secondary outcomes were the Cox retrospective symptom scale, verbal rating scale, pain total time, and proportion of participants using analgesics during three menstrual cycles. The primary comparison of the VAS scores demonstrated that patients receiving acupuncture ($P < 0.001$), unrelated acupoint ($P < 0.001$), and nonacupoint ($P < 0.01$) treatment presented significant improvements compared with the no-acupuncture group. There were no significant differences among the four groups with respect to secondary outcomes ($P > 0.05$). These trials indicated that acupuncture was superior to no acupuncture in relieving dysmenorrheal pain. However, no differences were detected between acupoint acupuncture and unrelated acupoint acupuncture; likewise,

no differences were observed between acupoint acupuncture and nonacupoint acupuncture [31]. The third RCT was implemented based on the results of the second trial. The sample size was expanded to 501 participants with PD, who were randomized into an acupoint group (*Sanyinjiao*, SP6), an unrelated acupoint group (*Xuanzhong*, GB39), and a nonacupoint group [31, 32]. Electro-acupuncture was applied for 30 minutes on the 1st day of the menstrual period when the VAS scores were greater than 40 mm. The treatment was administered once daily for 3 continuous days. With the first session of treatment, an immediate analgesic effect was observed by assessing the VAS score before treatment and 5 and 10 minutes after being connected to the Han's acupoint nerve stimulator; the VAS score was also recorded immediately after and 30 minutes after withdrawing the needles. With the second and third sessions of treatment, VAS was employed before treatment to confirm the cumulative analgesic effect; the same scoring method was conducted on the last day of treatment and before the next menstrual period to observe the cumulative and persistent analgesic effects. The results demonstrated that the immediate, cumulative, and persistent analgesic effects after the first, second, and third treatment sessions induced by *Sanyinjiao* (SP6) were significantly superior to those induced by *Xuanzhong* (GB39) and nonacupoint treatment ($P < 0.05$).

The seventh RCT consisted of 290 patients with ischemic stroke from four clinical centers who were randomized into acupoint and nonacupoint groups. They received "resuscitation therapy" ("*Xing Nao Kai Qiao*") on acupoints and nonacupoints once a day continuously for 4 weeks. The Barthel Index, National Institute of Health Stroke Scale, and Chinese Stroke Scale were used to assess the outcomes after treatment. Compared with the nonacupoint group, the primary outcome of the mean values for the Barthel index up to 6 months in the acupoint group showed a significant increase ($P < 0.01$), and the relapse rate was significantly reduced in the acupoint group ($P < 0.001$). However, there was no difference in the death rate between the two groups ($P > 0.05$). Additionally, acupuncture resulted in a significant difference between the two groups for the National Institute of Health Stroke Scale—not at 2 weeks ($P > 0.05$), but at 4 weeks ($P < 0.01$). There was a remarkable difference in the Chinese Stroke Scale at 4 weeks ($P < 0.001$) and the Stroke-Specific QOL Scale at 6 months ($P < 0.01$) between the acupoint and nonacupoint groups [33, 34].

4. Progress in Acupoint Specificity on Biological Structures

Anatomical structures act as the chief basis for action on the acupoints. Though no unique structures corresponding to the meridians or acupoints have been discovered, the points are always located on regions that are abundant in nerves and blood and lymph vessels; this is where nerve endings, nerve receptors, blood vessels, mucopolysaccharides, and mast cells are densely distributed.

By means of histological methods, Chinese researchers have conducted animal experiments to evaluate the analgesic

effect of acupuncture and analyzed the number of mast cells and their proportion in degranulation at both acupoints and nonacupoints areas. In addition, intensive systematic research has been conducted using morphological and molecular biological methods to determine the relation between the mast cells and acupoint effects; these studies have involved local anesthesia injections into the acupoint, patch clamps, and confocal laser scanning microscopy in addition to other techniques.

4.1. Degranulation of Mast Cells—Positive Correlation with Acupoint Specificity. Increased degranulation of mast cells has been observed at acupoint areas [35]. These granules would appear to stimulate the acupoint receptor to form an analgesic signal; the granules also appear to be diffused peripherally and participate in such phenomena as propagated sensation along the meridian. When cromolyn sodium was used to prevent degranulation of the mast cells at the acupoint, the analgesic effect induced by acupuncture was remarkably reduced. Therefore, degranulated mast cells appear to be involved in acupuncture analgesia, which is positively correlated with acupoint specificity. Degranulation of mast cells is one of the starting signals of acupuncture analgesia [35–37].

4.2. Activation of Mast Cells—Related to Collagen Fiber at Acupoints. At acupoints, collagen fibers are intertwined and form a three-dimensional net-like tissue. When an acupuncture needle is inserted into such points using a lifting, thrusting, or twisting technique, the needle stimulates the connective tissue at dense layer of the dermis, producing deformity of the collagen fibers, which in turn brings about mast cell degranulation. However, after the collagen fibers have been damaged, the needling manipulations are no longer able to produce this effect on the fibers; thus, acupuncture analgesia becomes reduced owing to decreased mast cell degranulation [38].

The analgesic effect was investigated in terms of the contrast in the afferent mechanism between hand acupuncture and electroacupuncture on *Zusanli* (ST36) in rats. Preprocessing of type I collagenase or cromolyn sodium significantly reduced the analgesic effect with hand acupuncture ($P < 0.05$), but this was not affected with electroacupuncture ($P > 0.05$). With the above two processing methods, the degranulation rate of mast cells induced by both hand acupuncture and electroacupuncture was significantly inhibited ($P < 0.05$) [39]. The results indicated that collagen fibers, as the recipient of the mechanical force with hand acupuncture, played an important role in peripheral signal transduction. It could be that the initiating signal caused by the hand acupuncture needle is mainly mediated by collagen fibers and mast cell activation; in this way, the acupuncture information is transmitted to the central nervous system. However, the signal with the electroacupuncture needle is directly mediated by the nerves through activation of the peripheral nerve receptors.

4.3. Location of Regional Elements—Acupoint Specificity. In one study, researchers measured the characteristic X-ray

emissions of Ca, Fe, Cu, and Zn at four different acupuncture points: *Jianshi* (PC5), *Ximen* (PC4), *Tiaokou* (ST38), and *Xiajuxu* (ST39) as well as in the surrounding tissues. The X-ray fluorescence analysis was used to study human tissue samples, and proton-induced X-ray emission and synchrotron X-ray fluorescence analysis were employed to detect tissue composition. The study determined differences in structure between acupoint and nonacupoints; with the former, there were high concentrations of mast cells as well as somewhat greater accumulation of microvessels. The contents of Ca, Fe, Cu, and Zn were significantly higher at three out of four acupoints examined than in the nonacupoint tissue, with closely similar ratios of Cu to Fe at points *Jianshi* (PC5), *Tiaokou* (ST38), and *Xiajuxu* (ST39), but not *Ximen* (PC4). Each acupoint seemed to be elliptical, with the long axis along the meridian. Therefore, it was assumed that reduction in the mineral content from acupoints to surrounding areas proceeded more slowly in the meridian direction [40].

5. Specific Reactions of Acupoints and Biophysical Properties

Studies examining biophysical properties, involving electrical and temperature features, have been used to investigate acupoint specificity. One study on the volt-ampere (V-A) characteristics of human acupoints indicated that there is a characteristic, nonlinear V-A curve associated with these points. Compared with control points, low electrical resistance was frequently found at acupoints. A cosine analysis and an amplitude test on acupoints on the six yin meridians of healthy participants showed that the acupoints underwent clear circadian changes, which reflected changes in body temperature circadian rhythms [41].

The skin temperature of uterine-related acupoints on three foot yin meridians, a uterine-relevant acupoint, and a nonpoint in 49 healthy female university students on the 1st day of menstruation and the 3rd day after menstruation were compared to examine the specific response of acupoints to menstruation (Table 2). The uterine-related acupoints *Xuehai* (SP10), *Diji* (SP8), *Zhongdu* (LR6), *Sanyinjiao* (SP6), *Taixi* (KI3), *Taibai* (SP3), *Taichong* (LR3), and *Shuiquan* (KI5), the uterine-unrelated acupoint *Xuanzhong* (GB39), and the nearby nonmeridian point *Xuanzhong* (GB39) were selected. The results showed that the temperature at *Taixi* (KI3)—the *yuan*-source point of the kidney meridian of the foot, *Shaoyin*—on the 1st day of menstruation was significantly lower than on the 3rd day after the menstruation ($P < 0.01$). There were no significant temperature differences at other measurement points between those 2 days ($P > 0.05$) [42].

One hundred healthy undergraduates were randomized into 10 groups. *Zusanli* (ST36), *Fenglong* (ST40), *Chongyang* (ST42), *Yinlingquan* (SP9), *Gongsun* (SP4), *Taibai* (SP3), *Guangming* (GB37), *Qiuxu* (GB40), and nonacupoints were acupunctured for 20 minutes, and gastric function before and after acupuncture was monitored by electrogastrogram. The results indicated that there were significant differences

TABLE 2: Biological basis studies of acupoint specificity in China.

Trial	Study carrier	Sample size	Groups	Primary indicator	Results
She et al. [42]	Healthy female	49	<i>Xuehai</i> (SP10), <i>Diji</i> (SP8), <i>Zhongdu</i> (LR6), <i>Sanyinjiao</i> (SP6), <i>Taixi</i> (KI3), <i>Taibai</i> (SP3), <i>Taichong</i> (LR3), <i>Shuiquan</i> (KI5), <i>Xuanzhong</i> (GB39), non-acupoint: located halfway between the stomach and gallbladder meridians lateral to <i>Xuanzhong</i> (GB39) horizontally	Skin temperature of acupoint/non-acupoint at the 1st day of menstruation and the 3rd day after menstruation.	<i>Taixi</i> (KI3) has specific response of menstruation.
Chen et al. [43]	Healthy undergraduates	100	<i>Zusanli</i> (ST36), <i>Fenglong</i> (ST40), <i>Chongyang</i> (ST42), <i>Yinlingquan</i> (SP9), <i>Gongsun</i> (SP4), <i>Taibai</i> (SP3), <i>Guangming</i> (GB37), <i>Quxu</i> (GB40) and non-acupoint: the edge of the tibia 1-2 cm lateral to the <i>Zusanli</i> (ST36) horizontally	Changes of average amplitude of gastric electrical activity.	<i>Zusanli</i> (ST36) has greatest impact on gastric function. Acupoints of stomach and spleen meridian have closely relation with stomach.
Deng et al. [44]	Volunteers	104	Bilateral <i>Taiyuan</i> (LU9), <i>Neiguan</i> (PC6), <i>Daling</i> (PC7), non-acupoint one: locates halfway between <i>Taiyuan</i> (LU9) and <i>Daling</i> (PC7), non-acupoint two: located halfway between the pericardium and lung meridians lateral to <i>Neiguan</i> (PC6) horizontally	FEV1, MVV	Left <i>Taiyuan</i> (LU9) can reflect the pulmonary function.
Liu et al. [49]	Patients with coronary heart disease	50	<i>Taiyuan</i> (LU9), <i>Shenmen</i> (HT7), <i>Daling</i> (PC7)	Detect the infrared radiation in the spectral range of 1.5-16 μm .	<i>Shenmen</i> (HT7) and <i>Daling</i> (PC7) can reflect the pathological state of myocardial ischemia.
Lai et al. [50], Zhang et al. [51], Huang et al. [52]	Healthy volunteers	36	<i>Waiguan</i> (TE5); sham needling in TE5; overt placebo needling in TE5; non-acupoint: located at the same level as <i>Waiguan</i> (TE5) and on the midline between the <i>Triple warmer</i> meridian of hand- <i>Shaoyang</i> and the <i>small intestine</i> meridian of hand- <i>Taiyan</i>	Cerebral responses by PET-CT or fMRI detected.	<i>Waiguan</i> (TE5) has relative specific effect in treating dysfunction of ear, cardiovascular disorders, upper limbs paralysis, and blood pressure fluctuation.

TABLE 2: Continued.

Trial	Study carrier	Sample size	Groups	Primary indicator	Results
Huang et al. [53, 54]	Ischemic stroke patients	55	<i>Waiguan</i> (TE5) needling group, <i>Waiguan</i> (TE5) sham needling group, sham point needling group, sham point sham needling group and non-needling group	Cerebral responses by PET-CT or fMRI detected.	<i>Waiguan</i> (TE5) can specific activate motor execution and vision-related cerebral regions in the healthy hemisphere and the limbic system of the affected hemisphere; can remarkable deactivate the motor execution-related cerebral region, emotion area and cognition region of the affected hemisphere for ischemic stroke patients.
Zeng et al. [56]	FD patients	20	Acupoints of stomach meridian: <i>Liangju</i> (ST34), <i>Zusanli</i> (ST36), <i>Fenglong</i> (ST40) and <i>Chongyang</i> (ST42); Non-acupoints: (1) At the medial arm on the anterior border of the insertion of the deltoid muscle at the junction of the deltoid and biceps muscles; (2) Halfway between the tip of the elbow and the axillae; (3) Ulnar side, halfway between the epicodyleus medialis of the humerus and the ulnar side of the wrist; (4) The edge of the tibia 1–2 cm lateral to the <i>Zusanli</i> (ST36) horizontally	Cerebral glycometabolism changes by PET-CT examined.	The more remarkable modulation on the homeostatic afferent network, including the insula, ACC, and hypothalamus, might be the specific mechanism of stomach-specific acupuncture for treating FD.

Notes: FEV1: Is forced expiratory volume; MVV: maximal voluntary ventilation.

in the rate of change of the gastric electrical area between needling acupoints and needling nonacupoints as well as between needling acupoints on different meridians ($P < 0.05$). There was a significant difference in needling different acupoints on different meridians on the rate of change of the gastric electrical area ($P < 0.05$). *Zusanli* (ST36) showed the strongest role with respect to gastric function ($P < 0.05$) [43].

A total of 104 volunteers were subjected to infrared radiation at bilateral *Taiyuan* (LU9), *Neiguan* (PC6), *Daling* (PC7), and nonacupoints as part of an investigation into pulmonary function. The results indicated that there was a correlation between infrared radiation and pulmonary function at six of the ten points. There was a correlation between the level of infrared radiation and 1-second forced expiratory volume and between infrared radiation and maximal voluntary ventilation at the left *Taiyuan* (LU9) ($P < 0.001$ or $P < 0.01$). Thus, infrared radiation at the left *Taiyuan* (LU9) was best able to reflect pulmonary function [44].

6. Correlation between Acupoint Specificity and Functional State

Acupoints can be used diagnostically to reveal the presence of pathogens and indicate therapies for curing disease. This diagnostic ability varies with changes in the body's constitution, which is manifest as an alternation between being physiologically "silent" or pathogenically "active." A number of researchers maintain that when some internal organs are affected by disease, acupoint sensitization has the potential for exerting dynamic functional changes, reflecting acupoint specificity [45].

Injecting mustard oil into the intragastric mucous membrane in rats resulted in massive mucous inflammation, as evidenced by histological examination, which revealed that the intragastric mucosa had become edematous and showed dilated blood vessels, and that there was ulceration of the endogastric lining. In all six rats that received the mustard oil injections into the intragastric mucosa, small blue dots appeared on the skin over the whole abdomen, but mainly in the perimidline upper and middle abdomen, and the middle back in addition to a few on the thigh and groin. The number and distribution of the blue dots varied considerably among the rats. The dots started to appear about 20 minutes after injecting the mustard oil, and the majority of dots were visible within 50 minutes. The dots were very small, usually ranging from 1 to 3 mm in diameter. However, several dots were more elongated and had a length of 3–6 mm. In contrast, two of the four control rats that received saline injections into the intragastric mucous membrane showed no skin color changes at all. The remaining two control rats showed only three to five small blue dots over the middle abdomen; this extravasation restricted to the abdominal skin in these two control rats may have been associated with the abdominal surgical incision. It may be speculated that cutaneous distribution of the blue dots reflected the distribution of gastric segmental innervations [46].

Acute gastric mucosal injury (AGMI) was modeled in the rat, and the plasma extravasated Evans blue (EB) points on the skin of the whole body were observed after removal of hair. The extravasated EB points showed the following distribution: 47.5% of the points were located at *Geshu* (BL17), 58.82% at *Jizhong* (GV6), 88.23% at *Pishu* (BL20), 82.35% at *Weishu* (BL21), 17.64% at *Zhongwan* (CV12), and 5.88% at *Shangwan* (CV13). The plasma extravasation of the EB points seldom appeared in normal control rats, and fewer points were observed in rats administered with 0.9% saline. Significant differences were found between model and normal control groups and also between model and normal saline groups in the number of extravasated EB points ($P < 0.01$, $P < 0.05$). The number of extravasated EB points was related to the phase of gastric mucosal injury, being greatest on the 2nd and 3rd days after modeling and disappearing gradually along with the natural repair of the AGMI [47].

A comparison was made between 31 patients with coronary artery disease and 31 healthy people to observe differences in the infrared spectra of the left *Neiguan* (PC6); significant differences in the wavelengths at 1.5–3.3 μm , 10.7–12.5 μm , and 14.1–15.9 μm were found ($P < 0.01$) [48]. In another study, 47 healthy subjects and 50 patients with coronary artery disease were compared to detect the infrared radiation at the *yuan*-source acupoint on the yin meridians of hand in the spectral range of 1.5–16 μm . Through a comparison of the spectral shape analysis and the infrared intensity, there was no significant difference on either side of the same bilateral acupoints in terms of infrared radiation intensity in healthy people ($P > 0.05$); there were, however, significant differences in infrared radiation intensity at *Daling* (PC7) and *Shenmen* (HT7) in patients with coronary heart disease ($P < 0.05$) [49].

7. Neuroimaging Research on Acupoint Specificity

In one study, 36 healthy volunteers participated in two neuroimaging experiments, which focused on cerebral responses following needling at *Waiguan* (TE5) on the right hand. The first part of the study examined the effect of true, sham, and overt placebo needling at *Waiguan* (TE5) on metabolic changes in cerebral regions by means of positron emission tomography (PET). This study showed that compared with sham acupuncture, the left temporal lobe (Brodmann area 42, BA42), insula (BA13), and cerebellum were activated by true acupuncture. Compared with placebo needling, BAs 13, 7, and 42, both parietal lobes, the occipital lobes, and cuneus were activated by true acupuncture. Cerebral glucose metabolism was changed by sham needling compared with placebo, mainly in the primary and supplementary motor cortex (BA4, BA6) and associative visual cortex (BA19) [50, 51]. The second part of the study observed the regional cerebral activation of the *Waiguan* (TE5) following true needling, sham needling, and true needling at a sham point using functional magnetic resonance imaging (fMRI). The results demonstrated that compared with sham needling,

true needling activated the right superior frontal gyrus (BA8) and the left cerebellum. Compared with needling at the sham point, true needling activated the right parietal lobe, the left cerebellum, and the right inferior semilunar lobule [52]. These results showed that the brain responses to true needling at *Waiguan* (TE5) were significantly different from the responses to needling at sham points or sham needling on true acupoints. It is well known that the insula regulates impulsive and aggressive behavior and that the temporal lobe regulates auditory functions. The parietal lobe receives nervous sensation from the opposite side of the body, and the superior frontal gyrus is involved in such activities as writing and movement of the upper limbs. The cerebellum regulates activities of the trunk muscles and plays an important role in maintaining balance and posture. These preliminary results provide some evidence for *Waiguan* (TE5) in the treatment of ear dysfunctions, cardiovascular disorders, paralysis of the upper limbs, and blood pressure problems.

In one study, 43 ischemic stroke patients with damage to the right hemisphere were randomly divided into a *Waiguan* (TE5) needling group, sham needling group, sham point needling group, sham point sham needling group, and nonneedling group. PET was used to detect cerebral functional regions during the needling process. Compared with the nonneedling group, the acupoint needling group showed activation of BA30. Sham needling at the sham point led to deactivation in BA6. Compared with sham needling at the acupoint, needling at TE5 activated BA13, 19, and 47. Compared with needling at the sham point, needling at the acupoint had a deactivating effect on BA9 [53]. Another fMRI study involved an analysis of 12 ischemic stroke patients who showed typical right-sided hemiplegia; they were randomly assigned to two groups: one group underwent sham needling and true needling at *Waiguan* (TE 5) in the healthy upper limb; the other group underwent sham and true needling at a sham point. Compared with sham needling at TE 5, true needling deactivated BA 4, 6, 24, and 32 areas. In addition, compared with needling at the sham point, true needling at TE 5 deactivated the bilateral hypothalamus [54]. In general, TE5 in stroke patients was able to activate motor execution- and vision-related cerebral regions in the healthy hemisphere and the limbic system of the affected hemisphere; it was also able to deactivate the motor execution-related cerebral region, emotion area, and cognition region of the affected hemisphere. This would appear to point to a key mechanism in the clinical treatment of ischemic stroke.

Six cases of chronic migraine were treated with acupuncture at *Fengchi* (GB20), *Waiguan* (TE5), and *Yanglingquan* (GB34) on the *shaoyang* meridian. PET was used for scanning, and Statistical Parametric Mapping software 2 was used to analyze the data and compare with healthy human brain function imaging and also to investigate changes in cerebral glucose metabolism in the migraine patients before and after acupuncture. The results suggested that after acupuncture, excited areas of the brain, such as the brain stem and insula, were obviously reduced, and brain areas with a lower level of glycometabolism changed from the right temporal lobe to the bilateral temporal lobes ($P < 0.005$). Such areas as the

pons, insula, and anterior frontal gyrus are possibly the target points of the analgesic effect for chronic migraine induced by acupuncture at the *Shaoyang* meridian. The reduction in metabolism in the bilateral temporal lobes is possibly the mechanism by which acupuncture at points on the *Shaoyang* meridian works in the treatment of migraine [55].

Neuroimaging studies have confirmed that compared with nonacupoints, acupoints had a much more extensive influence on brain functions in patients with FD, and that acupoint specificity was regulated by the central nervous system. In one study, 40 patients with FD and 20 healthy participants were scanned by PET-computed tomography (CT). The outcome showed that compared with healthy subjects, patients with FD had higher levels of glycometabolism in the bilateral insula, anterior cingulate cortex (ACC), middle cingulate cortex (MCC), cerebellum, thalamus, prefrontal cortex, precentral gyrus, postcentral gyrus, middle temporal gyrus, superior temporal gyrus, putamen, right parahippocampal gyrus, claustrum, and left precuneus ($P < 0.001$). The signal increase in the ACC, insula, MCC, and cerebellum was positively correlated with symptom index of dyspepsia scores ($P < 0.01$) and negatively correlated with NDI scores ($P < 0.01$). Therefore, it was concluded that the ACC, insula, thalamus, MCC, and cerebellum are closely related to the severity of FD [57]. In another study, 20 patients with FD were randomly assigned to receive either acupuncture or sham acupuncture therapy, and they were examined by PET-CT scan before and after treatment. The NDI and SID were used to evaluate the therapeutic effect. Acupuncture was performed on acupoints of the stomach meridian: *Liangqiu* (ST34), *Zusanli* (ST36), *Fenglong* (ST40), and *Chongyang* (ST42). The sham acupuncture was performed on four nonacupoints, which were the same as in the FD clinical trial mentioned above. The results indicated that acupuncture and sham acupuncture exerted different responses on the brain. In the acupuncture group, deactivation of the brainstem, ACC, insula, thalamus, and hypothalamus were largely related to the decrease in SID score and the increase in NDI score ($P < 0.05$, corrected) after treatment. In the sham acupuncture group, deactivation of the brainstem and thalamus tended to be associated with an increase in NDI score ($P < 0.1$, corrected) [56].

8. Metabolomic Study of Acupoint Specificity

A study was made of patients with FD, in whom plasma metabolites were measured by means of ^1H nuclear magnetic resonance (NMR) spectroscopy after the treatment at specific acupoints of the stomach meridian, nonspecific acupoints of the stomach meridian, specific acupoints of the gallbladder meridian, or nonacupoints. The acupoints and nonacupoints were selected in the same manner as in the FD clinical trial discussed in the previous section. The latent biomarkers, plasma phosphatidylcholine and leucine/isoleucine, were related to the NDI scores of patients with FD. Acupoints exerted a better effect on regulating the key metabolic substances than nonacupoints, and the specific acupoints

on the disease-pertinent meridian (stomach meridian) were superior to nonspecific acupoints or acupoints on the other meridian (gallbladder meridian) [58, 59]. In metabolic terms, the results confirmed that acupoints exerted a strong, targeted regulatory effect, whereas nonacupoints had a weaker effect and a narrow regulatory scope.

9. Discussion

As a critical theoretical foundation, acupoint specificity is of prime importance in point selection in acupuncture clinics, and it involves specificity in terms of clinical effect, biological structure, and biophysics. The specificity of the clinical effect is the basis of acupoint specificity, and therefore currently it is widely discussed both in China and overseas. Acupoint specificity focuses on differences in the indicative range and curative efficacy between real acupoints and nonacupoints as well as among real acupoints. In addition to a comparison of acupoints and nonacupoints, great attention has been paid to different acupoints and their meridian tropism. Thus, in some basic research efforts, the various effects of different acupoints that may be related to the same meridian have been investigated. With their particular characteristics, acupoints from one meridian can exert different impacts on the organ with which they are related. In different clinical situations, physicians perform meridian, regional, or visceral differentiation, and they carefully select the points on the affected regions, points corresponding to meridian terminals, or those with particular curative effects. If only the traveling pathway of the meridians and character of acupoints are taken into consideration, acupuncture is likely to achieve favorable results in clinical treatment. However, some non-Chinese studies have revealed that acupoint specificity does not exist since all parts of the body can obtain curative effects as a result of acupuncture. According to their hypothesis, nonacupoints exert identical therapeutic effects to acupoints when stimulated.

In recent years, many non-Chinese clinical and experimental studies have paid close attention to acupoint specificity, and they have produced mixed results. According to a systematic review of clinical trials on acupoint specificity from 1998 to 2009, six of the 12 studies positively pointed to the existence of acupoints; the other six were unable to confirm the existence of acupoints, and they suggested that conventional acupuncture was not different from sham acupuncture [60]. It is indisputable that positive reports about acupoint specificity from China far outnumber those from other countries. It is difficult to account for the different results obtained in China and overseas without examining issues of bias and the quality of the studies.

9.1. Design of Controls. In the opinion of the present authors, acupoints exert their effects in three ways: the main functions and indications of the acupoints; the manipulation techniques employed in needling; placebo effects, such as the interactions between doctors and patients; the expectation of the patients themselves.

The characteristics of the acupoint and its related meridian should be taken into consideration when examining

the therapeutic effects of acupoint specificity. Thus, a full analysis of the various clinical effects should be made at the following three levels: acupoints versus nonacupoints; different acupoints possessing the same property on different meridians; different acupoints from one meridian. Currently, properly controlled methods for studying acupoint specificity can be generalized into three categories: nonacupoints; minimal acupuncture (superficial needling); placebo needling (noninvasive needling). Comparisons are seldom made among acupoints on the same meridian or acupoints having the same property on different meridians.

Although minimal acupuncture is widely adopted in investigations of acupoint specificity, it has to be questioned whether it can be used as a control. Minimal acupuncture has a long history and is characterized by limited insertion of needles into the epidermis, dermis, or subcutaneous tissue. According to the theory of acupuncture, the place where minimal acupuncture exerts its effects is the cutaneous region (*pi bu*), which has definite divisions with respect to the system of the 12 regular meridians. A number of reports have verified that stimulating the cutaneous region can achieve specific curative effects [12, 61, 62]. Some basic studies have also demonstrated that both verum acupuncture and minimal acupuncture may induce activation of sensory afferents, which amounts to objective evidence of the clinical efficacy of minimal acupuncture [63–66]. However, in a study on the cardiovascular response to minimal acupuncture, some researchers viewed this procedure as a valid control method [67]. We believe that it is important to examine such investigations in terms of the following questions. Was minimal acupuncture appropriately used for the control group? What is the correlation between minimal acupuncture and the disease being treated and the stimulated part of the body? However, minimal acupuncture cannot be prioritized over other control methods in studies of acupoint specificity.

9.2. Objects of Studies. Studies on acupoint specificity, especially those conducted overseas using neuroimaging, have been carried out on healthy participants [11, 15, 68–70]. Studies on the correlation between the status and specificity of acupoints have demonstrated the following: acupoints are relatively “silent” under normal physiological conditions, yet they are relatively “sensitive” under pathological conditions [71]. With respect to the transmission of pathogens, manifest syndromes, regulatory organs, and balancing yin and yang, acupuncture plays its therapeutic role under pathological conditions, not normal physiological conditions. As a result, there are limitations to acupoint studies of physiological conditions that are not a concern with studies of pathological conditions.

Since it is widely acknowledged that acupuncture is effective in relieving pain, there have been many studies on acupoint specificity with respect to migraine [6, 12, 26, 61, 72], fibromyalgia [14, 73, 74], lumbago [62, 75–77], osteoarthritis [1, 78, 79], and other painful diseases. These studies produced mixed results. Pain is an objective sensation that is inevitably subject to individual variability; as such it can lead to study bias. Some researchers have suggested that

the studies on the efficacy of acupuncture in terms of pain produce uncertain results because of variability in measuring the outcomes [80].

We established clinical groups for needling acupoints on the affected meridian, acupoints on unaffected meridians, and nonacupoints in a study of the effect of acupuncture in migraine and FD. The results showed that with FD, the therapeutic effect in the acupoint group was greater than that in the nonacupoint group over the first 4 weeks. In the 8th week, and the acupoint group for the affected meridian (stomach meridian) showed a better therapeutic effect than the acupoint group on the other meridian (gallbladder meridian). Further, needling the acupoints on the affected meridian (stomach meridian) was more effective than stimulating the nonacupoints on that meridian [29]. In the case of migraine, the primary outcome was that in the 8th week, the acupoint group showed a superior therapeutic effect to the nonacupoint group. In the 16th week, the acupoint group on the affected meridian (*Shaoyang* meridian) showed a better therapeutic effect than the group for the other meridian (stomach meridian). Additionally, on the affected meridian (*Shaoyang* meridian), the specific acupoints were more sensitive than unspecific acupoints [72]. Accordingly, it was demonstrated that the sensitivity of the acupoints and the time when they exert their specific effects vary according to the type of illness.

Furthermore, *A-shi* points, which are typically used for localized treatment, are commonly adopted in treating pain. However, *A-shi* points are not regular acupuncture points in terms of traditional acupuncture theory, and they are unable to cure diseases. Thus, it might be assumed that acupoint specificity is influenced by the disease itself. However, further studies are necessary to determine how this effect operates.

9.3. Study Design of Clinical Trials. Two major types of clinical RCTs into acupuncture have been carried out in China and other countries—efficacy trials and effectiveness trials. There is a significant difference in these two types in terms of their objectives and interventions. “Efficacy” signifies the extent to which a specific intervention is beneficial under controlled conditions. An efficacy trial is typically an explanatory type of trial that is performed under experimentally controlled conditions. An efficacy trial primarily concentrates on the causal effects of a treatment, for example, by comparing it to a placebo. Effectiveness examines whether a treatment is beneficial under conditions close to those that operate in routine care, and effectiveness studies adopt a more pragmatic approach [81, 82]. Research into acupoint specificity in China always takes the form of efficacy trials [26, 29–32, 72], in which comparisons are made of acupoints and nonacupoints with respect to strong hypotheses and strict eligibility criteria. However, in other countries, researchers develop effectiveness trials by comparing intervention with both routine treatment and with sham acupuncture [83].

With regard to intervention, the therapeutic principle varies according to the objectives of the efficacy or effectiveness trial. As a rule, in an efficacy trial, the treatment protocol is often designed using a standardized or semistandardized

regimen, and every participant receives the same acupoint treatment—or the same treatment combined with adjunct points depending on their particular symptoms. An effectiveness trial reveals realistic results after clinical treatment, and it often employs a more flexible treatment protocol, whereby the acupuncturist carries out a unique treatment for the particular individual [81, 83]. In China, trials using standardized treatment [26, 29, 31, 72] are more frequently employed than those with semistandardized treatment [6, 34]; however, both types of treatment are used in trials overseas [84, 85], and a quite few trials overseas adopt individual treatment regimes [86].

Since the present study aims to explore the authenticity of acupoint specificity, the design of the efficacy trial is important. In terms of intervention, standardized treatment is appropriate for eliminating confounding factors and ensuring the reliability of the outcome. Although standardized treatment is poor in dealing with syndrome differentiation, it is not inconsistent with Traditional Chinese Medicine (TCM) because acupuncture therapy takes meridian differentiation as its principal, regional differentiation as its emphasis, and visceral differentiation as its supplementation [87]. The standardized treatment protocol is not something that is randomly mapped out; it depends on the particular features of the disorder, which determine the appropriate acupoints that should be used. For example, migraine is considered a disorder of the *Shaoyang* meridian; thus, acupoints on the *Shaoyang* meridian are the prime choice in acupuncture for treating this condition. FD is a disorder of the visceral organs, so the treatment protocol utilizes a visceral focus together with meridian differentiation, whereby application is made to the alarm and transport (*Fu* and *Mu*) points or other points of the stomach meridian.

Acupoint specificity and syndrome differentiation play a central role in acupuncture clinical practice. Acupoint selection according to syndrome differentiation is based on the specific effects of the various acupoints. As noted above, acupoint selection is linked to the common methods of meridian differentiation, regional differentiation, and visceral differentiation in acupuncture therapy. First, meridian differentiation reflects the meridian-propagated effect of points, which is highlighted in the ancient literature: “*the disorders along the traveling routes of meridian are indicated.*” Second, regional differentiation reflects the local effect of points, as stated in the ancient literature: “*the disorders of the point location are indicated.*” Visceral differentiation reflects the visceral specificity of acupoints, and special points, such as the back-*shu* points, front-*mu* points, lower-*he* points, and source-*yuan* points, are related to particular organs. Moreover, some acupoints, which are regarded as empirical points, are effective for particular diseases. Typical examples here are *Zhiyin* (BL67) for incorrect fetal positioning during pregnancy, *Chengshan* (GB57) for hemorrhoids, and *Liangqiu* (ST34) for stomachache.

9.4. Factors Influencing Acupoint Specificity

9.4.1. Manipulation Techniques. As noted above, manipulation of the needle, which is one of the most significant factors

in the curative effect of the acupoints, involves such factors as depth, intensity, and duration (course of acupuncture treatment). A large number of studies have indicated that the different depths employed in acupuncture can exert different effects on the central nervous system and different clinical effects; the intensity of the acupuncture likewise has a significant effect [88–95]. *De qi* (eliciting the needling sensation) is an essential factor in effective treatment, and it involves both depth and intensity. In the conventional theory of acupuncture, *de qi* is a prerequisite for acupoints in achieving their therapeutic effects. *De qi* may involve such factors as sensations of sourness, numbness, distention, and heaviness; if present, these phenomena may spread along the classical routes of the meridians and collaterals after needling. *De qi* is completely different from the pain that occurs during the acupuncture operation. Some fMRI studies have indicated that the response of the brain to acupuncture differs between subjects in whom the needling sensation is elicited and those who feel only a painful sensation [96, 97].

At present, the period of treatment with acupuncture differs between clinical practice in China and overseas. In China, patients prefer to receive therapy three to five times a week, which may be attributed to the impact of culture and treatment customs. Overseas, patients prefer to be treated once or twice a week [4, 12, 66]. It is supposed that the accumulative and sustained effects of acupuncture are linked to the weekly frequency of needling. However, thus far, the frequency of treatment with acupuncture has not been investigated.

The dose-effect relation of acupuncture consists of three main factors—depth, intensity, and time interval. Some researchers have made exploratory studies into the correlation between parameters and acupuncture specificity. They initially found that the therapeutic effect of acupoints was better than that of nonacupoints in rats with middle cerebral artery ischemia; the rats were treated using various stimulus parameters (frequency and time). In this way, the researchers were able to identify the optimal stimulus parameters for the acupoints [98]. This study revealed that the operative parameters of acupuncture are closely related to acupoint specificity. It would thus seem appropriate to examine such areas as the best needling parameters to adopt for acupoint specificity, whether these parameters are associated with acupoint specificity, and the exact influences of these parameters on specificity.

Acupuncture requires high clinical skill since the therapeutic effect of the acupoints can be seriously affected in several critical respects: the selection of acupoints; the application of reinforcing or reducing manipulation; the frequency of lifting, thrusting, and twirling operations; the depth of needling. Though the frequency and intensity employed can be relatively fixed, the operation still relies on practitioners appropriately selecting points and inserting needles before applying electroacupuncture. However, no systematic reviews have examined the influence of the acupuncturists' clinical skill upon acupoint clinical effect. In Chinese and non-Chinese clinical studies on acupoint specificity, differences in the professional experiences and

educational levels of practitioners may have affected the differences in the results obtained [60, 99].

9.4.2. Combination of Acupoints. The combination of acupoints is an essential element in acupuncture. In the classical theory of acupuncture, the combinations of back-*shu* and front-*mu* points, source and connecting points, and the confluence points of the eight vessels guide clinical practitioners in selecting points. Studies have demonstrated that a synergistic effect can be obtained when applying an appropriate combination of acupoints; conversely, an improper combination can produce an antagonistic effect [100, 101]. Semi-standardized treatment protocols, personalized treatment protocols (modifying the combination based on the patients' clinical symptoms and patterns of differentiation), and standardized treatment protocols have been employed in some clinical studies on acupoint specificity. As an example, in investigations into the treatment of migraine, the outcomes were different according to the different treatment protocols and acupoint combinations [6, 12, 61, 72]. We assume that the combination of acupoints exerts a definite effect on therapy, but as to the mechanism by which it does so, further studies are required.

9.5. Publication Bias. Interestingly, the majority of acupoint specificity studies implemented in China have produced positive results with regard to the efficacy. Among western researchers, there appears to be no general agreement with regard to acupoint specificity. It is undeniable that some investigators may feel personally inclined to report positive results. However, this phenomenon may reflect the different background of the researchers, for example, holding a general belief in the effects of acupoint specificity, confidence in the acupuncture treatment, subjects' compliance, and some social factors. On the other hand, publication bias may be due to such factors as the design of controls, the type of study adopted, and the study design of clinical trials.

10. Conclusions

Research into acupoint specificity is scientifically meaningful for enriching and developing acupuncture theory, and it is also pragmatically valuable for enhancing the clinical curative effect of the practice. Currently, research in this field in China has mostly confirmed acupoint specificity and its basic laws; however, modern technology should be fully used in terms of new techniques in genomics, epigenetics, and molecular imaging to investigate acupoint specificity. There is a need for multilevel research to be conducted into the universal applicability of acupoint specificity in an intensive, systematic, and comprehensive manner. It is necessary to expound the scientific foundation of acupuncture so as to elucidate the influence of acupoint combinations, needling techniques, and *qi* arrival on acupoint specificity and its underlying mechanism.

In addition, acupoint specificity has aroused international interest in acupuncture research, and many renowned universities, institutes, and research teams are conducting

work in this area. Thus, more collaborations and communication among different disciplines and international research teams should help integrate resources toward developing a theory for acupoint specificity in terms of reliable scientific language and achieving the sustainable development of acupuncture.

Authors' Contribution

L. Zhao and J. Chen contributed almost equally to this paper.

Conflict of Interests

The authors declare that they have no conflict of interests.

Acknowledgments

This study was supported by the National Basic Research Program of China (973 Program, nos. 2012CB518501, 2006CB504501), National Natural Science Foundations of China (nos. 30930112, 30901900), and the Project of Administration of TCM of Sichuan (no. 2012-E-038).

References

- [1] B. M. Berman, L. Lao, P. Langenberg, W. L. Lee, A. M. K. Gilpin, and M. C. Hochberg, "Effectiveness of acupuncture as adjunctive therapy in osteoarthritis of the knee. A randomized, controlled trial," *Annals of Internal Medicine*, vol. 141, no. 12, pp. 901–910, 2004.
- [2] K. Linde, G. Allais, B. Brinkhaus, E. Manheimer, A. Vickers, and A. R. White, "Acupuncture for migraine prophylaxis," *Cochrane Database of Systematic Reviews*, no. 1, Article ID CD001218, 2009.
- [3] A. Lee and L. T. Fan, "Stimulation of the wrist acupuncture point P6 for preventing postoperative nausea and vomiting," *Cochrane Database of Systematic Reviews*, no. 2, Article ID CD003281, 2009.
- [4] A. F. Molsberger, T. Schneider, H. Gotthardt, and A. Drabik, "German Randomized Acupuncture Trial for chronic shoulder pain (GRASP)—a pragmatic, controlled, patient-blinded, multi-centre trial in an outpatient care environment," *Pain*, vol. 151, no. 1, pp. 146–154, 2010.
- [5] H. Cao, X. Pan, H. Li, and J. Liu, "Acupuncture for treatment of insomnia: a systematic review of randomized Controlled trials," *Journal of Alternative and Complementary Medicine*, vol. 15, no. 11, pp. 1171–1186, 2009.
- [6] L. P. Wang, X. Z. Zhang, J. Guo et al., "Efficacy of acupuncture for migraine prophylaxis: a single-blinded, double-dummy, randomized controlled trial," *Pain*, vol. 152, no. 8, pp. 1864–1871, 2011.
- [7] W. Qin, J. Tian, L. Bai et al., "fMRI connectivity analysis of acupuncture effects on an amygdala-associated brain network," *Molecular Pain*, vol. 4, article 55, 2008.
- [8] F. Beissner, R. Deichmann, C. Henke, and K. J. Bar, "Acupuncture—deep pain with an autonomic dimension?" *Neuroimage*, vol. 60, no. 1, pp. 653–660, 2012.
- [9] T. Witzel, V. Napadow, N. W. Kettner, M. G. Vangel, M. S. Hamalainen, and R. P. Dhond, "Differences in cortical response to acupressure and electroacupuncture stimuli," *BMC Neuroscience*, vol. 12, article 73, 2011.
- [10] B. J. Na, G. H. Jahng, S. U. Park et al., "An fMRI study of neuronal specificity of an acupoint: electroacupuncture stimulation of Yanglingquan (GB34) and its sham point," *Neuroscience Letters*, vol. 464, no. 1, pp. 1–5, 2009.
- [11] K. K. S. Hui, O. Marina, J. D. Claunch et al., "Acupuncture mobilizes the brain's default mode and its anti-correlated network in healthy subjects," *Brain Research*, vol. 1287, pp. 84–103, 2009.
- [12] K. Linde, A. Streng, S. Jürgens et al., "Acupuncture for patients with migraine: a randomized controlled trial," *Journal of the American Medical Association*, vol. 293, no. 17, pp. 2118–2125, 2005.
- [13] N. E. Foster, E. Thomas, P. Barlas et al., "Acupuncture as an adjunct to exercise based physiotherapy for osteoarthritis of the knee: randomised controlled trial," *British Medical Journal*, vol. 335, no. 7617, pp. 436–440, 2007.
- [14] N. P. Assefi, K. J. Sherman, C. Jacobsen, J. Goldberg, W. R. Smith, and D. Buchwald, "A randomized clinical trial of acupuncture compared with sham acupuncture in fibromyalgia," *Annals of Internal Medicine*, vol. 143, no. 1, pp. 10–19, 2005.
- [15] J. Kong, T. J. Kaptchuk, J. M. Webb et al., "Functional neuroanatomical investigation of vision-related acupuncture point specificity—a multisession fMRI study," *Human Brain Mapping*, vol. 30, no. 1, pp. 38–46, 2009.
- [16] J. Pariente, P. White, R. S. J. Frackowiak, and G. Lewith, "Expectancy and belief modulate the neuronal substrates of pain treated by acupuncture," *NeuroImage*, vol. 25, no. 4, pp. 1161–1167, 2005.
- [17] H. M. Langevin, P. M. Wayne, H. Macpherson et al., "Paradoxes in acupuncture research: strategies for moving forward," *Evidence-Based Complementary and Alternative Medicine*, vol. 2011, Article ID 180805, 11 pages, 2011.
- [18] Y. L. Ren and F. R. Liang, "Review of literature on the specificity of therapeutic effects of acupoints on the basis of data mining," *Acupuncture Research*, vol. 34, no. 3, pp. 199–201, 2009.
- [19] Y. L. Ren, L. Zhao, Q. Chen, and F. R. Liang, "Application of data mining on selection and specificity of acupoints," *Journal of Traditional Chinese Medicine*, vol. 51, no. 1, pp. 47–51, 2010.
- [20] L. Zhao, F. R. Liang, Y. Li, F. W. Zhang, H. Zheng, and X. Wu, "Improved quality monitoring of multi-center acupuncture clinical trials in China," *Trials*, vol. 10, article 123, 2009.
- [21] Q. Chen, X. Wu, S. Lu et al., "Characteristics and related factors analysis on fourteen meridian Acupoints in migraine treatment," *Liaoning Journal of Traditional Chinese Medicine*, vol. 36, no. 9, pp. 1477–1480, 2009.
- [22] Y. L. Ren, L. Zhao, M. L. Liu, and F. R. Liang, "Data mining-based study on characteristics of Acupoints selection on ancient acupuncture treatment of functional dyspepsia," *Liaoning Journal of Traditional Chinese Medicine*, vol. 36, no. 2, pp. 259–262, 2009.
- [23] X. Xie, H. Zhu, X. Wu, Q. Chen, and F. Liang, "Regularity of acupoints' application in acupuncture and moxibustion clinical trials for functional dyspepsia," *Journal of Chengdu University of TCM*, vol. 31, no. 1, pp. 1–4, 2008.
- [24] X. Chen, J. P. Xie, J. Zhu et al., "Acupoint selection rules in dysmenorrhea treatment," *Shanghai Journal of Acupuncture and Moxibustion*, vol. 27, no. 6, pp. 45–46, 2008.
- [25] X. Chen, J. Zhu, J. Xie et al., "Rules of selection points on treating diseases related to uterus by acupuncture and moxibustion," *Chinese Archives of Traditional Chinese Medicine*, vol. 26, no. 9, pp. 1905–1906, 2008.

- [26] Y. Li, F. Liang, X. Yang et al., "Acupuncture for treating acute attacks of migraine: a randomized controlled trial," *Headache*, vol. 49, no. 6, pp. 805–816, 2009.
- [27] Y. Li, F. Liang, S. Yu et al., "Randomized controlled trial to treat migraine with acupuncture: design and protocol," *Trials*, vol. 9, article 57, 2008.
- [28] H. Zheng, X. P. Tian, Y. Li et al., "Acupuncture as a treatment for functional dyspepsia: design and methods of a randomized controlled trial," *Trials*, vol. 10, article 75, 2009.
- [29] T. T. Ma, S. Y. Yu, Y. Li, F. R. Liang et al., "Randomised clinical trial: an assessment of acupuncture on specific meridian or specific acupoint vs. sham acupuncture for treating functional dyspepsia," *Alimentary Pharmacology & Therapeutics*, vol. 35, pp. 552–561, 2012.
- [30] Y. P. Yu, L. X. Ma, Y. X. Ma et al., "Immediate effect of acupuncture at Sanyinjiao (SP6) and Xuanzhong (GB39) on Uterine arterial blood flow in primary dysmenorrhea," *Journal of Alternative and Complementary Medicine*, vol. 16, no. 10, pp. 1073–1078, 2010.
- [31] C. Z. Liu, J. P. Xie, L. P. Wang et al., "Immediate analgesia effect of single point acupuncture in primary dysmenorrhea: a randomized controlled trial," *Pain Medicine*, vol. 12, no. 2, pp. 300–307, 2011.
- [32] Y. X. Ma, L. X. Ma, X. L. Liu et al., "A comparative study on the immediate effects of electroacupuncture at sanyinjiao (SP6), xuanzhong (GB39) and a non-meridian point, on menstrual pain and uterine arterial blood flow, in primary dysmenorrhea patients," *Pain Medicine*, vol. 11, no. 10, pp. 1564–1575, 2010.
- [33] L.-W. Ni, P.-F. Shen, Z.-L. Zhang, J.-K. Guo, and J. Xiong, "Effect on neural function of Xingnao Kaiqiao and non-acupoint in treating acute cerebral infarction," *China Journal of Traditional Chinese Medicine and Pharmacy*, vol. 26, no. 5, pp. 891–897, 2011.
- [34] P. Shen, L. Kong, L. Ni et al. et al., "Acupuncture intervention in ischemic stroke: a randomized controlled prospective study," *The American Journal of Chinese Medicine*, vol. 40, no. 4, pp. 685–693, 2012.
- [35] D. Zhang, G. Ding, X. Shen et al., "Role of mast cells in acupuncture effect: a pilot study," *Explore*, vol. 4, no. 3, pp. 170–177, 2008.
- [36] D. Zhang, G. H. Ding, X. Y. Shen et al., "Influence of mast cell function on the analgesic effect of acupuncture of "Zusanli" (ST 36) in rats," *Acupuncture Research*, vol. 32, no. 3, pp. 147–152, 2007.
- [37] H. Huang, R. Zhan, X. J. Yu, D. Zhang, W. M. Li, and G. H. Ding, "Effects of acupoint-nerve block on mast cell activity, manual acupuncture- and electroacupuncture-induced analgesia in adjuvant arthritis rats," *Acupuncture Research*, vol. 34, no. 1, pp. 31–35, 2009.
- [38] X. Yu, G. Ding, H. Huang, J. Lin, W. Yao, and R. Zhan, "Role of collagen fibers in acupuncture analgesia therapy on rats," *Connective Tissue Research*, vol. 50, no. 2, pp. 110–120, 2009.
- [39] X. J. Yu, R. Zhan, H. Huang, and G. H. Ding, "Analysis on the difference of afferent mechanism of analgesic signals from manual acupuncture and electroacupuncture of "Zusanli" (ST 36)," *Acupuncture Research*, vol. 33, no. 5, pp. 310–315, 2008.
- [40] X. Yan, X. Zhang, C. Liu et al., "Do acupuncture points exist?" *Physics in Medicine and Biology*, vol. 54, no. 9, pp. N143–N150, 2009.
- [41] X. Y. Shen, J. Z. Wei, Y. H. Zhang et al., "Study on Volt-ampere (V-A) characteristics of human acupoints," *Chinese Acupuncture & Moxibustion*, vol. 26, no. 4, pp. 267–271, 2006.
- [42] Y. She, C. Qi, L. Ma et al., "A comparative study on skin temperature response to menstruation at uterine-related acupoint," *Zhong Hua Zhong Yi Yao Za Zhi*, vol. 26, no. 5, pp. 897–901, 2011.
- [43] T. Chen, X. Yu, and X. Liu, "Study on the effect of acupuncture different acupoints on area of gastric electrical activity of healthy people," *Chines Archives of Traditional Chinese Medicine*, vol. 28, no. 10, pp. 2054–2058, 2010.
- [44] H. Deng, X. Shen, G. Ding, H. Zhang, L. Zhao, and J. Ying, "Study on the speciality of the infrared radiation at LU9," *Chinese Archives of Traditional Chinese Medicine*, vol. 26, no. 10, pp. 494–495, 2008.
- [45] P. Rong, B. Zhu Y, X. Li, H. Gao, L. Ben, Li et al., "Mechanism of acupuncture regulating visceral sensation and mobility," *Frontiers of Medicine*, vol. 5, no. 2, pp. 151–156, 2011.
- [46] Y. Q. Li, B. Zhu, P. J. Rong, H. Ben, and Y. H. Li, "Effective regularity in modulation on gastric motility induced by different acupoint stimulation," *World Journal of Gastroenterology*, vol. 12, no. 47, pp. 7642–7648, 2006.
- [47] B. Cheng, H. Shi, C. F. Ji, J. H. Li, S. L. Chen, and X. H. Jing, "Distribution of the activated acupoints after acute gastric mucosal injury in the rat," *Acupuncture Research*, vol. 35, no. 3, pp. 193–197, 2010.
- [48] Y. Ding, G. Ding, X. Shen et al., "Observation on the characters of infrared radiation spectrum of acupoints in normal humans and CHD patients," *Journal of Biomedical Engineering*, vol. 23, no. 2, pp. 309–312, 2006.
- [49] H. Liu, X. Shen, H. Deng, and G. Ding, "The faint infrared radiation spectrum study on source-points of the three Yin meridian of hand in coronary heart disease," *Liaoning Journal of Traditional Chinese Medicine*, vol. 33, no. 5, pp. 519–520, 2006.
- [50] X. Lai, G. Zhang, Y. Huang et al., "A cerebral functional imaging study by positron emission tomography in healthy volunteers receiving true or sham acupuncture needling," *Neuroscience Letters*, vol. 452, no. 2, pp. 194–199, 2009.
- [51] G. Zhang, Y. Huang, C. Tang et al., "Study on cerebral functional images after puncturing Waiguan (TE5)," *Journal of Traditional Chinese Medicine*, vol. 50, no. 4, pp. 324–332, 2009.
- [52] Y. Huang, X. Lai, B. Shan et al., "Specific cerebral activation following true and sham Waiguan (SJ 5) needling: functional magnetic resonance imaging evidence," *Neural Regeneration Research*, vol. 5, no. 22, pp. 1712–1716, 2010.
- [53] Y. Huang, C. Tang, S. Wang et al. et al., "Acupuncture regulates the glucose metabolism in cerebral functional regions in chronic stage ischemic stroke patients—a PET-CT cerebral functional imaging study," *BMC Neuroscience*, vol. 13, no. 1, article 75, 2012.
- [54] Y. Huang, H. Xiao, J. Chen et al., "Needling at the Waiguan(SJ5) in healthy limbs deactivated functional brain areas in ischemic stroke patients," *Neural Regeneration Research*, vol. 6, no. 36, pp. 2829–2833, 2011.
- [55] X. Z. Li, X. G. Liu, W. Z. Song, Y. Tang, F. Zeng, and F. R. Liang, "Effect of acupuncture at acupoints of the Shaoyang Meridian on cerebral glucose metabolism in the patient of chronic migraine," *Chinese Acupuncture & Moxibustion*, vol. 28, no. 11, pp. 854–859, 2008.
- [56] F. Zeng, W. Qin, T. Ma et al. et al., "Influence of acupuncture treatment on cerebral activity in functional dyspepsia patients and its relationship with efficacy," *The American Journal of Gastroenterology*, vol. 107, no. 8, pp. 1236–1247, 2012.

- [57] F. Zeng, W. Qin, F. Liang et al., "Abnormal resting brain activity in patients with functional dyspepsia is related to symptom severity," *Gastroenterology*, vol. 141, no. 2, pp. 499–506, 2011.
- [58] Q. Wu, Q. Zhang, B. Sun et al., "¹H NMR-based metabonomic study on the metabolic changes in the plasma of patients with functional dyspepsia and the effect of acupuncture," *Journal of Pharmaceutical and Biomedical Analysis*, vol. 51, no. 3, pp. 698–704, 2010.
- [59] Q. F. Wu, S. Z. Xu, S. Yu, X. Z. Yan, Y. Tang, J. Liu et al., "Yangming Meridian specificity on ¹H NMR-based metabonomics," *Lishizhen Medicine and Materia Medica Research*, vol. 21, no. 10, pp. 2674–2676, 2010.
- [60] H. Zhang, Z. Bian, and Z. Lin, "Are acupoints specific for diseases? A systematic review of the randomized controlled trials with sham acupuncture controls," *Chinese Medicine*, vol. 5, article 1, 2010.
- [61] H. C. Diener, K. Kronfeld, G. Boewing et al., "Efficacy of acupuncture for the prophylaxis of migraine: a multicentre randomised controlled clinical trial," *The Lancet Neurology*, vol. 5, no. 4, pp. 310–316, 2006.
- [62] M. Haake, H. H. Müller, C. Schade-Brittinger et al., "German Acupuncture Trials (GERAC) for chronic low back pain: randomized, multicenter, blinded, parallel-group trial with 3 groups," *Archives of Internal Medicine*, vol. 167, no. 17, pp. 1892–1898, 2007.
- [63] I. Lund and T. Lundeberg, "Are minimal, superficial or sham acupuncture procedures acceptable as inert placebo controls?" *Acupuncture in Medicine*, vol. 24, no. 1, pp. 13–15, 2006.
- [64] H. Johansen-Berg, V. Christensen, M. Woolrich, and P. M. Matthews, "Attention to touch modulates activity in both primary and secondary somatosensory areas," *NeuroReport*, vol. 11, no. 6, pp. 1237–1241, 2000.
- [65] H. Olausson, Y. Lamarre, H. Backlund et al., "Unmyelinated tactile afferents signal touch and project to insular cortex," *Nature Neuroscience*, vol. 5, no. 9, pp. 900–904, 2002.
- [66] I. Lund, J. Näslund, and T. Lundeberg, "Minimal acupuncture is not a valid placebo control in randomised controlled trials of acupuncture: a physiologist's perspective," *Chinese Medicine*, vol. 4, article 1, 2009.
- [67] W. Zhou, L. W. Fu, S. C. Tjen-A-Looi, P. Li, and J. C. Longhurst, "Afferent mechanisms underlying stimulation modality-related modulation of acupuncture-related cardiovascular responses," *Journal of Applied Physiology*, vol. 98, no. 3, pp. 872–880, 2005.
- [68] V. Napadow, R. Dhond, K. Park et al., "Time-variant fMRI activity in the brainstem and higher structures in response to acupuncture," *NeuroImage*, vol. 47, no. 1, pp. 289–301, 2009.
- [69] D. D. Dougherty, J. Kong, M. Webb, A. A. Bonab, A. J. Fischman, and R. L. Gollub, "A combined [¹¹C]diprenorphine PET study and fMRI study of acupuncture analgesia," *Behavioural Brain Research*, vol. 193, no. 1, pp. 63–68, 2008.
- [70] C. E. Zyloney, K. Jensen, G. Polich et al., "Imaging the functional connectivity of the Periaqueductal Gray during genuine and sham electroacupuncture treatment," *Molecular Pain*, vol. 6, article 80, 2010.
- [71] X. Yu, B. Zhu, J. Gao et al., "The scientific basis of the dynamic process of acupoints," *Journal of Traditional Chinese Medicine*, vol. 48, no. 11, pp. 971–973, 2007.
- [72] Y. Li H Zheng, C. M. Witt et al., "Acupuncture for migraine prophylaxis: a randomized controlled trial," *Canadian Medical Association Journal*, vol. 184, no. 4, pp. 401–410, 2012.
- [73] C. Deluze, L. Bosia, A. Zirbs, A. Chantraine, and T. L. Vischer, "Electroacupuncture in fibromyalgia: results of a controlled trial," *British Medical Journal*, vol. 305, no. 6864, pp. 1249–1252, 1992.
- [74] R. E. Harris, X. Tian, D. A. Williams et al., "Treatment of fibromyalgia with formula acupuncture: investigation of needle placement, needle stimulation, and treatment frequency," *Journal of Alternative and Complementary Medicine*, vol. 11, no. 4, pp. 663–671, 2005.
- [75] B. Brinkhaus, C. M. Witt, S. Jena et al., "Acupuncture in patients with chronic low back pain: a randomized controlled trial," *Archives of Internal Medicine*, vol. 166, no. 4, pp. 450–457, 2006.
- [76] C. F. Meng, D. Wang, J. Ngeow, L. Lao, M. Peterson, and S. Paget, "Acupuncture for chronic low back pain in older patients: a randomized, controlled trial," *Rheumatology*, vol. 42, no. 12, pp. 1508–1517, 2003.
- [77] A. D. Wasan, J. Kong, L. D. Pham, T. J. Kaptchuk, R. Edwards, and R. L. Gollub, "The impact of placebo, psychopathology, and expectations on the response to acupuncture needling in patients with chronic low back pain," *Journal of Pain*, vol. 11, no. 6, pp. 555–563, 2010.
- [78] C. Witt, B. Brinkhaus, S. Jena et al., "Acupuncture in patients with osteoarthritis of the knee: a randomised trial," *The Lancet*, vol. 366, no. 9480, pp. 136–143, 2005.
- [79] B. Brinkhaus, C. M. Witt, S. Jena et al., "Physician and treatment characteristics in a randomised multicentre trial of acupuncture in patients with osteoarthritis of the knee," *Complementary Therapies in Medicine*, vol. 15, no. 3, pp. 180–189, 2007.
- [80] E. M. Choi, F. Jiang, and J. C. Longhurst, "Point specificity in acupuncture," *Chinese Medicine*, vol. 7, article 4, 2012.
- [81] C. M. Witt, "Efficacy, effectiveness, pragmatic trials—guidance on terminology and the advantages of pragmatic trials," *Forschende Komplementärmedizin*, vol. 16, no. 5, pp. 292–294, 2009.
- [82] Z. Deng, S. Zhou, Y. Li, and L. Zhao, "Thinking on the design scheme of clinical trial with the example of migraine treated by acupuncture," *Zhongguo Zhen Jiu*, vol. 32, no. 6, pp. 559–562, 2012.
- [83] J. Vas, Á. Rebollo, E. Perea-Milla et al., "Study protocol for a pragmatic randomised controlled trial in general practice investigating the effectiveness of acupuncture against migraine," *BMC Complementary and Alternative Medicine*, vol. 8, article 12, 2008.
- [84] M. Fink, E. Wolkenstein, M. Karst, and A. Gehrke, "Acupuncture in chronic epicondylitis: a randomized controlled trial," *Rheumatology*, vol. 41, no. 2, pp. 205–209, 2002.
- [85] A. Vincent, D. L. Barton, J. N. Mandrekar et al., "Acupuncture for hot flashes: a randomized, sham-controlled clinical study," *Menopause*, vol. 14, no. 1, pp. 45–52, 2007.
- [86] E. Facco, A. Liguori, F. Petti et al., "Traditional acupuncture in migraine: a controlled, randomized study," *Headache*, vol. 48, no. 3, pp. 398–407, 2008.
- [87] F. R. Liang, F. Zeng, and Y. Tang, "Thinking about building a clinical syndrome differentiation system of acupuncture and moxibustion," *Chinese Acupuncture & Moxibustion*, vol. 28, no. 8, pp. 551–553, 2008.
- [88] J. S. Han, X. H. Chen, S. L. Sun et al., "Effect of low- and high-frequency TENS on Met-enkephalin-Arg-Phe and dynorphin A immunoreactivity in human lumbar CSE," *Pain*, vol. 47, no. 3, pp. 295–298, 1991.

- [89] W. Y. Zhou, A. L. S. C. Tjen, and J. C. Longhurst, "lation of cardiovascular responses in rats," *Journal of Applied Physiology*, vol. 99, no. 3, pp. 851–860, 2005.
- [90] W. T. Zhang, Z. Jin, G. H. Cui et al., "Relations between brain network activation and analgesic effect induced by low vs. high frequency electrical acupoint stimulation in different subjects: a functional magnetic resonance imaging study," *Brain Research*, vol. 982, no. 2, pp. 168–178, 2003.
- [91] D. L. Somers and F. R. Clemente, "Contralateral high or a combination of high- and low-frequency transcutaneous electrical nerve stimulation reduces mechanical allodynia and alters dorsal horn neurotransmitter content in neuropathic rats," *Journal of Pain*, vol. 10, no. 2, pp. 221–229, 2009.
- [92] J. H. Lee, K. H. Kim, J. W. Hong, W. C. Lee, and S. Koo, "Comparison of electroacupuncture frequency-related effects on heart rate variability in healthy volunteers: a randomized clinical trial," *Journal of Acupuncture and Meridian Studies*, vol. 4, no. 2, pp. 107–115, 2011.
- [93] E. Kim, J. H. Cho, W. S. Jung, S. Lee, and S. C. Pak, "Effect of acupuncture on heart rate variability in primary dysmenorrheic women," *American Journal of Chinese Medicine*, vol. 39, no. 2, pp. 243–249, 2011.
- [94] M. T. Wu, J. C. Hsieh, J. Xiong et al., "Central nervous pathway for acupuncture stimulation: localization of processing with functional MR imaging of the brain—preliminary experience," *Radiology*, vol. 212, no. 1, pp. 133–141, 1999.
- [95] B. Xu, X. C. Yu, C. Y. Chen et al., "Relationship between efficacy of electroacupuncture and electroacupuncture stimulation of different acupoints and different tissue layers of acupoint area in hypotension plus bradycardia rats," *Acupuncture Research*, vol. 35, no. 6, pp. 422–428, 2010.
- [96] K. K. Hui, J. Liu, N. Makris, R. L. Gollub, A. J. Chen et al., "Acupuncture modulates the limbic system and subcortical gray structures of the human brain: evidence from fMRI studies in normal subjects," *Human Brain Mapping*, vol. 9, no. 1, pp. 13–25, 2000.
- [97] A. U. Asghar, G. Green, M. F. Lythgoe, G. Lewith, and H. MacPherson, "Acupuncture needling sensation: the neural correlates of deqi using fMRI," *Brain Research*, vol. 1315, pp. 111–118, 2010.
- [98] Y. Y. Wei, X. N. Fan, S. Wang, S. Yang, and X. M. Shi, "Specificity effect of acupuncture at "Shuigou" (GV 26) on brain infarction area in MCAO rats and the influence of acupuncture parameter," *Chinese Acupuncture & Moxibustion*, vol. 30, no. 3, pp. 221–225, 2010.
- [99] L. Zhao, F. W. Zhang, Y. Li et al., "Adverse events associated with acupuncture: three multicentre randomized controlled trials of 1968 cases in China," *Trials*, vol. 12, article 87, 2011.
- [100] S. Kong, Q. Shan, and A. Dong, "Synergetic and antagonistic effects of Shu-point and Mu-point of the lung on pulmonary functions," *Chinese Acupuncture & Moxibustion*, vol. 24, no. 12, pp. 840–842, 2004.
- [101] Y. Wang, "Clinical study on the synergic and antagonistic effects of pericardial Back-Shu and Front-Mu point compatibility," *Shanghai Journal of Acupuncture and Moxibustion*, vol. 24, no. 6, pp. 29–32.

Research Article

Effects of Electroacupuncture of Different Frequencies on the Release Profile of Endogenous Opioid Peptides in the Central Nerve System of Goats

Li-Li Cheng, Ming-Xing Ding, Cheng Xiong, Min-Yan Zhou, Zheng-Ying Qiu, and Qiong Wang

College of Veterinary Medicine, Huazhong Agricultural University, Wuhan 430070, China

Correspondence should be addressed to Ming-Xing Ding, dmx@mail.hzau.edu.cn

Received 25 July 2012; Revised 11 September 2012; Accepted 15 September 2012

Academic Editor: Wolfgang Schwarz

Copyright © 2012 Li-Li Cheng et al. This is an open access article distributed under the Creative Commons Attribution License, which permits unrestricted use, distribution, and reproduction in any medium, provided the original work is properly cited.

To investigate the release profile of met-enkephalin, β -endorphin, and dynorphin-A in ruminants' CNS, goats were stimulated by electroacupuncture of 0, 2, 40, 60, 80, or 100 Hz for 30 min. The pain threshold was measured using potassium iontophoresis. The peptide levels were determined with SABC immunohistochemistry. The results showed that 60 Hz increased pain threshold by 91%; its increasing rate was higher ($P < 0.01$) than any other frequency did. 2 Hz and 100 Hz increased met-enkephalin immunoactivities ($P < 0.05$) in nucleus accumbens, septal area, caudate nucleus, amygdala, paraventricular nucleus of hypothalamus, periaqueductal gray, dorsal raphe nucleus, and locus ceruleus. The two frequencies elicited β -endorphin release ($P < 0.05$) in nucleus accumbens, septal area, supraoptic nucleus, ventromedial nucleus of hypothalamus, periaqueductal gray, dorsal raphe nucleus, locus ceruleus, solitary nucleus and amygdala. 60 Hz increased ($P < 0.05$) met-enkephalin or β -endorphin immunoactivities in the nuclei and areas mentioned above, and habenular nucleus, substantia nigra, parabrachial nucleus, and nucleus raphe magnus. High frequencies increased dynorphin-A release ($P < 0.05$) in spinal cord dorsal horn and most analgesia-related nuclei. It suggested that 60 Hz induced the simultaneous release of the three peptides in extensive analgesia-related nuclei and areas of the CNS, which may be contributive to optimal analgesic effects and species variation.

1. Introduction

Acupuncture is a traditional therapeutic technique in Oriental medicine, which has a long history of 4000 years. As a modern version of hand acupuncture, electroacupuncture (EA) can provide a valid analgesic effect and has little physiological interference [1, 2]. It was successfully used to ameliorate pain not only in varieties of painful diseases [3, 4], but in various operations, such as cesarean section, gastrectomy, enterectomy, and castration, in animals during the 1970s [1, 5]. Since then, analgesia-regulating mechanism of EA has been extensively investigated. Previous studies found that electroacupuncture analgesia (EAA) was involved in modulations of neurotransmitters or neuromodulators in the central nerve system (CNS) [6], and most early studies focused on the role of neurotransmitters such as serotonin, noradrenaline, dopamine, and acetylcholine. Later, it was

certified that some endogenous opioid peptides (EOPs), mainly including enkephalin, β -endorphin, and dynorphin, played a more important role in EAA [7, 8]. EA of different frequencies can promote the release of different EOPs in the CNS. Studies showed that EAA induced by 2 Hz (low frequency) was mediated by the release of met-enkephalin (M-ENK) and β -endorphin (β -EP), while EAA by 100 Hz (high frequency) was mediated by the release of dynorphin-A (DYN-A) in the CNS in rats [9–11]. Although these results in rats above are extrapolated to give reasonable explanations for acupuncture analgesia phenomenon and its treatment of related diseases in human, there are still some unknown mechanisms to be investigated.

It has been proved that analgesia induced by EA varies in animal species. In order to quantitatively estimate the degree of acupuncture-induced analgesia, some researchers used an anesthetic to ensure a complete analgesia and to assess the

reduction of the amount of the anesthetics consumed in the EA plus anesthetic group as compared to the anesthetic group without acupuncture. Studies showed that EA in combination with anesthetics resulted in the reduction of the dosage of the anesthetics in human, rat, and goat by 45%–55%, 50%–60%, and over 75%, respectively [12, 13]. It is clear that the analgesic effect induced by EA in goats (ruminants) is superior to that in rats or human. Therefore, the modalities of EOP release elicited by different frequencies in ruminants could be different from those in rats. In the present study, goats were stimulated with EA of different frequencies to determine the analgesic efficacy and the release levels of M-ENK, β -EP, and DYN-A in the CNS in order to probe into the mechanisms of EA-induced analgesia in ruminants.

2. Materials and Methods

2.1. Animal Preparation. Forty-nine healthy 1- to 2-year-old hybrid male goats, weighing 23–28 kg, were purchased from the goat farm of Hubei Agricultural Academy of Science. All experimental goats were randomly divided into seven groups of seven each, maintained on dry grass diet which was supplemented with a cereal-based concentrate, and drank freely. They were dewormed and accustomed to being approached. Feed was withheld for 24 h before the start of the experiment. The experiment was performed in a quiet environment, and the ambient temperature fluctuated between 23°C and 24°C. The experimental protocol was approved by the Animal Care Center, College of Veterinary Medicine, Huazhong Agricultural University, Wuhan, China.

2.2. Electroacupuncture. A set of Baihui (hundred meetings), Santai (three platforms), Ergen (ear base), and Sanyangluo (three Yang communications) points was selected for EA. The anatomic location of these points has been described in detail in veterinary medicine [12, 14]. Needle insertion and EA were conducted with the method reported by Liu et al. [12]. Experimental animals were restrained in right recumbency, and stimulated with EA at 0, 2, 40, 60, 80, or 100 Hz for 30 min via WQ-6F Electronic Acupunctoscope (Beijing Xindonghua Electronic Instrument Co., Ltd., Beijing, China). The goats which were only dealt with needles left in the acupoints without electricity were used as the sham control.

2.3. Determination of Pain Threshold. Just before and after EA, the pain threshold was measured on the center of the left flank using the method of potassium iontophoresis [12, 15, 16]. The region used to measure pain threshold was shaved, cleaned with soap and water, and sterilized with 75% alcohol. Two electrodes soaked with saturated potassium chloride were placed 3 cm apart on the skin in position. A galvanofaradism apparatus (Shantou Medical Equipment Factory Co., Ltd., Shantou, China) was used to deliver pulsed direct current to the electrodes. The voltage was increased stepwise. Obvious contraction of the local skin and muscle was taken as the endpoint; the current was then terminated,

and the volt level was recorded. The procedure was repeated three times. The average volt level was obtained. Mean voltages before and after EA were expressed as V_0 and V_n , respectively. The change of percentage in pain threshold was calculated as follows: $\Delta(\%) = (V_n - V_0) / V_0 \times 100\%$.

2.4. Measurements of the Levels of Endogenous Opioid Peptides. The levels of M-ENK, β -EP, and DYN-A were measured through the method of SABC immunohistochemistry. The nuclei were identified according to the photographic atlas of the goat brain, and the morphological characteristics of the neurons [17–19].

Once the pain threshold was measured after EA, the goats were deeply anesthetized with intravenous administration of xylidinothiazoline at 3 mg/kg. Physiological saline was infused through bilateral carotid arteries at the same velocity with which the blood bled out from the jugular veins for about 5 min (until the blood fluid became colorless). Four percent paraformaldehyde instead of the physiological saline was infused for about 1 h. The brain and a part of the adjacent spinal cord were taken out of the skull and cervical vertebral canal. The brain was placed on a paraffin plate with the ventral surface up. Then it was transected into seven sections through the caudal edge of the residual part of the olfactory bulbs, the center of the optic chiasm, the caudal edge of the mamillary body, the sulcus between cerebral peduncles and pons, the sulcus between pons and medulla oblongata, and the caudal borderline between medulla oblongata and spinal cord, respectively. The first section with the residual part of the olfactory bulbs was discarded. The others were put into 4% paraformaldehyde to fix for 48 h. The cerebral cortex and cerebellum were stripped with the amygdala region left. Each of the second to fourth sections was evenly cut into three subsections (S1 to S9), while the fifth and the sixth sections were averagely divided into two and five subsections (S10 to S16), respectively. The seventh section was just spinal cord (S17). The sectionalization of the brain and the localization of nuclei and areas in subsections were illustrated in Figure 1. Each of the subsections was embedded in a paraffin block, sectioned at 5 μ m, mounted on polylysine-coated slides, deparaffinized, and rehydrated sequentially.

Twelve serial slides were chosen from near the middle of each subsection for immunohistochemical staining. Four of the twelve slides were randomly selected to detect the level of one of EOPs. Of these four slides, the three were incubated with one kind of rabbit-anti-M-ENK IgG (1:100), rabbit anti- β -endorphin IgG (1:200), or rabbit-anti-DYN-A IgG (1:100) (purchased from Wuhan Boster Biological Technology Ltd., Wuhan, China) while the rest was incubated with PBS instead of the corresponding antibody as negative control. Experimental procedures of SABC immunohistochemistry followed the instructions provided by the reagent company (Wuhan Boster Biological Technology Ltd., Wuhan, China). The cytoplasm of positive cells was stained as brown yellow. Optical density of the stained nuclei or area in the CNS was obtained with a light microscope connected to a video-based and computer-linked

system (high-resolution pathological image analysis system-1000, Wuhan Qianping Ltd., Wuhan, China). This system was programmed to calculate the mean optical density (MOD) for three fields of each slide examined under 400× magnification. The level of EOPs in each nucleus or area was represented with the mean value % of the mean optical density from the three slides.

2.5. Statistical Analysis. Statistical analysis was performed using SPSS version 18.0 (SPSS Inc., Chicago, IL, USA). All the data presented as mean ± SD. Pain threshold and EOP data were used for ANOVA followed by the Bonferroni's post hoc test. The correlation coefficient (Pearson's) was used to examine the relations between pain threshold and EOP level. Statistical significance was evaluated by determining if the *P* value was equal to or less than 0.05.

3. Results

3.1. Effects of EA of Different Frequencies on Pain Threshold. The analgesic effects of EA of different frequencies in goats were expressed as the pain threshold (Figure 2). After EA treatment for 30 min, the pain threshold increased as frequency increased, reached the highest at 60 Hz, but decreased at 80 Hz. Frequencies of 100, 80, 60, 40, and 2 Hz increased pain threshold by 42%, 41%, 91%, 69%, and 35% (*P* < 0.01), respectively. The pain threshold of goats stimulated by 60 Hz was higher (*P* = 0.001) than that by 40 Hz. The pain threshold by either 60 Hz or 40 Hz was higher (*P* = 0.001) than that by 80, 100, or 2 Hz. The pain threshold between goats in sham control and 0 Hz was no difference (*P* = 1.000). Because there was no difference (*P* = 1.000) in pain threshold between goats stimulated with 80 and 100 Hz, the effect of 80 Hz on the release of EOPs was not considered in the following experiment.

3.2. Level of M-ENK Release Induced by Different Frequencies in the CNS. The levels of M-ENK were measured in the analgesia-related nuclei or areas which included nucleus accumbens (ACB), septal area (SA), caudate nucleus (CAU), amygdala (AMY), supraoptic nucleus (SON), paraventricular nucleus of hypothalamus (PVH), ventromedial nucleus of hypothalamus (VMH), periaqueductal gray (PAG), dorsal raphe nucleus (DR), substantia nigra (SN), parabrachial nucleus (PBN), locus ceruleus (LC), nucleus raphe magnus (NRM), and spinal cord dorsal horn (SCD). The release levels of M-ENK between the sham control and 0 Hz were no differences (*P* > 0.05) in the measured nuclei and areas. EA of different frequencies facilitated M-ENK release significantly (*P* < 0.05) in the measured nuclei or areas except NRM, SON and SCD (Table 1). 60 Hz induced M-ENK immunoreactivities to increase by over 100% in the measured nuclei and areas except SN, SON, NRM, and SCD, and by over 300% in SA, AMY, and PAG. 100 Hz promoted M-ENK immunoreactivities to increase by over 100% in SA, AMY, PVH, VMH, PAG, PBN, and LC, and by over 300% in PBN. 2 Hz increased M-ENK immunoreactivities by over 100% in AMY, PVH and PAG. As frequency increased, M-ENK immunoreactivities of the forebrain nuclei, and AMY, VMH, and PAG increased,

reached the highest at 60 Hz, and then decreased at 100 Hz. There was no difference in M-ENK of VMH, SN or LC between goats stimulated by 60 Hz and 40 Hz, or by 60 Hz and 100 Hz. In DR, M-ENK immunoreactivities elicited by 40 or 60 Hz were higher than those by 2 Hz or 100 Hz. There was no difference in M-ENK immunoreactivities between goats stimulated by 40 Hz and 60 Hz in this nucleus. In PBN, M-ENK immunoreactivities induced by 100 Hz were higher than those by 40 or 2 Hz (*P* = 0.0001), but not higher (*P* = 0.663) than those by 60 Hz. In SCD, 2 Hz caused M-ENK immunoreactivities to increase (*P* = 0.0001) while the frequency of 40, 60 or 100 Hz did not. Statistic analysis showed that the pain thresholds correlated (*P* < 0.01) with M-ENK immunoreactivities in the measured nuclei and areas except SON, NRM, and SCD.

3.3. Level of β -EP Release Induced by Different Frequencies in the CNS. The β -EP levels were measured in the analgesia-related nuclei and areas which included ACB, SA, AMY, CAU, SON, arcuate nucleus (ARC), VMH, habenular nucleus (HB), PAG, DR, LC, PBN, NRM, solitary nucleus (SOL), and SCD. There were no differences (*P* > 0.05) in the β -EP immunoreactivities between the sham control and 0 Hz in these nuclei and areas. 60 Hz increased β -EP immunoreactivities by over 100% in the most measured nuclei and areas, and by over 300% in PAG and SOL, whereas 100 Hz increased β -EP immunoreactivities by over 100% in ACB, VMH, PAG, LC, SOL, and AMY. 2 Hz increased β -EP immunoreactivities by over 100% in PAG and SOL. Frequencies of 40, 60, and 100 Hz promoted β -EP immunoreactivities to decrease (*P* < 0.05) in ARC, but to increase (*P* < 0.05) in the other measured nuclei or areas. The β -EP immunoreactivities induced by 2 Hz were higher (*P* < 0.05) than those by 0 Hz in ACB, SA, SON, VMH, PAG, DR, LC, SCD, SOL, and AMY, but not in CAU, ARC, HB, PBN, and NRM. As frequency increased, EA promoted β -EP immunoreactivities to change in the measured nuclei and areas except CAU, SON, ARC, HB, PBN, and AMY. In CAU, PBN, and AMY, β -EP immunoreactivities induced by either 40 Hz or 60 Hz were higher (*P* < 0.05) than those by 2 Hz or 100 Hz. But no difference existed in β -EP immunoreactivities between goats stimulated by 40 Hz and 60 Hz. In SON, there were no differences in β -EP immunoreactivities between goats given with 60 Hz and 40 or 100 Hz. The pain thresholds correlated (*P* < 0.01) with β -EP immunoreactivities in the measured nuclei and areas (Table 2).

3.4. Level of DYN-A Release Induced by Different Frequencies in the CNS. The levels of DYN-A were measured in CAU, SA, AMY, SON, PVH, VMH, PAG, PBN, gigantocellular reticular nucleus (GI), and SCD. In these nuclei and areas, DYN-A immunoreactivities were no differences (*P* > 0.05) between the sham control and 0 Hz. DYN-A immunoreactivities in the CNS increased in a frequency-dependent manner. Frequency of 40, 60, or 100 Hz promoted DYN-A to increase significantly (*P* < 0.05) in the CNS. The DYN-A immunoreactivities induced by 100 Hz were different from those by 60 Hz in the measured nuclei and areas except VMH and GI. Statistic analysis showed that the pain thresholds correlated (*P* <

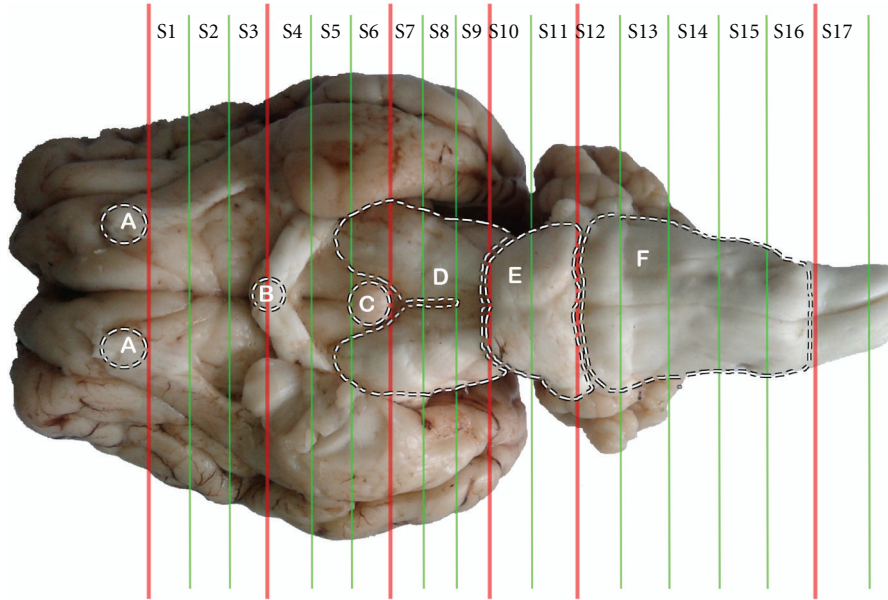


FIGURE 1: Brain sectionalization: (A) the residual part of the olfactory bulbs, (B) optic chiasm, (C) mamillary body, (D) cerebral peduncles, (E) Pons and (F) medulla oblongata. In the sections nuclei or areas: nucleus accumbens, septal area and caudate nucleus in S2, supraoptic nucleus, paraventricular nucleus of hypothalamus, and ventromedial nucleus of hypothalamus in S4, arcuate nucleus and amygdala in S5, habenular nucleus in S6, periaqueductal gray in S8, dorsal raphe nucleus and substantia nigra in S9, parabrachial nucleus and locus ceruleus in S10, nucleus raphe magnus in S13, solitary nucleus in S14, gigantocellular reticular nucleus in S15, and spinal cord dorsal horn in S17 are located.

TABLE 1: M-EMK immunoactivities induced by different frequencies in the CNS (mean \pm SD, $n = 7$).

Nuclei and areas	Sham control	0 Hz	2 Hz	40 Hz	60 Hz	100 Hz	Correlation coefficients
ACB	15.60 \pm 1.69 ^c	15.30 \pm 2.97 ^c	24.56 \pm 2.50 ^b	32.69 \pm 3.92 ^a	35.15 \pm 4.41 ^a	22.59 \pm 2.89 ^b	0.888**
SA	15.14 \pm 1.53 ^c	14.77 \pm 2.39 ^c	25.05 \pm 1.94 ^d	54.95 \pm 3.50 ^b	60.51 \pm 4.35 ^a	33.81 \pm 3.72 ^c	0.923**
CAU	15.00 \pm 1.92 ^c	14.35 \pm 3.18 ^c	22.78 \pm 2.92 ^b	25.24 \pm 5.64 ^b	32.66 \pm 3.47 ^a	26.88 \pm 5.48 ^b	0.724**
AMY	10.47 \pm 1.58 ^d	10.04 \pm 2.43 ^d	20.49 \pm 3.28 ^c	35.06 \pm 7.69 ^b	47.28 \pm 5.56 ^a	38.45 \pm 7.97 ^{a,b}	0.795**
SON	33.21 \pm 2.58	32.99 \pm 5.03	30.54 \pm 6.16	31.68 \pm 8.17	31.90 \pm 6.49	33.73 \pm 5.61	0.071
PVH	18.22 \pm 3.59 ^b	17.95 \pm 4.25 ^c	35.01 \pm 6.18 ^b	47.38 \pm 7.63 ^a	46.70 \pm 10.22 ^a	40.76 \pm 3.55 ^{a,b}	0.734**
VMH	11.95 \pm 1.72 ^b	11.09 \pm 3.29 ^b	18.47 \pm 2.56 ^b	36.56 \pm 8.99 ^a	40.65 \pm 10.10 ^a	38.19 \pm 9.27 ^a	0.735**
PAG	8.05 \pm 0.77 ^c	7.75 \pm 1.16 ^c	20.53 \pm 3.60 ^b	23.29 \pm 4.26 ^b	33.71 \pm 6.73 ^a	16.74 \pm 2.51 ^b	0.808**
DR	11.56 \pm 1.51 ^c	11.34 \pm 4.03 ^c	16.73 \pm 2.26 ^b	29.01 \pm 2.28 ^a	26.30 \pm 2.70 ^a	20.49 \pm 3.25 ^b	0.837**
SN	12.72 \pm 2.05 ^b	12.42 \pm 2.74 ^b	15.14 \pm 3.02 ^b	22.95 \pm 1.58 ^a	22.64 \pm 5.20 ^a	20.36 \pm 1.51 ^a	0.721**
PBN	7.69 \pm 1.04 ^c	7.18 \pm 1.61 ^c	9.71 \pm 1.52 ^c	18.90 \pm 2.93 ^b	26.44 \pm 3.53 ^a	29.13 \pm 3.01 ^a	0.656**
LC	11.69 \pm 1.15 ^c	10.93 \pm 0.89 ^c	15.68 \pm 2.97 ^b	27.49 \pm 2.11 ^a	27.80 \pm 3.60 ^a	25.15 \pm 3.31 ^a	0.799**
NRM	14.15 \pm 1.39	13.77 \pm 2.74	15.77 \pm 1.55	15.53 \pm 3.92	17.07 \pm 2.27	15.76 \pm 4.28	0.263
SCD	5.22 \pm 0.55 ^b	5.22 \pm 0.77 ^b	7.31 \pm 0.67 ^a	6.00 \pm 0.32 ^b	5.85 \pm 0.58 ^b	5.44 \pm 0.38 ^b	0.123

ACB: nucleus accumbens, SA: septal area, CAU: caudate nucleus, AMY: amygdala, SON: supraoptic nucleus, SN: substantia nigra, PAG: periaqueductal gray, NRM: nucleus raphe magnus, PBN: parabrachial nucleus, LC: locus ceruleus, DR: dorsal raphe nucleus, SCD: spinal cord dorsal horn, PVH: paraventricular nucleus of hypothalamus, VMH: ventromedial nucleus of hypothalamus.

Note: There was difference ($P < 0.05$) between the values with different letters, and no difference ($P > 0.05$) with the same letters in a line. * means the levels of the endogenous opioid peptides correlate with the pain thresholds at the 0.05 level, and the levels at the 0.01 level. **The letters and symbols in the following tables have the same meanings as the table above.

0.05) with DYN-A immunoactivities in the measured nuclei and areas except SCD (Table 3).

4. Discussion

4.1. *The Measurement for Pain Thresholds and the Acupoint Selection for Electroacupuncture.* There are a few methods to determine acupuncture-induced change in pain threshold.

The tail flick response or paw withdrawal reflex by radiant heat can be used for the measurement of nociceptive threshold in rats [20, 21]. But it is not applicable for larger experimental animals (such as cattle and goats) because of their thick skin and hard hoof structure. The level of analgesia in these animals is commonly determined by scores based on an animal's response to a pinprick at a particular

TABLE 2: β -EP immunoactivities induced by different frequencies in the CNS (mean \pm SD, $n = 7$).

Nuclei and areas	Sham control	0 Hz	2 Hz	40 Hz	60 Hz	100 Hz	Correlation coefficients
ACB	10.57 \pm 1.48 ^d	9.25 \pm 0.44 ^d	12.21 \pm 2.00 ^c	21.01 \pm 1.80 ^b	27.61 \pm 1.91 ^a	18.70 \pm 1.21 ^b	0.891**
CAU	20.90 \pm 1.99 ^c	20.84 \pm 3.87 ^c	24.05 \pm 2.99 ^{bc}	36.60 \pm 2.17 ^a	36.99 \pm 2.28 ^a	26.81 \pm 2.41 ^b	0.835**
SA	21.04 \pm 2.03 ^d	20.65 \pm 3.58 ^d	29.58 \pm 2.66 ^c	42.08 \pm 4.24 ^b	49.52 \pm 3.02 ^a	31.25 \pm 3.21 ^c	0.893**
AMY	18.46 \pm 2.45 ^d	18.21 \pm 3.33 ^d	32.95 \pm 4.16 ^c	53.15 \pm 2.74 ^{ab}	54.59 \pm 3.09 ^a	48.86 \pm 3.66 ^b	0.840**
SON	29.31 \pm 1.52 ^c	28.88 \pm 2.37 ^c	38.18 \pm 5.30 ^b	53.13 \pm 2.60 ^a	52.68 \pm 2.10 ^a	51.25 \pm 1.87 ^a	0.783**
ARC	33.45 \pm 2.11 ^a	33.42 \pm 2.34 ^a	35.13 \pm 2.02 ^a	26.83 \pm 1.13 ^{bc}	23.76 \pm 2.74 ^c	28.83 \pm 2.63 ^b	0.795**
VMH	19.81 \pm 2.10 ^e	18.86 \pm 1.79 ^e	34.41 \pm 2.82 ^d	56.30 \pm 3.77 ^b	61.17 \pm 2.35 ^a	47.94 \pm 1.66 ^c	0.897**
HB	17.57 \pm 2.42 ^c	16.12 \pm 1.63 ^c	18.44 \pm 1.49 ^c	22.59 \pm 2.05 ^b	26.37 \pm 1.20 ^a	27.46 \pm 1.30 ^a	0.647**
PAG	8.40 \pm 0.96 ^d	8.22 \pm 1.23 ^d	19.04 \pm 1.74 ^c	28.82 \pm 3.82 ^b	33.70 \pm 3.36 ^a	30.18 \pm 3.55 ^{ab}	0.871**
DR	18.63 \pm 1.83 ^d	17.82 \pm 2.34 ^d	29.07 \pm 1.94 ^c	34.06 \pm 3.09 ^{ab}	38.43 \pm 3.45 ^a	31.10 \pm 3.09 ^{bc}	0.808**
LC	14.90 \pm 2.21 ^d	13.72 \pm 2.95 ^d	21.01 \pm 2.37 ^c	30.13 \pm 2.66 ^b	35.14 \pm 2.42 ^a	30.35 \pm 1.80 ^b	0.855**
PBN	7.65 \pm 1.19 ^b	7.54 \pm 1.44 ^b	8.69 \pm 0.99 ^b	14.07 \pm 2.85 ^a	14.92 \pm 1.96 ^a	7.99 \pm 1.15 ^b	0.790**
NRM	17.37 \pm 2.20 ^c	16.52 \pm 2.23 ^c	17.93 \pm 1.21 ^c	23.50 \pm 1.65 ^b	30.25 \pm 2.91 ^a	24.89 \pm 1.76 ^b	0.779**
SOL	11.50 \pm 1.02 ^e	11.35 \pm 0.88 ^e	23.41 \pm 2.46 ^d	33.83 \pm 3.64 ^c	49.46 \pm 1.42 ^a	43.59 \pm 2.17 ^b	0.928**
SCD	7.25 \pm 1.13 ^d	6.80 \pm 0.26 ^d	10.91 \pm 1.00 ^c	14.42 \pm 1.18 ^b	17.72 \pm 1.03 ^a	10.30 \pm 1.26 ^c	0.795**

ACB: nucleus accumbens, SA: septal area, CAU: caudate nucleus, AMY: amygdala, SON: supraoptic nucleus, ARC: arcuate nucleus, LC: locus ceruleus, PAG: periaqueductal gray, DR: dorsal raphe nucleus, PBN: parabrachial nucleus, HB: habenular nucleus, NRM: nucleus raphe, SOL: solitary nucleus, VMH: ventromedial nucleus of hypothalamus magnus, SCD: spinal cord dorsal horn.

TABLE 3: DYN-A immunoactivities induced by different frequencies in the CNS (mean \pm SD, $n = 7$).

Nuclei and areas	Sham control	0 Hz	2 Hz	40 Hz	60 Hz	100 Hz	Correlation coefficients
CAU	9.03 \pm 0.57 ^d	8.89 \pm 0.27 ^d	9.77 \pm 0.34 ^d	17.22 \pm 1.05 ^c	20.91 \pm 1.81 ^b	25.37 \pm 1.14 ^a	0.573**
SA	14.93 \pm 1.29 ^d	14.68 \pm 1.11 ^d	14.88 \pm 0.97 ^d	19.82 \pm 2.00 ^c	26.61 \pm 1.30 ^b	35.75 \pm 1.58 ^a	0.400*
AMY	10.87 \pm 1.10 ^e	10.16 \pm 0.65 ^e	13.03 \pm 1.55 ^d	17.28 \pm 1.40 ^c	24.79 \pm 1.42 ^b	31.34 \pm 1.44 ^a	0.505**
SON	20.73 \pm 1.52 ^c	20.42 \pm 1.08 ^c	21.77 \pm 1.41 ^c	38.35 \pm 2.51 ^b	38.60 \pm 0.94 ^b	43.87 \pm 1.77 ^a	0.652**
PVH	8.74 \pm 0.83 ^d	8.65 \pm 0.39 ^d	8.85 \pm 0.57 ^d	17.53 \pm 1.39 ^c	19.87 \pm 1.13 ^b	23.24 \pm 1.92 ^a	0.606**
VMH	27.01 \pm 1.15 ^c	26.36 \pm 1.10 ^c	27.70 \pm 1.22 ^c	36.01 \pm 1.83 ^b	41.10 \pm 1.89 ^a	42.54 \pm 1.49 ^a	0.671**
PAG	12.27 \pm 1.27 ^d	12.02 \pm 1.28 ^d	12.87 \pm 1.12 ^d	16.94 \pm 2.05 ^c	19.68 \pm 1.90 ^b	23.72 \pm 1.52 ^a	0.457**
PBN	9.71 \pm 0.74 ^d	9.48 \pm 0.55 ^d	9.31 \pm 0.50 ^d	16.90 \pm 1.73 ^c	19.39 \pm 1.44 ^b	24.44 \pm 1.19 ^a	0.533**
GI	10.53 \pm 1.01 ^c	10.42 \pm 1.32 ^c	10.89 \pm 1.58 ^c	14.27 \pm 1.85 ^b	19.46 \pm 1.60 ^a	20.61 \pm 1.34 ^a	0.555**
SCD	3.73 \pm 0.26 ^c	3.68 \pm 0.27 ^c	4.06 \pm 0.22 ^c	5.86 \pm 0.19 ^b	6.05 \pm 0.46 ^b	10.27 \pm 0.60 ^a	0.275

CAU: caudate nucleus, SA: septal area, AMY: amygdala, SON: supraoptic nucleus, PAG: periaqueductal gray, PBN: parabrachial nucleus, GI: gigantocellular reticular nucleus, SCD: spinal cord dorsal horn, PVH: paraventricular nucleus of hypothalamus, VMH: ventromedial nucleus of hypothalamus.

region [22, 23]. Obviously, this method is influenced by subjective factors. Ludbrook et al. [24] and Grant and Upton [25] measured the pain threshold in goats by using an algometry method based on a leg-lifting response to a subcutaneous electric stimulus. This method is not an involuntary reflex but instead a learned cognitive behavior. Additionally, it cannot be used for restrained animals. Potassium iontophoresis is a convenient and reliable experimental pain stimulus that can be presented rapidly and repeatedly with minimal loss in consistency of a subject's reported pain level [16]. In our study, potassium iontophoresis provided a tool for investigating changes in the pain thresholds of EA-treated goats.

A potent analgesic effect induced by EA depends on proper prescriptions of specific acupoints. "Zusanli" (St.36) and "Sanyinjiao" (SP.6) acupoints are commonly chosen for EA to elevate the pain threshold of the traumatic rats

[26, 27]. A few sets of acupoints have been employed for EAA in ruminants. Numerous studies showed that EA at a set of Baihui, Santai, Ergen, and Sanyangluo acupoints elicited an effective analgesia in cattle [5]. Liu et al. [12] demonstrated that EA at this set of acupoints caused a potent analgesic effect in goats. In this study, we adopted this set of acupoints and obtained a similar analgesic effect as Liu did [12]. Experimental investigations showed that stimulation at different acupoints activated different nuclei and areas in rats [28–30]. However, whether acupoint specificities would change the releasing modalities of EOPs elicited by EA in the CNS of ruminants deserves to be investigated.

4.2. *Distribution of Endogenous Opioid Peptides in the CNS of Goats.* EOPs in the CNS include five families: enkephalins, endorphins, dynorphins, endomorphins, and orphanin FQ,

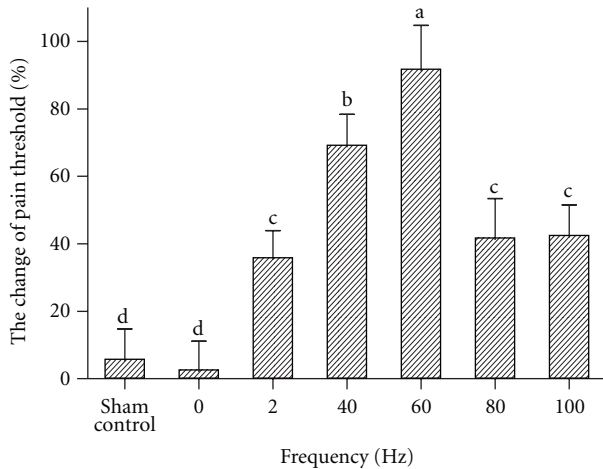


FIGURE 2: Pain threshold of goats stimulated by different frequencies (mean \pm SD, %, $n = 7$). The same letter indicated that no significant difference in pain threshold between two frequencies ($P > 0.05$), and different letter indicated significant difference ($P < 0.05$).

of which the roles of M-ENK, β -EP and DYN-A in EA-induced analgesia were best studied. Studies showed that M-ENK was mainly found in CAU, hypothalamus, SON, PVH, VMH, midbrain, formatio reticularis mesencephali, SN, pons, and formatio reticularis medullae oblongatae [31, 32]. β -EP existed in hypothalamus, SON, ARC, parafascicular nucleus, preoptic region, interpeduncular nucleus, olfactory bulb, pons, medulla oblongata, SCD, AMY, cortex, and hippocampus [33–35]. DYN-A existed in SOL, medullary lateral reticular structure, preoptic area, periventricular nucleus, SON, ARC, SCD, hypothalamus, midbrain, and forebrain [36–38]. In the present study, higher level of β -EP was seen in ARC and SON, as had been reported elsewhere [34]. The rank order of DYN-A levels in our results was VMH > SON > PAG > GI = AMY = PBN = CAU = PVH > SCD, which was similar to reports in human and rats [39, 40]. The highest immunoactivities of M-ENK existed in SON, followed by the lower levels in ACB, CAU, PVH, SA, NRM, and SN, and the lowest levels in PAG, and AMY. These results were some different from the report by Shi et al. [41] that higher level of M-ENK existed in ACB, CAU, SON, PAG and AMY in rats. This discrepancy might be caused by species variation.

4.3. Different Frequencies Induced the Release Profile of EOPs in the CNS of Goats. The veterinary practice proved that frequencies of 40 to 100 Hz are believed to be proper for analgesia of ruminants [5]. But there is a lack of studies to specify this frequency range. In the present study, the increasing magnitude of the pain threshold in goats stimulated by 60 Hz was greater than that by the frequency of 100, 80, 40, or 2 Hz. Obviously, the analgesic effect by 60 Hz was better than that by the others. It is well documented that EOPs exhibit a frequency-dependent response in EA-produced analgesia in rats [42–44]. Low frequency (2 Hz) exerts antinociceptive effects mainly by enhancing the release

of ENK and β -EP, whereas high frequency (100 Hz) produces antinociceptive effects by facilitating the release of DYN [44]. However, the release profile of goats' EOPs induced by different frequencies is not clear yet. In this study, 2 Hz and 100 Hz induced M-ENK to increase significantly in ACB, SA, CAU, AMY, PVH, PAG, DR, and LC and caused β -EP to increase significantly in ACB, SA, SON, VMH, PAG, DR, LC, SOL, and AMY. 60 Hz promoted the release of M-ENK or β -EP in the measured nuclei except in ARC. Therefore, 60 Hz activated more nuclei and areas to release M-ENK and β -EP than 2 or 100 Hz did in ruminants. EOPs participate in extensively physiological modulations. Their roles in EA-induced analgesia are verified by microinjecting EOP and its antagonist or antibody into some nuclei in rats. Levels of M-ENK in ACB [45], SA [46], CAU [47], PAG [48], or DR [48], AMY [49], and SN [50, 51] were proved to affect EA-induced analgesic effect. Either were the levels of β -EP in ACB [52], SA [46], CAU [53], PAG [54], DR [55], LC [56], NRM [56], HB [57], or ARC [58]. Our results showed that EA elevated the levels of M-ENK or β -EP in these nuclei of goats. Besides, we also found that M-ENK or β -EP immunoactivities increased in LC, PBN, VMH, SOL, SON, and PVH. It is seen that high frequencies can induce the simultaneous release of M-ENK or β -EP in a broader spectrum of nuclei in ruminants than in rats.

Role of DYN-A in EA-induced analgesia in the brain is controversial. Han and Xie [59] found that DYN-A did not produce EA-induced analgesia when it was microinjected into the cerebral ventricle of rats. Zhang et al. [60] made the opposite conclusion with DYN-A microinjection. In this study, EA induced DYN-A to increase in many analgesia-related nuclei in the CNS. The DYN-A immunoactivities induced by 100 Hz were significantly different from those by 60 Hz in the measured nuclei and areas except VMH and GI. It is shown that VMH and GI in the release of DYN-A were sensitive to both 100 Hz and 60 Hz. Whether the release of DYN-A takes part in EA analgesic modulation in the CNS of ruminants needs to be studied.

Release of DYN-A induced by 100 Hz in the SCD can produce a potent analgesic effect in rats [61]. In this study, EA of high frequencies induced DYN-A to increase in the SCD. This increase was in accordance with that of Han [61]. However, the increase in β -EP immunoactivities of the SCD and its correlation with the pain threshold values were different from the report of some studies in rats [62]. This discrepancy might be caused by the variation of the species or the studied spinal fragment. In this study, SCD samples were taken from the spinal cord adjacent to the medulla oblongata rather than the lumbar spinal cord.

Studies in rats showed that stimulation at 2 Hz and 100 Hz alternatively elicited the full release of M-ENK, β -EP, and DYN-A in the CNS, which produced a synergistic effect stronger than that at 2 Hz or 100 Hz alone [63]. Veterinary practice verifies that the mode of alternating stimulation with low and high frequencies can also induce more potent analgesic effect. However, the releasing modalities of EOPs which are induced by this stimulation mode in ruminants are worthy to be investigated.

4.4. *Animal Species Variation of EA-Induced Analgesia.* During the last decades, our understanding of how the brain processes acupuncture analgesia has undergone considerable development. But the major results of related researches are primarily obtained from small experimental animals such as rats, rabbits, dogs and monkeys. There are many factors which affect the EA-induced analgesic effect. Besides frequencies and acupoints, species-specificity has an important impact on EA analgesia. Studies showed that EA in combination with anesthetics led to reduce the dosage of the anesthetics in human, rat, and goat by 45%–55%, 50%–60%, and over 75%, respectively [12, 13]. Obviously, ruminants should be optimal model animals for research on the mechanisms of EA-induced analgesia. Our results showed that high frequencies motivated the simultaneous release of the three EOPs in the extensive analgesia-related nuclei and areas in the CNS, which may be conducive to explain why EA induced more potent analgesia in ruminants than in rats.

5. Conclusion

60 Hz was an optimal frequency for acupuncture-induced analgesia in goats and induced the simultaneous release of M-ENK, β -EP, and DYN-A in most of analgesia-related nuclei and areas in the CNS.

Acknowledgments

This study is supported by the funds from the National Natural Science Foundation of China (nos. 30771593 and 31072177) and by the Fundamental Research Funds for the Central Universities of China (no. 2012MBDX009).

References

- [1] H. Haltrecht, "Veterinary acupuncture," *Canadian Veterinary Journal*, vol. 40, no. 6, pp. 401–403, 1999.
- [2] R. Taguchi, "Acupuncture anesthesia and analgesia for clinical acute pain in Japan," *Evidence-Based Complementary and Alternative Medicine*, vol. 5, no. 2, pp. 153–158, 2008.
- [3] X. T. Zhang, Z. P. Ji, and J. S. Huang, *Acupuncture Studies of Acupuncture Anesthesia*, Science Press, 1986.
- [4] M. Inoue, H. Kitakoji, T. Yano, N. Ishizaki, M. Itoi, and Y. Katsumi, "Acupuncture treatment for low back pain and lower limb symptoms—the relation between acupuncture or electroacupuncture stimulation and sciatic nerve blood flow," *Evidence-Based Complementary and Alternative Medicine*, vol. 5, no. 2, pp. 133–143, 2008.
- [5] C. L. Chen, *Traditional Chinese Veterinary Medicine*, Chinese Agriculture Press, 1991.
- [6] X. T. Zhang, Z. P. Ji, and J. S. Huang, *Acupuncture Studies of Acupuncture Anesthesia*, Science Press, 1986.
- [7] J. S. Han, "Acupuncture and endorphins," *Neuroscience Letters*, vol. 361, no. 1–3, pp. 258–261, 2004.
- [8] H. Zhou, H. J. Yu, Y. Wan, Y. Wang, J. K. Chang, and J. S. Han, "Endomorphin-1 mediates 2 Hz but not 100 Hz electroacupuncture analgesia in the rat," *Neuroscience Letters*, vol. 274, no. 2, pp. 75–78, 1999.
- [9] J. S. Han and Q. Wang, "Mobilization of specific neuropeptides by peripheral stimulation of identified frequencies," *News in Physiological Sciences*, vol. 7, no. 4, pp. 176–180, 1992.
- [10] H. Fei, S. L. Sun, and J. S. Han, "New evidence supporting differential release of enkephalin and dynorphin by low and high frequency electro-acupuncture," *Chinese Science Bulletin*, vol. 33, no. 9, pp. 703–705, 1988.
- [11] H. Fei, G. X. Xie, and J. S. Han, "Low and high frequency electro-acupuncture stimulations release [met5] enkephalin and dynorphin A in rat spinal cord," *Chinese Science Bulletin*, vol. 32, no. 21, pp. 1496–1501, 1987.
- [12] D. M. Liu, Z. Y. Zhou, Y. Ding et al., "Physiologic effects of electroacupuncture combined with intramuscular administration of xylazine to provide analgesia in goats," *American Journal of Veterinary Research*, vol. 70, no. 11, pp. 1326–1332, 2009.
- [13] J. S. Han, "Acupuncture anesthesia versus Acupuncture-assisted anesthesia," *Acupuncture Research*, vol. 22, no. 1, pp. 97–102, 1997.
- [14] A. M. Klide and S. H. Kung, *Animal Acupuncture Points, Veterinary Acupuncture*, University of Pennsylvania, Philadelphia, Pa, USA, 2nd edition, 1982.
- [15] G. A. Ulett, S. Han, and J. S. Han, "Electroacupuncture: mechanisms and clinical application," *Biological Psychiatry*, vol. 44, no. 2, pp. 129–138, 1998.
- [16] S. A. Humphries, N. R. Long, and M. H. Johnson, "Ionophoretically applied potassium ions as an experimental pain stimulus for investigating pain mechanisms," *Perception and Psychophysics*, vol. 56, no. 6, pp. 637–648, 1994.
- [17] J. S. Tindal, G. S. Knaggs, and A. Turvey, "The forebrain of the goat in stereotaxic coordinates," *Journal of Anatomy*, vol. 103, no. 3, pp. 457–469, 1968.
- [18] J. S. Tindal, A. Turvey, and L. A. Blake, "A stereotaxic atlas of the medulla oblongata of the goat's brain," *Journal of Anatomy*, vol. 155, pp. 195–202, 1987.
- [19] T. Yoshikawa, *Atlas of the Brains of Domestic Animals*, University of Tokyo Press, Tokyo, Japan, 1967.
- [20] M. F. Ren and J. S. Han, "An improved tail-flick test and its application in the study of acupuncture analgesia," *Acta Physiologica Sinica*, vol. 30, no. 2, pp. 204–208, 1978.
- [21] K. Hargreaves, R. Dubner, F. Brown, C. Flores, and J. Joris, "A new and sensitive method for measuring thermal nociception in cutaneous hyperalgesia," *Pain*, vol. 32, no. 1, pp. 77–88, 1988.
- [22] R. DeRossi, E. B. Gaspar, A. L. Junqueira, and M. P. Beretta, "A comparison of two subarachnoid α 2-agonists, xylazine and clonidine, with respect to duration of antinociception, and hemodynamic effects in goats," *Small Ruminant Research*, vol. 47, no. 2, pp. 103–111, 2003.
- [23] P. Kinjavdekar, G. R. S. Amaral, H. P. Aithal, and A. M. Pawde, "Physiologic and biochemical effects of subarachnoidally administered xylazine and medetomidine in goats," *Small Ruminant Research*, vol. 38, no. 3, pp. 217–228, 2000.
- [24] G. Ludbrook, C. Grant, R. Upton, and C. Penhall, "A method for frequent measurement of sedation and analgesia in sheep using the response to a ramped electrical stimulus," *Journal of Pharmacological and Toxicological Methods*, vol. 33, no. 1, pp. 17–22, 1995.
- [25] C. Grant and R. N. Upton, "The anti-nociceptive efficacy of low dose intramuscular xylazine in lambs," *Research in Veterinary Science*, vol. 70, no. 1, pp. 47–50, 2001.
- [26] D. Zhang, G. H. Ding, X. Y. Shen et al., "Influence of mast cell function on the analgesic effect of acupuncture of "Zusanli"

- (ST 36) in rats,” *Acupuncture research*, vol. 32, no. 3, pp. 147–152, 2007.
- [27] V. Senna-Fernandes, D. L. M. França, D. De Souza et al., “Acupuncture at “zusuanli” (St.36) and “sanyinjiao” (SP.6) points on the gastrointestinal tract: a study of the bioavailability of ^{99m}Tc-sodium pertechnetate in rats,” *Evidence-based Complementary and Alternative Medicine*, vol. 2011, Article ID 823941, 2011.
- [28] S. S. Du, G. L. Du, Y. Q. Wang, M. Liu, Y. Bai, and Z. L. Guan, “Distribution of fos-Li neurons in the spinal trigeminal nucleus after stimulation at acupoints yifeng and fengchi in rats,” *Journal of Shanghai University of Traditional Chinese Medicine*, vol. 26, no. 2, pp. 78–82, 2012.
- [29] L. P. Yan, L. X. Ji, H. J. Wang et al., “Effects of “weibingfang” stimulated by electroacupuncture on expression of c-fos protein in medulla oblongata and hypothalamus of rats with acute gastric mucosal damage,” *Journal of Shanxi College of Traditional Chinese Medicine*, vol. 11, no. 5, pp. 9–11, 2010.
- [30] M. Qin, Y. X. Huang, J. J. Wang, L. Duan, R. Cao, and Z. R. Rao, “Effects of acupuncture at Tsusanli (He-Sea Point) on expression of FOS and GFAP in medullary visceral zone of rats under stress,” *Medical Journal of Chinese People’s Liberation Army*, vol. 30, no. 9, pp. 819–821, 2005.
- [31] C. Gramsch, V. Hoell, and P. Mehraein, “Regional distribution of methionine-enkephalin- and beta-endorphin-like immunoreactivity in human brain and pituitary,” *Brain Research*, vol. 171, no. 2, pp. 261–270, 1979.
- [32] H. Khachaturian, M. E. Lewis, and S. J. Watson, “Enkephalin systems in diencephalon and brainstem of the rat,” *Journal of Comparative Neurology*, vol. 220, no. 3, pp. 310–320, 1983.
- [33] F. Bloom, E. Battenberg, and J. Rossier, “Neurons containing β -endorphin in rat brain exist separately from those containing enkephalin: immunocytochemical studies,” *Proceedings of the National Academy of Sciences of the United States of America*, vol. 75, no. 3, pp. 1591–1595, 1978.
- [34] H. Akil, S. J. Watson, and E. Young, “Endogenous opioids: biology and function,” *Annual Review of Neuroscience*, vol. 7, pp. 223–255, 1984.
- [35] A. R. Karuri, S. Ayres, and M. S. A. Kumar, “Regional distribution of gonadotropin-releasing hormone-like, β -endorphin-like, and methionine-enkephalin-like immunoreactivities in the central nervous system of the goat,” *Brain Research Bulletin*, vol. 51, no. 1, pp. 63–68, 2000.
- [36] E. Weber and J. D. Barchas, “Immunohistochemical distribution of dynorphin B in rat brain: relation to dynorphin A and α -neo-endorphin systems,” *Proceedings of the National Academy of Sciences of the United States of America*, vol. 80, no. 4, pp. 1125–1129, 1983.
- [37] Z. H. Xiang and G. Q. Gu, “The morphology and distribution of DYN A 1-13 neuron in the rat hypothalamus,” *Chinese Journal of Anatomy*, vol. 14, no. 4, pp. 304–307, 1991.
- [38] J. S. Han and Q. Wang, “Arcuate nucleus (ARH) and parabrachial nucleus (PBN) mediate low-and high-frequency electroacupuncture analgesia,” *Acupuncture Research*, vol. 8, no. 4, pp. 181–182, 1991.
- [39] C. Gramsch, V. Hoell, and A. Pasi, “Immunoreactive dynorphin in human brain and pituitary,” *Brain Research*, vol. 233, no. 1, pp. 65–74, 1982.
- [40] V. Höllt, I. Haarmann, K. Bovermann, M. Jerlicz, and A. Herz, “Dynorphin-related immunoreactive peptides in rat brain and pituitary,” *Neuroscience Letters*, vol. 18, no. 2, pp. 149–153, 1980.
- [41] Y. L. Shi, J. P. Zhang, and W. Z. Bai, “The research progress of enkephalin,” *Journal of Hebei Medical University*, vol. 28, no. 2, pp. 148–150, 2007.
- [42] Z. Q. Zhao, “Neural mechanism underlying acupuncture analgesia,” *Progress in Neurobiology*, vol. 85, no. 4, pp. 355–375, 2008.
- [43] Z. H. Cho, S. C. Hwang, E. K. Wong et al., “Neural substrates, experimental evidences and functional hypothesis of acupuncture mechanisms,” *Acta Neurologica Scandinavica*, vol. 113, no. 6, pp. 370–377, 2006.
- [44] J. S. Han, “Acupuncture: neuropeptide release produced by electrical stimulation of different frequencies,” *Trends in Neurosciences*, vol. 26, no. 1, pp. 17–22, 2003.
- [45] W. Q. Jin, Z. F. Zhou, and J. S. Han, “Inhibition of enkephalins degradation in nucleus accumbens leads to potentiation of acupuncture and morphine analgesia,” *Acta Physiologica Sinica*, vol. 37, no. 4, pp. 377–382, 1985.
- [46] H. Y. Mo, S. P. Ou, and Y. F. Qiu, “Inhibitory effect of septal stimulation on cortical potentials evoked by tooth pulp stimulation in rabbits and its relationship with naloxone and acupuncture analgesia,” *Acta Academiae Medicinae Primae Shanghai*, vol. 10, no. 6, pp. 463–468, 1983.
- [47] C. W. Xie, W. Q. Zhang, X. J. Hong, and J. S. Han, “Relation between the content of central met-enkephalin and leu-enkephalin and the analgesic effect of electroacupuncture in rats,” *Acta Physiologica Sinica*, vol. 36, no. 2, pp. 192–197, 1984.
- [48] J. C. Zhao and D. N. Zhu, “The further analysis of the acupuncture analgesic role in Dorsal raphe nucleus and its adjacent gray region,” *Shaanxi Medical Journal*, vol. 9, no. 12, pp. 44–47, 1980.
- [49] D. Y. Xu, Z. F. Zhou, and J. S. Han, “Amygdaloid serotonin and endogenous opioid substances (OLS) are important for mediating electroacupuncture analgesia and morphine analgesia in the rabbit,” *Acta Physiologica Sinica*, vol. 37, no. 2, pp. 162–171, 1985.
- [50] A. A. Baumeister, T. G. Anticich, M. F. Hawkins, J. C. Liter, H. F. Thibodeaux, and E. C. Guillery, “Evidence that the substantia nigra is a component of the endogenous pain suppression system in the rat,” *Brain Research*, vol. 447, no. 1, pp. 116–121, 1988.
- [51] D. Y. Sun, W. Q. Wang, D. M. Gao, and Z. Q. Lu, “Influences of intranigral injection of kainic acid on electroacupuncture analgesia and morphine analgesia in the rabbits,” *Acupuncture research*, vol. 11, no. 2, pp. 113–118, 1986.
- [52] Q. P. Ma, Y. S. Shi, and J. S. Han, “Periaqueductal gray and nucleus Accumbens influence each other to promote the release of enkephalin and β -endorphin in rabbit brain,” *Chinese Science Bulletin*, vol. 11, pp. 855–858, 1991.
- [53] L. F. He, L. N. Du, X. G. Zhang, Z. Z. Shi, and J. W. Jiang, “Effect of intracaudate microinjection of naloxone on electroacupuncture analgesia,” *Acta Academic Medicine Prima Shanghai*, vol. 7, no. 5, pp. 332–337, 1980.
- [54] G. X. Xie, Z. F. Zhou, and J. S. Han, “Electro-acupuncture analgesia in the rabbit was partially blocked by anti- β -endorphin antiserum injected into periaqueductal grey, but not by its intrathecal injection,” *Acupuncture Research*, no. 4, pp. 275–280, 1981.
- [55] X. Y. Chen, W. P. Yin, and Q. Z. Yin, “The dorsal raphe nucleus is involved in the inhibitory effect of hypothalamic arcuate stimulation on pain-evoked unit discharges of the thalamic parafascicular nucleus,” *Acta Physiologica Sinica*, vol. 39, no. 1, pp. 46–53, 1987.

- [56] Z. D. You, C. Y. Song, C. H. Wang, and B. C. Lin, "Effect of stimulating the supraoptic nucleus and Electroacupuncture on β -endorphin contents in locus ceruleus and nucleus raphe magnus in rats," *Acupuncture Research*, vol. 19, no. 3, pp. 40–41, 1994.
- [57] Y. T. Xuan, Z. F. Zhou, W. Y. Wu, and J. S. Han, "Antagonism of acupuncture analgesia and morphine analgesia by microinjection of cinanserin into nucleus accumbens or habenula in the rabbit," *Journal of Beijing Medical College*, vol. 14, no. 1, pp. 23–26, 1982.
- [58] Q. L. Chen, H. C. Liu, F. Gu, and Q. Z. Yin, "Effects of neonatal administration of monosodium glutamate on acupuncture analgesia and beta-endorphin-immunoreactive neurons in the rat hypothalamic arcuate nucleus," *Acupuncture Research*, vol. 12, no. 3, pp. 235–238, 1987.
- [59] J. S. Han and C. W. Xie, "Dynorphin: potent analgesic effect in spinal cord of the rat," *Life Sciences*, vol. 31, no. 16-17, pp. 1781–1784, 1982.
- [60] W. Zhang, J. H. Tian, and J. S. Han, "Analgesic effect of dynorphin A (1~13) and its antagonistic effect on morphine analgesia in rat brain in the cold water tail flick test assay," *Chinese Journal of Neuroscience*, vol. 15, no. 2, pp. 120–124, 1999.
- [61] J. S. Han, X. H. Chen, S. L. Sun et al., "Effect of low- and high-frequency TENS on Met-enkephalin-Arg-Phe and dynorphin A immunoreactivity in human lumbar CSE," *Pain*, vol. 47, no. 3, pp. 295–298, 1991.
- [62] G. X. Xie, Z. F. Zhou, and J. S. Han, "Acupuncture analgesic effects of microinjection of enkephalin, β -endorphin and substance P antibodies into the CNS," *Acta Physiologica Sinica*, vol. 2, no. 1, pp. 10–11, 1982.
- [63] X. H. Chen, S. F. Guo, C. G. Chang, and J. S. Han, "Optimal conditions for eliciting maximal electroacupuncture analgesia with dense-and-disperse mode stimulation," *American Journal of Acupuncture*, vol. 22, no. 1, pp. 47–53, 1994.

Review Article

Patch Clamp: A Powerful Technique for Studying the Mechanism of Acupuncture

D. Zhang^{1,2}

¹Department of Mechanics and Engineering Science, Fudan University, Shanghai 200433, China

²Shanghai Research Center for Acupuncture and Meridians, Shanghai 201203, China

Correspondence should be addressed to D. Zhang, dizhang@fudan.edu.cn

Received 13 August 2012; Accepted 18 September 2012

Academic Editor: Guang-hong Ding

Copyright © 2012 D. Zhang. This is an open access article distributed under the Creative Commons Attribution License, which permits unrestricted use, distribution, and reproduction in any medium, provided the original work is properly cited.

Cellular and molecular events can be investigated using electrophysiological techniques. In particular, the patch-clamp method provides detailed information. In addition, the patch-clamp technique has become a powerful method for investigating the mechanisms underlying the effects of acupuncture. In this paper, recent researches on how acupuncture might modulate electrophysiological responses in the central nervous system (CNS) and affect peripheral structures are reviewed.

1. Introduction

The therapeutic mechanisms of acupuncture are based on the theory of acupuncture and meridians in traditional Chinese medicine (TCM). How to use modern medical research methods to clarify the mechanisms of acupuncture is one of the important subjects of current basic research in TCM. Currently, the microstructure of human tissue, including the complex relationship between cells and the interstitium, and the laws of information transmission in the human body are understood. However, the essence of acupuncture-effect mechanisms is still unclear.

Cellular signal transduction theory is critical for understanding the mechanisms that explain the effects and actions of acupuncture. Cells constitute the basic units of living organisms, and the synergy between cells facilitates the various functions of the body. Communication between cells relies on receptors and ion channels in the cell membrane. Using patch-clamp technology, the electrical changes of cell membrane ion channels can be observed to elucidate the cellular mechanisms of acupuncture. As a well-developed cellular electrophysiological method [1, 2], the patch-clamp technique has set the stage for further studies of the mechanisms of ion channels, signal transduction, and the nerve transduction system. This method is now widely used in the basic and applied research of various disciplines, such as physiology and pharmacology [3]. The patch-clamp

technique provides a fairly direct way to study the gating dynamics, permeability, and selectivity of ion channels in cell membranes. Acupuncture, which is based on meridian theory, can induce therapeutic effects throughout the entire body in a multi-action and multitarget fashion. These effects, as a type of biological information transfer, most likely involve cellular electrophysiological and biochemical changes similar to the effects of various drugs. The patch-clamp technique may deepen the study of acupuncture and clarify the underlying principles. The present paper reviews the application of patch-clamp technology in acupuncture research.

2. Study of Acupuncture-Induced Changes in the Central Nervous System

2.1. Recordings from Isolated Neurons. Acupuncture is a viable and complementary treatment for relieving pain; the treatment involves the insertion of needles to a certain depth at specific acupuncture points (acupoints) followed by manipulations or electrical stimuli [4–7]. Despite the widespread use and confirmed efficacy of acupuncture for specific areas of pain management, the mechanism of acupuncture-induced analgesia remains unclear [8, 9]. This ambiguity occurs because studying the characteristics and

regulatory function of the CNS network during acupuncture is rather complicated.

Researchers use different pain models to investigate the role of neuronal membrane receptors in the sensation, transmission, and modulation of pain [10, 11]. Unlike the evaluation of the tail flick reaction, which involves behavioral functions, electrophysiological recordings of extracellular single-unit discharges are relatively pure indicators of spinal nociceptive activity during acupuncture [12]. The *in vitro* patch-clamp technique more precisely demonstrates the interactions between multiple receptors [13].

The mechanisms of acupuncture-induced analgesia have been investigated since the 1950s as a key project of the Natural Science Development Plan in China [14]. The results of the research from the group led by Professor Han for more than 20 years showed that cholecystokinin octapeptide (CCK-8) in the CNS functions as an antiopioid substrate and antagonized opioid- or EA-induced analgesia [15, 16]. First, extracellular single-unit recordings were made from spinal dorsal horn wide dynamic range neurons in spinal-transected, urethane-anesthetized rats. EA at the ST-36 and SP-6 acupoints effectively suppressed the unit discharges elicited by noxious electrical stimulation of the hind paw. Local spinal superfusion with CCK-8 (10 ng/15 mL) attenuated, whereas the CCK-selective antagonists L365 and 260 (2.5 μ g/15 mL) enhanced the EA effect [17–19]. All three types of opioid receptors (μ , δ , and κ) in the spinal cord of rats play important roles in mediating the analgesia induced by EA [20]. Second, the sites of opioid-CCK interaction were precisely localized using the whole-cell patch-clamp technique on acutely dissociated dorsal root ganglion (DRG) neurons from rats. The dose-dependent inhibition relationship indicated that CCK-8 antagonized the μ - or κ -opioid-receptor-mediated depressant effect on the voltage-gated calcium current. The CCK receptors were presynaptically coexpressed with the opioid receptors in the same neuron [21, 22]. This finding could explain why the effect of EA subsided after prolonged (6 h) EA stimulation, suggesting the development of tolerance to EA [23]. Because CCK-8 has been shown to possess potent antiopioid activity at the spinal level, a blockade of the spinal CCK effect would be expected to potentiate EA-induced analgesia, which is known to be opioid mediated [24].

In neuropathic pain, adenosine 5'-triphosphate disodium- (ATP-) gated P2X receptors, especially the P2X3 subtype, play an important role in the transmission of pain signals [25, 26]. For electrophysiology recordings, a chronic constriction injury (CCI) model of neuropathic pain was induced by tying four ligature knots proximal to the sciatic trifurcation of the right nerve in rats [27]. After the CCI operation, EA was applied at the ST-36 and GB-34 acupoints for 30 min daily for one week. The DRG neurons were acutely isolated from the ganglia after enzymatic digestion, and a conventional whole-cell patch clamp was performed. As P2X3-receptor agonists, both ATP and α,β -methylene-ATP (α,β -meATP) evoked similar fast desensitizing inward currents in the DRG neurons. The amplitudes of the currents in the CCI group were larger than in the sham group and were significantly attenuated

by the EA treatment (no differences between ipsilateral and contralateral). EA may induce an apparent analgesic effect by decreasing the expression of and inhibiting P2X3 receptors in the DRG neurons of rats with CCI [27].

Visceral pain is difficult to be localized and easily transferred to cutaneous structures. Some natural stimuli are clearly associated with multisourced pain from the viscera, such as hollow organ distention, muscle spasm, ischemia, and inflammation [28]. EA is clinically used for the treatment of chronic visceral hyperalgesia (CVH). It is difficult to explain with the classical description in which there are segregated routes in the CNS for visceral and somatic inputs [29, 30]. Using the patch-clamp technique, the inhibitory effect of acupuncture on visceral sensory neuron excitability can be observed directly, which supports the interpretation of disorientated visceral pain and referred pain.

To investigate the effect of EA on colon-specific DRG neurons in rats with CVH and to clarify the interactions between somatic and visceral nociceptive inputs in the spinal dorsal horn, electrophysiological measurements were made [31]. Before perforated whole-cell recordings from DRG neurons were performed, a CVH model was induced by intracolonic injection of acetic acid in 10-day-old rats. EA was applied bilaterally at ST-36 in the hind limbs. The acutely dissociated colon-specific DRG neurons were prelabeled by injection of 1,1'-dioleyl-3,3,3',3'-tetramethylindocarbocyanine methanesulfonate (DiI) into the colon wall 10 days before acupuncture. The resting potentials and action potentials showed the passive and active membrane properties. The recordings from the CVH group displayed enhanced excitability of the colon DRG neurons; this enhancement was significantly suppressed in recordings from the EA group after treatment. Furthermore, the *in vitro* application of the μ -opioid receptor agonist (D-Ala (2), N-MePhe (4), and Gly (5)-Ol) enkephalin (DAMGO) mimicked the EA-mediated suppression. These findings revealed the endogenous opioid-related analgesic effects at the cellular level during EA treatment of visceral pain in functional gastrointestinal disorders.

2.2. Recording from Neurons in Living Slices. Patch-clamp recordings from brain slices have been utilized to analyze CNS function since the 1980s [32–34]. By applying the patch-clamp technique to brain slices, which constitute a simple network system *in vitro*, the effects of acupuncture on target cells can be directly observed because the blood-brain barrier is bypassed. With the proper conditions (increased oxygen supply and modified artificial cerebrospinal fluid (aCSF) content), the metabolic and biological properties of the brain slices can be maintained *in vitro* for a couple of hours [35], which forms an ideal system for recording electrophysiological activities. This system facilitates the investigation of the channels of the CNS and their physiological functions in neuroanatomical circuits.

An imbalance between the excitation and inhibition of gamma-aminobutyric acidergic (GABAergic) neurons caused by ischemia-induced neuron dysfunction has been suggested as an alternative mechanism for neuronal

excitotoxicity [36]. Stimulation of certain acupoints, such as Baihui (GV-20), has been found to improve the outcome of ischemic stroke [37, 38]. The function of GABAergic neurons can be evaluated based on their intrinsic properties as well as their response to excitatory synaptic inputs from other neurons [39]. EA was applied to FVB-Tg (Gad GFP) 4570 Swn/J mice at DV-20 for 20 min, twice daily for a week. Cortical slices (400 μ m) were sectioned from the acupuncture and sham groups and superfused with the aCSF oxygenated at 31°C. *In vitro* ischemia was generated by reducing the perfusion rate from 2 mL/min to 0.2 mL/min for 6 min. Ischemia generally induces increases in the threshold potential and absolute refractory periods of firing spikes in neurons that are measured in the whole-cell recording mode with sequential spikes induced by depolarizing current pulses; acupuncture prevented these increases. Meanwhile, spontaneous excitatory postsynaptic currents (sEPSCs) were recorded in the GFP-labeled GABAergic neurons. The impairment of active transmissions between neurons as a result of ischemia was significantly prevented with acupuncture. Acupuncture improves ischemic stroke via preventing this dysfunction by targeting voltage-gated sodium channels [40]. Modulation of GABAergic activity by inhibition of the GABA reuptake transporter GAT1 has also been suggested [41]. As discussed above, EA leads to an elevated release of endorphins [15]; it was also demonstrated that activation of δ -opioid receptors in the periaqueductal gray results in inhibition of GAT1-mediated current as measured in whole-cell recordings.

2.3. Recording from Neurons *In Vivo*. The *in vivo* patch-clamp technique is mainly used to study the characteristics and mechanisms of the sensory system in response to environmental stimuli [42]. The protocol for the blind patch-clamp method was first introduced *in vivo* for whole-cell recording. Later, the success rate was significantly improved by two-photon targeted patching (TPTP), in which the patch clamp is performed under direct visual control by imaging the fluorescence with two-photon microscopy (2PM) [34, 43]. The visualized operation of targeted patching allows a depth of 0.5 mm, which is approximately half of a young rat's cerebral cortex. In addition to the progress in labeling, the application of *in vivo* patch clamp has been broadened. Compared with *in vitro* isolated neurons, *in vivo* measurements on brain or spinal cord slices have a greater advantage: one can obtain not only the final outputs but also the subthreshold responses. With this information, analyzing the interaction between excitatory and inhibitory synaptic inputs activated by cutaneous stimulation becomes possible [44, 45]. The method provides an effective means for real-time observation of sensory neuronal transmission in the central and peripheral nervous systems.

The substantia gelatinosa (SG, lamina II of the spinal cord) may be a major site for the modification and integration of noxious sensation. A chronic pain model was established by complete Freund's adjuvant- (CFA-) induced inflammation in the right hind paw of rats. A lumbar laminectomy was performed on an anaesthetized rat at

the L4 or L5 level. The surface of the spinal cord was exposed by removal of the pia-arachnoid membrane and was irrigated with oxygenized Krebs solutions at 38°C. *In vivo* whole-cell voltage-clamp recordings were applied during acupuncture to the SG neurons, which were morphologically identified by injection of neurobiotin [46]. Spontaneous inhibitory postsynaptic currents (sIPSCs, $V_H = 0$ mV) and sEPSCs ($V_H = -70$ mV) were recorded from the same neurons by altering the holding potentials. In the CFA model group, sEPSCs with higher magnitudes were observed in the majority of SG neurons. The application of EA to the contralateral ST-36 point slightly decreased the amplitude and frequency of the sEPSCs. In contrast, a larger amplitude and higher frequency of sIPSCs were elicited with acupuncture frequencies from 2 to 10 Hz. This *in vivo* patch-clamp recording technique permits functional analyses of modality-dependent synaptic responses evoked by acupuncture. Therefore, the behavioral changes at the single-cell level can be explained with more certainty [47].

3. Study of the Mechanism of Peripheral Signaling Initiation in Acupoints and Related Structures Using Patch

3.1. Recording on Acupoint Enriched with Mast Cells. As the basic elements in meridian structure, acupoints are suggested to serve as the initiating points for acupuncture treatments [48]. Despite considerable efforts in probing the anatomy of acupoints, the structural characterization of acupoints remains elusive. Many methods have been employed to research the specificity of acupoints [49]. Compared with the surrounding tissue, acupoints were found to be richer in connective tissue structures [50], mast cells [51, 52], capillaries, and nerve endings [53]. In addition, significantly elevated concentrations of Ca, Fe, Cu, and Zn were reported [54]. The densities of mast cells in the acupoints of both skin and muscle tissues were approximately 50% higher than those in sham points [55]. Some researchers [56–58] have measured the sensitivities of different receptors on specific cells as a breakthrough point to explore the mechanism of peripheral signaling initiation in acupoints, including related structures, at the cellular and molecular levels.

Sensitivity to mechanical stimulation is an inherent property of many tissues and cells. The patch-clamp technique can directly study the responses of mechanosensitive (MS) ion channels [59], which are physiologically implicated in the processes of acupuncture manipulations in acupoints [60]. Along with the attenuation of analgesia or the regulatory effect from acupuncture at ST-36, pretreatment with collagenase significantly counteracted the acupuncture-induced increase in the number of degranulated mast cells [61, 62]. These results suggest that collagen fibers in the subcutaneous connective tissue act as a transduction medium for mechanical signals between manual acupuncture stimulation and mast cells. What is the underlying mechanism that triggers mast cell degranulation after the mechanical signals are received? Ion channels that are selective for K^+ , Na^+ , and Ca^{2+} , TREK and TRAAK [63], TRPV2 [64], and TRPV4 [65]

are typical proteins that mediate mechanosensitive cation movements across the lipid membrane. Cl^- channels are the primary mechanosensitive anion channels that play an important role in volume regulation [66].

Research on MS ion channels and the proteins that might play roles in the acupuncture effect was conducted at the cellular level using a human leukemia mast cell line (HMC-1) [56, 67]. In the whole-cell patch-clamp configuration, the mechanical stress applied to a cell membrane by hydrostatic pressure was increased (-30 to -90 cm H_2O applied via a patch pipette). This stress induced an inward-directed current along with cell degranulation [56]. The activation phenomenon was significantly blocked by Ruthenium Red (RuR), an inhibitor of the transient receptor potential vanilloid (TRPV) channel family, or by SKF96365, an inhibitor specific for TRPV2 [68]. The TRPV2-mediated current induced by mechanical stress exhibited a relatively low selectivity ratio (approximately 4) for divalent versus monovalent cations, as calculated from the reversal potential. Single-channel analysis in excised outside-out patches revealed strong outward rectifying, RuR- and SKF-insensitive events. Another component of the currents displayed single-channel events with chord conductance of 55 pS at positive potentials; this component strongly depended on Cl^- concentration, indicating that this current component may be mediated by Cl^- channels, possibly from the CLC family [67]. Further, the whole-cell current of mast cells was recorded *in situ* in connective tissue slices obtained from the ST-36 acupoint in rats. The resulting current to pressure gradient exhibited a similar outward rectification as for the activation of HMC-1 [57, 67]. Given that acupuncture-induced mast cell degranulation can be correlated with treatment effects, TRPV2 and Cl^- channels might be input receptors that contribute to the transduction process of the mechanical signal from acupuncture stimulations.

3.2. Recordings of Acupoint-Related Structures. As widely questioned in histological studies, the primo vascular system was first introduced as the anatomical structure of acupuncture meridians by Kim [69] and recently rediscovered in most tissues of the body [70]. As a semitranslucent thread-like structure, the PVS is composed of primo vessels (PV; Bonghan ducts) and primo nodes (PN; Bonghan corpuscles). The PNs were reported to contain cells such as mast cells, macrophages, and basophils [71]. The PNs were identified using confocal laser scanning microscopy in the epineurium along the rat sciatic nerve after subcutaneous injection of fluorescent nanoparticles at ST-36 [72]. Considering the close relationship between the peripheral nervous system and acupuncture treatment, further studying the primo vascular system to uncover its cellular properties may elucidate the mechanisms underlying acupuncture. Whole-cell recordings were performed on cells of a PN slice (200 μm in thickness) isolated from the surface of abdominal organs in rats. The small round PN cells had a low resting membrane potential (-39 mV) and spontaneous activities [73, 74]. Of the four types of IV relationships and kinetics, most (69%) cells were type I and showed outward rectification. In

current-clamp conditions, tetraethylammonium (TEA) dose dependently depolarized the membrane potential with an increase in input resistance [75]. The TEA-sensitive current with limited selectivity to K^+ contributed to the resting membrane potential of these cells.

4. Prospects

The patch-clamp technique allows for the study of the properties of single channels expressed in specific cell membranes; progress has also occurred in research on the mechanisms of acupuncture. However, the depth (and breadth) is insufficient for a clear understanding of the processes that occur in acupoints and along meridians. By applying specific agonists, antagonists, and allosteric modulators to different parts of the membrane (inside or outside) at different times with fast perfusion, differentiated ionic currents through single channels can be recorded. These currents, together with the dynamic properties of the receptors, may help to demonstrate the existence and function of the detected receptor.

Based on the technical potential of the patch-clamp method, the use of serum from acupunctured animals or humans [76] as a perfusate has been proposed to explore the mechanisms of acupuncture with regards to cellular electrophysiology. The serum may contain substances that act on targets such as cells or molecules in *in vivo* or *in vitro* tissues [77–79]. It will be informative to analyze the gating, ion selectivity, and regulation from single-channel currents before and after stimulation with serum. Further trials are required that vary the sampling time and method to determine the dilution and preservation of the serum and the involvement of the active ingredients from the reaction system. The application of serum to patch-clamp techniques requires further trials.

Additionally, by using *in vivo* patch-clamp technology, the functions and relationships of intracerebral nuclei or spinal cords can also be observed during acupuncture; thus, the acupuncture pathway and the signal transduction process can be explored. Compared with investigations using patch clamp on isolated cells, there are only a few reports of *in vivo* studies because there are still difficulties in controlling factors, such as the mechanical fixation, anesthesia, and physiological interference of animals.

The application of electrophysiological techniques to study the mechanisms of acupuncture at the molecular level first requires the establishment of an animal model corresponding to the disease at the organ level. Then, single cells must be obtained from crucial organs or acupoints using cell separation and cultivation. Finally, cellular models must be built from different organs under pathological circumstances. By combining that information with specific agonists and antagonists, it is possible to determine the pathway of electrophysiological signal changes caused by acupuncture and to preliminarily explore the mechanisms of disease at the molecular level.

Using modern measurement techniques to study the mechanisms of acupuncture is one of the most important

demonstrations of the modernization of Chinese medicine. The patch clamp can be combined with additional recordings to increase the analysis capabilities: with fluorescence measurement [80], the technique can be used to study the relationships between intracellular calcium concentration and secretion events; with the single cell reverse transcriptase-polymerase chain reaction (PCR) technique [81], patch clamp can be used to interpret why different cells of similar subtypes have different electrical activities. In addition, the patch-clamp technique can also reveal the pathways of intracellular information transmission and cell growth processes and even the complex interactions of central synapses. We believe that in the near future, patch-clamp methods will significantly contribute to unraveling the mystery of the mechanisms of acupuncture.

Acknowledgments

The author thanks Professor W. Schwarz and Professor G. H. Ding for helpful discussions. This work was supported by the National Natural Science Foundation of China (no. 81102630), the National Basic Research Program of China (973 Program, nos. 2012CB518502, 09CB522901), and the Science Foundation of Shanghai Municipal Commission of Science and Technology (no. 10DZ1975800).

References

- [1] M. Cahalan and E. Neher, "Patch clamp techniques: an overview," *Methods in Enzymology*, vol. 207, pp. 3–14, 1992.
- [2] M. Karmazinová and L. Lacinová, "Measurement of cellular excitability by whole cell patch clamp technique," *Physiological Research*, vol. 59, supplement 1, pp. S1–S7, 2010.
- [3] K. Jurkat-Rott and F. Lehmann-Horn, "The patch clamp technique in ion channel research," *Current Pharmaceutical Biotechnology*, vol. 5, no. 4, pp. 387–395, 2004.
- [4] "NIH Consensus Conference," *Acupuncture*, vol. 280, no. 17, pp. 1518–1524, 1998.
- [5] P. White, "A background to acupuncture and its use in chronic painful musculoskeletal conditions," *Journal of The Royal Society for the Promotion of Health*, vol. 126, no. 5, pp. 219–227, 2006.
- [6] Z. Q. Zhao, "Neural mechanism underlying acupuncture analgesia," *Progress in Neurobiology*, vol. 85, no. 4, pp. 355–375, 2008.
- [7] R. B. Kelly, "Acupuncture for pain," *American Family Physician*, vol. 80, no. 5, pp. 481–506, 2009.
- [8] C. J. Zaslowski, D. Cobbin, E. Lidums, and P. Petocz, "The impact of site specificity and needle manipulation on changes to pain pressure threshold following manual acupuncture: a controlled study," *Complementary Therapies in Medicine*, vol. 11, no. 1, pp. 11–21, 2003.
- [9] S. M. Wang, Z. N. Kain, and P. White, "Acupuncture analgesia: I. The scientific basis," *Anesthesia and Analgesia*, vol. 106, no. 2, pp. 602–610, 2008.
- [10] J. S. Mogil, "Animal models of pain: progress and challenges," *Nature Reviews Neuroscience*, vol. 10, no. 4, pp. 283–294, 2009.
- [11] A. S. Jaggi, V. Jain, and N. Singh, "Animal models of neuropathic pain," *Fundamental and Clinical Pharmacology*, vol. 25, no. 1, pp. 1–28, 2011.
- [12] J. S. Han, "Cholecystokinin octapeptide (CCK-8: a negative feedback control mechanism for opioid analgesia," *Progress in Brain Research*, vol. 105, pp. 263–271, 1995.
- [13] L. K. Liem, J. M. Simard, Y. Song, K. Tewari, W. Young, and R. G. Dacey, "The patch clamp technique," *Neurosurgery*, vol. 36, no. 2, pp. 382–392, 1995.
- [14] G. J. Wang, M. H. Ayati, and W. B. Zhang, "Meridian studies in China: a systematic review," *Journal of Acupuncture and Meridian Studies*, vol. 3, no. 1, pp. 1–9, 2010.
- [15] J. S. Han, X. Z. Ding, and S. G. Fan, "Is cholecystokinin octapeptide (CCK-8) a candidate for endogenous anti-opioid substrates?" *Neuropeptides*, vol. 5, no. 4–6, pp. 399–402, 1985.
- [16] J. S. Han, X. Z. Ding, and S. G. Fan, "Cholecystokinin octapeptide (CCK-8): antagonism to electroacupuncture analgesia and a possible role in electroacupuncture tolerance," *Pain*, vol. 27, no. 1, pp. 101–115, 1986.
- [17] J. T. Bian, M. Z. Sun, M. Y. Xu, and J. S. Han, "Antagonism by CCK-8 of the antinociceptive effect of electroacupuncture on pain-related neurons in nucleus parafascicularis of the rat," *Asia Pacific Journal of Pharmacology*, vol. 8, no. 2, pp. 89–97, 1993.
- [18] N. J. Liu, H. Bao, N. Li, Y. X. Yu, and J. S. Han, "Cholecystokinin octapeptide reverses the inhibitory effect induced by electroacupuncture on C-fiber evoked discharges," *International Journal of Neuroscience*, vol. 86, no. 3–4, pp. 241–247, 1996.
- [19] C. Huang, Z. P. Hu, S. Z. Jiang, H. T. Li, J. S. Han, and Y. Wan, "CCKB receptor antagonist L365,260 potentiates the efficacy to and reverses chronic tolerance to electroacupuncture-induced analgesia in mice," *Brain Research Bulletin*, vol. 71, no. 5, pp. 447–451, 2007.
- [20] X. H. Chen and J. S. Han, "All three types of opioid receptors in the spinal cord are important for 2/15 Hz electroacupuncture analgesia," *European Journal of Pharmacology*, vol. 211, no. 2, pp. 203–210, 1992.
- [21] N. J. Liu, T. Xu, C. Xu et al., "Cholecystokinin octapeptide reverses μ -opioid-receptor-mediated inhibition of calcium current in rat dorsal root ganglion neurons," *Journal of Pharmacology and Experimental Therapeutics*, vol. 275, no. 3, pp. 1293–1299, 1995.
- [22] T. Xu, N. J. Liu, C. Q. Li et al., "Cholecystokinin octapeptide reverses the κ -opioid-receptor-mediated depression of calcium current in rat dorsal root ganglion neurons," *Brain Research*, vol. 730, no. 1–2, pp. 207–211, 1996.
- [23] J. T. Bian, M. Z. Sun, and J. S. Han, "Reversal of electroacupuncture tolerance by CCK-8 antiserum: an electrophysiological study on pain-related neurons in nucleus parafascicularis of the rat," *International Journal of Neuroscience*, vol. 72, no. 1–2, pp. 15–29, 1993.
- [24] Y. Zhou, Y. H. Sun, J. M. Shen, and J. S. Han, "Increased release of immunoreactive CCK-8 by electroacupuncture and enhancement of electroacupuncture analgesia by CCK-B antagonist in rat spinal cord," *Neuropeptides*, vol. 24, no. 3, pp. 139–144, 1993.
- [25] R. A. North, "P2X₃ receptors and peripheral pain mechanisms," *Journal of Physiology*, vol. 554, no. 2, pp. 301–308, 2004.
- [26] Z. Xiao, S. Ou, W. J. He, Y. D. Zhao, X. H. Liu, and H. Z. Ruan, "Role of midbrain periaqueductal gray P2X₃ receptors in electroacupuncture-mediated endogenous pain modulatory systems," *Brain Research*, vol. 1330, pp. 31–44, 2010.
- [27] W. Z. Tu, R. D. Cheng, B. Cheng et al., "Analgesic effect of electroacupuncture on chronic neuropathic pain mediated

- by P2X₃ receptors in rat dorsal root ganglion neurons,” *Neurochemistry International*, vol. 60, no. 4, pp. 379–386, 2012.
- [28] M. P. Davis, “Drug management of visceral pain: concepts from basic research,” *Pain Research and Treatment*, vol. 2012, Article ID 265605, 18 pages, 2012.
- [29] X. Y. Tian, Z. X. Bian, X. G. Hu, X. J. Zhang, L. Liu, and H. Zhang, “Electro-acupuncture attenuates stress-induced defecation in rats with chronic visceral hypersensitivity via serotonergic pathway,” *Brain Research*, vol. 1088, no. 1, pp. 101–108, 2006.
- [30] J. Liu, W. Fu, W. Yi et al., “Extrasegmental analgesia of heterotopic electroacupuncture stimulation on visceral pain rats,” *Brain Research*, vol. 1373, pp. 160–171, 2011.
- [31] G. Y. Xu, J. H. Winston, and J. D. Z. Chen, “Electroacupuncture attenuates visceral hyperalgesia and inhibits the enhanced excitability of colon specific sensory neurons in a rat model of irritable bowel syndrome,” *Neurogastroenterology and Motility*, vol. 21, no. 12, pp. 1302–e125, 2009.
- [32] R. Gray and D. Johnston, “Rectification of single GABA-gated chloride channels in adult hippocampal neurons,” *Journal of Neurophysiology*, vol. 54, no. 1, pp. 134–142, 1985.
- [33] F. A. Edwards, A. Konnerth, B. Sakmann, and T. Takahashi, “A thin slice preparation for patch clamp recordings from neurones of the mammalian central nervous system,” *Pflügers Archiv European Journal of Physiology*, vol. 414, no. 5, pp. 600–612, 1989.
- [34] M. G. Blanton, J. J. Lo Turco, and A. R. Kriegstein, “Whole cell recording from neurons in slices of reptilian and mammalian cerebral cortex,” *Journal of Neuroscience Methods*, vol. 30, no. 3, pp. 203–210, 1989.
- [35] N. Hájos and I. Mody, “Establishing a physiological environment for visualized *in vitro* brain slice recordings by increasing oxygen supply and modifying aCSF content,” *Journal of Neuroscience Methods*, vol. 183, no. 2, pp. 107–113, 2009.
- [36] L. Huang, N. Chen, M. Ge, Y. Zhu, S. Guan, and J. H. Wang, “Ca²⁺ and acidosis synergistically lead to the dysfunction of cortical GABAergic neurons during ischemia,” *Biochemical and Biophysical Research Communications*, vol. 394, no. 3, pp. 709–714, 2010.
- [37] S. Choi, G. J. Lee, S. J. Chae et al., “Potential neuroprotective effects of acupuncture stimulation on diabetes mellitus in a global ischemic rat model,” *Physiological Measurement*, vol. 31, no. 5, pp. 633–647, 2010.
- [38] C. M. Chuang, C. L. Hsieh, T. C. Li, and J. G. Lin, “Acupuncture stimulation at Baihui acupoint reduced cerebral infarct and increased dopamine levels in chronic cerebral hypoperfusion and ischemia-reperfusion injured Sprague-Dawley rats,” *American Journal of Chinese Medicine*, vol. 35, no. 5, pp. 779–791, 2007.
- [39] J. H. Wang, “Short-term cerebral ischemia causes the dysfunction of interneurons and more excitation of pyramidal neurons in rats,” *Brain Research Bulletin*, vol. 60, no. 1-2, pp. 53–58, 2003.
- [40] S. Zhang, G. Li, X. Xu, M. Chang, C. Zhang, and F. Sun, “Acupuncture to point Baihui prevents ischemia-induced functional impairment of cortical GABAergic neurons,” *Journal of the Neurological Sciences*, vol. 307, no. 1-2, pp. 139–143, 2011.
- [41] W. Schwarz and Q. B. Gu, “Cellular mechanisms in acupuncture points and affected sites,” in *Current Research In Acupuncture*, Y. Xia, G. H. Ding, and G. C. Wu, Eds., Springer, New York, NY, USA, 2013.
- [42] D. Sugiyama, S. W. Hur, A. E. Pickering et al., “*In vivo* patch-clamp recording from locus coeruleus neurones in the rat brainstem,” *Journal of Physiology*, vol. 590, no. 10, pp. 2225–2231, 2012.
- [43] P. Theer, M. T. Hasan, and W. Denk, “Two-photon imaging to a depth of 1000 μm in living brains by use of a Ti:Al₂O₃ regenerative amplifier,” *Optics Letters*, vol. 28, no. 12, pp. 1022–1024, 2003.
- [44] K. Narikawa, H. Furue, E. Kumamoto, and M. Yoshimura, “*In vivo* patch-clamp analysis of IPSCs evoked in rat substantia gelatinosa neurons by cutaneous mechanical stimulation,” *Journal of Neurophysiology*, vol. 84, no. 4, pp. 2171–2174, 2000.
- [45] H. Furue, G. Kato, J. H. Kim, B. I. Min, T. Katafuchi, and M. Yoshimura, “*In vivo* patch-clamp analysis of sensory neuronal circuit in the rat superficial spinal dorsal horn,” in *Brain- Inspired IT I International Congress Series No. 1269*, H. Nakagawa, K. Ishii, and H. Miyamoto, Eds., pp. 69–72, Elsevier Science B.V., 2004.
- [46] G. Q. Bi, V. Bolshakov, G. Bu et al., “Recent advances in basic neurosciences and brain disease: from synapses to behavior,” *Molecular Pain*, vol. 2, article 38, 2006.
- [47] M. Yoshimura, A. Doi, M. Mizuno, H. Furue, and T. Katafuchi, “*In vivo* and *in vitro* patch-clamp recording analysis of the process of sensory transmission in the spinal cord and sensory cortex,” *Journal of Physiological Anthropology and Applied Human Science*, vol. 24, no. 1, pp. 93–97, 2005.
- [48] V. Napadow, A. Ahn, J. Longhurst et al., “The status and future of acupuncture clinical research,” *Journal of Alternative and Complementary Medicine*, vol. 14, no. 7, pp. 861–869, 2008.
- [49] G. H. Ding, D. Zhang, M. Huang, L. N. Wang, and W. Yao, “Function of collagen and mast cells in acupuncture points,” in *Current Research in Acupuncture*, Y. Xia, G. H. Ding, and G. C. Wu, Eds., Springer, New York, NY, USA, 2012.
- [50] H. M. Langevin, D. L. Churchill, and M. J. Cipolla, “Mechanical signaling through connective tissue: a mechanism for the therapeutic effect of acupuncture,” *The FASEB Journal*, vol. 15, no. 12, pp. 2275–2282, 2001.
- [51] D. Zhang, G. H. Ding, X. Y. Shen, W. Yao, and J. Lin, “Study on correlation between meridians acupoints and mast cells,” *Acupuncture Research*, vol. 30, no. 2, pp. 115–118, 2005.
- [52] A. M. Zhong, J. L. Wu, Y. L. Hu, Y. Feng, and X. G. Deng, “Study on correlation between the mast cell and the acupoint,” *World Journal of Acupuncture and Moxibustion*, vol. 4, no. 4, pp. 53–58, 1994.
- [53] L. Fei, H. Cheng, D. Cai et al., “Experimental exploration and research prospect of physical bases and functional characteristics of meridians,” *Chinese Science Bulletin*, vol. 43, no. 15, pp. 1233–1252, 1998.
- [54] X. Yan, X. Zhang, C. Liu et al., “Do acupuncture points exist?” *Physics in Medicine and Biology*, vol. 54, no. 9, pp. N143–N150, 2009.
- [55] D. Zhang, G. H. Ding, X. Y. Shen et al., “Role of mast cells in acupuncture effect: a pilot study,” *Explore*, vol. 4, no. 3, pp. 170–177, 2008.
- [56] D. Zhang, A. Spielmann, G. H. Ding, and W. Schwarz, “Activation of mast-cell degranulation by different physical stimuli involves activation of the transient-receptor-potential channel TRPV2,” *Physiological Research*, vol. 61, no. 1, pp. 113–124, 2012.
- [57] L. N. Wang, W. Schwarz, Q. B. Gu, and G. H. Ding, “Skin slice used as a model for investigating acupuncture effects,” *Acupuncture Research*, vol. 34, no. 5, pp. 291–296, 2009.
- [58] W. Z. Yang, J. Y. Chen, J. T. Yu, and L. W. Zhou, “Effects of low power laser irradiation on intracellular calcium and histamine release in RBL-2H3 mast cells,” *Photochemistry and Photobiology*, vol. 83, no. 4, pp. 979–984, 2007.

- [59] B. G. Kornreich, "The patch clamp technique: principles and technical considerations," *Journal of Veterinary Cardiology*, vol. 9, no. 1, pp. 25–37, 2007.
- [60] T. S. Abraham, M. L. Chen, and S. X. Ma, "TRPV1 expression in acupuncture points: response to electroacupuncture stimulation," *Journal of Chemical Neuroanatomy*, vol. 41, no. 3, pp. 129–136, 2011.
- [61] X. J. Yu, G. H. Ding, H. Huang, J. Lin, W. Yao, and R. Zhan, "Role of collagen fibers in acupuncture analgesia therapy on rats," *Connective Tissue Research*, vol. 50, no. 2, pp. 110–120, 2009.
- [62] H. G. Wu, B. Jiang, E. H. Zhou et al., "Regulatory mechanism of electroacupuncture in irritable bowel syndrome: preventing MC activation and decreasing SP VIP secretion," *Digestive Diseases and Sciences*, vol. 53, no. 6, pp. 1644–1651, 2008.
- [63] F. Lesage, F. Maingret, and M. Lazdunski, "Cloning and expression of human TRAAK, a polyunsaturated fatty acids-activated and mechano-sensitive K⁺ channel," *FEBS Letters*, vol. 471, no. 2-3, pp. 137–140, 2000.
- [64] K. Muraki, Y. Iwata, Y. Katanosaka et al., "TRPV2 is a component of osmotically sensitive cation channels in murine aortic myocytes," *Circulation Research*, vol. 93, no. 9, pp. 829–838, 2003.
- [65] Y. Jia, X. Wang, L. Varty et al., "Functional TRPV4 channels are expressed in human airway smooth muscle cells," *American Journal of Physiology*, vol. 287, no. 2, pp. L272–L278, 2004.
- [66] A. Sardini, J. S. Amey, K. H. Weylandt, M. Nobles, M. A. Valverde, and C. F. Higgins, "Cell volume regulation and swelling-activated chloride channels," *Biochimica et Biophysica Acta*, vol. 1618, no. 2, pp. 153–162, 2003.
- [67] L. Wang, G. Ding, Q. Gu, and W. Schwarz, "Single-channel properties of a stretch-sensitive chloride channel in the human mast cell line HMC-1," *European Biophysics Journal*, vol. 39, no. 5, pp. 757–767, 2010.
- [68] D. Clapham, "Transient receptor potential (TRP) channels," in *Encyclopedia of Neuroscience*, R. L. Squire, Ed., pp. 1109–1133, Academic Press, Oxford, UK, 2009.
- [69] B. H. Kim, "On the kyungrak system," *Journal of Academy of Medical Sciences*, vol. 90, pp. 1–41, 1963.
- [70] K. S. Soh, "Bonghan circulatory system as an extension of acupuncture meridians," *Journal of Acupuncture and Meridian Studies*, vol. 2, no. 2, pp. 93–106, 2009.
- [71] B. C. Lee, J. S. Yoo, V. Ogay et al., "Electron microscopic study of novel threadlike structures on the surfaces of mammalian organs," *Microscopy Research and Technique*, vol. 70, no. 1, pp. 34–43, 2007.
- [72] Z. F. Jia, B. C. Lee, K. H. Eom et al., "Fluorescent nanoparticles for observing primo vascular system along sciatic nerve," *Journal of Acupuncture and Meridian Studies*, vol. 3, no. 3, pp. 150–155, 2010.
- [73] S. H. Park, B. C. Lee, C. J. Choi et al., "Bioelectrical study of bonghan corpuscles on organ surfaces in rats," *Journal of the Korean Physical Society*, vol. 55, no. 2, pp. 688–693, 2009.
- [74] T. H. Han, C. J. Lim, J. H. Choi, S. Y. Lee, and P. D. Ryu, "viability assessment of primo-node slices from organ surface primo-vascular tissues in rats," *Journal of Acupuncture and Meridian Studies*, vol. 3, no. 4, pp. 241–248, 2010.
- [75] J. H. Choi, C. J. Lim, T. H. Han, S. K. Lee, S. Y. Lee, and P. D. Ryu, "TEA-sensitive currents contribute to membrane potential of organ surface primo-node cells in rats," *Journal of Membrane Biology*, vol. 239, no. 3, pp. 167–175, 2011.
- [76] H. H. Zhou, F. Lu, S. D. Chen, Z. H. Zhou, Y. Z. Han, and J. Y. Hu, "Effect of electroacupuncture on serum copper, zinc, calcium and magnesium levels in the depression rats," *Journal of Traditional Chinese Medicine*, vol. 31, no. 2, pp. 112–114, 2011.
- [77] N. Goldman, M. Chen, T. Fujita et al., "Adenosine A1 receptors mediate local anti-nociceptive effects of acupuncture," *Nature Neuroscience*, vol. 13, no. 7, pp. 883–888, 2010.
- [78] G. Burnstock, "Acupuncture: a novel hypothesis for the involvement of purinergic signalling," *Medical Hypotheses*, vol. 73, no. 4, pp. 470–472, 2009.
- [79] T. H. Joh, H. J. Park, S. N. Kim, and H. Lee, "Recent development of acupuncture on Parkinson's disease," *Neurological Research*, vol. 32, supplement 1, pp. S5–S9, 2010.
- [80] M. K. Park, A. V. Tepikin, and O. H. Petersen, "What can we learn about cell signalling by combining optical imaging and patch clamp techniques?" *Pflugers Archiv European Journal of Physiology*, vol. 444, no. 3, pp. 305–316, 2002.
- [81] N. J. Sucher, D. L. Deitcher, D. J. Baro, R. M. Harris Warrick, and E. Guenther, "Genes and channels: patch/voltage-clamp analysis and single-cell RT-PCR," *Cell and Tissue Research*, vol. 302, no. 3, pp. 295–307, 2000.

Review Article

Systems Biology of Meridians, Acupoints, and Chinese Herbs in Disease

Li-Ling Lin,¹ Ya-Hui Wang,² Chi-Yu Lai,² Chan-Lao Chau,³ Guan-Chin Su,⁴ Chun-Yi Yang,⁴ Shu-Ying Lou,¹ Szu-Kai Chen,⁵ Kuan-Hao Hsu,⁵ Yen-Ling Lai,¹ Wei-Ming Wu,⁶ Jian-Long Huang,⁷ Chih-Hsin Liao,¹ and Hsueh-Fen Juan^{1,5,7}

¹ Department of Life Science, National Taiwan University, No. 1, Section 4, Roosevelt Road, Taipei 106, Taiwan

² Graduate Institute of Epidemiology and Preventive Medicine, National Taiwan University, Taipei 100, Taiwan

³ Department of Bioenvironmental Systems Engineering, National Taiwan University, Taipei 106, Taiwan

⁴ Institute of Biochemical Sciences, National Taiwan University, Taipei 106, Taiwan

⁵ Institute of Molecular and Cellular Biology, National Taiwan University, No. 1, Section 4, Roosevelt Road, Taipei 106, Taiwan

⁶ Department of Biochemical Science and Technology, National Taiwan University, Taipei 106, Taiwan

⁷ Graduate Institute of Biomedical Electronic and Bioinformatics, National Taiwan University, No. 1, Section 4, Roosevelt Road, Taipei 106, Taiwan

Correspondence should be addressed to Hsueh-Fen Juan, yukijuan@ntu.edu.tw

Received 2 August 2012; Accepted 26 September 2012

Academic Editor: Wolfgang Schwarz

Copyright © 2012 Li-Ling Lin et al. This is an open access article distributed under the Creative Commons Attribution License, which permits unrestricted use, distribution, and reproduction in any medium, provided the original work is properly cited.

Meridians, acupoints, and Chinese herbs are important components of traditional Chinese medicine (TCM). They have been used for disease treatment and prevention and as alternative and complementary therapies. Systems biology integrates omics data, such as transcriptional, proteomic, and metabolomics data, in order to obtain a more global and complete picture of biological activity. To further understand the existence and functions of the three components above, we reviewed relevant research in the systems biology literature and found many recent studies that indicate the value of acupuncture and Chinese herbs. Acupuncture is useful in pain moderation and relieves various symptoms arising from acute spinal cord injury and acute ischemic stroke. Moreover, Chinese herbal extracts have been linked to wound repair, the alleviation of postmenopausal osteoporosis severity, and anti-tumor effects, among others. Different acupoints, variations in treatment duration, and herbal extracts can be used to alleviate various symptoms and conditions and to regulate biological pathways by altering gene and protein expression. Our paper demonstrates how systems biology has helped to establish a platform for investigating the efficacy of TCM in treating different diseases and improving treatment strategies.

1. Introduction

According to traditional Chinese medicine (TCM), acupoints are linked in a network of meridians running along the surface of the body. The meridian system is a special channel network that consists of skin with a high concentration of nerves, various nociceptive receptors, and deeper connective tissues inside the body [1]. Moreover, “ q_i ” (vital energy) in TCM is transferred by meridians, and its flow around the body can reflect the health status of individuals [2]. Acupoints are special locations in the body where the “ q_i ” of

viscera and meridians infuses and effuses. This phenomenon is thought to be similar to how signals are passed through neural networks. Acupoints are also considered reflection points (i.e., points on the body whose reflexes provide diagnostic information) for certain diseases and are the targets for clinical acupuncture [3].

Acupuncture is an alternative medicine methodology that originated in ancient China. It uses thin metal needles to pierce through skin into acupoints to regulate the flow of q_i around the whole body [4]. Needling at appropriate points can induce effects in locations remote from the insertion

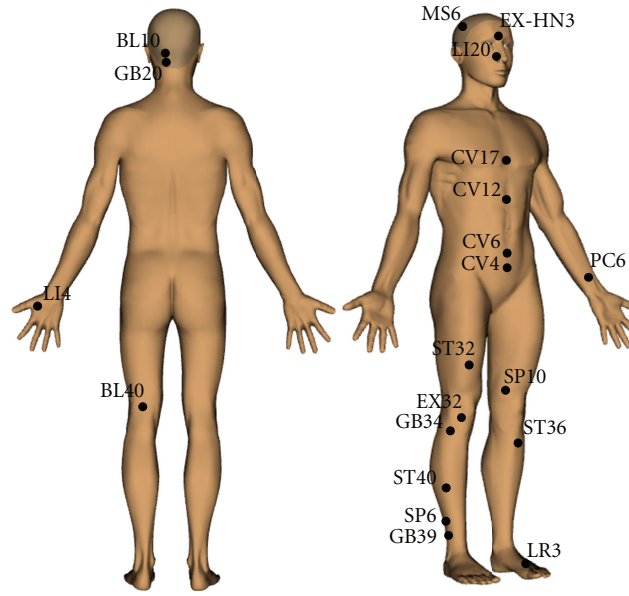


FIGURE 1: The approximate locations of acupoints on the human body reviewed in this paper. Images are created by Acu3D Ver.1.0.2011.0218.

site [5]. Many recent brain imaging studies have shown that acupuncture has a specific correlation with the human nervous system. Using functional magnetic resonance imaging (fMRI) to scan the brains of subjects undergoing needling, researchers found that different acupoints corresponded to different cerebral areas and conditioned reactions [3, 6]. Therefore, it has the potential to provide therapy for many diseases. Recent studies have found that electroacupuncture (EA) improved the pathology of motor disorders in a Parkinsonian rat model by restoring homeostasis in the basal ganglia circuit [7, 8]. In other reports, the effects of EA treatment on neuropathic pain [9], acute spinal cord injury [10], acute ischemic stroke [11], and reducing inflammation [12, 13] were also rigorously studied. We review the relevant literature below and have depicted the human acupoints described in this paper in Figure 1.

Another important aspect of TCM is Chinese herbal medicine (CHM), which has been used for thousands of years as a major preventive and therapeutic strategy against disease [14]. Currently, more than 3,200 species of medicinal plants are used in CHM treatments. A fundamental feature of TCM is TCM compound formulas, which are composed of many kinds of herbs and sometimes minerals or animal components, similar to a cocktail therapy [15]. Each TCM compound formula is usually designed to combat specific symptoms and combined with other herbs or prescriptions to tailor to individual needs. Herbal extracts have been investigated for use in treating various diseases and have been used as a complementary or alternative form of medical therapy for cancer patients [16–18]. In other studies that focus on chronic kidney disease [19], neurodegenerative disease [20], and diabetes mellitus [21], Chinese herbs have been reported to alleviate symptoms and mediate signal transduction.

Systems biology, which combines computational and experimental approaches to analyze complex biological

systems, focuses on understanding functional activities from a systems-wide perspective [22]. With the advent of high-throughput global gene expression, proteomics, and metabolomic technologies, systems biology has become a viable approach for improving our knowledge of health and disease [23, 24]. In this paper, we review recent research articles on acupuncture and Chinese herbal therapy performed in conjunction with omics technologies to analyze and investigate the regulatory mechanisms of the treatments and their therapeutic applications.

2. Systems Biology and Omics Data

Systems biology is the computational integration of huge datasets to explore biomolecular functional networks [22, 25]. The field offers many approaches and models for searching for biological pathways and predicting their effects and implications [26, 27]. More recently, academic research has focused on developing basic informatics tools that can integrate large quantities of global gene expression, proteomic, and metabolomic data to mimic regulatory networks and cell function [26, 28]. The principle of systems biology is to understand and compare physiology and disease, first from the level of molecular pathways and regulatory networks, then moving up through the cell, tissue, and organ, and finally whole organism levels [29, 30]. It has the potential to provide new concepts to reveal unknown functions at all levels of the organism being studied.

Omics data helps to explore the different levels in systems biology from a holistic perspective. The suffix “-omics” is added to the object of study or the level of biological process to form new terms to describe that information—for example, genomics from gene data, proteomics from protein data, metabolomics from metabolic data [31]. With

rapid progress in sequencing and computational methods, omics techniques have become powerful tools for researching biological mechanisms and diseases and for interdisciplinary applications, for example, biologics, mathematics, and informatics [32–34].

3. Genomic Studies of Acupuncture in Diseases

Many individual transcriptional profiles of animals or patients have been mined to search for target molecules of acupuncture treatments. Candidate genes or pathways associated with the protective effect of acupuncture treatments have been revealed through genomic analysis for several diseases and symptoms. We list the acupoints and related symptoms in Table 1.

3.1. Analgesia. Acupuncture was reported to reduce pain during surgery in the 1950s [35] and can treat different types of pain in many cases [36, 37]. Particularly, previous reports have indicated a major role for acupoint ST36, whose therapeutic properties include analgesia [38]. Gao et al. compared the hypothalamus transcriptional profiles of rats that responded or did not respond to EA analgesia treatment at ST36 [39]. They found that genes for glutamatergic receptors, ghrelin precursor peptides, the melanocortin 4 receptor, and neuroligin 1 may all be new targets for pain management. Moreover, Chae et al. found 375 genes showing significant variation in response to the analgesic effect of acupuncture (on LI4) [40]. Among these genes, cold shock domain protein A and kruppel-like factor 5 were identified as potential targets for investigating the mechanisms behind acupuncture-induced analgesia.

3.2. Antiaging. In an anti-aging study, Ding et al. analyzed the hippocampus gene expression profiles in senescence-accelerated mice given acupuncture treatment [41]. Following applied acupuncture at the CV17, CV12, CV6, ST36, and SP10 acupoints, the researchers observed eight genes affected by age. They found that acupuncture could completely or partially alter the gene expression of heat-shock proteins (Hsp84 and Hsp86) and Y-box binding protein 1—genes related to oxidative damage—in senescence-accelerated mice, indicating that acupuncture may show promise in retarding aging in mammals.

3.3. Hypercholesterolemia. Li and Zhang stimulated C57BL/6j mice, which are used in diabetes and obesity research, at the ST40 acupoint and found that cholesterol 7 α hydroxylase was upregulated following EA, while sodium taurocholate cotransporting polypeptide was downregulated [42]. Each of these variations in gene expression might alter the balance of cholesterol metabolism and reduce cholesterol by regulating bile salt biosynthesis and flux, respectively [43, 44].

3.4. Knee Osteoarthritis. Tan et al. compared the transcriptional profiles of four patients stimulated at the CV4, CV6, ST36, EX32, and GB34 acupoints [45]. They collected samples from the peripheral blood of patients after acupuncture

TABLE 1: List of the acupuncture points (acupoints) reviewed in this paper.

Acupoint Chinese name	Acupoint name	Function/target	References
Weizhong	BL40	Acute ischemic stroke	[11]
Tianzhu	BL10	Acute ischemic stroke	[11]
Guanyuan	CV4	Knee osteoarthritis	[45]
Qihai	CV6	Antiaging, knee osteoarthritis	[41, 45]
Zhongwan	CV12	Antiaging	[41]
Danzhong	CV17	Antiaging	[41]
Yintang	EX-HN3	Allergic rhinitis	[56]
Xiyan	EX32	Knee osteoarthritis	[45]
Fengchi	GB20	Acute ischemic stroke	[11]
Yanglingquan	GB34	Knee osteoarthritis, Parkinson's disease	[45, 49–52, 63, 64]
Xuanzhong	GB39	Spinal cord injury, Parkinson's disease,	[46, 64]
Hegu	LI4	Allergic rhinitis, analgesia, and acute ischemic stroke	[11, 40, 56]
Yingxiang	LI20	Allergic rhinitis	[46, 56]
Taichong	LR3	Parkinson's disease	[49, 50]
Motor Area	MS6	Acute ischemic stroke	[11]
Neiguan	PC6	Acute ischemic stroke	[11]
Sanyinjiao	SP6	Spinal cord injury, acute ischemic stroke	[11, 46]
Xuehai	SP10	Anti-aging	[41]
Futu	ST32	Spinal cord injury	[46]
Zusanli	ST36	Neuropathic pain, spinal cord injury, immune modulation, allergic rhinitis, analgesia, anti-aging, knee osteoarthritis, and acute ischemic stroke	[9, 11, 38–41, 45–47, 53–56]
Fenglong	ST40	Hypercholesterolemia	[42]

treatments. Among differentially expressed genes involved in the pathways, oxidative phosphorylation (ATP synthesis) was found in all patients. Analysis of profiles with respect to the Kyoto Encyclopedia of Genes and Genomes (KEGG) pathway database showed that the majority of differentially expressed genes were associated with seven types of metabolic pathways, particularly the primary, cellular, and energy metabolism pathways. These results showed that acupuncture treatment may regulate gene expression to balance energy metabolism of knee osteoarthritis patients.

3.5. Neuronal Diseases. In a spinal cord injury (SCI) study, EA treatment on rats at four acupoints—ST36, GB39, ST32,

and SP6—was seen to restore sensory function by microarray analysis [46]. In this study, they found that extending the EA treatment time for SCI rats could result in more changes in gene expression. After EA stimulation, the gene expression of calcitonin gene-related polypeptide (CGRP) and neuropeptide Y (NPY) were up-regulated and functionally annotated with the recovery of sensory functions. Acupuncture treatment at ST36 has also been reported to reduce neuropathic pain. Using microarray analysis, opioid receptor sigma was one of differentially expressed genes and involved in opioid signaling which has been implicated in neuropathic pain and the analgesic effects of EA at ST36 in neuropathic pain model rats [47].

Parkinson's disease is a neurodegenerative disease caused by the death of dopaminergic neurons [48]. Several studies have performed acupuncture treatments on different acupoints in 1-methyl-4-phenyl-1, 2, 3, 6-tetrahydropyridine (MPTP-) induced Parkinson's models. These models were used to evaluate the effects of acupuncture treatment at the GB34 and LR3 acupoints by analyzing the transcriptional profiles from cervical spinal cord or brain bilateral striatal tissues [49, 50]. Among the genes downregulated by acupuncture treatment, proplatelet basic protein (Ppbbp) was functionally annotated with cytokine-cytokine receptor interaction pathways, and cytotoxic T lymphocyte-associated protein 2 alpha (Ctla2a) was associated with a pathway relevant to Parkinson's disease according to KEGG analysis [49]. Similar results were observed from substantia nigra tissue of MPTP mice following treatment at the GB34 acupoint [51]. In previous studies, myelin basic protein, a major constituent of the axonal myelin sheath, has been reported to be up-regulated in MPTP mice and Parkinson's patients stimulated at the GB34 acupoint [52]. In the bilateral striatal tissue of mice brain following acupuncture at the GB34 and LR3 acupoints, the gene expression levels of gap junction alpha 4 protein (Gja4) and tubulin alpha 8 (Tuba8) were down-regulated and annotated with the cell communication and gap junction pathway, respectively. Furthermore, an up-regulated gene, neurotrophin-3 (Ntf3), was annotated with the mitogen-activated protein kinases (MAPK) signaling pathway [50].

3.6. Immune Modulation and Allergic Rhinitis. Evidence from mouse models has demonstrated that EA or acupuncture stimulation at ST36 can modulate the immune response [53–55]. Two studies using a 2,4-dinitrophenylated keyhole limpet protein (DNP-KLH) immunized mouse model have shown that gene expression patterns can change in the spleen [55] and hypothalamus [54] after EA treatment. Using Sprague Dawley (SD) rats, Kim et al. found that the genes altered following EA at ST36 play crucial roles in natural killer cell activation in spleen tissue [53]. However, the effects of EA treatments remain diverse, partly because of variation in immune responses when triggered in different types of tissues or models (e.g., DNP-KLH immunized mice versus SD rats).

Acupuncture treatment has also demonstrated some effectiveness against allergic rhinitis in clinical settings,

presumably through immune modulation [56, 57]. Allergic rhinitis occurs when an allergen is inhaled and generates an immune response in an individual. Its symptoms can be reduced by acupuncture treatment at the EX-HN3, LI4, LI20, and ST36 acupoints [56]. The effectiveness of the treatment could be accounted for by modulation of pro- and anti-inflammatory genes observed through microarray analyses of blood samples. Immune responses to allergic rhinitis may vary depending on types of allergen. Shiue et al. have used the Phadiatop (Ph) assay, an effective screening tool that detects a diverse range of allergens, to demonstrate that patients with Ph-positive (+) and Ph-negative (–) allergic rhinitis display different gene expression profiles after acupuncture treatment [57]. A hierarchical clustering analysis revealed that three gene groups—those for active immune response, regulatory T cell differential, and apoptosis—were differentially expressed in the Ph (+) and Ph (–) patients after treatment [57]. These results also indicate the importance of personalized medicine for future investigations.

4. Proteomic Studies of Acupuncture in Diseases

Proteomic technologies, such as two-dimensional electrophoresis (2-DE), can screen for proteins differentially expressed between individuals responsive and nonresponsive to acupuncture treatments. These proteins were identified by various mass spectrometry (MS) techniques, and their related pathways were explored to determine the mechanism of the acupuncture treatments. The results clarify the relationships between different acupoints and functions (Table 1).

4.1. Acute Ischemic Stroke. EA efficacy has been studied by comparing levels of serum proteins in response to EA or drug treatments in acute ischemic stroke patients [11]. Patients were treated with EA at eight acupoints (MS6, BL10, GB20, LI4, PC6, B40, SP6, and ST36) once daily for ten consecutive days. The protein profiles were analyzed using 2-DE; SerpinG1 was up-regulated, while gelsolin, complement component 1 (C1), C3, C4B, and beta-2-glycoprotein I were all down-regulated. Other studies have indicated that platelet C4 expression is associated with acute ischemic stroke by comparing serum proteins from healthy individuals and ischemic stroke patients [58].

4.2. Neuronal Diseases. Using matrix-assisted laser desorption/ionization time-of-flight mass spectroscopy (MALDI TOF-MS) and subsequent protein database mining, Li et al. identified fifteen candidate proteins whose expression levels varied with acupuncture treatment for SCI [59]. Among them, annexin A5 (ANXA5) and collapsin response modifier protein 2 (CRMP2) were determined to be beneficial for neuronal survival and axonal regeneration. ANXA5 is a member of the annexin superfamily of calcium- and phospholipid-binding proteins, which are related to apoptosis and inflammation [60]. CRMP2 is a member of the collapsin response mediator protein family and is expressed

exclusively in the nervous system, especially during development [61]. Additionally, among up-regulated proteins, heat shock protein beta-1 (HSPB1) has a reported role in cell stress/neuroprotection as well as in axonal regeneration [62]. These results reveal the potential for proteomics research to supplement and guide the treatment of SCI with acupuncture in future research.

Moreover, Sung et al. applied EA at ST36 in a SD rat model, and subsequent 2-DE was used to identify signaling pathways involved in neuropathic pain [9]. Thirty-six differentially expressed proteins were identified in the neuropathic pain model, and the normal expression levels of their corresponding genes could be restored following EA treatment. Furthermore, Jeon et al. performed EA at GB34 in an MPTP mouse model of Parkinson's disease [63]. They observed restoration of behavioral impairment and rescued tyrosine hydroxylase-positive dopaminergic neurodegeneration after the treatment. In previous studies, the expression of myelin basic protein can also be restored to normal levels after EA treatment [63]. Kim et al. performed similar studies at GB34 and GB39 [64]. They identified thirteen differentially expressed proteins using MS, and four of these proteins—cytosolic malate dehydrogenase, munc18-1, hydroxyacylglutathione hydrolase, and cytochrome c oxidase subunit Vb—were restored to normal expression levels following EA treatment. These proteins are involved in cell metabolism, and may reduce MPTP-induced dopaminergic neuronal destruction by decreasing oxidative stress. Taken together, these results suggest that acupuncture treatment is likely to have a neuroprotective effect on neuronal diseases through cell metabolic and nervous tissue developmental pathways, among others.

5. Genomic Studies of Chinese Herbs in Diseases

Many studies have investigated genes impacted by Chinese herb extracts from transcriptional profiles after treatment and analyzed their functions using pathway databases. These results were used to evaluate whether Chinese herb extracts could be used as a complementary drug to treat specific symptoms. Here, we review Chinese herbal treatment-related studies that incorporated genomic analysis and interpret the efficacy of Chinese herb extracts for various symptoms and conditions (Table 2).

5.1. Immunomodulatory Function. It is generally agreed that the fungus *Ganoderma lucidum* contains an abundance of polysaccharides with immunostimulatory properties [65], and these have been investigated using human CD14 (+) (cluster of differentiation 14) derived dendritic cells [66, 67]. Dendritic cells are antigen-presenting cells that play a critical role in the regulation of the adaptive immune response. A comparison of transcriptional profiles from the polysaccharide of *G. lucidum*-treated dendritic cells and untreated dendritic cells showed a decrease in the expression of some phagocytosis-related genes, for example, CD36, CD206, and CD209. The expression of proinflammatory chemokines was increased, that is, chemokine (C-C motif) ligands (CCL)

CCL20, CCL5, and CCL19; interleukins (IL) IL-27, IL-23A, IL-12A, and IL-12B; costimulatory molecules CD40, CD54, CD80, and CD86 [67]. Additionally, altered expression levels of CD209, CCL20, CCL5, IL-27, CD54, CD80, and CD86 in cells after treatment with F3 (a polysaccharide fraction extracted from lingzhi) have been observed by Lai et al., with CD209 expression down-regulated proportional to treatment time [66]. Another study investigated the treatment of human CD14+ monocytes with polysaccharide fractions extracted from North American ginseng [68]. The MAPK (extracellular regulated protein kinases-1/2), phosphoinositide-3-kinase, p38, and nuclear factor-kappaB (NF- κ B) cascades are key signaling pathways that may trigger immunomodulatory functions, as determined by Ingenuity Pathway Analysis [68]. With regard to other extracts, Cheng et al. reported that the NF- κ B pathway was up-regulated in THP-1 by treatment with ethanol extracts of *G. sinense*, but not by *G. lucidum* [69]. Moreover, protosapannin A treatment (an ethanol extract of *Caesalpinia sappan*) has been reported to induce an immunosuppressive effect via the NF- κ B pathway in a heart transplantation rat model [70].

5.2. Wound Repair. Herbal formulas containing extracts of *Astragali radix*, *Rehmanniae radix*, and *Angelica sinensis* show potential therapeutic benefits for wound repair [72]. For example, the formula NF3, which consists of a 2:1 ratio of *A. radix* and *R. radix*, has been found to affect cell proliferation, angiogenesis, extracellular matrix formation, and inflammation in the Hs27 skin fibroblast cell line through microarray analysis [72]. Another study in human skin substitutes revealed that SBD.4 extracts of *A. sinensis* possesses skin- and wound-healing activity [73]. After SBD.4 stimulation, the gene expression of collagen XVI and XVII, laminin γ -2 and 5, claudin 1 and 4, hyaluronan synthase 3, superoxide dismutase 2, and heparin-binding EGF was up-regulated and ADAM 9 was down-regulated in EpiDermFT skin substitute tissues. The elevation of collagen XVI and XVII can enhance collagen fibril organization and the reduction of ADAM9 may stimulate collagen deposition [89, 90]. These results suggest that these skin- and wound-healing related genes function in cell-substrate junction assembly.

5.3. Postmenopausal Osteoporosis. Traditional Chinese herbalists have been treating patients with chronic kidney disease for thousands of years [19]. The effect of an herbal mixture consisting of *Herba Epimedii*, *Fructus Ligustri Lucidi*, and *Fructus Psoraleae* was investigated in aged ovariectomy and calcium deficiency-induced osteoporotic rats [74]. A comparison of the transcriptional profiles between nontreated and herbal formula-treated ovariectomized rats found that some genes specifically activated by the herbal mixture, such as prostaglandin EP3 receptor and osteoprotegerin, were involved in bone remodeling and bone protection. Moreover, they identified the involvement of estrogen-related proteins and suggested that the herbal formula may act like estrogens.

5.4. Diabetes Mellitus. Type 2 diabetes mellitus (T2DM) is characterized by insufficient insulin secretion and insulin

TABLE 2: List of Chinese herbal studies that have incorporated genomic and proteomic analysis.

Authors	Herb name	Extracts	Common functions
Sliva [65], Lai et al. [66], Lin et al. [67], Cheng et al. [71]	<i>G. lucidum (lingzhi)</i>	Polysaccharide fraction/F3	Immunomodulatory, antitumor activity
Cheng et al. [69]	<i>G. sinense (lingzhi)</i>	Ethanol extracts	Immunomodulatory
Wu et al. [70]	<i>C. sappan</i>	Protosappanin A	Immunomodulatory
Zhang et al. [72]	A. Radix and R. Radix	NF3 (A. Radix and R. Radix in the ratio of 2 : 1)	Wound repair
Zhao et al. [73]	<i>A. Sinensis</i>	SBD.4	Wound repair
Sun et al. [74]	Herba Epimedii, Fructus Ligustri Lucidi, and Fructus Psoraleae		Postmenopausal osteoporosis
Han et al. [21]	C.A. Meyer	CK	Diabetes mellitus
Luo et al. [75], King and Murphy [76]	American <i>ginseng</i> (<i>P. quinquefolius</i> L.)	Ginsenoside Rg3/ginseng extracts	Antitumor activity
Hara et al. [77], Iizuka et al. [78]	<i>C. rhizome</i>	Benzodioxoloquinolizine alkaloids/berberine	Anti-tumor activity
Wang et al. [79]	<i>L. rubescens</i>	Oridonin	Anti-tumor activity
Xu et al. [80]	Franquet	TBMS1	Anti-tumor activity
Cheng et al. [81]	<i>R. paridis</i>	RPTS	Anti-tumor activity
Yue et al. [82]	<i>P. ginseng</i>	Rg1	Angiogenesis
Konkimalla et al. [83]	Artemisinin		Nitric oxide biosynthesis
Su et al. [20, 84]	<i>P. suffruticosa</i>	Paeonol	Neurodegenerative disease
Wang et al. [85]	<i>S. miltiorrhiza</i>	SAL or TAN	Acute myocardial infarction
Lo et al. [86]	<i>U. rhynchophylla</i>		Convulsive disorders
Hung et al. [87, 88]	<i>S. miltiorrhiza</i>	SMAE	Cardiovascular disorder

resistance, such that the liver lacks the ability to regulate glycolysis and gluconeogenesis [91]. Han et al. compared gene expression profiles of C57BL/KsJ-*db/db* mice (insulin-resistant model of insulin-dependent diabetes and obesity) following treatment with compound K (CK), a final metabolite of *Panax ginseng* C.A. Meyer [21]. They found that some differentially expressed genes in liver tissue were associated with glycolysis/gluconeogenesis and pentose phosphate pathways, for example, upregulation of aldolase 2, B isoform and phosphogluconate dehydrogenase for glycolysis and pentose phosphate pathways, and downregulation of fructose biphosphatase 1 for gluconeogenesis pathways after CK treatment. In adipose tissue, on the other hand, they found differentially expressed genes there was linked to adipocytokine signaling and fatty acid synthesis/metabolism pathways, for example, upregulation of peroxisome proliferator-activated receptor gamma for adipocytokine signaling and fatty acid synthase for fatty acid synthesis pathways after CK treatment.

Plasma adiponectin, a hormone responsible for increasing neoglucogenesis, is secreted from adipocytes and might play a key role in linking obesity, insulin resistance, and the T2DM syndrome. A higher adiponectin expression has been observed in conjunction with lowered obesity levels in

human studies [92]. Furthermore, Fu et al. have found that adiponectin increases total glucose transporter 4 expression, which can aid in the response to insulin at the plasma membrane [93]. These results suggest that CK might be a potential target for antidiabetic drugs.

5.5. Antitumor Activity. Chinese herbs have been known to possess anti-tumor activity, and some studies have investigated this functionality and its mechanisms in cancer treatments. F3-treated human leukemia THP-1 cells have been found to undergo apoptosis through death receptor pathways as determined through microarray analysis [71]. Furthermore, F3 induces macrophage-like differentiation by caspase cleavage and p53 activation in THP-1 cells [94]. Another study using a microarray approach determined that 25% of genes regulated by two lingzhi (*G. lucidum* and *G. sinense*) was determined to be similar [69]. *G. sinense* was observed to regulate inflammation and immune response pathways, while *G. lucidum* appeared to increase the expression levels of NF- κ B pathway genes. Therefore, lingzhi appears to have efficacy as an anti-tumor agent against THP-1 cells.

Other Chinese herbs have also been associated with anti-tumor effects [95–101]. Two studies have shown that

American ginseng (*Panax quinquefolius* L.) extracts can inhibit tumor growth in HCT-116 [75] and MCF-7 cells [76]. A-kinase (PKA) and anchor protein 8-like (AKAP8L) gene expression were up-regulated, and phosphatidylinositol transfer protein alpha (PITPNA) gene expression was down-regulated after ginsenoside Rg3 treatment in HCT-116 cells [75]. The inhibition of the MAPK pathway and the up-regulation of Raf-1 kinase inhibitor protein (RKIP) expression were determined in the ginseng extract of hot water-extracted American ginseng-treated MCF-7 cells [76]. These genes have anticancer potential and are considered to be involved in anti-tumor mechanism of America ginseng. A comparison of transcriptional profiles between mouse macrophage RAW 264.7 cells before and after artemisinin treatments [83] found that the differentially expressed genes were most associated with the nitric oxide, cAMP, and Wnt/beta-catenin pathways. They suggested that the tumor regulation function of artemisinin might arise from its effect on nitric oxide biosynthesis. Nitric oxide has been proved that it can suppress tumorigenesis [102].

In another study, Hara et al. examined eight benzodioxoloquinolizine alkaloids extracted from *Coptidis rhizome* and assessed the strength of their antiproliferative activity in eight human pancreatic cancer cell lines [77]. These results indicated that berberine is the major compound behind boosting the anti-proliferative response. However, the anti-tumor effect of berberine isolated from *C. rhizome* was poorer than that of whole *C. rhizome*, suggesting other components of the fungus are to some degree responsible as well [78]. MCF-7 cells treated with *Coptidis* extracts also displayed increased activation of anti-tumor pathways. Two critical anti-tumor cytokines were identified—interferon- β and tumor necrosis factor- α —and *Coptidis* extracts were also found to induce cell growth arrest and apoptosis [103]. These studies suggest that *C. rhizome* or *Coptidis* extracts are able to inhibit cell proliferation by reducing tumor cell growth and promoting apoptosis.

5.6. Angiogenesis. Some Chinese herbs have been reported to promote angiogenesis. Ginseng refers to both *Panax ginseng* C.A. Meyer and *Panax quinquefolius* L. (Araliaceae), which contain similar components. Rg1, a *P. ginseng* extract, can promote angiogenesis by modulating cytoskeletal-related genes and enhancing endothelial nitric oxide synthase activities in human umbilical vein endothelial cells (HUVEC) [82]. Chan et al. also illustrated that Rg1-induced down-regulation of miR-214 led to an increase in the expression of eNOS in HUVEC through miRNA microarray analysis [104]. Taken together, the findings suggest that Rg1, the major component ginsenoside from *P. ginseng*, can promote angiogenesis in HUVEC.

5.7. Cardiovascular Disease. *Salvia miltiorrhiza* is widely used for human cardiovascular disorders in Asia, but the cellular mechanism by which it attenuates the growth of aortic smooth muscle under oxidative stress remains unclear. Salvianolic acid (SAL) or tanshinone (TAN) purified from *S. miltiorrhiza* was used to treat acute myocardial infarction

in Wistar rats [85]. SAL decreases the gene expression of apoptosis-related genes at a later period after ischemia, for example, BCL2 modifying factor (Bmf). TAN decreases the gene expression of intracellular calcium pathways-related genes at an early stage after ischemic injury, for example, voltage-dependent calcium channel alpha 1 (CACNA1). Intracellular calcium and apoptosis pathways have been reported to be associated with ischemic cardiac injury and repair [105, 106]. These results suggest that SAL and TAN could be used to prevent injury and involved in after injury repair of acute myocardial infarction.

5.8. Neuronal Diseases. Su et al. compared gene expression profiles of H₂O₂-exposed human neuroblastoma SH-SY5Y cells following treatment with paeonol, which is extracted from *Paeonia suffruticosa* [20, 84]. They identified that the extract up-regulated the mature T-cell gene set and found that paeonol was able to reduce H₂O₂-induced NF- κ B activity. These data indicate that paeonol might have antioxidative related properties and could be used to treat neurodegenerative diseases, for example, Alzheimer's disease [107].

6. Proteomic Studies of Chinese Herbs in Diseases

Compared with studies investigating Chinese herbs using genomic analysis, proteomic analytic studies have been performed far less and on fewer herbs. Tumors and convulsive disorders are the major subjects of analysis by proteomic technologies to date. The Chinese herbs used for these conditions and related references are documented in Table 2.

6.1. Antitumor Activity. HepG2 liver cancer cells were treated with oridonin extracted from *Isodon rubescens* and analyzed by 2-DE and MALDI-TOF-MS [79]. Proteomic data showed that expression levels of heat shock 70 kDa protein 1, Sti1h, and hnRNP-E1 were altered after treatment; these proteins are associated with apoptosis pathways. An extract from Franquet (Cucurbitaceae), tubeimoside-1 (TBMS1), has also been used as an anticancer treatment [108]. Xu et al. found 15 proteins differentially expressed between TBMS-treated or -untreated HeLa cells through MALDI-TOF-MS analysis [80]. These proteins were associated with mitochondrial dysfunction and ER stress-induced cell death pathways and participated in TBMS1-induced cytotoxicity [80].

The major component of *Rhizoma paridis*, *Rhizoma paridis* total saponin (RPTS), is responsible for the antitumor effects of this herb. Using MALDI-TOF-MS, Cheng et al. identified 15 proteins altered in HepG2 cells differentially expressed between RPTS-treated or untreated HepG2 cells, with most of them implicated in tumor initiation, promotion, and progression [81]. These results suggest that proteomic approaches could be useful tools to elucidate pharmacological mechanisms responsible for anti-cancer drug activities.

Moreover, Hung et al. found that *S. miltiorrhiza* aqueous extract (SMAE) inhibited the proliferation of rat aortic

smooth muscle cell line A10 under homocysteine (Hcy)-induced oxidative stress [87, 88]. Furthermore, the intracellular reactive oxygen species concentration significantly decreased in A10 cells after SMAE treatment. Using MALDI-TOF-MS, the researchers suggested that the SMAE-induced inhibition of growth in Hcy-stimulated A10 cells occurred via the PKC/MAPK-dependent pathway [87, 88].

6.2. Convulsive Disorders. *Uncaria rhynchophylla* (UR) and its major component, rhynchophylline, have demonstrated effectiveness in treating convulsive disorders [109]. Lo et al. used SD rats with kainic acid (KA)-induced epileptic seizures and treated them with UR [86]. They then analyzed proteomic profiles from the frontal cortex and hippocampus of rat brain tissues and identified proteins differentially expressed between treated and untreated tissue. Macrophage migration inhibitory factor (MIF) and cyclophilin A were down-regulated and restored to normal levels in epileptic seizure rats after UR treatment. MIF has been considered as a counterregulator of normal neuronal actions and increases its expression level to reduce the chronotropic actions in SD rats [110]. Cyclophilin A is a phylogenetically-conserved protein and regulates immunosuppression [111]. These results showed that MIF and cyclophilin A involved in the mechanism of anticonvulsive effect of UR.

7. Metabolomics Studies of Chinese Herbs in Diseases

Another platform for systems biology research is metabolomics, involving the study of targeted small molecule metabolites (<1500 Da). In 1998, the metabolome was first introduced in the elucidation of yeast gene function [112]. However, the application of this concept can be traced back to the development of traditional medicine; while metabonomics chemically tracks metabolites in urine, feces, and so forth, traditional medicine used color, smell, and taste to facilitate diagnoses. Over genomics and proteomics, metabolomics can provide a more solid link between genotype and phenotype.

7.1. NMR-Based Metabolomics Analysis. NMR-based metabolomics is an attractive method for the study of medicinal herb efficacy on disease symptoms. Using this method, nonselective and comprehensive analysis was performed on ginkgo extracts [113]. Moreover, Zhang et al. found that ginkgo extracts have multidirectional lipid-lowering effects on the rat metabolome [114]. They suggested that ginkgo extracts possess metabolomic functions, including limitation of cholesterol absorption, inactivation of HMGCoA, and favorable regulation of essential polyunsaturated fatty acid profiles [114].

7.2. Liquid Chromatography (LC)-TOF MS-Based Metabolomics. LC-MS-based metabolomics have been explored in many studies to date. Tan et al. performed LC-TOF MS to investigate the metabolites of aconitum alkaloids in rat urine after oral administration of aconite root extracts [115].

They found 10 metabolites and 24 parent components and suggested that metabolomic approaches may prove useful in exploring the efficacy of CHM. Moreover, Yan et al. investigated the antiaging effect of flavones contained in *Epimedium* extract in rats through LC-MS [116]. They were able to identify differences in multiple age-related metabolites in serum, including carnosine, ergothioneine, unsaturated fatty acids, saturated fatty acids, and nucleotides. The expression levels of these age-related proteins were restored to levels found in younger rats after *Epimedium* treatment.

Terpenoids, a group of important secondary metabolites in plants, are found in *Ganoderma* sp., which have high cytotoxic and anti-tumor activity. Ganoderiol F, a tetracyclic triterpene, has been analyzed by LC/MS/MS and administered to rats for metabolomics and pharmacokinetics experiments [117]. Analysis of the metabolites of ganoderiol F by HPLC/MS/MS from orally or i.v.-treated rats showed good viability and low acute toxicity. According to these reports, ganoderiol F may show potential as an anti-cancer drug.

8. Summary and Future Perspectives

In this paper, we described and discussed omics research to date combined with acupuncture or CHM, performed at the systems biology level. We found that the ST36 acupoint is the most widely used acupoints, and that it has multiple therapeutic functions and targets, including spinal cord injury [46], allergic rhinitis [56], analgesia [38], neuropathic pain [9, 47], antiaging [41], knee osteoarthritis [45], and acute ischemic stroke [11]. Different from other therapies, acupuncture treatments show variation in the transcriptional profiles and perceived effect of their subjects, whether rats [39] or humans [40]. Gao et al. reported that approximately 30% of rats demonstrated no analgesic effects during EA [39]. Similarly, Chae et al. reported that 40% of their participants felt only low analgesic effects during acupuncture, an observation that is more likely caused by genetic variation rather than differences in psychology [40]. Individual variance in treatment response is becoming an important issue when deciding whether it is suitable or not to administer acupuncture therapy. Based on this paper results, we suggest that system biology approaches can be performed to construct exhaustive clinical data of patients with acupuncture or CHM treatments, for example, up-regulated or down-regulated genes of Ph (+) or Ph (-) allergic rhinitis patients with acupuncture treatments, and provide useful information for improving future therapeutic strategies. In term of acupuncture treatment, one acupoint commonly used for different symptoms, for example, LI4 acupoint could be performed for allergic rhinitis, analgesia, and acute ischemic stroke. Compared with acupuncture treatments, Chinese herbal treatments are more often investigated for their effectiveness on specific diseases, and studies focus on the pharmacological mechanisms of different herbal extracts, for example, benzodioxoloquinolizine alkaloids has anti-tumor activity [77] or CK has anti-diabetic efficacy [21]. In summary, we suggest appropriate therapies—whether

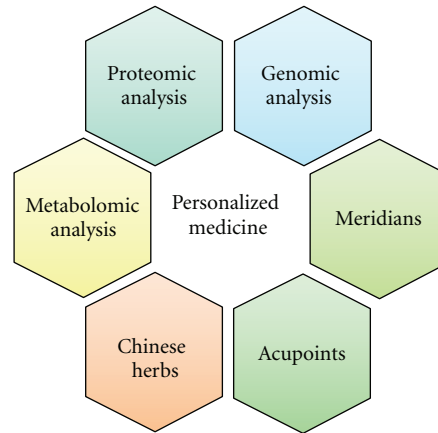


FIGURE 2: The composition of “personalized medicine in TCM.” Combining genomic, proteomic, and metabolomic information can provide more comprehensive strategies for TCM therapies.

acupuncture, TCM, or a combination—can be personalized to individuals through analyzing their transcriptional or proteomic profiles (Figure 2). “Personalized medicine in TCM” can be developed even further and provide important information for therapeutic strategies in managing various diseases and conditions.

Acknowledgments

This work was supported by the National Taiwan University Cutting-Edge Steering Research Project (101R7602C3) and the National Science Council of Taiwan (NSC99-2621-B-010-001-MY3, and NSC99-2621-B-002-005-MY3).

References

- [1] P. C. W. Fung, “Probing the mystery of Chinese medicine meridian channels with special emphasis on the connective tissue interstitial fluid system, mechanotransduction, cells durotaxis and mast cell degranulation,” *Chinese Medicine*, vol. 4, article 10, 2009.
- [2] S. J. Birch and R. L. Felt, *Understanding Acupuncture*, Churchill Livingstone, New York, NY, USA, 1999.
- [3] L. Bai, J. Tian, C. Zhong et al., “Acupuncture modulates temporal neural responses in wide brain networks: evidence from fMRI study,” *Molecular Pain*, vol. 6, article 73, 2010.
- [4] M. V. Madsen, P. C. Gøtzsche, and A. Hróbjartsson, “Acupuncture treatment for pain: systematic review of randomised clinical trials with acupuncture, placebo acupuncture, and no acupuncture groups,” *BMJ*, vol. 338, p. a3115, 2009.
- [5] H. M. Langevin and J. A. Yandow, “Relationship of acupuncture points and meridians to connective tissue planes,” *Anatomical Record*, vol. 269, no. 6, pp. 257–265, 2002.
- [6] J. Kong, T. J. Kaptchuk, G. Polich et al., “An fMRI study on the interaction and dissociation between expectation of pain relief and acupuncture treatment,” *NeuroImage*, vol. 47, no. 3, pp. 1066–1076, 2009.
- [7] J. Jia, B. Li, Z. L. Sun, F. Yu, X. Wang, and X. M. Wang, “Electro-acupuncture stimulation acts on the basal ganglia output pathway to ameliorate motor impairment in parkinsonian model rats,” *Behavioral Neuroscience*, vol. 124, no. 2, pp. 305–310, 2010.
- [8] J. Jia, Z. Sun, B. Li et al., “Electro-acupuncture stimulation improves motor disorders in Parkinsonian rats,” *Behavioural Brain Research*, vol. 205, no. 1, pp. 214–218, 2009.
- [9] H. J. Sung, Y. S. Kim, I. S. Kim et al., “Proteomic analysis of differential protein expression in neuropathic pain and electroacupuncture treatment models,” *Proteomics*, vol. 4, no. 9, pp. 2805–2813, 2004.
- [10] X. C. Yuan, J. L. Song, G. H. Tian, S. H. Shi, and Z. G. Li, “Proteome analysis on the mechanism of electroacupuncture in relieving acute spinal cord injury at different time courses in rats,” *Chinese Acupuncture & Moxibustion*, vol. 34, no. 2, pp. 75–82, 2009.
- [11] S. Pan, X. Zhan, X. Su, L. Guo, L. Lv, and B. Su, “Proteomic analysis of serum proteins in acute ischemic stroke patients treated with acupuncture,” *Experimental Biology and Medicine*, vol. 236, no. 3, pp. 325–333, 2011.
- [12] J. Q. Fang, E. Aoki, Y. Yu, T. Sohma, T. Kasahara, and T. Hisamitsu, “Inhibitory effect of electroacupuncture on murine collagen arthritis and its possible mechanisms,” *In Vivo*, vol. 13, no. 4, pp. 311–318, 1999.
- [13] S. P. Zhang, J. S. Zhang, K. K. L. Yung, and H. Q. Zhang, “Non-opioid-dependent anti-inflammatory effects of low frequency electroacupuncture,” *Brain Research Bulletin*, vol. 62, no. 4, pp. 327–334, 2004.
- [14] S. Fulder, *The Handbook of Alternative and Complementary Medicine*, Oxford University Press, Oxford, UK, 1996.
- [15] X. Xu, K. You, X. Bao, and K. Kang, *Essentials of Traditional Chinese Medicine English-Chinese Encyclopedia of Practical Tcm*, Higher Education Press, Beijing, China, 1991.
- [16] M. A. Richardson, T. Sanders, J. L. Palmer, A. Greisinger, and S. E. Singletary, “Complementary/alternative medicine use in a comprehensive cancer center and the implications for oncology,” *Journal of Clinical Oncology*, vol. 18, no. 13, pp. 2505–2514, 2000.
- [17] S. Gözümlü, A. Tezel, and M. Koc, “Complementary alternative treatments used by patients with cancer in Eastern Turkey,” *Cancer Nursing*, vol. 26, no. 3, pp. 230–236, 2003.
- [18] O. DePeyer, *Herbal Extracts Help Fight Cancer*, Nature News, 2000.

- [19] K. Wojcikowski, D. W. Johnson, and G. Gobe, "Herbs or natural substances as complementary therapies for chronic kidney disease: ideas for future studies," *Journal of Laboratory and Clinical Medicine*, vol. 147, no. 4, pp. 160–166, 2006.
- [20] S. Y. Su, C. Y. Cheng, T. H. Tsai, C. Y. Hsiang, T. Y. Ho, and C. L. Hsieh, "Paenolol attenuates H₂O₂-induced NF- κ B-associated amyloid precursor protein expression," *American Journal of Chinese Medicine*, vol. 38, no. 6, pp. 1171–1192, 2010.
- [21] G. C. Han, S. K. Ko, J. H. Sung, and S. H. Chung, "Compound K enhances insulin secretion with beneficial metabolic effects in db/db mice," *Journal of Agricultural and Food Chemistry*, vol. 55, no. 26, pp. 10641–10648, 2007.
- [22] H. F. Juan and H. C. Huang, *System Biology: Applications in Cancer-Related Research*, World Scientific, Singapore, 2012.
- [23] Z. L. Whichard, C. A. Sarkar, M. Kimmel, and S. J. Corey, "Hematopoiesis and its disorders: a systems biology approach," *Blood*, vol. 115, no. 12, pp. 2339–2347, 2010.
- [24] Y. Rudy, M. J. Ackerman, D. M. Bers et al., "Systems approach to understanding electromechanical activity in the human heart a national heart, lung, and blood institute workshop summary," *Circulation*, vol. 118, no. 11, pp. 1202–1211, 2008.
- [25] H. Y. Chuang, M. Hofree, and T. Ideker, "A decade of systems biology," *Annual Review of Cell and Developmental Biology*, vol. 26, pp. 721–744, 2010.
- [26] E. C. Butcher, E. L. Berg, and E. J. Kunkel, "Systems biology in drug discovery," *Nature Biotechnology*, vol. 22, no. 10, pp. 1253–1259, 2004.
- [27] C. W. Hu, Y. L. Chang, S. J. Chen et al., "Revealing the functions of the transketolase enzyme isoforms in *Rhodospseudomonas palustris* using a systems biology approach," *PloS One*, vol. 6, no. 12, article e28329, 2011.
- [28] R. Hall, M. Beale, O. Fiehn, N. Hardy, L. Sumner, and R. Bino, "Plant metabolomics: the missing link in functional genomics strategies," *Plant Cell*, vol. 14, no. 7, pp. 1437–1440, 2002.
- [29] H. V. Westerhoff and B. O. Palsson, "The evolution of molecular biology into systems biology," *Nature Biotechnology*, vol. 22, no. 10, pp. 1249–1252, 2004.
- [30] C. C. Lin, J. T. Hsiang, C. Y. Wu, Y. J. Oyang, H. F. Juan, and H. C. Huang, "Dynamic functional modules in co-expressed protein interaction networks of dilated cardiomyopathy," *BMC Systems Biology*, vol. 4, article 138, 2010.
- [31] D. Greenbaum, N. M. Luscombe, R. Jansen, J. Qian, and M. Gerstein, "Interrelating different types of genomic data, from proteome to secretome: 'Oming in on function,'" *Genome Research*, vol. 11, no. 9, pp. 1463–1468, 2001.
- [32] L. L. Lin, H. C. Huang, and H. F. Juan, "Discovery of biomarkers for gastric cancer: a proteomics approach," *Journal of Proteomics*, vol. 75, no. 11, pp. 3081–3097, 2012.
- [33] C. C. Lin, Y. J. Chen, C. Y. Chen, Y. J. Oyang, H. F. Juan, and H. C. Huang, "Crosstalk between transcription factors and microRNAs in human protein interaction network," *BMC Systems Biology*, vol. 6, article 18, 2012.
- [34] C. W. Tseng, C. C. Lin, C. N. Chen, H. C. Huang, and H. F. Juan, "Integrative network analysis reveals active microRNAs and their functions in gastric cancer," *BMC Systems Biology*, vol. 5, article 99, 2011.
- [35] G. A. Ulett, J. Han, and S. Han, "Traditional and evidence-based acupuncture: history, mechanisms, and present status," *Southern Medical Journal*, vol. 91, no. 12, pp. 1115–1120, 1998.
- [36] S. L. Cantwell, "Traditional Chinese veterinary medicine: the mechanism and management of acupuncture for chronic pain," *Topics in Companion Animal Medicine*, vol. 25, no. 1, pp. 53–58, 2010.
- [37] C. A. Smith, C. T. Collins, C. A. Crowther, and K. M. Levett, "Acupuncture or acupressure for pain management in labour," *Cochrane Database of Systematic Reviews*, no. 7, article CD009232, 2011.
- [38] F. C. Chang, H. Y. Tsai, M. C. Yu, P. L. Yi, and J. G. Lin, "The central serotonergic system mediates the analgesic effect of electroacupuncture on Zusanli (ST36) acupoints," *Journal of Biomedical Science*, vol. 11, no. 2, pp. 179–185, 2004.
- [39] Y. Z. Gao, S. Y. Guo, Q. Z. Yin, T. Hisamitsu, and X. H. Jiang, "An individual variation study of electroacupuncture analgesia in rats using microarray," *American Journal of Chinese Medicine*, vol. 35, no. 5, pp. 767–778, 2007.
- [40] Y. Chae, H. J. Park, D. H. Hahm, S. H. Yi, and H. Lee, "Individual differences of acupuncture analgesia in humans using cDNA microarray," *Journal of Physiological Sciences*, vol. 56, no. 6, pp. 425–431, 2006.
- [41] X. Ding, J. Yu, T. Yu, Y. Fu, and J. Han, "Acupuncture regulates the aging-related changes in gene profile expression of the hippocampus in senescence-accelerated mouse (SAMP10)," *Neuroscience Letters*, vol. 399, no. 1–2, pp. 11–16, 2006.
- [42] M. Li and Y. Zhang, "Modulation of gene expression in cholesterol-lowering effect of electroacupuncture at Fenglong acupoint (ST40): a cDNA microarray study," *International Journal of Molecular Medicine*, vol. 19, no. 4, pp. 617–629, 2007.
- [43] Z. R. Vlahcevic, S. K. Jairath, D. M. Heuman et al., "Transcriptional regulation of hepatic sterol 27-hydroxylase by bile acids," *American Journal of Physiology*, vol. 270, no. 4, pp. G646–G652, 1996.
- [44] H. Wolters, B. M. Elzinga, J. F. W. Baller et al., "Effects of bile salt flux variations on the expression of hepatic bile salt transporters in vivo in mice," *Journal of Hepatology*, vol. 37, no. 5, pp. 556–563, 2002.
- [45] C. Tan, J. Wang, W. Feng, W. Ding, and M. Wang, "Preliminary correlation between warm needling treatment for knee osteoarthritis of deficiency-cold syndrome and metabolic functional genes and pathways," *JAMS Journal of Acupuncture and Meridian Studies*, vol. 3, no. 3, pp. 173–180, 2010.
- [46] X. Y. Wang, X. L. Li, S. Q. Hong, Y. B. Xi, and T. H. Wang, "Electroacupuncture induced spinal plasticity is linked to multiple gene expressions in dorsal root deafferented rats," *Journal of Molecular Neuroscience*, vol. 37, no. 2, pp. 97–110, 2009.
- [47] J. Ko, D. S. Na, H. L. Young et al., "cDNA microarray analysis of the differential gene expression in the neuropathic pain and electroacupuncture treatment models," *Journal of Biochemistry and Molecular Biology*, vol. 35, no. 4, pp. 420–427, 2002.
- [48] W. Dauer and S. Przedborski, "Parkinson's disease: mechanisms and models," *Neuron*, vol. 39, no. 6, pp. 889–909, 2003.
- [49] Y. G. Choi, S. Yeo, Y. M. Hong, S. H. Kim, and S. Lim, "Changes of gene expression profiles in the cervical spinal cord by acupuncture in an MPTP-intoxicated mouse model: microarray analysis," *Gene*, vol. 481, no. 1, pp. 7–16, 2011.
- [50] Y. G. Choi, S. Yeo, Y. M. Hong, and S. Lim, "Neuroprotective changes of striatal degeneration-related gene expression by acupuncture in an MPTP mouse model of Parkinsonism: microarray analysis," *Cellular and Molecular Neurobiology*, vol. 31, no. 3, pp. 377–391, 2011.

- [51] M. S. Hong, H. K. Park, J. S. Yang et al., "Gene expression profile of acupuncture treatment in 1-methyl-4-phenyl-1,2,3,6-tetrahydropyridine-induced Parkinson's disease model," *Neurological Research*, vol. 32, Supplement 1, pp. S74–S78, 2010.
- [52] M. A. Nouredine, Y. J. Li, J. M. van der Walt et al., "Genomic convergence to identify candidate genes for Parkinson's disease: SAGE analysis of the substantia nigra," *Movement Disorders*, vol. 20, no. 10, pp. 1299–1309, 2005.
- [53] C. K. Kim, G. S. Choi, S. D. Oh et al., "Electroacupuncture up-regulates natural killer cell activity: identification of genes altering their expressions in electroacupuncture induced up-regulation of natural killer cell activity," *Journal of Neuroimmunology*, vol. 168, no. 1-2, pp. 144–153, 2005.
- [54] S. K. Kim, J. Kim, E. Ko et al., "Gene expression profile of the hypothalamus in DNP-KLH immunized mice following electroacupuncture stimulation," *Evidence-Based Complementary and Alternative Medicine*, vol. 2011, Article ID 508689, 8 pages, 2011.
- [55] S. H. Sohn, S. K. Kim, E. Ko et al., "The genome-wide expression profile of electroacupuncture in DNP-KLH immunized mice," *Cellular and Molecular Neurobiology*, vol. 30, no. 4, pp. 631–640, 2010.
- [56] H. S. Shiue, Y. S. Lee, C. N. Tsai, Y. M. Hsueh, J. R. Sheu, and H. H. Chang, "DNA microarray analysis of the effect on inflammation in patients treated with acupuncture for allergic rhinitis," *Journal of Alternative and Complementary Medicine*, vol. 14, no. 6, pp. 689–698, 2008.
- [57] H. S. Shiue, Y. S. Lee, C. N. Tsai, Y. M. Hsueh, J. R. Sheu, and H. H. Chang, "Gene expression profile of patients with phadiatop-positive and -negative allergic rhinitis treated with acupuncture," *Journal of Alternative and Complementary Medicine*, vol. 16, no. 1, pp. 59–68, 2010.
- [58] I. M. Cojocar, M. Cojocar, R. Tănăsescu et al., "Changes in plasma levels of complement in patients with acute ischemic stroke," *Romanian Journal of Internal Medicine*, vol. 46, no. 1, pp. 77–80, 2008.
- [59] W. J. Li, S. Q. Pan, Y. S. Zeng et al., "Identification of acupuncture-specific proteins in the process of electroacupuncture after spinal cord injury," *Neuroscience Research*, vol. 67, no. 4, pp. 307–316, 2010.
- [60] C. P. M. Reutelingsperger and W. L. Van Heerde, "Annexin V, the regulator of phosphatidylserine-catalyzed inflammation and coagulation during apoptosis," *Cellular and Molecular Life Sciences*, vol. 53, no. 6, pp. 527–532, 1997.
- [61] L. H. Wang and S. M. Strittmatter, "A family of rat CRMP genes is differentially expressed in the nervous system," *Journal of Neuroscience*, vol. 16, no. 19, pp. 6197–6207, 1996.
- [62] J. R. Siebert, F. A. Middleton, and D. J. Stelzner, "Long descending cervical propriospinal neurons differ from thoracic propriospinal neurons in response to low thoracic spinal injury," *BMC Neuroscience*, vol. 11, article 148, 2010.
- [63] S. Jeon, J. K. Youn, S. T. Kim et al., "Proteomic analysis of the neuroprotective mechanisms of acupuncture treatment in a Parkinson's disease mouse model," *Proteomics*, vol. 8, no. 22, pp. 4822–4832, 2008.
- [64] S. T. Kim, W. Moon, Y. Chae, Y. J. Kim, H. Lee, and H. J. Park, "The effect of electroacupuncture for 1-methyl-4-phenyl-1,2,3,6-tetrahydropyridine-induced proteomic changes in the mouse striatum," *Journal of Physiological Sciences*, vol. 60, no. 1, pp. 27–34, 2010.
- [65] D. Sliva, "Cellular and physiological effects of *Ganoderma lucidum* (Reishi)," *Mini-Reviews in Medicinal Chemistry*, vol. 4, no. 8, pp. 873–879, 2004.
- [66] C. Y. Lai, J. T. Hung, H. H. Lin et al., "Immunomodulatory and adjuvant activities of a polysaccharide extract of *Ganoderma lucidum* in vivo and in vitro," *Vaccine*, vol. 28, no. 31, pp. 4945–4954, 2010.
- [67] Y. L. Lin, S. S. Lee, S. M. Hou, and B. L. Chiang, "Polysaccharide purified from *Ganoderma lucidum* induces gene expression changes in human dendritic cells and promotes T helper 1 immune response in BALB/c mice," *Molecular Pharmacology*, vol. 70, no. 2, pp. 637–644, 2006.
- [68] H. R. Lemmon, J. Sham, L. A. Chau, and J. Madrenas, "High molecular weight polysaccharides are key immunomodulators in North American ginseng extracts: characterization of the ginseng genetic signature in primary human immune cells," *Journal of Ethnopharmacology*, vol. 142, no. 1, pp. 1–13, 2012.
- [69] C. H. Cheng, A. Y. Leung, and C. F. Chen, "The effects of two different ganoderma species (Lingzhi) on gene expression in human monocytic THP-1 cells," *Nutrition and Cancer*, vol. 62, no. 5, pp. 648–658, 2010.
- [70] J. Wu, M. Zhang, H. Jia et al., "Protosappanin A induces immunosuppression of rats heart transplantation targeting T cells in grafts via NF- κ B pathway," *Naunyn-Schmiedeberg's Archives of Pharmacology*, vol. 381, no. 1, pp. 83–92, 2010.
- [71] K. C. Cheng, H. C. Huang, J. H. Chen et al., "Ganoderma lucidum polysaccharides in human monocytic leukemia cells: from gene expression to network construction," *BMC Genomics*, vol. 8, article 411, 2007.
- [72] Q. Zhang, F. Wei, C. C. Fong et al., "Transcriptional profiling of human skin fibroblast cell line Hs27 induced by herbal formula *Astragalii Radix* and *Rehmanniae Radix*," *Journal of Ethnopharmacology*, vol. 138, no. 3, pp. 668–675, 2011.
- [73] H. Zhao, J. Deneau, G. O. Che et al., "Angelica sinensis isolate SBD. 4: composition, gene expression profiling, mechanism of action and effect on wounds, in rats and humans," *European Journal of Dermatology*, vol. 22, no. 1, pp. 58–67, 2012.
- [74] Y. Sun, S. M. Y. Lee, Y. M. Wong et al., "Dosing effects of an antiosteoporosis herbal formula—a preclinical investigation using a rat model," *Phytotherapy Research*, vol. 22, no. 2, pp. 267–273, 2008.
- [75] X. Luo, C. Z. Wang, J. Chen et al., "Characterization of gene expression regulated by American ginseng and ginsenoside Rg3 in human colorectal cancer cells," *International Journal of Oncology*, vol. 32, no. 5, pp. 975–983, 2008.
- [76] M. L. King and L. L. Murphy, "American ginseng (*Panax quinquefolius* L.) extract alters mitogen-activated protein kinase cell signaling and inhibits proliferation of MCF-7-cells," *Journal of Experimental Therapeutics and Oncology*, vol. 6, no. 2, pp. 147–155, 2007.
- [77] A. Hara, N. Iizuka, Y. Hamamoto et al., "Molecular dissection of a medicinal herb with anti-tumor activity by oligonucleotide microarray," *Life Sciences*, vol. 77, no. 9, pp. 991–1002, 2005.
- [78] N. Iizuka, M. Oka, K. Yamamoto et al., "Identification of common or distinct genes related to antitumor activities of a medicinal herb and its major component by oligonucleotide microarray," *International Journal of Cancer*, vol. 107, no. 4, pp. 666–672, 2003.
- [79] H. Wang, Y. Ye, S. Y. Pan et al., "Proteomic identification of proteins involved in the anticancer activities of oridonin in HepG2 cells," *Phytomedicine*, vol. 18, no. 2-3, pp. 163–169, 2011.
- [80] Y. Xu, J. F. Chiu, Q. Y. He, and F. Chen, "Tubeimoside-1 exerts cytotoxicity in heLa cells Through mitochondrial dysfunction and endoplasmic reticulum stress pathways,"

- Journal of Proteome Research*, vol. 8, no. 3, pp. 1585–1593, 2009.
- [81] Z. X. Cheng, B. R. Liu, X. P. Qian et al., “Proteomic analysis of anti-tumor effects by *Rhizoma Paridis* total saponin treatment in HepG2 cells,” *Journal of Ethnopharmacology*, vol. 120, no. 2, pp. 129–137, 2008.
- [82] P. Y. K. Yue, D. Y. L. Wong, W. Y. Ha et al., “Elucidation of the mechanisms underlying the angiogenic effects of ginsenoside Rg1 in vivo and in vitro,” *Angiogenesis*, vol. 8, no. 3, pp. 205–216, 2005.
- [83] V. B. Konkimalla, M. Blunder, B. Korn et al., “Effect of artemisinins and other endoperoxides on nitric oxide-related signaling pathway in RAW 264.7 mouse macrophage cells,” *Nitric Oxide*, vol. 19, no. 2, pp. 184–191, 2008.
- [84] S. Y. Su, C. Y. Cheng, T. H. Tsai, C. Y. Hsiang, T. Y. Ho, and C. L. Hsieh, “Paeonol attenuates H₂O₂-induced NF- κ B-associated amyloid precursor protein expression,” *American Journal of Chinese Medicine*, vol. 38, no. 6, pp. 1171–1192, 2010.
- [85] X. Wang, Y. Wang, M. Jiang et al., “Differential cardioprotective effects of salvianolic acid and tanshinone on acute myocardial infarction are mediated by unique signaling pathways,” *Journal of Ethnopharmacology*, vol. 135, no. 3, pp. 662–671, 2011.
- [86] W. Y. Lo, F. J. Tsai, C. H. Liu et al., “*Uncaria rhynchophylla* upregulates the expression of MIF and cyclophilin A in kainic acid-induced epilepsy rats: a proteomic analysis,” *American Journal of Chinese Medicine*, vol. 38, no. 4, pp. 745–759, 2010.
- [87] Y. C. Hung, P. W. Wang, and T. L. Pan, “Functional proteomics reveal the effect of *Salvia miltiorrhiza* aqueous extract against vascular atherosclerotic lesions,” *Biochimica et Biophysica Acta*, vol. 1804, no. 6, pp. 1310–1321, 2010.
- [88] Y. C. Hung, P. W. Wang, T. L. Pan, G. Bazylak, and Y. L. Leu, “Proteomic screening of antioxidant effects exhibited by *Radix Salvia miltiorrhiza* aqueous extract in cultured rat aortic smooth muscle cells under homocysteine treatment,” *Journal of Ethnopharmacology*, vol. 124, no. 3, pp. 463–474, 2009.
- [89] H. Zhao, R. Mortezaei, Y. Wang, X. Sheng, F. Aria, and K. Bojanowski, “SBD.4 stimulates regenerative processes in vitro, and wound healing in genetically diabetic mice and in human skin/severe-combined immunodeficiency mouse chimera,” *Wound Repair and Regeneration*, vol. 14, no. 5, pp. 593–601, 2006.
- [90] C. Prost-Squarcioni, S. Fraitag, M. Heller, and N. Boehm, “Functional histology of dermis,” *Annales De Dermatologie Et De Venereologie*, vol. 135, no. 1, Part 2, pp. 1–20, 2008.
- [91] A. R. Saltiel, “New perspectives into the molecular pathogenesis and treatment of type 2 diabetes,” *Cell*, vol. 104, no. 4, pp. 517–529, 2001.
- [92] R. S. Lindsay, T. Funahashi, R. L. Hanson et al., “Adiponectin and development of type 2 diabetes in the Pima Indian population,” *The Lancet*, vol. 360, no. 9326, pp. 57–58, 2002.
- [93] Y. Fu, N. Luo, R. L. Klein, and W. T. Garvey, “Adiponectin promotes adipocyte differentiation, insulin sensitivity, and lipid accumulation,” *Journal of Lipid Research*, vol. 46, no. 7, pp. 1369–1379, 2005.
- [94] J. W. Hsu, H. C. Huang, S. T. Chen, C. H. Wong, and H. F. Juan, “*Ganoderma lucidum* polysaccharides induce macrophage-like differentiation in human leukemia THP-1 cells via caspase and p53 activation,” *Evidence-Based Complementary and Alternative Medicine*, vol. 2011, Article ID 358717, 13 pages, 2011.
- [95] J. Jiang, I. Eliaz, and D. Sliva, “Suppression of growth and invasive behavior of human prostate cancer cells by ProstaCaid: mechanism of activity,” *International Journal of Oncology*, vol. 38, no. 6, pp. 1675–1682, 2011.
- [96] J. Jiang and D. Sliva, “Novel medicinal mushroom blend suppresses growth and invasiveness of human breast cancer cells,” *International Journal of Oncology*, vol. 37, no. 6, pp. 1529–1536, 2010.
- [97] S. M. Y. Lee, M. L. Y. Li, Y. C. Tse et al., “*Paeoniae Radix*, a Chinese herbal extract, inhibit hepatoma cells growth by inducing apoptosis in a p53 independent pathway,” *Life Sciences*, vol. 71, no. 19, pp. 2267–2277, 2002.
- [98] H. Li, N. Takai, A. Yuge et al., “Novel target genes responsive to the anti-growth activity of triptolide in endometrial and ovarian cancer cells,” *Cancer Letters*, vol. 297, no. 2, pp. 198–206, 2010.
- [99] A. N. Pham, P. E. Blower, O. Alvarado, R. Ravula, P. W. Gout, and Y. Huang, “Pharmacogenomic approach reveals a role for the xc-cystine/glutamate antiporter in growth and celestrol resistance of glioma cell lines,” *Journal of Pharmacology and Experimental Therapeutics*, vol. 332, no. 3, pp. 949–958, 2010.
- [100] E. Wang, S. Bussom, J. Chen et al., “Interaction of a traditional Chinese Medicine (PHY906) and CPT-11 on the inflammatory process in the tumor microenvironment,” *BMC Medical Genomics*, vol. 4, article 38, 2011.
- [101] J. H. Yoo, H. C. Kwon, Y. J. Kim, J. H. Park, and H. O. Yang, “KG-135, enriched with selected ginsenosides, inhibits the proliferation of human prostate cancer cells in culture and inhibits xenograft growth in athymic mice,” *Cancer Letters*, vol. 289, no. 1, pp. 99–110, 2010.
- [102] S. P. Hussain, G. E. Trivers, L. J. Hofseth et al., “Nitric oxide, a mediator of inflammation, suppresses tumorigenesis,” *Cancer Research*, vol. 64, no. 19, pp. 6849–6853, 2004.
- [103] J. X. Kang, J. Liu, J. Wang, C. He, and F. P. Li, “The extract of huanglian, a medicinal herb, induces cell growth arrest and apoptosis by upregulation of interferon- β and TNF- α in human breast cancer cells,” *Carcinogenesis*, vol. 26, no. 11, pp. 1934–1939, 2005.
- [104] L. S. Chan, P. Y. K. Yue, N. K. Mak, and R. N. S. Wong, “Role of MicroRNA-214 in ginsenoside-Rg1-induced angiogenesis,” *European Journal of Pharmaceutical Sciences*, vol. 38, no. 4, pp. 370–377, 2009.
- [105] H. Yaoita, K. Ogawa, K. Maehara, and Y. Maruyama, “Apoptosis in relevant clinical situations: contribution of apoptosis in myocardial infarction,” *Cardiovascular Research*, vol. 45, no. 3, pp. 630–641, 2000.
- [106] K. Ito, X. Yan, M. Tajima, Z. Su, W. H. Barry, and B. H. Lorell, “Contractile reserve and intracellular calcium regulation in mouse myocytes from normal and hypertrophied failing hearts,” *Circulation Research*, vol. 87, no. 7, pp. 588–595, 2000.
- [107] D. Praticò, “Oxidative stress hypothesis in Alzheimer’s disease: a reappraisal,” *Trends in Pharmacological Sciences*, vol. 29, no. 12, pp. 609–615, 2008.
- [108] F. Wang, R. Ma, and L. Yu, “Role of mitochondria and mitochondrial cytochrome c in tubeimoside I-mediated apoptosis of human cervical carcinoma HeLa cell line,” *Cancer chemotherapy and pharmacology*, vol. 57, no. 3, pp. 389–399, 2006.
- [109] J. Lee, D. Son, P. Lee et al., “Protective effect of methanol extract of *Uncaria rhynchophylla* against excitotoxicity induced by N-methyl-D-aspartate in rat hippocampus,” *Journal Pharmacological Sciences*, vol. 92, no. 1, pp. 70–73, 2003.

- [110] H. Li, Y. Gao, C. D. Freire, M. K. Raizada, G. M. Toney, and C. Sumners, "Macrophage migration inhibitory factor in the PVN attenuates the central pressor and dipsogenic actions of angiotensin II," *The FASEB Journal*, vol. 20, no. 10, pp. 1748–1750, 2006.
- [111] J. Liu, J. D. Farmer Jr., W. S. Lane, J. Friedman, I. Weissman, and S. L. Schreiber, "Calcineurin is a common target of cyclophilin-cyclosporin A and FKBP-FK506 complexes," *Cell*, vol. 66, no. 4, pp. 807–815, 1991.
- [112] S. G. Oliver, M. K. Winson, D. B. Kell, and F. Baganz, "Systematic functional analysis of the yeast genome," *Trends in Biotechnology*, vol. 16, no. 9, pp. 373–378, 1998.
- [113] S. Agnolet, J. W. Jaroszewski, R. Verpoorte, and D. Staerk, "1H NMR-based metabolomics combined with HPLC-PDA-MS-SPE-NMR for investigation of standardized Ginkgo biloba preparations," *Metabolomics*, vol. 6, no. 2, pp. 292–302, 2010.
- [114] Q. Zhang, G. J. Wang, J. Y. A et al., "Application of GC/MS-based metabonomic profiling in studying the lipid-regulating effects of Ginkgo biloba extract on diet-induced hyperlipidemia in rats," *Acta Pharmacologica Sinica*, vol. 30, no. 12, pp. 1674–1687, 2009.
- [115] G. Tan, Z. Lou, J. Jing et al., "Screening and analysis of aconitum alkaloids and their metabolites in rat urine after oral administration of aconite roots extract using LC-TOFMS-based metabolomics," *Biomedical Chromatography*, vol. 25, no. 12, pp. 1343–1351, 2011.
- [116] S. Yan, B. Wu, Z. Lin et al., "Metabonomic characterization of aging and investigation on the anti-aging effects of total flavones of Epimedium," *Molecular BioSystems*, vol. 5, no. 10, pp. 1204–1213, 2009.
- [117] Q. Zhang, F. Zuo, N. Nakamura, C. M. Ma, and M. Hattori, "Metabolism and pharmacokinetics in rats of ganoderiol F, a highly cytotoxic and antitumor triterpene from *Ganoderma lucidum*," *Journal of Natural Medicines*, vol. 63, no. 3, pp. 304–310, 2009.

Research Article

NMDA Receptor-Dependent Synaptic Activity in Dorsal Motor Nucleus of Vagus Mediates the Enhancement of Gastric Motility by Stimulating ST36

Xinyan Gao,¹ Yongfa Qiao,² Baohui Jia,³ Xianghong Jing,¹ Bin Cheng,⁴ Lei Wen,⁵ Qiwen Tan,⁴ Yi Zhou,⁶ Bing Zhu,¹ and Haifa Qiao^{1,4,6}

¹Institute of Acupuncture and Moxibustion, China Academy of Chinese Medical Sciences, 16 Nanxiaojie Street, Dongzhimennei, Beijing 100700, China

²Qingdao Haici Medical Group, 4 Renmin Road, Qingdao 266033, China

³Guanganmen Hospital, China Academy of Chinese Medical Sciences, Beijing 100053, China

⁴The Affiliated Hospital, Shandong University of Traditional Chinese Medicine, Jinan 250014, China

⁵Department of Pharmacology, Southern Medical University, Guangzhou 510515, China

⁶Department of Biomedical Sciences, Florida State University College of Medicine, Tallahassee, FL 32306, USA

Correspondence should be addressed to Bing Zhu, zhubing@mail.cintcm.ac.cn and Haifa Qiao, haifa.qiao@med.fsu.edu

Received 12 July 2012; Revised 4 September 2012; Accepted 8 September 2012

Academic Editor: Ying Xia

Copyright © 2012 Xinyan Gao et al. This is an open access article distributed under the Creative Commons Attribution License, which permits unrestricted use, distribution, and reproduction in any medium, provided the original work is properly cited.

Previous studies have demonstrated the efficacy of electroacupuncture at ST36 for patients with gastrointestinal motility disorders. While several lines of evidence suggest that the effect may involve vagal reflex, the precise molecular mechanism underlying this process still remains unclear. Here we report that the intragastric pressure increase induced by low frequency electric stimulation at ST36 was blocked by AP-5, an antagonist of N-methyl-D-aspartate receptors (NMDARs). Indeed, stimulating ST36 enhanced NMDAR-mediated, but not 2-amino-3-(5-methyl-3-oxo-1,2-oxazol-4-yl)propanoic-acid-(AMPA-) receptor-(AMPA-) mediated synaptic transmission in gastric-projecting neurons of the dorsal motor nucleus of the vagus (DMV). We also identified that suppression of presynaptic μ -opioid receptors may contribute to upregulation of NMDAR-mediated synaptic transmission induced by electroacupuncture at ST36. Furthermore, we determined that the glutamate-receptor-2a-(NR2A-) containing NMDARs are essential for NMDAR-mediated enhancement of gastric motility caused by stimulating ST36. Taken together, our results reveal an important role of NMDA receptors in mediating enhancement of gastric motility induced by stimulating ST36.

1. Introduction

Gastric motility disorders are clinically characterized by impaired accommodation, gastroparesis, and dumping syndrome. A large number of studies has been conducted to explore the efficacy of somatic stimulation for the treatment of gastrointestinal motility disorders [1–5]. Reproducible results were generated in both clinical and research settings [6, 7], and several lines of evidence suggest that the gastric motility regulation induced by stimulating ST36 seems to be mediated via vagal reflex in the supraspinal pathway [5, 8–10]. However, how stimulating ST36 regulates gastric motility through relay nuclei and the molecular mechanism

employed in this process still remain unclear. Addressing this question can provide valuable clues for the development of effective therapeutics against gastrointestinal motility disorders.

Vagal motor innervation to the major portion of the gastrointestinal (GI) tract is provided by neurons in the dorsal motor nucleus of the vagus (DMV) [11, 12]. Nucleus of the solitary tract (NTS) neurons can potentially contribute input to the DMV and induce potent effects on vagus-mediated gastric function through excitatory glutamatergic and inhibitory GABAergic synaptic connections [13, 14]. Neuropharmacological studies have demonstrated changes in gastric function in response to localized application

of gamma-aminobutyric acid (GABA) and glutamate (via GABA_A and NMDA receptors) within the DMV [15–18].

In this study, we directly examined the functional role of NMDAR-mediated synaptic transmission in mediating the upregulation of gastric motility by stimulating ST36. Our data reveal that electroacupuncture at ST36 upregulates gastric motility by specifically enhancing the glutamate-receptor-2a-(NR2A-) containing N-Methyl-D-aspartate-receptors-(NMDAR-) mediated synaptic transmission in gastric-projecting DMV neurons.

2. Materials and Methods

2.1. Animals and Surgical Preparation for In Vivo Experiments. Adult male Sprague Dawley (250–300 g) rats were purchased from the Institute of Laboratory Animal Sciences, CAMS and PUMC (Beijing, China). In this study, all manipulations and procedures were carried out in accordance with The Guide for Care and Use of Laboratory Animals issued by USA National Institutes of Health and were approved by the Institutional Animal Care and Use Committee of China Academy of Chinese Medical Sciences. As described previously [19, 20], rats were housed ($23 \pm 1^\circ\text{C}$) in groups and maintained under a 12 hours light/dark cycle with food and water available *ad libitum*. The rats were fasted overnight with free access to water in *proxima luce*, and anesthetized with an intraperitoneal injection of urethane (1.0 g/kg, Sigma-Aldrich, St. Louis, USA). The left common carotid artery was cannulated with a polyethylene catheter filled with physiological saline containing heparin (200 IU/mL, LEO, Denmark) for recording of arterial pressure (AP) via a blood pressure transducer (TSD104A) and amplifier (MP150, DA100C, BIOPEC, Goleta, USA). The trachea was cannulated but not immobilized, to avoid respiratory tract congestion and a catheter was inserted into the left jugular vein for solution. A 2-mm-diameter polyurethane tube attached to a 1-cm-diameter latex balloon was inserted into the stomach through the mouth and esophagus. A syringe was attached to the cannula to inflate and deflate the balloon with water. The balloon was filled with 0.5–1.5 mL warm-water (37°C), which is equal to 80–150 mm H₂O pressure, and the pressure was measured by a transducer connected to an amplifier through a thin polyethylene tube (1.5-mm in o.d.) and recorded by a multichannel data acquisition workstation (Micro1401-3, Cambridge Electronic Design, England). Offline data analysis was conducted with spike2 software. Semifasting gastric motor activity was recorded as a control for at least 1 hour before somatic stimulation. C57BL/6J or NR2A knockout mice (6–8 weeks) were purchased from Riken Bioresource Center, Japan and were treated with the protocol similar to the above.

2.2. Microinjection in DMV. A glass micropipette (i.d.: 0.04 mm; o.d.: 0.12 mm; WPI, Sarasota, USA) with a tip diameter of $\sim 30\ \mu\text{m}$ was stereotaxically placed at 0.1 to 0.6 mm rostral to calamus scriptorius (CS), 0.3 to 0.6 mm lateral from the midline, and 0.5 to 0.9 mm below the dorsal surface of the medulla. Microinjections of glutamate or GABA receptor (GABAR) antagonist were performed

bilaterally via a Hamilton syringe (Mode 75) connected to the micropipette, with the movement of the meniscus monitored by a dissecting microscope. Injections were given in volumes of 20 nL over a period of 10–15 seconds. Somatic-stimulation-evoked responses were repeated 5 minutes after the DMV microinjection. The locations of microinjection were confirmed by histological verification.

2.3. Histological Verification of Injection Sites. The microinjection site in the brainstem was marked by pontamine sky blue. After fixing *in vivo* with 2% paraformaldehyde and 1% glutaraldehyde in 0.1 M PBS (pH 7.4), the brainstem was sectioned at $30\ \mu\text{m}$, and the sections were stained with 0.3% neutral red. The marked microinjection site was located by microscopic examination. Only those data with histological and chemical confirmation were accepted.

2.4. Electroacupuncture. The stimulation electrode was placed at ST36, a hind limb point at which electroacupuncture or manual acupuncture enhances gastric motility [20]. Based on the descriptions in previous reports [21], the location is on the anterolateral side of the hind limb near the anterior crest of the tibia below the knee under the tibialis anterior muscle. This point was bilaterally stimulated with a 2–3 mA pulse of 0.5 ms duration at a frequency of 4 Hz for 30 seconds or 20 min by a pair of needle-electrodes inserted 3 mm depth into the skin. As a control, we selected CV12 which is located on the median line of the upper abdomen, 1.5 cm above the umbilicus, and could inhibit gastric motility [19]. The abdomen point was also inserted to a depth of 3 mm and stimulated with the same protocol. The electrical current for somatic stimulation was generated by a stimulator (SEN-7203, NIHON KOHDEN, Tokyo, Japan). For the recording of intragastric pressure *in vivo*, electroacupuncture was given at least 1 hour after stable basal recording or 10 min after drug administration. In brain slice experiments, we stimulated ST36 for 20 minutes in rats with retrograde labeling after anesthetization and then cut brain slices.

2.5. Retrograde Labeling. Retrograde neuronal tracer 1,1'-diiododecyl-3,3',3'-tetramethylindocarbocyanine perchlorate (DiI₁₈(3); DiI) (Molecular Probes) was used to label gastric-projecting neurons of the DMV in 14-day-old male Sprague Dawley rats (Institute of Laboratory Animal Sciences, CAMS and PUMC, Beijing, China). As described previously [11, 22], after anesthetizing deeply with urethane and performing an abdominal laparotomy, DiI crystals were applied to one gastric region per rat (either the major curvature of the fundus or corpus or the antrum-pylorus). To confine the site of application, the crystals were embedded to the application site using a fast-settling epoxy resin that was allowed to harden for several minutes. After closing the laparotomy with 5/0 suture, the animals were placed in the chamber warmed under a radiant heat lamp until normal activity was restored. The animals were then returned to their home cages and allowed to recover for 10–15 days before brain slices were collected.

2.6. Brain Slice Preparation. Thin brainstem slices were prepared from retrograde-labeled rats as described previously with several modifications [11, 22]. Briefly, the rat was sacrificed after being deeply anesthetized with urethane. The whole brain was then removed and placed in ice-cold artificial cerebrospinal fluid (ACSF) containing (mM): 124 NaCl, 3 KCl, 1.25 NaH₂PO₄, 1.3 MgSO₄, 2 CaCl₂, 26 NaHCO₃, 10 glucose, bubbled with 95% O₂/5% CO₂, osmolality 300–310 mOsm. After removing the cerebellum, the brainstem was transected rostrally at the level of the pons and again at a point several millimeters caudal to the CS. A vibratome (VT1200S, Leica, German) was used to cut four to five coronal slices (250 μ m thickness) containing the DMV. The slices were incubated at 37°C for at least 45 minutes in oxygenated ACSF before use.

2.7. Whole Cell Recording. A single slice was transferred to the recording chamber and kept in place with a slice anchor (Warner Instruments, Hamden, USA). The retrograde-labeled DMV neurons were identified under a Nikon E600 microscope (Nikon, Tokyo, Japan) equipped with tetramethylrhodamine isothiocyanate epifluorescence filters. Electrophysiological recordings were made under brightfield illumination after the identity of a labeled neuron was confirmed. The slice was continuously superfused with oxygenated ACSF (2 mL/min) at room temperature. Recording solution containing (in mM): 145 K-gluconate, 7.5 KCl, 9 NaCl, 1 MgSO₄, 10 HEPES, 0.2 EGTA, 2 Na-ATP, 0.25 Na-GTP, adjusted to pH 7.4 with KOH, osmolality 290–300 mOsm, was used to back-fill recording electrodes (DC resistance: 5–7 M Ω). Currents were recorded with a MultiClamp700B amplifier (Molecular Devices) and filtered at 2 kHz with a lowpass filter, and data were digitized at 10 kHz and stored online using the pClamp10 software.

For recording of mini-EPSC (mEPSC), the perfusion solution contained 30 μ M bicuculline and 1 μ M TTX, and the membrane was held at –60 mV. Data were analyzed with the Mini Analysis program (Synaptosoft, Leonia, USA).

For electrical stimulation-induced EPSCs, a concentric tungsten bipolar stimulating electrode (WPI, Sarasota, USA) was placed in the centralis or medialis subnuclei of the NTS. Single stimulus pulse (200 μ s, 10–500 μ A) or pairs of stimuli (200 μ s, 10–500 μ A, 100 ms interval) were applied every 20 seconds to evoke EPSCs. The above stimulation intensity is a range which can induce 50% of maximum AMPAR- or NMDAR-mediated EPSC. Series resistance ranged from 12 to 16 M Ω , and input resistance is 260–290 M Ω . The series and input resistances were monitored using voltage steps (5 mV, 50 ms) at 20-second intervals throughout the whole recording. If the membrane resistance changes more than 20% relative to an initial 3-minute period of recordings, the neuron will be rejected from the statistical analysis. Non-NMDAR- (AMPA/kainite-) and NMDAR-mediated EPSCs were recorded at a holding potential of –60 mV and +40 mV. 30 μ M bicuculline or 20 μ M 6,7-dinitroquinoxaline-2,3-dione (DNQX) was bath-applied to block GABAR or AMPA receptor (AMPA) current. 5 mM QX314 was added to recording solution to prevent antidromically activated action potentials. Neurons were allowed to recover fully

between additions of antagonists (minimum washout period of 10 minutes). Antagonists were superfused for at least 5 minutes. All chemicals or drugs are purchased from Sigma-Aldrich (St Louis, USA) if not stated otherwise.

2.8. Data Analysis. Data are shown as mean \pm SEM. For significance evaluation, data sets with normal distribution were analyzed by paired or unpaired *t* test for two groups or one-way ANOVA followed by *q* test or Dunnett's test for more than two groups, and *P* < 0.05 was considered statistical significance.

3. Results

3.1. Electroacupuncture at ST36 Increases Gastric Motility through Activating DMV Neurons. To determine whether electroacupuncture at ST36 may affect gastric motility in rats, we designed an experiment in which an electrical stimulation with 2–3 mA pulse of 0.2 ms duration at a frequency of 4 Hz was applied to ST36 or CV12. As shown in Figure 1(a), gastric pressure was dramatically increased by the low frequency stimulation at ST36. On the contrary, stimulating CV12 caused a marked reduction in gastric pressure. On average, gastric pressure was increased 24.15 ± 1.02 mm H₂O (*P* < 0.05, *n* = 9) by stimulation at ST36, but decreased 13.43 ± 3.16 mm H₂O (*P* < 0.05, *n* = 9) by stimulating CV12. Thus, these data suggested that low frequency stimulation at ST36 can regulate gastric motility in a location-specific manner.

To identify the role of glutamate or GABA receptors of DMV neurons in mediating the enhancement of gastric motility by electroacupuncture at ST36, we stereotaxically microinjected antagonists for either GABA_A receptor bicuculline (2 nL, 30 μ M), or glutamate receptor including DNQX (2 nL, 20 μ M) for AMPARs and AP5 (2 nL, 50 μ M) for NMDARs into DMV. The increased gastric pressure induced by stimulating ST36 was significantly reduced by AP5 (2.18 ± 1.85 mm H₂O, *P* < 0.05, *n* = 9), but not by bicuculline (25.89 ± 3.07 mm H₂O, *P* > 0.05, *n* = 9) or DNQX (23.47 ± 2.05 mm H₂O, *P* > 0.05, *n* = 9) (Figures 1(a) and 1(b)), suggesting that low frequency stimulation at ST36 increases gastric motility through activating NMDARs, rather than AMPARs or GABARs in DMV neurons.

3.2. Electroacupuncture at ST36 Enhances NMDAR-Mediated EPSCs in Gastric-Projecting DMV Neurons. To address whether electroacupuncture at ST36 specifically affects the NMDAR-mediated synaptic responses in gastric-projecting DMV neurons, we first used a retrograde tracing marker to label gastric-projecting DMV neurons. Similar to previous reports [11, 23, 24], a majority of labeled neurons were localized at the medial DMV and had small somas and few branches (Figure 2(a)). We then stimulated ST36 for 20 minutes in rats with retrograde labeling, and carried out whole cell recording in acute brainstem slices. In labeled DMV neurons, NMDAR-mediated EPSC in ST36 group was significantly larger than that in the control group without stimulation (91.49 ± 8.12 pA versus 68.50 ± 4.76 pA, *P* < 0.05, *n* = 12) (Figures 2(b) and 2(c)). By contrast, no

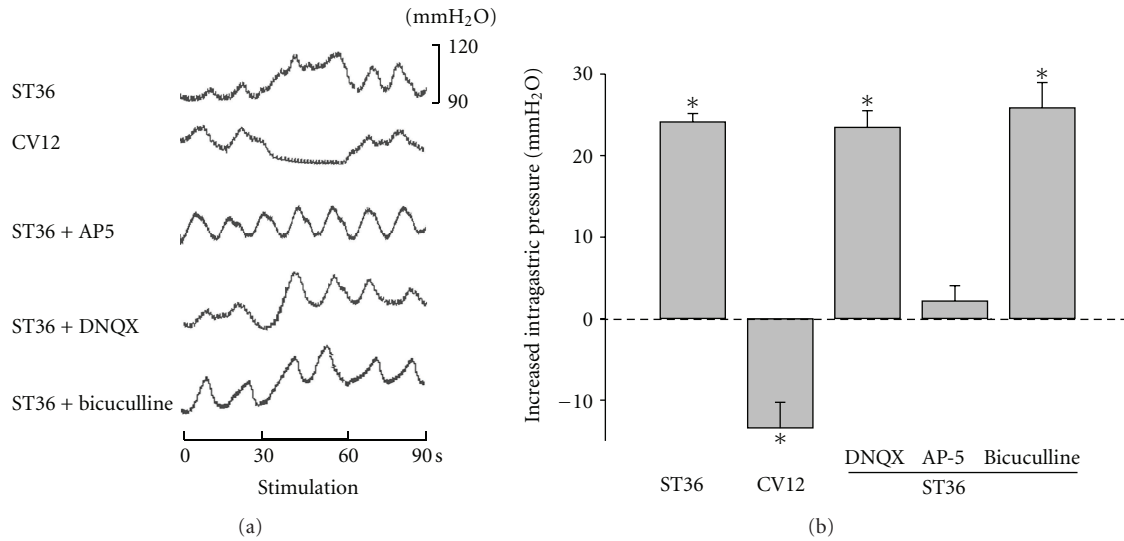


FIGURE 1: Low frequency stimulation at ST36 increases intragastric pressure. (a) Representative waves of intragastric pressure of rats induced by stimulating CV12 and ST36 with or without AP5, DNQX, or bicuculline. (b) Summarized data for the effect of low frequency stimulation at CV12 and ST36 with or without AP5, DNQX, or bicuculline on intragastric pressure. * $P < 0.05$, $n = 9$ for each group, one-way ANOVA followed by Dunnett's test.

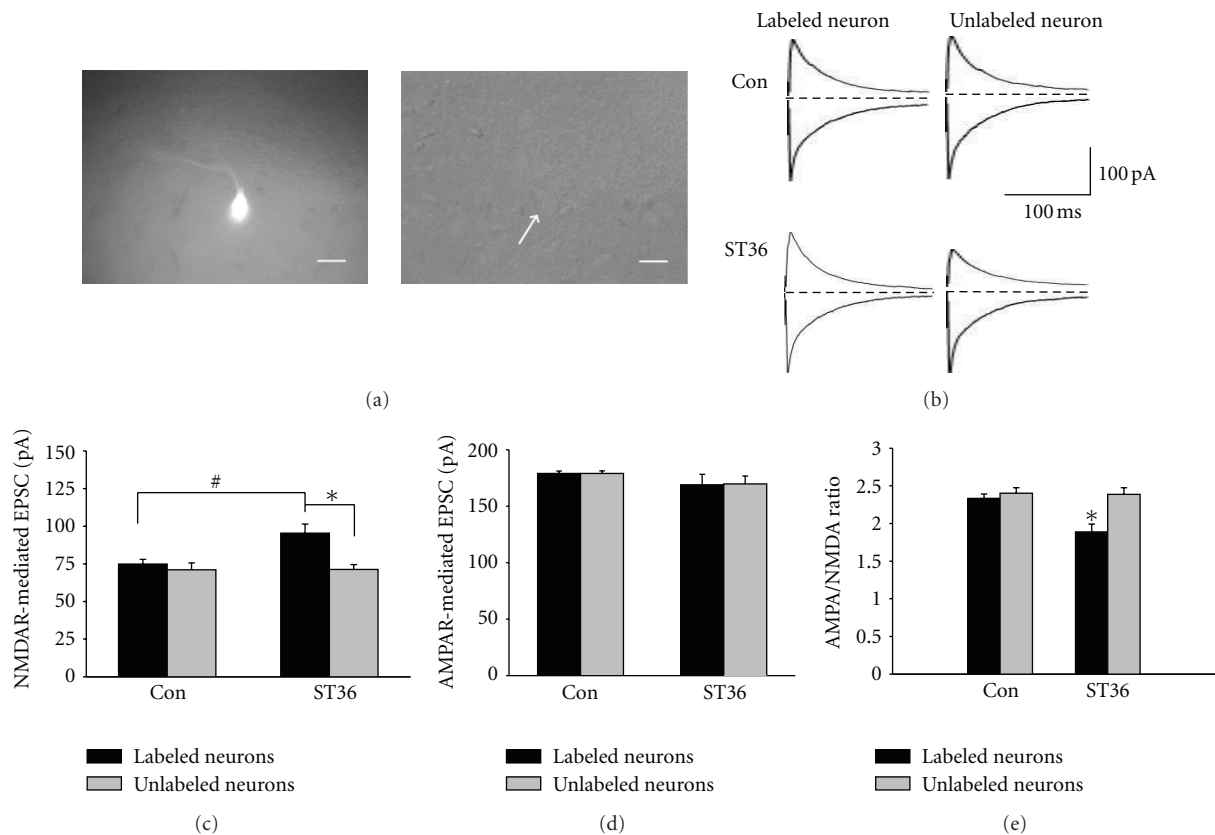


FIGURE 2: Low frequency stimulation at ST36 increases NMDAR-mediated EPSCs in gastric-projecting neurons. (a) Representative gastric-projecting neuron which is labeled with retrograde tracer. Left: under fluorescent light; right: under bright-field illumination. The arrows point to the same neuron. Calibration bar: 20 μm . (b) Representative traces of labeled and unlabeled neurons in the brain slices from rats with and without low frequency stimulation at ST36. (c) NMDAR-mediated EPSCs are increased in labeled neurons from the stimulated rats. * $P < 0.05$, compared to unlabeled neurons from the stimulated rats, unpaired t test; # $P < 0.05$, compared to the labeled neurons from control rats (without stimulation), $n = 12$, unpaired t test. (d) The low frequency stimulation at ST36 does not change AMPAR-receptor-(AMPA)-mediated EPSCs in either labeled or unlabeled neurons, unpaired t test. (e) The low frequency stimulation at ST36 does not change the AMPA/NMDA ratio.

significant difference was found in AMPAR-mediated EPSCs between ST36 and control groups in labeled DMV neurons (170.58 ± 11.74 pA versus 181.37 ± 4.19 pA, $P > 0.05$, $n = 12$) (Figures 2(b) and 2(d)). On the other hand, neither NMDAR nor AMPAR mediated EPSC in unlabeled DMV neurons had significant changes in either ST36 or control group (NMDAR-mediated EPSC: 69.17 ± 4.31 pA for stimulated versus 71.03 ± 5.89 pA for control, $P > 0.05$, $n = 12$; AMPAR-mediated EPSC: 182.05 ± 2.98 pA for stimulation versus 171.27 ± 8.42 pA for control, $P > 0.05$, $n = 12$) (Figures 2(b)–2(d)). As shown in Figure 2(e), AMPA/NMDA current ratio of labeled neurons in ST36 group decreased significantly compared to the unlabeled neurons (1.89 ± 0.10 for labeled neurons versus 2.39 ± 0.09 for unlabeled neurons, $P < 0.05$, $n = 12$); in control, no significant difference between labeled and unlabeled neurons was found (2.33 ± 0.06 for labeled neurons versus 2.40 ± 0.07 for unlabeled neurons). Thus, these results demonstrated that low frequency stimulation at ST36 selectively increased the NMDAR-mediated synaptic responses in gastric-projecting DMV neurons.

3.3. Electroacupuncture at ST36 Increases NMDAR-Mediated Synaptic Transmission through Presynaptic Regulation. It is well documented that excitatory amino acid inputs from the NTS mediate vagal gastric motor excitation via NMDA and kainite/AMPA receptors in vagal motor neurons [25, 26]. Having identified that low frequency stimulation at ST36 increased NMDAR-mediated EPSCs between NTS and DMV EPSC, we went on to identify the pre- or postsynaptic mechanism responsible for the impact of electroacupuncture at ST36 on synaptic transmission. At first, mEPSCs were recorded in acute brainstem slices from rats subjected to ST36 stimulation. Although mEPSC amplitude did not differ between retrogradely labeled and unlabeled DMV neurons (51.41 ± 8.02 pA versus 50.07 ± 5.12 pA, $P > 0.05$, $n = 11$) (Figures 3(a)–3(d)), the frequency of mEPSC was significantly greater in labeled neurons (labeled neurons: 2.43 ± 0.07 Hz versus unlabeled neurons: 1.64 ± 0.05 Hz, $P < 0.05$, $n = 11$) (Figures 3(a)–3(c), and 3(e)). In control animals without somatic stimulation, we did not observe any significant difference in either mEPSC amplitude or frequency between labeled and unlabeled DMV neurons (amplitude: 51.38 ± 6.29 pA and frequency: 1.78 ± 0.10 Hz for labeled neurons versus 51.67 ± 9.88 pA and 1.74 ± 0.07 Hz for unlabeled neurons, $P > 0.05$, $n = 8$) (Figures 3(a), 3(b), 3(d), and 3(e)).

In addition, we assessed the site of action by measuring the ratio of the amplitudes of two postsynaptic currents in DMV neurons using a paired-pulse protocol. By delivering paired-pulse (10 Hz) stimulation to presynaptic NTS, we consistently observed a substantial change in paired-pulse ratio (PPR) of NMDAR-mediated currents in labeled and unlabeled neurons. As shown in Figures 4(a) and 4(c), the PPR of NMDAR-mediated EPSCs recorded from the retrogradely labeled DMV neurons was significantly larger in ST36 group than that in control (1.03 ± 0.11 versus 0.71 ± 0.02 ; $P < 0.01$, $n = 10$). In fact, there was a paired-pulse facilitation in labeled neurons compared to paired-pulse depression in unlabeled neurons. For the ST36 group, there

was also a significant difference between PPR of NMDAR-mediated EPSCs in labeled and unlabeled neurons (1.03 ± 0.11 for labeled neurons versus 0.74 ± 0.07 for unlabeled neurons, $P < 0.01$, $n = 10$) (Figures 4(a) and 4(c)). By contrast, there was little change in PPR of AMPAR-mediated EPSCs after ST36 stimulation, as the PPR recorded from labeled neuron in stimulated rats was not different with that either recorded from labeled neurons in the control group or unlabeled neurons in ST36 group (0.66 ± 0.04 for labeled neurons in ST36 group versus 0.72 ± 0.07 for labeled neurons in control; and 0.69 ± 0.07 for unlabeled neurons: $P > 0.05$, $n = 10$) (Figures 4(a)–4(d)). Given that a PPR change is indicative of a presynaptic site of action [27], these data suggested that stimulating ST36 increased NMDAR-mediated synaptic transmission via a presynaptic mechanism.

3.4. Electroacupuncture at ST36 Inhibits Presynaptic μ -Opioid Receptors. Previous evidence indicates that increasing activity of the presynaptic μ -opioid receptors attenuates the excitatory synaptic transmission from the NTS to GI-projecting DMV neurons [28]. Here we set out to detect whether stimulating ST36 can affect presynaptic μ -opioid receptors and hence increase NMDAR-mediated synaptic transmission. As shown in Figures 5(a) and 5(c), the NMDAR-mediated EPSCs in labeled neurons were significantly reduced by perfusion of the brain slice with a competitive agonist of μ -opioid receptors, D-Ala², N-MePhe⁴, Gly⁵-ol-enkephalin (DAMGO) (95.73 ± 4.89 pA versus 70.34 ± 7.22 pA, $P < 0.05$, $n = 12$ –14), and the reduction in NMDAR-mediated EPSCs by DAMGO was reversed by $0.2 \mu\text{M}$ naloxonazine, a selective μ -opioid receptor antagonist (93.39 ± 3.97 pA, $n = 14$). In addition, we found that the enhanced PPR by ST36 stimulation was abolished by DAMGO (stimulation: 1.12 ± 0.10 versus stimulation + DAMGO: 0.78 ± 0.13 , $P < 0.05$, $n = 7$ –8), and reversed by naloxonazine (1.18 ± 0.09 , $P < 0.05$, $n = 7$) (Figures 5(b) and 5(d)). Taken together, these data suggested that low frequency stimulation at ST36 inhibits the presynaptic μ -opioid receptor.

3.5. Electroacupuncture at ST36 Increases NR2A-Containing NMDAR-Mediated Synaptic Transmission of Gastric-Projecting DMV Neurons. To further characterize the role of specific subunits of NMDAR in mediating regulation of gastric motility by stimulating ST36, we applied selective antagonists which block either NR2A or NR2B containing NMDARs during whole-cell recording in the retrograde labeling neurons. Figures 6(a) and 6(b) show that in the presence of a NR2A-specific antagonist, ((R)-((S)-1-(4-bromophenyl)-ethylamino)-(2,3-dioxo-1,2,3,4-tetrahydroquinoloxalin-5-yl)-methyl)-phosphonic acid (NVP-AAM077) ($0.4 \mu\text{M}$), the facilitation of NMDAR-mediated EPSCs induced by ST36 stimulation in labeled neurons was abolished completely (stimulation: 95.73 ± 4.89 pA, $n = 12$; NVP-AAM077: 70.47 ± 7.87 pA, $n = 8$; $P < 0.05$). Conversely, no significant difference was observed between pre- and postapplication of $3 \mu\text{M}$ ifenprodil, a NR2B antagonist [29] (92.59 ± 4.07 pA, $n = 7$). Another NR2B-specific antagonist Ro25-6981 ($0.5 \mu\text{M}$) [30] also did not cause

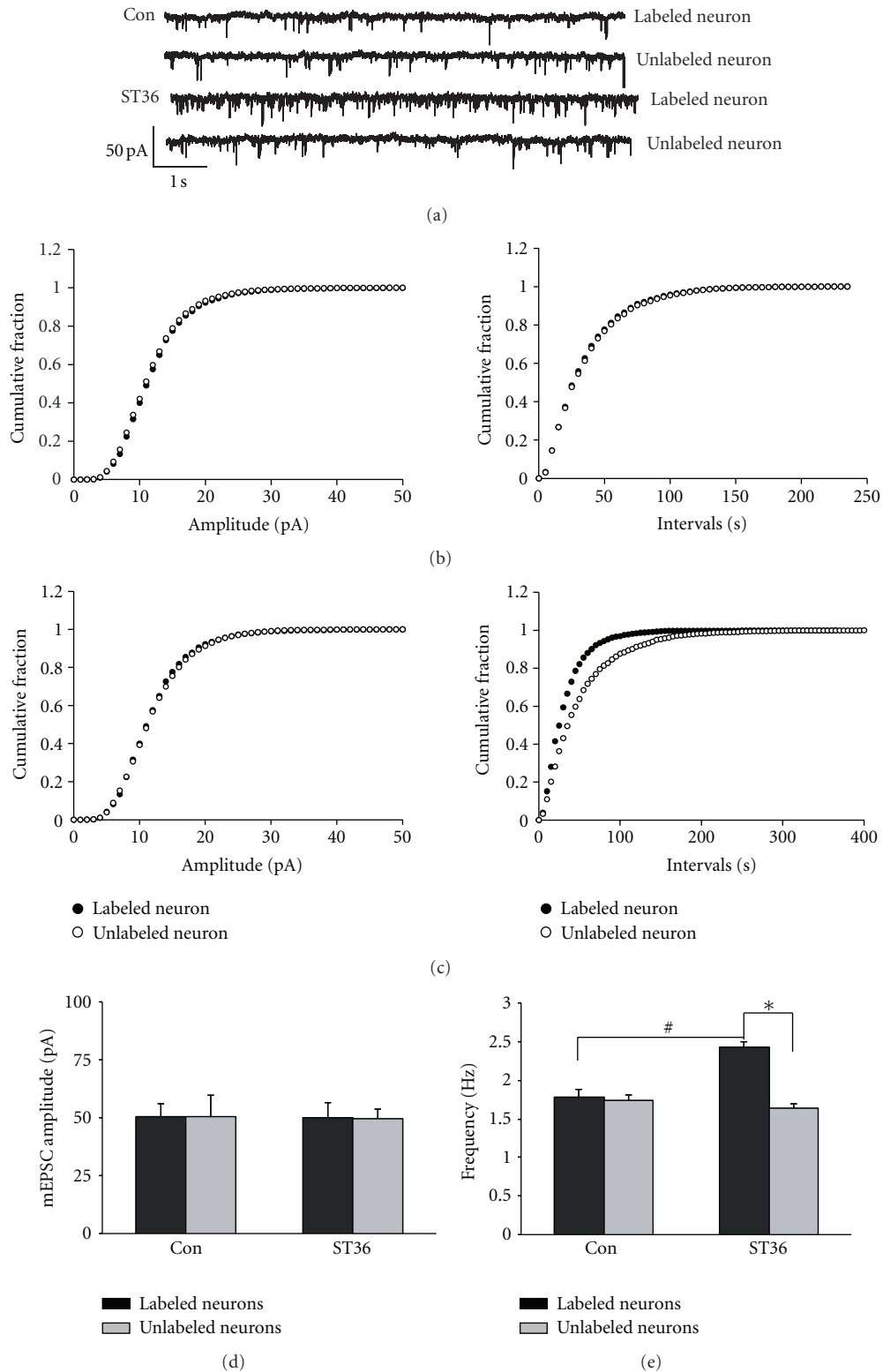


FIGURE 3: Low frequency stimulation at ST36 increases frequency of mEPSC. (a) Representative traces of mEPSC. (b) Cumulative plots of mEPSC amplitude and frequency of control. (c) Cumulative plots of mEPSC amplitude and frequency of low frequency stimulation at ST36. (d) Summarized amplitudes of mEPSC of labeled and unlabeled neuron in control and stimulated group. Unpaired t test shows no significant difference between labeled and unlabeled neurons in both groups. (e) Summarized frequencies of mEPSC of labeled and unlabeled neuron in control and stimulated rats. * $P < 0.05$, compared to the unlabeled neurons from the stimulated rats; # $P < 0.05$, compared to the labeled neurons from control; $n = 8-11$, unpaired t test.

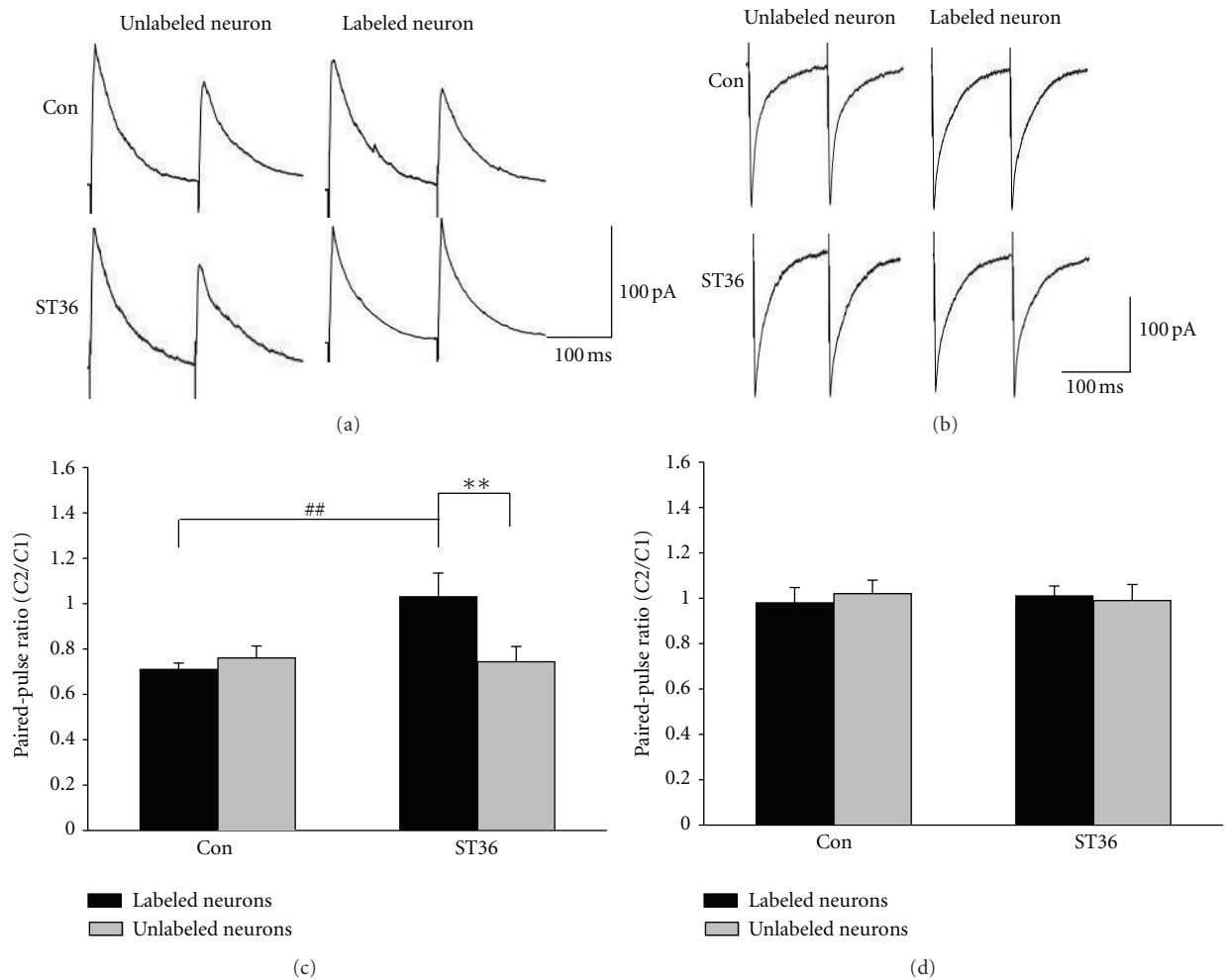


FIGURE 4: Low frequency stimulation at ST36 decreases paired-pulse ratio (PPR) of NMDAR-mediated EPSC. (a), (b) Representative traces of NMDAR- or AMPAR-mediated EPSC induced by paired-pulse stimulation in NTS. (c) ST36 stimulation decreases PPR of NMDAR-mediated EPSC in labeled DMV neurons. $**P < 0.01$, compared to the unlabeled neurons from the stimulated group; $##P < 0.01$, compared to the labeled neurons from control; $n = 10$, unpaired t test. (d) ST36 stimulation fails to cause significant change of PPR of AMPAR-mediated EPSC in labeled and unlabeled neurons in both groups, unpaired t test.

a significant change in evoked NMDAR-mediated EPSCs (95.39 ± 7.94 pA, $n = 7$), suggesting that NR2A-containing NMDARs are essential for NMDAR-mediated increase of gastric motility by stimulating ST36.

3.6. NVP-AAM077 Microinjection Diminishes the Enhancement of Gastric Motility Induced by Electroacupuncture at ST36 in Anesthetized Rats and Transgenic Mice. To examine whether these findings for the role of NR2A-containing NMDARs observed *in vitro* could be reproduced *in vivo*, NVP-AAM077 (2 nL, $0.4 \mu\text{M}$) was microinjected into DMV before ST36 stimulation in anesthetized rats. As shown in Figures 7(a) and 7(b), the increase of the intragastric pressure induced by stimulating ST36 was diminished significantly after microinjection of NVP-AAM077 ($135.15 \pm 7.06\%$ versus $87.04 \pm 8.32\%$, $P < 0.05$, $n = 5$). To further verify a specific role of NR2A in mediating the regulation of gastric motility by stimulating ST36, we performed the same stimulation

protocol in both wild-type and NR2A knockout mice. As shown in Figures 7(c) and 7(d), low frequency stimulation at ST increased gastric motility in the wild-type littermates, but not in the NR2A knockout mice ($100.00 \pm 3.96\%$, versus $67.97 \pm 4.13\%$, $P < 0.01$, $n = 5$), providing additional evidence that NR2A-containing NMDARs of DMV neurons are required for the increase of gastric motility induced by stimulating ST36.

4. Discussion

In the present study, we discovered that NMDARs of gastric-projecting DMV neurons play a critical role in mediating the enhancement of gastric motility induced by electroacupuncture at ST36 in anesthetized rats. Stimulating ST36 enhances NMDAR-mediated synaptic transmission through inhibiting presynaptic μ -opioid receptors. We also determined that the enhancement of NR2A-containing NMDAR-mediated

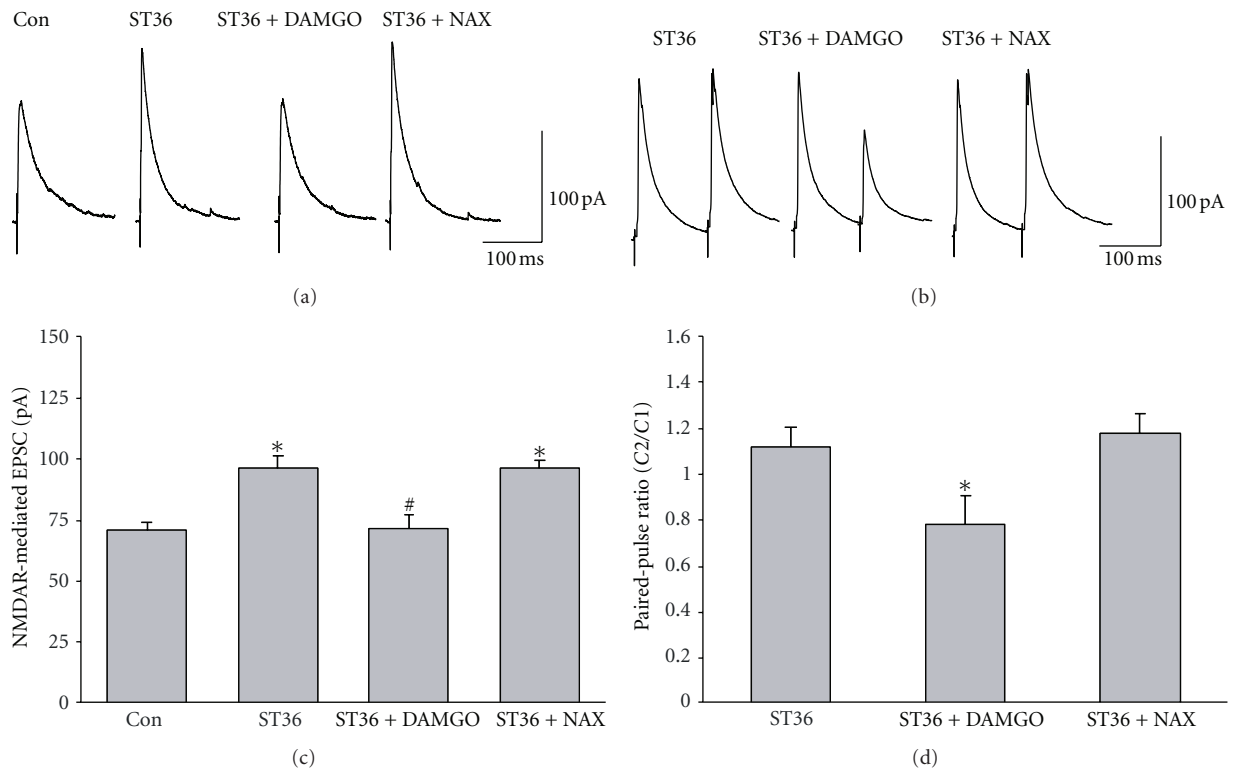


FIGURE 5: μ -opioid receptor agonist DAMGO abolishes the increase in NMDAR-mediated EPSC induced by low frequency stimulation at ST36. (a) Representative traces of NMDAR-mediated EPSC. (b) The increase of NMDAR-mediated EPSC in labeled DMV neurons induced by ST36 stimulation is reduced by bath perfusion of μ -opioid receptor agonist DAMGO and reversed by a specific μ -opioid receptor antagonist naloxonazine. * $P < 0.05$, compared to control; # $P < 0.05$, compared to the stimulated rats, $n = 12-14$, one-way ANOVA followed by q test. (c) Representative traces of NMDAR-mediated EPSC induced by paired-pulse. (d) The PPR decreased by ST36 stimulation is increased by DAMGO. * $P < 0.05$, $n = 7-8$, compared to ST36 stimulation and ST36 stimulation with naloxonazine, one-way ANOVA followed by q test.

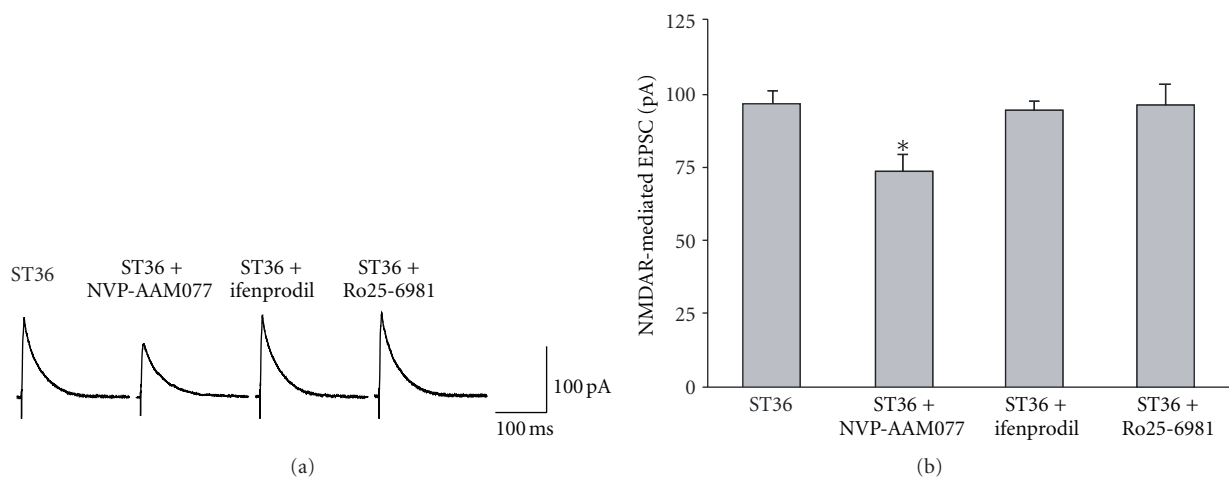


FIGURE 6: The increased NMDAR-mediated EPSC by low frequency stimulation at ST36 is diminished by NR2A antagonist NVP-AAM077. (a) Representative trace of NMDA-mediated EPSC with ST36 stimulation and different drugs. (b) The increased NMDAR-mediated EPSC by ST36 stimulation is diminished by NR2A antagonist NVP-AAM077, but not by NR2B antagonist ifenprodil and Ro25-6981. * $P < 0.05$, $n = 7-12$, one-way ANOVA followed by Dunnett's test.

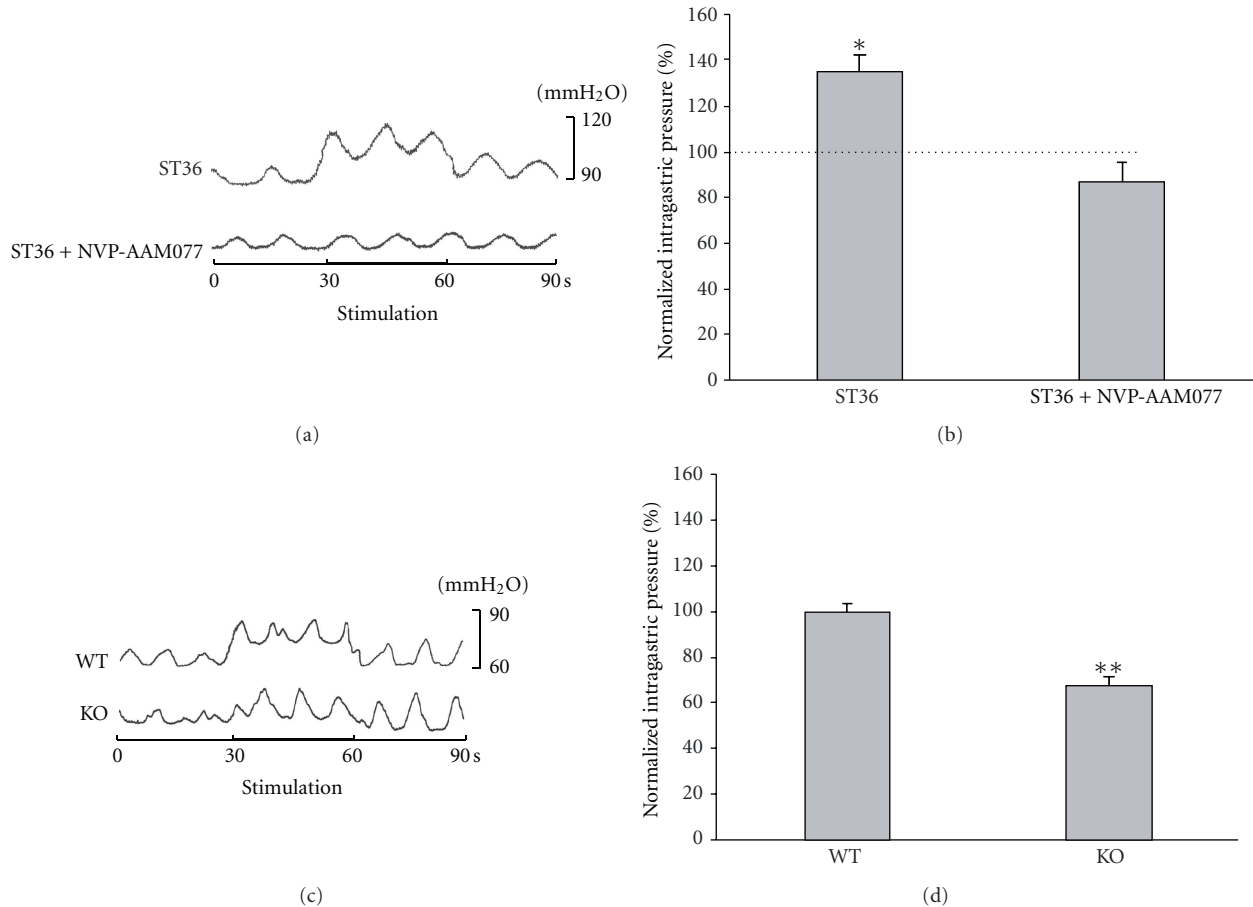


FIGURE 7: NVP-AAM077 microinjection of DMV reduced intragastric pressure enhanced by low frequency stimulation at ST36. (a) Representative waves of intragastric pressure under different conditions in anesthetized rats. (b) NVP-AAM077 abolishes the increase of intragastric pressure caused by ST36 stimulation. * $P < 0.05$, $n = 5$, one-way ANOVA followed by q test. Dotted line represents the control. (c) Representative waves of gastric motility of NR2A knockout mouse and its littermate wildtype. (d) ST36 stimulation increases intragastric pressure in wildtype mice but not in NR2A knockout mice. ** $P < 0.01$, $n = 5$, unpaired t test.

synaptic transmission between NTS and gastric-projecting DMV neurons is an absolute requirement for this potent regulation of gastric motility. Therefore, our study unveiled a novel molecular mechanism by which stimulating ST36 upregulates gastric motility via the vagal pathway.

Somatovisceral reflexes responsible for regulation of visceral organs are strongly associated with the effects of acupuncture. Application of acupuncture to the abdominal region inhibits gastric motility in anesthetized rats via a spinal reflex that activates sympathetic efferent nerve fibers, while stimulating a limb increases gastric motility via a supra-spinal reflex that activates vagal nerve fibers [19, 31, 32]. Here, we found that low frequency stimulation at ST36 can significantly increase gastric motility, but stimulating CV12 decreases gastric motility significantly. Our results are consistent with previous reports and provide strong support for the location specificity of somatic stimulation in regulating gastric motility.

It is well documented that somatic stimulation upregulates gastric motility through the vagal reflex pathway [5, 19]. However, little is known regarding the anatomic circuit

and functional changes underlying the somatic stimulation induced regulation of gastric motility. In the vagal reflex pathway, DMV plays a pivotal role in controlling the motility of the GI tract, as it sends efferent projections to the GI tract. NTS neurons also regulate gastric motility by providing direct inhibitory and excitatory inputs to preganglionic parasympathetic neurons in the DMV. Based on previous studies in brainstem slice preparations, endogenously occurring glutamate and GABA are the major neurotransmitters controlling the excitability of DMV motor neurons [24], while their inhibitory and excitatory effects on the excitability of DMV neurons are mediated directly via activation of postsynaptic GABA_A receptors and both NMDA- and non-NMDA-type glutamatergic receptors [26, 33, 34]. Our finding that the increase in intragastric pressure induced by low frequency stimulation at ST36 was diminished by NMDAR antagonist AP5 indicates that low frequency stimulation at ST36 upregulates gastric motility through the excitatory synaptic transmission between NTS and DMV, especially through NMDARs rather than non-NMDARs of DMV neurons.

The distinct distribution and morphology are characteristics of a subpopulation of DMV neurons that project to the stomach [13]. Our finding that stimulating ST36 enhances NMDAR-mediated EPSCs specifically in the retrogradely labeled neurons suggests that NMDARs of gastric-projecting DMV neurons mediate the regulation of gastric motility by somatic stimulation. We also determined that the ST36 stimulation induced enhancement of NMDAR-mediated synaptic transmission in DMV neurons is through presynaptic regulation, and propose inhibition of presynaptic μ -opioid receptors as one of the potential mechanisms. This hypothesis is supported by previous observations that opioid peptides attenuate excitatory synaptic transmission to gastric-projecting DMV neurons via interactions with presynaptic μ -opioid receptors [27]. In addition, opioid pathway may contribute to long-lasting effects of acupuncture on gastric motility [35]. The current result that μ -opioid receptor agonist DAMGO inhibited EPSCs of the gastric-projecting DMV neurons also suggests that increasing NMDAR-mediated synaptic transmission may be attributed to the inhibition of presynaptic μ -opioid receptors. However, the data that low frequency stimulation at ST36 did not change AMPAR-mediated synaptic transmission implies that other mechanisms might be involved and also need to be clarified in the future.

In the present work, we demonstrate that NMDAR-mediated excitation of DMV neurons evoked by ST36 stimulation is primarily mediated by NR1/NR2A receptors, as NR2A preferential antagonist *in vitro* decreases NMDAR-mediated synaptic response and *in vivo* abolishes the increase of gastric motility induced by low frequency somatic stimulation. The observed involvement of NR2A receptors in NMDAR-mediated upregulation of gastric motility by low frequency stimulation at ST36 is in agreement with previous reports that, in the adult brainstem, NR2A is predominantly expressed among the four NR2 subunits [36, 37] and the functional change in NMDAR properties is correlated with an increase in the NR2A subunit ratio [37, 38].

5. Conclusions

To sum, our study establishes that low frequency somatic stimulation at ST36 enhances NMDAR-mediated synaptic transmission via suppressing presynaptic μ -opioid receptors, and in turn increases NR2A-containing NMDAR-mediated synaptic transmission in gastric-projecting DMV neurons. While future studies are needed to clarify how low frequency stimulation at ST36 inhibits presynaptic μ -opioid receptors and thus increases NMDAR-mediated synaptic transmission, our data provide an important insight into the mechanism for ST36 stimulation enhanced gastric motility. In the future, this finding may also help to develop treatment strategy for gastric motility disorders by an NR2A-containing NMDAR-based activation approach.

Conflict of Interests

No conflict of interests, financial or otherwise, is declared by the author(s).

Authors' Contribution

The experiments were performed in the laboratories of H. Qiao and B. Zhu; X. Gao, H. Qiao, and B. Zhu made conception and design of research; X. Gao, Y. Qiao, B. Jia, X. Jing, B. Cheng, and Q. Tan performed experiments; X. Gao, B. Cheng, L. Wen, and H. Qiao analyzed data; X. Gao, Y. Zhou, B. Zhu, and H. Qiao interpreted results of experiments; X. Gao, B. Zhu, and H. Qiao prepared figures; X. Gao, and H. Qiao drafted the manuscript; X. Gao, Y. Zhou, B. Zhu, and H. Qiao edited and revised the manuscript; X. Gao, B. Cheng, B. Jia, X. Jing, L. Wen, Q. Tan, Y. Zhou, B. Zhu, and H. Qiao approved the final version of the paper.

Acknowledgments

This work was supported by National Natural Science Foundation of China Grants to H. Qiao (nos. 30772706 and 81273831), X. Gao (no. 30371804) and X. Jing (no. 30873241), intramural program of China Academy of Chinese Medical Sciences Institute of Acupuncture and Moxibustion to H. Qiao (ZZ12006), and the National Basic Research Program of China Grant to B. Zhu (no. 2011CB505201) and X. Jing (no. 2010CB530507). The authors thank Matthew Davis for word polishing.

References

- [1] X. Lin, J. Liang, J. Ren, F. Mu, M. Zhang, and J. D. Chen, "Electrical stimulation of acupuncture points enhances gastric myoelectrical activity in humans," *American Journal of Gastroenterology*, vol. 92, no. 9, pp. 1527–1530, 1997.
- [2] C. S. Chang, C. W. Ko, C. Y. Wu, and G. H. Chen, "Effect of electrical stimulation on acupuncture points in diabetic patients with gastric dysrhythmia: a pilot study," *Digestion*, vol. 64, no. 3, pp. 184–190, 2001.
- [3] H. Ouyang and J. D. Z. Chen, "Review article: therapeutic roles of acupuncture in functional gastrointestinal disorders," *Alimentary Pharmacology and Therapeutics*, vol. 20, no. 8, pp. 831–841, 2004.
- [4] T. Takahashi, "Acupuncture for functional gastrointestinal disorders," *Journal of Gastroenterology*, vol. 41, no. 5, pp. 408–417, 2006.
- [5] J. Yin and J. D. Z. Chen, "Gastrointestinal motility disorders and acupuncture," *Autonomic Neuroscience*, vol. 157, no. 1-2, pp. 31–37, 2010.
- [6] Y. Li, G. Tougas, S. G. Chiverton, and R. H. Hunt, "The effect of acupuncture on gastrointestinal function and disorders," *American Journal of Gastroenterology*, vol. 87, no. 10, pp. 1372–1381, 1992.
- [7] G. Lux, J. Hagel, P. Bäcker et al., "Acupuncture inhibits vagal gastric acid secretion stimulated by sham feeding in healthy subjects," *Gut*, vol. 35, no. 8, pp. 1026–1029, 1994.
- [8] H. Ouyang, J. Yin, Z. Wang, P. J. Pasricha, and J. D. Z. Chen, "Electroacupuncture accelerates gastric emptying in association with changes in vagal activity," *American Journal of Physiology*, vol. 282, no. 2, pp. G390–G396, 2002.
- [9] M. Tatewaki, M. Harris, K. Uemura et al., "Dual effects of acupuncture on gastric motility in conscious rats," *American Journal of Physiology*, vol. 285, no. 4, pp. R862–R872, 2003.
- [10] J. Chen, G. Q. Song, J. Yin, T. Koothan, and J. D. Z. Chen, "Electroacupuncture improves impaired gastric motility and

- slow waves induced by rectal distension in dogs,” *American Journal of Physiology*, vol. 295, no. 3, pp. G614–G620, 2008.
- [11] K. N. Browning, W. E. Renahan, and R. A. Travagli, “Electrophysiological and morphological heterogeneity of rat dorsal vagal neurones which project to specific areas of the gastrointestinal tract,” *Journal of Physiology*, vol. 517, Part 2, pp. 521–532, 1999.
 - [12] R. A. Gillis, J. A. Quest, F. D. Pagani et al., “Control centers in the central nervous system for regulating gastrointestinal motility,” in *Comprehensive Physiology*, R. Terjung, Ed., pp. 621–683, Wiley Online Library, 2011.
 - [13] R. A. Travagli, G. E. Hermann, K. N. Browning, and R. C. Rogers, “Brainstem circuits regulating gastric function,” *Annual Review of Physiology*, vol. 68, pp. 279–305, 2006.
 - [14] H. Gao and B. N. Smith, “Tonic GABA_A receptor-mediated inhibition in the rat dorsal motor nucleus of the vagus,” *Journal of Neurophysiology*, vol. 103, no. 2, pp. 904–914, 2010.
 - [15] H. E. Raybould, L. J. Jakobsen, D. Novin, and Y. Tache, “TRH stimulation and L-glutamic acid inhibition of proximal gastric motor activity in the rat dorsal vagal complex,” *Brain Research*, vol. 495, no. 2, pp. 319–328, 1989.
 - [16] H. S. Feng, R. B. Lynn, J. Han, and F. P. Brooks, “Gastric effects of TRH analogue and bicuculline injected into dorsal motor vagal nucleus in cats,” *American Journal of Physiology*, vol. 259, no. 2, pp. G321–G326, 1990.
 - [17] R. A. Travagli, R. A. Gillis, and S. Vicini, “Effects of thyrotropin-releasing hormone on neurons in rat dorsal motor nucleus of the vagus, in vitro,” *American Journal of Physiology*, vol. 263, no. 4, pp. G508–G517, 1992.
 - [18] R. J. Washabau, M. Fudge, W. J. Price, and F. C. Barone, “GABA receptors in the dorsal motor nucleus of the vagus influence feline lower esophageal sphincter and gastric function,” *Brain Research Bulletin*, vol. 38, no. 6, pp. 587–594, 1995.
 - [19] Y. Q. Li, B. Zhu, P. J. Rong, H. Ben, and Y. H. Li, “Neural mechanism of acupuncture-modulated gastric motility,” *World Journal of Gastroenterology*, vol. 13, no. 5, pp. 709–716, 2007.
 - [20] X. Y. Gao, S. P. Zhang, B. Zhu, and H. Q. Zhang, “Investigation of specificity of auricular acupuncture points in regulation of autonomic function in anesthetized rats,” *Autonomic Neuroscience*, vol. 138, no. 1-2, pp. 50–56, 2008.
 - [21] S. Cheng, *Chinese Acupuncture and Moxibustion*, Foreign Language Press, Beijing, China, 1996.
 - [22] K. N. Browning, A. E. Kalyuzhny, and R. A. Travagli, “ μ -opioid receptor trafficking on inhibitory synapses in the rat brainstem,” *Journal of Neuroscience*, vol. 24, no. 33, pp. 7344–7352, 2004.
 - [23] Z. K. Krowicki, K. A. Sharkey, S. C. Serron, N. A. Nathan, and P. J. Hornby, “Distribution of nitric oxide synthase in rat dorsal vagal complex and effects of microinjection of nitric oxide compounds upon gastric motor function,” *The Journal of Comparative Neurology*, vol. 377, pp. 49–69, 1997.
 - [24] R. C. Rogers, G. E. Hermann, and R. A. Travagli, “Brainstem pathways responsible for oesophageal control of gastric motility and tone in the rat,” *Journal of Physiology*, vol. 514, no. 2, pp. 369–383, 1999.
 - [25] P. J. Hornby, “Receptors and transmission in the brain-gut axis. II. Excitatory amino acid receptors in the brain-gut axis,” *American Journal of Physiology*, vol. 280, no. 6, pp. G1055–G1060, 2001.
 - [26] X. Zhang and R. Fogel, “Glutamate mediates an excitatory influence of the paraventricular hypothalamic nucleus on the dorsal motor nucleus of the vagus,” *Journal of Neurophysiology*, vol. 88, no. 1, pp. 49–63, 2002.
 - [27] K. N. Browning and R. A. Travagli, “The peptide TPH uncovers the presence of presynaptic 5-HT_{1A} receptors via activation of a second messenger pathway in the rat dorsal vagal complex,” *Journal of Physiology*, vol. 531, no. 2, pp. 425–435, 2001.
 - [28] K. N. Browning, A. E. Kalyuzhny, and R. A. Travagli, “Opioid peptides inhibit excitatory but not inhibitory synaptic transmission in the rat dorsal motor nucleus of the vagus,” *Journal of Neuroscience*, vol. 22, no. 8, pp. 2998–3004, 2002.
 - [29] Y. Liu, T. P. Wong, M. Aarts et al., “NMDA receptor subunits have differential roles in mediating excitotoxic neuronal death both in vitro and in vivo,” *Journal of Neuroscience*, vol. 27, no. 11, pp. 2846–2857, 2007.
 - [30] V. Mutel, D. Buchy, A. Klingelschmidt et al., “In vitro binding properties in rat brain of [3H] Ro 25-6981, a potent and selective antagonist of NMDA receptors containing NR2B subunits,” *Journal of Neurochemistry*, vol. 70, no. 5, pp. 2147–2155, 1998.
 - [31] A. Sato, Y. Sato, A. Suzuki, and S. Uchida, “Neural mechanisms of the reflex inhibition and excitation of gastric motility elicited by acupuncture-like stimulation in anesthetized rats,” *Neuroscience Research*, vol. 18, no. 1, pp. 53–62, 1993.
 - [32] E. Noguchi, “Acupuncture regulates gut motility and secretion via nerve reflexes,” *Autonomic Neuroscience*, vol. 156, no. 1-2, pp. 15–18, 2010.
 - [33] A. Willis, M. Mihalevich, R. A. Neff, and D. Mendelowitz, “Three types of postsynaptic glutamatergic receptors are activated in DMNX neurons upon stimulation of NTS,” *American Journal of Physiology*, vol. 271, no. 6, pp. R1614–R1619, 1996.
 - [34] D. L. Broussard, H. Li, and S. M. Altschuler, “Colocalization of GABA(A) and NMDA receptors within the dorsal motor nucleus of the vagus nerve (DMV) of the rat,” *Brain Research*, vol. 763, no. 1, pp. 123–126, 1997.
 - [35] M. Tatewaki, M. Harris, K. Uemura et al., “The stimulatory effects of acupuncture on gastric motility is mediated via vagal cholinergic and opioid pathways in conscious rats,” *Gastroenterology*, vol. 124, Supplement 1, pp. A669–A670, 2003.
 - [36] H. Monyer, R. Sprengel, R. Schoepfer et al., “Heteromeric NMDA receptors: molecular and functional distinction of subtypes,” *Science*, vol. 256, no. 5060, pp. 1217–1221, 1992.
 - [37] J. Nabekura, T. Ueno, S. Katsurabayashi, A. Furuta, N. Akaike, and M. Okada, “Reduced NR2A expression and prolonged decay of NMDA receptor-mediated synaptic current in rat vagal motoneurons following axotomy,” *Journal of Physiology*, vol. 539, no. 3, pp. 735–741, 2002.
 - [38] S. Vicini, J. F. Wang, J. H. Li et al., “Functional and pharmacological differences between recombinant N-methyl-D-aspartate receptors,” *Journal of Neurophysiology*, vol. 79, no. 2, pp. 555–566, 1998.

Research Article

Evaluation of the Effect of Laser Acupuncture and Cupping with Ryodoraku and Visual Analog Scale on Low Back Pain

Mu-Lien Lin,^{1,2} Hung-Chien Wu,³ Ya-Hui Hsieh,⁴ Chuan-Tsung Su,⁵ Yong-Sheng Shih,⁵ Chii-Wann Lin,¹ and Jih-Huah Wu⁵

¹Institute of Biomedical Engineering, National Taiwan University, No. 1, Section 4, Roosevelt Road, Taipei City 10617, Taiwan

²Department of Pain Management, Taipei City Hospital Zhong Xing Branch, Zheng Zhou Road, No.145, Taipei 103, Taiwan

³Yi Sheng Chinese Medicine Clinic, Room 3, 4 Floor, No. 333, Fuxing N. Road, Songshan District, Taipei City 105, Taiwan

⁴Department of Healthcare Information and Management, Ming Chuan University, No. 5, Deming Road, Gweishan Township, Taoyuan 333, Taiwan

⁵Department of Biomedical Engineering, Ming Chuan University, No. 5, Deming Road., Gweishan Township, Taoyuan 333, Taiwan

Correspondence should be addressed to Jih-Huah Wu, wujh@mail.mcu.edu.tw

Received 6 April 2012; Revised 6 July 2012; Accepted 9 July 2012

Academic Editor: Di Zhang

Copyright © 2012 Mu-Lien Lin et al. This is an open access article distributed under the Creative Commons Attribution License, which permits unrestricted use, distribution, and reproduction in any medium, provided the original work is properly cited.

The purpose of this study was to evaluate the effect of laser acupuncture (LA) and soft cupping on low back pain. In this study, the subjects were randomly assigned to two groups: active group (real LA and soft cupping) and placebo group (sham laser and soft cupping). Visual analog scale (VAS) and Ryodoraku were used to evaluate the effect of treatment on low back pain in this trial. Laser, 40 mW, wavelength 808 nm, pulse rate 20 Hz, was used to irradiate Weizhong (BL40) and Ashi acupoints for 10 minutes. And the Ryodoraku values were measured 2 times, that is, before and 15 minutes after treatment. The results show that there were significant difference between the first day baseline and the fifth day treatment in VAS in the two groups. Therefore, LA combined with soft cupping or only soft cupping was effective on low back pain. However, the Ryodoraku values of Bladder Meridian of the placebo group have been decreased apparently, and didn't come back to their original values. It means that "cupping" plays the role of "leak or purge" in traditional Chinese medicine (TCM). On the other hand, the Ryodoraku values of Bladder Meridian of the active group have been turned back to almost their original values; "mend or reinforcing" effect is attributed to the laser radiation.

1. Introduction

Most people often disregard the severity and the impact of low back pain (LBP). However, the influences of LBP can be very widespread, especially in the aspect of quality of life. And the impact of LBP will lead to spinal instability finally. It will produce more uncomfortable status and lead to chronic LBP eventually [1].

Acupuncture was the oldest and also an important therapy of TCM. It has been accepted for pain relief, and it was regarded as a complementary therapy in most countries [2]. At present, there was sufficient evidences to prove the clinical value of acupuncture [3, 4] and encourage further studies to elucidate the relationship between physiological changes and clinical outcomes. For instance, needle acupuncture has 80% subjective improvement on osteoarthritis of the knee [5]. Moreover, various studies have shown that needle

acupuncture has efficacy for the treatment of long-term disease of neck pain [6]. Ahsin et al. also showed that the electroacupuncture active group was more effective than the placebo group for improvement of stiffness and disability on osteoarthritis of the knee [7]. However, for those people who were afraid of needles, they do not will to endure the tingling of acupuncture. Some researchers tried to replace the needles by using laser; therefore, it was called "laser acupuncture" (LA). LA has the characteristics of being noninvasive, noninfectious, easy to use, and it can avoid the pain and psychological fear of traditional acupuncture. Thus, LA was chosen in this trial.

After laser biostimulation was published by a Hungarian professor, Dr. Mester, in 1969, low level laser therapy (LLLT) has gradually gained popularity from eastern Europe to the whole world. Many scholars also used Nd:YAG laser or semiconductor diode laser as laser source to treat lower

back pain and musculoskeletal back pain [8, 9]. In 2002, Molsberger et al. showed that acupuncture (fixed points) plus conventional orthopedic therapy versus sham plus conventional orthopedic therapy was statistically significant ($P = 0.013$) after test [10]. LA was widely used for treatment of acute or chronic pain, such as chronic myofascial pain in the neck [11]. Shen et al. showed that the pain of osteoarthritis was reduced on active laser treatment group [12]. There was another therapy called cupping, and it can remove the wind-cold-dampness, stagnant blood. In addition, the combination of acupuncture and cupping was an appropriate therapy with a shorter treatment course [13]. After conducting the LA and cupping in the painful area, it can facilitate the flow of QI in meridians. According to Arndt-Schulz Biological Law [14], when energy densities were too small, no significant effect can be observed. Higher energy densities resulted in the inhibition of cellular functions. Thus, low energy laser was used in this study.

The Ryodoraku (meridian) theory was developed by Nakatani [15], and the values of Ryodoraku can reflect the conditions of the relative meridians and organs by analyzing and comparing their changes with microelectrical current. The Ryodoraku gives a clear definition of its measuring. The electrical current between two acupoints was larger than $90 \mu\text{A}$ or smaller than $50 \mu\text{A}$, and it represented their the relative meridian is excess syndrome or deficiency syndrome, respectively. In 1998, Ulett et al. noted that acupuncture includes many techniques such as acupressure, shiatsu, laser acupuncture, Ryodoraku, electro-acupuncture, and more [16]. In 2003, Wang et al. used acupuncture with Ryodoraku for hypertension patients, and the result indicated that the Ryodoraku value, blood pressure, and pulse rate were reduced after stimulating at Zusanli acupoints [17]. In the study of Sancier, the subjects practiced QI gong approximately five hours for two days, and the results revealed that the balance of improvement of body energy for the group was observed through the Ryodoraku value [18]. In 2005, Weng et al. used Ryodoraku to evaluate the effect of tennis elbow pain and back pain [19, 20].

Furthermore, the LA plus soft cupping on the efficacy of back pain has not been published yet. And to measure the Ryodoraku of the meridians of the subjects is a good way to understand the variation of meridians before and after using laser acupuncture and soft cupping [15]. Thus, in this study, low level laser acupuncture and soft cupping were used to stimulate the patient's acupoints, and Ryodoraku and VAS were used to evaluate the improvement of the symptoms of chronic LBP.

2. Materials and Methods

2.1. Subjects. A total of 60 patients of either sex with LBP for at least three months were recruited in the study from Taipei Municipal Chung-Hsin Hospital. Ethical approval was granted by Taipei Municipal Chung-Hsin Hospital ethical committee. All the patients were diagnosed by a doctor. The patients with other complications like heart attack, kidney problem, including pregnancy, were excluded from this study. They were randomly assigned to active group

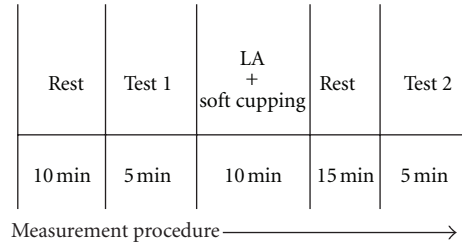


FIGURE 1: Protocol in this study.

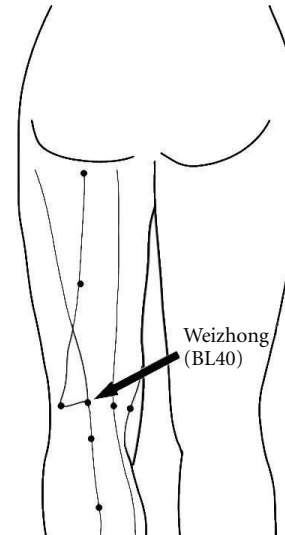


FIGURE 2: Weizhong (BL40) acupoint.

(real LA with soft cupping) and placebo group (sham LA with soft cupping). After the diagnosis, each patient included in the study was explained the procedure of study. Written informed consent was taken, and relevant history of each patient was recorded.

2.2. Procedure. All patients lied down on the bed in the room air-conditioned (25°C) and kept quiet. The protocol in this study was followed in Figure 1. Every patient received one treatment (five continuous days). First, we recorded the visual analog scale and measured the Ryodoraku values for all patients before the trial. Second, we used 4-channel laser therapy instrument LA400 (manufactured by United Integrated Services Co., Ltd., Taiwan) to treat Weizhong acupoints (BL40) on two feet and Ashi points on dorsal for 10 minutes, see Figures 2 and 3. The sham group has the same procedure as the laser group, however, without laser radiation. The two groups also received soft cupping treatment at the same time. After treatment the patients took a break of about 15 minutes; finally, we recorded the VAS and measured the Ryodoraku values again.

2.3. Instrument. The depth of penetration of laser varies with wavelength. Generally, near infrared light has deeper tissue penetration than that of the visible light. The laser therapy instrument LA-400 that operated with a pulsed laser beam



FIGURE 3: The treatment combining LA with soft cupping in this study.

(40 mW output power, wavelength 808 nm, spot size 0.8 cm^2 , pulse rate 20 Hz, 50% duty cycle of the pulse, 10 minutes treatment) was used in this study. Thus, the dosage in this study is approximately 15 J/cm^2 .

2.4. Measurement. A Ryodoraku measurement device, Health Director, Model HD747, manufactured by Nay Yuan technology Co., Ltd. in Taiwan, was used in this study. According to the instruction, when the current was less than $50 \mu\text{A}$, it represented that the relative meridian was “deficiency” syndrome, when the current was greater than $90 \mu\text{A}$, it represented that the relative meridian was “excess” syndrome. The average and standard error of such values were determined and expressed as “Mean \pm STD” for statistical analysis.

2.5. Statistical Analysis. The scores of VAS in each group before and after the treatment were compared with paired-sample *t*-test. The 12 meridians, lung, pericardium, heart, small intestine, triple energizer, large intestine, spleen, liver, kidney, bladder, gallbladder and stomach, of groups were analyzed by using the paired-sample *t*-test. The difference between the values of patients in the two groups measured before and after treatment was analyzed. All the statistical tests were two-tailed. A statistical significance was recognized as *P* value < 0.05 .

3. Results

In this study, 60 patients who have chronic LBP were recruited, in total. 28 patients were recruited for active group of which 21 completed the study protocol. In the control placebo (or sham) group, 29 patients were recruited in total, but failure to complete was 8, see Figure 4 for demographic details. There was no significant difference of age, weight, height, and BMI between the two groups as shown in Table 1. After the collection of data, we compared and analyzed the value of active group and placebo group. Baseline measurements of 12 meridians showed that there were no significant differences between these two groups as listed in Table 2.

TABLE 1: Demographic data for the study groups.

	Age	Weight (Kg)	Height (cm)	BMI (kg/m^2)
Active (<i>n</i> = 21)	63.35 ± 11.23	69.04 ± 12.17	160.00 ± 8.74	26.98 ± 4.33
Control (<i>n</i> = 21)	64.65 ± 13.57	64.41 ± 15.50	159.68 ± 9.26	25.07 ± 4.24

The result reveals that the Ryodoraku values of 12 meridians were reduced by cupping in both groups. In active group, most of the Ryodoraku values of 12 meridians were reduced in the first day due to the combination of LA and cupping. On the fifth day, most of the Ryodoraku values of 12 meridians were raised back to almost original values due to the irradiation of laser light. However, in placebo group, most of the Ryodoraku values of 12 meridians were also reduced on the first day, but not obviously. On the fifth day, most of the Ryodoraku values of 12 meridians were not raised back to original values without the irradiation of laser light. In this study, Weizhong acupoint (BL40) which belongs to bladder Meridian was chosen. It is worthy to mention the variations of Ryodoraku value of Bladder Meridian after treatment in two groups. In active group, the Ryodoraku value of Bladder was raised back on the fifth day, but it has not been raised back in placebo group. It means that “cupping” plays “leak or purge” role in TCM, as shown in Figure 5. And laser acupuncture plays “mend or reinforcing” role in TCM.

The VAS scales of all patients are decreased in these two groups after 5 times of treatment, but it had no significant difference between these two groups in each treatment, see Figure 6 and Table 3. However, it had been statistically significant ($P < 0.01$) for VAS compared with the first day and the fifth day in active group and placebo group, see Tables 4 and 5. The results show that there were significant differences between the first day baseline and the fifth day treatment in VAS in the two groups.

4. Discussion

LBP was the most common disease in the world [21]. 70%–85% people suffer LBP at some time in life, and the prevalence per year was 15%–45% [22]. There are many etiologies of LBP, for example, acute or chronic strain, sprain contusion, and degenerative disease of lumbar spine. In our study, most of the patients (42/60) were caused by degenerative disease of lumbar spine and finally disc pain, facet pain, or radicular pain happened; others (18/60) were myofascial pain caused by sprain or strain injury. From TCM point of view, Xiong et al. used factor analysis to explore patterns of symptoms and signs from patients with chronic low-back pain based on the TCM theory. They found that four factors were extracted from LBP patients, including (1) Qi and/or blood stagnation, (2) cold/damp, (3) a part of “kidney deficiency,” and (4) warm/heat [23]. The research of Sherman et al. also showed that Qi and blood stagnation or Qi stagnation was found for 85% of LBP patients and kidney deficiency was found for 33–51% of LBP patients [24].

TABLE 2: Comparisons between the Ryodoraku values of 12 meridians at baseline and that after therapy from the first day to the fifth day in two groups.

12 meridians <i>n</i> =21	Active		Placebo		Active group					Placebo group						
	Baseline		Baseline		Combine LA with soft cupping		Soft cupping			Soft cupping			Soft cupping		Soft cupping	
	First day	First day	First day	First day	Second day	Third day	Fourth day	Fifth day	First day	Second day	Third day	Fourth day	Fifth day	Third day	Fourth day	Fifth day
Lung	47.55 ± 19.71	46.54 ± 18.71	35.25 ± 20.73*	37.13 ± 21.69	45.80 ± 26.33	35.74 ± 17.30	52.81 ± 24.37	40.24 ± 23.04	32.40 ± 19.65*	34.23 ± 19.81*	31.39 ± 18.71**	38.08 ± 2.86	33.50 ± 22.23	30.34 ± 17.29*	29.58 ± 18.21**	29.73 ± 21.37
Pericardium	43.47 ± 16.19	40.12 ± 17.22	34.42 ± 19.83	33.59 ± 20.38	41.24 ± 25.18	33.41 ± 19.55	42.48 ± 20.02	36.12 ± 19.65	29.31 ± 17.01*	30.34 ± 17.29*	29.58 ± 18.21**	33.50 ± 22.23	29.73 ± 21.37	25.76 ± 16.28*	24.74 ± 15.55**	34.04 ± 21.93
Heart	37.84 ± 13.51	35.96 ± 15.81	28.16 ± 16.19*	27.35 ± 16.14*	34.22 ± 16.54	28.30 ± 13.55*	35.44 ± 15.58	31.33 ± 16.93	24.92 ± 15.76*	25.76 ± 16.28*	24.74 ± 15.55**	29.73 ± 21.37	34.04 ± 21.93	30.14 ± 17.79*	29.48 ± 19.86**	37.12 ± 20.08
Small intestine	45.84 ± 16.61	41.74 ± 18.14	34.85 ± 20.43*	34.47 ± 21.38*	40.13 ± 22.14	35.46 ± 17.94	45.36 ± 21.79	37.11 ± 19.86	28.45 ± 17.30*	34.72 ± 18.94*	29.56 ± 18.36*	37.12 ± 20.08	34.04 ± 21.93	34.71 ± 17.20*	31.77 ± 18.67**	35.24 ± 18.39*
Triple energizer	47.54 ± 22.36	45.08 ± 19.83	39.89 ± 23.45	40.08 ± 22.95	47.04 ± 26.78	39.27 ± 18.25	52.90 ± 27.02	38.18 ± 22.25	31.31 ± 18.96*	34.72 ± 18.94*	29.56 ± 18.36*	37.12 ± 20.08	34.04 ± 21.93	34.71 ± 17.20*	31.77 ± 18.67**	35.24 ± 18.39*
Large intestine	46.33 ± 20.28	46.48 ± 19.65	29.23 ± 21.28	38.34 ± 20.22	47.17 ± 26.00	36.17 ± 14.98	50.29 ± 21.21	37.82 ± 22.04	30.60 ± 18.93**	34.71 ± 17.20*	31.77 ± 18.67**	35.24 ± 18.39*	34.04 ± 21.93	22.03 ± 12.40**	24.12 ± 15.40*	24.65 ± 13.55*
Spleen	36.86 ± 13.3	38.42 ± 23.62	28.02 ± 19.37**	30.76 ± 20.70	35.94 ± 24.89	29.53 ± 15.82	34.73 ± 19.97	29.17 ± 13.47	24.67 ± 15.31	22.03 ± 12.40**	24.12 ± 15.40*	24.65 ± 13.55*	34.04 ± 21.93	25.64 ± 16.01*	22.03 ± 15.64**	25.76 ± 15.85*
Liver	34.96 ± 15.12	33.96 ± 17.06	24.58 ± 18.91**	25.66 ± 18.49**	36.71 ± 24.23	26.55 ± 14.50	34.81 ± 20.47	29.06 ± 16.78	24.25 ± 14.85*	25.64 ± 16.01*	22.03 ± 15.64**	24.65 ± 13.55*	34.04 ± 21.93	21.24 ± 13.87*	20.46 ± 13.40**	25.03 ± 16.22
Kidney	25.05 ± 13.27	30.23 ± 15.88	22.52 ± 18.19	25.04 ± 18.77	28.65 ± 20.06	24.19 ± 15.74	28.51 ± 16.36	28.58 ± 15.32	19.40 ± 13.58*	21.24 ± 13.87*	20.46 ± 13.40**	25.03 ± 16.22	34.04 ± 21.93	19.84 ± 12.48*	20.51 ± 12.52*	20.91 ± 12.05*
Bladder	31.93 ± 12.37	32.93 ± 19.79	23.36 ± 16.94**	24.32 ± 17.66**	30.34 ± 20.63	25.76 ± 15.36*	28.08 ± 13.87	25.09 ± 12.50	22.43 ± 13.50	19.84 ± 12.48*	20.51 ± 12.52*	20.91 ± 12.05*	34.04 ± 21.93	22.04 ± 14.84	19.74 ± 14.02*	21.78 ± 11.85
Gallbladder	25.49 ± 12.59	27.66 ± 15.55	21.10 ± 17.01	22.75 ± 17.33	28.31 ± 19.03	23.90 ± 13.04	28.51 ± 17.49	25.62 ± 15.65	18.82 ± 12.11*	22.04 ± 14.84	19.74 ± 14.02*	21.78 ± 11.85	34.04 ± 21.93	23.63 ± 15.71*	21.90 ± 13.76*	21.72 ± 14.08*
Stomach	31.27 ± 13.08	30.94 ± 16.74	21.10 ± 17.01	25.76 ± 18.59	33.02 ± 20.83	26.85 ± 16.13	29.15 ± 18.75	25.70 ± 14.03	21.23 ± 12.39*	23.63 ± 15.71*	21.90 ± 13.76*	21.72 ± 14.08*	34.04 ± 21.93			

* *P* < 0.05 by paired-samples *t*-test.** *P* < 0.01 by paired-samples *t*-test.

Data are expressed as means ± standard deviation.

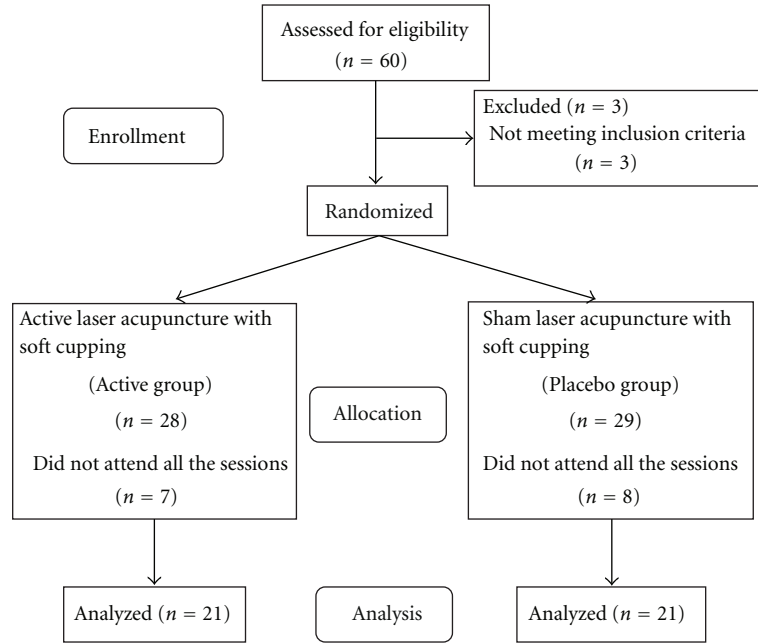


FIGURE 4: Consort flow diagram.

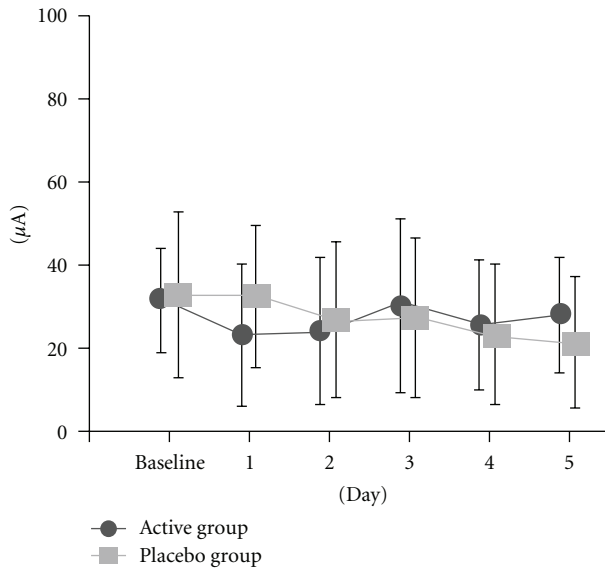


FIGURE 5: The change of Ryodoraku value of Bladder Meridian after treatment in two groups.

TABLE 3: Comparison of the two groups in VAS in each treatment.

	Active group	Placebo group	P value
First day	5.00 ± 1.96	5.46 ± 1.96	0.214
Second day	4.60 ± 2.11	5.09 ± 2.12	0.182
Third day	4.03 ± 2.03	4.49 ± 1.96	0.126
Forth day	3.60 ± 1.58	3.85 ± 1.97	0.088
Fifth day	3.11 ± 1.54	3.20 ± 1.84	0.145

** P < 0.01 by paired-samples t-test.

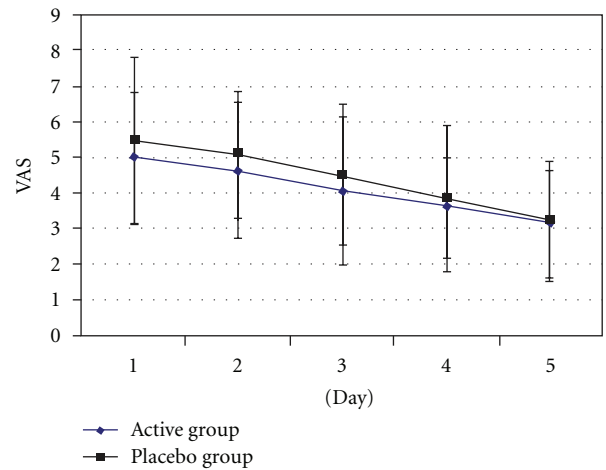


FIGURE 6: Statistics and analysis VAS of patients after the treatment in two groups.

TABLE 4: VAS comparison of active group.

	Active group		P value
	First day	Fifth day	
Before	6.25 ± 1.75	4.25 ± 1.72	0.000**
After	5.00 ± 1.96	3.11 ± 1.54	0.000**

** P < 0.01 by paired-samples t-test.

LA was a kind of phototherapy at acupoint similar to needle acupuncture with different kind of perturbation energy. Low level laser has been used for acupuncture treatment to replace traditional acupuncture, and it had been

TABLE 5: VAS comparison of placebo group.

	Placebo group		P value
	First day	Fifth day	
Before	6.54 ± 2.05	3.72 ± 1.67	0.000**
After	5.46 ± 1.96	3.20 ± 1.84	0.000**

** $P < 0.01$ by paired-samples t -test.

reported that LA was effective in many diseases, such as osteoarthritis of the knees, a kind of degenerative disease [12]. The near infrared laser range of about 600–1400 nm was the most suitable wavelength for LA, because it can infiltrate the skin 2–5 mm, and dosage can be cumulated if irradiating at the same location. So far, LA combined with soft cupping treatment on LBP has not been reported yet, but previous studies have shown that LA can stimulate acupuncture points [12]. In this study, 60 patients who have chronic LBP were recruited from outpatient visits, and 42 patients completed the trial. We recorded the VAS and measured the Ryodoraku values for all patients before and after the treatment. There was no significant difference between these two groups of Bladder Meridian before LA and soft cupping. But the Ryodoraku value in the active group was decreased apparently; however, on the fifth day, it almost returned to original value after laser irradiation, which might be due to the dosage that was cumulated by LA. Karu et al. noted the continuing effects and delayed effects of laser irradiation [25]. We found that the Ryodoraku value of Bladder Meridian had significantly changed in active group after the treatment, and it had statistically significance on first two days. However, there was no statistically significance of Bladder Meridian on the baseline and the fifth day after treatment due to the effect of laser acupuncture, as shown in Figure 5. In addition, the scores of VAS decreased after the trial in both groups. Besides, the scores of VAS had statistically significance before and after LA and soft cupping on the first day baseline and the fifth day in two groups in this trial.

According to TCM acupuncture theory, some kind of energy or information worked in our body was called qi. The source points of Ryodoraku were most associated with the internal organs in the body and the energetic level of the meridians. Thus, these points are effective for measuring meridian energy, or QI. In addition, there were some subjects who received acupuncture treatment experienced sensations of soreness for needle acupuncture and obtaining of QI [26]. We found that the QI-blood can be reactivated after irradiated with the laser acupuncture at Weizhong acupoint of Bladder Meridian of Foot Taiyang. According to TCM, cupping on the human body will cause warm and stimulating effect on local skin and improved local blood circulation. It was well known that the Ryodoraku value of Bladder Meridian would be increased based on the complementary functions of TCM. Thus, we thought that the improvement of LA at Weizhong acupoint was similar to the effect caused by traditional acupuncture. From these studies, we do believe that continuous treatment with LA for a consecutive time can improve LBP and influence the relative meridians. And

the results indicated that LA combined with soft cupping at the Weizhong acupoint and Ashi acupoint can relieve the symptom of LBP. Therefore, treatment with LA and soft cupping at the Weizhong and Ashi acupoints was effective on LBP.

5. Conclusion

After five days, the Ryodoraku values of some meridians decreased significantly in placebo group. On the other hand, most of the Ryodoraku values of twelve meridians changed back to almost original values in active group. The cupping seems can “leak or purge” the relative meridians, its effect on relieving low back pain is positive, but the relative meridians seem to be changed to deficiency syndrome. However, the laser acupuncture can raise the Ryodoraku values of the relative meridians. Hence, the findings in this study found that LA and soft cupping can be a suitable treatment choice for patients with LBP.

Acknowledgments

The authors wish to thank the Department of Health, Taipei City Government, for its expenditure support (the application number is 099XDAA00076). They also thank to United Integrated Services Co., Ltd for instruments support.

References

- [1] M. M. Panjabi, “Clinical spinal instability and low back pain,” *Journal of Electromyography and Kinesiology*, vol. 13, no. 4, pp. 371–379, 2003.
- [2] S. Andersson and T. Lundberg, “Acupuncture—from empiricism to science functional background to acupuncture effects in pain and disease,” *Medical Hypotheses*, vol. 45, no. 3, pp. 271–281, 1995.
- [3] G. Litscher, “Ten years evidence-based High-tech acupuncture—a short review of peripherally measured effects,” *Evidence-Based Complementary and Alternative Medicine*, vol. 6, no. 2, pp. 153–158, 2009.
- [4] G. Litscher, “Ten years evidence-based high-tech acupuncture—a short review of centrally measured effects (part II),” *Evidence-Based Complementary and Alternative Medicine*, vol. 6, no. 3, pp. 305–314, 2009.
- [5] B. V. Christensen, I. U. Iuhl, H. Vilbek, H. H. Bülow, N. C. Dreijer, and H. F. Rasmussen, “Acupuncture treatment of severe knee osteoarthritis. A long-term study,” *Acta Anaesthesiologica Scandinavica*, vol. 36, no. 6, pp. 519–525, 1992.
- [6] P. White, G. Lewith, P. Prescott, and J. Conway, “Acupuncture versus placebo for the treatment of chronic mechanical neck pain. A randomized, controlled trial,” *Annals of Internal Medicine*, vol. 141, no. 12, pp. 911–919, 2004.
- [7] S. Ahsin, S. Saleem, A. M. Bhatti, R. K. Iles, and M. Aslam, “Clinical and endocrinological changes after electroacupuncture treatment in patients with osteoarthritis of the knee,” *Pain*, vol. 147, no. 1–3, pp. 60–66, 2009.
- [8] F. Soriano and R. Rios, “Gallium arsenide laser treatment of chronic low back pain: a prospective, randomized and double blind study,” *Laser Therapy*, vol. 10, pp. 178–180, 1998.
- [9] J. R. Basford, C. G. Sheffield, and W. S. Harmsen, “Laser therapy: a randomized, controlled trial of the effects of low-intensity Nd:YAG laser irradiation on musculoskeletal back

- pain," *Archives of Physical Medicine and Rehabilitation*, vol. 80, no. 6, pp. 647–652, 1999.
- [10] A. F. Molsberger, J. Mau, D. B. Pawelec, and J. A. Winkler, "Does acupuncture improve the orthopedic management of chronic low back pain—a randomized, blinded, controlled trial with 3 months follow up," *Pain*, vol. 99, no. 3, pp. 579–587, 2002.
- [11] A. Gur, A. J. Sarac, R. Cevik, O. Altindag, and S. Sarac, "Efficacy of 904 nm gallium arsenide low level laser therapy in the management of chronic myofascial pain in the neck: a double-blind and randomize-controlled trial," *Lasers in Surgery and Medicine*, vol. 35, no. 3, pp. 229–235, 2004.
- [12] X. Shen, L. Zhao, G. Ding et al., "Effect of combined laser acupuncture on knee osteoarthritis: a pilot study," *Lasers in Medical Science*, vol. 24, no. 2, pp. 129–136, 2009.
- [13] X. W. Wan, "Clinical observation on treatment of cervical spondylosis with combined acupuncture and cupping therapies," *Journal of Acupuncture and Tuina Science*, vol. 5, no. 6, pp. 345–347, 2007.
- [14] A. P. Sommer, A. L. B. Pinheiro, A. R. Mester, R. P. Franke, and H. T. Whelan, "Biostimulatory windows in low-intensity laser activation: lasers, scanners, and NASA's light-emitting diode array system," *Journal of Clinical Laser Medicine and Surgery*, vol. 19, no. 1, pp. 29–33, 2001.
- [15] Y. Nakatani, "Skin electric resistance and ryodoraku," *Journal of the Autonomic Nervous System*, vol. 6, p. 52, 1956.
- [16] G. A. Ulett, J. Han, and S. Han, "Traditional and evidence-based acupuncture: history, mechanisms, and present status," *Southern Medical Journal*, vol. 91, no. 12, pp. 1115–1120, 1998.
- [17] S. H. Wang, Y. T. Chen, C. S. Weng, P. H. Tsui, J. L. Huang, and K. C. Chiang, "A clinical therapeutic assessment for the administration of different modes of ultrasounds to stimulate the Zusanli acupuncture point of hypertension patients," *Journal of Medical and Biological Engineering*, vol. 23, no. 4, pp. 221–228, 2003.
- [18] K. M. Sancier, "Electrodermal measurements for monitoring the effects of a Qigong workshop," *Journal of Alternative and Complementary Medicine*, vol. 9, no. 2, pp. 235–241, 2003.
- [19] C. S. Weng, S. H. Shu, C. C. Chen, Y. S. Tsai, W. C. Hu, and Y. H. Chang, "The evaluation of two modulated frequency modes of acupuncture-like tens on the treatment of tennis elbow pain," *Biomedical Engineering—Applications, Basis and Communications*, vol. 17, no. 5, pp. 236–242, 2005.
- [20] C. S. Weng, Y. S. Tsai, S. H. Shu, C. C. Chen, and M. F. Sun, "The treatment of upper back pain by two modulated frequency modes of acupuncture-like TENS," *Journal of Medical and Biological Engineering*, vol. 25, no. 1, pp. 21–25, 2005.
- [21] J. N. Katz, "Lumbar disc disorders and low-back pain: socioeconomic factors and consequences," *Journal of Bone and Joint Surgery A*, vol. 88, no. 2, pp. 21–24, 2006.
- [22] N. Bogduk and B. McGuirk, *Medical Management of Acute and Chronic Low Back Pain: An Evidence-Based Approach*, Pain Research and Clinical Management, 1999.
- [23] G. Xiong, C. Virasakdi, A. Geater, Y. Zhang, M. Li, and S. Lerkiatbundit, "Factor analysis on symptoms and signs of chronic low-back pain based on traditional Chinese medicine theory," *Journal of Alternative and Complementary Medicine*, vol. 17, no. 1, pp. 51–55, 2011.
- [24] K. J. Sherman, D. C. Cherkin, and C. J. Hogeboom, "The diagnosis and treatment of patients with chronic low-back pain by traditional Chinese medical acupuncturists," *Journal of Alternative and Complementary Medicine*, vol. 7, no. 6, pp. 641–650, 2001.
- [25] T. I. Karu, N. I. Afanasyeva, S. F. Kolyakov, L. V. Pyatibrat, and L. Welser, "Changes in absorbance of monolayer of living cells induced by laser radiation at 633, 670, and 820 nm," *IEEE Journal on Selected Topics in Quantum Electronics*, vol. 7, no. 6, pp. 982–988, 2001.
- [26] S. Y. Liu, C. L. Hsieh, T. S. Wei, P. T. Liu, Y. J. Chang, and T. C. Li, "Acupuncture stimulation improves balance function in stroke patients: a single-blinded controlled, randomized study," *American Journal of Chinese Medicine*, vol. 37, no. 3, pp. 483–494, 2009.

Research Article

Acupuncture Alleviates Colorectal Hypersensitivity and Correlates with the Regulatory Mechanism of TrpV1 and p-ERK

Shao-Jun Wang,¹ Hao-Yan Yang,² and Guo-Shuang Xu³

¹*Institute of Acupuncture and Moxibustion, China Academy of Chinese Medical Sciences, Beijing 100700, China*

²*Basic Medicine, School of Basic Medical Science, Capital Medical University, Beijing 100069, China*

³*Department of Nephrology, Xijing Hospital, The Fourth Military Medical University, Xi'an 710032, China*

Correspondence should be addressed to Shao-Jun Wang, ddwsj5@sina.com

Received 11 June 2012; Revised 16 August 2012; Accepted 12 September 2012

Academic Editor: Ying Xia

Copyright © 2012 Shao-Jun Wang et al. This is an open access article distributed under the Creative Commons Attribution License, which permits unrestricted use, distribution, and reproduction in any medium, provided the original work is properly cited.

Here we used a mouse model of zymosan-induced colorectal hypersensitivity, a similar model of IBS in our previous work, to evaluate the effectiveness of the different number of times of acupuncture and elucidate its potential mechanism of EA treatment. Colorectal distension (CRD) tests show that intracolonic zymosan injection does, while saline injection does not, induce a typical colorectal hypersensitivity. EA treatment at classical acupoints Zusanli (ST36) and Shangjuxu (ST37) in both hind limbs for 15 min slightly attenuated and significantly blunted the hypersensitive responses after first and fifth acupunctures, respectively, to colorectal distension in zymosan treatment mice, but not in saline treatment mice. Western blot results indicated that ion channel and TrpV1 expression in colorectum as well as ERK1/2 MAPK pathway activation in peripheral and central nerve system might be involved in this process. Hence, we conclude that EA is a potential therapeutic tool in the treatment and alleviation of chronic abdominal pain, and the effectiveness of acupuncture analgesia is accumulative with increased number of times of acupuncture when compared to that of a single time of acupuncture.

1. Introduction

IBS is characterized by chronic abdominal pain and altered bowel habits in the relative absence of signs of gastrointestinal inflammation. The pathophysiology of IBS is likely multifactorial [1–4], and the mechanism(s) contributing to discomfort and pain remains unclear, which continues to stimulate the study of peripheral and central nociceptive mechanisms and mediators of hypersensitivity.

Acupuncture is a procedure in which fine needles are inserted into an individual at discrete points and then manipulated, with the intent of relieving pain. The clinical practice of acupuncture is growing in popularity worldwide. More than 40 disorders have been endorsed by the World Health Organization (WHO) as conditions that can benefit

from acupuncture treatment [5–7]. Pain is particularly sensitive to acupuncture. Acupuncture at ST36 and ST37 exerts an antinociceptive effect in rats pain model with PFA injection into the left hind paw [8]. Combined EA at the different acupoints had improving symptoms in IBS patients [9, 10]. Due to previous lack of an ideal experimental animal model suitable for acupuncture research which simulates the human model of chronic visceral hypersensitivity, the mechanism of EA treatment on pain relief in IBS remained unclear. Here we used a mouse model of zymosan-induced colorectal hypersensitivity, a similar model of IBS in Gebhart previous work, and a noninflammatory model of visceral hypersensitivity [11]. In the application of this model in our study, we developed a methodology to assess the effect of different number of times of acupuncture being applied to

the same animal which was awake and elucidate its potential mechanism of EA treatment on pain relief in model of visceral hypersensitivity in the mouse.

2. Materials and Methods

2.1. Animals. In total, 20 adult male mice (20–30 g, 7 weeks) of C57BL/6 (Taconic, Germantown, NY) were used in this experiment. All procedures were approved by the University of Pittsburgh Institutional Animal Care and Use Committee.

The mice were divided into four groups as follows.

- (1) Saline injection via intracolonic route with EA (S+A).
- (2) Saline injection via intracolonic route without EA (S + C).
- (3) Zymosan injection via intracolonic route with EA (Z + A).
- (4) Zymosan injection via intracolonic route without EA (Z + C).

Five mice were used in each group. Zymosan induced colorectal hypersensitivity animal model and EA interference was shown by schematic diagram in Figure 1.

2.2. Intracolonic Treatments. Mice were anesthetized with 2% isoflurane (Hospira Inc., Lake Forest, IL). Either 0.2 mL of vehicle (saline) or a suspension of 30 mg/mL zymosan (a protein-carbohydrate cell wall derivative of the yeast *Saccharomyces cerevisiae* in saline; Sigma Chemical Co, St. Louis, MO) was administered transanally via a 22-gauge, 24 mm long stainless-steel feeding needle. Intracolonic treatment with saline or zymosan was performed daily for 3 consecutive days after obtaining baseline response measures to colorectal distension (CRD) before assessing colorectal hypersensitivity.

2.3. Electromyographic Electrode Implantation and CRD Testing. Electromyographic Electrode Implantation was performed at day 0. Following anesthesia, the left abdominal musculature was exposed by incision of the skin, and the bare ends of 2 lengths of Teflon-coated (Cooner Wire Sales, Chatsworth, CA) stainless-steel wire (Cooner Wire Sales, Chatsworth, CA) were inserted into the abdominal muscles and secured in place with 5–0 polyglactin sutures (Ethicon, Somerville, NJ). The other wire ends were tunneled subcutaneously to a small incision made on the nape of the neck and externalized for access during testing. Four days was allowed for recovery from surgery before initiating the CRD protocol. On the day of testing, mice were briefly sedated with isoflurane for balloon insertion. Distension balloons were made from polyethylene (length, 1.5 cm; diameter, 0.9 cm) [11] coated with lubricant, inserted transanally until the proximal end of the balloon was 0.5 cm from the anal verge (total balloon insertion 2 cm), and secured to the mouse tail with tape. Mice were placed in a restraint device (manufactured as described previously [12]) inside a sound-attenuating, dark chamber and allowed to recover from isoflurane sedation (30 minutes) before CRD

testing. CRD was performed as previously described [12]. Briefly, electromyographic (EMG) activity was recorded for 10 seconds before and during phasic balloon inflation (15, 30, 45, or 60 mmHg) of the colorectum. Each distension lasted 10 seconds, and each pressure was tested 3 times with 5 minutes apart and between distensions. EMG electrode activity was amplified, filtered, rectified, and quantified using Spike 2 software (Cambridge Electronic Design, Cambridge, UK) and recorded on a computer. Responses to CRD were quantified as the total area of EMG activity during balloon inflation minus baseline activity in the 10 seconds prior to distension.

The first time CRD test was performed on day 4 as a baseline (CRD₀) and after which saline or zymosan was injected via intracolonic route. Subsequently, the CRD tests were recorded on day 8 (CRD₁), day 10 (CRD₂), day 12 (CRD₃), day 14 (CRD₄), day 17 (CRD₅), and day 20 (CRD₆). EA or SA was performed on day 14, day 16, day 17, day 19, and day 20 (Figure 1). Mice were sacrificed immediately after the last CRD test (CRD₆), and the fresh tissues of brain (thalamic area), spinal cord (L₅-S₂), and colorectum (the lengths 1 cm above anorectal line) were collected.

2.4. EA Treatment. EA was applied by two pair of stainless steel needles (0.25 mm in diameter) inserted bilaterally at a depth of 3 mm into the skin and underlying muscles at ST36 (2 mm lateral to the anterior tubercle of the tibia and 3 mm below the knee joint plus) [13, 14] and ST37 (2 mm lateral to the anterior tubercle of the tibia and 6 mm below the knee joint, minus) (Figure 3. Acupoints). The needles, which were inserted into acupoints, were stimulated by an EA apparatus (#HANS-100A, Nan Jing Ji Sheng Medical Treatment Science and Technology Co., China) with a constant rectangular current of alternating trains of dense-sparse frequency (2/100 Hz, pulse width, 0.2–0.6 msec). This combination of dense-sparse frequency would maximally induce opioid release of met-enkephalin and dynorphin A [15]. Electrical stimulus intensity was set at the threshold for a detectable muscle twitch (approximately 1 mA). The stimulation was delivered for 15 min. For sham EA group, the needle set was same EA group, but no electrical stimulation was applied. CRD tests were performed 30 min after termination of EA.

2.5. Western Blot Analysis. Western blot analysis was performed as follows [16]: mice tissues of colorectum, spinal cord, or brain were homogenized on ice in RIPA buffer (50 mol/L Tris-Cl, pH 7.6, 5 mol/L ethylenediaminetetraacetic acid, 150 mol/L NaCl, 0.5% Nonidet P-40, 0.5% Triton X-100) containing protease inhibitor cocktail and phosphatase inhibitor cocktails I/II (Sigma-Aldrich). The homogenate was centrifuged at 12,000 ×g for 30 minutes at 4°C. The supernatant was collected and the protein concentration was measured using the Bradford assay. Twenty micrograms of the sample was separated with 10% polyacrylamide gel blotted on a PVDF film (Millipore Corp). The blotted film was blocked for 2 hours at 4°C in blocking solution (1 × TBS with 5% nonfat milk and 0.02% Tween

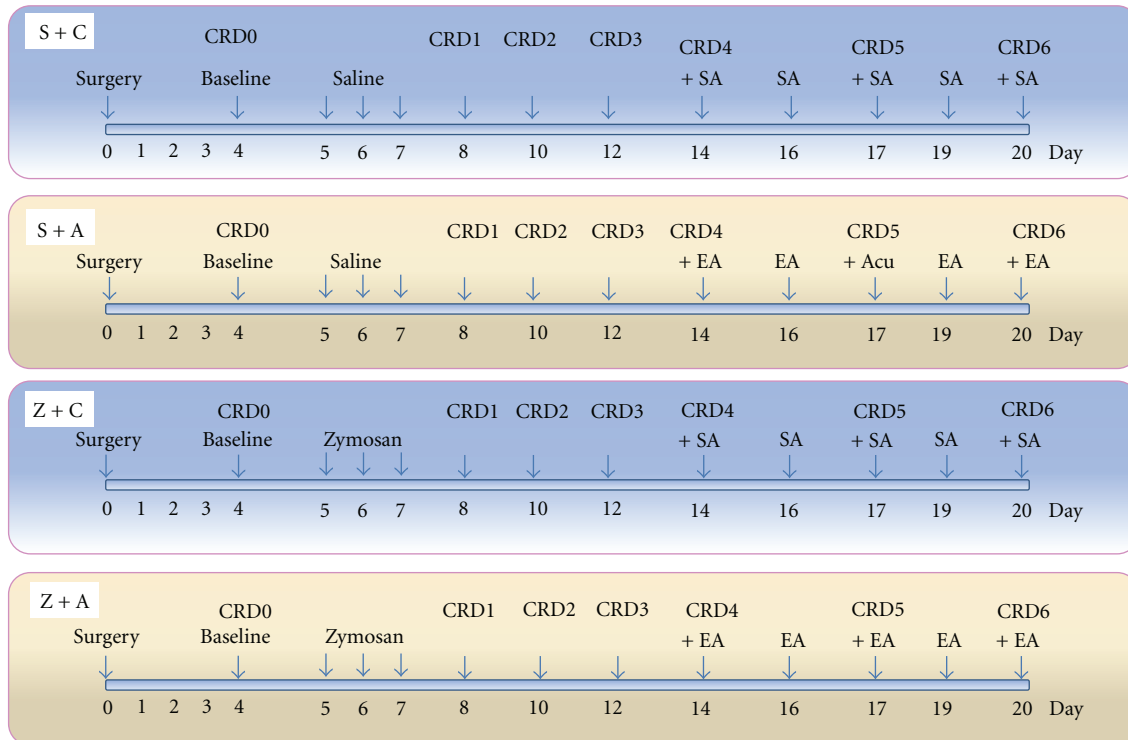


FIGURE 1: Experimental protocol, 20 mice are used. 5 mice in each group. There are 4 groups. S + C: saline + sham-acupuncture (SA), S + A: saline + EA, Z + C: zymosan + SA, Z + A: zymosan + EA.

20). The blocked film was shaken overnight at 4°C using primary antibodies in blocking solution. Following three times of washing with TBST (1 × TBS with 0.02% Tween 20), the film was shaken for 1 hour at room temperature with peroxidase-conjugated secondary antibody and then washed three times with TBST. Detection was performed using an ECL kit (Santa Cruz Biotech) according to the manufacturer's instructions. The western blots shown are representative of at least three independent experiments.

The antibodies used included the following: anti-TrpV1 (Alomone Labs, #Acc-030) (1:800), antiphospho- and anti-total ERK_{1/2} (cell signaling, #9109 and #4695,) (1:2000), anti-PGP9.5 (Neuromics, #RA12103) (1:20000), anti-β-Actin (Sigma, A5316) (1:100000), HRP-conjugated IgG secondary antibodies (1:2000) (GE Healthcare Life Sciences). All western blot data were analyzed by Image J software.

2.6. Statistical Analysis. All CRD test data were expressed as mean ± SEM. Statistical significance of visceromotor response (VMR) values of the area under the curve (AUC) from EMG recording was determined using two way analysis of variance (ANOVA) with repeated-measures via GraphPad Prism (Avenida de la Playa La Jolla California).

All results with *P* values less than 0.05 were considered statistically significant.

3. Results

3.1. Zymosan-Induced Visceral Hypersensitivity. Visceromotor responses (VMR) to colorectal distension were recorded as EMG measurements before (day 4) and after intracolonic administration of saline or zymosan (days 8, 10, and 12), and only on 3 days after acupuncture treatment (days 14, 17, and 20), though EA treatment was administered on days 14, 16, 17, 19, and 20. The measurement of EMG on days 17 had additional assessment value for consecutive EA treatment of 2 days. In addition EMG measurement at days 20 will shed light on the cumulative therapeutic effect of the entire duration of EA therapy.

On day 4 (baseline, before any intracolonic treatment or CRD₀), groups S + C, S + A, Z + C, and Z + A of mice all responded in a graded manner to increasing pressures of colorectal distension. However, visceromotor responses (VMRs) to distension among 4 groups had no significant difference, revealing that all mice from different groups had similar response to pressures of colorectal distension before any intracolonic treatment. To compare VMR to distension overtime, responses within four groups of mice are normalized to 60 mm Hg in subsequent data presentations.

After 3 times of intracolonic injection of saline or zymosan on days 5, 6 and 7, CRD tests were performed on days 8 (CRD₁), 10 (CRD₂), and 12 (CRD₃).

Figure 2 CRD1 showed that intracolonic saline or zymosan treatment did not produce persistent colorectal

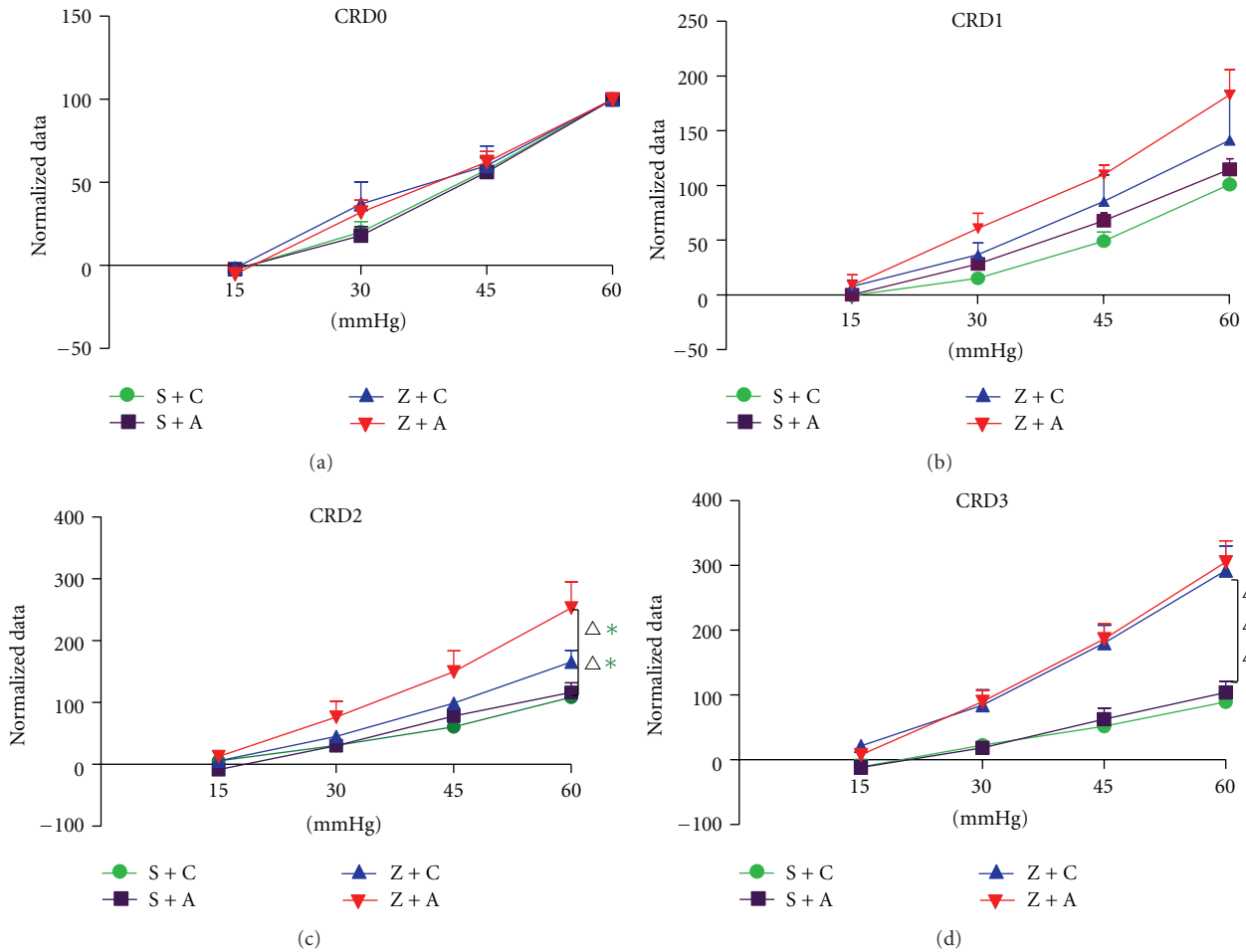


FIGURE 2: CRD test results before EA. CRD0: responses to colorectal distension in 4 groups before (baseline) saline or zymosan treatment ($F_{3,16} = 0.542$, $P > 0.05$); CRD1: responses to colorectal distension in 4 groups after intracolonic treatment with saline or zymosan ($F_{3,16} = 2.593$, $P > 0.05$) on day 8; CRD2: responses to colorectal distension in 4 groups after intracolonic treatment with saline or zymosan ($F_{3,16} = 6.021$, $P = 0.006$, in Z + C versus S + A and Z + C versus S + C) on day 10; CRD3: Responses to colon distension in 4 groups after intracolonic treatment with saline or zymosan ($F_{3,16} = 15.24$, $P < 0.001$, in Z + C versus S + A, Z + C versus S + C, Z + A versus S + A, and Z + A versus S + C) on day 12. Colorectal hypersensitivity did not develop in saline-treated mice. Data are expressed as percentage (mean \pm SEM) of the VMR to colorectal distension on the day of baseline testing (day 4) for each animal and normalized to the response to 60 mm Hg distension (100%) to generate stimulus-response functions.

hypersensitivity in 4 groups of mice. CRD₂ showed that intracolonic saline treatment did not produce, whereas intracolonic zymosan treatment did produce, persistent colorectal hypersensitivity in group Z + A mice. However, one of the zymosan treatment groups, Z + C, showed increasing of colorectal hypersensitivity but had no significant difference compared with saline treatment group. On day 12, CRD₃ showed that both saline treatment groups did not, while both zymosan treatment groups did, exhibit persistent colorectal hypersensitivity, suggesting that at least 4–8 days' time period was required for maturing of zymosan-induced colorectal hypersensitivity.

3.2. EA Treatment Suppressed Zymosan-Induced Visceral Hypersensitivity in Mice. Figure 3 showed the CRD tests results after acupuncture. CRD4 showed EMG activity in

group Z + C was significantly increased than that in group S + C and S + A after first time EA. However, there was no significant difference among the four groups. CRD5 showed EMG activity in group Z + C was significantly increased than those in saline groups S + C and S + A. CRD6 showed EMG activity in group Z + C was significantly increased than that in saline groups S + C and S + A, while the elevation of EMG activity was significantly blunted in group Z + A after fifth time EA, as shown by the EMG results in Figures 4(a) and 4(b). These data demonstrated that EA treatment suppresses zymosan-induced visceral hypersensitivity, which is in agreement with previous studies that EA treatment attenuated chronic visceral hyperalgesia induced by neonatal colonic injection of acetic acid [17]. As expected, the relief of visceral hypersensitivity-induced pain increased with more EA treatments.

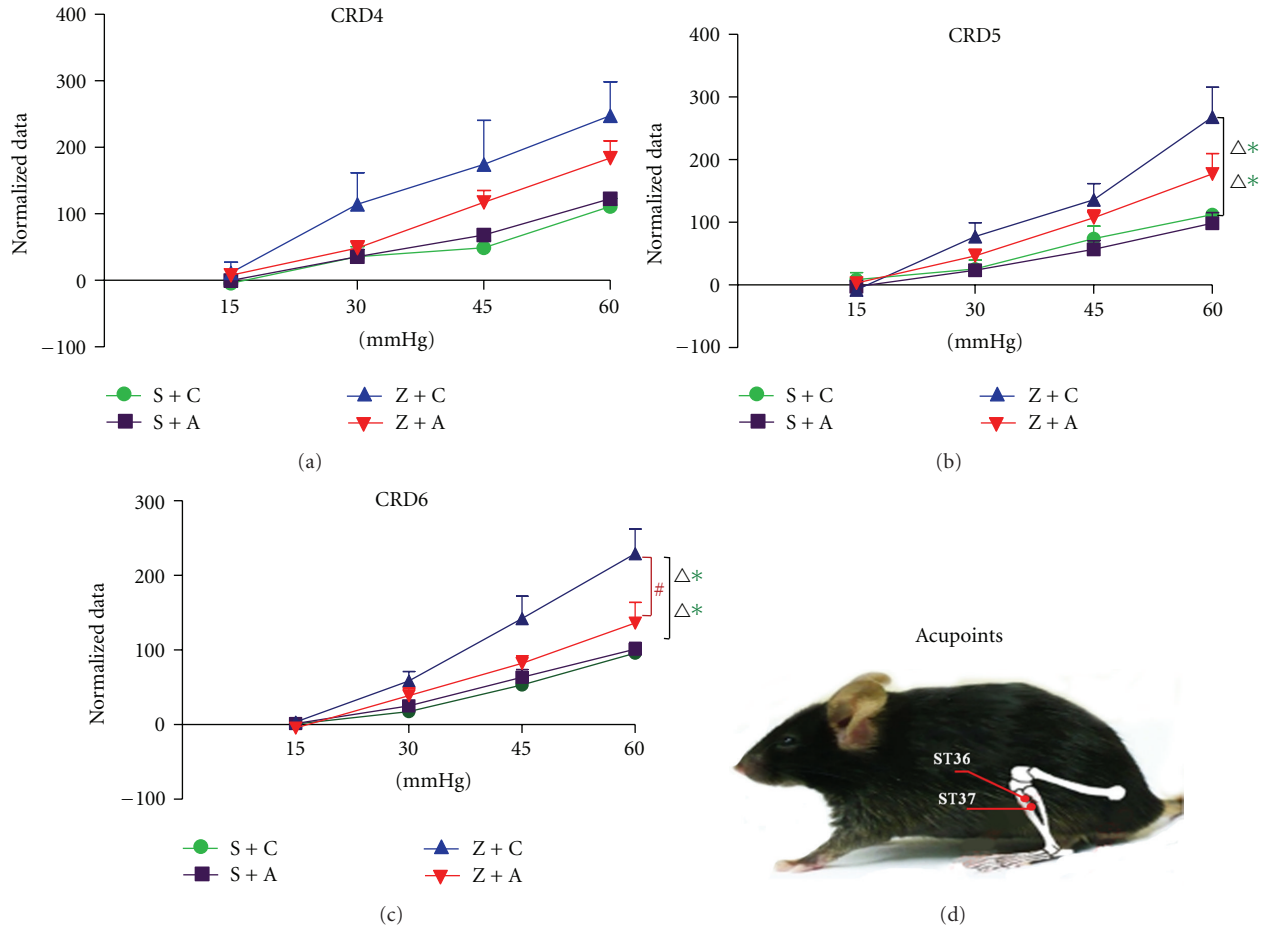


FIGURE 3: CRD test results after EA. CRD4: responses to colorectal distension in 4 groups after first time EA ($F_{3,16} = 3.216, P = 0.051$); CRD5: responses to colorectal distension in 4 groups after third-time EA ($F_{3,16} = 5.853, P = 0.007$, in Z + C versus S + A, Z + C versus S + C); CRD6: responses to colorectal distension in 4 groups after fifth-time EA ($F_{3,16} = 10.541, P < 0.001$, in Z + C versus S + C, Z + C versus S + A, and Z + C versus Z + A). Acupoints: schematic representation of the ST36 and ST37.

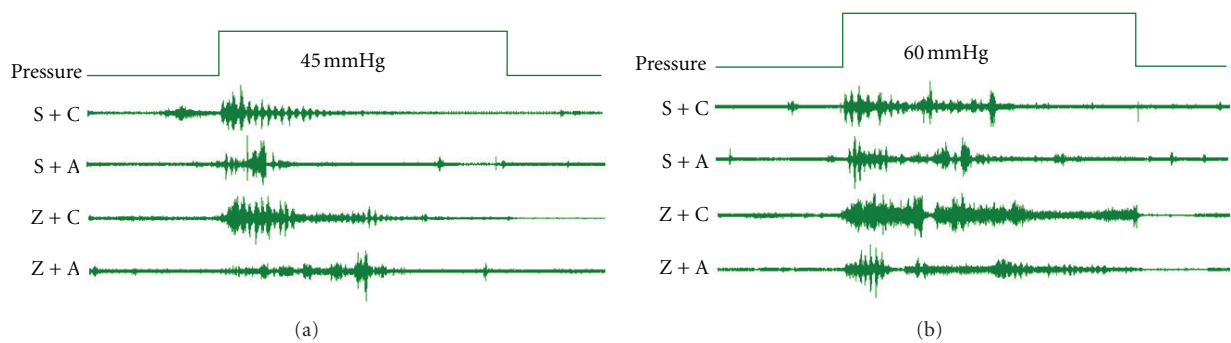


FIGURE 4: Examples of EMG activity in mice with or without EA. (a) indicates EMG activity results under 45 mmHg; (b) indicates EMG activity results under 60 mmHg.

3.3. EA Blunts Zymosan-Induced Expression of TRPV1. Western blot analysis showed that there was a detectable signal of transient receptor potential vanilloid 1 (TrpV1) in the colorectum (Figure 5). TrpV1 expression was only slightly increased in response to acupuncture in group S + A,

while it was dramatically induced by zymosan injection. EA obviously compromises zymosan-induced upregulation of TrpV1. The Z + C group displayed an obviously higher expression of TrpV1 when compared with the S + C group, by 80%. However, the TrpV1 level in S + A group manifested

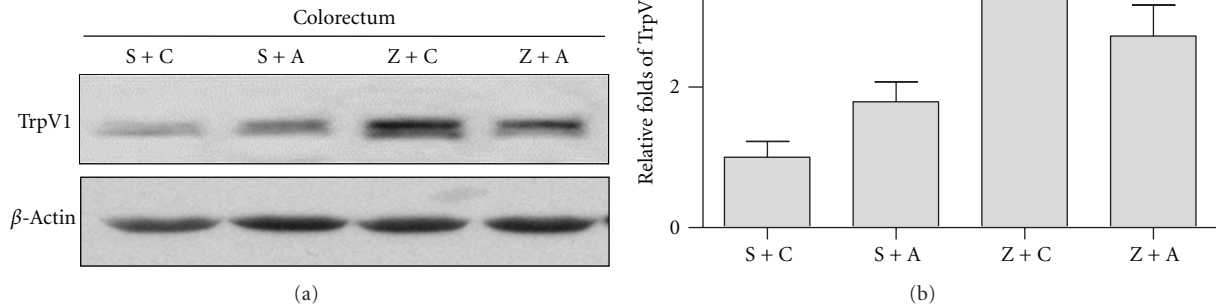


FIGURE 5: EA blunts zymosan-induced expression of TrpV1. Western blot shows detectable signal of TrpV1 in colon. TrpV1 expression slightly increased in response of EA in group S + A (S + A versus Z + C, $P < 0.01$), while it is dramatically induced by zymosan injection (S + C versus Z + C, $P < 0.001$). EA obviously compromises zymosan-induced upregulation of TrpV1 (Z + A versus Z + C, $P < 0.05$) (#Acc-030, Alomone Labs, 150KD, delusion: 1 : 800).

44.43% up-regulation, when compared with the S + C group. This in turn demonstrated that EA greatly compromised zymosan-induced up-regulation of TrpV1 by 87.58%.

These data suggested that TrpV1 is involved in zymosan-induced visceral hypersensitivity and EA suppressed visceral hypersensitivity. We found that TrpV1 protein is detectable only in colorectal tissue by Western blot. EA treatment alone can slightly induce TrpV1 in S + A group.

3.4. EA Blunts Zymosan-Induced ERK1/2 Activation. Extracellular signal-regulated kinase1/2 (ERK1/2) is protein kinase signaling pathways. ERK1/2 activation is presented by phosph-ERK1/2 (p-ERK) versus their related total ERK1/2 (Figure 6). ERK1, and ERK2 activation was induced by acupuncture in group S + A by 56.59% and 71.32%, 48.27% and 29.98%, 40.79%, and 25.89% when compared with group S + C in colorectum, spinal cord, and hypothalamus, respectively. It was dramatically increased in Z + C group by 87.63% and 83.68%, 72.22% and 44.68%, 76.28% and 70.83% compared with the S + C group in colorectum, spinal cord, and hypothalamus, respectively. However, zymosan-induced ERK1 and ERK2 activation is obviously compromised by EA. The Z + A group displayed a reduction of p-ERK expression by 160.32% and 167.19%, 47.34% and 30.63%, 96.98% and 337.05% when compared with the Z + C group in colorectum, spinal cord and hypothalamus, respectively. These data suggested that the processing of EA analgesia information occurs at central as well as at peripheral sites in the mice with zymosan induction.

3.5. Zymosan Could Not Induce PGP9.5 Activation. Protein gene product (PGP) is neuron specific protein, structurally and immunologically distinct from neuron specific enolase.

PGP9.5 is in neurones and nerve fibers at all levels of the central and peripheral nervous system. As a pan-neuronal marker, it may also be expressed by nonneural cells such as enteroendocrine cells.

Therefore we determined that PGP9.5 is involved in colorectal distention process. The results showed that PGP9.5 (Figure 7) is predominantly expressed in colorectum, spinal cord, and hypothalamus. However, there is no significant difference in PGP9.5 expression among the 4 groups in colorectum, spinal cord, and hypothalamus, respectively.

4. Discussion

The principal findings were as follows: (1) zymosan-induced elevation of visceromotor responses to colorectal distension is significantly attenuated by EA, suggesting that EA blunts zymosan-produced colorectal hypersensitivity; (2) visceral hypersensitivity-related molecules' results showed that TrpV1 expression in colorectum is slightly increased in response of EA in mice without zymosan injection. Zymosan dramatically induces TrpV1 expression, and the induction of TrpV1 is greatly blunted by EA in colorectum. Consistently, ERK1/2 phosphorylation in colorectum, spinal cord, and hypothalamus is also slightly increased in response to EA in mice without zymosan injection and is dramatically induced by zymosan injection. EA greatly compromised zymosan-induced ERK1/2 phosphorylation. However, after Western blot analysis, we did not detect any difference in PGP9.5 expression among the 4 groups in colorectum, spinal cord, and hypothalamus. These findings support the fact that the processing of EA analgesia information occurs at central as well as at peripheral sites in the mice with zymosan induction.

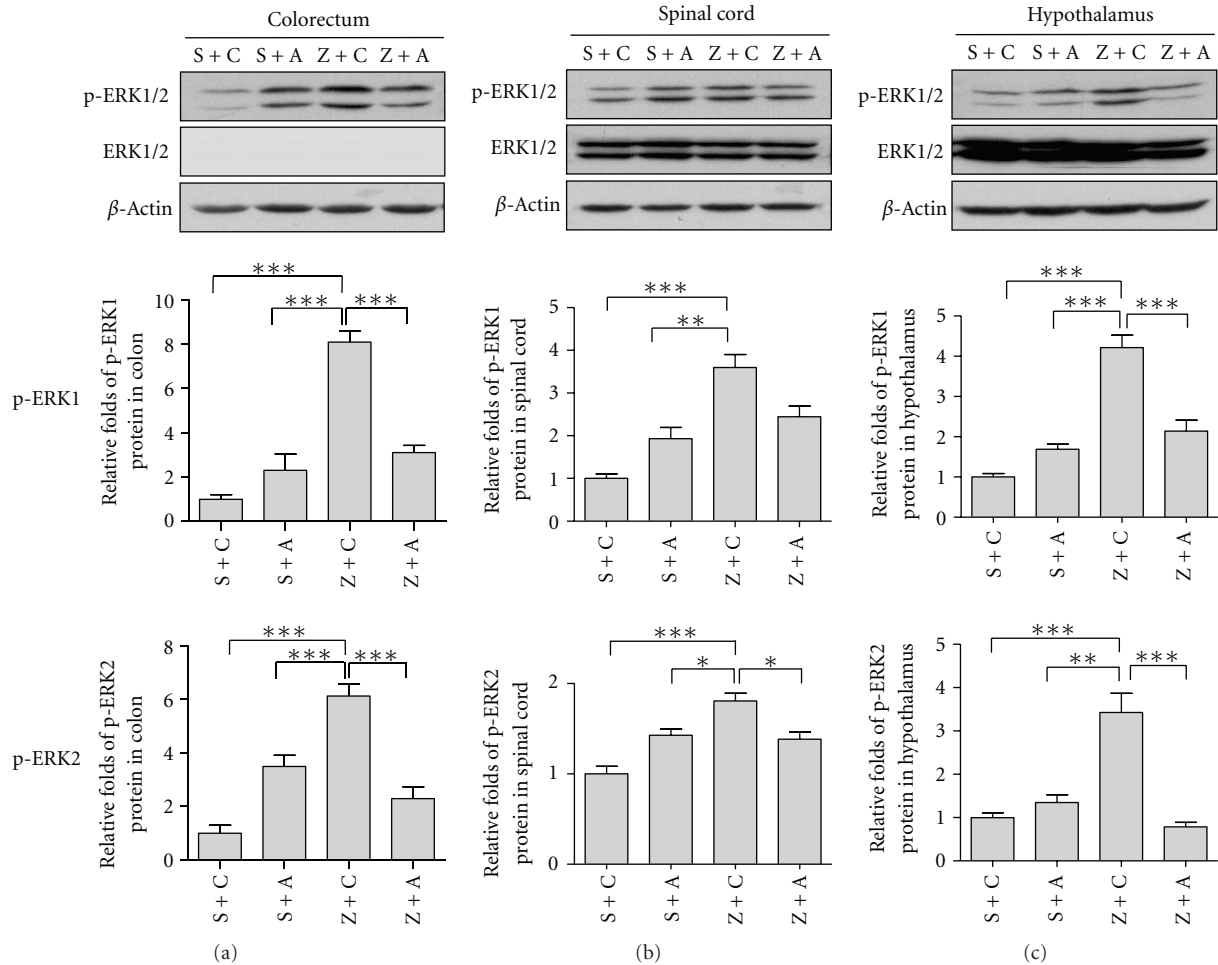


FIGURE 6: EA blunts zymosan-induced ERK1 and ERK2 activation. ERK1 and ERK2 activation is presented by phosph-ERK1 and ERK2 versus their related total ERK1 and ERK2. ERK1 and ERK2 activation is slightly induced by EA in group S + A, while it is dramatically induced by zymosan injection. Zymosan-induced ERK1 and ERK2 activation is obviously compromised by EA in colorectum ($P < 0.001$), spinal cord ($P < 0.05$), and hypothalamus ($P < 0.001$). EA in alleviating hypersensitivity is probably associated with external signaling (p-ERK1/2: #9109, cell signaling, 42/44 KD, delusion: 1 : 2000; ERK1/2: #4695, cell signaling, 42/44 KD, delusion: 1 : 2000).

4.1. *This Animal Model Suits for Acupuncture Research.* Acupuncture and EA are widely used in pain relief in clinic [18, 19] and in relieving inflammation-induced hypersensitivity in rat models [8, 20]. However, in the treatment of visceral hypersensitivity, the use of acupuncture once is often not enough. The use of an animal model that can be assessed for cumulating effect of different number of times of acupuncture in the same animal, which is awake, is important in the research evaluation of acupuncture treatment in IBS and the elucidation of the involved mechanism(s). In the current study, we developed a noninflammatory colorectal hypersensitivity model in which an intracolonic treatment with zymosan, a protein-carbohydrate cell wall derivative of the yeast *Saccharomyces cerevisiae*, was capable of producing a robust and chronic behavioral hypersensitivity to colorectal distention [21, 22]. It is noteworthy that in this animal model there were two electrodes in between the two ears of each mouse; the other ends of these two electrodes were fixed

on the abdominal muscles; hence, we can use this animal model for real-time monitoring of effect of acupuncture on visceral hypersensitivity in the awaked animal by EMG, with continuous observation of the effect of different number of times of acupuncture in vivo in the same animal. This has not been achieved in other animal models.

4.2. *EA Treatment Suppressed Zymosan-Induced Visceral Hypersensitivity in Mice.* The EA procedures may stimulate the somatic afferent nerves innervating the skin and muscles of the body, which are thought to be specific points that reflect visceral conditions and organs [23]. We found that EA treatment significantly reduced and suppressed EMG responses to colorectal distention in zymosan-induced non-inflammatory colorectal hypersensitivity (Figures 4(a) and 4(b)) in the present study. Moreover, the effectiveness of acupuncture analgesia increases with the increase in number of times of acupuncture (Figure 3 CRD4, CRD5, and CRD6),

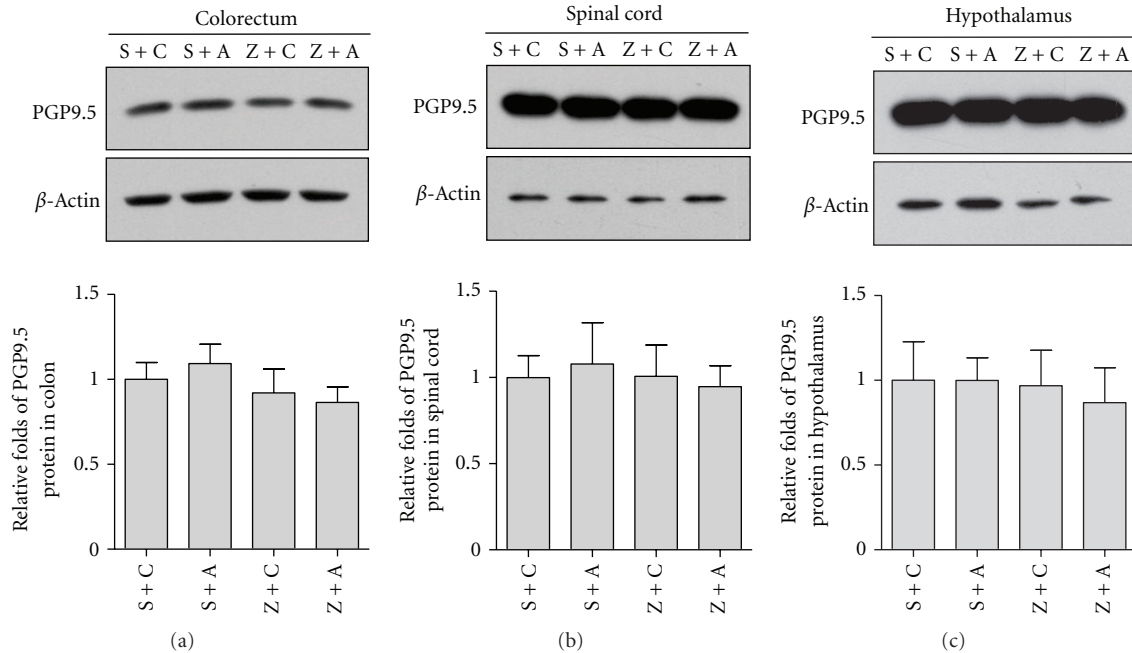


FIGURE 7: Zymosan could not induce PGP9.5 activation. There are no big differences in PGP9.5 expression among the 4 groups in colorectum, spinal cord, and hypothalamus, respectively. (#RA12103, Neuromics, 27KD, delusion: 1 : 20000).

indicating that EA had an analgesic effect in this model. These findings clearly showed the effectiveness of EA at the ST36 and ST37 acupoints on anti-non-inflammatory pain.

4.3. EA Blunts Zymosan-Induced Expression of TrpV1. The transient receptor potential vanilloid 1 (TrpV1) is an important protein for ligand-gated ion channels formation in peripheral sensory neurons [24, 25] and is believed to play a pivotal role in visceral hypersensitivity [26]. TrpV1 upregulation was found in colorectal samples from patients with inflammatory bowel disease and Crohn's disease [27], as well as in sensory fibers from patients with rectal hypersensitivity [28]. This present study concurs with our previous work [21] that TrpV1 was involved in zymosan-induced an noninflammation-independent colorectal hypersensitivity. Interestingly, EA treatment compromised zymosan-induced TrpV1 up-regulation in colorectum, suggesting that EA, partially through regulating TrpV1 expression, reduces zymosan-induced colorectal hypersensitivity. However, when compared with complete blockage of EMG activity in mice with zymosan injection, EA treatment only partially retarded TrpV1 protein level, suggesting that other molecules or central nerves system is likely to be involved in the processing of acupuncture analgesia.

4.4. EA Blunts Zymosan-Induced ERK1/2 Activation. ERK, activated by neurotrophins or neuronal activity in the central or peripheral nervous system, plays an essential role in the generation and maintenance of inflammation-induced hyperalgesia by regulating nociceptive activities in primary sensory pathways [29, 30]. Increased phosphorylation of ERK1/2 has been observed in rat spinal cord dorsal horn

neurons in response to noxious stimulation of the peripheral tissue or electrical stimulation to the peripheral nerve [31, 32]. Moreover, intrathecal injection of MEK/ERK inhibitor U_{0126} or PD_{98059} alleviated pain behaviour induced by inflammation of the hind paw [32] or viscera [31], suggesting a prominent role of ERK in the regulation of peripheral inflammation. We found that both EA treatment and zymosan injection alone greatly induced ERK1/2 phosphorylation in colorectum, spinal cord, and brain, suggesting that ERK1/2 MAP kinase pathway is involved in transduction of pain signal in peripheral as well as in central nervous system. However, ERK1/2 phosphorylation was obviously suppressed both in colorectum and in spinal cord by EA treatment. Importantly, it was completely blocked by EA treatment in hypothalamus. These results highly suggested that EA treatment might have an increased blocking capacity for pain signal from peripheral to central nervous system in colorectal hypersensitivity mouse model via blocking of ERK1/2 MAPK activation, while it has no effects on pain signal transduction in CNS or even enhancing signal of peripheral nervous system in normal control mice.

4.5. Zymosan Could Not Induce PGP9.5 Activation. PGP9.5 nerve fibres are believed to be involved in IBS [33]. It was detected in the myenteric plexus, but PGP 9.5-immunoreactive cell bodies did not colocalize with TrpV1 [26], suggesting that PGP 9.5 and TrpV1 play different roles in pain signal transmission. In our present study, PGP9.5 was not significantly different among the 4 groups in colorectum, spinal cord and hypothalamus, suggesting that PGP9.5 is not involved in zymosan-induced noninflammatory colorectal

hypersensitivity and in the processing of acupuncture analgesia.

4.6. *Possible Roles of p-ERK1/2 and TrpV1 in Zymosan-Induced Visceral Hypersensitivity and EA-Induced Analgesia in IBS.* Activation of the ERK signaling pathway in the periphery is likely necessary for the maintenance of a spinally sensitized state, while activation of ERK1/2 in the primary injury site may regulate TrpV1, leading to dorsal horn hypersensitivity to thermal and chemical stimuli [34]. Activation of ERK in primary afferent neurons is mediated, at least in part by TrpV1 [35]. In agreement with these two studies, our result shows that both p-ERK1/2 and TrpV1 in the periphery are involved in zymosan-induced hypersensitivity and EA-induced analgesia in IBS. However, in central nerves system, we detected a strong signal of p-ERK1/2 in response to zymosan treatment and this signal was greatly blunted by EA treatment, while TrpV1 was undetectable, suggesting that p-ERK1/2 is more important than TrpV1 in central nerves system in those processes. Further studies by using either ERK or TrpV1 knockout mice are necessary to clarify their correlation in the mechanism of EA in the future.

5. Conclusions

EA significantly compromises zymosan-induced colorectal hypersensitivity, and the effectiveness of acupuncture analgesia is accumulative with increased number of times of acupuncture when compared to that of a single time of acupuncture. Ion channel, TrpV1 expression in colorectal, and ERK1/2 MAPK pathway activation in peripheral and central nerve system might be involved in this process. These results suggested that EA is a potential therapeutic tool to treat the abdominal pain or discomfort.

Abbreviations

CRD: Colorectal distension
EA: Electroacupuncture
IBS: Irritable bowel syndrome
VMR: Visceral motor response
EMG: Electromyographic.

Acknowledgments

S.-J. Wang is supported by the scholarship of the China Scholarship Council. The research described here was carried out at the University of Pittsburgh while the author was a visiting fellow. The authors thank Drs. Bin Feng and Gerald F. Gebhart for their advice and support and Guo-Shuang Xu for assistance with Western blot. They also thank Dr. Li-Yun Ke for assistance in the paper preparation and H.-Y. Yang in the analysis. This work was supported by Grant from National Nature Science Foundation of China (81072856/H2718) to S.-J. Wang.

References

- [1] D. A. Drossman, W. E. Whitehead, and M. Camilleri, "Irritable bowel syndrome: a technical review for practice guideline development," *Gastroenterology*, vol. 112, no. 6, pp. 2120–2137, 1997.
- [2] J. Fan, X. Wu, Z. Cao, S. Chen, C. Owyang, and Y. Li, "Up-regulation of anterior cingulate cortex NR2B receptors contributes to visceral pain responses in rats," *Gastroenterology*, vol. 136, no. 5, pp. 1732–e3, 2009.
- [3] Z. Cao, X. Wu, S. Chen et al., "Anterior cingulate cortex modulates visceral pain as measured by visceromotor responses in visceroally hypersensitive rats," *Gastroenterology*, vol. 134, no. 2, pp. 535–543, 2008.
- [4] N. Yan, B. Cao, J. Xu, C. Hao, X. Zhang, and Y. Li, "Glutamatergic activation of anterior cingulate cortex mediates the affective component of visceral pain memory in rats," *Neurobiology of Learning and Memory*, vol. 97, no. 1, pp. 156–164, 2012.
- [5] J. S. Han, "Acupuncture analgesia: areas of consensus and controversy," *Pain*, vol. 152, no. 3, supplement 1, pp. S41–S48, 2011.
- [6] J. H. Tu, W. C. Chung, C. Y. Yang, and D. S. Tzeng, "A comparison between acupuncture versus zolpidem in the treatment of primary insomnia," *Asian Journal of Psychiatry*, vol. 5, no. 3, pp. 231–235, 2012.
- [7] F. Y. Kong, Q. Y. Zhang, Q. Guan, F. Q. Jian, W. Sun, and Y. Wang, "Effects of electroacupuncture on embryo implanted potential for patients with infertility of different symptom complex," *Zhong Guo Zhen Jiu*, vol. 32, no. 2, pp. 113–116, 2012.
- [8] T. Murotani, T. Ishizuka, H. Nakazawa et al., "Possible involvement of histamine, dopamine, and noradrenalin in the periaqueductal gray in electroacupuncture pain relief," *Brain Research*, vol. 1306, pp. 62–68, 2010.
- [9] Y. H. Chen, X. K. Chen, and X. J. Yin, "Comparison of the therapeutic effects of electroacupuncture and probiotics combined with deanxit in treating diarrhea-predominant irritable bowel syndrome," *Zhong Guo Zhen Jiu*, vol. 32, no. 5, pp. 594–598, 2012.
- [10] J. Xing, B. Larive, N. Mekhail, and E. Soffer, "Transcutaneous electrical acustimulation can reduce visceral perception in patients with the irritable bowel syndrome: a pilot study," *Alternative Therapies in Health and Medicine*, vol. 10, no. 1, pp. 38–42, 2004.
- [11] J. A. Christianson and G. F. Gebhart, "Assessment of colon sensitivity by luminal distension in mice," *Nature Protocols*, vol. 2, no. 10, pp. 2624–2631, 2007.
- [12] E. H. Kamp, R. C. W. Jones, S. R. Tillman, and G. F. Gebhart, "Quantitative assessment and characterization of visceral nociception and hyperalgesia in mice," *American Journal of Physiology-Gastrointestinal and Liver Physiology*, vol. 284, no. 3, pp. G434–G444, 2003.
- [13] M. J. Kim, U. Namgung, and K. E. Hong, "Regenerative effects of moxibustion on skeletal muscle in collagen-induced arthritic mice," *Journal of Acupuncture and Meridian Studies*, vol. 5, no. 3, pp. 126–135, 2012.
- [14] M. J. Kim, U. K. Namgung, and K. E. Hong, "Regenerative effects of moxibustion on skeletal muscle in collagen-induced arthritic mice," *Acupuncture and Meridian Studies*, vol. 5, no. 6, pp. 126–135, 2012.
- [15] J. S. Han, "Acupuncture: neuropeptide release produced by electrical stimulation of different frequencies," *Trends in Neurosciences*, vol. 26, no. 1, pp. 17–22, 2003.

- [16] G. Xu, A. Liu, and X. Liu, "Aldosterone induces collagen synthesis via activation of extracellular signal-regulated kinase 1 and 2 in renal proximal tubules," *Nephrology*, vol. 13, no. 8, pp. 694–701, 2008.
- [17] G. Y. Xu, J. H. Winston, and J. D. Z. Chen, "Electroacupuncture attenuates visceral hyperalgesia and inhibits the enhanced excitability of colon specific sensory neurons in a rat model of irritable bowel syndrome," *Neurogastroenterology and Motility*, vol. 21, no. 12, pp. 1302–e125, 2009.
- [18] J. H. Sun, X. L. Wu, C. Xia, L. X. Pei, H. Li, and G. Y. Han, "Clinical evaluation of Soothing Gan and invigorating Pi acupuncture treatment on diarrhea-predominant irritable bowel syndrome," *Chinese Journal of Integrative Medicine*, vol. 17, no. 10, pp. 780–785, 2011.
- [19] L. L. Wu, C. H. Su, and C. F. Liu, "Effects of noninvasive electroacupuncture at Hegu (LI4) and Sanyinjiao (SP6) acupoints on dysmenorrhea: a randomized controlled trial," *Journal of Alternative and Complementary Medicine*, vol. 18, no. 2, pp. 137–142, 2012.
- [20] R. Taguchi, T. Taguchi, and H. Kitakoji, "Involvement of peripheral opioid receptors in electroacupuncture analgesia for carrageenan-induced hyperalgesia," *Brain Research C*, vol. 1355, pp. 97–103, 2010.
- [21] R. C. W. Jones III, E. Otsuka, E. Wagstrom, C. S. Jensen, M. P. Price, and G. F. Gebhart, "Short-term sensitization of colon mechanoreceptors is associated With long-term hypersensitivity to colon distention in the mouse," *Gastroenterology*, vol. 133, no. 1, pp. 184–194, 2007.
- [22] M. Shinoda, B. Feng, and G. F. Gebhart, "Peripheral and central P2X3 receptor contributions to colon mechanosensitivity and hypersensitivity in the mouse," *Gastroenterology*, vol. 137, no. 6, pp. 2096–2104, 2009.
- [23] Z. Chen, Y. Yan, K. Wang, W. Xu, and T. Shi, "An analysis of neuronal responses in nucleus centrum medianum to electrical stimulation of the superficial peroneal nerve.," *Zhen ci Yan Jiu*, vol. 16, no. 1, pp. 15–47, 1991.
- [24] L. Yu, F. Yang, H. Luo et al., "The role of TRPV1 in different subtypes of dorsal root ganglion neurons in rat chronic inflammatory nociception induced by complete Freund's adjuvant," *Molecular Pain*, vol. 4, p. 61, 2008.
- [25] H. Luo, J. Cheng, J. S. Man, and Y. Wan, "Change of vanilloid receptor 1 expression in dorsal root ganglion and spinal dorsal horn during inflammatory nociception induced by complete Freund's adjuvant in rats," *NeuroReport*, vol. 15, no. 4, pp. 655–658, 2004.
- [26] K. Matsumoto, E. Kurosawa, H. Terui et al., "Localization of TRPV1 and contractile effect of capsaicin in mouse large intestine: high abundance and sensitivity in rectum and distal colon," *American Journal of Physiology-Gastrointestinal and Liver Physiology*, vol. 297, no. 2, pp. G348–G360, 2009.
- [27] Y. Yiangou, P. Facer, N. H. C. Dyer et al., "Vanilloid receptor 1 immunoreactivity in inflamed human bowel," *The Lancet*, vol. 357, no. 9265, pp. 1338–1339, 2001.
- [28] C. L. H. Chan, P. Facer, J. B. Davis et al., "Sensory fibres expressing capsaicin receptor TRPV1 in patients with rectal hypersensitivity and faecal urgency," *The Lancet*, vol. 361, no. 9355, pp. 385–391, 2003.
- [29] R. R. Ji, H. Baba, G. J. Brenner, and C. J. Woolf, "Nociceptive-specific activation of ERK in spinal neurons contributes to pain hypersensitivity," *Nature Neuroscience*, vol. 2, no. 12, pp. 1114–1119, 1999.
- [30] X. J. Zhang, H. L. Chen, Z. Li et al., "Analgesic effect of paeoniflorin in rats with neonatal maternal separation-induced visceral hyperalgesia is mediated through adenosine A1 receptor by inhibiting the extracellular signal-regulated protein kinase (ERK) pathway," *Pharmacology Biochemistry and Behavior*, vol. 94, no. 1, pp. 88–97, 2009.
- [31] A. Galan, F. Cervero, and J. M. A. Laird, "Extracellular signaling-regulated kinase-1 and -2 (ERK 1/2) mediate referred hyperalgesia in a murine model of visceral pain," *Molecular Brain Research*, vol. 116, no. 1-2, pp. 126–134, 2003.
- [32] R. R. Ji, K. Befort, G. J. Brenner, and C. J. Woolf, "ERK MAP kinase activation in superficial spinal cord neurons induces prodynorphin and NK-1 upregulation and contributes to persistent inflammatory pain hypersensitivity," *Journal of Neuroscience*, vol. 22, no. 2, pp. 478–485, 2002.
- [33] A. Akbar, Y. Yiangou, P. Facer, J. R. F. Walters, P. Anand, and S. Ghosh, "Increased capsaicin receptor TRPV1-expressing sensory fibres in irritable bowel syndrome and their correlation with abdominal pain," *Gut*, vol. 57, no. 7, pp. 923–929, 2008.
- [34] M. M. Li, Y. Q. Yu, H. Fu, F. Xie, L. X. Xu, and J. Chen, "Extracellular signal-regulated kinases mediate melittin-induced hypersensitivity of spinal neurons to chemical and thermal but not mechanical stimuli," *Brain Research Bulletin*, vol. 77, no. 5, pp. 227–232, 2008.
- [35] Y. Chen, H. H. Willcockson, and J. G. Valtchanoff, "Vanilloid receptor TRPV1-mediated phosphorylation of ERK in murine adjuvant arthritis," *Osteoarthritis and Cartilage*, vol. 17, no. 2, pp. 244–251, 2009.

Research Article

Are Primo Vessels (PVs) on the Surface of Gastrointestine Involved in Regulation of Gastric Motility Induced by Stimulating Acupoints ST36 or CV12?

Xiaoyu Wang,¹ Hong Shi,¹ Hongyan Shang,¹ Yangshuai Su,¹ Juanjuan Xin,^{1,2} Wei He,¹ Xianghong Jing,¹ and Bing Zhu¹

¹Institute of Acupuncture and Moxibustion, China Academy of Chinese Medical Sciences, Beijing 100700, China

²Shandong University of Traditional Chinese Medicine, Jinan 250355, China

Correspondence should be addressed to Xianghong Jing, xianghongjing@hotmail.com and Bing Zhu, zhubing@mail.cintcm.ac.cn

Received 27 July 2012; Accepted 7 September 2012

Academic Editor: Di Zhang

Copyright © 2012 Xiaoyu Wang et al. This is an open access article distributed under the Creative Commons Attribution License, which permits unrestricted use, distribution, and reproduction in any medium, provided the original work is properly cited.

Previous studies showed primo vessels (PVs), which were referred to as Bonhan ducts (BHDs) and a part of circulatory system by Kim, located in different places of the body. The BHDs system was once considered as the anatomical basis of classical acupuncture meridian but not clearly identified by other investigators. In the present study, we tried to address the relationship between PVs and meridians through detecting the modulation of gastric motility by stimulating the PVs on the surface of stomach or intestine, as well as acupoints Zusanli (ST36) and Zhongwan (CV12). The results showed electric stimulation of the PVs had no effect on the gastric motility. While stimulating CV12 inhibited gastric motility significantly in PVs-intact and PVs-cut rats, there is no significant difference between the inhibition rate of the PVS-intact and the PVS-cut rats. Stimulating at ST36 increased gastric motility significantly in both the PVs-intact and the PVs-cut rats, yet there was no significant difference between the facilitation rate of the both groups. Taken together, the PVs on the surface of stomach or intestine did not mediate the regulation of gastric motility induced by stimulating at the acupoints ST36 or CV12.

1. Introduction

Acupuncture, as an important part of traditional Chinese medicine, is believed to restore the balance of *qi* and blood, as well as yin and yang, regulates functions of the viscera by dredging meridians. The meridian system plays a pivotal role in regulation and maintenance of physiological functions, and mediation of effects of acupuncture and moxibustion on visceral organs. So far there are many hypotheses explaining the mechanism and phenomena of acupuncture or meridian. Many researchers in this field tend to believe that the scientific bases of meridian and acupuncture can be explained by neurophysiological theories [1–3]. Langevin and Yandow and Langevin et al. proposed that acupoints and meridians were parts of a network formed by interstitial connective tissues [4, 5]. Another study provided evidence that the liquid-crystal collagen fibers that formed the bulk of connective tissue may conduct sound or electricity [6]. In

addition, Zhang et al. proposed the low hydraulic resistance channel theory [7]. However, the anatomical structures of meridians still remain elusive.

Recently a series of studies from Prof. Soh KS reported that the primo vessels (PVs) are located in different places of the body, like the surface of the internal organs of rats, rabbits, and swine [8–10], inside the blood and lymphatic vessels [11, 12], in the epineurium, running along the sciatic nerve [13], and below the skin [14]. These PVs, also referred to as Bonhan ducts (BHDs), were part of a circulatory system that was first reported by Kim [15, 16] in the early 1960s. The BHDs system, which included several subsystems, was once considered as the anatomical basis of classical acupuncture meridians. The structure was also found by Fujiwara's followup [17]. Unfortunately, Bonghan theory was not clearly confirmed by most investigators [18]. The main reason is that the method employed by Kim was not disclosed, and the experiments were hard to reproduce.

In addition, nobody addressed the role of BHD in the effect of acupuncture. The structure of the PVs is distinct from the well-known tissues, such as nerves, blood vessels, lymph-vessels, and blood capillaries. But there is still no research focusing on the relationship between the PVs and acupuncture meridian. In order to elucidate the relationship between the PVs and acupuncture meridians, the possible impacts of the PVs on the effectiveness of acupuncture should be investigated.

Acupuncture has been widely used for treating functional gastrointestinal (GI) disorders [19]. Previous studies showed that acupuncture at the lower limbs (ST36) causes muscle contractions via the somatoparasymphathetic pathway, while acupuncture at the upper abdomen (CV-12) causes muscle relaxation via the somatoparasymphathetic pathway [20, 21]. Are the PVs on the surface of gastrointestine involved in regulating process of gastro motility induced by stimulating ST36 or CV12? In this paper, we detected the effects of stimulating the PVs on gastric motility and whether the PVs play a role in the regulation of gastric motility by stimulating ST36 or CV12, and tried to address the relationship between the PVs and meridians.

2. Materials and Methods

2.1. Animal Preparation and Methods for Identifying PVs. Thirty Sprague-Dawley (SD) rats (both sexes, 200–230 g) were purchased from Institute of Animal, Academy of Chinese Medical Sciences. The animals were housed under a 12 h light/dark with free access to food and water. All animals were treated according to the Guide for Use and Care of Medical Laboratory Animals from Ministry of Public Health of People's Republic of China.

The animals were fasted overnight with free drinking of water in proxima luce and were anesthetized with urethane (1.5 g kg^{-1}), and all surgical procedures were performed under anesthesia. About 1 h after the urethane administration, the rats were under deep anesthesia, and the trachea was cannulated but not immobilized to keep respiratory tract unobstructed and a catheter was inserted into one of the jugular veins for infusion. The abdominal sides of the rats were incised, and the identification of the PVs was carried out under a stereomicroscope (Nikon SMZ750) according to the method reported by Lee et al. [22]. The images of the PVs on the organ surfaces were recorded using a CCD camera in situ and in vivo (Nikon SMZ750).

When the PVs were located, 0.2% diluted Trypan blue solution 1–2 mL was dropped to stain them on the internal organs such as the stomach, the small intestine, the large intestine, and the urinary bladder and the wall of the peritoneum of the rat for 20–30 sec, and then the internal organs were washed for several times with 10 mL of phosphate-buffered saline, PH 7.4 (PBS) for detection of the PVs. Under a stereomicroscope with a CCD camera (Nikon SMZ750), the stained PVs were observed, and the images were taken.

2.2. Gastric Motility Recording. After identifying the PVs, gastric motility were recorded. A small longitudinal incision

was made in the duodenum about 2–3 cm from the pylorus. A small balloon made of flexible condom rubber was inserted via incision of the duodenum into the pyloric area of rat and kept in position by tying the connecting catheter to the duodenum, and another catheter (inner diameter of 1 mm) was also inserted into the same hole by incision in order to drain digestive juices secreted from stomach. The balloon was filled with warm-water about 0.2–0.5 mL, which gave about 80–150 mmH₂O pressures. Pressure in the balloon was measured by a transducer (NeuroLog, NL900D) for low pressure through a thin polyethylene tube (1.5 mm in outer diameter) and then input on a polygraph (NeuroLog, NL900D) amplifier and led into a data acquisition system (Power-Lab) for further analysis. Demifasting gastric motor activity was recorded as a control for at least 1 h before acupuncture stimulation [20, 21].

The changes of gastric motility induced by the stimulation were compared with the basal activity recorded before any stimulation. If the change rates of gastric motility during stimulation were 15–20% of the basal activity, the response was then considered to have an excitatory or inhibitory regulation, respectively. Systemic blood pressure and heart rate were continuously monitored by using of Biopac data acquisition system (MP150, USA). Both signals were analyzed offline using the CED 1401-plus data system and the Spike 2 package (Cambridge Electronic Devices, Cambridge, UK), Rectal temperature was kept constantly around 37°C by a temperature controller (DC, USA).

2.3. Acupuncture and Electroacupuncture Stimulation of CV12 or ST36. A needle (0.3 mm in diameter) was inserted into the skin and its underlying muscles at acupoints Zhongwan (CV12) and Zusanli (ST36) on the body. CV12 was located at center of abdomen, in middle line of the body. ST36 was located bilaterally at the anterior tibia muscles near the knees. For the manual acupuncture (MA), the needle was rotated clockwise and anticlockwise at 2 Hz for 3 min. In electroacupuncture (EA) experiments, acupoints were stimulated by a pair of needle-electrodes inserted 0.3–0.5 cm deep into the skin, and electroacupuncture intensities were set as 5 mA, with frequency of 2/15 Hz alternatively for 3 min. Procedure of the experiments was performed as follows: (1) firstly manual acupuncture or electroacupuncture at ST36 or CV12, (2) then stimulated the PVs with different frequency, (3) manual acupuncture or electroacupuncture at ST36 or CV12 after PVs was cut. Besides the heart rate and the blood pressure, the gastric pressure should be kept stable before stimulating the acupoint.

2.4. Electrostimulation of PVs in Different Intensities. Bipolar stainless-steel electrodes were placed at the PVs for stimulation. Stimuli were given at different intensities of 1–20 mA, increments 2 mA, duration 2 ms, and 20 Hz for 30 s.

2.5. Statistical Analysis. The data obtained before and after treatment in the same group or different group was compared statistically by a paired *t*-test or unpaired *t*-test.

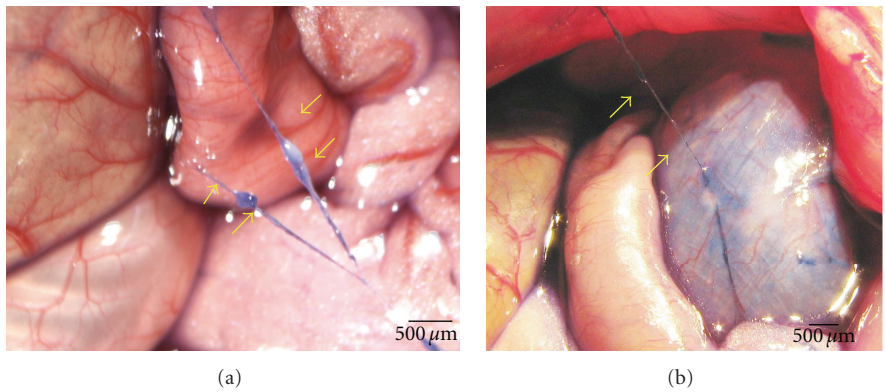


FIGURE 1: In situ and in vivo stereomicroscopic image of a typical primo vessel (arrow) and a corpuscle (arrow). (a) The primo vessel on the surface of intestine was stained with Trypan blue. (b) The primo vessel on the surface of stomach stained with Trypan blue. The primo vessels are semitransparent, freely movable strands irregularly fixed on the peritonea.

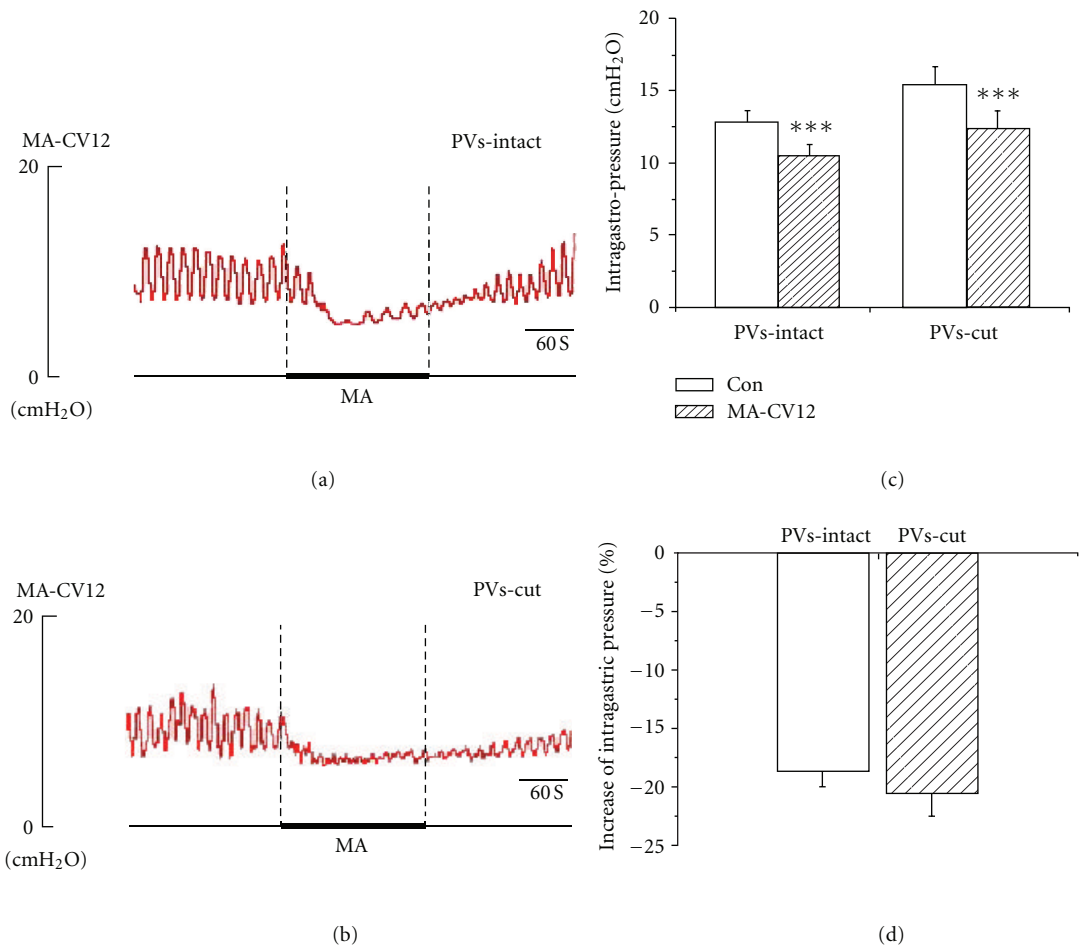


FIGURE 2: The response of gastric motility to the MA stimulation of CV12 in PVs-intact and PVs-cut rats. (a) and (b) Representative recording of gastric pressure during MA stimulation of CV12 before and after PVs-cut, respectively. (c) The inhibition of gastric motility induced by stimulating CV12 was of great significance in PVs-intact rats ($n = 6, P < 0.01$) and PVs-cut rats ($n = 6, P < 0.01$). (d) Comparing the inhibition effect between PVS-intact and PVS-cut, the inhibition rate was not significantly changed ($n = 6, P > 0.05$).

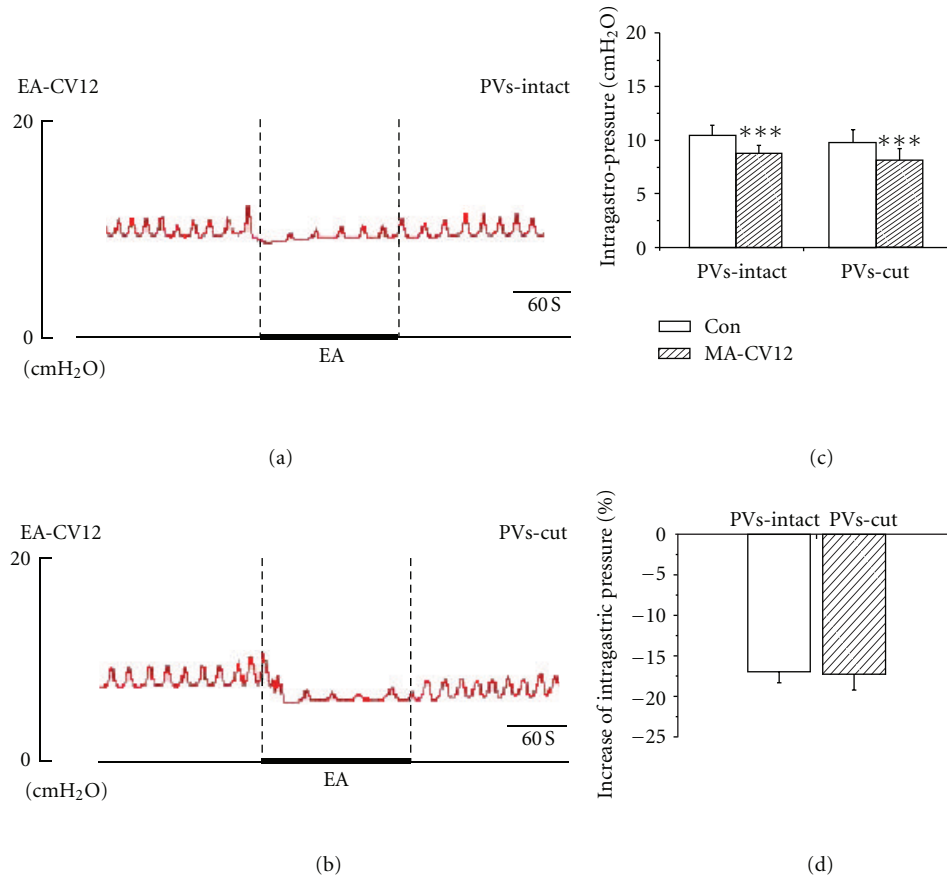


FIGURE 3: The response of gastric motility to the EA of CV12 in PVs-intact and PVs cut rats. (a) and (b) Representative recording of gastric pressure during EA stimulation of CV12 before and after PVs-cut, respectively. (c) The inhibition of gastric motility induced by stimulating CV12 was of great significance in PVs-intact rats ($n = 9$, $P < 0.001$) and PVs-cut rats ($n = 9$, $P < 0.001$). (d) Comparing the inhibition effect between PVS-intact and PVS-cut, the inhibition rate was not significantly changed ($n = 9$, $P > 0.05$).

$P < 0.05$ was considered as a statistical significance. All data are expressed as mean \pm SE.

3. Results

3.1. Distribution of PVs on the Surface of the Internal Organs and the Amount. The PVs and the corpuscles were observed on surfaces of different internal organs, such as the stomach, liver, large and small intestines, and bladder. Figure 1 showed a representative stereomicroscopic image of a PV (arrow) and its corpuscles (arrow) on the surface of the stomach and small intestine, respectively. The PVs observed in the present work are thin, semitransparent, freely movable strands that are randomly fixed on the peritonea, same as described by Lee et al. [22]. Among the total 30 rats, the PVS was observed in 23 rats. There is no difference between sexes. The percentage of the PVs emergence was 76.67%. There were 1 or 2 PVs observed on the surface of the gastrointestinal in most rats, sometimes 1 PV was observed on the surface of the liver.

3.2. PVs Cut Did Not Change the Inhibition of Gastric Motility Induced by CV12. The Gastric motility was detected in 23

rats by recording the intragastric pressure. Sometimes the gastric pressure did not recover to the baseline after stimulation of acupoints. Only two rats underwent all the manipulations, the other rats underwent two or more of the manipulations. When the intrapyloric balloon pressure was increased to about 80–200 mmH₂O, the rhythmic waves of contractions in pyloric area were observed. With regard to gastric motor characteristics, it was noteworthy both the changes of intragastric pressure and rhythmic contraction. Generally, the intragastric pressure represents the index of gastric tone motility and rhythmic contraction represents gastric peristalsis induced by circular muscle contractions, similar to slow wave of gastric motor activity. The pressure was maintained at about 100 mmH₂O as a baseline by expanding the volume of the balloon with warm water, rhythmic contractions occurred at a rate of four to six per minute, and these rhythmically gastric contractions could be recorded in both the PVS intact and PVs-cut rats.

MA and EA stimulation resulted in high suppression of gastric tonic motility with a rapid onset, followed by an obvious inhibition of rhythmic contraction waves, consistent with previous reports [20, 21]. These suppressions lasted throughout the period of acustimulation and even lasted

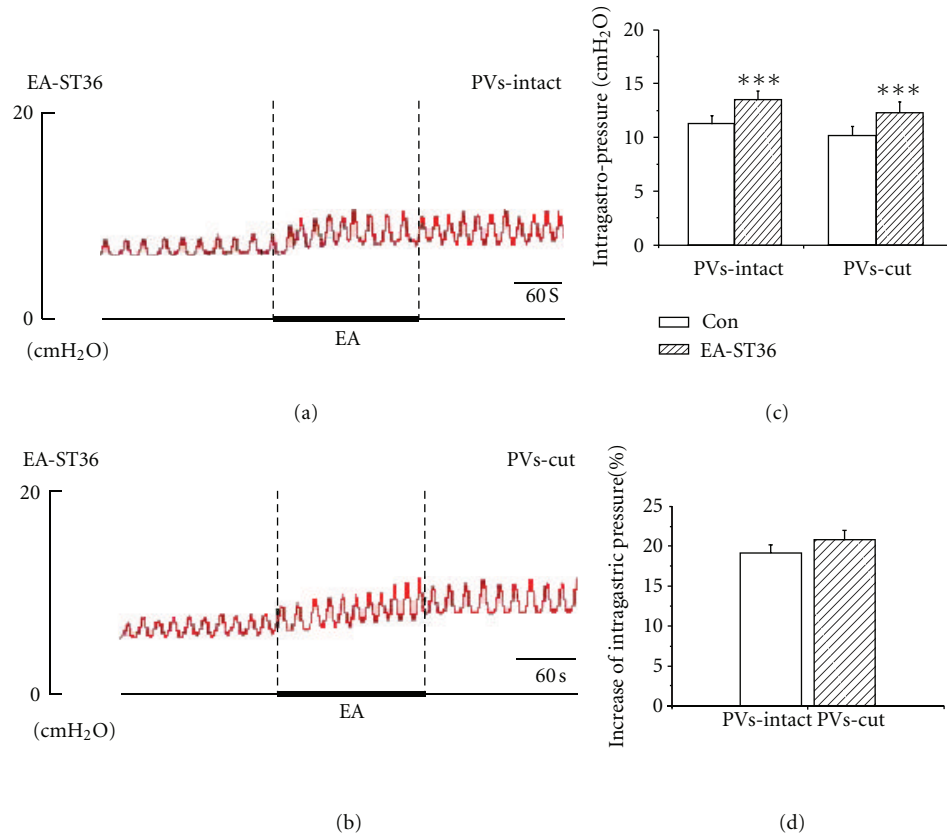


FIGURE 4: The response of gastric motility to the MA of ST36 in PVs-intact and PVs-cut rats. (a) and (b) Representative recording of gastric pressure during MA stimulating ST36 before and after PVs-cut, respectively. (c) The facilitation of gastric motility induced by stimulating ST36 was of great significance in PVs-intact rats ($n = 5$, $P < 0.001$) and PVs-cut rats ($n = 5$, $P < 0.001$). (d) Comparing the facilitation effect between PVS-intact and PVS-cut, the facilitation rate was not significantly changed ($n = 5$, $P > 0.05$).

about 3 min after withdrawing the needles in most cases. As shown in Figures 2(a), 2(c), 3(a), and 3(c), the intragastric pressure decreased from 12.82 ± 0.83 mmH₂O to 10.46 ± 0.79 mmH₂O in MA of CV12, the inhibition rate was $18.66 \pm 1.28\%$. For EA stimulation of CV12, the intragastric pressure decreased from 10.51 ± 0.86 mmH₂O to 8.75 ± 0.77 mmH₂O, the inhibition rate was $17.02 \pm 1.31\%$. Compared to the basal pressure, both inhibition effects were of great significance ($***P < 0.001$). In order to detect the contribution of the PVs to the inhibition of gastric motility, we designed an experiment in which the PVs were removed and then the effects of MA and EA stimulation at CV12 on gastric motility were examined. As shown in Figures 2(b), 2(d), 3(b), and 3(d), the inhibition of CV12 was not changed significantly after the PVs was cut. The intragastric pressure decreased from 15.48 ± 1.22 mmH₂O to 12.38 ± 1.20 mmH₂O by MA CV12, the inhibition rate was $20.21 \pm 1.89\%$. For EA CV12, the intragastric pressure decreased from 9.84 ± 1.16 mmH₂O to 8.18 ± 1.06 mmH₂O, the inhibition rate was $17.34 \pm 1.86\%$. Both inhibition effects were of great significance ($***P < 0.001$). Regardless of MA or EA, the inhibition rate was not significantly changed after removing the PVs ($P > 0.05$).

3.3. PVs Did Not Mediate the Facilitation of Gastric Motility Induced by ST36. MA and EA stimulation at ST36 caused a slight-moderate facilitation of gastric motility with a rapid onset and followed by a tonic motor that lasted throughout the period of acustimulation. The facilitation lasted throughout the period of acustimulation and even lasted about 1-2 min after withdrawing the needles in most cases. Figures 4(a), 4(c), 5(a), and 5(c), showed that both MA ($n = 5$) and EA ($n = 9$) at ST36 induced facilitation of gastric motility, consistent with the previous reports [20, 21]. The intragastric pressure increased from 11.63 ± 1.33 mmH₂O to 13.64 ± 1.52 mmH₂O in MA ST36, the facilitation rate was $17.47 \pm 1.33\%$. For EA stimulation of ST36, the intragastric pressure increased from 11.34 ± 0.72 mmH₂O to 13.47 ± 0.80 mmH₂O, the facilitation rate was $19.13 \pm 1.01\%$. Both reinforcement effects were of great significance ($**P < 0.01$, $***P < 0.001$). We also examined the contribution of the PVs to the facilitation of gastric motility by removing the PVs here. Interestingly, as shown in Figures 4(b), 4(d), 5(b), and 5(d), the facilitation effect of needling ST36 did not change after the PVs was cut, the intragastric pressure increased from 11.81 ± 1.41 mmH₂O to 13.77 ± 1.67 mmH₂O by MA stimulation at ST36 after removing the PVs, with

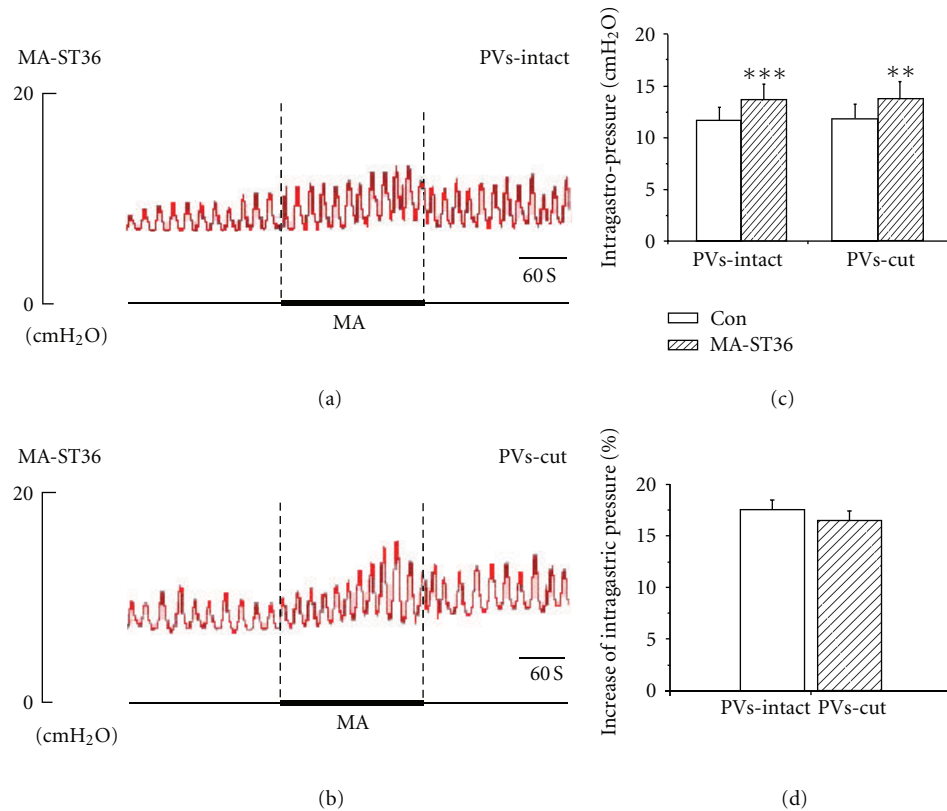


FIGURE 5: The response of gastric motility to the EA of ST36 in PVs-intact and PVs-cut rats. (a) and (b) Representative recording of intragastric pressure during MA stimulation of ST36 before and after PVs-cut, respectively. (c) The facilitation of gastric motility induced by stimulating ST36 was of great significance in PVs-intact rats ($n = 9$, $P < 0.01$) and PVs-cut rats ($n = 9$, $P < 0.01$). (d) Comparing the facilitation effect between PVS-intact and PVS-cut, the facilitation rate was not significantly changed ($n = 9$, $P > 0.05$).

a facilitation rate of $16.50 \pm 0.51\%$. For EA ST36, the intragastric pressure increased from 10.23 ± 0.83 mmH₂O to 12.32 ± 0.93 mmH₂O after removing the PVs, and the facilitation rate was $20.79 \pm 1.21\%$. Both facilitation effects were still of great significance (** $P < 0.01$, *** $P < 0.01$). The results suggested that removing PVs did not change the enhanced effects of gastric motility induced by ST36.

3.4. Electrostimulation of PVs Did Not Affect the Changes of Gastric Motility Induced by ST36 or CV12. From above, we knew that the PVs were not involved in the regulation of gastric motility by EA/MA at CV12 or ST36. A recent study [23] showed that the action potentials of the PVs had two types of pulses that are different from those of smooth muscle. Because action potentials occur in excitable cells, the electrophysiological characteristics of the PVs indicate that the PVs are excitable. To observe the changes of intragastric pressure induced by electro-stimulating the PVs with different intensities, here the bipolar stainless-steel electrodes were placed at the PVs for stimulus. As shown in Figure 6, the gastric pressure was not changed significantly by electro-stimulating the PVs with different intensities from 1–19 mA ($P > 0.05$). The result indicated that the gastric motility was not affected by electrostimulating the PVs.

4. Discussion

In this study, we investigated the effects of stimulating the PVs on gastric motility in situ and in vivo, the role of PVs in the regulation of gastric motility by stimulating acupoints ST36 or CV12, and the relationship between the PVs and meridians. Stimulating the PVs with different intensities did not change the intragastric pressure in comparison with baseline. The results indicated that although the PVs were an excitable tissue [23], the PVs on the surface of internal organs did not show an effect on the regulation of gastric motility. To confirm whether the PVs in the internal organs play a role in the regulation of gastric motility by stimulating ST36 or CV12, the effects of acupuncturing at CV12 or ST36 on gastric motility were observed in PVs intact and PVs-removing rats. The results indicated that MA/EA-stimulating CV12 actually caused inhibition effect on gastric motility, otherwise MA/EA stimulating ST36 caused facilitation effect on gastric motility. This was in accordance with previous reports [24]. After the electric stimulation of the PVs was finished and the PVs were removed, the inhabitation and facilitation of gastric motility induced by acupuncturing CV12 or ST36 did not change significantly. These results showed that the PVs were not involved in the regulation of gastric motility by stimulation of CV12 or ST36.

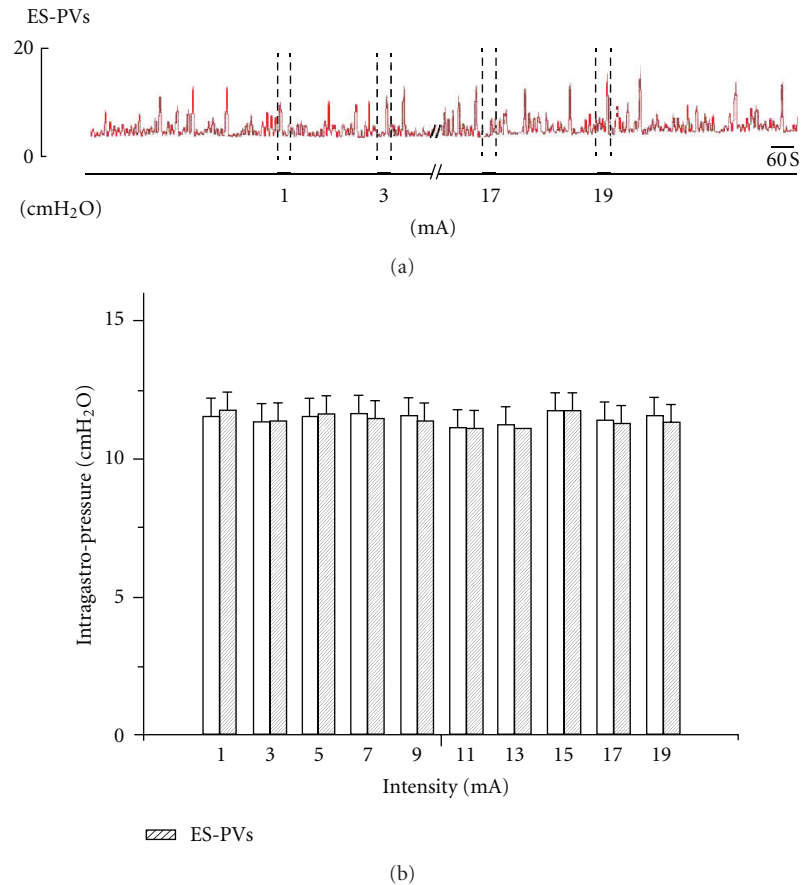


FIGURE 6: Electro-stimulation of PVs with different intensities by bipolar stainless-steel electrodes. Stimuli were given with different intensities from 1 to 19 mA, increments 2 mA, duration 2 ms, 20 Hz for 30 s. (a) A representative recording of the intragastric pressure under electro-stimulation of PVs with different intensities. (b) The intragastric pressure was not changed significantly by electro-stimulating PVs with different intensities from 1–19 mA ($n = 11$, $P > 0.05$).

PVs, which were widely distributed and had a lot of characteristics and medical significance [25], are speculated to be involved in many processes of life, such as circulatory function, excitability, hormone path, immune function, hematopoiesis, regeneration and sanal, obesity and cancer, and so on. Therefore, the PVs may play endocrine and immunological roles, which might be involved in therapeutic effects of acupuncture. However, our current study provides evidence that the PVs were not essential for the regulation of gastric motility by stimulating CV12 or ST36.

The anatomical structure of meridian had attracted many scientists since Dr. Kim declared that he found BHD and BHC in 1963 [15]. Some scientists taking part in the work recorded and narrated the process of the repeating experiments [18]. Combined with the restricted data at that time in China, the BHD was just found in a navel of an infant rabbit, including chromaffin cells, with smooth muscle outside. But when a rabbit grew up, the structure disappeared, suggesting that the structure of BHD is a degenerative tissue. Although the existence of the phenomena of meridians has been confirmed [26], the physical structure of meridian still remains controversial. Yet it is accepted by most researchers that there is relevance between the acupoints and

internal organs. Different visceral diseases can be reflected in different acupoints. And acupuncture at different acupoints can regulate the functions of different visceral diseases. The meridians play important roles in the relevance between the acupoints and internal organs. So, in the present study, we try to investigate the relationship between the PVs and meridians by investigating the relationship between the PVs and acupoints. Now the question is: although Soh et al.'s findings provide the evidence that the PVs exist in the internal organs, these findings did not address the function of the PVs, and thus are not enough to verify the relationship between the PVs and meridians. Our data also did not support an existence of the relationship between the PVs and the effects of acupuncture stimulation. In the future, we will have to further study the function of the PVs and their role in the regulation of visceral organs by acupuncture, and then elucidate the relationship between the PVs and the effects of acupuncture stimulation.

5. Conclusions

The PVs in surface of internal organs did not have an effect in regulating gastric motility. The PVs in the surface of internal

organs were involved neither in the inhibition of the gastric motility induced by acupuncture at CV12 nor in the facilitation of gastric motility induced by acupuncture at ST36. Further research about the functional relationship between the PVs and meridian is needed in the future.

Authors' Contributions

X. Wang and H. Shi contributed equally to this work.

Acknowledgments

This work was supported by National Key Basic Research Program 973 (no. 2010CB530507) and National Natural Science Foundation of China (no. 81173205). The authors thank Dr. Haifa Qiao and Prof. Junling Liu for word polishing.

References

- [1] B. Zhu, P. Rong, H. Ben, Y. Li, W. Xu, and X. Gao, "Generating-sensation and propagating-myoelectrical responses along the meridian," *Science in China C*, vol. 45, no. 1, pp. 105–112, 2002.
- [2] Y. Xie, H. Li, and W. Xiao, "Neurobiological mechanisms of the meridian and the propagation of needle feeling along the meridian pathway," *Science in China C*, vol. 39, no. 1, pp. 99–112, 1996.
- [3] K. Liu, A. H. Li, W. Wang, and Y. K. Xie, "Dense innervation of acupoints and its easier reflex excitatory character in rats," *Zhen Ci Yan Jiu*, vol. 34, no. 1, pp. 36–42, 2009 (Chinese).
- [4] H. M. Langevin and J. A. Yandow, "Relationship of acupuncture points and meridians to connective tissue planes," *Anatomical Record*, vol. 269, no. 6, pp. 257–265, 2002.
- [5] H. M. Langevin, D. L. Churchill, J. Wu et al., "Evidence of connective tissue involvement in acupuncture," *The FASEB Journal*, vol. 16, no. 8, pp. 872–874, 2002.
- [6] M.-W. Ho and D.-P. Knight, "The acupuncture system and the liquid crystalline collagen fibers of the connective tissues," *American Journal of Chinese Medicine*, vol. 26, no. 3-4, pp. 251–263, 1998.
- [7] W. B. Zhang, Y.-Y. Tian, H. Li et al., "A discovery of low hydraulic resistance channel along meridians," *JAMS Journal of Acupuncture and Meridian Studies*, vol. 1, no. 1, pp. 20–28, 2008.
- [8] S.-J. Cho, B.-S. Kim, and Y. S. Park, "Threadlike structures in the aorta and coronary artery of swine," *Journal of International Society of Life Information Science*, vol. 22, no. 2, pp. 609–611, 2004.
- [9] K. J. Lee, S. Kim, T. E. Jung, D. Jin, D.-H. Kim, and H.-W. Kim, "Unique duct system and the corpuscle-like structures found on the surface of the liver," *Journal of International Society of Life Information Science*, vol. 22, no. 2, pp. 460–462, 2004.
- [10] H.-S. Shin, H.-M. Johng, B.-C. Lee et al., "Feulgen reaction study of novel threadlike structures (Bonghan ducts) on the surfaces of mammalian organs," *Anatomical Record B*, vol. 284, no. 1, pp. 35–40, 2005.
- [11] B.-C. Lee, K.-Y. Baik, H.-M. Johng et al., "Acridine orange staining method to reveal the characteristic features of an intravascular threadlike structure," *Anatomical Record B*, vol. 278, no. 1, pp. 27–30, 2004.
- [12] B.-C. Lee, J.-S. Yoo, K.-Y. Baik, K.-W. Kim, and K.-S. Soh, "Novel threadlike structures (Bonghan ducts) inside lymphatic vessels of rabbits visualized with a Janus Green B staining method," *Anatomical Record B*, vol. 286, no. 1, pp. 1–7, 2005.
- [13] Z. F. Jia, B.-C. Lee, K.-H. Eom et al., "Fluorescent nanoparticles for observing primo vascular system along sciatic nerve," *JAMS Journal of Acupuncture and Meridian Studies*, vol. 3, no. 3, pp. 150–155, 2010.
- [14] J. P. Jones and Y. K. Bae, "Ultrasonic visualization and stimulation of classical oriental acupuncture points," *Med Acupunct*, vol. 15, no. 2, pp. 24–26, 2004.
- [15] B. H. Kim, "On the Kyungrak system," *Journal of Academy of Medical Sciences*, vol. 90, pp. 1–41, 1963.
- [16] B. H. Kim, "Sanal theory," *Journal of Academy of Medical Sciences*, vol. 168, pp. 5–38, 1965.
- [17] S. Fujiwara and S. B. Yu, "'Bonghan theory' morphological studies," *Igaku no Ayumi*, vol. 60, pp. 567–577, 1967.
- [18] X. Liu, "Verification and confirmation about 'Bonghan ducts' as meridian," *Zhen Ci Yan Jiu*, vol. 34, pp. 353–354, 2009.
- [19] T. Takahashi, "Acupuncture for functional gastrointestinal disorders," *Journal of Gastroenterology*, vol. 41, no. 5, pp. 408–417, 2006.
- [20] Y. Q. Li, B. Zhu, P. J. Rong, H. Ben, and Y. H. Li, "Effective regularity in modulation on gastric motility induced by different acupoint stimulation," *World Journal of Gastroenterology*, vol. 12, no. 47, pp. 7642–7648, 2006.
- [21] Y. Q. Li, B. Zhu, P. J. Rong, H. Ben, and Y. H. Li, "Neural mechanism of acupuncture-modulated gastric motility," *World Journal of Gastroenterology*, vol. 13, no. 5, pp. 709–716, 2007.
- [22] B.-C. Lee, K.-W. Kim, and K.-S. Soh, "Visualizing the network of bonghan ducts in the omentum and peritoneum by using trypan blue," *Journal of Acupuncture and Meridian Studies*, vol. 2, no. 1, pp. 66–70, 2009.
- [23] S.-J. Cho, S.-H. Lee, W. J. Zhang et al., "Mathematical distinction in action potential between primo-vessels and smooth muscle," *Evidence-Based Complementary and Alternative Medicine*, vol. 2012, Article ID 269397, 6 pages, 2012.
- [24] E. Noguchi, "Mechanism of reflex regulation of the gastroduodenal function by acupuncture," *Evidence-Based Complementary and Alternative Medicine*, vol. 5, no. 3, pp. 251–256, 2008.
- [25] K.-S. Soh, "Bonghan circulatory system as an extension of acupuncture meridians," *Journal of Acupuncture and Meridian Studies*, vol. 2, no. 2, pp. 93–106, 2009.
- [26] G. J. Wang, M. H. Ayati, and W. B. Zhang, "Meridian studies in China: a systematic review," *Journal of Acupuncture and Meridian Studies*, vol. 3, no. 1, pp. 1–9, 2010.

Research Article

Measurements of Location-Dependent Nitric Oxide Levels on Skin Surface in relation to Acupuncture Point

Yejin Ha,¹ Misun Kim,¹ Jiseon Nah,¹ Minah Suh,^{2,3} and Youngmi Lee¹

¹Department of Chemistry and Nano Science, Ewha Womans University, Seoul 120-750, Republic of Korea

²Department of Biological Science, Sungkyunkwan University, Suwon 440-746, Republic of Korea

³Samsung Advanced Institute for Health Sciences and Technology, Graduate School of Health Sciences and Technology, Sungkyunkwan University, Suwon 440-746, Republic of Korea

Correspondence should be addressed to Minah Suh, minahsuh@skku.edu and Youngmi Lee, youngmilee@ewha.ac.kr

Received 20 July 2012; Accepted 28 August 2012

Academic Editor: Di Zhang

Copyright © 2012 Yejin Ha et al. This is an open access article distributed under the Creative Commons Attribution License, which permits unrestricted use, distribution, and reproduction in any medium, provided the original work is properly cited.

Location-dependent skin surface's partial nitric oxide pressure (pNO) is studied using highly sensitive amperometric NO microsensor with a small sensing area (diameter = 76 μm). The pNO level of LI4 (Hegu) acupuncture point is measured and compared with the pNO level of nonacupuncture point. In addition, the mapping of pNO is carried out over the left wrist skin area one- as well as two-dimensionally. Statistically higher pNO levels near the position of acupuncture points than non-acupuncture points are observed consistently, implying tight relationship between the level of NO release of skin and acupuncture points. The amperometric planar NO microsensor successfully monitors the heterogeneity of skin pNO distribution in high spatial resolution due to its advantageous features such as high sensitivity and small sensing dimension. The current study suggests the direct connection between NO and acupuncture points and possibly provides beneficial information to understand physiological roles and basis of the acupuncture points.

1. Introduction

Traditional eastern medicine describes meridians as physical channels which Qi flows through, connect body internal organs, and link the specified body skin locations, called acupuncture points [1]. The stimulation of acupuncture points by placing small needles is called acupuncture which is a medical treatment carried out to attain harmonious and balanced Qi flow and thus to improve health [2]. Acupuncture has been practiced as a medical treatment for over 2500 years in traditional eastern medicine. Nowadays, acupuncture treatment became to be employed more widely as a complementary and alternative therapy not only in eastern but in western countries [1]. In 1997, the National Institute of Health (NIH) published a consensus on the curative effect of acupuncture for some pain symptoms such as postoperative nausea and vomiting [3]. However, the definite efficacy and mechanism of the acupuncture action in relieving pain are still disputable.

The distinctive biophysical features of acupuncture points and meridians, such as the high electrical conductance [4, 5] and possible relationship with connective tissue planes [6] and perivascular space [7], have been studied over the last few decades. Nonetheless, more direct scientific evidence of the physical existence as well as physiological functions of acupuncture points and meridians is still to seek particularly for humans, mainly due to the limitation of noninvasive technology.

In ancient acupuncture meridian theory, Qi has long been believed to be essential for sustaining life [8] and considered to be related with air and food intake, and inheritance [1]. Oxygen in air is definitely essential for our lives. Therefore, we supposed the possible relationship between acupuncture points and body oxygen supply and studied the heterogeneity of skin surface oxygen levels in relation to the acupuncture points [9]. The localized oxygen levels at acupuncture points and adjacent non-acupuncture points were measured using a highly sensitive electrochemical oxygen microsensor (sensing diameter = 25 μm) [9]. Relatively

higher oxygen levels were measured at the acupuncture points on hand skin surface, LI4 (Hegu) and PC8 (Laogong), than those at the corresponding non-acupuncture points. Our previous results provide a direct evidence for the presence of acupuncture points, which are possibly linked to the oxygenation of body. More recently, we also reported the mapping of oxygen levels in a fixed one- as well as two-dimensional areas of wrist skin surface [10]. The oxygen mapping demonstrated that the higher oxygen levels are, indeed, related with acupuncture points [10].

NO is known to be a signaling gas molecule mediating vasodilation and thus regulating blood flow and volume [11]. There are some previous studies on the relationship between NO and acupuncture points/meridians, reporting that acupuncture treatment increases blood flow [12] and expression of NO synthase (NOS), enzyme producing NO, is higher around skin acupuncture points and meridians of rat [13]. NO was also proposed as a prime candidate as a signaling molecule in the meridian system [14]. In addition, the quantification of NO_x^- collected from the skin surface along meridian lines using NO collecting solutions containing NO absorbing compounds was reported [15]. However, these works include rather complicated methods (e.g., postmortem immunohistochemical analysis) which may have restrictions in future application for humans thus are not applicable in investigation of direct evidence of the NO and acupuncture point relations. Herein, we map the skin nitric oxide (NO) levels of human wrist area with a sensitive electrochemical NO microsensor. Since the present technique uses a tiny, yet high-resolution NO microsensor positioned over a fixed skin surface with a certain distance (~ 1 mm) to measure skin NO levels, it is advantageous towards human study of acupuncture points.

2. Materials and Methods

2.1. Electrochemical NO Microsensor. A planar amperometric microsensor highly selective for nitric oxide was prepared as described elsewhere [16]. The nitric oxide microsensor is composed of a glass-sealed Pt disc anode (Pt diameter = $76 \mu\text{m}$, Sigma Aldrich) and a coiled Ag/AgCl wire cathode ($127\text{-}\mu\text{m}$ diameter, Sigma Aldrich) immersed in an internal solution and covered with PTFE gas-permeable membrane (W. L. Gore & Associates, thickness $< 19 \mu\text{m}$, porosity 50%, pore size $0.05 \mu\text{m}$). The internal solution contained 30 mM NaCl and 0.3 mM HCl in deionized water. The surface of the Pt disc anode was electrochemically deposited with additional porous Pt layer by cyclic voltammetry carried out in 3% H_2PtCl_6 solution (YSI Inc., USA) to obtain the enhanced sensitivity to NO. A potential of $+0.75$ V (versus Ag/AgCl anode) was applied to the platinized Pt anode to induce the favorable electrochemical NO oxidation. NO oxidation current was measured between the cathode and anode, as a function of time using CHI1000A electrochemical analyzer (CH Instruments Inc., USA). For the calibration of the prepared NO microsensor, the sensor current was measured while the concentration of NO was increased in deoxygenated phosphate-buffered saline (PBS, pH 7.4, Fisher

Scientific) solution by successive several injections of a given amount of NO standard solution. NO standard solution was prepared by bubbling deoxygenated PBS solution (pH 7.4) with NO gas (Dong-A Gas Co., Seoul, Republic of Korea) for 30 min. The concentrations of the standard solution was calculated as 1.91 mM using Henry's law assuming ideal dilute solutions and Henry's law constants for NO of 526.3 atom/M [17].

2.2. Skin NO Measurements. Skin NO measurements, NO mapping, were performed similarly to the skin oxygen measurements described previously [9, 10]. Briefly, as-prepared planar NO microsensor was positioned above the skin location of interest to which a drop of PBS (pH = 7.4) solution ($15 \mu\text{L}$) was applied. The vertical distance between the sensor and plane and skin surface separation was maintained as ~ 1 mm using a micromanipulator (World Precision Instrumentation Inc., Sarasota, FL, USA). The sensor current proportional to the partial NO pressure (pNO) was monitored. Once a stable current signal was achieved, the sensor was moved and positioned over the second skin point of interest with the same vertical distance, ~ 1 mm, while the sensor current was monitored continuously. After the stable current was acquired at the second point, the sensor was moved to the third point to measure the pNO level at that location. This whole procedure was repeated until the measurements of pNO levels for all the projected points were completed. The measured sensor currents were converted to the corresponding pNO levels using prior calibration curves recorded before the measurements.

The measurements of pNO levels were carried out in three different designs. First, pNO levels between acupuncture point and non-acupuncture point were compared. The pNO was measured over an acupuncture point (LI 4, Hegu) and then nearby non-acupuncture point ~ 3 cm apart with three-time repetition as shown in Figure 1(a). Second, the pNO was monitored along one-dimensional single line over left wrist in a blind fashion. The pNO levels were measured at 10 different points along the line on the anterior aspect of the left hand-wrist transverse crease. The 10 points were evenly distributed with the same separation ($d = 4.5 - 5.5$ mm depending on individual subject) between two adjacent points. The first point and the last tenth point were positioned 5 mm apart from the left and right sides of the wrist as shown in Figure 1(b). Last, the pNO measurements were performed on 25 different points equally partitioning a square area of the left wrist (Figure 1(c)). The first five points were located over the lateral line on the anterior aspect of the left hand-wrist boundary crease while the first point and the fifth point were positioned 5 mm apart from the left and right sides, respectively.

The measurements were carried out for five healthy volunteers (average age = 23.7) in calm and restful conditions at room temperature. All the volunteers washed the projected body parts with an antibacterial hand soap, rinsed out thoroughly with water, and then fully dried before the skin pNO measurements. Any of the subjects were never treated

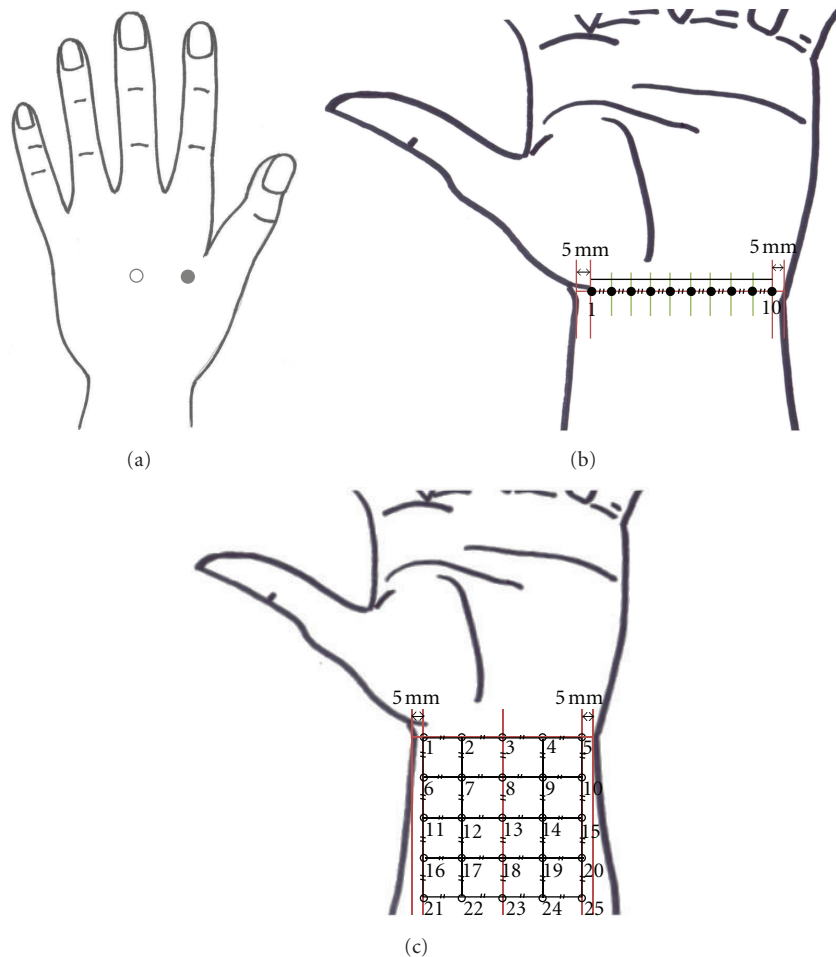


FIGURE 1: Schematic illustration for the points on the skin where a NO microsensor was positioned for pNO measurement: (a) at LI4 acupoint (solid circle) and non-acupoint (open circle); (b) 10 points along one-dimensional line on left wrist transverse crease; (c) at 25 different points within two-dimensional square area. The points, No. 1, 10 in (b) and the points, No. 1, 5 in (c) were positioned 5 mm apart from the left and right sides of the wrist. Symbol// represents the same separation.

with acupuncture needle insertion at the skin locations investigated prior to the experiments.

2.3. Data Analysis and Statistics. At each point of each subject, the average of the data acquired for the last 50 s before the sensor movement to another point was taken as the pNO value corresponding to that point. This verifies that sufficiently equilibrated pNO value is measured. The averaged data for the same skin location of five different subjects were also averaged with standard deviation calculation. The data for some points showing relatively higher pNO values were compared with those at other points exhibiting relatively lower pNO values using a paired *t*-test with a Bonferroni correction. *P* value < 0.05 was considered significantly different in statistical meaning.

3. Results and Discussion

Figure 2(a) shows the dynamic amperometric response of a NO sensor to the increased pNO in deoxygenated PBS

solution. The sensor current induced by NO oxidation linearly increases as the pNO increases. High sensitivity of 5.36 ± 0.34 nA/mmHg ($n = 5$) with good linearity ($R^2 > 0.99$) is observed in the corresponding calibration curve (Figure 2(b)). The sensor showed no discernible responses to the addition of some biological interferences such as nitrite, indicating the selectivity to NO achieved with the aid of sensor covering PTFE gas-permeable membrane [16]. The sensor sensitivity varied within $< \sim 5\%$ before and after the skin pNO measurements and $< 0.5\%$ for the temperature change between 25 and 35°C, confirming the sensor stability.

Figure 3 presents a typical pNO recording obtained as a function of time, while the sensor is moved between LI4 acupoint (gray-colored region) and non-acupoint (noncolored region). The measurements were repeated for three times. Sharp current peaks are noise signals caused by the sensor repositioning from one to the other points. Relatively higher pNO levels were measured over the LI4 point than non-acupoint consistently for all five subjects without exceptions. The absolute pNO,

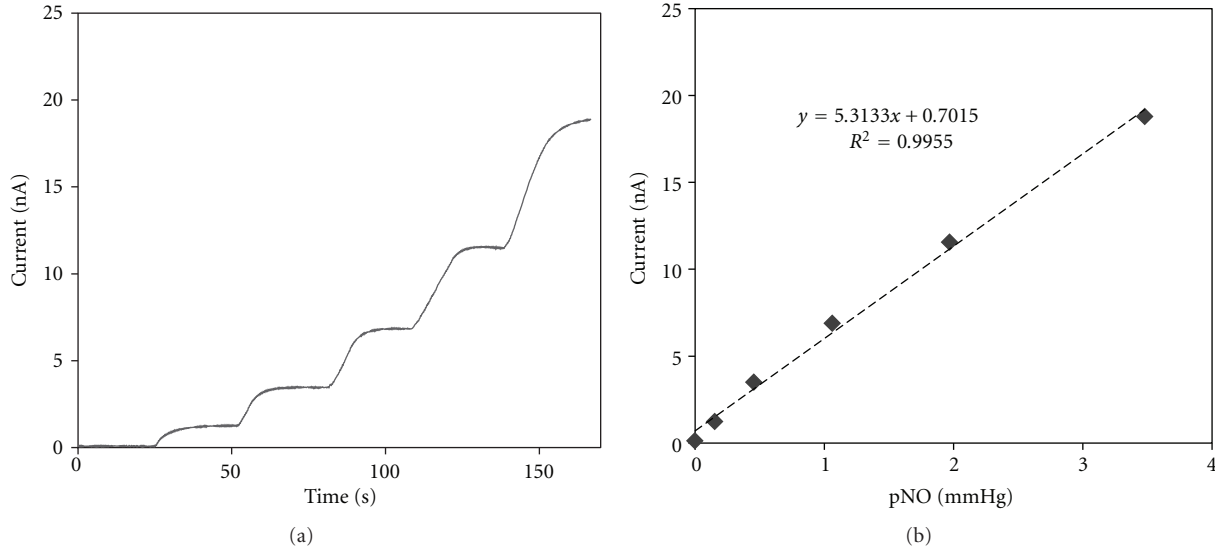


FIGURE 2: (a) A typical dynamic amperometric response curve of a NO microsensor to the varying NO concentration. (b) Corresponding calibration curve in terms of pNO.

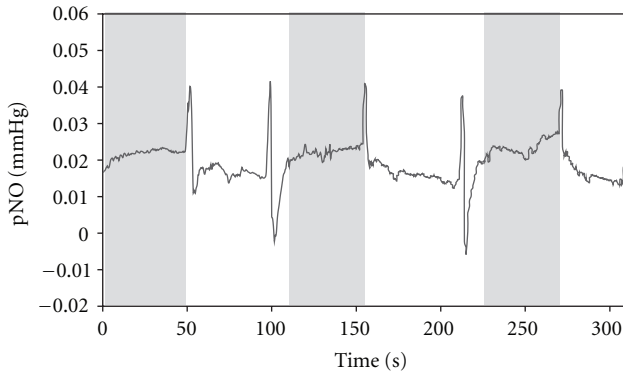


FIGURE 3: A representative pNO measurement as a function of time when the sensor was moved between LI4 acupuncture point (gray-colored) and nonacupuncture point (noncolored) indicated in Figure 1(a). The sensor end plane to skin surface distance, ~ 1 mm.

however, has a wide range of the values depending on subject entities presumably due to individual physiological conditions of the volunteers. Thus, for the statistics and comparison, the pNO value was normalized to the average of the pNO measured during a course of the overall measurement for each subject as follows:

$$\text{pNO}_{\text{norm}} = \frac{\text{pNO}}{\text{pNO}_{\text{avg}}}, \quad (1)$$

where pNO_{norm} is the normalized pNO; pNO is the measured pNO value at each time point; pNO_{avg} is the average of all the pNO values measured throughout the overall experiment for each subject. Thus, the pNO_{norm} values less or greater than one represent the measured absolute pNO values lower or higher than the average, respectively.

The averaged pNO_{norm} for five subjects were 1.239 (± 0.067) at LI4 and 0.755 (± 0.060) at non-acupuncture point. The measured pNO level at LI4 point was significantly different ($P < 0.001$) compared to the corresponding non-acupuncture point.

Figure 4(a) demonstrates a representative pNO measurement at 10 different locations along the transverse wrist crease line as shown in Figure 1(b). The measurement at each location is differentiated with vertical-dashed line in Figure 4(a). Again, sharp current noise signals are observed due to the repositioning of sensor. The data clearly shows the relatively higher pNO levels at the points No. 1, 5, and 10 compared to the other parts. Similar trends of the location-dependent pNO levels were observed for all five different subjects without exceptions. Figure 4(b) displays the pNO_{norm} (normalized pNO for each subject as in (1)) averaged for five entire subjects (with standard deviation) corresponding to the indicated specific point. These statistically treated data for five different subjects also exhibit the close relation of the pNO values to the skin location. In fact, higher pNO levels were measured at the points near to the acupuncture points: there are three acupuncture points, LU9 (Taiyuan), PC7 (Daling), and HT7 (Shenmen) from left to right side along the wrist transverse crease line. Rather large standard deviations of the averaged pNO_{norm} values could be ascribed to the interindividual variation such as wrist circumference and health condition. In the one-dimensional study over wrist transverse crease, the range of measured pNO values was in between 0.0243 and 0.0069 mmHg, while the greatest difference between the highest and lowest pNO was 0.0051–0.0149 mmHg depending on the individual subject.

In addition, the pNO levels at eight representative points (No. 1, 2, 4, 5, 6, 7, 8, and 9) were compared with one another. A paired t -test with a Bonferroni correction verifies

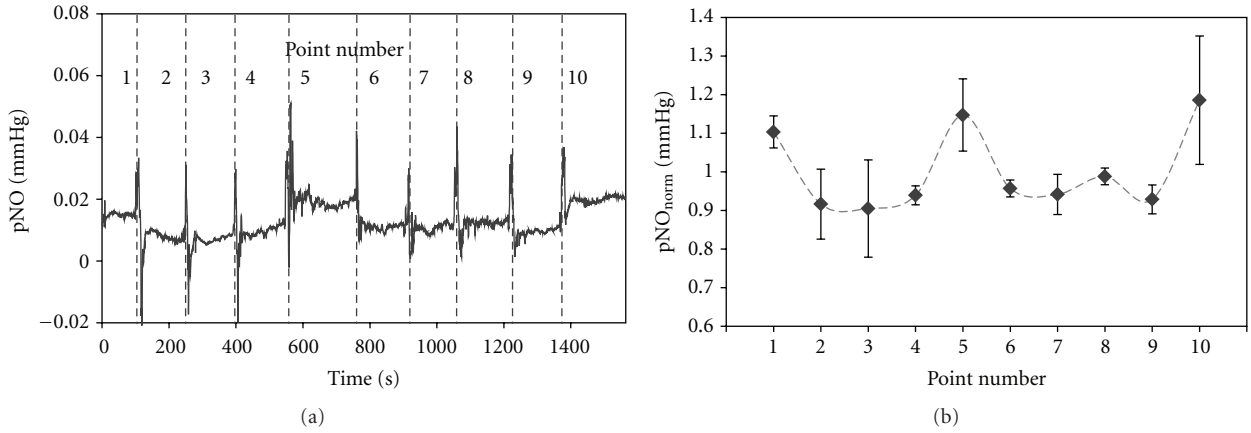


FIGURE 4: (a) A representative pNO measurement along the left wrist transverse crease as shown in Figure 1(b). The pNO values were measured continuously at 10 different points with the one-dimensional sensor movement in the direction of point No. 1 to 10. (b) Averaged pNO_{norm} levels ($n = 5$) for 10 different points. The sensor’s measurements at each point were averaged across five subjects. A paired t -test with a Bonferroni correction was conducted for eight representative points (No. 1, 2, 4, 5, 6, 7, 8, and 9), and the P values are summarized in Table 1.

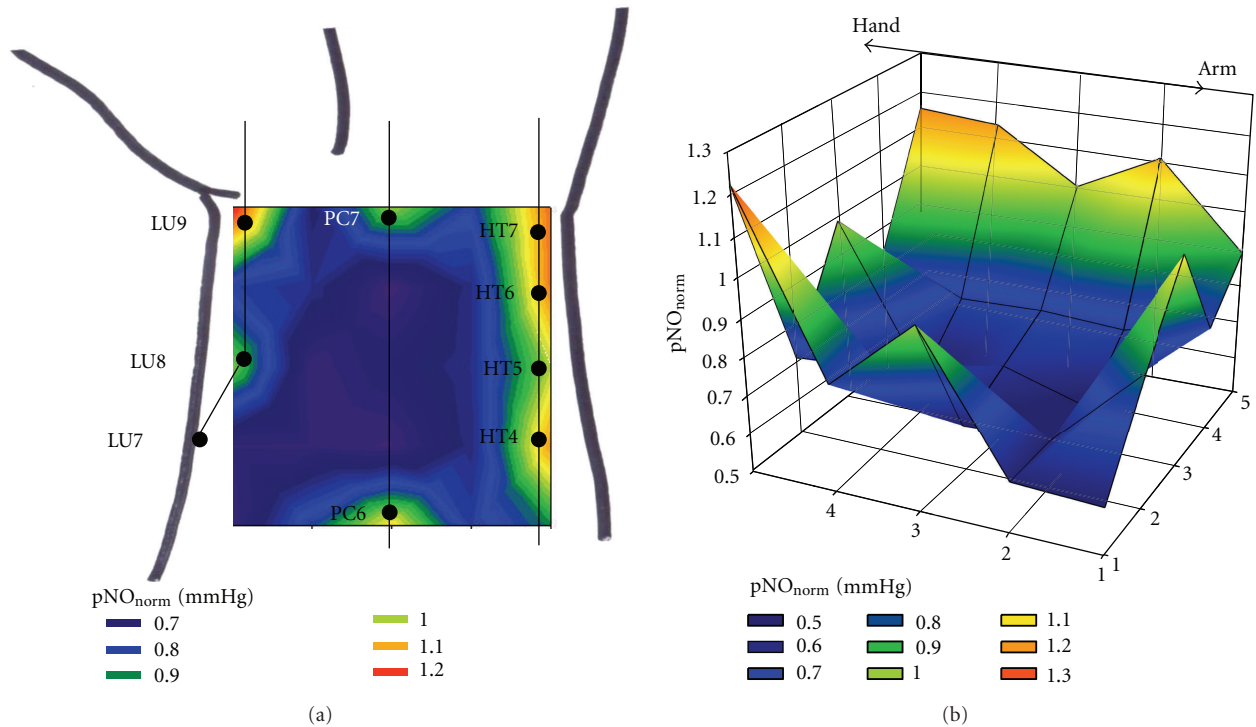


FIGURE 5: (a) 2D and (b) 3D illustrations for the color-coded contour plot of a typical example of the two-dimensional pNO measurement over the left wrist skin. A linear change in the pNO_{norm} values was assumed between two adjacent points.

that the relatively higher pNO values at the points No. 1 and 5 are significantly different from the lower pNO values at the points No. 2, 4, 6, 7, 8, and 9 (Table 1).

Figure 5 is the color-coded contour plots for a typical mapping example of pNO measurement over 25 different points in two-dimensional square area of the wrist as depicted in Figure 1(c). For these contour plots, a linear change in pNO was assumed between two adjacent points. The pNO values were varied depending on the locations,

showing the heterogenous skin pNO distribution. Being in good agreement with the results shown in Figures 3 and 4, the points measured with comparatively higher pNO levels were closely related to the positions of acupuncture points. There are eight acupuncture points present in the wrist skin region where the pNO was measured: LU9 (Taiyuan) and LU8 (Jingqu) on the lung meridian; PC7 (Daling) and PC6 (Neiguan) on the pericardium meridian; HT7 (Shenmen), HT6 (Yinxi), HT5 (Tongli), and HT4 (Lingdao)

TABLE 1: Calculated P values for the paired t -test ($*P < 0.05$).

Point number	P2	P4	P5	P6	P7	P8	P9
P1	0.0315	0.0042*	0.5010	0.0057*	0.0136*	0.0129*	0.0057*
P2		0.6975	0.0375*	0.4950	0.6994	0.2547	0.8391
P4			0.0205*	0.4066	0.9465	0.0616	0.7087
P5				0.0267*	0.0293*	0.0456*	0.02*
P6					0.6622	0.1556	0.3249
P7						0.2262	0.7472
P8							0.0765

on the heart meridian as indicated in Figure 5(a). Since the pNO_{norm} instead of absolute pNO was used for this contour plots, the higher pNO level than the average is easily recognized by the pNO_{norm} value greater than 1. In fact, the $pNO_{norm} > 1$ is found at the points closely located to the area where these acupuncture points are supposed to exist. Although the measured pNO values showed very large inter-individual variation, presumably due to the subject body size difference and physiological condition, similar pNO distribution patterns, that is, higher pNO near acupuncture points, were observed for the entire three subjects.

The observed higher pNO levels near acupuncture points in the present study are well consistent with the previous reports on higher expression of NOS enzyme around skin acupuncture points and meridians of rat [13] and higher concentration of NO metabolite along meridian lines of humans [15]. Our current work provides a clear and direct evidence of the strong relationship between high pNO and acupuncture points by *in vivo* measuring location-dependent pNO in higher spatial resolution with the aid of a highly selective tiny NO microsensor in real time. Since the NO level in atmosphere is negligible, the higher pNO over some specific skin locations suggests the emission of endogenous NO from those skin locations. In fact, the measured pNO is dependent on the sensor-to-skin surface distance, the higher pNO , the shorter sensor-skin separation is, also supporting the skin emission of NO. It should be noted that the pNO difference caused by a slight difference in the sensor-to-skin separation during the experimental course was relatively small (<0.0005 mmHg) compared to the pNO difference between acupuncture and non-acupuncture points (>0.005 mmHg), confirming the reliability of the sensor movement/reposition procedure. Importantly, the observed heterogeneous pNO distribution can be reasonably considered to be true because the pNO change caused by the sensor vertical positioning is much smaller than the location-dependent pNO difference.

There are some reports regarding the connection between gas and acupuncture points: higher pO_2 measured in the tissue below some chosen acupuncture points of rabbit [18] and higher transcutaneous CO_2 emission at 12 acupuncture points on the pericardium meridian of humans [19]. Our group also reported the relatively higher pO_2 levels around acupuncture points of humans [9, 10]. Along with these previous works, the higher pNO levels near acupuncture points possibly suggest the existence of large blood

vessels or main junction underneath the skin acupuncture points. Further research, however, for example, pNO analysis combined with anatomical study of vasculature, needs to be performed to clarify the possible relationship between blood vessels and acupuncture points.

4. Conclusions

The skin surface pNO levels as a function of location were studied using a non-invasive method with the aid of a highly sensitive NO microsensor. Both the comparison study between LI4 acupuncture and non-acupuncture points and one-, two-dimensional mapping studies for the anterior aspect of the left wrist exhibit relatively higher pNO around acupuncture points consistently with statistical significant. The amperometric NO microsensor possessed high sensitivity and small sensing dimension (diameter = $76 \mu m$) is sufficient to monitor pNO level difference depending on the skin surface location. The observed tight relationship between high skin surface pNO levels and the positions of acupuncture points provides direct and scientific evidence on the physical existence of acupuncture points and may contribute to elucidating their possible physiological/biological functions believed in eastern medicine for ages.

Acknowledgment

This research was supported by Basic Science Research Program through the National Research Foundation of Korea (NRF) funded by the Ministry of Education, Science and Technology (2012-0003779 and 2012-0005062).

References

- [1] M. W. Beal, "Acupuncture and Oriental body work: traditional and biomedical concepts in holistic care: history and basic concepts," *Holistic Nursing Practice*, vol. 14, no. 3, pp. 69–78, 2000.
- [2] S. H. H. Chan, "What is being stimulated in acupuncture: evaluation of the existence of a specific substrate," *Neuroscience and Biobehavioral Reviews*, vol. 8, no. 1, pp. 25–33, 1984.
- [3] National Institutes of Health and U.S. Department of Health and Human Services, "Acupuncture: NIH consensus statement," in *Consensus Development Conference Statement*, vol. 15, pp. 1–34, 1997.

- [4] H. M. Johng, J. H. Cho, H. S. Shin et al., "Frequency dependence of impedances at the acupuncture point Quze (PC3)," *IEEE Engineering in Medicine and Biology Magazine*, vol. 21, no. 2, pp. 33–36, 2002.
- [5] M. S. Lee, S. Y. Jeong, Y. H. Lee, D. M. Jeong, Y. G. Eo, and S. B. Ko, "Differences in electrical conduction properties between meridians and non-meridians," *American Journal of Chinese Medicine*, vol. 33, no. 5, pp. 723–728, 2005.
- [6] H. M. Langevin and J. A. Yandow, "Relationship of acupuncture points and meridians to connective tissue planes," *The Anatomical Record*, vol. 269, no. 6, pp. 257–265, 2002.
- [7] W. Ma, H. Tong, W. Xu et al., "Perivascular space: possible anatomical substrate for the meridian," *Journal of Alternative and Complementary Medicine*, vol. 9, no. 6, pp. 851–859, 2003.
- [8] W. A. Rickett, *Guanzi: Political, Economic, and Philosophical Essays from Early China*, Princeton University Press, 1998.
- [9] Y. Lee, G. Lee, S. S. Park, A. Jang, and G.-J. Jhon, "Heterogeneity of skin oxygen density distribution: relation to location of acupuncture points," *JAMS Journal of Acupuncture and Meridian Studies*, vol. 2, no. 4, pp. 269–272, 2009.
- [10] M. Hong, S. S. Park, Y. Ha et al., "Heterogeneity of skin surface oxygen level of wrist in relation to acupuncture point," *Evidence-Based Complementary and Alternative Medicine*, vol. 2012, Article ID 106762, 7 pages, 2012.
- [11] F. M. Faraci, "Role of nitric oxide in regulation of basilar artery tone in vivo," *American Journal of Physiology*, vol. 259, no. 4, pp. H1216–H1221, 1990.
- [12] M. Sandberg, T. Lundberg, L. G. Lindberg, and B. Gerdle, "Effects of acupuncture on skin and muscle blood flow in healthy subjects," *European Journal of Applied Physiology*, vol. 90, no. 1-2, pp. 114–119, 2003.
- [13] S. X. Ma, "Enhanced nitric oxide concentrations and expression of nitric oxide synthase in acupuncture points/meridians," *Journal of Alternative and Complementary Medicine*, vol. 9, no. 2, pp. 207–215, 2003.
- [14] D. Ralt, "Intercellular communication, NO and the biology of Chinese medicine," *Cell Communication and Signaling*, vol. 3, article 8, 2005.
- [15] S.-X. Ma, X.-Y. Li, T. Sakurai, and M. Pandjaitan, "Evidence of enhanced non-enzymatic generation of nitric oxide on the skin surface of acupuncture points: an innovative approach in humans," *Nitric Oxide*, vol. 17, no. 2, pp. 60–68, 2007.
- [16] Y. Lee, B. K. Oh, and M. E. Meyerhoff, "Improved planar amperometric nitric oxide sensor based on platinized platinum anode. 1. experimental results and theory when applied for monitoring NO release from diazeniumdiolate-doped polymeric films," *Analytical Chemistry*, vol. 76, no. 3, pp. 536–544, 2004.
- [17] S. E. Manahan, *Environmental Chemistry*, CRC Press, Boca Raon, Fla, USA, 8th edition, 2004.
- [18] W. Xu, W. Ma, K. Li et al., "A needle-electrochemical micro-sensor for in vivo measurement of the partial pressure of oxygen in acupuncture points," *Sensors and Actuators B*, vol. 86, no. 2-3, pp. 174–179, 2002.
- [19] W. B. Zhang, Y. Y. Tian, Z. X. Zhu, and R. M. Xu, "The distribution of transcutaneous CO₂ emission and correlation with the points along the pericardium meridian," *JAMS Journal of Acupuncture and Meridian Studies*, vol. 2, no. 3, pp. 197–201, 2009.

Research Article

Evaluate Laser Needle Effect on Blood Perfusion Signals of Contralateral Hegu Acupoint with Wavelet Analysis

Guangjun Wang,¹ Yuying Tian,¹ Shuyong Jia,¹ Gerhard Litscher,^{1,2} and Weibo Zhang¹

¹Institute of Acupuncture and Moxibustion, China Academy of Chinese Medical Sciences, Beijing 100700, China

²Stronach Research Unit for Complementary and Integrative Laser Medicine, Research Unit of Biomedical Engineering in Anesthesia and Intensive Care Medicine, and TCM Research Center Graz, Medical University of Graz, Auenbruggerplatz 29, 8036 Graz, Austria

Correspondence should be addressed to Weibo Zhang, zhangweibo@hotmail.com

Received 7 June 2012; Revised 1 August 2012; Accepted 3 August 2012

Academic Editor: Wolfgang Schwarz

Copyright © 2012 Guangjun Wang et al. This is an open access article distributed under the Creative Commons Attribution License, which permits unrestricted use, distribution, and reproduction in any medium, provided the original work is properly cited.

Our previous studies suggested that the MBF in contralateral Hegu acupoint (LI4) increased after ipsilateral Hegu acupoint was stimulated with manual acupuncture. In this study, twenty-eight (28) healthy volunteers were recruited and were randomly divided into Hegu acupoint stimulation group and Non-Hegu stimulation group. All subjects received the same model stimulation of the laser needle for 30 min in right Hegu acupoint and Non-Hegu acupoint, respectively. MBF of left LI4 was measured by the laser Doppler perfusion imaging system. The original data dealt with morlet wavelet analysis and the average amplitude and power spectral density of different frequency intervals was acquired. The results indicated that right Hegu stimulation with the laser needle might result in the increase of left Hegu acupoint MBF. 40 min later after ceased stimulation, the MBF is still increasing significantly, whereas the MBF has no significantly change in Non-Hegu stimulation group. The wavelet analysis result suggested that compared to Non-Hegu stimulation, stimulated to right Hegu acupoint might result in the increase of average amplitude in frequency intervals of 0.0095–0.02 Hz, 0.02–0.06 Hz, and 0.06–0.15 Hz, which might be influenced by the endothelial, neurogenic, and the intrinsic myogenic activity of the vessel wall, respectively.

1. Introduction

Acupuncture has been widely used to the treatment of diseases in clinical practice at least for 2000 years [1]. According to the principles of *Huang Di Nei Jing Su Wen* [2], acupuncture effects might be related to the appropriate acupoints selection during the treatment. However, many researchers firmly believe that placebo effect may be the best explanation for acupuncture [3]. A large number of clinical trials have reported that true acupuncture is superior to usual care, but is not significantly better than sham acupuncture, findings apparently at odds with acupoint specificity [4]. On the contrary, many researchers pointed out that distribution of blood perfusion has specificity in acupoint and meridians compared with no acupoint or no meridian areas. Assuming the acupoint was stimulated adequately, the blood flow of this point increased whereas the blood flow of non-acupoint only changed slightly by the same stimulation [5]. Needling

the LI4 significantly increased perfusion at Hegu acupoint but not at nearby nonacupoint [6].

Our previous studies have shown that thermostimulation could result in an increase of blood perfusion not only in the local area, but also in the same area of contralateral side. This phenomenon can be observed both in the upper limb and lower limb, but not around the periumbilicus area. It indicated that bilateral blood perfusion of same area might be special relationships. We have reported that stimulation on side LI4 by the manual acupuncture might result in the increase of blood perfusion on the contralateral LI4, which indicated that there might be intrinsic correlation between contra and ipsilateral parts [7, 8]. Our work was supported by Kubo et al. [9]. Furthermore, we explored the MBF of bilateral LI4 with system identification algorithm and found that the LI4 has lateralized specificity. Stimulating right LI4 by manual acupuncture might produce the more forceful amplifactory effect than stimulating left LI4 [7, 8].

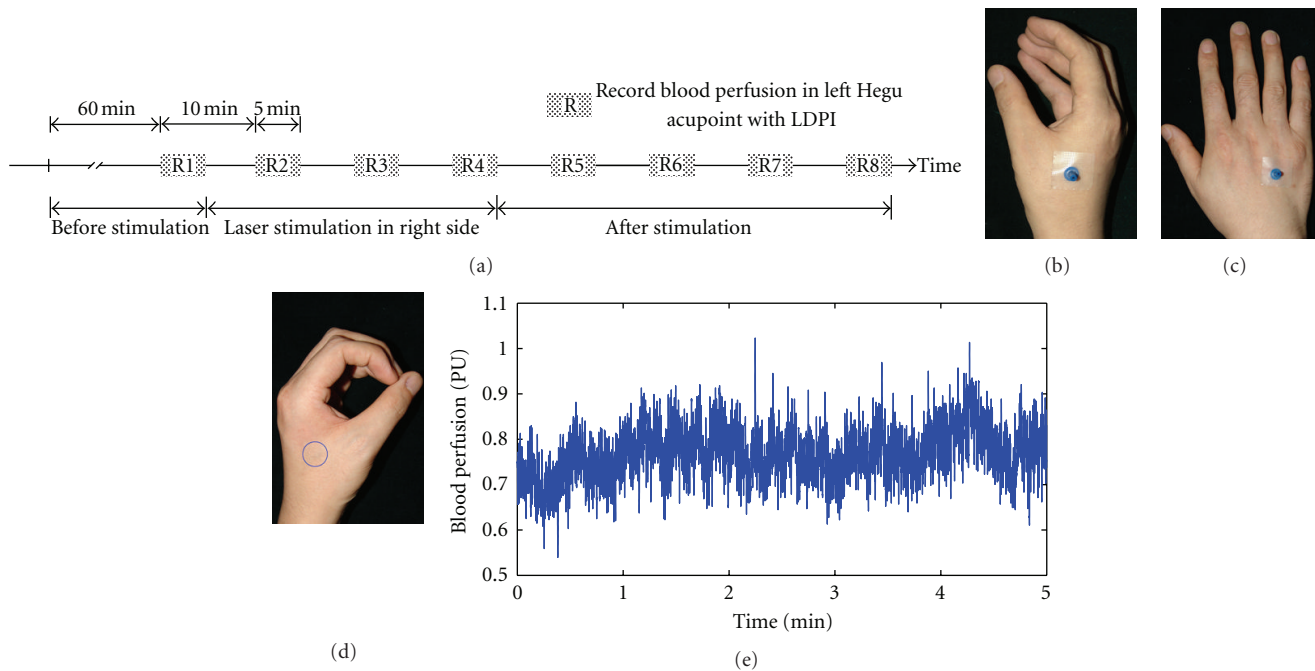


FIGURE 1: Illustration of the study design. Measurement and stimulation procedures (a); Hegu acupoint stimulation site (b); Non-Hegu stimulation site (c); measurement site of left Hegu acupoint marked as blue circle (d); the original signal of blood flux (e).

Recently, the laser needle as an alternative method of manual acupuncture was used in many studies because it is effective not only as a treatment method, but also as a research tool [10–12]. It can simulate traditional acupuncture while reducing the stress effect resulted from the mental needle. So in this study, we select laser needle as stimulation tool and observe the contralateral effect which resulted from laser acupuncture.

2. Methods

2.1. Ethics Statement. This study was reviewed and approved by the Institutional Review Board of the Institute of Acupuncture and Moxibustion, China Academy of Chinese Medical Sciences. Each study participant read and signed an informed consent form.

2.2. Subjects. Twenty-eight (28) healthy volunteers were recruited in this study. All subjects were students from the China Academy of Chinese Medical Sciences and Beijing University of TCM and all of them had no history of diseases and had not taken any medicine in the past six months before study. The detail information of subjects is shown in Table 1. Each subject provided informed consent and had an adequate understanding of the procedure and purpose of this study.

2.3. Protocol for MBF Measurement. Before arrival to the laboratory, subjects were placed in a temperature-controlled

room (24–26°C) as a resting state for 60 minutes. Measurements of skin blood perfusion in left LI4 (as shown in Figure 1(d)) were carried out using laser doppler perfusion imager (LDPI, PeriScan PIM II system, Perimed AB, Sweden). Before recording, left hands were immobilized with a cylindrical object to ensure positioning. The measurement parameters were as follows: NR model; duplex mode; one measurement site; 100 Hz sample rate. Measurement was carried out every 5 minutes over a total of 80 min (as shown in Figure 1(a)). During the experiment, the laboratory room was kept in dark light condition and the protocol for measurement operation was abided strictly. In recording process, ensuring the laser beam was inside the selected area marked by a blue circle (Figure 1(d)). MBF (symbolized as \bar{R}_i ($i = 1, 2, 3, \dots, 8$)) was defined as mean of blood flux in 5 min. The change of MBF was defined as $(\bar{R}_i - \bar{R}_1)/\bar{R}_1$ ($i = 1, 2, 3, \dots, 8$).

2.4. Laser Acupuncture Protocol. For acupuncture, the position of LI4 was confirmed according to the previous studies [13, 14], as shown in Figure 1(b). Non-Hegu position was defined as between thirty-four metacarpal, in the same plane of LI4 (Figure 1(c)). In H-S group and N-HS group, the laser needle was attached to right LI4 and Non-Hegu position, respectively. Just in the H-S group, the appliance was switched on, and the lasers were activated. The radiation model is continuous radiation (CW) and radiation power is ca. 50 mW. The radiation time keeps 30 min continuously (Figure 1(a)).

TABLE 1: Subjects' gender composition, average age, and body mass index.

Group	n	Gender (female/male)	Age (years, mean \pm SD)	Body mass index (mean \pm SD)
H-S group	14	13/1	24.36 \pm 2.06	21.35 \pm 3.19
NH-S group	14	11/3	24.43 \pm 1.74	20.61 \pm 1.66

H-S: Hegu acupoint stimulation; NH-S: Non-Hegu acupoint stimulation.

TABLE 2: MBF in different group (PU, Mean \pm SEM).

Record point	H-S group	NH-S group
R1	0.587 \pm 0.041	0.716 \pm 0.071
R4	0.651 \pm 0.031**	0.744 \pm 0.046
R8	0.731 \pm 0.032###	0.784 \pm 0.046

** $P < 0.01$ R4 versus R1; ### $P < 0.01$ R8 versus R4.

TABLE 3: Change of MBF in different group (Mean \pm SEM).

Record point	H-S group	NH-S group
R1	0.000 \pm 0.000	0.000 \pm 0.000
R2	0.068 \pm 0.016	0.035 \pm 0.038
R3	0.113 \pm 0.031	0.062 \pm 0.037
R4	0.142 \pm 0.042	0.089 \pm 0.045
R5	0.165 \pm 0.050	0.121 \pm 0.063
R6	0.241 \pm 0.056	0.156 \pm 0.057
R7	0.275 \pm 0.059	0.180 \pm 0.075
R8	0.294 \pm 0.062	0.175 \pm 0.077

Change of MBF in different time point is defined as $(\bar{R}_i - \bar{R}_1)/\bar{R}_1$ ($i = 1, 2, 3, \dots, 8$).
 $P > 0.05$.

2.5. Data Analysis. For every record epoch of 5 min, the MBF was calculated to elucidate the effect of contralateral laser needle stimulation. According to previous studies, microvascular blood perfusion signal can be separated into five components, which were influenced by the endothelial activity, the neurogenic activity, the intrinsic myogenic activity, the respiration, and the heartbeat, respectively [6, 15–17]. Morlet mother wavelet was applied to improve the low-frequency resolution. In frequency domain, five characteristic frequency components were separated by 0.0095–0.02, 0.02–0.06, 0.06–0.15, 0.15–0.4, and 0.4–1.6 Hz frequency bands (symbolized as FR1 to FR5, resp.) and the average amplitude (symbolized as \bar{A}_i ($i = 1, 2, 3, \dots, 8$)) in every frequency band was calculated with morlet wavelet analysis method [6]. The change of average amplitude was defined as $(\bar{A}_i - \bar{A}_1)/\bar{A}_1$ ($i = 1, 2, 3, \dots, 8$). The energy distribution was symbolized as P_i ($i = 1, 2, 3, \dots, 8$) in every frequency band, and for every FR, the change of energy distribution from R1 to R8 which defined as $(P_i - P_1)/P_1$ ($i = 1, 2, 3, \dots, 8$) was also calculated. All signal processing was performed with MATLAB (MathWorks, Natick, MA, USA). Two-tailed paired t -test and independent t -test were used to verify the statistical significance. Differences were considered significant when $P < 0.05$.

3. Results

3.1. MBF Response. The MBF in different time was compared both in H-S group and NH-S Group (as shown in Table 2 and Figure 2). In H-S group, the MBF of left Hegu acupoint was significantly increased after laser stimulation ($P < 0.01$, R1 versus R4, paired t -test). 40 min later after ceased laser stimulation, the MBF was significantly increased ($P < 0.01$, R4 versus R8, paired t -test). However, in NH-S group, there is no significant increase of MBF both in R1 versus R4 and in R4 versus R8 (Table 2 and Figure 2(a)). In every time point, there is no significant difference in change of MBF between H-S and NH-S groups (as shown in Table 3 and Figure 2(b)).

3.2. LDF Flux Spectra. The result of wavelet analysis is shown in Table 4 and Figure 3. The time-frequency relationship is shown in Figure 3(a), and the frequency-amplitude relationship is shown in Figure 3(b). Change of average amplitude in the different frequency intervals following laser stimulation at the different time points is compared in Figure 4. 40 min later after ceased laser stimulation, the change of average amplitude in frequency intervals of FR1 (0.0095–0.02 Hz), FR2 (0.02–0.06), and FR3 (0.06–0.15) was significantly different between H-S group and NH-S group ($P < 0.05$, two-tailed t -test), as shown in Table 4 and

TABLE 4: Change of average amplitude in different frequency intervals (Mean \pm SEM).

Frequency intervals	Record point	H-S group	NH-S group
FR1	R1	0.000 \pm 0.000	0.000 \pm 0.000
	R2	0.722 \pm 0.323	0.722 \pm 0.947
	R3	0.338 \pm 0.266	0.029 \pm 0.253
	R4	1.032 \pm 0.480	0.476 \pm 0.475
	R5	1.505 \pm 0.928	0.234 \pm 0.374
	R6	0.923 \pm 0.426	0.398 \pm 0.369
	R7	1.886 \pm 1.495	0.105 \pm 0.280
	R8	1.399 \pm 0.543*	0.076 \pm 0.329
FR2	R1	0.000 \pm 0.000	0.000 \pm 0.000
	R2	0.498 \pm 0.225	1.174 \pm 1.267
	R3	0.358 \pm 0.201	0.086 \pm 0.213
	R4	0.875 \pm 0.320	0.422 \pm 0.332
	R5	0.791 \pm 0.432	0.241 \pm 0.273
	R6	0.808 \pm 0.273	0.255 \pm 0.228
	R7	1.225 \pm 0.975	0.265 \pm 0.259
	R8	1.293 \pm 0.417*	0.103 \pm 0.222
FR3	R1	0.000 \pm 0.000	0.000 \pm 0.000
	R2	0.253 \pm 0.134	0.989 \pm 1.031
	R3	0.296 \pm 0.126	0.073 \pm 0.131
	R4	0.577 \pm 0.206	0.165 \pm 0.141
	R5	0.423 \pm 0.203	0.115 \pm 0.231
	R6	0.567 \pm 0.195	0.074 \pm 0.145
	R7	0.737 \pm 0.580	0.295 \pm 0.324
	R8	0.853 \pm 0.276*	0.056 \pm 0.192
FR4	R1	0.000 \pm 0.000	0.000 \pm 0.000
	R2	0.089 \pm 0.090	0.643 \pm 0.669
	R3	0.234 \pm 0.097	0.086 \pm 0.114
	R4	0.369 \pm 0.145	0.124 \pm 0.114
	R5	0.187 \pm 0.106	0.101 \pm 0.206
	R6	0.281 \pm 0.111	0.109 \pm 0.135
	R7	0.356 \pm 0.293	0.242 \pm 0.298
	R8	0.455 \pm 0.168	0.035 \pm 0.169
FR5	R1	0.000 \pm 0.000	0.000 \pm 0.000
	R2	0.051 \pm 0.043	0.282 \pm 0.298
	R3	0.126 \pm 0.050	0.101 \pm 0.112
	R4	0.193 \pm 0.065	0.098 \pm 0.104
	R5	0.086 \pm 0.057	0.133 \pm 0.184
	R6	0.148 \pm 0.051	0.141 \pm 0.127
	R7	0.175 \pm 0.135	0.223 \pm 0.263
	R8	0.251 \pm 0.086	0.051 \pm 0.146

* $P < 0.05$, H-S group versus NH-S group; The change of average amplitude is defined as $(\bar{A}_i - \bar{A}_1)/\bar{A}_1 (i = 1, 2, 3, \dots, 8)$.

Figures 4(a), 4(b), and 4(c). In other time point and other frequency intervals, there are no significant differences between H-S group and NH-S group (as shown in Table 4 and Figures 4(d) and 4(e)). The result of energy distribution was shown in Table 5 and Figure 5. It can be found that the change of energy distribution in frequency intervals of FR2 (0.02–0.06) and FR3 (0.06–0.15) was significantly different between H-S group and NH-S group ($P < 0.05$, two-tailed t -test).

4. Discussion

Up to now, it is difficult to evaluate the activation of acupoints, and as a result, it is also difficult to analyse the specificity of acupoints after meridians stimulated. Recently, more and more attention has been focused on the relationship of acupuncture and circulation [18–20]. In Traditional Chinese Medical (TCM) theory, one of the definitive causes of acupuncture effect is the special sensation

TABLE 5: Change of energy distribution in different frequency intervals (Mean \pm SEM).

Frequency intervals	Record point	H-S group	NH-S group
FR1	R1	0.000 \pm 0.000	0.000 \pm 0.000
	R2	0.877 \pm 0.420	1.104 \pm 1.162
	R3	0.558 \pm 0.368	0.715 \pm 0.706
	R4	1.831 \pm 0.956	1.280 \pm 1.268
	R5	2.965 \pm 1.798	0.870 \pm 0.854
	R6	1.169 \pm 0.506	0.394 \pm 0.357
	R7	3.086 \pm 2.635	0.937 \pm 1.022
	R8	2.416 \pm 1.095	0.679 \pm 0.988
FR2	R1	0.000 \pm 0.000	0.000 \pm 0.000
	R2	0.527 \pm 0.362	4.479 \pm 4.244
	R3	0.463 \pm 0.232	0.384 \pm 0.342
	R4	0.981 \pm 0.352	0.767 \pm 0.322
	R5	0.596 \pm 0.331	0.633 \pm 0.355
	R6	1.046 \pm 0.358	0.576 \pm 0.321
	R7	1.678 \pm 1.347	0.728 \pm 0.489
	R8	1.850 \pm 0.619*	0.438 \pm 0.262
FR3	R1	0.000 \pm 0.000	0.000 \pm 0.000
	R2	0.293 \pm 0.121	1.305 \pm 1.302
	R3	0.357 \pm 0.127	0.080 \pm 0.152
	R4	0.555 \pm 0.179	0.126 \pm 0.138
	R5	0.481 \pm 0.179	0.092 \pm 0.268
	R6	0.543 \pm 0.223	-0.006 \pm 0.152
	R7	0.934 \pm 0.709	0.279 \pm 0.386
	R8	0.766 \pm 0.290*	0.028 \pm 0.208
FR4	R1	0.000 \pm 0.000	0.000 \pm 0.000
	R2	-0.093 \pm 0.082	0.422 \pm 0.341
	R3	0.233 \pm 0.141	0.154 \pm 0.105
	R4	0.171 \pm 0.109	0.198 \pm 0.114
	R5	0.045 \pm 0.102	0.082 \pm 0.129
	R6	0.072 \pm 0.108	0.209 \pm 0.146
	R7	0.195 \pm 0.167	0.139 \pm 0.103
	R8	0.209 \pm 0.167	0.102 \pm 0.145
FR5	R1	0.000 \pm 0.000	0.000 \pm 0.000
	R2	0.098 \pm 0.035	0.010 \pm 0.088
	R3	0.124 \pm 0.036	0.039 \pm 0.126
	R4	0.154 \pm 0.047	0.004 \pm 0.098
	R5	0.078 \pm 0.035	0.093 \pm 0.177
	R6	0.163 \pm 0.044	0.101 \pm 0.144
	R7	0.138 \pm 0.063	0.185 \pm 0.248
	R8	0.201 \pm 0.054	0.019 \pm 0.127

* $P < 0.05$, H-S group versus NH-S group.

in local acupoint after stimulation, which might be related to the blood perfusion changes in acupoints or meridians [13]. According to the previous study, the MBF was larger at the acupoints than in their surrounding tissues, which indicates that the MBF can be used as an index for discriminating differences in the microcirculatory conditions between acupoints and their surrounding tissues [21]. It

has also been shown that acupuncture cannot only increase general circulation [22] and circulation in specific organs [23], but change the skin microcirculation as well [14, 19, 24, 25]. When an acupoint was stimulated adequately, the blood perfusion of this point continued to increase, whereas the blood perfusion of non-acupoint only changed slightly by the same acupuncture stimulation [5]. These results indicated

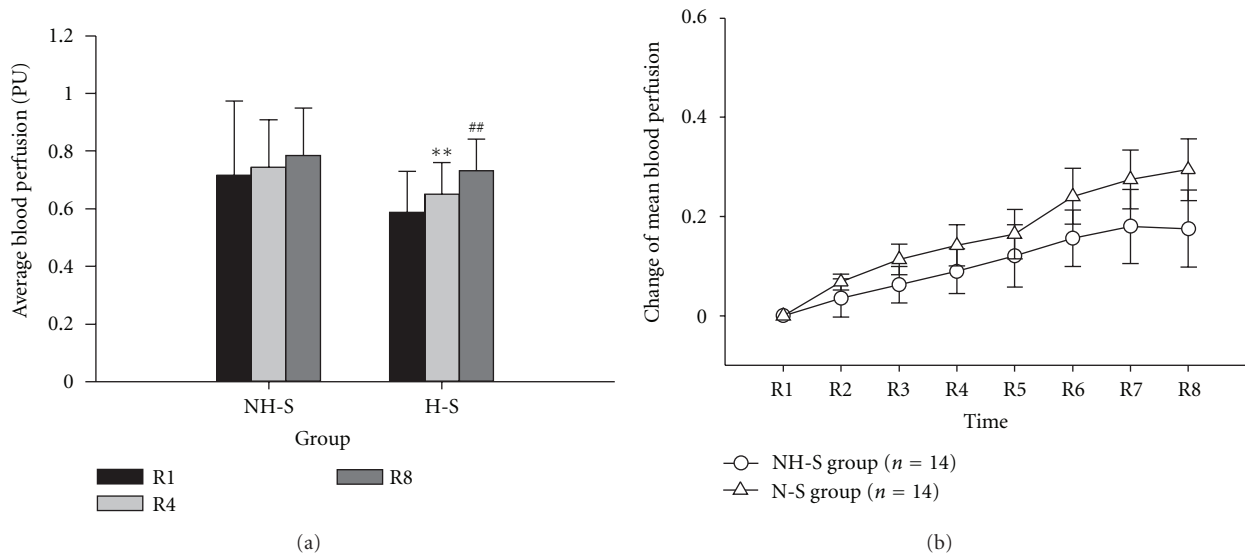


FIGURE 2: Change of MBF in left Hegu acupoint. All data expressed as Mean \pm SEM. NH-S: Non-Hegu stimulation; H-S: Hegu acupoint stimulation; (a) shows the average blood flux in NH-S group and H-S group, $**P < 0.01$, R1 versus R4; $##P < 0.01$, R4 versus R8. (b) shows the change of MBF in different time period, which defined as $(\bar{R}_i - \bar{R}_1)/\bar{R}_1$ ($i = 1, 2, 3, \dots, 8$). In every time, the change of MBF between two group has not significant difference ($P > 0.05$).

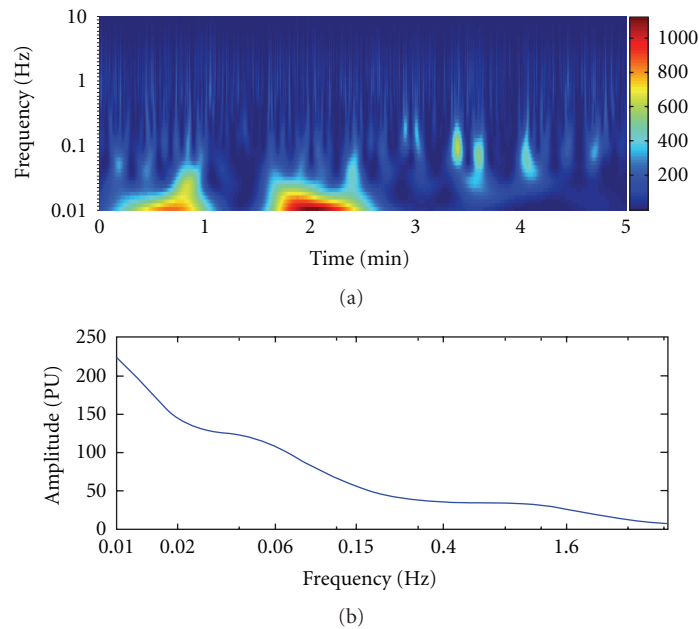


FIGURE 3: Morlet wavelet analysis result of original signal. (a) shows the time-frequency relationship; (b) shows the frequency-amplitude relationship.

that the blood perfusion in acupoints can be recommended as a candidate index for acupuncture effect evaluation.

Recently, Laser Doppler flowmetry (LDF) is widely used for monitoring the microcirculation due to its advantages of a good frequency response and is suited for noninvasive

investigations of microvascular responses to acupuncture [18, 26]. In this study, the result suggested that stimulated right LI4 with laser needle and the BMF in left Hegu acupoint increased significantly, which brings into correspondence with our previous study [27, 28]. In this study, when laser

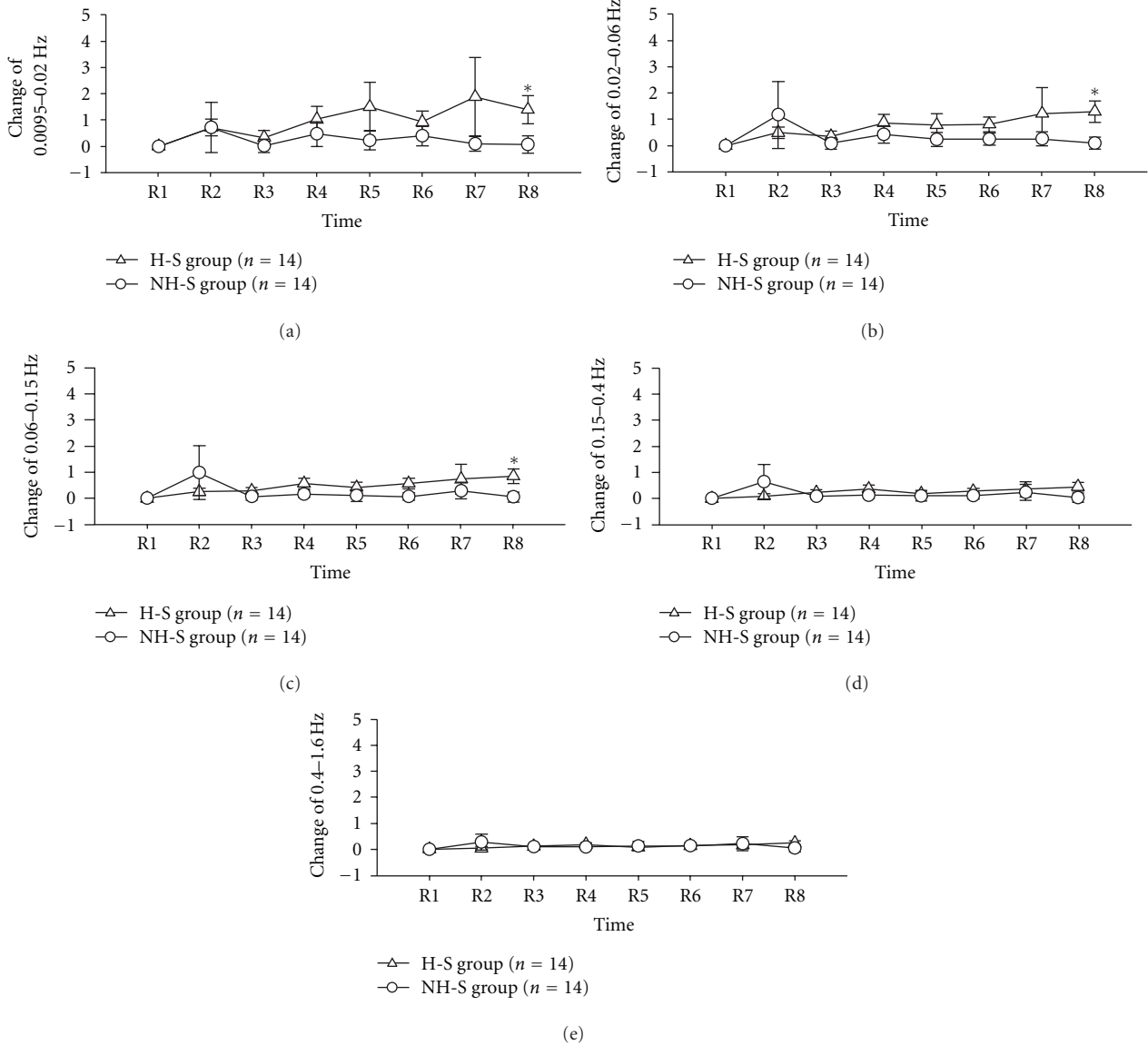


FIGURE 4: Change of average amplitude in left Hegu acupoint. The change of average amplitude is defined as $(\bar{A}_i - \bar{A}_1)/\bar{A}_1$ ($i = 1, 2, 3, \dots, 8$). All data expressed as Mean \pm SEM. NH-S: Non-Hegu stimulation; H-S: Hegu acupoint stimulation; (a) shows the frequency interval of 0.0095–0.02 Hz; (b) shows the frequency interval of 0.02–0.06 Hz; (c) shows the frequency interval of 0.06–0.15 Hz; (d) shows the frequency interval of 0.15–0.4 Hz; (e) shows the frequency interval of 0.4–1.6 Hz; * $P < 0.05$, H-S versus NH-S.

stimulation was ceased, the MBF increased in the symmetric area, while Non-Hegu acupoint stimulation has no effect in left LI4, which suggested that the laser needle effect might have area specificity.

Spectral analysis of LDF signals reveals that blood-flow oscillations at frequencies from 0.009 to 1.6 Hz might reflect various physiological rhythms [17, 29]. In this study, LDF signals spectral were analyzed with morlet wavelet analysis [6, 14, 19]. The results indicated that right LI4 stimulation with laser needle just affect the amplitude of FR1, FR2, and FR3, which can be influenced by the endothelial, neurogenic, and the intrinsic myogenic activity of vascular smooth muscle, respectively. After analyzed energy distribution, we found from R1 to R8 that the change of energy in different

FRs has the same change trend as amplitude. In accord with the suggestion that the skin microvasculature mirrors the vascular function of other parts of the body [30–32], we also can suppose that the vascular function of left LI4 is the mirror of the right LI4, or partly the mirror of right LI4. From our study, the FR1, FR2, and FR3 take part in the action of laser stimulation, which means that the endothelial activity, the neurogenic activity, and the intrinsic myogenic activity might be the candidates of the underlying physiological mechanism of this function mirror. Compared to NH-S group, the laser needle effect observed 80 min later after laser stimulation, which suggested that laser stimulation in special acupoint might have resulted in slow

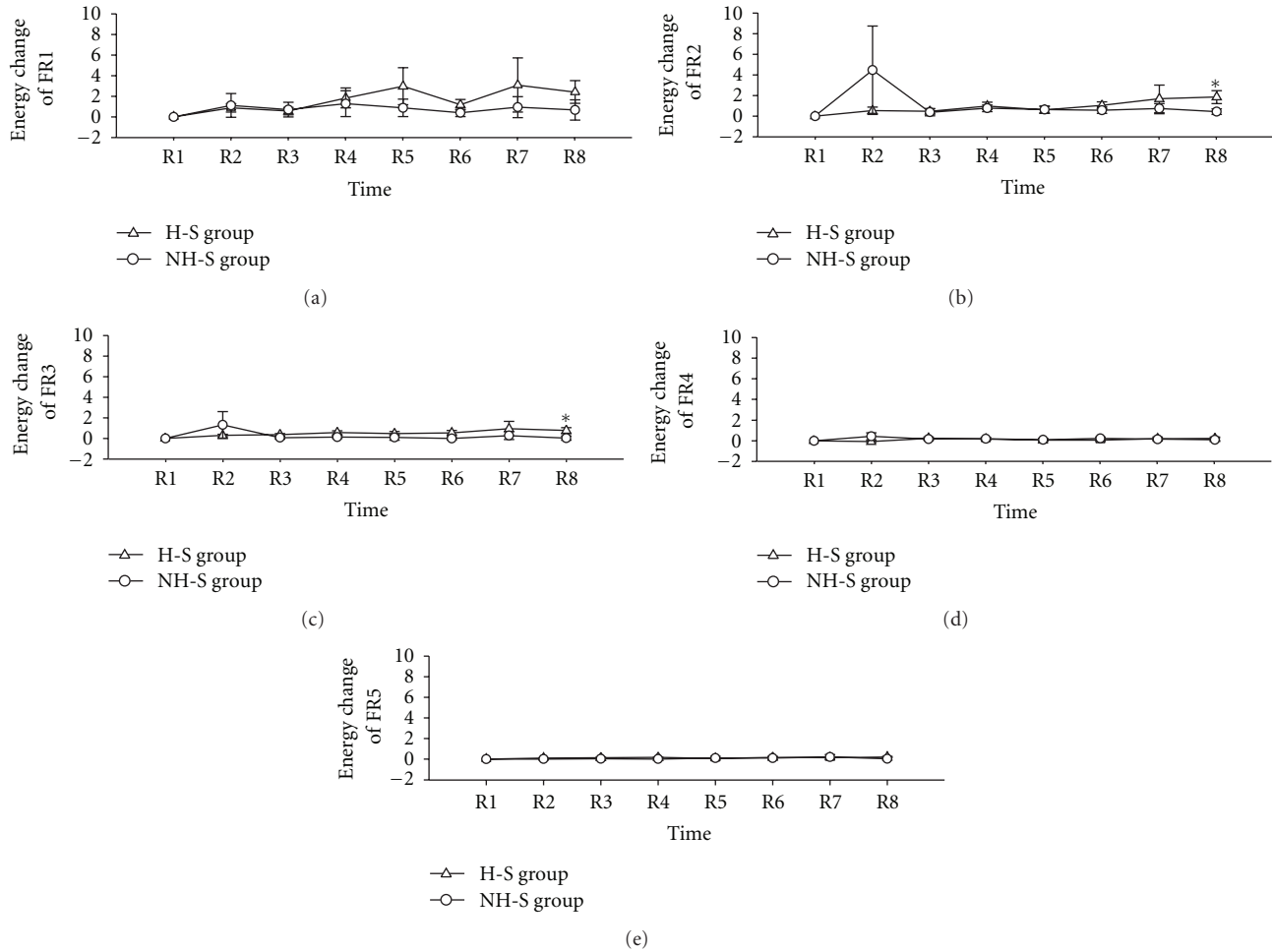


FIGURE 5: Change of energy distribution in left Hegu acupoint. The energy distribution in every frequency band was symbolized as P_i ($i = 1, 2, 3, \dots, 8$), and for every FR, the change of energy distribution from R1 to R8 was defined as $(P_i - P_1)/P_1$ ($i = 1, 2, 3, \dots, 8$). All data expressed as Mean \pm SEM. NH-S: Non-Hegu stimulation; H-S: Hegu acupoint stimulation; (a) shows the frequency interval of 0.0095–0.02 Hz; (b) shows the frequency interval of 0.02–0.06 Hz; (c) shows the frequency interval of 0.06–0.15 Hz; (d) shows the frequency interval of 0.15–0.4 Hz; (e) shows the frequency interval of 0.4–1.6 Hz; * $P < 0.05$, H-S versus NH-S.

and complicated reaction and this mirror function is not happened at once after stimulation.

Conflict of Interests

The authors declare that they have no competing interests.

Acknowledgments

The authors are grateful to Dr. Li Zhe and Dr. Che Yanqiu for providing the matlab code for data analysis and to Dr Zhou Mei for her useful comments on the data analysis with Matlab software. This research was supported by the National Natural Science Foundation of China (Grant no. 81001553) and a Sino-Austrian cooperating project on high-tech acupuncture. The research activities at the TCM Research Center Graz are partly supported by the German Academy of Acupuncture (President Dr. Gerhard Opitz). Professor G. Litscher is also a Visiting Professor at the

Institute of Acupuncture and Moxibustion at the China Academy of Chinese Medical Sciences.

References

- [1] G. D. Lu and J. Needham, *Celestial Lancets: A History and Rationale of Acupuncture and Moxa*, Cambridge University Press, New York, NY, USA, 1980.
- [2] P. U. Unschuld, *Huang Di Nei Jing Su Wen: Nature, Knowledge, Imagery in an Ancient Chinese Medical Text, with an Appendix, the Doctrine of the Five Periods and Six Qi in the HuAng Di Nei Jing Su Wen*, University of California Press, Berkeley, Calif, USA, 2003.
- [3] M. Rossi, A. Carpi, C. Di Maria, F. Franzoni, F. Galetta, and G. Santoro, "Skin blood flowmotion and microvascular reactivity investigation in hypercholesterolemic patients without clinically manifest arterial diseases," *Physiological Research*, vol. 58, no. 1, pp. 39–47, 2009.
- [4] H. M. Langevin, P. M. Wayne, H. MacPherson et al., "Paradoxes in acupuncture research: strategies for moving forward,"

- Evidence-based Complementary and Alternative Medicine*, vol. 2011, Article ID 180805, 11 pages, 2011.
- [5] T. C. Kuo, Z. S. Chen, C. H. Chen, F. M. Ho, C. W. Lin, and Y. J. Chen, "The physiological effect of DE QI during acupuncture," *Journal of Health Science*, vol. 50, no. 4, pp. 336–342, 2004.
 - [6] H. Hsiu, W. C. Hsu, C. L. Hsu, and S. M. Huang, "Assessing the effects of acupuncture by comparing needling the hegu acupoint and needling nearby nonacupoints by spectral analysis of microcirculatory laser Doppler signals," *Evidence-Based Complementary and Alternative Medicine*, vol. 2011, Article ID 435928, 9 pages, 2011.
 - [7] G. J. Wang, Y. Y. Tian, S. Y. Jia, T. Huang, and W. B. Zhang, "Change of blood perfusion in hegu acupoint after contralateral hegu acupoint was stimulated," *The Journal of Alternative and Complementary Medicine*, vol. 18, no. 8, pp. 784–788, 2012.
 - [8] G. Wang, J. Han, G. Litscher, and W. Zhang, "System identification algorithm analysis of acupuncture effect on mean blood flux of contralateral hegu acupoint," *Evidence-Based Complementary and Alternative Medicine*, vol. 2012, Article ID 951928, 7 pages, 2012.
 - [9] K. Kubo, H. Yajima, M. Takayama, T. Ikebukuro, H. Mizoguchi, and N. Takakura, "Changes in blood circulation of the contralateral Achilles tendon during and after acupuncture and heating," *International Journal of Sports Medicine*, vol. 32, no. 10, pp. 807–813, 2011.
 - [10] G. Litscher and G. Opitz, "Technical parameters for laser acupuncture to elicit peripheral and central effects: state-of-the-art and short guidelines based on results from the medical university of Graz, the German Academy of Acupuncture, and the scientific literature," *Evidence-Based Complementary and Alternative Medicine*, vol. 2012, Article ID 697096, 5 pages, 2012.
 - [11] G. Litscher, G. Bauernfeind, G. Mueller-Putz, and C. Neuper, "Laser-induced evoked potentials in the brain after nonperceptible optical stimulation at the neiguan acupoint: a preliminary report," *Evidence-Based Complementary and Alternative Medicine*, vol. 2012, Article ID 292475, 6 pages, 2012.
 - [12] G. Litscher, "Integrative laser medicine and high-tech acupuncture at the medical university of Graz, Austria, Europe," *Evidence-Based Complementary and Alternative Medicine*, vol. 2012, Article ID 103109, 21 pages, 2012.
 - [13] T. C. Kuo, C. W. Lin, and F. M. Ho, "The soreness and numbness effect of acupuncture on skin blood flow," *American Journal of Chinese Medicine*, vol. 32, no. 1, pp. 117–129, 2004.
 - [14] H. Hsiu, W. C. Hsu, B. H. Chen, and C. L. Hsu, "Differences in the microcirculatory effects of local skin surface contact pressure stimulation between acupoints and nonacupoints: possible relevance to acupressure," *Physiological Measurement*, vol. 31, no. 6, pp. 829–841, 2010.
 - [15] C. E. Thorn, S. J. Matcher, I. V. Meglinski, and A. C. Shore, "Is mean blood saturation a useful marker of tissue oxygenation?" *American Journal of Physiology—Heart and Circulatory Physiology*, vol. 296, no. 5, pp. H1289–H1295, 2009.
 - [16] A. Bernjak, P. B. M. Clarkson, P. V. E. McClintock, and A. Stefanovska, "Low-frequency blood flow oscillations in congestive heart failure and after β 1-blockade treatment," *Microvascular Research*, vol. 76, no. 3, pp. 224–232, 2008.
 - [17] P. Kvandal, S. A. Landsverk, A. Bernjak, A. Stefanovska, H. D. Kvernmo, and K. A. Kirkebøen, "Low-frequency oscillations of the laser Doppler perfusion signal in human skin," *Microvascular Research*, vol. 72, no. 3, pp. 120–127, 2006.
 - [18] G. Litscher, L. Wang, E. Huber, and G. Nilsson, "Changed skin blood perfusion in the fingertip following acupuncture needle introduction as evaluated by Laser Doppler Perfusion Imaging," *Lasers in Medical Science*, vol. 17, no. 1, pp. 19–25, 2002.
 - [19] H. Hsiu, W. C. Hsu, S. L. Chang, C. L. Hsu, S. M. Huang, and Y. Y. W. Lin, "Microcirculatory effect of different skin contacting pressures around the blood pressure," *Physiological Measurement*, vol. 29, no. 12, pp. 1421–1434, 2008.
 - [20] G. Litscher, "Bioengineering assessment of acupuncture, part 2: monitoring of microcirculation," *Critical Reviews in Biomedical Engineering*, vol. 34, no. 4, pp. 273–293, 2006.
 - [21] H. Hsiu, S. M. Huang, P. T. Chao et al., "Microcirculatory characteristics of acupuncture points obtained by laser Doppler flowmetry," *Physiological Measurement*, vol. 28, no. 10, pp. N77–N86, 2007.
 - [22] H. Niimi and H. S. Yuwono, "Asian traditional medicine: from molecular biology to organ circulation," *Clinical Hemorheology and Microcirculation*, vol. 23, no. 2–4, pp. 123–125, 2000.
 - [23] H. Tsuru and K. Kawakita, "Acupuncture on the blood flow of various organs measured simultaneously by colored microspheres in rats," *Evidence-based Complementary and Alternative Medicine*, vol. 6, no. 1, pp. 77–83, 2009.
 - [24] H. Hsiu, W. C. Hsu, C. L. Hsu, M. Y. Jan, and Y. Y. Wang-Lin, "Effects of acupuncture at the Hoku acupoint on the pulsatile laser Doppler signal at the heartbeat frequency," *Lasers in Medical Science*, vol. 24, no. 4, pp. 553–560, 2009.
 - [25] M. L. Sandberg, M. K. Sandberg, and J. Dahl, "Blood flow changes in the trapezius muscle and overlying skin following transcutaneous electrical nerve stimulation," *Physical Therapy*, vol. 87, no. 8, pp. 1047–1055, 2007.
 - [26] C. L. Hsieh, Y. M. Chang, N. Y. Tang et al., "Time course of changes in nail fold microcirculation induced by acupuncture stimulation at the Waiguan acupoints," *American Journal of Chinese Medicine*, vol. 34, no. 5, pp. 777–785, 2006.
 - [27] Y. Q. Zhang, Y. L. Ding, Y. Y. Tian, T. Huang, W. B. Zhang, and G. J. Wang, "Change of blood perfusion on contra-lateral lower limb after electro-bian stone intervention," *Jiangsu Journal of Traditional Chinese Medicine*, vol. 42, no. 4, pp. 48–49, 2010.
 - [28] G. J. Wang, Y. Q. Zhang, R. H. Wang et al., "The study of interaction based on the thermostimulation," *Chinese Journal of Basic Medicine in Traditional Chinese Medicine*, vol. 16, no. 9, pp. 803–804, 2010.
 - [29] L. Bernardi, M. Rossi, P. Fratino, G. Finardi, E. Mevio, and C. Orlandi, "Relationship between phasic changes in human skin blood flow and autonomic tone," *Microvascular Research*, vol. 37, no. 1, pp. 16–27, 1989.
 - [30] L. A. Holowatz, C. S. Thompson-Torgerson, and W. L. Kenney, "The human cutaneous circulation as a model of generalized microvascular function," *Journal of Applied Physiology*, vol. 105, no. 1, pp. 370–372, 2008.
 - [31] J. Stewart, A. Kohen, D. Brouder et al., "Noninvasive interrogation of microvasculature for signs of endothelial dysfunction in patients with chronic renal failure," *American Journal of Physiology—Heart and Circulatory Physiology*, vol. 287, no. 6, pp. H2687–H2696, 2004.
 - [32] M. Rossi, A. Bradbury, A. Magagna, M. Pesce, S. Taddei, and A. Stefanovska, "Investigation of skin vasoreactivity and blood flow oscillations in hypertensive patients: effect of short-term antihypertensive treatment," *Journal of Hypertension*, vol. 29, no. 8, pp. 1569–1576, 2011.